TARGETING NEUROINFLAMMATION IN CENTRAL NERVOUS SYSTEM DISORDERS: UNCOVERING MECHANISMS, PHARMACOLOGICAL TARGETS, AND NEUROPHARMACEUTICAL DEVELOPMENTS

EDITED BY: Mariela Fernanda Perez, Claudia Bregonzio,
Maria Graciela Castro and Flavia Eugenia Saravia

PUBLISHED IN: Frontiers in Pharmacology, Frontiers in Neuroscience,
Frontiers in Neurology and Frontiers in Cellular Neuroscience

frontiers Research Topics

Frontiers eBook Copyright Statement

The copyright in the text of individual articles in this eBook is the property of their respective authors or their respective institutions or funders. The copyright in graphics and images within each article may be subject to copyright of other parties. In both cases this is subject to a license granted to Frontiers.

The compilation of articles constituting this eBook is the property of Frontiers.

Each article within this eBook, and the eBook itself, are published under the most recent version of the Creative Commons CC-BY licence. The version current at the date of publication of this eBook is CC-BY 4.0. If the CC-BY licence is updated, the licence granted by Frontiers is automatically updated to the new version.

When exercising any right under the CC-BY licence, Frontiers must be attributed as the original publisher of the article or eBook, as applicable.

Authors have the responsibility of ensuring that any graphics or other materials which are the property of others may be included in the CC-BY licence, but this should be checked before relying on the CC-BY licence to reproduce those materials. Any copyright notices relating to those materials must be complied with.

Copyright and source acknowledgement notices may not be removed and must be displayed in any copy, derivative work or partial copy which includes the elements in question.

All copyright, and all rights therein, are protected by national and international copyright laws. The above represents a summary only. For further information please read Frontiers' Conditions for Website Use and Copyright Statement, and the applicable CC-BY licence.

ISSN 1664-8714
ISBN 978-2-88974-107-6
DOI 10.3389/978-2-88974-107-6

About Frontiers

Frontiers is more than just an open-access publisher of scholarly articles: it is a pioneering approach to the world of academia, radically improving the way scholarly research is managed. The grand vision of Frontiers is a world where all people have an equal opportunity to seek, share and generate knowledge. Frontiers provides immediate and permanent online open access to all its publications, but this alone is not enough to realize our grand goals.

Frontiers Journal Series

The Frontiers Journal Series is a multi-tier and interdisciplinary set of open-access, online journals, promising a paradigm shift from the current review, selection and dissemination processes in academic publishing. All Frontiers journals are driven by researchers for researchers; therefore, they constitute a service to the scholarly community. At the same time, the Frontiers Journal Series operates on a revolutionary invention, the tiered publishing system, initially addressing specific communities of scholars, and gradually climbing up to broader public understanding, thus serving the interests of the lay society, too.

Dedication to Quality

Each Frontiers article is a landmark of the highest quality, thanks to genuinely collaborative interactions between authors and review editors, who include some of the world's best academicians. Research must be certified by peers before entering a stream of knowledge that may eventually reach the public - and shape society; therefore, Frontiers only applies the most rigorous and unbiased reviews.
Frontiers revolutionizes research publishing by freely delivering the most outstanding research, evaluated with no bias from both the academic and social point of view. By applying the most advanced information technologies, Frontiers is catapulting scholarly publishing into a new generation.

What are Frontiers Research Topics?

Frontiers Research Topics are very popular trademarks of the Frontiers Journals Series: they are collections of at least ten articles, all centered on a particular subject. With their unique mix of varied contributions from Original Research to Review Articles, Frontiers Research Topics unify the most influential researchers, the latest key findings and historical advances in a hot research area! Find out more on how to host your own Frontiers Research Topic or contribute to one as an author by contacting the Frontiers Editorial Office: frontiersin.org/about/contact

TARGETING NEUROINFLAMMATION IN CENTRAL NERVOUS SYSTEM DISORDERS: UNCOVERING MECHANISMS, PHARMACOLOGICAL TARGETS, AND NEUROPHARMACEUTICAL DEVELOPMENTS

Topic Editors:
Mariela Fernanda Perez, National University of Cordoba, Argentina
Claudia Bregonzio, CCT CONICET Córdoba, Argentina
Maria Graciela Castro, University of Michigan, United States
Flavia Eugenia Saravia, Universidad de Buenos Aires, Argentina

Citation: Perez, M. F., Bregonzio, C., Castro, M. G., Saravia, F. E., eds. (2022). Targeting Neuroinflammation in Central Nervous System Disorders: Uncovering Mechanisms, Pharmacological Targets, and Neuropharmaceutical Developments. Lausanne: Frontiers Media SA. doi: 10.3389/978-2-88974-107-6

Table of Contents

06 ***Editorial: Targeting Neuroinflammation in Central Nervous System Disorders: Uncovering Mechanisms, Pharmacological Targets, and Neuropharmaceutical Developments***
Mariela Fernanda Pérez, Flavia Saravia, María Graciela Castro and Claudia Bregonzio

09 ***Triumeq Increases Excitability of Pyramidal Neurons in the Medial Prefrontal Cortex by Facilitating Voltage-Gated Ca^{2+} Channel Function***
Lihua Chen, Lena Al-Harthi and Xiu-Ti Hu

22 ***Cerebrospinal Fluid Inflammatory Cytokine Levels in Patients With Major Psychiatric Disorders: A Multiplex Immunoassay Study***
Shinsuke Hidese, Kotaro Hattori, Daimei Sasayama, Takuya Tsumagari, Tomoko Miyakawa, Ryo Matsumura, Yuuki Yokota, Ikki Ishida, Junko Matsuo, Sumiko Yoshida, Miho Ota and Hiroshi Kunugi

31 ***The Complexity of the cGAS-STING Pathway in CNS Pathologies***
Amelia L. Fryer, Amar Abdullah, Juliet M. Taylor and Peter J. Crack

42 ***Venlafaxine Attenuated the Cognitive and Memory Deficit in Mice Exposed to Isoflurane Alone***
Liang Li and Chunhai Zhang

51 ***Effects of Interleukin-1β in Glycinergic Transmission at the Central Amygdala***
Jocelyn Solorza, Carolina A. Oliva, Karen Castillo, Gabriela Amestica, María Constanza Maldifassi, Xaviera A. López-Cortés, Rafael Barra, Jimmy Stehberg, Matthias Piesche, Patricio Sáez-Briones, Wendy González, Mauricio Arenas-Salinas and Trinidad A. Mariqueo

61 ***Chronic Voluntary Alcohol Drinking Causes Anxiety-like Behavior, Thiamine Deficiency, and Brain Damage of Female Crossed High Alcohol Preferring Mice***
Hong Xu, Hui Li, Dexiang Liu, Wen Wen, Mei Xu, Jacqueline A. Frank, Jing Chen, Haining Zhu, Nicholas J. Grahame and Jia Luo

79 ***Neuroimmune Mechanisms as Novel Treatment Targets for Substance Use Disorders and Associated Comorbidities***
Mark D. Namba, Jonna M. Leyrer-Jackson, Erin K. Nagy, M. Foster Olive and Janet L. Neisewander

106 ***Fenofibrate (a PPAR-α Agonist) Administered During Ethanol Withdrawal Reverts Ethanol-Induced Astrogliosis and Restores the Levels of Glutamate Transporter in Ethanol-Administered Adolescent Rats***
Francisca Villavicencio-Tejo, Osvaldo Flores-Bastías, Lucas Marambio-Ruiz, Diliana Pérez-Reytor and Eduardo Karahanian

114 ***Inflammation and Insulin Resistance as Risk Factors and Potential Therapeutic Targets for Alzheimer's Disease***
Angeles Vinuesa, Carlos Pomilio, Amal Gregosa, Melisa Bentivegna, Jessica Presa, Melina Bellotto, Flavia Saravia and Juan Beauquis

139 ***CNS-Draining Meningeal Lymphatic Vasculature: Roles, Conundrums and Future Challenges***
Sofia Pereira das Neves, Nickoleta Delivanoglou and Sandro Da Mesquita

156 ***Amphetamine Induces Oxidative Stress, Glial Activation and Transient Angiogenesis in Prefrontal Cortex via AT_1-R***
Osvaldo M. Basmadjian, Victoria B. Occhieppo, Natalia A. Marchese, M. Jazmin Silvero C., María Cecilia Becerra, Gustavo Baiardi and Claudia Bregonzio

173 ***Anti-Inflammatory Effects of Dimethyl Fumarate in Microglia via an Autophagy Dependent Pathway***
Young-Sun Lee, Deepak Prasad Gupta, Sung Hee Park, Hyun-Jeong Yang and Gyun Jee Song

184 ***Maternal Nicotine Exposure Alters Hippocampal Microglia Polarization and Promotes Anti-inflammatory Signaling in Juvenile Offspring in Mice***
Li Zhou, Xinrong Tao, Gang Pang, Min Mu, Qixian Sun, Fei Liu, Yuting Hu, Huihui Tao, Bing Li and Keyi Xu

202 ***Neuroinflammation as a Therapeutic Target for Mitigating the Long-Term Consequences of Acute Organophosphate Intoxication***
Peter M. Andrew and Pamela J. Lein

218 ***Methylene Blue Application to Lessen Pain: Its Analgesic Effect and Mechanism***
Seung Won Lee and Hee Chul Han

230 ***Discovery of a Highly Conserved Peptide in the Iron Transporter Melanotransferrin that Traverses an Intact Blood Brain Barrier and Localizes in Neural Cells***
Chaahat S. B. Singh, Brett A. Eyford, Thomas Abraham, Lonna Munro, Kyung Bok Choi, Mark Okon, Timothy Z. Vitalis, Reinhard Gabathuler, Chieh-Ju Lu, Cheryl G. Pfeifer, Mei Mei Tian and Wilfred A. Jefferies

245 ***Early IGF-1 Gene Therapy Prevented Oxidative Stress and Cognitive Deficits Induced by Traumatic Brain Injury***
Agustín. J. Montivero, Marisa. S. Ghersi, M. Jazmín Silvero C, Emilce Artur de la Villarmois, Johanna Catalan-Figueroa, Macarena Herrera, María Cecilia Becerra, Claudia. B. Hereñú and Mariela. F. Pérez

257 ***Pathological Neuroinflammatory Conversion of Reactive Astrocytes Is Induced by Microglia and Involves Chromatin Remodeling***
Alejandro Villarreal, Camila Vidos, Matías Monteverde Busso, María Belén Cieri and Alberto Javier Ramos

272 ***Connecting Neuroinflammation and Neurodegeneration in Multiple Sclerosis: Are Oligodendrocyte Precursor Cells a Nexus of Disease?***
Morgan W. Psenicka, Brandon C. Smith, Rachel A. Tinkey and Jessica L. Williams

301 ***Effect of Ulinastatin on Early Postoperative Cognitive Dysfunction in Elderly Patients Undergoing Surgery: A Systemic Review and Meta-Analysis***
Mei Duan, Fangyan Liu, Huiqun Fu, Shuai Feng, Xue Wang and Tianlong Wang

312 ***Baicalin Attenuates Oxygen–Glucose Deprivation/Reoxygenation–Induced Injury by Modulating the BDNF-TrkB/PI3K/Akt and MAPK/Erk1/2 Signaling Axes in Neuron–Astrocyte Cocultures***
Changxiang Li, Conglu Sui, Wei Wang, Juntang Yan, Nan Deng, Xin Du, Fafeng Cheng, Xiaona Ma, Xueqian Wang and Qingguo Wang

326 ***A Computational Exploration of the Molecular Network Associated to Neuroinflammation in Alzheimer's Disease***
Fatima El Idrissi, Bernard Gressier, David Devos and Karim Belarbi

338 ***Glucagon-Like Peptide-1 Analog Exendin-4 Ameliorates Cocaine-Mediated Behavior by Inhibiting Toll-Like Receptor 4 Signaling in Mice***
Changliang Zhu, Hong Tao, Shikuo Rong, Lifei Xiao, Xinxiao Li, Shucai Jiang, Baorui Guo, Lei Wang, Jiangwei Ding, Caibing Gao, Haigang Chang, Tao Sun and Feng Wang

355 ***Long-Lasting Changes in Glial Cells Isolated From Rats Subjected to the Valproic Acid Model of Autism Spectrum Disorder***
Marianela Evelyn Traetta, Nonthué Alejandra Uccelli, Sandra Cristina Zárate, Dante Gómez Cuautle, Alberto Javier Ramos and Analía Reinés

375 ***Galectin-3 Deletion Reduces LPS and Acute Colitis-Induced Pro-Inflammatory Microglial Activation in the Ventral Mesencephalon***
Ana M. Espinosa-Oliva, Pablo García-Miranda, Isabel María Alonso-Bellido, Ana E. Carvajal, Melania González-Rodríguez, Alejandro Carrillo-Jiménez, Arturo J. Temblador, Manuel Felices-Navarro, Irene García-Domínguez, María Angustias Roca-Ceballos, María D. Vázquez-Carretero, Juan García-Revilla, Marti Santiago, María J. Peral, José Luis Venero and Rocío M. de Pablos

frontiers in Pharmacology

EDITORIAL
published: 01 December 2021
doi: 10.3389/fphar.2021.771610

Editorial: Targeting Neuroinflammation in Central Nervous System Disorders: Uncovering Mechanisms, Pharmacological Targets, and Neuropharmaceutical Developments

Mariela Fernanda Pérez[1†], *Flavia Saravia*[2†], *María Graciela Castro*[3†] and *Claudia Bregonzio*[1*†]

[1]Instituto de Farmacología Experimental Córdoba (IFEC-CONICET), Departamento de Farmacología, Facultad de Ciencias Químicas, Universidad Nacional de Córdoba, Córdoba, Argentina, [2]Facultad de Ciencias Exactas y Naturales, Universidad de Buenos Aires, Cordoba, Argentina, [3]Department of Neurosurgery, School of Medicine, University of Michigan, Ann Arbor, MI, United States

Keywords: neuroinflammation, Alzheimer´s disease, drug abuse and addiction, traumatic brain injury, autophagic dysfunction, lymphatic drainage and uptake

OPEN ACCESS

Edited and reviewed by:
Nicholas M. Barnes, University of Birmingham, United Kingdom

***Correspondence:**
Claudia Bregonzio
claubregonzio@unc.edu.ar

†ORCID:
Mariela Fernanda Pérez, orcid.org/0000-0002-7337-9248;
Flavia Saravia, orcid.org/0000-0002-0781-0140;
Maria Graciela Castro, orcid.org/0000-0003-2237-2756;
Claudia Bregonzio, orcid.org/0000-0003-3542-2177

Specialty section:
This article was submitted to Neuropharmacology, a section of the journal Frontiers in Pharmacology

Received: *06 September 2021*
Accepted: *16 November 2021*
Published: *01 December 2021*

Citation:
Pérez MF, Saravia F, Castro MG and Bregonzio C (2021) Editorial: Targeting Neuroinflammation in Central Nervous System Disorders: Uncovering Mechanisms, Pharmacological Targets, and Neuropharmaceutical Developments. Front. Pharmacol. 12:771610. doi: 10.3389/fphar.2021.771610

Editorial on the Research Topic

Targeting Neuroinflammation in Central Nervous System Disorders: Uncovering Mechanisms, Pharmacological Targets, and Neuropharmaceutical Developments

In this special issue we present a series of reviews and research papers written from leading authors highlighting neuroinflammation as a common target to overcome and understand brain disorders. Neuroinflammation plays a key role in Parkinson, Alzheimer, schizophrenia, major depression and drug addiction, among others. Some threads include: autophagic dysfunction (essential for the removal of unnecessary cellular constituents and dysfunctional components), dysfunctional central nervous system (CNS) lymphatic drainage (dampened cleansing of molecules prone to aggregation and reduced immune cell egress into the draining cervical lymphatic nodes), traumatic brain injury and psychostimulants and alcohol abuse disorders. The growing evidence shows that attenuation of neuroinflammation brings beneficial effects against neurodegeneration and cognitive deficits associated with a plethora of CNS disorders. Considering this last issue, the identification of its most relevant biological processes and possible pharmacological targets remains a major challenge.

Keeping in mind the role of neuroinflammation in psychiatric disorders and its implications in mediating worsening of the symptoms, it is important to highlight the search of biomarkers for early diagnosis and improved treatment. In this sense it is important to consider a recent study performed in patients with major psychiatric disorders showing alterations in cerebrospinal fluid (CSF) inflammatory cytokine levels. Hidese et al. found that CSF interferon-β levels, among 19 cytokines tested was significantly higher in patients with schizophrenia, or bipolar disorder when compared to healthy controls. This represents novel evidence showing prominent statistical differences between psychiatric groups and healthy controls. Along the same lines, in a very interesting computational exploration of the molecular network associated to neuroinflammation in Alzheimer's disease (AD), Idrissi et al. found that 94 proteins were significantly associated. Over the scientific literature they identified eleven key proteins with the highest ability to control neuroinflammatory processes significantly associated with AD and

pharmacological compounds with single or pleiotropic actions acting on them. These results could help in the prioritization of diagnostic and target-engagement biomarkers as well as in the development of therapeutic strategies against neuroinflammation in AD.

The autophagic process is implicated in the removal of unnecessary or dysfunctional proteins and damaged organelles *via* the lysosomal machinery. For this reason, it is critical for the maintenance of neuronal function and to provide neuroprotection in neurodegenerative disorders. Adequate regulation of autophagy is associated with beneficial outcomes in neurodegenerative diseases (Nixon, 2013; Cho et al., 2020). The interplay between autophagy and inflammation is complex, although neuroinflammation is implicated in autophagic dysfunction. In this sense, it is known that upregulation of autophagy promotes microglial polarization toward the M2 phenotype by the suppression of M1 markers (Jin et al., 2018; Cho et al., 2020). In this respect, Lee et al. found that dimethyl fumarate reduced NO production and the expression levels of genes associated with the M1 phenotype, including TNF-α and IL-6 and phagocytosis in microglia, both associated with the M2 phenotype. These data suggest that this compound leads to the induction of autophagy in microglia and its anti-inflammatory effects are partially mediated through an autophagy-dependent pathway.

It is well known that following brain injury or in neurodegenerative diseases, astrocytes become reactive and may suffer pathological remodeling, they lose their homeostatic functions facilitating neurodegeneration by maintenance of the pro-inflammatory environment. A deeper understanding of the cellular and molecular mechanisms involved in the astroglial response and neuroinflammation are needed to develop pharmacological interventions that will lead to novel therapeutic strategies. In this regard, Villarreal et al. showed that pathological neuroinflammatory conversion of reactive astrocytes is induced by microglia and involves chromatin remodeling. These results open a new perspective in pharmacological interventions that affect astroglial pathological remodeling and point out to epigenetic changes as a potential pharmacological target to interfere with pathological astroglial phenotype stabilization.

Neuroinflammation is also a risk factor for neurodegenerative disease such as AD. Vinuesa et al. compiled data supporting the role of inflammation and insulin resistance as risk factors for AD and explored potential therapeutic targets. Considering that there has been a global rise of type II diabetes and obesity prevalence, it becomes necessary to understand how changes in metabolic function can lead to an increased risk for premature brain aging and the development of neurodegenerative disorders such as AD. In this respect, the interplay between inflammation and insulin resistance could represent a potential therapeutic target to prevent or ameliorate neurodegeneration and cognitive impairment.

The morphology and unique functional features of meningeal lymphatics have a close relation with several brain disorders. Recent studies have tested the effects of boosting the function of the meningeal lymphatics in mouse models of AD. Since a pathological hallmark of AD is the accumulation of extracellular amyloid plaques rich in aggregated amyloid beta (Aβ) peptides (Ittner and Gotz, 2011) impairment in Aβ clearance could contribute to its accumulation (Wisniewski and Goni, 2014). Moreover, the presence of intracellular neurofibrillary tangles is another pathological hallmark of this neurodegenerative disease, which is composed by hyperphosphorylated forms of the microtubule-associated protein Tau (Ittner and Gotz, 2011). Pereira das Neves et al. highlighted and exhaustively described the evidence supporting the notion that an impaired meningeal lymphatic drainage in AD could promote both Aβ and Tau accumulation in the brain, affecting disease severity and aggravating cognitive decline. Induction of traumatic brain injury (TBI) in mice resulted in a substantial decrease in meningeal lymphatic drainage as early as 2 hours post-injury, which was only fully restored 2 months later (Bolte et al., 2020). In accordance, CSF flow was altered in TBI (Johanson et al., 2011), and intracranial pressure was markedly increased 2 hours post-injury (Bolte et al., 2020). These data suggest that there is an early temporal window right after brain injury, suitable for pharmacological interventions, in order to prevent secondary injury mechanisms and reduce the development of long-term disabilities, including cognitive, affective and physical impairments, as well as neurodegenerative pathologies. Regrettably, none of the pharmacological agents used in the clinic to manage the TBI sequelae can inhibit the neuroinflammatory cascade (Carney et al., 2017). Montivero et al. proposed brain insulin-like growth factor 1 (IGF-1) over-expression, considering IGF-1 neuroprotective and anti-inflammatory effects (Zheng et al., 2000; Carlson and Saatman 2018; Serhan et al., 2019). This treatment, performed as early as 15 min after TBI, was effective not only in reducing oxidative-stress markers, but also in improving the cognitive deficits observed long-term after mild TBI in adult rats.

In a very interesting review, Namba et al. describe the neuroimmune mechanisms as novel treatment targets for substance abuse disorders and associated comorbidities. This report presents recent studies analyzing the neurobiology of substance abuse that have exposed a significant role in neuroimmune signaling as a mechanism for drugs of abuse changes in synaptic plasticity and contribute to drug abuse-related behaviors. In the same lines, Xu et al. showed in a study performed in female mice, that alcohol consumption increased the expression of neuroinflammation markers. Accordingly, Villavicencio-Tejo et al. found that fenofibrate (peroxisome proliferator-activated receptor alpha agonist) administered during ethanol withdrawal blunted ethanol-induced astrogliosis and restores the levels of glutamate transporter in ethanol-administered adolescent rats. Moreover, the activation of PPARα by fibrates inhibits neuroinflammation, in models other than ethanol consumption. In relation to other drug of abuse, Basmadjian et al. showed that D-amphetamine is able to induce oxidative stress, transient angiogenesis, and long-lasting astroglial and microglial reactivity in the prefrontal cortex. These effects were prevented with an angiotensin II AT1 receptor blocker, candesartan. To this respect, it was shown that AT1-R blockade exerts protective effects over gliosis and pro-

inflammatory compounds released in several animal models of neuroinflammation.

Taken together all findings presented in the Research Topic, point out that neuroinflammation is a common denominator between diverse CNS-associated pathologies such as neurodegenerative diseases, acute injuries, metabolic, psychiatric and drug abuse induced disorders. The ability to modulate neuroinflammation could provide a novel therapeutic opportunity to improve the outcomes in these devasting conditions.

AUTHOR CONTRIBUTIONS

All authors listed have made a substantial, direct, and intellectual contribution to the work and approved it for publication.

REFERENCES

Bolte, A. C., Dutta, A. B., Hurt, M. E., Smirnov, I., Kovacs, M. A., McKee, C. A., et al. (2020). Meningeal Lymphatic Dysfunction Exacerbates Traumatic Brain Injury Pathogenesis. *Nat. Commun.* 11 (1), 4524. doi:10.1038/s41467-020-18113-4

Carlson, S. W., and Saatman, K. E. (2018). Central Infusion of Insulin-like Growth Factor-1 Increases Hippocampal Neurogenesis and Improves Neurobehavioral Function after Traumatic Brain Injury. *J. Neurotrauma* 35 (13), 1467–1480. doi:10.1089/neu.2017.5374

Carney, N., Totten, A. M., O'Reilly, C., Ullman, J. S., Hawryluk, G. W., Bell, M. J., et al. (2017). Guidelines for the Management of Severe Traumatic Brain Injury, Fourth Edition. *Neurosurgery* 80 (1), 6–15. doi:10.1227/NEU.0000000000001432Fourth Edition

Cho, K. S., Lee, J. H., Cho, J., Cha, G. H., and Song, G. J. (2020). Autophagy Modulators and Neuroinflammation. *Curr. Med. Chem.* 27 (6), 955–982. doi:10.2174/0929867325666181031144605

Ittner, L. M., and Götz, J. (2011). Amyloid-β and tau--a toxic pas de deux in Alzheimer's disease. *Nat. Rev. Neurosci.* 12 (2), 65–72. doi:10.1038/nrn2967

Jin, M. M., Wang, F., Qi, D., Liu, W. W., Gu, C., Mao, C. J., et al. (2018). A Critical Role of Autophagy in Regulating Microglia Polarization in Neurodegeneration. *Front. Aging Neurosci.* 10, 378. doi:10.3389/fnagi.2018.00378

Johanson, C., Stopa, E., Baird, A., and Sharma, H. (2011). Traumatic Brain Injury and Recovery Mechanisms: Peptide Modulation of Periventricular Neurogenic Regions by the Choroid Plexus-CSF Nexus. *J. Neural Transm. (Vienna)* 118 (1), 115–133. doi:10.1007/s00702-010-0498-0

Nixon, R. A. (2013). The Role of Autophagy in Neurodegenerative Disease. *Nat. Med.* 19 (8), 983–997. doi:10.1038/nm.3232

Serhan, A., Boddeke, E., and Kooijman, R. (2019). Insulin-Like Growth Factor-1 Is Neuroprotective in Aged Rats with Ischemic Stroke. *Front. Aging Neurosci.* 11, 349. doi:10.3389/fnagi.2019.00349

Wisniewski, T., and Goñi, F. (2014). Immunotherapy for Alzheimer's Disease. *Biochem. Pharmacol.* 88 (4), 499–507. doi:10.1016/j.bcp.2013.12.020

Zheng, W. H., Kar, S., Doré, S. R., and Quirion, R. (2000). Insulin-like Growth Factor-1 (IGF-1): a Neuroprotective Trophic Factor Acting via the Akt Kinase Pathway. *J. Neural Transm. Suppl.* 1 (60), 261–272. doi:10.1007/978-3-7091-6301-6_17

Conflict of Interest: The authors declare that the research was conducted in the absence of any commercial or financial relationships that could be construed as a potential conflict of interest.

Publisher's Note: All claims expressed in this article are solely those of the authors and do not necessarily represent those of their affiliated organizations, or those of the publisher, the editors and the reviewers. Any product that may be evaluated in this article, or claim that may be made by its manufacturer, is not guaranteed or endorsed by the publisher.

Copyright © 2021 Pérez, Saravia, Castro and Bregonzio. This is an open-access article distributed under the terms of the Creative Commons Attribution License (CC BY). The use, distribution or reproduction in other forums is permitted, provided the original author(s) and the copyright owner(s) are credited and that the original publication in this journal is cited, in accordance with accepted academic practice. No use, distribution or reproduction is permitted which does not comply with these terms.

frontiers in Pharmacology

ORIGINAL RESEARCH
published: 28 January 2021
doi: 10.3389/fphar.2020.617149

Triumeq Increases Excitability of Pyramidal Neurons in the Medial Prefrontal Cortex by Facilitating Voltage-Gated Ca^{2+} Channel Function

*Lihua Chen, Lena Al-Harthi and Xiu-Ti Hu**

Department of Microbial Pathogens and Immunity, Rush University Medical Center, Chicago, IL, United States

Combination antiretroviral therapy (cART) suppresses HIV-1 replication, improves immune function, and prolongs the life of people living with HIV (PLWH). However, cART also induces neurotoxicity that could complicate HIV-induced neurodegeneration while reduce its therapeutic efficacy in treating HIV/AIDS. Triumeq is a first-line cART regimen, which is co-formulated by three antiretroviral drugs (ARVs), lamivudine (3TC), abcavir (ABC), and dolutegravir (DTG). Little is known about potential side effects of ARVs on the brain (including those co-formulating Triumeq), and their mechanisms impacting neuronal activity. We assessed acute (*in vitro*) and chronic (*in vivo*) effects of Triumeq and co-formulating ARVs on pyramidal neurons in rat brain slices containing the medial prefrontal cortex (mPFC) using patch-clamp recording approaches. We found that acute Triumeq or 3TC *in vitro* significantly increased firing of mPFC neurons in a concentration- and time-dependent manner. This neuronal hyperactivity was associated with enhanced Ca^{2+} influx through voltage-gated Ca^{2+} channels (VGCCs). Additionally, chronic treatment with Triumeq *in vivo* for 4 weeks (4 wks) also significantly increased firing and Ca^{2+} influx via VGCCs in mPFC neurons, which was not shown after 2 wks treatment. Such mPFC neuronal hyperexcitability was not found after 4 weeks treatments of individual ARVs. Further, chronic Triumeq exposure *in vivo* significantly enhanced mRNA expression of low voltage-activated (LVA) L-type Ca^{2+} channels ($Ca_v1.3$ L-channels), while changes in high voltage-activated (HVA) Cav1.2 L-channels were not observed. Collectively, these novel findings demonstrate that chronic cART induces hyperexcitability of mPFC pyramidal neurons by abnormally promoting VGCC overactivation/overexpression of VGCCs (including, but may not limited to, LVA-$Ca_v1.3$ L-channels), which could complicate HIV-induced neurotoxicity, and ultimately may contribute to HIV-associated neurocognitive disorders (HAND) in PLWH. Determining additional target(s) of cART in

OPEN ACCESS

Edited by:
Flavia Eugenia Saravia, University of Buenos Aires, Argentina

Reviewed by:
Yan Dong, University of Pittsburgh, United States
Vinod Tiwari, Indian Institute of Technology (BHU), India

***Correspondence:**
Xiu-Ti Hu
xiu-ti_hu@rush.edu

Specialty section:
This article was submitted to Neuropharmacology, a section of the journal Frontiers in Pharmacology

Received: *14 October 2020*
Accepted: *30 December 2020*
Published: *28 January 2021*

Citation:
Chen L, Al-Harthi L and Hu X-T (2021) Triumeq Increases Excitability of Pyramidal Neurons in the Medial Prefrontal Cortex by Facilitating Voltage-Gated Ca^{2+} Channel Function. Front. Pharmacol. 11:617149. doi: 10.3389/fphar.2020.617149

Abbreviations: PLWH, People living with HIV; HAND, HIV-associated neurocognitive disorders; cART, combined antiretroviral therapy; ARVs, antiretroviral drugs; mPFC, medial prefrontal cortex; VGCC, voltage-gated Ca2+ channel; WHO, World Health Organization; 3TC, lamivudine; ABC, abcavir; DTG, dolutegravir; NRTI, nucleotide reverse transcriptase inhibitor; INSTI, integrase strand transfer inhibitor; wk, week; RMP, resting membrane potential; AP, action potential; ×, fold; rm, repeated measures; L-channels, L-type VGCCs; LVA, low voltage-activated; HVA, high voltage-activated; Hipp, hippocampal; nNRTI, non-NRTI.

mPFC pyramidal neurons may help to improve the therapeutic strategies by minimizing the side effects of cART for treating HIV/AIDS.

Keywords: HIV-1, neurodegenerative disease, CART, neurotoxicity, hyperactivity, calcium dysregulation, voltage-gated calcium channel, electrophysiology

INTRODUCTION

Combination antiretroviral therapy (cART) effectively suppresses HIV replication, improves immune function, and prolongs life of people living with HIV (PLWH), which transformed HIV infection from a fatal disease to a lifelong chronic, but manageable disease. However, the prevalence of HIV-associated neurocognitive disorders (HAND) occurs in up to ~50% of PLWH in the era of cART (Antinori et al., 2007; Tozzi et al., 2007; McArthur et al., 2010). A growing body of evidence suggests that cART may be a contributing factor to the neurodegenerative HAND, likely by altering the function of the brain regions that regulate cognition (Heaton et al., 2010; Robertson et al., 2010; Simioni et al., 2010). It is unknown if this high prevalence of HAND is due to the legacy effects in the pre-cART era, low level of HIV below the limit of detection of sensitive assays, or the side effects of cART that could complicate HIV-induced neurotoxicity, or both (Kranick and Nath, 2012; Manji et al., 2013; Underwood et al., 2015), especially during aging (Brew et al., 2009; Cysique and Brew, 2009; Vance et al., 2011; Jiang et al., 2016; Clifford et al., 2017). Therefore, understanding how and to what extent chronic cART affects the functional activity of neurons in the key brain regions that regulate neurocognition in PLWH warrants a thorough investigation.

The medial prefrontal cortex (mPFC) plays a critical role in regulating neurocognition; but it is profoundly altered by HIV-1 (Ferris et al., 2008; Hu, 2016). HIV-1 induces hyperactivity of glutamatergic pyramidal neurons in the mPFC by causing overactivation of voltage-gated Ca^{2+} channels (VGCCs) (Khodr et al., 2016; 2018; Napier et al., 2014; Wayman et al., 2015; 2016; 2012), in addition to glutamate and NMDA receptor (NMDAR) dysfunction (Gonzalez-Scarano and Martin-Garcia, 2005; King et al., 2006). Such Ca^{2+} dysregulation-mediated neurotoxicity resulting from NMDAR/VGCC dysfunction may contribute to the underlying mechanism of HAND (Hu, 2016). Other studies also suggest a negative impact of antiretroviral drugs (ARVs) on cortical neurons that may worsen HIV-induced neurotoxicity and HIV/AIDS-associated neurodegenerative consequences (Akay et al., 2011; Birbeck et al., 2012; Robertson et al., 2012; Romo et al., 2012; Manji et al., 2013; Akay et al., 2014; Jensen et al., 2015). Whether, how, and to what extent chronic cART alters neuronal activity in the mPFC, or in other brain regions that also regulate neurocognition, and therefore complicates HIV neurotoxicity, is not known.

Triumeq is a first-line cART regimen recommended by the World Health Organization (WHO) for treating HIV/AIDS (Walmsley et al., 2013; Calcagno et al., 2014; Greig and Deeks, 2015; Nwogu et al., 2016). It is a single-tablet co-formulated by three ARVs: lamivudine (3TC), abcavir (ABC) and dolutegravir (DTG) (Walmsley et al., 2013). 3TC and ABC are nucleoside reverse transcriptase inhibitor (NRTI), while DTG is an integrase strand transfer inhibitor (INSTI). Together, they effectively inhibit HIV replication. However, despite the required therapeutic effects, many ARVs also induce neurotoxicity, which could exacerbate HIV-induced neurodegeneration and brain dysfunction (Gonzalez et al., 2020). Clinical studies report that chronic treatments of ABC, DTG, efavirenz, and some other ARVs are also associated with neuropsychiatric disorders (Maxwell et al., 1988; Blanch et al., 2001; Colebunders et al., 2002; Wise et al., 2002; Mengato et al., 2020). Other studies show that some side effects of 3TC and DTG disappear when HIV^+ patients stop taking ARVs (Zamora et al., 2019). Moreover, a recent clinical study also reveals that HIV^+ women with consistent viral suppression following continuous cART show significantly more cognitive deficits than HIV^- or HIV^+ women without chronic cART (Rubin et al., 2017).

Pre-clinical studies using lab animals also reveal ARVs-induced neurotoxicity in the brain, including, but not limited to, loss of the dendritic processes, cytoplasmic shrinkage, mitochondrial dysfunction, and death of prefrontal cortical neurons in SIV^+ macaques and rats after chronic cART *in vivo* (Robertson et al., 2012; Akay et al., 2014). Chronic treatment with tenovovir, 3TC, and efavirenz also disturbs activity of hippocampal pyramidal neurons and memory impairments in rats (Akang, 2019), while acute ARV treatment reduces bioenergetic function in nerve terminals isolated from the striatum (Stauch et al., 2017). It is worth noting that 1) the prefrontal cortex, hippocampus, and striatum are the key regulators of cognition; but they are also most susceptible and vulnerable to HIV (Ferris et al., 2008; Manji et al., 2013; Hu, 2016); and (ii) neurotoxicity induced by ARVs appears to be associated with dysregulation of neuronal Ca^{2+} homeostasis (i.e., excessive intracellular free calcium, $[Ca^{2+}]_{in}$) (Robertson et al., 2012; Romo et al., 2012; Akay et al., 2014; Apostolova et al., 2015; Underwood et al., 2015; Vivithanaporn et al., 2016), similar to that induced by HIV (Wayman et al., 2012, 2015, 2016; Napier et al., 2014; Khodr et al., 2016, 2018; Chen et al., 2019). Collectively, these studies suggest that the site effects of cART disturb neuronal activity in the brain regions that regulate neurocognition, and therefore indicate the necessity to elucidate the mechanism by which ARVs disrupt the brain function. Understanding such mechanism could help us to improve the therapeutic strategies for treating HIV/AIDS by minimizing the side effects of cART through pharmacological intervene.

In this study, we assessed the impact of Triumeq, both acutely (*in vitro*) and chronically (*in vivo*), and the three individual ARVs (3TC, ABC, and DTG) co-formulating it, on the functional activity of mPFC pyramidal neurons in rat brain slices. We also defined the mechanism (i.e., overactivation of VGCCs) by which Triumeq induces abnormal neuronal hyperactivity that may complicate HIV-induced neurotoxicity in the mPFC.

MATERIALS AND METHODS

Animals

Male F344 rats (3–4 weeks old, wk) were purchased from Charles River (Wilmington, MA) and group-housed at Rush University Medical Center animal facility on a 12-hour light/dark cycle. Food and water were available *ad libitum*. Animal care and use procedures were conducted with the Institutional Animal Care and Use Committee, and in accordance with NIH, USDA and institutional guidelines.

Whole-Cell Current-Clamp Recording

Brain slices of rats were prepared, and then evoked action potential (firing) and VGCC activity were assessed among pyramidal neurons from the layer V-VI of the mPFC as described in our previous studies (Nasif et al., 2005a; Wayman et al., 2005b; Napier et al., 2014; Wayman et al., 2015; Wayman et al., 2016, Chen et al., 2019; Khodr et al., 2018).

To access the normal action potential, glass electrodes (4–6 MΩ) were filled with an internal solution (in mM: 120 K-gluconate, 10 HEPES, 20 KCl, 2 $MgCl_2$, 3 Na_2ATP, 0.3 NaGTP, and 0.1 EGTA; pH: 7.3–7.35; with 280–285 mOsm). All neurons met the criteria of a resting membrane potential (RMP) at least −60 mV and action potential (AP) amplitude ≥60 mV. The recording protocol included a series of 500 ms current pulses with the intensity ranged from 0 to +300 pA with a 25-pA.

VGCC activity was accessed after ~10 min perfusion of aCSF containing selective blockers for voltage-sensitive Na^+ channels (tetrodotoxin, TTX, 0.5 μM), K^+ channels (tetraethylammonium, TEA, 20 mM; Sigma), NMDA/AMPA receptors (kynurenic acid, 3 mM), and $GABA_A$ receptors ($GABA_AR$; picrotoxin, 100 μM). The internal solution used in the recording of VGCC activity consisted of (in mM) 140 Cs-gluconate, 10 HEPES, 2 $MgCl_2$, 3 Na_2ATP and 0.3 NaGTP (pH: 7.3–7.35; with 280–285 mOsm). V_m was held at ~−68 mV (around average RMP). 40 ms depolarizing rheobase currents were determined and used to elicit Ca^{2+} plateau potentials (reflecting Ca^{2+} influx through VGCCs).

Drug Application

For 3TC study *in vitro*, 3TC (from NIH AIDS reagent program) was dissolved in ddH_2O to make 10 mg/ml or 100 mg/ml stock solution. For Triumeq study *in vitro*, 1-fold (1×) Triumeq contained 1 μM (300 ng/ml) ABC, 1.3 μM (300 ng/ml) 3TC, and 50 nM (20 ng/ml) DTG dissolved in ddH_2O, ddH_2O and DMSO (vehicle), respectively. Such drug concentrations are equivalent or comparable to the levels of these ARVs reported in the CSF of cART-treated HIV^+ patients (Calcagno et al., 2014; Van den Hof et al., 2018). To access the drug(s) effects on firing and VGCC activity, at least 1000x higher concentrated stock solution of the compound(s) were diluted in the aCSF to make the final concentration. Recording was performed after ≥10 min perfusion of each concentration from low to higher concentration using a continuous perfusion system.

During *in vivo* study, ABC and 3TC (Sigma, St. Louis, MO) were dissolved in saline (SAL) to make 12 mg/ml and 6 mg/ml stock solution, respectively. DTG were first dissolved in 100% DMSO and then diluted to 70% DMSO with SAL (vehicle). The final DTG stock concentration was 1 mg/ml. During chronic experiment, rats received one daily s. c. injection of each compound based on their body weight. As a result, animals received a combined daily dosage of 12 mg/kg ABC, 6 mg/kg 3TC, and 1 mg/kg DTG. The combined dosage was similar to the Triumeq pill taken by PLWH. All drugs were purchased from Sigma unless specified.

Quantitative Real-Time PCR

Anesthetized rats were perfused transcardially with ice-cold saline. The brain was removed and dissected mPFC tissues were stored at −80°C for RNA extraction. Total RNA was extracted using a miRNeasy Mini kit (Qiagen Inc., Germantown, MD). DNA was removed using the RNase-free DNase set (Qiagen Inc.). mRNA level was measured on an Applied Biosystems (Foster City, CA) QuantStudio 7 Flex real-time PCR system using the Power SYBR® Green RNA-to-C_T™ 1-Step kit (Applied Biosystems). The 20 μL reaction mixture contained 25 ng of total RNA, 10 μL of 2X Power SYBR® Green RT-PCR Mix, 0.14 μL of RT enzyme mix, and 0.2 μL of each primer (10 μM forward β-actin, or 20 μM forward *CACNA1c* or *CACNA1d* and 20 μM reverse β-actin, *CACNA1C* or *CACNA1D*). Primers used are as follows: rat β-actin (forward primer: ccgcgagtacaaccttcttgc, reverse primer: atatcgtcatccatggcgaac tgg); rat *CACNA1C* (forward primer: ggcatcaccaacttcgaca, reverse primer: tacacccagggcaactcata); rat *CACNA1D* (forward primer: gag aggagggcaaacgaaaca, reverse primer: tcttttccaccagcaccagaga). Reactions were incubated at 48°C for 30 min; 95°C for 10 min, then 40 cycles of 95°C for 15 s and 60°C for 1 min, followed by a dissociation curve in order to confirm primer specificity. The mRNA levels shown as fold change ($2^{-\Delta\Delta Ct}$) were normalized to β-actin Ct and to vehicle (4 wk).

Statistical Analysis

Prism (GraphPad Software Inc., La Jolla, CA) and SigmaPlot (Systat Software Inc., San Jose, CA) were used to analyze data. One-way ANOVA with repeated measures (rm) was used to analyze the membrane properties and VGCC activity, followed by Dunnett's *post-hoc* test. Two-way rm ANOVA was used to analyze the firing frequency followed by Newman-Keuls *post-hoc* test. Statistical significance was set at $p \leq 0.05$. Student *t*-test was used to analyze the mRNA level of L-type Ca^{2+} channels. Data was presented as mean ± standard error. Outlier was identified as more than 2× of the standard deviation from the mean and was excluded from analysis.

RESULT

Acute Lamivudine Treatment *in vitro* Increases Firing and Voltage-Gated Ca2+ Channel Activity of Medial Prefrontal Cortex Pyramidal Neurons in a Dose-dependent Manner

To determine the impact of Triumeq on mPFC neuronal activity, we first assessed the acute effects of lamivudine (a.k.a. 3TC, one of

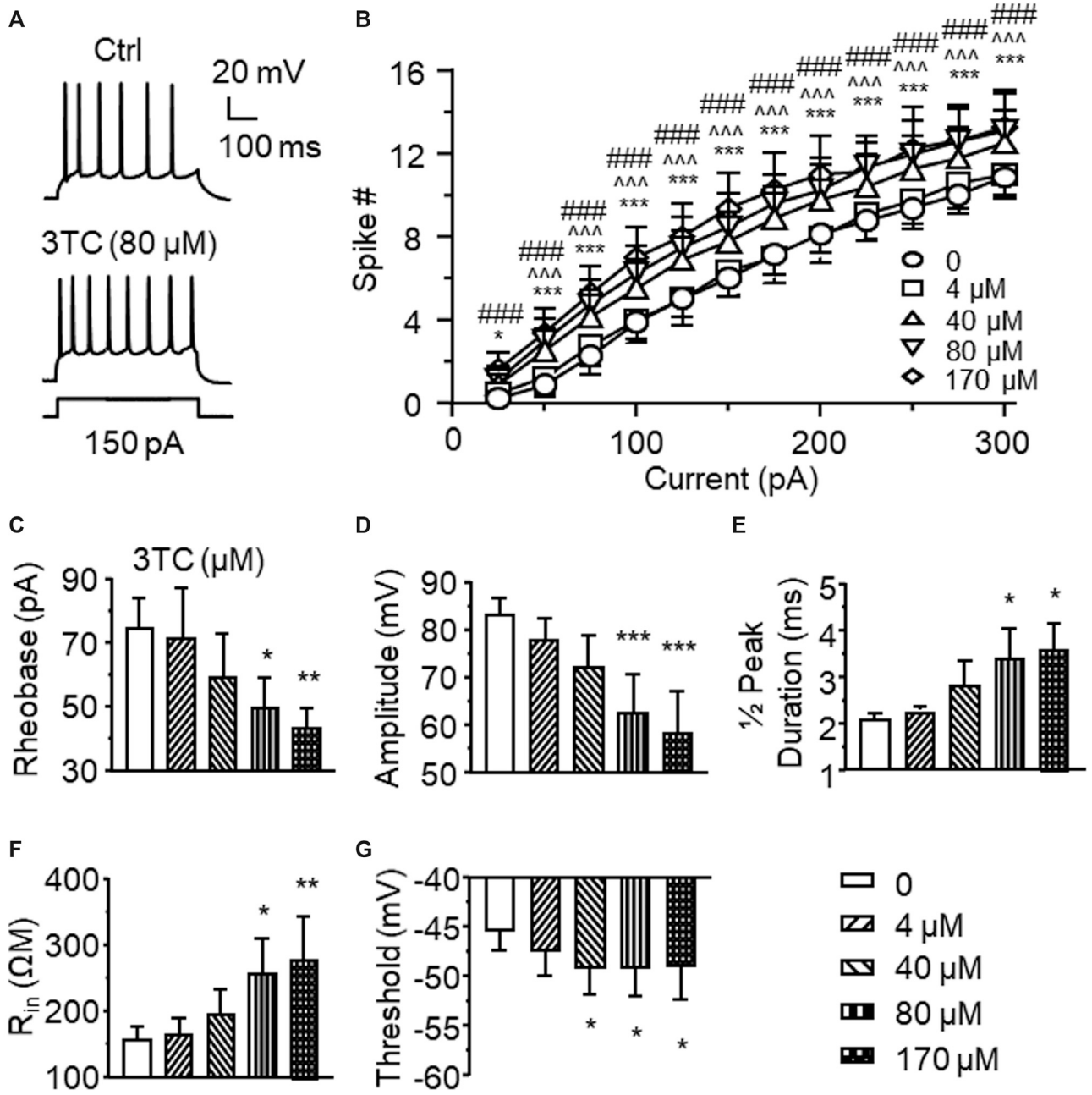

Figure 1 | Acute treatment of lamivudine (3TC) *in vitro* increases firing of mPFC pyramidal neurons **(A)** Sample traces showing that a moderate depolarizing current pulse (150pA, which mimicked physiological excitatory inputs) evoked more action potentials in a 3TC-treated neuron compared to one without 3TC treatment **(B)** The current-spike relationships indicate a significant increase in the firing frequency of neurons treated with 3TC in a concentration-dependent manner (40–170 μM) compared to those without this ARV (n = 8/ea. ***$p < 0.001$ between 0 vs 44 μM; ^$p < 0.05$ or 0.001 between 0 and 80 μM; ###$p < 0.001$ between 0 and 170 μM). 3TC-Associated with increased firing, higher concentrations of 3TC also altered the membrane properties by reducing the rheobase **(C)** and peak amplitude **(D)**, increasing the ½ peak duration **(E)** and inward resistance R_{in} **(F)**, while decreasing the threshold **(G)** (n = 8/ea. *,**,***$p < 0.05$, 0.01 or 0.001).

the ARVs that co-formulates Triumeq) on firing of mPFC pyramidal neurons evoked by depolarizing current pulses (25–400 pA). We found that 3TC at the concentrations of 40, 80 and 170 μM, though not 4 μM, significantly increased neuron's firing (n = 8/ea. 3TC effect: $F_{(4,28)} = 10.77$, $p < 0.001$; Current effect: $F_{(11,77)} = 123.3$, $p < 0.001$; Interaction: $F_{(44,308)} = 1.725$, $p = 0.004$; **Figures 1A,B**). Certain membrane properties were altered in association with the increased firing, which were also in a concentration-dependent manner. For example, the rheobase (the minimal current required for evoking firing, n = 8/each group (ea), $F_{(4,28)} = 5.174$, $p = 0.003$) and peak amplitude (n = 8/ea, $F_{(4,28)} = 11.512$, $p<0.001$) were significantly reduced by 3TC at

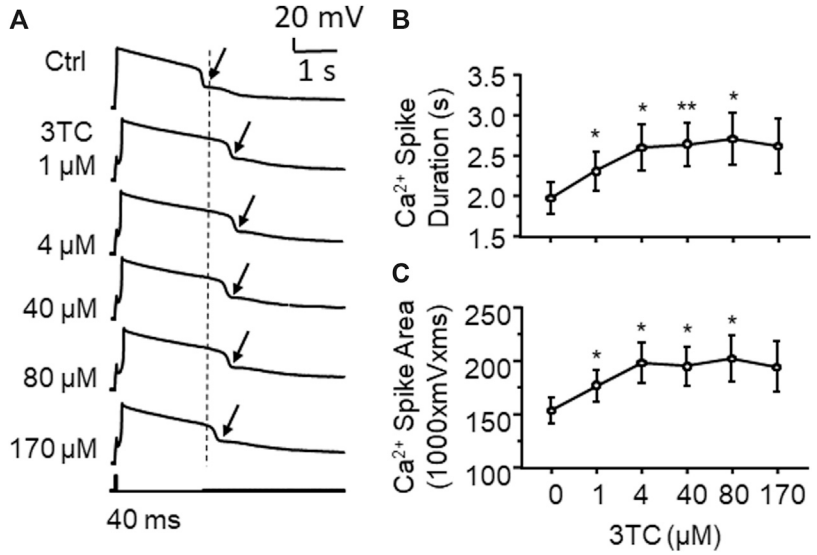

Figure 2 | 3TC enhances Ca^{2+} influx through overactive VGCCs **(A)** Sample traces showing that acute exposure to 3TC *in vitro* induced a prolongation of Ca^{2+} spikes in mPFC neurons (pointed by the arrows), indicating an increased functional activity of VGCCs in mPFC neurons **(B)** The acute effect of 3TC on Ca^{2+} spikes was also concentration-dependent, showing that the duration of Ca^{2+} spike was gradually increased at lower concentrations (1–80 μM), but begun to decrease in response to a high concentration (170 μM) (n = 9/ea. $^{*,**}p < 0.05$ or 0.01).

higher doses (80 and 170 μM) (**Figures 1C,D**), the half-peak duration (n = 8/ea, $F_{(4,28)} = 4.080$, $p = 0.01$) and inward resistance (R_{in}, n = 8/ea, $F_{(4,28)} = 4.665$, $p = 0.005$) were significantly increased by 80 and 170 μM 3TC (**Figures 1E,F**), while the threshold was reduced by 40, 80 and 170 μM 3TC (n = 8/ea, $F_{(4,28)} = 2.989$, $p = 0.036$; **Figure 1G**). All these alterations indicate an increased membrane excitability among these neurons.

VGCCs are one of the key regulators in mediating neuronal excitability. To determine if alterations in Ca^{2+} channel activity contribute to 3TC-induced increase of firing, voltage-sensitive Ca^{2+} spikes (reflecting Ca^{2+} influx *via* activated VGCCs) were evaluated with blockade of voltage-gated Na^+/K^+ channels, as well as glutamate and GABA-mediated excitatory and inhibitory inputs, respectively. We found that voltage-sensitive Ca^{2+} influx through VGCCs in mPFC pyramidal neurons was significantly enhanced by 3TC in a concentration-dependent manner (1, 4, 40 and 80 μM), evidenced by increased Ca^{2+} spike duration (n = 9/ea. $F_{(5,40)} = 5.052$, $p = 0.001$) and area (n = 9/ea. $F_{(5,40)} = 4.068$, $p = 0.004$) (**Figure 2A**). But 170 μM 3TC begun to reduce the previously prolonged Ca^{2+} spike (**Figures 2B,C**), likely due to overactivation-induced inactivation of VGCCs. The lowest concentration (1 μM) used here was equivalent to the reported level of 3TC in the CSFs of HIV^+ patients taking this ARV, while the higher concentrations (4~40 μM) were comparable to the plasma levels of this ARV detected in HIV^+ individuals (Johnson et al., 1999; Van den Hof et al., 2018). The highest concentrations of 3TC (80 and 170) were used to assess potential neurotoxic effect of this ARV on dysregulating neuronal Ca^{2+} homeostasis mediated by VGCCs, as done in our previous studies (Napier et al., 2014; Wayman et al., 2015; Wayman et al., 2016). These results reveal a 3TC-induced increase in VGCC activity and Ca^{2+} influx, which contributes to increase firing.

Acute Triumeq Exposure *in vitro* Increases Firing of Medial Prefrontal Cortex Neurons and Voltage-Sensitive Ca^{2+} Influx *in vitro* in a Dose-Dependent Manner

To access the acute effects of Triumeq on functional activity of mPFC neurons, we evaluated the firing frequency of neurons in response to depolarizing current pulses (25–400 pA) after ≥10 min perfusion with different concentrations of Triumeq in the bath. Similar to our 3TC study, we assessed the acute effects of Triumeq on mPFC neurons using different concentrations. The low concentration (1×) was the same as ×that found in the CSFs of HIV^+ patients on this cART, while higher concentrations (up to 100×) were comparable to that found in the plasma of HIV^+ on this cART since different ARVs have different plasma:CSF ratios (e.g., the plasma level of 3TC was about twice of that in CSF, and the plasma level of DTG was 236× higher than it in CSF) (Letendre et al., 2014). We found that the 1× Triumeq induced no alteration in firing; but at the concentrations that were 10- and 100-fold (10× and 100×, respectively) higher than the levels found in the CSFs of PLWH, Triumeq significantly increased firing of mPFC neurons compared to vehicle-treated controls (n = 8 neurons in 8 rats per group data; Triumeq effect: $F_{(3,21)} = 5.986$, $p = 0.004$; current effect: $F_{(11,77)} = 93.88$, $p < 0.001$; interaction: $F_{(33,231)} = 3.697$, $p < 0.001$; **Figure 3A,B**). Moreover, we also assessed the effects of Triumeq *in vitro* on the functional activity of VGCCs. We found that Ca^{2+} spike was significantly increased by acute Triumeq, also in a dose-dependent manner (**Figure 4A**). For example, the duration and/or area were significantly prolonged and enlarged by higher concentrations of Triumeq (10× and 100×, both $^*p < 0.05$), but not by 1× Triumeq, in the bath (**Figures 4B,C**).

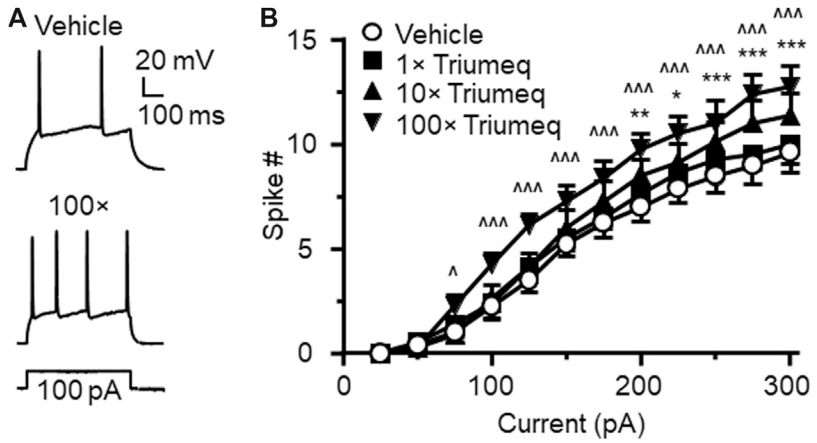

Figure 3 | Acute Triumeq treatment *in vitro* also increases firing of mPFC pyramidal neurons in a dose-dependent manner **(A)** Sample traces showing the firing numbers evoked by a moderate depolarizing current (150 pA) in mPFC neurons with or without Triumeq in the bath **(B)** The current-spike relationships indicate a significant increase in mPFC neuronal firing in response to 10× or 100×, but not 1×, of acute Triumeq compared to vehicle-treated controls (n = 8/ea. Triumeq effect: $F_{3,21} = 5.986$, $p = 0.004$; current effect: $F_{11,77} = 93.88$, $p < 0.001$; interaction: $F_{33,231} = 3.697$, $p < 0.001$. *post-hoc* test: $^{*,**,***}p < 0.05$, 0.01 or 0.001 between 0 vs 10× Triumeq; $^{\wedge}p < 0.05$ or 0.001 between 0 vs 100× Triumeq). 1× Triumeq (containing 0.3 μg/ml ABC, 0.3 μg/ml 3TC, and 20 ng/ml DTG) equals to the concentrations of these ARVs found in the CSF of PLWH on Triumeq. 10× and 100× Triumeq refers to 10-fold and 100-fold of which, respectively.

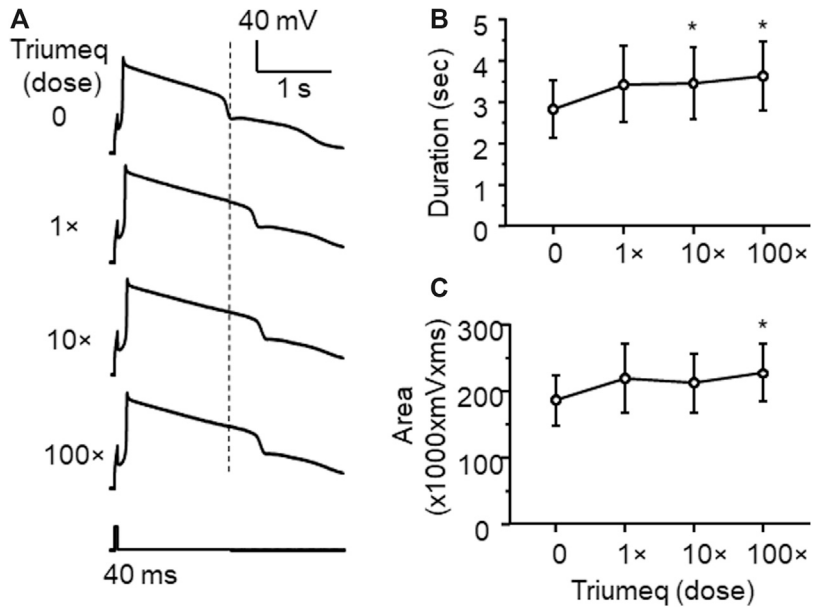

Figure 4 | Acute Triumeq treatment also increases VGCC activity in mPFC pyramidal neurons in a dose-dependent manner **(A)** Sample traces showing the acute effects of Triumeq (1×, 10×, and 100×) on evoked Ca^{2+} spikes **(B–C)** High concentrations of Triumeq *in vitro* significantly increased the duration **(B)** (n = 8/ea. $F_{3,21} = 7.089$, $p = 0.002$) and the area of Ca^{2+} spikes **(C)** (n = 8/ea. $F_{3,21} = 4.201$, $p = 0.018$). $^{*}p<0.05$ compared to the baseline prior to acute exposure to Triumeq.

Chronic Triumeq Treatment *in vivo* Increases Firing of Medial Prefrontal Cortex Neurons

To access the chronic effects of Triumeq *in vivo* on neuronal excitability, we evaluated the firing frequency of mPFC pyramidal neurons in rats after 2 wks (subchronic) or 4 wks (chronic) once daily s. c. injections of Triumeq. There was no significant difference in evoked firing between mPFC neurons from rats pretreated with vehicle and Triumeq for 2 wks (**Figures 5A,B**); but firing was significantly increased following chronic Triumeq treatment for 4 wks ($^{*,**,***}p$ < 0.05, 0.01, and 0.001, **Figures 5C,D**). These findings suggest that chronic exposure to Triumeq *in vivo* for 4 wks significantly increases mPFC neuronal excitability, while earlier changes in neuronal excitability induced by acute or

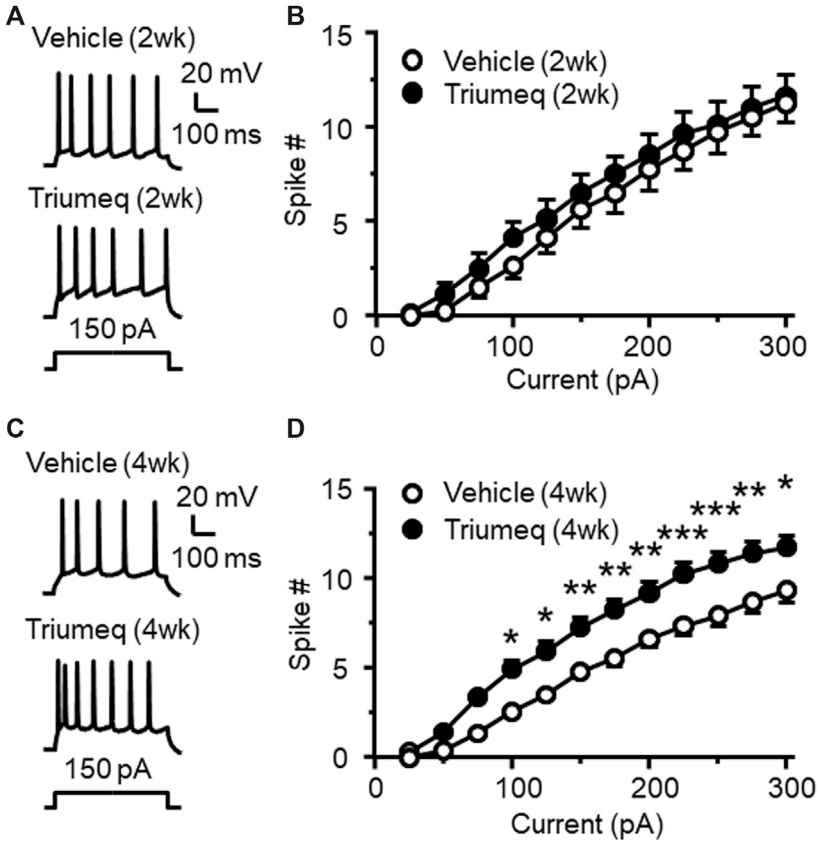

Figure 5 | Chronic, but not subchronic, treatment of Triumeq *in vivo* significantly increases firing of mPFC pyramidal neurons **(A)** Sample traces showing firing of mPFC neurons evoked by V_m depolarization after a 2 wks subchronic vehicle **(upper panel)** or Triumeq **(lower panel)** treatment *in vivo* **(B)** The current-spike relationships indicate that there was no significant difference in the firing between mPFC neurons from 2 wks Triumeq-pretreated rats and those from 2 wks vehicle-pretreated controls (n = 8/ea. Triumeq effect: $F_{1,14} = 0.424$, $p = 0.426$; current effect: $F_{11,154} = 187.8$, $p < 0.001$; interaction: $F_{11,154} = 0.418$, $p = 0.947$) **(C)** Sample traces showing the changes in firing evoked by V_m depolarization in mPFC neurons after 4 wks of vehicle **(upper panel)** or Triumeq **(lower panel)** treatment *in vivo* **(D)** The current-spike relationships indicate a significant increase in firing of mPFC neurons in rats after 4 wks Triumeq pretreatment compared to those in 4 wks vehicle-pretreated rats (14/ea. Triumeq effect: $F_{1,26} = 12.59$, $p = 0.002$; current effect: $F_{11,286} = 398.9$, $p < 0.001$; interaction: $F_{11,286} = 4.851$, $p < 0.001$; *post-hoc* test, *·**·***$p < 0.05$, 0.01 or 0.001).

TABLE 1 | Chronic Triumeq treatment significantly alters some membrane properties in mPFC pyramidal neurons.

	Vehicle (4 wks)	Triumeq (4 wks)
RMP (mV)	–64.4 ± 1.1	–62.4 ± 0.7
R_{in} (MΩ)	208.5 ± 14.0	242.8 ± 14.9
Rheobase (pA)	71.7 ± 5.9	53.3 ± 5.4*
Threshold (mV)	–40.6 ± 1.2	–42.7 ± 0.8
Amplitude (mV)	79.1 ± 2.4	71.7 ± 3.3
½ peak duration (ms)	2.2 ± 0.1	2.5 ± 0.1*
Time constant (ms)	39.1 ± 4.0	34.5 ± 2.4
AHP (mV)	11.6 ± 1.0	9.4 ± 1.2

t-*test:* *p < *0.5.*

subchronic (2 wks) treatment of Triumeq might be compensated by a negative-feedback mechanism in these neurons.

The increased firing following 4 wks treatment of Triumeq *in vivo* was associated with alterations in some membrane properties (**Table 1**). For example, the rheobase was significantly decreased in mPFC neurons from 4 wks Triumeq-pretreated rats (n = 15 neurons in 4 rats per group data; $t_{28} = 2.294$, $p = 0.0295$), while the ½ peak duration was significantly increased after 4 wks Triumeq-pretreatment compared to vehicle-pretreated controls (Vehicle vs Triumeq-4 wks: n = 14 vs. 15 neurons in 4 rats; $t_{27} = 2.29$, $p = 0.0301$). The reduced rheobase suggests an increased mPFC neuronal excitability, which is in agreement with 4 wks Triumeq-induced increase of firing. The ½ peak duration is partly mediated by VGCCs, and therefore, a prolonged ½ peak duration following 4 wks Triumeq-pretreatment suggests increased activity of VGCCs.

Chronic Triumeq Treatment Enhances Ca^{2+} Influx via Voltage-Gated Ca2+ Channel

To determine the chronic effects of Triumeq *in vivo* on VGCC activity, we assessed Ca^{2+} spikes evoked in mPFC pyramidal neurons of rats after 4 wks Triumeq or vehicle pretreatment. We found that Ca^{2+} spike was significantly prolonged by chronic Triumeq treatment for 4 wks (**Figure 6A**). Both the duration

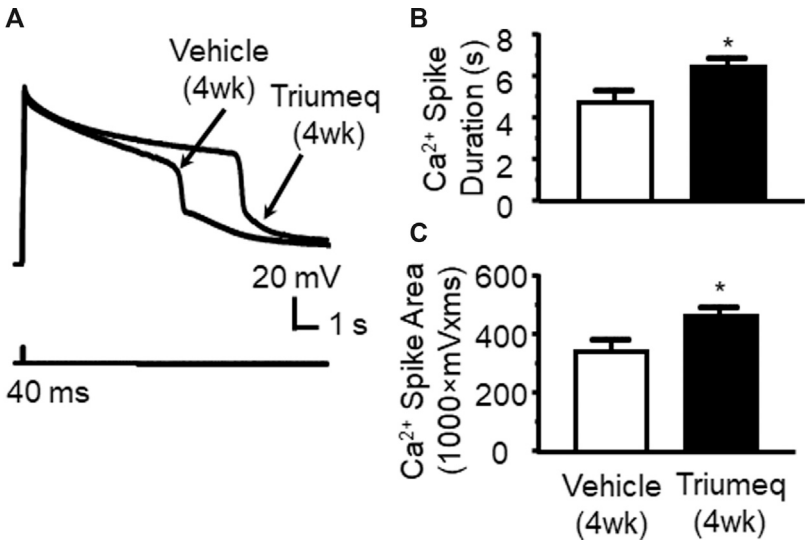

Figure 6 | Chronic Triumeq treatment *in vivo* for 4 wks increases Ca^{2+} influx via VGCCs in mPFC pyramidal neurons compared to those from vehicle-pretreated controls **(A)** Sample traces showing Ca^{2+} spikes evoked by V_m depolarization (indicating Ca^{2+} influx *via* VGCCs) in mPFC neurons from a vehicle-pretreated rat compared to a Triumeq-pretreated rat **(B)–(C)** The bar graphs indicate that the duration **(B)** and area **(C)** of Ca^{2+} spikes were significantly prolonged and enlarged, respectively, after a 4 wks Triumeq pretreatment (the duration: vehicle vs. Triumeq: n = 8 vs. 11; $t_{17} = 2.141$, $p = 0.047$; and the area: vehicle vs. Triumeq: n = 8 vs. 11; $t_{17} = 2.272$, $p = 0.036$).

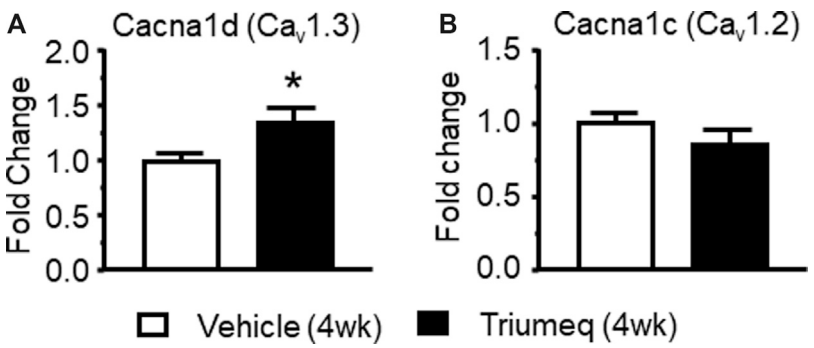

Figure 7 | Chronic Triumeq treatment *in vivo* for 4 wk significantly increases the mRNA expression of $Ca_v1.3$, but not Cav1.2, L-channels in the mPFC **(A)** The mRNA level of the $Ca_v1.3$ L-channel (Cacna1d gene) was significantly increased in the mPFC following 4 wks treatment of Triumeq compared to chronic treatment of vehicle (n = 8 rat/ea: $t_{14} = 2.161$, $p = 0.0485$) **(B)** There was no significant change in the mRNA level of $Ca_v1.2$ (Cacna1c gene) L-channels in the mPFC after 4 wks treatment of Triumeq (n = 8 rat/ea: $t_{14} = 1.249$, $p = 0.232$).

($p < 0.05$; **Figure 6B**) and spike area ($p < 0.05$; **Figure 6C**) were significantly increased in mPFC neurons from rats pretreated with Triumeq for 4 wks compared to those from vehicle-pretreated rats. These findings indicate that chronic Triumeq treatment increases VGCC activity in mPFC neurons; and such change in intracellular Ca^{2+} ($[Ca^{2+}]_{in}$) could contribute to the abnormal increase of firing.

Chronic Triumeq Treatment *in vivo* Increases the mRNA Expression of $Ca_v1.3$ L-Channels

There are different subtypes of VGCCs (Brini et al., 2014), including the L-type (L-channel). In the brain, L-channels consist of a high voltage-activated (HVA-$Ca_v1.2$) and a low voltage-activated (LVA-$Ca_v1.3$) form (Lipscombe, 2002). To better understand which subtype of L-channels contributes to the Triumeq-induced increase of Ca^{2+} spikes, we assessed the mRNA expression levels of $Ca_v1.2$ (a LVA L-channel) and $Ca_v1.3$ (a HVA L-channel) using qRT-PCR. We found that the $Ca_v1.3$ mRNA level was significantly increased in the mPFC from rats after chronic Triumeq pretreatment compared to vehicle-pretreatment rats (*$p < 0.05$; **Figure 7A**), while the $Ca_v1.2$ was not changes (**Figure 7B**). These results demonstrate that LVA-$Ca_v1.3$ L-channels mediate Triumeq-induced increase of mPFC neuronal excitability.

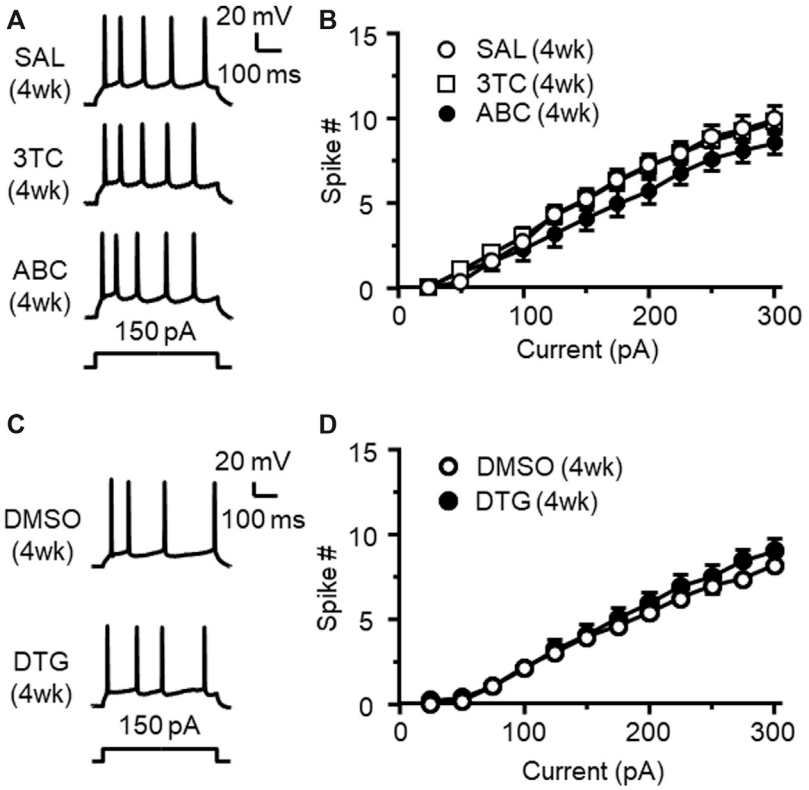

Figure 8 | Chronic treatment of individual 3TC, ABC, or DTG alone *in vivo* for 4 wks does not alter firing of mPFC pyramidal neurons **(A)** Samples traces showing firing in response to V_m hyperpolarization in mPFC neurons following 4 wks chronic treatment of SAL (upper panel), 3TC (middle panel) or ABC (lower panel) treatment *in vivo* **(B)** The current-spike relationships indicate that there was no significant difference in firing among mPFC neurons from 3TC, ABC or SAL-pretreated rats (SAL vs. 3TC: n = 9 vs. 12. 3TC effect: $F_{(1,19)} = 0.009$, $p = 0.925$; current effect: $F_{(11,209)} = 309.6$, $p<0.001$; interaction: $F_{(11,206)} = 0.502$, $p = 0.901$; SAL vs. ABC: n = 9 vs. 12. ABC effect: $F_{(1,19)} = 1.136$, $p = 0.300$; current effect: $F_{(11,209)} = 211.4$, $p<0.001$; interaction: $F_{(11,206)} = 2.557$, $p = 0.005$). **(C)** Sample traces showing the firing in response to V_m hyperpolarization in mPFC neurons following 4 wks pretreatment of 70% DMSO (the solvent for DTG, upper panel), or DTG (lower panel). **(D)** The current-spike relationships indicate that there was no significant difference in firing between neurons from 4 wks DTG-pretreated and 4 wks DMSO-pretreated rats (n = 14/ea. DTG effect: $F_{(1,26)} = 0.587$, $p = 0.450$; current effect: $F_{(11,286)} = 308.1$, $p<0.001$; interaction: $F_{(11,286)} = 1.04$, $p = 0.411$).

Chronic Treatment of Individual Antiretroviral Drugs Alone Does Not Alter Firing of Medial Prefrontal Cortex Neurons

Triumeq is co-formulated by three individual ARVs, including 3TC, ABC, and DTG. To identify the influence of each ARV alone on mPFC neuronal activity, we further assessed firing of mPFC pyramidal neurons in rats that have received daily s. c. pretreatment of either 3TC, ABC, or DTG respectively for 4 wks. We found that none of the 3 individual ARVs was able to significantly alter firing of mPFC neurons (**Figures 8A–D**). These results differ from that after 4 wks chronic treatment of Triumeq, suggesting that there may be additive or interactive effects among these ARVs in affecting mPFC neuronal excitability. Alternatively, longer period of treatment time may be needed for the individual ARVs to induce hyperexcitability among mPFC neurons.

DISCUSSION

Our study indicates that Triumeq (a first-line cART regimen for treating HIV/AIDS) alters the functional activity of mPFC pyramidal neurons, and it does so through increasing Ca^{2+} influx via overactivation/overexpression of VGCCs, including, but may not be limited to, LVA-Cav1.3 L-channels. Specifically, exposure to Triumeq, either acutely *in vitro* or chronically *in vivo*, increased firing of mPFC neurons in a dose- and/or time-dependent manner. This Triumeq-induced neuronal hyperexcitability is mediated by Ca^{2+} dysregulation resulting from VGCC overactivation and increased mRNA expression of LVA Cav1.3 L-channels. Acute exposure to lamivudine (a.k.a. 3TC), one of the three ARVs that co-formulate Triumeq, also increased firing and Ca^{2+} influx via VGCCs in hyperactive mPFC pyramidal neurons. In contrast, neither a subchronic (2 wks) treatment of Triumeq *in vivo*, nor chronic (4 wks) treatment of individual ARVs that co-formulate Triumeq *in vivo*, significantly alters mPFC neuronal activity. Collectively, these novel findings indicate that chronic Triumeq *in vivo* abnormally increases excitability of mPFC pyramidal neurons, which is mediated by overactivation and/or overexpression of VGCCs, including, but may not limited to, L-type Ca^{2+} channels.

We demonstrated that Triumeq-induced increase of mPFC neuronal firing is dosage- and time-dependent, which could have bi-directional, therapeutic and/or neurotoxic consequences, respectively. For instance, neither the lowest concentrations of acute Triumeq *in vitro* (which were equivalent to that found in the CSFs of PLWH on these ARVs) (Calcagno et al., 2014), nor a subchronic treatment (2 wks) of Triumeq *in vivo*, instantaneously affected firing of mPFC neurons. However, higher concentrations of acute Triumeq, or chronic treatment (4 wks) of this cART *in vivo*, facilitated mPFC neuronal activity. These findings suggest that an acute or subchronic clinical dosage of Triumeq is well-tolerated by glutamatergic mPFC pyramidal neurons, which allow them to maintain normal functional activity. Nevertheless, neuronal activity could be increased by raising the dosages (reflected by higher concentrations) of Triumeq in the brain, or prolonging the period of this particular cART. Therefore, it is likely that under the circumstances in which the mPFC function begins to be diminished by aging (Chen et al., 2019), or by HIV-induced overactivation that ultimately leads to inactivation of some mPFC neurons (Wayman et al., 2012; Napier et al., 2014; Wayman et al., 2015; Khodr et al., 2016; Wayman et al., 2016; Khodr et al., 2018), such an increased neuronal activity may exert a positive role in maintaining normal function of the mPFC, or delaying progression of HAND. Both may contribute to the therapeutic effects of Triumeq, in addition to suppressing HIV replication.

However, chronic Triumeq exposure to the brain could gradually and persistently increase the excitability of mPFC neurons, rendering them more susceptible and vulnerable to deleterious excitatory stimuli in the CNS HIV reservoirs. Our previous studies demonstrate that in the context of neuroHIV, in which HIV-1 and neuroinflammation induce neuronal hyperactivity, persistent neuronal hyperexcitability drives mPFC neurons from overactivation to inactivation (Wayman et al., 2012; Napier et al., 2014; Wayman et al., 2015; Khodr et al., 2016; Wayman et al., 2016; Khodr et al., 2018; Chen et al., 2019); and such dysregulation is exacerbated by psychostimulants, which also induce hyperactivity. Under these comorbid conditions, chronic Triumeq-induced neuronal hyperactivity could enhance HIV-induced neurotoxicity by further disturbing neuronal Ca^{2+} dysregulation (see below); and that may ultimately contribute to the underlying mechanism of HAND. In addition, our study also suggests a dysfunction of voltage-gated sodium channels (VGSCs, reflected by reduced firing threshold) in these hyperactive mPFC neurons. In combination with Triumeq-induced VGCC overactivation, such a reduction in firing threshold could further promote neuronal hyperactivity. On the other side, our findings also suggest a self-protective mechanism, by which the acute effects of individual ARVs (that co-formulate Triumeq) on facilitating firing were restricted, and normal activity was maintained in response to chronic treatment of each ARV alone. This potential mechanism may work during a subchronic treatment of Triumeq. Alternatively, they also suggest additive or interactive effects of these ARVs on inducing neuronal hyperactivity following persistent treatment *in vivo*.

Another important finding of the present study is that Triumeq-induced mPFC neuronal hyperexcitability is associated with a significant increase in Ca^{2+} influx through overactive VGCCs. This Ca^{2+} dysregulation was found both *in vitro* in response to acute Triumeq exposure, and *in vivo* following chronic Triumeq treatment. Similar to its effects on firing, a lower concentration of Triumeq *in vitro*, which was equivalent to the drug level found in the CSF of PLWH on this cART (Calcagno et al., 2014) and described here as 1-fold (1×), did not alter Ca^{2+} spikes. But higher concentrations (10× or 100× greater than a clinical dosage) significantly increases Ca^{2+} influx via VGCCs. Equal importantly, the increased firing was associated with enhanced Ca^{2+} influx via overactive VGCCs. Moreover, the widened action potentials and reduced rheobase found in hyperactive mPFC neurons were also in agreement with this increased Ca^{2+} influx. Together, these results not only indicate that a regular clinical dosage of Triumeq, either given acutely or for a relatively short period of time, does not induce neuronal hyperactivity and overactivation of VGCCs, but also suggest that mPFC neurons are able to integratively contain Triumeq-induced hyperexcitability by keeping neuronal Ca^{2+} homeostasis under control, though only for a short period of time.

Similar changes in neuronal Ca^{2+} homeostasis was also induced by lower concentrations of 3TC (1–4 μM) *in vitro*, which significantly enhanced Ca^{2+} influx via overactive VGCCs. Interestingly, at concentrations that were comparable to that found in CSF of PLWH receiving this ARV (Johnson et al., 1999), 3TC was *unable* to increase firing, either acutely *in vitro* or chronically *in vivo*. This finding suggests that although a regular clinical dosage of 3TC promotes VGCC activity, it is incapable to cause neuronal hyperactivity. However, higher concentrations of, persistent exposure to, or combined treatment of other ARVs with this ARV, could drive mPFC neurons to hyperactivity mediated by deteriorated neuronal Ca^{2+} dysregulation.

Cumulative evidence suggests that neuronal Ca^{2+} dysregulation (excessive $[Ca^{2+}]_{in}$) plays a critical role in neurotoxicity induced by ARVs (Robertson et al., 2012; Romo et al., 2012; Akay et al., 2014; Apostolova et al., 2015; Underwood et al., 2015; Vivithanaporn et al., 2016). Ironically, such neuronal Ca^{2+} dysregulation is similar to that found in the context of neuroAIDS; both are mediated by dysfunction of VGCCs (Hu, 2016), in addition to NMDARs (Haughey and Mattson, 2002; Gonzalez-Scarano and Martin-Garcia, 2005; Mattson et al., 2005). VGCCs include several different subtypes, including L-type of Ca^{2+} channels that are involved in Ca^{2+}-induced signaling processes and gene expression in neurons (Ikeda, 2001; Brini et al., 2014). Our previous studies demonstrate that overactivation and overexpression of L-channels contributes to abnormal hyperactivity of mPFC pyramidal neurons in the context of neuroHIV (Khodr et al., 2016; Khodr et al., 2018; Napier et al., 2014; Wayman et al., 2015; 2016; 2012). There are two subtypes of L-channels expressed in the brain, include a

HVA-$Ca_v1.2$ (Cacna1c) L-channel and a LVA-$Ca_v1.3$ (Cacna1d) L-channel (Lipscombe, 2002). Our previous studies suggest that overactivation and overexpression of both HVA-Ca^{2+} and LVA-Ca^{2+} channels mediates mPFC neuronal hyperactivity in the context of neuroHIV and aging (Wayman et al., 2012; Napier et al., 2014; Wayman et al., 2015; Khodr et al., 2016; Wayman et al., 2016; Khodr et al., 2018). The present study further reveals the involvement of increased mRNA expression of LVA-$Ca_v1.3$ L-channels following chronic Triumeq treatment. Together, these findings indicate that, even at regular clinical dosages, persistent exposure to Triumeq *in vivo*, or to any other chronic cART regimen which is likely a common situation for PLWH, may eventually complicate HIV-induced neuronal hyperactivity by targeting L-channels to exacerbate neuronal Ca^{2+} dysregulation in the brain of PLWH.

However, even though many ARVs induce neurotoxicity (Kranick and Nath, 2012; Manji et al., 2013; Underwood et al., 2015), cART is still absolutely needed for treating HIV/AIDS. Thus, how to minimize the site effects of ARVs should receive a thoughtful consideration. To avoid or minimize cART-induced neurotoxicity, a better understanding of ARVs' site effects is undeniably required. The present study, in combination with previous studies of others, indicates that the responses of pyramidal neurons in the mPFC to Triumeq differ considerably from those in the hippocampal (Hipp) CA1 region to efavirenz, a non-NRTI, nNRTI (Ciavatta et al., 2017). The CSF levels of efavirenz found in PLWH taking this ARV are in the range of 23–450 nM (Tashima et al., 1999; Yilmaz et al., 2012; Aouri et al., 2016; Ciavatta et al., 2017), depending upon the condition of studies (e.g., the time point for sample collection). In contrast to the effects of Triumeq (10× or 100×) on inducing initial *increase* of neuronal activity, efavirenz (20μM, ~40× higher than its CSF level) significantly *suppresses* firing and causes severer dendritic injury in Hipp pyramidal neurons (Ciavatta et al., 2017). Together, these findings suggest that certain ARV(s), like efavirenz, is more toxic than other ARVs (Kranick and Nath, 2012). Our findings are in agreement with this proposition. In fact, Atripla, another cART regimen co-formulated by efavirenz, 3TC, and tenofovir disoproxiln fumarate, is reported to have significantly greater site effects and less efficacy than Triumeq in treating HIV/AIDS (Walmsley et al., 2013); and therefore, has no longer been recommended as a first-line cART regimen for treating HIV/AIDS. In a parallel study, we also examined acute effects of 1× Atripla on mPFC pyramidal neurons; and found a significant increase in firing (unpublished data). This data also suggests a greater side effect of Atripla compared to Triumeq (e.g., causing mPFC neuronal hyperactivity by a low clinical dosage). However, given that almost all ARVs have a similar site effect in inducing neurotoxicity, especially with higher dosages and/or after persistent treatment either *in vitro* or *in vivo*, the present study will not exclude the likelihood that enduring Triumeq treatment could also induce neuronal dysfunction and injury in the key brain regions that regulate neurocognition. Thus, out study also suggests that caution should be taken seriously to raise levels of ARVs in the brain of PLWH.

In summary, the present study demonstrates that chronic Triumeq treatment *in vivo* induces mPFC neuronal hyperactivity, which is due partly to neuronal Ca^{2+} dysregulation mediated by overactivation/overexpression of VGCCs, including, but not limited to, LVA-$Ca_v1.3$ L-channels. Our novel findings also suggest that, while cART effectively inhibits HIV-1 replication, chronic exposure to Triumeq *in vivo* could complicate HIV-induced neurotoxicity due to abnormal increase of Ca^{2+} influx and excessive $[Ca^{2+}]_{in}$. Therefore, there may be an increasing risk for PLWH who are on chronic cART to eventually experience an undeserved impact from the site effects of ARVs on neurons in the brain region(s) that regulate neurocognition; and that may contribute to the underlying mechanism of HAND. Nevertheless, because cART is unreplaceable for treating HIV/AIDS, such side effects of ARVs will not restrict cART for PLWH. Understanding this reality and elucidating the mechanism underlying ARVs-induced neurotoxicity should ultimately help us to develop new and more effective therapeutic strategies to combating against HIV/AIDS, while minimizing the side effects of cART.

DATA AVAILABILITY STATEMENT

The raw data supporting the conclusions of this article will be made available by the authors, without undue reservation.

ETHICS STATEMENT

The animal study was reviewed and approved by the IACUC of Rush University Medical Center.

AUTHOR CONTRIBUTIONS

LC and X-TH conceived and designed the study. LC performed experiments, analyzed data and prepared the original manuscript draft. LC, LA-H, and XH reviewed and edited the manuscript. LA-H and XH acquired funding to perform the projects.

FUNDING

This work was supported by the National Institutes of Health (NIH) [grants number: NS084817, DA044552 and DA044552-03S1 (X-TH), DA033966, MH122241, and NS060632 (LA-H)].

ACKNOWLEDGMENTS

The authors would also like to thank NIH AIDS Reagent program for providing 3TC.

REFERENCES

Akang, E. N. (2019). Combination antiretroviral therapy (cART)-induced hippocampal disorders: highlights on therapeutic potential of Naringenin and Quercetin. *IBRO Rep*. 6, 137–146. doi:10.1016/j.ibror.2019.04.002

Akay, C., Cooper, M., Odeleye, A., Jensen, B. K., White, M. G., Vassoler, F., et al. (2014) Antiretroviral drugs induce oxidative stress and neuronal damage in the central nervous system. *J. Neurovirol.* 20:39–53. doi:10.1007/s13365-013-0227-1

Akay, C., Lindl, K. A., Wang, Y., White, M. G., Isaacman-Beck, J., Kolson, D. L., et al. (2011). Site-specific hyperphosphorylation of pRb in HIV-induced neurotoxicity. *Mol. Cell. Neurosci.* 47, 154–165. doi:10.1016/j.mcn.2011.04.001

Antinori, A., Arendt, G., Becker, J. T., Brew, B. J., Byrd, D. A., Cherner, M., et al. (2007) Updated research nosology for HIV-associated neurocognitive disorders. *Neurology*. 69:1789–1799. doi:10.1212/01.WNL.0000287431.88658.8b

Aouri, M., Barcelo, C., Ternon, B., Cavassini, M., Anagnostopoulos, A., Yerly, S., et al. (2016). In Vivo profiling and distribution of known and novel phase I and phase II metabolites of efavirenz in plasma, urine, and cerebrospinal fluid. *Drug Metab. Dispos.* 44, 151–161. doi:10.1124/dmd.115.065839

Apostolova, N., Funes, H. A., Blas-Garcia, A., Galindo, M. J., Alvarez, A., and Esplugues, J. V. (2015). Efavirenz and the CNS: what we already know and questions that need to be answered. *J. Antimicrob. Chemother.* 70, 2693–2708. doi:10.1093/jac/dkv183

Birbeck, G. L., French, J. A., Perucca, E., Simpson, D. M., Fraimow, H., George, J. M., et al. (2012). Antiepileptic drug selection for people with HIV/AIDS: evidence-based guidelines from the ILAE and AAN. *Epilepsia*. 53, 207–214. doi:10.1111/j.1528-1167.2011.03335.x

Blanch, J., Martínez, E., Rousaud, A., Blanco, J. L., García-Viejo, M. A., Peri, J. M., et al. (2001). Preliminary data of a prospective study on neuropsychiatric side effects after initiation of efavirenz. *J. Acquir. Immune Defic. Syndr.* 27, 336–343. doi:10.1097/00126334-200108010-00003

Brew, B. J., Crowe, S. M., Landay, A., Cysique, L. A., and Guillemin, G. (2009). Neurodegeneration and ageing in the HAART era. *J. Neuroimmune Pharmacol.* 4, 163–174. doi:10.1007/s11481-008-9143-1

Brini, M., Calì, T., Ottolini, D., and Carafoli, E. (2014). Neuronal calcium signaling: function and dysfunction. *Cell. Mol. Life Sci.* 71, 2787–2814. doi:10.1007/s00018-013-1550-7

Calcagno, A., Di Perri, G., and Bonora, S. (2014). Pharmacokinetics and pharmacodynamics of antiretrovirals in the central nervous system. *Clin. Pharmacokinet.* 53, 891–906. doi:10.1007/s40262-014-0171-0

Chen, L., Khodr, C. E., Al-Harthi, L., and Hu, X. T. (2019) Aging and HIV-1 alter the function of specific K (+) channels in prefrontal cortex pyramidal neurons. *Neurosci. Lett.* 708: 134341. doi:10.1016/j.neulet.2019.134341

Ciavatta, V. T., Bichler, E. K., Speigel, I. A., Elder, C. C., Teng, S. L., Tyor, W. R., et al. (2017). In vitro and ex vivo neurotoxic effects of efavirenz are greater than those of other common antiretrovirals. *Neurochem. Res.* 42, 3220–3232. doi:10.1007/s11064-017-2358-x

Clifford, K. M., Samboju, V., Cobigo, Y., Milanini, B., Marx, G. A., Hellmuth, J. M., et al. (2017). Progressive brain atrophy despite persistent viral suppression in HIV patients older than 60 years. *J. Acquir. Immune Defic. Syndr.* 76, 289–297. doi:10.1097/QAI.0000000000001489

Colebunders, R., Hilbrands, R., De Roo, A., and Pelgrom, J. (2002). Neuropsychiatric reaction induced by abacavir. *Am. J. Med.* 113, 616. doi:10.1016/s0002-9343(02)01259-7

Cysique, L. A., and Brew, B. J. (2009). Neuropsychological functioning and antiretroviral treatment in HIV/AIDS: a review. *Neuropsychol. Rev.* 19, 169–185. doi:10.1007/s11065-009-9092-3

Ferris, M. J., Mactutus, C. F., and Booze, R. M. (2008). Neurotoxic profiles of HIV, psychostimulant drugs of abuse, and their concerted effect on the brain: current status of dopamine system vulnerability in neuroAIDS. *Neurosci. Biobehav. Rev.* 32, 883–909. doi:10.1016/j.neubiorev.2008.01.004

Gonzalez, H., Podany, A., Al-Harthi, L., and Wallace, J. (2020). The far-reaching HAND of cART: cART effects on astrocytes. *J. Neuroimmune Pharmacol.* [Epub ahead of print] doi:10.1007/s11481-020-09907-w

González-Scarano, F., and Martín-García, J. (2005). The neuropathogenesis of AIDS. *Nat. Rev. Immunol.* 5, 69–81. doi:10.1038/nri1527

Grant, X. T. (2016). HIV-1 tat-mediated calcium dysregulation and neuronal dysfunction in vulnerable brain regions. *Curr. Drug Targets.* 17, 4–14. doi:10.2174/1389450116666150531162212

Greig, S. L., and Deeks, E. D. (2015). Abacavir/dolutegravir/lamivudine single-tablet regimen: a review of its use in HIV-1 infection. *Drugs*. 75, 503–514. doi:10.1007/s40265-015-0361-6

Haughey, N. J., and Mattson, M. P. (2002). Calcium dysregulation and neuronal apoptosis by the HIV-1 proteins Tat and gp120. *J. Acquir. Immune Defic. Syndr.* 31 (Suppl. 2), S55–S61. doi:10.1097/00126334-200210012-00005

Heaton, R. K., Clifford, D. B., Franklin, D. R., Woods, S. P., Ake, C., Vaida, F., et al. (2010). HIV-associated neurocognitive disorders persist in the era of potent antiretroviral therapy: charter study. *Neurology*. 75, 2087–2096. doi:10.1212/WNL.0b013e318200d727

Ikeda, S. R. (2001). Signal transduction. Calcium channels--link locally, act globally. *Science*. 294, 318–319. doi:10.1126/science.1066160

Jensen, B. K., Monnerie, H., Mannell, M. V., Gannon, P. J., Espinoza, C. A., Erickson, M. A., et al. (2015). Altered oligodendrocyte maturation and myelin maintenance: the role of antiretrovirals in HIV-associated neurocognitive disorders. *J. Neuropathol. Exp. Neurol.* 74, 1093–1118. doi:10.1097/NEN.0000000000000255

Jiang, X., Barasky, R., Olsen, H., Riesenhuber, M., and Magnus, M. (2016). Behavioral and neuroimaging evidence for impaired executive function in "cognitively normal" older HIV-infected adults. *AIDS Care*. 28, 436–440. doi:10.1080/09540121.2015.1112347

Johnson, M. A., Moore, K. H., Yuen, G. J., Bye, A., and Pakes, G. E. (1999). Clinical pharmacokinetics of lamivudine. *Clin. Pharmacokinet.* 36, 41–66. doi:10.2165/00003088-199936010-00004

Khodr, C. E., Chen, L., Al-Harthi, L., and Hu, X. T. (2018). Aging alters voltage-gated calcium channels in prefrontal cortex pyramidal neurons in the HIV brain. *J. Neurovirol.* 24, 113–118. doi:10.1007/s13365-017-0588-y

Khodr, C. E., Chen, L., Dave, S., Al-Harthi, L., and Hu, X. T. (2016). Combined chronic blockade of hyper-active L-type calcium channels and NMDA receptors ameliorates HIV-1 associated hyper-excitability of mPFC pyramidal neurons. *Neurobiol. Dis.* 94, 85–94. doi:10.1016/j.nbd.2016.06.008

King, J. E., Eugenin, E. A., Buckner, C. M., and Berman, J. W. (2006). HIV tat and neurotoxicity. *Microb. Infect.* 8, 1347–1357. doi:10.1016/j.micinf.2005.11.014

Kranick, S. M., and Nath, A. (2012). Neurologic complications of HIV-1 infection and its treatment in the era of antiretroviral therapy. *Continuum.* 18, 1319–1337. doi:10.1212/01.CON.0000423849.24900.ec

Letendre, S. L., Mills, A. M., Tashima, K. T., Thomas, D. A., Min, S. S., Chen, S., et al. (2014). ING116070: a study of the pharmacokinetics and antiviral activity of dolutegravir in cerebrospinal fluid in HIV-1-infected, antiretroviral therapy-naive subjects. *Clin. Infect. Dis.* 59, 1032–1037. doi:10.1093/cid/ciu477

Lipscombe, D. (2002). L-type calcium channels: highs and new lows. *Circ. Res.* 90, 933–935. doi:10.1161/01.res.0000019740.52306.92

Manji, H., Jäger, H. R., and Winston, A. (2013). HIV, dementia and antiretroviral drugs: 30 years of an epidemic. *J. Neurol. Neurosurg. Psychiatry*. 84, 1126–1137. doi:10.1136/jnnp-2012-304022

Mattson, M. P., Haughey, N. J., and Nath, A. (2005). Cell death in HIV dementia. *Cell Death Differ.* 12 Suppl 1 (Suppl. 1), 893–904. doi:10.1038/sj.cdd.4401577

Maxwell, S., Scheftner, W. A., Kessler, H. A., and Busch, K. (1988). Manic syndrome associated with zidovudine treatment. *J. Am. Med. Assoc.* 259, 3406–3407. doi:10.1001/jama.1988.03720230018014

McArthur, J. C., Steiner, J., Sacktor, N., and Nath, A. (2010). Human immunodeficiency virus-associated neurocognitive disorders: mind the gap. *Ann. Neurol.* 67, 699–714. doi:10.1002/ana.22053

Mengato, D., Binazzi, R., Unterholzner, I., Erne, E. M., and Tavella, A. (2020). Psychiatric disorders after switching to dolutegravir: a case report of a 59-year-old virosuppressed HIV-1 positive woman. *Case Rep Infect Dis*. 2020, 9708913. doi:10.1155/2020/9708913

Napier, T. C., Chen, L., Kashanchi, F., and Hu, X. T. (2014). Repeated cocaine treatment enhances HIV-1 Tat-induced cortical excitability via over-activation of L-type calcium channels. *J. Neuroimmune Pharmacol.* 9, 354. doi:10.1007/s11481-014-9524-6

Nasif, F. J., Hu, X. T., and White, F. J. (2005a). Repeated cocaine administration increases voltage-sensitive calcium currents in response to membrane depolarization in medial prefrontal cortex pyramidal neurons. *J. Neurosci.* 25, 3674–3679. doi:10.1523/JNEUROSCI.0010-05.2005

Nasif, F. J., Sidiropoulou, K., Hu, X. T., and White, F. J. (2005b). Repeated cocaine administration increases membrane excitability of pyramidal neurons in the rat medial prefrontal cortex. *J. Pharmacol. Exp. Therapeut.* 312, 1305–1313. doi:10.1124/jpet.104.075184

Nwogu, J. N., Ma, Q., Babalola, C. P., Adedeji, W. A., Morse, G. D., and Taiwo, B. (2016). Pharmacokinetic, pharmacogenetic, and other factors influencing CNS penetration of antiretrovirals. *AIDS Res Treat*. 2016, 2587094. doi:10.1155/2016/2587094

Robertson, K., Liner, J., and Meeker, R. B. (2012). Antiretroviral neurotoxicity. *J. Neurovirol.* 18, 388–399. doi:10.1007/s13365-012-0120-3

Robertson, K. R., Su, Z., Margolis, D. M., Krambrink, A., Havlir, D. V., Evans, S., et al. (2010). Neurocognitive effects of treatment interruption in stable HIV-positive patients in an observational cohort. *Neurology*. 74, 1260–1266. doi:10.1212/WNL.0b013e3181d9ed09

Rubin, L. H., Maki, P. M., Springer, G., Benning, L., Anastos, K., Gustafson, D., et al. (2017). Cognitive trajectories over 4 years among HIV-infected women with optimal viral suppression. *Neurology*. 89, 1594–1603. doi:10.1212/WNL.0000000000004491

Simioni, S., Cavassini, M., Annoni, J. M., Rimbault Abraham, A., Bourquin, I., Schiffer, V., et al. (2010). Cognitive dysfunction in HIV patients despite long-standing suppression of viremia. *AIDS*. 24, 1243–1250. doi:10.1097/QAD.0b013e3283354a7b

Stauch, K. L., Emanuel, K., Lamberty, B. G., Morsey, B., and Fox, H. S. (2017). Central nervous system-penetrating antiretrovirals impair energetic reserve in striatal nerve terminals. *J. Neurovirol.* 23, 795–807. doi:10.1007/s13365-017-0573-5

Tashima, K. T., Caliendo, A. M., Ahmad, M., Gormley, J. M., Fiske, W. D., Brennan, J. M., et al. (1999). Cerebrospinal fluid human immunodeficiency virus type 1 (HIV-1) suppression and efavirenz drug concentrations in HIV-1-infected patients receiving combination therapy. *J. Infect. Dis.* 180, 862–864. doi:10.1086/314945

Tovar-y-Romo, L. B., Bumpus, N. N., Pomerantz, D., Avery, L. B., Sacktor, N., McArthur, J. C., et al. (2012). Dendritic spine injury induced by the 8-hydroxy metabolite of efavirenz. *J. Pharmacol. Exp. Therapeut.* 343, 696–703. doi:10.1124/jpet.112.195701

Tozzi, V., Balestra, P., Bellagamba, R., Corpolongo, A., Salvatori, M. F., Visco-Comandini, U., et al. (2007). Persistence of neuropsychologic deficits despite long-term highly active antiretroviral therapy in patients with HIV-related neurocognitive impairment: prevalence and risk factors. *J. Acquir. Immune Defic. Syndr.* 45, 174–182. doi:10.1097/QAI.0b013e318042e1ee

Underwood, J., Robertson, K. R., and Winston, A. (2015). Could antiretroviral neurotoxicity play a role in the pathogenesis of cognitive impairment in treated HIV disease?. *AIDS*. 29, 253–261. doi:10.1097/QAD.0000000000000538

Van den Hof, M., Blokhuis, C., Cohen, S., Scherpbier, H. J., Wit, F. W. N. M., Pistorius, M. C. M., et al. (2018). CNS penetration of ART in HIV-infected children. *J. Antimicrob. Chemother*. 73(2), 484–489. doi:10.1093/jac/dkx396

Vance, D. E., McGuinness, T., Musgrove, K., Orel, N. A., and Fazeli, P. L. (2011). Successful aging and the epidemiology of HIV. *Clin. Interv. Aging*. 6, 181–192. doi:10.2147/CIA.S14726

Vivithanaporn, P., Asahchop, E. L., Acharjee, S., Baker, G. B., and Power, C. (2016). HIV protease inhibitors disrupt astrocytic glutamate transporter function and neurobehavioral performance. *AIDS*. 30, 543–552. doi:10.1097/QAD.0000000000000955

Walmsley, S. L., Antela, A., Clumeck, N., Duiculescu, D., Eberhard, A., Gutiérrez, F., et al. (2013). Dolutegravir plus abacavir-lamivudine for the treatment of HIV-1 infection. *N. Engl. J. Med.* 369, 1807–1818. doi:10.1056/NEJMoa1215541

Wayman, W. N., Chen, L., Hu, X. T., and Napier, T. C. (2016). HIV-1 transgenic rat prefrontal cortex hyper-excitability is enhanced by cocaine self-administration. *Neuropsychopharmacology*. 41, 1965–1973. doi:10.1038/npp.2015.366

Wayman, W. N., Chen, L., Napier, T. C., and Hu, X. T. (2015). Cocaine self-administration enhances excitatory responses of pyramidal neurons in the rat medial prefrontal cortex to human immunodeficiency virus-1 Tat. *Eur. J. Neurosci.* 41, 1195–1206. doi:10.1111/ejn.12853

Wayman, W. N., Dodiya, H. B., Persons, A. L., Kashanchi, F., Kordower, J. H., Hu, X. T., et al. (2012). Enduring cortical alterations after a single in-vivo treatment of HIV-1 Tat. *Neuroreport*. 23, 825–829. doi:10.1097/WNR.0b013e3283578050

Wise, M. E., Mistry, K., and Reid, S. (2002). Drug points: neuropsychiatric complications of nevirapine treatment. *BMJ*. 324, 879. doi:10.1136/bmj.324.7342.879

Yilmaz, A., Watson, V., Dickinson, L., and Back, D. (2012). Efavirenz pharmacokinetics in cerebrospinal fluid and plasma over a 24-hour dosing interval. *Antimicrob. Agents Chemother.* 56, 4583–4585. doi:10.1128/AAC.06311-11

Zamora, F. J., Dowers, E., Yasin, F., and Ogbuagu, O. (2019). Dolutegravir and lamivudine combination for the treatment of HIV-1 infection. *HIV AIDS (Auckl)*. 11, 255–263. doi:10.2147/HIV.S216067

Conflict of Interest: The authors declare that the research was conducted in the absence of any commercial or financial relationships that could be construed as a potential conflict of interest.

Copyright © 2021 Chen, Al-Harthi and Hu. This is an open-access article distributed under the terms of the Creative Commons Attribution License (CC BY). The use, distribution or reproduction in other forums is permitted, provided the original author(s) and the copyright owner(s) are credited and that the original publication in this journal is cited, in accordance with accepted academic practice. No use, distribution or reproduction is permitted which does not comply with these terms.

frontiers in Pharmacology

ORIGINAL RESEARCH
published: 01 February 2021
doi: 10.3389/fphar.2020.594394

Cerebrospinal Fluid Inflammatory Cytokine Levels in Patients With Major Psychiatric Disorders: A Multiplex Immunoassay Study

*Shinsuke Hidese[1], Kotaro Hattori[1,2], Daimei Sasayama[1], Takuya Tsumagari[1,2], Tomoko Miyakawa[2], Ryo Matsumura[2], Yuuki Yokota[1,2], Ikki Ishida[1], Junko Matsuo[1], Sumiko Yoshida[2,3], Miho Ota[1] and Hiroshi Kunugi[1,4]**

[1]Department of Mental Disorder Research, National Institute of Neuroscience, National Center of Neurology and Psychiatry, Tokyo, Japan, [2]Medical Genome Center, National Center of Neurology and Psychiatry, Tokyo, Japan, [3]Department of Psychiatry, National Center Hospital, National Center of Neurology and Psychiatry, Tokyo, Japan, [4]Department of Psychiatry, Teikyo University School of Medicine, Tokyo, Japan

OPEN ACCESS

Edited by:
Mariela Fernanda Perez, National University of Cordoba, Argentina

Reviewed by:
Dietmar Fuchs, Innsbruck Medical University, Austria
Anindya Bhattacharya, Janssen Research and Development, United States
Agustin Montivero, CCT Conicet Córdoba, Argentina

***Correspondence:**
Hiroshi Kunugi
hkunugi@ncnp.go.jp

Specialty section:
This article was submitted to Neuropharmacology, a section of the journal Frontiers in Pharmacology

Received: 13 August 2020
Accepted: 29 December 2020
Published: 01 February 2021

Citation:
Hidese S, Hattori K, Sasayama D, Tsumagari T, Miyakawa T, Matsumura R, Yokota Y, Ishida I, Matsuo J, Yoshida S, Ota M and Kunugi H (2021) Cerebrospinal Fluid Inflammatory Cytokine Levels in Patients With Major Psychiatric Disorders: A Multiplex Immunoassay Study. Front. Pharmacol. 11:594394. doi: 10.3389/fphar.2020.594394

Aim: Accumulating evidence suggests that neural inflammation plays an important role in psychiatric disorders. We aimed to identify inflammatory cytokines involved in the pathophysiology of such disorders by quantifying them in cerebrospinal fluid (CSF) samples from a large sample of patients with major psychiatric disorders and healthy controls.

Methods: The subjects included 94 patients with schizophrenia, 68 with bipolar disorder, 104 with major depressive disorder, and 118 healthy controls, matched for age, sex, and ethnicity (Japanese). Lumbar puncture was performed to collect these CSF samples. A multiplex immunoassay was then performed to measure CSF cytokine levels using magnetic on-bead antibody conjugation for 19 inflammatory cytokines.

Results: CSF interferon-β level was significantly higher in total psychiatric patients than in healthy controls (corrected p = 0.000029). In diagnostic group comparisons, CSF interferon-β level was significantly higher in patients with schizophrenia, or bipolar disorder (corrected p = 0.000047 or 0.0034) than in healthy controls.

Conclusion: We present novel evidence that CSF IFN-β level showed prominent statistical differences between psychiatric groups and healthy controls. This suggests IFN-β as the most important player among the 19 cytokines tested here in the inflammation-related pathophysiology of major psychiatric disorders.

Keywords: bipolar disorder, cerebrospinal fluid, cytokine, major depressive disorder, multiplex, schizophrenia

Abbreviations: ANOVA, analysis of variance; BD, bipolar disorder; BMI, body mass index; CD, cluster of differentiation; CNS, central nervous system; CSF, cerebrospinal fluid; IFN, interferon; IL, interleukin; MDD, major depressive disorder; NCNP, National Center of Neurology; PANSS, Positive and Negative Syndrome Scale; TNFSF, tumor necrosis factor superfamily; TSLP, thymic stromal lymphopoietin.

INTRODUCTION

Inflammation has been suggested to play a key role in the pathogenesis and pathophysiology of psychiatric disorders (Khandaker et al., 2017; Bauer and Teixeira, 2018), including schizophrenia (Horvath and Mirnics, 2014; Na et al., 2014; Muller et al., 2015; Khandaker and Dantzer, 2016; Muller, 2018), bipolar disorder (BD) (Rosenblat and McIntyre, 2015; Walther et al., 2017), and major depressive disorder (MDD) (Sperner-Unterweger et al., 2014; Kunugi et al., 2015; Adzic et al., 2018; Misiak et al., 2018). In the pathophysiology of these disorders, a bidirectional interplay between the brain and the immune system has been suggested (Dantzer, 2018).

Cerebrospinal fluid (CSF) is the optimal biomaterial to examine the molecular status of the central nervous system (CNS) (Veening and Barendregt, 2010; Sakka et al., 2011). Previous meta-analyses have reported altered CSF cytokine levels (e.g., interleukin [IL]-1β, IL-6, and IL-8) in patients with schizophrenia, BD, or MDD (Orlovska-Waast et al., 2018; Wang and Miller, 2018). Our research group has also reported elevations in inflammation-related molecules in the CSF of patients with schizophrenia, BD, or MDD using the enzyme-linked immunosorbent assays (Sasayama et al., 2013; Hattori et al., 2015; Ishii et al., 2018). However, there are many other candidate molecules related to inflammation.

Multiplex immunoassays (Bio-Plex and V-plex®) have been validated for the simultaneous measurement of multiple cytokine levels using blood samples from patients with MDD and healthy control subjects (Belzeaux et al., 2017). The bead-based Luminex® (Bio-Rad Laboratories, Inc.) platform has been used for CSF sample to measure 8 cytokine levels in 43 patients with BD or MDD (Haroon et al., 2016), while the immunoassay-based protein array multiplex system has been used for CSF samples to measure 10 cytokine levels in 30 patients with BD and 30 controls (Soderlund et al., 2011). The electro-chemiluminescence-based V-plex® (MesoScale Discovery) platform has also been used for CSF samples to measure 10 cytokine levels in 23 patients with chronic schizophrenia and 37 controls (Schwieler et al., 2015), 5 cytokine levels in 11 patients with recent-onset schizophrenia and 12 controls (Coughlin et al., 2016), 2 cytokine levels in 19 patients with current depression and 67 subjects without depression among older women (Kern et al., 2014), and 11 cytokine levels in 16 patients with schizophrenia and 15 with affective disorders (Maxeiner et al., 2014).

Although prior studies have conducted multiplex immunoassays to measure CSF cytokine levels in psychiatric disorders (Soderlund et al., 2011; Kern et al., 2014; Maxeiner et al., 2014; Schwieler et al., 2015; Coughlin et al., 2016; Haroon et al., 2016), the highest number of cytokines measured was at once was 11, and sample sizes of patients and controls were not very large (at most 43 and 67, respectively). This warrants to obtain more solid evidence for the role of inflammatory cytokines in the pathophysiology of major psychiatric disorders. We aimed to accomplish simultaneous quantification of a much larger number of cytokines using the bead-based Luminex® in a much larger CSF sample from patients with schizophrenia, BD, or MDD and healthy controls. We hypothesized that a variety of inflammatory changes would be detected in the CSF of patients with psychiatric disorders.

MATERIALS AND METHODS

Participants

This study involved 94 patients with schizophrenia (mean age: 40.5 ± 10.1 years, 56 males and 38 females), 68 with BD (mean age: 43.6 ± 12.2 years, 33 males and 35 females), 104 with MDD (mean age: 43.4 ± 11.0 years, 49 males and 55 females), and 118 healthy controls (mean age: 42.4 ± 15.3 years, 66 males and 52 females) who were matched for age, sex, and ethnicity (Japanese). The BD group included 22 patients with BD I and 46 with BD II. A total of 384 samples were not based on any power analyses since we have not had data on pre-obtained effect size. All participants were recruited at the National Center of Neurology (NCNP), via advertisements at the NCNP Hospital, on our website, and in local free magazines. Participants were screened for psychiatric disorders by qualified psychiatrists using the Japanese version of the Mini International Neuropsychiatric Interview (Sheehan et al., 1998; Otsubo et al., 2005). Consensus diagnoses were determined according to the criteria laid out in the Diagnostic and Statistical Manual of Mental Disorders, 4th edition (American Psychiatric Association, 1994), based on the information from the Mini International Neuropsychiatric Interview, additional unstructured interviews, and medical records, if available. Healthy controls had no history of contact with any psychiatric services. Participants were excluded if they had a medical history of CNS diseases, severe head injury, substance abuse, or mental retardation. After providing them with a description of the study, written informed consent was obtained from every participant. The study protocol was approved by the ethics committee of the NCNP. The study was performed in accordance with the Declaration of Helsinki (World Medical Association, 2013).

Clinical Assessments

The Positive and Negative Syndrome Scale (PANSS) was used to evaluate symptoms in patients with schizophrenia (Kay et al., 1987), and the Young Mania Rating Scale was used to evaluate manic symptoms in patients with BD (Young et al., 1978). The 21-item version of the GRID Hamilton Depression Rating Scale was used to assess depressive symptoms in patients with BD and MDD (Williams et al., 2008). Symptoms were assessed by board-qualified psychiatrists. Daily doses of antipsychotics were converted to chlorpromazine-equivalent doses, and doses of antidepressants were converted to imipramine-equivalent doses according to a published guideline (Inada and Inagaki, 2015). Every patient's medication status was recorded at the time of the lumbar puncture.

Lumbar Puncture

Lumbar puncture was performed in the left lateral decubitus or a sitting position. Each participant received local anesthesia by lidocaine hydrochloride injection before the puncture. CSF was withdrawn from the L3–L4 or L4–L5 interspace using an atraumatic pencil-point needle (Universe 22 or 23G, 75 mm, Unisis Corp., Tokyo, Japan). The CSF was collected in a low protein absorption tube (PROTEOSAVE SS, 15 ml Conicaltube, Sumitomo Bakelite Co., Tokyo, Japan) and immediately

transferred on ice. The CSF was centrifuged (4,000 × *g* for 10 min) at 4°C and the supernatant was dispended in 0.5-ml aliquots and stored at −80°C in a deep freezer. After a single melting and re-freeze of the sample for the preparation of the 96-well plates, multiplex immunoassays were performed.

Multiplex Immunoassays

CSF protein levels were measured with the MAGPIX CCD imaging system (Bio-Rad Laboratories, Inc.) using magnetic on-bead antibody conjugation for 37 inflammatory cytokines (171AL001M, Bio-Plex Pro™ Human Inflammation Panel 1, 37-Plex, Bio-Rad Laboratories, Inc.) according to the manufacturer's instructions. CSF samples were diluted to 1:2, and 2 standard samples (S9 and S10) were newly created to extend the assay working range on the basis of the results of a verification assay. The assay was performed on the same day using 384 single CSF samples to secure a large number after confirming that the intra-run and inter-run coefficients of variance for the 37 proteins accounted for less than 10% of the variance in the verification assay (intra-run: one set, maximum 9.7%, quadruplicate; inter-run: 16 sets, maximum 5.7%, duplicate). A VIAFLO 96/384 system (INTEGRA Biosciences, Corp.) was used to apply samples simultaneously into the 96-well plates. To adjust the inter-assay variations between the 96-well plates, 13 randomly selected CSF diluted to 1:2, 2 standards (S4 and S10), and one blank were used as margin samples to fit measures of four plates to those of 1 standard plate that included 8 standard dilution (S4–10) and blank samples. Based on the measures of the margin samples, regression equations were calculated for the 37 proteins using 2-dimensional scatter diagrams between the standard and the other four plates for the inter-plate adjustment. Among the 37 assayed proteins, the measurements of 19 cytokines satisfied the following three criteria and were thus deemed reliable: 1) within the assay working range, 2) coefficients accounting for less than 15% median inter-run variance, and 3) strong Pearson's correlation coefficients ($r > 0.70$) in the regression equations of the inter-plate adjustment. The assay data for the 18 remaining cytokines (i.e., chitinase3-like 1, gp130/soluble IL-6 receptor β, interferon [IFN]-γ, IL-2, IL-12(p70), IL-20, IL-22, IL-27(p28), IL-28A/IFN-λ1, IL-32, IL-34, IL-35, LIGHT/tumor necrosis factor superfamily (TNFSF) 14, matrix metalloproteinases-1, matrix metalloproteinases-2, osteopontin, pentraxin-3, and tumor necrosis factor-related weak inducer of apoptosis/TNFSF12) did not meet some of the criteria and were thus excluded from the following statistical analyses. CSF cytokine levels are represented as pg/ml.

Statistical Analyses

Categorical and continuous variables were compared between the four diagnostic groups using chi-square tests and analysis of variance (ANOVA), respectively. CSF cytokine levels were compared between patient (both three diagnoses combined and each diagnosis) and control groups and between drug free and non-drug free groups using Mann–Whitney U tests, while effect sizes are shown using r. Kruskal-Wallis tests were used when comparing CSF cytokine levels across the four diagnostic groups. Correlation between CSF cytokine levels and clinical variables were assessed using Pearson's correlation coefficients, while CSF cytokine levels were compared using unpaired (Student's or Welch's) -t tests between sexes. Correlations between CSF cytokine levels and symptom scores or CSF total protein level were assessed using Pearson's partial correlation coefficient controlled for age, sex, and drug use (only for patients). The correlation matrix for CSF cytokine levels was also assessed with Pearson's partial correlation coefficient controlled for age, sex, and drug use (only for patients). Bonferroni corrections for multiple testing were applied for 3 ANOVAs for comparison of clinical variables (i.e., age, BMI, and education level) between each diagnostic and control groups ($p < 0.05/3 = 0.016$), Mann–Whitney U tests, Kruskal-Wallis tests, and correlational analyses on measured 19 CSF cytokine levels ($p < 0.05/19 = 0.0026$). Hence, corrected *p*-values were calculated 19 x nominal *p*-values for group comparisons and correlational analyses on the CSF cytokine levels. All statistical tests were 2-tailed and $p < 0.05$ was considered significant. Statistical analyses were performed using the Statistical Package for the Social Sciences version 25.0 and 27.0 (IBM Japan, Ltd., Tokyo, Japan).

RESULTS

Association Between Clinical Variables and Cerebrospinal Fluid Cytokine Levels

The clinical characteristics of the participants are shown in **Table 1**. There were no significant differences in the distributions of age and sex, while body mass index (BMI) and education level were significantly higher and lower, respectively, in patients with schizophrenia than in healthy controls (corrected $p = 0.004$ and 0.006). There were 11, 5, and 26 drug-free patients with schizophrenia, BD, and MDD, respectively. Correlations between CSF cytokine levels and clinical variables in patients with schizophrenia, BD, or MDD and healthy controls are shown in **Supplementary Tables S1–S4**, respectively. BMI was significantly and negatively correlated with CSF IL-12(p40) level in patients with schizophrenia (corrected $p < 0.05$). Age was significantly and positively correlated with CSF soluble CD163 and soluble TNF-receptor one levels, while age of onset was significantly and positively correlated with CSF soluble CD163 level in patients with MDD (corrected $p < 0.05$).

Group Comparisons of Cerebrospinal Fluid Cytokine Levels

Comparisons of CSF cytokine levels between the patient group (3 diagnoses combined; $n = 266$) and the control group are shown in **Table 2**. CSF IFN-β level was significantly higher in the psychiatric patients than in the controls (corrected $p = 0.000029$, **Figure 1A**). Comparisons across the four diagnostic groups are shown in **Table 3**. CSF IFN-β level was significantly higher in patients with schizophrenia or BD than in healthy controls (corrected $p = 0.000047$ or 0.0034, respectively, **Figure 1B**). Comparisons of CSF cytokine levels between drug free and non-drug free patients with schizophrenia, BD, or MDD

TABLE 1 | The clinical characteristics of the participants.

	Schizophrenia (*n* = 94)		Bipolar disorder (*n* = 68)		Major depressive disorder (*n* = 104)		Control (*n* = 118)	
	Mean ± Standard deviation	**Range**	**Mean ± Standard deviation**	**Range**	**Mean ± Standard deviation**	**Range**	**Mean ± Standard deviation**	**Range**
Age (years)	40.5 ± 10.1	18-65	43.6 ± 12.2	20-74	43.4 ± 11.0	18-71	42.4 ± 15.3	19-77
Sex, male (%)	56 (59.6)		33 (48.5)		49 (47.1)		66 (55.9)	
Body mass index (kg/m^2)	24.7 ± 5.5	15.3-46.7	23.9 ± 4.8	13.9-35.6	22.3 ± 3.4	15.6-33.8	22.6 ± 3.4	15.8-32.5
Education (years)	13.6 ± 2.7	9-22	14.8 ± 2.6	9-21	15.0 ± 2.5	10-26	14.9 ± 2.6	10-23
Age of onset (years)	24.2 ± 7.5	5-46	31.5 ± 11.5	15-57	33.9 ± 11.2	13-59		
Duration of illness (years)	15.7 ± 9.6	2-47	10.4 ± 7.7	0-30	7.2 ± 7.6	0-38		
Chlorpromazine-equivalent dose (mg/day)								
Total	950.7 ± 929.9	0-2750.0	175.0 ± 303.1	0-1409.1	70.0 ± 156.7	0-823.0		
Typical	99.8 ± 387.1	0-2750.0	7.4 ± 25.9	0-150.0	6.3 ± 25.1	0-150.0		
Atypical	850.8 ± 715.7	0-3645.5	171.3 ± 306.1	0-1409.1	63.7 ± 150.3	0-803.0		
Imipramine-equivalent dose (mg/day)	21.4 ± 46.4	0-225.0	51.9 ± 99.1	0-456.3	164.0 ± 143.0	0-525.0		
Drug free, n (%)	11 (11.7)		5 (7.3)		26 (25.0)			
Positive and negative syndrome scale								
Total	61.0 ± 16.1	33-115						
Positive	14.2 ± 5.1	7-27						
Negative	16.3 ± 5.2	7-28						
General	30.5 ± 8.9	16-60						
Young mania rating scale			6.2 ± 7.5	0-33				
Hamilton depression rating scale, 21-item version			11.4 ± 7.7	0-35	11.3 ± 9.2			

Drug free was counted if psychotropic medication was not used.

TABLE 2 | Comparisons of cerebrospinal fluid cytokine levels between patient (three diagnoses combined) and control groups.

	Patient (*n* = 266)	Control (*n* = 118)	Statistical comparison
	Mean ± Standard deviation	**Mean ± Standard deviation**	
APRIL/TNFSF13	20,589.0 ± 6,672.6	19,726.6 ± 5,419.7	U = 14710, p = 0.33, r = −0.051
BAFF/TNFSF13B	3,017.6 ± 905.4	2,811.3 ± 561.4	U = 14178.5, p = 0.13, r = −0.078
Soluble CD30/TNFSF8	347.3 ± 158.5	308.2 ± 136.0	U = 13401, p = 0.022, r = −0.117
Soluble CD163	3,514.1 ± 1,161.8	3,229.2 ± 1,151.9	U = 13474, p = 0.027, r = −0.113
IFN-α2	5.2 ± 2.6	5.0 ± 3.2	U = 14792, p = 0.37, r = −0.046
IFN-β	48.0 ± 7.8	44.0 ± 7.6	U = 10868.5, **p = 1.5.E−06**, r = −0.246
Soluble IL-6 receptor α	993.4 ± 299.3	975.9 ± 280.7	U = 15275.5, p = 0.67, r = −0.022
IL-8	23.7 ± 4.1	22.8 ± 4.5	U = 13888, p = 0.07, r = −0.092
IL-10	5.5 ± 1.4	5.6 ± 1.3	U = 15104, p = 0.56, r = −0.032
IL-11	3.5 ± 1.0	3.4 ± 1.4	U = 13753, p = 0.053, r = −0.099
IL-12 (p40)	42.2 ± 10.9	44.3 ± 9.7	U = 13980, p = 0.09, r = −0.088
IL-19	20.2 ± 2.7	20.2 ± 2.9	U = 15500.5, p = 0.85, r = −0.010
IL-26	37.7 ± 14.9	36.6 ± 17.1	U = 15052.5, p = 0.52, r = −0.033
IL-29/IFN-λ1	151.1 ± 44.5	160.0 ± 40.8	U = 13880, p = 0.07, r = −0.093
Matrix metalloproteinase-3	730.2 ± 84.1	715.8 ± 87.8	U = 14392.5, p = 0.19, r = −0.067
Osteocalcin	94.0 ± 52.5	88.6 ± 44.9	U = 14926, p = 0.44, r = −0.040
soluble TNF-receptor 1	999.1 ± 289.4	957.3 ± 243.4	U = 14902.5, p = 0.43, r = −0.041
Soluble TNF-receptor 2	365.5 ± 173.3	336.5 ± 170.5	U = 14322, p = 0.17, r = −0.070
TSLP	22.0 ± 8.2	21.2 ± 10.0	U = 14640.5, p = 0.29, r = −0.054

APRIL, A proliferation-inducing ligand; BAFF, B-cell activating factor; CD, cluster of differentiation; IFN, interferon; IL, interleukin; TNF, tumor necrosis factor; TNFSF, tumor necrosis factor superfamily; TSLP, thymic stromal lymphopoietin. A correctedly significant p-value is shown in a bold exponent (p < 0.0026), while nominally significant p-values are shown in underlined cases (p < 0.05). Values are represented as pg/ml.

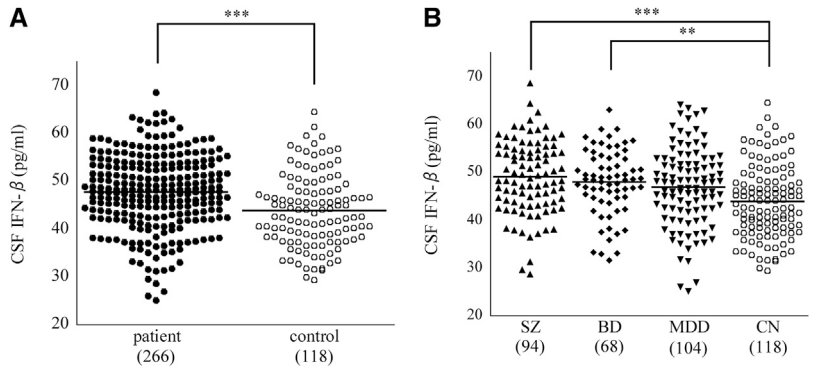

FIGURE 1 | Dot plots showing that cerebrospinal fluid (CSF) cytokine interferon (IFN)-β level. CSF IFN-β level was significantly higher in the patient (3 diagnoses combined) group than in the control group **(A)**. CSF IFN-β level was significantly higher in patients with SZ, or BD than in healthy controls **(B)**. Horizontal lines in the dot plots signify mean values, while numbers in parentheses represent those of the participants. $^{**}p < 0.01$, $^{***}p < 0.001$ (corrected). BD, bipolar disorder; CN, control; MDD, major depressive disorder; SZ, schizophrenia.

are shown in **Supplementary Tables S5–S7**, respectively. CSF IL-11 level was significantly lower in drug free patients than in non-drug free patients with schizophrenia (corrected $p < 0.05$).

Correlational Analyses of Cerebrospinal Fluid Cytokine Levels

Correlations between CSF cytokine levels and symptom scores are shown in **Supplementary Table S8**. Significantly negative correlations between IL-11, IL-29/IFN-λ1, and thymic stromal lymphopoietin (TSLP) levels and PANSS scores were found in patients with schizophrenia (corrected $p < 0.05$), while no significant correlations were found in patients with BD or MDD. Correlations between CSF cytokine and total protein levels are shown in **Supplementary Table 9S**. There were no significant correlations in patients with schizophrenia or BD or in healthy controls, while CSF osteocalcin level was significantly and positively corelated with CSF total protein level in patients with MDD (corrected $p < 0.05$). Correlation matrices for CSF cytokine levels are shown in **Supplementary Tables 10S–S13**. As expected, many CSF cytokine levels showed significantly positive correlation with each other in patients with schizophrenia, those with BD, those with MDD, and healthy controls (corrected $p < 0.05$).

DISCUSSION

To our knowledge, this is the largest multiplex immunoassay study in terms of both the number of cytokines measured ($n = 19$) and the patient (schizophrenia: $n = 94$, BD: $n = 68$, MDD: $n = 104$) and controls ($n = 118$) sample size. Among the 19 reliably measured cytokines, CSF IFN-β level was higher in psychiatric patients than in healthy controls. Even when comparing across all four diagnostic groups, we found that CSF IFN-β level was higher in patients with schizophrenia and in those with BD, in this order, than in healthy controls. Notably, CSF IFN-α2 and IFN-λ1 levels were not significantly altered. These results suggest that CSF IFN-β could be a useful biomarker for psychiatric disorders.

When all four diagnostic groups were compared with the controls, the elevation in IFN-β level reached the statistical significance even after corrections for multiple testing, suggesting that elevation of IFN-β could be involved in the pathophysiology of schizophrenia. Some earlier studies suggested that IFN-γ, rather than IFN-β, could be a trait maker of schizophrenia; the source, however, included peripheral IFN-γ (Na et al., 2014; Steiner et al., 2014). A meta-analysis (Miller et al., 2011) and a review (Mohammadi et al., 2018) reported CSF cytokine levels in patients with schizophrenia, but did not include data on CSF IFN-β level. Regarding other cytokines, CSF IL-6 level was found to be elevated (Coughlin et al., 2016), while CSF IL-8 level was unaltered in patients with schizophrenia compared to controls (Schwieler et al., 2015) in the V-plex® assays, which, since IL-6 is synonymous to IFN-β2, is consistent with the findings of our study.

CSF IFN-β level was higher in patients with BD than in healthy controls. Although IFN has been suggested as an inflammatory cytokine in patients with BD (Rosenblat and McIntyre, 2015), IFN-β was not identified as a significantly elevated cytokine in a recent systematic review (Knorr et al., 2018). The present study indicates that CSF IFN-β could be involved in the pathophysiology of BD as well. Regarding other cytokines, increased CSF IL-1β and decreased CSF IL-6 levels in patients with BD compared with healthy volunteers were found in a multiplex assay (Soderlund et al., 2011). While IL-1β was not assayed in this study, our finding on IL-6 (i.e., IFN-β2) are in contrast to this earlier study. This inconsistency may be, due at least in part, to the fact that the study of Soderlund et al. (2011) examined euthymic patients with BD. To draw any firm conclusions, further studies in a large sample with the stratification by patients' state will be necessary.

Although statistical significance could not be obtained (corrected $p = 0.061$), CSF IFN-β level was tended to be higher in patients with MDD than in healthy controls. In line with this finding, CSF IL-6 (i.e., IFN-β2) level was increased in a geriatric depression group compared with a non-depression

TABLE 3 | Comparisons across the four diagnostic groups.

	Schizophrenia (*n* = 94)		Bipolar disorder (*n* = 68)		Major depressive disorder (*n* = 104)		Control (*n* = 118)	Statistical comparison
	Mean ± Standard deviation	vs. control	Mean ± Standard deviation	vs. control	Mean ± Standard deviation	vs. control	Mean ± Standard deviation	
APRIL/TNFSF13	20,072.0 ± 6,131.0	U = 5341, p = 0.64, r = −0.032	20,660.2 ± 7,234.7	U =3847, p = 0.64, r = −0.035	21,009.7 ± 6,792.5	U = 5522, p = 0.20, r = −0.087	19,726.6 ± 5,419.7	H = 1.65, p = 0.65
BAFF/TNFSF13B	29,25.7 ± 892.0	U = 5350, p = 0.66, r = −0.031	3,076.3 ± 835.7	U = 3442.5, p = 0.11, r = −0.119	3,062.5 ± 961.5	U = 5386, p = 0.12, r = −0.106	2,811.3 ± 561.4	H = 3.85, p = 0.28
Soluble CD30/ TNFSF8	367.2 ± 175.5	U = 4590, p = 0.031, r = −0.148	344.3 ± 154.4	U = 3432, p = 0.10, r = −0.121	331.3 ± 143.7	U = 5379, p = 0.11, r = −0.107	308.2 ± 136.0	H = 6.18, p = 0.10
Soluble CD163	3,487.8 ± 1,154.3	U = 4841.5, p = 0.11, r = -0.110	3,604.1 ± 1,236.6	U = 3324, p = 0.052, r = −0.143	3,479.0 ± 1126.1	U = 5308.5, p = 0.08, r = −0.117	3,229.2 ± 1,151.9	H = 5.18, p = 0.16
IFN-α2	5.6 ± 2.5	U = 4842.5, p = 0.11, r = -0.109	5.1 ± 2.7	U = 3946.5, p = 0.85, r = −0.014	5.0 ± 2.5	U = 6003, p = 0.78, r = −0.019	5.0 ± 3.2	H = 3.18, p = 0.37
IFN-β	49.1 ± 7.7	U = 3452.5, **p = 2.4.E−06**, r = −0.325	48.0 ± 6.9	U = 2689.5, **p = 1.8.E−04**, r = −0.275	46.9 ± 8.3	U = 4726.5, p = 0.0032, r = −0.199	44.0 ± 7.6	H = 26.57, **p = 7.3.E−06**
Soluble IL-6 receptor α	965.1 ± 265.3	U = 5453.5, p = 0.84, r = −0.015	947.5 ± 261.6	U = 3828.5, p = 0.60, r = −0.039	1,048.9 ± 342.2	U = 5441.5, p = 0.15, r = −0.098	975.9 ± 280.7	H = 4.11, p = 0.25
IL-8	24.3 ± 3.8	U = 4293.5, p = 0.0046, r = −0.194	23.5 ± 4.2	U = 3714.5, p = 0.40, r = −0.062	23.4 ± 4.4	U = 5880, p = 0.59, r = −0.036	22.8 ± 4.5	H = 8.36, p = 0.039
IL-10	5.4 ± 1.5	U = 5374.5, p = 0.70, r = −0.024	5.4 ± 1.6	U = 3805.5, p = 0.56, r = −0.043	5.5 ± 1.3	U = 5924, p = 0.66, r = 0.030	5.6 ± 1.3	H = 0.41, p = 0.94
IL-11	3.4 ± 0.8	U = 4692, p = 0.054, r = -0.133	3.4 ± 0.9	U = 3697.5, p = 0.37, r = −0.066	3.5 ± 1.2	U = 5363.5, p = 0.11, r = −0.109	3.4 ± 1.4	H = 4.62, p = 0.20
IL-12 (p40)	41.0 ± 11.7	U = 4699.5, p = 0.056, r = -0.132	42.1 ± 11.0	U = 3493, p = 0.14, r = −0.108	43.3 ± 10.1	U = 5787.5, p = 0.47, r = −0.050	44.3 ± 9.7	H = 4.73, p = 0.19
IL-19	20.8 ± 2.6	U = 4866, p = 0.13, r = −0.106	20.2 ± 2.9	U = 3936.5, p = 0.83, r = −0.016	19.7 ± 2.6	U = 5574, p = 0.24, r = −0.079	20.2 ± 2.9	H = 7.62, p = 0.055
IL-26	39.8 ± 13.9	U = 4971.5, p = 0.20, r = −0.089	38.5 ± 15.2	U = 3698, p = 0.38, r = −0.066	35.3 ± 15.4	U = 5889, p = 0.61, r = −0.035	36.6 ± 17.1	H = 4.05, p = 0.26
IL-29/IFN-λ1	149.3 ± 47.7	U = 4759, p = 0.08, r = −0.122	147.0 ± 45.2	U = 3288.5, p = 0.041, r = −0.151	155.3 ± 41.0	U = 5832.5, p = 0.53, r = −0.043	160.0 ± 40.8	H = 5.64, p = 0.13
Matrix metalloproteinase-3	731.4 ± 81.7	U = 5138, p = 0.36, r = −0.064	724.4 ± 79.5	U = 3764.5, p = 0.48, r = −0.052	732.9 ± 89.5	U = 5490, p = 0.18, r = −0.091	715.8 ± 87.8	H = 2.00, p = 0.57
Osteocalcin	96.7 ± 54.7	U = 5148, p = 0.37, r = −0.062	88.6 ± 54.7	U = 3931, p = 0.82, r = −0.017	95.0 ± 49.1	U = 5685, p = 0.35, r = −0.064	88.6 ± 44.9	H = 1.94, p = 0.59
Soluble TNF-receptor 1	971.2 ± 287.6	U = 5418, p = 0.77, r = −0.020	997.5 ± 279.8	U = 3858.5, p = 0.66, r = −0.032	1,025.4 ± 297.4	U = 5370, p = 0.11, r = −0.108	957.3 ± 243.4	H = 3.65, p = 0.30
Soluble TNF-receptor 2	347.6 ± 163.0	U = 5338.5, p = 0.64, r = −0.033	374.6 ± 179.5	U = 3548, p = 0.19, r = −0.097	375.8 ± 178.5	U = 5435.5, p = 0.14, r = −0.099	336.5 ± 170.5	H = 3.10, p = 0.38
TSLP	22.9 ± 7.5	U = 4871, p = 0.13, r = −0.105	21.9 ± 10.1	U = 3885, p = 0.72, r = −0.027	21.2 ± 7.2	U = 5884.5, p = 0.60, r = −0.036	21.2 ± 10.0	H = 2.36, p = 0.50

APRIL, A proliferation-inducing ligand; BAFF, B-cell activating factor; CD, cluster of differentiation; IFN, interferon; IL, interleukin;TNF; tumor necrosis factor; TNFSF, tumor necrosis factor superfamily; TSLP, thymic stromal lymphopoietin Correctedly significant p-values are shown in bold exponents (p < 0.0026), while nominally significant p-values are shown in underlined cases (p < 0.05). Values are represented as pg/ml.

group in an earlier V-plex® assay (Kern et al., 2014). Remarkably, exogenous IFN-α and IFN-β used for hepatitis C treatment have been reported to induce depressive states as a side effect (Loftis and Hauser, 2004; Machado et al., 2017); this is partially in accordance with our data, since CSF IFN-α2 and IFN-λ1 levels showed no significant differences between our patients and controls. Two multiplex immunoassays (Luminex® and V-plex®) reported CSF cytokine levels (Maxeiner et al., 2014;

Haroon et al., 2016) in patients with affective/mood disorder; however, levels for healthy controls were not reported.

We found, for the first time, that soluble CD163 was elevated in the total psychiatric group, compared with the controls, although this finding was statistically nominal. A previous clinical study reported that CD163-positive perivascular macrophages, which is a feasible origin of soluble CD163, were abundantly detected in the brain of patients with schizophrenia with high inflammation (Cai et al., 2018). Relatedly, a macrophage-derived product neopterin (Oxenkrug, 2011) level were reported to increase in the CSF of patients with psychiatric disorders (Bechter et al., 2010; Kuehne et al., 2013; Ghisoni and Latini, 2015). Our results of increases in CD163 thus imply activation of monocytes-macrophages and may provide additional support for the involvement of inflammation in psychiatric disorders.

Negative correlations were observed between CSF IL-11, IL-29/IFN-λ1, and TSLP levels and PANSS scores in patients with schizophrenia. Unexpectedly, these results suggest that brain inflammation is not positively associated with symptom severity in patients with psychiatric disorders, which is inconsistent with previous reports including animal models (Loftis et al., 2010; Na et al., 2014; Muller et al., 2015; Rosenblat and McIntyre, 2015; Adzic et al., 2018; Misiak et al., 2018; Muller, 2018). Considering the fact that the correlations were sporadic and that significant cytokines that were identified as significant in group comparisons (i.e., IFN-β) were not included, the effects of CSF cytokines on symptom severity in schizophrenia are considerably limited. Taken together with the results of our group comparisons, these findings suggest that IFN-β is related with the pathology, but not with symptom severity, in patients with psychiatric disorders.

No significant correlations were observed between CSF cytokine and total protein levels in patients and controls, despite CSF osteocalcin level showing a positive correlation only in patients with MDD. Although direct relationship between CSF and plasma cytokine levels could not presented in this study, blood-brain barrier dysfunction and CSF total protein elevation have been reported in psychiatric disorders (Orlovska-Waast et al., 2018; Pollak et al., 2018). Since plasma cytokine levels are generally equal or higher than CSF cytokine levels (Maxeiner et al., 2014; Coughlin et al., 2016; Haroon et al., 2016), the absence of a correlation between CSF cytokine and total protein levels may suggest that the origin of most of cytokines measured in this study was central rather than peripheral. This supports a role of central inflammation in the pathology of psychiatric disorders (Na et al., 2014; Anderson and Maes, 2017).

There are following limitations. First, the majority of patients (schizophrenia: 88.3%, BD: 92.7%, MDD: 75.0%) had taken some form of psychotropic medication, although the effects on CSF cytokines were confirmed to be small in statistical comparisons. Second, 19 (51.4%) among the 37 cytokines could only be measured using a Bio-Plex assay kit. Similarly, prior studies have reported that a variety of targeted cytokines cannot be measured with V-plex® (Schwieler et al., 2015; Coughlin et al., 2016) or multiplex (Soderlund et al., 2011) assays. This implies that multiplex immunoassays are not flawless when it comes to measuring, especially if they have been designed for measurements of plasma or other tissues that contain higher levels of target molecules than the CSF. Third, significant biomarkers were rarely reported among limited cytokines measured in this multiplex immunoassay, suggesting that relatively lower number of immunocompetent cells may be involved in the pathology of psychiatric disorders. Otherwise, any prominent biomarkers may exist among cytokines which have not been included in the measurement of this study. Fourth, CSF may not be the best biological sample for seeking cytokine abnormalities in patients with psychiatric disorders. Peripheral metabolic and microbiome alternations (Aizawa et al., 2016; Rosenblat and McIntyre, 2017; Hidese et al., 2018; Horne and Foster, 2018; Kraeuter et al., 2020) may rather be more sensitive than central immunological disturbances to elucidate inflammatory changes in the pathogenesis of psychiatric disorders. Fifth, since general laboratory data about inflammatory status (e.g., CSF or plasma C-reactive protein levels) were not included, this study could not address systemic inflammation in patient groups. Sixth, this study revealed that IFN-β was significantly increased in patients with psychiatric disorders; however, dot plots of patient (both all and each diagnostic) and control groups are widely overlapped. Therefore, IFN-β will not still be used as a biomarker to distinguish 'psychiatric disease' from 'normal population'. Finally, the cross-sectional nature of this study does not allow us to clearly link the etiology of psychiatric disorders to CSF inflammatory cytokines. Further studies are warranted to address the pathogenesis of brain inflammation in patients with psychiatric disorders.

In conclusion, CSF IFN-β level showed most prominent increases in psychiatric groups compared with healthy controls. Our data suggest that IFN-β could be a useful biomarker in the inflammation-related pathophysiology of major psychiatric disorders.

DATA AVAILABILITY STATEMENT

The original contributions presented in the study are included in the article/**Supplementary Material**, further inquiries can be directed to the corresponding author.

ETHICS STATEMENT

The studies involving human participants were reviewed and approved by the ethics committee of the NCNP. The patients/participants provided their written informed consent to participate in this study.

AUTHOR CONTRIBUTIONS

SH and KH designed and HK supervised, the study. SH, KH, DS, and MO evaluated the symptoms and determined the diagnoses. SY helped to recruit participants among clinic patients. YY, II, and

JM conducted interviews and psychological assessments of the participants. SH, KH, and DS conducted the lumbar punctures to collect CSF samples. KH selected and TM prepared the CSF sample set. RM created and maintained the biobank database system. SH performed laboratory experiments with the assistance of TT. SH performed the statistical analyses and wrote the manuscript, which was revised and approved by all authors.

FUNDING

This work was supported by Intramural Research Grants for Neurological and Psychiatric Disorders from the NCNP (27-6, 30-1, and 30-7 for KH and HK) and by grants from the Japan Agency for Medical Research and Development (18dk0307062h0003, 18dk0307081h0001, 18dm0107100h0003, and 19ak0101043h0205 for KH and HK). These funding sources were only financially involved in the study.

ACKNOWLEDGMENTS

We thank Masashi Hashimoto, Chie Kimizuka, Takahiro Tomizawa, Naoko Ishihara, Tomoko Kuroshio, Moeko Hiraishi, and Chiori Maeda for their assistance in the recruitment of participants, the clinical assessments, and the lumbar punctures. We also thank Yuko Yamaoka, Ayumi Fujisawa, Izumi Sato, Misao Nakano, Yurika Adachi, and Megumi Tatsumi for their sample management. This paper was proofread by a scientific editor at Editage (Tokyo, Japan).

SUPPLEMENTARY MATERIAL

The Supplementary Material for this article can be found online at: https://www.frontiersin.org/articles/10.3389/fphar.2020.594394/full#supplementary-material.

REFERENCES

Adzic, M., Brkic, Z., Mitic, M., Francija, E., Jovicic, M. J., Radulovic, J., et al. (2018). Therapeutic strategies for treatment of inflammation-related depression. *Curr. Neuropharmacol.* 16, 176–209. doi:10.2174/1570159X15666170828163048

Aizawa, E., Tsuji, H., Asahara, T., Takahashi, T., Teraishi, T., Yoshida, S., et al. (2016). Possible association of Bifidobacterium and Lactobacillus in the gut microbiota of patients with major depressive disorder. *J. Affect. Disord.* 202, 254–257. doi:10.1016/j.jad.2016.05.038

American Psychiatric Association (1994). *Diagnostic and statistical manual of mental disorders*. 4th Ed. Washington, DC: American Psychiatric Association.

Anderson, G., and Maes, M. (2017). How immune-inflammatory processes link CNS and psychiatric disorders: classification and treatment implications. *CNS Neurol. Disord.* 16, 266–278. doi:10.2174/1871527315666161122144659

Bauer, M. E., and Teixeira, A. L. (2018). Inflammation in psychiatric disorders: what comes first?. *Ann. N. Y. Acad. Sci.* 1437 (1), 57–67. doi:10.1111/nyas.13712

Bechter, K., Reiber, H., Herzog, S., Fuchs, D., Tumani, H., and Maxeiner, H. G. (2010). Cerebrospinal fluid analysis in affective and schizophrenic spectrum disorders: identification of subgroups with immune responses and blood-CSF barrier dysfunction. *J. Psychiatr. Res.* 44, 321–330. doi:10.1016/j.jpsychires.2009.08.008

Belzeaux, R., Lefebvre, M. N., Lazzari, A., Le Carpentier, T., Consoloni, J. L., Zendjidjian, X., et al. (2017). How to: measuring blood cytokines in biological psychiatry using commercially available multiplex immunoassays. *Psychoneuroendocrinology* 75, 72–82. doi:10.1016/j.psyneuen.2016.10.010

Cai, H. Q., Catts, V. S., Webster, M. J., Galletly, C., Liu, D., O'donnell, M., et al. (2018). Increased macrophages and changed brain endothelial cell gene expression in the frontal cortex of people with schizophrenia displaying inflammation. *Mol. Psychiatr.* 25 (4), 761–775. doi:10.1038/s41380-018-0235-x

Coughlin, J. M., Wang, Y., Ambinder, E. B., Ward, R. E., Minn, I., Vranesic, M., et al. (2016). *In vivo* markers of inflammatory response in recent-onset schizophrenia: a combined study using [(11)C]DPA-713 PET and analysis of CSF and plasma. *Transl. Psychiatry* 6, e777. doi:10.1038/tp.2016.40

Dantzer, R. (2018). Neuroimmune interactions: from the brain to the immune system and vice versa. *Physiol. Rev.* 98, 477–504. doi:10.1152/physrev.00039.2016

Ghisoni, K., Latini, A., Kuehne, L. K., Reiber, H., Bechter, K., and Hagberg, L. (2015). Cerebrospinal fluid neopterin is brain-derived and not associated with blood-CSF barrier dysfunction in non-inflammatory affective and schizophrenic spectrum disorders. *J. Psychiatr. Res.* 63 (Issue 10), 141–142. doi:10.1016/j.jpsychires.2015.02.002

Haroon, E., Fleischer, C. C., Felger, J. C., Chen, X., Woolwine, B. J., Patel, T., et al. (2016). Conceptual convergence: increased inflammation is associated with increased basal ganglia glutamate in patients with major depression. *Mol. Psychiatr.* 21, 1351–1357. doi:10.1038/mp.2015.206

Hattori, K., Ota, M., Sasayama, D., Yoshida, S., Matsumura, R., Miyakawa, T., et al. (2015). Increased cerebrospinal fluid fibrinogen in major depressive disorder. *Sci. Rep.* 5, 11412. doi:10.1038/srep11412

Hidese, S., Asano, S., Saito, K., Sasayama, D., and Kunugi, H. (2018). Association of depression with body mass index classification, metabolic disease, and lifestyle: a web-based survey involving 11,876 Japanese people. *J. Psychiatr. Res.* 102, 23–28. doi:10.1016/j.jpsychires.2018.02.009

Horne, R., and Foster, J. A. (2018). Metabolic and microbiota measures as peripheral biomarkers in major depressive disorder. *Front. Psychiatr.* 9, 513. doi:10.3389/fpsyt.2018.00513

Horváth, S., and Mirnics, K. (2014). Immune system disturbances in schizophrenia. *Biol. Psychiatr.* 75, 316–323. doi:10.1016/j.biopsych.2013.06.010

Inada, T., and Inagaki, A. (2015). Psychotropic dose equivalence in Japan. *Psychiatr. Clin. Neurosci.* 69, 440–447. doi:10.1111/pcn.12275

Ishii, T., Hattori, K., Miyakawa, T., Watanabe, K., Hidese, S., Sasayama, D., et al. (2018). Increased cerebrospinal fluid complement C5 levels in major depressive disorder and schizophrenia. *Biochem. Biophys. Res. Commun.* 497, 683–688. doi:10.1016/j.bbrc.2018.02.131

Kay, S. R., Fiszbein, A., and Opler, L. A. (1987). The positive and negative syndrome scale (PANSS) for schizophrenia. *Schizophr. Bull.* 13, 261–276. doi:10.1093/schbul/13.2.261

Kern, S., Skoog, I., Börjesson-Hanson, A., Blennow, K., Zetterberg, H., Ostling, S., et al. (2014). Higher CSF interleukin-6 and CSF interleukin-8 in current depression in older women. Results from a population-based sample. *Brain Behav. Immun.* 41, 55–58. doi:10.1016/j.bbi.2014.05.006

Khandaker, G. M., and Dantzer, R. (2016). Is there a role for immune-to-brain communication in schizophrenia?. *Psychopharmacology* 233, 1559–1573. doi:10.1007/s00213-015-3975-1

Khandaker, G. M., Dantzer, R., and Jones, P. B. (2017). Immunopsychiatry: important facts. *Psychol. Med.* 47, 2229–2237. doi:10.1017/S0033291717000745

Knorr, U., Simonsen, A. H., Zetterberg, H., Blennow, K., Hasselbalch, S. G., and Kessing, L. V. (2018). Biomarkers in cerebrospinal fluid of patients with bipolar disorder versus healthy individuals: a systematic review. *Eur. Neuropsychopharmacol* 28, 783–794. doi:10.1016/j.euroneuro.2018.04.002

Kraeuter, A. K., Phillips, R., and Sarnyai, Z. (2020). The gut microbiome in psychosis from mice to men: a systematic review of preclinical and clinical studies. *Front. Psychiatr.* 11, 799. doi:10.3389/fpsyt.2020.00799

Kuehne, L. K., Reiber, H., Bechter, K., Hagberg, L., and Fuchs, D. (2013). Cerebrospinal fluid neopterin is brain-derived and not associated with blood-CSF barrier dysfunction in non-inflammatory affective and schizophrenic spectrum disorders. *J. Psychiatr. Res.* 47, 1417–1422. doi:10.1016/j.jpsychires.2013.05.027

Kunugi, H., Hori, H., and Ogawa, S. (2015). Biochemical markers subtyping major depressive disorder. *Psychiatr. Clin. Neurosci.* 69, 597–608. doi:10.1111/pcn.12299

Loftis, J. M., and Hauser, P. (2004). The phenomenology and treatment of interferon-induced depression. *J. Affect. Disord.* 82, 175–190. doi:10.1016/j.jad.2004.04.002

Loftis, J. M., Huckans, M., and Morasco, B. J. (2010). Neuroimmune mechanisms of cytokine-induced depression: current theories and novel treatment strategies. *Neurobiol. Dis.* 37, 519–533. doi:10.1016/j.nbd.2009.11.015

Machado, M. O., Oriolo, G., Bortolato, B., Köhler, C. A., Maes, M., Solmi, M., et al. (2017). Biological mechanisms of depression following treatment with interferon for chronic hepatitis C: a critical systematic review. *J. Affect. Disord.* 209, 235–245. doi:10.1016/j.jad.2016.11.039

Maxeiner, H. G., Marion Schneider, E., Kurfiss, S. T., Brettschneider, J., Tumani, H., and Bechter, K. (2014). Cerebrospinal fluid and serum cytokine profiling to detect immune control of infectious and inflammatory neurological and psychiatric diseases. *Cytokine* 69, 62–67. doi:10.1016/j.cyto.2014.05.008

Miller, B. J., Buckley, P., Seabolt, W., Mellor, A., and Kirkpatrick, B. (2011). Meta-analysis of cytokine alterations in schizophrenia: clinical status and antipsychotic effects. *Biol. Psychiatr.* 70, 663–671. doi:10.1016/j.biopsych.2011.04.013

Misiak, B., Beszłej, J. A., Kotowicz, K., Szewczuk-Bogusławska, M., Samochowiec, J., Kucharska-Mazur, J., et al. (2018). Cytokine alterations and cognitive impairment in major depressive disorder: from putative mechanisms to novel treatment targets. *Prog. Neuro-Psychopharmacol. Biol. Psychiatry* 80, 177–188. doi:10.1016/j.pnpbp.2017.04.021

Mohammadi, A., Rashidi, E., and Amooeian, V. G. (2018). Brain, blood, cerebrospinal fluid, and serum biomarkers in schizophrenia. *Psychiatr. Res.* 265, 25–38. doi:10.1016/j.psychres.2018.04.036

Müller, N. (2018). Inflammation in schizophrenia: pathogenetic aspects and therapeutic considerations. *Schizophr. Bull.* 44, 973–982. doi:10.1093/schbul/sby024

Müller, N., Weidinger, E., Leitner, B., and Schwarz, M. J. (2015). The role of inflammation in schizophrenia. *Front. Neurosci.* 9, 372. doi:10.3389/fnins.2015.00372

Na, K. S., Jung, H. Y., and Kim, Y. K. (2014). The role of pro-inflammatory cytokines in the neuroinflammation and neurogenesis of schizophrenia. *Prog. Neuro-Psychopharmacol. Biol. Psychiatry* 48, 277–286. doi:10.1016/j.pnpbp.2012.10.022

Orlovska-Waast, S., Kohler-Forsberg, O., Brix, S. W., Nordentoft, M., Kondziella, D., Krogh, J., et al. (2018). Cerebrospinal fluid markers of inflammation and infections in schizophrenia and affective disorders: a systematic review and meta-analysis. *Mol. Psychiatr.* 24 (6), 869–887. doi:10.1038/s41380-018-0220-4

Otsubo, T., Tanaka, K., Koda, R., Shinoda, J., Sano, N., Tanaka, S., et al. (2005). Reliability and validity of Japanese version of the mini-international neuropsychiatric interview. *Psychiatr. Clin. Neurosci.* 59, 517–526. doi:10.1111/j.1440-1819.2005.01408.x

Oxenkrug, G. F. (2011). Interferon-gamma-inducible kynurenines/pteridines inflammation cascade: implications for aging and aging-associated psychiatric and medical disorders. *J. Neural. Transm.* 118, 75–85. doi:10.1007/s00702-010-0475-7

Pollak, T. A., Drndarski, S., Stone, J. M., David, A. S., Mcguire, P., and Abbott, N. J. (2018). The blood-brain barrier in psychosis. *Lancet Psychiatry* 5, 79–92. doi:10.1016/S2215-0366(17)30293-6

Rosenblat, J. D., and Mcintyre, R. S. (2015). Are medical comorbid conditions of bipolar disorder due to immune dysfunction?. *Acta Psychiatr. Scand.* 132, 180–191. doi:10.1111/acps.12414

Rosenblat, J. D., and Mcintyre, R. S. (2017). Bipolar disorder and immune dysfunction: epidemiological findings, proposed pathophysiology and clinical implications. *Brain Sci.* 7, 144. doi:10.3390/brainsci7110144

Sakka, L., Coll, G., and Chazal, J. (2011). Anatomy and physiology of cerebrospinal fluid. *Eur. Ann. Otorhinolaryngol. Head Neck Dis.* 128, 309–316. doi:10.1016/j.anorl.2011.03.002

Sasayama, D., Hattori, K., Wakabayashi, C., Teraishi, T., Hori, H., Ota, M., et al. (2013). Increased cerebrospinal fluid interleukin-6 levels in patients with schizophrenia and those with major depressive disorder. *J. Psychiatr. Res.* 47, 401–406. doi:10.1016/j.jpsychires.2012.12.001

Schwieler, L., Larsson, M. K., Skogh, E., Kegel, M. E., Orhan, F., Abdelmoaty, S., et al. (2015). Increased levels of IL-6 in the cerebrospinal fluid of patients with chronic schizophrenia--significance for activation of the kynurenine pathway. *J. Psychiatry Neurosci.* 40, 126–133. doi:10.1503/jpn.140126

Sheehan, D. V., Lecrubier, Y., Sheehan, K. H., Amorim, P., Janavs, J., Weiller, E., et al. (1998). The Mini-International Neuropsychiatric Interview (M.I.N.I.): the development and validation of a structured diagnostic psychiatric interview for DSM-IV and ICD-10. *J. Clin. Psychiatr.* 59 (Suppl. 20), 22–57.

Söderlund, J., Olsson, S. K., Samuelsson, M., Walther-Jallow, L., Johansson, C., Erhardt, S., et al. (2011). Elevation of cerebrospinal fluid interleukin-1ss in bipolar disorder. *J. Psychiatry Neurosci.* 36, 114–118. doi:10.1503/jpn.100080

Sperner-Unterweger, B., Kohl, C., and Fuchs, D. (2014). Immune changes and neurotransmitters: possible interactions in depression?. *Prog. Neuro Psychopharmacol. Biol. Psychiatry* 48, 268–276. doi:10.1016/j.pnpbp.2012.10.006

Steiner, J., Bernstein, H. G., Schiltz, K., Müller, U. J., Westphal, S., Drexhage, H. A., et al. (2014). Immune system and glucose metabolism interaction in schizophrenia: a chicken-egg dilemma. *Prog. Neuro Psychopharmacol. Biol. Psychiatry* 48, 287–294. doi:10.1016/j.pnpbp.2012.09.016

Veening, J. G., and Barendregt, H. P. (2010). The regulation of brain states by neuroactive substances distributed via the cerebrospinal fluid; a review. *Cerebrospinal Fluid Res.* 7, 1. doi:10.1186/1743-8454-7-1

Walther, A., Penz, M., Ijacic, D., and Rice, T. R. (2017). Bipolar spectrum disorders in male youth: the interplay between symptom severity, inflammation, steroid secretion, and body composition. *Front. Psychiatr.* 8, 207. doi:10.3389/fpsyt.2017.00207

Wang, A. K., and Miller, B. J. (2018). Meta-analysis of cerebrospinal fluid cytokine and tryptophan catabolite alterations in psychiatric patients: comparisons between schizophrenia, bipolar disorder, and depression. *Schizophr. Bull.* 44, 75–83. doi:10.1093/schbul/sbx035

Williams, J. B., Kobak, K. A., Bech, P., Engelhardt, N., Evans, K., Lipsitz, J., et al. (2008). The GRID-HAMD: standardization of the Hamilton depression rating scale. *Int. Clin. Psychopharmacol.* 23, 120–129. doi:10.1097/YIC.0b013e3282f948f5

World Medical Association (2013). World Medical Association Declaration of Helsinki: ethical principles for medical research involving human subjects. *J. Am. Med. Assoc.* 310, 2191–2194. doi:10.1001/jama.2013.281053

Young, R. C., Biggs, J. T., Ziegler, V. E., and Meyer, D. A. (1978). A rating scale for mania: reliability, validity and sensitivity. *Br. J. Psychiatry* 133, 429–435. doi:10.1192/bjp.133.5.429

Conflict of Interest: The authors declare that the research was conducted in the absence of any commercial or financial relationships that could be construed as a potential conflict of interest.

Copyright © 2021 Hidese, Hattori, Sasayama, Tsumagari, Miyakawa, Matsumurra, Yokota, Ishida, Matsuo, Yoshida, Ota and Kunugi. This is an open-access article distributed under the terms of the Creative Commons Attribution License (CC BY). The use, distribution or reproduction in other forums is permitted, provided the original author(s) and the copyright owner(s) are credited and that the original publication in this journal is cited, in accordance with accepted academic practice. No use, distribution or reproduction is permitted which does not comply with these terms.

frontiers in Neuroscience

REVIEW
published: 09 February 2021
doi: 10.3389/fnins.2021.621501

The Complexity of the cGAS-STING Pathway in CNS Pathologies

Amelia L. Fryer, Amar Abdullah, Juliet M. Taylor and Peter J. Crack**

Neuropharmacology Laboratory, Department of Pharmacology and Therapeutics, University of Melbourne, Melbourne, VIC, Australia

Neuroinflammation driven by type-I interferons in the CNS is well established to exacerbate the progression of many CNS pathologies both acute and chronic. The role of adaptor protein Stimulator of Interferon Genes (STING) is increasingly appreciated to instigate type-I IFN-mediated neuroinflammation. As an upstream regulator of type-I IFNs, STING modulation presents a novel therapeutic opportunity to mediate inflammation in the CNS. This review will detail the current knowledge of protective and detrimental STING activity in acute and chronic CNS pathologies and the current therapeutic avenues being explored.

Keywords: STING, neuroinflammation, interferon, central nervous system, cGAS

OPEN ACCESS

Edited by:
Flavia Eugenia Saravia, Universidad de Buenos Aires, Argentina

Reviewed by:
Pavel Katsel, Icahn School of Medicine at Mount Sinai, United States
Anindya Bhattacharya, Janssen Research and Development (United States), United States

****Correspondence:***
Juliet M. Taylor
juliett@unimelb.edu.au
Peter J. Crack
pcrack@unimelb.edu.au

Specialty section:
This article was submitted to Neuropharmacology, a section of the journal Frontiers in Neuroscience

Received: *26 October 2020*
Accepted: *19 January 2021*
Published: *09 February 2021*

Citation:
Fryer AL, Abdullah A, Taylor JM and Crack PJ (2021) The Complexity of the cGAS-STING Pathway in CNS Pathologies. Front. Neurosci. 15:621501. doi: 10.3389/fnins.2021.621501

INTRODUCTION

Type-I interferons (IFNs) have been strongly implicated in the progression of neuroinflammation in a host of central nervous system (CNS) pathologies including Alzheimer's disease (Taylor et al., 2014; Minter et al., 2016; Roy et al., 2020), Parkinson's disease (Main et al., 2016; Qin et al., 2016), traumatic brain injury (Karve et al., 2016; Barrett et al., 2020) and amyotrophic lateral sclerosis (ALS) (Oakes et al., 2017; Shelkovnikova et al., 2019). However, the role of the type-I IFN upstream regulator, the stimulator of interferon genes (STING), in driving this response in the CNS remains largely unknown. Over the last 10 years, STING signalling has been identified as a therapeutic target in autoinflammatory disorders and cancer with its role in neuroinflammation being increasingly recognised. Therefore, a greater understanding of STING signalling in driving a neuroinflammatory response in the diseased brain may also uncover similar therapeutic potential in treating acute and chronic CNS pathologies.

TYPE-I INTERFERON SIGNALLING

The type-I IFN response is known to be a key in the innate immune response to viral infection. However, this response has also been associated with a potent inflammatory response in the absence of pathogen invasion. In the context of viral infection, pathogen-associated molecular patterns (PAMPs) are produced by the invading pathogen and bind to pattern recognition receptors (PRRs) including toll-like receptors (TLR) and cyclic GMP-AMP synthase (cGAS) on the surface of resident immune cells such as microglia and astrocytes in the CNS (Bowman et al., 2003; Olson and Miller, 2004; Jack et al., 2005). This elicits an array of innate anti-viral responses, notably the production of pleiotropic pro-inflammatory cytokines known collectively as the type-I IFNs (Koyama et al., 2008; Murira and Lamarre, 2016). PRRs on CNS immune cells are capable of mounting a similar pro-inflammatory response upon detection of endogenous damage-associated

molecular patterns (DAMP) released during injury and stress (Loane et al., 2014; Cox et al., 2015; Kumar, 2019).

Following binding to their cognate receptor, IFNAR (composed of the IFNAR1 and IFNAR2 subunits), the type-I IFNs signal through the Janus kinase (JAK)-signal transducer and activator of transcription (STAT) pathway to elicit an anti-viral, anti-proliferative and immunostimulatory response through interferon-stimulated gene (ISG) induction (Platanias, 2005; Schneider et al., 2014). This results in the secretion of proinflammatory cytokines and chemokines, including tumour necrosis factor-α (TNF-α), interleukin-6 (IL-6), interleukin-1β (IL-1β) and the type-I IFNs themselves (IFN-alpha [IFN-α] and IFN-beta [IFN-β]) (Lousberg et al., 2010).

THE cGAS-STING PATHWAY

A DNA sensor known as cGAS was recently shown to be critical in type-I IFN induction (Sun et al., 2013). cGAS detects circulating double-stranded DNA (dsDNA) in the cytosol and mounts a potent type-I IFN response through the adaptor protein STING (Sun et al., 2013; Zhang et al., 2013). Exogenous DNA introduced into the cells by invading pathogens is recognised as a PAMP by cGAS, activating STING, a transmembrane adaptor protein located on the endoplasmic reticulum and eliciting a potent type-I IFN response (Li et al., 2013; Watson et al., 2015). Endogenous DNA found outside of the nucleus, in the absence of pathogen invasion, is strongly immunogenic and prompts a pro-inflammatory response, termed sterile inflammation. Released from the nucleus and mitochondria, this DNA can be the result of cell death or genotoxic, mitochondrial or endoplasmic reticulum (ER) stress (Jahr et al., 2001; Kono and Rock, 2008; Petrasek et al., 2013; West et al., 2015; Motwani and Fitzgerald, 2017). This cytosolic DNA is recognised by cGAS as a DAMP and initiates the type-I IFN response through STING (Ishikawa and Barber, 2008; Ishikawa et al., 2009; Sun et al., 2013; Chen et al., 2016b). Once bound to dsDNA, cGAS facilitates the production of a cyclic dinucleotide, 2′5-cyclic adenosine monophosphate guanosine monophosphate (2′5′-cGAMP) from adenosine triphosphate (ATP) and guanosine triphosphate (GTP) (Ablasser et al., 2013); 2′5′-cGAMP is the endogenous agonist of STING, inducing STING phosphorylation and oligomerisation (Ablasser et al., 2013; Shang et al., 2019). Alternatively, STING can be activated by directly binding to bacterial cyclic dinucleotides (CDNs) (Burdette et al., 2011).

Once activated, the STING oligomer translocates to the Golgi apparatus where it recruits and phosphorylates kinases tank binding kinase 1 (TBK1) and IκB kinase (IKK), forming multimeric dimers at the cytosolic domain of STING (Tanaka and Chen, 2012; Liu et al., 2015; Haag et al., 2018; Zhang et al., 2019). Activated STING, TBK1 and IKK recruit and phosphorylate interferon regulatory factor 3 (IRF3) and nuclear factor kappa-light-chain-enhancer of activated B cells (NF-κB) at the C-terminal tail of STING (Tanaka and Chen, 2012; Abe and Barber, 2014; Liu et al., 2015). IRF3 once activated migrates to the nucleus, binds to IFN promoter regions and potently upregulates type-I IFN production (Liu et al., 2015). Following activation by TBK1 and IKK, NF-κB also translocates to the nucleus to upregulate the production of proinflammatory cytokines and chemokines including TNF-α, IL-1β and IL-6, all implicated in driving the neuroinflammatory response in the CNS (Barnes and Karin, 1997) (**Figure 1**).

STING ACTIVITY IN VIRAL INFECTIONS

Much of our knowledge of STING signalling in the brain originates from mouse models of viral infections. A protective role of STING signalling in mice has been reported following Herpes simplex virus (HSV) and West Nile virus (WNV) infection. Herpes simplex encephalitis (HSE) is a sporadic and fatal form of necrotising encephalitis caused by infection with herpes simplex virus 1 and 2 (Gnann and Whitley, 2017). STING knockout ($STING^{-/-}$) mice demonstrate a markedly increased susceptibility and lethality to HSV-1 infection (Ishikawa et al., 2009). Furthermore, increased HSV-1 viral loads have been detected in the brains of $STING^{-/-}$, STING loss of function ($STING^{gt/gt}$) and cGAS knockout ($cGAS^{-/-}$) mice compared to wild-type controls, indicating increased HSE susceptibility (Ishikawa et al., 2009; Reinert et al., 2016). Microglia were the primary producers of the type-I IFNs following HSV-1 infection, and this IFN production was found to be STING dependent (Reinert et al., 2016). STING-deficient mice also display increased morbidity and mortality following WNV infection compared to their wild-type counterparts (You et al., 2013; McGuckin Wuertz et al., 2019). Infection with WNV can progress to West Nile Neuroinvasive Disease (WNND) resulting in meningitis, encephalitis and Parkinsonian-like symptoms (Sejvar et al., 2003). Taken together, these results support a neuroprotective role of STING following HSV-1 and WNV infection.

STING ACTIVITY IN ACUTE CNS PATHOLOGIES

In direct contrast with acute viral infections, STING signalling has recently been shown to be a key instigator of the detrimental prolonged neuroinflammation that ensues following traumatic brain injury (TBI), subarachnoid haemorrhage (SAH) and hypoxia-ischemia (HI) (**Table 1**). Increased STING signalling was detected in post-mortem human TBI samples (Abdullah et al., 2018) and 24 and 72 h post-CNS injury in mice in a controlled cortical impact model of TBI (Abdullah et al., 2018; Barrett et al., 2020). Additionally, $STING^{-/-}$ mice showed a significantly smaller lesion size compared to wild-type mice suggesting that STING is a driver of TBI-induced neurodegeneration (Abdullah et al., 2018). Sen et al. (2020) identified a possible upstream activator of STING in TBI, a protein produced in response to endoplasmic reticulum stress known as protein kinase R-like ER kinase (PERK). As STING is localised on the endoplasmic reticulum in its resting state, this supports a connection between the ER stress response and STING. Significantly, the TBI-induced activation of STING was attenuated in mice administered a PERK inhibitor (GSK2656157), with reduced

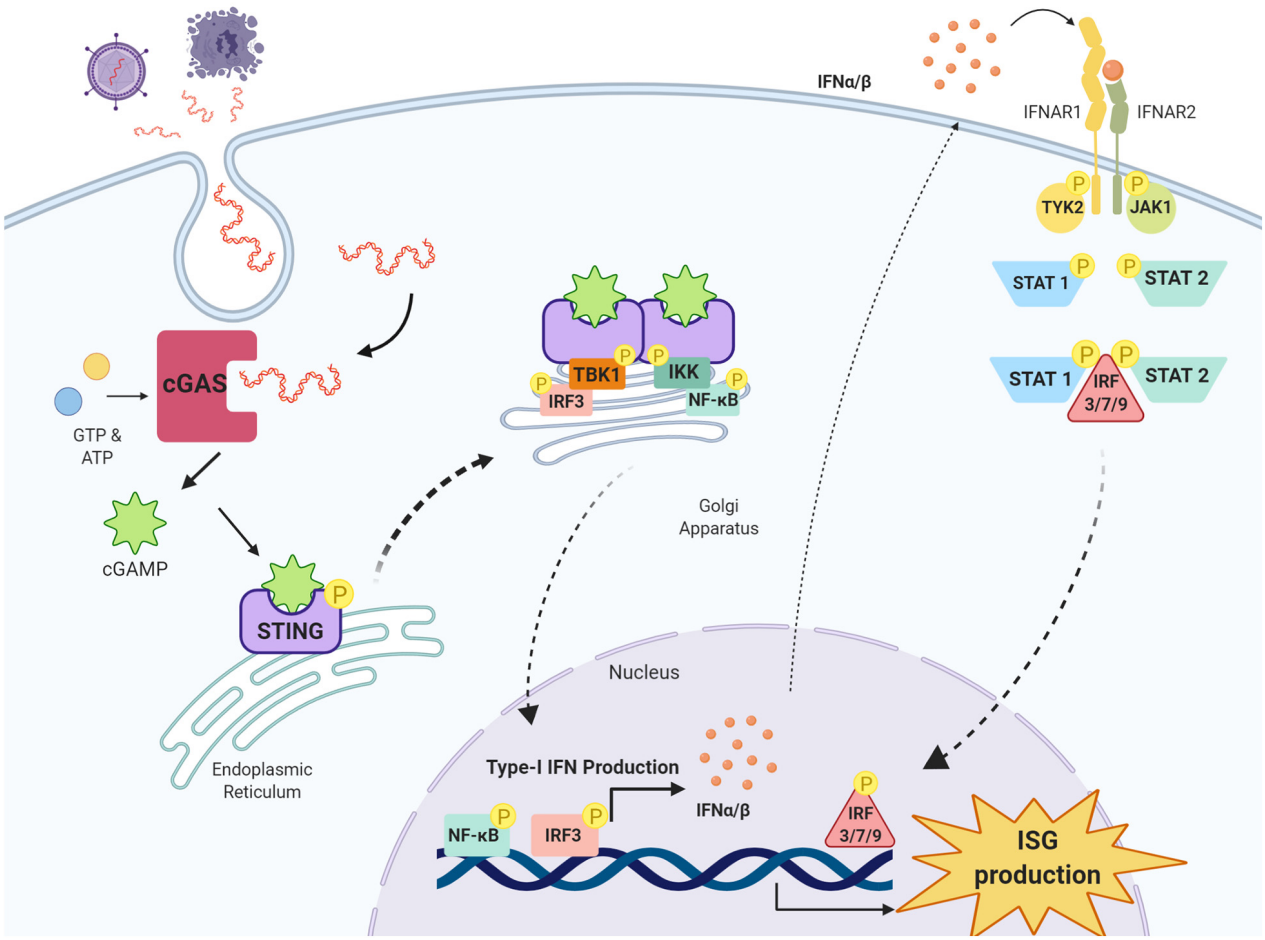

FIGURE 1 | cGAS-STING pathway and type-I IFN signaling. Double-stranded DNA (dsDNA) released from damaged cells or following pathogen infection is taken up cells into the cytosol where it is detected by the enzyme cyclic GMP-AMP synthase (cGAS) which synthesises the cyclic di-nucleotide 2′3′-cGAMP from GTP and ATP. 2′3′-cGAMP is detected by stimulator of interferon genes (STING) residing on the endoplasmic reticulum, and once activated, STING oligomerises and translocates to the Golgi apparatus where it recruits kinases tank binding kinase 1 (TBK1) and IκB kinase (IKK). TBK1 recruits and phosphorylates interferon regulatory factor 3 (IRF3) and IKK recruits and phosphorylates nuclear factor kappa-light-chain-enhancer of activated B cells (NF-κB). IRF3 and NF-κB translocate to the nucleus and upregulate the production of type-I IFNs, which through their receptors interferon alpha and beta receptor subunits 1 and 2 (IFNAR1 and IFNAR2) activate Janus kinase 1 (JAK1) and tyrosine kinase 2 (TYK2). JAK1 and TYK2 activate signal transducer and activator of transcription 1 and 2 (STAT1 and STAT2), which phosphorylate IRF3, IRF7 and IRF9 to stimulate the transcription of interferon stimulated genes (ISG) in the nucleus. Image created with BioRender.com.

lesion volume as well as improvements in anxiety and depression tests reported (Sen et al., 2020). SAH is a form of stroke often resulting from a ruptured aneurism or CNS injury (Tenny and Thorell, 2020). Recently, Peng et al. (2020) found increased STING and p-TBK1 protein expression 12 h post-injury in a mouse model of SAH. The administration of a STING agonist, CMA in SAH mice worsened the neuronal damage and neurobehavioral deficits when compared to vehicle-treated mice. In contrast, administration of a small-molecule STING inhibitor C-176 shortly after SAH modelling conferred neuroprotection by reducing brain oedema, neuronal damage and attenuated the upregulation of pro-inflammatory microglial markers including IL-1β, iNOS and caspase-1 (Peng et al., 2020). Upregulation of STING signalling has also been reported in rats 48–72 h after neonatal HI (Gamdzyk et al., 2020). Furthermore, silencing of STING signalling using siRNA was found to reduce infarct size and neurological impairments 48 h after HI. The significant reduction in TBI lesion size, HI infarct size and neuronal damage through both direct and indirect inhibition of STING signalling suggests a critical role of the STING signalling pathway in perpetuating neurodegeneration with potential therapeutic opportunities to treat acute CNS injuries such as TBI and stroke.

STING ACTIVITY IN CHRONIC CNS PATHOLOGIES

STING signalling has recently been associated with worsened disease progression in a number of chronic neurodegenerative disease models (**Table 2**). The ME7 prion disease model is a widely used mouse model for studying chronic

TABLE 1 | STING activity in acute CNS pathologies.

Pathology	Rodent models	Human	Genetic/pharmacological intervention	References
Traumatic brain injury (TBI)	Increased cortical mRNA and protein expression of STING 24 and 72 h post-TBI in mice	Increased STING mRNA expression reported in post-mortem brain tissue of TBI patients	Smaller TBI-induced lesion size measured in STING$^{-/-}$ mice Small-molecule inhibition of ER-stress protein PERK reduced white matter injury and improved mouse behavioural outcomes by attenuating STING dependent signalling	Abdullah et al., 2018; Barrett et al., 2020; Sen et al., 2020
Subarachnoid haemorrhage (SAH)	Increased STING and p-TBK1 protein expression 12–72 h post-injury in mice	N/A	Administration of small-molecule STING inhibitor C-176 in mice attenuated brain oedema, neuronal injury, and expression of microglial proinflammatory markers and improved neurobehavioral outcomes Administration of STING agonist CMA worsened neurobehavioral performance, exacerbated neuronal damage, and upregulated microglial proinflammatory markers in mice	Peng et al., 2020
Hypoxia-ischemia (HI)	STING upregulated in neonatal rats 24–48 h post-HI	N/A	Inhibition of STING signalling using siRNA attenuated the size of the infarct, neurodegeneration and neurological impairments in rats	Gamdzyk et al., 2020

TABLE 2 | STING activity in chronic CNS pathologies.

Pathology	Rodent models	Human	Genetic/pharmacological intervention	References
Parkinson's disease (PD)	STING pathway implicated in the onset of neuroinflammation, neurodegeneration and motor deficits in Parkin$^{-/-}$ mice	N/A	Genetic deletion of STING attenuates the loss of dopaminergic neurons and motor deficits seen in Parkin$^{-/-}$ mice	Sliter et al., 2018
Ataxia telangiectasia (AT)	STING drives type-I IFN induction in ATM$^{-/-}$ mice	N/A	Genetic deletion of STING reduced type-I IFN response caused by loss of ATM gene	Hartlova et al., 2015
Huntington's disease (HD)	Increased cGAS, p-TBK1 and p-STING expression found in Hdh$^{Q111/Q111}$ mice	Increased cGAS protein expression found in HD striatal neurons	N/A	Sharma et al., 2020
Multiple Sclerosis (MS)	STING-induced type-I IFN production attenuates EAE pathology Mice lacking functional STING display attenuated EAE development	cGAS and STING gene expression is downregulated in relapsed MS patients	Use of STING agonist c-di-GMP delayed disease onset and severity in EAE mouse model Activating STING using antiviral therapeutic ganciclovir was able to attenuate disease progression in EAE mice	Lemos et al., 2014; Mathur et al., 2017; Masanneck et al., 2020
Systemic lupus erythematosus (SLE)	Loss of STING accelerates mortality and disease progression in Lupus prone mice (MRL-Fas^{lpr})	ISG inducing activity of sera derived from SLE patients is STING dependent	N/A	Sharma et al., 2015; Kato et al., 2018
Amyotrophic lateral sclerosis (ALS)	Increased cGAS and cGAMP detected in the spinal cords of Prp-TDP-43$^{Tg/+}$ mice Genetic deletion of STING in Prp-TDP-43$^{Tg/+}$ mice increased average lifespan by 40%	Elevated levels of cGAMP detected in the spinal cords of ALS patients	Administration of small-molecule STING inhibitor H-151 reduced cortical and spinal cord proinflammatory cytokine gene expression and reduced neurodegeneration in ALS mice. Death of ALS patient iPSC -derived motor neurons was prevented following H-151 administration	Yu et al., 2020

neurodegeneration. Nazmi et al. (2019) confirmed STING is a critical driver of the type-I IFN mediated neurodegeneration in this model with mice deficient in STING or IFNAR1 displaying attenuated neuroinflammation (Nazmi et al., 2019). STING has also been reported to exacerbate the neuropathology of a mouse model of Parkinson's disease (PD). Mutations in *PARKIN*, a ubiquitin ligase, are the most common cause of early-onset PD and have been linked in mouse models to the inefficient removal or autophagy of dysfunctional mitochondria (Pickrell and Youle, 2015). In a model of PD, Parkin$^{-/-}$ mice lacking STING displayed attenuated neuroinflammation and neurodegeneration with improvements in motor function compared Parkin$^{-/-}$ mice (Sliter et al., 2018). This suggests an interplay between mitochondrial stress and STING signalling in PD. Specifically, the inefficient clearing of damaged mitochondria by parkin leads to increased circulating cytosolic mtDNA which when recognised by cGAS initiates the STING signalling cascade. Similarly, a detrimental role for STING in ataxia telangiectasia (AT), an autosomal recessive disorder caused by mutations in the ataxia-telangiectasia (*ATM*) gene, has been reported. AT is clinically characterised by cerebellar degeneration, telangiectasia and immunodeficiency (Amirifar et al., 2019). Mutations in the *ATM* gene in mice have been associated with the accumulation of DNA in the cytoplasm, leading to increased

type-I IFN production through a STING-mediated pathway (Hartlova et al., 2015). However, the implications of targeting this STING-mediated IFN production in terms of reducing the cerebellar degeneration and improving motor control in this mouse model are still unknown. Recently, Sharma et al. (2020) identified upregulated cGAS-STING signalling in Huntington's disease (HD). Increased cGAS protein expression was found in human HD striatal neurons and in neurons derived from $Hdh^{Q111/Q111}$ mice. Furthermore, increased expression of p-TBK1 and p-STING, downstream of cGAS was detected in the striatal neurons of the HD mice (Sharma et al., 2020). Increased mRNA levels of *Ccl5* and *Cxcl10* was found to be cGAS dependent in both human and mouse striatal HD tissue further implicating the cGAS-STING pathway in driving the neuroinflammatory response in HD (Sharma et al., 2020). A relationship between STING and TDP-43, a hallmark protein of ALS has recently been established with TDP-43 found to trigger mtDNA release into the cytoplasm, activating the cGAS-STING pathway (Yu et al., 2020). Increased cGAS and cGAMP, the STING activating molecule produced by cGAS was detected in spinal cords and in the cortex of ALS mice overexpressing TDP-43 (Prp-TDP-$43^{Tg/+}$). When STING was genetically deleted from these mice, the average lifespan increased by 40% and the mice exhibited improved rotarod performance compared to Prp-TDP-$43^{Tg/+}$ mice with intact STING (Yu et al., 2020). Furthermore, elevated levels of the STING activator cGAMP were detected in spinal cord samples from ALS patients (Yu et al., 2020). Together these findings implicate the cGAS-STING pathway in driving the damaging inflammatory processes present in ALS.

In contrast to other chronic neurodegenerative diseases, the type-I IFNs have been implicated in a neuroprotective role in Multiple Sclerosis (MS). Intramuscular IFN-β1 is used therapeutically in patients with relapsing and remitting MS to reduce the number and volume of brain lesions; however, its exact mechanism of action remains to be fully elucidated (Kieseier, 2011). More recently, a protective effect of STING activation has been reported in experimental autoimmune encephalitis (EAE), a mouse model of MS. The CDN STING activator c-di-GMP and DNA nanoparticles (DNPs) were able to delay EAE and reduce the overall disease severity (Lemos et al., 2014). A later study confirmed the therapeutic potential of activating STING in EAE mice using a clinically approved antiviral, ganciclovir (GCV), which has been previously shown to attenuate EAE pathology in mice. The study found that STING was required for GCV to elicit its neuroprotective and anti-inflammatory activity in EAE mice (Mathur et al., 2017). This is supported by a gene expression analysis of peripheral blood mononuclear cells from relapsing remitting MS patients and healthy donors. cGAS and STING gene expression was downregulated in relapsed MS patients compared to both patients in remission and healthy donors, further suggesting a neuroprotective role of cGAS-STING signalling in MS (Masanneck et al., 2020). Together these results support the therapeutic potential of upregulating STING mediated-type-I IFN production through the use of STING agonists as an adjunct to antivirals such as GCV used in MS. Although upregulating IFN production through STING shows promise in mouse models of MS, this same efficacy may not translate to humans. Long-term IFN-β therapy has been associated with the increased incidence of adverse CNS effects including depression and 'flu-like symptoms' such as fever, muscle aches and headaches, which have been noted as a major factor for MS patients to discontinue IFN-β therapy in addition to poorly perceived efficacy (Neilley et al., 1996; O'Rourke and Hutchinson, 2005; Fox et al., 2013).

The role of STING in systemic lupus erythematosus (SLE) is also less clear, with both detrimental and beneficial effects in the disease progression reported. SLE is an autoimmune disease that can present as neuropsychiatric lupus (NPSLE) in approximately 20% of cases causing a range of syndromes including aseptic meningitis, cerebrovascular disease, seizure disorders and cognitive dysfunction (Manson and Rahman, 2006). Lupus prone mice (MRL-Fas^{lpr}) lacking STING display an accelerated disease progression and mortality compared to lupus-prone mice (Sharma et al., 2015). However, a later study with apoptosis-derived vesicles (AdMVs) from the sera of patients with SLE identified dampened ISG induction in $STING^{-/-}$ reporter cells compared to parental cells when challenged with these AdMVs (Kato et al., 2018). This suggests that ISG induction in human SLE is amplified in the presence of STING. The contrasting roles of STING in promoting disease susceptibility and severity whilst amplifying the autoinflammatory response in SLE warrant further investigation. In addition, these studies failed to study the role STING may play in the CNS and lupus progression.

STING ACTIVITY IN THE AGEING BRAIN

Ageing is a major risk factor for the development of neurodegenerative diseases. Cell senescence is a hallmark feature of ageing as senescent cells perpetuate chronic low-level inflammation by adopting the senescence-associated secretory phenotype (SASP), resulting in the release of proinflammatory cytokines, chemokines, growth factors and extracellular matrix proteins (Coppé et al., 2010; McHugh and Gil, 2018). Increasing evidence has implicated cGAS-STING signalling in the chronic inflammation associated with age-induced cell senescence. Increased cytosolic DNA has been found in aged diploid fibroblasts when compared to younger cells (Lan et al., 2019). The inflammation observed in these cells was cGAS-STING dependent, suggesting aging triggers cGAS-STING mediated inflammation through the accumulation of cytosolic DNA (Lan et al., 2019). This idea was further supported using murine embryonic fibroblast cells, where genetic deletion of cGAS attenuated senesce processes in these cells (Glück et al., 2017). Furthermore, upregulation of proinflammatory markers IL-6 and CXCL-10 following irradiation *in vitro* and *in vivo* was found to be dependent on intact cGAS-STING signalling (Glück et al., 2017). Further supporting cGAS-STING signalling as a driver of age-induced inflammation, cells from AT and Hutchinson-Gilford progeria patients have been shown to have increased cytosolic DNA compared to healthy donor cells (Lan et al., 2019). AT and Hutchinson-Gilford

progeria are genetically inherited disorders characterised by premature ageing (Merideth et al., 2008; Rothblum-Oviatt et al., 2016). Together these findings implicate cGAS-STING signalling as a driver of detrimental chronic inflammation associated with ageing.

THERAPEUTIC POTENTIAL OF TARGETING STING

IFN-α and IFN-β are abundantly expressed and highly implicated in normal and pathological conditions (González-Navajas et al., 2012; Malireddi and Kanneganti, 2013; Cho and Kelsall, 2014). As a result, targeting type-I IFN signalling has shown to be promising in the treatment of infectious diseases, various cancers, and autoimmune diseases including multiple sclerosis, SLE and psoriasis (Di Domizio and Cao, 2013; Aricò et al., 2019). However, their therapeutic success in clinical trials have been variable and is severely limited due to side effects which include fever, cognitive dysfunction, depression and in some cases death. With mounting evidence implicating the cGAS-STING pathway in driving neuroinflammation in both acute and chronic neurological diseases, modulation of type-I IFN signalling by targeting cGAS-STING pathways represents a viable therapeutic in the treatment of CNS disorders.

The development of small-molecule agonists and antagonists to target STING signalling in mice and humans is a growing area of research (**Table 3**). Small-molecule agonists and CDN analogues are currently being developed, with several in phase I and II clinical trials for use against viral infections such as human papillomavirus (HPV) and in cancer immunotherapy with a focus on solid tumours (**Figure 2**) (Feng et al., 2020; Zhang et al., 2020). The use of bacterial and synthetic CDNs such as c-di-GMP and 3′3′cGMP as vaccine adjuvants have displayed promising anti-tumour activity in mouse models of metastatic breast cancer, melanoma and colon carcinoma (Chandra et al., 2014; Fu et al., 2015). STING activating nanoparticles is an increasingly active area of research in treating solid tumours as nanoparticles may be able to overcome the translational challenges of using CDNs, which include their negative charge and susceptibility to being rapidly enzymatically degraded (Wilson et al., 2018; Luo et al., 2019; Su et al., 2019).

Currently, there is limited research on the use of STING agonists and antagonists in the CNS. Nonetheless, STING activation in astrocytes has been reported to promote the growth of brain metastatic cancer cells in mice (Chen et al., 2016a). This study found that brain metastatic cells co-cultured with astrocytes transported cGAMP into the neighbouring astrocytes via *Cx43* gap junctions to activate STING. Astrocytic production of IFN-α and TNF-α was correlated with the inhibition of apoptosis in the metastatic brain cells when exposed to chemotherapy, suggesting that STING activation in astrocytes promotes survival of brain metastatic cancer cells in mice (Chen et al., 2016a). Further studies elucidating the impact of STING activation and the development of brain cancers will be required to assess the suitability of STING agonists for the treatment of these CNS pathologies.

STING inhibitors in the form of competitive antagonists and covalent inhibitors have also been developed to treat autoinflammatory conditions such as Aicardi Goutières syndrome (AGS) and STING-associated vasculopathy with onset in infancy (SAVI) (Haag et al., 2018; Hansen et al., 2018). These compounds are nitrofuran and nitro-fatty acid derivatives and have shown promising results in reducing serum type-I IFN concentrations in a $Trex1^{-/-}$ mouse model of AGS and SAVI patient-derived fibroblasts (Haag et al., 2018; Hansen et al., 2018). C-176 was shown by Haag et al. (2018) to ablate STING activity through the blockade of activation-induced palmitoylation, impeding STING's ability to translocate to the Golgi in response to CDN binding. Administration of C-176 intraperitoneally in SAH induced mice has also been shown to improve neurobehavioural outcomes and reduced the expression pro-inflammatory microglial markers including IL-1β, TNF-α and IL-6 (Peng et al., 2020). Peng et al. (2020) reported that inhibition of adenosine monophosphate-activated protein kinase (AMPK), a regulator of cellular energy homoeostasis (Hardie, 2011) reversed the anti-inflammatory activity of C-176 *in vitro* and *in vivo*, suggesting that AMPK has a role in the inhibition of STING through C-176.

Gain of function mutations in the STING gene, *TMEM173*, is associated with autoinflammatory disorders including familial chilblain lupus and STING-associated vasculopathy with onset in infancy (SAVI). A heterozygous mutation in *TMEM173* has been linked to familial chilblain lupus, a rare autoinflammatory pathology characterised by early onset arthralgia and lymphopenia (König et al., 2017). This gain of function mutation enhanced the ability of STING to dimerise in the absence of cGAMP, resulting in constitutive IFN activation (König et al., 2017); *de novo* germline mutations in STING have been identified in SAVI patients, causing a hypersensitivity to ligand activation in STING, resulting in constitutive production of type-I IFNs (Liu et al., 2014). This mutation manifested clinically in the onset of systemic inflammation, acral necrosis and interstitial lung in infants and children (Liu et al., 2014).

Multiple STING allele variants have been detected in the human population, with one variant *R293Q*, known to impair the function of STING (Patel and Jin, 2019). A multicentre study carried out in Polish Caucasians over 65 years of age, found individuals carrying the *R293Q* STING allele were less susceptible to age-related chronic lung disease due to the lowered immune sensitivity associated with the dysfunctional STING (Hamann et al., 2019). Given that mutations in the STING gene correlate with disease prognosis, genetic screening for STING mutants may serve as potential biomarker in diseases linked to impaired STING function. In addition, changes in expression levels of molecules downstream in the STING pathway have also been associated with various diseases. Exome sequencing has identified TBK1 as a risk factor in ALS and fronto-temporal dementia with mutations in the human TBK1 gene implicated in neuroinflammatory disorders (Cirulli et al., 2015; Ahmad et al., 2016; Wilke et al., 2017). Unregulated levels of IRF3 and the type-IFNs have been implicated in tumorigenesis and progression of autoimmune disorders including rheumatoid arthritis (RA), SLE and primary Sjogren's syndrome (Gottenberg et al., 2006;

TABLE 3 | STING modulators.

Compound	Affinity	Disease model	Disease outcome	References
STING activator CDNs	mSTING; Kd~110 nM, hSTING; ~4.59 nM	Viral infection^{+}; Cancer^{+}; EAE^{+}	Protective against viral infections; shows anti-tumour activity in mouse models of various cancers; delays EAE and reduce the overall disease severity	Burdette et al., 2011; Chandra et al., 2014; Lemos et al., 2014; Li et al., 2014
STING activator DMXAA	mSTING; Kd~130 nM	Cancer^{+}	Shows potent anti-tumour activity in mouse models of lung cancer and mesothelioma	Conlon et al., 2013; Kim et al., 2013
STING activator CMA	mSTING; Kd:3.5 μM	SAH^{-}	Exacerbates neuronal damage and neurobehavioral deficits in a mouse model of SAH	Zhang et al., 2015; Peng et al., 2020
STING activator GCV	m/hSTING; Kd:N/A	EAE^{+}; Viral infection^{+}	Attenuates EAE pathology in mice; protective against cytomegalovirus infections	Mathur et al., 2017
STING inhibitor GSK2656157	N/A	TBI^{+}	Reduces lesion volume and improves neurobehavioral outcome	Sen et al., 2020
STING inhibitor C-176	mSTING; IC_{50} < 50 nM	AGS^{+}; SAH^{+}	Ameliorates STING associated-inflammation in AGS mouse model; reduces brain oedema, neuronal damage and neuroinflammatory response in SAH mouse model	Haag et al., 2018; Peng et al., 2020

Kd (dissociation constant) indicates the affinity of STING binding to the compound ligand.
Half-maximal inhibitory concentration (IC_{50}) is the concentration of an inhibitor where the response (or binding) is reduced by half.
$^{(+)}$ denotes beneficial and $^{(-)}$ denotes detrimental effects of STING compound in disease outcome.
mSTING, mouse STNG; hSTING, human STING.

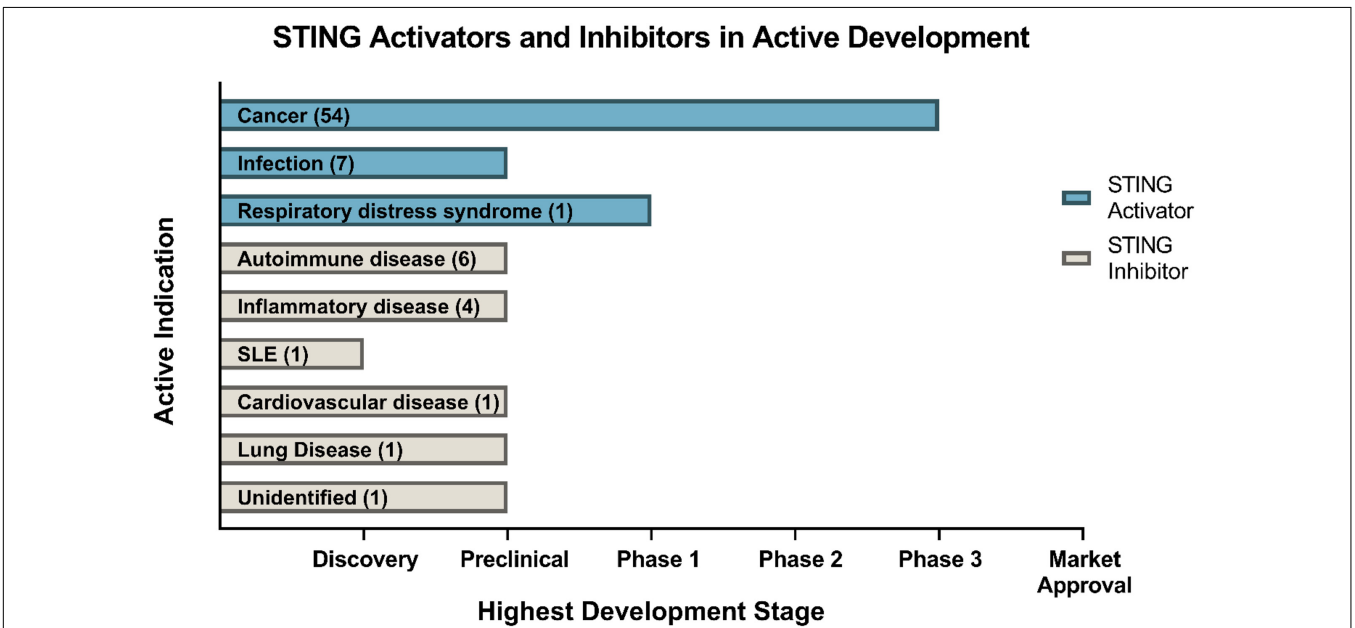

FIGURE 2 | Drugs targeting STING currently in development. Data obtained through Cortellis search (Clarivate Analytics). Data correct as of December 2020.

Crow, 2014; Muvaffak et al., 2014; Jiao et al., 2018; Barrat et al., 2019; Petro, 2020). Together these results implicate genetic alterations in STING and its downstream mediators in the progression of autoinflammatory disorders and highlight the importance of genetic characterisation of STING to gain a deeper insight into the mechanisms of STING dysregulation in neurodegeneration.

Key challenges in targeting STING include the high heterogeneity of STING in the human population and the differences in structure and signalling between mouse and human STING. There are multiple alleles present for the gene that encodes STING (*TMEM173*) and these alleles have been found to exhibit a high degree of population stratification (Patel et al., 2017). Markedly different *TMEM173* genotypes have been detected in different ethnic groups and differential STING protein expression has been found in cells of these different genotypes (Patel et al., 2017). Further characterisation of the variants of STING present in different populations is required to ensure the accurate development of STING compounds. The structural difference in mice (mSTING) and humans (hSTING) is also a challenge in STING targeted therapies and has been attributed to the clinical failure of the small-molecule STING activator DMXAA. This initially displayed promising anti-tumour capability in mice but failed to translate

to human studies due to the compound's inability to bind to hSTING (Conlon et al., 2013). This highlights the importance of developing animal and cell culture models that can accurately mimic the activity of hSTING with the binding capabilities of the compound with hSTING tested. The use of rats instead of mice has also been proposed to be a more accurate model to study compounds targeting STING as rat STING (rSTING) has been found to mimic the substrate binding properties of hSTING more so than mSTING (Zhang et al., 2015). Moreover, the double-edge sword of the immune system in suppressing and promoting tumour growth poses a challenge in targeting STING as a cancer therapy. Prolonged activation of STING can result in a tolerogenic immune response, chronic neuroinflammation, increased tumour growth and impaired T-lymphocyte function all of which are detrimental in cancer treatment (Huang et al., 2013; Ahn et al., 2014; Larkin et al., 2017; Lemos et al., 2020). Conversely, prolonged suppression of the neuroinflammatory response by STING inhibition may be detrimental in the treatment of diseases that require an acute, beneficial initial neuroinflammatory response as seen in spinal cord injury, stroke, and traumatic brain injury (DiSabato et al., 2016; Simon et al., 2017; Shields et al., 2020). Given the multifaceted role of STING and the magnitude of STING signalling pathways still remains to be determined, caution should be taken in the development and application of STING modulators. The optimal therapeutic window for STING activation and inhibition will be essential in allowing STING modulators to exert their protective effects whilst minimising toxicity in any disease treatment.

CONCLUSION

Recent studies on STING signalling in the brain have increased our understanding of the role of this pathway in neural innate immunity and inflammation-mediated neurodegeneration. STING activation occurs in response to a wide array of stressors, from viral infection to ER and mitochondrial stress, suggesting it is a major player in a number of neuropathologies. With both beneficial and detrimental effects of STING reported, it appears there will be complexity in targeting this pathway. However, with multiple small-molecule agonists and antagonists of STING emerging and the critical validation of findings from mouse models in humans, we are gaining an increased understanding of the therapeutic potential of targeting STING in specific CNS disorders.

AUTHOR CONTRIBUTIONS

ALF, AA, JMT, and PJC contributed to the writing of this manuscript. All authors contributed to the article and approved the submitted version.

FUNDING

NHMRC project grant funding to JMT and PJC.

REFERENCES

Abdullah, A., Zhang, M., Frugier, T., Bedoui, S., Taylor, J. M., and Crack, P. J. (2018). STING-mediated type-I interferons contribute to the neuroinflammatory process and detrimental effects following traumatic brain injury. *Neuroinflamm. J.* 15:17. doi: 10.1186/s12974-018-1354-7

Abe, T., and Barber, G. N. (2014). Cytosolic-DNA-mediated, STING-dependent proinflammatory gene induction necessitates canonical NF-kappaB activation through TBK1. *J. Virol.* 88, 5328–5341. doi: 10.1128/JVI.00037-14

Ablasser, A., Goldeck, M., Caviar, T., Deimling, T., Witte, G., Rohl, I., et al. (2013). cGAS produces a 2′-5′-linked cyclic dinucleotide second messenger that activates STING. *Nature* 498, 380–384. doi: 10.1038/naturel2306

Ahmad, L., Zhang, S. Y., Casanova, J. L., and Sancho-Shimizu, V. (2016). Human TBK1: a gatekeeper of neuroinflammation. *Trends Mol. Med.* 22, 511–527. doi: 10.1016/j.molmed.2016.04.006

Ahn, J., Xia, T., Konno, H., Konno, K., Ruiz, P., and Barber, G. N. (2014). Inflammation-driven carcinogenesis is mediated through STING. *Nat. Commun.* 5:5166. doi: 10.1038/ncomms6166

Amirifar, P., Ranjouri, M. R., Yazdani, R., Abolhassani, H., and Aghamohammadi, A. (2019). Ataxia-telangiectasia: a review of clinical features and molecular pathology. *Pediatr. Allergy Immunol.* 30, 277–288. doi: 10.1111/pai.13020

Aricò, E., Castiello, L., Capone, I., Gabriele, L., and Belardelli, F. (2019). Type I interferons and cancer: an evolving story demanding novel clinical applications. *Cancers* 11:1943. doi: 10.3390/cancers11121943

Barnes, P. J., and Karin, M. (1997). Nuclear factor-kappaB: a pivotal transcription factor in chronic inflammatory diseases. *N. Engl. J. Med.* 336, 1066–1071. doi: 10.1056/NEJM199704103361506

Barrat, F. J., Crow, M. K., and Ivashkiv, L. B. (2019). Interferon target-gene expression and epigenomic signatures in health and disease. *Nat. Immunol.* 20, 1574–1583. doi: 10.1038/s41590-019-0466-2

Barrett, J. P., Henry, R. J., Shirey, K. A., Doran, S. J., Makarevich, O. D., Ritzel, R. M., et al. (2020). Interferon-beta plays a detrimental role in experimental traumatic brain injury by enhancing neuroinflammation that drives chronic neurodegeneration. *J. Neurosci.* 40, 2357–2370. doi: 10.1523/JNEUROSCI.2516-19.2020

Bowman, C. C., Rasley, A., Tranguch, S. L., and Marriott, I. (2003). Cultured astrocytes express toll-like receptors for bacterial products. *Glia* 43, 281–291. doi: 10.1002/glia.10256

Burdette, D. L., Monroe, K. M., Sotelo-Troha, K., Iwig, J. S., Eckert, B., Hyodo, M., et al. (2011). STING is a direct innate immune sensor of cyclic di-GMP. *Nature* 478, 515–518. doi: 10.1038/nature10429

Chandra, D., Quispe-Tintaya, W., Jahangir, A., Asafu-Adjei, D., Ramos, I., Sintim, H. O., et al. (2014). STING ligand c-di-GMP improves cancer vaccination against metastatic breast cancer. *Cancer Immunol. Res.* 2, 901–910. doi: 10.1158/2326-6066.CIR-13-0123

Chen, Q., Boire, A., Jin, X., Valiente, M., Er, E. E., Lopez-Soto, A., et al. (2016a). Carcinoma-astrocyte gap junctions promote brain metastasis by cGAMP transfer. *Nature* 533, 493–498. doi: 10.1038/nature18268

Chen, Q., Sun, L., and Chen, Z. J. (2016b). Regulation and function of the cGAS-STING pathway of cytosolic DNA sensing. *Nat. Immunol.* 17, 1142–1149. doi: 10.1038/ni.3558

Cho, H., and Kelsall, B. L. (2014). The role of type I interferons in intestinal infection, homeostasis, and inflammation. *Immunol. Rev.* 260, 145–167.

Cirulli, E. T., Lasseigne, B. N., Petrovski, S., Sapp, P. C., Dion, P. A., Leblond, C. S., et al. (2015). Exome sequencing in amyotrophic lateral sclerosis identifies risk genes and pathways. *Science* 347, 1436–1441. doi: 10.1126/science.aaa3650

Conlon, J., Burdette, D. L., Sharma, S., Bhat, N., Thompson, M., Jiang, Z., et al. (2013). Mouse, but not human STING, binds and signals in response to the vascular disrupting agent 5,6-dimethylxanthenone-4-acetic acid. *J. Immunol.* 190, 5216–5225. doi: 10.4049/jimmunol.1300097

Coppé, J.-P., Desprez, P.-Y., Krtolica, A., and Campisi, J. (2010). The senescence-associated secretory phenotype: the dark side of tumor suppression. *Annu. Rev. Pathol.* 5, 99–118. doi: 10.1146/annurev-pathol-121808-102144

Cox, D. J., Field, R. H., Williams, D. G., Baran, M., Bowie, A. G., Cunningham, C., et al. (2015). DNA sensors are expressed in astrocytes and microglia in vitro and are upregulated during gliosis in neurodegenerative disease. *Glia* 63, 812–825. doi: 10.1002/glia.22786

Crow, M. K. (2014). Type I interferon in the pathogenesis of lupus. *J. Immunol.* 192, 5459–5468. doi: 10.4049/jimmunol.1002795

Di Domizio, J., and Cao, W. (2013). Fueling autoimmunity: type I interferon in autoimmune diseases. *Expert Rev. Clin. Immunol.* 9, 201–210. doi: 10.1586/eci.12.106

DiSabato, D. J., Quan, N., and Godbout, J. P. (2016). Neuroinflammation: the devil is in the details. *J. Neurochem.* 139(Suppl. 2), 136–153. doi: 10.1111/jnc.13607

Feng, X., Liu, D., Li, Z., and Bian, J. (2020). Bioactive modulators targeting STING adaptor in cGAS-STING pathway. *Drug Discov. Today* 25, 230–237. doi: 10.1016/j.drudis.2019.11.007

Fox, R. J., Salter, A. R., Tyry, T., Sun, J., You, X., Laforet, G., et al. (2013). Treatment discontinuation and disease progression with injectable disease-modifying therapies: findings from the north american research committee on multiple sclerosis database. *Int. J. MS Care* 15, 194–201. doi: 10.7224/1537-2073.2012-034

Fu, J., Kanne, D. B., Leong, M., Glickman, L. H., McWhirter, S. M., Lemmens, E., et al. (2015). STING agonist formulated cancer vaccines can cure established tumors resistant to PD-1 blockade. *Sci. Transl. Med.* 7:283ra52. doi: 10.1126/scitranslmed.aaa4306

Gamdzyk, M., Doycheva, D. M., Araujo, C., Ocak, U., Luo, Y., Tang, J., et al. (2020). cGAS/STING pathway activation contributes to delayed neurodegeneration in neonatal hypoxia-ischemia rat model: possible involvement of LINE-1. *Mol. Neurobiol.* 57, 2600–2619. doi: 10.1007/s12035-020-01904-7

Glück, S., Guey, B., Gulen, M. F., Wolter, K., Kang, T.-W., Schmacke, N. A., et al. (2017). Innate immune sensing of cytosolic chromatin fragments through cGAS promotes senescence. *Nat. Cell Biol.* 19, 1061–1070. doi: 10.1038/ncb3586

Gnann, J. W. Jr., and Whitley, R. J. (2017). Herpes simplex encephalitis: an update. *Curr. Infect. Dis. Rep.* 19:13. doi: 10.1007/s11908-017-0568-7

González-Navajas, J. M., Lee, J., David, M., and Raz, E. (2012). Immunomodulatory functions of type I interferons. *Nat. Rev. Immunol.* 12, 125–135.

Gottenberg, J.-E., Cagnard, N., Lucchesi, C., Letourneur, F., Mistou, S., Lazure, T., et al. (2006). Activation of IFN pathways and plasmacytoid dendritic cell recruitment in target organs of primary Sjögren's syndrome. *Proc. Natl. Acad. Sci. U.S.A.* 103, 2770–2775. doi: 10.1073/pnas.0510837103

Haag, S. M., Gulen, M. F., Reymond, L., Gibelin, A., Abrami, L., Decout, A., et al. (2018). Targeting STING with covalent small-molecule inhibitors. *Nature* 559, 269–273. doi: 10.1038/s41586-018-0287-8

Hamann, L., Ruiz-Moreno, J. S., Szwed, M., Mossakowska, M., Lundvall, L., Schumann, R. R., et al. (2019). STING SNP R293Q is associated with a decreased risk of aging-related diseases. *Gerontology* 65, 145–154. doi: 10.1159/000492972

Hansen, A. L., Buchan, G. J., Ruhl, M., Mukai, K., Salvatore, S. R., Ogawa, E., et al. (2018). Nitro-fatty acids are formed in response to virus infection and are potent inhibitors of STING palmitoylation and signaling. *Proc. Natl. Acad. Sci. U.S.A.* 115, E7768–E7775. doi: 10.1073/pnas.1806239115

Hardie, D. G. (2011). AMP-activated protein kinase: an energy sensor that regulates all aspects of cell function. *Genes Dev.* 25, 1895–1908. doi: 10.1101/gad.17420111

Hartlova, A., Erttmann, S. F., Raffi, F. A., Schmalz, A. M., Resch, U., Anugula, S., et al. (2015). DNA damage primes the type I interferon system via the cytosolic DNA sensor STING to promote anti-microbial innate immunity. *Immunity* 42, 332–343. doi: 10.1016/j.immuni.2015.01.012

Huang, L., Li, L., Lemos, H., Chandler, P. R., Pacholczyk, G., Baban, B., et al. (2013). Cutting edge: DNA sensing via the STING adaptor in myeloid dendritic cells induces potent tolerogenic responses. *J. Immunol.* 191, 3509–3513. doi: 10.4049/jimmunol.1301419

Ishikawa, H., and Barber, G. N. (2008). STING is an endoplasmic reticulum adaptor that facilitates innate immune signalling. *Nature* 455, 674–678. doi: 10.1038/nature07317

Ishikawa, H., Ma, Z., and Barber, G. N. (2009). STING regulates intracellular DNA-mediated, type I interferon-dependent innate immunity. *Nature* 461, 788–792. doi: 10.1038/nature08476

Jack, C. S., Arbour, N., Manusow, J., Montgrain, V., Blain, M., McCrea, E., et al. (2005). TLR signaling tailors innate immune responses in human microglia and astrocytes. *J. Immunol.* 175, 4320–4330. doi: 10.4049/jimmunol.175.7.4320

Jahr, S., Hentze, H., Englisch, S., Hardt, D., Fackelmayer, F. O., Hesch, R. D., et al. (2001). DNA fragments in the blood plasma of cancer patients: quantitations and evidence for their origin from apoptotic and necrotic cells. *Cancer Res.* 61, 1659–1665.

Jiao, S., Guan, J., Chen, M., Wang, W., Li, C., Wang, Y., et al. (2018). Targeting IRF3 as a YAP agonist therapy against gastric cancer. *J. Exp. Med.* 215, 699–718. doi: 10.1084/jem.20171116

Karve, I. P., Zhang, M., Habgood, M., Frugier, T., Brody, K. M., Sashindranath, M., et al. (2016). Ablation of Type-1 IFN signaling in hematopoietic cells confers protection following traumatic brain injury. *eNeuro* 3:ENEURO.128-ENEURO.115. doi: 10.1523/ENEURO.0128-15.2016

Kato, Y., Park, J., Takamatsu, H., Konaka, H., Aoki, W., Aburaya, S., et al. (2018). Apoptosis-derived membrane vesicles drive the cGAS-STING pathway and enhance type I IFN production in systemic lupus erythematosus. *Ann. Rheum. Dis.* 77, 1507–1515. doi: 10.1136/annrheumdis-2018-212988

Kieseier, B. C. (2011). The mechanism of action of interferon-beta in relapsing multiple sclerosis. *CNS Drugs* 25, 491–502. doi: 10.2165/11591110-000000000-00000

Kim, S., Li, L., Maliga, Z., Yin, Q., Wu, H., and Mitchison, T. J. (2013). Anticancer flavonoids are mouse-selective STING agonists. *ACS Chem. Biol.* 8, 1396–1401. doi: 10.1021/cb400264n

König, N., Fiehn, C., Wolf, C., Schuster, M., Cura Costa, E., Tüngler, V., et al. (2017). Familial chilblain lupus due to a gain-of-function mutation in STING. *Ann. Rheum. Dis.* 76, 468–472. doi: 10.1136/annrheumdis-2016-209841

Kono, H., and Rock, K. L. (2008). How dying cells alert the immune system to danger. *Nat. Rev. Immunol.* 8, 279–289. doi: 10.1038/nri2215

Koyama, S., Ishii, K. J., Coban, C., and Akira, S. (2008). Innate immune response to viral infection. *Cytokine* 43, 336–341. doi: 10.1016/j.cyto.2008.07.009

Kumar, V. (2019). Toll-like receptors in the pathogenesis of neuroinflammation. *J. Neuroimmunol.* 332, 16–30. doi: 10.1016/j.jneuroim.2019.03.012

Lan, Y. Y., Heather, J. M., Eisenhaure, T., Garris, C. S., Lieb, D., Raychowdhury, R., et al. (2019). Extranuclear DNA accumulates in aged cells and contributes to senescence and inflammation. *Aging Cell* 18:e12901. doi: 10.1111/acel.12901

Larkin, B., Ilyukha, V., Sorokin, M., Buzdin, A., Vannier, E., and Poltorak, A. (2017). Cutting edge: activation of STING in T cells induces type I IFN responses and cell death. *J. Immunol.* 199, 397–402. doi: 10.4049/jimmunol.1601999

Lemos, H., Huang, L., Chandler, P. R., Mohamed, E., Souza, G. R., Li, L., et al. (2014). Activation of the STING adaptor attenuates experimental autoimmune encephalitis. *J. Immunol.* 192, 5571–5578. doi: 10.4049/jimmunol.1303258

Lemos, H., Ou, R., McCardle, C., Lin, Y., Calver, J., Minett, J., et al. (2020). Overcoming resistance to STING agonist therapy to incite durable protective antitumor immunity. *J. Immunother. Cancer* 8:e001182. doi: 10.1136/jitc-2020-001182

Li, L., Yin, Q., Kuss, P., Maliga, Z., Millán, J. L., Wu, H., et al. (2014). Hydrolysis of 2′3′-cGAMP by ENPP1 and design of nonhydrolyzable analogs. *Nat. Chem. Biol.* 10, 1043–1048. doi: 10.1038/nchembio.1661

Li, X. D., Wu, J., Gao, D., Wang, H., Sun, L., and Chen, Z. J. (2013). Pivotal roles of cGAS-cGAMP signaling in antiviral defense and immune adjuvant effects. *Science* 341, 1390–1394. doi: 10.1126/science.1244040

Liu, S., Cai, X., Wu, J., Cong, Q., Chen, X., Li, T., et al. (2015). Phosphorylation of innate immune adaptor proteins MAVS, STING, and TRIF induces IRF3 activation. *Science* 347:aaa2630. doi: 10.1126/science.aaa2630

Liu, Y., Jesus, A. A., Marrero, B., Yang, D., Ramsey, S. E., Montealegre Sanchez, G. A., et al. (2014). Activated STING in a vascular and pulmonary syndrome. *N. Engl. J. Med.* 371, 507–518. doi: 10.1056/nejmoa1312625

Loane, D. J., Kumar, A., Stoica, B. A., Cabatbat, R., and Faden, A. I. (2014). Progressive neurodegeneration after experimental brain trauma: association with chronic microglial activation. *J. Neuropathol. Exp. Neurol.* 73, 14–29. doi: 10.1097/NEN.0000000000000021

Lousberg, E. L., Fraser, C. K., Tovey, M. G., Diener, K. R., and Hayball, J. D. (2010). Type I interferons mediate the innate cytokine response to recombinant

fowlpox virus but not the induction of plasmacytoid dendritic cell-dependent adaptive immunity. *J. Virol.* 84, 6549–6563. doi: 10.1128/JVI.02618-09

Luo, M., Liu, Z., Zhang, X., Han, C., Samandi, L. Z., Dong, C., et al. (2019). Synergistic STING activation by PC7A nanovaccine and ionizing radiation improves cancer immunotherapy. *J. Control. Release* 300, 154–160. doi: 10.1016/j.jconrel.2019.02.036

Main, B. S., Zhang, M., Brody, K. M., Ayton, S., Frugier, T., Steer, D., et al. (2016). Type-1 interferons contribute to the neuroinflammatory response and disease progression of the MPTP mouse model of Parkinson's disease. *Glia* 64, 1590–1604. doi: 10.1002/glia.23028

Malireddi, R. K., and Kanneganti, T. D. (2013). Role of type I interferons in inflammasome activation, cell death, and disease during microbial infection. *Front. Cell. Infect. Microbiol.* 3:77. doi: 10.3389/fcimb.2013.00077

Manson, J. J., and Rahman, A. (2006). Systemic lupus erythematosus. *Orphanet J. Rare Dis.* 1:6. doi: 10.1186/1750-1172-1-6

Masanneck, L., Eichler, S., Vogelsang, A., Korsen, M., Wiendl, H., Budde, T., et al. (2020). The STING-IFN-beta-Dependent axis is markedly low in patients with relapsing-remitting multiple sclerosis. *Int. J. Mol. Sci.* 21:9249. doi: 10.3390/ijms21239249

Mathur, V., Burai, R., Vest, R. T., Bonanno, L. N., Lehallier, B., Zardeneta, M. E., et al. (2017). Activation of the STING-dependent type I interferon response reduces microglial reactivity and neuroinflammation. *Neuron* 96, 1290–1302.

McGuckin Wuertz, K., Treuting, P. M., Hemann, E. A., Esser-Nobis, K., Snyder, A. G., Graham, J. B., et al. (2019). STING is required for host defense against neuropathological West Nile virus infection. *PLoS Pathog.* 15:e1007899. doi: 10.1371/journal.ppat.1007899

McHugh, D., and Gil, J. (2018). Senescence and aging: causes, consequences, and therapeutic avenues. *J. Cell Biol.* 217, 65–77. doi: 10.1083/jcb.201708092

Merideth, M. A., Gordon, L. B., Clauss, S., Sachdev, V., Smith, A. C. M., Perry, M. B., et al. (2008). Phenotype and course of hutchinson–gilford progeria syndrome. *N. Engl. J. Med.* 358, 592–604. doi: 10.1056/nejmoa0706898

Minter, M. R., Moore, Z., Zhang, M., Brody, K. M., Jones, N. C., Shultz, S. R., et al. (2016). Deletion of the type-1 interferon receptor in APPSWE/PS1DeltaE9 mice preserves cognitive function and alters glial phenotype. *Acta Neuropathol. Commun.* 4, 016–0341.

Motwani, M., and Fitzgerald, K. A. (2017). cGAS micro-manages genotoxic stress. *Immunity* 47, 616–617. doi: 10.1016/j.immuni.2017.09.020

Murira, A., and Lamarre, A. (2016). Type-I interferon responses: from friend to foe in the battle against chronic viral infection. *Front. Immunol.* 7:609. doi: 10.3389/fimmu.2016.00609

Muvaffak, A., Pan, Q., Yan, H., Fernandez, R., Lim, J., Dolinski, B., et al. (2014). Evaluating TBK1 as a therapeutic target in cancers with activated IRF3. *Mol. Cancer Res.* 12, 1055–1066. doi: 10.1158/1541-7786.Mcr-13-0642

Nazmi, A., Field, R. H., Griffin, E. W., Haugh, O., Hennessy, E., Cox, D., et al. (2019). Chronic neurodegeneration induces type I interferon synthesis via STING, shaping microglial phenotype and accelerating disease progression. *Glia* 67, 1254–1276.

Neilley, L. K., Goodin, D. S., Goodkin, D. E., and Hauser, S. L. (1996). Side effect profile of interferon beta-1b in MS: results of an open label trial. *Neurology* 46, 552–554. doi: 10.1212/wnl.46.2.552

Oakes, J. A., Davies, M. C., and Collins, M. O. (2017). TBK1: a new player in ALS linking autophagy and neuroinflammation. *Mol. Brain* 10:5. doi: 10.1186/s13041-017-0287-x

Olson, J. K., and Miller, S. D. (2004). Microglia initiate central nervous system innate and adaptive immune responses through multiple TLRs. *J. Immunol.* 173, 3916–3924. doi: 10.4049/jimmunol.173.6.3916

O'Rourke, K. E., and Hutchinson, M. (2005). Stopping beta-interferon therapy in multiple sclerosis: an analysis of stopping patterns. *Mult. Scler.* 11, 46–50. doi: 10.1191/1352458505ms1131oa

Patel, S., Blaauboer, S. M., Tucker, H. R., Mansouri, S., Ruiz-Moreno, J. S., Hamann, L., et al. (2017). The common R71H-G230A-R293Q human TMEM173 is a null allele. *J. Immunol.* 198, 776–787. doi: 10.4049/jimmunol.1601585

Patel, S., and Jin, L. (2019). TMEM173 variants and potential importance to human biology and disease. *Genes Immun.* 20, 82–89. doi: 10.1038/s41435-018-0029-9

Peng, Y., Zhuang, J., Ying, G., Zeng, H., Zhou, H., Cao, Y., et al. (2020). Stimulator of IFN genes mediates neuroinflammatory injury by suppressing AMPK signal in experimental subarachnoid hemorrhage. *J. Neuroinflammation* 17:165. doi: 10.1186/s12974-020-01830-4

Petrasek, J., Iracheta-Vellve, A., Csak, T., Satishchandran, A., Kodys, K., Kurt-Jones, E. A., et al. (2013). STING-IRF3 pathway links endoplasmic reticulum stress with hepatocyte apoptosis in early alcoholic liver disease. *Proc. Natl. Acad. Sci. U.S.A.* 110, 16544–16549. doi: 10.1073/pnas.1308331110

Petro, T. M. (2020). IFN regulatory factor 3 in health and disease. *J. Immunol.* 205, 1981–1989. doi: 10.4049/jimmunol.2000462

Pickrell, A. M., and Youle, R. J. (2015). The roles of PINK1, parkin, and mitochondrial fidelity in Parkinson's disease. *Neuron* 85, 257–273. doi: 10.1016/j.neuron.2014.12.007

Platanias, L. C. (2005). Mechanisms of type-I- and type-II-interferon-mediated signalling. *Nat. Rev. Immunol.* 5, 375–386.

Qin, H., Buckley, J. A., Li, X., Liu, Y., Fox, T. H. III, Meares, G. P., et al. (2016). Inhibition of the JAK/STAT pathway protects against alpha-synuclein-induced neuroinflammation and dopaminergic neurodegeneration. *J. Neurosci.* 36, 5144–5159. doi: 10.1523/JNEUROSCI.4658-15.2016

Reinert, L. S., Lopusna, K., Winther, H., Sun, C., Thomsen, M. K., Nandakumar, R., et al. (2016). Sensing of HSV-1 by the cGAS-STING pathway in microglia orchestrates antiviral defence in the CNS. *Nat. Commun.* 7:13348. doi: 10.1038/ncomms13348

Rothblum-Oviatt, C., Wright, J., Lefton-Greif, M. A., McGrath-Morrow, S. A., Crawford, T. O., and Lederman, H. M. (2016). Ataxia telangiectasia: a review. *Orphanet J. Rare Dis.* 11:159. doi: 10.1186/s13023-016-0543-7

Roy, E. R., Wang, B., Wan, Y. W., Chiu, G., Cole, A., Yin, Z., et al. (2020). Type I interferon response drives neuroinflammation and synapse loss in Alzheimer disease. *J. Clin. Invest.* 130, 1912–1930. doi: 10.1172/JCI133737

Schneider, W. M., Chevillotte, M. D., and Rice, C. M. (2014). Interferon-stimulated genes: a complex web of host defenses. *Annu. Rev. Immunol.* 32, 513–545. doi: 10.1146/annurev-immunol-032713-120231

Sejvar, J. J., Haddad, M. B., Tierney, B. C., Campbell, G. L., Marfin, A. A., Van Gerpen, J. A., et al. (2003). Neurologic manifestations and outcome of West Nile virus infection. *JAMA* 290, 511–515. doi: 10.1001/jama.290.4.511

Sen, T., Saha, P., Gupta, R., Foley, L. M., Jiang, T., Abakumova, O. S., et al. (2020). Aberrant ER stress induced neuronal-IFNbeta elicits white matter injury due to microglial activation and T-cell infiltration after TBI. *J. Neurosci.* 40, 424–446. doi: 10.1523/JNEUROSCI.0718-19.2019

Shang, G., Zhang, C., Chen, Z. J., Bai, X.-C., and Zhang, X. (2019). Cryo-EM structures of STING reveal its mechanism of activation by cyclic GMP–AMP. *Nature* 567, 389–393. doi: 10.1038/s41586-019-0998-5

Sharma, M., Rajendrarao, S., Shahani, N., Ramirez-Jarquin, U. N., and Subramaniam, S. (2020). Cyclic GMP-AMP synthase promotes the inflammatory and autophagy responses in Huntington disease. *Proc. Natl. Acad. Sci. U.S.A.* 117, 15989–15999. doi: 10.1073/pnas.2002144117

Sharma, S., Campbell, A. M., Chan, J., Schattgen, S. A., Orlowski, G. M., Nayar, R., et al. (2015). Suppression of systemic autoimmunity by the innate immune adaptor STING. *Proc. Natl. Acad. Sci. U.S.A.* 112, E710–E717. doi: 10.1073/pnas.1420217112

Shelkovnikova, T. A., An, H., Skelt, L., Tregoning, J. S., Humphreys, I. R., and Buchman, V. L. (2019). Antiviral immune response as a trigger of FUS proteinopathy in amyotrophic lateral sclerosis. *Cell Rep.* 29, 4496–4508.e4. doi: 10.1016/j.celrep.2019.11.094

Shields, D. C., Haque, A., and Banik, N. L. (2020). Neuroinflammatory responses of microglia in central nervous system trauma. *J. Cereb. Blood Flow Metab.* 40, S25–S33. doi: 10.1177/0271678X20965786

Simon, D. W., McGeachy, M. J., Bayır, H., Clark, R. S. B., Loane, D. J., and Kochanek, P. M. (2017). The far-reaching scope of neuroinflammation after traumatic brain injury. *Nat. Rev. Neurol.* 13, 171–191. doi: 10.1038/nrneurol.2017.13

Sliter, D. A., Martinez, J., Hao, L., Chen, X., Sun, N., Fischer, T. D., et al. (2018). Parkin and PINK1 mitigate STING-induced inflammation. *Nature* 561, 258–262. doi: 10.1038/s41586-018-0448-9

Su, T., Zhang, Y., Valerie, K., Wang, X. Y., Lin, S., and Zhu, G. (2019). STING activation in cancer immunotherapy. *Theranostics* 9, 7759–7771. doi: 10.7150/thno.37574

Sun, L., Wu, J., Du, F., Chen, X., and Chen, Z. J. (2013). Cyclic GMP-AMP synthase is a cytosolic DNA sensor that activates the type I interferon pathway. *Science* 339, 786–791. doi: 10.1126/science.1232458

Tanaka, Y., and Chen, Z. J. (2012). STING specifies IRF3 phosphorylation by TBK1 in the Cytosolic DNA signaling pathway. *Sci. Signal.* 5:ra20. doi: 10.1126/scisignal.2002521

Taylor, J. M., Minter, M. R., Newman, A. G., Zhang, M., Adlard, P. A., and Crack, P. J. (2014). Type-1 interferon signaling mediates neuro-inflammatory events in models of Alzheimer's disease. *Neurobiol. Aging* 35, 1012–1023. doi: 10.1016/j.neurobiolaging.2013.10.089

Tenny, S., and Thorell, W. (2020). *Intracranial Hemorrhage*. Treasure Island, FL: StatPearls.

Watson, R. O., Bell, S. L., MacDuff, D. A., Kimmey, J. M., Diner, E. J., Olivas, J., et al. (2015). The cytosolic sensor cGAS detects *Mycobacterium tuberculosis* DNA to induce type i interferons and activate autophagy. *Cell Host Microbe* 17, 811–819. doi: 10.1016/j.chom.2015.05.004

West, A. P., Khoury-Hanold, W., Staron, M., Tal, M. C., Pineda, C. M., Lang, S. M., et al. (2015). Mitochondrial DNA stress primes the antiviral innate immune response. *Nature* 520, 553–557. doi: 10.1038/nature14156

Wilke, C., Baets, J., Bleecker, J., Deconinck, T., Biskup, S., Hayer, S., et al. (2017). Beyond ALS and FTD: The phenotypic spectrum of TBK1 mutations includes PSP-like and cerebellar phenotypes. *Neurobiol. Aging* 62, 244.e9–244.e13. doi: 10.1016/j.neurobiolaging.2017.10.010

Wilson, D. R., Sen, R., Sunshine, J. C., Pardoll, D. M., Green, J. J., and Kim, Y. J. (2018). Biodegradable STING agonist nanoparticles for enhanced cancer immunotherapy. *Nanomedicine* 14, 237–246. doi: 10.1016/j.nano.2017.10.013

You, F., Wang, P., Yang, L., Yang, G., Zhao, Y. O., Qian, F., et al. (2013). ELF4 is critical for induction of type I interferon and the host antiviral response. *Nat. Immunol.* 14, 1237–1246. doi: 10.1038/ni.2756

Yu, C. H., Davidson, S., Harapas, C. R., Hilton, J. B., Mlodzianoski, M. J., Laohamonthonkul, P., et al. (2020). TDP-43 triggers mitochondrial DNA release via mPTP to Activate cGAS/STING in ALS. *Cell* 183, 636–649.e18. doi: 10.1016/j.cell.2020.09.020

Zhang, C., Shang, G., Gui, X., Zhang, X., Bai, X.-C., and Chen, Z. J. (2019). Structural basis of STING binding with and phosphorylation by TBK1. *Nature* 567, 394–398. doi: 10.1038/s41586-019-1000-2

Zhang, H., Han, M. J., Tao, J., Ye, Z. Y., Du, X. X., Deng, M. J., et al. (2015). Rat and human STINGs profile similarly towards anticancer/antiviral compounds. *Sci. Rep.* 5:18035. doi: 10.1038/srep18035

Zhang, H., You, Q. D., and Xu, X. L. (2020). Targeting stimulator of interferon genes (STING): a medicinal chemistry perspective. *J. Med. Chem.* 63, 3785–3816. doi: 10.1021/acs.jmedchem.9b01039

Zhang, X., Shi, H., Wu, J., Zhang, X., Sun, L., Chen, C., et al. (2013). Cyclic GMP-AMP containing mixed Phosphodiester linkages is an endogenous high-affinity ligand for STING. *Mol. Cell* 51, 226–235. doi: 10.1016/j.molcel.2013.05.022

Conflict of Interest: The authors declare that the research was conducted in the absence of any commercial or financial relationships that could be construed as a potential conflict of interest.

Copyright © 2021 Fryer, Abdullah, Taylor and Crack. This is an open-access article distributed under the terms of the Creative Commons Attribution License (CC BY). The use, distribution or reproduction in other forums is permitted, provided the original author(s) and the copyright owner(s) are credited and that the original publication in this journal is cited, in accordance with accepted academic practice. No use, distribution or reproduction is permitted which does not comply with these terms.

frontiers in Neurology

ORIGINAL RESEARCH
published: 23 February 2021
doi: 10.3389/fneur.2021.591223

Venlafaxine Attenuated the Cognitive and Memory Deficit in Mice Exposed to Isoflurane Alone

Liang Li[1] *and Chunhai Zhang*[2]*

[1] Department of Orthopedics, Shenzhen Hospital, South Medical University, Shenzhen, China, [2] Department of Thyroid Surgery, China-Japan Union Hospital of Jilin University, Changchun, China

Post-operative cognitive dysfunction (POCD) is a common complication during the post-operative period. It affects the recovery time of the patient after surgery and the stay time in hospital, which causes a great deal of burden to patients and families emotionally and financially. However, there is no specific and effective treatment available for this disorder. Recent study indicated exposure to general anesthetics contributed to POCD by triggering gamma-amino butyric acid type A ($GABA_A$) receptors hyperactivities that persisted even the anesthetic compounds have been eliminated. Here, we investigated the antidepressant, venlafaxine (VLX), in a mouse model of POCD and studied whether VLX attenuated the cognitive dysfunction of mice exposed to general anesthetic, isoflurane (ISO). We found that ISO significantly induced an increased surface expression of the $GABA_A$ receptor subunit, α5, in the hippocampus of the mice. However, VLX treatment reduced the increase in α5 subunit expression. Meanwhile, we found the expression levels of interleukin (IL)-1β, tumor necrosis factor alpha (TNF-α), and IL-6 in the brains of mice exposed to ISO were significantly increased. However, VLX could prevent the increase in these cytokines. We also investigated the memory deficit of these mice by using a Y maze behavioral test. Mice with ISO exposure showed decreased alternation performance that could be prevented by the VLX treatment. Collectively, our results here are in line with the previous findings that α5 subunit plays an important role of the formation of POCD, but VLX may be a promising candidate compound for the treatment of POCD.

Keywords: POCD, GABAA receptors α5, neuroinflammation, Y maze, memory

OPEN ACCESS

Edited by:
Flavia Eugenia Saravia, Universidad de Buenos Aires, Argentina

Reviewed by:
Bruno Pierre Guiard, Université de Toulouse, France
Valeria Carlini, National University of Cordoba, Argentina

***Correspondence:**
Chunhai Zhang
chunhai@jlu.edu.cn

Specialty section:
This article was submitted to Neuropharmacology, a section of the journal Frontiers in Neurology

Received: *04 August 2020*
Accepted: *26 January 2021*
Published: *23 February 2021*

Citation:
Li L and Zhang C (2021) Venlafaxine Attenuated the Cognitive and Memory Deficit in Mice Exposed to Isoflurane Alone. Front. Neurol. 12:591223. doi: 10.3389/fneur.2021.591223

INTRODUCTION

Post-operative cognitive dysfunction (POCD) is featured with cognitive decline, such as memory and executive functions after surgeries, including thyroid cancers, especially in elderly patients. It could last days, weeks, and months even longer than several years (1). Statistical data suggest that the proportion of POCD after surgery in elderly patients is as high as 10% at 3 months after surgery (2). The persistent cognitive dysfunction adversely affects the life quality of patients, such as long time bedridden stage and recovery time, which could cause heavy burden to the patients and their families (3). Multiple factors are considered to predispose POCD, such as aging and other pre-existing medical conditions (4). However, the underlying mechanisms of this disorder remain ambiguous so far. Few options of the treatment are specifically for POCD so far due to lack of the extensive knowledge of this disorder. Recent studies indicated that the type of anesthetics, anesthetic method, and the duration of anesthetics were critical factors that contributed

to the development of POCD (3, 5), which suggested that understanding the anesthetics action mechanism might lead to important clinical significance for the prevention and treatment of POCD in the future. Meanwhile, a promising treatment strategy could be developed based on the further understanding of the pathogenesis of POCD. Therefore, the study aimed to explore the etiology of POCD after anesthesia treatment and the possible treatment option of the disorder.

In the central nervous system (CNS), gamma-amino butyric acid type A receptors ($GABA_ARs$) are critical inhibitory receptors, and most general anesthetics are positive allosteric modulators of $GABA_ARs$ by increasing the inhibition in the brain, which causes amnesia and loss of consciousness (6). Among them, $GABA_ARs$ containing an a5 subunit are relevant in the POCD after exposure to general anesthesia (3, 7). One of the general anesthetics, etomidate, could cause sustained increase in $\alpha5GABA_AR$ activity and impair memory performance and synaptic plasticity. Furthermore, inhibition of the $\alpha5GABA_AR$ could prevent the mentioned memory deficits (3). Established studies have suggested that neuroinflammation resulting from anesthesia or surgery significantly contributed to the development of POCD (8). In human, general anesthesia was associated with cognitive dysfunction and the increased expression of interleukin (IL)-6 and tumor necrosis factor alpha (TNF-α), which could be attenuated by dexmedetomidine (9). In rat model, ISO exposure alone could cause the higher expression levels of cytokines in the hippocampus (10). In another pre-clinical study, ISO could boost the release of IL-1β in the hippocampal CA1 region of rats (11). However, the specific relationship between neuroinflammation and POCD treatment is still not profiled yet.

Venlafaxine (VLX) is one of the widely used antidepressants due to its relatively safe profile and efficacy on depressive and anxiety disorders (12). Study also implicated that VLX could improve the cognitive performance in patients and animals (13, 14). These results promoted us to postulate whether VLX could be a potential compound for the treatment of POCD. This assumption was also supported by the fact that VLX has been post-operatively used for the patients in a variety of clinical settings (15, 16). Moreover, VLX has been found to possess neuroprotective effects (17), which could be another important property to support the potential treatment for POCD since POCD was associated with synaptic protein dysfunction (18).

In the present study, we investigated the possible effect of VLX on the prevention of POCD in mice exposed to ISO. We found that ISO could cause decreased spontaneous alternation of mice in a Y maze test that is a behavioral assay of working memory (19), but VLX could effectively protect the mice from the above memory loss. We also explored the underlying mechanism by which VLX could exert these beneficial effects.

MATERIALS AND METHODS

Animals and Drug Treatments

All procedures involving animals were approved by the Experimental Animal Ethics Committee of China–Japan Union Hospital of Jilin University, Jilin Province, China. Male C57BL/6 mice at the age of 12 weeks old were used in the present experiments. Mice were kept in the standard laminal-flow cabinets with pathogen-free conditions. Mice were randomly grouped into multiple groups: control group, venlafaxine alone group (VLX), ISO alone group (ISO), and ISO plus venlafaxine group (ISO + VLX). VLX was purchased from Sigma-Aldrich and dissolved in normal saline. For the ISO treatment, the mice were anesthetized with inhalation of 4% ISO for the induction phase and then 1.3% for 3 h in a chamber on a heating pad to keep body temperature with 100% oxygen (20). The breath and heartbeat of the mice were closely monitored by an experimenter. VLX (16 mg/kg) and normal saline were administrated intraperitoneally on a daily basis till the day when behavioral test was completed. For the control group and VLX alone group, mice were either injected with normal saline or VLX intraperitoneally and then went through 3 h in chambers with 100% oxygen but without ISO on the first day. The concentration of VLX used here was adapted from the previous report (21). A brief diagram of the experimental design was presented (**Figure 1**).

Tissue Collection

Mice were sacrificed on the day when the behavioral tests were completed. After perfusion with 0.9% normal saline, the hippocampal tissues from the mice brains were collected for the determination of protein concentration with Western blot, ELISA, and biotinylation.

Y Maze

Working memory was assessed in a Y maze apparatus consisting of three arms, which was a 1-day test. The Y maze test was carried out for 3 days and 1 week later after the anesthesia. Each arm of the Y maze was 35 cm long, 25 cm high, and 10 cm wide and positioned at an equal angle as previously reported (22). The three arms were labeled as A, B, and C. During the test, mice were put at the end of one arm randomly and allowed to explore freely the arms in 8 min. We manually recorded the sequence of arm entries during the test. The alternation and total arms entries were analyzed and compared among groups.

Western Blot

To measure the protein expression level of p-STAT3 and STAT3, tissues from the hippocampus of mice were lysed with radioimmunoprecipitation assay (RIPA) buffer and then centrifuged at 12,000 g at cold condition. The supernatant containing equal amount of total protein was separated in sodium dodecyl sulfate–polyacrylamide gel electrophoresis (SDS-PAGE) gel for 2 h. After transferring to polyvinylidene fluoride (PVDF) membranes and blocking with 5% bovine serum albumin (BSA) in Tris-buffered saline with Tween 20 (TBST) buffer, the membranes were incubated with primary antibodies of p-STAT3 (1:1,000, Cell Signaling, #9145), STAT3 (1:1,000, Cell Signaling, #9132), and β-actin (1:4,000, Santa Cruz Biotechnology, sc-517582) in cold room for overnight and then in secondary antibodies for 2 more hours at room temperature after washing with TBST. Chemiluminescence with enhanced chemiluminescence (ECL) solution was used to visualize the

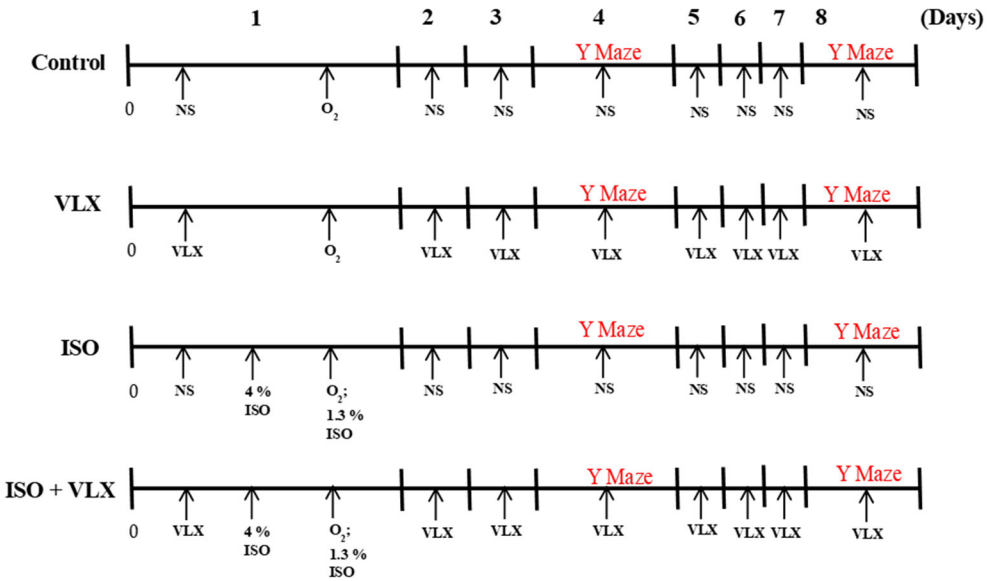

FIGURE 1 | Brief diagram of the experimental protocol. NS, normal saline; O_2, 100% oxygen; VLX, venlafaxine; ISO, isoflurane.

signal from the membranes. The expression level of each protein in statistical analysis was presented as the relative ratio compared to the internal control protein, β-actin.

ELISA

Cytokines were measured with the commercial ELISA kits (Thermo Scientific) according to manufacturer's protocols, respectively. Briefly, the total protein was isolated from hippocampal tissues as above mentioned in the Western blot, and the supernatant was used for ELISA assay after concentration was determined. All samples were assayed with duplication. Standard curve for each cytokine was established with their standard samples provided in the kits. The values of these cytokines were normalized as a relative ratio compared to the total protein.

Cell-Surface Biotinylation

Cell-surface biotinylation was carried out as previously reported (3). Briefly, 350-μm coronal slices were prepared with a vibratome and then immediately transferred to ice-cold artificial cerebrospinal fluid (ACSF) oxygenation with 95% O_2/5% CO_2. The slices were then incubated twice in ice-cold 0.75 mg/ml NHS-SS-biotin (Thermo Scientific) for 45 min. Then, slices were washed several times to stop the excess biotin reaction followed by adding lysis buffer with protease inhibitors. Hi-Capacity NeutrAvidin beads (Thermo Scientific) was used to incubate supernatant for 16–18 h at 4°C to pull down and elute the proteins with elution buffer. The protein concentration was determined, and equal amount protein was subjected to SDS-PAGE analysis as Western blot assay. $GABA_A$ receptor α5 subunit antibody (1:1,000, Millipore, ab9678), β-actin antibody (1:4,000, Santa Cruz Biotechnology, sc-517582), and anti-Na+/K+ ATPase antibody (1:500, Abcam, ab58475) were used for Western blot analysis. The expression of α5 was normalized to its respective loading controls in the surface (NKA) and total (β-actin). The purity of extracted surface protein was determined by probing the presence of β-actin with antibody.

Statistical Analysis

All statistical analysis was completed with Prism software. Data were expressed as the mean ± SEM. The significance of differences was determined by two-way ANOVA, followed by Tukey's *post-hoc* test for multiple comparisons. A $p < 0.05$ was deemed to show statistical significance.

RESULTS

VLX Ameliorated the Memory Deficit of Mice Exposed to ISO in a Y Maze Test

To test the protective effects of VLX on memory deficit, we carried out a Y maze behavioral test to assess the status of working memory of the mice with ISO treatment. We carried out the test on day 3 and 1 week after the anesthesia. On day 3, we found that ISO caused a lower alternation performance in the transition of A, B, and C arms, which indicated compromised working memory of these mice. However, the deterioration of cognitive function could be significantly prevented when we employed the VLX treatment to these mice. Two-way ANOVA analysis demonstrated that ISO [$F_{1,44} = 14.12$, $p < 0.001$] and VLX [$F_{1,44} = 4.297$, $p < 0.05$] exerted a significant change in the alternation performance. There was an interaction between ISO and VLX [$F_{1,44} = 7.738$, $p < 0.01$] in day 3. A *post-hoc* analysis indicated that the alternation behavior in the ISO-treated mice was less than that of the control mice ($p < 0.001$), and VLX significantly prevented the reduction in the alternation performance ($p < 0.01$) (**Figure 2A**). Interestingly, the treatments of VLX and ISO did not affect the total arm entries

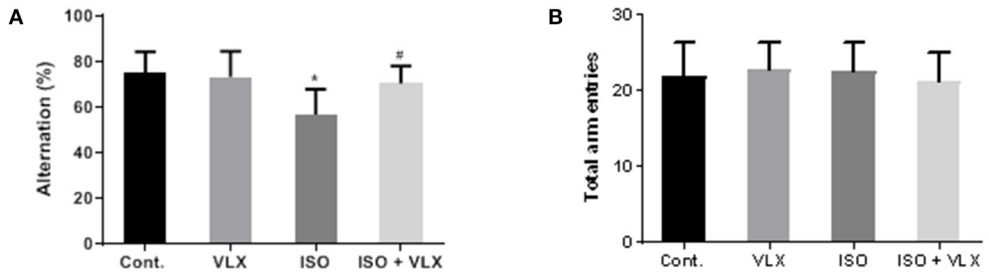

FIGURE 2 | Venlafaxine (VLX) ameliorated the memory deficit in Y maze test of mice exposed to isoflurane (ISO) (day 3). **(A)** The effect of VLX on the alternation of mice in Y maze test. **(B)** The effect of VLX on the total arm entries of mice in Y maze test. Data were expressed as mean ± SEM. $^{*}p < 0.05$ compared to control; $^{\#}p < 0.05$ compared to ISO, $n = 12$.

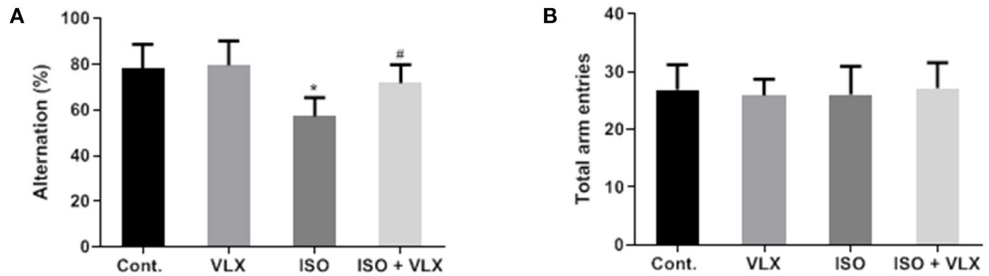

FIGURE 3 | Venlafaxine (VLX) attenuated the memory deficit in Y maze test of mice exposed to isoflurane (ISO) (1 week). **(A)** The effect of VLX on the alternation of mice in Y maze test. **(B)** The effect of VLX on the total arm entries of mice in Y maze test. Data were expressed as mean ± SEM. $^{*}p < 0.05$ compared to control; $^{\#}p < 0.05$ compared to ISO, $n = 12$.

among all groups, which suggested that the changes in alternation were not due to the alteration of the motor function of these mice (**Figure 2B**). Moreover, the total arm entries in all groups were comparable, which indicated neither ISO nor VLX treatment was able to affect the motor function of mice (**Figure 2B**). On the time point of 1 week after anesthesia, we observed the similar results. Two-way ANOVA analysis demonstrated that ISO [$F_{1,44} = 28.18$, $p < 0.0001$] and VLX [$F_{1,44} = 8.531$, $p < 0.01$] exerted a significant change in the alternation performance. There was an interaction between ISO and VLX [$F_{1,44} = 5.787$, $p < 0.05$] in 1 week. A *post-hoc* analysis indicated that the alternation behavior in the ISO-treated mice was less than that of the control mice ($p < 0.0001$), and VLX significantly prevented the reduction in the alternation performance ($p < 0.01$) (**Figure 3A**). ISO and VLX showed no effect on the total arm entries (**Figure 3B**). These above results suggested that ISO exposure could adversely affect the working memory in mice, but VLX could rescue the mice from the ISO-induced memory deficit.

VLX Reduced the Phosphorylation of STAT3 in Mice Exposed to ISO

JAK2/STAT3 axis has been considered as an important signaling pathway that was disturbed in the memory loss under certain circumstance (23). In addition, STAT3 was one of the key players in neuroinflammatory response that was found to be responsible for memory and cognitive impairment in certain extent (24, 25). Therefore, we performed Western blot assay to measure whether there was a change in STAT3 expression level in the mouse hippocampus. Our results demonstrated that ISO exposure did not affect the expression level of total STAT3 protein but significantly increased the expression level of phosphorylated STAT3 (p-STAT3). Importantly, we found that VLX could inhibit the upregulation of p-STAT3 expression level. Two-way ANOVA analysis demonstrated that ISO [$F_{1,20} = 44.60$, $p < 0.0001$] and VLX [$F_{1,20} = 9.073$, $p < 0.01$] exerted a significant change in the protein level of p-STAT3. There was an interaction between ISO and VLX [$F_{1,20} = 10.79$, $p < 0.01$] on the change of p-STAT3 protein. A *post-hoc* analysis indicated that p-STAT3 protein in the ISO-treated mice was higher than that of the control mice ($p < 0.0001$), and VLX significantly prevented the increase in the p-STAT3 protein ($p < 0.01$) (**Figure 4**). These above results indicated that ISO might activate the STAT3 signaling pathway via enhancing its phosphorylation, and VLX could exert its beneficial effect by preventing the phosphorylation.

VLX Attenuated the Levels of Cytokines in the Hippocampus of Mice Exposed to ISO

Based on the above findings and the fact that STAT3 activation was closely associated with neuroinflammation (26), we postulated that VLX might regulate the inflammatory response in the brains of these mice. We carried out ELISA assays to measure the cytokine products in the hippocampal tissues of the mice. We found that the levels of IL-1β and IL-6 were significantly increased by ISO, but there was no change

in TNF-α in these mice (**Figure 5**), which suggested that IL-1β and IL-6 not TNF-α were activated by ISO treatment. For IL-6, two-way ANOVA analysis demonstrated that ISO [$F_{1,24} = 24.80$, $p < 0.0001$] and VLX [$F_{1,24} = 5.140$, $p < 0.05$] exerted a significant change in the IL-6 protein level. There was an interaction between ISO and VLX [$F_{1,24} = 12.32$, $p < 0.01$] on the changes of IL-6 protein level. A *post-hoc* analysis indicated that the IL-6 protein level in the ISO-treated mice was higher than that of control mice ($p < 0.0001$), and VLX significantly prevented the increase in the IL-6 protein level ($p < 0.01$) (**Figure 5A**). For IL-1β, two-way ANOVA analysis demonstrated that ISO [$F_{1,24} = 50.62$, $p < 0.0001$] and VLX [$F_{1,24} = 12.48$, $p < 0.01$] exerted a significant change in the IL-1β protein level. There was an interaction between ISO and VLX [$F_{1,24} = 4.271$, $p < 0.05$] on the changes in IL-1β protein level. A *post-hoc* analysis indicated that the IL-1β protein level in the ISO-treated mice was higher than that of the control mice ($p < 0.0001$), and VLX significantly prevented the increase in the IL-1β protein level ($p < 0.01$) (**Figure 5B**). For TNF-α, ISO and VLX showed no effect on its protein expression level (**Figure 5C**). These results implied that VLX might exert anti-inflammatory effects in these mice exposed to ISO by inhibiting the levels of IL-1β and IL-6 in their hippocampus.

VLX Decreased the Surface Expression of $GABA_A$ Receptor α5 in Mice Exposed to ISO

Increased surface expression of $GABA_A$ receptor α5 was shown to be responsible for the changes in tonic current that was considered as the molecular mechanism of memory impairment in POCD (3). Here, we investigated whether VLX regulated the response process of α5 receptor in the mice stimulated with ISO. In line with the previous findings, we found that ISO could increase the surface expression level of α5 receptor (**Figure 6A**), which suggested that ISO might influence tonic current and then affect the memory and cognitive deficits as suggested by a previous study (3). As anticipated, VLX could decrease the expression level of α5 receptor on cell surface of the hippocampus in mice with ISO. Two-way ANOVA analysis demonstrated that ISO [$F_{1,16} = 16.11$, $p < 0.01$] and VLX [$F_{1,16} = 10.40$, $p < 0.01$] exerted a significant change in the surface expression level of α5. There was an interaction between ISO and VLX [$F_{1,16} = 4.573$, $p < 0.05$] on the changes in the surface expression level of α5. A *post-hoc* analysis indicated that the surface expression level of α5 in the ISO-treated mice was higher than that of the control mice ($p < 0.01$), and VLX significantly prevented the increase in the surface expression level of α5 ($p < 0.01$) (**Figure 6A**). There was no β-actin expression detected in the surface protein samples as shown in **Figure 6A**. Meanwhile, we also employed the Western blot analysis in the total protein to probe the expression level of α5. We found that ISO and VLX showed no effect on total protein of α5 (**Figure 6B**), which suggested that ISO did not affect the total protein expression of α5 but increased the surface expression only.

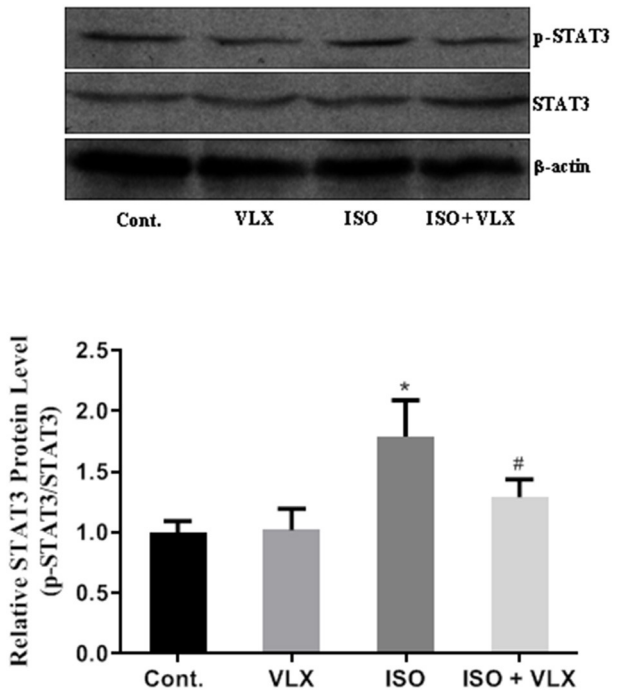

FIGURE 4 | Venlafaxine (VLX) reduced the phosphorylation of STAT3 in mice exposed to isoflurane (ISO) in Western blot assay. Data were expressed as mean ± SEM. $^{*}p < 0.05$ compared to control; $^{\#}p < 0.05$ compared to ISO, $n = 6$.

DISCUSSION

POCD happens frequently following major surgery. The incidence of this disorder is around one-third in major surgeries and much higher in elderly patients. However, there is no specific treatment option for it yet.

In the present study, we found that the antidepressant, VLX, could be a promising candidate compound to handle the disorder. Cotreatment of VLX could prevent the cognitive and memory deterioration in the mice exposed to anesthetic compound, isoflurane. Our study validated the previous findings by highlighting the involvement of $GABA_A$ receptor α5 in the anesthetics-induced POCD. The mouse model used here has been verified by several recent studies from other groups by using single dose of etomidate, which caused memory and cognitive impairment, POCD (3, 7). More importantly, we also found that the protective effects of VLX could last at least 1 week (**Figure 3**). Mice are often affected by the acute sedative effect of ISO, and to further investigate whether the effect could last longer, we carried out the Y maze test on day 3 and 1 week after the anesthesia. The average total arm entries among all groups were less in day 3 than 1 week (**Figures 2, 3**). We postulated that it might be due to the acute influence of ISO on the mouse motivation. The repeated effects shown on both day 3 and 1 week from our results made us to claim the protective effects of VLX in the POCD mouse model. Although there existed controversial conclusion of the

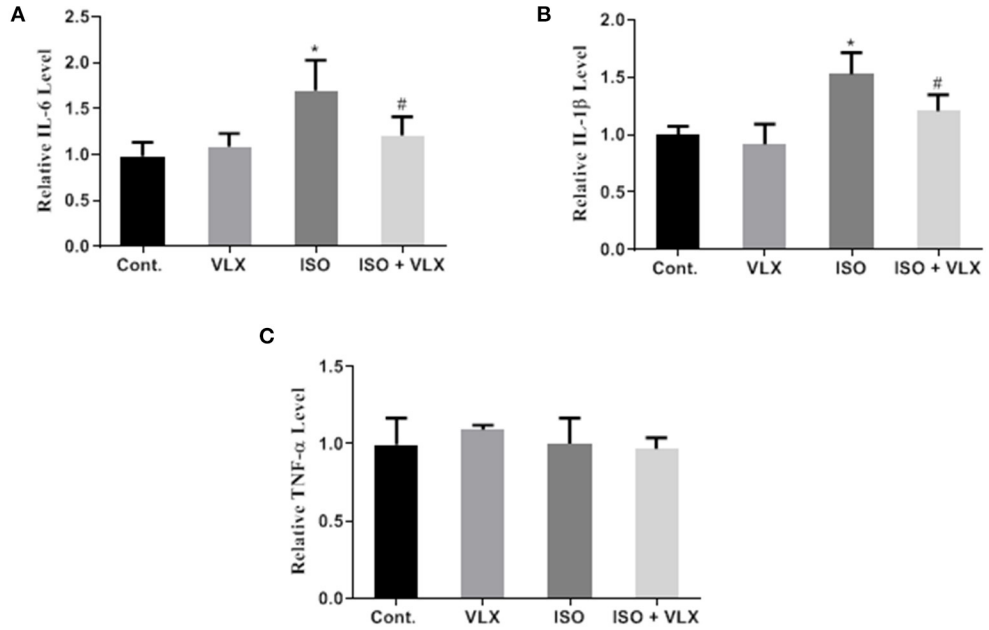

FIGURE 5 | Venlafaxine (VLX) attenuated the products of cytokine in hippocampus of mice exposed to isoflurane (ISO) in ELISA assay. **(A)** The effect of VLX on the expression of IL-6 of mice exposed to ISO. **(B)** The effect of VLX on the expression of IL-1β of mice exposed to ISO. **(C)** The effect of VLX on the expression of tumor necrosis factor alpha (TNF-α) of mice exposed to ISO. Data were expressed as mean ± SEM. $^{*}p < 0.05$ compared to control; $^{\#}p < 0.05$ compared to ISO, $n = 7$.

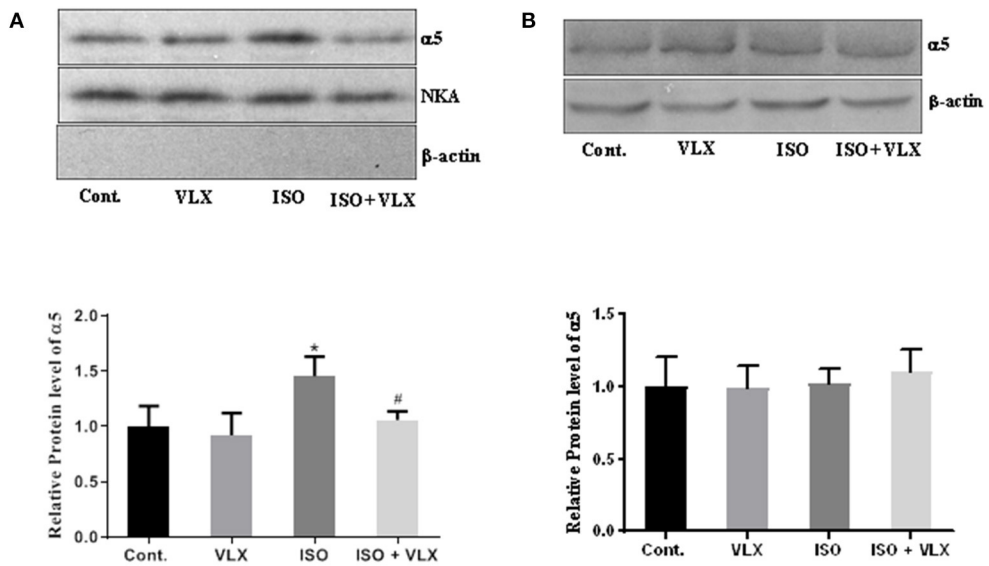

FIGURE 6 | Venlafaxine (VLX) decreased the surface expression of $GABA_A$ receptor α5 in mice exposed to isoflurane (ISO). **(A)** The effect of VLX on the surface expression of α5 receptor in mice exposed to ISO. **(B)** The effect of VLX on the total expression of α5 receptor in mice exposed to ISO. Data were expressed as mean ± SEM. $^{*}p < 0.05$ compared to control; $^{\#}p < 0.05$ compared to ISO, $n = 6$.

effects of VLX on memory and cognitive function in clinical studies (27–29), findings from some early stage preclinical studies favored the beneficial roles of VLX (14, 30). Especially, a recent study revealed that VLX rescued the memory loss in the Y maze test in a demyelination mouse model (31), which promoted us to evaluate the possible role of VLX in POCD with the Y maze test.

The dose of VLX used in the present study was based on the previous reports. One report claimed that higher doses (75, 100, and 150 mg/kg) of venlafaxine could lower the threshold of

convulsion in animals and suggested the use of 25 and 50 mg/kg for animal study (32). Another study found that venlafaxine exerted stimulant effect on mouse activity in a locomotor test from the dose of 16 mg/kg (33). More importantly, a study indicated that 16 mg/kg could significantly affect the function of the hippocampus (21). The common mechanism of VLX is blocking the reuptake of serotonin and norepinephrine in CNS and leaving more these neurotransmitters in the synapse. In the dose of 16 mg/kg, VLX could reduce the noradrenaline but not serotonin level in pre-synapse (33). Another study suggested that lower dose of VLX (15 mg/kg) was not able to elicit 5-HT1A receptors-stimulated G protein activation (34). Levels of noradrenaline are obviously lowered in several areas in older mice brains, including the hypothalamus (35). In human, reduction in noradrenergic-dependent functions in locus coeruleus is associated with impaired cognitive and behavioral function (36). Based on the above previous reports and our findings here, we assumed that the beneficial effects of VLX in this mouse model might not be derived from the direct effects on neurotransmitters. Inflammatory responses and immune reaction play role in cognitive decline after surgery (37). Therefore, we wondered whether VLX regulate the inflammatory response in this mouse model. Our assumption was further encouraged by the recent publication that indicated VLX could alleviate the neuroinflammation and depressive-like behaviors in a mouse model of demyelination (31).

It has been well-established that tissue trauma released damage-associated cytokines, including TNF-α, could break the blood–brain barrier (BBB) and result in neuroinflammation and concomitant cognitive decline (38). Moreover, recent studies have demonstrated that anesthetic alone could cause damages to the hippocampus, which led to memory and cognitive dysfunction (3, 39). Therefore, we investigated the pathological hippocampal tissue and the hippocampus related behavioral performance in this mouse model. Current studies of neuropsychiatric diseases, including POCD, were primarily on the disturbance of neurotransmitters, but recent studies emphasized the importance of neuroinflammation (8).

The inhibitory neurotransmitter, GABA, is a prominent player in regulating learning and memory (40). Particularly, the $GABA_A$ receptor α5 subunit plays a key role in POCD (3, 7). A previous study also suggested that α5 could actively regulate the memory deficits induced by inflammation (41). Therefore, we postulated that preventing the ISO-induced activation of α5 could inhibit the inflammation as well. STAT3 is a key player in regulating inflammatory gene expression and glial reactivity in CNS to various insults and stimulations (42). Specifically, JAK2/STAT3 signaling pathway was involved in POCD in rat model by increasing their phosphorylation, and inhibiting the levels of p-JAK2 and p-STAT3 could attenuate the symptoms of POCD in rats (43). A study has shown that VLX possesses anti-inflammation property (44). Consistent with the previous findings, we demonstrated that VLX could inhibit the expression of p-STAT3 and reduce the expression of some cytokines (**Figure 4**). It has been well-established that VLX could protect neurons against insults in CNS. Combined with anti-inflammation effect, VLX might exert therapeutic effects by targeting multiple ways in the CNS to prevent the memory and cognitive loss in POCD. Impaired spatial learning memory caused by ISO has been reported (45). Neuroinflammation could be attributed to the development of the deficits (45). Studies have indicated that anesthetics alone could cause POCD in several models (3, 46). A study also suggested that ISO caused POCD via triggering neuroinflammation (46). Our study further confirmed this property of ISO in a mouse model. More importantly, here, we demonstrated an effective method to rescue these mice from the neuronal damage on the behavioral level. The most important finding in our study was the molecular mechanism by which VLX prevented the surface expression of one of $GABA_A$ receptors, α5. The persistent increased surface expression of this receptor has been shown to be closely associated with the increase in tonic current, which might eventually cause the memory and cognitive impairment of these mice (3). Here, we found that ISO could induce the surface expression of α5 in mice, and the increased expression could be modulated by the treatment of VLX. These findings were consistent with previous reports. More importantly, our results indicated that VLX, an available compound, could prevent the increased surface expression of α5 that was validated to be associated with the POCD (3). Accordingly, we found the VLX treatment could effectively ameliorate the impairment of working memory induced by ISO in a Y maze test. Since there is no report of the direct effect of VLX on the $GABA_A$ receptors, the indirect regulation of VLX on α5 subunit is quite possible. As a typical serotonin–norepinephrine reuptake inhibitor (SNRI) antidepressant, VLX has potent effect on serotonin receptor and increase the content of serotonin. Serotonin has been found to be a modulator of GABA neurotransmission (47), and therefore, serotonin receptor may mediate the effect of VLX to $GABA_A$ receptors α5 subunit.

VLX possesses obvious therapeutic effect on mood disorders, and meanwhile, it exerts anti-inflammatory effect in CNS (48). A study has indicated that VLX was able to exert obvious neuroprotective effects in brain injuries (17). In addition, STAT3 activation is essential for neuronal regeneration (49). By working on both neurotransmitters and inflammation in CNS, VLX may open a new road to explore the treatment options. Although multiple factors may predispose POCD, only aging is identified as an important one so far (50). Therefore, we admitted the limitations of the present study such as the young age of mice, which was not the best scenario for mimicking the patients clinically since POCD occurs more often in the elderly patients. However, young mice are more suitable for further cellular and molecular mechanism study (3, 50, 51). Old mice were usually used to compare the age effects on the mice response (39). Future studies involving the relative old mice are warranted for this purpose. In addition, memory and cognitive dysfunctions induced by anesthetics could be affected by several factors, including treatment protocol (anesthetic alone or combining with surgical procedure) and the age of mouse used in the studies. For example, a previous study found that ISO exposure could affect acquisition in a water maze test but influence the retention in young not older rats (52). In the present study, we attempted to explore the effects of ISO on the reference memory of mice by carrying out a water maze test. We found under our specific

treatment protocol that there was no significant difference in either acquisition or retention trials in water maze test among the control and ISO treatment group (**Supplementary Figure 1**). To further confirm the protective effects of VLX in the mouse model, efforts on other behavioral assays of the memory and cognitive function should be put on future studies, such as puzzle box test, which was recently claimed by a research group with using the etomidate in a mouse model of POCD (7).

DATA AVAILABILITY STATEMENT

The original contributions presented in the study are included in the article/**Supplementary Material**, further inquiries can be directed to the corresponding author/s.

ETHICS STATEMENT

The animal study was reviewed and approved by The Experimental Animal Ethics Committee of China-Japan Union Hospital of Jilin University, Jilin Province, China.

AUTHOR CONTRIBUTIONS

LL designed the study, wrote the draft, and finalized the manuscript. CZ performed the assays and edited the manuscript. LL was a visiting scholar in CZ's team (Department of Thyroid Surgery, China–Japan Union Hospital of Jilin University, Changchun, Jilin Province, China). Both authors contributed to the article and approved the submitted version.

FUNDING

CZ was supported financially by the China Scholarship Council, China.

ACKNOWLEDGMENTS

Authors thank the support to this study from the Department of Orthopedics, Shenzhen Hospital, South Medical University, Shenzhen, Guangdong Province, China and Department of Thyroid Surgery, China–Japan Union Hospital of Jilin University, Changchun, Jilin Province, China.

SUPPLEMENTARY MATERIAL

The Supplementary Material for this article can be found online at: https://www.frontiersin.org/articles/10.3389/fneur.2021.591223/full#supplementary-material

REFERENCES

1. Plas M, Rotteveel E, Izaks GJ, Spikman JM, van der Wal-Huisman H, van Etten B, et al. Cognitive decline after major oncological surgery in the elderly. *Eur J Cancer*. (2017) 86:394–402. doi: 10.1016/j.ejca.2017.09.024
2. Moller JT, Cluitmans P, Rasmussen LS, Houx P, Rasmussen H, Canet J, et al. Long-term postoperative cognitive dysfunction in the elderly ISPOCD1 study. ISPOCD investigators. International study of post-operative cognitive dysfunction. *Lancet*. (1998) 351:857–61. doi: 10.1016/S0140-6736(97)07382-0
3. Zurek AA, Yu J, Wang DS, Haffey SC, Bridgwater EM, Penna A, et al. Sustained increase in α5GABAA receptor function impairs memory after anesthesia. *J Clin Invest*. (2014) 124:5437–541. doi: 10.1172/JCI76669
4. Shoair OA, Grasso Ii MP, Lahaye LA, Daniel R, Biddle CJ, Slattum PW. Incidence and risk factors for postoperative cognitive dysfunction in older adults undergoing major noncardiac surgery: a prospective study. *J Anaesthesiol Clin Pharmacol*. (2015) 31:30–6. doi: 10.4103/0970-9185.150530
5. Jiang Y, Gao H, Yuan H, Xu H, Tian M, Du G, et al. Amelioration of postoperative cognitive dysfunction in mice by mesenchymal stem cell-conditioned medium treatments is associated with reduced inflammation, oxidative stress and increased BDNF expression in brain tissues. *Neurosci Lett*. (2019) 709:134372. doi: 10.1016/j.neulet.2019.134372
6. Zhao ZF, Du L, Gao T, Bao L, Luo Y, Yin YQ, et al. Inhibition of α5 GABAA receptors has preventive but not therapeutic effects on isoflurane-induced memory impairment in aged rats. *Neural Regen Res*. (2019) 14:1029–36. doi: 10.4103/1673-5374.250621
7. Wang DS, Kaneshwaran K, Lei G, Mostafa F, Wang J, Lecker I, et al. Dexmedetomidine prevents excessive γ-aminobutyric acid type A receptor function after anesthesia. *Anesthesiology*. (2018) 129:477–89. doi: 10.1097/ALN.0000000000002311
8. Safavynia SA, Goldstein PA. The role of neuroinflammation in postoperative cognitive dysfunction: moving from hypothesis to treatment. *Front Psychiatry*. (2019) 9:752. doi: 10.3389/fpsyt.2018.00752
9. Yang W, Kong LS, Zhu XX, Wang RX, Liu Y, Chen LR. Effect of dexmedetomidine on postoperative cognitive dysfunction and inflammation in patients after general anaesthesia: A PRISMA-compliant systematic review and meta-analysis. *Medicine*. (2019) 98:e15383. doi: 10.1097/MD.0000000000015383
10. Chen L, Xie W, Xie W, Zhuang W, Jiang C, Liu N. Apigenin attenuates isoflurane-induced cognitive dysfunction via epigenetic regulation and neuroinflammation in aged rats. *Arch Gerontol Geriatr*. (2017) 73:29–36. doi: 10.1016/j.archger.2017.07.004
11. Kong F, Chen S, Cheng Y, Ma L, Lu H, Zhang H, et al. Minocycline attenuates cognitive impairment induced by isoflurane anesthesia in aged rats. *PLoS ONE*. (2013) 8:e61385. doi: 10.1371/journal.pone.0061385
12. Montoya A, Bruins R, Katzman MA, Blier P. The noradrenergic paradox: implications in the management of depression and anxiety. *Neuropsychiatr Dis Treat*. (2016) 12:541–57. doi: 10.2147/NDT.S91311
13. Tian Y, Du J, Spagna A, Mackie MA, Gu X, Dong Y, et al. Venlafaxine treatment reduces the deficit of executive control of attention in patients with major depressive disorder. *Sci Rep*. (2016) 6:28028. doi: 10.1038/srep28028
14. Lapmanee S, Charoenphandhu J, Teerapornpuntakit J, Krishnamra N, Charoenphandhu N. Agomelatine, venlafaxine, and running exercise effectively prevent anxiety- and depression-like behaviors and memory impairment in restraint stressed rats. *PLoS ONE*. (2017) 12:e0187671. doi: 10.1371/journalpone0187671
15. Mansouri MT, Naghizadeh B, Ghorbanzadeh B, Alboghobeish S, Amirgholami N, Houshmand G, et al. Venlafaxine prevents morphine antinociceptive tolerance: the role of neuroinflammation and the l-arginine-nitric oxide pathway. *Exp Neurol*. (2018) 303:134–41. doi: 10.1016/j.expneurol.2018.02.009
16. Mansouri MT, Naghizadeh B, Ghorbanzadeh B, Alboghobeish S, Houshmand G, Amirgholami N. Venlafaxine attenuates the development of morphine tolerance and dependence: role of L-arginine/nitric oxide/cGMP pathway. *Endocr Metab Immune Disord Drug Targets*. (2018) 18:362–70. doi: 10.2174/1871530318666171213153920
17. Zepeda R, Contreras V, Pissani C, Stack K, Vargas M, Owen GI, et al. Venlafaxine treatment after endothelin-1-induced cortical stroke modulates growth factor expression and reduces tissue damage in rats. *Neuropharmacology*. (2016) 107:131–45. doi: 10.1016/j.neuropharm.2016.03.011

18. Wang P, Cao J, Liu N, Ma L, Zhou X, Zhang H, et al. Protective effects of edaravone in adult rats with surgery and lipopolysaccharide administration-induced cognitive function impairment. *PLoS ONE*. (2016) 11:e0153708. doi: 10.1371/journal.pone.0153708
19. Kraeuter AK, Guest PC, Sarnyai Z. The Y-maze for assessment of spatial working and reference memory in mice. *Methods Mol Biol*. (2019) 1916:105–11. doi: 10.1007/978-1-4939-8994-2_10
20. Fang X, Xia T, Xu F, Wu H, Ma Z, Zhao X, et al. Isoflurane aggravates peripheral and central insulin resistance in high-fat diet/streptozocin-induced type 2 diabetic mice. *Brain Res*. (2020) 1727:146511. doi: 10.1016/j.brainres.2019.146511
21. Shen P, Hu Q, Dong M, Bai S, Liang Z, Chen Z, et al. Venlafaxine exerts antidepressant effects possibly by activating MAPK-ERK1/2 and P13K-AKT pathways in the hippocampus. *Behav Brain Res*. (2017) 335:63–70. doi: 10.1016/j.bbr.2017.08.011
22. Xiao L, Xu H, Zhang Y, Wei Z, He J, Jiang W, et al. Quetiapine facilitates oligodendrocyte development and prevents mice from myelin breakdown and behavioral changes. *Mol Psychiatry*. (2008) 13:697–708. doi: 10.1038/sjmp4002064
23. Chiba T, Yamada M, Sasabe J, Terashita K, Shimoda M, Matsuoka M, et al. Amyloid-beta causes memory impairment by disturbing the JAK2/STAT3 axis in hippocampal neurons. *Mol Psychiatry*. (2009) 14:206–22. doi: 10.1038/mp.2008.105
24. Chen X, Nie X, Mao J, Zhang Y, Yin K, Jiang S. Perfluorooctanesulfonate induces neuroinflammation through the secretion of TNF-α mediated by the JAK2/STAT3 pathway. *Neurotoxicology*. (2018) 66:32–42. doi: 10.1016/j.neuro.2018.03.003
25. Pfau ML, Russo SJ. Neuroinflammation Regulates cognitive impairment in socially defeated mice. *Trends Neurosci*. (2016) 39:353–5. doi: 10.1016/j.tins.2016.04.004
26. Yang X, He G, Hao Y, Chen C, Li M, Wang Y, et al. The role of the JAK2-STAT3 pathway in pro-inflammatory responses of EMF-stimulated N9 microglial cells. *J Neuroinflammation*. (2010) 7:54. doi: 10.1186/1742-2094-7-54
27. Chavant F, Favrelière S, Lafay-Chebassier C, Plazanet C, Pérault-Pochat MC. Memory disorders associated with consumption of drugs: updating through a case/noncase study in the French PharmacoVigilance database. *Br J Clin Pharmacol*. (2011) 72:898–904. doi: 10.1111/j.1365-2125.2011.04009.x
28. Mokhber N, Abdollahian E, Soltanifar A, Samadi R, Saghebi A, Haghighi MB, et al. Comparison of sertraline, venlafaxine and desipramine effects on depression, cognition and the daily living activities in Alzheimer patients. *Pharmacopsychiatry*. (2014) 47:131–40. doi: 10.1055/s-0034-1377041
29. Szkutnik-Fiedler D, Kus k, Ratajczak P, Antoniów M, Nowakowska E, Grześkowiak E. Coadministration of tramadol with aripiprazole and venlafaxine–The effect on spatial memory functions in male rats. *Pharmacol Rep*. (2016) 68:451–6. doi: 10.1016/j.pharep.2015.11.003
30. Nowakowska E, Kus K, Bobkiewicz-Kozłowska T, Hertmanowska H. Role of neuropeptides in antidepressant and memory improving effects of venlafaxine. *Pol J Pharmacol*. (2002) 54:605–13.
31. Zhang Y, Bi X, Adebiyi O, Wang J, Mooshekhian A, Cohen J, et al. Venlafaxine improves the cognitive impairment and depression-like behaviors in a cuprizone mouse model by alleviating demyelination and neuroinflammation in the brain. *Front Pharmacol*. (2019) 10:332. doi: 10.3389/fphar.2019.00332
32. Santos Jr JG, Do Monte FHM, Russi M, Agustine PE, Lanziotti VMNB. Proconvulsant effects of high doses of venlafaxine in pentylenetetrazole-convulsive rats. *Braz J Med Biol Res*. (2002) 35:469–72. doi: 10.1590/S0100-879X2002000400010
33. Redrobe JP, Bourin M, Colombel MC, Baker GB. Dose-dependent noradrenergic and serotonergic properties of venlafaxine in animal models indicative of antidepressant activity. *Psychopharmacology*. (1998) 138:1–8. doi: 10.1007/s002130050638
34. Rossi DV, Valdez M, Gould GG, Hensler JG. Chronic administration of venlafaxine fails to attenuate 5-HT1A receptor function at the level of receptor-G protein interaction. *Int J Neuropsychopharmacol*. (2006) 9:393–406. doi: 10.1017/S1461145705005754
35. Ida Y, Tanaka M, Kohno Y, Nakagawa R, Iimori K, Tsuda A, et al. Effects of age and stress on regional noradrenaline metabolism in the rat brain. *Neurobiol Aging*. (1982) 3:233–6. doi: 10.1016/0197-4580(82)90044-6
36. Liu KY, Kievit RA, Tsvetanov KA, Betts MJ, Düzel E, Rowe JB, Howard RCC, Hämmerer D. Noradrenergic-dependent functions are associated with age-related locus coeruleus signal intensity differences. *Nat Commun*. (2020) 11:1712. doi: 10.1038/s41467-020-15410-w
37. Cibelli M, Fidalgo AR, Terrando N, Ma D, Monaco C, Feldmann M, et al. Role of interleukin-1beta in postoperative cognitive dysfunction. *Ann Neurol*. (2010) 68:360–8. doi: 10.1002/ana.22082
38. Vacas S, Degos V, Feng X, Maze M. The neuroinflammatory response of postoperative cognitive decline. *Br Med Bull*. (2013) 106:161–78. doi: 10.1093/bmb/ldt006
39. Wang Z, Meng S, Cao L, Chen Y, Zuo Z, Peng S. Critical role of NLRP3-caspase-1 pathway in age-dependent isoflurane-induced microglial inflammatory response and cognitive impairment. *J Neuroinflammation*. (2018) 151:109. doi: 10.1186/s12974-018-1137-1
40. Collinson N, Kuenzi FM, Jarolimek W, Maubach KA, Cothliff R, Sur C, et al. Enhanced learning and memory and altered GABAergic synaptic transmission in mice lacking the alpha 5 subunit of the GABAA receptor. *J Neurosci*. (2002) 22:5572–80. doi: 10.1523/JNEUROSCI.22-13-05572.2002
41. Wang DS, Zurek AA, Lecker I, Yu J, Abramian AM, Avramescu S, et al. Memory deficits induced by inflammation are regulated by α5-subunit-containing GABAA receptors. *Cell Rep*. (2012) 2:488–96. doi: 10.1016/j.celrep.2012.08.022
42. Chen S, Dong Z, Cheng M, Zhao Y, Wang M, Sai N, et al. Homocysteine exaggerates microglia activation and neuroinflammation through microglia localized STAT3 overactivation following ischemic stroke. *J Neuroinflammation*. (2017) 14:187. doi: 10.1186/s12974-017-0963-x
43. Li X, Sun Y, Jin Q, Song D, Diao Y. Kappa opioid receptor agonists improve postoperative cognitive dysfunction in rats via the JAK2/STAT3 signaling pathway. *Int J Mol Med*. (2019) 44:1866–76. doi: 10.3892/ijmm.2019.4339
44. Hajhashemi V, Minaiyan M, Banafshe HR, Mesdaghinia A, Abed A. The anti-inflammatory effects of venlafaxine in the rat model of carrageenan-induced paw edema. *Iran J Basic Med Sci*. (2015) 18:654–8.
45. Wang HL, Ma RH, Fang H, Xue ZG, Liao QW. Impaired spatial learning memory after isoflurane anesthesia or appendectomy in aged mice is associated with microglia activation. *J Cell Death*. (2015) 8:9–19. doi: 10.4137/JCD.S30596
46. Cao Y, Li Z, Ma L, Ni C, Li L, Yang N, et al. Isoflurane-induced postoperative cognitive dysfunction is mediated by hypoxia-inducible factor-1α-dependent neuroinflammation in aged rats. *Mol Med Rep*. (2018) 17:7730–6. doi: 10.3892/mmr.2018.8850
47. Ciranna L. Serotonin as a modulator of glutamate- And GABA-mediated neurotransmission: implications in physiological functions and in pathology. *Curr Neuropharmacol*. (2006) 4:101–14. doi: 10.2174/157015906776359540
48. Kalkman HO, Feuerbach D. Antidepressant therapies inhibit inflammation and microglial M1-polarization. *Pharmacol Ther*. (2016) 163:82–93. doi: 10.1016/j.pharmthera.2016.04.001
49. Leibinger M, Andreadaki A, Diekmann H, Fischer D. Neuronal STAT3 activation is essential for CNTF- and inflammatory stimulation-induced CNS axon regeneration. *Cell Death Dis*. (2013) 4:e805. doi: 10.1038/cddis.2013.310
50. Guéniot L, Lepere V, De Medeiros GF, Danckaert A, Flamant P, Le Dudal M, et al. Muscle injury induces postoperative cognitive dysfunction. *Sci Rep*. (2020) 10:2768. doi: 10.1038/s41598-020-59639-3
51. Feng X, Valdearcos M, Uchida Y, Lutrin D, Maze M, Koliwad SK. Microglia mediate postoperative hippocampal inflammation and cognitive decline in mice. *JCI Insight*. (2017) 2:e91229. doi: 10.1172/jci.insight.91229
52. Callaway JK, Jones NC, Royse CF. Isoflurane induces cognitive deficits in the morris water maze task in rats. *Eur J Anaesthesiol*. (2012) 29:239–45. doi: 10.1097/EJA.0b013e32835103c1

Conflict of Interest: The authors declare that the research was conducted in the absence of any commercial or financial relationships that could be construed as a potential conflict of interest.

Copyright © 2021 Li and Zhang. This is an open-access article distributed under the terms of the Creative Commons Attribution License (CC BY). The use, distribution or reproduction in other forums is permitted, provided the original author(s) and the copyright owner(s) are credited and that the original publication in this journal is cited, in accordance with accepted academic practice. No use, distribution or reproduction is permitted which does not comply with these terms.

frontiers in Pharmacology

ORIGINAL RESEARCH
published: 05 March 2021
doi: 10.3389/fphar.2021.613105

Effects of Interleukin-1β in Glycinergic Transmission at the Central Amygdala

*Jocelyn Solorza[1,2†], Carolina A. Oliva[3†], Karen Castillo[4†], Gabriela Amestica[1], María Constanza Maldifassi[4], Xaviera A. López-Cortés[5], Rafael Barra[6], Jimmy Stehberg[7], Matthias Piesche[8,9], Patricio Sáez-Briones[10], Wendy González[2,11], Mauricio Arenas-Salinas[2] and Trinidad A. Mariqueo[1]**

[1]Center for Medical Research, Laboratory of Neuropharmacology, School of Medicine, Universidad de Talca, Talca, Chile, [2]Centro de Bioinformática, Simulación y Modelado (CBSM), Facultad de Ingeniería, Universidad de Talca, Talca, Chile, [3]Institute of Biomedical Sciences, Faculty of Medicine, Universidad Andrés Bello, Santiago, Chile, [4]Centro Interdisciplinario de Neurociencia de Valparaíso, Facultad de Ciencias, Universidad de Valparaíso, Valparaíso, Chile, [5]Department of Computer Science and Industries, Faculty of Engineering Science, Universidad Católica del Maule, Talca, Chile, [6]Centro de Investigación Biomédica y Aplicada (CIBAP), Escuela de Medicina, Facultad de Ciencias Médicas, Universidad de Santiago de Chile (USACH), Santiago, Chile, [7]Faculty of Biological Sciences and Faculty of Medicine, Instituto de Ciencias Biomédicas, Universidad Andres Bello, Santiago, Chile, [8]Laboratory of Biomedical Research, Medicine Faculty, Universidad Católica del Maule, Talca, Chile, [9]Oncology Center, Medicine Faculty, Universidad Católica del Maule, Talca, Chile, [10]Laboratory of Neuropharmacology and Behavior, School of Medicine, Faculty of Medical Sciences, Universidad de Santiago de Chile (USACH), Santiago, Chile, [11]Millennium Nucleus of Ion Channels-Associated Diseases (MiNICAD), Universidad de Talca, Talca, Chile*

OPEN ACCESS

Edited by:
Flavia Eugenia Saravia, Universidad de Buenos Aires, Argentina

Reviewed by:
Thomas Heinbockel, Howard University, United States
Marco Milanese, University of Genoa, Italy

***Correspondence:**
Trinidad A. Mariqueo
tmariqueo@utalca.cl
tmc@ciq.uchile.cl

†These authors have contributed equally to this work

Specialty section:
This article was submitted to Neuropharmacology, a section of the journal Frontiers in Pharmacology

Received: *01 October 2020*
Accepted: *19 January 2021*
Published: *05 March 2021*

Citation:
Solorza J, Oliva CA, Castillo K, Amestica G, Maldifassi MC, López-Cortés XA, Barra R, Stehberg J, Piesche M, Sáez-Briones P, González W, Arenas-Salinas M and Mariqueo TA (2021) Effects of Interleukin-1β in Glycinergic Transmission at the Central Amygdala. Front. Pharmacol. 12:613105. doi: 10.3389/fphar.2021.613105

Interleukin-1β (IL-1β) is an important cytokine that modulates peripheral and central pain sensitization at the spinal level. Among its effects, it increases spinal cord excitability by reducing inhibitory Glycinergic and GABAergic neurotransmission. In the brain, IL-1β is released by glial cells in regions associated with pain processing during neuropathic pain. It also has important roles in neuroinflammation and in regulating NMDA receptor activity required for learning and memory. The modulation of glycine-mediated inhibitory activity via IL-1β may play a critical role in the perception of different levels of pain. The central nucleus of the amygdala (CeA) participates in receiving and processing pain information. Interestingly, this nucleus is enriched in the regulatory auxiliary glycine receptor (GlyR) β subunit (βGlyR); however, no studies have evaluated the effect of IL-1β on glycinergic neurotransmission in the brain. Hence, we hypothesized that IL-1β may modulate GlyR-mediated inhibitory activity via interactions with the βGlyR subunit. Our results show that the application of IL-1β (10 ng/ml) to CeA brain slices has a biphasic effect; transiently increases and then reduces sIPSC amplitude of CeA glycinergic currents. Additionally, we performed molecular docking, site-directed mutagenesis, and whole-cell voltage-clamp electrophysiological experiments in HEK cells transfected with GlyRs containing different GlyR subunits. These data indicate that IL-1β modulates GlyR activity by establishing hydrogen bonds with at least one key amino acid residue located in the back of the loop C at the ECD domain of the βGlyR subunit. The present results suggest that IL-1β in the CeA controls glycinergic neurotransmission, possibly via interactions with the βGlyR subunit. This effect could be relevant for understanding how IL-1β released by glia modulates central processing of pain, learning and memory, and is involved in neuroinflammation.

Keywords: interleukin-1β, auxiliary subunit, glycine receptors, beta subunit, central amygdala (CeA), neuroimmune communication

INTRODUCTION

The Central Nervous System (CNS) performs an orchestrated innate immune response to painful injury (Watkins and Maier, 2002; Xu et al., 2020). During chronic pain development, several inflammatory mediators participate in the loss of spinal and supra-spinal inhibition, leading to hyperexcitability of pain-associated circuits (Ji et al., 2018; Maydych, 2019; Mariqueo and Zúñiga-Hernández, 2020). Proinflammatory cytokines including IL-1β, participate actively in pain sensitization (Ferreira et al., 1988; Sommer and Kress, 2004), inducing hyperalgesia and allodynia (Tadano et al., 1999; Wei et al., 2012). These effects are mediated via spinal modulation of GABAergic and glycinergic inhibitory synaptic transmission (Kawasaki et al., 2008; Chirila et al., 2014; Patrizio et al., 2017), by decreasing glycine receptor activity in lamina II postsynaptic interneurons (Chirila et al., 2014), and hence, reducing glycinergic inhibitory control of spinal excitability.

While the role of spinal IL-1β in pain processing has been widely studied, information on the effects of IL-1β at the supra-spinal level is rather precarious. In the brain, IL-1β is released by astrocytes and microglia in response to various proinflammatory stimuli (Sugama et al., 2011; González et al., 2014). Increased IL-1β in brain regions relevant for pain processing such as the hippocampus, prefrontal cortex and amygdala have been reported during neuropathic pain establishment (del Rey et al., 2011; Al-Amin et al., 2011; Gui et al., 2016).

No study to date has evaluated the effects of IL-1β on glycinergic activity at supra-spinal regions. Together with $GABA_A$ receptors, GlyRs regulate neuronal excitability in the CNS, including regions that are critical for central nociceptive processing, such as the spinal cord (Gradwell et al., 2017), thalamus (Molchanova et al., 2018), prefrontal cortex (Liu et al., 2015), nucleus accumbens (Muñoz et al., 2018), hippocampus (Aroeira et al., 2011), periaqueductal gray (PAG) (Choi et al., 2013) and amygdala (Delaney et al., 2010).

Glycine receptors are pentameric ligand-gated chloride channels that control synaptic inhibition in the CNS (Thompson et al., 2010; Burgos et al., 2016). GlyRs can be assembled as homopentamers of four types of α subunits (α(1–4)GlyR subunits), or heteropentamers forming complexes with the auxiliary β subunit (βGlyR), in a proposed 3α2β or 2α3β conformation (Grudzinska et al., 2005). The auxiliary βGlyR subunit is unable to form functional channels without αGlyR subunits (Galaz et al., 2015). However, βGlyR affects the establishment of inhibitory synapses by an intracellular interaction with the scaffolding protein Gephyrin (Maric et al., 2011) and modulates the pharmacological profile of glycinergic currents (Bormann et al., 1993). Both αGlyR and βGlyR subunits share common structural characteristics, including a N-terminal extracellular domain (ECD), four transmembrane domains (TMD), and a large intracellular loop (ICD) between TM3 and TM4 (Lynch, 2004).

The role of spinal GlyRs in chronic pain sensitization has been broadly investigated. Using Prostaglandin E2 (PGE2) as a pro-inflammatory mediator to induce peripheral and central inflammatory pain sensitization, it was reported that PGE2 stimulates the intracellular phosphorylation of α3GlyR subunits to reduce glycinergic inhibitory neurotransmission control (Moraga-Cid et al., 2020). The role of α3GlyR subunits in PGE2-induced pain sensitization is further supported by a study showing that PGE2-induced pain sensitization was reduced in mice lacking α3GlyR subunits (*Glra3*−/− Knockout mice) (Harvey et al., 2004). Interestingly, it has been proposed that the auxiliary βGlyR subunit blocks α3GlyR subunit phosphorylation by steric hindrance, as the βGlyR ICD loop is larger than that of α3GlyR subunits (Acuña et al., 2016). The βGlyR subunit shows widespread expression in the CeA nucleus (Delaney et al., 2010), which is involved in the cognitive and emotional integration of peripheral nociceptive pain (Cai et al., 2018). CeA neural circuits integrate cortical inputs to assign valence to peripheral nociceptive stimuli (Pessoa and Adolphs, 2010), and increased excitability in CeA circuits has been associated to reduced inhibitory control during the establishment of neuropathic pain (Ikeda et al., 2007; Jiang et al., 2014). The role of GlyRs at the CeA level has not been explored to date. Given that IL-1β induces hyperalgesia by reducing glycinergic activity in the spinal cord, here we studied whether IL-1β can modulate GlyR activity in the CeA. Furthermore, we evaluated the possibility that IL-1β modulates GlyR activity via interactions with the βGlyR auxiliary subunit.

MATERIALS AND METHODS

Animals

Male Sprague-Dawley (SD) rats (250–350 g) were obtained from the Animal Facility of University of Chile. Animal care and experimental protocols for this study were approved by the Institutional Animal Use Committee of University of Chile (N°17027-MED-UCH) and followed the guidelines for ethical protocols and animal care established by the National Institute of Health, MD, United States and the International Association for the Study of Pain in conscious animals. Every effort was made to minimize animal suffering.

Animals were bred and housed in controlled laboratory conditions, received standard rat chow diet and water *ad libitum* and were housed on a 12-h light/dark cycle at a constant room temperature of 23°C.

Homology Modeling and Molecular Simulations

We constructed a three-dimensional (3D) molecular model of the heteropentameric GlyR (2α1:3β) based on the X ray crystal structure of α1GlyR subunits from zebrafish (Du et al., 2015a) (Protein Data Bank ID code: 3JAE; Resolution: 3.9 Å). The software MODELLER version 9.18 was used to build the homology models for all sets of receptors (Šali and Blundell, 1993). The GlyR was oriented towards the z axis and embedded in a membrane composed by POPC (1-palmitoyl-2-oleoyl-sn-glycero-3-phosphocholine) lipids. The system was solvated in a water periodic box (162 × 160 × 123 Å) of TIP3 water molecules and ionized at 0.15 mM NaCl. The initial conformations of each

system were subjected to cycles of energy minimization of 10,000 steps and further equilibrated by molecular dynamics of 20 ns with α carbons restrained, in order to relax the conformation of the lateral chains and avoid conformation tension generated during the construction of the model. The calculations were performed using NAMD software and the CHARMM36 united-atom force field for membrane lipids and the CHARMM27 force field with the CMAP correction for proteins (Phillips et al., 2005). All analyses were performed using the VMD software (Humphrey et al., 1996). To study the interaction of IL-1β with the GlyR, the crystal structure of the IL-1β Receptor complex bound to IL-1β (ID code: 3O4O; Resolution: 3.3 Å; RValue: 0.29) was used to build the IL-1β homology model. All models were validated using PROCHEK (Laskowski et al., 1993).

Docking Simulations

Protein-protein interactions between GlyR with IL-1β were explored. The system was named 2α1:3β-IL-1β (heteropentameric α1βGlyR conformation bound to IL-1β). In order to study the putative interactions between IL-1β and the 2α1:3β GlyR the ClusPro2.0 server was used (https://cluspro.org). ClusPro2.0 is based on three key computational stages. First, an extensive sampling of conformations on a rigid-body docking was performed. Then, resulting conformations were grouped by RMSD according to those with the lowest energy, and finally, a refinement of the structures was performed by energy minimizations. Clusters were classified using electrostatic and Van der Waals interactions. Clusters with sizes greater than the sum of their average plus twice their standard deviation were considered representative, as previously reported (Bottegoni et al., 2006).

Site Directed Mutagenesis

Point mutations in the βGlyR subunit were made using a QuikChange kit from Agilent Technologies (Santa Clara, CA, United States), following the manufacturer's instructions, and checked by sequencing (Macrogen), using the following primers GlyRY240A: Forward: tgatattaaaaaggaggatatcgaagctggcaactgtac aaaat and Reverse: attttgtacagttgccagcttcgatatcctccttttaatatca.

Cell Culture and Expression of Recombinant GlyRs

Human embryonic kidney 293 cells (HEK293T) were cultured in Dulbecco's modified Eagle's medium supplemented with L-glutamine DMEM-GlutaMAX (Gibco) and 10% fetal bovine serum (Lonza Basel, Switzerland) at 37 °C and 5% CO_2. Once the cells reached 60–70% confluence, they were transfected with a pcDNA3.1 plasmid containing either the rat αGlyR subunit, rat βGlyR subunit (NovoPro Biosciences) or site mutated rat Y240AβGlyR subunits, using the Effectene transfection kit (Qiagen). GlyR subunits were co-transfected with CD-8 as reporter, and labeled using Dynabeads coupled with anti-CD8 antibody (Invitrogen). Cells were transfected with 0.3 μg total DNA at a co-transfection ratio 1:2:0.1 or 1:0.1 for heteropentameric α1GlyR:βGly:CD8 or homopentameric α1GlyR:CD8, respectively. Cell cultures were incubated for 24 h with the Effectene-DNA complexes, followed by trypsinization and seeding in poly-l coated 12 mm coverslips at a density of 300,000 cells/μl. Electrophysiology experiments were performed 48 h after transfection, in 12-mm glass coverslips coated with poly-lysine (Sigma-Aldrich).

Patch Clamp Recordings in Cultured Cells

Patch Clamp recordings in whole cell configuration where used to measure evoked current amplitudes on transiently transfected HEK293T cells at −60 mV holding potential. Patch electrodes (3.0–5.0 MΩ) were pulled from borosilicate glass (World Precision Instruments, INC 1B150F-4) in a Sutter P97 puller (Sutter Instruments, Novato, CA, United States) and filled with an internal solution buffer composed of (in mM): 140 CsCl, 10 BAPTA, 10 HEPES, 4 $MgCl_2$, 2 ATP, 0.5 GTP. The external solution buffer was composed of (in mM): 140 NaCl, 3 KCl, 10 HEPES, 1.3 Mg_2Cl and 2.4 $CaCl_2$ and 10 glucose. Axopatch 200B amplifier (Molecular Devices, Sunnyvale, CA, United States) in conjunction with an I/O board NI 6221 PCI (National Instruments) and the Strathclyde electrophysiology software WinWCP (University of Strathclyde, UK) were used for data acquisition. EC_{50} and nHill values were obtained experimentally from a normalized dose response curve using data points from the evoked currents in response to 30, 50, 100, 300 and 1,000 μM of glycine, using a nonlinear algorithm in the GraphPad Prism 6 software. The dose-response curves were fitted to Hill's equation:

$$Iglycine = Imax * \frac{[glycine]}{EC_{50}^{nHill} + [glycine]^{nHill}}$$

The current evoked at a determined concentration (I glycine), the maximal current obtained at saturating concentrations of glycine (I max), the concentration of glycine to reach the half maximal current response (EC_{50}) and the Hill coefficient (nHill), which indicates cooperativity in the binding of glycine to GlyR (Hussein et al., 2019), were estimated from the dose response curves. Perfusion experiments were performed by evoking currents with 50 μM glycine pulses. Then IL-1β (10 ng/ml) was perfused for 60 s, followed by intermittent 50 μM glycine pulses in 10 s intervals until sensitivity was restored. All experiments were performed at room temperature (20°–21°C). These currents were analyzed by fitting a single exponential function to adjust the decay time constant.

Patch Clamp Recordings in Central Amygdala Slices: Rat Brain Slice Preparation and Electrophysiological Measurements

Four male SD rats were anesthetized with isoflurane and then decapitated. Their brains were rapidly removed and placed in a beaker with cold artificial cerebrospinal solution (ACSF) composed of (in mM): 85 NaCl, 75 sucrose, 3 KCl, 1.25 NaH_2PO_4, 25 $NaHCO_3$, 10 dextrose, 3.5 $MgSO_4$, 0.5 $CaCl_2$, 3 sodium pyruvate, 0.5 sodium L-ascorbate and 3 myo-inositol (305 mOsm, pH 7.4 with 95% O_2/5% CO_2). Two coronal slices of

300 μm from each hemisphere were obtained from each animal using a vibratome and left for 1 h at 36°C in the ACSF solution. Then the ACSF solution was replaced with a "recording solution," composed of (in mM): 126 NaCl, 3.5 KCl, 1.25 NaH_2PO_4, 25 $NaHCO_3$, 10 dextrose, 1 $MgSO_4$, 2 $CaCl_2$, 3 sodium pyruvate, 0.5 sodium L-ascorbate and 3 myo-inositol (305 mOsm, pH 7.4 with 95% O_2/5% CO_2) at room temperature (22°C). Slices were recorded in a submerged-style chamber solution with recording solution at 30–32°C, under an upright infrared-differential interference contrast (IR-DIC) fluorescence microscope (Eclipse FNI, Nikon) equipped with a 40× water objective. Voltage-clamp whole cell recordings were performed in the soma of visually identified neurons in the CeA. We used a borosilicate glass electrode (World Precision Instruments, Sarasota, FL, United States) pulled on a P-97 Flaming/Brown Micropipette Puller (Sutter Instruments, Novato, CA, United States). The glass pipette, ranging from 3.5 to 4.2 MΩ, was filled with intracellular solution containing the following (in mM): 130 Cs-gluconate, 3.5 CsCl, 4 ATP-Mg, 0.3 GTP-Na, 10 Na-phosphocreatine, 1 EGTA, 10 HEPES and 0.4% Biocytin (286 mOsm, pH 7.4 adjusted with CsOH). After seal formation and successful transition to whole-cell configuration, access resistance usually between 4 and 15 MΩ, was continuously monitored; series resistance was monitored and compensated between 75 and 80%. Glycine-mediated currents were isolated in the presence of synaptic blockers CNQX (10 μM), APV (50 μM), and picrotoxin (50 μM) to block AMPAR, NMDAR and $GABA_A$ receptors, respectively. The spontaneous inhibitory postsynaptic currents (sIPSCs) obtained as outward currents were recorded at a holding potential of +20 mV. The remaining sIPSCs obtained after further application of bicuculline (10 μM) was considered glycine-based sIPSC. At the end of the recordings, strychnine was applied to block glycinergic currents and thus confirm that the observed currents were glycinergic. We used PClamp detection events to choose single events of about 3–10 pA that were greater than peak to peak noise, to analyze their amplitude, area, and decay constant. Spontaneous synaptic events were detected over 100 s of continuous recording, and two different times following IL-1β application were analyzed (10 ng/ml, at 5 and 15 min). For these experiments, 16 slices out of 4 animals were recorded, and 13 cells were selected for the calculations (the criterium was the recording with stable input resistance (R_{in}) along the experiment). Voltage-clamp signals were acquired using a MultiClamp 700B amplifier (Axon CNS, Molecular Devices LLC), low-pass filtered at 10 kHz, digitally sampled at 30 kHz and recorded through a Digidata-1440A interface (Axon CNS, Molecular Devices) and PClamp 10.3 software.

Statistical Analysis

The results are expressed as mean ± standard error of the mean (SEM). We used one-way analysis of variance (ANOVA) to determine the effects of IL-1β treatment, followed by a Bonferroni's *post hoc* test. The threshold for statistical significance was set at $p < 0.05$, with a 95% confidence interval. Statistical analyses were performed using Prism software (GraphPad, United States).

RESULTS

IL-1β Modulated Glycinergic Currents in Central Amygdala Slices

To determine whether IL-1β can modulate GlyR activity in the CeA, we performed whole-cell voltage-clamp recordings in CeA neurons from brain slices. Representative traces of isolated spontaneous inhibitory postsynaptic glycinergic currents (sIPSCs), before (Control) and during the application of IL-1β, are presented in **Figure 1A**. We generated an amplitude distribution plot of the events recorded in all the slices/cells. We observed that the application of IL-1β induced a significant change in the amplitude distribution of sIPSCs, from the beginning of IL-1β perfusion (5 min), and up to 15 min afterward (**Figure 1B**). GlyR currents transiently shifted toward events of higher amplitude after 5 min of IL-1β perfusion, and reduced the events in all the amplitudes after 15 min (See the table with summarized values). The cumulative probability distribution of the amplitudes showed that the half-probability is transiently shifted to the right at the beginning of IL-1β perfusion. At 15 min, the half-probability is similar to the control. However, the curve is accelerated by the effects of IL-1β (**Figure 1C**).

The analysis of the mean current amplitude, frequency, and decay constant (tau) is summarized in **Figure 1D**. We compared the control average with the 5 and 15 min time points after IL-1β perfusion. The data showed that IL-1β transiently and significantly modulated spontaneous glycine current amplitudes (control: 20.4 ± 0.22 pA; IL-1β 5 min: 23.7 ± 0.18 pA; IL-1β 15 min: 19.5 ± 0.23 pA; $*p < 0.05$, $***p < 0.001$; **Figure 1D**, left). Instead, IL-1β did not significantly change the frequency of spontaneous glycinergic activity (control: 0.15 ± 0.01 Hz; IL-1β 5 min: 0.18 ± 0.02 Hz; IL-1β 15 min: 0.15 ± 0.02 Hz; **Figure 1D**, middle). However, the presence of IL-1β did transiently increase the decay time constant of the current (control: 7.2 ± 0.72 ms; IL-1β $_{5min}$: 18.4 ± 0.5 ms; IL-1β $_{15min}$: 8.6 ± 0.9 ms; $***p < 0.001$). These analyses suggest that IL-1β can dynamically modulate the amplitude and decay time constant of spontaneous isolated glycinergic currents, suggesting a modulatory effect on GlyR subunits in the CeA.

The Effects of IL-1β on GlyRs is Mediated by an Interaction with the Auxiliary βGlyR Subunit

Previous studies demonstrated that auxiliary βGlyR subunit is broadly expressed in the CeA (Delaney et al., 2010). To determine if βGlyR subunit could be involved in the effects of IL-1β, we constructed a three-dimensional (3D) molecular model of the heteropentameric GlyR (2α1:3β) and IL-1β based on the most complete X-ray crystal structure of α1GlyR available, which was obtained from zebrafish (PDBid: 3JAE) and the IL-1β (PDBid: 3o4o). Several three-dimensional reconstructions of αGlyR structure are available, but they are only partial (Du et al., 2015b; Huang et al., 2017; Moraga-Cid et al., 2015). We modeled the ECD and TMD of the βGlyR subunit since there is no available crystallographic structure of the ICD. The sequence identity between both proteins is nearly 50%, which is acceptable

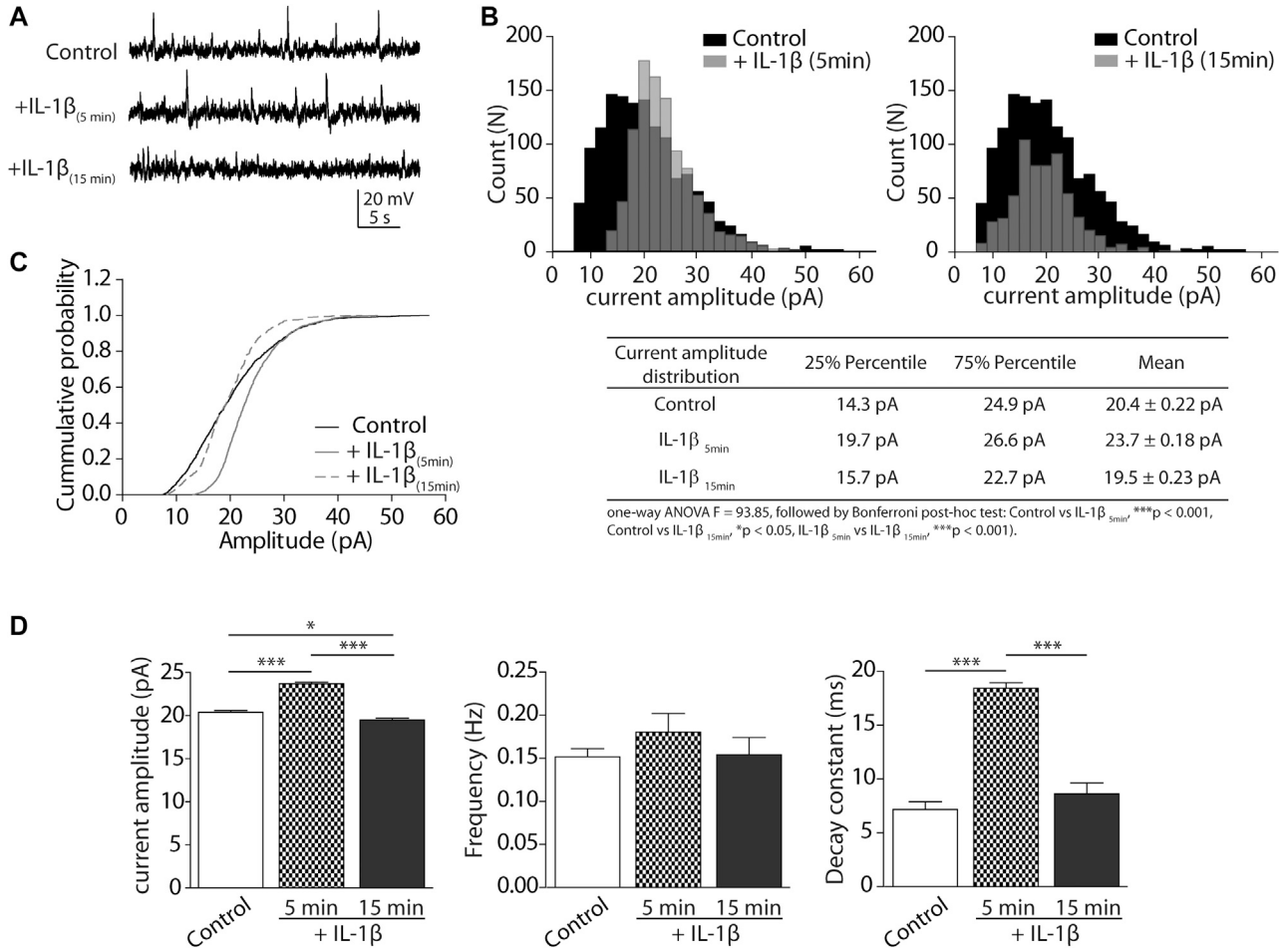

Current amplitude distribution	25% Percentile	75% Percentile	Mean
Control	14.3 pA	24.9 pA	20.4 ± 0.22 pA
IL-1β $_{5min}$	19.7 pA	26.6 pA	23.7 ± 0.18 pA
IL-1β $_{15min}$	15.7 pA	22.7 pA	19.5 ± 0.23 pA

one-way ANOVA F = 93.85, followed by Bonferroni post-hoc test: Control vs IL-1β $_{5min}$, ***p < 0.001, Control vs IL-1β $_{15min}$, *p < 0.05, IL-1β $_{5min}$ vs IL-1β $_{15min}$, ***p < 0.001).

FIGURE 1 | Glycinergic sIPSCs are modulated by IL-1β in CeA neurons of rat. **(A)** Representative synaptic sIPSC glycinergic currents in the presence of CNQX (10 μM), APV (50 μM), picrotoxin (50 μM), bicuculline (10 μM), clamped at +20 mV, 5 and 15 min after incubation with IL-1β. **(B)** Upper: Event distribution histograms of sIPSCs amplitudes before (black bars) and after IL-1β application (gray bars). Below: table with summarized analysis and statistics of distribution histograms **(C)** Cumulative probability histogram of amplitude in CeA neurons before (black line), 5 min (gray line) and 15 min (discontinuous line) after incubation with IL-1β. **(D)** Graphical representation of the mean ± SEM (n = 4 rats, 13 cells) of glycinergic sIPSC currents parameters: amplitude (pA), frequency (Hz) and decay time (ms). One-way ANOVA and Bonferroni post-hoc test (*p < 0.05 and ***p < 0.001).

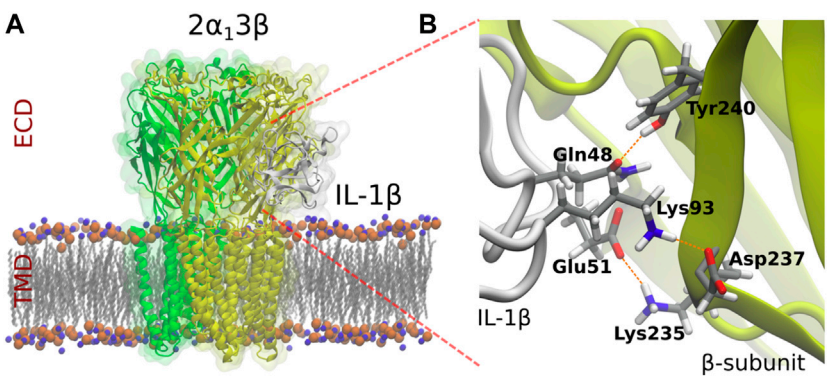

FIGURE 2 | Molecular model of heteropentameric 2α1:3β GlyRs and identification of the residues which putatively interact with IL-1β. αGlyR, βGlyR subunits and IL-1β are represented in green, yellow and grey, respectively.

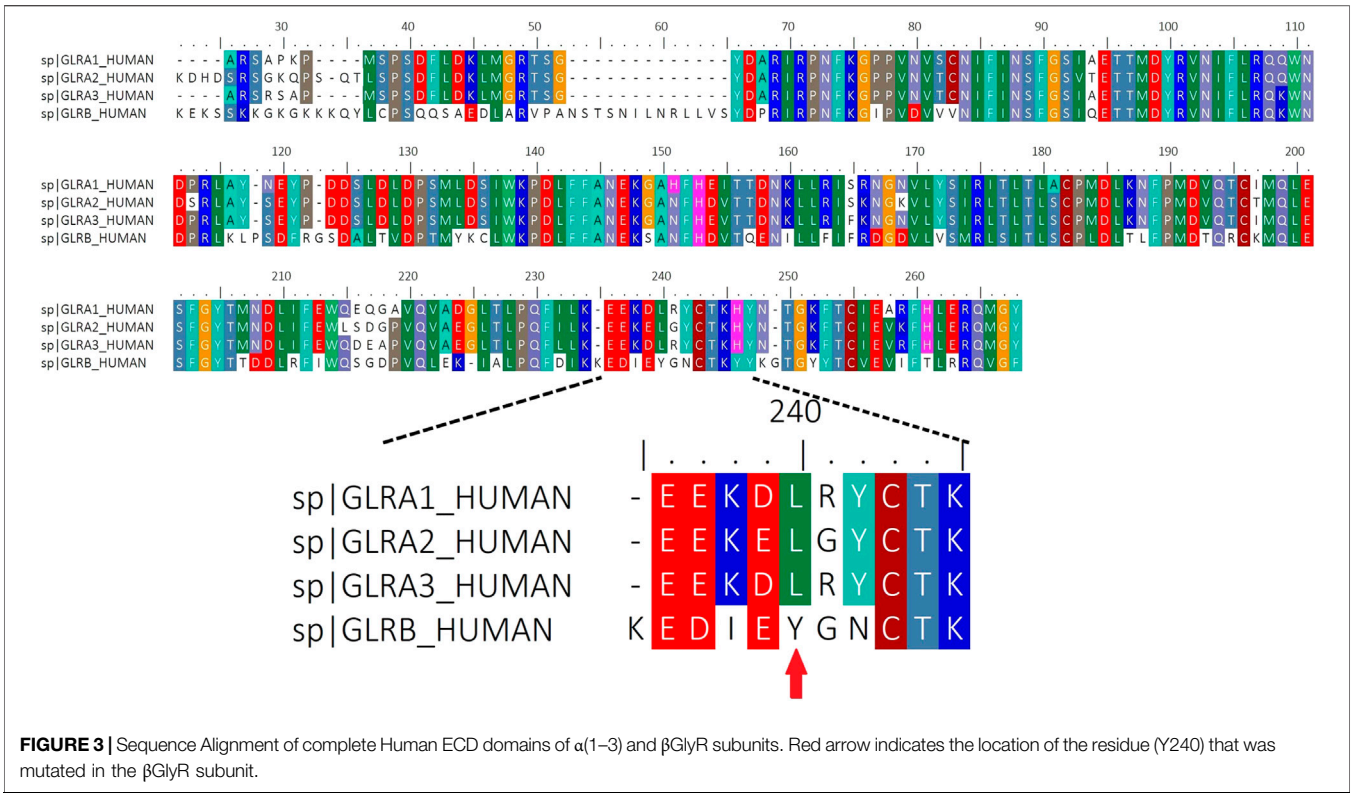

FIGURE 3 | Sequence Alignment of complete Human ECD domains of α(1–3) and βGlyR subunits. Red arrow indicates the location of the residue (Y240) that was mutated in the βGlyR subunit.

for this type of procedure (Burgos et al., 2016). We carried out protein-protein coupling experiments to predict the binding modes of IL-1β on the heteromeric GlyR. The system 2α1:3β-IL-1β showed a representative cluster (*See* **Supplementary Appendix S1**). Finally, the result was enhanced on Rosie (Rosseta Online Server, https://rosie.graylab.jhu.edu/docking2). The relevant site identified in the interaction with the IL-1β, corresponded to the back of the loop C of β-subunit in the system 2α1:3β. Molecular Docking suggested that the residues Tyrosine 240, Lysine 235 and Aspartate 237 in the back of loop C of the ECD domain of the βGlyR subunit could have a predominant role in the modulation of IL-1β, mostly interacting through hydrogen bonds (**Figure 2A**). These residues were identified as hot spots for interactions with IL-1β (Wang et al., 2010). Besides, three important putative interactions between β-subunit and IL-1β through hydrogen bonds were described. These interactions correspond to the hydrogen bonds that were established between residues Gln48 (IL-1β)-Tyr240 (βGlyR), Glu51 (IL-1 β)-Lys235 (βGlyR) and Lys93 (IL-1β)-Asp237 (βGlyR), and showed as red dotted lines in **Figure 2B**. These results suggested that IL-1β may modulate GlyRs currents by interacting with the βGlyR auxiliary subunit, however to prove it we performed site-directed mutations.

The Modulation of Glycinergic Currents by IL-1β Is Impaired by Site-Directed Mutation in the Auxiliary βGlyR Subunit

We performed an alignment of human ECD domains of αGlyR and βGlyR subunits focusing on the domain that contains the amino acids proposed to interact with IL-1β (**Figure 3**). The Tyrosine 240 residue that was divergent in βGlyR was selected to perform a site directed mutagenesis. Then, whole-cell patch clamp electrophysiological recordings were performed on HEK293T cells transfected with α1 alone, α1β wild type (α1βWT) or α1β mutated (α1βY240A), and perfused with glycine (50 μM) and IL-1β (10 ng/ml) as already described (Kawasaki et al., 2008) (**Figure 4**). The heteropentameric α1βWT exhibited greater current decay time constant when compared to the mutated α1βY240A GlyR (**Figure 4A**; τ = 35,420 ± 2,671 ms and τ = 3,367 ± 1,684 ms, respectively (n = 3 cells from three different cultures; one-way ANOVA, $^{****}p < 0.0001$). The plotted current decay time constants of glycine-activated currents in homo- and heteropentameric GlyRs after the application of glycine or glycine + IL-1β are shown in **Figure 4B**. The effect of IL-1β significantly increases the decay time of the chloride currents in the presence of a βGlyR subunit in heteropentameric GlyRs; whereas, when the βGlyR was mutated (βY240A) the effect of IL-1β was abolished. This data shows that this subunit is important for the cytokine-induced effect in the GlyRs kinetics. Remarkably, it also suggests that the Tyrosine 240 residue from the βGlyR subunit is critical for IL-1β effects on GlyRs (**Figure 4B**). On the other hand, the EC_{50} for glycine was not affected by the mutated subunit (comparing EC_{50} of α1βWT with α1βY240A; **Figure 4C** and table), showing that the mutation affects the modulation of GlyRs by IL-1β without altering the pharmacological properties of the channel. Altogether these results suggest that IL-1β modulates GlyR activity through an interaction with the βGlyR subunit.

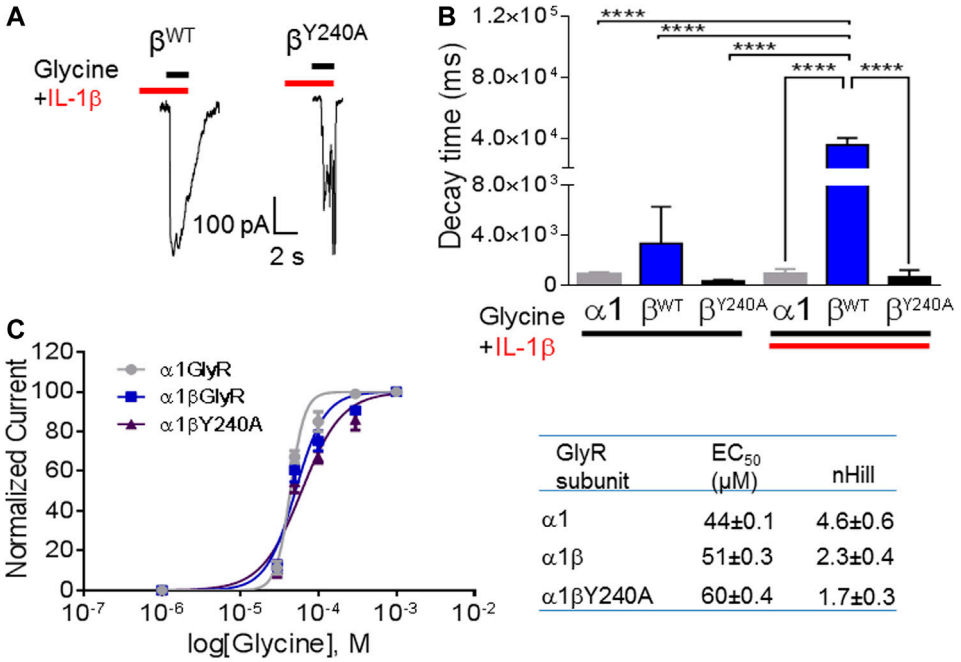

GlyR subunit	EC_{50} (μM)	nHill
α1	44±0.1	4.6±0.6
α1β	51±0.3	2.3±0.4
α1βY240A	60±0.4	1.7±0.3

FIGURE 4 | The effects of IL-1β are mediated by interaction with auxiliary βGlyR. **(A)** Representative glycine-activated currents of α1β wild type and α1βY240A after the perfusion of glycine (black line) + IL-1β (red line). **(B)**: Graphical representation of effects of glycine or glycine + IL-1β in homo and heteropentameric GlyRs. **(C)** Graphical representation of dose-response curve. Glycine activated currents at different glycine concentrations (10–1,000 μM) were normalized to a percentage of the maximal response to the application of glycine 1,000 μM in HEK293T cells transfected with different subunits of GlyRs. Data are presented as mean ± SEM.

DISCUSSION

Here, we showed that IL-1β modulates glycinergic transmission in the CeA, which is in line with previous studies showing that IL-1β decreases spinal glycinergic inhibitory neurotransmission by reducing the number and amplitude of sIPSCs events (Kawasaki et al., 2008; Chirila et al., 2014; Patrizio et al., 2017). We recorded spontaneous currents (sIPSC), this is, spontaneous postsynaptic currents generated in the absence of experimental stimulation, but by action-potential-dependent and the spontaneous release of neurotransmitter. Changes in current frequency are related to vesicular release from presynaptic sites, whereas changes in current amplitude are dependent upon activation of the postsynaptic receptors. Our results show a transient effect of IL-1β in CeA neurons lasting for minutes, suggesting that the modulation of glycinergic transmission induced by IL-1β could be modulatory and dynamic, affecting channel kinetic parameters at postsynaptic sites. Thus, in our analysis, we observed a transient increase in the amplitude of sIPSCs, probably due to increased activation of postsynaptic GlyRs, with a later reduction (after 15 min) due to a reduced activation, or inhibition, of postsynaptic GlyR. No changes related to frequency were observed, suggesting that presynaptic release of glycine was not affected by IL-1β.

Previous evidence demonstrated that clustering of GlyR is dynamically regulated depending on the subunit composition, and its mobility along the synapse is strongly dependent on the presence of α1 and β subunits (Patrizio et al., 2017). Moreover, in that report, the authors showed that IL-1β affects GlyR currents when α1β, but no other α subunits (α2,3) are present, suggesting that the effect of IL-1β is dependent on subunit-specific tissue expression. In the amygdala, the presence of α1GlyR and βGlyR is relevant, specifically in CeA, where the expression of βGlyR subunit is particularly high (Delaney et al., 2010). Our data indicate that in this region, GlyR currents are dynamically modulated by IL-1β, and this effect is specifically dependent on the presence of βGlyR. The amplitude distribution histograms were built two times after IL-1β, where we observed a shift toward the higher events. We suggest that this is part of the dynamic effect of IL-1β in the particular tissue as the amygdala. The unusual high expression of βGlyR subunit in the CeA induces the clustering of GlyRs, transiently increasing the postsynaptic currents. Later, the inhibition caused by IL-1β exerts its effect reducing significantly the currents, disaggregating the clusters. The clustering of GlyRs found in synapses is a process regulated by the auxiliary βGlyR subunit via an intracellular interaction with the scaffolding protein Gephyrin (Maric et al., 2011). The exact mechanism by which IL-1β modulates the GlyRs is unknown; however, we propose that IL-1β exerts a conformational change at the extracellular protein domain that causes changes both in channel opening and receptor clustering. Based on previous studies and our present results, it is possible to propose that IL-1β reduces glycinergic inhibitory control in CeA neurons by disaggregation of glycinergic clusters.

We performed *in silico* docking experiments using the α1βGlyR 3D structure because α1β is the predominant GlyR conformation in the mature central nervous system (Aguayo et al., 2004). Our molecular docking results show that IL-1β may

interact with the loop C at the ECD of βGlyR subunits. This structure has been implicated in the conformational rearrangement necessary for the closing of the channel (Huang et al., 2017). Accordingly, our data in transfected HEK cells show that application of IL-1β slows down the recovery of glycine activated currents in the α1βWT. A similar effect was observed in CeA slices, a region with elevated levels of βGlyR, where the decay constant was significantly increased in response to IL-1β. The effect of IL-1β on the glycine current recovery was abolished in channels formed by the βGlyR containing the Y240A mutation. This result supports the idea that IL-1β is interacting with the GlyR in a β subunit dependent binding.

Given that the release of IL-1β is increased in brain regions associated to pain processing including the amygdala in different models of chronic pain (del Rey et al., 2011; Al-Amin et al., 2011; Gui et al., 2016), it is probable that the modulation of glycinergic currents induced by IL-1β may be relevant for pain processing in the CeA. Further studies will be required to assess the role of inhibitory glycinergic currents in the processing of pain at the CeA.

However, the relevance of the present report is not limited to pain processing. The expression of IL-1β has also been reported to increase after LTP induction in the hippocampus (Schneider et al., 1998); while its blockade has been shown to facilitate hippocampus-dependent memory (Yirmiya, 2002; Avital et al., 2003; Depino et al., 2004). The expression of IL-1β in brain regions associated to pain processing, mood, and memory (such as the hippocampus and amygdala) can be associated with chronic pain perception, but also with learning deficits and depression triggered by chronic pain. How the modulation of glycinergic currents by IL-1β in the CeA and other brain regions contributes to learning impairments and mood disorders is a matter of further investigation.

In conclusion, GlyRs activity is modulated by IL-1β in the CeA, possibly via interactions with the βGlyRs auxiliary subunit. This subunit may play a critical role in central pain sensitization. Elucidation of the binding mode between IL-1β and the βGlyR subunit may offer novel possibilities for the development of new pharmacological agents with potential analgesic activity to treat chronic pain and its associated pathologies.

HIGHLIGHTS

- IL-1β modulates inhibitory synaptic transmission in the Central Amygdala
- The effect of IL-1β is mediated by the auxiliary βGlyR subunit

DATA AVAILABILITY STATEMENT

The raw data supporting the conclusions of this article will be made available by the authors, without undue reservation.

ETHICS STATEMENT

The animal study was reviewed and approved by the Institutional Animal Use Committee of the University of Chile (N17027-MED-UCH).

AUTHOR CONTRIBUTIONS

JS, KC, GA, MM, XL-C, RB, MP, PS-B, WG, and MA-S designed or performed experiments, discussed the results, reviewed the final manuscript. CO, JS, and TM designed and performed experiments, discussed the results and wrote the manuscript.

FUNDING

This work was supported by PIEI QUIMBIO University of Talca (TM), FONDECYT grant No. 3170690 (TM). CONICYT Doctoral Program Scholarship Grant No.21201001 (JS). FONDECYT Grant No.1180999 (KC). The Centro Interdisciplinario de Neurociencia de Valparaiso is a Millennium Institute supported by the Millennium Scientific Initiative of the Chilean Ministry of Economy, Development, and Tourism (P029-022-F) (KC). FONDECYT grant 1200452 (JS), FONDECYT grant No.1191133 (WG), Millennium Nucleus of Ion Channels-Associated Diseases (MiNICAD) and FONDEQUIP (WG).

SUPPLEMENTARY MATERIAL

The Supplementary Material for this article can be found online at: https://www.frontiersin.org/articles/10.3389/fphar.2021.613105/full#supplementary-material.

REFERENCES

Acuña, M. A., Yévenes, G. E., Ralvenius, W. T., Benke, D., Di Lio, A., Lara, C. O., et al. (2016). Phosphorylation state-dependent modulation of spinal glycine receptors alleviates inflammatory pain. *J. Clin. Invest.* 126, 2547–2560. doi:10.1172/JCI83817

Aguayo, L. G., van Zundert, B., Tapia, J. C., Carrasco, M. A., and Alvarez, F. J. (2004). Changes on the properties of glycine receptors during neuronal development. *Brain Res. Rev.* 47, 33–45. doi:10.1016/j.brainresrev.2004.06.007

Al-Amin, H., Sarkis, R., Atweh, S., Jabbur, S., and Saadé, N. (2011). Chronic dizocilpine or apomorphine and development of neuropathy in two animal models II: effects on brain cytokines and neurotrophins. *Exp. Neurol.* 228, 30–40. doi:10.1016/j.expneurol.2010.11.005

Aroeira, R. I., Ribeiro, J. A., Sebastião, A. M., and Valente, C. A. (2011). Age-related changes of glycine receptor at the rat hippocampus: from the embryo to the adult. *J. Neurochem.* 118, 339–353. doi:10.1111/j.1471-4159.2011.07197.x

Avital, A., Goshen, I., Kamsler, A., Segal, M., Iverfeldt, K., Richter-Levin, G., et al. (2003). Impaired interleukin-1 signaling is associated with deficits in hippocampal memory processes and neural plasticity. *Hippocampus* 13, 826–834. doi:10.1002/hipo.10135

Bormann, J., Rundström, N., Betz, H., and Langosch, D. (1993). Residues within transmembrane segment M2 determine chloride conductance of glycine receptor homo- and hetero-oligomers. *EMBO J.* 12, 3729–3737. Available at: http://www.ncbi.nlm.nih.gov/pubmed/8404844.

Bottegoni, G., Cavalli, A., and Recanatini, M. (2006). A comparative study on the application of hierarchical-agglomerative clustering approaches to organize outputs of reiterated docking runs. *J. Chem. Inf. Model.* 46, 852–862. doi:10.1021/ci050141q

Burgos, C. F., Yévenes, G. E., and Aguayo, L. G. (2016). Structure and pharmacologic modulation of inhibitory glycine receptors. *Mol. Pharmacol.* 90, 318–325. doi:10.1124/mol.116.105726

Cai, Y. Q., Wang, W., Paulucci-Holthauzen, A., and Pan, Z. Z. (2018). Brain circuits mediating opposing effects on emotion and pain. *J. Neurosci.* 38, 6340–6349. doi:10.1523/JNEUROSCI.2780-17.2018

Chirila, A. M., Brown, T. E., Bishop, R. A., Bellono, N. W., Pucci, F. G., and Kauer, J. A. (2014). Long-term potentiation of glycinergic synapses triggered by interleukin 1β. *Proc. Natl. Acad. Sci. USA* 111, 8263–8268. doi:10.1073/pnas.1401013111

Choi, K.-H., Nakamura, M., and Jang, I.-S. (2013). Presynaptic Glycine receptors increase GABAergic neurotransmission in rat periaqueductal gray neurons. *Neural Plast.* 2013, 954302. doi:10.1155/2013/954302

del Rey, A., Yau, H.-J., Randolf, A., Centeno, M. V., Wildmann, J., Martina, M., et al. (2011). Chronic neuropathic pain-like behavior correlates with IL-1β expression and disrupts cytokine interactions in the hippocampus. *Pain* 152, 2827–2835. doi:10.1016/j.pain.2011.09.013

Delaney, A. J., Esmaeili, A., Sedlak, P. L., Lynch, J. W., and Sah, P. (2010). Differential expression of glycine receptor subunits in the rat basolateral and central amygdala. *Neurosci. Lett.* 469, 237–242. doi:10.1016/j.neulet.2009.12.003

Depino, A. M., Alonso, M., Ferrari, C., del Rey, A., Anthony, D., Besedovsky, H., et al. (2004). Learning modulation by endogenous hippocampal IL-1: blockade of endogenous IL-1 facilitates memory formation. *Hippocampus* 14, 526–535. doi:10.1002/hipo.10164

Du, J., Lü, W., Wu, S., Cheng, Y., and Gouaux, E. (2015a). Glycine receptor mechanism elucidated by electron cryo-microscopy. *Nature* 526, 224–229. doi:10.1038/nature14853

Du, J., Lü, W., Wu, S., Cheng, Y., and Gouaux, E. (2015b). Glycine receptor mechanism elucidated by electron cryo-microscopy. *Nature* 526, 224–229. doi:10.1038/nature14853

Ferreira, S. H., Lorenzetti, B. B., Bristow, A. F., and Poole, S. (1988). Interleukin-1 beta as a potent hyperalgesic agent antagonized by a tripeptide analogue. *Nature* 334, 698–700. doi:10.1038/334698a0

Galaz, P., Barra, R., Figueroa, H., and Mariqueo, T. (2015). Advances in the pharmacology of lGICs auxiliary subunits. *Pharmacol. Res.* 101, 65–73. doi:10.1016/j.phrs.2015.07.026

González, H., Elgueta, D., Montoya, A., and Pacheco, R. (2014). Neuroimmune regulation of microglial activity involved in neuroinflammation and neurodegenerative diseases. *J. Neuroimmunol.* 274, 1–13. doi:10.1016/j.jneuroim.2014.07.012

Gradwell, M. A., Boyle, K. A., Callister, R. J., Hughes, D. I., and Graham, B. A. (2017). Heteromeric α/β glycine receptors regulate excitability in parvalbumin-expressing dorsal horn neurons through phasic and tonic glycinergic inhibition. *J. Physiol.* 595, 7185–7202. doi:10.1113/JP274926

Grudzinska, J., Schemm, R., Haeger, S., Nicke, A., Schmalzing, G., Betz, H., et al. (2005). The beta subunit determines the ligand binding properties of synaptic glycine receptors. *Neuron* 45, 727–739. doi:10.1016/j.neuron.2005.01.028

Gui, W.-S., Wei, X., Mai, C.-L., Murugan, M., Wu, L.-J., Xin, W.-J., et al. (2016). Interleukin-1β overproduction is a common cause for neuropathic pain, memory deficit, and depression following peripheral nerve injury in rodents. *Mol. Pain* 12, 174480691664678. doi:10.1177/1744806916646784

Harvey, R. J., Depner, U. B., Wässle, H., Ahmadi, S., Heindl, C., Reinold, H., et al. (2004). GlyR alpha3: an essential target for spinal PGE2-mediated inflammatory pain sensitization. *Science* 304, 884–887. doi:10.1126/science.1094925

Huang, X., Shaffer, P. L., Ayube, S., Bregman, H., Chen, H., Lehto, S. G., et al. (2017). Crystal structures of human glycine receptor α3 bound to a novel class of analgesic potentiators. *Nat. Struct. Mol. Biol.* 24, 108–113. doi:10.1038/nsmb.3329

Humphrey, W., Dalke, A., and Schulten, K. (1996). VMD: visual molecular dynamics. *J. Mol. Graph.* 14, 33–38. doi:10.1016/0263-7855(96)00018-5

Hussein, R. A., Ahmed, M., Breitinger, H.-G., and Breitinger, U. (2019). Modulation of glycine receptor-mediated pain signaling *in vitro* and *in vivo* by glucose. *Front. Mol. Neurosci.* 12, 280. doi:10.3389/fnmol.2019.00280

Ikeda, R., Takahashi, Y., Inoue, K., and Kato, F. (2007). NMDA receptor-independent synaptic plasticity in the central amygdala in the rat model of neuropathic pain. *Pain* 127, 161–172. doi:10.1016/j.pain.2006.09.003

Ji, R.-R., Nackley, A., Huh, Y., Terrando, N., and Maixner, W. (2018). Neuroinflammation and central sensitization in chronic and widespread pain. *Anesthesiology* 129, 343–366. doi:10.1097/ALN.0000000000002130

Jiang, H., Fang, D., Kong, L.-Y., Jin, Z.-R., Cai, J., Kang, X.-J., et al. (2014). Sensitization of neurons in the central nucleus of the amygdala via the decreased GABAergic inhibition contributes to the development of neuropathic pain-related anxiety-like behaviors in rats. *Mol. Brain* 7, 72. doi:10.1186/s13041-014-0072-z

Kawasaki, Y., Zhang, L., Cheng, J.-K., and Ji, R.-R. (2008). Cytokine mechanisms of central sensitization: distinct and overlapping role of interleukin-1beta, interleukin-6, and tumor necrosis factor-alpha in regulating synaptic and neuronal activity in the superficial spinal cord. *J. Neurosci.* 28, 5189–5194. doi:10.1523/JNEUROSCI.3338-07.2008

Laskowski, R. A., MacArthur, M. W., Moss, D. S., and Thornton, J. M. (1993). PROCHECK: a program to check the stereochemical quality of protein structures. *J. Appl. Crystallogr.* 26, 283–291. doi:10.1107/S0021889892009944

Liu, Y., Huang, D., Wen, R., Chen, X., and Yi, H. (2015). Glycine receptor-mediated inhibition of medial prefrontal cortical pyramidal cells. *Biochem. Biophys. Res. Commun.* 456, 666–669. doi:10.1016/j.bbrc.2014.12.014

Lynch, J. W. (2004). Molecular structure and function of the glycine receptor chloride channel. *Physiol. Rev.* 84, 1051–1095. doi:10.1152/physrev.00042.2003

Maric, H.-M., Mukherjee, J., Tretter, V., Moss, S. J., and Schindelin, H. (2011). Gephyrin-mediated γ-aminobutyric acid type A and glycine receptor clustering relies on a common binding site. *J. Biol. Chem.* 286, 42105–421114. doi:10.1074/jbc.M111.303412

Mariqueo, T., and Zúñiga-Hernández, J. (2020). Omega-3 derivatives, specialized pro-resolving mediators: promising therapeutic tools for the treatment of pain in chronic liver disease. *Prostaglandins, Leukot. Essent. Fat. Acids* 158, 102095. doi:10.1016/j.plefa.2020.102095

Maydych, V. (2019). The interplay between stress, inflammation, and emotional attention: relevance for depression. *Front. Neurosci.* 13, 384. doi:10.3389/fnins.2019.00384

Molchanova, S. M., Comhair, J., Karadurmus, D., Piccart, E., Harvey, R. J., Rigo, J.-M., et al. (2017). Tonically active α2 subunit-containing Glycine receptors regulate the excitability of striatal medium spiny neurons. *Front. Mol. Neurosci.* 10, 442. doi:10.3389/fnmol.2017.00442

Moraga-Cid, G., San Martín, V. P., Lara, C. O., Muñoz, B., Marileo, A. M., Sazo, A., et al. (2020). Modulation of glycine receptor single-channel conductance by intracellular phosphorylation. *Sci. Rep.* 10, 4804. doi:10.1038/s41598-020-61677-w

Moraga-Cid, G., Sauguet, L., Huon, C., Malherbe, L., Girard-Blanc, C., Petres, S., et al. (2015). Allosteric and hyperekplexic mutant phenotypes investigated on an α1 glycine receptor transmembrane structure. *Proc. Natl. Acad. Sci.* 112, 2865–2870. doi:10.1073/pnas.1417864112

Muñoz, B., Yevenes, G. E., Förstera, B., Lovinger, D. M., and Aguayo, L. G. (2018). Presence of inhibitory glycinergic transmission in medium spiny neurons in the nucleus accumbens. *Front. Mol. Neurosci.* 11, 228. doi:10.3389/fnmol.2018.00228

Patrizio, A., Renner, M., Pizzarelli, R., Triller, A., and Specht, C. G. (2017). Alpha subunit-dependent glycine receptor clustering and regulation of synaptic receptor numbers. *Sci. Rep.* 7, 10899. doi:10.1038/s41598-017-11264-3

Pessoa, L., and Adolphs, R. (2010). Emotion processing and the amygdala: from a 'low road' to 'many roads' of evaluating biological significance. *Nat. Rev. Neurosci.* 11, 773–782. doi:10.1038/nrn2920

Phillips, J. C., Braun, R., Wang, W., Gumbart, J., Tajkhorshid, E., Villa, E., et al. (2005). Scalable molecular dynamics with NAMD. *J. Comput. Chem.* 26, 1781–1802. doi:10.1002/jcc.20289

Šali, A., and Blundell, T. L. (1993). Comparative protein modelling by satisfaction of spatial restraints. *J. Mol. Biol.* 234, 779–815. doi:10.1006/jmbi.1993.1626

Schneider, H., Pitossi, F., Balschun, D., Wagner, A., del Rey, A., and Besedovsky, H. O. (1998). A neuromodulatory role of interleukin-1beta in the hippocampus. *Proc. Natl. Acad. Sci.USA* 95, 7778–7783. doi:10.1073/pnas.95.13.7778

Sommer, C., and Kress, M. (2004). Recent findings on how proinflammatory cytokines cause pain: peripheral mechanisms in inflammatory and neuropathic hyperalgesia. *Neurosci. Lett.* 361, 184–187. doi:10.1016/j.neulet.2003.12.007

Sugama, S., Takenouchi, T., Sekiyama, K., Kitani, H., and Hashimoto, M. (2011). Immunological responses of astroglia in the rat brain under acute stress: interleukin 1 beta co-localized in astroglia. *Neuroscience* 192, 429–437. doi:10.1016/j.neuroscience.2011.06.051

Tadano, T., Namioka, M., Nakagawasai, O., Tan-No, K., Matsushima, K., Endo, Y., et al. (1999). Induction of nociceptive responses by intrathecal injection of interleukin-1 in mice. *Life Sci.* 65, 255–261. doi:10.1016/S0024-3205(99)00244-1

Thompson, A. J., Lester, H. A., and Lummis, S. C. R. (2010). The structural basis of function in Cys-loop receptors. *Q. Rev. Biophys.* 43, 449–499. doi:10.1017/S0033583510000168

Wang, D., Zhang, S., Li, L., Liu, X., Mei, K., and Wang, X. (2010). Structural insights into the assembly and activation of IL-1β with its receptors. *Nat. Immunol.* 11, 905–911. doi:10.1038/ni.1925

Watkins, L. R., and Maier, S. F. (2002). Beyond neurons: evidence that immune and glial cells contribute to pathological pain States. *Physiol. Rev.* 82, 981–1011. doi:10.1152/physrev.00011.2002

Wei, X.-H., Yang, T., Wu, Q., Xin, W.-J., Wu, J.-L., Wang, Y. Q., et al. (2012). Peri-sciatic administration of recombinant rat IL-1β induces mechanical allodynia by activation of src-family kinases in spinal microglia in rats. *Exp. Neurol.* 234, 389–397. doi:10.1016/j.expneurol.2012.01.001

Xu, M., Bennett, D. L. H., Querol, L. A., Wu, L.-J., Irani, S. R., Watson, J. C., et al. (2020). Pain and the immune system: emerging concepts of IgG-mediated autoimmune pain and immunotherapies. *J. Neurol. Neurosurg. Psychiatry* 91, 177–188. doi:10.1136/jnnp-2018-318556

Yirmiya, R. (2002). Brain interleukin-1 is involved in spatial memory and passive avoidance conditioning. *Neurobiol. Learn. Mem.* 78, 379–389. doi:10.1006/nlme.2002.4072

Conflict of Interest: The authors declare that the research was conducted in the absence of any commercial or financial relationships that could be construed as a potential conflict of interest.

Copyright © 2021 Solorza, Oliva, Castillo, Amestica, Maldifassi, López-Cortés, Barra, Stehberg, Piesche, Sáez-Briones, González, Arenas-Salinas and Mariqueo. This is an open-access article distributed under the terms of the Creative Commons Attribution License (CC BY). The use, distribution or reproduction in other forums is permitted, provided the original author(s) and the copyright owner(s) are credited and that the original publication in this journal is cited, in accordance with accepted academic practice. No use, distribution or reproduction is permitted which does not comply with these terms.

frontiers in Pharmacology

ORIGINAL RESEARCH
published: 09 March 2021
doi: 10.3389/fphar.2021.614396

Chronic Voluntary Alcohol Drinking Causes Anxiety-like Behavior, Thiamine Deficiency, and Brain Damage of Female Crossed High Alcohol Preferring Mice

*Hong Xu[1], Hui Li[2], Dexiang Liu[3], Wen Wen[2], Mei Xu[1], Jacqueline A. Frank[1], Jing Chen[4], Haining Zhu[4], Nicholas J. Grahame[5] and Jia Luo[2,6]**

[1]Department of Pharmacology and Nutritional Sciences, University of Kentucky College of Medicine, Lexington, KY, United States, [2]Department of Pathology, University of Iowa Carver College of Medicine, Iowa City, IA, United States, [3]Department of Medical Psychology, Shandong University School of Medicine, Jinan, China, [4]Department of Molecular and Cellular Biochemistry, University of Kentucky College of Medicine, Lexington, KY, United States, [5]Department of Psychology, Indiana University-Purdue University Indianapolis, Indianapolis, IN, United States, [6]Iowa City VA Health Care System, Iowa City, IA, United States

OPEN ACCESS

Edited by:
Mariela Fernanda Perez, National University of Cordoba, Argentina

Reviewed by:
Fawaz Alasmari, King Saud University, Saudi Arabia
Ricardo Marcos Pautassi, Medical Research Institute Mercedes and Martín Ferreyra (INIMEC), Argentina
Rosana Camarini, University of São Paulo, Brazil

***Correspondence:**
Jia Luo
jia-luo@uiowa.edu

Specialty section:
This article was submitted to Neuropharmacology, a section of the journal Frontiers in Pharmacology

Received: 06 October 2020
Accepted: 29 January 2021
Published: 09 March 2021

Citation:
Xu H, Li H, Liu D, Wen W, Xu M, Frank JA, Chen J, Zhu H, Grahame NJ and Luo J (2021) Chronic Voluntary Alcohol Drinking Causes Anxiety-like Behavior, Thiamine Deficiency, and Brain Damage of Female Crossed High Alcohol Preferring Mice. Front. Pharmacol. 12:614396. doi: 10.3389/fphar.2021.614396

The central nervous system is vulnerable to chronic alcohol abuse, and alcohol dependence is a chronically relapsing disorder which causes a variety of physical and mental disorders. Appropriate animal models are important for investigating the underlying cellular and molecular mechanisms. The crossed High Alcohol Preferring mice prefer alcohol to water when given free access. In the present study, we used female cHAP mice as a model of chronic voluntary drinking to evaluate the effects of alcohol on neurobehavioral and neuropathological changes. The female cHAP mice had free-choice access to 10% ethanol and water, while control mice had access to water alone at the age of 60-day-old. The mice were exposed to alcohol for 7 months then subjected to neurobehavioral tests including open field (OF), elevated plus maze (EPM), and Morris water maze (MWM). Results from OF and EPM tests suggested that chronic voluntary drinking caused anxiety-like behaviors. After behavior tests, mice were sacrificed, and brain tissues were processed for biochemical analyses. Alcohol altered the levels of several neurotransmitters and neurotrophic factors in the brain including gamma-Aminobutyric acid (GABA), corticotropin-releasing factor, cAMP response element-binding protein (CREB) and brain-derived neurotrophic factor. Alcohol increased the expression of neuroinflammation markers including interleukin-6 (IL-6), tumor necrosis factor alpha (TNF-α), monocyte chemoattractant protein-1 (MCP-1) and

Abbreviations: AUD, alcohol use disorders; BrdU, Bromodeoxyuridine; BDNF, Brain-derived neurotrophic factor; CCR2, C-C chemokine receptor 2; cHAP mice, Crossed High Alcohol Preferring mice; CNS, central nervous system; CREB, cAMP response element-binding protein; CRF, Corticotropin-releasing factor; DCX, doublecortin; DG, dentate gyrus of the hippocampus; ER, endoplasmic reticulum; GPR30, G protein-coupled estrogen receptor 1; GFAP, Glial fibrillary acidic protein; IHC, immunohistochemistry; Iba-1, Ionized calcium binding adaptor molecule 1; IL-6, Interleukin-6; MANF, Mesencephalic astrocyte-derived neurotrophic factor; MCP-1, monocyte chemoattractant protein-1; OCT1, Organic cation transporter 1; PBS, phosphate buffered saline; SGZ, subgranular zone; SLC19A2, Solute Carrier Family 19 Member 2 (Thiamine transporter 1); SLC19A3, Solute Carrier Family 19 Member 2 (Thiamine transporter 2); SVZ, subventricular zone; TNFα, tumor necrosis factor alpha.

C-C chemokine receptor 2 (CCR2). Alcohol also induced cleaved caspase-3 and glial fibrillary acidic protein, indicative of neurodegeneration and gliosis. In addition, alcohol inhibited the expression of thiamine transporters in the brain and reduced thiamine levels in the blood. Alcohol also caused oxidative stress and endoplasmic reticulum (ER) stress, and stimulated neurogenesis.

Keywords: alcohol use disorder, endoplasmic reticulum stress, oxidative stress, neurodegeneration, neuroinflammation

INTRODUCTION

Alcohol use disorder (AUD) is a chronically relapsing disorder characterized by compulsive alcohol consumption that can cause a variety of physical and mental problems (Grant et al., 2004; Bouchery et al., 2011). It is one of the most prevalent mental disorders in the United States with nearly one-third of adults experiencing it at some point in their lifetime (Grant et al., 2004; Grant et al., 2006; Grant et al., 2015). AUD is comorbid with other mental disorders, particularly anxiety disorder (Kushner et al., 2000; Burns and Teesson, 2002; Petry et al., 2005; Schneier et al., 2010). Anxiety is another common psychiatric condition characterized by excessive fear of the situation (McLean and Anderson, 2009; Bandelow and Michaelis, 2015). Clinical studies have shown AUD and anxiety can both act to initiate and reinforce each other (Kushner et al., 2000; Schneier et al., 2010). Many population surveys have consistently shown that AUD is more common in men whereas anxiety is more prevalent in women (Lewis et al., 1996; Kessler et al., 1997; Hasin et al., 2007). However, the national survey on gender-specific comorbidity rates for AUD and anxiety has indicated that alcohol-dependent women may almost double the risk of developing co-occurring anxiety relative to alcohol-dependent men (Kessler et al., 1997). Although much progress has been made in understanding AUD and many treatment options are available, patients with AUD tend to relapse and their recovery is often compromised, which may result from the failure to treat the comorbid anxiety (Randall et al., 2001; Terra et al., 2006; Schneier et al., 2010).

It is important to investigate whether there is a causative role of alcohol-induced brain injury or neurochemical alterations in the anxiety associated with alcohol abuse. Neurotransmitters are chemical molecules that are synthesized and released by neurons to transmit a message by binding to their receptors of target cells across the synapse. Disruption of neurotransmitter systems is associated with alcohol abuse and anxiety. Alcohol affects multiple neurotransmitter systems and neuropeptides in the brain's reward and stress circuits including gamma-aminobutyric acid (GABA) and corticotropin-releasing factor (CRF) systems. GABA is the primary inhibitory neurotransmitter in the brain. Alcohol can act on the presynaptic neurons to increase GABA release or act on the postsynaptic neurons to enhance the activity of GABA receptor (Banerjee, 2014). GABAergic inhibitory transmission is involved in alcohol drinking behavior (Roberto et al., 2003; Roberto et al., 2004) and anxiety (Kalueff and Nutt, 2007). CRF is a neuropeptide that can function as a neurotransmitter in stress-related behaviors in mood and anxiety disorders (Koob and Thatcher-Britton, 1985; Risbrough and Stein, 2006; Binder and Nemeroff, 2010). CFR signaling in the amygdala has been shown to mediate alcohol-induced GABA release (Bajo et al., 2008). In addition, CRF signaling has been shown to play a role in drinking behavior in alcoholism and is associated with anxiety-like behavior (Zorrilla et al., 2014).

As suggested by clinical studies and research using animal models, alcohol-induced neurodegeneration in multiple brain regions may underlie neurocognitive deficits in AUD (Harper, 1998; Crews, 2008; Kamal et al., 2020). However, the cellular and molecular mechanisms underlying alcohol-induced neurodegeneration remains unclear. There are several proposed mechanisms for alcohol-induced neurodegeneration. Oxidative stress has been implicated as a key mechanism underlying alcohol-induced neurodegeneration (Chen and Luo, 2010; Yang and Luo, 2015). Oxidative stress is defined as the imbalance between the reactive oxygen species (ROS) and antioxidants. Moreover, oxidative stress is associated with alcohol-induced anxiety-like behavior (Brocardo et al., 2012). Endoplasmic reticulum (ER) stress is another potential mechanism for alcohol-induced brain damage in both developing and adult brains (Yang and Luo, 2015). In addition, neuroinflammation is often associated with neurodegeneration and has been implicated in the pathophysiology of AUD (Hurley and Tizabi, 2013; Ramesh et al., 2013; Kempuraj et al., 2016; Coppens et al., 2019; Erickson et al., 2019). It is therefore important to establish appropriate animal models to elucidate these potential mechanisms.

Mice that are willing to voluntarily drink alcohol over an extended period, achieving pharmacologically relevant blood alcohol concentrations (BACs), may model chronic alcohol abuse in humans. The selectively bred crossed High Alcohol Preferring (cHAP) mice, bred for high ethanol intake when 10% ethanol and water are concurrently available for a month, have been shown to voluntarily consume high amounts of alcohol and demonstrate relatively high BACs that are comparable to those observed in alcohol-dependent humans (Matson and Grahame, 2013; Matson et al., 2014; Xu et al., 2019). We have previously used male cHAP mice to determine the effect of chronic voluntary alcohol on neurochemical alterations and thiamine contents in the brain. We demonstrated that chronic voluntary alcohol exposure increased oxidative stress, endoplasmic reticulum (ER) stress and neuronal apoptosis, and decreased thiamine levels in the brain of male cHAP mice. In the present study, we sought to determine the neurobehavioral

and biochemical consequences of chronic alcohol voluntary exposure in female cHAP mice. For the comparison to male cHAP, we also investigated the effects of alcohol on neurochemical changes and thiamine contents in female cHAP mice.

MATERIALS AND METHODS

Materials

Bromodeoxyuridine (BrdU) was obtained from Thermo Fisher Scientific (Rockford, IL). CREB, GFAP, Anti-cleaved caspase-3 and anti-Ki-67 antibodies were obtained from Cell Signaling Technology (Danvers, MA). Anti-BrdU antibody was obtained from Thermo Fisher Scientific (Waltham, MA). Antibodies directed against BDNF, CCR2, MCP-1, MANF, GPR30, TNFα, doublecortin, and OCT1 were obtained from Abcam (Cambridge, MA). Biotinylated goat anti-rabbit IgG was obtained from Vector Laboratories Inc. (Burlingame, CA). Alexa 488-conjugated goat anti-rabbit IgG was obtained from Invitrogen (Carlsbad, CA). Antibodies directed against CRF, NRG1, ErbB4, Caspase-12, CHOP, XBP-1s, ATF6, DNP, and HNE were obtained from Santa Cruz Biotech (Santa Cruz, CA). Anti-SLC19A2 antibody and 3, 3′-diaminobenzidine (DAB) were obtained from Sigma-Aldrich (St. Louis, MO). Anti-IL-6 and anti-SLC19A3 antibodies were obtained from Proteintech (Rosemont, IL). GABA ELISA kit (gAB; RK00663) was obtained from ABclonal (Woburn, MA). Anti-Iba-1 antibody was obtained from Wako Chemicals United States (Richmond, VA).

Experimental Design

The female cHAP mice were maintained in a 12:12 reverse light cycle colony room (lights on at 21:00 h and off at 09:00 h) with free access to 10% ethanol (v/v) solution and water during the period of 7-month alcohol drinking. After that, alcohol solution was removed, and animals were switched to standard light-dark cycle (lights on at 07:00 h and off at 21:00 h) for 1 week. The animals were then subjected to various behavioral tests including open field (OF), elevated plus maze (EPM), and Morris water maze (MWM) tests. EPM was conducted a week after OF and MWM was performed 4 days after EPM. After MWM, animals were injected with BrdU for 2 days, and then sacrificed. The and brain tissues and blood were collected and subjected to neurochemical analyses.

Animals and Alcohol Exposure Method

Female cHAP mice from the 31st generation of selection were obtained from Dr. Nicholas J. Grahame at Indiana University Purdue University Indianapolis (Indianapolis, IN, United States) and housed in the University of Kentucky Medical Center Animal Care Facilities. Two-month-old mice were used because they are comparable to human young adults; alcohol usage during this period more likely develops alcohol dependence (Lundahl et al., 1997; Grant, 1998; Hingson et al., 2006; Nair et al., 2016). Female mice were chosen to model the comorbidity of anxiety and AUD because alcohol-dependent women are more likely to develop anxiety than alcohol-dependent men (Kessler et al., 1997), and to compare to the results obtained from male mice (Xu et al., 2019). Animals were maintained in a reverse light cycle colony room in which lights were in 12:12 reverse light-dark cycle. The dark cycle started at 9:00 am. All mice had ad libitum access to food and water throughout the experiment. All experimental procedures were approved by the Institutional Animal Care and Use Committee (IACUC) at the University of Kentucky and performed following regulations for the Care and Use of Laboratory Animals set forth by the National Institutes of Health (NIH) Guide. Mice were given access to alcohol at 60 days of age. The mice had 24-hour-free-choice access to 10% ethanol (v/v) solution and water. Alcohol and drinking water were provided with 50 ml test tube water bottle (#20872, Arcata Pet Supplies, Arcata, CA) fit with a stainless-steel sipper tube (Model OCT-100, Ancare, Belmont, NY). The water bottles were changed every 2 days with freshly prepared ethanol in drinking water or drinking water. The average intake of alcohol was 10.88 ± 0.20 g/kg/d. Mice were weighed before and after alcohol drinking and there was no significant difference between the control and alcohol drinking group (data not shown). After 7 months of alcohol consumption, mice were tested for behavioral scoring, then sacrificed and the brain tissues were harvested for neurochemical studies. The whole blood was also collected for LC-MS analysis of thiamine concentration.

Determination of Blood Alcohol Concentrations (BACs)

Blood samples were collected at 26 weeks of free-choice access to alcohol and water. The blood was drawn from the tail veins 4 h after the onset of the dark cycle. The time point was selected because the cHAP mice drink more in the dark and peak BECs were observed in the dark cycle (Matson and Grahame, 2013; Matson et al., 2014). The plasma supernatant was extracted, and BACs were measured using an Analox Alcohol Analyzer (Analox Instruments, Lunenburg, MA).

Behavior Tests

All behavior tests were conducted one week after the alcohol drinking had ended and they were 4–7 days apart to ensure adequate rest and stress relief of animals. Open field (OF) was the first test and it was conducted in two consecutive days; then Elevated plus maze (EPM) was applied in 1 day; whereas Morris water maze (MWM) was completed in five consecutive days. With the lights on at 07:00 h, off at 21:00 h, OF and EPM were conducted at similar times in the morning between 08:00–12:00 h, whereas MWM was conducted between at 12:00–16:00 h according to the standard protocol of rodent behavior core at United Kingdom.

Open Field

Open field (OF) test is commonly used to measure the levels of exploration and anxiety-like behavior in response to novel environment in mice (Seibenhener and Wooten, 2015). OF was performed in the Rodent Behavior Core (RBC) at the University of Kentucky following the standard procedure for

two consecutive days. Prior to the test, animals were brought into the testing room and placed in cleaning cages for 10 min as habituation period. Each mouse was then placed in a square chamber measured 50 cm (length) × 50 cm (width) × 38 cm height with opaque white walls in a multi-unit open field maze (San Diego Instruments), and its activity was recorded for 15 min using EthoVision XT 8.0 video tracking software (Noldus Information Technology, Leesburg, VA, United States). The distance traveled (cm), movement time (s), velocity (cm/s) and time spent in the center zone (s) were recorded and automatically calculated. Center zone is defined as the central area of the chamber measured 25 cm (length) × 25 cm (width). Distance traveled and movement speeds are measures of locomotor activity, whereas the time spent in the center zone is a measure of anxiety in mice.

Elevated Plus Maze

Elevated plus maze (EPM) is primarily used to assess anxiety-related behavior in rodents (Walf and Frye, 2007). It was conducted under low ambient light conditions with white noise to minimize extraneous auditory stimuli. The EPM apparatus consisted of four arms, two without walls, two enclosed with walls, and each arm measured 30 cm (length) × 6 cm (width). Each mouse was tested in a single session of 5 min to explore the maze. The maze was cleaned after each test with Nature's Miracle enzymatic cleaning solution to remove animal odors. Animal movements were recorded using EthoVision XT 8.0 video tracking software (Noldus Information Technology, Leesburg, VA, United States). The time spent in each arm and the entries into each arm were analyzed.

Morris Water Maze

The Morris water maze (MWM) is one of most common behavioral tests of spatial learning for rodents (Vorhees and Williams, 2006). The MWM was performed based on a previously published method with some modifications (Xu et al., 2018). Briefly, each mouse was placed in a round plastic tub with a diameter of 108 cm filled with white-painted water at the temperature of 22–23°C to locate and escape onto a submerged platform. Four visible cues were placed at different points around the tub. Each animal was placed at random locations distal to the platform and allowed to swim to find the hidden platform. If the animal failed to locate the platform within 1 min, it would be gently guided to and remained on the platform for 10 s. Each animal was then placed in a warm cage with a heating pad underneath. There were approximately 5 min in between trials. Each mouse was given four daily trials for five consecutive days. Animal movements were recorded and analyzed using EthoVision XT 8.0 video tracking software (Noldus Information Technology, Leesburg, VA, United States).

Quantification of Thiamine Concentrations in the Whole Blood

The determination of thiamine concentration in the blood was performed based on a previously described method with some modifications (Kato et al., 2015; Xu et al., 2019). Briefly, whole blood (100 μL) was mixed with 100 μL of 1.2 M ice-cold perchloric acid and kept at 0°C for 15 min. The mixture was centrifuged for 30 min at 15,000 g. 150 μL of supernatant was collected and incubated with 150 μL of 0.6 M KOH/1.8 M potassium acetate for neutralization; then the mixture was centrifuged for 30 min at 15,000 g for desalting. The supernatant (250 μL) was mixed with 250 μL of 4% phosphatase acid and hydrolyzed overnight at room temperature. After that, the supernatant (90 μL) was collected and analyzed for thiamine content. A quadruple volume of acetonitrile/methanol (9:1; v/v) containing an internal standard thiamine-D3 was added to the 90 μL supernatant. The mixture was vortexed and centrifuged for 10 min at 12,000 g. The supernatant was transferred to a new vial, dried with SpeedVac until the final volume was 90 μL. An aliquot of the samples was injected into a LC-MS/MS for the analysis of thiamine concentration.

BrdU Labeling, Immunohistochemistry and Immunofluorescent Staining

BrdU incorporation labels mitotic cells in the S phase and is used to monitor cell proliferation in the brain. After the last behavioral test (MWM), mice received an intraperitoneal injection of BrdU (50 mg/kg) for two consecutive days. Mice were then anesthetized by intraperitoneal injection of ketamine/xylazine (100 mg/kg/10 mg/kg) and perfused with 0.1 M potassium phosphate buffer (pH 7.2), followed by 4% paraformaldehyde in PBS (pH 7.4). The brain tissues were dissected and postfixed in 4% paraformaldehyde for 48 h followed by cryoprotection in 30% sucrose in PBS. Brains were sectioned (sagittal or coronal section) on a sliding microtome (Leica Microsystems, Wetzlar, Germany) at a thickness of 10 μm at an interval of 20 μm. The sections were then mounted onto Superfrost Plus slides (Fisher).

The immunohistochemical (IHC) staining for NGR1, GPR30, CREB, GFAP, Iba-1, BrdU, doublecortin (DCX), Ki67, and cleaved-caspase-3 in the whole brain was performed as previously described (Xu et al., 2019). Neurochemical alterations in some brain regions, such as PFC and hippocampus, were examined and analyzed. Briefly, the mounted sections were incubated in 0.3% H_2O_2 in methanol for 30 min at room temperature and then treated with 0.1% Triton X-100 for 10 min in PBS. The sections were washed with PBS three times and then blocked with 1% BSA and 0.01% Triton X-100 for 1 h at room temperature. The sections were incubated with anti-NGR1 (1:200), anti-GPR30 (1:100), anti-CREB (1:200), anti-GFAP (1:200), anti-Iba-1(1:200), anti-cleaved caspase-3 (1:200), anti-BrdU antibody (1:50), anti-DCX (1:1,000), or anti-Ki-67 antibodies (1:400) overnight at 4°C. Negative controls were performed by omitting the primary antibody. After rinsing in PBS, sections were incubated with a biotinylated goat anti-rabbit IgG (1:200) for 1 h at room temperature. The sections were washed 3 times with PBS, then incubated in avidin–biotin–peroxidase complex (1:100 in PBS) for 1 h and developed in 0.05% 3,3′-diaminobenzidine (DAB) containing 0.003% H2O2 in PBS. To quantify positive cells, the positive cells were counted at ×20 magnification from five microscopic

fields in the SVZ or DG area from each brain. The average of the positive cells from 4-5 consecutive sections were analyzed using the software of Image lab 5.2 (Bio-Rad Laboratories, Hercules, CA) for each brain.

Immunoblotting

The brain tissues from the whole brain were frozen in liquid nitrogen and stored at −80°C. Proteins were extracted as previously described (Xu et al., 2019). In brief, the tissues were homogenized using an ice-cold lysis buffer containing 50 mM Tris-HCl (pH 7.5), 150 mM NaCl, 1 mM EGTA, 1 mM PMSF, 0.5% NP-40, 0.25% SDS, 5 μg/ml leupeptin, and 5 μg/ml aprotinin. Homogenates were centrifuged at 20,000 g for 30 min at 4°C and the supernatant fraction was collected. Aliquots of the protein samples (30 μg) were separated on an SDS-polyacrylamide gel by electrophoresis. The separated proteins were transferred to nitrocellulose membranes. The membranes were blocked with either 5% milk or 5% bovine serum albumins (BSA) or at room temperature for 1 h. Subsequently, the membranes were probed with primary antibodies directed against target proteins overnight at 4°C. After three quick washes in TPBS, the membranes were incubated with a secondary antibody conjugated to horseradish peroxidase. The immune complexes were detected by the enhanced chemiluminescence method. The density of immunoblotting was quantified with the software of Quantity One (Bio-Rad Laboratories, Hercules, CA).

Quantitative Real-Time RT-PCR

Total RNA from the brain was extracted using Trizol Reagent (Life Technologies) and treated with RNA-free DNAase I to remove remnant DNA as described previously (Kim et al., 2014). 1 μg of total RNA was used for first strand cDNA synthesis (Promega, A3500). Quantitative real-time RT-PCR was performed on a Light cycler 480 system (Roche) using a Power SYBR Green PCR Master kit (Invitrogen, 4368706) with cDNA and primers (1 μM) according to the manufacturer's recommendation. The primers used for this study were purchased from Fisher Scientific and were as follows: TNF-α, Mm099999068; IL-6, Mm00446190. The relative difference between control and treatment group was expressed and calculated as relative increases using 2-ΔΔCt and setting control as 1.

Measurement of Estradiol, Progesterone and GABA

General Gamma-Aminobutyric Acid ELISA Kit was used to measure GABA concentrations in the homogenized brain tissues. The brain tissues were homogenized in an ice-cold lysis buffer containing 50 mM Tris-HCl (pH 7.5), 150 mM NaCl, 1 mM EGTA, 1 mM PMSF, 0.5% NP-40, 0.25% SDS, 5 μg/ml leupeptin, and 5 μg/ml aprotinin. Homogenates were centrifuged at 20,000 g for 30 min at 4°C and the supernatant fraction was collected. After 100-fold dilution, the optical density of glutamate and GABA was measured at 450 nm using Beckman Coulter DTX880 Multimode Detector according to the manufacturer's protocol. The concentrations of GABA were calculated based on a standard optical density.

The measurement of estradiol and progesterone in blood plasma was performed by the Ligand Assay and Analysis Core in Center for Research in Reproduction (CRR) at University of Virginia. The plasma in mouse blood was collected following the standard protocol published by CRR. Briefly, whole mouse blood was collected with anticoagulant. The blood sample was then centrifuged at 2000 × g for 15 min at room temperature. The plasma was then transferred into a polypropylene tube and stored at −20°C until shipment for analysis.

Statistical Analysis

All values were reported as mean ± SEM. A statistical analysis was performed using Graphpad Prism 6 (San Diego, CA, United States) and SPSS software 19 (IBM, Armonk, NY, YSA). *t*-test was used for the data analysis of and EPM, protein markers and molecules between control and alcohol groups. ANOVA was performed to compare difference between treatments with repeated measure factors being day. The Greenhouse–Geisser correction was used to correct the F statistic and assess significance if necessary. Differences were considered significant if the p value was smaller than 0.05.

RESULTS

Chronic Voluntary Alcohol Exposure Causes Anxiety-like Behaviors in Female cHAP Mice

The animals were weighed before alcohol drinking and 3.5 months after alcohol drinking. The mean body weight of the control and the alcohol drinking group before alcohol drinking was 22.8 ± 0.4 g and 22.2 ± 0.5 g, respectively. The mean body weight of the control and the alcohol drinking group after 3.5 months of alcohol drinking was 22.2 ± 0.3 g and 23.0 ± 0.5 g, respectively.

The blood alcohol concentrations (BACs) were determined 26 weeks into the alcohol drinking history. The mean BAC was 77.9 ± 8.51 mg/dl. In the open field (OF) test, we measured the total distance traveled and time spent in the center in two consecutive days. Because the data are similar in both days, we averaged the data, so each data point represents the mean of the measurements of 2 days in **Figure 1A**. The total distance traveled by the control mice was 7,132 ± 368.4 cm (mean ± SEM) (n = 7) which was not significantly different from that by the alcohol-exposed mice (7,294 ± 1,237 cm, n = 7) [t (12) = 0.1255, $p = 0.902$] (**Figure 1A**). The time spent in the center by the alcohol-exposed mice (98.11 ± 13.46 s, n = 7), however, was significantly lower than that by the control mice (182.0 ± 15.77 s, n = 7) [t (12) = 4.047, $p = 0.002$] (**Figure 1B**), suggesting anxiety-like behaviors.

We then conducted elevated plus maze (EPM) and measured the time and entry number in open and closed arms. The percentage of time in open arms for the alcohol-exposed mice was measured as 18.90% ± 3.11% (n = 7) which was significantly lower than that for the control mice 31.69% ± 3.31% (n = 7)

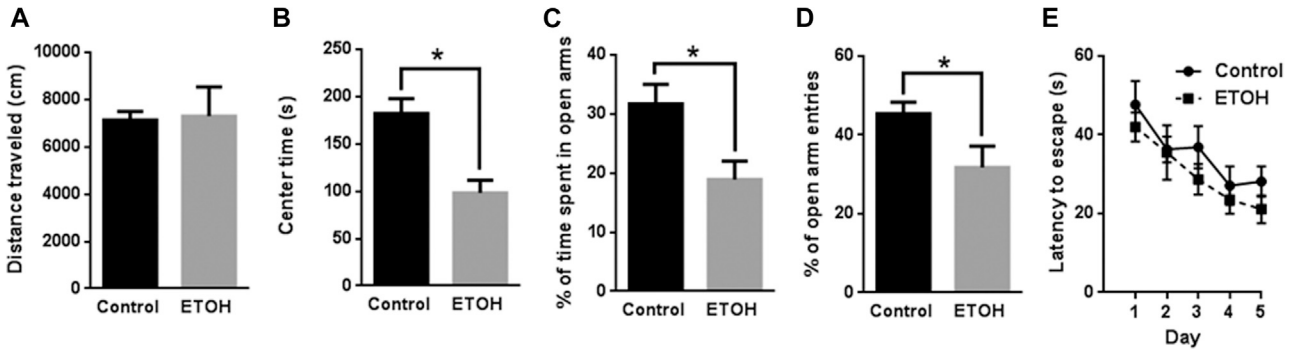

FIGURE 1 | Effects of 7 months of voluntary alcohol drinking on anxiety-like behavior in female cHAP mice. After that, mice were subjected to Open Field (OF) test **(A,B)**, Elevated Plus Maze (EPM) test **(C,D)**, and Morris Water Maze (MWM) test **(E)**. The total distance traveled **(A)** and the time spent in the center **(B)** in OF was measured and presented as the mean ± SEM (n = 7) in each group. The percentage of time spent in open arms **(C)** and percentage of entry numbers into open arms **(D)** in EPM were quantified and presented the mean ± SEM (n = 7). **(E)** The spatial learning and memory were evaluated by MWM. The total latency escape time was measured and presented as the mean ± SEM (n = 7). Unpaired student t-test was used to assess the difference between control and alcohol-exposed group. *$p < 0.05$ denotes a statistically significant difference from the control group.

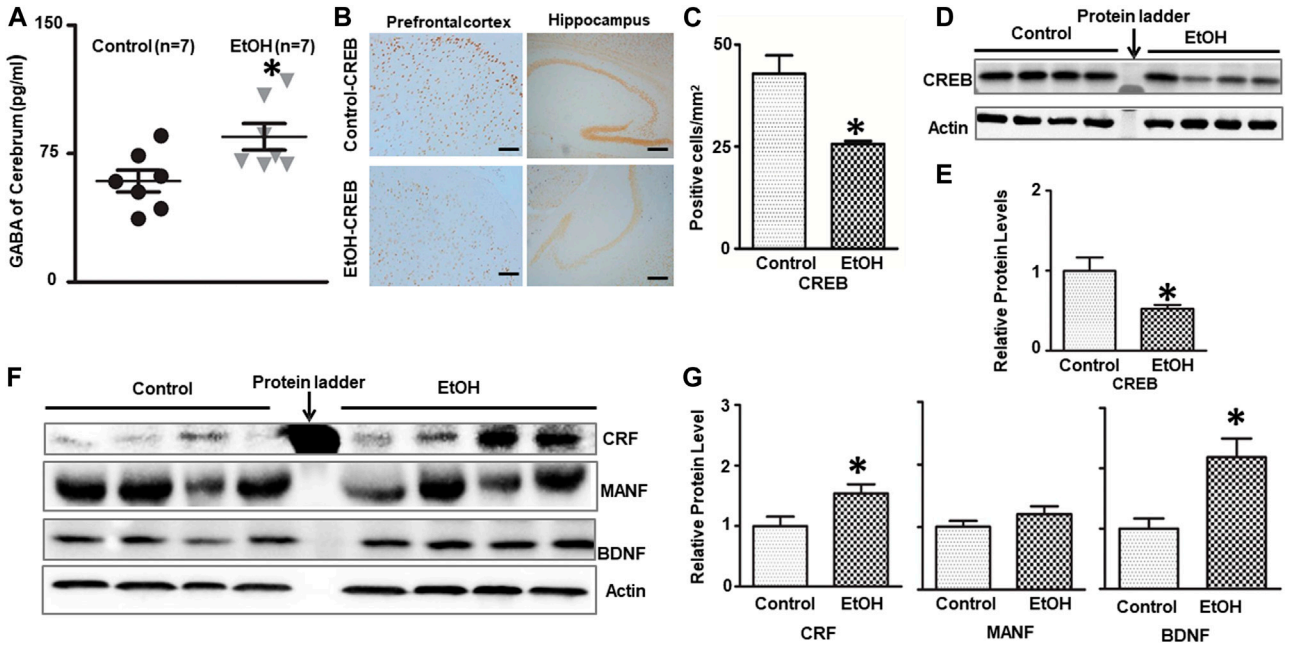

FIGURE 2 | Effects of chronic alcohol exposure on the levels of GABA and neurotrophic factors in the brain. **(A)** The concentration of GABA in the brain was determined by ELISA as described in the *Materials and Methods*. n = 7, *$p < 0.05$ denotes a statistically significant difference from the control. **(B)** The expression of CREB in the cerebrum was determined by immunohistochemistry (IHC). **(C)** The numbers of CREB-positive cells in the hippocampus or prefrontal cortex (PFC) were determined. The results were expressed as the mean ± SEM; n = 4, *$p < 0.05$ denotes a statistically significant difference from the control group. **(D)** The expression of CREB was determined by immunoblotting (IB). **(E)** The relative amounts of CREB were quantified and normalized to the expression of actin. **(F)** The expression of CRF, BDNF and MANF in the cerebrum was determined by IB. **(G)** The relative amounts of CRF, BDNF and MANF were quantified and normalized to the expression of actin. The results were expressed as the mean ± SEM, n = 4 for each group. *$p < 0.05$ denotes a statistically significant difference from the control group.

[t (12) = 2.816, $p = 0.016$] (**Figure 1C**). The percentage of entry numbers of open arms for the alcohol-exposed mice was 31.75% ± 5.40% (n = 7) which was also significantly lower than that for the control mice 45.33% ± 2.97% (n = 7) [t (12) = 2.202, $p = 0.048$] (**Figure 1D**). These results indicated anxiety-like behavior in alcohol-exposed mice.

In addition, we applied Morris water maze (MWM) to determine whether spatial learning was affected by alcohol exposure. Animals were trained with four trials per day for 5 days and the time required to locate the hidden platform in water maze were analyzed and presented in **Figure 1E**. The statistical analysis indicated there was a significant main effect

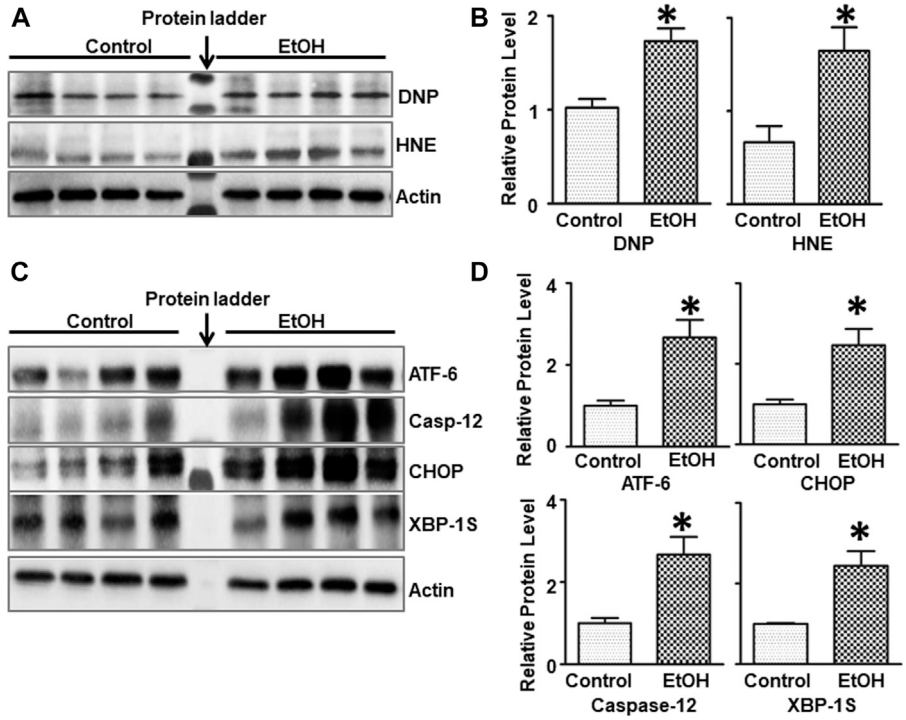

FIGURE 3 | Effects of chronic alcohol exposure on oxidative stress and ER stress in the brain. **(A)** The expression of 4-HNE and DNP in the cerebrum was determined by IB. **(B)** The relative amounts of 4-HNE and DNP were quantified and normalized to the expression of actin. **(C)** The expression of ER stress markers, ATF-6, CHOP, Caspase-12, and XBP-1s in the cerebrum was determined by IB. The relative amounts of expression were quantified and normalized to the expression of actin. **(D)** The relative amounts of ER stress markers were quantified and normalized to the expression of actin. The results were expressed as the mean ± SEM; n = 4 for each group. *$p < 0.05$ denotes a statistically significant difference from the control group.

of day [F (4, 48) = 7.294, $p < 0.001$] but not treatment [F (1, 12) = 1.959, $p = 0.187$]. The interaction of day by treatment was not significant [F (4, 48) = 0.226, $p = 0.922$]. Therefore, alcohol exposure did not alter spatial learning.

Chronic Voluntary Alcohol Exposure Alters the Levels of Neurotransmitters and Neurotrophic Factors That Are Related to the Regulation of Anxiety

γ-Aminobutyric acid (GABA) is the major inhibitory neurotransmitter controlling synaptic transmission and neuronal excitability. GABAergic inhibitory transmission is involved in the effects of alcohol exposure on the brain and anxiety behaviors (Roberto et al., 2003; Roberto et al., 2004; Kalueff and Nutt, 2007). We measured the GABA concentration in the brain after 7 months of alcohol exposure. As shown in **Figure 2A**, alcohol exposure significantly increased the concentration of GABA in the brain; it was 84.82 ± 7.72 (pg/ml) in the alcohol-exposed group (n = 7) and 58.89 ± 6.39 (pg/ml) in the control mice (n = 7) [t (12) = 2.587, $p = 0.024$].

We next examined the expression of several neurotrophic factors/growth factors that are known to play a role in anxiety and alcoholism, such as CRF, CREB, and BDNF (Bolaños and Nestler, 2004; Pandey et al., 2004; Govindarajan et al., 2006; Uddin and Singh, 2007; Baiamonte et al., 2014; Roberto et al., 2017). As shown in **Figures 2B–E**, chronic alcohol exposure decreased the number of CREB-positive cells in the prefrontal cortex (PFC) and hippocampus [t (6) = 3.758, $p = 0.0094$], and down-regulated the expression of CREB in the brain [t (6) = 2.660, $p = 0.038$]. On the other hand, alcohol exposure increased the levels of CRF [t (6) = 2.481, $p = 0.048$] and BDNF [t (6) = 3.143, $p = 0.016$] in the brain without affecting MANF [t (6) = 1.360, $p = 0.229$], a protein involved in ER function (**Figures 2F,G**).

Chronic Voluntary Alcohol Exposure Causes Oxidative Stress, ER Stress and Apoptosis in the Brain

Since oxidative stress and ER stress play an important role in alcohol-induced damage to the CNS (Yang and Luo, 2015), we sought to investigate the effect of chronic alcohol exposure on oxidative stress and ER stress in the brain. 4-hydroxynonenal (4-HNE) and 2, 4-dinitrophenol (DNP) are reliable biomarkers for lipid peroxidation and protein oxidation, respectively (Perluigi et al., 2014). As shown in **Figures 3A,B**, chronic alcohol drinking significantly increased the expression of 4-HNE [t (6) = 2.925, $p = 0.026$], and DNP [t (6) = 3.915, $p = 0.008$] in the brain, indicating the induction of oxidative stress. Furthermore, chronic alcohol drinking upregulated the expression of a number of markers for ER stress, such as ATF-6 [t (6) = 2.822, $p = 0.030$], CHOP [t (6) = 2.718, $p = 0.035$], Caspase-12 [t (6) = 3.341, $p = 0.01$], and XBP-1s [t (6) = 3.016, $p = 0.024$] in the brain, indicative of ER stress (**Figures 3C,D**).

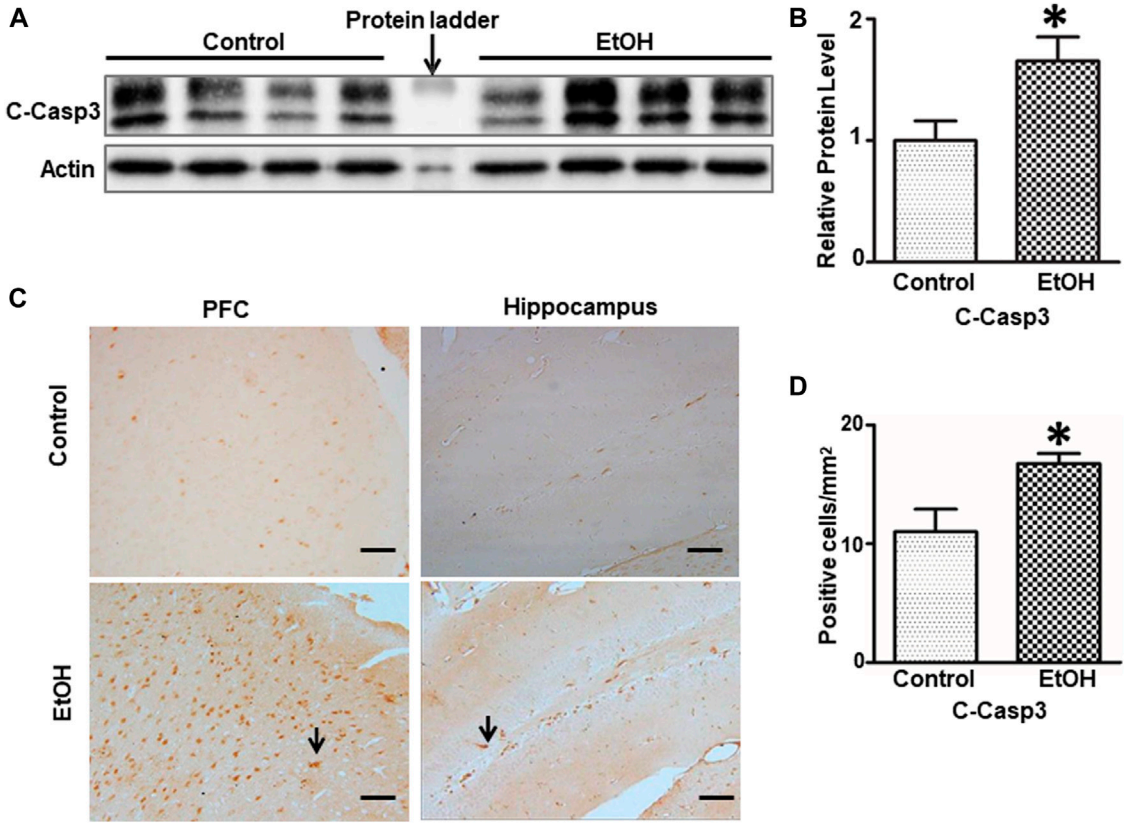

FIGURE 4 | Effects of chronic alcohol exposure on the expression of activated caspase-3. **(A)** The expression of cleaved caspase-3 in the cerebrum was determined by IB. **(B)** The relative amounts of expression were quantified and normalized to the expression of actin. The result was expressed as the mean ± SEM; n = 4. *$p < 0.05$ denotes a statistically significant difference from the control group. **(C)** The expression of cleaved caspase-3 in the prefrontal cortex (PFC) and the dentate gyrus (DG) of the hippocampus was examined by IHC; bar = 50 μm. Arrows indicate cells that are positive for cleaved caspase-3. **(D)** The numbers of cleaved caspase 3-positive cells in the hippocampus and PFC were determined. The results were expressed as the mean ± SEM; n = 4.

We next sought to determine whether alcohol caused neuronal apoptosis in the brain. As shown in **Figures 4A**,**B**, the alcohol-induced increase in cleaved-caspase-3 was shown by immunoblotting analysis [t (6) = 2.567, p = 0.043], indicating apoptosis in the brain. Consistently, alcohol increased the expression of cleaved-caspase-3 in the PFC and the dentate gyrus (DG) of hippocampus was revealed by IHC [t (6) = 2.756, p = 0.033] (**Figures 4C,D**).

Chronic Voluntary Exposure Induces Neuroinflammation and Glial Activation in the Brain

Alcohol-induced damage to the brain is usually accompanied by neuroinflammation (Chastain and Sarkar, 2014; Zhang and Luo, 2019). We sought to determine whether chronic alcohol exposure induced neuroinflammation. Interleukin-6 (IL-6), tumor necrosis factor alpha (TNFα), monocyte chemoattractant protein-1 (MCP-1) and its receptor CCR2 are major pro-inflammatory cytokines/chemokines that are involved alcohol-induced in injuries in the CNS (Vallières and Rivest, 1999; Alfonso-Loeches et al., 2016; Zhang et al., 2018). Alcohol exposure significantly increased the protein levels of TNFα [t (6) = 3.172, p = 0.019] but not IL-6 [t (6) = 0.502, p = 0.634] in the brain of female cHAP mice (**Figures 5A**,**B**). Chronic alcohol drinking also significantly upregulated the expression of MCP-1 [t (6) = 3.039, p = 0.023] and CCR2 [t (6) = 2.916, p = 0.027] in the brain (**Figures 5C,D**), indicating the induction of neuroinflammation.

We further determined whether chronic alcohol exposure activated astrocytes or microglia. As shown in **Figure 6**, the IHC study indicated that GFAP positive cells were increased in the hippocampus of alcohol-exposed mice [t (6) = 4.77, p = 0.008] (**Figures 6A–C**). This was confirmed by immunoblotting analysis which indicated that chronic alcohol exposure increased the expression of GFAP [t (6) = 3.123, p = 0.020] (**Figures 6D,E**), suggesting gliosis in the brain. However, alcohol exposure did not activate microglia and alter Iba1 expression (data not shown).

Chronic Voluntary Alcohol Exposure Reduces Thiamine Concentration in the Blood, and the Expression of GPR30 in the Brain

Thiamine deficiency (TD) has long been associated with alcohol-induced brain damages (Leevy and Baker, 1968;

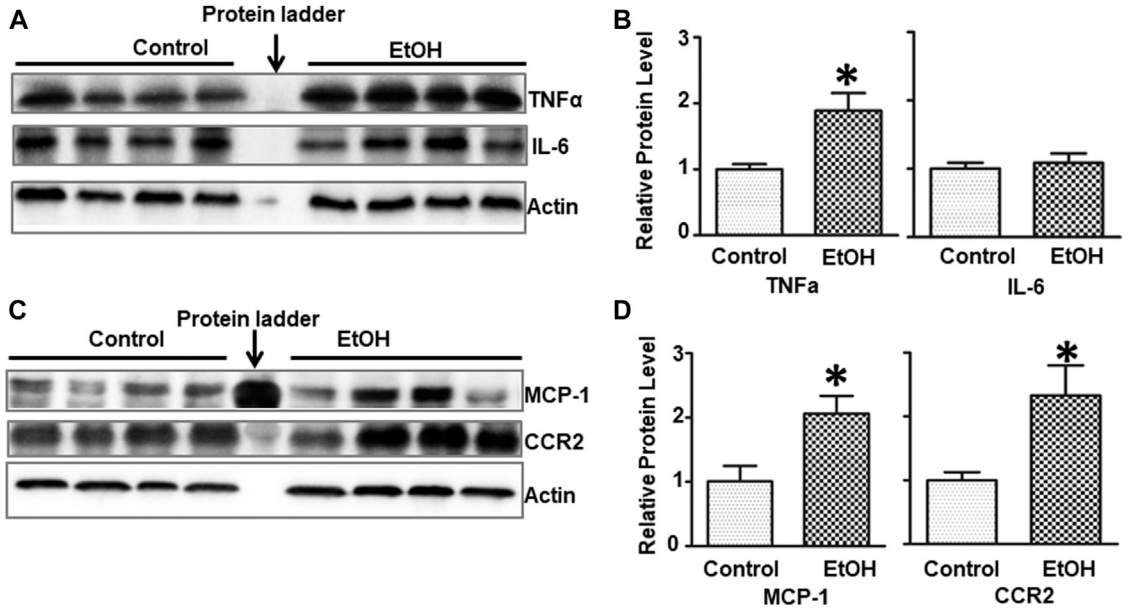

FIGURE 5 | Effects of chronic alcohol exposure on inflammatory cytokines/chemokines in the brain. **(A)** The expression of IL-6 and TNFα in the brain was determined with IB. **(B)** The relative expression of IL-6 and TNFα was quantified as described above. Each data point was the mean ± SEM; n = 4. *$p < 0.05$, statistically significant difference from the control group. **(C)** The expression of MCP-1 and CCR2 in the brain was determined with IB. **(D)** The relative expression of MCP-1 and CCR2 was quantified. Each data point was the mean ± SEM; n = 4. *$p < 0.05$, statistically significant difference from control group.

Woodhill and Nobile, 1972; Butterworth, 1995). We sought to determine whether alcohol exposure reduced thiamine level in the blood. As shown in **Table 1**, the concentration of thiamine in alcohol-exposed mice was 0.03 + 0.003 nmol/ml (n = 8), while it was 0.66 ± 0.15 nmol/ml in control animals (n = 8) [t (14) = 4.25, $p = 0.001$]. Alcohol exposure also significantly reduced the expression of thiamine transporters SLC19A2 [t (6) = 2.656, $p = 0.038$], SLC19A3 [t (6) = 3.056, $p = 0.022$], and OCT1 [t (6) = 2.502, $p = 0.046$] in the brain (**Figure 7**). However, alcohol did not alter these thiamine transporters in the liver (data not shown).

There is a gender difference in the neurobiology of anxiety, and females face twice the risk of anxiety disorder as males (Lebron-Milad and Milad, 2012; Cover et al., 2014; Bale and Epperson, 2015), which suggests that sexual hormones may play a role. G-protein-coupled estrogen receptor (ER) known as GPR30 has been implicated in the rodent anxiety response. We determined the expression of GPR30 in the brain. Chronic alcohol exposure significantly decreased the level of GPR30 [t (6) = 2.484, $p = 0.048$] (**Figures 8A**,**B**) in the brain. However, there was no significant difference of estradiol and progesterone concentrations in the blood between control and alcohol-exposed mice. The concentration of estradiol in the blood was 6.31 ± 1.75 (pg/ml)(n = 5), and 5.18 ± 0.84 (pg/ml) in alcohol-exposed (n = 5) and control group (n = 5), respectively [t (8) = 0.581, $p = 0.577$] (**Figure 8C**). The concentration of progesterone in the blood was 4.13 ± 1.36 (ng/ml), and 2.59 ± 0.68 (ng/ml) in alcohol-exposed (n = 8) and control group (n = 8) for respectively [t (14) = 1.01, $p = 0.329$] (**Figure 8D**).

Chronic Voluntary Alcohol Exposure Stimulated Neurogenesis in the Brain

We investigated the effect of chronic alcohol exposure on the neurogenesis in the subventricular zone (SVZ) and the dentate gyrus (DG) of the hippocampus. As shown in **Figure 9**, alcohol exposure increased the number of BrdU-positive cells [t (4) = 3.16 , $p = 0.034$] and DCX-positive cells [t (4) = 4.50 , $p = 0.011$] in the DG; Alcohol exposure also increased the number of BrdU-positive cells (t (5) = 3.17 , $p = 0.025$] and Ki67-positive cells [t (6) = 3.62 , $p = 0.01$] in the SVZ, indicating enhanced proliferation of neural progenitors.

DISCUSSION

In the present study, we used female cHAP mice to investigate chronic voluntary alcohol drinking-induced neurobehavioral and neurochemical alterations. The mice drank alcohol for 7 months, which is roughly equivalent to 20 years of drinking in humans extrapolated as a proportion of the lifespan. These are the first data showing behavioral symptoms of alcohol withdrawal in these mice, which are quite resistant to more conventional measures of withdrawal, such as handling induced convulsions following multiple rounds of chronic vapor exposure and withdrawal over several weeks (Lopez et al., 2011). Our study suggests that cHAP mice are valuable in their ability to use voluntary drinking to model both behavioral and biochemical effects of chronic alcohol consumption and subsequent short-term withdrawal in human AUD.

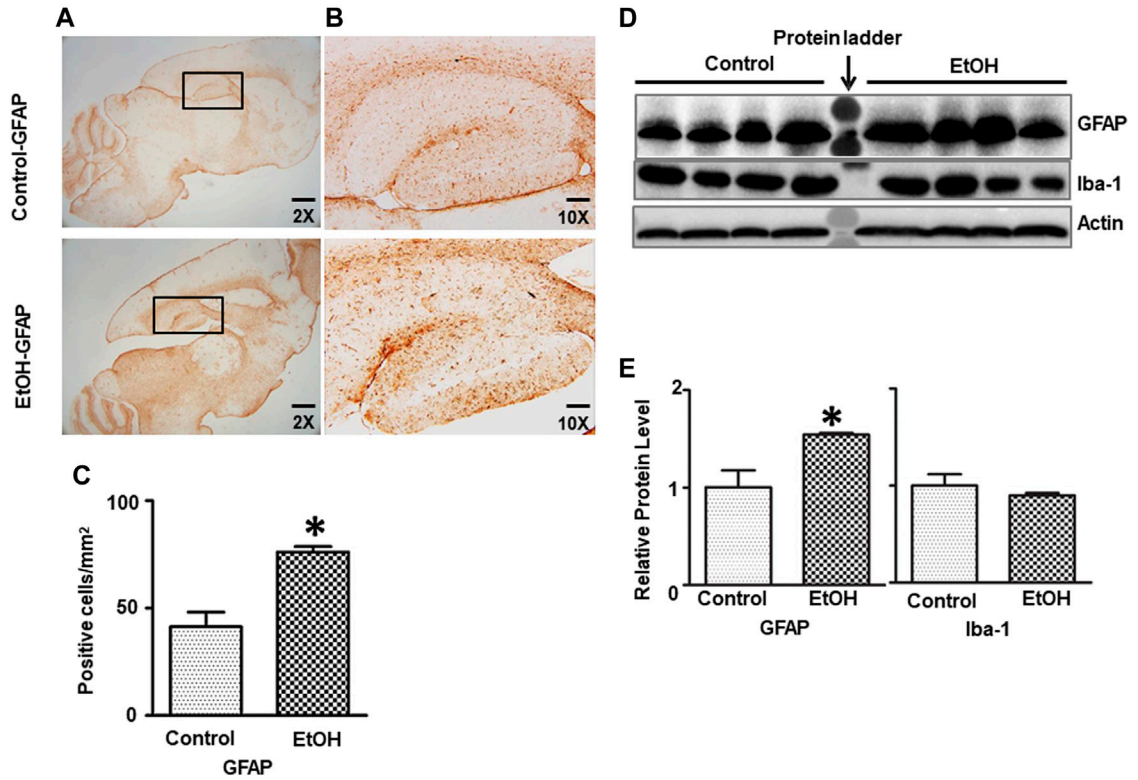

FIGURE 6 | Effects of chronic ethanol exposure on astrocyte activation. **(A)** The expression of GFAP in the mouse brain was examined by IHC. The rectangle insets indicate an area of the hippocampus. **(B)** The rectangle insets in **(A)** are shown in higher magnifications. **(C)** The GFAP-positive cells in the hippocampus were quantified. The result was expressed as the mean ± SEM, n = 3 for each group. *$p < 0.05$ denotes a statistically significant difference from the control group. **(D)** The protein levels of GFAP were examined by IB. **(E)** The relative amounts of GFAP expression were quantified and normalized to the expression of actin. The result was expressed as the mean ± SEM, n = 4 for each group. *$p < 0.05$ denotes a statistically significant difference from the control group.

Chronic Voluntary Alcohol Drinking Induces Anxiety-like Behaviors

We conducted three behavioral tests: Open Field (OF), Elevated Plus Maze (EPM) and Morris water maze (MWM) to evaluate the neurobehavioral consequences of 7-month voluntarily alcohol drinking on female cHAP mice (**Figure 1**). In OF, the female cHAP mice after 7 months of voluntarily alcohol drinking showed no deficits in their locomotor activity but displayed anxiety-like behaviors by spending less time in the center (46.1% reduction). In EPM, the alcohol-exposed animals demonstrated anxiety-like behaviors by spending 40.4% less time and 30.0% less entry number in the open arms. These findings are consistent with a broad range of literature indicating changes in anxiety and stress sensitivity following chronic ethanol exposure (Becker, 2012), but is the first time that any behavioral symptoms of withdrawal have been observe in cHAP mice. In MWM, however, there was no effect of a history of alcohol drinking on latency to escape, suggesting that spatial learning was not affected by alcohol exposure. Previous studies demonstrating decreased MWM learning after alcohol exposure were in rats (Lukoyanov et al., 1999; Novier et al., 2016), and it is unclear why we did not observe these changes in this study, but species may be a factor. Besides species, the age of animals being studied is a potential factor. For example, adolescents are more sensitive to alcohol-induced impairments in the acquisition of spatial learning and memory than adult rats (Acheson et al., 2001). Moreover, the duration of withdrawal may also be a factor. Chronic alcohol consumption for 8 weeks (20% ethanol in liquid diet) followed by a three or 12-weeks of withdrawal period produced significant deficits in learning and memory in male mice (Farr et al., 2005).

Overall, these findings may be of particular interest because comorbidity of AUD and anxiety is more common in women (Kessler et al., 1997) though AUD is more common in men (Lewis et al., 1996; Kessler et al., 1997; Hasin et al., 2007). Given that mice

TABLE 1 | Thiamine concentrations in the whole blood.

Average thiamine concentration (nmol/ml)	Control	EtOH
Mean	0.66	0.03*
SEM	0.15	0.003

*Effects of chronic alcohol exposure on thiamine concentrations in the blood. The concentration of thiamine in the blood was determined by LC-MS/MS as described in the "*Materials and Methods*". The results were expressed as mean ± SEM;* n = *8 for both control and EtOH group. *denotes a statistical difference,* $p < 0.05$.

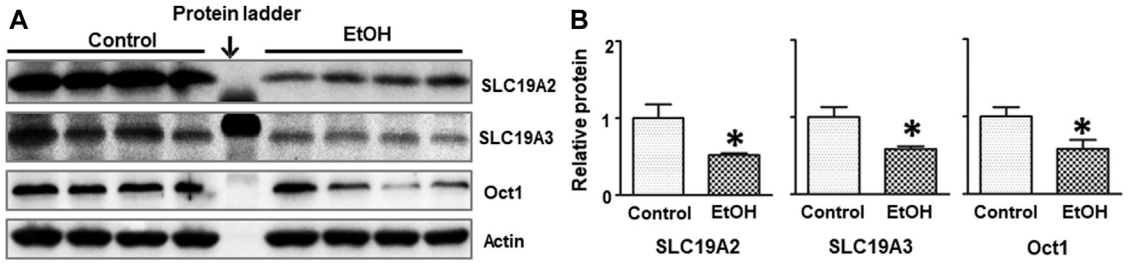

FIGURE 7 | Effects of chronic alcohol exposure on the expression of thiamine transporters in the brain. **(A)** The expression of thiamine transporters (SLC19A2, SLC19A3, and OCT1) in the cerebrum was determined by IB. **(B)** The relative amounts of expression were quantified and normalized to the expression of actin. The results were expressed as the mean ± SEM, n = 4 for each group. *$p < 0.05$ denotes a statistically significant difference from the control group.

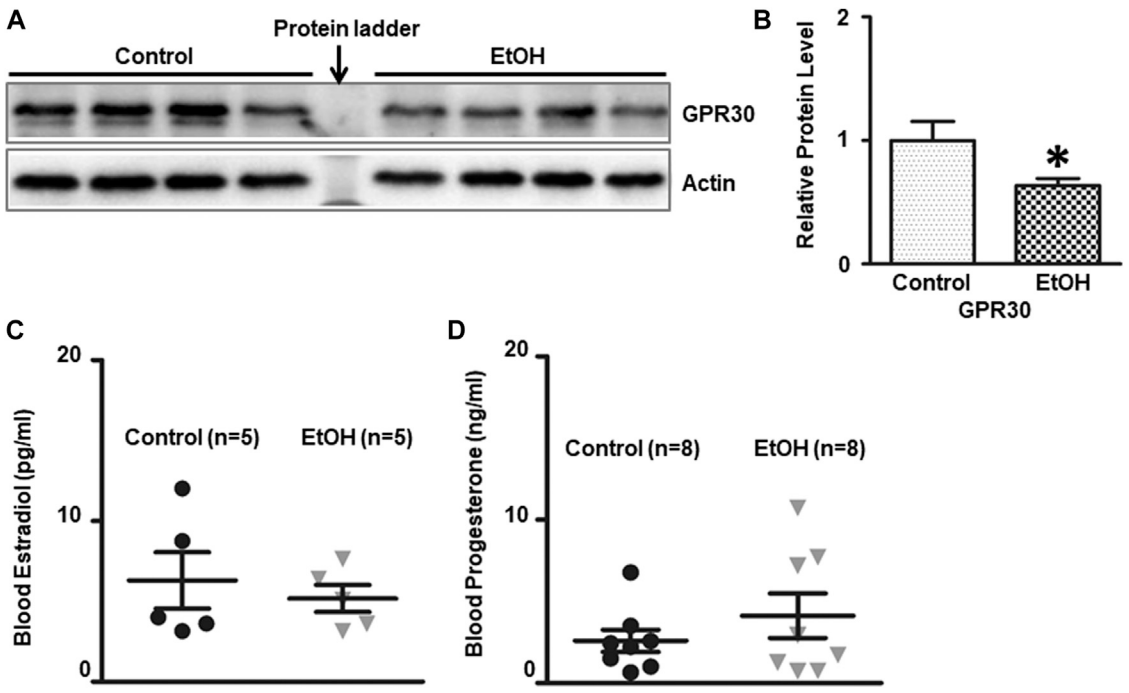

FIGURE 8 | Effects of chronic alcohol exposure on the expression of G-protein-coupled estrogen receptor (GPR30) in the brain, and estradiol/progesterone levels in the blood. **(A)** The expression of GPR30 in the cerebrum was determined by IB. **(B)** The relative amounts of expression were quantified and normalized to the expression of actin. The results were expressed as the mean ± SEM, n = 4 for each group. *$p < 0.05$ denotes a statistically significant difference from the control group. The concentration of estradiol **(C)** and progesterone **(D)** in the blood was determined by ELISA as described in the *Materials and Methods*. n = 5 for estradiol test, and n = 8 for progesterone test.

were showing elevated anxiety at least a week following the cessation of voluntary alcohol access, these findings are consistent with the idea that chronic drug self-administration causes homeostatic alterations in reward and stress systems that persist following cessation of drug use (Breese et al., 2005; Koob et al., 2014), and may drive subsequent relapse. In our previous study using male cHAP, we did not evaluate the effects of alcohol exposure on neurobehavioral outcomes, and therefore cannot make a conclusion whether this is a sex-specific effect. Nonetheless, the model of chronic voluntarily alcohol exposure in female cHAP mice could be useful to study the comorbidity of AUD with anxiety.

We examined several molecules/proteins that are known to be alcohol-sensitive and related to the control of anxiety behavior. We found that alcohol exposure increased GABA, CRF and BDNF, while decreasing CREB in the brain (**Figure 2**). GABAergic inhibitory transmission has been implicated as a contributory factor to the complex relationship between alcoholism and anxiety (Silberman et al., 2009). While some previous studies have showed that chronic alcohol exposure reduces GABA transmission (Hunt, 1983), other have demonstrated that chronic alcohol treatment increases GABA transmission in central amygdala (CeA) which is a brain region involved in anxiety and alcohol consumption behavior (Roberto

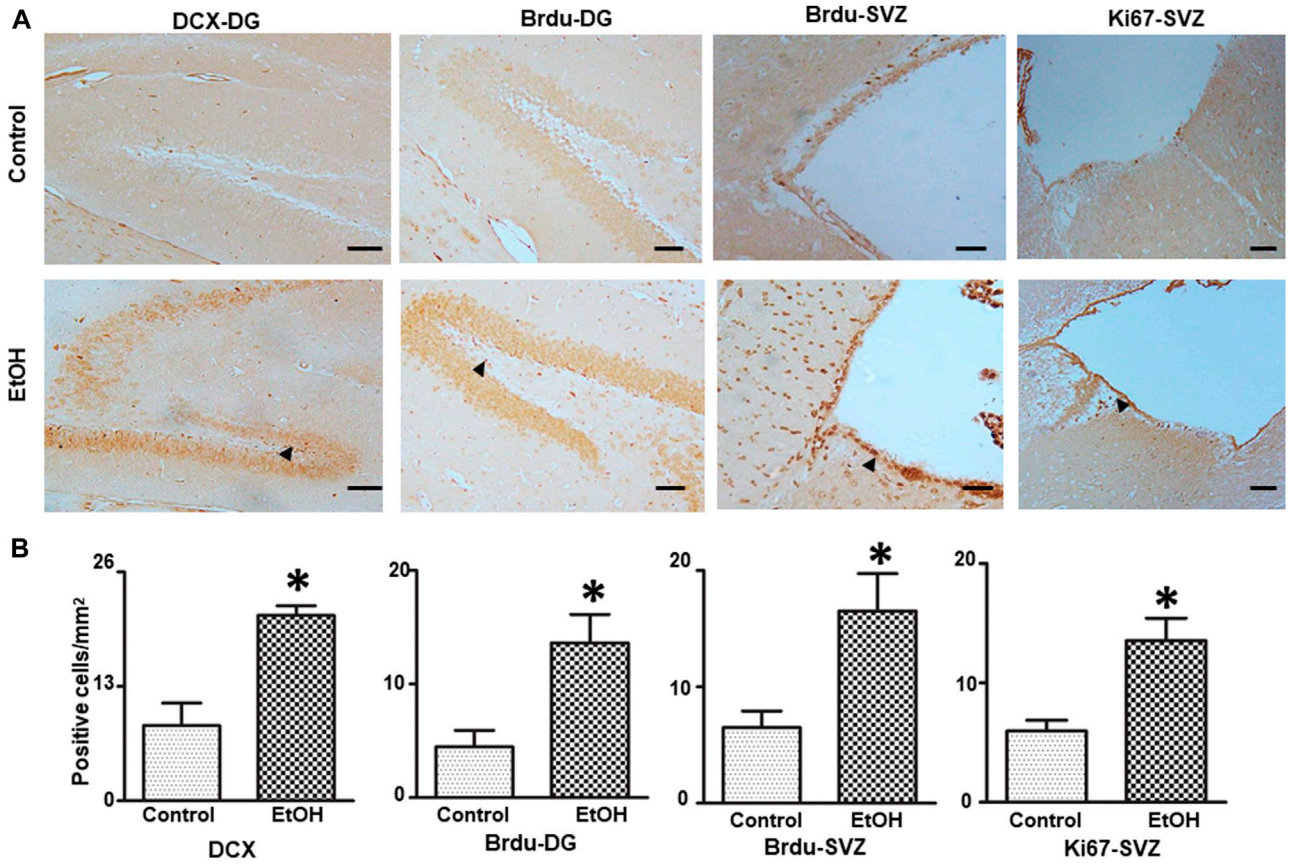

FIGURE 9 | Effects of chronic alcohol exposure on neurogenesis in the subventricular zone (SVZ) and dentate gyrus (DG) of the hippocampus. Both control and alcohol-exposed mice received BrdU injection. **(A)** BrdU-positive cells in the DG and SVZ were determined by IHC. Arrows indicate BrdU-positive cells; bar = 50 μm. The expression of doublecortin (DCX) in the DG of the hippocampus and Ki67 in the SVZ were examined by IHC. Arrows indicate DCX- and Ki67-positive cells; bar = 20 μm. **(B)** The number of DCX-, BrdU-, and Ki67-positive cells in the DG and SVZ was quantified as described in the "*Materials and Methods*" section. The results were expressed as mean ± SEM, n = 3 or 4 for each group. *$p < 0.05$ denotes a statistically significant difference from the control group.

et al., 2003; Koob, 2004; Roberto et al., 2004). We showed that chronic voluntarily alcohol drinking increased the levels of GABA in the brain tissues of female cHAP mice. A further study examining some brain structures specifically involved in the anxiety response, such as the amygdala may be necessary to establish a role of altered GABA levels in anxiety-like behaviors in this model. In addition, it may be desirable to treat these alcohol-exposed cHAP mice with GABA antagonists to determine whether GABA signaling is indeed involved in alcohol-induced anxiety.

CRF has been identified as a mediator of alcohol's action on GABA signaling in the CeA as alcohol-enhanced GABA signaling was blocked in CeA neurons in CRF1 receptor knockout mice (Nie et al., 2004). CRF and CRFR1 receptors have been implied in alcohol consumption (Lodge and Lawrence, 2003; Hansson et al., 2006; Cippitelli et al., 2012; Lowery-Gionta et al., 2012). Chronic feeding of alcoholic liquid diet increased the mRNA level of CRF in the CeA (Läck et al., 2005). CRF signaling may also be involved in anxiety behavior as CRF administration caused anxiety (Dunn and Berridge, 1990), whereas CRFR1 antagonists or knock-out of CRFR1 reduced anxiety-like behavior (Timpl et al., 1998; Zorrilla et al., 2002; Müller et al., 2003; Henckens et al., 2016). Therefore, the increased CRF level in alcohol-exposed cHAP mice, may contribute to alcohol consumption and anxiety-like behaviors. However, as discussed above, it is desirable to examine the levels of CRF in some brain regions that are involved in the regulation of anxiety, such as the amygdala. Further experiments using CRFR1 antagonists or knock out of CFR/CRFR1 in this model are necessary to confirm its role.

The neurotrophin BDNF is affected by alcohol exposure and associated with alcohol drinking behaviors (McGough et al., 2004; Jeanblanc et al., 2009; Logrip et al., 2009; Tapocik et al., 2014; Stragier et al., 2015). BDNF expression appears to have an inverse correlation with alcohol intake. There were a number of studies showing decreased BDNF level promoted behavioral responses to alcohol whereas increased level of BDNF attenuated alcohol preference (McGough et al., 2004; Jeanblanc et al., 2009). However, the findings regarding the relationship between BDNF level and anxiety disorder are not consistent in either animal models (Chen et al., 2006; Govindarajan et al., 2006; Monteggia et al., 2007) or human studies (Maina et al., 2010; Molendijk et al., 2011; Wang et al., 2011). The increased BDNF

level observed in the alcohol-exposed cHAP in this study, may account for the neurogenesis observed in the DG and SVZ (**Figure 9**). However, the impact of increased BDNF levels on anxiety in this study is unclear. Therefore, future studies using BDNF knockout mice or knockdown in this model will be desired to further determine the role of BDNF.

CREB is an alcohol-sensitive transcription factor (Uddin and Singh, 2007). Reduced levels of CREB and pCREB have been linked to the high anxiety and excessive alcohol intake in alcohol-preferring rats (Pandey et al., 2005). In addition, partial deletion of CREB caused alcohol-drinking and anxiety-like behaviors in mice (Pandey et al., 2004). We showed that the expression of CREB protein was decreased in the brain, particularly in the hippocampus and prefrontal cortex (PFC), the two brain regions that are involved in the control of stress-related behaviors (Russo and Nestler, 2013) and alcohol drinking behaviors (Koob and Roberts, 1999). A further study on the levels of CREB in other brain regions, such as the CeA and medial nuclei of amygdala (MeA), may be necessary to draw a conclusion. In addition, to determine whether the reduced CREB level contributes to alcohol-induced anxiety of in cHAP mice, we may infuse activators for CREB's upstream protein kinase PKA, or Neuropeptide Y, one of the CREB-targeted genes, into the amygdala, hippocampus or prefrontal cortex in future study.

The female sex hormones and their receptors have been proposed to modulate anxiety in both humans (Maeng and Milad, 2015; Li and Graham, 2017) and rodents (Zimmerberg and Farley, 1993; Toufexis, 2007; Domonkos et al., 2017). We demonstrate that chronic voluntary alcohol drinking decreased G-protein-coupled estrogen receptor GPR30 in the brain while had little effect on estradiol/progesterone levels in the blood. It has been shown that administration of GPR30 agonist G-1 can decrease anxiety in female mice suggesting anxiolytic effects of GPR30 (Tian et al., 2013; Anchan et al., 2014; Liu et al., 2015). Future experiments using GPR30 agonist G-1 will be able to determine the role of GPR30 in alcohol-induced anxiety in female cHAP mice.

Chronic Voluntary Alcohol Drinking Induced Oxidative Stress, ER Stress, Neuroinflammation and Neurodegeneration.

Oxidative stress, ER stress, neuroinflammation have been proposed as potential mechanisms for alcohol-induced neurodegeneration. For example, oxidative stress is associated with alcohol-induced neurodegeneration *in vitro* and *in vivo* (Chen and Luo, 2010; Hernández et al., 2016). There have been many studies showing a correlation between oxidative stress and alcohol dependence (Thome et al., 1997; Das et al., 2007; Haorah et al., 2008; Galicia-Moreno and Gutierrez-Reyes, 2014; Muñiz Hernandez et al., 2014). The link between oxidative stress and anxiety has been established in human patients or animal models and oxidative stress has been suggested to play a causative role in anxiety (Bouayed et al., 2009; Hovatta et al., 2010). Similar to our previous findings in male cHAP mice (Xu et al., 2019), chronic voluntary alcohol drinking also caused oxidative stress in female cHAP mice. Therefore, alcohol-induced oxidative stress in cHAP mice is not gender-specific. To further determine whether oxidative stress is involved in the alcohol dependence and anxiety in this model, future studies could use antioxidants or free radical scavengers in alcohol-drinking cHAP mice.

ER stress is another potential mechanism for alcohol-induced brain damage in both developing and adult brains (Yang and Luo, 2015). Similar to our previous findings in male cHAP mice (Xu et al., 2019), chronic voluntary alcohol drinking caused ER stress in female cHAP mice. There is little information regarding the role of ER stress in alcohol-drinking behaviors. However, ER stress may play a critical role in stress-related behaviors as treatment of 4-phenylbutyrate (4-PBA), a known ER stress inhibitor, alleviated anxiety-like behaviors in a mouse model for diffuse axonal injury (Huang et al., 2019). The administration of 4-PBA, and edaravone, a free radical scavenger, improved chronic restraint stress (CRS)-induced anxiety-like behaviors in mice which were accompanied with inhibition of oxidative stress, neuroinflammation and ER stress (Jangra et al., 2017).

In addition, chronic alcohol voluntary drinking caused caspase-3 activation in the brain, particularly the PFC and hippocampus, indicative of apoptosis. The PFC and hippocampus are parts of the brain reward circuitry that is vulnerable to alcohol exposure (Sunkesula et al., 2008; Wang et al., 2018; Xu et al., 2019). Again, these findings are consistent with our previous results obtained from male cHAP mice (Xu et al., 2019).

The alcohol-induced neurodegeneration in both adult and developing brain is often accompanied by neuroinflammation and gliosis (Alfonso-Loeches et al., 2013; Pascual et al., 2014; Tajuddin et al., 2014; Zhang and Luo, 2019). We showed that chronic alcohol exposure induced neuroinflammation which was demonstrated by the increased expression of proinflammatory TNFα, MCP-1 and its receptor CCR2 but not IL-6; alcohol also increased gliosis which was indicated by increased GFAP-labeled astrocytes (He and Crews, 2008; Sullivan and Zahr, 2008). The alcohol-induced neuroinflammation may also contribute to the anxiety-like behavior as higher basal levels of TNFα and MCP-1 were observed in patients with anxiety (Vogelzangs et al., 2016). Treatment TNFα inhibitors have been shown to improve the symptoms of anxiety in patients (Ertenli et al., 2012) and animals (Haji et al., 2012).

Chronic Voluntary Alcohol Drinking Reduced Thiamine in the Blood

Thiamine deficiency (TD) has long been associated with alcoholism (Leevy and Baker, 1968; Woodhill and Nobile, 1972; Butterworth, 1995) and has been implicated as a key factor for alcohol-induced brain damages (Martin et al., 2003; Liu et al., 2017). Our recent publication indicated thiamine deficiency can cause anxiety-like behaviors (Li et al., 2020). Xu et al. showed chronic voluntary alcohol drinking caused a significant decrease in the levels of thiamine in the brain but not the blood of male cHAP mice (Xu et al., 2019). In the present study, alcohol drinking

significantly reduced thiamine concentration in the blood of female cHAP (**Table 1**), and decreased the expression of thiamine transporters (SLC19A2, SLC19A3, and OCT1) in female cHAP mice (**Figure 7**). Our previous study showed that alcohol exposure down-regulated the expression of SLC19A3, but not SLC19A2 and OCT1 in male cHAP mice (Xu et al., 2019). Due to some technical problems, we were unable to detect and quantify thiamine in the brain of female cHAP mice. Further effort is needed to evaluate thiamine levels in the brain of female cHAP mice. The reduced levels of thiamine either in the brain and blood may contribute to anxiety-like behaviors.

Chronic Voluntary Alcohol Drinking Stimulated Neurogenesis in the Brain

Depending on the paradigms of alcohol exposure and experimental models employed, alcohol exposure could either inhibit or stimulate neurogenesis (Nixon and Crews, 2002; He et al., 2005; Ieraci and Herrera, 2007; Klintsova et al., 2007; Morris et al., 2010; Hamilton et al., 2011). In the current study, we used multiple markers, such as DCX, BrdU and Ki67 to monitor neurogenesis and demonstrated that chronic voluntary alcohol drinking increased the neurogenesis in the DG and SVZ of female cHAP mice. This findings is consistent with the result obtained from male cHAP mice (Xu et al., 2019). Therefore, the effect of chronic voluntary alcohol drinking on the neurogenesis in cHAP mice is not gender specific. The enhanced neurogenesis observed in these two regions may result from the increased BDNF expression and/or compensatory response to alcohol-induced neuronal damage.

In summary, chronic voluntary alcohol drinking caused anxiety-like behaviors, and altered the expression of several neurotransmitters and neurotrophic factors associated with the regulation of anxiety in female cHAP mice. In comparison with our previous study in male cHAP mice, the current results indicate that alcohol-induced damage and neurochemical changes to the brain, such as oxidative stress, ER stress, neurodegeneration and neurogenesis, are similar between male and female mice and not gender-specific. It appears that the effect of alcohol exposure on thiamine concentrations in the blood and the expression of thiamine transporters is different between male and female cHAP mice. Further studies are needed to investigate the underlying mechanisms.

DATA AVAILABILITY STATEMENT

The original data that support the findings of this study are available from the corresponding author upon reasonable request.

ETHICS STATEMENT

The animal study was reviewed and approved by the Institutional Animal Care and Use Committee (IACUC) at the University of Kentucky.

AUTHOR CONTRIBUTIONS

HX and JL were responsible for the study concept and design. HX, HL, DL, WW, MX, JF, and JC contributed to the acquisition of data. HX and JL drafted the manuscript. HZ and NG provided critical revision of the manuscript for important intellectual content. All authors reviewed content and approved the final version for publication.

FUNDING

This research is supported by the Department of Veterans Affairs, Veterans Health Administration, Office of Research and Development (Biomedical Laboratory Research and Development: Merit Review (BX001721)) to JL. It is also supported in part by grants from the National Institutes of Health (NIH) (AA017226 and AA015407) to JL. Provision of cHAP mice was supported by the NIH grant AA015512 to Richard Bell at the Indiana University Purdue University Indianapolis. It is also supported by the University of Kentucky Center of Biomedical Research Excellence (COBRE) grant P30 GM127211/GM/NIGMS NIH HHS/United States.

REFERENCES

Acheson, S. K., Ross, E. L., and Swartzwelder, H. S. (2001). Age-independent and dose-response effects of ethanol on spatial memory in rats. *Alcohol* 23, 167–175. doi:10.1016/s0741-8329(01)00127-6

Alfonso-Loeches, S., Pascual, M., and Guerri, C. (2013). Gender differences in alcohol-induced neurotoxicity and brain damage. *Toxicology* 311, 27–34. doi:10.1016/s0741-8329(01)00127-6

Alfonso-Loeches, S., Urena-Peralta, J., Morillo-Bargues, M. J., Gómez-Pinedo, U., and Guerri, C. (2016). Ethanol-induced TLR4/NLRP3 neuroinflammatory response in microglial cells promotes leukocyte infiltration across the BBB. *Neurochem. Res.* 41, 193–209. doi:10.1007/s11064-015-1760-5

Anchan, D., Clark, S., Pollard, K., and Vasudevan, N. (2014). GPR30 activation decreases anxiety in the open field test but not in the elevated plus maze test in female mice. *Brain Behav.* 4, 51–59. doi:10.1007/s11064-015-1760-5

Baiamonte, B. A., Valenza, M., Roltsch, E. A., Whitaker, A. M., Baynes, B. B., Sabino, V., et al. (2014). Nicotine dependence produces hyperalgesia: role of corticotropin-releasing factor-1 receptors (CRF1Rs) in the central amygdala (CeA). *Neuropharmacology* 77, 217–223. doi:10.1016/j.neuropharm.2013.09.025

Bajo, M., Cruz, M. T., Siggins, G. R., Messing, R., and Roberto, M. (2008). Protein kinase C epsilon mediation of CRF-and ethanol-induced GABA release in central amygdala. *Proc. Natl. Acad. Sci. U.S.A.* 105, 8410–8415. doi:10.1073/pnas.0802302105

Bale, T. L., and Epperson, C. N. (2015). Sex differences and stress across the lifespan. *Nat. Neurosci.* 18, 1413–1420. doi:10.1038/nn.4112

Bandelow, B., and Michaelis, S. (2015). Epidemiology of anxiety disorders in the 21st century. *Dialogues Clin. Neurosci.* 17, 327–335. doi:10.31887/DCNS.2015.17.3/bbandelow

Banerjee, N. (2014). Neurotransmitters in alcoholism: a review of neurobiological and genetic studies. *Indian J. Hum. Genet.* 20, 20–31. doi:10.4103/0971-6866.132750

Becker, H. C. (2012). Effects of alcohol dependence and withdrawal on stress responsiveness and alcohol consumption. *Alcohol Res. Curr. Rev.* 34, 448–458.

Binder, E. B., and Nemeroff, C. B. (2010). The CRF system, stress, depression and anxiety—insights from human genetic studies. *Mol. Psychiatry* 15, 574–588. doi:10.4103/0971-6866.132750

Bolaños, C. A., and Nestler, E. J. (2004). Neurotrophic mechanisms in drug addiction. *Neuromol. Med.* 5, 69–83. doi:10.1385/NMM:5:1:069

Bouayed, J., Rammal, H., and Soulimani, R. (2009). Oxidative stress and anxiety: relationship and cellular pathways. *Oxid. Med. Cell. Longevity* 2, 63–67. doi:10.4161/oxim.2.2.7944

Bouchery, E. E., Harwood, H. J., Sacks, J. J., Simon, C. J., and Brewer, R. D. (2011). Economic costs of excessive alcohol consumption in the US, 2006. *Am. J. Prev. Med.* 41, 516–524. doi:10.1016/j.amepre.2011.06.045

Breese, G. R., Chu, K., Dayas, C. V., Funk, D., Knapp, D. J., Koob, G. F., et al. (2005). Stress enhancement of craving during sobriety: a risk for relapse. *Alcohol. Clin. Exp. Res.* 29, 185–195. doi:10.1097/01.alc.0000153544.83656.3c

Brocardo, P. S., Boehme, F., Patten, A., Cox, A., Gil-Mohapel, J., and Christie, B. R. (2012). Anxiety-and depression-like behaviors are accompanied by an increase in oxidative stress in a rat model of fetal alcohol spectrum disorders: protective effects of voluntary physical exercise. *Neuropharmacology* 62, 1607–1618. doi:10.1016/j.amepre.2011.06.045

Burns, L., and Teesson, M. (2002). Alcohol use disorders comorbid with anxiety, depression and drug use disorders: findings from the Australian National Survey of Mental Health and Well Being. *Drug Alcohol Depend.* 68, 299–307. doi:10.1016/s0376-8716(02)00220-x

Butterworth, R. F. (1995). Pathophysiology of alcoholic brain damage: synergistic effects of ethanol, thiamine deficiency and alcoholic liver disease. *Metab. Brain Dis.* 10, 1–8. doi:10.1007/BF01991777

Chastain, L. G., and Sarkar, D. K. (2014). Role of microglia in regulation of ethanol neurotoxic action. *Int. Rev. Neurobiol.* 118, 81–103. doi:10.1016/B978-0-12-801284-0.00004-X

Chen, G., and Luo, J. (2010). Anthocyanins: are they beneficial in treating ethanol neurotoxicity?. *Neurotoxic. Res.* 17, 91–101. doi:10.1007/s12640-009-9083-4

Chen, Z.-Y., Jing, D., Bath, K. G., Ieraci, A., Khan, T., Siao, C.-J., et al. (2006). Genetic variant BDNF (Val66Met) polymorphism alters anxiety-related behavior. *Science* 314, 140–143. doi:10.1126/science.1129663

Cippitelli, A., Damadzic, R., Singley, E., Thorsell, A., Ciccocioppo, R., Eskay, R. L., et al. (2012). Pharmacological blockade of corticotropin-releasing hormone receptor 1 (CRH1R) reduces voluntary consumption of high alcohol concentrations in non-dependent Wistar rats. *Pharmacol. Biochem. Behav.* 100, 522–529. doi:10.1016/j.pbb.2011.10.016

Coppens, V., Morrens, M., Destoop, M., and Dom, G. (2019). The interplay of inflammatory processes and cognition in alcohol use disorders-A systematic review. *Front. Psychiatry* 10, 632. doi:10.3389/fpsyt.2019.00632

Cover, K., Maeng, L., Lebrón-Milad, K., and Milad, M. (2014). Mechanisms of estradiol in fear circuitry: implications for sex differences in psychopathology. *Transl. Psychiatry* 4, e422. doi:10.3389/fpsyt.2019.00632

Crews, F. T. (2008). Alcohol-related neurodegeneration and recovery: mechanisms from animal models. *Alcohol Res. Health* 31, 377–388.

Das, S. K., Hiran, K., Mukherjee, S., and Vasudevan, D. (2007). Oxidative stress is the primary event: effects of ethanol consumption in brain. *Indian J. Clin. Biochem.* 22, 99–104. doi:10.1007/BF02912890

Domonkos, E., Borbélyová, V., Csongová, M., Bosý, M., Kačmárová, M., Ostatníková, D., et al. (2017). Sex differences and sex hormones in anxiety-like behavior of aging rats. *Horm. Behav.* 93, 159–165. doi:10.1016/j.yhbeh.2017.05.019

Dunn, A. J., and Berridge, C. W. (1990). Physiological and behavioral responses to corticotropin-releasing factor administration: is CRF a mediator of anxiety or stress responses?. *Brain Res. Rev.* 15, 71–100. doi:10.1016/0165-0173(90)90012-d

Erickson, E. K., Grantham, E. K., Warden, A. S., and Harris, R. A. (2019). Neuroimmune signaling in alcohol use disorder. *Pharmacol. Biochem. Behav.* 177, 34–60. doi:10.1016/j.pbb.2018.12.007

Ertenli, I., Ozer, S., Kiraz, S., Apras, S., Akdogan, A., Karadag, O., et al. (2012). Infliximab, a TNF-alpha antagonist treatment in patients with ankylosing spondylitis: the impact on depression, anxiety and quality of life level. *Rheumatol. Int.* 32, 323–330. doi:10.1007/s00296-010-1616-x

Farr, S. A., Scherrer, J. F., Banks, W. A., Flood, J. F., and Morley, J. E. (2005). Chronic ethanol consumption impairs learning and memory after cessation of ethanol. *Alcohol Clin. Exp. Res.* 29, 971–982. doi:10.1097/01.alc.0000171038.03371.56

Galicia-Moreno, M., and Gutierrez-Reyes, G. (2014). The role of oxidative stress in the development of alcoholic liver disease. *Rev. Gastroenterol. México* 79, 135–144. doi:10.1016/j.rgmx.2014.03.001

Govindarajan, A., Rao, B. S., Nair, D., Trinh, M., Mawjee, N., Tonegawa, S., et al. (2006). Transgenic brain-derived neurotrophic factor expression causes both anxiogenic and antidepressant effects. *Proc. Natl. Acad. Sci. U.S.A.* 103, 13208–13213. doi:10.1073/pnas.0605180103

Grant, B. F. (1998). The impact of a family history of alcoholism on the relationship between age at onset of alcohol use and DSM–IV alcohol dependence: results from the national longitudinal alcohol epidemiologic survey. *Alcohol Health Res. World* 22, 144–147.

Grant, B. F., Dawson, D. A., Stinson, F. S., Chou, S. P., Dufour, M. C., and Pickering, R. P. (2004). The 12-month prevalence and trends in DSM-IV alcohol abuse and dependence: United States, 1991–1992 and 2001–2002. *Drug and alcohol dependence* 74, 223–234. doi:10.1016/j.drugalcdep.2004.02.004

Grant, B. F., Dawson, D. A., Stinson, F. S., Chou, S. P., Dufour, M. C., and Pickering, R. P. (2006). The 12-month prevalence and trends in DSM–IV alcohol abuse and dependence: United States, 1991–1992 and 2001–2002. *Alcohol Res. Health* 29, 79–91.

Grant, B. F., Goldstein, R. B., Saha, T. D., Chou, S. P., Jung, J., Zhang, H., et al. (2015). Epidemiology of DSM-5 alcohol use disorder: results from the national epidemiologic survey on alcohol and related conditions III. *JAMA Psychiatry* 72, 757–766. doi:10.1073/pnas.0605180103

Haji, N., Mandolesi, G., Gentile, A., Sacchetti, L., Fresegna, D., Rossi, S., et al. (2012). TNF-α-mediated anxiety in a mouse model of multiple sclerosis. *Exp. Neurol.* 237, 296–303. doi:10.1016/j.expneurol.2012.07.010

Hamilton, G., Murawski, N., Cyr, S. S., Jablonski, S., Schiffino, F., Stanton, M., et al. (2011). Neonatal alcohol exposure disrupts hippocampal neurogenesis and contextual fear conditioning in adult rats. *Brain Res.* 1412, 88–101. doi:10.1016/j.brainres.2011.07.027

Hansson, A. C., Cippitelli, A., Sommer, W. H., Fedeli, A., Björk, K., Soverchia, L., et al. (2006). Variation at the rat Crhr1 locus and sensitivity to relapse into alcohol seeking induced by environmental stress. *Proc. Natl. Acad. Sci. U.S.A.* 103, 15236–15241. doi:10.1016/j.brainres.2011.07.027

Haorah, J., Ramirez, S. H., Floreani, N., Gorantla, S., Morsey, B., and Persidsky, Y. (2008). Mechanism of alcohol-induced oxidative stress and neuronal injury. *Free Radic. Biol. Med.* 45, 1542–1550. doi:10.1016/j.freeradbiomed.2008.08.030

Harper, C. (1998). The neuropathology of alcohol-specific brain damage, or does alcohol damage the brain?. *J. Neuropathol. Exp. Neurol.* 57, 101–110. doi:10.1097/00005072-199802000-00001

Hasin, D. S., Stinson, F. S., Ogburn, E., and Grant, B. F. (2007). Prevalence, correlates, disability, and comorbidity of DSM-IV alcohol abuse and dependence in the United States: results from the National Epidemiologic Survey on Alcohol and Related Conditions. *Arch. Gen. Psychiatry* 64, 830–842. doi:10.1001/archpsyc.64.7.830

He, J., and Crews, F. T. (2008). Increased MCP-1 and microglia in various regions of the human alcoholic brain. *Exp. Neurol.* 210, 349–358. doi:10.1016/j.expneurol.2007.11.017

He, J., Nixon, K., Shetty, A. K., and Crews, F. T. (2005). Chronic alcohol exposure reduces hippocampal neurogenesis and dendritic growth of newborn neurons. *Eur. J. Neurosci.* 21, 2711–2720. doi:10.1111/j.1460-9568.2005.04120.x

Henckens, M. J., Deussing, J. M., and Chen, A. (2016). Region-specific roles of the corticotropin-releasing factor–urocortin system in stress. *Nat. Rev. Neurosci.* 17, 636–651. doi:10.1038/nrn.2016.94

Hernández, J. A., López-Sánchez, R. C., and Rendón-Ramírez, A. (2016). Lipids and oxidative stress associated with ethanol-induced neurological damage. *Oxid. Med. Cell. Longevity* 2016, 1543809. doi:10.1155/2016/1543809

Hingson, R. W., Heeren, T., and Winter, M. R. (2006). Age at drinking onset and alcohol dependence: age at onset, duration, and severity. *Arch. Pediatr. Adolesc. Med.* 160, 739–746. doi:10.1001/archpedi.160.7.739

Hovatta, I., Juhila, J., and Donner, J. (2010). Oxidative stress in anxiety and comorbid disorders. *Neurosci. Res.* 68, 261–275. doi:10.1016/j.neures.2010.08.007

Huang, G.-H., Chen, K., Sun, Y.-Y., Zhu, L., Sun, Z.-L., and Feng, D.-F. (2019). 4-Phenylbutyrate ameliorates anxiety disorder by inhibiting endoplasmic

reticulum stress after diffuse axonal injury. *J. Neurotrauma* 36, 1856–1868. doi:10.1089/neu.2018.6048

Hunt, W. A. (1983). The effect of ethanol on GABAergic transmission. *Neurosci. Biobehav Rev.* 7, 87–95. doi:10.1016/0149-7634(83)90009-x

Hurley, L. L., and Tizabi, Y. (2013). Neuroinflammation, neurodegeneration, and depression. *Neurotoxic. Res.* 23, 131–144. doi:10.1016/0149-7634(83)90009-x

Ieraci, A., and Herrera, D. G. (2007). Single alcohol exposure in early life damages hippocampal stem/progenitor cells and reduces adult neurogenesis. *Neurobiol. Dis.* 26, 597–605. doi:10.1016/j.nbd.2007.02.011

Jangra, A., Sriram, C. S., Dwivedi, S., Gurjar, S. S., Hussain, M. I., Borah, P., et al. (2017). Sodium phenylbutyrate and edaravone abrogate chronic restraint stress-induced behavioral deficits: implication of oxido-nitrosative, endoplasmic reticulum stress cascade, and neuroinflammation. *Cell Mol. Neurobiol.* 37, 65–81. doi:10.1007/s10571-016-0344-5

Jeanblanc, J., He, D.-Y., Carnicella, S., Kharazia, V., Janak, P. H., and Ron, D. (2009). Endogenous BDNF in the dorsolateral striatum gates alcohol drinking. *J. Neurosci.* 29, 13494–13502. doi:10.1523/JNEUROSCI.2243-09.2009

Kalueff, A. V., and Nutt, D. J. (2007). Role of GABA in anxiety and depression. *Depress. Anxiety* 24, 495–517. doi:10.1002/da.20262

Kamal, H., Tan, G. C., Ibrahim, S. F., Shaikh, M. F., Mohamed, I. N., Mohamed, R. M. P., et al. (2020). Alcohol use disorder, neurodegeneration, Alzheimer's and Parkinson's disease: interplay between oxidative stress, neuroimmune response and excitotoxicity. *Front. Cell. Neurosci.* 14, 282. doi:10.1002/da.20262

Kato, K., Moriyama, C., Ito, N., Zhang, X., Hachiuma, K., Hagima, N., et al. (2015). Involvement of organic cation transporters in the clearance and milk secretion of thiamine in mice. *Pharm. Res.* 32, 2192–2204. doi:10.1007/s11095-014-1608-8

Kempuraj, D., Thangavel, R., Natteru, P., Selvakumar, G., Saeed, D., Zahoor, H., et al. (2016). Neuroinflammation induces neurodegeneration. *J. Neurol. Neurosurg. Spine* 1, 1003.

Kessler, R. C., Crum, R. M., Warner, L. A., Nelson, C. B., Schulenberg, J., and Anthony, J. C. (1997). Lifetime co-occurrence of DSM-III-R alcohol abuse and dependence with other psychiatric disorders in the National Comorbidity Survey. *Arch. Gen. Psychiatry* 54, 313–321. doi:10.1001/archpsyc.1997.01830160031005

Kim, M. J., Nagy, L. E., and Park, P.-H. (2014). Globular adiponectin inhibits ethanol-induced reactive oxygen species production through modulation of NADPH oxidase in macrophages: involvement of liver kinase B1/AMP-activated protein kinase pathway. *Mol. Pharmacol.* 86, 284–296. doi:10.1124/mol.114.093039

Klintsova, A. Y., Helfer, J. L., Calizo, L. H., Dong, W. K., Goodlett, C. R., and Greenough, W. T. (2007). Persistent impairment of hippocampal neurogenesis in young adult rats following early postnatal alcohol exposure. *Alcohol. Clin. Exp. Res.* 31, 2073–2082. doi:10.1111/j.1530-0277.2007.00528.x

Koob, G. F. (2004). A role for GABA mechanisms in the motivational effects of alcohol. *Biochem. Pharmacol.* 68, 1515–1525. doi:10.1016/j.bcp.2004.07.031

Koob, G. F., and Roberts, A. J. (1999). Brain reward circuits in alcoholism. *CNS Spectrums* 4, 23–37. doi:10.1017/s1092852900011196

Koob, G., and Thatcher-Britton, K. (1985). Stimulant and anxiogenic effects of corticotropin releasing factor. *Prog. Clin. Biol. Res.* 192, 499–506.

Koob, G. F., Buck, C. L., Cohen, A., Edwards, S., Park, P. E., Schlosburg, J. E., et al. (2014). Addiction as a stress surfeit disorder. *Neuropharmacology* 76, 370–382. doi:10.1016/j.bcp.2004.07.031

Kushner, M. G., Abrams, K., and Borchardt, C. (2000). The relationship between anxiety disorders and alcohol use disorders: a review of major perspectives and findings. *Clin. Psychol. Rev.* 20, 149–171. doi:10.1016/s0272-7358(99)00027-6

Läck, A. K., Floyd, D. W., and Mccool, B. A. (2005). Chronic ethanol ingestion modulates proanxiety factors expressed in rat central amygdala. *Alcohol* 36, 83–90. doi:10.1016/j.alcohol.2005.07.004

Lebron-Milad, K., and Milad, M. R. (2012). Sex differences, gonadal hormones and the fear extinction network: implications for anxiety disorders. *Biol. Mood Anxiety Disord.* 2, 3. doi:10.1186/2045-5380-2-3

Leevy, C. M., and Baker, H. (1968). Vitamins and alcoholism. Introduction. *Am. J. Clin. Nutr.* 21, 1325–1328. doi:10.1093/ajcn/21.11.1325

Lewis, C. E., Bucholz, K. K., Spitznagel, E., and Shayka, J. J. (1996). Effects of gender and comorbidity on problem drinking in a community sample. *Alcohol. Clin. Exp. Res.* 20, 466–476. doi:10.1111/j.1530-0277.1996.tb01077.x

Li, S. H., and Graham, B. M. (2017). Why are women so vulnerable to anxiety, trauma-related and stress-related disorders? The potential role of sex hormones. *Lancet Psychiatry* 4, 73–82. doi:10.1016/S2215-0366(16)30358-3

Li, H., Xu, H., Wen, W., Wu, L., Xu, M., and Luo, J. (2020). Thiamine deficiency causes long-lasting neurobehavioral deficits in mice. *Brain Sci.* 10, 565. doi:10.3390/brainsci10080565

Liu, D., Ke, Z., and Luo, J. (2017). Thiamine deficiency and neurodegeneration: the interplay among oxidative stress, endoplasmic reticulum stress, and autophagy. *Mol. Neurobiol.* 54, 5440–5448. doi:10.1007/s12035-016-0079-9

Liu, S.-B., Tian, Z., Guo, Y.-Y., Zhang, N., Feng, B., and Zhao, M.-G. (2015). Activation of GPR30 attenuates chronic pain-related anxiety in ovariectomized mice. *Psychoneuroendocrinology* 53, 94–107. doi:10.1016/j.psyneuen.2014.12.021

Lodge, D. J., and Lawrence, A. J. (2003). The CRF1 receptor antagonist antalarmin reduces volitional ethanol consumption in isolation-reared fawn-hooded rats. *Neuroscience* 117, 243–247. doi:10.1016/s0306-4522(02)00793-5

Logrip, M. L., Janak, P. H., and Ron, D. (2009). Escalating ethanol intake is associated with altered corticostriatal BDNF expression. *J. Neurochem.* 109, 1459–1468. doi:10.1111/j.1471-4159.2009.06073.x

Lopez, M. F., Grahame, N. J., and Becker, H. C. (2011). Development of ethanol withdrawal-related sensitization and relapse drinking in mice selected for high- or low-ethanol preference. *Alcohol. Clin. Exp. Res.* 35, 953–962. doi:10.1111/j.1530-0277.2010.01426.x

Lowery-Gionta, E. G., Navarro, M., Li, C., Pleil, K. E., Rinker, J. A., Cox, B. R., et al. (2012). Corticotropin releasing factor signaling in the central amygdala is recruited during binge-like ethanol consumption in C57BL/6J mice. *J. Neurosci.* 32, 3405–3413. doi:10.1523/JNEUROSCI.6256-11.2012

Lukoyanov, N. V., Madeira, M. D., and Paula–Barbosa, M. M. (1999). Behavioral and neuroanatomical consequences of chronic ethanol intake and withdrawal. *Physiol. Behav.* 66, 337–346. doi:10.1016/s0031-9384(98)00301-1

Lundahl, L. H., Davis, T. M., Adesso, V. J., and Lukas, S. E. (1997). Alcohol expectancies: effects of gender, age, and family history of alcoholism. *Addict. Behav.* 22, 115–125. doi:10.1016/s0306-4603(96)00022-6

Maeng, L. Y., and Milad, M. R. (2015). Sex differences in anxiety disorders: interactions between fear, stress, and gonadal hormones. *Horm. Behav.* 76, 106–117. doi:10.1016/j.yhbeh.2015.04.002

Maina, G., Rosso, G., Zanardini, R., Bogetto, F., Gennarelli, M., and Bocchio-Chiavetto, L. (2010). Serum levels of brain-derived neurotrophic factor in drug-naive obsessive–compulsive patients: a case–control study. *J. Affective Disord.* 122, 174–178. doi:10.1016/j.jad.2009.07.009

Martin, P. R., Singleton, C. K., and Hiller-Sturmhöfel, S. (2003). The role of thiamine deficiency in alcoholic brain disease. *Alcohol Res. Health* 27, 134–142.

Matson, L. M., and Grahame, N. J. (2013). Pharmacologically relevant intake during chronic, free-choice drinking rhythms in selectively bred high alcohol-preferring mice. *Addict. Biol.* 18, 921–929. doi:10.1111/j.1369-1600.2011.00412.x

Matson, L. M., Kasten, C. R., Boehm, S. L., and Grahame, N. J. (2014). Selectively bred crossed high-alcohol-preferring mice drink to intoxication and develop functional tolerance, but not locomotor sensitization during free-choice ethanol access. *Alcohol. Clin. Exp. Res.* 38, 267–274. doi:10.1111/acer.12216

Mcgough, N. N., He, D.-Y., Logrip, M. L., Jeanblanc, J., Phamluong, K., Luong, K., et al. (2004). RACK1 and brain-derived neurotrophic factor: a homeostatic pathway that regulates alcohol addiction. *J. Neurosci.* 24, 10542–10552. doi:10.1523/JNEUROSCI.3714-04.2004

Mclean, C. P., and Anderson, E. R. (2009). Brave men and timid women? A review of the gender differences in fear and anxiety. *Clin. Psychol. Rev.* 29, 496–505. doi:10.1016/j.cpr.2009.05.003

Molendijk, M. L., Bus, B. A., Spinhoven, P., Penninx, B. W., Kenis, G., Prickaerts, J., et al. (2011). Serum levels of brain-derived neurotrophic factor in major depressive disorder: state–trait issues, clinical features and pharmacological treatment. *Mol. Psychiatry* 16, 1088–1095. doi:10.1038/mp.2010.98

Monteggia, L. M., Luikart, B., Barrot, M., Theobold, D., Malkovska, I., Nef, S., et al. (2007). Brain-derived neurotrophic factor conditional knockouts show gender differences in depression-related behaviors. *Biol. Psychiatry* 61, 187–197. doi:10.1016/j.biopsych.2006.03.021

Morris, S. A., Eaves, D. W., Smith, A. R., and Nixon, K. (2010). Alcohol inhibition of neurogenesis: a mechanism of hippocampal neurodegeneration in an

adolescent alcohol abuse model. *Hippocampus* 20, 596–607. doi:10.1002/hipo.20665

Müller, M. B., Zimmermann, S., Sillaber, I., Hagemeyer, T. P., Deussing, J. M., Timpl, P., et al. (2003). Limbic corticotropin-releasing hormone receptor 1 mediates anxiety-related behavior and hormonal adaptation to stress. *Nat. Neurosci.* 6, 1100–1107. doi:10.1038/nn1123

Muñiz Hernandez, S., Velazquez Fernandez, J. B., Diaz Chavez, J., Lopez Sanchez, R. C., Hernandez, J. A., and Rendon Ramirez, A. (2014). Alcoholism: common and oxidative damage biomarkers. *J. Clin. Toxicol.* S7, S7-006. doi:10.4172/2161-0495.S7-006

Nair, U. R., Vidhukumar, K., and Prabhakaran, A. (2016). Age at onset of alcohol use and alcohol use disorder: time-trend study in patients seeking de-addiction services in Kerala. *Indian J. Psychol. Med.* 38, 315–319. doi:10.4103/0253-7176.185958

Nie, Z., Schweitzer, P., Roberts, A. J., Madamba, S. G., Moore, S. D., and Siggins, G. R. (2004). Ethanol augments GABAergic transmission in the central amygdala via CRF1 receptors. *Science* 303, 1512–1514. doi:10.1126/science.1092550

Nixon, K., and Crews, F. T. (2002). Binge ethanol exposure decreases neurogenesis in adult rat hippocampus. *J. Neurochem.* 83, 1087–1093. doi:10.1046/j.1471-4159.2002.01214.x

Novier, A., Ornelas, L. C., Diaz-Granados, J. L., and Matthews, D. B. (2016). Differences in behavioral responding in adult and aged rats following chronic ethanol exposure. *Alcohol. Clin. Exp. Res.* 40, 1462–1472. doi:10.1111/acer.13098

Pandey, S. C., Roy, A., Zhang, H., and Xu, T. (2004). Partial deletion of the cAMP response element-binding protein gene promotes alcohol-drinking behaviors. *J. Neurosci.* 24, 5022–5030. doi:10.1046/j.1471-4159.2002.01214.x

Pandey, S. C., Zhang, H., Roy, A., and Xu, T. (2005). Deficits in amygdaloid cAMP-responsive element–binding protein signaling play a role in genetic predisposition to anxiety and alcoholism. *J. Clin. Invest.* 115, 2762–2773. doi:10.1172/JCI24381

Pascual, M., Pla, A., Miñarro, J., and Guerri, C. (2014). Neuroimmune activation and myelin changes in adolescent rats exposed to high-dose alcohol and associated cognitive dysfunction: a review with reference to human adolescent drinking. *Alcohol Alcohol.* 49, 187–192. doi:10.1093/alcalc/agt164

Perluigi, M., Swomley, A. M., and Butterfield, D. A. (2014). Redox proteomics and the dynamic molecular landscape of the aging brain. *Ageing Res. Rev.* 13, 75–89. doi:10.1016/j.arr.2013.12.005

Petry, N. M., Stinson, F. S., and Grant, B. F. (2005). Comorbidity of DSM-IV pathological gambling and other psychiatric disorders: results from the National Epidemiologic Survey on Alcohol and Related Conditions. *J. Clin. Psychiatry* 66, 564–574. doi:10.4088/jcp.v66n0504

Ramesh, G., Maclean, A. G., and Philipp, M. T. (2013). Cytokines and chemokines at the crossroads of neuroinflammation, neurodegeneration, and neuropathic pain. *Mediators Inflamm.* 2013, 480739. doi:10.1155/2013/480739

Randall, C. L., Thomas, S., and Thevos, A. K. (2001). Concurrent alcoholism and social anxiety disorder: a first step toward developing effective treatments. *Alcohol. Clin. Exp. Res.* 25, 210–220. doi:10.1111/j.1530-0277.2001.tb02201.x

Risbrough, V. B., and Stein, M. B. (2006). Role of corticotropin releasing factor in anxiety disorders: a translational research perspective. *Horm. Behav.* 50, 550–561. doi:10.1016/j.yhbeh.2006.06.019

Roberto, M., Madamba, S. G., Moore, S. D., Tallent, M. K., and Siggins, G. R. (2003). Ethanol increases GABAergic transmission at both pre-and postsynaptic sites in rat central amygdala neurons. *Proc. Natl. Acad. Sci. U.S.A.* 100, 2053–2058. doi:10.1073/pnas.0437926100

Roberto, M., Madamba, S. G., Stouffer, D. G., Parsons, L. H., and Siggins, G. R. (2004). Increased GABA release in the central amygdala of ethanol-dependent rats. *J. Neurosci.* 24, 10159–10166. doi:10.1523/JNEUROSCI.3004-04.2004

Roberto, M., Spierling, S. R., Kirson, D., and Zorrilla, E. P. (2017). Corticotropin-releasing factor (CRF) and addictive behaviors. *Int. Rev. Neurobiol.* 136, 5–51. doi:10.1016/bs.irn.2017.06.004

Russo, S. J., and Nestler, E. J. (2013). The brain reward circuitry in mood disorders. *Nat. Rev. Neurosci.* 14, 609–625. doi:10.1038/nrn3381

Schneier, F. R., Foose, T. E., Hasin, D. S., Heimberg, R. G., Liu, S.-M., Grant, B. F., et al. (2010). Social anxiety disorder and alcohol use disorder co-morbidity in the National Epidemiologic Survey on Alcohol and Related Conditions. *Psychol. Med.* 40, 977–988. doi:10.1017/S0033291709991231

Seibenhener, M. L., and Wooten, M. C. (2015). Use of the Open Field Maze to measure locomotor and anxiety-like behavior in mice. *J. Vis. Exp.* e52434. doi:10.3791/52434

Silberman, Y., Bajo, M., Chappell, A. M., Christian, D. T., Cruz, M., Diaz, M. R., et al. (2009). Neurobiological mechanisms contributing to alcohol–stress–anxiety interactions. *Alcohol* 43, 509–519. doi:10.1016/j.alcohol.2009.01.002

Stragier, E., Massart, R., Salery, M., Hamon, M., Geny, D., Martin, V., et al. (2015). Ethanol-induced epigenetic regulations at the Bdnf gene in C57BL/6J mice. *Mol. Psychiatry* 20, 405–412. doi:10.1038/mp.2014.38

Sullivan, E. V., and Zahr, N. M. (2008). Neuroinflammation as a neurotoxic mechanism in alcoholism: commentary on" Increased MCP-1 and microglia in various regions of human alcoholic brain. *Exp. Neurol.* 213, 10–17. doi:10.1016/j.expneurol.2008.05.016

Sunkesula, S. R. B., Swain, U., and Babu, P. P. (2008). Cell death is associated with reduced base excision repair during chronic alcohol administration in adult rat brain. *Neurochem. Res.* 33, 1117–1128. doi:10.1007/s11064-007-9560-1

Tajuddin, N., Moon, K.-H., Marshall, S. A., Nixon, K., Neafsey, E. J., Kim, H.-Y., et al. (2014). Neuroinflammation and neurodegeneration in adult rat brain from binge ethanol exposure: abrogation by docosahexaenoic acid. *PLoS One* 9, e101223. doi:10.1371/journal.pone.0101223

Tapocik, J. D., Barbier, E., Flanigan, M., Solomon, M., Pincus, A., Pilling, A., et al. (2014). microRNA-206 in rat medial prefrontal cortex regulates BDNF expression and alcohol drinking. *J. Neurosci.* 34, 4581–4588. doi:10.1523/JNEUROSCI.0445-14.2014

Terra, M. B., Barros, H. M., Stein, A. T., Figueira, I., Jorge, M. R., Palermo, L. H., et al. (2006). Social anxiety disorder in 300 patients hospitalized for alcoholism in Brazil: high prevalence and undertreatment. *Compr. Psychiatry* 47, 463–467. doi:10.1016/j.comppsych.2006.02.004

Thome, J., Zhang, J., Davids, E., Foley, P., Weijers, H. G., Wiesbeck, G. A., et al. (1997). Evidence for increased oxidative stress in alcohol-dependent patients provided by quantification of *in vivo* salicylate hydroxylation products. *Alcohol. Clin. Exp. Res.* 21, 82–85. doi:10.1111/j.1530-0277.1997.tb03732.x

Tian, Z., Wang, Y., Zhang, N., Guo, Y.-Y., Feng, B., Liu, S.-B., et al. (2013). Estrogen receptor GPR30 exerts anxiolytic effects by maintaining the balance between GABAergic and glutamatergic transmission in the basolateral amygdala of ovariectomized mice after stress. *Psychoneuroendocrinology* 38, 2218–2233. doi:10.1016/j.psyneuen.2013.04.011

Timpl, P., Spanagel, R., Sillaber, I., Kresse, A., Reul, J. M., Stalla, G. K., et al. (1998). Impaired stress response and reduced anxiety in mice lacking a functional corticotropin-releasing hormone receptor 1. *Nat. Genet.* 19, 162–166. doi:10.1038/520

Toufexis, D. (2007). Region-and sex-specific modulation of anxiety behaviours in the rat. *J. Neuroendocrinol.* 19, 461–473. doi:10.1111/j.1365-2826.2007.01552.x

Uddin, R., and Singh, S. (2007). Ethanol-responsive genes: identification of transcription factors and their role in metabolomics. *Pharmacogenomics J.* 7, 38–47. doi:10.1038/sj.tpj.6500394

Vallières, L., and Rivest, S. (1999). Interleukin-6 is a needed proinflammatory cytokine in the prolonged neural activity and transcriptional activation of corticotropin-releasing factor during endotoxemia. *Endocrinology* 140, 3890–3903. doi:10.1210/endo.140.9.6983

Vogelzangs, N., De Jonge, P., Smit, J., Bahn, S., and Penninx, B. (2016). Cytokine production capacity in depression and anxiety. *Transl. Psychiatry* 6, e825. doi:10.1038/tp.2016.92

Vorhees, C. V., and Williams, M. T. (2006). Morris water maze: procedures for assessing spatial and related forms of learning and memory. *Nat. Protoc.* 1, 848–858. doi:10.1038/nprot.2006.116

Walf, A. A., and Frye, C. A. (2007). The use of the elevated plus maze as an assay of anxiety-related behavior in rodents. *Nat. Protoc.* 2, 322–328. doi:10.1038/nprot.2007.44

Wang, X., Yu, H., You, J., Wang, C., Feng, C., Liu, Z., et al. (2018). Memantine can improve chronic ethanol exposure-induced spatial memory impairment in male C57BL/6 mice by reducing hippocampal apoptosis. *Toxicology* 406, 21–32. doi:10.1016/j.tox.2018.05.013

Wang, Y., Mathews, C. A., Li, Y., Lin, Z., and Xiao, Z. (2011). Brain-derived neurotrophic factor (BDNF) plasma levels in drug-naïve OCD patients are lower than those in healthy people, but are not lower than those in drug-treated OCD patients. *J. Affective Disord.* 133, 305–310. doi:10.1016/j.jad.2011.04.002

Woodhill, J., and Nobile, S. (1972). Thiamine in the 1970 Australian diet with special reference to cereals and the assessment of thiamine statusInternationale

Zeitschrift fur Vitamin-und Ernahrungsforschung. *Int. J. Vitam. Nutr. Res.* 42, 435–443.

Xu, H., Liu, D., Chen, J., Li, H., Xu, M., Wen, W., et al. (2019). Effects of chronic voluntary alcohol drinking on thiamine concentrations, endoplasmic reticulum stress, and oxidative stress in the brain of crossed high alcohol preferring mice. *Neurotoxicity Res.* 36, 777–787. doi:10.1007/s12640-019-00032-y

Xu, W., Hawkey, A. B., Li, H., Dai, L., Brim, H. H., Frank, J. A., et al. (2018). Neonatal ethanol exposure causes behavioral deficits in young mice. *Alcohol. Clin. Exp. Res.* 42, 743–750. doi:10.1111/acer.13598

Yang, F., and Luo, J. (2015). Endoplasmic reticulum stress and ethanol neurotoxicity. *Biomolecules* 5, 2538–2553. doi:10.3390/biom5042538

Zhang, K., and Luo, J. (2019). Role of MCP-1 and CCR2 in alcohol neurotoxicity. *Pharmacol. Res.* 139, 360–366. doi:10.1016/j.phrs.2018.11.030

Zhang, K., Wang, H., Xu, M., Frank, J. A., and Luo, J. (2018). Role of MCP-1 and CCR2 in ethanol-induced neuroinflammation and neurodegeneration in the developing brain. *J. Neuroinflammation* 15, 197. doi:10.1186/s12974-018-1241-2

Zimmerberg, B., and Farley, M. J. (1993). Sex differences in anxiety behavior in rats: role of gonadal hormones. *Physiol. Behav.* 54, 1119–1124. doi:10.1016/0031-9384(93)90335-d

Zorrilla, E. P., Logrip, M. L., and Koob, G. F. (2014). Corticotropin releasing factor: a key role in the neurobiology of addiction. *Front. Neuroendocrinol.* 35, 234–244. doi:10.1016/j.yfrne.2014.01.001

Zorrilla, E. P., Valdez, G. R., Nozulak, J., Koob, G. F., and Markou, A. (2002). Effects of antalarmin, a CRF type 1 receptor antagonist, on anxiety-like behavior and motor activation in the rat. *Brain Res.* 952, 188–199. doi:10.1016/s0006-8993(02)03189-x

Conflict of Interest: The authors declare that the research was conducted in the absence of any commercial or financial relationships that could be construed as a potential conflict of interest.

Copyright © 2021 Xu, Li, Liu, Wen, Xu, Frank, Chen, Zhu, Grahame and Luo. This is an open-access article distributed under the terms of the Creative Commons Attribution License (CC BY). The use, distribution or reproduction in other forums is permitted, provided the original author(s) and the copyright owner(s) are credited and that the original publication in this journal is cited, in accordance with accepted academic practice. No use, distribution or reproduction is permitted which does not comply with these terms.

frontiers in Neuroscience

REVIEW
published: 15 April 2021
doi: 10.3389/fnins.2021.650785

Neuroimmune Mechanisms as Novel Treatment Targets for Substance Use Disorders and Associated Comorbidities

Mark D. Namba[1], Jonna M. Leyrer-Jackson[2], Erin K. Nagy[2], M. Foster Olive[2] and Janet L. Neisewander[1]**

[1] School of Life Sciences, Arizona State University, Tempe, AZ, United States, [2] Department of Psychology, Arizona State University, Tempe, AZ, United States

OPEN ACCESS

Edited by:
Flavia Eugenia Saravia, Universidad de Buenos Aires, Argentina

Reviewed by:
Marcello Solinas, Institut National de la Santé et de la Recherche Médicale (INSERM), France
Karen K. Szumlinski, University of California, Santa Barbara, United States

***Correspondence:**
Janet L. Neisewander
janet.neisewander@asu.edu
Mark D. Namba
mnamba@asu.edu

Specialty section:
This article was submitted to Neuropharmacology, a section of the journal Frontiers in Neuroscience

Received: 08 January 2021
Accepted: 24 March 2021
Published: 15 April 2021

Citation:
Namba MD, Leyrer-Jackson JM, Nagy EK, Olive MF and Neisewander JL (2021) Neuroimmune Mechanisms as Novel Treatment Targets for Substance Use Disorders and Associated Comorbidities. Front. Neurosci. 15:650785. doi: 10.3389/fnins.2021.650785

Recent studies examining the neurobiology of substance abuse have revealed a significant role of neuroimmune signaling as a mechanism through which drugs of abuse induce aberrant changes in synaptic plasticity and contribute to substance abuse-related behaviors. Immune signaling within the brain and the periphery critically regulates homeostasis of the nervous system. Perturbations in immune signaling can induce neuroinflammation or immunosuppression, which dysregulate nervous system function including neural processes associated with substance use disorders (SUDs). In this review, we discuss the literature that demonstrates a role of neuroimmune signaling in regulating learning, memory, and synaptic plasticity, emphasizing specific cytokine signaling within the central nervous system. We then highlight recent preclinical studies, within the last 5 years when possible, that have identified immune mechanisms within the brain and the periphery associated with addiction-related behaviors. Findings thus far underscore the need for future investigations into the clinical potential of immunopharmacology as a novel approach toward treating SUDs. Considering the high prevalence rate of comorbidities among those with SUDs, we also discuss neuroimmune mechanisms of common comorbidities associated with SUDs and highlight potentially novel treatment targets for these comorbid conditions. We argue that immunopharmacology represents a novel frontier in the development of new pharmacotherapies that promote long-term abstinence from drug use and minimize the detrimental impact of SUD comorbidities on patient health and treatment outcomes.

Keywords: neuroinflammation, addiction, PTSD, MDD, chronic pain, HIV

INTRODUCTION

Substance Use Disorders (SUDs) are a significant public health concern and remain a leading cause of preventable death in the United States (US) and worldwide. Moreover, the economic burden of SUDs is substantial, amounting to more than $740 billion annually within the US in health care costs, lost productivity, and crime (National Institute on Drug Abuse [NIDA], 2020d).

Current FDA-approved pharmacotherapies used to treat SUDs primarily function to reduce withdrawal symptoms via partial receptor stimulation or to prevent drug reinforcement through receptor inhibition. Such strategies can reduce drug cravings and promote abstinence, yet relapse rates remain high even for individuals receiving such treatments (National Institute on Drug Abuse [NIDA], 2020b). Impediments to successful treatment include comorbidities such as depression, anxiety, and other physical ailments that are not adequately addressed by current treatment strategies (Swendsen et al., 2010). Thus, new and effective treatments that target shared mechanisms underlying these comorbidities may enhance treatment outcomes.

Decades of research have revealed distinct neural mechanisms involved in various phases of SUD development. Early work utilizing animal models focused on the effects of drug exposure on mesolimbic dopamine transmission originating from the ventral tegmental area (VTA) and terminating in corticolimbic structures such as the nucleus accumbens (see Koob and Volkow, 2010 for review). More recent studies have expounded the role of other molecular pathways and cellular circuitries that are involved in the cycle of addiction (Koob and Volkow, 2016). For example, the role of glial cells in modulating drug-induced neural plasticity and behavior has emerged as an important topic in the study of the pathophysiology of SUDs (Miguel-Hidalgo, 2009). Specifically, glia within the CNS and immune cells within the periphery are capable of modulating brain plasticity and behavior through complex interactions, and mounting evidence suggests that these interactions may underlie substance abuse and relapse vulnerability (Crews and Vetreno, 2011; Crews et al., 2011; Clark et al., 2013; Cui et al., 2014).

There are several recent and thorough reviews on neuroimmune mechanisms of SUDs (Cui et al., 2014; Bachtell et al., 2015; Jacobsen et al., 2016; Crews et al., 2017; Hofford et al., 2019) and other neuropsychiatric disorders (Hodes et al., 2015; Wohleb et al., 2016; Bekhbat and Neigh, 2018; Brenhouse et al., 2019). Here, we focus on literature from within the last 5 years when possible to highlight the most recent advances in neuroimmune mechanisms of SUDs across several common drugs of abuse. As well, we highlight recent studies on neuroimmune mechanisms of psychiatric and non-psychiatric comorbidities and discuss how these studies reveal intersections with the SUD literature. Specifically, we discuss the neuroimmune mechanisms that are associated with addiction-related processes, first focusing on neuron-glia interactions and how they underlie synaptic plasticity, learning, and memory with cytokine signaling as a case in point. Next, we highlight recent preclinical studies that have identified immune processes that are associated with drug-induced neural plasticity and behavior. We then discuss how recent studies have implicated neuroimmune mechanisms in the comorbidity of SUDs with other diseases and disorders, and we describe how targeting these underlying neuroimmune mechanisms may represent a novel approach toward improving treatment outcomes. Lastly, we provide recommendations for future studies that aim to identify and describe neuroimmune mechanisms underlying SUDs and associated comorbidities.

CYTOKINES CRITICALLY REGULATE SYNAPTIC PLASTICITY, LEARNING, AND MEMORY

Glia play diverse roles in dynamically modulating synaptic plasticity, learning, and memory beyond their "traditional" roles in supporting tissue homeostasis (Temburni and Jacob, 2001; Ben Achour and Pascual, 2010; Perea et al., 2014). For example, neurochemical signaling molecules such as glutamate mediate neuron-glia crosstalk that can alter downstream immunomodulatory signaling. As illustrated in **Figure 1**, microglia, which continuously survey their environment with ramified processes, express both ionotropic and metabotropic glutamate receptors and can release proinflammatory factors in response to rapid changes in extracellular glutamate levels (Hagino et al., 2004; Murugan et al., 2011; Liu H. et al., 2016). Similarly, astrocytes express such receptors and dynamically respond to rapid changes in synaptic glutamate levels through modulation of glutamate uptake (Duan et al., 1999) and through gliotransmission via adenosine triphosphate (ATP) and other transmitters (Harada et al., 2016). As well, astrocytes are highly sensitive to immunomodulatory signals and this has indirect consequences on astrocytic regulation of synaptic transmission (Cekanaviciute and Buckwalter, 2016). Together, microglia and astrocytes can orchestrate potent modulatory control over synaptic plasticity through glial cell-derived immunomodulatory factors such as cytokines.

Cytokines have been extensively studied for their role in learning, memory, and synaptic plasticity (Levin and Godukhin, 2017), and the outcome of these processes depend on the specific cytokine, its concentration within the brain, receptors available for cytokine binding and activation of signal transduction pathways, and the conditions underlying cytokine release (Goshen and Yirmiya, 2007). For example, Beattie et al. (2002) and Stellwagen et al. (2005) have demonstrated that glial tumor necrosis factor alpha (TNFα) facilitates membrane insertion of calcium-permeable α-amino-3-hydroxy-5-methyl-4-isoxazolepropionic acid (AMPA) glutamate receptors (CP-AMPARs) and internalization of γ-aminobutyric acid type A ($GABA_A$) receptors within the hippocampus, leading to enhanced excitatory synaptic transmission. In contrast, Lewitus et al. (2014) found that TNFα exerts an opposite effect at striatal synapses, where TNFα internalizes CP-AMPARs and reduces corticostriatal synaptic strength. These investigators demonstrated that microglia-induced TNFα release depresses excitatory synaptic activity within the ventral striatum through internalization of AMPARs and that this process is associated with cocaine-induced locomotor sensitization (Lewitus et al., 2016). Another example of region-specific regulation of synaptic plasticity showed that TNFα secretion in response to peripheral nerve injury enhances excitatory synaptic connectivity within the spinal cord but impairs this connectivity within the hippocampus (Liu et al., 2017). These studies provide clear

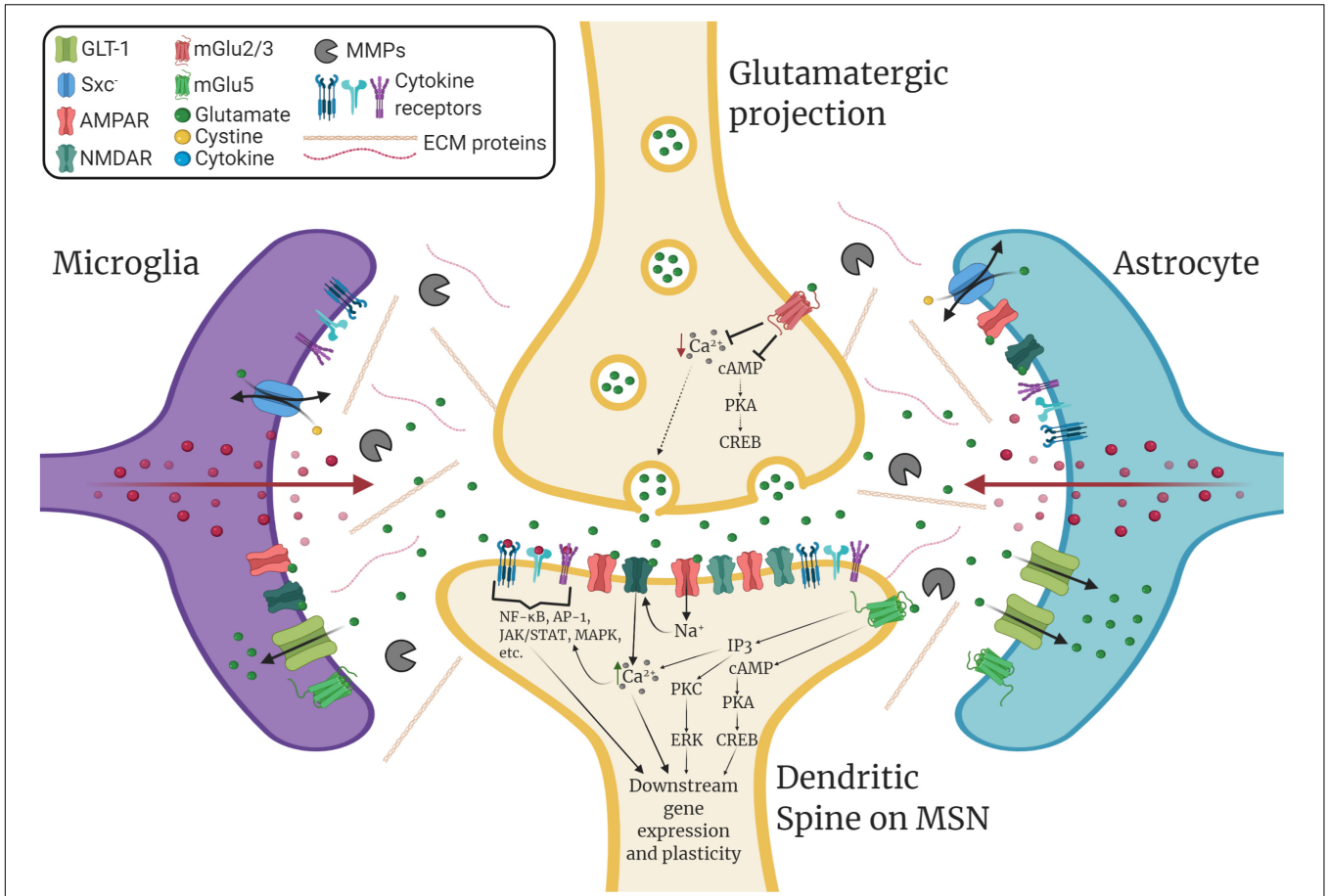

FIGURE 1 | Immunomodulation of striatal glutamatergic synaptic plasticity. GABAergic medium spiny neurons (MSNs) within the nucleus accumbens (NAc) receive glutamatergic inputs from various corticolimbic structures that drive drug-seeking behavior, which includes the prelimbic cortex (PrL), the amygdala (AMY), and the hippocampus (HPC). Glutamatergic plasticity at dendritic spines on MSNs is regulated by glia and extracellular matrix signaling. Glial cell-derived neuroimmune signals such as cytokines play a significant role in modulating this plasticity. Additionally, glutamate transporters such as GLT-1 and the cystine-glutamate exchanger, system xc- (Sxc$^-$), which are found on both astrocytes and microglia, tightly regulate extracellular levels of glutamate. Microglia and astrocytes express ionotropic and metabotropic glutamate receptors (e.g., mGlu5) and can release neuroimmune factors in response to glutamatergic stimulation. Within the extracellular matrix (ECM), enzymes such as matrix metalloproteinases (MMPs), which are predominantly produced by microglia and astrocytes, can remodel the ECM to facilitate dendritic spine plasticity. Cytokines can promote the expression and activation of MMPs, which are associated with learning, memory, and synaptic plasticity. Cytokines also bind directly to receptors located on both neurons and glia, which can directly influence downstream gene expression and synaptic plasticity. This can result in changes in glutamate transporter expression, glutamate receptor surface expression, intracellular signaling, gene expression, dendritic spine morphology, and post-synaptic excitability.

evidence that immunomodulatory signals such as TNFα crucially regulate synaptic plasticity in a brain region-specific manner, which may have important implications for understanding the pathophysiology of SUDs.

Like TNFα, microglia and astrocytes also release interleukin-6 (IL-6) within the CNS, a cytokine involved in modulating learning and memory (Ye and Johnson, 1999; Dong and Benveniste, 2001; Choi et al., 2014). Early studies demonstrated that acute IL-6 exposure inhibits long-term potentiation (LTP) within the hippocampus likely through inhibition of mitogen-activated protein kinase/extracellular signal-regulated kinase (MAPK/ERK) signaling (Li et al., 1997; Tancredi et al., 2002). In addition, overexpression of IL-6 in astrocytes of mice results in reduced LTP in the dentate gyrus (Bellinger et al., 1995). However, *in vitro* and *in vivo* studies examining IL-6 expression during the induction of hippocampal LTP show that LTP induces an upregulation of IL-6 mRNA that is localized to non-neuronal cells such as astrocytes (Jankowsky et al., 2000; Balschun et al., 2004) and inhibition of IL-6 signaling results in improved performance in hippocampus-dependent memory tasks (del Rey et al., 2013). Consistent with this finding, IL-6 knockout mice exhibit enhanced performance in a radial arm maze task compared to wild type mice, which is correlated with hippocampal choline acetyltransferase activity (Braida et al., 2004).

Interleukin-1β (IL-1β) is also critically involved in hippocampal-dependent learning and synaptic plasticity. Within the hippocampus, fear conditioning and LTP upregulate IL-1β and systemic administration of small concentrations of IL-1β can enhance learning and memory (Schneider et al., 1998;

Balschun et al., 2003; Goshen et al., 2007; del Rey et al., 2013). Additionally, acute intra-hippocampal administration and chronic overexpression of IL-1β can impair fear conditioning and spatial learning as well as hippocampal LTP similar to IL-6 (Vereker et al., 2000; Loscher et al., 2003; Ross et al., 2003; Gonzalez et al., 2009; Moore et al., 2009; Hein et al., 2010; MacHado et al., 2010). Despite these seemingly convergent and consistent findings, studies examining learning (e.g., fear conditioning) and hippocampal plasticity using IL-1 receptor (IL-1R) knockout mice have demonstrated mixed effects (Avital et al., 2003; Koo and Duman, 2009; Murray et al., 2013). This is likely the result of complex interactions with other cytokines within the IL-1 family, which is a very broad family of closely related cytokines (Dinarello, 2018).

These studies provide clear evidence that cytokines can exert a dynamic modulatory role within the nervous system over synaptic plasticity, learning, and memory. They also highlight that the specific cytokine and conditions in which neural circuits are exposed to them are paramount when interpreting these findings. This complexity is a primary reason why elucidating the role of immunomodulation and neuron-glia crosstalk in facilitating the formation and persistence of addiction-related behaviors remains challenging. Below we highlight recent preclinical studies, within the last 5 years when possible, that demonstrate the diverse nature of immunomodulation in regulating addiction-related behaviors and underscore some of the remaining gaps in our understanding of these processes.

RECENT PRECLINICAL STUDIES EXAMINING IMMUNOMODULATION OF ADDICTION-RELATED BEHAVIORS AND ASSOCIATED NEUROPLASTICITY

Since 2015, hundreds of articles related to immune mechanisms involved in SUDs have been published, ranging from cellular and molecular studies exploring novel neuroimmune mechanisms of addiction-related behaviors to clinical studies examining the efficacy of immunopharmacology in the treatment of SUDs and associated comorbidities. For example, a PubMed search conducted at the time of preparation of this manuscript for all articles within the last 5 years containing the keywords "addiction" and "immune" yielded over 900 results, showing the exponential growth of research in this area. Of relevance to the current review, preclinical animal models of SUDs have proven invaluable in advancing our understanding of the social, psychological, and biological etiology of SUDs (Lynch et al., 2010; Kuhn et al., 2019), and recent studies utilizing these models have revealed valuable insights into the significant role neuroimmune mechanisms play in regulating drug reward and motivation. Here, we highlight key preclinical research developments in this area, focusing on cocaine, methamphetamine, nicotine, alcohol, and opioids. This review is by no means intended to be exhaustive, but rather serves to highlight recent advances, common themes, and lingering gaps within the literature geared to inform future investigations into the neuroimmune mechanisms of SUDs.

Cocaine

Since 2015, cocaine overdose deaths, particularly those involving synthetic opioids, have risen sharply to over 15,000 as of 2019 in the United States (National Institute on Drug Abuse [NIDA], 2021), highlighting a resurgence of psychostimulant abuse in the wake of the opioid epidemic. Importantly, no effective medications exist that successfully treat cocaine use disorders (CUDs). Studies in humans have demonstrated that CUDs are associated with altered serum levels of pro- and anti-inflammatory cytokines (Moreira et al., 2016; Zaparte et al., 2019). As well, serum cytokine levels may be useful indicators for assessing the severity for CUDs and identifying effective treatment strategies, although sex differences and psychiatric comorbidity are important factors to consider (Araos et al., 2015; Pedraz et al., 2015; Maza-Quiroga et al., 2017; Pianca et al., 2017). Thus, preclinical investigation into the impact of cocaine on immune function may reveal novel targets for pharmacotherapy development. In a recent study by Calipari et al. (2018), both non-contingent cocaine exposure and cocaine self-administration in mice were found to upregulate serum levels of granulocyte-colony stimulating factor (G-CSF), a known growth factor regulator of granulocytes, which positively correlated with cocaine-induced locomotor sensitization. This study also found that both acute and sub-chronic cocaine exposure increased G-CSF mRNA expression within the nucleus accumbens (NAc) and medial prefrontal cortex (mPFC) and that G-CSF potentiates cocaine self-administration. This effect is likely not specific to cocaine, as this same group also demonstrated that G-CSF enhances sucrose motivation and cognitive flexibility, which they hypothesize may be through indirect modulation of mesolimbic dopamine transmission via other immunomodulators such as TNFα (Kutlu et al., 2018). As well, the role of G-CSF in cocaine-induced dopaminergic plasticity was also shown to be dependent on estrous cycle phase in female mice (Brady et al., 2019), suggesting important sex differences underlying immunomodulation of drug-induced neural and behavioral plasticity.

As mentioned above, TNFα is a critical modulator of synaptic plasticity and specifically cocaine-induced neuroadaptations. A recent study demonstrated that non-contingent cocaine exposure in mice activated microglia and increased TNFα in the NAc, leading to depressed excitatory synaptic strength at striatal synapses (Lewitus et al., 2016). Interestingly, this study showed that treatment with a weak agonist of toll-like receptor 4 (TLR4) resulted in microglia activation, reduced cocaine-induced locomotor sensitization, and decreased excitatory activity within the NAc. This study suggests that TNFα plays an adaptive role in suppressing cocaine-induced neurobehavioral plasticity. Nevertheless, the effects of TNFα on downstream cell signaling and subsequent changes in gene expression and cellular physiology are sensitive to the concentration and duration of exposure to these immunomodulators. For example, nuclear factor kappa B (NF-κB), which is a DNA-binding protein complex that is induced by TNFα, exhibits autoregulatory

feedback and oscillatory nuclear translocation with prolonged upstream receptor stimulation. This allows cells to discriminate against multiple levels of cytokine input and subsequently fine-tune downstream gene transcription (Inoue et al., 2016; Zambrano et al., 2016; Zhang Q. et al., 2017). Moreover, the effects of immunomodulators such as TNFα are likely drug-specific and dependent on the preclinical behavioral model (e.g., see Araos et al., 2015 for comparison to nicotine). Indeed, attention to these considerations is important for understanding the role of neuroimmune signaling in the pathophysiology of SUDs. Recent studies examining mesolimbic neuroimmune signaling implicate proinflammatory signaling mechanisms as an important regulator of cocaine-induced neurobehavioral plasticity. For example, Brown et al. (2018) demonstrated that antagonism of TLR4 within the ventral tegmental area (VTA), which sends dopaminergic projections to corticolimbic structures such as the striatum to drive drug-seeking, reduces cocaine-primed reinstatement of drug seeking with no effect on sucrose seeking. As well, stimulation of the VTA with lipopolysaccharide (LPS), which activates TLR4, modestly reinstates cocaine seeking, and inhibition of cocaine-induced elevations in IL-1β within the VTA reduces cocaine seeking (Brown et al., 2018). This study corroborates a previous study demonstrating that cocaine binds uniquely with the TLR4 receptor complex within the VTA to modulate dopamine input into the NAc and subsequent cocaine-seeking behavior (Northcutt et al., 2015). TLR4 knockout mice exhibit attenuated cocaine conditioned place preference (CPP), which may be due to impairments in excitatory synaptic plasticity within the NAc core (Kashima and Grueter, 2017). These findings are consistent with the hypothesis that dopamine input into the NAc and cocaine-mediated activation of TLR4 stimulate microglial activation, resulting in TNFα release that serves as a feedback mechanism to scale down drug-induced increases in synaptic strength. Nevertheless, whether these neuroimmune mechanisms play a significant role in abstinence-dependent changes in mesocorticolimbic plasticity and subsequent relapse remains unclear.

Like cytokines, chemokines are immunomodulators that are influenced by cocaine and may be important regulators of cocaine-induced neurobehavioral plasticity. Traditionally, chemokines promote cellular chemotaxis and are important for directing both homeostatic and inflammatory immune responses. Kim et al. (2017) recently demonstrated that inhibiting the chemokine receptor CXCR4 with the antagonist AMD3100 reduces cocaine CPP and cocaine-induced locomotion. Similar effects are also observed with the synthetic cathinone methylenedioxypyrovalerone (MDPV) (Oliver et al., 2018), which mimics cocaine in its physiological and behavioral effects. Interestingly, this same group has recently provided the first evidence that the chemokine receptor CCR5, which is highly implicated in the pathophysiology of human immunodeficiency virus (HIV), is upregulated by cocaine and regulates the formation of cocaine CPP (Nayak et al., 2020). Cocaine is known to facilitate HIV invasion and viral replication within the brain (Zhang et al., 1998; Sahu et al., 2015; Tyagi et al., 2016) and HIV may also potentiate the reinforcing properties of cocaine (McIntosh et al., 2015). Thus, these studies highlight how neuroimmune mechanisms may underly the intersection between SUDs and other comorbidities, including non-psychiatric comorbidities such as HIV. As discussed below, other psychostimulants such as methamphetamine also exhibit similar qualities.

Methamphetamine

Over the last decade, methamphetamine (METH) use has risen sharply, particularly among individuals that also use opioids. Specifically, the number of psychostimulant overdoses (consisting primarily of METH), both with and without opioids, has been sharply rising within the United States over the last decade in the wake of the opioid epidemic (Mattson et al., 2021). This highlights an important need for novel therapeutic strategies to treat psychostimulant use disorders, which currently have no FDA-approved pharmacological treatments. METH has a profound impact on immune system function through disruption of the blood–brain barrier, dysregulation of both central and peripheral immune signaling, epigenetic modifications, and perturbation to the gut microbiome (for a recent review, see Prakash et al., 2017). For instance, METH alters the expression of microRNAs (miRNAs) that regulate immune- and addiction-related genes (Zhu et al., 2015, 2016). A recent study demonstrated that METH exposure in mice downregulates miR-29b and miR-124 within the NAc, which is consistent with previous observations in animals treated with cocaine (Chandrasekar and Dreyer, 2009; Eipper-Mains et al., 2011; Zhu et al., 2016). These miRNAs are crucial regulators of immune system function (Liston et al., 2012; Qin et al., 2016), suggesting that METH (and possibly psychostimulants in general) may exert aberrant immunomodulatory effects over mesocorticolimbic reward pathway signaling through dysregulation of miRNA expression. In addition to indirect immunomodulation of drug-induced plasticity via miRNA regulation, METH interacts directly with immune cells to promote neuroinflammation and alter reward learning. Indeed, a recent report examining METH's effects on TLR4 signaling and VTA-NAc dopamine transmission provides convincing evidence of this fact. In this study, Wang X. et al. (2019) report that METH can bind to lymphocyte antigen 96 (i.e., MD-2), which interacts directly with TLR4 to confer receptor responsiveness to LPS, and that inhibition of TLR4 attenuated METH-induced NF-κB activation in microglia. In addition, this study also showed that METH upregulates IL-6 within the VTA and that this is associated with enhanced extracellular dopamine within the NAc, and treatment with the TLR4 inhibitor (+) naloxone or an intra-VTA IL-6 antibody reduces METH-induced increases in NAc dopamine (Wang X. et al., 2019). This study parallels findings described above by Brown et al. (2018), which demonstrated reduced cocaine-primed reinstatement following intra-VTA treatment with a TLR4 antagonist. These findings collectively suggest that psychostimulants such as METH and cocaine may alter dopamine transmission and reward processing through similar immunomodulatory mechanisms such as TLR4 signaling.

Another recent study examining the potential role of dopamine D1 receptors (D1Rs) in mediating METH's immunomodulatory effects found that acute METH exposure

increases LPS-induced IL-6 and TNFα release within the NAc, hippocampus (HPC), and caudate-putamen (CPu), and that systemic inhibition of D1Rs suppresses this effect (Wang B. et al., 2019). This study suggests that METH primes neuroimmune responses to inflammatory stimuli within the mesocorticolimbic reward circuitry and that METH-induced dopamine transmission may be involved in this process. Nevertheless, whether these processes confer increased susceptibility to METH relapse remains unclear. An intriguing pair of studies has attempted to address this gap within the literature, where investigators used a CPP paradigm to probe whether cannabidiol (CBD) reduces reinstatement of METH seeking in animals that experienced sleep deprivation and if CBD modulates cytokine expression within the prefrontal cortex (PFC) and HPC (Karimi-Haghighi and Haghparast, 2018; Karimi-Haghighi et al., 2020). These studies collectively showed that METH-induced reinstatement is accompanied by increased expression of TNFα and the anti-inflammatory cytokine IL-10 within the PFC and HPC, and CBD treatment significantly reduces reinstatement as well as proinflammatory cytokine levels within these brain regions. Interestingly, CBD treatment before sleep deprivation elevated TNFα, IL-1β, IL-6, and IL-10 levels within the HPC but reduced IL-10 levels within the PFC. These results indicate that CBD may attenuate METH-seeking behavior through immunomodulatory mechanisms. However, the clear heterogeneity of cytokine expression profiles across the brain raise important questions regarding the functional role of these cytokines within specific neural circuits. Thus, further studies that attempt to dissect possible circuit-specific mechanisms of immunomodulation are warranted.

One limitation of the studies above is that METH was experimenter-delivered to the animals, as opposed to self-administered. Previous studies demonstrate that the magnitude of METH effects on the CNS, such as on dopamine transporter (DAT) expression, is larger in experimenter-delivered METH exposure models as compared to human clinical and post-mortem studies (Wilson et al., 1996; Volkow et al., 2001a,b; Sekine et al., 2003). Indeed, self-administration models better recapitulate the effects of METH on striatal DAT function and expression observed in humans (McFadden et al., 2012). As well, experimenter-delivered METH models do not allow investigators to correlate drug-induced neuroplasticity with behavioral measures such as escalation of drug intake and cue-motivated drug seeking. Thus, self-administration models examining the neuroimmune consequences of chronic METH use provide a clearer understanding of how these immune mechanisms facilitate METH abuse and relapse vulnerability in humans.

Recent investigations using self-administration paradigms implicate neuroinflammation and disruption of blood-brain barrier (BBB) integrity as a consequences of chronic METH use. For example, Gonçalves et al. (2017) examined the impact of extended-access METH self-administration and abstinence on BBB integrity and neuroinflammation within the HPC and striatum. This study found that METH self-administration and abstinence downregulated tight junction proteins and collagen IV, indicating reduced BBB integrity, as well as astrogliosis, microgliosis, and upregulated proinflammatory mediators such as TNFα, IL-1β, and matrix metalloproteinase-9 (MMP-9) (Gonçalves et al., 2017). While this study did not examine whether these METH-induced neuroadaptations are directly involved in METH-seeking behaviors, many other studies discussed previously have implicated TNFα and IL-1β in regulating learning, memory, and synaptic plasticity, and MMP-9 in particular has also been implicated in these processes as well as in cue-motivated drug seeking specifically (Mizoguchi et al., 2007; Knapska and Kaczmarek, 2015; Smith et al., 2015). METH-induced impairments on the BBB are well documented, and the consequences of these proinflammatory effects of METH on the BBB can exacerbate invasion of viruses as well as peripheral immune cells into the brain (see Northrop and Yamamoto, 2015 for review). Indeed, individuals who use METH are significantly more vulnerable to HIV and the neurocognitive dysfunctions associated with chronic HIV infection (Borgmann and Ghorpade, 2015; Kesby et al., 2015a). Recent preclinical animal studies demonstrate that HIV and its proteins exacerbate METH-induced deficits in learning and memory (Hoefer et al., 2015; Kesby et al., 2015a,b) as well as METH reward sensitivity and behavioral sensitization (Liu et al., 2009; Kesby et al., 2014). Taken together, METH produces significant perturbations to cellular systems within the mesocorticolimbic reward system through immunomodulation and, akin to cocaine, these immunomodulatory mechanisms may underlie the co-morbidity of chronic METH use and both psychiatric and non-psychiatric diseases.

Nicotine

Unlike other drugs of abuse such as alcohol, cocaine, and methamphetamine, relatively little preclinical research exists on the role of immunomodulation in nicotine addiction-related behaviors. Previous work demonstrates that nicotine produces predominantly anti-inflammatory and pro-cognitive effects, which has been largely attributed to nicotine's full-agonist activity at α7-containing nicotinic acetylcholine receptors (Kalra et al., 2004; Shytle et al., 2004; Foucault-Fruchard and Antier, 2017) (nAChRs; although see Thomsen and Mikkelsen, 2012). For example, recent studies suggest that nicotine's acute anti-inflammatory effects via α7-containing nAChR signaling may improve learning and memory and reduce the severity of neurocognitive symptoms associated with neurodegenerative diseases such as Alzheimer's disease. Specifically, a recent study demonstrated that nicotine attenuates LPS-induced neuroinflammation within the HPC and associated cognitive deficits in spatial learning (Wei et al., 2015). As well, another study showed that inhibition of α7-containing nAChRs with an α7-specific antibody is sufficient to produce neuroinflammation, accumulation of β-amyloid, and memory impairments in mice (Lykhmus et al., 2015). While these studies suggest that nicotine may be therapeutic within certain clinical contexts (e.g., Alzheimer's disease), there are a number of caveats to consider. Firstly, individuals who are dependent on nicotine largely smoke tobacco, which can produce profoundly different effects on cognition and neuroinflammation when compared to nicotine alone (Swan and Lessov-Schlaggar, 2007). This complicates the interpretations one can make from preclinical

nicotine studies regarding the neuroimmune and neurocognitive effects of smoking in humans. Additionally, acute versus chronic nicotine, as well as varying withdrawal periods, are all associated with significant differences in whether they are associated with neuroinflammation and cognitive deficits. For example, a recent study revealed cognitive impairment and neuroinflammation within the PFC and HPC of mice 4 days after mecamylamine-precipitated nicotine withdrawal, which was reversed by cannabidiol (Saravia et al., 2019). This contrasts the studies described above demonstrating anti-inflammatory and cognition-enhancing effects of acute or sub-chronic nicotine treatment in inflammatory disease models. Furthermore, these disparate findings in the literature may be attributed to the heterogenous distribution of nAChRs throughout the CNS (Gotti et al., 2009). Given the significant role of nAChRs in immune system function [particularly the α7-containing nAChR (Fujii et al., 2017)], the heterogeneity of nAChR distribution within the CNS could have significant implications for immunomodulation of nicotine addiction-related behaviors.

Several recent studies have attempted to address these significant gaps in the literature by investigating whether neuroimmune mechanisms within mesocorticolimbic reward circuitry are involved in nicotine addiction-related behaviors. In our recent study, we attempted to investigate whether changes in NAc core neuroimmune signaling were associated with nicotine self-administration, extinction, and cue-induced reinstatement as well as the therapeutic efficacy of the antioxidant compound *N*-acetylcysteine (NAC). NAC, which has been used traditionally as a mucolytic and as a treatment for acetaminophen overdose, is known to reverse drug-induced perturbations in glutamatergic homeostasis within the NAc and to inhibit cue-motivated drug seeking (Baker et al., 2003; Moran et al., 2005; Moussawi et al., 2009; Deepmala et al., 2015; Reissner et al., 2015; Elbini Dhouib et al., 2016; Powell et al., 2019). We demonstrated that 2 weeks of extinction training following nicotine self-administration was associated with enhanced TNFα expression within the NAc core and concomitant downregulation of the astrocytic glutamate transporter GLT-1. As well, we showed that NAC ameliorated these deficits and blocked cue-induced reinstatement of nicotine seeking through GLT-1- and NF-κB-dependent mechanisms within the NAc core (Namba et al., 2019). Unlike TNFα, IL-6 was not upregulated after a period of extinction and cue reinstatement testing, although glial fibrillary acidic protein (GFAP) expression was downregulated at these timepoints. No changes in TNFα and GFAP expression were observed immediately following nicotine self-administration when compared to yoked saline controls. This is consistent with a previous report showing downregulated NAc GFAP expression following 2 weeks of cocaine extinction (Scofield et al., 2016). Our findings were also corroborated by another recent study demonstrating that withdrawal from experimenter-delivered nicotine exposure in mice upregulates TNFα and IL-1β mRNA within the NAc and increases anxiety-like behavior, both of which are prevented by pharmacological depletion of microglia with a colony-stimulating factor 1 receptor inhibitor (Adeluyi et al., 2019). Moreover, another recent study showed that co-administration of the non-steroidal anti-inflammatory drug acetylsalicylic acid with NAC significantly attenuates oral nicotine self-administration as well as consumption of nicotine following a period of nicotine deprivation (Quintanilla et al., 2021).

Taken together, the above findings highlight the need for future studies to evaluate multiple timepoints when attempting to describe neuroimmune mechanisms of addiction-related behaviors. As well, these data underscore the need for investigators to exhibit caution when describing their findings related to the neuroimmune consequences of nicotine exposure. While it can be tempting to ascribe labels such as "neuroinflammation" to processes that upregulate proinflammatory cytokines such as TNFα, the studies above illustrate that these immunomodulators exhibit diverse functions that serve to fine-tune neuronal plasticity and behavior, and dysregulation of a specific cytokine may not be indicative of a net "inflammatory" or "anti-inflammatory" process *per se*. Significant gaps remain in the understanding of whether nicotine alters neuroimmune signaling within the brain's mesocorticolimbic reward circuitry and whether such changes are relevant to the reinforcing and incentive motivational properties of nicotine. However, α7-containing nAChRs are critically involved in nicotine addiction-related behaviors, and it is possible that neuroimmune mechanisms downstream of α7-containing nAChRs mediate the modulatory role of this receptor type over nicotine reward and reinforcement.

The α7 nAChR subunit plays a critical yet complex role in mediating the effects of nicotine on immune system function. For example, a recent study demonstrated that an α7-containing nAChR agonist inhibits LPS-induced astroglial release of proinflammatory cytokines and NF-κB activation *in vitro* (Patel et al., 2017). Moreover, another recent study showed that α7-containing nAChR agonist treatment improves neuronal survival and reduces microglial activation in rats treated with an excitotoxic lesion within the striatum (Foucault-Fruchard et al., 2017). While many studies demonstrate an anti-inflammatory and protective role of α7-containing nAChR stimulation in a variety of disease models, other studies offer conflicting conclusions (Thomsen and Mikkelsen, 2012). In addition to its role in regulating neuroimmune signaling, the α7 nAChR subunit has also been implicated in the reinforcing properties of nicotine (Levin et al., 2009; Besson et al., 2012; Brunzell and McIntosh, 2012). In a recent study examining nicotine-induced changes in α7 expression within the striatum and frontal cortex of mice, experimenter-delivered, nicotine-containing electronic cigarette vapor exposure upregulated α7 expression within these brain regions (Alasmari et al., 2017). In contrast, another recent study demonstrated that nicotine consumption in rats is negatively correlated with α7 expression within the HPC, which is most prominent in females (Gozen et al., 2016). Indeed, the heterogeneity of nAChR expression throughout the brain as well as the differential neurobehavioral impact of experimenter-delivered drug exposure versus self-administration likely contributed to these seemingly discrepant findings (Gotti et al., 2009; Namba et al., 2018). Additionally, such differences may suggest that nicotine alters α7-containing nAChR expression differentially throughout the brain, which could produce brain region-specific differences

in downstream neuroimmune signaling. Varenicline, which is a popular smoking-cessation medication, has been reported to be a full agonist at α7-containing nAChRs in addition to a partial agonist at α4β2* nAChRs (Mihalak et al., 2006). Interestingly, a recent study demonstrated that combination therapy of varenicline with the weak monoamine reuptake inhibitor bupropion reduced nicotine self-administration in rats (Hall et al., 2015), and bupropion has been shown to exhibit anti-inflammatory properties in mice (Hajhashemi and Khanjani, 2014). However, another recent study concluded that discontinuation of varenicline treatment may increase relapse vulnerability. Specifically, this study showed that rats receiving varenicline treatment exhibited impaired extinction learning, which was particularly evident in varenicline-treated rats that underwent a second cycle of nicotine self-administration and extinction training without continued varenicline treatment (Macnamara et al., 2016). Perturbations to α7-containing nAChRs and subsequent α7-mediated neuroimmune responses may also come from flavor additives in tobacco products such as menthol, which has been shown to inhibit α7-containing nAChR receptor function (Ashoor et al., 2013) and facilitate nicotine self-administration (Biswas et al., 2016). Ultimately, it remains unclear whether immunomodulatory mechanisms, such as those elicited by α7-containing nAChRs, are relevant to the formation and persistence of nicotine addiction-related behaviors. As well, it is unclear if such mechanisms would be effective targets for medications development. While recent preclinical studies have attempted to shed light on this gap in the literature (Adeluyi et al., 2019; Namba et al., 2019), future research that utilizes preclinical models of volitional drug self-administration, withdrawal, and cue-motivated nicotine seeking is needed to better understand whether neuroimmune mechanisms underly the pathophysiology of nicotine addiction-related behaviors.

Alcohol

Similar to cocaine and methamphetamine, alcohol (ethanol) promotes inflammation and immune system dysfunction. Alcohol and its metabolites induce oxidative stress, increase systemic endotoxin levels, and promote the release of inflammatory peptides. Together, these effects contribute to liver disease, bone and muscle disease, cardiovascular disease, reproductive disorders, and neuroinflammation (González-Reimers et al., 2014). Many studies have revealed alcohol-induced changes in immunoregulatory miRNAs, cytokines, and other signaling pathways associated with neuroinflammation, and increasing evidence suggests that alcohol-induced neuroinflammation contributes to brain damage and neurodegeneration that is observed in individuals with severe alcohol use disorders (AUDs) (Vallés et al., 2006; Tajuddin et al., 2014; Orio et al., 2019).

NF-κB regulates alcohol-induced changes in immune-related gene expression, either through direct interactions with NF-κB-specific binding sites on many immune-related genes (e.g., IL-1β, TNFα, and MCP1) or with miRNAs to indirectly regulate immune-related gene expression. For example, the miRNA miR-155 is induced by NF-κB activation and plays a role in alcohol-induced dysregulation of TNFα and MCP1 expression. Specifically, chronic alcohol intake increases TNFα and MCP1 expression within the cerebellum, an effect mediated by alcohol-induced activation of miR-155 (Lippai et al., 2013). This effect was further validated in this study using miR-155 knockout mice, where alcohol-induced TNFα and MCP1 elevations were prevented in these animals following alcohol treatment. Also known for its role in alcohol-induced liver diseases (for review see Hartmann and Tacke, 2016), miR-155 has been shown to promote cytokine release through TLR4 activation (Lippai et al., 2013). TLR4, which is a potent mediator of alcohol-induced neuroinflammation (Alfonso-Loeches et al., 2010), participates in alcohol-induced, long-term synaptic remodeling during adolescence (Montesinos et al., 2016), promotes leukocyte infiltration across the blood–brain barrier (BBB) in the presence of alcohol (Alfonso-Loeches et al., 2016), and participates in alcohol-induced autophagy and synaptic dysfunction during development (Montesinos et al., 2018). Furthermore, alcohol increases the release of TLR4 and cytokines from astrocytes by mediating the release of astrocyte-derived extracellular vesicles (EVs) containing these inflammation-related proteins (Ibáñez et al., 2019). Such mechanisms are capable of altering the physiological state of neurons and has the ability to enhance alcohol-induced neuroinflammation. Interestingly, alcohol does not induce EV release in TLR4-deficient astrocytes, further implicating TLR4 as an important component of alcohol-induced neuroinflammation (Ibáñez et al., 2019). Additionally, genetic elimination of TLR4 prevents damage to myelin and synapses within the PFC as well as neuroinflammatory processes induced by intermittent alcohol treatment (Montesinos et al., 2015), and inhibition of TLR4 using the opioid antagonist nalmefene has been shown to prevent alcohol-induced neuroinflammation (Montesinos et al., 2017). Taken together, TLR4 plays an essential role in mediating alcohol-induced neuroinflammation and may serve as a promising target for treatment in patients with AUDs.

Similar to other drugs of abuse, alcohol consumption increases LPS-induced inflammation, which has known interactions with TLR4 located within the hepatic system as well as on microglia and astrocytes (Monnig, 2017). Interestingly, while alcohol increases proinflammatory cytokine release within the mouse hippocampus, including TNFα, IL-1β and MCP-1, co-treatment with LPS (alcohol + LPS) further increases MCP-1 and IL-1β (Qin et al., 2008). Additionally, alcohol + LPS significantly decreases the number of cells within the dentate gyrus relative to controls, an effect not observed with alcohol or LPS treatment alone (Qin et al., 2008). The ionized calcium binding adapter molecule 1 (Iba-1) protein is expressed within microglia and is elevated in post-mortem brains of patients with AUD (He and Crews, 2008). Iba-1 expression is increased in a TLR4-dependent manner in response to ethanol, where 35 days of chronic intermittent ethanol (CIE) exposure enhanced Iba-1 expression within the PFC (Sanchez-Alavez et al., 2019). Conversely, a recent study showed that 15 days of CIE exposure plus 10 h of withdrawal decreases Iba-1 immunoreactivity within the prelimbic cortex (PrL), whereas no changes are observed in the NAc. This study also demonstrated that LPS exposure produces an enlargement of soma volume in Iba-1-expressing microglia within the PrL and NAc and a decrease in microglial

density within the NAc (Siemsen et al., 2020). Taken together, these studies suggest that chronic alcohol exposure may prime both central and peripheral immune mechanisms to exhibit exacerbated immune responses to inflammatory insults such as LPS. As well, these studies suggest that alcohol exposure produces a unique profile of neuroimmune effects that are distinct from classic proinflammatory stimuli such as LPS and that the duration of alcohol exposure and withdrawal are important factors when considering alcohol-induced changes in neuroimmune function.

In addition to processes described above, alcohol activates nicotinamide adenine dinucleotide phosphate (NADHP) oxidase, an enzyme known to produce reactive oxygen species, thus contributing to oxidative stress, alcohol-induced cell damage, and neuroinflammation (Qin and Crews, 2012). As a common activator of glial cells within the brain, oxidative stress is promoted by inducible nitric oxide synthase (iNOS), a gene activated by pro-inflammatory cytokines induced by alcohol (Sun and Sun, 2001). Further, iNOS catalyzes the oxidation of alcohol into acetaldehyde and α-hydroxyethyl radicals (Porasuphatana et al., 2006), and acetyladehyde production promotes reactive oxygen species (ROS) formation that contributes to unbalanced cellular oxidative stress (Hernández et al., 2016; Yan et al., 2016). Through its activation of p38 mitogen-activated protein kinase (MAPK) and inhibition of extracellular signal-regulated kinases, acetaldehyde induces cytotoxicity by promoting apoptotic signaling and inhibiting cell survival pathways (Yan et al., 2016). Interestingly, inhibition of the phosphoinositide 3-kinase/protein kinase B (PI3K/Akt) pathway with glycine inhibits ROS production in young rats and reduces alcohol-induced neuroinflammation (Amin et al., 2016). Altogether, these studies highlight the complexities of ROS and oxidative stress induced by alcohol, and more studies investigating the role of these processes in alcohol addiction-related behaviors are warranted.

Preclinical models of alcohol consumption are largely reliant on three forms of self-administration paradigms, which include drinking-in-the-dark (DID), two-bottle choice (2BC), and operant conditioning for oral alcohol consumption. Each paradigm allows rodents to self-administer alcohol-containing solutions and have varying degrees of translational value. Pharmacological and genetic manipulations of neuroinflammatory targets have yielded promising results in reducing alcohol consumption across these different paradigms. For example, inhibition of microglia activation reduces alcohol consumption during the DID task in C57/BL6 male mice (Lainiola and Linden, 2017) and prevents relapse-like drinking in the 2BC task in male rats (Gajbhiye et al., 2018). Further, inhibition of microglial P2X7 receptor signaling also reduces alcohol consumption in C57/BL6 male mice during the DID paradigm (Lainiola and Linden, 2017). Dual knockout of IL-1 and TNFα receptors reduces social stress-induced increases in alcohol consumption during the 2BC task in male mice (Karlsson et al., 2017), and IL-6 knockout mice also show similar reductions (Blednov et al., 2012). Likewise, antagonism of the IL-1 receptor within the basolateral amygdala reduces alcohol consumption during DID in male C57/BL6 mice (Marshall et al., 2016). Similar reductions in alcohol consumption have also been observed using peroxisome proliferator activated receptor (PPAR) agonists, which generally promote anti-inflammatory responses. Specifically, PPARα activation with fenofibrate decreases alcohol consumption during the 2BC and DID tasks in both UChB male rats and C57/BL6 male mice (Karahanian et al., 2014; Blednov et al., 2016). PPARα activation with gemfibrozil also decreases 2BC alcohol consumption in male Sprague-Dawley rats (Barson et al., 2009). Lastly, treatment with ceftriaxone [a beta-lactam antibiotic with immunomodulatory mechanisms (Wei et al., 2012; Kaur and Prakash, 2017; Ochoa-Aguilar et al., 2018)] or the antioxidant *N*-acetylcysteine reduces relapse-like drinking in alcohol preferring P rats (Qrunfleh et al., 2013; Alhaddad et al., 2014) as well as alcohol seeking and alcohol-reinforced responding in Long-Evans rats (Lebourgeois et al., 2018). Altogether, these findings provide a critical foundation for future investigations into anti-inflammatory compounds that may reduce alcohol motivation and consumption. However, most of the studies discussed here were conducted in male subjects only, making it difficult to determine whether these effects would also be observed in females. Thus, further characterization of potential sex differences in both alcohol-induced neuroimmune responses as well as the effects of pharmacological and genetic manipulations on these responses are warranted.

While much preclinical evidence exists demonstrating alcohol-induced neuroinflammation and cellular toxicity as well as the effects of anti-inflammatory agents in reducing alcohol consumption, studies examining pharmacotherapies for treating alcohol-induced neuroinflammation in humans are lacking. *N*-acetylcysteine (NAC) prevents alcohol-induced neuroinflammation in rats (Schneider et al., 2017) and human studies suggest that NAC may be useful for treating AUDs. Preclinically, NAC prevents alcohol withdrawal-induced increases in TNFα, IL-1β, IL-6, and IL-18 within the hippocampus and medial prefrontal cortex of rats (Schneider et al., 2017). As well, co-treatment with aspirin and NAC restores alcohol-induced impairments in glial glutamate transporter expression within the prefrontal cortex and prevents microglial activation (as measured through morphological alterations) within the hippocampus of rats (Israel et al., 2019). Parallel to these preclinical findings, NAC has also shown efficacy within humans with AUDs for reducing alcohol intake and withdrawal symptoms (Back et al., 2016; Squeglia et al., 2016, 2018); however, studies have not examined whether NAC reduces inflammation in humans. NAC's poor bioavailability is a significant clinical limitation that may impair its efficacy. Thus, improving its bioavailability with novel delivery vectors such as nanoparticles may enhance its anti-inflammatory properties and, consequently, its therapeutic efficacy (Markoutsa and Xu, 2017). Similar to NAC, the lipid transmitter oleoylethanolamide (OEA), which is primarily generated by phospholipid cleavage, reduces alcohol-mediated neuroinflammation. By modulating oxidative stress, neuroinflammation, glial cell activation, as well as neurotransmission, OEA has neuroprotective properties, such as blocking alcohol-induced upregulation of TLR4 and subsequent proinflammatory signaling (Orio et al., 2019; Orio, 2020). OEA provides neuroprotection of the frontal cortex in alcohol-exposed rats by inhibiting NF-κB and TLR4 signaling pathways (Antón et al., 2017). Interestingly, systemic OEA treatment reduces

operant responding for alcohol and prevents alcohol-induced withdrawal symptoms in rodents (Bilbao et al., 2016).

Another novel treatment target that is being investigated both clinically and preclinically for its use in treating AUDs is phosphodiesterases (PDEs). PDEs are upstream modulators of intracellular cyclic nucleotides, such as cyclic AMP (cAMP) and cyclic GMP (cGMP), as well as immunomodulators that underly alcohol reward and toxicity (Wen et al., 2018). Specifically, PDEs catalyze the hydrolysis of cAMP and cGMP, decreasing their intracellular levels and thus downstream signal transduction. As well, PDEs (e.g., PDE4) are involved in ethanol-mediated inflammatory responses (Gobejishvili et al., 2008; Avila et al., 2017). Evidence suggests that ethanol exposure alters cAMP signal transduction by modulating adenylate cyclase (Yang et al., 1996; Asher et al., 2002; Asyyed et al., 2006). This modulatory effect may depend on the amount of ethanol exposure as acute ethanol promotes cAMP signal transduction whereas chronic ethanol attenuates this signaling (Saito et al., 1987; Yang et al., 1996, 1998; Pandey, 2004). Preclinical studies show that reductions in cAMP and cGMP levels, caused by hyperactivity of PDEs, promote excessive ethanol use. Given their link to alcohol seeking, several studies have attempted to pharmacologically identify which PDEs modulate alcohol consumption (Hu et al., 2011; Wen et al., 2012; Blednov et al., 2014; Bell et al., 2015; Logrip, 2015). Other studies have attempted to describe genetic differences in PDEs between alcohol-preferring and non-preferring mouse lines (Mulligan et al., 2006). Importantly, pharmacological inhibition of PDE4 (Hu et al., 2011; Wen et al., 2012; Blednov et al., 2014) and PDE10 (Bell et al., 2015; Logrip, 2015) reduce ethanol intake in rodents. Given the results of these preclinical findings, two PDE inhibitors are undergoing clinical trials for their therapeutic efficacy in treating AUDs. Specifically, the PDE inhibitor Ibudilast, a non-specific PDE inhibitor that targets PDE3, PDE4, PDE10, and PDE11, is currently within Phase I (ClinicalTrials.gov, 2021a), while the PDE4 inhibitor Apremilast is currently within Phase II (ClinicalTrials.gov, 2021b). For additional information regarding PDEs and alcohol, see the in-depth review by Wen et al. (2018). Taken together, targeting neuroinflammation and reducing oxidative stress may be a promising therapeutic strategy for individuals with AUDs by reducing the underlying effects of alcohol on neuroinflammation.

Opioids

Opioids are a class of drugs that possess a very high abuse liability and have been at the center of an ongoing public health crisis. Between the years 2000 and 2017, yearly opioid overdose-related deaths rose to more than 47,000 within the United States, and 21–29 percent of individuals who are prescribed opioids to manage chronic pain misuse them (Vowles et al., 2015; National Institute on Drug Abuse [NIDA], 2020c). In response to this crisis, considerable preclinical research has revealed many neuronal and non-neuronal mechanisms underlying opioid reward and reinforcement, including neuroimmune mechanisms. This research has advanced our understanding of the pathophysiology of opioid use disorders (OUDs) as well as other comorbid chronic pain and inflammatory conditions. For example, the opioid receptor antagonist naltrexone, which has been used as a medication to treat both OUDs and AUDs, attenuates inflammation and pain associated with chronic autoimmune disorders and cancer (Li et al., 2018; Patten et al., 2018). Several groups have recently provided thorough, in-depth reviews of the many neuroimmune mechanisms involved in OUDs (Plein and Rittner, 2018; Eidson and Murphy, 2019; Hofford et al., 2019; Zhang et al., 2020). Thus, for the purposes of this review, we will summarize key findings within the last 5 years, and emphasize recent advancements within the last 2 years where possible, to highlight current trends in the field and offer our perspectives on future directions regarding novel neuroimmune mechanisms of OUDs.

TLR4 is known to play a critical role in the rewarding and reinforcing effects of opioids, and TLR4 antagonists may be efficacious pharmacotherapies to treat OUDs (Hutchinson et al., 2012; Wang et al., 2012; Bachtell et al., 2015). Specifically, a study by Hutchinson et al. (2012) showed that inhibition of TLR4 and its downstream myeloid differentiation primary response 88 (MyD88)-dependent signaling suppresses opioid-conditioned place preference and self-administration as well as morphine-induced increases in NAc extracellular dopamine. This study was paralleled by another study demonstrating that morphine induces neuroinflammation through activation of TLR4 signaling and that inhibition of TLR4 signaling can enhance the analgesic properties of morphine (Wang et al., 2012). TLR4 is also involved in opioid reinforcement, tolerance, and withdrawal. For example, knockdown of TLR4 within the ventrolateral periaqueductal gray (vlPAG) increases glutamic acid decarboxylase mRNA within the PAG and decreases withdrawal symptoms in morphine-exposed rats (Liu Q.F. et al., 2016). As well, chronic morphine exposure stimulates TLR4 and recruits TNFα signaling within the PAG to enhance neuroinflammation, downregulate glutamate transporters, and increase morphine tolerance (Eidson et al., 2017). Within the VTA, TLR4 signaling also facilitates the acquisition and maintenance opioid CPP, which may depend on downstream signal transducer and activator of transcription 3 (STAT3) signaling (Chen et al., 2017). Interestingly, genetic deletion of Myd88, in microglia of mice impairs extinction learning and enhances reinstatement of morphine CPP (Rivera et al., 2019). These findings are seemingly conflicting with those of Hutchinson et al. (2012) as highlighted above which used a Myd88 knockout mouse model that lacked cell-type specificity. Nevertheless, it is likely that neuroimmune influences over addiction-related behaviors, such as those mediated by TLR4-Myd88 signaling, are cell type-specific and brain region-dependent. Moreover, there are likely sex-specific neuroimmune mechanisms that may influence opioid addiction-related behaviors and opioid treatment outcomes for chronic pain (Posillico et al., 2015; Doyle et al., 2017). While there is still some conflicting evidence regarding the efficacy of TLR4 antagonists for reducing opioid craving and relapse (Yue et al., 2020), future research should explore the efficacy of TLR4 antagonists as medications that supplement other treatment approaches for OUDs and comorbid chronic pain.

Several recent investigations have identified many cytokines and other immune-related signaling mechanisms that may regulate opioid reinforcement and motivation. For example, a

recent study using a rodent model of fentanyl self-administration showed that the NAc and HPC are particularly vulnerable to changes in the expression of a number of immune markers, such as increased IL-1β, TNFα, and IFN-γ within the NAc and decreased GM-CSF and IFN-γ in the HPC (Ezeomah et al., 2020). While this study did not directly manipulate any of these neuroimmune substrates, expression of IL-1β and IL-6 within the NAc, as well as IFN-β and various interleukins within the HPC, correlate positively and negatively (respectively) with fentanyl intake. Similarly, another study using single-cell qRT-PCR analyses demonstrated that morphine withdrawal is associated with increased expression of neuroinflammatory genes, such as *Tnf,* as well as increased TNFα protein expression within neurons, microglia, and astrocytes from the central amygdala. Among these cell types, astrocytes exhibited the largest changes in neuroimmune gene expression (O'Sullivan et al., 2019). Such findings implicate opioid-induced neuroinflammatory interactions with neural reward systems that are known to drive drug-seeking behavior (Koob and Volkow, 2016). Rodent self-administration models with the prescription opioid oxycodone have shown upregulation within both the dorsal and ventral striatum of numerous immune-related genes using RNAseq and qPCR techniques [e.g., *Ccr5*, *Icam1*, *Cybb* (Zhang Y. et al., 2017)], as well as changes within the NAc and CPu in the expression of various integrin, semaphorin, and ephrin genes that play a role in neurodevelopment, cell migration, structural regulation of synapses, and immune signaling (Yuferov et al., 2018).

Several studies examining the efficacy of various immunomodulatory treatments have also provided evidence for immune signaling as an important mechanism underlying opioid addiction-related behaviors. For example, *N*-acetylcysteine effectively inhibits heroin-seeking behavior akin to other drugs of abuse (Zhou and Kalivas, 2008; Hodebourg et al., 2019). Similarly, IL-10 overexpression within the NAc reduces remifentanil self-administration in rats (Lacagnina et al., 2017) and intra-NAc treatment with the antibiotic and microglia inhibitor minocycline inhibits drug-primed reinstatement of morphine CPP in rats (Arezoomandan and Haghparast, 2016). Clinical studies also support the use of anti-inflammatory medications to treat OUDs. For instance, the anti-inflammatory phosphodiesterase inhibitor ibudilast reduces heroin cravings and self-reported pain ratings among opioid-dependent individuals (Metz et al., 2017). Another study suggests beneficial effects of ibudilast on withdrawal symptoms in opioid-dependent individuals undergoing detoxification (Cooper et al., 2016). The cyclooxygenase-2 (COX-2) inhibitor celecoxib may also reduce opioid cravings among individuals undergoing detoxification (Jafari et al., 2017). Overall, the studies described here provide evidence supporting the conclusion that neuroimmune mechanisms may be involved in the pathophysiology of OUDs, particularly regarding tolerance to both the rewarding and analgesic properties of opioids, as well as withdrawal from chronic opioid use. Nevertheless, there is still a significant gap in the literature regarding the efficacy of novel immunomodulatory medications, and particularly anti-inflammatory agents, in reducing opioid craving and relapse as well as tolerance to the analgesic effects of opioids. Specifically, the changes in neuroimmune function in acute versus protracted abstinence from chronic opioid self-administration and the functional role of such changes on opioid craving and relapse are not well understood. As well, sex differences within these processes are poorly understood. Future studies are needed to improve our understanding of how neuroimmune mechanisms may contribute to opioid relapse.

NEUROIMMUNE MECHANISMS AND SUBSTANCE USE DISORDER COMORBIDITIES

Many individuals who are diagnosed with a SUD often suffer from other physical or psychiatric comorbidities that can hinder successful treatment outcomes. According to the United States Substance Abuse and Mental Health Services Administration (SAMHSA), over 9.2 million American adults had both a SUD and a comorbid mental illness such as anxiety or depression as of 2018 (Substance Abuse and Mental Health Services Administration, 2019). Furthermore, physical comorbidities such as chronic pain and HIV are more difficult to treat among those with SUDs (National Institute on Drug Abuse [NIDA], 2020a). Convergent findings from numerous clinical and preclinical studies have implicated immune dysfunction as a possible shared mechanism linking these comorbidities to the pathophysiology of SUDs. Here, we briefly highlight recent studies demonstrating immune system dysfunction in disorders that are commonly comorbid with SUDs, focusing primarily on major depressive disorder (MDD), posttraumatic stress disorder (PTSD), chronic pain, and HIV. The studies discussed here may provide useful insights into commonly shared mechanisms that facilitate the pathogenesis of these comorbidities as well as increase SUD vulnerability.

Depression

The idea that depression (also referred to as Major Depressive Disorder, or MDD) may be influenced by immune system dysfunction dates back to the early 1990's, when Ronald Smith published his seminal paper on the "macrophage theory of depression" (Smith, 1991). Among the evidence described by Smith included the observations that experimental volunteers who were administered monocyte/macrophage-derived cytokines developed many of the symptoms of MDD and that individuals with chronic inflammatory diseases such as rheumatoid arthritis are more likely to have depression. Ahead of his time, Smith also postulated that the "food-gut-allergy" axis may be involved in the pathogenesis of MDD. While outside the scope of this review, recent studies have elucidated key mechanisms of the gut microbiome in human health and disease, including its role in the etiology of psychiatric illnesses (Singh et al., 2017; Cryan and de Wit, 2019). Both systemic inflammation induced by xenobiotic substances and inflammatory disease states, such as in multiple sclerosis and spinal cord injury, are associated with depressive symptoms in humans (Allison and Ditor, 2015; Engler et al., 2017; Morris et al., 2018). Other inflammatory conditions such as irritable bowel syndrome and psoriasis are associated with higher prevalence

rates of depression, anxiety, and substance abuse, suggesting that inflammatory mechanisms may reside at the intersection between these disorders (Hayes and Koo, 2010; Fond et al., 2014; Knight et al., 2015). MDD is often comorbid with AUDs in particular, and many studies implicate neuroimmune dysfunction as a significant pathophysiological feature of this comorbidity (for review, see Neupane, 2016). Individuals with MDD also show elevated serum levels of various immune factors such as IL-6 (Engler et al., 2017; Ye et al., 2018) and TNFα (Fan et al., 2017; Zou et al., 2018), and IL-6 in particular has been implicated in depression across a number of clinical and preclinical studies (for review, see Hodes et al., 2016). A recent example is that stress-susceptible mice treated systemically with an IL-6 antibody show significant reductions in depressive-like behaviors in the chronic social defeat stress model of depression, which generally upregulates systemic levels of IL-6 (Hodes et al., 2014; Stewart et al., 2015; Zhang J.C. et al., 2017). As well, social stress and drugs of abuse can downregulate the expression of cell adhesion and tight junction proteins such as collagen-IV and claudin-5, leading to infiltration of immune factors like IL-6 from the periphery (Menard et al., 2017; Rodríguez-Arias et al., 2017). In a recent preclinical study, mice exposed to chronic unpredictable stress exhibited elevated levels of TNFα within the HPC and increased depressive- and anxiety-like behaviors, which were attenuated by minocycline treatment (Zhang et al., 2019). Interestingly, minocycline has also been shown to reduce both METH- and alcohol-seeking behavior in rodents (Fujita et al., 2012; Attarzadeh-Yazdi et al., 2014; Gajbhiye et al., 2017).

Serum levels of TNFα are also elevated in individuals with MDD (Tuglu et al., 2003), and elevated levels of TNFα may be associated with treatment-resistance, particularly with selective serotonin reuptake inhibitors (SSRIs) (Tuglu et al., 2003; O'Brien et al., 2007; Eller et al., 2008). Interestingly, TNFα levels are positively correlated with midbrain serotonin transporter (SERT) availability in humans (Krishnadas et al., 2016), suggesting a possible immunomodulatory mechanism that underlies dysregulated serotonin neurotransmission in depression. The SSRIs fluoxetine and escitalopram inhibit M1 proinflammatory activation and promote M2 anti-inflammatory activation of microglia *in vitro* (Su et al., 2015). As well, rats experiencing chronic mild stress exhibit elevated plasma levels of proinflammatory cytokines (IL-1β, IL-17, and TNFα), which are prevented by chronic fluoxetine treatment (Lu et al., 2017). This is mirrored by a recent meta-analysis demonstrating that patients with MDD who respond to antidepressant treatment show significantly decreased peripheral TNFα levels (Liu et al., 2020).

The studies above highlight that antidepressant SERT inhibitors exert immunomodulatory effects, and these effects may be related to their therapeutic efficacy. As well, several recent preclinical studies suggest that changes in SERT expression and/or activity alters glutamatergic plasticity and addiction-related behaviors. For example, SERT knockout ($SERT^{-/-}$) rats, which exhibit depression- and anxiety-like behaviors (Kalueff et al., 2010), show decreased mRNA expression of key glutamatergic substrates within the habenula, including GLT-1, NMDA subunits (GluN1, GluN2A, and GluN2B), and AMPA subunits (GluA1 and GluA2) (Caffino et al., 2019). Moreover, $SERT^{-/-}$ rats exhibit greater cocaine self-administration, and cocaine self-administering $SERT^{+/+}$ rats showed reduced mRNA levels of genes encoding for GLT-1 and GluN1 to the levels of $SERT^{-/-}$ rats (Caffino et al., 2019). Another recent study utilizing the bilateral olfactory bulbectomy (OBX) model of depression in combination with cocaine self-administration showed that treatment with escitalopram dose-dependently reduces cue-induced cocaine-seeking behavior in both OBX and sham control rats as well as burst responding on day 1 of extinction training (Jastrzêbska et al., 2017). As illustrated in **Figure 1**, glutamatergic signaling interfaces with neuroimmune function in glial cells, and serotonergic dysfunction in MDD (e.g., altered SERT function) could lead to dysregulated glutamatergic signaling and, subsequently, altered neuroimmune function. Nevertheless, this remains largely speculative, and more studies are needed to fully investigate whether serotonergic substrates directly or indirectly alter neuroimmune function within animal models of MDD and SUDs and if such neuroimmune mechanisms are relevant to the pathophysiology of this comorbidity.

Although it is unclear whether specific cytokine inhibitors alone would be broadly effective treatments for MDD (Raison et al., 2013; Smolen et al., 2014), these studies support the notion that immunopharmacology may be an efficacious adjunctive treatment strategy in combination with existing anti-depressants for treating co-morbid MDD and SUDs. Ketamine, which has demonstrated efficacy in cases of chronic, treatment-resistant depression, exhibits a broad spectrum of anti-inflammatory effects (e.g., TNFα and IL-6 inhibition) in both clinical and preclinical studies (Murrough et al., 2013; Tan et al., 2017; Chen et al., 2018). Indeed, broad-spectrum immunomodulators, as opposed to cytokine-specific antibodies for example, may prove to be effective treatment strategies for MDD. For instance, drugs that confer a wide range of antioxidant and anti-inflammatory effects, such as the cysteine prodrug *N*-acetylcysteine, show clinical promise as adjunctive treatments for MDD, bipolar depression, and for SUDs (Berk et al., 2011, 2014; Magalhães et al., 2011; Carvalho et al., 2013; Tomko et al., 2018). Nevertheless, more studies are needed to further examine whether such treatment strategies are effective in cases of comorbid MDD and SUDs.

Posttraumatic Stress Disorder

Akin to MDD, posttraumatic stress disorder (PTSD) is a comorbidity experienced by many individuals with SUDs. PTSD is associated with systemic elevation of inflammatory markers that may underly the pathophysiology of the disorder (for review, see Hori and Kim, 2019). A recent meta-analysis by Passos et al. (2015) revealed that serum IL-6, IL-1β, and interferon gamma (IFN-γ) are all elevated in individuals with PTSD compared to healthy controls. IL-6 is also positively correlated with disease severity and IL-1β with disease duration. Furthermore, when MDD comorbidity is controlled for, individuals with PTSD show elevated TNFα, IL-6, and IL-1β (Passos et al., 2015). Genetic studies in humans also provide converging evidence in support of immune dysregulation in PTSD. For example, a

recent genome-wide association study identified significant gene loci (e.g., ANKRD55) associated with immune disorders such as rheumatoid arthritis and psoriasis in individuals with PTSD (Stein et al., 2016).

Preclinical studies also implicate both central and peripheral immune activation in the pathophysiology of PTSD. For instance, fear memory retrieval in mice is associated with increased circulating IL-6 and inhibition of IL-6 signaling can improve extinction learning (Young et al., 2018). In addition, many inflammatory and innate immune pathways such as interferons, interleukins, and TNFα remain activated long after social stress exposure in mice, while anti-inflammatory mediators such as TGFβ are inhibited (Muhie et al., 2017). Interestingly, predator stress exposure in mice induces a state of immunosuppression within the brain, but acute "priming" of the immune system with LPS prior to this form of stress exposure has no effect on later avoidance behavior (Deslauriers et al., 2017). This suggests that chronic stress experienced with PTSD, as opposed to acute trauma exposure itself, may underly the persistence of immune dysregulation seen in individuals with PTSD.

Other studies utilizing predator-based psychosocial stress models also highlight the significance of prior drug experience in modulating the effects of stress on drug taking later in life. For example, a recent study demonstrated that rats exposed to chronic predator stress showed enhanced ethanol preference (over sucrose) compared to unstressed controls only when they had ethanol experience with two-bottle choice *prior* to stress exposure (Zoladz et al., 2018). A question that remains is whether prior stress and drug experience interact to dysregulate immune signaling in a way that promotes stress susceptibility and/or subsequent increases in addiction-related behaviors. One recent study sheds some light on this topic, demonstrating that early life stress in the form of maternal separation increases PFC and NAc TNFα levels in males, but not females, and enhances cocaine CPP in maternally stressed males. As well, this study showed that systemic inhibition of TNFα restores cocaine CPP to control levels (Ganguly et al., 2019). This supports another recent study showing that early life social stress in mice can sensitize both central and peripheral immune responses to cocaine within the VTA and that humans with CUDs that experienced childhood social stress show elevated expression of inflammatory markers (e.g., TLR4, TNFα, IL-1β, and IL-6) (Lo Iacono et al., 2018). Indeed, these findings highlight that a history of chronic stress or trauma, especially during adolescence, may cause aberrant changes in immune function that could increase SUD susceptibility later in life.

As highlighted throughout this review and illustrated in **Figure 1**, glutamate dysfunction is a consistent feature observed across drugs of abuse and recent evidence implicates metabotropic glutamate receptor 5 (mGlu5) in the pathophysiology of PTSD and neuroimmune function. Indeed, dysfunction of glutamatergic plasticity is also thought to be involved in pathophysiology of PTSD (for review, see Averill et al., 2017). Microglia, astrocytes, and peripheral immune cells express mGlu5, which promotes anti-inflammatory responses (Fazio et al., 2018). Interestingly, a recent study showed that neuroinflammation induced by traumatic brain injury in mice is reduced by mGlu5 PAM treatment and that the mechanism of action involves Akt/GSK-3β/CREB signaling (Bhat et al., 2021). This corroborates previous evidence showing that stimulation of mGlu5 reduces LPS-induced microglial activation and proinflammatory signaling (Byrnes et al., 2009). A recent study by Schwendt et al. (2018) showed that rats resilient to stress induced by predator odor exposure exhibit increased *mGlu5* gene expression within the amygdala and mPFC. As well, stress-susceptible animals show enhanced cue-induced reinstatement of cocaine seeking that is not attenuated by the β-lactam antibiotic ceftriaxone, which is a drug known to reliably suppress this behavior (Knackstedt et al., 2010; LaCrosse et al., 2016; Schwendt et al., 2018). Importantly, treating stress-susceptible animals with a mGlu5 positive allosteric modulator (PAM) along with ceftriaxone and fear extinction successfully prevented cue-induced reinstatement of cocaine seeking (Schwendt et al., 2018). Another recent study parallels these findings, showing that early life stress in rats causes these animals to spend less time in the light area of a light-dark box and to exhibit lower *mGlu5* gene expression within the amygdala. This study also showed that time spent in the light area is positively correlated with *mGlu5* gene expression within the amygdala (Buonaguro et al., 2020). One question that remains is whether such mGlu5-mediated neuroimmune mechanisms are therapeutic in cases of comorbid PTSD and SUDs. Given the putative role of glutamatergic substrates such as mGlu5 in both PTSD and SUDs, further investigation into the neuroimmune mechanisms of this receptor system within animal models of comorbid PTSD and SUDs is warranted.

Novel drugs that modulate immune signaling have shown stress-reducing effects in preclinical models. For example, a recent study showed that intranasal oxytocin treatment following single prolonged stress (SPS) exposure is sufficient to reverse physiological and behavioral deficits such as increased central and peripheral proinflammatory cytokine expression, reduced plasma corticosterone levels, and impaired extinction learning (Wang S.C. et al., 2018). Additionally, SPS in rats treated with a cyclooxygenase-2 (COX-2) inhibitor exhibit decreased apoptosis in the HPC, reduced levels of proinflammatory cytokines in the HPC, and decreased anxiety-like behavior (Wang M. et al., 2018). Other preclinical studies have also shown similar effects on anxiety-like behavior and proinflammatory cytokine expression within the brain using COX-2 inhibitors (Gamble-George et al., 2016; Lee et al., 2016), and human studies suggest that anti-inflammatory treatments such as COX-2 inhibitors may be effective in reducing depression symptoms (Köhler et al., 2014). Interestingly, the antioxidant *N*-acetylcysteine (NAC) was recently shown to inhibit conditioned stress-induced cocaine and alcohol seeking when administered during or immediately following restraint stress (Garcia-Keller et al., 2020), which raises the question as to whether suppression of oxidative stress and inflammation via NAC treatment is therapeutic in this context. Importantly, NAC is currently being investigated clinically for its use in treating comorbid AUDs and PTSD (Back et al., 2020). Drugs with immunomodulatory activity, such as monoclonal antibodies, glucocorticoids, and cannabinoids, are also being investigated for their use in

the treatment of PTSD (Hori and Kim, 2019). Overall, these studies provide a firm rationale for future investigations into immunomodulatory medications to treat symptoms of PTSD. However, it remains largely unknown whether such treatment strategies are efficacious in treating cases of comorbid PTSD and SUDs. Indeed, use of psychotropic substances can explain a significant degree of heterogeneity across studies examining proinflammatory cytokine expression in individuals with PTSD (Passos et al., 2015). Thus, future investigations should consider the neuroimmune intersections of comorbid PTSD and SUDs that may impact the therapeutic efficacy of treatments.

Chronic Pain

Substance abuse and misuse, particularly with opioids, is more common among individuals with chronic pain. For example, an estimated 10% of individuals living with chronic pain also misuse prescription opioids, and chronic pain interacts with mesocorticolimbic reward circuits and stress pathways to increase SUD vulnerability (for review, see Elman and Borsook, 2016; Garland et al., 2013). Chronic pain, defined as pain lasting longer than 3 months or beyond the period of normal tissue healing, affects as much as 43% of adults within the United States (Dowell et al., 2016). While the prescribing of opioids has declined since 2012 (Zhu et al., 2019), these medications are still commonly used to treat chronic pain and opioid-related overdoses and deaths still remain high (Scholl et al., 2018). Inflammation and immune system dysfunction are defining features of many forms of chronic pain (Marchand et al., 2005; Totsch and Sorge, 2017) and several recent studies have identified immunomodulatory pain mechanisms that may extend our understanding of the pathophysiology of SUDs (particularly OUDs). For example, a recent preclinical study using the complete Freund's adjuvant (CFA) model of inflammation found that rats experiencing chronic inflammation require higher doses of heroin (150 μg/kg) to achieve significant increases in NAc core dopamine release. As well, this study showed that inflammatory pain impairs MOR-mediated inhibition of GABA transmission within the VTA and enhances heroin self-administration at higher doses without impacting sucrose self-administration (Hipólito et al., 2015). This is consistent with another study demonstrating that chronic neuropathic pain decreases MOR1 availability and expression within the rat CPu and motor cortex, which correlates positively with sucrose preference in nerve-injured animals (Thompson et al., 2018). Converging evidence suggests that chronic inflammatory pain may also impair the analgesic effects of opioids (Steele et al., 2002; DeLeo et al., 2004; Zhang et al., 2004). Studies also show that the MOR antagonist naltrexone may reduce chronic inflammatory pain through inhibition of T and B cell proliferation and TLR4 signaling (Tawfik et al., 2016; Patten et al., 2018), suggesting a potentially promising role for adjunctive immunomodulatory therapies in chronic pain management. Taken together, inflammatory mechanisms can lead to dysregulations in endogenous opioid receptor signaling that can facilitate chronic pain and lead to escalated drug intake over time and, subsequently, increased risk for drug dependence and substance abuse. Thus, use of anti-inflammatory medications as adjunctive therapies to improve chronic pain management may have the added benefit of reducing the risk of addiction to opioid pain medications.

Chronic pain and antinociceptive opioid drugs are subject to important sex differences that may have underlying neuroimmune mechanisms. Indeed, some of the most common chronic pain conditions such as migraine, low back pain, and neck pain, are vastly overexpressed in women (Mogil, 2012). In fact, women are overall more likely to use prescription opioids than men (Serdarevic et al., 2017) and women may also experience greater levels of pain than men in a manner that may be dependent on opioid withdrawal (Huhn et al., 2019). Preclinical studies have identified sexual dimorphism of cellular responses to opioids that may explain some of the sex differences in pain observed in humans. For example, a recent study demonstrated that female rats exhibit increased basal and LPS-induced microglial activation within the PAG, and that basal activation of microglia is a significant predictor of the ED_{50} of morphine's antinociceptive effects (Doyle et al., 2017). Moreover, this study showed that naloxone inhibition of TLR4 within the PAG significantly improves the antinociceptive effects of morphine. T cells may also underly observed sex differences in opioid analgesia, with one recent study demonstrating that T-cell-deficient mice exhibit impaired opioid-induced analgesia that is more pronounced in females (Rosen et al., 2019). Other non-opioidergic, sex-specific neuroimmune mechanisms underlying chronic pain have been identified, which could have significant implications for clinical treatment of pain and SUDs in human populations. For instance, ATP signaling via P2X4 receptors on microglia has been shown to be essential for nerve injury-induced allodynia in males but not in females (Mapplebeck et al., 2018). However, human studies have shown that the serotonin and norepinephrine reuptake inhibitor duloxetine, which also inhibits P2X4 signaling (Yamashita et al., 2016), reduces pain in women with fibromyalgia (Arnold et al., 2007; Bidari et al., 2019). This highlights the complexity of sex differences in the neuroimmune regulation of pain and suggests that perhaps dynamic immune interactions with monoamine neurotransmitter systems play a significant modulatory role in chronic pain between males and females (Lei et al., 2011; Packiasabapathy and Sadhasivam, 2018).

Neuromodulatory systems such as the endocannabinoid system (ECS) have also garnered significant attention for their role in chronic pain. Conflicting clinical and preclinical studies exist regarding sex differences in the efficacy of cannabinoids as chronic pain treatments (for review, see Cooper and Craft, 2018). The efficacy of such treatments likely depend upon the route of administration, type of pain, and locus of pain (Romero-Sandoval et al., 2017). Nevertheless, the ECS is well regarded for its role in regulating neuroimmune signaling and pain. For example, cannabinoid receptors such as CB1 and CB2 are expressed in CNS regions involved in nociception (e.g., PAG, amygdala, dorsal root ganglion, thalamus, etc.) and these receptors exert primarily anti-inflammatory effects (Burstein and Zurier, 2009; Barrie and Manolios, 2017). Cannabis has been proposed as a potential adjunctive or alternative therapeutic for OUDs, particularly in cases of

comorbid chronic pain (Wiese and Wilson-Poe, 2018), although this has been disputed (Olfson et al., 2018; Wilson et al., 2018; McBrien et al., 2019). Nevertheless, cannabidiol (CBD), which is a specific chemical constituent of cannabis that has no intoxicating psychoactive properties, exerts anti-inflammatory activity (Nichols and Kaplan, 2020) that has shown significant promise as a potential therapeutic for OUDs (Hurd et al., 2015). Altogether, these studies underscore the need for future investigations into the use of immunomodulatory therapeutics in the treatment of chronic pain, either alone or as adjunctive therapies. Importantly, these medications may be useful in the treatment of comorbid chronic pain and SUDs, where common immune mechanisms may underly the pathophysiology of both conditions.

Human Immunodeficiency Virus (HIV)

HIV is another physical comorbidity that can significantly impede treatment outcomes for SUDs and vice versa. According to the United States Centers for Disease Control and Prevention (CDC), over 1 million people in the United States are currently living with HIV and 1 in 7 of those affected are unaware of their HIV status (Centers for Disease Control and Prevention, 2019). Globally, nearly 40 million people are currently living with HIV, and individuals who inject drugs are at a 22 times greater risk for acquiring HIV (UNAIDS, 2019). Importantly, HIV still remains a significant public health concern among minority and socioeconomically disadvantaged populations (National Institute on Drug Abuse [NIDA], 2012; Durvasula and Miller, 2014). As well, drug abuse (particularly psychostimulant abuse) is associated with higher rates of risky behaviors such as unsafe sexual practices that can increase HIV risk (Centers for Disease Control and Prevention, 2018).

Modern antiretroviral therapy (ART) has proven successful at suppressing viral load and mitigating the transition to acquired immunodeficiency syndrome (AIDS), allowing many individuals living with HIV to live relatively normal lives. However, ART does not readily cross the BBB, rendering the brain vulnerable to chronic HIV infection (Atluri et al., 2015). Specifically, drugs of abuse such as cocaine can increase BBB permeability (Zhang et al., 1998) and facilitate invasion (An and Scaravilli, 1997) and viral replication (Sahu et al., 2015) of HIV in the brain even during the early asymptomatic stages of HIV infection. This process can happen rapidly and lead to chronic CNS infection that results in neuroimmune activation and, in many cases, HIV-associated neurocognitive disorders (HAND) (Hong and Banks, 2015; Zayyad and Spudich, 2015). Cocaine facilitates HIV replication through a NF-κB-dependent mechanism (Fiume et al., 2012; Sahu et al., 2015) and impairs the innate immune response of astrocytes to infiltrating viruses such as HIV through increased oxidative stress when tested *in vitro* (Cisneros et al., 2018). Drugs of abuse also exacerbate the effects of the HIV proteins *trans*-activator of transcription (Tat) and gp120 in inducing oxidative stress, microgliosis, and astrogliosis (Aksenov et al., 2001, 2003; Shah et al., 2013; Samikkannu et al., 2015; Zeng et al., 2018). Moreover, HIV Tat primes and activates proinflammatory responses in microglia via the NLR family pyrin domain containing 3 (NLRP3) inflammasome (Chivero et al., 2017), and dopamine can activate NF-κB and prime the NLRP3 inflammasome in macrophages (Nolan et al., 2020) (however, see Zhu et al., 2018). This could be exacerbated by drugs of abuse that promote dopamine transmission within areas of the brain that are particularly vulnerable to HIV, such as the striatum (Nolan and Gaskill, 2019). Clinically, the mitochondrial protein translocator protein (TSPO), which has garnered interest as a biomarker of neuroinflammation in human imaging studies (Werry et al., 2019), is upregulated in people living with HIV (PLWH) and increased TSPO within the hippocampus, amygdala, and thalamus is associated with impaired cognition (Vera et al., 2016). Other studies suggest that impaired cognitive function is associated with enhanced TSPO binding in frontal and temporal regions of the brain in PLWH (Garveya et al., 2014; Rubin et al., 2018). It remains unclear whether combined HIV and active drug use, compared to drug abstinence, produces differential profiles of neuroinflammation and immune activation to confer increased vulnerability to HAND and drug relapse. Nevertheless, many preclinical studies suggest that HIV and its protein products may exacerbate drug reward and reinforcement as well as drug-induced neuroadaptations that may impede successful SUD treatment outcomes.

Growing evidence suggests that HIV and its protein products interact with brain reward circuitry to contribute to dysregulated reward-seeking behavior and cognition. For example, HIV-1 transgenic rats, which constitutively express HIV-1 viral proteins and model many HIV-associated neurological abnormalities observed in humans (Moran et al., 2014; Vigorito et al., 2015; McLaurin et al., 2018), exhibit increased dopamine affinity at striatal dopamine transporters and a leftward shift in the ascending limb of the cocaine dose response function, suggesting enhanced sensitivity to the reinforcing properties of cocaine (McIntosh et al., 2015). Another study using this transgenic rat model showed that these animals exhibit enhanced hyperexcitability of pyramidal neurons within the PFC following abstinence from cocaine (Wayman et al., 2016). As well, inducible Tat expression within the brain of transgenic mice is associated with enhanced METH-induced microglia activation as well as METH-induced locomotor sensitization (Kesby et al., 2017). Other studies using the inducible Tat mouse model have shown that induced Tat expression within the brain increases the magnitude of cocaine CPP and is sufficient to reinstate extinguished cocaine CPP (Paris et al., 2014a). Similar effects have been observed in females, albeit in an estrous cycle phase-dependent manner (Paris et al., 2014b). Similarly, inducible gp120 expression within the mouse brain is associated with the formation of METH conditioned place preference at lower METH doses compared to non-transgenic controls (Kesby et al., 2014). Many other preclinical studies have also demonstrated impaired cognitive function in animals exposed to HIV proteins and drugs of abuse, mimicking the cognitive dysfunction observed in humans with HAND (Moran et al., 2014; Kesby et al., 2015a,b, 2016; Paydary et al., 2016). Taken together, such studies suggest that HIV and its protein products may increase one's sensitivity to the rewarding and reinforcing properties of psychostimulants and impair cognitive function.

In contrast to the studies above, a recent study using the HIV transgenic rat model suggests that HIV many promote a

motivational state of apathy (Bertrand et al., 2018). However, one significant limitation to this study and studies like it is that the HIV transgenic rat model constitutively expresses HIV proteins throughout the CNS *prior* to the establishment of stable drug self-administration, which may produce profoundly different effects on mesocorticolimbic circuit function and neuroimmune signaling compared to the induction of viral protein expression within the CNS *after* drug self-administration is established or during a period of abstinence. Indeed, some individuals with preexisting SUDs contract HIV collaterally through drug use and risky behaviors associated with drug use (Centers for Disease Control and Prevention, 2018). Regardless, it is possible that HIV-induced perturbations to neuroimmune signaling described above may underly these neurobehavioral intersections between HIV and SUDs. Thus, immunopharmacology may be a promising avenue of future research into medications that inhibit the long-term neurocognitive deficits observed with chronic HIV infection as well as drug craving and relapse in cases of comorbid SUDs (Roederer et al., 1992; Ambrosius et al., 2019; Tripathi et al., 2020). Interestingly, ART itself possess anti-inflammatory properties (Hileman and Funderburg, 2017), but drugs of abuse may interact pharmacologically with ART to reduce its effectiveness in both suppressing viral load and minimizing cognitive deficits associated with HAND (Kumar et al., 2015). Future studies should examine the efficacy of anti-inflammatory adjunctive therapeutics in reducing HIV-associated neurocognitive deficits and promoting long-term abstinence from drug use.

CONCLUSION

Throughout this review, we have highlighted recent studies that demonstrate functionally significant immunomodulatory mechanisms that may underlie the pathophysiology of SUDs and associated comorbidities. While immunomodulation of learning, memory, and synaptic plasticity is not a new concept *per se*, recent research has greatly expounded the role of immune signaling in neuropsychiatric disorders and diseases, providing a firm foundation for future investigations into novel treatment targets. The literature presented herein suggests that central and peripheral immune mechanisms may represent a common thread underlying the interactions between SUDs and associated comorbidities. Indeed, the clinical and preclinical findings discussed here underscore the need for future investigations into the efficacy of adjunctive immunomodulatory medications that may be therapeutically efficacious in the treatment of SUDs and associated comorbidities such as MDD, PTSD, chronic pain, and HIV. Despite these advances, one major gap in the literature that demands future investigation is how neuroimmune signaling within mesocorticolimbic circuits is altered across the entire addiction cycle. For example, very few studies to date have examined how neuroimmune signaling is altered across a protracted period of abstinence compared to acute and chronic drug exposure, and if such changes are causally linked to drug-seeking behavior. Moreover, very few studies to date have thoroughly examined how comorbidities impact neuroimmune function during periods of active drug taking versus periods of protracted abstinence. Abstinence represents a critical period of vulnerability within the addiction cycle, and the neuroimmune sequelae of chronic drug use and abstinence remains poorly understood. Investigation of these processes could improve our understanding of how motivation for drug increases (or "incubates") over time throughout a protracted period of abstinence to increase relapse vulnerability (Pickens et al., 2011). As mentioned numerous times throughout this review, the role of sex differences in the neuroimmune mechanisms of SUDs and associated comorbidities remains poorly understood. Indeed, there are significant sex differences in the prevalence rates of individual conditions such as SUDs, MDD, PTSD, chronic pain, etc. As thoroughly reviewed by others (Rosen et al., 2017; Bekhbat and Neigh, 2018; Osborne et al., 2018; McCarthy, 2019), there are sex-specific neuroimmune mechanisms involved in the pathophysiology of these conditions that may be suitable targets for medications development. Nevertheless, whether these sex-specific neuroimmune mechanisms drive the comorbidity of these disorders and diseases and contribute to their disparate prevalence rates is largely unknown and future research is needed to address this gap. Many of the studies discussed herein are largely observational in nature and few have attempted to experimentally manipulate neuroimmune mechanisms using drug self-administration animal models, which is another remaining gap in the field. For example, there are significant differences in the neurobiological mechanisms underlying cue-induced drug-seeking behavior between animal models involving experimenter-delivered drug versus self-administration of drug (Namba et al., 2018), and these mechanisms may be differentially regulated by distinct neuroimmune mechanisms. Overall, we suggest that future research needs to address the gaps mentioned above to better assess whether putative neuroimmune targets are suitable candidates for medications development to treat SUDs and associated comorbidities.

AUTHOR CONTRIBUTIONS

MN conceptualized this review. MN and JL-J wrote the first draft. EN, MO, and JN subsequently contributed to the content, ideas, and editing of the manuscript. All authors contributed to the article and approved the submitted version.

FUNDING

This work was supported by National Institutes of Health grants F31 DA047072 (MN), R21 DA048651 (JN), R01 DA043172 and R01 AA025590 (MO), F32 AA027962 (JL-J), Sigma Xi grant G2019100191831450 (MN), Arizona State University Institute for Social Science Research seed grant (JN), and ARCS Foundation Scholar Award (MN).

ACKNOWLEDGMENTS

Figure 1 was created with BioRender.com.

REFERENCES

Adeluyi, A., Guerin, L., Fisher, M. L., Galloway, A., Cole, R. D., Chan, S. S. L., et al. (2019). Microglia morphology and proinflammatory signaling in the nucleus accumbens during nicotine withdrawal. *Sci. Adv.* 5:eaax7031. doi: 10.1126/sciadv.aax7031

Aksenov, M. Y., Hasselrot, U., Bansal, A. K., Wu, G., Nath, A., Anderson, C., et al. (2001). Oxidative damage induced by the injection of HIV-1 Tat protein in the rat striatum. *Neurosci. Lett.* 305, 5–8. doi: 10.1016/s0304-3940(01)01786-4

Aksenov, M. Y., Hasselrot, U., Wu, G., Nath, A., Anderson, C., Mactutus, C. F., et al. (2003). Temporal relationships between HIV-1 Tat-induced neuronal degeneration, OX-42 immunoreactivity, reactive astrocytosis, and protein oxidation in the rat striatum. *Brain Res.* 987, 1–9. doi: 10.1016/s0006-8993(03)03194-9

Alasmari, F., Crotty Alexander, L. E., Nelson, J. A., Schiefer, I. T., Breen, E., Drummond, C. A., et al. (2017). Effects of chronic inhalation of electronic cigarettes containing nicotine on glial glutamate transporters and α-7 nicotinic acetylcholine receptor in female CD-1 mice. *Prog. Neuro Psychopharmacol. Biol. Psychiatry* 77, 1–8. doi: 10.1016/j.pnpbp.2017.03.017

Alfonso-Loeches, S., Pascual-Lucas, M., Blanco, A. M., Sanchez-Vera, I., and Guerri, C. (2010). Pivotal role of TLR4 receptors in alcohol-induced neuroinflammation and brain damage. *J. Neurosci.* 30, 8285–8295. doi: 10.1523/jneurosci.0976-10.2010

Alfonso-Loeches, S., Ureña-Peralta, J., Morillo-Bargues, M. J., Gómez-Pinedo, U., and Guerri, C. (2016). Ethanol-induced TLR4/NLRP3 neuroinflammatory response in microglial cells promotes leukocyte infiltration across the BBB. *Neurochem. Res.* 41, 193–209. doi: 10.1007/s11064-015-1760-5

Alhaddad, H., Das, S. C., and Sari, Y. (2014). Effects of ceftriaxone on ethanol intake: a possible role for xCT and GLT-1 isoforms modulation of glutamate levels in P rats. *Psychopharmacology* 231, 4049–4057. doi: 10.1007/s00213-014-3545-y

Allison, D. J., and Ditor, D. S. (2015). Targeting inflammation to influence mood following spinal cord injury: a randomized clinical trial. *J. Neuroinflamm.* 12:204.

Ambrosius, B., Gold, R., Chan, A., and Faissner, S. (2019). Antineuroinflammatory drugs in HIV-associated neurocognitive disorders as potential therapy. *Neurol. Neuroimmunol. Neuroinflamm.* 6:e551. doi: 10.1212/nxi.0000000000000551

Amin, F. U., Shah, S. A., and Kim, M. O. (2016). Glycine inhibits ethanol-induced oxidative stress, neuroinflammation and apoptotic neurodegeneration in postnatal rat brain. *Neurochem. Int.* 96, 1–12. doi: 10.1016/j.neuint.2016.04.001

An, S. F., and Scaravilli, F. (1997). Early HIV-1 infection of the central nervous system. *Arch. Anat. Cytol. Pathol.* 45, 94–105.

Antón, M., Alén, F., Gómez de Heras, R., Serrano, A., Pavón, F. J., Leza, J. C., et al. (2017). Oleoylethanolamide prevents neuroimmune HMGB1/TLR4/NF-kB danger signaling in rat frontal cortex and depressive-like behavior induced by ethanol binge administration. *Addict. Biol.* 22, 724–741. doi: 10.1111/adb.12365

Araos, P., Pedraz, M., Serrano, A., Lucena, M., Barrios, V., García-Marchena, N., et al. (2015). Plasma profile of pro-inflammatory cytokines and chemokines in cocaine users under outpatient treatment: influence of cocaine symptom severity and psychiatric co-morbidity. *Addict. Biol.* 20, 756–772. doi: 10.1111/adb.12156

Arezoomandan, R., and Haghparast, A. (2016). Administration of the glial cell modulator, minocycline, in the nucleus accumbens attenuated the maintenance and reinstatement of morphine-seeking behavior. *Can. J. Physiol. Pharmacol.* 94, 257–264. doi: 10.1139/cjpp-2015-0209

Arnold, L. M., Pritchett, Y. L., D'Souza, D. N., Kajdasz, D. K., Iyengar, S., and Wernicke, J. F. (2007). Duloxetine for the treatment of fibromyalgia in women: pooled results from two randomized, placebo-controlled clinical trials. *J. Women Heal.* 16, 1145–1156. doi: 10.1089/jwh.2006.0213

Asher, O., Cunningham, T. D., Yao, L., Gordon, A. S., and Diamond, I. (2002). Ethanol stimulates cAMP-responsive element (CRE)-mediated transcription via CRE-binding protein and cAMP-dependent protein kinase. *J. Pharmacol. Exp. Ther.* 301, 66–70. doi: 10.1124/jpet.301.1.66

Ashoor, A., Nordman, J. C., Veltri, D., Yang, K. H. S., Al Kury, L., Shuba, Y., et al. (2013). Menthol binding and inhibition of α7-nicotinic acetylcholine receptors. *PLoS One* 8:e67674. doi: 10.1371/journal.pone.0067674

Asyyed, A., Storm, D., and Diamond, I. (2006). Ethanol activates cAMP response element-mediated gene expression in select regions of the mouse brain. *Brain Res.* 1106, 63–71. doi: 10.1016/j.brainres.2006.05.107

Atluri, V. S. R., Hidalgo, M., Samikkannu, T., Kurapati, K. R. V., Jayant, R. D., Sagar, V., et al. (2015). Effect of human immunodeficiency virus on blood-brain barrier integrity and function: an update. *Front. Cell. Neurosci* 9:212. doi: 10.3389/fncel.2015.00212

Attarzadeh-Yazdi, G., Arezoomandan, R., and Haghparast, A. (2014). Minocycline, an antibiotic with inhibitory effect on microglial activation, attenuates the maintenance and reinstatement of methamphetamine-seeking behavior in rat. *Prog. Neuro Psychopharmacol. Biol. Psychiatry* 53, 142–148. doi: 10.1016/j.pnpbp.2014.04.008

Averill, L. A., Purohit, P., Averill, C. L., Boesl, M. A., Krystal, J. H., and Abdallah, C. G. (2017). Glutamate dysregulation and glutamatergic therapeutics for PTSD: evidence from human studies. *Neurosci. Lett.* 649, 147–155. doi: 10.1016/j.neulet.2016.11.064

Avila, D. V., Myers, S. A., Zhang, J. W., Kharebava, G., McClain, C. J., Kim, H. Y., et al. (2017). Phosphodiesterase 4b expression plays a major role in alcohol-induced neuro-inflammation. *Neuropharmacology* 125, 376–385. doi: 10.1016/j.neuropharm.2017.08.011

Avital, A., Goshen, I., Kamsler, A., Segal, M., Iverfeldt, K., Richter-Levin, G., et al. (2003). Impaired interleukin-1 signaling is associated with deficits in hippocampal memory processes and neural plasticity. *Hippocampus* 13, 826–834. doi: 10.1002/hipo.10135

Bachtell, R., Hutchinson, M. R., Wang, X., Rice, K. C., Maier, S. F., and Watkins, L. R. (2015). Targeting the toll of drug abuse: the translational potential of toll-like receptor 4. *CNS Neurol. Disord. Drug Targets* 14, 692–699. doi: 10.2174/1871527314666150529132503

Back, S. E., Gray, K., Santa Ana, E., Jones, J. L., Jarnecke, A. M., Joseph, J. E., et al. (2020). acetylcysteine for the treatment of comorbid alcohol use disorder and posttraumatic stress disorder: design and methodology of a randomized clinical trial. *Contemp. Clin. Trials* 91:105961. doi: 10.1016/j.cct.2020.105961

Back, S. E., McCauley, J. L., Korte, K. J., Gros, D. F., Leavitt, V., Gray, K. M., et al. (2016). double-blind, randomized, controlled pilot trial of N-acetylcysteine in veterans with posttraumatic stress disorder and substance use disorders. *J. Clin. Psychiatry* 77, e1439–e1446.

Baker, D. A., McFarland, K., Lake, R. W., Shen, H., Tang, X.-C., Toda, S., et al. (2003). Neuroadaptations in cystine-glutamate exchange underlie cocaine relapse. *Nat. Neurosci.* 6, 743–749. doi: 10.1038/nn1069

Balschun, D., Randolf, A., Pitossi, F., Schneider, H., Del Rey, A., and Besedovsky, H. O. (2003). Hippocampal interleukin-1β gene expression during long-term potentiation decays with age. *Ann. N. Y. Acad. Sci.* 992, 1–8. doi: 10.1111/j.1749-6632.2003.tb03132.x

Balschun, D., Wetzel, W., del Rey, A., Pitossi, F., Schneider, H., Zuschratter, W., et al. (2004). Interleukin-6: a cytokine to forget. *FASEB J.* 18, 1788–1790. doi: 10.1096/fj.04-1625fje

Barrie, N., and Manolios, N. (2017). The endocannabinoid system in pain and inflammation: its relevance to rheumatic disease. *Eur. J. Rheumatol.* 4, 210–218. doi: 10.5152/eurjrheum.2017.17025

Barson, J. R., Karatayev, O., Chang, G. Q., Johnson, D. F., Bocarsly, M. E., Hoebel, B. G., et al. (2009). Positive relationship between dietary fat, ethanol intake, triglycerides, and hypothalamic peptides: counteraction by lipid-lowering drugs. *Alcohol* 43, 433–441. doi: 10.1016/j.alcohol.2009.07.003

Beattie, E. C., Stellwagen, D., Morishita, W., Bresnahan, J. C., Ha, B. K., Von Zastrow, M., et al. (2002). Control of synaptic strength by glial TNFalpha. *Science* 295, 2282–2285. doi: 10.1126/science.1067859

Bekhbat, M., and Neigh, G. N. (2018). Sex differences in the neuro-immune consequences of stress: focus on depression and anxiety. *Brain Behav. Immun.* 67, 1–12. doi: 10.1016/j.bbi.2017.02.006

Bell, R. L., Lopez, M. F., Cui, C., Egli, M., Johnson, K. W., Franklin, K. M., et al. (2015). Ibudilast reduces alcohol drinking in multiple animal models of alcohol dependence. *Addict. Biol.* 20, 38–42. doi: 10.1111/adb.12106

Bellinger, F. P., Madamba, S. G., Campbell, I. L., and Siggins, G. R. (1995). Reduced long-term potentiation in the dentate gyrus of transgenic mice with cerebral overexpression of interleukin-6. *Neurosci. Lett.* 198, 95–98. doi: 10.1016/0304-3940(95)11976-4

Ben Achour, S., and Pascual, O. (2010). Glia: the many ways to modulate synaptic plasticity. *Neurochem. Int.* 57, 440–445. doi: 10.1016/j.neuint.2010.02.013

Berk, M., Dean, O. M., Cotton, S. M., Jeavons, S., Tanious, M., Kohlmann, K., et al. (2014). The efficacy of adjunctive N-acetylcysteine in major depressive disorder: a double-blind, randomized, placebo-controlled trial. *J. Clin. Psychiatry* 75, 628–636.

Berk, M., Dean, O., Cotton, S. M., Gama, C. S., Kapczinski, F., Fernandes, B. S., et al. (2011). The efficacy of N-acetylcysteine as an adjunctive treatment in bipolar depression: an open label trial. *J. Affect. Disord.* 135, 389–394. doi: 10.1016/j.jad.2011.06.005

Bertrand, S. J., Mactutus, C. F., Harrod, S. B., Moran, L. M., and Booze, R. M. (2018). HIV-1 proteins dysregulate motivational processes and dopamine circuitry. *Sci. Rep.* 8, 1–17.

Besson, M., David, V., Baudonnat, M., Cazala, P., Guilloux, J.-P., Reperant, C., et al. (2012). Alpha7-nicotinic receptors modulate nicotine-induced reinforcement and extracellular dopamine outflow in the mesolimbic system in mice. *Psychopharmacology* 220, 1–14. doi: 10.1007/s00213-011-2422-1

Bhat, S. A., Henry, R. J., Blanchard, A. C., Stoica, B. A., Loane, D. J., and Faden, A. I. (2021). Enhanced Akt/GSK-3β/CREB signaling mediates the anti-inflammatory actions of mGluR5 positive allosteric modulators in microglia and following traumatic brain injury in male mice. *J. Neurochem.* 156, 225–248. doi: 10.1111/jnc.14954

Bidari, A., Moazen-Zadeh, E., Ghavidel-Parsa, B., Rahmani, S., Hosseini, S., and Hassankhani, A. (2019). Comparing duloxetine and pregabalin for treatment of pain and depression in women with fibromyalgia: an open-label randomized clinical trial. *DARU J. Pharm. Sci.* 27, 149–158. doi: 10.1007/s40199-019-00257-4

Bilbao, A., Serrano, A., Cippitelli, A., Pavón, F. J., Giuffrida, A., Suárez, J., et al. (2016). Role of the satiety factor oleoylethanolamide in alcoholism. *Addict. Biol.* 21, 859–872. doi: 10.1111/adb.12276

Biswas, L., Harrison, E., Gong, Y., Avusula, R., Lee, J., Zhang, M., et al. (2016). Enhancing effect of menthol on nicotine self-administration in rats. *Psychopharmacology* 233, 3417–3427. doi: 10.1007/s00213-016-4391-x

Blednov, Y. A., Benavidez, J. M., Black, M., and Harris, R. A. (2014). Inhibition of phosphodiesterase 4 reduces ethanol intake and preference in C57BL/6J mice. *Front. Neurosci.* 8:129. doi: 10.3389/fnins.2014.00129

Blednov, Y. A., Black, M., Benavidez, J. M., Stamatakis, E. E., and Harris, R. A. (2016). PPAR agonists: II. Fenofibrate and Tesaglitazar alter behaviors related to voluntary alcohol consumption. *Alcohol. Clin. Exp. Res.* 40, 563–571. doi: 10.1111/acer.12972

Blednov, Y. A., Ponomarev, I., Geil, C., Bergeson, S., Koob, G. F., and Harris, R. A. (2012). Neuroimmune regulation of alcohol consumption: behavioral validation of genes obtained from genomic studies. *Addict. Biol.* 17, 108–120. doi: 10.1111/j.1369-1600.2010.00284.x

Borgmann, K., and Ghorpade, A. (2015). HIV-1, methamphetamine and astrocytes at neuroinflammatory crossroads. *Front. Microbiol.* 6:1143. doi: 10.3389/fmicb.2015.01143

Brady, L. J., Hofford, R. S., Tat, J., Calipari, E. S., and Kiraly, D. D. (2019). Granulocyte-colony stimulating factor alters the Pharmacodynamic properties of cocaine in female mice. *ACS Chem. Neurosci.* 10, 4213–4220. doi: 10.1021/acschemneuro.9b00309

Braida, D., Sacerdote, P., Panerai, A. E., Bianchi, M., Aloisi, A. M., Iosuè, S., et al. (2004). Cognitive function in young and adult IL (interleukin)-6 deficient mice. *Behav. Brain Res.* 153, 423–429. doi: 10.1016/j.bbr.2003.12.018

Brenhouse, H. C., Danese, A., and Grassi-Oliveira, R. (2019). Neuroimmune impacts of early-life stress on development and psychopathology. *Curr. Top. Behav. Neurosci.* 43, 423–447. doi: 10.1007/7854_2018_53

Brown, K. T., Levis, S. C., O'Neill, C. E., Northcutt, A. L., Fabisiak, T. J., Watkins, L. R., et al. (2018). Innate immune signaling in the ventral tegmental area contributes to drug-primed reinstatement of cocaine seeking. *Brain. Behav. Immun.* 67, 130–138. doi: 10.1016/j.bbi.2017.08.012

Brunzell, D. H., and McIntosh, J. M. (2012). Alpha7 nicotinic acetylcholine receptors modulate motivation to self-administer nicotine: implications for smoking and schizophrenia. *Neuropsychopharmacology* 37, 1134–1143. doi: 10.1038/npp.2011.299

Buonaguro, E. F., Morley-Fletcher, S., Avagliano, C., Vellucci, L., Iasevoli, F., Bouwalerh, H., et al. (2020). Glutamatergic postsynaptic density in early life stress programming: topographic gene expression of mGlu5 receptors and Homer proteins. *Prog. Neuro Psychopharmacol. Biol. Psychiatry* 96:109725. doi: 10.1016/j.pnpbp.2019.109725

Burstein, S. H., and Zurier, R. B. (2009). Cannabinoids, endocannabinoids, and related analogs in inflammation. *AAPS J.* 11, 109–119.

Byrnes, K. R., Stoica, B., Loane, D. J., Riccio, A., Davis, M. I., and Faden, A. I. (2009). Metabotropic glutamate receptor 5 activation inhibits microglial associated inflammation and neurotoxicity. *Glia* 57, 550–560. doi: 10.1002/glia.20783

Caffino, L., Verheij, M. M. M., Que, L., Guo, C., Homberg, J. R., and Fumagalli, F. (2019). Increased cocaine self-administration in rats lacking the serotonin transporter: a role for glutamatergic signaling in the habenula. *Addict. Biol.* 24, 1167–1178. doi: 10.1111/adb.12673

Calipari, E. S., Godino, A., Peck, E. G., Salery, M., Mervosh, N. L., Landry, J. A., et al. (2018). Granulocyte-colony stimulating factor controls neural and behavioral plasticity in response to cocaine. *Nat. Commun.* 9, 1–14.

Carvalho, A. F., Macêdo, D. S., Goulia, P., and Hyphantis, T. N. N. - (2013). Acetylcysteine augmentation to tranylcypromine in treatment-resistant major depression. *J. Clin. Psychopharmacol.* 33, 719–720. doi: 10.1097/jcp.0b013e31829839c6

Cekanaviciute, E., and Buckwalter, M. S. (2016). Astrocytes: integrative regulators of neuroinflammation in stroke and other neurological diseases. *Neurotherapeutics* 13, 685–701. doi: 10.1007/s13311-016-0477-8

Centers for Disease Control and Prevention (2018). *HIV and Substance Use in the United States*. Available online at: https://www.cdc.gov/hiv/risk/substanceuse.html (accessed August 16, 2019).

Centers for Disease Control and Prevention (2019). *Estimated HIV Incidence and Prevalence in the United States, 2010-2016*. HIV Surveillance Supplemental Report 24. Atlanta, GA: Centers for Disease Control and Prevention.

Chandrasekar, V., and Dreyer, J. L. (2009). microRNAs miR-124, let-7d and miR-181a regulate cocaine-induced plasticity. *Mol. Cell. Neurosci.* 42, 350–362. doi: 10.1016/j.mcn.2009.08.009

Chen, J. X., Huang, K. M., Liu, M., Jiang, J. X., Liu, J. P., Zhang, Y. X., et al. (2017). Activation of TLR4/STAT3 signaling in VTA contributes to the acquisition and maintenance of morphine-induced conditioned place preference. *Behav. Brain Res.* 335, 151–157. doi: 10.1016/j.bbr.2017.08.022

Chen, M. H., Li, C. T., Lin, W. C., Hong, C. J., Tu, P. C., Bai, Y. M., et al. (2018). Rapid inflammation modulation and antidepressant efficacy of a low-dose ketamine infusion in treatment-resistant depression: a randomized, double-blind control study. *Psychiatry Res.* 269, 207–211. doi: 10.1016/j.psychres.2018.08.078

Chivero, E. T., Guo, M.-L., Periyasamy, P., Liao, K., Callen, S. E., and Buch, S. (2017). HIV-1 Tat primes and activates Microglial NLRP3 inflammasome-Mediated neuroinflammation. *J. Neurosci.* 37, 3599–3609. doi: 10.1523/JNEUROSCI.3045-16.2017

Choi, S. S., Lee, H. J., Lim, I., Satoh, J. I., and Kim, S. U. (2014). Human astrocytes: secretome profiles of cytokines and Chemokines. *PLoS One* 9:e92325. doi: 10.1371/journal.pone.0092325

Cisneros, I. E., Erdenizmenli, M., Cunningham, K. A., Paessler, S., and Dineley, K. T. (2018). Cocaine evokes a profile of oxidative stress and impacts innate antiviral response pathways in astrocytes. *Neuropharmacology* 135, 431–443. doi: 10.1016/j.neuropharm.2018.03.019

Clark, K. H., Wiley, C. A., and Bradberry, C. W. (2013). Psychostimulant abuse and neuroinflammation: emerging evidence of their interconnection. *Neurotox. Res.* 23, 174–188. doi: 10.1007/s12640-012-9334-7

ClinicalTrials.gov (2021a). *Development of Ibudilast for Alcohol Use Disorder - Full Text View*. Available online at: https://clinicaltrials.gov/ct2/show/NCT02025998?term=Ibudilast&cond=alcohol&draw=1&rank=1 (accessed March 12, 2021).

ClinicalTrials.gov (2021b). *Medication Development in Alcoholism: Apremilast Versus Placebo - Full Text View*. Available online at: https://clinicaltrials.gov/ct2/show/NCT03175549?term=apremilast&cond=alcohol&draw=2&rank=1 (accessed March 12, 2021).

Cooper, Z. D., and Craft, R. M. (2018). Sex-dependent effects of cannabis and cannabinoids: a translational perspective. *Neuropsychopharmacology* 43, 34–51. doi: 10.1038/npp.2017.140

Cooper, Z. D., Johnson, K. W., Pavlicova, M., Glass, A., Vosburg, S. K., Sullivan, M. A., et al. (2016). The effects of ibudilast, a glial activation inhibitor, on opioid withdrawal symptoms in opioid-dependent volunteers. *Addict. Biol.* 21, 895–903. doi: 10.1111/adb.12261

Crews, F. T., and Vetreno, R. P. (2011). Addiction, adolescence, and innate immune gene induction. *Front. Psychiatry* 2:19. doi: 10.3389/fpsyt.2011.00019

Crews, F. T., Lawrimore, C. J., Walter, T. J., and Coleman, L. G. (2017). The role of neuroimmune signaling in alcoholism. *Neuropharmacology* 122, 56–73. doi: 10.1016/j.neuropharm.2017.01.031

Crews, F. T., Zou, J., and Qin, L. (2011). Induction of innate immune genes in brain create the neurobiology of addiction. *Brain. Behav. Immun.* 25, S4–S12.

Cryan, J. F., and de Wit, H. (2019). The gut microbiome in psychopharmacology and psychiatry. *Psychopharmacology* 236, 1407–1409. doi: 10.1007/s00213-019-05288-y

Cui, C., Shurtleff, D., and Harris, R. A. (2014). Neuroimmune mechanisms of alcohol and drug addiction. *Int. Rev. Neurobiol.* 118, 1–12. doi: 10.1016/b978-0-12-801284-0.00001-4

Deepmala, Slattery, J., Kumar, N., Delhey, L., Berk, M., Dean, O., et al. (2015). Clinical trials of N-acetylcysteine in psychiatry and neurology: a systematic review. *Neurosci. Biobehav. Rev.* 55, 294–321. doi: 10.1016/j.neubiorev.2015.04.015

del Rey, A., Balschun, D., Wetzel, W., Randolf, A., and Besedovsky, H. O. (2013). A cytokine network involving brain-borne IL-1β, IL-1ra, IL-18, IL-6, and TNFα operates during long-term potentiation and learning. *Brain. Behav. Immun.* 33, 15–23. doi: 10.1016/j.bbi.2013.05.011

DeLeo, J. A., Tanga, F. Y., and Tawfik, V. L. (2004). Neuroimmune activation and neuroinflammation in chronic pain and opioid tolerance/hyperalgesia. *Neuroscientist* 10, 40–52. doi: 10.1177/1073858403259950

Deslauriers, J., van Wijngaarde, M., Geyer, M. A., Powell, S., and Risbrough, V. B. (2017). Effects of LPS-induced immune activation prior to trauma exposure on PTSD-like symptoms in mice. *Behav. Brain Res.* 323, 117–123. doi: 10.1016/j.bbr.2017.01.048

Dinarello, C. A. (2018). Overview of the IL-1 family in innate inflammation and acquired immunity. *Immunol. Rev.* 281, 8–27. doi: 10.1111/imr.12621

Dong, Y., and Benveniste, E. N. (2001). Immune function of astrocytes. *Glia* 36, 180–190. doi: 10.1002/glia.1107

Dowell, D., Haegerich, T. M., and Chou, R. C. D. C. (2016). Guideline for prescribing opioids for chronic pain - United States, 2016. *MMWR Recomm. Rep.* 65, 1–49. doi: 10.15585/mmwr.rr6501e1er

Doyle, H. H., Eidson, L. N., Sinkiewicz, D. M., and Murphy, A. Z. (2017). Sex differences in microglia activity within the periaqueductal gray of the rat: a potential mechanism driving the dimorphic effects of morphine. *J. Neurosci.* 37, 3202–3214. doi: 10.1523/jneurosci.2906-16.2017

Duan, S., Anderson, C. M., Stein, B. A., and Swanson, R. A. (1999). Glutamate induces rapid upregulation of astrocyte glutamate transport and cell-surface expression of GLAST. *J. Neurosci.* 19, 10193–10200. doi: 10.1523/jneurosci.19-23-10193.1999

Durvasula, R., and Miller, T. R. (2014). Substance abuse treatment in persons with HIV/AIDS: challenges in managing triple diagnosis. *Behav. Med.* 40, 43–52. doi: 10.1080/08964289.2013.866540

Eidson, L. N., and Murphy, A. Z. (2019). Inflammatory mediators of opioid tolerance: implications for dependency and addiction. *Peptides* 115, 51–58. doi: 10.1016/j.peptides.2019.01.003

Eidson, L. N., Inoue, K., Young, L. J., Tansey, M. G., and Murphy, A. Z. (2017). Toll-like receptor 4 mediates morphine-induced neuroinflammation and tolerance via soluble tumor necrosis factor signaling. *Neuropsychopharmacology* 42, 661–670. doi: 10.1038/npp.2016.131

Eipper-Mains, J. E., Kiraly, D. D., Palakodeti, D., Mains, R. E., Eipper, B. A., and Graveley, B. R. (2011). microRNA-Seq reveals cocaine-regulated expression of striatal microRNAs. *RNA* 17, 1529–1543. doi: 10.1261/rna.2775511

Elbini Dhouib, I., Jallouli, M., Annabi, A., Gharbi, N., Elfazaa, S., and Lasram, M. M. (2016). A minireview on N-acetylcysteine: an old drug with new approaches. *Life Sci.* 151, 359–363. doi: 10.1016/j.lfs.2016.03.003

Eller, T., Vasar, V., Shlik, J., and Maron, E. (2008). Pro-inflammatory cytokines and treatment response to escitaloprsam in major depressive disorder. *Prog. Neuro Psychopharmacol. Biol. Psychiatry* 32, 445–450. doi: 10.1016/j.pnpbp.2007.09.015

Elman, I., and Borsook, D. (2016). Common brain mechanisms of chronic pain and addiction. *Neuron* 89, 11–36. doi: 10.1016/j.neuron.2015.11.027

Engler, H., Brendt, P., Wischermann, J., Wegner, A., Röhling, R., Schoemberg, T., et al. (2017). Selective increase of cerebrospinal fluid IL-6 during experimental systemic inflammation in humans: association with depressive symptoms. *Mol. Psychiatry* 22, 1448–1454. doi: 10.1038/mp.2016.264

Ezeomah, C., Cunningham, K. A., Stutz, S. J., Fox, R. G., Bukreyeva, N., Dineley, K. T., et al. (2020). Fentanyl self-administration impacts brain immune responses in male Sprague-Dawley rats. *Brain. Behav. Immun.* 87, 725–738. doi: 10.1016/j.bbi.2020.03.003

Fan, N., Luo, Y., Ou, Y., and He, H. (2017). Altered serum levels of TNF-α, IL-6, and IL-18 in depressive disorder patients. *Hum. Psychopharmacol.* 32:2588.

Fazio, F., Ulivieri, M., Volpi, C., Gargaro, M., and Fallarino, F. (2018). Targeting metabotropic glutamate receptors for the treatment of neuroinflammation. *Curr. Opin. Pharmacol.* 38, 16–23. doi: 10.1016/j.coph.2018.01.010

Fiume, G., Vecchio, E., De Laurentiis, A., Trimboli, F., Palmieri, C., Pisano, A., et al. (2012). Human immunodeficiency virus-1 Tat activates NF-κB via physical interaction with IκB-α and p65. *Nucleic Acids Res.* 40, 3548–3562. doi: 10.1093/nar/gkr1224

Fond, G., Loundou, A., Hamdani, N., Boukouaci, W., Dargel, A., Oliveira, J., et al. (2014). Anxiety and depression comorbidities in irritable bowel syndrome (IBS): a systematic review and meta-analysis. *Eur. Arch. Psychiatry Clin. Neurosci.* 264, 651–660. doi: 10.1007/s00406-014-0502-z

Foucault-Fruchard, L., and Antier, D. (2017). Therapeutic potential of α7 nicotinic receptor agonists to regulate neuroinflammation in neurodegenerative diseases. *Neural Regen. Res.* 12, 1418–1421. doi: 10.4103/1673-5374.215244

Foucault-Fruchard, L., Doméné, A., Page, G., Windsor, M., Emond, P., Rodrigues, N., et al. (2017). Neuroprotective effect of the alpha 7 nicotinic receptor agonist PHA 543613 in an in vivo excitotoxic adult rat model. *Neuroscience* 356, 52–63. doi: 10.1016/j.neuroscience.2017.05.019

Fujii, T., Mashimo, M., Moriwaki, Y., Misawa, H., Ono, S., Horiguchi, K., et al. (2017). Expression and function of the cholinergic system in immune cells. *Front. Immunol.* 8:1085. doi: 10.3389/fimmu.2017.01085

Fujita, Y., Kunitachi, S., Iyo, M., and Hashimoto, K. (2012). The antibiotic minocycline prevents methamphetamine-induced rewarding effects in mice. *Pharmacol. Biochem. Behav.* 101, 303–306. doi: 10.1016/j.pbb.2012.01.005

Gajbhiye, S. V., Tripathi, R. K., Petare, A., Potey, A. V., and Shankar, A. (2018). Minocycline in alcohol withdrawal induced anxiety and alcohol relapse in rats. *Curr. Clin. Pharmacol.* 13, 65–72. doi: 10.2174/1574884713666180228110310

Gajbhiye, S. V., Tripathi, R. K., Salve, B., Petare, A., and Potey, A. V. (2017). Evaluation of effect of minocycline on rewarding potential and alcohol relapse in place preference model in mice. *Neurosci. Lett.* 649, 28–33. doi: 10.1016/j.neulet.2017.04.007

Gamble-George, J. C., Baldi, R., Halladay, L., Kocharian, A., Hartley, N., Silva, C., et al. (2016). Cyclooxygenase-2 inhibition reduces stress-induced affective pathology. *eLife* 5:e14137.

Ganguly, P., Honeycutt, J. A., Rowe, J. R., Demaestri, C., and Brenhouse, H. C. (2019). Effects of early life stress on cocaine conditioning and AMPA receptor composition are sex-specific and driven by TNF. *Brain. Behav. Immun.* 78, 41–51. doi: 10.1016/j.bbi.2019.01.006

Garcia-Keller, C., Smiley, C., Monforton, C., Melton, S., Kalivas, P. W., and Gass, J. N. (2020). -Acetylcysteine treatment during acute stress prevents stress-induced augmentation of addictive drug use and relapse. *Addict. Biol.* 25:e12798.

Garland, E. L., Froeliger, B., Zeidan, F., Partin, K., and Howard, M. O. (2013). The downward spiral of chronic pain, prescription opioid misuse, and addiction: cognitive, affective, and neuropsychopharmacologic pathways. *Neurosci. Biobehav. Rev.* 37, 2597–2607. doi: 10.1016/j.neubiorev.2013.08.006

Garveya, L. J., Pavese, N., Politis, M., Ramlackhansingh, A., Brooks, D. J., Taylor-Robinson, S. D., et al. (2014). Increased microglia activation in neurologically asymptomatic HIV-infected patients receiving effective ART. *AIDS* 28, 67–72. doi: 10.1097/01.aids.0000432467.54003.f7

Gobejishvili, L., Barve, S., Joshi-Barve, S., and McClain, C. (2008). Enhanced PDE4B expression augments LPS-inducible TNF expression in ethanol-primed monocytes: relevance to alcoholic liver disease. *Am. J. Physiol. Gastrointest. Liver Physiol.* 295:G718.

Gonçalves, J., Leitão, R. A., Higuera-Matas, A., Assis, M. A., Coria, S. M., Fontes-Ribeiro, C., et al. (2017). Extended-access methamphetamine self-administration elicits neuroinflammatory response along with blood-brain barrier breakdown. *Brain. Behav. Immun.* 62, 306–317. doi: 10.1016/j.bbi.2017.02.017

Gonzalez, P. V., Schiöth, H. B., Lasaga, M., and Scimonelli, T. N. (2009). Memory impairment induced by IL-1β is reversed by α-MSH through central

melanocortin-4 receptors. *Brain. Behav. Immun.* 23, 817–822. doi: 10.1016/j.bbi.2009.03.001

González-Reimers, E., Santolaria-Fernández, F., Martín-González, M. C., Fernández-Rodríguez, C. M., and Quintero-Platt, G. (2014). Alcoholism: a systemic proinflammatory condition. *World J. Gastroenterol.* 20, 14660–14671. doi: 10.3748/wjg.v20.i40.14660

Goshen, I., and Yirmiya, R. (2007). "The role of pro-inflammatory cytokines in memory processes and neural plasticity," in *Psychoneuroimmunology*, Vol. 1, ed. R. Ader (Amsterdam: Elsevier), 337–377. doi: 10.1016/b978-012088576-3/50021-6

Goshen, I., Kreisel, T., Ounallah-Saad, H., Renbaum, P., Zalzstein, Y., Ben-Hur, T., et al. (2007). A dual role for interleukin-1 in hippocampal-dependent memory processes. *Psychoneuroendocrinology* 32, 1106–1115. doi: 10.1016/j.psyneuen.2007.09.004

Gotti, C., Clementi, F., Fornari, A., Gaimarri, A., Guiducci, S., Manfredi, I., et al. (2009). Structural and functional diversity of native brain neuronal nicotinic receptors. *Biochem. Pharmacol.* 78, 703–711. doi: 10.1016/j.bcp.2009.05.024

Gozen, O., Nesil, T., Kanit, L., Koylu, E. O., and Pogun, S. (2016). Nicotinic cholinergic and dopaminergic receptor mRNA expression in male and female rats with high or low preference for nicotine. *Am. J. Drug Alcohol Abuse* 42, 556–566. doi: 10.1080/00952990.2016.1198799

Hagino, Y., Kariura, Y., Manago, Y., Amano, T., Wang, B., Sekiguchi, M., et al. (2004). Heterogeneity and potentiation of AMPA type of glutamate receptors in rat cultured microglia. *Glia* 47, 68–77. doi: 10.1002/glia.20034

Hajhashemi, V., and Khanjani, P. (2014). Analgesic and anti-inflammatory activities of bupropion in animal models. *Res. Pharm. Sci.* 9, 251–257.

Hall, B. J., Slade, S., Wells, C., Rose, J. E., and Levin, E. D. (2015). Bupropion-varenicline interactions and nicotine self-administration behavior in rats. *Pharmacol. Biochem. Behav.* 130, 84–89. doi: 10.1016/j.pbb.2015.01.009

Harada, K., Kamiya, T., and Tsuboi, T. (2016). Gliotransmitter release from astrocytes: functional, developmental, and pathological implications in the brain. *Front. Neurosci.* 9:499. doi: 10.3389/fnins.2015.00499

Hartmann, P., and Tacke, F. (2016). Tiny RNA with great effects: MiR-155 in alcoholic liver disease. *J. Hepatol.* 64, 1214–1216. doi: 10.1016/j.jhep.2016.02.039

Hayes, J., and Koo, J. (2010). Psoriasis: depression, anxiety, smoking, and drinking habits. *Dermatol. Ther.* 23, 174–180. doi: 10.1111/j.1529-8019.2010.01312.x

He, J., and Crews, F. T. (2008). Increased MCP-1 and microglia in various regions of the human alcoholic brain. *Exp. Neurol.* 210, 349–358. doi: 10.1016/j.expneurol.2007.11.017

Hein, A. M., Stasko, M. R., Matousek, S. B., Scott-McKean, J. J., Maier, S. F., Olschowka, J. A., et al. (2010). Sustained hippocampal IL-1β overexpression impairs contextual and spatial memory in transgenic mice. *Brain. Behav. Immun.* 24, 243–253. doi: 10.1016/j.bbi.2009.10.002

Hernández, J. A., López-Sánchez, R. C., and Rendón-Ramírez, A. (2016). Lipids and oxidative stress associated with ethanol-induced neurological damage. *Oxid. Med. Cell. Longev.* 2016:1543809.

Hileman, C. O., and Funderburg, N. T. (2017). Inflammation, immune activation, and antiretroviral therapy in HIV. *Curr. HIV/AIDS Rep.* 14, 93–100. doi: 10.1007/s11904-017-0356-x

Hipólito, L., Wilson-Poe, A., Campos-Jurado, Y., Zhong, E., Gonzalez-Romero, J., Virag, L., et al. (2015). Inflammatory pain promotes increased opioid self-administration: role of dysregulated ventral tegmental area μ opioid receptors. *J. Neurosci.* 35:12217. doi: 10.1523/jneurosci.1053-15.2015

Hodebourg, R., Murray, J. E., Fouyssac, M., Puaud, M., Everitt, B. J., and Belin, D. (2019). Heroin seeking becomes dependent on dorsal striatal dopaminergic mechanisms and can be decreased by N-acetylcysteine. *Eur. J. Neurosci.* 50, 2036–2044. doi: 10.1111/ejn.13894

Hodes, G. E., Kana, V., Menard, C., Merad, M., and Russo, S. J. (2015). Neuroimmune mechanisms of depression. *Nat. Neurosci.* 18, 1386–1393. doi: 10.1038/nn.4113

Hodes, G. E., Ménard, C., and Russo, S. J. (2016). Integrating interleukin-6 into depression diagnosis and treatment. *Neurobiol. Stress* 4, 15–22. doi: 10.1016/j.ynstr.2016.03.003

Hodes, G. E., Pfau, M. L., Leboeuf, M., Golden, S. A., Christoffel, D. J., Bregman, D., et al. (2014). Individual differences in the peripheral immune system promote resilience versus susceptibility to social stress. *Proc. Natl. Acad. Sci. U.S.A.* 111, 16136–16141. doi: 10.1073/pnas.1415191111

Hoefer, M. M., Sanchez, A. B., Maung, R., de Rozieres, C. M., Catalan, I. C., Dowling, C. C., et al. (2015). Combination of methamphetamine and HIV-1 gp120 causes distinct long-term alterations of behavior, gene expression, and injury in the central nervous system. *Exp. Neurol.* 263, 221–234. doi: 10.1016/j.expneurol.2014.09.010

Hofford, R. S., Russo, S. J., and Kiraly, D. D. (2019). Neuroimmune mechanisms of psychostimulant and opioid use disorders. *Eur. J. Neurosci.* 50, 2562–2573. doi: 10.1111/ejn.14143

Hong, S., and Banks, W. A. (2015). Role of the immune system in HIV-associated neuroinflammation and neurocognitive implications. *Brain Behav. Immun.* 45, 1–12. doi: 10.1016/j.bbi.2014.10.008

Hori, H., and Kim, Y. (2019). Inflammation and post-traumatic stress disorder. *Psychiatry Clinical Neurosci.* 73, 143–153.

Hu, W., Lu, T., Chen, A., Huang, Y., Hansen, R., Chandler, L. J., et al. (2011). Inhibition of phosphodiesterase-4 decreases ethanol intake in mice. *Psychopharmacology* 218, 331–339. doi: 10.1007/s00213-011-2290-8

Huhn, A. S., Tompkins, D. A., Campbell, C. M., and Dunn, K. E. (2019). Individuals with chronic pain who misuse prescription opioids report sex-based differences in pain and opioid withdrawal. *Pain Med.* 20, 1942–1947. doi: 10.1093/pm/pny295

Hurd, Y. L., Yoon, M., Manini, A. F., Hernandez, S., Olmedo, R., Ostman, M., et al. (2015). Early phase in the development of Cannabidiol as a treatment for addiction: opioid relapse takes initial center stage. *Neurotherapeutics* 12, 807–815. doi: 10.1007/s13311-015-0373-7

Hutchinson, M. R., Northcutt, A. L., Hiranita, T., Wang, X., Lewis, S. S., Thomas, J., et al. (2012). Opioid activation of toll-like receptor 4 contributes to drug reinforcement. *J. Neurosci.* 32, 11187–11200.

Ibáñez, F., Montesinos, J., Ureña-Peralta, J. R., Guerri, C., and Pascual, M. (2019). TLR4 participates in the transmission of ethanol-induced neuroinflammation via astrocyte-derived extracellular vesicles. *J. Neuroinflamm.* 16:136.

Inoue, K., Shinohara, H., Behar, M., Yumoto, N., Tanaka, G., Hoffmann, A., et al. (2016). Oscillation dynamics underlie functional switching of NF-κB for B-cell activation. *NPJ Syst. Biol. Appl.* 2, 1–9.

Israel, Y., Quintanilla, M. E., Ezquer, F., Morales, P., Santapau, D., Berríos-Cárcamo, P., et al. (2019). Aspirin and N-acetylcysteine co-administration markedly inhibit chronic ethanol intake and block relapse binge drinking: role of neuroinflammation-oxidative stress self-perpetuation. *Addict. Biol* 26:e12853. doi: 10.1111/adb.12853

Jacobsen, J. H. W., Hutchinson, M. R., and Mustafa, S. (2016). Drug addiction: targeting dynamic neuroimmune receptor interactions as a potential therapeutic strategy. *Curr. Opin. Pharmacol.* 26, 131–137. doi: 10.1016/j.coph.2015.10.010

Jafari, S., Khajehpour, S., Razzaghi, E. M., Heidari, K., Soleimani, M., and Ghaeli, P. (2017). Craving and drug reward: a comparison of Celecoxib and ibuprofen in detoxifying opiate addicts. *Iran. J. Psychiatry* 12, 229–235.

Jankowsky, J. L., Derrick, B. E., and Patterson, P. H. (2000). Cytokine responses to LTP induction in the rat hippocampus: a comparison of in vitro and in vivo techniques. *Learn. Mem.* 7, 400–412. doi: 10.1101/lm.32600

Jastrzêbska, J., Frankowska, M., Suder, A., Wydra, K., Nowak, E., Filip, M., et al. (2017). Effects of escitalopram and imipramine on cocaine reinforcement and drug-seeking behaviors in a rat model of depression. *Brain Res.* 1673, 30–41. doi: 10.1016/j.brainres.2017.07.016

Kalra, R., Singh, S. P., Pena-Philippides, J. C., Langley, R. J., Razani-Boroujerdi, S., and Sopori, M. L. (2004). Immunosuppressive and anti-inflammatory effects of nicotine administered by patch in an animal model. *Clin. Diagn. Lab. Immunol.* 11, 563–568. doi: 10.1128/cdli.11.3.563-568.2004

Kalueff, A. V., Olivier, J. D. A., Nonkes, L. J. P., and Homberg, J. R. (2010). Conserved role for the serotonin transporter gene in rat and mouse neurobehavioral endophenotypes. *Neurosci. Biobehav. Rev.* 34, 373–386. doi: 10.1016/j.neubiorev.2009.08.003

Karahanian, E., Quintanilla, M. E., Fernandez, K., and Israel, Y. (2014). Fenofibrate - A lipid-lowering drug - reduces voluntary alcohol drinking in rats. *Alcohol* 48, 665–670. doi: 10.1016/j.alcohol.2014.08.004

Karimi-Haghighi, S., and Haghparast, A. (2018). Cannabidiol inhibits priming-induced reinstatement of methamphetamine in REM sleep deprived rats. *Prog. Neuro Psychopharmacol. Biol. Psychiatry* 82, 307–313. doi: 10.1016/j.pnpbp.2017.08.022

Karimi-Haghighi, S., Dargahi, L., and Haghparast, A. (2020). Cannabidiol modulates the expression of neuroinflammatory factors in stress- and drug-induced reinstatement of methamphetamine in extinguished rats. *Addict. Biol.* 25:e12740.

Karlsson, C., Schank, J. R., Rehman, F., Stojakovic, A., Björk, K., Barbier, E., et al. (2017). Proinflammatory signaling regulates voluntary alcohol intake and stress-induced consumption after exposure to social defeat stress in mice. *Addict. Biol.* 22, 1279–1288. doi: 10.1111/adb.12416

Kashima, D. T., and Grueter, B. A. (2017). Toll-like receptor 4 deficiency alters nucleus accumbens synaptic physiology and drug reward behavior. *Proc. Natl. Acad. Sci. U.S.A.* 114, 8865–8870. doi: 10.1073/pnas.1705974114

Kaur, B., and Prakash, A. (2017). Ceftriaxone attenuates glutamate-mediated neuro-inflammation and restores BDNF in MPTP model of Parkinson's disease in rats. *Pathophysiology* 24, 71–79. doi: 10.1016/j.pathophys.2017.02.001

Kesby, J. P., Heaton, R. K., Young, J. W., Umlauf, A., Woods, S. P., Letendre, S. L., et al. (2015a). Methamphetamine exposure combined with HIV-1 disease or gp120 expression: comparison of learning and executive functions in humans and mice. *Neuropsychopharmacology* 40, 1899–1909. doi: 10.1038/npp.2015.39

Kesby, J. P., Hubbard, D. T., Markou, A., and Semenova, S. (2014). Expression of HIV gp120 protein increases sensitivity to the rewarding properties of methamphetamine in mice. *Addict. Biol.* 19, 593–605. doi: 10.1111/adb.12023

Kesby, J. P., Markou, A., and Semenova, S. (2015b). Cognitive deficits associated with combined HIV gp120 expression and chronic methamphetamine exposure in mice. *Eur. Neuropsychopharmacol.* 25, 141–150. doi: 10.1016/j.euroneuro.2014.07.014

Kesby, J. P., Markou, A., and Semenova, S. (2016). The effects of HIV-1 regulatory TAT protein expression on brain reward function, response to psychostimulants and delay-dependent memory in mice. *Neuropharmacology* 109, 205–215. doi: 10.1016/j.neuropharm.2016.06.011

Kesby, J. P., Najera, J. A., Romoli, B., Fang, Y., Basova, L., Birmingham, A., et al. (2017). HIV-1 TAT protein enhances sensitization to methamphetamine by affecting dopaminergic function. *Brain. Behav. Immun.* 65, 210–221. doi: 10.1016/j.bbi.2017.05.004

Kim, J., Connelly, K. L., Unterwald, E. M., and Rawls, S. M. (2017). Chemokines and cocaine: CXCR4 receptor antagonist AMD3100 attenuates cocaine place preference and locomotor stimulation in rats. *Brain. Behav. Immun.* 62, 30–34. doi: 10.1016/j.bbi.2016.08.015

Knackstedt, L. A., Melendez, R. I., and Kalivas, P. W. (2010). Ceftriaxone restores glutamate homeostasis and prevents relapse to cocaine seeking. *Biol. Psychiatry* 67, 81–84. doi: 10.1016/j.biopsych.2009.07.018

Knapska, E., and Kaczmarek, L. (2015). "Matrix metalloproteinase 9 (MMP-9) in learning and memory," in *Novel Mechanisms of Memory*, eds K. P. Giese, and K. Radwanska (Cham: Springer International Publishing), 161–181. doi: 10.1007/978-3-319-24364-1_9

Knight, J. R., Locke, G. R., Zinsmeister, A. R., Schleck, C. D., and Talley, N. J. (2015). Family history of mental illness or alcohol abuse and the irritable bowel syndrome. *J. Psychosom. Res.* 78, 237–241. doi: 10.1016/j.jpsychores.2014.11.021

Köhler, O., Benros, E. M., Nordentoft, M., Farkouh, M. E., Iyengar, R. L., Mors, O., et al. (2014). Effect of anti-inflammatory treatment on depression, depressive symptoms, and adverse effects a systematic review and meta-analysis of randomized clinical trials. *JAMA Psychiatry* 71, 1381–1391. doi: 10.1001/jamapsychiatry.2014.1611

Koo, J. W., and Duman, R. S. (2009). Interleukin-1 receptor null mutant mice show decreased anxiety-like behavior and enhanced fear memory. *Neurosci. Lett.* 456, 39–43. doi: 10.1016/j.neulet.2009.03.068

Koob, G. F., and Volkow, N. D. (2010). Neurocircuitry of addiction. *Neuropsychopharmacology* 35, 217–238. doi: 10.1038/npp.2009.110

Koob, G. F., and Volkow, N. D. (2016). Neurobiology of addiction: a neurocircuitry analysis. *Lancet Psychiatry* 3, 760–773. doi: 10.1016/s2215-0366(16)00104-8

Krishnadas, R., Nicol, A., Sassarini, J., Puri, N., Burden, A. D., Leman, J., et al. (2016). Circulating tumour necrosis factor is highly correlated with brainstem serotonin transporter availability in humans. *Brain. Behav. Immun.* 51, 29–38. doi: 10.1016/j.bbi.2015.08.005

Kuhn, B. N., Kalivas, P. W., and Bobadilla, A. C. (2019). Understanding addiction using animal models. *Front. Behav. Neurosci.* 13:262. doi: 10.3389/fnbeh.2019.00262

Kumar, S., Rao, P. S. S., Earla, R., and Kumar, A. (2015). Drug-drug interactions between anti-retroviral therapies and drugs of abuse in HIV systems. *Expert Opin. Drug Metab. Toxicol.* 11, 343–355. doi: 10.1517/17425255.2015.996546

Kutlu, M. G., Brady, L. J., Peck, E. G., Hofford, R. S., Yorgason, J. T., Siciliano, C. A., et al. (2018). Granulocyte colony stimulating factor enhances reward learning through potentiation of mesolimbic dopamine system function. *J. Neurosci.* 38, 8845–8859. doi: 10.1523/jneurosci.1116-18.2018

Lacagnina, M. J., Kopec, A. M., Cox, S. S., Hanamsagar, R., Wells, C., Slade, S., et al. (2017). Opioid Self-administration is attenuated by early-life experience and gene therapy for anti-inflammatory IL-10 in the nucleus Accumbens of male rats. *Neuropsychopharmacology* 42, 2128–2140. doi: 10.1038/npp.2017.82

LaCrosse, A. L., Hill, K., and Knackstedt, L. A. (2016). Ceftriaxone attenuates cocaine relapse after abstinence through modulation of nucleus accumbens AMPA subunit expression. *Eur. Neuropsychopharmacol.* 26, 186–194. doi: 10.1016/j.euroneuro.2015.12.022

Lainiola, M., and Linden, A.-M. (2017). Alcohol intake in two different mouse drinking models after recovery from the lipopolysaccharide-induced sickness reaction. *Alcohol* 65, 1–10. doi: 10.1016/j.alcohol.2017.06.002

Lebourgeois, S., González-Marín, M. C., Jeanblanc, J., Naassila, M., and Vilpoux, C. (2018). Effect of N-acetylcysteine on motivation, seeking and relapse to ethanol self-administration. *Addict. Biol.* 23, 643–652. doi: 10.1111/adb.12521

Lee, B., Sur, B., Yeom, M., Shim, I., Lee, H., and Hahm, D. H. (2016). Effects of systemic administration of ibuprofen on stress response in a rat model of post-traumatic stress disorder. *Korean J. Physiol. Pharmacol.* 20, 357–366. doi: 10.4196/kjpp.2016.20.4.357

Lei, J., Jin, L., Zhao, Y., Sui, M. Y., Huang, L., Tan, Y. X., et al. (2011). Sex-related differences in descending norepinephrine and serotonin controls of spinal withdrawal reflex during intramuscular saline induced muscle nociception in rats. *Exp. Neurol.* 228, 206–214. doi: 10.1016/j.expneurol.2011.01.004

Levin, E. D., Petro, A., Rezvani, A. H., Pollard, N., Christopher, N. C., Strauss, M., et al. (2009). Nicotinic α7- or β2-containing receptor knockout: effects on radial-arm maze learning and long-term nicotine consumption in mice. *Behav. Brain Res.* 196, 207–213. doi: 10.1016/j.bbr.2008.08.048

Levin, S. G., and Godukhin, O. V. (2017). Modulating effect of cytokines on mechanisms of synaptic plasticity in the brain. *Biochemistry* 82, 264–274. doi: 10.1134/s000629791703004x

Lewitus, G. M., Konefal, S. C., Greenhalgh, A. D., Pribiag, H., Augereau, K., and Stellwagen, D. (2016). Microglial TNF-α Suppresses Cocaine-Induced Plasticity and Behavioral Sensitization. *Neuron* 90, 483–491. doi: 10.1016/j.neuron.2016.03.030

Lewitus, G. M., Pribiag, H., Duseja, R., St-Hilaire, M., and Stellwagen, D. (2014). An adaptive role of TNFα in the regulation of striatal synapses. *J. Neurosci.* 34, 6146–6155. doi: 10.1523/jneurosci.3481-13.2014

Li, A. J., Katafuchi, T., Oda, S., Hori, T., and Oomura, Y. (1997). Interleukin-6 inhibits long-term potentiation in rat hippocampal slices. *Brain Res.* 748, 30–38. doi: 10.1016/s0006-8993(96)01283-8

Li, Z., You, Y., Griffin, N., Feng, J., and Shan, F. (2018). Low-dose naltrexone (LDN): a promising treatment in immune-related diseases and cancer therapy. *Int. Immunopharmacol.* 61, 178–184. doi: 10.1016/j.intimp.2018.05.020

Lippai, D., Bala, S., Csak, T., Kurt-Jones, E. A., and Szabo, G. (2013). Chronic alcohol-induced microRNA-155 contributes to neuroinflammation in a TLR4-dependent manner in mice. *PLoS One* 8:e70945. doi: 10.1371/journal.pone.0070945

Liston, A., Papadopoulou, A. S., Danso-Abeam, D., and Dooley, J. (2012). MicroRNA-29 in the adaptive immune system: setting the threshold. *Cell. Mol. Life Sci.* 69, 3533–3541. doi: 10.1007/s00018-012-1124-0

Liu, H., Leak, R. K., and Hu, X. (2016). Neurotransmitter receptors on microglia. *Stroke Vasc. Neurol.* 1, 52–58. doi: 10.1136/svn-2016-000012

Liu, J. J., Bin, W. Y., Strawbridge, R., Bao, Y., Chang, S., Shi, L., et al. (2020). Peripheral cytokine levels and response to antidepressant treatment in depression: a systematic review and meta-analysis. *Mol. Psychiatry* 25, 339–350. doi: 10.1038/s41380-019-0474-5

Liu, Q. F., Li, L., Guo, Y. Q., Li, X., Mou, Z. D., Wang, X., et al. (2016). Injection of Toll-like receptor 4 siRNA into the ventrolateral periaqueductal gray attenuates withdrawal syndrome in morphine-dependent rats. *Arch. Ital. Biol.* 154, 133–142. doi: 10.12871/00039829201644

Liu, X., Chang, L., Vigorito, M., Kass, M., Li, H., and Chang, S. L. (2009). Methamphetamine-induced behavioral sensitization is enhanced in the HIV-1 transgenic rat. *J. Neuroimmun. Pharmacol.* 4, 309–316. doi: 10.1007/s11481-009-9160-8

Liu, Y., Zhou, L.-J., Wang, J., Li, D., Ren, W.-J., Peng, J., et al. (2017). TNF-differentially regulates synaptic plasticity in the hippocampus and spinal cord by microglia-dependent mechanisms after peripheral nerve injury. *J. Neurosci.* 37, 871–881. doi: 10.1523/jneurosci.2235-16.2016

Lo Iacono, L., Catale, C., Martini, A., Valzania, A., Viscomi, M. T., Chiurchiù, V., et al. (2018). From traumatic childhood to cocaine abuse: the critical function of the immune system. *Biol. Psychiatry* 84, 905–916. doi: 10.1016/j.biopsych.2018.05.022

Logrip, M. L. (2015). Phosphodiesterase regulation of alcohol drinking in rodents. *Alcohol* 49, 795–802. doi: 10.1016/j.alcohol.2015.03.007

Loscher, C. E., Mills, K. H. G., and Lynch, M. A. (2003). Interleukin-1 receptor antagonist exerts agonist activity in the hippocampus independent of the interleukin-1 type I receptor. *J. Neuroimmunol.* 137, 117–124. doi: 10.1016/s0165-5728(03)00072-9

Lu, Y., Ho, C. S., Liu, X., Chua, A. N., Wang, W., McIntyre, R. S., et al. (2017). Chronic administration of fluoxetine and pro-inflammatory cytokine change in a rat model of depression. *PLoS One* 12:e0186700. doi: 10.1371/journal.pone.0186700

Lykhmus, O., Voytenko, L., Koval, L., Mykhalskiy, S., Kholin, V., Peschana, K., et al. (2015). α7 nicotinic acetylcholine receptor-specific antibody induces inflammation and amyloid β42 accumulation in the mouse brain to impair memory. *PLoS One* 10:e0122706. doi: 10.1371/journal.pone.0122706

Lynch, W. J., Nicholson, K. L., Dance, M. E., Morgan, R. W., and Foley, P. L. (2010). Animal models of substance abuse and addiction: implications for science, animal welfare, and society. *Compar. Med.* 60, 177–188.

MacHado, I., González, P., Schiöth, H. B., Lasaga, M., and Scimonelli, T. N. (2010). α-Melanocyte-stimulating hormone (α-MSH) reverses impairment of memory reconsolidation induced by interleukin-1 beta (IL-1 beta) hippocampal infusions. *Peptides* 31, 2141–2144. doi: 10.1016/j.peptides.2010.07.018

Macnamara, C. L., Holmes, N. M., Westbrook, R. F., and Clemens, K. J. (2016). Varenicline impairs extinction and enhances reinstatement across repeated cycles of nicotine self-administration in rats. *Neuropharmacology* 105, 463–470. doi: 10.1016/j.neuropharm.2016.02.023

Magalhães, P. V., Dean, O. M., Bush, A. I., Copolov, D. L., Malhi, G. S., Kohlmann, K. K., et al. (2011). acetylcysteine for major depressive episodes in bipolar disorder. *Rev. Bras. Psiquiatr.* 33, 374–378. doi: 10.1590/s1516-44462011000400011

Mapplebeck, J. C. S., Dalgarno, R., Tu, Y., Moriarty, O., Beggs, S., Kwok, C. H. T., et al. (2018). Microglial P2X4R-evoked pain hypersensitivity is sexually dimorphic in rats. *Pain* 159, 1752–1763. doi: 10.1097/j.pain.0000000000001265

Marchand, F., Perretti, M., and McMahon, S. B. (2005). Role of the immune system in chronic pain. *Nat. Rev. Neurosci.* 6, 521–532. doi: 10.1038/nrn1700

Markoutsa, E., and Xu, P. (2017). Redox Potential-Sensitive N-Acetyl cysteine-prodrug nanoparticles inhibit the activation of microglia and improve neuronal survival. *Mol. Pharm.* 14, 1591–1600. doi: 10.1021/acs.molpharmaceut.6b01028

Marshall, S. A., Casachahua, J. D., Rinker, J. A., Blose, A. K., Lysle, D. T., and Thiele, T. E. (2016). IL-1 receptor signaling in the basolateral amygdala modulates binge-like ethanol consumption in male C57BL/6J mice. *Brain. Behav. Immun.* 51, 258–267. doi: 10.1016/j.bbi.2015.09.006

Mattson, C. L., Tanz, L. J., Quinn, K., Kariisa, M., Patel, P., and Davis, N. L. (2021). Trends and geographic patterns in drug and synthetic opioid overdose deaths — United States, 2013-2019. *MMWR Morb. Mortal. Wkly. Rep.* 70, 202–207. doi: 10.15585/mmwr.mm7006a4

Maza-Quiroga, R., García-Marchena, N., Romero-Sanchiz, P., Barrios, V., Pedraz, M., Serrano, A., et al. (2017). Evaluation of plasma cytokines in patients with cocaine use disorders in abstinence identifies transforming growth factor alpha (tgfα) as a potential biomarker of consumption and dual diagnosis. *PeerJ* 5:e3926. doi: 10.7717/peerj.3926

McBrien, H., Luo, C., Sanger, N., Zielinski, L., Bhatt, M., Zhu, X. M., et al. (2019). Cannabis use during methadone maintenance treatment for opioid use disorder: a systematic review and meta-analysis. *C. Open* 7, E665–E673.

McCarthy, M. M. (2019). Sex differences in neuroimmunity as an inherent risk factor. *Neuropsychopharmacology* 44, 38–44. doi: 10.1038/s41386-018-0138-1

McFadden, L. M., Hadlock, G. C., Allen, S. C., Vieira-Brock, P. L., Stout, K. A., Ellis, J. D., et al. (2012). Methamphetamine self-administration causes persistent striatal dopaminergic alterations and mitigates the deficits caused by a subsequent methamphetamine exposure. *J. Pharmacol. Exp. Ther.* 340, 295–303. doi: 10.1124/jpet.111.188433

McIntosh, S., Sexton, T., Pattison, L. P., Childers, S. R., and Hemby, S. E. (2015). Increased sensitivity to cocaine self-administration in HIV-1 transgenic rats is associated with changes in striatal dopamine transporter binding. *J. Neuroimmun. Pharmacol.* 10, 493–505. doi: 10.1007/s11481-015-9594-0

McLaurin, K. A., Booze, R. M., and Mactutus, C. F. (2018). Evolution of the HIV-1 transgenic rat: utility in assessing the progression of HIV-1-associated neurocognitive disorders. *J. Neurovirol.* 24, 229–245. doi: 10.1007/s13365-017-0544-x

Menard, C., Pfau, M. L., Hodes, G. E., Kana, V., Wang, V. X., Bouchard, S., et al. (2017). Social stress induces neurovascular pathology promoting depression. *Nat. Neurosci.* 20, 1752–1760. doi: 10.1038/s41593-017-0010-3

Metz, V. E., Jones, J. D., Manubay, J., Sullivan, M. A., Mogali, S., Segoshi, A., et al. (2017). Effects of ibudilast on the subjective, reinforcing, and analgesic effects of oxycodone in recently detoxified adults with opioid dependence. *Neuropsychopharmacology* 42, 1825–1832. doi: 10.1038/npp.2017.70

Miguel-Hidalgo, J. J. (2009). The role of glial cells in drug abuse. *Curr. Drug Abuse Rev.* 2, 76–82. doi: 10.2174/1874473710902010076

Mihalak, K. B., Carroll, F. I., and Luetje, C. W. (2006). Varenicline is a partial agonist at α4β2 and a full agonist at α7 neuronal nicotinic receptors. *Mol. Pharmacol.* 70, 801–805. doi: 10.1124/mol.106.025130

Mizoguchi, H., Yamada, K., Mouri, A., Niwa, M., Mizuno, T., Noda, Y., et al. (2007). Role of matrix metalloproteinase and tissue inhibitor of MMP in methamphetamine-induced behavioral sensitization and reward: implications for dopamine receptor down-regulation and dopamine release. *J. Neurochem.* 102, 1548–1560.

Mogil, J. S. (2012). Sex differences in pain and pain inhibition: multiple explanations of a controversial phenomenon. *Nat. Rev. Neurosci.* 13, 859–866. doi: 10.1038/nrn3360

Monnig, M. A. (2017). Immune activation and neuroinflammation in alcohol use and HIV infection: evidence for shared mechanisms. *Am. J. Drug Alcohol Abuse* 43, 7–23. doi: 10.1080/00952990.2016.1211667

Montesinos, J., Gil, A., and Guerri, C. (2017). Nalmefene prevents alcohol-induced neuroinflammation and alcohol drinking preference in adolescent female mice: role of TLR4. *Alcohol. Clin. Exp. Res.* 41, 1257–1270. doi: 10.1111/acer.13416

Montesinos, J., Pascual, M., Millán-Esteban, D., and Guerri, C. (2018). Binge-like ethanol treatment in adolescence impairs autophagy and hinders synaptic maturation: role of TLR4. *Neurosci. Lett.* 682, 85–91. doi: 10.1016/j.neulet.2018.05.049

Montesinos, J., Pascual, M., Pla, A., Maldonado, C., Rodríguez-Arias, M., Miñarro, J., et al. (2015). TLR4 elimination prevents synaptic and myelin alterations and long-term cognitive dysfunctions in adolescent mice with intermittent ethanol treatment. *Brain. Behav. Immun.* 45, 233–244. doi: 10.1016/j.bbi.2014.11.015

Montesinos, J., Pascual, M., Rodríguez-Arias, M., Miñarro, J., and Guerri, C. (2016). Involvement of TLR4 in the long-term epigenetic changes, rewarding and anxiety effects induced by intermittent ethanol treatment in adolescence. *Brain. Behav. Immun.* 53, 159–171. doi: 10.1016/j.bbi.2015.12.006

Moore, A. H., Wu, M., Shaftel, S. S., Graham, K. A., and O'Banion, M. K. (2009). Sustained expression of interleukin-1β in mouse hippocampus impairs spatial memory. *Neuroscience* 164, 1484–1495. doi: 10.1016/j.neuroscience.2009.08.073

Moran, L. M., Booze, R. M., and Mactutus, C. F. (2014). Modeling deficits in attention, inhibition, and flexibility in HAND. *J. Neuroimmune Pharmacol.* 9, 508–521. doi: 10.1007/s11481-014-9539-z

Moran, M. M., McFarland, K., Melendez, R. I., Kalivas, P. W., and Seamans, J. K. (2005). Cystine/glutamate exchange regulates metabotropic glutamate receptor presynaptic inhibition of excitatory transmission and vulnerability to cocaine seeking. *J. Neurosci.* 25, 6389–6393. doi: 10.1523/jneurosci.1007-05.2005

Moreira, F. P., Medeiros, J. R. C., Lhullier, A. C., Souza, L. D., de, M., Jansen, K., et al. (2016). Cocaine abuse and effects in the serum levels of cytokines IL-6 and IL-10. *Drug Alcohol Depend.* 158, 181–185. doi: 10.1016/j.drugalcdep.2015.11.024

Morris, G., Reiche, E. M. V., Murru, A., Carvalho, A. F., Maes, M., Berk, M., et al. (2018). Multiple immune-inflammatory and oxidative and nitrosative stress pathways explain the frequent presence of depression in multiple sclerosis. *Mol. Neurobiol.* 55, 6282–6306. doi: 10.1007/s12035-017-0843-5

Moussawi, K., Pacchioni, A., Moran, M., Olive, M. F., Gass, J. T., Lavin, A., et al. (2009). N-Acetylcysteine reverses cocaine-induced metaplasticity. *Nat. Neurosci.* 12, 182–189. doi: 10.1038/nn.2250

Muhie, S., Gautam, A., Chakraborty, N., Hoke, A., Meyerhoff, J., Hammamieh, R., et al. (2017). Molecular indicators of stress-induced neuroinflammation in a mouse model simulating features of post-traumatic stress disorder. *Transl. Psychiatry* 7:e1135. doi: 10.1038/tp.2017.91

Mulligan, M. K., Ponomarev, I., Hitzemann, R. J., Belknap, J. K., Tabakoff, B., Harris, R. A., et al. (2006). Toward understanding the genetics of alcohol drinking through transcriptome meta-analysis. *Proc. Natl. Acad. Sci. U.S.A.* 103, 6368–6373. doi: 10.1073/pnas.0510188103

Murray, C. L., Obiang, P., Bannerman, D., and Cunningham, C. (2013). Endogenous IL-1 in cognitive function and anxiety: a study in IL-1RI-/-mice. *PLoS One* 8:e78385. doi: 10.1371/journal.pone.0078385

Murrough, J. W., Iosifescu, D. V., Chang, L. C., Al Jurdi, R. K., Green, C. E., Perez, A. M., et al. (2013). Antidepressant efficacy of ketamine in treatment-resistant major depression: a two-site randomized controlled trial. *Am. J. Psychiatry* 170, 1134–1142. doi: 10.1176/appi.ajp.2013.13030392

Murugan, M., Sivakumar, V., Lu, J., Ling, E. A., and Kaur, C. (2011). Expression of N-methyl D-aspartate receptor subunits in amoeboid microglia mediates production of nitric oxide via NF-κB signaling pathway and oligodendrocyte cell death in hypoxic postnatal rats. *Glia* 59, 521–539. doi: 10.1002/glia.21121

Namba, M. D., Kupchik, Y. M., Spencer, S. M., Garcia Keller, C., Goenaga, J. G., Powell, G. L., et al. (2019). Accumbens neuroimmune signaling and dysregulation of astrocytic glutamate transport underlie conditioned nicotine seeking. *Addict. Biol.* 25:e12797.

Namba, M. D., Tomek, S. E., Olive, M. F., Beckmann, J. S., and Gipson, C. D. (2018). The winding road to relapse: forging a new understanding of cue-induced reinstatement models and their associated neural mechanisms. *Front. Behav. Neurosci.* 12:17. doi: 10.3389/fnbeh.2018.00017

National Institute on Drug Abuse [NIDA] (2012). *Who Is at Risk for HIV Infection and Which Populations Are Most Affected?*. Available online at: https://www.drugabuse.gov/publications/research-reports/hivaids/who-risk-hiv-infection-which-populations-are-most-affected (accessed June 28, 2019).

National Institute on Drug Abuse [NIDA] (2020a). *Common Comorbidities with Substance Use Disorders*. Available online at: https://www.drugabuse.gov/publications/research-reports/common-comorbidities-substance-use-disorders/part-2-co-occurring-substance-use-disorder-physical-comorbidities (accessed April 2, 2020).

National Institute on Drug Abuse [NIDA] (2020b). *How Effective is Drug Addiction Treatment?*. Available online at: https://www.drugabuse.gov/publications/principles-drug-addiction-treatment-research-based-guide-third-edition/frequently-asked-questions/how-effective-drug-addiction-treatment (accessed May 7, 2020).

National Institute on Drug Abuse [NIDA] (2020c). *Opioid Overdose Crisis*. Available online at: https://www.drugabuse.gov/drugs-abuse/opioids/opioid-overdose-crisis#six (accessed April 19, 2020).

National Institute on Drug Abuse [NIDA] (2020d). *Trends & Statistics*. Available online at: https://www.drugabuse.gov/related-topics/trends-statistics (accessed May 7, 2020).

National Institute on Drug Abuse [NIDA] (2021). *Overdose Death Rates*. Available online at: https://www.drugabuse.gov/drug-topics/trends-statistics/overdose-death-rates (accessed March 15, 2021).

Nayak, S. U., Cicalese, S., Tallarida, C., Oliver, C. F., and Rawls, S. M. (2020). Chemokine CCR5 and cocaine interactions in the brain: cocaine enhances mesolimbic CCR5 mRNA levels and produces place preference and locomotor activation that are reduced by a CCR5 antagonist. *Brain. Behav. Immun.* 83, 288–292. doi: 10.1016/j.bbi.2019.09.017

Neupane, S. P. (2016). Neuroimmune interface in the comorbidity between alcohol use disorder and major depression. *Front. Immunol.* 7:655. doi: 10.3389/fimmu.2016.00655

Nichols, J. M., and Kaplan, B. L. F. (2020). Immune responses regulated by Cannabidiol. *Cannabis Cannabinoid Res.* 5, 12–31. doi: 10.1089/can.2018.0073

Nolan, R. A., Reeb, K. L., Rong, Y., Matt, S. M., Johnson, H. S., Runner, K., et al. (2020). Dopamine activates NF-κB and primes the NLRP3 inflammasome in primary human macrophages. *Brain, Behav. Immun. Heal.* 2:100030. doi: 10.1016/j.bbih.2019.100030

Nolan, R., and Gaskill, P. J. (2019). The role of catecholamines in HIV neuropathogenesis. *Brain Res.* 1702, 54–73. doi: 10.1016/j.brainres.2018.04.030

Northcutt, A. L., Hutchinson, M. R., Wang, X., Baratta, M. V., Hiranita, T., Cochran, T. A., et al. (2015). DAT isn't all that: cocaine reward and reinforcement require Toll-like receptor 4 signaling. *Mol. Psychiatry* 20, 1525–1537. doi: 10.1038/mp.2014.177

Northrop, N. A., and Yamamoto, B. K. (2015). Methamphetamine effects on blood-brain barrier structure and function. *Front. Neurosci.* 9:69. doi: 10.3389/fnins.2015.00069

O'Brien, S. M., Scully, P., Fitzgerald, P., Scott, L. V., and Dinan, T. G. (2007). Plasma cytokine profiles in depressed patients who fail to respond to selective serotonin reuptake inhibitor therapy. *J. Psychiatr. Res.* 41, 326–331. doi: 10.1016/j.jpsychires.2006.05.013

O'Sullivan, S. J., Malahias, E., Park, J., Srivastava, A., Reyes, B. A. S., Gorky, J., et al. (2019). Single-Cell glia and neuron gene expression in the central amygdala in opioid withdrawal suggests inflammation with correlated gut Dysbiosis. *Front. Neurosci.* 13:665. doi: 10.3389/fnins.2019.00665

Ochoa-Aguilar, A., Ventura-Martinez, R., Sotomayor-Sobrino, M. A., Jaimez, R., Coffeen, U., Jiménez-González, A., et al. (2018). Ceftriaxone and clavulanic acid induce antiallodynia and anti-inflammatory effects in rats using the carrageenan model. *J. Pain Res.* 11, 977–985. doi: 10.2147/jpr.s154661

Olfson, M., Wall, M. M., Liu, S.-M., and Blanco, C. (2018). Cannabis use and risk of prescription opioid use disorder in the United States. *Am. J. Psychiatry* 175, 47–53. doi: 10.1176/appi.ajp.2017.17040413

Oliver, C. F., Simmons, S. J., Nayak, S. U., Smith, G. R., Reitz, A. B., and Rawls, S. M. (2018). Chemokines and 'bath salts': CXCR4 receptor antagonist reduces rewarding and locomotor-stimulant effects of the designer cathinone MDPV in rats. *Drug Alcohol Depend.* 186, 75–79. doi: 10.1016/j.drugalcdep.2018.01.013

Orio, L. (2020). The multifaceted potential of the lipid transmitter oleoylethanolamide to treat alcohol-induced neuroinflammation and alcohol use disorders. *Neural Regen. Res.* 15, 71–72. doi: 10.4103/1673-5374.264457

Orio, L., Alen, F., Pavón, F. J., Serrano, A., and García-Bueno, B. (2019). Oleoylethanolamide, neuroinflammation, and alcohol abuse. *Front. Mol. Neurosci.* 11:490. doi: 10.3389/fnmol.2018.00490

Osborne, B. F., Turano, A., and Schwarz, J. M. (2018). Sex differences in the neuroimmune system. *Curr. Opin. Behav. Sci.* 23, 118–123. doi: 10.1016/j.cobeha.2018.05.007

Packiasabapathy, S., and Sadhasivam, S. (2018). Gender, genetics, and analgesia: understanding the differences in response to pain relief. *J. Pain Res.* 11, 2729–2739. doi: 10.2147/jpr.s94650

Pandey, S. C. (2004). The gene transcription factor cyclic AMP-responsive element binding protein: role in positive and negative affective states of alcohol addiction. *Pharmacol. Therap.* 104, 47–58. doi: 10.1016/j.pharmthera.2004.08.002

Paris, J. J., Carey, A. N., Shay, C. F., Gomes, S. M., He, J. J., and McLaughlin, J. P. (2014). Effects of conditional central expression of HIV-1 tat protein to potentiate cocaine-mediated psychostimulation and reward among male mice. *Neuropsychopharmacology* 39, 380–388. doi: 10.1038/npp.2013.201

Paris, J. J., Fenwick, J., and McLaughlin, J. P. (2014). Estrous cycle and HIV-1 Tat protein influence cocaine-conditioned place preference and induced locomotion of female mice. *Curr. HIV Res.* 12, 388–396. doi: 10.2174/1570162x13666150121105221

Passos, I. C., Vasconcelos-Moreno, M. P., Costa, L. G., Kunz, M., Brietzke, E., Quevedo, J., et al. (2015). Inflammatory markers in post-traumatic stress disorder: A systematic review, meta-analysis, and meta-regression. *Lancet Psychiatry* 2, 1002–1012. doi: 10.1016/s2215-0366(15)00309-0

Patel, H., McIntire, J., Ryan, S., Dunah, A., and Loring, R. (2017). Anti-inflammatory effects of astroglial α7 nicotinic acetylcholine receptors are mediated by inhibition of the NF-κB pathway and activation of the Nrf2 pathway. *J. Neuroinflamm.* 14, 192.

Patten, D. K., Schultz, B. G., and Berlau, D. J. (2018). The safety and efficacy of low-dose naltrexone in the management of chronic pain and inflammation in multiple sclerosis, fibromyalgia, crohn's disease, and other chronic pain disorders. *Pharmacother. J. Hum. Pharmacol. Drug Ther.* 38, 382–389. doi: 10.1002/phar.2086

Paydary, K., Mahin Torabi, S., SeyedAlinaghi, S., Noori, M., Noroozi, A., Ameri, S., et al. (2016). Impulsivity, sensation seeking, and risk-taking behaviors among

hiv-positive and HIV-negative heroin dependent persons. *AIDS Res. Treat.* 2016, 1–8. doi: 10.1155/2016/5323256

Pedraz, M., Araos, P., García-Marchena, N., Serrano, A., Romero-Sanchiz, P., Suárez, J., et al. (2015). Sex differences in psychiatric comorbidity and plasma biomarkers for cocaine addiction in abstinent cocaine-addicted subjects in outpatient settings. *Front. Psychiatry* 6:17. doi: 10.3389/fpsyt.2015.00017

Perea, G., Sur, M., and Araque, A. (2014). Neuron-glia networks: integral gear of brain function. *Front. Cell. Neurosci.* 8:378. doi: 10.3389/fncel.2014.00378

Pianca, T. G., Rosa, R. L., Ceresér, K. M. M., de Aguiar, B. W., de Abrahão, R. C., Lazzari, P. M., et al. (2017). Differences in biomarkers of crack-cocaine adolescent users before/after abstinence. *Drug Alcohol Depend.* 177, 207–213. doi: 10.1016/j.drugalcdep.2017.03.043

Pickens, C. L., Airavaara, M., Theberge, F., Fanous, S., Hope, B. T., and Shaham, Y. (2011). Neurobiology of the incubation of drug craving. *Trends Neurosci.* 34, 411–420. doi: 10.1016/j.tins.2011.06.001

Plein, L. M., and Rittner, H. L. (2018). Opioids and the immune system - friend or foe. *Br. J. Pharmacol.* 175, 2717–2725. doi: 10.1111/bph.13750

Porasuphatana, S., Weaver, J., and Rosen, G. M. (2006). Inducible nitric oxide synthase catalyzes ethanol oxidation to α-hydroxyethyl radical and acetaldehyde. *Toxicology* 223, 167–174. doi: 10.1016/j.tox.2006.02.022

Posillico, C. K., Terasaki, L. S., Bilbo, S. D., and Schwarz, J. M. (2015). Examination of sex and minocycline treatment on acute morphine-induced analgesia and inflammatory gene expression along the pain pathway in Sprague-Dawley rats. *Biol. Sex Differ.* 6, 1–12.

Powell, G. L., Leyrer-Jackson, J. M., Goenaga, J., Namba, M. D., Piña, J., Spencer, S., et al. (2019). Chronic treatment with N-acetylcysteine decreases extinction responding and reduces cue-induced nicotine-seeking. *Physiol. Rep.* 7:e13958. doi: 10.14814/phy2.13958

Prakash, M. D., Tangalakis, K., Antonipillai, J., Stojanovska, L., Nurgali, K., and Apostolopoulos, V. (2017). Methamphetamine: effects on the brain, gut and immune system. *Pharmacol. Res.* 120, 60–67. doi: 10.1016/j.phrs.2017.03.009

Qin, L., and Crews, F. T. (2012). NADPH oxidase and reactive oxygen species contribute to alcohol-induced microglial activation and neurodegeneration. *J. Neuroinflamm.* 9:5.

Qin, L., He, J., Hanes, R. N., Pluzarev, O., Hong, J. S., and Crews, F. T. (2008). Increased systemic and brain cytokine production and neuroinflammation by endotoxin following ethanol treatment. *J. Neuroinflamm.* 5:10. doi: 10.1186/1742-2094-5-10

Qin, Z., Wang, P. Y., Su, D. F., and Liu, X. (2016). miRNA-124 in immune system and immune disorders. *Front. Immunol.* 7:406. doi: 10.3389/fimmu.2016.00406

Qrunfleh, A. M., Alazizi, A., and Sari, Y. (2013). Ceftriaxone, a beta-lactam antibiotic, attenuates relapse-like ethanol-drinking behavior in alcohol-preferring rats. *J. Psychopharmacol.* 27, 541–549. doi: 10.1177/0269881113482529

Quintanilla, M. E., Morales, P., Ezquer, F., Ezquer, M., Herrera-Marschitz, M., and Israel, Y. (2021). Administration of N-acetylcysteine Plus acetylsalicylic acid markedly inhibits nicotine reinstatement following chronic oral nicotine intake in female rats. *Front. Behav. Neurosci.* 14:617418.

Raison, C. L., Rutherford, R. E., Woolwine, B. J., Shuo, C., Schettler, P., Drake, D. F., et al. (2013). randomized controlled trial of the tumor necrosis factor antagonist infliximab for treatment-resistant depression: the role of baseline inflammatory biomarkers. *Arch. Gen. Psychiatry* 70, 31–41. doi: 10.1001/2013.jamapsychiatry.4

Reissner, K. J., Gipson, C. D., Tran, P. K., Knackstedt, L. A., Scofield, M. D., and Kalivas, P. W. (2015). Glutamate transporter GLT-1 mediates N-acetylcysteine inhibition of cocaine reinstatement. *Addict. Biol.* 20, 316–323. doi: 10.1111/adb.12127

Rivera, P. D., Hanamsagar, R., Kan, M. J., Tran, P. K., Stewart, D., Jo, Y. C., et al. (2019). Removal of microglial-specific MyD88 signaling alters dentate gyrus doublecortin and enhances opioid addiction-like behaviors. *Brain. Behav. Immun.* 76, 104–115. doi: 10.1016/j.bbi.2018.11.010

Rodríguez-Arias, M., Montagud-Romero, S., Rubio-Araiz, A., Aguilar, M. A., Martín-García, E., Cabrera, R., et al. (2017). Effects of repeated social defeat on adolescent mice on cocaine-induced CPP and self-administration in adulthood: integrity of the blood-brain barrier. *Addict. Biol.* 22, 129–141. doi: 10.1111/adb.12301

Roederer, M., Ela, S. W., Staal, F. J. T., Herzenberg, L. A., and Herzenberg, L. A. (1992). . *AIDS Res. Hum. Retroviruses* 8, 209–217.

Romero-Sandoval, E. A., Kolano, A. L., and Alvarado-Vázquez, P. A. (2017). Cannabis and cannabinoids for chronic pain. *Curr. Rheumatol. Rep.* 19, 1–10. doi: 10.1159/000489029

Rosen, S. F., Ham, B., Haichin, M., Walters, I. C., Tohyama, S., Sotocinal, S. G., et al. (2019). Increased pain sensitivity and decreased opioid analgesia in T-cell-deficient mice and implications for sex differences. *Pain* 160, 358–366. doi: 10.1097/j.pain.0000000000001420

Rosen, S., Ham, B., and Mogil, J. S. (2017). Sex differences in neuroimmunity and pain. *J. Neurosci. Res.* 95, 500–508. doi: 10.1002/jnr.23831

Ross, F. M., Allan, S. M., Rothwell, N. J., and Verkhratsky, A. (2003). A dual role for interleukin-1 in LTP in mouse hippocampal slices. *J. Neuroimmunol.* 144, 61–67. doi: 10.1016/j.jneuroim.2003.08.030

Rubin, L. H., Sacktor, N., Creighton, J., Du, Y., Endres, C. J., Pomper, M. G., et al. (2018). Microglial activation is inversely associated with cognition in individuals living with HIV on effective antiretroviral therapy. *AIDS* 32, 1661–1667. doi: 10.1097/qad.0000000000001858

Sahu, G., Farley, K., El-Hage, N., Aiamkitsumrit, B., Fassnacht, R., Kashanchi, F., et al. (2015). Cocaine promotes both initiation and elongation phase of HIV-1 transcription by activating NF-κB and MSK1 and inducing selective epigenetic modifications at HIV-1 LTR. *Virology* 483, 185–202. doi: 10.1016/j.virol.2015.03.036

Saito, T., Lee, J. M., Hoffman, P. L., and Tabakoff, B. (1987). Effects of chronic ethanol treatment on the β-adrenergic receptor-coupled adenylate cyclase system of mouse cerebral cortex. *J. Neurochem.* 48, 1817–1822. doi: 10.1111/j.1471-4159.1987.tb05741.x

Samikkannu, T., Ranjith, D., Rao, K. V. K., Atluri, V. S. R., Pimentel, E., El-Hage, N., et al. (2015). HIV-1 gp120 and morphine induced oxidative stress: role in cell cycle regulation. *Front. Microbiol.* 6:614. doi: 10.3389/fmicb.2015.00614

Sanchez-Alavez, M., Nguyen, W., Mori, S., Wills, D. N., Otero, D., Ehlers, C. L., et al. (2019). Time course of microglia activation and brain and blood cytokine/chemokine levels following chronic ethanol exposure and protracted withdrawal in rats. *Alcohol* 76, 37–45. doi: 10.1016/j.alcohol.2018.07.005

Saravia, R., Ten-Blanco, M., Grande, M. T., Maldonado, R., and Berrendero, F. (2019). Anti-inflammatory agents for smoking cessation? Focus on cognitive deficits associated with nicotine withdrawal in male mice. *Brain. Behav. Immun.* 75, 228–239. doi: 10.1016/j.bbi.2018.11.003

Schneider, H., Pitossi, F., Balschun, D., Wagner, A., Del Rey, A., and Besedovsky, H. O. (1998). A neuromodulatory role of interleukin-1β in the hippocampus. *Proc. Natl. Acad. Sci. U.S.A.* 95, 7778–7783. doi: 10.1073/pnas.95.13.7778

Schneider, R., Bandiera, S., Souza, D. G., Bellaver, B., Caletti, G., Quincozes-Santos, A., et al. (2017). acetylcysteine prevents alcohol related neuroinflammation in rats. *Neurochem. Res.* 42, 2135–2141. doi: 10.1007/s11064-017-2218-8

Scholl, L., Seth, P., Kariisa, M., Wilson, N., and Baldwin, G. (2018). Drug and opioid-involved overdose deaths - United States, 2013-2017. *MMWR Morb. Mortal. Wkly. Rep.* 67, 1419–1427.

Schwendt, M., Shallcross, J., Hadad, N. A., Namba, M. D., Hiller, H., Wu, L., et al. (2018). novel rat model of comorbid PTSD and addiction reveals intersections between stress susceptibility and enhanced cocaine seeking with a role for mGlu5 receptors. *Transl. Psychiatry* 8:209.

Scofield, M. D., Li, H., Siemsen, B. M., Healey, K. L., Tran, P. K., Woronoff, N., et al. (2016). Cocaine Self-administration and extinction leads to reduced glial fibrillary acidic protein expression and morphometric features of astrocytes in the nucleus accumbens core. *Biol. Psychiatry* 80, 207–215. doi: 10.1016/j.biopsych.2015.12.022

Sekine, Y., Minabe, Y., Ouchi, Y., Takei, N., Iyo, M., Nakamura, K., et al. (2003). Association of dopamine transporter loss in the orbitofrontal and dorsolateral prefrontal cortices with methamphetamine-related psychiatric symptoms. *Am. J. Psychiatry* 160, 1699–1701. doi: 10.1176/appi.ajp.160.9.1699

Serdarevic, M., Striley, C. W., and Cottler, L. B. (2017). Sex differences in prescription opioid use. *Curr. Opin. Psychiatry* 30, 238–246. doi: 10.1097/yco.0000000000000337

Shah, A., Kumar, S., Simon, S. D., Singh, D. P., and Kumar, A. (2013). HIV gp120- and methamphetamine-mediated oxidative stress induces astrocyte apoptosis via cytochrome P450 2E1. *Cell Death Dis.* 4, e850–e850.

Shytle, R. D., Mori, T., Townsend, K., Vendrame, M., Sun, N., Zeng, J., et al. (2004). Cholinergic modulation of microglial activation by α7 nicotinic receptors. *J. Neurochem.* 89, 337–343. doi: 10.1046/j.1471-4159.2004.02347.x

Siemsen, B. M., Landin, J. D., McFaddin, J. A., Hooker, K. N., Chandler, L. J., and Scofield, M. D. (2020). Chronic intermittent ethanol and lipopolysaccharide exposure differentially alter Iba1-derived microglia morphology in the prelimbic cortex and nucleus accumbens core of male Long-Evans rats. *J. Neurosci. Res.* doi: 10.1002/jnr.24683 [Epub ahead of print].

Singh, R. K., Chang, H. W., Yan, D., Lee, K. M., Ucmak, D., Wong, K., et al. (2017). Influence of diet on the gut microbiome and implications for human health. *J. Transla. Med.* 15, 1–17. doi: 10.1016/b978-0-12-811440-7.00001-6

Smith, A. C. W., Scofield, M. D., and Kalivas, P. W. (2015). The tetrapartite synapse: extracellular matrix remodeling contributes to corticoaccumbens plasticity underlying drug addiction. *Brain Res.* 1628, 29–39. doi: 10.1016/j.brainres.2015.03.027

Smith, R. S. (1991). The macrophage theory of depression. *Med. Hypotheses* 35, 298–306. doi: 10.1016/0306-9877(91)90272-z

Smolen, J. S., Weinblatt, M. E., Sheng, S., Zhuang, Y., and Hsu, B. (2014). Sirukumab, a human anti-interleukin-6 monoclonal antibody: a randomised, 2-part (proof-of-concept and dose-finding), phase II study in patients with active rheumatoid arthritis despite methotrexate therapy. *Ann. Rheum. Dis.* 73, 1616–1625. doi: 10.1136/annrheumdis-2013-205137

Squeglia, L. M., Baker, N. L., McClure, E. A., Tomko, R. L., Adisetiyo, V., and Gray, K. M. (2016). Alcohol use during a trial of N-acetylcysteine for adolescent marijuana cessation. *Addict. Behav.* 63, 172–177. doi: 10.1016/j.addbeh.2016.08.001

Squeglia, L. M., Tomko, R. L., Baker, N. L., McClure, E. A., Book, G. A., and Gray, K. M. (2018). The effect of N-acetylcysteine on alcohol use during a cannabis cessation trial. *Drug Alcohol Depend.* 185, 17–22. doi: 10.1016/j.drugalcdep.2017.12.005

Steele, A. D., Szabo, I., Bednar, F., and Rogers, T. J. (2002). Interactions between opioid and chemokine receptors: heterologous desensitization. *Cytokine Growth Fact. Rev.* 13, 209–222. doi: 10.1016/s1359-6101(02)00007-2

Stein, M. B., Chen, C. Y., Ursano, R. J., Cai, T., Gelernter, J., Heeringa, S. G., et al. (2016). Genome-wide association studies of posttraumatic stress disorder in 2 cohorts of US army soldiers. *JAMA Psychiatry* 73, 695–704. doi: 10.1001/jamapsychiatry.2016.0350

Stellwagen, D., Beattie, E. C., Seo, J. Y., and Malenka, R. C. (2005). Differential regulation of AMPA receptor and GABA receptor trafficking by tumor necrosis factor-α. *J. Neurosci.* 25, 3219–3228. doi: 10.1523/jneurosci.4486-04.2005

Stewart, A. M., Roy, S., Wong, K., Gaikwad, S., Chung, K. M., and Kalueff, A. V. (2015). Cytokine and endocrine parameters in mouse chronic social defeat: implications for translational 'cross-domain' modeling of stress-related brain disorders. *Behav. Brain Res.* 276, 84–91. doi: 10.1016/j.bbr.2014.08.037

Su, F., Yi, H., Xu, L., and Zhang, Z. (2015). Fluoxetine and S-citalopram inhibit M1 activation and promote M2 activation of microglia in vitro. *Neuroscience* 294, 60–68. doi: 10.1016/j.neuroscience.2015.02.028

Substance Abuse and Mental Health Services Administration (2019). Key substance use and mental health indicators in the United States: Results from the 2018 National Survey on Drug Use and Health (HHS Publication No. PEP19-5068, NSDUH Series H-54). Rockville, MD: Center for Behavioral Health Statistics and Quality, Substance Abuse and Mental Health Services Administration. Available online at: https://www.samhsa.gov/data/

Sun, A. Y., and Sun, G. Y. (2001). Ethanol and oxidative mechanisms in the brain. *J. Biomed. Sci.* 8, 37–43. doi: 10.1007/bf02255969

Swan, G. E., and Lessov-Schlaggar, C. N. (2007). The effects of tobacco smoke and nicotine on cognition and the brain. *Neuropsychol. Rev.* 17, 259–273. doi: 10.1007/s11065-007-9035-9

Swendsen, J., Conway, K. P., Degenhardt, L., Glantz, M., Jin, R., Merikangas, K. R., et al. (2010). Mental disorders as risk factors for substance use, abuse and dependence: results from the 10-year follow-up of the National Comorbidity Survey. *Addiction* 105, 1117–1128. doi: 10.1111/j.1360-0443.2010.02902.x

Tajuddin, N., Moon, K. H., Marshall, S. A., Nixon, K., Neafsey, E. J., Kim, H. Y., et al. (2014). Neuroinflammation and neurodegeneration in adult rat brain from binge ethanol exposure: abrogation by docosahexaenoic acid. *PLoS One* 9:e101223. doi: 10.1371/journal.pone.0101223

Tan, S., Wang, Y., Chen, K., Long, Z., and Zou, J. (2017). Ketamine alleviates depressive-like behaviors via down-regulating inflammatory cytokines induced by chronic restraint stress in mice. *Biol. Pharm. Bull.* 40, 1260–1267. doi: 10.1248/bpb.b17-00131

Tancredi, V., D'Antuono, M., Cafè, C., Giovedì, S., Buè, M. C., D'Arcangelo, G., et al. (2002). The inhibitory effects of interleukin-6 on synaptic plasticity in the rat hippocampus are associated with an inhibition of mitogen-activated protein kinase ERK. *J. Neurochem.* 75, 634–643. doi: 10.1046/j.1471-4159.2000.0750634.x

Tawfik, D. I., Osman, A. S., Tolba, H. M., Khattab, A., Abdel-Salam, L. O., and Kamel, M. M. (2016). Evaluation of therapeutic effect of low dose naltrexone in experimentally-induced Crohn's disease in rats. *Neuropeptides* 59, 39–45. doi: 10.1016/j.npep.2016.06.003

Temburni, M. K., and Jacob, M. H. (2001). New functions for glia in the brain. *Proc. Natl. Acad. Sci. U.S.A.* 98, 3631–3632. doi: 10.1073/pnas.081073198

Thompson, S. J., Pitcher, M. H., Stone, L. S., Tarum, F., Niu, G., Chen, X., et al. (2018). Chronic neuropathic pain reduces opioid receptor availability with associated anhedonia in rat. *Pain* 159, 1856–1866. doi: 10.1097/j.pain.0000000000001282

Thomsen, M. S., and Mikkelsen, J. D. (2012). The α7 nicotinic acetylcholine receptor ligands methyllycaconitine, NS6740 and GTS-21 reduce lipopolysaccharide-induced TNF-α release from microglia. *J. Neuroimmunol.* 251, 65–72. doi: 10.1016/j.jneuroim.2012.07.006

Tomko, R. L., Jones, J. L., Gilmore, A. K., Brady, K. T., Back, S. E., and Gray, K. M. (2018). N-acetylcysteine: a potential treatment for substance use disorders. *Curr. Psychiatr.* 17, 30–55.

Totsch, S. K., and Sorge, R. E. (2017). Immune system involvement in specific pain conditions. *Mol. Pain* 13:1744806917724559.

Tripathi, A., Thangaraj, A., Chivero, E. T., Periyasamy, P., Burkovetskaya, M. E., Niu, F., et al. (2020). N-Acetylcysteine reverses antiretroviral-mediated microglial activation by attenuating autophagy-lysosomal dysfunction. *Front. Neurol.* 11:840. doi: 10.3389/fneur.2020.00840

Tuglu, C., Kara, S. H., Caliyurt, O., Vardar, E., and Abay, E. (2003). Increased serum tumor necrosis factor-alpha levels and treatment response in major depressive disorder. *Psychopharmacology* 170, 429–433. doi: 10.1007/s00213-003-1566-z

Tyagi, M., Weber, J., Bukrinsky, M., and Simon, G. L. (2016). The effects of cocaine on HIV transcription. *J. Neurovirol.* 22, 261–274. doi: 10.1007/s13365-015-0398-z

UNAIDS (2019). *Global HIV & AIDS Statistics — 2019 Fact Sheet*. Available online at: https://www.unaids.org/en/resources/fact-sheet (accessed April 8, 2020).

Vallés, S. L., Blanco, A. M., Pascual, M., and Guerri, C. (2006). Chronic ethanol treatment enhances inflammatory mediators and cell death in the brain and in astrocytes. *Brain Pathol.* 14, 365–371. doi: 10.1111/j.1750-3639.2004.tb00079.x

Vera, J. H., Guo, Q., Cole, J. H., Boasso, A., Greathead, L., Kelleher, P., et al. (2016). Neuroinflammation in treated HIV-positive individuals: a TSPO PET STUDY. *Neurology* 86, 1425–1432. doi: 10.1212/wnl.0000000000002485

Vereker, E., O'Donnell, E., and Lynch, M. A. (2000). The inhibitory effect of interleukin-1β on long-term potentiation is coupled with increased activity of stress-activated protein kinases. *J. Neurosci.* 20, 6811–6819. doi: 10.1523/jneurosci.20-18-06811.2000

Vigorito, M., Connaghan, K. P., and Chang, S. L. (2015). The HIV-1 transgenic rat model of neuroHIV. *Brain. Behav. Immun.* 48, 336–349. doi: 10.1016/j.bbi.2015.02.020

Volkow, N. D., Chang, L., Wang, G. J., Fowler, J. S., Franceschi, D., Sedler, M., et al. (2001a). Loss of dopamine transporters in methamphetamine abusers recovers with protracted abstinence. *J. Neurosci.* 21, 9414–9418. doi: 10.1523/jneurosci.21-23-09414.2001

Volkow, N. D., Chang, L., Wang, G. J., Fowler, J. S., Leonido-Yee, M., Franceschi, D., et al. (2001b). Association of dopamine transporter reduction with psychomotor impairment in methamphetamine abusers. *Am. J. Psychiatry* 158, 377–382. doi: 10.1176/appi.ajp.158.3.377

Vowles, K. E., McEntee, M. L., Julnes, P. S., Frohe, T., Ney, J. P., and Van Der Goes, D. N. (2015). Rates of opioid misuse, abuse, and addiction in chronic pain: a systematic review and data synthesis. *Pain* 156, 569–576. doi: 10.1097/01.j.pain.0000460357.01998.f1

Wang, B., Chen, T., Xue, L., Wang, J., Jia, Y., Li, G., et al. (2019). Methamphetamine exacerbates neuroinflammatory response to lipopolysaccharide by activating dopamine D1-like receptors. *Int. Immunopharmacol.* 73, 1–9. doi: 10.1016/j.intimp.2019.04.053

Wang, M., Duan, F., Wu, J., Min, Q., Huang, Q., Luo, M., et al. (2018). Effect of cyclooxygenase-2 inhibition on the development of post-traumatic stress disorder in rats. *Mol. Med. Rep.* 17, 4925–4932.

Wang, S. C., Lin, C. C., Chen, C. C., Tzeng, N. S., and Liu, Y. P. (2018). Effects of oxytocin on fear memory and neuroinflammation in a rodent model of posttraumatic stress disorder. *Int. J. Mol. Sci.* 19:3848. doi: 10.3390/ijms19123848

Wang, X., Loram, L. C., Ramos, K., De Jesus, A. J., Thomas, J., Cheng, K., et al. (2012). Morphine activates neuroinflammation in a manner parallel to endotoxin. *Proc. Natl. Acad. Sci. U.S.A.* 109, 6325–6330. doi: 10.1073/pnas.1200130109

Wang, X., Northcutt, A. L., Cochran, T. A., Zhang, X., Fabisiak, T. J., Haas, M. E., et al. (2019). Methamphetamine activates toll-like receptor 4 to induce central immune signaling within the ventral tegmental area and contributes to extracellular dopamine increase in the nucleus accumbens shell. *ACS Chem. Neurosci.* 10, 3622–3634. doi: 10.1021/acschemneuro.9b00225

Wayman, W. N., Chen, L., Hu, X. T., and Napier, T. C. (2016). HIV-1 transgenic rat prefrontal cortex hyper-excitability is enhanced by cocaine self-administration. *Neuropsychopharmacology* 41, 1965–1973. doi: 10.1038/npp.2015.366

Wei, J., Pan, X., Pei, Z., Wang, W., Qiu, W., Shi, Z., et al. (2012). The beta-lactam antibiotic, ceftriaxone, provides neuroprotective potential via anti-excitotoxicity and anti-inflammation response in a rat model of traumatic brain injury. *J. Trauma Acute Care Surg.* 73, 654–660. doi: 10.1097/ta.0b013e31825133c0

Wei, P., Liu, Q., Li, D., Zheng, Q., Zhou, J., and Li, J. (2015). Acute nicotine treatment attenuates lipopolysaccharide-induced cognitive dysfunction by increasing BDNF expression and inhibiting neuroinflammation in the rat hippocampus. *Neurosci. Lett.* 604, 161–166. doi: 10.1016/j.neulet.2015.08.008

Wen, R. T., Zhang, F. F., and Zhang, H. T. (2018). Cyclic nucleotide phosphodiesterases: potential therapeutic targets for alcohol use disorder. *Psychopharmacology* 235, 1793–1805. doi: 10.1007/s00213-018-4895-7

Wen, R. T., Zhang, M., Qin, W. J., Liu, Q., Wang, W. P., Lawrence, A. J., et al. (2012). The phosphodiesterase-4 (PDE4) inhibitor rolipram decreases ethanol seeking and consumption in alcohol-preferring fawn-hooded rats. *Alcohol. Clin. Exp. Res.* 36, 2157–2167. doi: 10.1111/j.1530-0277.2012.01845.x

Werry, E. L., Bright, F. M., Piguet, O., Ittner, L. M., Halliday, G. M., Hodges, J. R., et al. (2019). Recent developments in TSPO PET imaging as a biomarker of neuroinflammation in neurodegenerative disorders. *Intern. J. Mol. Sci.* 20:3161. doi: 10.3390/ijms20133161

Wiese, B., and Wilson-Poe, A. R. (2018). Emerging evidence for Cannabis'. Role in Opioid Use Disorder. *Cannabis Cannabinoid Res.* 3, 179–189. doi: 10.1089/can.2018.0022

Wilson, J. M., Kalasinsky, K. S., Levey, A. I., Bergeron, C., Reiber, G., Anthony, R. M., et al. (1996). Striatal dopamine nerve terminal markers in human, chronic methamphetamine users. *Nat. Med.* 2, 699–703. doi: 10.1038/nm0696-699

Wilson, M., Gogulski, H. Y., Cuttler, C., Bigand, T. L., Oluwoye, O., Barbosa-Leiker, C., et al. (2018). Cannabis use moderates the relationship between pain and negative affect in adults with opioid use disorder. *Addict. Behav.* 77, 225–231. doi: 10.1016/j.addbeh.2017.10.012

Wohleb, E. S., Franklin, T., Iwata, M., and Duman, R. S. (2016). Integrating neuroimmune systems in the neurobiology of depression. *Nat. Rev. Neurosci.* 17, 497–511. doi: 10.1038/nrn.2016.69

Yamashita, T., Yamamoto, S., Zhang, J., Kometani, M., Tomiyama, D., Kohno, K., et al. (2016). Duloxetine inhibits microglial P2X4 receptor function and alleviates neuropathic pain after peripheral nerve injury. *PLoS One* 11:e0165189. doi: 10.1371/journal.pone.0165189

Yan, T., Zhao, Y., and Zhang, X. (2016). Acetaldehyde induces Cytotoxicity of SH-SY5Y cells via inhibition of Akt activation and induction of oxidative stress. *Oxid. Med. Cell. Longev.* 2016:4512309.

Yang, X., Diehl, A. M., and Wand, G. S. (1996). Ethanol exposure alters the phosphorylation of cyclic AMP responsive element binding protein and cyclic AMP responsive element binding activity in rat cerebellum. *J. Pharmacol. Exp. Ther.* 278, 338–346.

Yang, X., Horn, K., Baraban, J. M., and Wand, G. S. (1998). Chronic ethanol administration decreases phosphorylation of cyclic AMP response element-binding protein in granule cells of rat cerebellum. *J. Neurochem.* 70, 224–232. doi: 10.1046/j.1471-4159.1998.70010224.x

Ye, G., Yin, G. Z., Tang, Z., Fu, J. L., Chen, J., Chen, S. S., et al. (2018). Association between increased serum interleukin-6 levels and sustained attention deficits in patients with major depressive disorder. *Psychol. Med.* 48, 2500–2507.

Ye, S. M., and Johnson, R. W. (1999). Increased interleukin-6 expression by microglia from brain of aged mice. *J. Neuroimmunol.* 93, 139–148. doi: 10.1016/s0165-5728(98)00217-3

Young, M. B., Howell, L. L., Hopkins, L., Moshfegh, C., Yu, Z., Clubb, L., et al. (2018). peripheral immune response to remembering trauma contributes to the maintenance of fear memory in mice. *Psychoneuroendocrinology* 94, 143–151. doi: 10.1016/j.psyneuen.2018.05.012

Yue, K., Tanda, G., Katz, J. L., and Zanettini, C. A. (2020). further assessment of a role for Toll-like receptor 4 in the reinforcing and reinstating effects of opioids. *Behav. Pharmacol.* 31, 186–195. doi: 10.1097/fbp.0000000000000474

Yuferov, V., Zhang, Y., Liang, Y., Zhao, C., Randesi, M., and Kreek, M. J. (2018). Oxycodone self-administration induces alterations in expression of integrin, Semaphorin and Ephrin genes in the mouse striatum. *Front. Psychiatry* 9:257. doi: 10.3389/fpsyt.2018.00257

Zambrano, S., de Toma, I., Piffer, A., Bianchi, M. E., and Agresti, A. (2016). NF-κB oscillations translate into functionally related patterns of gene expression. *eLife* 5:e09100.

Zaparte, A., Schuch, J. B., Viola, T. W., Baptista, T. A. S., Beidacki, A. S., do Prado, C. H., et al. (2019). Cocaine use disorder is associated with changes in Th1/Th2/Th17 cytokines and lymphocytes subsets. *Front. Immunol.* 10:2435. doi: 10.3389/fimmu.2019.02435

Zayyad, Z., and Spudich, S. (2015). Neuropathogenesis of HIV: from initial neuroinvasion to HIV-associated neurocognitive disorder (HAND). *Curr. HIV/AIDS Rep.* 12, 16–24. doi: 10.1007/s11904-014-0255-3

Zeng, X. F., Li, Q., Li, J., Wong, N., Li, Z., Huang, J., et al. (2018). HIV-1 Tat and methamphetamine co-induced oxidative cellular injury is mitigated by N-acetylcysteine amide (NACA) through rectifying mTOR signaling. *Toxicol. Lett.* 299, 159–171. doi: 10.1016/j.toxlet.2018.09.009

Zhang, C., Zhang, Y. P., Li, Y. Y., Liu, B. P., Wang, H. Y., Li, K. W., et al. (2019). Minocycline ameliorates depressive behaviors and neuro-immune dysfunction induced by chronic unpredictable mild stress in the rat. *Behav. Brain Res.* 356, 348–357. doi: 10.1016/j.bbr.2018.07.001

Zhang, H., Largent-Milnes, T. M., and Vanderah, T. W. (2020). Glial neuroimmune signaling in opioid reward. *Brain Res. Bull.* 155, 102–111. doi: 10.1016/j.brainresbull.2019.11.012

Zhang, J. C., Yao, W., Dong, C., Yang, C., Ren, Q., Ma, M., et al. (2017). Blockade of interleukin-6 receptor in the periphery promotes rapid and sustained antidepressant actions: a possible role of gut-microbiota-brain axis. *Transl. Psychiatry* 7:e1138. doi: 10.1038/tp.2017.112

Zhang, L., Looney, D., Taub, D., Chang, S. L., Way, D., Witte, M. H., et al. (1998). Cocaine opens the blood-brain barrier to HIV-1 invasion. *J. Neurovirol.* 4, 619–626. doi: 10.3109/13550289809114228

Zhang, N., Rogers, T. J., Caterina, M., and Oppenheim, J. J. (2004). Proinflammatory chemokines, such as C-C Chemokine Ligand 3, desensitize μ-Opioid receptors on dorsal root ganglia neurons. *J. Immunol.* 173, 594–599. doi: 10.4049/jimmunol.173.1.594

Zhang, Q., Gupta, S., Schipper, D. L., Kowalczyk, G. J., Mancini, A. E., Faeder, J. R., et al. (2017). C. NF-κB dynamics discriminate between TNF doses in single cells. *Cell Syst.* 5, 638–645.e5.

Zhang, Y., Liang, Y., Levran, O., Randesi, M., Yuferov, V., Zhao, C., et al. (2017). Alterations of expression of inflammation/immune-related genes in the dorsal and ventral striatum of adult C57BL/6J mice following chronic oxycodone self-administration: a RNA sequencing study. *Psychopharmacology* 234, 2259–2275. doi: 10.1007/s00213-017-4657-y

Zhou, W., and Kalivas, P. W. N. - (2008). Acetylcysteine reduces extinction responding and induces enduring reductions in cue- and heroin-induced drug-seeking. *Biol. Psychiatry* 63, 338–340. doi: 10.1016/j.biopsych.2007.06.008

Zhu, J., Hu, Z., Han, X., Wang, D., Jiang, Q., Ding, J., et al. (2018). Dopamine D2 receptor restricts astrocytic NLRP3 inflammasome activation via enhancing the interaction of β-arrestin2 and NLRP3. *Cell Death Differ.* 25, 2037–2049. doi: 10.1038/s41418-018-0127-2

Zhu, L., Li, J., Dong, N., Guan, F., Liu, Y., Ma, D., et al. (2016). MRNA changes in nucleus accumbens related to methamphetamine addiction in mice. *Sci. Rep.* 6:36993.

Zhu, L., Zhu, J., Liu, Y., Chen, Y., Li, Y., Chen, S., et al. (2015). Chronic methamphetamine regulates the expression of MicroRNAs and putative target genes in the nucleus accumbens of mice. *J. Neurosci. Res.* 93, 1600–1610. doi: 10.1002/jnr.23605

Zhu, W., Chernew, M. E., Sherry, T. B., and Maestas, N. (2019). Initial Opioid Prescriptions among U.S. Commercially Insured Patients, 2012-2017. *N. Engl. J. Med.* 380, 1043–1052. doi: 10.1056/nejmsa1807069

Zoladz, P. R., Eisenmann, E. D., Rose, R. M., Kohls, B. A., Johnson, B. L., Robinson, K. L., et al. (2018). Predator-based psychosocial stress model of PTSD differentially influences voluntary ethanol consumption depending on methodology. *Alcohol* 70, 33–41.

Zou, W., Feng, R., and Yang, Y. (2018). Changes in the serum levels of inflammatory cytokines in antidepressant drug-naïve patients with major depression. *PLoS One* 13:e0197267. doi: 10.1371/journal.pone.0197267

Conflict of Interest: The authors declare that the research was conducted in the absence of any commercial or financial relationships that could be construed as a potential conflict of interest.

Copyright © 2021 Namba, Leyrer-Jackson, Nagy, Olive and Neisewander. This is an open-access article distributed under the terms of the Creative Commons Attribution License (CC BY). The use, distribution or reproduction in other forums is permitted, provided the original author(s) and the copyright owner(s) are credited and that the original publication in this journal is cited, in accordance with accepted academic practice. No use, distribution or reproduction is permitted which does not comply with these terms.

frontiers in Pharmacology

BRIEF RESEARCH REPORT
published: 20 April 2021
doi: 10.3389/fphar.2021.653175

Fenofibrate (a PPAR-α Agonist) Administered During Ethanol Withdrawal Reverts Ethanol-Induced Astrogliosis and Restores the Levels of Glutamate Transporter in Ethanol-Administered Adolescent Rats

Francisca Villavicencio-Tejo, Osvaldo Flores-Bastías, Lucas Marambio-Ruiz, Diliana Pérez-Reytor and Eduardo Karahanian *

Institute of Biomedical Sciences, Faculty of Health Sciences, Universidad Autónoma de Chile, Santiago, Chile

OPEN ACCESS

Edited by:
Mariela Fernanda Perez, National University of Cordoba, Argentina

Reviewed by:
Miriam Beatriz Virgolini, Universidad Nacional de Córdoba, Argentina
Kathryn J. Reissner, University of North Carolina at Chapel Hill, United States

***Correspondence:**
Eduardo Karahanian
eduardo.karahanian@uautonoma.cl

Specialty section:
This article was submitted to Neuropharmacology, a section of the journal Frontiers in Pharmacology

Received: *13 January 2021*
Accepted: *31 March 2021*
Published: *20 April 2021*

Citation:
Villavicencio-Tejo F, Flores-Bastías O, Marambio-Ruiz L, Pérez-Reytor D and Karahanian E (2021) Fenofibrate (a PPAR-α Agonist) Administered During Ethanol Withdrawal Reverts Ethanol-Induced Astrogliosis and Restores the Levels of Glutamate Transporter in Ethanol-Administered Adolescent Rats. Front. Pharmacol. 12:653175. doi: 10.3389/fphar.2021.653175

High-ethanol intake induces a neuroinflammatory response, which has been proposed as responsible for the maintenance of chronic ethanol consumption. Neuroinflammation decreases glutamate transporter (GLT-1) expression, increasing levels of glutamate that trigger dopamine release at the corticolimbic reward areas, driving long-term drinking behavior. The activation of peroxisome proliferator-activated receptor alpha (PPARα) by fibrates inhibits neuroinflammation, in models other than ethanol consumption. However, the effect of fibrates on ethanol-induced neuroinflammation has not yet been studied. We previously reported that the administration of fenofibrate to ethanol-drinking rats decreased ethanol consumption. Here, we studied whether fenofibrate effects are related to a decrease in ethanol-induced neuroinflammation and to the normalization of the levels of GLT-1. Rats were administered ethanol on alternate days for 4 weeks (2 g/kg/day). After ethanol withdrawal, fenofibrate was administered for 14 days (50 mg/kg/day) and the levels of glial fibrillary acidic protein (GFAP), phosphorylated NF-κB-inhibitory protein (pIκBα) and GLT-1, were quantified in the prefrontal cortex, hippocampus, and hypothalamus. Ethanol treatment increased the levels of GFAP in the hippocampus and hypothalamus, indicating a clear astrocytic activation. Similarly, ethanol increased the levels of pIκBα in the three areas. The administration of fenofibrate decreased the expression of GFAP and pIκBα in the three areas. These results indicate that fenofibrate reverts both astrogliosis and NF-κB activation. Finally, ethanol decreased GLT-1 expression in the prefrontal cortex and hippocampus. Fenofibrate normalized the levels of GLT-1 in both areas, suggesting that its effect in reducing ethanol consumption could be due to the normalization of glutamatergic tone.

Keywords: fibrates, alcohol use disorder, alcoholism, treatment, neuroinflammation

INTRODUCTION

The health and social consequences of ethanol use disorder (AUD) have been widely recognized (World Health Organization, 2018). Currently, there are no effective pharmacological therapies to treat AUD since, despite the existence of medications such as naltrexone and acamprosate to reduce the craving for ethanol, most patients relapse in the short or medium-term after initial detoxification (Maisel et al., 2013; Plosker, 2015), suggesting that chronic and abusive consumption of ethanol leaves long-term imprints on the brain, possibly perpetuating the addictive state. This raises the urgent need to find new and better drugs for the treatment of AUD.

Neuroinflammation has been implicated in the consolidation of long-term addiction to ethanol (Coller and Hutchinson, 2012; Flores-Bastías and Karahanian, 2018). The activation of the brain's innate immune system triggers long-lasting neurobiological changes, e.g., increased glutamate-induced hyperexcitability and excitotoxicity, decreased neurogenesis, and behavioral changes such as anxiety and depression, all of which are related to ethanol abuse (Crews et al., 2011). Although the fact that ethanol intake causes neuroinflammation had been reported (Blanco and Guerri, 2007; Flores-Bastías et al., 2019), the first evidence that neuroinflammation would be a major cause of ethanol addiction came from experiments by Blednov et al. (2011), who reported that the i. p. administration of bacterial lipopolysaccharide (LPS) to mice increased voluntary ethanol intake for a prolonged time. The consumption of ethanol increases the permeability of the intestinal mucosa, enabling the diffusion of bacterial LPS into circulation (Ferrier et al., 2006). LPS entering the body triggers the release of tumor necrosis factor-alpha (TNF-α) to blood, which crosses the blood-brain barrier and activates microglial and astrocytic TNF-α receptors, inducing neuroinflammation through a signaling pathway that leads to NF-κB activation (Qin et al., 2007; Crews and Vetreno 2016). This state of neuroinflammation is maintained for several months (Qin et al., 2007), suggesting the existence of long-lasting mechanisms that perpetuate it. In addition, ethanol upregulates cytochrome P4502E1 (CYP2E1) activity and expression in the brain, and CYP2E1 oxidation of ethanol increases ROS levels which in turn activate NF-κB. Also, NF-κB activation induces the expression of NADPH oxidase (NOX), an enzyme that produces even more ROS, thus creating an activation loop that rapidly induces genes that lead to the activation of the innate immune response (Crews et al., 2011; Flores-Bastías and Karahanian, 2018).

The hippocampus is the brain region most pathologically affected by chronic ethanol ingestion (Franke et al., 1997), which leads to the loss of control over drinking in humans (Crews, 2008; Hermens et al., 2015). The activity of astrocytes and microglia in the hippocampus is exacerbated in alcoholics (He and Crews, 2008). This activation promotes the release of pro-inflammatory cytokines and ROS which in turn, promote neuronal death in the hippocampus and other brain regions (Ward et al., 2009). The sustained activation of neuroinflammation plus the exacerbated production of ROS would lead to neurodegeneration of key areas involved in excessive ethanol intake (Flores-Bastías and Karahanian, 2018). The prefrontal cortex (PFC) is a region that operates within the mesocorticolimbic circuit to exert executive control over ethanol-seeking behavior. Besides the hippocampus, ethanol-induced cell death in other regions such as PFC and the hypothalamus may lead to lack of inhibition of reward areas, reducing behavioral inhibition and increasing motivation to drink (Crews et al., 2011; Crews et al., 2015). Interestingly, it is reported that adolescence is when the greatest damage associated with ethanol-induced neuroinflammation occurs in hippocampal, cortical, and hypothalamic structures, both in humans and in murine models (Crews and Vetreno, 2011; Crews et al., 2016; Pascual et al., 2018). In adolescents, the typical pattern of ethanol consumption corresponds to binge drinking, where a large amount is consumed in a short period time.

The excitatory neurotransmitter glutamate is strongly implicated in the maintenance of chronic ethanol intake, as well as with relapse (Reissner and Kalivas, 2010). Ethanol increases levels of glutamate within corticolimbic structures (Dahchour and De Witte, 2000). Repeated administration of ethanol elicits a progressive increase in the capacity of ethanol to stimulate glutamate release, leading to glutamate sensitization (Szumlinski et al., 2007; Carrara-Nascimento et al., 2011). After chronic ethanol intake and following abstinence, relapse is elicited by cues previously associated with the ethanol effect, which activate glutamate release in several brain areas involved in the memory of the addictive-drug cues. After this memory association, the glutamatergic drive is transferred to PFC, increasing dopamine release at the reward system driving the drinking behavior (Rao et al., 2015; Bell et al., 2016). Glutamate transporter 1 (GLT-1), also known as excitatory amino acid transporter 2 (EAAT2) or solute carrier family 1 member 2 (SLC1A2), is the main transporter that allows re-uptake of glutamate from the extracellular space by astrocytes at tripartite glutamatergic synapses. Glutamate reuptake is imperative to prevent neuronal damage due to exacerbated activity of glutamate receptors. Interestingly, animals that consume ethanol chronically show reduced levels of GLT-1 and marked increases in extracellular levels of glutamate (Sari et al., 2013a). The administration of ceftriaxone (a drug that increases the levels of GLT-1) to ethanol-drinking rats restored extracellular glutamate concentration and reduced chronic ethanol intake by 70% (Sari et al., 2013b; Das et al., 2015). In addition to ethanol consumption, neuroinflammation induced by direct administration of LPS or TNF-α also reduces the levels of GLT-1, leading to an increase in extracellular glutamate; blockade of the signaling produced by proinflammatory cytokines normalized GLT-1 and levels of glutamate (Fang et al., 2012). Thus, it is conceivable that the reduction in GLT-1 expression produced by ethanol is mediated by the activation of the neuroinflammatory response.

Peroxisome proliferator-activated receptor alpha (PPAR-α) is a nuclear receptor that has essential functions in the metabolism of lipids (Berger and Moller, 2002). PPAR-α can be activated by fibrate drugs, which include fenofibrate, bezafibrate, gemfibrozil, ciprofibrate, and clofibrate (Schoonjans et al., 1996). Fibrates increase the oxidation rate of fatty acids; therefore, they are widely used clinically for the treatment of hypertriglyceridemia

(Cignarella et al., 2006). Several authors have reported that fenofibrate decreases ethanol intake in rodents (Barson et al., 2009; Karahanian et al., 2014; Blednov et al., 2015, 2016; Haile and Kosten, 2017; Rivera-Meza et al., 2017). We were able to demonstrate that fenofibrate increases catalase and alcohol dehydrogenase activities in the liver, which leads to rapid acetaldehyde accumulation when the animals drink ethanol (Karahanian et al., 2014; Rivera-Meza et al., 2017; Muñoz et al., 2020). Acetaldehyde that accumulates in the blood produces unpleasant effects that lead to an aversion to ethanol consumption in animal models and humans (Mizoi et al., 1979). Additionally, fenofibrate would have effects at the central level that decrease the craving to drink ethanol after a period of abstinence (Rivera-Meza et al., 2017). Interestingly, astrocytes are the cell type where PPARα is most expressed in the brain (Cullingford et al., 1998). This opens the possibility that the activation of PPARα in astrocytes by fenofibrate could be mediating its effects at the central level. Given the central role of astrocytes in the neuroimmune system, we hypothesized that fenofibrate should have a modulating effect on neuroinflammation induced by ethanol consumption.

To date, the effect of the activation of PPAR-α on ethanol-induced neuroinflammation has not been reported. However, the decrease in neuroinflammation mediated by PPAR-α activation has been reported in brain injury models other than ethanol abuse (aging, ischemia/reperfusion injury, and traumatic brain injury) (Poynter and Daynes, 1998; Bordet et al., 2006; Collino et al., 2006; Chen et al., 2007; Shehata et al., 2020). Activation of PPAR-α by the administration of fibrates downregulates NF-κB activity (Staels et al., 1998; Delerive et al., 1999, 2000; Marx et al., 1999; Collino et al., 2006), decreasing the production of proinflammatory cytokines and enzymes (Poynter and Daynes, 1998; Pahan et al., 2002; Bordet et al., 2006; Chen et al., 2007).

Here, we aimed to evaluate whether fenofibrate administered during ethanol withdrawal would be capable of reducing neuroinflammation induced by binge ethanol ingestion in adolescent rats and of restoring the levels of GLT-1 in the hippocampus, hypothalamus, and prefrontal cortex, which could help to explain the protracted effects of this drug on reducing the craving to drink ethanol after periods of abstinence. To evaluate the anti-neuroinflammatory effects of fenofibrate after a prolonged period of administration of ethanol, we quantified by western blot the levels of the neuroinflammation marker proteins GFAP and inhibitor of κB alpha (IκBα) phosphorylated. GFAP increases its expression when astrocytes become activated in neuroinflammatory processes. On the other hand, IκBα is the protein that binds to and inhibits NF-κB, masking its nuclear localization signal which keeps it sequestered in the cytoplasm. When inflammatory processes are triggered, IκBα is phosphorylated (pIκBα), which causes it to become detached from NF-κB, which is now free to enter the nucleus where it can activate the expression of specific genes related to the immune response.

METHOD

Male Sprague-Dawley rats were purchased from Pontificia Universidad Católica de Chile. Rats were housed in individual cages in a temperature-controlled room on a 12-h light/12-h dark cycle, with food and water provided *ad libitum*. The binge-like administration of ethanol was started by esophageal gavage in 30-day-old adolescent rats (n = 4 per group). Administration of ethanol was carried out for 4 weeks on Mondays, Wednesdays, and Fridays, starting the first week with a dose of 1 g/k/day ethanol and continuing the following 3 weeks with a dose of 2 g/k/day (both doses as a 30% v/v ethanol solution). Control groups were intragastrical given only water (n = 4 per group). At the end of 4 weeks, the administration of ethanol was terminated, and ethanol-treated animals and controls were randomly separated into two groups each. One ethanol group and one control group were administered micronized fenofibrate 50 mg/k/day (Fibronil, Royal Pharma, Chile) by esophageal gavage for 14 days. The other two groups were given only vehicle.

One day after the last dose of fenofibrate or vehicle, the animals were anesthetized with ketamine/xylazine (10:1 mg/kg of body weight, i. p.), decapitated and the brains removed. *Hippocampus*, hypothalamus, and prefrontal cortex tissues were extracted and homogenized with an Ultra-Turrax homogenizer in buffer containing Tris-HCl 100 mM pH 7.4, EDTA 5 mM, SDS 1%, PMSF 1 μM and a protease inhibitor cocktail (Pierce) (1 ml lysis buffer per 0.1 g tissue). Then, the samples were centrifuged at 14.000 x g for 10 min at 4 °C to remove tissue debris. Protein concentration was determined in the supernatants with the Bio-Rad protein assay kit. SDS-PAGE was performed loading the same amount of total protein per lane (100 μg). The expression levels of GLT-1, pIκBα and GFAP were determined by western blot with the following antibodies: anti-GLT-1 (PA5-19706 ThermoFisher Scientific), anti-pIκBα (SC8404, Santa Cruz Biotechnology, detects specifically IκBα phosphorylated at Ser 32), and anti-GFAP (G3893 Sigma-Aldrich). As a loading control, the levels of *ß*-actin were also determined in the same blots (anti-β-actin SC47778, Santa Cruz Biotechnology). All primary antibodies were used at 1:3,000 dilution, and were incubated at 4 °C overnight, except for *ß*-actin and GLT-1, which were incubated for 1:30 h at room temperature. After the incubation with the corresponding HRP-conjugated secondary antibodies (diluted 1:5,000), blotting membranes were revealed with Luminata Western HRP Chemiluminescence Substrate (Merck Millipore). The different proteins and *ß*-actin were all quantified in the same blotting membranes, which were previously stripped of the preceding antibodies by incubation for 10 min in Restore Western Blot Stripping Buffer (ThermoFisher Scientific) (the detection sequence was: pIκBα, GFAP, GLT-1 and finally *ß*-actin). Bands were quantified by densitometry with ImageJ software. The levels of each protein were expressed as percentages of their water-administered controls, normalized by the levels of *ß*-actin. For statistical analysis, two-way ANOVA was used followed by Bonferroni's post-hoc analysis.

RESULTS

One-month ethanol treatment increased the levels of GFAP in the hippocampus and hypothalamus (to 640 ± 14% and 190 ± 13% of their controls without ethanol, respectively), indicating a clear astrocytic activation in these areas of the brain (**Figure 1A**). In

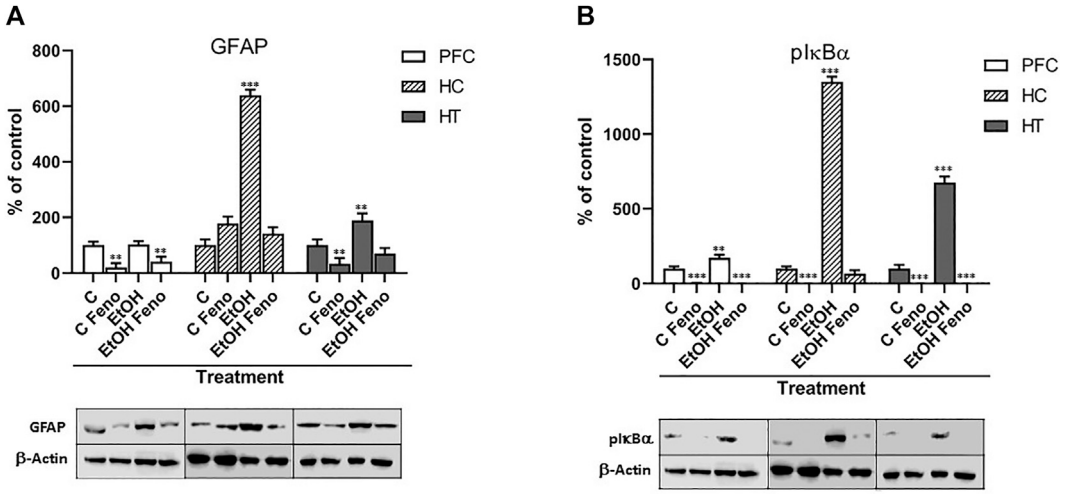

FIGURE 1 | Expression levels of GFAP **(A)** and pIκBα **(B)** in prefrontal cortex (PFC), hippocampus (HC) and hypothalamus (HT) in rats that were administered alcohol for one month and then were treated with fenofibrate for 14 days. C = water-administered controls; C Feno = water-administered controls treated with fenofibrate; EtOH = alcohol-treated rats; EtOH Feno = alcohol-treated rats then treated with fenofibrate. The graphs show the protein levels expressed as percentages of their water-administered controls, normalized by the levels of *β*-actin. Representative blots from each group are shown below each respective bar. ANOVA $^{**}p < 0.01$; $^{***}p < 0.001$. GFAP PFC: $F_{(3,12)} = 23.50$ for Feno effect; GFAP HC: $F_{(3,12)} = 131.10$ for EtOH effect; GFAP HT: $F_{(3,12)} = 34.07$ for EtOH effect, $F_{(3,12)} = 75.40$ for Feno effect. pIκBα PFC: $F_{(3,12)} = 9.76$ for EtOH effect, $F_{(3,12)} = 149.90$ for Feno effect; pIκBα HC: $F_{(3,12)} = 1,190.00$ for EtOH effect, $F_{(3,12)} = 1,314.00$ for Feno effect; pIκBα HT: $F_{(3,12)} = 594.40$ for EtOH effect, $F_{(3,12)} = 1,080.00$ for Feno effect. The error bars correspond to SD, $n = 4$. The absolute values, normalized by *β*-actin, obtained from the quantification of the bands are **(A)** GFAP: PFC (C = 0.98 ± 0.33; C FENO = 0.20 ± 0.08; EtOH = 1.00 ± 0.13; EtOH FENO = 0.40 ± 0.09); HC (C = 0.31 ± 0.11; C FENO = 0.55 ± 0.03; EtOH = 1.98 ± 0.04; EtOH FENO = 0.44 ± 0.03); HT (C = 0.56 ± 0.19; C FENO = 0.19 ± 0.05; EtOH = 1.06 ± 0.08; EtOH FENO = 0.39 ± 0.05) **(B)** pIκBα: PFC (C = 0.35 ± 0.12; C FENO = 0.00 ± 0.00; EtOH = 0.60 ± 0.05; EtOH FENO = 0.00 ± 0.00); HC (C = 0.12 ± 0.04; C FENO = 0.00 ± 0.00; EtOH = 1.62 ± 0.02; EtOH FENO = 0.08 ± 0.01); HT (C = 0.16 ± 0.06; C FENO = 0.00 ± 0.00; EtOH = 1.08 ± 0.02; EtOH FENO = 0.00 ± 0.00).

contrast, the levels of GFAP were not altered by ethanol in the PFC. It should be noted that these effects were measured 14 days after finishing the administration of ethanol. The administration of fenofibrate for 14 days to rats that were previously treated with ethanol markedly decreased the expression of GFAP in the PFC, hippocampus, and hypothalamus (to 40 ± 7, 141 ± 9 and 69 ± 7% of their controls without ethanol, respectively), which indicates that fenofibrate reverses ethanol-induced glial activation. Interestingly, in PFC and hypothalamus, fenofibrate was able to reduce the expression levels of GFAP even in rats that had not been treated with ethanol. In the hippocampus, there appears to be a slight increase in GFAP expression in rats that were treated with fenofibrate, however, this is not statistically significant.

The levels of pIκBα increased in the PFC, hippocampus, and hypothalamus due to the administration of ethanol (to 170 ± 11, 1,350 ± 14 and 675 ± 13% of their controls without ethanol, respectively) (**Figure 1B**). Again, it is important to note that this effect was measured 14 days after finishing the administration of ethanol. Administration of fenofibrate to rats that had previously been treated with ethanol decreased the inactivation of IκBα to levels even lower than its controls without ethanol, in the three brain areas. Furthermore, fenofibrate reduced the levels of pIκBα to undetectable values in control animals, as well as in the PFC and hypothalamus of ethanol-treated rats. These results indicate that ethanol treatment induces phosphorylation of IκBα, which would allow the activation of NF-κB, triggering the neuroinflammatory response. Fenofibrate markedly reverts this effect, again showing its ability to reverse neuroinflammation induced by the administration of ethanol.

Administration of ethanol decreased the levels of the glutamate transporter GLT-1, both in the PFC and in the hippocampus (to 14 ± 7% and 52 ± 12% of their controls without ethanol, respectively), but not in the hypothalamus (**Figure 2**). The administration of fenofibrate for 14 days to rats that had previously been treated with ethanol normalized the expression of GLT-1 in both the PFC and hippocampus (to 82 ± 9 and 80 ± 9% of their controls without ethanol, respectively), which indicates that fenofibrate reverses the ethanol-induced decrease in the levels of GLT-1 which could be leading to the normalization of glutamatergic tone increased by excessive ethanol intake.

DISCUSSION

The main findings in this study are that the administration of fenofibrate can reverse in the PFC, hippocampus, and hypothalamus, both neuroinflammation and the decrease in the expression of GLT-1, induced by high binge-like administration of ethanol to adolescent rats. Since neuroinflammation has been strongly implicated in the activation of brain mechanisms that perpetuate chronic ethanol consumption, and since fenofibrate is a drug approved for many years by the FDA for the clinical treatment of

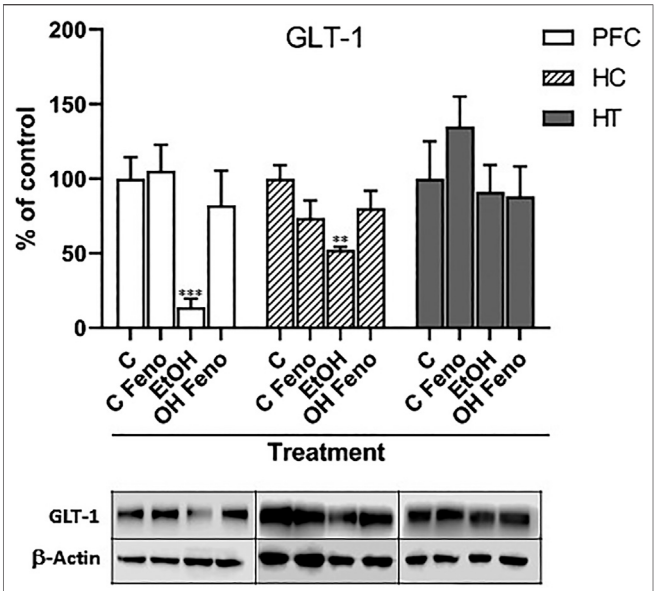

FIGURE 2 | Expression levels of GLT-1 in prefrontal cortex (PFC), hippocampus (HC) and hypothalamus (HT) in rats that were administered alcohol for one month and then were treated with fenofibrate for 14 days. C = water-administered controls; C Feno = water-administered controls treated with fenofibrate; EtOH = alcohol-treated rats; EtOH Feno = alcohol-treated rats then treated with fenofibrate. The graphs show the protein levels expressed as percentages of their water-administered controls, normalized by the levels of *β*-actin. Representative blots from each group are shown below each respective bar. ANOVA $^{**}p < 0.01$; $^{***}p < 0.001$. PFC: $F_{(3,12)} = 14.81$ for EtOH effect; HC: $F_{(3,12)} = 6.39$ for EtOH effect. The error bars correspond to SD, $n = 4$. The absolute values, normalized by *β*-actin, obtained from the quantification of the bands are: PFC (C = 1.30 ± 0.44; C FENO = 1.37 ± 0.11; EtOH = 0.18 ± 0.10; EtOH FENO = 1.07 ± 0.12); HC (C = 0.61 ± 0.21; C FENO = 0.45 ± 0.05; EtOH = 0.32 ± 0.08; EtOH FENO = 0.49 ± 0.06); HT (C = 0.34 ± 0.12; C FENO = 0.51 ± 0.03; EtOH = 0.31 ± 0.05; EtOH FENO = 0.30 ± 0.03).

hypertriglyceridemia, our findings could have a great translational value for the treatment of AUD.

The hippocampus is the brain region that suffers the greatest damage due to neuroinflammation induced by ethanol consumption (Franke et al., 1997; He and Crews, 2008). The exacerbated activation of the glia finally leads to neuronal death in this area (Ward et al., 2009). In agreement with this, we found in our model that the hippocampus is where the greatest increase (640 ± 14%) in the expression of GFAP is detected because of the administration of ethanol (**Figure 1A**). Besides, we also observed a significant increase in the levels of GFAP in the hypothalamus (190 ± 13%), which agrees with what was observed in the brains of alcoholics where a greater number of GFAP-positive astrocytes exist in hypothalamic tissue compared to non-alcoholic individuals (Cullen and Halliday, 1994). Administration of fenofibrate to rats that had been treated with ethanol reduced GFAP expression to similar levels as their non-ethanol controls, demonstrating that fenofibrate is capable of completely reversing ethanol-induced glial activation. On the other hand, we did not observe changes in the levels of GFAP in PFC of rats treated with ethanol. Interestingly, even though ethanol did not increase GFAP expression in PFC, fenofibrate was still able to reduce the levels of GFAP in control animals and in those that were treated with ethanol (to 20 ± 8 and 40 ± 9% of the controls without ethanol, respectively). A similar effect was observed in the hypothalamus, where fenofibrate also reduced GFAP expression in control animals (to 34 ± 8% of their controls without fenofibrate).

We also evaluated the ability of fenofibrate to inhibit ethanol-induced phosphorylation of IκBα, and thus inhibit NF-κB activation and neuroinflammatory response. As with GFAP, we observed that the administration of ethanol produced the most marked effects in the hippocampus (increase in pIκBα to 1,350 ± 14% compared to its controls without ethanol), followed by the hypothalamus (675 ± 13%) and PFC (170 ± 11%). This would indicate that the neuroinflammatory response is exacerbated mainly in the hippocampus, which agrees with the fact that this brain region is the one that suffers the greatest damage because excessive ethanol consumption. In all three areas, the administration of fenofibrate reduced the levels of pIκBα to undetectable values, which demonstrates its effectiveness in reducing neuroinflammation induced by the administration of ethanol. Even in non-ethanol control rats, fenofibrate showed effects by completely inhibiting IκBα phosphorylation. PPAR-α can act as a negative regulator of several pro-inflammatory genes via inhibiting the activation of NF-κB (Delerive et al., 2000; Kleemann et al., 2003; Gervois et al., 2004). Activation of NF-κB is initiated by the proinflammatory signal-induced phosphorylation of IκB. This occurs primarily via activation of a kinase called IκB kinase (IKK). Okayasu et al. 2008 demonstrated that TNF-α stimulates IκB phosphorylation by inducing IKK activity, and fenofibrate inhibits TNFα-induced IKK activity and IκB phosphorylation. However, the direct mechanism by which fenofibrate inhibits IKK has not yet been found; apparently, there could be an indirect mechanism mediated by the activation of AMP-activated protein kinase (AMPK), which in fact would phosphorylate IKK, inactivating it (Okayasu et al., 2008).

It is worth analyzing the notorious increase in pIκBα levels produced by ethanol administration, especially in the hippocampus and hypothalamus. Once proinflammatory signals are present due to ethanol consumption, NF-κB is activated and commands the expression of its own repressor, IκBα. The newly synthesized IκBα then re-inhibits NF-κB and, thus, forms a feedback loop of regulation (Nelson et al., 2004). Thereby, as long as NF-κB is active the levels of IκBα increase, which in turn will be phosphorylated by IKK that is active due to the proinflammatory signals present due to ethanol consumption. Thus, the more active NF-κB is maintained, the higher the levels of phosphorylated IκBα are present.

In this study, PFC was the area that showed the least neuroinflammatory response due to alcohol administration, evidenced by the non-increase in the levels of GFAP and a lower phosphorylation response of IκBα (compared to the hippocampus and hypothalamus). It should be emphasized that the measurements were made 2 weeks after finishing with the administration of ethanol; Bull et al. 2015 reported that after 3 weeks of ethanol abstinence, the number of GFAP-positive astrocytes in PFC decreased to the same levels as in control rats that had not consumed ethanol. Similarly, it is conceivable in our studies that 2 weeks of abstinence would have been enough for

GFAP expression to normalize in the PFC of rats that had been treated with ethanol. Another possibility is that PFC has a lower capacity to induce an inflammatory response against exposure to ethanol, or that it has a greater anti-inflammatory and/or antioxidant capacity against the injuries produced by ethanol. Consistent with this idea, Kane et al. (2014) reported that ethanol did not increase the expression of pro-inflammatory molecules such as CCL2, IL-6, or TNF-α in adolescent mice cerebral cortex.

As indicated above, ethanol intake increases the levels of glutamate within corticomesolimbic structures, mainly PFC, hippocampus, and nucleus accumbens (Dahchour and De Witte, 2000). This hyper glutamatergic state is responsible for craving in individuals addicted to ethanol and can trigger the neurobiological mechanisms responsible for relapse after a period of abstinence. These mechanisms are related to the memory of ethanol-related cues, which once presented in this hyper glutamatergic context in the hippocampus, the drive is exacerbated transmitted to the PFC, enhancing the behavior of ethanol consumption (Bell et al., 2016). As indicated above, the main cause of this hyper glutamatergic state is the decreased expression of GLT-1. In accordance with what was reported by other research groups (Sari et al., 2013a; Israel et al., 2021), in our studies we observed that ethanol greatly decreased the levels of GLT-1 in PFC and the hippocampus. Interestingly, the administration of fenofibrate reversed this decrease in both areas. On the contrary, in the hypothalamus, we did not observe statistically significant changes in the expression of GLT-1 due to the administration of ethanol or treatment with fenofibrate. To our level of knowledge, alterations of the levels of GLT-1 in the hypothalamus due to the administration of ethanol have not yet been reported. Interestingly, multiple PPAR response elements (PPREs) in the promoter region of the GLT-1 (EAAT2) gene have been found (Romera et al., 2007), suggesting that the activation of PPAR-α by fenofibrate would have a direct effect on the increase of the expression of this gene.

Although GLT-1 is responsible for >90% of the glutamate transport activity in the brain (Holmseth et al., 2009), there are other glutamate transporters, such as the cystine-glutamate antiporter (xC^-), that participate in the homeostasis of this neurotransmitter. xC^- promotes the release of glutamate to the extracellular space while cystine is taken up by the cell. Although its importance in maintaining the levels of glutamate in the synaptic space may not be as relevant as that of GLT-1, the uptake of cystine by glial cells promotes the synthesis of glutathione (of which cystine is its precursor), which is one of the main antioxidant agents that counteract oxidative stress in the brain (Danbolt, 2001). Thus, we cannot rule out that, at least in part, the anti-inflammatory effects of fenofibrate may be due to an upregulation of xC^- and an increased synthesis of glutathione.

Although our studies suggest that the decrease in neuroinflammation together with the normalization of the levels of GLT-1 could be responsible for the effects of fenofibrate on alcohol consumption at the central level, we cannot rule out that there are other mechanisms involved. In a previous study (Rivera-Meza et al., 2017), we reported that fenofibrate is also capable of reducing the consumption of another reinforcing substance (saccharin) that a priori would not be related to alcohol; however, there is evidence that ethanol and palatable foods (e.g., sweet taste) ingestion share common mechanisms involving μ-opioid receptors and dopaminergic transmission in the brain reward system (Di Chiara, 1998; Kelley et al., 2002; Hajnal et al., 2004). Therefore, this effect of fenofibrate on saccharin consumption could probably be related to a decrease in the dopaminergic response in the limbic reward system. It has been reported that the activation of PPARα induces some tyrosine kinase(s) which has not yet been identified, which phosphorylates and negatively regulates α4β2-type nicotinic acetylcholine receptors, thus decreasing the dopaminergic activity of neurons in the ventral tegmental area (Melis et al., 2008; Melis et al., 2013). These results suggest that fenofibrate-mediated activation of PPARα would also diminish dopamine release in the mesolimbic pathway, thereby decreasing its rewarding activity. We intend to address this hypothesis in future studies.

Overall, our studies show that the administration of fenofibrate to rats that were administered ethanol reverses: (i) the increase in the expression of an astrocyte-activation marker protein (GFAP) in the hippocampus and hypothalamus, (ii) the increase in the levels of phosphorylation of the inhibitory protein of NF-κB (IκB) in PFC, hippocampus, and hypothalamus, which would prevent the activation of neuroinflammation-related genes, and (iii) the decrease in the expression of the glutamate transporter GLT-1, which could possibly lead to the restoration of normal glutamatergic tone, which was altered by ethanol consumption. The latter would lead to a decrease in ethanol craving, which is the main cause of relapse in patients who have detoxified. These findings suggest that the administration of fenofibrate in the withdrawal period after ethanol detoxification could be a good therapeutic alternative to avoid or reduce the severity of relapse.

DATA AVAILABILITY STATEMENT

The original contributions presented in the study are included in the article/Supplementary Material, further inquiries can be directed to the corresponding author.

ETHICS STATEMENT

The animal study was reviewed and approved by Scientific Ethics Committee and Animal Bioethics, Universidad Autónoma de Chile.

AUTHOR CONTRIBUTIONS

FV-T, OF-B, LM-R, DP-R and EK performed the experiments. EK wrote the manuscript. OF-B proofread the manuscript.

FUNDING

This work was supported by DIUA222–2021 and DIUA191-2020 (Universidad Autónoma de Chile).

REFERENCES

Barson, J. R., Karatayev, O., Chang, G.-Q., Johnson, D. F., Bocarsly, M. E., Hoebel, B. G., et al. (2009). Positive relationship between dietary fat, ethanol intake, triglycerides, and hypothalamic peptides: counteraction by lipid-lowering drugs. *Alcohol* 43 (6), 433–441. doi:10.1016/j.alcohol.2009.07.003

Bell, R. L., Hauser, S. R., McClintick, J., Rahman, S., Edenberg, H. J., Szumlinski, K. K., et al. (2016). Ethanol-associated changes in glutamate reward neurocircuitry: a minireview of clinical and preclinical genetic findings. *Prog. Mol. Biol. Transl. Sci.* 137, 41–85. doi:10.1016/bs.pmbts.2015.10.018

Berger, J., and Moller, D. E. (2002). The mechanisms of action of PPARs. *Annu. Rev. Med.* 53, 409–435. doi:10.1146/annurev.med.53.082901.104018

Blanco, A. M., and Guerri, C. (2007). Ethanol intake enhances inflammatory mediators in brain: role of glial cells and TLR4/IL-1RI receptors. *Front. Biosci.* 12, 2616–2630. doi:10.2741/2259

Blednov, Y. A., Benavidez, J. M., Black, M., Ferguson, L. B., Schoenhard, G. L., Goate, A. M., et al. (2015). Peroxisome proliferator-activated receptorsαandγare linked with alcohol consumption in mice and withdrawal and dependence in humans. *Alcohol. Clin. Exp. Res.* 39 (1), 136–145. doi:10.1111/acer.12610

Blednov, Y. A., Benavidez, J. M., Geil, C., Perra, S., Morikawa, H., and Harris, R. A. (2011). Activation of inflammatory signaling by lipopolysaccharide produces a prolonged increase of voluntary alcohol intake in mice. *Brain Behav. Immun.* 25 (Suppl 1), S92–S105. doi:10.1016/j.bbi.2011.01.008

Blednov, Y. A., Black, M., Benavidez, J. M., Stamatakis, E. E., and Harris, R. A. (2016). PPAR agonists: II. fenofibrate and tesaglitazar alter behaviors related to voluntary alcohol consumption. *Alcohol. Clin. Exp. Res.* 40 (3), 563–571. doi:10.1111/acer.12972

Bordet, R., Ouk, T., Petrault, O., Gelé, P., Gautier, S., Laprais, M., et al. (2006). PPAR: a new pharmacological target for neuroprotection in stroke and neurodegenerative diseases. *Biochem. Soc. Trans.* 34 (Pt 6), 1341–1346. doi:10.1042/BST0341341

Bull, C., Syed, W. A., Minter, S. C., and Bowers, M. S. (2015). Differential response of glial fibrillary acidic protein-positive astrocytes in the rat prefrontal cortex following ethanol self-administration. *Alcohol. Clin. Exp. Res.* 39 (4), 650–658. doi:10.1111/acer.12683

Carrara-Nascimento, P. F., Griffin, W. C., 3rd, Pastrello, D. M., Olive, M. F., and Camarini, R. (2011). Changes in extracellular levels of glutamate in the nucleus accumbens after ethanol-induced behavioral sensitization in adolescent and adult mice. *Alcohol* 45 (5), 451–460. doi:10.1016/j.alcohol.2011.01.002

Chen, X. R., Besson, V. C., Palmier, B., Garcia, Y., Plotkine, M., and Marchand-Leroux, C. (2007). Neurological recovery-promoting, anti-inflammatory, and anti-oxidative effects afforded by fenofibrate, a PPAR alpha agonist, in traumatic brain injury. *J. Neurotrauma* 24 (7), 1119–1131. doi:10.1089/neu.2006.0216

Cignarella, A., Bellosta, S., Corsini, A., and Bolego, C. (2006). Hypolipidemic therapy for the metabolic syndrome. *Pharmacol. Res.* 53 (6), 492–500. doi:10.1016/j.phrs.2006.03.012

Coller, J. K., and Hutchinson, M. R. (2012). Implications of central immune signaling caused by drugs of abuse: mechanisms, mediators and new therapeutic approaches for prediction and treatment of drug dependence. *Pharmacol. Ther.* 134 (2), 219–245. doi:10.1016/j.pharmthera.2012.01.008

Collino, M., Aragno, M., Mastrocola, R., Benetti, E., Gallicchio, M., Dianzani, C., et al. (2006). Oxidative stress and inflammatory response evoked by transient cerebral ischemia/reperfusion: effects of the PPAR-α agonist WY14643. *Free Radic. Biol. Med.* 41 (4), 579–589. doi:10.1016/j.freeradbiomed.2006.04.030

Crews, F. T., Sarkar, D. K., Qin, L., Zou, J., Boyadjieva, N., and Vetreno, R. P. (2015). Neuroimmune function and the consequences of alcohol exposure. *Alcohol. Res.* 37 (2), 331–351. doi:10.1007/978-1-4614-4729-0_10

Crews, F. T. (2008). Alcohol-related neurodegeneration and recovery: mechanisms from animal models. *Alcohol. Res. Health* 31 (4), 377–388. doi:10.1002/0470022574.ch11

Crews, F. T., and Vetreno, R. P. (2011). Addiction, adolescence, and innate immune gene induction. *Front. Psychiatry* 2, 19. doi:10.3389/fpsyt.2011.00019

Crews, F. T., Vetreno, R. P., Broadwater, M. A., and Robinson, D. L. (2016). Adolescent alcohol exposure persistently impacts adult neurobiology and behavior. *Pharmacol. Rev.* 68 (4), 1074–1109. doi:10.1124/pr.115.012138

Crews, F. T., and Vetreno, R. P. (2016). Mechanisms of neuroimmune gene induction in alcoholism. *Psychopharmacology* 233, 1543–1557. doi:10.1007/s00213-015-3906-1

Crews, F. T., Zou, J., and Qin, L. (2011). Induction of innate immune genes in brain create the neurobiology of addiction. *Brain Behav. Immun.* 25 (Suppl. 1), S4–S12. doi:10.1016/j.bbi.2011.03.003

Cullen, K. M., and Halliday, G. M. (1994). Chronic alcoholics have substantial glial pathology in the forebrain and diencephalon. *Alcohol. Alcohol. Suppl.* 2, 253–257.

Cullingford, T. E., Bhakoo, K., Peuchen, S., Dolphin, C. T., Patel, R., and Clark, J. B. (1998). Distribution of mRNAs encoding the peroxisome proliferator-activated receptor α, β, and γ and the retinoid X receptor α, β, and γ in rat central nervous system. *J. Neurochem.* 70, 1366–1375. doi:10.1046/j.1471-4159.1998.70041366.x

Dahchour, A., and De Witte, P. (2000). Taurine blocks the glutamate increase in the nucleus accumbens microdialysate of ethanol-dependent rats. *Pharmacol. Biochem. Behav.* 65, 345–350. doi:10.1016/s0091-3057(99)00197-5

Danbolt, N. C. (2001). Glutamate uptake. *Prog. Neurobiol.* 65, 1–105. doi:10.1016/s0301-0082(00)00067-8

Das, S. C., Yamamoto, B. K., Hristov, A. M., and Sari, Y. (2015). Ceftriaxone attenuates ethanol drinking and restores extracellular glutamate concentration through normalization of GLT-1 in nucleus accumbens of male alcohol-preferring rats. *Neuropharmacol* 97, 67–74. doi:10.1016/j.neuropharm.2015.05.009

Delerive, P., Gervois, P., Fruchart, J. C., and Staels, B. (2000). Induction of IkappaBalpha expression as a mechanism contributing to the anti-inflammatory activities of peroxisome proliferator-activated receptor-alpha activators. *J. Biol. Chem.* 275, 36703–36707. doi:10.1074/jbc.M004045200

Delerive, P., De Bosscher, K., Besnard, S., Vanden Berghe, W., Peters, J. M., Gonzalez, F. J., et al. (1999). Peroxisome proliferator-activated receptor α negatively regulates the vascular inflammatory gene response by negative cross-talk with transcription factors NF-Kb and AP-1. *J. Biol. Chem.* 274, 32048–32054. doi:10.1074/jbc.274.45.32048

Di Chiara, G. (1998). A motivational learning hypothesis of the role of mesolimbic dopamine in compulsive drug use. *J. Psychopharmacol.* 12, 54–67. doi:10.1177/026988119801200108

Fang, J., Han, D., Hong, J., Tan, Q., and Tian, Y. (2012). The chemokine, macrophage inflammatory protein-2γ, reduces the expression of glutamate transporter-1 on astrocytes and increases neuronal sensitivity to glutamate excitotoxicity. *J. Neuroinflammation.* 9, 267. doi:10.1186/1742-2094-9-267

Ferrier, L., Bérard, F., Debrauwer, L., Chabo, C., Langella, P., Buéno, L., et al. (2006). Impairment of the intestinal barrier by ethanol involves enteric microflora and mast cell activation in rodents. *Am. J. Pathol.* 168 (4), 1148–1154. doi:10.2353/ajpath.2006.050617

Flores-Bastías, O., Gómez, G. I., Orellana, J. A., and Karahanian, E. (2019). Activation of melanocortin-4 receptor by a synthetic agonist inhibits ethanolinduced neuroinflammation in rats. *Curr. Pharm. Des.* 25, 4799–4805. doi:10.2174/1381612825666191216145153

Flores-Bastías, O., and Karahanian, E. (2018). Neuroinflammation produced by heavy alcohol intake is due to loops of interactions between toll-like 4 and TNF receptors, peroxisome proliferator-activated receptors and the Central Melanocortin system: a novel hypothesis and new therapeutic avenues. *Neuropharmacol.* 128, 401–407. doi:10.1016/j.neuropharm.2017.11.003

Franke, H., Kittner, H., Berger, P., Wirkner, K., and Schramek, J. (1997). The reaction of astrocytes and neurons in the hippocampus of adult rats during chronic ethanol treatment and correlations to behavioral impairments. *Alcohol* 14, 445–454. doi:10.1016/s0741-8329(96)00209-1

Gervois, P., Kleemann, R., Pilon, A., Percevault, F., Koenig, W., Staels, B., et al. (2004). Global suppression of IL-6-induced acute phase response gene expression after chronic in vivo treatment with the peroxisome proliferator-activated receptor-α activator fenofibrate. *J. Biol. Chem.* 279, 16154–16160. doi:10.1074/jbc.M400346200

Haile, C. N., and Kosten, T. A. (2017). The peroxisome proliferator-activated receptor alpha agonist fenofibrate attenuates alcohol self-administration in rats. *Neuropharmacology* 116, 364–370. doi:10.1016/j.neuropharm.2017.01.007

Hajnal, A., Smith, G. P., and Norgren, R. (2004). Oral sucrose stimulation increases accumbens dopamine in the rat. *Am. J. Physiology-Regulatory, Integr. Comp. Physiol.* 286 (1), R31–R37. doi:10.1152/ajpregu.00282.2003

He, J., and Crews, F. T. (2008). Increased MCP-1 and microglia in various regions of the human alcoholic brain. *Exp. Neurol.* 210, 349–358. doi:10.1016/j.expneurol.2007.11.017

Hermens, D. F., Chitty, K. M., Lee, R. S., Tickell, A., Haber, P. S., Naismith, S. L., et al. (2015). Hippocampal glutamate is increased and associated with risky drinking in young adults with major depression. *J. Affective Disord.* 186, 95–98. doi:10.1016/j.jad.2015.07.009

Holmseth, S., Scott, H. A., Real, K., Lehre, K. P., Leergaard, T. B., Bjaalie, J. G., et al. (2009). The concentrations and distributions of three C-terminal variants of the GLT1 (EAAT2; Slc1a2) glutamate transporter protein in rat brain tissue suggest differential regulation. *Neuroscience* 162 (4), 1055–1071. doi:10.1016/j.neuroscience.2009.03.048

Israel, Y., Quintanilla, M. E., Ezquer, F., Morales, P., Santapau, D., Berríos-Cárcamo, P., et al. (2021). Aspirin and N-acetylcysteine Co-administration Markedly inhibit chronic ethanol intake and block relapse binge drinking: role of neuroinflammation-oxidative stress self-perpetuation. *Addict. Biol.* 26, e12853. doi:10.1111/adb.12853

Kane, C. J. M., Phelan, K. D., Douglas, J. C., Wagoner, G., Johnson, J. W., Xu, J., et al. (2014). Effects of ethanol on immune response in the brain: region-specific changes in adolescent versus adult mice. *Alcohol. Clin. Exp. Res.* 38, 384–391. doi:10.1111/acer.12244

Karahanian, E., Quintanilla, M. E., Fernandez, K., and Israel, Y. (2014). Fenofibrate—a lipid-lowering drug—reduces voluntary alcohol drinking in rats. *Alcohol* 48, 665–670. doi:10.1016/j.alcohol.2014.08.004

Kelley, A. E., Bakshi, V. P., Haber, S. N., Steininger, T. L., Will, M. J., and Zhang, M. (2002). Opioid modulation of taste hedonics within the ventral striatum. *Physiol. Behav.* 76 (3), 365–377. doi:10.1016/s0031-9384(02)00751-5

Kleemann, R., Gervois, P. P., Verschuren, L., Staels, B., Princen, H. M. G., and Kooistra, T. (2003). Fibrates down-regulate IL-1-stimulated C-reactive protein gene expression in hepatocytes by reducing nuclear P50-Nfκb-C/ebp-β complex formation. *Blood* 101 (2), 545–551. doi:10.1182/blood-2002-06-1762

Maisel, N. C., Blodgett, J. C., Wilbourne, P. L., Humphreys, K., and Finney, J. W. (2013). Meta-analysis of naltrexone and acamprosate for treating alcohol use disorders: when are these medications most helpful? *Addiction* 108 (2), 275–293. doi:10.1111/j.1360-0443.2012.04054.x

Marx, N., Sukhova, G. K., Collins, T., Libby, P., and Plutzky, J. (1999). PPARα activators inhibit cytokine-induced vascular cell adhesion molecule-1 expression in human endothelial cells. *Circulation* 99 (24), 3125–3131. doi:10.1161/01.cir.99.24.3125

Melis, M., Pillolla, G., Luchicchi, A., Muntoni, A. L., Yasar, S., Goldberg, S. R., et al. (2008). Endogenous fatty acid ethanolamides suppress nicotine-induced activation of mesolimbic dopamine neurons through nuclear receptors. *J. Neurosci.* 28, 13985–13994. doi:10.1523/JNEUROSCI.3221-08.2008

Melis, M., Scheggi, S., Carta, G., Madeddu, C., Lecca, S., Luchicchi, A., et al. (2013). PPAR regulates cholinergic-driven activity of midbrain dopamine neurons via a novel mechanism involving 7 nicotinic acetylcholine receptors. *J. Neurosci.* 33, 6203–6211. doi:10.1523/JNEUROSCI.4647-12.2013

Mizoi, Y., Ijiri, I., Tatsuno, Y., Kijima, T., Fujiwara, S., Adachi, J., et al. (1979). Relationship between facial flushing and blood acetaldehyde levels after alcohol intake. *Pharmacol. Biochem. Behav.* 10 (2), 303–311. doi:10.1016/0091-3057(79)90105-9

Muñoz, D., Rivera-Meza, M., Flores-Bastías, O., Quintanilla, M. E., and Karahanian, E. (2020). Fenofibrato -un Agonista De PPARα- incrementa Los Niveles de la Alcohol Deshidrogenasa Hepática: Implicaciones Para su Posible Uso Como una Droga de Aversión al Etanol. *Adicciones* 32, 208–215. doi:10.20882/adicciones.1226

Nelson, D. E., Ihekwaba, A. E., and Elliott, M. (2004). Oscillations in NF-B signaling control the dynamics of gene expression. *Science* 306, 704–708. doi:10.1126/science.1099962

Okayasu, T., Tomizawa, A., Suzuki, K., Manaka, K.-i., and Hattori, Y. (2008). PPARα activators upregulate eNOS activity and inhibit cytokine-induced NF-Kb activation through AMP-activated protein kinase activation. *Life Sci.* 82, 884–891. doi:10.1016/j.lfs.2008.02.002

Pahan, K., Jana, M., Liu, X., Taylor, B. S., Wood, C., and Fischer, S. M. (2002). Gemfibrozil, a lipid-lowering drug, inhibits the induction of nitric-oxide synthase in human astrocytes. *J. Biol. Chem.* 277, 45984–45991. doi:10.1074/jbc.M200250200

Pascual, M., Montesinos, J., and Guerri, C. (2018). Role of the innate immune system in the neuropathological consequences induced by adolescent binge drinking. *J. Neuro Res.* 96, 765–780. doi:10.1002/jnr.24203

Plosker, G. L. (2015). Acamprosate: a review of its use in alcohol dependence. *Drugs* 75, 1255–1268. doi:10.1007/s40265-015-0423-9

Poynter, M. E., and Daynes, R. A. (1998). Peroxisome proliferator-activated receptor α activation modulates cellular redox status, represses nuclear factor-Kb signaling, and reduces inflammatory cytokine production in aging. *J. Biol. Chem.* 273, 32833–32841. doi:10.1074/jbc.273.49.32833

Qin, L., Wu, X., Block, M. L., Liu, Y., Breese, G. R., Hong, J.-S., et al. (2007). Systemic LPS causes chronic neuroinflammation and progressive neurodegeneration. *Glia* 55, 453–462. doi:10.1002/glia.20467

Rao, P. S. S., Bell, R. L., Engleman, E. A., and Sari, Y. (2015). Targeting glutamate uptake to treat alcohol use disorders. *Front. Neurosci.* 9, 144. doi:10.3389/fnins.2015.00144

Reissner, K. J., and Kalivas, P. W. (2010). Using glutamate homeostasis as a target for treating addictive disorders. *Behav. Pharmacol.* 21, 514–522. doi:10.1097/FBP.0b013e32833d41b2

Rivera-Meza, M., Muñoz, D., Jerez, E., Quintanilla, M. E., Salinas-Luypaert, C., Fernandez, K., et al. (2017). Fenofibrate administration reduces alcohol and saccharin intake in rats: possible effects at peripheral and central levels. *Front. Behav. Neurosci.* 11, 133. doi:10.3389/fnbeh.2017.00133

Romera, C., Hurtado, O., Mallolas, J., Pereira, M. P., Morales, J. R., Romera, A., et al. (2007). Ischemic preconditioning reveals that GLT1/EAAT2 glutamate transporter is a novel PPARγ target gene involved in neuroprotection. *J. Cereb. Blood Flow. Metab.* 27, 1327. doi:10.1038/sj.jcbfm.9600438

Sari, Y., Franklin, K. M., Alazizi, A., Rao, P. S. S., and Bell, R. L. (2013b). Effects of ceftriaxone on the acquisition and maintenance of ethanol drinking in peri-adolescent and adult female alcohol-preferring (P) rats. *Neuroscience* 241, 229–238. doi:10.1016/j.neuroscience.2013.03.016

Sari, Y., Sreemantula, S. N., Lee, M. R., and Choi, D.-S. (2013a). Ceftriaxone treatment affects the levels of GLT1 and ENT1 as well as ethanol intake in alcohol-preferring rats. *J. Mol. Neurosci.* 51, 779–787. doi:10.1007/s12031-013-0064-y

Schoonjans, K., Staels, B., and Auwerx, J. (1996). Role of the Peroxisome Proliferator-Activated Receptor (PPAR) in mediating the effects of fibrates and fatty acids on gene expression. *J. Lipid Res.* 37, 907–925. doi:10.1016/s0022-2275(20)42003-6

Shehata, A. H. F., Ahmed, A.-S. F., Abdelrehim, A. B., and Heeba, G. H. (2020). The impact of single and combined PPAR-α and PPAR-γ activation on the neurological outcomes following cerebral ischemia reperfusion. *Life Sci.* 252, 117679. doi:10.1016/j.lfs.2020.117679

Staels, B., Koenig, W., Habib, A., Merval, R., Lebret, M., Torra, I. P., et al. (1998). Activation of human aortic smooth-muscle cells is inhibited by PPARα but not by PPARγ activators. *Nature* 393, 790–793. doi:10.1038/31701

Szumlinski, K. K., Diab, M. E., Friedman, R., Henze, L. M., Lominac, K. D., and Bowers, M. S. (2007). Accumbens neurochemical adaptations produced by binge-like alcohol consumption. *Psychopharmacology* 190 (4), 415–431. doi:10.1007/s00213-006-0641-7

Ward, R. J., Colivicchi, M. A., Allen, R., Schol, F., Lallemand, F., de Witte, P., et al. (2009). Neuro-inflammation induced in the hippocampus of 'binge Drinking' rats may be mediated by elevated extracellular glutamate content. *J. Neurochem.* 111, 1119–1128. doi:10.1111/j.1471-4159.2009.06389.x

World Health Organization. (2018). *Global Status Report on Alcohol and Health 2018*. www.who.int/substance_abuse/publications/global_alcohol_report/en/ (Accessed 02 11, 2020).

Conflict of Interest: The authors declare that the research was conducted in the absence of any commercial or financial relationships that could be construed as a potential conflict of interest.

Copyright © 2021 Villavicencio-Tejo, Flores-Bastías, Marambio-Ruiz, Pérez-Reytor and Karahanian. This is an open-access article distributed under the terms of the Creative Commons Attribution License (CC BY). The use, distribution or reproduction in other forums is permitted, provided the original author(s) and the copyright owner(s) are credited and that the original publication in this journal is cited, in accordance with accepted academic practice. No use, distribution or reproduction is permitted which does not comply with these terms.

frontiers in Neuroscience

REVIEW
published: 23 April 2021
doi: 10.3389/fnins.2021.653651

Inflammation and Insulin Resistance as Risk Factors and Potential Therapeutic Targets for Alzheimer's Disease

*Angeles Vinuesa[1,2], Carlos Pomilio[1,2], Amal Gregosa[1,2], Melisa Bentivegna[1,2], Jessica Presa[1,2], Melina Bellotto[1,2], Flavia Saravia[1,2] and Juan Beauquis[1,2]**

[1] Laboratorio de Neurobiología del Envejecimiento, Instituto de Biología y Medicina Experimental, Consejo Nacional de Investigaciones Científicas y Técnicas, Buenos Aires, Argentina, [2] Departamento de Química Biológica, Facultad de Ciencias Exactas y Naturales, Universidad de Buenos Aires, Buenos Aires, Argentina

OPEN ACCESS

Edited by:
Con Stough,
Swinburne University of Technology, Australia

Reviewed by:
Maite Solas,
University of Navarra, Spain
Dubravka Svob Strac,
Rudjer Boskovic Institute, Croatia

***Correspondence:**
Juan Beauquis
juanbeauquis@gmail.com

Specialty section:
This article was submitted to Neuropharmacology, a section of the journal Frontiers in Neuroscience

Received: 14 January 2021
Accepted: 31 March 2021
Published: 23 April 2021

Citation:
Vinuesa A, Pomilio C, Gregosa A, Bentivegna M, Presa J, Bellotto M, Saravia F and Beauquis J (2021) Inflammation and Insulin Resistance as Risk Factors and Potential Therapeutic Targets for Alzheimer's Disease. Front. Neurosci. 15:653651. doi: 10.3389/fnins.2021.653651

Overnutrition and modern diets containing high proportions of saturated fat are among the major factors contributing to a low-grade state of inflammation, hyperglycemia and dyslipidemia. In the last decades, the global rise of type 2 diabetes and obesity prevalence has elicited a great interest in understanding how changes in metabolic function lead to an increased risk for premature brain aging and the development of neurodegenerative disorders such as Alzheimer's disease (AD). Cognitive impairment and decreased neurogenic capacity could be a consequence of metabolic disturbances. In these scenarios, the interplay between inflammation and insulin resistance could represent a potential therapeutic target to prevent or ameliorate neurodegeneration and cognitive impairment. The present review aims to provide an update on the impact of metabolic stress pathways on AD with a focus on inflammation and insulin resistance as risk factors and therapeutic targets.

Keywords: Alzheimer's disease, metabolic disorders, cognitive impairment, insulin resistance, inflammation, therapies

INTRODUCTION

Modern lifestyle is associated with detrimental behavioral and dietary habits such as sedentarism and high dietary intake of saturated fats and refined sugars. These, among other habits, are determinants for the development of obesity, type 2 diabetes (T2D) and associated conditions that have a straightforward impact on several systems including the central nervous system (CNS), thereby heightening the risk for cognitive impairment and neuropsychiatric diseases.

Obesity is a multifactorial disease mainly defined as an excessive accumulation and abnormal distribution of adipose tissue in the body. In terms of prevalence, overweight and obesity rates have increased alarmingly in the last decades currently reaching global epidemic levels (Who, 2018). Almost 40% of the world's adult population was overweight in 2016 and 13% was obese, with the aggravating fact of this trend being featured also at juvenile stages. Moreover, overweight

and obesity constitute the major risk factors for the development of T2D and metabolic syndrome (MetS). As for diabetes, the main hallmark is the presence of increased blood glucose levels and its prevalence was estimated to be close to 9% of the world's population (Idf, 2017). The most common form is the T2D, representing 85–95% of the cases, closely associated with metabolic factors such as obesity. Metabolic syndrome encompasses a variety of conditions associated with cardiometabolic risk, a cluster of alterations including high blood pressure, hyperglycemia, hyperinsulinemia, dyslipidemia and increased abdominal fat or obesity. However, these conditions may not manifest in the same way in all patients. Its prevalence has dramatically increased in a similar fashion as obesity in all age groups (Bussler et al., 2017). Although each of the pathologies stated above has its own features, they are intimately related, sharing components, common risk factors and also being part of the etiology of one another. Therefore, one could attempt to focus on their shared pathways in order to discuss potential mechanisms involved in the development of associated pathologies.

Inflammation and insulin resistance are among the most common phenomena underlying the pathophysiology of obesity- and T2D- related diseases and, interestingly, also consistently found in several neuropsychiatric conditions (Parimisetty et al., 2016; O'Brien et al., 2017; Ying et al., 2020). As it will be further discussed ahead, in neurodegenerative conditions associated with brain aging, the hippocampus is one of the most vulnerable and primarily affected structures, showing atrophy and alterations in neuroplasticity mechanisms related to synaptic connectivity and adult neurogenesis leading to cognitive dysfunction (Mu and Gage, 2011). The fact that chronic metabolic disturbances can also negatively affect such plasticity mechanisms in addition to their association with cognitive deficits and mood alterations (Biro and Wien, 2010; Puder and Munsch, 2010), suggests there are converging pathways of metabolic stress and aging.

In the last decades, it has been reported that T2D, obesity, hypertension and sedentarism are among the main modifiable risk factors for neurodegenerative diseases (Bruce-Keller et al., 2009). In particular, in this review we will focus on Alzheimer's disease (AD) as it is the most prevalent neurodegenerative disease, the major cause of dementia and has a strong association with metabolic disorders and related cardiovascular risk factors.

From several points of view, AD and obesity constitute very relevant public health concerns due to the economic and social burden of the diseases. The economic burden of AD, that was estimated to be more than $300 billion in 2020 only in the United States, is not only related to direct costs such as diagnosis, drug therapy, hospitalization and specialized nursing or home care but also with the quality of life of both patients and caregivers in such a progressive and long- term disease (Alzheimer's-Association., 2020). Global obesity economic burden has been estimated to be two trillion USD in 2014, accounting for a 20% of the total health care and is also related to decreased productivity due to associated disease disability and promotion of premature aging (Tremmel et al., 2017). These diseases' impact over public health could be even much greater if we considered at least four important factors: increasing obesity rates in younger generations, diagnosis underestimation, obesity comorbidities and the lack of effective therapies to mitigate AD-like neurodegeneration.

Taking the above into account, the relevance and interrelation of both metabolic and neurodegenerative health domains leads to the development of a research field devoted to the study of shared pathways in order to better comprehend their dynamics and identify potential solutions (**Figure 1**). Obesity-induced brain inflammation, as a common phenomenon involved in the increased risk for brain dysfunction, could act as a trigger and also as an exacerbating factor in the development of neurodegenerative disorders. Therefore, in this review we will discuss the particular effect of the mentioned metabolic disorders on brain plasticity and the potentiality for inflammatory and associated insulin-resistance mediators as therapeutic targets in AD. Analyzing existing interventions that address either insulin signaling or inflammation might contribute to the understanding of brain

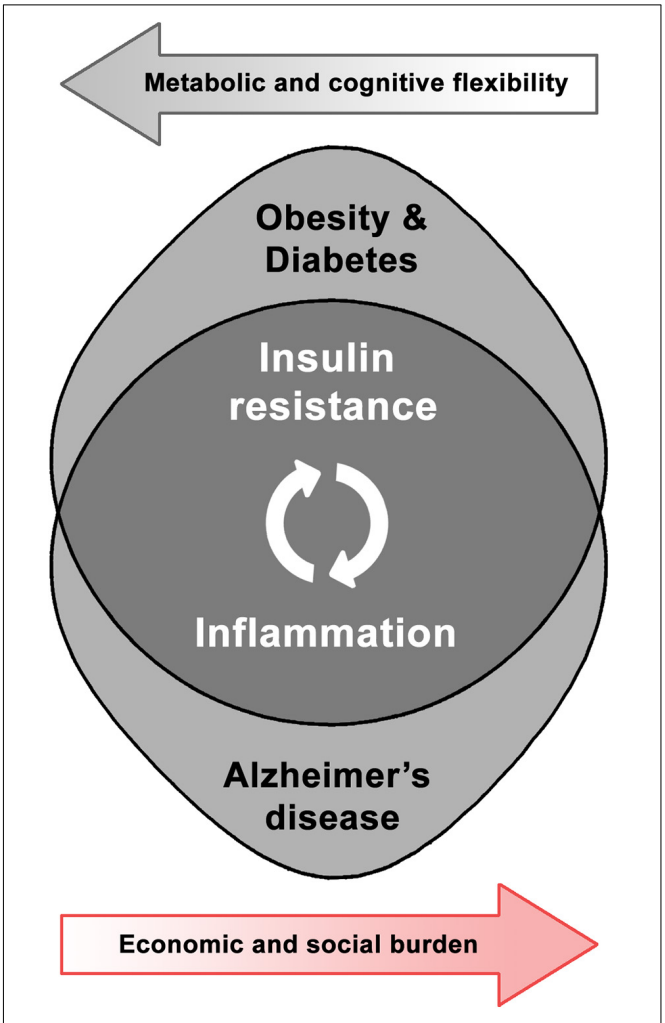

FIGURE 1 | Shared pathophysiological pathways and synergic burden of obesity-related disorders and Alzheimer's disease.

dysfunction mechanisms and neurodegenerative diseases as potential metabolic pathologies.

NEUROLOGICAL CONSEQUENCES OF OBESITY-RELATED DERANGEMENTS: METABOLIC RISK FACTORS FOR ALZHEIMER'S DISEASE

Together with obesity, both mood and neurocognitive disorders are highly prevalent public health concerns and a bidirectional relationship among them has been suggested. Several studies have recently shown a strong association between metabolic disturbances and the development of anxiety-related disorders and poor cognitive outcomes (Avinun and Hariri, 2019; Ronan et al., 2019; van Duinkerken and Ryan, 2019), with higher rates of anxiety and depression found in overweight and obese people (Luppino et al., 2010; Gomes et al., 2019; James et al., 2020). Interestingly, both anxiety and depression are associated with an increased likelihood of developing AD (Becker et al., 2018; Canton-Habas et al., 2020).

As life expectancy has constantly grown, brain aging-related diseases have increased in a similar fashion. Among neurodegenerative disorders, AD is the most common form of age-related dementia. There are approximately 50 million people worldwide suffering from dementia and 60–70% of the cases may be attributed to AD, according to the World Health Organization (Who, 2020). While age is the main risk factor associated to the development of sporadic AD, increasing the chances by 50% every 5 years after 65 years old and reaching a 30–50% prevalence after 85 years of age (Alzheimer's-Association., 2020), it has been reported that T2D and obesity, independently, are associated with an approximate two-to-threefold increased chance of developing AD (Bruce-Keller et al., 2009). Other risk factors for sporadic AD, which constitute more than 95% of AD cases, are the presence of the ε4 allele for apolipoprotein E (APOE) (Morris et al., 2017), hypertension, atherosclerosis, hypercholesterolemia, traumatic brain injury, among others (Edwards et al., 2019). Familial AD, which accounts for 5% of total AD cases, is associated with inherited mutations in the amyloid precursor protein (APP) gene or in the genes for the enzymes that process APP to produce amyloid β (Aβ). Clinically, AD is characterized by the progressive loss of memory and cognitive abilities that ultimately lead to severe impairments in daily life activities. Cerebral extracellular accumulation of Aβ peptide plaques and intraneuronal neurofibrillary tangles of hyperphosphorylated Tau are the main histopathological hallmarks. Among the shared brain alterations between metabolic pathologies and neurodegeneration, insulin resistance constitutes one of the main factors. A considerable body of evidence suggests a relevant overlap across T2D and AD including risk, comorbidity and pathophysiological pathways. As a matter of fact, though controversial, some authors propose that AD might represent the so-called "Type 3 diabetes," given that initial stages of the disease related to cognitive dysfunction go along with multiple alterations of the insulin pathway in the hippocampus (de la Monte and Tong, 2014; Arnold et al., 2018).

The impact of midlife obesity in cognitive decline has been extensively studied and even considered to be an early predictor of AD (Dahl et al., 2010; Chuang et al., 2016; Gottesman et al., 2017). High levels of saturated fatty acid in the cerebrospinal fluid (CSF) of overweight patients with related metabolic comorbidities correlate with amnestic mild cognitive impairment (MCI) (Melo et al., 2020). However, the relevance of obesity may be somewhat controversial across different age groups, particularly depending on the phenotypic parameter assessed. For instance, while a high body mass index (BMI $>$ 25 kg/m^2) in early and midlife obese patients has been associated with the development of cognitive impairment, it is more controversial in the elderly since some reports support the same relationship between both phenomena (Biro and Wien, 2010; Benito-Leon et al., 2013; Melo et al., 2020) while others have not found a significant association (Dahl and Hassing, 2013; Wang et al., 2016; Deckers et al., 2017). In that sense, some studies claim that indirect parameters associated with obesity, such as body fat distribution, hyperglycemia or high-fat diet (HFD) consumption, exhibit higher correlation with cognitive dysfunction in aged cohorts (Assuncao et al., 2018). A large longitudinal analysis by Mac Giollabhui et al. (2020) has shown that higher BMI in a cohort of adolescents predicts a worse performance of executive function and greater depression risk, in a context of peripheral inflammation.

Another obesity-related factor that has been associated with an increased risk of AD is dyslipidemia. Studies in animal models have shown that high consumption of cholesterol and hypercholesterolemia are associated with increased Aβ aggregation and neuroinflammation (Sparks et al., 1994; Zatta et al., 2002; Xue et al., 2007). Correspondingly, high cholesterolemia in middle-aged humans is linked with an increased risk for AD in later life compared with a control population (Solomon et al., 2009) and a lipid profile showing high levels of low-density lipoprotein (LDL) cholesterol and low levels of high-density lipoprotein (HDL) cholesterol is associated with increased Aβ levels in the brain (Reed et al., 2014). However, a recent meta-analysis has found that AD risk is increased in individuals with high LDL cholesterol blood levels but not in those with high levels of HDL cholesterol, total cholesterol or triglycerides (Saiz-Vazquez et al., 2020). Even though cholesterol does not cross the blood–brain barrier (BBB) in physiological conditions, cholesterol oxidized products like oxysterols can cross it and may play a role in memory consolidation and AD pathophysiology (Lutjohann et al., 1996; Kotti et al., 2006).

Regarding experimental data, our group and others have shown neurological consequences associated with cognitive dysfunction and emotional processing alterations in obesogenic contexts. Exposure to a HFD promotes an altered behavioral profile with diminished spatial memory, impaired daily life activities, as well as anxiety and depressive-like behaviors in young adult mice (Vinuesa et al., 2016) and cognitive decline in aged mice (Wei et al., 2018). Likewise, HFD has shown to exacerbate brain pathology and related behavioral impairment in APP/PS1 and 3xTg-AD mouse models of AD (Theriault

et al., 2016; Sah et al., 2017; Bracko et al., 2020), reinforcing the relevant crosstalk between metabolic and age-associated brain dysfunction.

In the following sections of this review, we will provide an overview of the phenomena in common between the aforementioned metabolic and neurodegenerative domains and associated therapeutic approaches, in order to ascertain the relevance of metabolic derangements as drivers of brain dysfunction in AD.

COMMON PATHOPHYSIOLOGICAL FEATURES: INFLAMMATION AND INSULIN RESISTANCE IN THE INTERFACE BETWEEN METABOLIC AND NEURODEGENERATIVE CONDITIONS

Systemic Inflammation

Although many cellular and molecular pathways are affected in the context of diabetes, obesity and metabolic syndrome, one of the primarily occurring phenomena is inflammation. High peripheral levels of inflammatory biomarkers such as C-reactive protein (CRP), IL-6 and TNF-α have been described in obesogenic contexts (Ellulu et al., 2017). Low-grade systemic inflammation is one of the earliest and main pathological events that might lead to the development of insulin resistance in most insulin-sensitive tissues (Kloting and Bluher, 2014; Parimisetty et al., 2016). The activation of the immune system and chronic inflammation are not only featured by increased circulating pro-inflammatory molecules but also by infiltration of macrophages and other immune cells into the affected tissues.

In the context of obesity, the hypertrophied adipose tissue experiments a functional switch, changing the secretory profile of endocrine factors from homeostatic to pathologic or pro-inflammatory, thereby leading to a decreased metabolic flexibility (Ronan et al., 2019), with lower levels of the pro-homeostatic adiponectin and increased levels of pro-inflammatory adipokines, generating a context of chronic low grade inflammation affecting not only adipose tissue but also the liver, insulin-producing pancreatic β-cells, skeletal muscle, the heart and the brain (Ridker et al., 2000; Aleffi et al., 2005; Le et al., 2011). Regarding systemic inflammatory markers, a positive association has been found not only with high BMI and obesity-related parameters but also with CNS impairment. In fact, Mac Giollabhui et al. (2020) reported increased levels of the proinflammatory cytokine IL-6 as a relevant predictor factor of both depression and executive dysfunction in individuals with elevated BMI. In fact, chronic sterile, low-grade inflammation is associated with aging and age-related diseases, leading to the emergent concept of "inflamm-aging" in order to describe a dysregulation in the homeostasis of cytokines and oxidative stress (Franceschi et al., 2018). In the case of AD for instance, there have been described certain genetic variants leading to increased levels of IL-1β, IL-6, and TNF-α that are associated with a greater risk of developing the disease (Wang, 2015; Miwa et al., 2016; Mun et al., 2016). Circulating levels of these mediators, together with CRP, constitute relevant damage biomarkers connecting chronic metabolic diseases such as obesity and T2D with incident dementia or late-onset AD (Franceschi and Campisi, 2014). Moreover, in preclinical AD models, peripheral immune challenges with lipopolysaccharides (LPS) or polyI:C have shown to accelerate or increase Aβ deposition in 3xTg-AD mice and APPswe Tg2576 (Sheng et al., 2003; Kitazawa et al., 2005; Krstic et al., 2012), supporting a role for peripheral inflammatory mediators in brain pathology.

Additionally, in reference to the metabolic-induced inflammatory response, alterations in gut microbiota have also emerged critical for pathogenesis. In the last decade, the gut microbiome has gained increasing interest due to its role in the physiology of humans and several animal models including rodents (Bruce-Keller et al., 2009). The composition and diversity of gut microbiota can be modulated by a wide range of factors including colonization at birth and lifestyle events across the lifespan such as feeding behavior, toxins and antibiotic exposure in addition to aging, experiencing a shift to a decreased diversity in the elderly and thereby contributing to systemic inflammation and detrimental signaling to the brain (Claesson et al., 2012; Bokulich et al., 2016; Sochocka et al., 2019). For instance, HFD exposure has shown to reduce microbiome diversity and transplantation of obese-derived microbiota into control germ-free mice was able to induce metabolic alterations associated with obesity (Turnbaugh et al., 2006; Cani et al., 2008). An unhealthy microbiome could promote a "leaky gut" and thus enable the increase of immunogenic components such as LPS in plasma, a phenomenon known as endotoxemia, contributing to the metabolic inflammation (Carvalho et al., 2012). In a similar fashion, as the gastrointestinal barrier disruption could lead to the increase of potentially toxic effectors in circulation, the BBB integrity has also shown to be affected in the context of metabolic disorders, aging and neurodegeneration (Erickson and Banks, 2013; Salameh et al., 2019). Therefore, the gut-brain axis disruption might as well contribute to the negative impact of peripheral insults on the CNS.

Inflammation in the CNS

Neuroinflammation is a shared hallmark among diverse pathologies and should not be considered an isolated or independent phenomenon from systemic inflammation since different experimental approaches have shown that peripheral inflammatory challenges as well as chronic low grade inflammation trigger inflammation in the CNS (Heneka et al., 2015). In relation to obesity for instance, circulating pro-inflammatory cytokines, free-fatty acids and ceramides have shown to impact also on limbic structures. This effect could be worsened by BBB increased permeability, as it has been described in HFD exposed rodents, leading to the alteration of hippocampal function (Hargrave et al., 2016). Hypothalamic inflammation has been found to be involved in the development as well as in the maintenance of an obese phenotype, promoting and perpetuating unhealthy feeding behavior, altering the reward circuitry (Guillemot-Legris and Muccioli, 2017) and has actually been acutely detected after high-fat feeding, even before the establishment of obesity (Maric et al., 2014). In this context,

reactive gliosis can be found in the arcuate nucleus, being microglial cells the main cell type proposed to sense nutrient overload and trigger the inflammatory response since long-chain fatty acids bind to toll-like receptors (TLR4) and downstream cytokine synthesis and endoplasmic reticulum stress (ERS) pathway (Milanski et al., 2009). On the other hand, several reports have shown that metabolic-induced inflammation is also present in extra-hypothalamic structures such as hippocampus, cortex and amygdala, constituting a relevant link between the neuropsychiatric alterations and obesity or insulin resistance-associated disorders (Parimisetty et al., 2016; Vinuesa et al., 2016; Solas et al., 2017).

As regards age-related cognitive decline, neuroinflammation and oxidative stress are known to be present in the hippocampus and potentially related to the reduced plasticity and associated memory impairment (Frank et al., 2006; Patterson, 2015; Stebbings et al., 2016). Nevertheless, in the particular case of AD-like aging, it is not yet elucidated if inflammation should be considered a trigger, consequence or aggravating factor. Neuroinflammation (mostly given by hyperreactivity of glial cells secreting pro-inflammatory molecules) is consistently found in AD patients and animal models (Heneka et al., 2015). In fact, in the case of animal models, neuroinflammation has been detected even prior to amyloid deposition (Heneka et al., 2005; Beauquis et al., 2013). Reactive glial cells and increased pro-inflammatory mediators have shown to affect both Aβ production and clearance, two processes directly associated with the main histopathological hallmark of AD. For instance, acute neuroinflammation after traumatic brain injury or hypoxia have shown to increase levels of relevant actors for APP amyloidogenic enzymatic cleavage such as the beta-site amyloid precursor protein cleaving enzyme 1 (BACE1), as well as presenilin 1 (PS1) or nicastrin, components of the γ-secretase complex in rodents and pigs (Blasko et al., 2004; Chen et al., 2004; Nadler et al., 2008). Moreover, the deletion of TNF-α in transgenic 5XFAD mice promoted a decreased deposition of Aβ in association with a decreased expression of PS1 and β-secretase (Paouri et al., 2017). Interestingly, Aβ *per se* acts as an important TLR4 ligand, constituting a positive feed-forward loop with neuroinflammation thus contributing to Aβ plaque formation (Stewart et al., 2010). In reference to Aβ clearance, there are several mechanisms affected in the context of chronic or unsolved inflammatory response. Microglial cells, as the first-line defense brain cells, are mostly in charge of removing Aβ deposits by phagocytosis and intracellular proteolysis mechanisms such as proteasome-degradation and autophagy.

During the last decades, several authors emphasized the relevance of the autophagy-lysosomal system and its regulation in age-associated diseases like AD, proposing the modulation of cellular metabolism and the activation of autophagy as a valid therapeutic approach. Autophagy involves the semi-specific isolation of intracellular content -mainly misfolded proteins and dysfunctional organelles- into a double-membrane vesicle called autophagosome. Later, the autophagosome is fused to a lysosome, forming the autolysosome, where the content of the vesicle is degraded and further recycled into the cytosol (Liu and Li, 2019). Autophagy is negatively affected by age, and particularly impaired in AD. The impairment of autophagy involves the accumulation of autophagosomes that do not evolve into autolysosomes, as it was evidenced in neuronal and glial cells, both in patients and experimental models of AD (Gregosa et al., 2019; Uddin et al., 2019; Pomilio et al., 2020; Stavoe and Holzbaur, 2020). While there is no concluding information regarding if autophagy impairment is a cause or a consequence for AD, its dysfunction is related to a loss of amyloid degradation capacity and an accumulation of toxic waste that could lead to reduced neuronal viability and neuroinflammation, reinforcing the degenerative character of this pathology. Chronic activation of autophagy by rapamycin administration is associated with cognitive improvement, decreased amyloid pathology and enhanced autophagy in transgenic mouse models of AD (Spilman et al., 2010; Majumder et al., 2011). Neuroinflammation is also associated with this scenario. Our group has recently shown that microglial autophagy is impaired in AD patients and experimental models (Pomilio et al., 2020), and that this condition is associated with the assembly of inflammasomes and the production of the proinflammatory cytokine IL-1β (Cho et al., 2014). Interestingly, a recent article by Liu et al. (2020) showed that promoting microglial autophagy in APP/PS1 mice using nanoparticles not only enhances amyloid degradation but also reduces neuroinflammation by causing a decrease in brain levels of proinflammatory cytokines and an increase in anti inflammatory cytokines, finally conducing to a better performance in cognitive tests.

Autophagy in the brain is not independent of peripheral stimuli. In the last years, several studies showed that gut microbiota is altered in transgenic mouse models of AD, and that restoring microbiota enhances the autophagic flux in the brain, amyloid degradation and cognitive performance (Bonfili et al., 2017, 2018; Chen et al., 2017). Particularly, Bonfili et al. (2017) showed that microbiota restoration causes a decrease in plasma levels of proinflammatory cytokines, suggesting that peripheral inflammation, brain autophagy and neurodegeneration are closely related.

Alterations of Insulin Signaling Pathways

Insulin Resistance Triggers

Overall, the canonical function of insulin is to maintain glucose homeostasis and to regulate cellular division and growth through the PI3K/Akt pathway and mitogenic activity through the RAS/MAPK signal transduction pathway. The concept of insulin resistance emerges when insulin levels, whether elevated or within normal range, are associated with a diminished metabolic response or sensitivity (Wilcox, 2005).

Several reports indicate that inflammation affects insulin signaling pathways in insulin-sensitive tissues (Kloting and Bluher, 2014; Parimisetty et al., 2016). Hence, it seems evident that obesity-induced inflammation is closely related to the development of T2D, mainly featured by an inefficient action of insulin or insulin resistance, thus placing insulin in the center of the scene. Among the candidate molecules involved in this inflammatory response are reactive oxygen species (ROS), pro-inflammatory cytokines such as TNF-α, IL-1β, IL-6 and

stress kinases as Jun N-terminal kinase (JNK), inhibitor of kappaB kinase (IKK) and protein kinase C (PKC) (Boucher et al., 2014). Regarding IL-1β, there are relevant factors to be considered particularly associated with acute and chronic effects in relation to glycemic control. It has been shown that postprandial-induced hyperglycemia triggers inflammasome-mediated maturation and secretion of IL-1β in adipose macrophages as an homeostatic mechanism to favor insulin-dependent glucose uptake and protect the organism against potential food microbes (Dror et al., 2017). Nonetheless, when the pro-inflammatory cytokine levels together with hyperglycemia-induced ROS are sustained chronically, deleterious effects arise and contribute to the development of insulin resistance (Maedler et al., 2002). The latter has been proposed not only for IL-1β but other inflammatory cytokines such as TNF-α and IL-6. Hotamisligil et al. (1993), one of the first groups in assigning a relevant role for inflammatory cytokines such as TNF-α in the context of experimental obesity or diabetes, also proposed that the endoplasmic reticulum (ER) should be considered as an essential component in the coordination of metabolic responses (Hotamisligil, 2010; Kloting and Bluher, 2014) and could also be involved in the disruption of insulin signaling. Under physiological conditions, proteins are synthesized at the ER, folded, modified and ultimately targeted to the appropriate cellular compartment. However, when there is an uncontrolled or excessive increase in protein synthesis and presence of incorrectly folded proteins, the ERS response or unfolded protein response (UPR) is triggered to activate JNK/AP1, IKK, NFκB and oxidative stress pathways. In the context of metabolic stress, nutrient overload or elevated free fatty acids constitute potential inductors of this response (Velloso et al., 2015).

Another relevant phenomenon underlying inflammation-induced insulin resistance is the activation of TLRs, members of the pattern recognition receptor family responsible for the innate immune response. Interestingly, different rodent models of TLR4 ablation, either genetically modified by knock-out approaches (Poggi et al., 2007; Jia et al., 2014; Li et al., 2014) or by pharmacological inhibition (Zhang et al., 2015), have shown to prevent HFD-induced insulin resistance. As for TLR4 ligands in obesogenic contexts, it has been reported that long chain fatty acids increased in obesity-related contexts are able to stimulate TLR4 signaling leading to the development of insulin resistance (Velloso et al., 2015). Regarding lipotoxic stimuli as insulin-resistance inducers, ceramides have also been found to be very relevant. Ceramides are important bioactive lipidic messengers regulating cellular functions such as stress response, inflammation and survival. Levels are increased in obesogenic and diabetogenic contexts and were found to induce insulin resistance both *in vitro* and *in vivo* (Holland et al., 2011; Chavez et al., 2014). Even though ERS and TLRs activation have been originally studied as independent mechanisms in the pathophysiology of metabolic disorders, there is a considerable body of evidence suggesting a constant crosstalk between them in the modulation of metabolic dysfunction and inflammation associated to a decreased insulin sensitivity and downstream actions (Guillemot-Legris and Muccioli, 2017).

During insulin resistance, the activity of Akt -a main effector of the insulin receptor pathway- remains low. Akt is a multi-substrate kinase that regulates the activity of the AMP-dependent kinase (AMPK). Although AMPK is activated by several stimuli, it acts as a master regulator for cellular metabolism and its activation is necessary as a mediator for insulin effects on skeletal muscle and adipose tissue, as it was recently reviewed by Chen et al. (2020). Particularly, AMPK activation directly inhibits *de novo* lipid synthesis and enhances fatty acid oxidation, linking its activity with insulin resistance and macrophage activation in the context of obesity and T2D (Herzig and Shaw, 2018). In fact, activation of AMPK is proposed as the mechanism responsible for the therapeutic effects of metformin and other antidiabetic treatments, as it is mentioned ahead in Section "Therapeutic Approaches." Akt and AMPK altogether regulate the activity of the mammalian target of rapamycin (mTOR) complex. The activation of Akt leads to the activation of mTOR, while AMPK directly inhibits its function. When activated, mTOR upregulates major anabolic pathways like protein synthesis while inhibiting protein degradation through the downregulation of the autophagic-lysosomal system (Herzig and Shaw, 2018).

Insulin sensitivity, among other factors, is regulated by a number of small insulin-sensitive adipocytes (Leonardini et al., 2009), via PPARγ, a member of the peroxisome proliferator-activated receptors (PPAR) family that regulates the expression of several genes, mainly related to metabolism and inflammation. It is highly expressed in adipose tissue, and also in the liver and skeletal muscle (Vidal-Puig et al., 1996). The endogenous ligands of PPARs are free fatty acids and eicosanoids, favoring lipid storage in adipose tissue while reducing lipotoxicity, promoting an anti-inflammatory response and enhancing insulin sensitivity (Varga et al., 2011). It has been hypothesized that PPARγ function is also neuroprotective. It was found to be expressed in the hippocampus, cortex and hypothalamus and is associated with decreased levels of pro-inflammatory mediators, ROS and Aβ in AD models (Inestrosa et al., 2005; Warden et al., 2016).

Insulin Effects on the Brain

Mainly known for its role in peripheral glucose homeostasis, insulin also has a significant impact within the brain, functioning as a key neuromodulator in behavioral, cellular, biochemical and molecular studies. Emerging evidence from human and animal studies indicate that insulin influences cerebral bioenergetics and neural functioning (Kellar and Craft, 2020). The brain is now regarded as an insulin-sensitive organ with widespread, yet selective, expression of the insulin receptor in the olfactory bulb, hypothalamus, hippocampus, cerebellum, amygdala and cerebral cortex. In the hypothalamus, insulin signaling modulates metabolism, food intake and energy balance (Lee and Mattson, 2014), while in extra-hypothalamic structures such as the hippocampus, insulin actions are associated with neurotrophic and neuromodulatory functions. Insulin receptor signaling in the brain is important for neuronal development, glucose regulation, feeding behavior, body weight, and cognitive processes such as executive functioning, learning and memory (Kellar and Craft, 2020). Insulin receptors are abundantly expressed in neurons and glial cells (Frolich et al., 1998) and,

together with insulin-like growth factors (IGFs) and receptors, regulate functions like neuron differentiation, dendritic growth, neuronal survival, circuit development, synaptic plasticity and postsynaptic neurotransmitter receptor trafficking (Kleinridders et al., 2014; Gralle, 2017), playing a key role in memory and learning (Blazquez et al., 2014; Ferrario and Reagan, 2017). Consistently, individuals with diabetes or insulin resistance show hippocampal atrophy, alterations in brain connectivity and variable degrees of cognitive impairment, shared phenomena between metabolic and neurodegenerative disorders (Beauquis et al., 2008, 2010; Dey et al., 2017).

Insulin signaling has been shown to be impaired in experimental models of AD (Chua et al., 2012; Ferreira et al., 2018) and in patients (Baker et al., 2011). Brain insulin resistance is a cause for dysregulation of brain bioenergetics, and also leads to enhanced Aβ production, impaired axonal transport, apoptosis and neuroinflammation, as it was recently reviewed by Nguyen et al. (2020). Particularly, impaired hippocampal insulin signaling is associated with impairments in memory and other executive functions, and it is proposed as a mediator between peripheral insulin resistance in T2D and brain dysfunction in AD. In line with this, Li et al. (2018) demonstrated that an animal model presenting both T2D and AD exhibits accelerated neurodegeneration and cognitive impairment, in association with dysregulation of the insulin degrading enzyme (IDE) expression. IDE is an extracellular protease that degrades not only insulin, but also Aβ, in a competitive way. Several authors have proposed that Aβ clearance by IDE could be impaired as IDE is saturated by the high insulin levels in the extracellular space due to insulin resistance, finally leading to Aβ accumulation and aggregation (Qiu and Folstein, 2006; Mayeux and Stern, 2012; Li et al., 2018).

Insulin resistance has also been associated with the modulation of amyloid production, tau phosphorylation and neuroinflammation through the regulation of glycogen synthase kinase (GSK)−3 activity (Jope et al., 2007). This kinase is one of the main targets of the PI3K/Akt pathway and is inactive upon phosphorylation by Akt. Hence, it has been hypothesized that a defect in insulin signaling would lead to GSK3 activation through diminished PI3K/Akt signaling. Subsequently, activation of GSK3 would lead to a number of effects among which tau hyperphosphorylation (Ishiguro et al., 1993) and increased Aβ production through BACE1 activation (Ly et al., 2013) or APP phosphorylation (Rockenstein et al., 2007) could play a significant role in AD pathogenesis. However, there are conflicting results in studies addressing this issue. While some support this hypothesis (Steen et al., 2005) others have found that inactive forms of GSK3 are present in AD brains (Griffin et al., 2005) and this discrepancy would depend on the progression (early vs. late stages) of the disease (Jimenez et al., 2011).

It has been shown that insulin resistance, induced by chronic exposure to a HFD promotes short-term memory impairments and decreases brain-derived neurotrophic factor (BDNF) and phospho-Akt levels in the prefrontal cortex and hippocampus. BDNF, a neurotrophin associated with synaptic and neural plasticity, shares components of the PI3K/Akt insulin pathway through the interaction with tropomyosin receptor kinase B (TrkB) (Kowianski et al., 2018). This fact stresses the relevance of these signaling cascades' crosstalk and the consequent impact of the potential impairment induced by metabolic alterations.

Even though there is a solid body of literature supporting a mainly pro-homeostatic role of insulin on brain function, contradicting evidence in relation to aging and neurodegeneration should not be ignored. Particularly, and in conflict with the previously mentioned deleterious effects of insulin resistance, there is evidence from animal models suggesting that the downregulation of insulin signaling may have protective effects in aging and AD. In Tg2576 mice, a commonly used model of AD, neuronal deletion of insulin receptor substrate 2 (IRS2) is associated with decreased Aβ deposition in the brain, improved cognitive performance and increased survival of adult animals (Freude et al., 2009; Stohr et al., 2013). However, it should be noted that the expression of Akt and other downstream components of the insulin signaling pathway are unaffected by the deletion of IRS2 in this model. Similarly, using the nematode *Caenorhabditis elegans* expressing a minigene for human $A\beta_{1-42}$, Cohen et al. (2006) have shown that amyloid aggregation is decreased and aging is slowed when insulin signaling is reduced after a treatment with a *daf-2* RNAi. Regarding human studies, Harries et al. (2012) have shown that the expression of genes participating in insulin signaling as PI3K, PTEN, FOXO and PDK1 is decreased in aged human populations in a similar fashion to that seen under the pro-longevity mTOR inhibition therapy. Thus, these results may suggest that decreased insulin signaling may have a role extending lifespan and modulating amyloid aggregation, in potential conflict with therapeutic strategies aimed at promoting insulin signaling. However it is not clear yet if the impairment of insulin signaling is a consequence of neurodegeneration or a protective response, stressing the need for more mechanistic and functional studies to clarify this central point.

Alterations of Neural Plasticity

The brain is exposed to a highly dynamic environment and requires concerted mechanisms to exert appropriate responses. In that sense, brain plasticity represents the CNS intrinsic ability to act upon constantly changing conditions by means of structural and functional processes. Among the phenomena involved in such flexibility, synapse formation, elimination or strength modulation, as well as the promotion of hippocampal neurogenesis are essential mechanisms (Kelly et al., 2006; Selemon, 2013; Lucassen et al., 2015). In line with this, alterations of such mechanisms of structural plasticity are associated with cognitive decline and memory dysfunction in aging and neurodegenerative disorders.

Adult Hippocampal Neurogenesis

Hippocampal neurogenesis is a key neuroplastic process that involves the proliferation of neural precursor cells (NPCs) in the subgranular zone (SGZ), differentiation, survival and proper integration into the hippocampal circuit. It is a thoroughly relevant process underlying emotional behavior and cognitive function mainly associated with memory and learning (Clelland et al., 2009; Toda and Gage, 2017). Neurogenesis occurs during

development and continues throughout life, persisting even in aged adults and AD patients. Nevertheless, it declines with age and is strongly affected by the environment (Klempin and Kempermann, 2007). Tobin et al. (2019) recently showed that adult neurogenesis exhibits a positive correlation with cognitive status in MCI and AD versus aged patients and could render an early sign of the disease. Animal models of AD show decreased rates of hippocampal neurogenesis (Mu and Gage, 2011; Myhre et al., 2019). Interestingly, overactivation of GSK3β by genetic blockade of the kinase inhibition in NPCs has been associated with diminished neurogenesis together with impaired hippocampus-dependent behavior in mice (Eom and Jope, 2009; Pardo et al., 2016), reinforcing the relevance of neurotrophin-induced signaling in hippocampal plasticity affected in age-related neurodegeneration.

Taking into account metabolic disturbances as negative modulating factors, the aforementioned conditions associated with obesity and T2D, insulin resistance and sustained inflammation have consistently shown to promote neural connectivity dysfunction. Several studies from our group and others have reported alterations in hippocampal neurogenesis as a consequence of HFD exposure, occurring in association with impaired cognitive and emotional processing (Boitard et al., 2012; Hao et al., 2016; Vinuesa et al., 2016, 2019). In particular, the early-onset of HFD exposure in rodents has shown to be especially detrimental; both C57BL6/J mice after 6 (Vinuesa et al., 2019) or 11 (Boitard et al., 2012) weeks of HFD exposure and 12-week-old rats exposed to a cafeteria diet (Ferreira et al., 2018), showed a drastic reduction of the total number of doublecortin (DCX+) cells in the SGZ of the DG. Besides, hippocampal neurogenesis appears to be affected also in genetic models of obesity such as the leptin-deficient ob/ob mice, with alteration of proliferation and differentiation processes in the SGZ (Bracke et al., 2019). Leptin receptor-deficient db/db mice, that develop diabetes in addition to obesity, also show a reduction of neurogenic capability in association to a cognitively impaired phenotype (Stranahan et al., 2008).

Synaptic Plasticity

As regards structural changes in dendritic spines and synaptic plasticity upon metabolic disturbances, HFD exposure for instance has been associated to cause alterations either in the density or the morphology patterns of dendritic spines in the hippocampus. Hao et al. (2016) showed that animals exposed to HFD since 6 weeks of age suffered a decrease in the density of dendritic spines in dentate granule neurons in adulthood which was reversible by switching to a low fat diet. Additionally, work from our group has shown that a moderate HFD exposure since weaning, was associated with a predominance of immature dendritic spines in CA1 pyramidal neurons in young adult C57BL/6 mice, even though the total density of dendritic spines remained unchanged (Vinuesa et al., 2019). Moreover, dendritic spine reduction was also detected in pyramidal neurons of the parietal cortex in the context of streptozotocin-induced diabetes in hyperglycemic rats, together with an impaired memory performance assessed by the Morris Water Maze (MWM) (Malone et al., 2008).

Synaptic failure and loss are key factors underlying cognitive impairment in AD patients (Scheff et al., 2006, 2015). Progressive dendritic spine alterations were found to correlate with intracellular Tau deposits in postmortem analysis (Merino-Serrais et al., 2013), thereby associating functional and histological hallmarks of the disease. Several studies have also shown dendritic spine loss and synaptic dysfunction in animal models of AD, where Aβ toxicity appears to be the main contributor (Tu et al., 2014; Subramanian et al., 2020). Apart from Aβ-induced toxicity, dendritic spine and associated synaptic alterations could be associated with reduced levels of BDNF in MCI and AD patients, reinforced by the neuroprotective effects of the neurotrophin reported in experimental AD models (Peng et al., 2005; O'Bryant et al., 2009; Caccamo et al., 2010; Jiao et al., 2016). BDNF signaling through TRKB receptor and PI3K-Akt-GSK3β pathway are central regulators mediating synaptic plasticity-required dendritic spine turnover and preserving long-term potentiation (LTP) (Peineau et al., 2007; Kowianski et al., 2018). The fact that neurotrophin-induced regulation shares the main components of insulin pathway and is counteracted by proinflammatory mediators such as IL-1β (Tong et al., 2012), stresses the relevance of insulin resistance in AD pathophysiology.

The fact that the mentioned alterations of structural plasticity present in AD are also induced by metabolic pathologies would support a further exacerbation of neuroplasticity decline by interaction of age-related neurodegeneration with obesity and associated disturbances.

THERAPEUTIC APPROACHES

Given the relevance of insulin resistance and its close association with inflammation as common pathophysiological mechanisms present in metabolic and neurological disorders, in the following sections we will address the aforementioned phenomena as potential therapeutic targets for CNS dysfunction in AD-related pathology. The crosstalk between these pathways on the brain is schematized in **Figure 2**, showing the main actors involved and identifying with letters A-I the potential targets that will be discussed below, classified as insulin signaling-, inflammation- or lifestyle-based approaches.

Insulin Signaling-Based Approaches

Among the existing treatments that address insulin resistance mainly used in diabetic patients, several clinical and pre-clinical studies have assessed the effect of insulin signaling-based approaches as potential mitigators of brain dysfunction and cognitive impairment.

Intranasal Insulin

As it was previously mentioned, the bioavailability and downstream actions of insulin in the brain can be diminished in the context of MCI, dementia and particularly in AD, supporting the concept of the disease as "Type 3 Diabetes." The administration of insulin in the context of diabetes is a well-known treatment. Nevertheless, regarding potentially positive

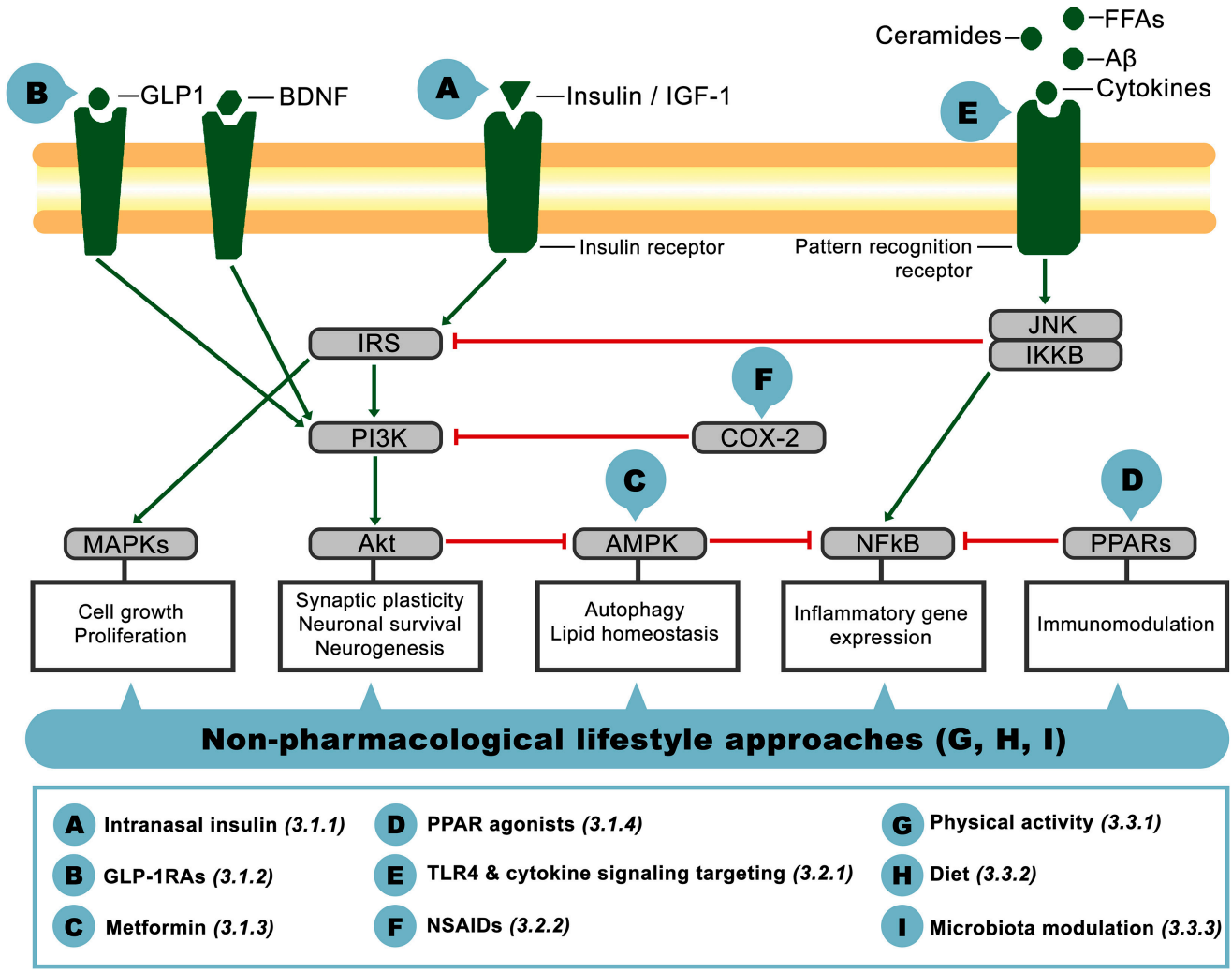

FIGURE 2 | Schematic representation of interacting components of the insulin signaling and inflammatory pathways on the brain. Pointed-head arrows depict activation and blunt-end arrows inhibition, while letter circles A-I point the level at which the potential therapeutic approaches discussed in this article would act. Treatment definition and corresponding reference section are defined in the inferior square.

neurological outcomes, the systemic administration of insulin results in low transport levels to the brain and, on the other hand, may account for undesirable side effects such as hypoglycemia (Schmid et al., 2018). In that sense, intranasal (IN) insulin delivery represents a safe and non-invasive method that has gained increased interest in neurodegeneration research, both in patients and animal models. Intranasal administration of insulin has shown a rapid and widespread distribution through perineural spaces of the trigeminal nerve and the ability to activate the insulin receptor (Lochhead et al., 2019). The common doses of IN insulin range from 20 to 160 IU according to different studies, with different outcomes even though there is a growing consensus that IN administration is able to promote changes on CNS as well as peripheral pathways. There are many positive metabolic effects of IN insulin such as body weight management, food intake and fat composition, with variations according to sex, age and protocol of administration (Derkach et al., 2017). However, in this review we will focus on cognitive-related outcomes. Several clinical studies, some of which are explicated in **Table 1**, have shown that either IN insulin or its long-lasting analog Detemir were associated with memory improvement both in cognitively intact (Benedict et al., 2004) and impaired individuals. Memory amelioration in AD subjects was observed for different doses of IN insulin and treatment duration with APOE-ε4 allele being a strong though controversial moderating factor. Different trials assessing acute (Reger et al., 2008) or 4-month chronic IN insulin treatment (Craft et al., 2017) showed improved memory outcomes for APOE-ε4 non-carriers, albeit the latter report also exhibited minor but significant changes in APOE-ε4 carriers. Contrary to these studies, Claxton et al. (2015) only detected IN insulin positive modulation of verbal and visuospatial working memory in AD or MCI adults carrying APOE-ε4 genetic variant. Additionally, in this cohort of patients a greater degree of insulin resistance at baseline

TABLE 1 | Clinical trials targeting insulin resistance and/or inflammation for the treatment of cognitive impairment and AD.

Study	Subjects	Age	Treatment	Observations	Main outcomes
Insulin signaling- based approaches					
Benedict et al. (2004)	38	18–34	8w IN insulin (4 × 40 IU)/day	Healthy subjects	Enhanced long-term declarative memory Better mood rating
Reger et al. (2008)	92	74–77	IN insulin dose (0, 10, 20, 40, or 60 IU)across 5w	MCI, AD subjects	Improved verbal memory in APOE ε4- but no APOE ε4 + MCI and AD adults
Claxton et al. (2015)	60	–	21d IN insulin Detemir (0, 20, 40 IU)	MCI, AD subjects	No memory changes with 20 IU Improved memory in APOE ε4 + but reduced in APOE ε4- with 40 IU
Craft et al. (2017)	36	60–80	4m IN insulin or Detemir (0, 40 IU)	MCI to moderate AD subjects	Improved delayed memory composite scores for regular insulin compared to placebo Greater improvement in insulin treated APOE ε4 non-carriers No memory changes with Detemir
Gejl et al. (2016)	38	50–80	26w GLP1-RA liraglutide	AD patients	No significant differences in cognitive scores or Aβ levels Improved cerebral glucose metabolism
Mullins et al. (2019)	27	71–74	18m GLP1-RA exenatide	MCI/early AD (early terminated trial)	Reduced BMI and improved glucose tolerance; No significant differences in cognitive test or AD CSF biomarkers; Reduced $A\beta_{1-42}$ in neuronal-derived plasma EVs
Koo et al. (2019)	732	≥60	Metformin	Non-diabetic and diabetic subjects	Association of metformin with rapid cognitive deterioration
Koenig et al. (2017)	20	55–80	8w metformin/placebo	Non-diabetic MCI/early AD	Improvement in executive function, with a trend in amelioration of learning and memory No changes in CSF levels of Aβ, Tau or pTau
Luchsinger et al. (2016)	80	55–90	12m metformin/placebo	Non-diabetic, overweight/obese, MCI patients	Decreased inflammatory marker CRP Improved scores in total recall tests No changes in plasma levels of Aβ-42
Ryan et al. (2006)	141	43–75	Metformin monotherapy + rosiglitazone/glyburide	T2D patients	Improved working memory, no changes in learning ability or mood Improved blood glucose with both drugs Decreased CRP and fasting insulin with rosiglitazone
Sato et al. (2011)	42	77	6m Pioglitazone	Mild AD patients with T2D	Improved scores in MMSE, ADAS-J-cog, and WMS-R logical memory-I Improved rCBF and insulin sensitivity
Watson et al. (2005)	30	55–85	6m Rosiglitazone	Mild-to-moderate cognitive impaired patients	Improved delayed recall and selective attention Decreased plasma Aβ levels in the placebo group but no changes with RSG
Risner et al. (2006)	511	50–85	24w placebo, 2–4–8 mg Rosiglitazone	Mild-to-moderate AD patients	No effect of RSG but interaction with APOε-4 genotype, with an improvement in the ADAS-cog of APOε-4 positive patients
Gold et al. (2010)	693		24w placebo/2 or 8 mg RSG XR/10 mg donepezil	Mild-to-moderate AD patients	No significant differences in cognitive outcome or Aβ levels
Inflammation- based approaches					
Larsen et al. (2007)	70	50–70	Anakinra (IL1β receptor antagonist)	T2D patients	Decreased glycemia and β cell function Decreased CRP and IL6
Cavelti-Weder et al. (2012)	98	34–70	Gevokizumab	T2D patients	Improved glycemia and reduced systemic inflammation
Aisen et al. (2003)	351	>50	One year rofecoxib/naproxen/placebo	Mild-to-moderate AD patients	No changes in ADAS-Cog scores
Pasqualetti et al. (2009)	132	≥65	One year-ibuprofen/placebo	Probable mild/moderate AD patients	No effect on cognitive decline Less cognitive worsening in APOE-ε4 carriers than APOE-ε4 non-carriers

(Continued)

TABLE 1 | Continued

Study	Subjects	Age	Treatment	Observations	Main outcomes
Non-pharmacological lifestyle approaches					
Hoffmann et al. (2016)	200	50–90	16w–60 min moderate-to-high PA x3/w or control	Mild-to-moderate AD patients	Less severe neuropsychiatric symptoms in intervention group Potential cognitive improvement in high-intensity maintenance group
Jensen et al. (2019)	200	50–90	16w–60 min moderate-to-high PA x3/w or control	Mild-to-moderate AD patients	Increased sTREM2 in exercise group CSF and IL6 in plasma Reduced plasma IFNγ in control vs. exercise APOE-ε4 carriers
Sobol et al. (2018)	49	69 (52–83)	16w–60 min moderate-to-high PA x3/w or control	Mild-to-moderate AD patients	Increased cardiorespiratory capacity (VO2 peak) Positive association of VO2 peak with cognitive and neuropsychiatric symptoms
Napoli et al. (2014)	107	≥65	52wPA, diet or both and control	Obese and sedentary patients	Weight loss and exercise positively associated with improved scores in cognitive status
Shellington et al. (2018)	25	≥50	24wSSE (square stepping exercise)	T2D, non-demented but cognitive alterations self-reported	Improved executive function
Quinn et al. (2010)	402	76 (9.3)	18m DHA	Mild-to-moderate AD patients	No beneficial behavioral or functional changes found
Freund-Levi et al. (2006)	174	76 (9)	6–12m DHA and EPA	Mild-to-moderate AD patients	Positive effect in cognitive decline rate only in small subgroup with very-mild AD
Shinto et al. (2014)	34	>55	12mDHA and EPA	Probable AD patients	Decrease decline in MMSE score
Eriksdotter et al. (2015)	174		6m DHA and EPA	Mild-to-moderate AD patients	Inverse association between omega 3 seric PUFAs and cognitive deterioration rate
Reger et al. (2004)	20	74.7	Ketogenic MCT (medium chain triglycerides)	aMCI or probable AD	Improved ADAS-cog scores in APOE-ε4 non-carriers
Taylor et al. (2018)	15	73.1	3m KD supplemented with MCT	Very mild/mild/moderate AD patients	Improved ADAS-cog scores in KD group
Henderson et al. (2009)	152	51–93 (76.8)	Ketogenic compound AC-1202	Mild-to-moderate AD patients	No overall cognitive changes, improvement in APOE ε4 non-carriers
Tamtaji et al. (2019)	79	(77.8) 55–100	12w probiotics + selenium/selenium/placebo	AD patients	Probiotics + selenium group exhibited improved MMSE scores than placebo or Selenium only
Kobayashi et al. (2019a)	27	82.5 (5.3)	24w *Bifidobacterium breve* A1	MCI elder patients	Improved cognitive and mood scores
Kobayashi et al. (2019)	117	61.6 (6.83)	12w *Bifidobacterium breve* A1	MCI elder patients	Improved scores at neuropsychological tests

was associated with greater cognitive improvement after the treatment (Claxton et al., 2015).

As regards animal models, IN insulin treatment has been associated with positive results in the behavioral profile, brain metabolic pathways, neuroinflammation and plasticity of several rodent models of AD-like aging. For instance, 4- to 5-month-old APP/PS1 transgenic mice treated with IN insulin for 6 weeks presented enhanced memory performance and decreased anxiety-like behavior, along with improved histopathological signs such as decreased levels of soluble Aβ and Aβ plaques in the hippocampus and cortex, insulin-signaling rescue and enhanced hippocampal neurogenesis in relation to vehicle-treated mice (Mao et al., 2016). Moreover, IN insulin treatment has shown beneficial effects in the non-transgenic model SAMP8 AD-like mice. Twelve-month-old AD-like mice exhibited cognitive improvement assessed by spatial memory and object recognition paradigms (Salameh et al., 2015). The same insulin dose rendered hippocampal gene expression changes associated with the inflammatory response in young and aged SAMP8 mice (Rhea et al., 2019). Consistent with this, IN insulin treatment exhibited a positive cognitive, metabolic and histopathological outcome in 14-month-old HFD-induced 3xTG-AD mice (Sanguinetti et al., 2019). Furthermore, in the intracerebroventricular (i.c.v) streptozotocin-induced model, claimed by several authors to promote an AD-like phenotype, IN insulin has shown to prevent memory impairment, neuroinflammation and insulin resistance in the hippocampus and cortex (Rajasekar et al., 2017a), as well as promoting restored cerebral blood flow (CBF), decreased ROS and increased BDNF expression (Rajasekar et al., 2017b).

Glucagon-Like Peptide 1 Receptor Analogs (GLP-1 RAs)

Glucagon-like peptide 1 is a peptide hormone mainly synthesized in intestinal L-cells and is one of the incretin hormones promoting glucose-induced insulin secretion by the pancreas after food intake, reducing the release of glucagon and also protecting the pancreas by preventing apoptosis of β-cells (Farilla et al., 2003; de Heer et al., 2008). Apart from these effects, it has been shown that this hormone plays an important role in different organs. For instance, GLP-1 receptors are also present in the liver, heart and brain. GLP-1 function has been associated to the prevention of cardiovascular diseases (Bethel et al., 2018) and constitutes a key component of the gut-brain axis, behaving as a relevant neuropeptide, not only for the regulation of food intake and glucose homeostasis but as a neuroprotective factor in relation to synaptic function and plasticity (Gault and Holscher, 2008). As regards T2D and obesity treatment, there are currently approved GLP-1 RAs such as exenatide, liraglutide and lixisenatide which are resistant to the enzymatic cleavage of dipeptidyl peptidase-4 (DPP-4), thus accounting for an increased half-life in comparison to endogenous GLP-1, that have shown positive management of the disease (Aroda, 2018). Given the pleiotropic character of GLP-1 R and in particular its role in neuromodulation and associated cognitive-related outcome, the use of GLP-1 RAs has been proposed as a potential therapy for neurodegenerative diseases (Gejl et al., 2016). Interestingly, Parkinson's disease patients that participated in a randomized controlled trial (RCT) for exenatide exhibited improved motor and cognitive scores 12 months after the trial endpoint (Aviles-Olmos et al., 2014).

Although there is an important research gap regarding clinical evidence in AD given the limitation of sample size or unfinished trials (Mullins et al., 2019), as it is shown in **Table 1** for the GLP-1RAs exenatide and liraglutide, there is very promising data drawn mainly from preclinical animal models of AD.

In that sense, Cai et al. (2018) showed that the GLP-1 RA lixisenatide treatment for 60 days in 12-month-old APP/PS1/Tau AD female mice promoted a decreased Aβ plaque load and p-Tau levels in the hippocampus, along with a decreased neuroinflammatory status. In a previous work, the same group also showed the ability of lixisenatide to ameliorate memory performance assessed by the MWM in intrahippocampal Aβ-injected rats (Cai et al., 2014). Regarding exenatide and cognitive outcome in AD rodent models, its use has been associated to memory improvement in i.c.v streptozotocin (STZ)-induced rats when treated during 2 weeks (Solmaz et al., 2015) and Bomba et al. (2013) showed that 3-month-old PS1-KI mice treated for 9 months with the GLP-1RA had improved performance in MWM while the 3xTg-AD assessed within the same protocol, did not show cognitive amelioration. Despite the lack of cognitive improvement in 3xTg-AD mice, the authors later showed that exenatide promoted an enhanced BDNF signaling and reduced inflammation in HFD-induced 3xTg-AD mice (Bomba et al., 2019). Moreover, Batista et al. (2018) have recently reported neuroprotective features of liraglutide not only in mice i.c.v-injected with Aβ oligomers (AβO) but also in non-human primates (NHP). Interestingly, the GLP-1 RA was able to revert AβO-induced cognitive impairment as well as to prevent insulin receptor loss in mice hippocampus, the latter also being found in NHP, along with synapse loss prevention and decreased p-Tau levels (Batista et al., 2018). Finally, a dual therapy targeting both GLP-1 and GIP incretin receptors, proposed as improved candidates for T2D treatment, has shown to ameliorate memory impairment, Aβ deposition, glial reactivity and expression of synaptic marker PSD95 in 10-month-old APP/PS1 mice, potentially due to the rescue of proteostatic functions associated to the enhancement of autophagy and decreased ERS response (Panagaki et al., 2018).

Metformin

Metformin constitutes one of the most common treatments for T2D. It is an oral biguanide and anti-hyperglycemic drug that acts as an insulin sensitizer, lowering blood glucose by increasing its uptake and reducing hepatic gluconeogenesis (Zhou et al., 2001). Although metformin's mechanism of action is not thoroughly understood, it has been associated with the activation of Ampk. The use of metformin in diabetic patients has been associated not only with blood glucose control but also with an improved lipidic profile and decreased inflammatory markers (Lin et al., 2018). Concerning the impact of metformin in cognitive decline, either induced in the context of diabetes or among age-related AD patients, there is promising evidence albeit contradictory data should be also taken into account. In **Table 1**, we can find a representative selection of clinical studies addressing brain-related outcomes of metformin treatment in aged patients with/without diabetic medical history. For instance, in a pilot study, Koenig et al. (2017) showed that metformin exposure in non-diabetic patients with MCI or early signs of AD was associated with an ameliorated cognitive function, even though no changes in AD CSF biomarkers such as Aβ, Tau or p-Tau levels were observed. Moreover, in non-diabetic patients with amnestic MCI co-occurring with overweight or obesity, metformin appeared to ameliorate systemic inflammation lowering CRP levels and a partial improvement in recall memory (Luchsinger et al., 2016). However, in a prospective cohort report with a 1–7.6 years range follow-up, comparing older non-diabetic patients and diabetic patients treated or not with metformin, the exposure to the biguanide drug was not associated with changes in Ad assessment as shown by the Korean version of the Consortium to Establish a Registry for Alzheimer's Disease Assessment Packet (Cerad-K), the short geriatric depression scale (SGDS) or activities of daily living score (Barthel ADL index). In fact, when analyzing annual "rapid deterioration" among diabetic patients, the authors found metformin to be associated with a more marked deterioration (Koo et al., 2019). Nonetheless, more longitudinal and larger cohort studies should be assessed since there are confounding factors such as other antidiabetic treatments and lifestyle factors (diet and exercise), that may account for the variability and conclusions of such complex studies.

Concerning experimental assessment of metformin in animal models, the use of the anti-hyperglycemic drug has shown to rescue hippocampal plasticity alterations and associated cognitive outcomes in both metabolic dysfunction-induced

and AD-like paradigms. As an example, oral administration of metformin in middle-aged C57BL/6J mice was able to rescue spatial memory impairment, adult neurogenesis in the DG, presumably by the enhanced signaling of IR/IRS1 and AMPK/PKC detected in the hippocampus of metformin chronic exposure (Tanokashira et al., 2018). In the same line, db/db mice exposed to metformin exhibited an improved spatial memory assessed by the MWM and a lesser degree of hippocampal atrophy (Chen et al., 2019). In the context of experimental AD, 26-week-old APP/PS1 female mice were treated during 14 days with i.p metformin and several pathophysiological parameters were changed. Along with hippocampus-dependent memory improvement, metformin exposure in APP/PS1 mice was associated with an increased neurogenic ability, reduced Aβ soluble levels and deposits as well as an amelioration of the inflammatory status in hippocampus and cortex, in relation to vehicle-treated APP/PS1 mice. As regards the potential mechanisms involved, the authors showed the relevance of the reported induction of AMPK/mTOR/PKC pathway since at least the inflammatory response and soluble Aβ levels decreased by metformin in the hippocampus and cortex of APP/PS1 mice was impaired in the presence of AMPK inhibitor (Ou et al., 2018). Interestingly, in a sporadic AD model, 12-month-old SAMP8 mice treated with metformin for 8 weeks, also exhibited an ameliorated behavioral profile with improved learning and memory parameters together with decreased levels of Aβ and p-Tau, even though pGSK3β was found to be slightly increased (Farr et al., 2019).

PPAR Agonists

Among insulin sensitizing drugs, another relevant category is represented by thiazolidinediones such as rosiglitazone (RSG) and pioglitazone (PIO). Such compounds, commonly used in the management of T2D, are agonists/ligands of PPARγ receptor, a master regulator of adipose tissue differentiation. As regards clinical evidence of pharmacological ligands of PPARγ, several reports addressed the impact of glitazones on the cognitive status of patients with diabetes and/or MCI-AD (**Table 1**). Ryan et al. (2006) analyzed diabetic patients with metformin monotherapy that were exposed during 24 weeks to RSG or glyburide treatment. In the metabolic sphere, both drugs were able to improve blood glucose and fasting insulin levels and C-peptide were only reduced in the rosiglitazone group. Both drugs were associated with improved working memory, even though no differences were registered in learning ability or mood assessment (Ryan et al., 2006). Concerning T2D patients co-occurring with mild AD, antidiabetic add-on therapy with PIO for 6 months enhanced insulin sensitivity, improved patients performance in the following cognitive tests: Mini- Mental State Examination (MMSE), Alzheimer's Disease Assessment Scale- Cognitive Subscale Japanese version (ADAS-J-Cog), and Wechsler Memory Scale-revised (WMS-R) logical memory-I and regional CBF in the parietal lobe (Sato et al., 2011). The effect of RSG in AD patients is rather controversial yet. Although certain preliminary or explorative analyses showed an association with cognitive improvement (Watson et al., 2005) or an interaction of the treatment with APOE-ε4 genotype (Risner et al., 2006), this was not further supported by Gold et al. (2010) in their large clinical study and future clinical evidence is needed.

In relation to experimental data from animal models and potential mechanisms involved, PPAR agonists have shown positive effects in AD pathophysiology and cognitive status. For instance, the treatment of 3xTG-AD female mice with PIO was associated with several beneficial effects such as learning improvement, decreased Aβ and Tau deposits in the hippocampus and enhanced hippocampal plasticity shown by increased LTP, along with decreased plasma cholesterol levels (Searcy et al., 2012). Neuroprotective outcomes in AD models were also found by combining different PPAR agonists. For example, the use of PPAR-δ and PPAR-γ agonists L165,041 and F-L-Leu, respectively, has shown positive changes in brain slices from i.c.v STZ injected rats: decreased inflammation, improved mitochondrial function and reduced Aβ neurotoxicity, although lipid peroxidation and cholinergic function were not rescued (Reich et al., 2018), suggesting that PPAR ligand therapies should be thought as complementary treatments in AD-like pathology. In the same line, a recent report showed that targeting PPAR-α with fenofibrate and PPAR-γ with PIO during 21 days ameliorated memory impairment induced by $A\beta_{1-40}$ i.c.v injection. Additionally, authors found the Wnt/β catenin to be enhanced with the treatment, proposing this signaling pathway relevant for neuron plasticity and synaptic remodeling altered in AD and mood disorders to be involved (Assaf et al., 2020).

Inflammation-Based Approaches

As mentioned in previous sections, inflammation is a crucial phenomenon in the development of insulin resistance-related pathologies and targeting different components of the inflammatory response has been a promising yet challenging approach in chronic metabolic pathologies such as obesity and diabetes. Furthermore, taking into consideration that inflammation is a common factor occurring also in a wide variety of neuropsychiatric pathologies, and with microglia being a fundamental element in such response, many authors have undertaken experimental animal approaches to inhibit inflammation and ultimately microglial cells with the aim to reverse cognitive decline. In the present section, we will analyze available inflammation-based therapies used in diabetes or obesity and the impact as potential treatment for AD.

TLR4 and Cytokine-Signaling Targeting

As it was previously described, inflammatory mediators are intimately related to the promotion and propagation of metabolic-induced damage in insulin-resistant contexts both in the periphery and the CNS. Even though anti-inflammatory therapies are not primary treatments for diabetes, obesity or AD, there is interesting clinical and preclinical evidence that may as well contribute to strengthen the role of inflammation and enable the design of future strategies.

As regards TLR4 direct targeting, neurological available data is scarce and comes mostly from animal models possibly due to its relevance in innate immunity and potential secondary effects. Moser et al. (2018) showed that in pathologic contexts such as

diet-induced obesity, pharmacological microglia TLR4 inhibition with TAK-242 prevented adverse neurological outcomes by decreasing microgliosis, enhancing neurogenesis and potentially modifying amyloidogenic pathways. Consistent with this, the neutralization of HMGB1, a TLR4 ligand has shown to reverse cognitive decline and brain pathology in the 5xFAD mouse model. The subcutaneous administration of HMGB1 monoclonal antibody was able to recover dendritic spine density and decrease DNA damage in 6-month-old 5xFAD cortex (Fujita et al., 2016). In the same line, inhibiting obesity-induced microglia activation has shown to ameliorate cognitive decline in two different approaches: pharmacologically with the use of minocycline and genetically by the downregulation of microglial fractalkine receptor (Cope et al., 2018). Accordingly, in a very recent report, Melo et al. (2020) showed that targeting microglia inflammation induced by the exposure to the saturated fatty acid palmitate prevented both the defective insulin signaling in hippocampal cultures and also in rodents, in addition to amelioration of the cognitively impaired phenotype. This was achieved by the use of two different approaches: minocycline or TNFα- neutralizing antibody therapy with infliximab. The latter also prevented memory impairment in mice exposed to chronic HFD feeding (Melo et al., 2020), reinforcing the role of pro-inflammatory cytokines as mediators of metabolic-induced impairment of hippocampal flexibility, as it will be further discussed.

In relation to TLR4 downstream signaling, there is an increasing body of literature addressing NFκB induced-cytokines targeting. One of the most studied is IL-1β due to its close association with metabolic inflammation and insulin resistance. IL-1β receptor antagonists (IL-1β RA) have been used in clinical trials focused both on diabetic and AD-like scenarios as it can be seen in **Table 1**. For instance, T2D adult patients treated with the IL-1β RA anakinra presented ameliorated glucose levels and pancreatic function with decreased systemic inflammation markers such as CRP and IL6 (Larsen et al., 2007) and similar results were observed with the use of IL-1β neutralizing antibody Gevokizumab (Cavelti-Weder et al., 2012). As regards the impact of cytokine inhibition in cognitive decline and AD pathology, evidence comes mostly from animal models. APP/PS1 mice lacking either NLRP3 or caspase 1, which are key components for the maturation and secretion of IL-1β, showed improved spatial memory, synaptic plasticity and decreased Aβ levels (Heneka et al., 2013), suggesting a relevant role of the pro-inflammatory cytokine in the progression of AD pathology. In the same line, LTP analysis in a rat model of amyloidosis (McGill-RThy1- APP TG rat) showed improved synaptic plasticity when animals were treated with NLRP3 inhibitor Mcc950, IL-1β RA anakinra or anti- TNF-α (etanercept) (Qi et al., 2018). TNF-α is also one of the most relevant pro-inflammatory cytokines and its neutralization has been associated with improved cognition and synaptic flexibility in different AD models. XPro 1595 anti- TNF-α antibody rescued LTP, Aβ deposition and inflammatory response in 5xFAD (MacPherson et al., 2017) and the neutralization TNFSF10 pro-apoptotic cytokine belonging to TNF family was also able to improve spatial memory, decrease Aβ levels and inflammation in the hippocampus of 3xTG-AD mice (Cantarella et al., 2015). Interestingly, XPro 1595 anti- TNF-α antibody also exhibited interesting results in a diet-induced obesity paradigm by exposing C57BL/6 mice to a high-fat high-carbohydrate diet. Authors have recently found not only an improvement of metabolic parameters associated to dyslipidemia and insulin resistance in the periphery but also central insulin signaling was improved in the hypothalamus and prefrontal cortex, together with behavioral changes in anxiety-like behavior (De Sousa Rodrigues et al., 2019), reinforcing the potential of anti-inflammatory strategies in metabolic- and brain-dysfunction contexts.

Non-steroidal Anti-inflammatory Drugs (NSAIDs)

Non-steroidal anti-inflammatory drugs (NSAIDs) constitute a well-known strategy for targeting both acute and chronic inflammation in diverse contexts. There are different types of compounds in this category with primarily anti-inflammatory and analgesic consequences, associated with the inhibition of cyclooxygenase (COX) activity and downstream prostaglandin synthesis (Rao and Knaus, 2008). Given the relevance of the inflammatory response in the pathophysiology and progression of chronic metabolic diseases such as obesity and T2D as well as in the context of AD-like dementia, there has been a genuine interest in preclinical and clinical exploration of NSAIDs as potential therapies. However, there is controversial or insufficient data as regards their efficacy. In relation to AD risk and progression, there is observational data suggesting a potential benefit of NSAIDs usage in the prevention of the disease (Etminan et al., 2003) and small clinical trials providing evidence in the same line (Rogers et al., 1993), albeit further RCTs should be conducted. For instance, in a quite large multicenter RCT, Aisen et al. (2003) showed that the selective Cox-2 inhibitor rofecoxib or traditional NSAID naproxen failed to ameliorate cognitive decline after 12-month exposure to the drugs in mild-to-moderate AD patients. Additionally, drug-exposed groups reported adverse effects such as dizziness, hypertension and fatigue more frequently than placebo (Aisen et al., 2003). Consistent with this work, 12-month exposure to ibuprofen was also unable to slow time-dependent cognitive decline, even though an interestingly favorable different outcome was seen for APOE-ε4 carriers in comparison with non-carriers (Pasqualetti et al., 2009). In the same line, the large longitudinal trial assessing naproxen or celecoxib NSAIDs contributed to the "non-beneficial" body of evidence of these drugs for improvement of AD cognitive impairment (Group et al., 2008).

Despite the predominance of disappointing clinic results, animal models of AD have shown positive effects of NSAIDs in the progression of the disease. For example, ibuprofen treatment was associated to decreased Aβ deposition, microglial activation and inflammatory cytokine levels in the APP Tg2576 AD mice model, together with improved signs of degeneration shown by decreased dystrophic neurites (Lim et al., 2000; Yan et al., 2003). Likewise, decreased microglial activation and Aβ deposition was observed in 12-month-old APP/PS1 transgenic mice treated with the NCX-2216 NSAID agent (Jantzen et al., 2002). Moreover, and in relation to diabetes and cognitive impairment, Wang et al. (2011) showed that aspirin treatment during 4 and 8 weeks

promoted decreased levels of pro-inflammatory cytokines in the hippocampus and improved spatial memory in STZ-induced diabetic mice.

Liver X Receptor (LXR) Agonists and Cholesterol Targeting

As mentioned, cholesterol and its oxidized forms called oxysterols are associated with increased risk for AD, promotion of amyloid pathology and induced inflammation. Oxysterols are ligands for liver X receptors (LXRs), nuclear receptors that function as lipid-activated transcription factors and regulate cholesterol homeostasis (Wang and Tontonoz, 2018). Besides their role on lipid metabolism, LXRs can regulate inflammation and neuroinflammation. Evidence from *in vitro* models showed that LXR agonists inhibit the production of pro-inflammatory mediators from microglia and astroglia at least in part through interfering with the capacity of NFκB to bind DNA and induce transcription (Zhang-Gandhi and Drew, 2007). Also LXR agonists can interfere with Aβ production and decrease soluble amyloid peptides in the brain of the APP23 mouse model of AD (Koldamova et al., 2005). Some drug candidates have been proposed for AD treatment but due to the mixed nature of LXRs effects and adverse effects such as dyslipidemia and hepatic steatosis (Grefhorst et al., 2002; Tai et al., 2014), clinical translation of these strategies has been unsuccessful. Novel agonists overcoming these effects can have potential as AD therapies.

A more direct approach has been proposed using statins and cholesterol lowering therapies. First known for their protective effects on cardiovascular disease, statins were then proposed as risk-reducing therapies for AD, with many studies describing protection against the risk of dementia and AD but failing when tested in controlled randomized trials, probably due to the complexity of AD, to the variety of lipids involved (HDL cholesterol, LDL-cholesterol, triglycerides) and the separate cholesterol pools (circulation vs. brain) that coexist (reviewed in Reitz, 2013; Samant and Gupta, 2021). Another strategy aims at enhancing CYP46A1 activity, the enzyme that converts cholesterol to 24S-hydroxycholesterol (24S-OHC), the major oxysterol in the brain. This oxysterol, besides its effects on cholesterol metabolism and function as LXR agonist, is an α-secretase activator that hence decreases the rate of Aβ production and plaque formation (Bjorkhem et al., 2009). Efavirenz, L-glutamine and dapagliflozin are some of the CYP46A1 activators that showed promising results in experimental models and are being tested in clinical trials (Mast et al., 2017; van der Kant et al., 2019; Samant and Gupta, 2021).

Non-pharmacological Lifestyle Approaches

As it can be appreciated in the previous sections, on a general basis insulin function-based therapies appear to downregulate inflammation and inflammation-based therapies seem to improve insulin sensitivity, supporting the notion of inflammation and insulin resistance as bidirectionally affecting phenomena. In that line, in the present section we will discuss non-pharmacological lifestyle approaches mainly associated to diet and physical activity interventions in aged adults either with obesity comorbidity or age-related cognitive impairment. Interestingly, such approaches can be potentially proposed not only as treatments but also as relevant preventive strategies in order to promote a healthier aging and improved quality of life.

Physical Activity (PA)

Among lifestyle modifiable risk factors associated with AD, great attention has been devoted to physical activity since sedentarism is a crucial risk factor for obesity, cardiovascular disease and is also associated with impaired cognitive function. Sustained physical activity has shown to ameliorate overall health and particularly maintain cognitive function in disease-free elders even when taken up at late stages (Elosua et al., 2005; Hamer et al., 2014). Moreover, non-demented patients with physical and cognitive frailty exhibited positive results regarding both physical parameters such as muscle strength and speed and also in cognitive flexibility when exposed to a 4 months high-speed resistance exercise training (Yoon et al., 2018). Given the lack of successful therapies for age-related dementia, and in particular due to AD, several clinical trials have addressed exercise-based interventions as a potential treatment of AD symptoms, some of which are cited in **Table 1**. For instance, a RCT assessing the impact of high-to-moderate exercise in patients diagnosed with probable mild or moderate AD has shown to improve neuropsychiatric symptoms and cognitive status after 16 weeks of continuous attendance to the program (Hoffmann et al., 2016). From the same trial, Jensen et al. (2019) recently reported the effect of the intervention on inflammatory biomarkers. Although they did not find many significant changes, the exercise group presented increased CSF levels of sTREM2 and IL-6 in plasma and, interestingly, APOE-ε4 non-carriers had reduced levels of IFNγ than APOE-ε4 carriers after exercise intervention (Jensen et al., 2019). A subgroup of the patients enrolled in the trial were subjected to cardiorespiratory fitness assessment and an improvement was found in the intervention group, together with a positive association with mood and cognitive outcomes (Sobol et al., 2018). In close association with the physical activity approach, dance therapy constitutes a non-pharmacological alternative that has exhibited positive outcomes in the amelioration of several symptoms related to AD pathology. Exposure to different types of dance sessions has shown to promote improvement in diverse domains including physical well-being, mood and cognitive status, irrespective of the practice duration (Lazarou et al., 2017; Marquez et al., 2017). However, it should be noted that this kind of intervention not only entails moderate exercise but also social interaction. Therefore, the improvement assessed would be the result of mixed stimuli resembling an enriched sensory-motor environment, as proposed by Kattenstroth et al. (2010).

In reference to the interaction with obesity or insulin resistance in the older population, lifestyle interventions also showed to ameliorate cognitive function. Even though the impact of weight loss in the elderly is controversial, in the case of obese older patients, weight loss associated to diet and exercise has shown positive outcomes in several measures assessing global cognition. In fact, the combination of both

interventions appeared to be better, although for several parameters the combination of diet and exercise was no different than exercise alone (Napoli et al., 2014). Additionally, albeit being a rather small sample-sized study, a light exercise intervention promoted mild improvement in executive functioning in non-demented T2D patients with self-reported cognitive impairment (Shellington et al., 2018).

Regarding experimental models, there is an extensive body of literature addressing the impact of exercise paradigms on brain function (Ryan and Kelly, 2016). Exercise has elicited positive effects on cognition, brain metabolism and plasticity. For instance, 6-month-old APP/PS1 mice subjected to regular exercise during 4 weeks exhibited improved learning and spatial memory together with decreased levels of Aβ and p-Tau in the cortex and hippocampus. Additionally, it promoted enhanced mitochondrial function and increased synaptic density (Pang et al., 2019). Likewise, it was recently reported that hippocampus-dependent memory and synaptic puncta were positively modulated in 12-month-old mice of the same strain subjected to running during 4 months (Zhang et al., 2020). Furthermore, running in the 5xFAD mice promoted beneficial effects in spatial memory and Aβ burden along with increased BDNF levels and enhanced adult neurogenesis. Interestingly enough, these effects were partially mimicked by the combination of adult neurogenesis enhancement via NPCs' pharmacologically induced survival and BDNF overexpression in the hippocampus. These effects were not detected when neurogenesis alone was stimulated, suggesting a crucial role for BDNF in the exercise-induced response (Choi et al., 2018). Moreover, exercise has also shown to ameliorate hippocampus-dependent behavior, together with inflammation and oxidative stress in the "sporadic" rat model of AD induced with SZT (Lu et al., 2017). Finally, exercise has also promoted pro-cognitive, pro-neuroplastic and anti-inflammatory effects in metabolically challenged contexts such as diabetes or diet-induced obesity (Ruegsegger et al., 2019; Wang et al., 2019), becoming a quite strongly recommendable lifestyle approach not only to prevent the development of the mentioned chronic disorders but also being potential therapies in the amelioration of life quality by targeting inflammation and insulin resistance derangements.

Diet

In the same sense that highly processed fat and sugar-enriched western diets negatively affect metabolism, inflammatory status and cognitive function, modulating dietary composition can be a powerful strategy to positively modify the aforementioned health domains. For instance, Mediterranean diet (MD) has been associated with general wellbeing and preserved cognitive function in the elderly (McGrattan et al., 2019). MD is predominantly constituted by fruits, vegetables, wholegrains and legumes, fish and poultry to a lesser extent and a very low intake of red meats and processed food where olive oil is the main source of fat, thereby associated with antioxidant and anti-inflammatory components. Although MD has exhibited an important adherence among commonly proposed diets, the use of certain supplements addressing some of its components has also been related to beneficial effects. As an example, lycopene is a potent antioxidant carotenoid present in fruits and vegetables that has shown protective effects in several chronic diseases such as cancer, cardiovascular disease and neurodegeneration (Saini et al., 2020). As regards dietary interventions, CNS impact of lipid metabolism-based supplements was given attention. Not only approaches to decrease cholesterol levels were studied (Chu et al., 2018) but also administration of fish oil or similar supplements containing omega3 polyunsaturated fatty acids (PUFAs) for their potentiality to maintain cognitive function. The most commonly used PUFAs are docosahexaenoic acid (DHA), eicosapentaenoic acid (EPA), and alpha-linolenic acid (ALA), which are reported as relevant precursors of neuronal membrane components, fluidity and signaling (Chappus-McCendie et al., 2019). As it can be appreciated in **Table 1**, several clinical trials analyzed the impact of DHA and EPA in patients with mild-to-moderate AD and mixed results were obtained. Quinn et al. (2010) were not able to find significant effects of DHA in a quite large RCT. Nevertheless, when administration of DHA was combined with EPA, other clinical studies found either a subtle cognitive improvement in a subgroup of very-mild AD (Freund-Levi et al., 2006) or a decrease of cognitive decline rates in mild-to-moderate AD patients (Shinto et al., 2014; Eriksdotter et al., 2015).

Among dietary interventions, fasting, calorie restriction and ketogenic diets (KD) have also been widely proposed to reverse obesity and T2D, being able not only to promote weight loss but also to enhance insulin sensitivity and reduce inflammation (Harvie et al., 2011; Myette-Cote et al., 2018). In the present section, we will discuss the impact of these particular dietary approaches on brain plasticity and pathological hallmarks as potential therapies for AD-like neurodegeneration. Fasting can be defined as a period of food deprivation. It has been associated with different socio-cultural factors from religion to periods of food scarcity and it was later related to increased lifespan in several species (Brandhorst et al., 2015). There are different fasting protocols described in the literature, mainly due to length and frequency variations. Essentially, intermittent or periodic fasting and dietary restriction are very similar approaches since the main phenomenon is the time restriction of food intake. At the level of the metabolic response and in a similar fashion as ketogenic diets, these dietary interventions lead to an increase of ketone bodies, producing relevant changes in glucose metabolism (Wilhelmi de Toledo et al., 2019). Ketogenic diet is mainly featured by a very high-fat and low-carbohydrate intake and can be difficult to sustain, therefore the increase of ketone bodies can also be achieved by administering medium chain triglycerides (MCT) without changing the diet (Reger et al., 2004; Henderson et al., 2009; Taylor et al., 2018). In **Table 1**, we can find a selection of relevant clinical studies addressing their impact on cognitive function.

As regards experimental studies, KD, intermittent fasting (IF) or dietary restriction (DR) have shown to promote improved glucose metabolism together with anti-inflammatory and cognitive amelioration in animal models of AD. For instance, KD exposed 3xTg-AD mice exhibited enhanced memory and learning ability in addition to decreased hippocampal Aβ deposition (Kashiwaya et al., 2013), while APP/V7/171 transgenic female mice also showed decreased levels of Aβ along with

positive metabolic changes in response to KD, though the behavioral alterations were not significantly improved (Van der Auwera et al., 2005). As for intermittent fasting, it was recently shown that App NL-G-F mice maintained in an IF protocol alternating *ad libitum* and fasting days for a month, exhibited an adaptive response to acute fasting with improved memory and anxiety-related outcomes. The behavioral profile amelioration occurred concomitantly with synaptic remodeling dependent of SIRT3 mitochondrial deacetylase (Liu et al., 2019), suggesting that IF can modulate oxidative stress, thereby constituting a potential approach to mitigate AD-related cognitive impairment and synaptic dysfunction. In the same line, our group and others have shown that DR represents a moderate and feasible schedule capable of improving cognitive function in aged wild type (Ma et al., 2018) and PDAPP-J20 transgenic mice (Gregosa et al., 2019). In the latter, we found that three cycles of DR alternated with *ad libitum* feeding between 6.5 and 8 months of age not only was able to improve spatial memory but was also associated with enhanced neurogenesis and decreased Aβ load in the hippocampus. Moreover, periodic DR prevented microglial activation and promoted a decrease in the levels of hippocampal IL-1β, thus counteracting the neuroinflammatory status.

Microbiota Modulation

The inflammatory status in the mentioned structures of the CNS present in the context of metabolic diseases has been associated with a low-grade chronic inflammation response both detected and potentially triggered in the periphery. One of the possible mechanisms corresponds to alterations of the gut microbiota affecting the microbiome-gut-brain axis. Obesity-related disorders are often reported to co-occur with dysbiosis-associated inflammation and interventions with probiotics and related bioactive compounds have been able to reverse inflammatory parameters and ameliorate cognitive decline and hippocampal plasticity alterations, such as LTP and synaptic activity (Solas et al., 2017). Gut microbiome diversity alterations have been associated with the AD-like pathological context, not only in relation to the gut but also BBB dysfunction (Vogt et al., 2017). Therefore, probiotic supplementation has been proposed as a potentially beneficial strategy to improve AD symptoms by modulating microbiota and ultimately the gut-brain axis. Probiotics are living microorganisms that have shown to elicit beneficial effects in the host, preventing infections, obesity-related alterations as well as promoting CNS positive modulation (Hutchinson et al., 2020). As it can be appreciated in the studies cited in **Table 1**, different probiotic formulations have shown to ameliorate cognitive function in patients with MCI or AD. For instance, Tamtaji et al. (2019) showed that the administration of a probiotic therapy containing *L. acidophilus*, *B. bifidum*, and *Bifidobacterium longum* co-supplemented with selenium, present in several beneficial probiotic formulations, was able to promote improved cognitive performance as well as an ameliorated metabolic profile. Peripheral inflammation decreased together with enhanced insulin sensitivity and an ameliorated lipidemic profile (Tamtaji et al., 2019). Consistently with this data, there is also experimental evidence of positive outcomes in 3x-Tg mice that were given selenium-enriched yeast for 3 months. Interestingly, spatial memory was improved concomitantly with reduced neuroinflammation, GSK3β-dependent Tau phosphorylation and increased expression of synaptic proteins in the cortex and hippocampus (Zhang et al., 2017). In the same line, in a pilot study and a larger RCT (Kobayashi et al., 2019a,b), analyzed the impact of a 6- or 3-month probiotic supplementation with *Bifidobacterium breve* A1 in aged patients with MCI, respectively. In both cases, administration of the probiotics resulted in improved scores at neuropsychological tests assessing cognitive and mood status. Likewise, *Bifidobacterium breve* A1 administration to mice that were i.c.v- injected with Aβ elicited an anti-inflammatory response, along with an improvement of cognitive decline (Kobayashi et al., 2017). Taken together, this experimental and clinical data suggests that probiotic supplementation may constitute a beneficial lifestyle approach to enrich and reshape gut microbiome, thereby exerting an anti-inflammatory and anti-neurodegenerative response to AD pathological context.

CONCLUDING REMARKS

The alarming prevalence of both AD and obesity- related metabolic disorders and the consequent implications in public health strongly require the rise of efficient therapeutic solutions. The fact that metabolic alterations are risk factors for the development of age-related dementia not only reinforces the relevance of the problem but also provides useful insight as regards potential research fields to further explore. Therefore, this review intended to highlight the shared pathways at the interface of these pathologies as potential targets to override AD burden.

Insulin resistance and chronic inflammation are two synergic phenomena underlying the pathogenesis of metabolic diseases as well as the development of the wide variety of associated disorders, including AD-like neurodegeneration. Therapeutic approaches targeting these interacting factors could be proposed as potential AD treatments even though data is variable and there is an important gap between experimental evidence from animal models and replication in clinical trials. Several factors should be taken into account. Firstly, the specific origin or etiology of the diseased context might differ considerably, with a variable substrate to address mainly according to age but also as regards pre-existing or co-occurring morbidities, namely developmental traits, obesity, diabetes and genetic predisposition. Secondly, and in association with the lack of etiology certainty in AD patients, the proposed therapies may be targeting either causes or mere symptoms, with an additional factor: the targeted pathways redundancy and compensatory mechanisms. In that sense, lifestyle approaches may tackle different pathological components in a more extensive/holistic manner, serving also as powerful preventive strategies.

AUTHOR CONTRIBUTIONS

AV, CP, AG, MnB, JP, MsB, FS, and JB discussed, wrote and reviewed this manuscript. All authors contributed to the article and approved the submitted version.

FUNDING

This work was supported by Williams, René Barón and Alberto J. Roemmers Foundations, ANPCyT PICT Grants 2013-2645, 2014-1168, 2016-1046, and 2016-1572, CONICET PIP Grant 2013-2015, and UBACyT 2018.

ACKNOWLEDGMENTS

AV and CP are postdoctoral CONICET fellows, MsB is Ph.D. CONICET fellow, AG and JP are Ph.D. ANPCyT fellows, FS and JB are CONICET researchers.

REFERENCES

Aisen, P. S., Schafer, K. A., Grundman, M., Pfeiffer, E., Sano, M., Davis, K. L., et al. (2003). Effects of rofecoxib or naproxen vs placebo on Alzheimer disease progression: a randomized controlled trial. *JAMA* 289, 2819–2826. doi: 10.1001/jama.289.21.2819

Aleffi, S., Petrai, I., Bertolani, C., Parola, M., Colombatto, S., Novo, E., et al. (2005). Upregulation of proinflammatory and proangiogenic cytokines by leptin in human hepatic stellate cells. *Hepatology* 42, 1339–1348. doi: 10.1002/hep.20965

Alzheimer's-Association. (2020). *2020 Alzheimer's disease facts and figures. Alzheimer's and Dementia. The Journal of the Alzheimer's Association*.

Arnold, S. E., Arvanitakis, Z., Macauley-Rambach, S. L., Koenig, A. M., Wang, H. Y., Ahima, R. S., et al. (2018). Brain insulin resistance in type 2 diabetes and Alzheimer disease: concepts and conundrums. *Nat Rev Neurol* 14, 168–181. doi: 10.1038/nrneurol.2017.185

Aroda, V. R. (2018). A review of GLP-1 receptor agonists: Evolution and advancement, through the lens of randomised controlled trials. *Diabetes. Obes. Metab* 20(Suppl. 1), 22–33. doi: 10.1111/dom.13162

Assaf, N., El-Shamarka, M. E., Salem, N. A., Khadrawy, Y. A., and El Sayed, N. S. (2020). Neuroprotective effect of PPAR alpha and gamma agonists in a mouse model of amyloidogenesis through modulation of the Wnt/beta catenin pathway via targeting alpha- and beta-secretases. *Prog Neuropsychopharmacol Biol Psychiatry* 97, 109793. doi: 10.1016/j.pnpbp.2019.109793

Assuncao, N., Sudo, F. K., Drummond, C., De Felice, F. G., and Mattos, P. (2018). Metabolic Syndrome and cognitive decline in the elderly: A systematic review. *PLoS ONE* 13, e0194990. doi: 10.1371/journal.pone.0194990

Aviles-Olmos, I., Dickson, J., Kefalopoulou, Z., Djamshidian, A., Kahan, J., Ell, P., et al. (2014). Motor and cognitive advantages persist 12 months after exenatide exposure in Parkinson's disease. *J Parkinsons Dis* 4, 337–344. doi: 10.3233/jpd-140364

Avinun, R., and Hariri, A. R. (2019). A polygenic score for body mass index is associated with depressive symptoms via early life stress: Evidence for gene-environment correlation. *J. Psychiatr. Res.* 118, 9–13. doi: 10.1016/j.jpsychires.2019.08.008

Baker, L. D., Cross, D. J., Minoshima, S., Belongia, D., Watson, G. S., and Craft, S. (2011). Insulin resistance and Alzheimer-like reductions in regional cerebral glucose metabolism for cognitively normal adults with prediabetes or early type 2 diabetes. *Arch. Neurol.* 68, 51–57.

Batista, A. F., Forny-Germano, L., Clarke, J. R., Lyra, E. S. N. M., Brito-Moreira, J., Boehnke, S. E., et al. (2018). The diabetes drug liraglutide reverses cognitive impairment in mice and attenuates insulin receptor and synaptic pathology in a non-human primate model of Alzheimer's disease. *J. Pathol.* 245, 85–100. doi: 10.1002/path.5056

Beauquis, J., Homo-Delarche, F., Giroix, M. H., Ehses, J., Coulaud, J., Roig, P., et al. (2010). Hippocampal neurovascular and hypothalamic-pituitary-adrenal axis alterations in spontaneously type 2 diabetic GK rats. *Exp.Neurol.* 222, 125–134. doi: 10.1016/j.expneurol.2009.12.022

Beauquis, J., Pomilio, C., Vinuesa, A., Pavía, P., Galvan, V., and Saravia, F. (2013). "Early astroglial and neuronal changes in the hippocampus of PDAPP-J20 transgenic mice, model of Alzheimer's disease," in *Comunicación oral en la Reunión Anual de la Society for Neuroscience, noviembre* 2013, (San Diego).

Beauquis, J., Saravia, F., Coulaud, J., Roig, P., Dardenne, M., Homo-Delarche, F., et al. (2008). Prominently decreased hippocampal neurogenesis in a spontaneous model of type 1 diabetes, the nonobese diabetic mouse. *Exp.Neurol.* 210, 359–367. doi: 10.1016/j.expneurol.2007.11.009

Becker, E., Orellana Rios, C. L., Lahmann, C., Rucker, G., Bauer, J., and Boeker, M. (2018). Anxiety as a risk factor of Alzheimer's disease and vascular dementia. *Br. J. Psychiatry* 213, 654–660.

Benedict, C., Hallschmid, M., Hatke, A., Schultes, B., Fehm, H. L., Born, J., et al. (2004). Intranasal insulin improves memory in humans. *Psychoneuroendocrinology* 29, 1326–1334. doi: 10.1016/j.psyneuen.2004.04.003

Benito-Leon, J., Mitchell, A. J., Hernandez-Gallego, J., and Bermejo-Pareja, F. (2013). Obesity and impaired cognitive functioning in the elderly: a population-based cross-sectional study (NEDICES). *Eur. J. Neurol.* 20.

Bethel, M. A., Patel, R. A., Merrill, P., Lokhnygina, Y., Buse, J. B., Mentz, R. J., et al. (2018). Cardiovascular outcomes with glucagon-like peptide-1 receptor agonists in patients with type 2 diabetes: a meta-analysis. *Lancet Diabetes Endocrinol* 6, 105–113.

Biro, F. M., and Wien, M. (2010). Childhood obesity and adult morbidities. *Am.J.Clin.Nutr.* 91, 1499S–1505S.

Bjorkhem, I., Cedazo-Minguez, A., Leoni, V., and Meaney, S. (2009). Oxysterols and neurodegenerative diseases. *Mol. Aspects Med.* 30, 171–179. doi: 10.1016/j.mam.2009.02.001

Blasko, I., Beer, R., Bigl, M., Apelt, J., Franz, G., Rudzki, D., et al. (2004). Experimental traumatic brain injury in rats stimulates the expression, production and activity of Alzheimer's disease beta-secretase (BACE-1). *J Neural Transm (Vienna)* 111, 523–536. doi: 10.1007/s00702-003-0095-6

Blazquez, E., Velazquez, E., Hurtado-Carneiro, V., and Ruiz-Albusac, J. M. (2014). Insulin in the brain: its pathophysiological implications for States related with central insulin resistance, type 2 diabetes and Alzheimer's disease. *Front Endocrinol (Lausanne)* 5, 161.

Boitard, C., Etchamendy, N., Sauvant, J., Aubert, A., Tronel, S., Marighetto, A., et al. (2012). Juvenile, but not adult exposure to high-fat diet impairs relational memory and hippocampal neurogenesis in mice. *Hippocampus* 22, 2095–2100. doi: 10.1002/hipo.22032

Bokulich, N. A., Chung, J., Battaglia, T., Henderson, N., Jay, M., Li, H., et al. (2016). Antibiotics, birth mode, and diet shape microbiome maturation during early life. *Sci Transl Med* 8, 343ra382.

Bomba, M., Ciavardelli, D., Silvestri, E., Canzoniero, L. M., Lattanzio, R., Chiappini, P., et al. (2013). Exenatide promotes cognitive enhancement and positive brain metabolic changes in PS1-KI mice but has no effects in 3xTg-AD animals. *Cell Death Dis* 4, e612. doi: 10.1038/cddis.2013.139

Bomba, M., Granzotto, A., Castelli, V., Onofrj, M., Lattanzio, R., Cimini, A., et al. (2019). Exenatide Reverts the High-Fat-Diet-Induced Impairment of BDNF Signaling and Inflammatory Response in an Animal Model of Alzheimer's Disease. *J. Alzheimers. Dis.* 70, 793–810. doi: 10.3233/jad-190237

Bonfili, L., Cecarini, V., Berardi, S., Scarpona, S., Suchodolski, J. S., Nasuti, C., et al. (2017). Microbiota modulation counteracts Alzheimer's disease progression influencing neuronal proteolysis and gut hormones plasma levels. *Sci Rep* 7, 2426.

Bonfili, L., Cecarini, V., Cuccioloni, M., Angeletti, M., Berardi, S., Scarpona, S., et al. (2018). SLAB51 Probiotic Formulation Activates SIRT1 Pathway Promoting Antioxidant and Neuroprotective Effects in an AD Mouse Model. *Mol. Neurobiol.* 55, 7987–8000. doi: 10.1007/s12035-018-0973-4

Boucher, J., Kleinridders, A., and Kahn, C. R. (2014). Insulin receptor signaling in normal and insulin-resistant states. *Cold Spring Harb. Perspect. Biol* 6.

Bracke, A., Domanska, G., Bracke, K., Harzsch, S., Van Den Brandt, J., Broker, B., et al. (2019). Obesity Impairs Mobility and Adult Hippocampal Neurogenesis. *J Exp Neurosci* 13, 1179069519883580.

Bracko, O., Vinarcsik, L. K., Cruz Hernandez, J. C., Ruiz-Uribe, N. E., Haft-Javaherian, M., Falkenhain, K., et al. (2020). High fat diet worsens Alzheimer's disease-related behavioral abnormalities and neuropathology in APP/PS1 mice, but not by synergistically decreasing cerebral blood flow. *Sci Rep* 10, 9884.

Brandhorst, S., Choi, I. Y., Wei, M., Cheng, C. W., Sedrakyan, S., Navarrete, G., et al. (2015). A Periodic Diet that Mimics Fasting Promotes Multi-System Regeneration, Enhanced Cognitive Performance, and Healthspan. *Cell Metab* 22, 86–99. doi: 10.1016/j.cmet.2015.05.012

Bruce-Keller, A. J., Keller, J. N., and Morrison, C. D. (2009). Obesity and vulnerability of the CNS. *Biochim. Biophys. Acta* 1792, 395–400.

Bussler, S., Penke, M., Flemming, G., Elhassan, Y. S., Kratzsch, J., Sergeyev, E., et al. (2017). Novel Insights in the Metabolic Syndrome in Childhood and Adolescence. *Horm Res Paediatr* 88, 181–193.

Caccamo, A., Maldonado, M. A., Bokov, A. F., Majumder, S., and Oddo, S. (2010). CBP gene transfer increases BDNF levels and ameliorates learning and memory deficits in a mouse model of Alzheimer's disease. *Proc. Natl. Acad. Sci. U.S.A.* 107, 22687–22692. doi: 10.1073/pnas.1012851108

Cai, H. Y., Holscher, C., Yue, X. H., Zhang, S. X., Wang, X. H., Qiao, F., et al. (2014). Lixisenatide rescues spatial memory and synaptic plasticity from amyloid beta protein-induced impairments in rats. *Neuroscience* 277, 6–13. doi: 10.1016/j.neuroscience.2014.02.022

Cai, H. Y., Yang, J. T., Wang, Z. J., Zhang, J., Yang, W., Wu, M. N., et al. (2018). Lixisenatide reduces amyloid plaques, neurofibrillary tangles and neuroinflammation in an APP/PS1/tau mouse model of Alzheimer's disease. *Biochem. Biophys. Res. Commun.* 495, 1034–1040. doi: 10.1016/j.bbrc.2017.11.114

Cani, P. D., Bibiloni, R., Knauf, C., Waget, A., Neyrinck, A. M., Delzenne, N. M., et al. (2008). Changes in gut microbiota control metabolic endotoxemia-induced inflammation in high-fat diet-induced obesity and diabetes in mice. *Diabetes Metab. Res. Rev* 57, 1470–1481. doi: 10.2337/db07-1403

Cantarella, G., Di Benedetto, G., Puzzo, D., Privitera, L., Loreto, C., Saccone, S., et al. (2015). Neutralization of TNFSF10 ameliorates functional outcome in a murine model of Alzheimer's disease. *Brain* 138, 203–216. doi: 10.1093/brain/awu318

Canton-Habas, V., Rich-Ruiz, M., Romero-Saldana, M., and Carrera-Gonzalez, M. D. P. (2020). Depression as a Risk Factor for Dementia and Alzheimer's Disease. *Biomedicines* 8.

Carvalho, B. M., Guadagnini, D., Tsukumo, D. M. L., Schenka, A. A., Latuf-Filho, P., Vassallo, J., et al. (2012). Modulation of gut microbiota by antibiotics improves insulin signalling in high-fat fed mice. *Diabetologia* 55, 2823–2834. doi: 10.1007/s00125-012-2648-4

Cavelti-Weder, C., Babians-Brunner, A., Keller, C., Stahel, M. A., Kurz-Levin, M., Zayed, H., et al. (2012). Effects of gevokizumab on glycemia and inflammatory markers in type 2 diabetes. *Diabetes Care* 35, 1654–1662. doi: 10.2337/dc11-2219

Chappus-McCendie, H., Chevalier, L., Roberge, C., and Plourde, M. (2019). Omega-3 PUFA metabolism and brain modifications during aging. *Prog Neuropsychopharmacol Biol Psychiatry* 94, 109662. doi: 10.1016/j.pnpbp.2019.109662

Chavez, J. A., Siddique, M. M., Wang, S. T., Ching, J., Shayman, J. A., and Summers, S. A. (2014). Ceramides and glucosylceramides are independent antagonists of insulin signaling. *J. Biol. Chem.* 289, 723–734. doi: 10.1074/jbc.m113.522847

Chen, D., Yang, X., Yang, J., Lai, G., Yong, T., Tang, X., et al. (2017). Prebiotic Effect of Fructooligosaccharides from Morinda officinalis on Alzheimer's Disease in Rodent Models by Targeting the Microbiota-Gut-Brain Axis. *Front Aging Neurosci* 9, 403.

Chen, J. L., Luo, C., Pu, D., Zhang, G. Q., Zhao, Y. X., Sun, Y., et al. (2019). Metformin attenuates diabetes-induced tau hyperphosphorylation in vitro and in vivo by enhancing autophagic clearance. *Exp. Neurol.* 311, 44–56. doi: 10.1016/j.expneurol.2018.09.008

Chen, M., Huang, N., Liu, J., Huang, J., Shi, J., and Jin, F. (2020). AMPK: A bridge between diabetes mellitus and Alzheimer's disease. *Behav. Brain Res.* 400, 113043. doi: 10.1016/j.bbr.2020.113043

Chen, X. H., Siman, R., Iwata, A., Meaney, D. F., Trojanowski, J. Q., and Smith, D. H. (2004). Long-term accumulation of amyloid-beta, beta-secretase, presenilin-1, and caspase-3 in damaged axons following brain trauma. *Am. J. Pathol.* 165, 357–371. doi: 10.1016/s0002-9440(10)63303-2

Cho, M. H., Cho, K., Kang, H. J., Jeon, E. Y., Kim, H. S., Kwon, H. J., et al. (2014). Autophagy in microglia degrades extracellular beta-amyloid fibrils and regulates the NLRP3 inflammasome. *Autophagy.* 10, 1761–1775. doi: 10.4161/auto.29647

Choi, S. H., Bylykbashi, E., Chatila, Z. K., Lee, S. W., Pulli, B., Clemenson, G. D., et al. (2018). Combined adult neurogenesis and BDNF mimic exercise effects on cognition in an Alzheimer's mouse model. *Science* 361.

Chu, C. S., Tseng, P. T., Stubbs, B., Chen, T. Y., Tang, C. H., Li, D. J., et al. (2018). Use of statins and the risk of dementia and mild cognitive impairment: A systematic review and meta-analysis. *Sci Rep* 8, 5804.

Chua, L. M., Lim, M. L., Chong, P. R., Hu, Z. P., Cheung, N. S., and Wong, B. S. (2012). Impaired neuronal insulin signaling precedes Abeta42 accumulation in female AbetaPPsw/PS1DeltaE9 mice. *J. Alzheimers. Dis.* 29, 783–791. doi: 10.3233/jad-2012-111880

Chuang, Y. F., An, Y., Bilgel, M., Wong, D. F., Troncoso, J. C., O'brien, R. J., et al. (2016). Midlife adiposity predicts earlier onset of Alzheimer's dementia, neuropathology and presymptomatic cerebral amyloid accumulation. *Mol. Psychiatry* 21, 910–915. doi: 10.1038/mp.2015.129

Claesson, M. J., Jeffery, I. B., Conde, S., Power, S. E., O'connor, E. M., Cusack, S., et al. (2012). Gut microbiota composition correlates with diet and health in the elderly. *Nature* 488, 178–184.

Claxton, A., Baker, L. D., Hanson, A., Trittschuh, E. H., Cholerton, B., Morgan, A., et al. (2015). Long Acting Intranasal Insulin Detemir Improves Cognition for Adults with Mild Cognitive Impairment or Early-Stage Alzheimer's Disease Dementia. *J. Alzheimers. Dis.* 45, 1269–1270. doi: 10.3233/jad-159002

Clelland, C. D., Choi, M., Romberg, C., Clemenson, G. D. Jr., Fragniere, A., et al. (2009). A functional role for adult hippocampal neurogenesis in spatial pattern separation. *Science* 325, 210–213. doi: 10.1126/science.1173215

Cohen, E., Bieschke, J., Perciavalle, R. M., Kelly, J. W., and Dillin, A. (2006). Opposing activities protect against age-onset proteotoxicity. *Science* 313, 1604–1610. doi: 10.1126/science.1124646

Cope, E. C., Lamarca, E. A., Monari, P. K., Olson, L. B., Martinez, S., Zych, A. D., et al. (2018). Microglia Play an Active Role in Obesity-Associated Cognitive Decline. *J. Neurosci.* 38, 8889–8904. doi: 10.1523/jneurosci.0789-18.2018

Craft, S., Claxton, A., Baker, L. D., Hanson, A. J., Cholerton, B., Trittschuh, E. H., et al. (2017). Effects of Regular and Long-Acting Insulin on Cognition and Alzheimer's Disease Biomarkers: A Pilot Clinical Trial. *J. Alzheimers. Dis.* 57, 1325–1334. doi: 10.3233/jad-161256

Dahl, A., Hassing, L. B., Fransson, E., Berg, S., Gatz, M., Reynolds, C. A., et al. (2010). Being overweight in midlife is associated with lower cognitive ability and steeper cognitive decline in late life. *J. Gerontol. A Biol. Sci. Med. Sci.* 65, 57–62. doi: 10.1093/gerona/glp035

Dahl, A. K., and Hassing, L. B. (2013). Obesity and cognitive aging. *Epidemiol. Rev.* 35, 22–32. doi: 10.1093/epirev/mxs002

de Heer, J., Rasmussen, C., Coy, D. H., and Holst, J. J. (2008). Glucagon-like peptide-1, but not glucose-dependent insulinotropic peptide, inhibits glucagon secretion via somatostatin (receptor subtype 2) in the perfused rat pancreas. *Diabetologia* 51, 2263–2270. doi: 10.1007/s00125-008-1149-y

de la Monte, S. M., and Tong, M. (2014). Brain metabolic dysfunction at the core of Alzheimer's disease. *Biochem. Pharmacol* 88, 548–559. doi: 10.1016/j.bcp.2013.12.012

De Sousa Rodrigues, M. E., Houser, M. C., Walker, D. I., Jones, D. P., Chang, J., Barnum, C. J., et al. (2019). Targeting soluble tumor necrosis factor as a potential intervention to lower risk for late-onset Alzheimer's disease associated with obesity, metabolic syndrome, and type 2 diabetes. *Alzheimers Res Ther* 12, 1. doi: 10.1007/s11010-011-0917-z

Deckers, K., Van Boxtel, M. P. J., Verhey, F. R. J., and Kohler, S. (2017). Obesity and Cognitive Decline in Adults: Effect of Methodological Choices and Confounding by Age in a Longitudinal Study. *J. Nutr. Health Aging* 21, 546–553. doi: 10.1007/s12603-016-0757-3

Derkach, K. V., Ivantsov, A. O., Chistyakova, O. V., Sukhov, I. B., Buzanakov, D. M., Kulikova, A. A., et al. (2017). Intranasal Insulin Restores Metabolic Parameters and Insulin Sensitivity in Rats with Metabolic Syndrome. *Bull. Exp. Biol. Med.* 163, 184–189. doi: 10.1007/s10517-017-3762-6

Dey, A., Hao, S., Wosiski-Kuhn, M., and Stranahan, A. M. (2017). Glucocorticoid-mediated activation of GSK3beta promotes tau phosphorylation and impairs memory in type 2 diabetes. *Neurobiol. Aging* 57, 75–83. doi: 10.1016/j.neurobiolaging.2017.05.010

Dror, E., Dalmas, E., Meier, D. T., Wueest, S., Thevenet, J., Thienel, C., et al. (2017). Postprandial macrophage-derived IL-1beta stimulates insulin, and both synergistically promote glucose disposal and inflammation. *Nat. Immunol.* 18, 283–292. doi: 10.1038/ni.3659

Edwards, P. K., Mears, S. C., Stambough, J. B., Foster, S. E., and Barnes, C. L. (2019). Response to Letter to the Editor on "Choices, Compromises, and Controversies

in Total Knee and Total Hip Arthroplasty Modifiable Risk Factors: What You Need to Know". . *J. Arthroplasty* 34, 1039. doi: 10.1016/j.arth.2019.02.015

Ellulu, M. S., Patimah, I., Khaza'ai, H., Rahmat, A., and Abed, Y. (2017). Obesity and inflammation: the linking mechanism and the complications. *Arch Med Sci* 13, 851–863. doi: 10.5114/aoms.2016.58928

Elosua, R., Bartali, B., Ordovas, J. M., Corsi, A. M., Lauretani, F., Ferrucci, L., et al. (2005). Association between physical activity, physical performance, and inflammatory biomarkers in an elderly population: the InCHIANTI study. *J Gerontol A Biol Sci Med Sci* 60, 760–767. doi: 10.1093/gerona/60.6.760

Eom, T. Y., and Jope, R. S. (2009). Blocked inhibitory serine-phosphorylation of glycogen synthase kinase-3alpha/beta impairs in vivo neural precursor cell proliferation. *Biol. Psychiatry* 66, 494–502. doi: 10.1016/j.biopsych.2009.04.015

Erickson, M. A., and Banks, W. A. (2013). Blood-brain barrier dysfunction as a cause and consequence of Alzheimer's disease. *J. Cereb. Blood Flow Metab.* 33, 1500–1513. doi: 10.1038/jcbfm.2013.135

Eriksdotter, M., Vedin, I., Falahati, F., Freund-Levi, Y., Hjorth, E., Faxen-Irving, G., et al. (2015). Plasma Fatty Acid Profiles in Relation to Cognition and Gender in Alzheimer's Disease Patients During Oral Omega-3 Fatty Acid Supplementation: The OmegAD Study. *J. Alzheimers. Dis.* 48, 805–812. doi: 10.3233/jad-150102

Etminan, M., Gill, S., and Samii, A. (2003). Effect of non-steroidal anti-inflammatory drugs on risk of Alzheimer's disease: systematic review and meta-analysis of observational studies. *BMJ* 327, 128. doi: 10.1136/bmj.327.7407.128

Farilla, L., Bulotta, A., Hirshberg, B., Li Calzi, S., Khoury, N., Noushmehr, H., et al. (2003). Glucagon-like peptide 1 inhibits cell apoptosis and improves glucose responsiveness of freshly isolated human islets. *Endocrinology* 144, 5149–5158. doi: 10.1210/en.2003-0323

Farr, S. A., Roesler, E., Niehoff, M. L., Roby, D. A., Mckee, A., and Morley, J. E. (2019). Metformin Improves Learning and Memory in the SAMP8 Mouse Model of Alzheimer's Disease. *J. Alzheimers. Dis.* 68, 1699–1710. doi: 10.3233/jad-181240

Ferrario, C. R., and Reagan, L. P. (2017). Insulin-mediated synaptic plasticity in the CNS: Anatomical, functional and temporal contexts. *Neuropharmacology.*

Ferreira, L. S. S., Fernandes, C. S., Vieira, M. N. N., and De Felice, F. G. (2018). Insulin Resistance in Alzheimer's Disease. *Front Neurosci* 12, 830.

Franceschi, C., and Campisi, J. (2014). Chronic inflammation (inflammaging) and its potential contribution to age-associated diseases. *J. Gerontol. A Biol. Sci. Med. Sci.* 69(Suppl. 1), S4–S9.

Franceschi, C., Garagnani, P., Parini, P., Giuliani, C., and Santoro, A. (2018). Inflammaging: a new immune-metabolic viewpoint for age-related diseases. *Nat Rev Endocrinol* 14, 576–590. doi: 10.1038/s41574-018-0059-4

Frank, M. G., Barrientos, R. M., Biedenkapp, J. C., Rudy, J. W., Watkins, L. R., and Maier, S. F. (2006). mRNA up-regulation of MHC II and pivotal pro-inflammatory genes in normal brain aging. *Neurobiol. Aging* 27, 717–722. doi: 10.1016/j.neurobiolaging.2005.03.013

Freude, S., Hettich, M. M., Schumann, C., Stohr, O., Koch, L., Kohler, C., et al. (2009). Neuronal IGF-1 resistance reduces Abeta accumulation and protects against premature death in a model of Alzheimer's disease. *FASEB J.* 23, 3315–3324. doi: 10.1096/fj.09-132043

Freund-Levi, Y., Eriksdotter-Jonhagen, M., Cederholm, T., Basun, H., Faxen-Irving, G., Garlind, A., et al. (2006). Omega-3 fatty acid treatment in 174 patients with mild to moderate Alzheimer disease: OmegAD study: a randomized double-blind trial. *Arch. Neurol.* 63, 1402–1408. doi: 10.1001/archneur.63.10.1402

Frolich, L., Blum-Degen, D., Bernstein, H. G., Engelsberger, S., Humrich, J., Laufer, S., et al. (1998). Brain insulin and insulin receptors in aging and sporadic Alzheimer's disease. *J Neural Transm (Vienna)* 105, 423–438. doi: 10.1007/s007020050068

Fujita, K., Motoki, K., Tagawa, K., Chen, X., Hama, H., Nakajima, K., et al. (2016). HMGB1, a pathogenic molecule that induces neurite degeneration via TLR4-MARCKS, is a potential therapeutic target for Alzheimer's disease. *Sci Rep* 6, 31895.

Gault, V. A., and Holscher, C. (2008). GLP-1 agonists facilitate hippocampal LTP and reverse the impairment of LTP induced by beta-amyloid. *Eur. J. Pharmacol* 587, 112–117. doi: 10.1016/j.ejphar.2008.03.025

Gejl, M., Gjedde, A., Egefjord, L., Moller, A., Hansen, S. B., Vang, K., et al. (2016). In Alzheimer's Disease, 6-Month Treatment with GLP-1 Analog Prevents Decline of Brain Glucose Metabolism: Randomized, Placebo-Controlled, Double-Blind Clinical Trial. *Front Aging Neurosci* 8, 108.

Gold, M., Alderton, C., Zvartau-Hind, M., Egginton, S., Saunders, A. M., Irizarry, M., et al. (2010). Rosiglitazone monotherapy in mild-to-moderate Alzheimer's disease: results from a randomized, double-blind, placebo-controlled phase III study. *Dement. Geriatr. Cogn. Disord* 30, 131–146. doi: 10.1159/000318845

Gomes, A. P., Soares, A. L. G., Menezes, A. M. B., Assuncao, M. C., Wehrmeister, F. C., Howe, L. D., et al. (2019). Adiposity, depression and anxiety: interrelationship and possible mediators. *Rev Saude Publica* 53, 103. doi: 10.11606/s1518-8787.2019053001119

Gottesman, R. F., Albert, M. S., Alonso, A., Coker, L. H., Coresh, J., Davis, S. M., et al. (2017). Associations Between Midlife Vascular Risk Factors and 25-Year Incident Dementia in the Atherosclerosis Risk in Communities (ARIC) Cohort. *JAMA Neurol* 74, 1246–1254. doi: 10.1001/jamaneurol.2017.1658

Gralle, M. (2017). The neuronal insulin receptor in its environment. *J. Neurochem.* 140, 359–367. doi: 10.1111/jnc.13909

Grefhorst, A., Elzinga, B. M., Voshol, P. J., Plosch, T., Kok, T., Bloks, V. W., et al. (2002). Stimulation of lipogenesis by pharmacological activation of the liver X receptor leads to production of large, triglyceride-rich very low density lipoprotein particles. *J. Biol. Chem.* 277, 34182–34190. doi: 10.1074/jbc.m204887200

Gregosa, A., Vinuesa, A., Todero, M. F., Pomilio, C., Rossi, S. P., Bentivegna, M., et al. (2019). Periodic dietary restriction ameliorates amyloid pathology and cognitive impairment in PDAPP-J20 mice: Potential implication of glial autophagy. *Neurobiol. Dis* 104542. doi: 10.1016/j.nbd.2019.104542

Griffin, R. J., Moloney, A., Kelliher, M., Johnston, J. A., Ravid, R., Dockery, P., et al. (2005). Activation of Akt/PKB, increased phosphorylation of Akt substrates and loss and altered distribution of Akt and PTEN are features of Alzheimer's disease pathology. *J. Neurochem.* 93, 105–117. doi: 10.1111/j.1471-4159.2004.02949.x

Group, A. R., Martin, B. K., Szekely, C., Brandt, J., Piantadosi, S., Breitner, J. C., et al. (2008). Cognitive function over time in the Alzheimer's Disease Anti-inflammatory Prevention Trial (ADAPT): results of a randomized, controlled trial of naproxen and celecoxib. *Arch. Neurol.* 65, 896–905. doi: 10.1001/archneur.2008.65.7.nct70006

Guillemot-Legris, O., and Muccioli, G. G. (2017). Obesity-Induced Neuroinflammation: Beyond the Hypothalamus. *Trends Neurosci* 40, 237–253. doi: 10.1016/j.tins.2017.02.005

Hamer, M., Lavoie, K. L., and Bacon, S. L. (2014). Taking up physical activity in later life and healthy ageing: the English longitudinal study of ageing. *Br. J. Sports Med.* 48, 239–243. doi: 10.1136/bjsports-2013-092993

Hao, S., Dey, A., Yu, X., and Stranahan, A. M. (2016). Dietary obesity reversibly induces synaptic stripping by microglia and impairs hippocampal plasticity. *Brain Behav. Immun.* 51, 230–239. doi: 10.1016/j.bbi.2015.08.023

Hargrave, S. L., Davidson, T. L., Zheng, W., and Kinzig, K. P. (2016). Western diets induce blood-brain barrier leakage and alter spatial strategies in rats. *Behav. Neurosci.* 130, 123–135. doi: 10.1037/bne0000110

Harries, L. W., Fellows, A. D., Pilling, L. C., Hernandez, D., Singleton, A., Bandinelli, S., et al. (2012). Advancing age is associated with gene expression changes resembling mTOR inhibition: evidence from two human populations. *Mech. Ageing Dev.* 133, 556–562. doi: 10.1016/j.mad.2012.07.003

Harvie, M. N., Pegington, M., Mattson, M. P., Frystyk, J., Dillon, B., Evans, G., et al. (2011). The effects of intermittent or continuous energy restriction on weight loss and metabolic disease risk markers: a randomized trial in young overweight women. *Int J Obes (Lond)* 35, 714–727. doi: 10.1038/ijo.2010.171

Henderson, S. T., Vogel, J. L., Barr, L. J., Garvin, F., Jones, J. J., and Costantini, L. C. (2009). Study of the ketogenic agent AC-1202 in mild to moderate Alzheimer's disease: a randomized, double-blind, placebo-controlled, multicenter trial. *Nutr Metab (Lond)* 6, 31. doi: 10.1186/1743-7075-6-31

Heneka, M. T., Carson, M. J., El Khoury, J., Landreth, G. E., Brosseron, F., Feinstein, D. L., et al. (2015). Neuroinflammation in Alzheimer's disease. *Lancet Neurol.* 14, 388–405.

Heneka, M. T., Kummer, M. P., Stutz, A., Delekate, A., Schwartz, S., Vieira-Saecker, A., et al. (2013). NLRP3 is activated in Alzheimer's disease and contributes to pathology in APP/PS1 mice. *Nature* 493, 674–678. doi: 10.1038/nature11729

Heneka, M. T., Sastre, M., Dumitrescu-Ozimek, L., Dewachter, I., Walter, J., Klockgether, T., et al. (2005). Focal glial activation coincides with increased

BACE1 activation and precedes amyloid plaque deposition in APP[V717I] transgenic mice. *J Neuroinflammation* 2, 22.

Herzig, S., and Shaw, R. J. (2018). AMPK: guardian of metabolism and mitochondrial homeostasis. *Nat. Rev. Mol. Cell Biol.* 19, 121–135. doi: 10.1038/nrm.2017.95

Hoffmann, K., Sobol, N. A., Frederiksen, K. S., Beyer, N., Vogel, A., Vestergaard, K., et al. (2016). Moderate-to-High Intensity Physical Exercise in Patients with Alzheimer's Disease: A Randomized Controlled Trial. *J. Alzheimers. Dis.* 50, 443–453.

Holland, W. L., Bikman, B. T., Wang, L. P., Yuguang, G., Sargent, K. M., Bulchand, S., et al. (2011). Lipid-induced insulin resistance mediated by the proinflammatory receptor TLR4 requires saturated fatty acid-induced ceramide biosynthesis in mice. *J. Clin. Invest.* 121, 1858–1870. doi: 10.1172/jci43378

Hotamisligil, G. S. (2010). Endoplasmic reticulum stress and the inflammatory basis of metabolic disease. *Cell* 140, 900–917. doi: 10.1016/j.cell.2010.02.034

Hotamisligil, G. S., Shargill, N. S., and Spiegelman, B. M. (1993). Adipose expression of tumor necrosis factor-alpha: direct role in obesity-linked insulin resistance. *Science* 259, 87–91. doi: 10.1126/science.7678183

Hutchinson, A. N., Tingo, L., and Brummer, R. J. (2020). The Potential Effects of Probiotics and omega-3 Fatty Acids on Chronic Low-Grade Inflammation. *Nutrients* 12.

Idf. (2017). *IDF DIABETES ATLAS [Online]*. Available: https://www.diabetesatlas.org/en/[Accessed] (accessed December 20, 2020).

Inestrosa, N. C., Godoy, J. A., Quintanilla, R. A., Koenig, C. S., and Bronfman, M. (2005). Peroxisome proliferator-activated receptor gamma is expressed in hippocampal neurons and its activation prevents beta-amyloid neurodegeneration: role of Wnt signaling. *Exp. Cell Res.* 304, 91–104. doi: 10.1016/j.yexcr.2004.09.032

Ishiguro, K., Shiratsuchi, A., Sato, S., Omori, A., Arioka, M., Kobayashi, S., et al. (1993). Glycogen synthase kinase 3 beta is identical to tau protein kinase I generating several epitopes of paired helical filaments. *FEBS Lett.* 325, 167–172. doi: 10.1016/0014-5793(93)81066-9

James, S. L., Lucchesi, L. R., Bisignano, C., Castle, C. D., Dingels, Z. V., Fox, J. T., et al. (2020). Morbidity and mortality from road injuries: results from the Global Burden of Disease Study 2017. *Inj. Prev.* 26, i46–i56.

Jantzen, P. T., Connor, K. E., Dicarlo, G., Wenk, G. L., Wallace, J. L., Rojiani, A. M., et al. (2002). Microglial activation and beta -amyloid deposit reduction caused by a nitric oxide-releasing nonsteroidal anti-inflammatory drug in amyloid precursor protein plus presenilin-1 transgenic mice. *J. Neurosci.* 22, 2246–2254. doi: 10.1523/jneurosci.22-06-02246.2002

Jensen, C. S., Bahl, J. M., Ostergaard, L. B., Hogh, P., Wermuth, L., Heslegrave, A., et al. (2019). Exercise as a potential modulator of inflammation in patients with Alzheimer's disease measured in cerebrospinal fluid and plasma. *Exp. Gerontol.* 121, 91–98. doi: 10.1016/j.exger.2019.04.003

Jia, L., Vianna, C. R., Fukuda, M., Berglund, E. D., Liu, C., Tao, C., et al. (2014). Hepatocyte Toll-like receptor 4 regulates obesity-induced inflammation and insulin resistance. *Nat Commun* 5, 3878.

Jiao, S. S., Shen, L. L., Zhu, C., Bu, X. L., Liu, Y. H., Liu, C. H., et al. (2016). Brain-derived neurotrophic factor protects against tau-related neurodegeneration of Alzheimer's disease. *Transl Psychiatry* 6, e907. doi: 10.1038/tp.2016.186

Jimenez, S., Torres, M., Vizuete, M., Sanchez-Varo, R., Sanchez-Mejias, E., Trujillo-Estrada, L., et al. (2011). Age-dependent accumulation of soluble amyloid beta (Abeta) oligomers reverses the neuroprotective effect of soluble amyloid precursor protein-alpha (sAPP(alpha)) by modulating phosphatidylinositol 3-kinase (PI3K)/Akt-GSK-3beta pathway in Alzheimer mouse model. *J. Biol. Chem.* 286, 18414–18425. doi: 10.1074/jbc.m110.209718

Jope, R. S., Yuskaitis, C. J., and Beurel, E. (2007). Glycogen synthase kinase-3 (GSK3): inflammation, diseases, and therapeutics. *Neurochem. Res.* 32, 577–595. doi: 10.1007/s11064-006-9128-5

Kashiwaya, Y., Bergman, C., Lee, J. H., Wan, R., King, M. T., Mughal, M. R., et al. (2013). A ketone ester diet exhibits anxiolytic and cognition-sparing properties, and lessens amyloid and tau pathologies in a mouse model of Alzheimer's disease. *Neurobiol. Aging* 34, 1530–1539. doi: 10.1016/j.neurobiolaging.2012.11.023

Kattenstroth, J. C., Kolankowska, I., Kalisch, T., and Dinse, H. R. (2010). Superior sensory, motor, and cognitive performance in elderly individuals with multi-year dancing activities. *Front Aging Neurosci* 2.

Kellar, D., and Craft, S. (2020). Brain insulin resistance in Alzheimer's disease and related disorders: mechanisms and therapeutic approaches. *Lancet Neurol.* 19, 758–766. doi: 10.1016/s1474-4422(20)30231-3

Kelly, K. M., Nadon, N. L., Morrison, J. H., Thibault, O., Barnes, C. A., and Blalock, E. M. (2006). The neurobiology of aging. *Epilepsy Res.* 68(Suppl. 1), S5–S20.

Kitazawa, M., Oddo, S., Yamasaki, T. R., Green, K. N., and Laferla, F. M. (2005). Lipopolysaccharide-induced inflammation exacerbates tau pathology by a cyclin-dependent kinase 5-mediated pathway in a transgenic model of Alzheimer's disease. *J. Neurosci.* 25, 8843–8853. doi: 10.1523/jneurosci.2868-05.2005

Kleinridders, A., Ferris, H. A., Cai, W., and Kahn, C. R. (2014). Insulin action in brain regulates systemic metabolism and brain function. *Diabetes Metab. Res. Rev* 63, 2232–2243. doi: 10.2337/db14-0568

Klempin, F., and Kempermann, G. (2007). Adult hippocampal neurogenesis and aging. *Eur. Arch. Psychiatry Clin. Neurosci.* 257, 271–280.

Kloting, N., and Bluher, M. (2014). Adipocyte dysfunction, inflammation and metabolic syndrome. *Rev Endocr Metab Disord* 15, 277–287. doi: 10.1007/s11154-014-9301-0

Kobayashi, Y., Kinoshita, T., Matsumoto, A., Yoshino, K., Saito, I., and Xiao, J. Z. (2019a). Bifidobacterium Breve A1 Supplementation Improved Cognitive Decline in Older Adults with Mild Cognitive Impairment: An Open-Label, Single-Arm Study. *J Prev Alzheimers Dis* 6, 70–75.

Kobayashi, Y., Kuhara, T., Oki, M., and Xiao, J. Z. (2019b). Effects of Bifidobacterium breve A1 on the cognitive function of older adults with memory complaints: a randomised, double-blind, placebo-controlled trial. *Benef Microbes* 10, 511–520. doi: 10.3920/bm2018.0170

Kobayashi, Y., Sugahara, H., Shimada, K., Mitsuyama, E., Kuhara, T., Yasuoka, A., et al. (2017). Therapeutic potential of Bifidobacterium breve strain A1 for preventing cognitive impairment in Alzheimer's disease. *Sci Rep* 7, 13510.

Koenig, A. M., Mechanic-Hamilton, D., Xie, S. X., Combs, M. F., Cappola, A. R., Xie, L., et al. (2017). Effects of the Insulin Sensitizer Metformin in Alzheimer Disease: Pilot Data From a Randomized Placebo-controlled Crossover Study. *Alzheimer Dis. Assoc. Disord.* 31, 107–113. doi: 10.1097/wad.0000000000000202

Koldamova, R. P., Lefterov, I. M., Staufenbiel, M., Wolfe, D., Huang, S., Glorioso, J. C., et al. (2005). The liver X receptor ligand T0901317 decreases amyloid beta production in vitro and in a mouse model of Alzheimer's disease. *J. Biol. Chem.* 280, 4079–4088. doi: 10.1074/jbc.m411420200

Koo, B. K., Kim, L. K., Lee, J. Y., and Moon, M. K. (2019). Taking metformin and cognitive function change in older patients with diabetes. *Geriatr Gerontol Int* 19, 755–761. doi: 10.1111/ggi.13692

Kotti, T. J., Ramirez, D. M., Pfeiffer, B. E., Huber, K. M., and Russell, D. W. (2006). Brain cholesterol turnover required for geranylgeraniol production and learning in mice. *Proc. Natl. Acad. Sci. U.S.A.* 103, 3869–3874. doi: 10.1073/pnas.0600316103

Kowianski, P., Lietzau, G., Czuba, E., Waskow, M., Steliga, A., and Morys, J. (2018). BDNF: A Key Factor with Multipotent Impact on Brain Signaling and Synaptic Plasticity. *Cell Mol. Neurobiol* 38, 579–593. doi: 10.1007/s10571-017-0510-4

Krstic, D., Madhusudan, A., Doehner, J., Vogel, P., Notter, T., Imhof, C., et al. (2012). Systemic immune challenges trigger and drive Alzheimer-like neuropathology in mice. *J Neuroinflammation* 9, 151.

Larsen, C. M., Faulenbach, M., Vaag, A., Volund, A., Ehses, J. A., Seifert, B., et al. (2007). Interleukin-1-receptor antagonist in type 2 diabetes mellitus. *N. Engl. J. Med.* 356, 1517–1526.

Lazarou, I., Parastatidis, T., Tsolaki, A., Gkioka, M., Karakostas, A., Douka, S., et al. (2017). International Ballroom Dancing Against Neurodegeneration: A Randomized Controlled Trial in Greek Community-Dwelling Elders With Mild Cognitive impairment. *Am. J. Alzheimers Dis. Other Demen.* 32, 489–499. doi: 10.1177/1533317517725813

Le, K. A., Ventura, E. E., Fisher, J. Q., Davis, J. N., Weigensberg, M. J., Punyanitya, M., et al. (2011). Ethnic differences in pancreatic fat accumulation and its relationship with other fat depots and inflammatory markers. *Diabetes Care* 34, 485–490. doi: 10.2337/dc10-0760

Lee, E. B., and Mattson, M. P. (2014). The neuropathology of obesity: insights from human disease. *Acta Neuropathol.* 127, 3–28. doi: 10.1007/s00401-013-1190-x

Leonardini, A., Laviola, L., Perrini, S., Natalicchio, A., and Giorgino, F. (2009). Cross-Talk between PPARgamma and Insulin Signaling and Modulation of Insulin Sensitivity. *PPAR Res* 2009, 818945.

Li, H., Yang, S., Wu, J., Ji, L., Zhu, L., Cao, L., et al. (2018). cAMP/PKA signaling pathway contributes to neuronal apoptosis via regulating IDE expression in a mixed model of type 2 diabetes and Alzheimer's disease. *J. Cell. Biochem.* 119, 1616–1626. doi: 10.1002/jcb.26321

Li, J., Chen, S., Qiang, J., Wang, X., Chen, L., and Zou, D. (2014). Diet-induced obesity mediates a proinflammatory response in pancreatic beta cell via toll-like receptor 4. *Cent Eur J Immunol* 39, 306–315. doi: 10.5114/ceji.2014.45940

Lim, G. P., Yang, F., Chu, T., Chen, P., Beech, W., Teter, B., et al. (2000). Ibuprofen suppresses plaque pathology and inflammation in a mouse model for Alzheimer's disease. *J. Neurosci.* 20, 5709–5714. doi: 10.1523/jneurosci.20-15-05709.2000

Lin, S. H., Cheng, P. C., Tu, S. T., Hsu, S. R., Cheng, Y. C., and Liu, Y. H. (2018). Effect of metformin monotherapy on serum lipid profile in statin-naive individuals with newly diagnosed type 2 diabetes mellitus: a cohort study. *PeerJ* 6, e4578. doi: 10.7717/peerj.4578

Liu, J., and Li, L. (2019). Targeting Autophagy for the Treatment of Alzheimer's Disease: Challenges and Opportunities. *Front Mol Neurosci* 12, 203.

Liu, R., Yang, J., Liu, L., Lu, Z., Shi, Z., Ji, W., et al. (2020). An "Amyloid-beta Cleaner" for the Treatment of Alzheimer's Disease by Normalizing Microglial Dysfunction. *Adv Sci (Weinh)* 7, 1901555. doi: 10.1002/advs.201901555

Liu, Y., Cheng, A., Li, Y. J., Yang, Y., Kishimoto, Y., Zhang, S., et al. (2019). SIRT3 mediates hippocampal synaptic adaptations to intermittent fasting and ameliorates deficits in APP mutant mice. *Nat Commun* 10, 1886.

Lochhead, J. J., Kellohen, K. L., Ronaldson, P. T., and Davis, T. P. (2019). Distribution of insulin in trigeminal nerve and brain after intranasal administration. *Sci Rep* 9, 2621.

Lu, Y., Dong, Y., Tucker, D., Wang, R., Ahmed, M. E., Brann, D., et al. (2017). Treadmill Exercise Exerts Neuroprotection and Regulates Microglial Polarization and Oxidative Stress in a Streptozotocin-Induced Rat Model of Sporadic Alzheimer's Disease. *J. Alzheimers. Dis.* 56, 1469–1484. doi: 10.3233/jad-160869

Lucassen, P. J., Oomen, C. A., Naninck, E. F., Fitzsimons, C. P., Van Dam, A. M., Czeh, B., et al. (2015). Regulation of Adult Neurogenesis and Plasticity by (Early) Stress, Glucocorticoids, and Inflammation. *Cold Spring Harb. Perspect. Biol.* 7, a021303. doi: 10.1101/cshperspect.a021303

Luchsinger, J. A., Perez, T., Chang, H., Mehta, P., Steffener, J., Pradabhan, G., et al. (2016). Metformin in Amnestic Mild Cognitive Impairment: Results of a Pilot Randomized Placebo Controlled Clinical Trial. *J. Alzheimers. Dis.* 51, 501–514. doi: 10.3233/jad-150493

Luppino, F. S., De Wit, L. M., Bouvy, P. F., Stijnen, T., Cuijpers, P., Penninx, B. W., et al. (2010). Overweight, obesity, and depression: a systematic review and meta-analysis of longitudinal studies. *Arch. Gen. Psychiatry* 67, 220–229. doi: 10.1001/archgenpsychiatry.2010.2

Lutjohann, D., Breuer, O., Ahlborg, G., Nennesmo, I., Siden, A., Diczfalusy, U., et al. (1996). Cholesterol homeostasis in human brain: evidence for an age-dependent flux of 24S-hydroxycholesterol from the brain into the circulation. *Proc. Natl. Acad. Sci. U.S.A.* 93, 9799–9804. doi: 10.1073/pnas.93.18.9799

Ly, P. T., Wu, Y., Zou, H., Wang, R., Zhou, W., Kinoshita, A., et al. (2013). Inhibition of GSK3beta-mediated BACE1 expression reduces Alzheimer-associated phenotypes. *J. Clin. Invest.* 123, 224–235. doi: 10.1172/jci64516

Ma, L., Wang, R., Dong, W., and Zhao, Z. (2018). Caloric restriction can improve learning and memory in C57/BL mice probably via regulation of the AMPK signaling pathway. *Exp. Gerontol.* 102, 28–35. doi: 10.1016/j.exger.2017.11.013

Mac Giollabhui, N., Swistun, D., Murray, S., Moriarity, D. P., Kautz, M. M., Ellman, L. M., et al. (2020). Executive dysfunction in depression in adolescence: the role of inflammation and higher body mass. *Psychol Med* 50, 683–691. doi: 10.1017/s0033291719000564

MacPherson, K. P., Sompol, P., Kannarkat, G. T., Chang, J., Sniffen, L., Wildner, M. E., et al. (2017). Peripheral administration of the soluble TNF inhibitor XPro1595 modifies brain immune cell profiles, decreases beta-amyloid plaque load, and rescues impaired long-term potentiation in 5xFAD mice. *Neurobiol. Dis.* 102, 81–95. doi: 10.1016/j.nbd.2017.02.010

Maedler, K., Sergeev, P., Ris, F., Oberholzer, J., Joller-Jemelka, H. I., Spinas, G. A., et al. (2002). Glucose-induced beta cell production of IL-1beta contributes to glucotoxicity in human pancreatic islets. *J. Clin. Invest.* 110, 851–860. doi: 10.1172/jci200215318

Majumder, S., Richardson, A., Strong, R., and Oddo, S. (2011). Inducing autophagy by rapamycin before, but not after, the formation of plaques and tangles ameliorates cognitive deficits. *PLoS ONE* 6, e25416. doi: 10.1371/journal.pone.0025416

Malone, J. I., Hanna, S., Saporta, S., Mervis, R. F., Park, C. R., Chong, L., et al. (2008). Hyperglycemia not hypoglycemia alters neuronal dendrites and impairs spatial memory. *Pediatr. Diabetes* 9, 531–539. doi: 10.1111/j.1399-5448.2008.00431.x

Mao, Y. F., Guo, Z., Zheng, T., Jiang, Y., Yan, Y., Yin, X., et al. (2016). Intranasal insulin alleviates cognitive deficits and amyloid pathology in young adult APPswe/PS1dE9 mice. *Aging Cell* 15, 893–902. doi: 10.1111/acel.12498

Maric, T., Woodside, B., and Luheshi, G. N. (2014). The effects of dietary saturated fat on basal hypothalamic neuroinflammation in rats. *Brain Behav. Immun.* 36, 35–45. doi: 10.1016/j.bbi.2013.09.011

Marquez, D. X., Wilson, R., Aguinaga, S., Vasquez, P., Fogg, L., Yang, Z., et al. (2017). Regular Latin Dancing and Health Education May Improve Cognition of Late Middle-Aged and Older Latinos. *J Aging Phys Act* 25, 482–489. doi: 10.1123/japa.2016-0049

Mast, N., Saadane, A., Valencia-Olvera, A., Constans, J., Maxfield, E., Arakawa, H., et al. (2017). Cholesterol-metabolizing enzyme cytochrome P450 46A1 as a pharmacologic target for Alzheimer's disease. *Neuropharmacology* 123, 465–476. doi: 10.1016/j.neuropharm.2017.06.026

Mayeux, R., and Stern, Y. (2012). Epidemiology of Alzheimer disease. *Cold Spring Harb Perspect Med* 2.

McGrattan, A. M., Mcguinness, B., Mckinley, M. C., Kee, F., Passmore, P., Woodside, J. V., et al. (2019). Diet and Inflammation in Cognitive Ageing and Alzheimer's Disease. *Curr Nutr Rep* 8, 53–65.

Melo, H. M., Seixas, Da Silva, G. D. S., Sant'ana, M. R., Teixeira, C. V. L., Clarke, J. R., et al. (2020). Palmitate Is Increased in the Cerebrospinal Fluid of Humans with Obesity and Induces Memory Impairment in Mice via Pro-inflammatory TNF-alpha. *Cell Rep* 30.

Merino-Serrais, P., Benavides-Piccione, R., Blazquez-Llorca, L., Kastanauskaite, A., Rabano, A., Avila, J., et al. (2013). The influence of phospho-tau on dendritic spines of cortical pyramidal neurons in patients with Alzheimer's disease. *Brain* 136, 1913–1928. doi: 10.1093/brain/awt088

Milanski, M., Degasperi, G., Coope, A., Morari, J., Denis, R., Cintra, D. E., et al. (2009). Saturated fatty acids produce an inflammatory response predominantly through the activation of TLR4 signaling in hypothalamus: implications for the pathogenesis of obesity. *J. Neurosci.* 29, 359–370. doi: 10.1523/jneurosci.2760-08.2009

Miwa, K., Okazaki, S., Sakaguchi, M., Mochizuki, H., and Kitagawa, K. (2016). Interleukin-6, interleukin-6 receptor gene variant, small-vessel disease and incident dementia. *Eur. J. Neurol.* 23, 656–663. doi: 10.1111/ene.12921

Morris, J. K., Uy, R. A. Z., Vidoni, E. D., Wilkins, H. M., Archer, A. E., Thyfault, J. P., et al. (2017). Effect of APOE epsilon4 Genotype on Metabolic Biomarkers in Aging and Alzheimer's Disease. *J. Alzheimers. Dis* 58, 1129–1135. doi: 10.3233/jad-170148

Moser, V. A., Uchoa, M. F., and Pike, C. J. (2018). TLR4 inhibitor TAK-242 attenuates the adverse neural effects of diet-induced obesity. *J Neuroinflammation* 15, 306.

Mu, Y., and Gage, F. H. (2011). Adult hippocampal neurogenesis and its role in Alzheimer's disease. *Mol.Neurodegener.* 6, 85. doi: 10.1186/1750-1326-6-85

Mullins, R. J., Mustapic, M., Chia, C. W., Carlson, O., Gulyani, S., Tran, J., et al. (2019). A Pilot Study of Exenatide Actions in Alzheimer's Disease. *Curr Alzheimer Res* 16, 741–752. doi: 10.2174/1567205016666190913155950

Mun, M. J., Kim, J. H., Choi, J. Y., and Jang, W. C. (2016). Genetic polymorphisms of interleukin genes and the risk of Alzheimer's disease: An update meta-analysis. *Meta Gene* 8, 1–10. doi: 10.1016/j.mgene.2016.01.001

Myette-Cote, E., Durrer, C., Neudorf, H., Bammert, T. D., Botezelli, J. D., Johnson, J. D., et al. (2018). The effect of a short-term low-carbohydrate, high-fat diet with or without postmeal walks on glycemic control and inflammation in type 2 diabetes: a randomized trial. *Am. J. Physiol. Regul. Integr. Comp. Physiol.* 315, R1210–R1219.

Myhre, C. L., Thygesen, C., Villadsen, B., Vollerup, J., Ilkjaer, L., Krohn, K. T., et al. (2019). Microglia Express Insulin-Like Growth Factor-1 in the Hippocampus of Aged APPswe/PS1DeltaE9 Transgenic Mice. *Front Cell Neurosci* 13, 308.

Nadler, Y., Alexandrovich, A., Grigoriadis, N., Hartmann, T., Rao, K. S., Shohami, E., et al. (2008). Increased expression of the gamma-secretase components

presenilin-1 and nicastrin in activated astrocytes and microglia following traumatic brain injury. *Glia* 56, 552–567. doi: 10.1002/glia.20638

Napoli, N., Shah, K., Waters, D. L., Sinacore, D. R., Qualls, C., and Villareal, D. T. (2014). Effect of weight loss, exercise, or both on cognition and quality of life in obese older adults. *Am. J. Clin. Nutr.* 100, 189–198. doi: 10.3945/ajcn.113.082883

Nguyen, T. T., Ta, Q. T. H., Nguyen, T. T. D., Le, T. T., and Vo, V. G. (2020). Role of Insulin Resistance in the Alzheimer's Disease Progression. *Neurochem. Res.* 45, 1481–1491.

O'Brien, P. D., Hinder, L. M., Callaghan, B. C., and Feldman, E. L. (2017). Neurological consequences of obesity. *Lancet Neurol.* 16, 465–477.

O'Bryant, S. E., Hobson, V., Hall, J. R., Waring, S. C., Chan, W., Massman, P., et al. (2009). Brain-derived neurotrophic factor levels in Alzheimer's disease. *J. Alzheimers. Dis.* 17, 337–341.

Ou, Z., Kong, X., Sun, X., He, X., Zhang, L., Gong, Z., et al. (2018). Metformin treatment prevents amyloid plaque deposition and memory impairment in APP/PS1 mice. *Brain Behav. Immun.* 69, 351–363. doi: 10.1016/j.bbi.2017.12.009

Panagaki, T., Gengler, S., and Holscher, C. (2018). The Novel DA-CH3 Dual Incretin Restores Endoplasmic Reticulum Stress and Autophagy Impairments to Attenuate Alzheimer-Like Pathology and Cognitive Decrements in the APPSWE/PS1DeltaE9 Mouse Model. *J. Alzheimers. Dis.* 66, 195–218. doi: 10.3233/jad-180584

Pang, R., Wang, X., Pei, F., Zhang, W., Shen, J., Gao, X., et al. (2019). Regular Exercise Enhances Cognitive Function and Intracephalic GLUT Expression in Alzheimer's Disease Model Mice. *J. Alzheimers. Dis.* 72, 83–96. doi: 10.3233/jad-190328

Paouri, E., Tzara, O., Zenelak, S., and Georgopoulos, S. (2017). Genetic Deletion of Tumor Necrosis Factor-alpha Attenuates Amyloid-beta Production and Decreases Amyloid Plaque Formation and Glial Response in the 5XFAD Model of Alzheimer's Disease. *J. Alzheimers. Dis.* 60, 165–181. doi: 10.3233/jad-170065

Pardo, M., Abrial, E., Jope, R. S., and Beurel, E. (2016). GSK3beta isoform-selective regulation of depression, memory and hippocampal cell proliferation. *Genes Brain Behav.* 15, 348–355. doi: 10.1111/gbb.12283

Parimisetty, A., Dorsemans, A. C., Awada, R., Ravanan, P., Diotel, N., and Lefebvre D'hellencourt, C. (2016). Secret talk between adipose tissue and central nervous system via secreted factors-an emerging frontier in the neurodegenerative research. *J Neuroinflammation* 13, 67.

Pasqualetti, P., Bonomini, C., Dal Forno, G., Paulon, L., Sinforiani, E., Marra, C., et al. (2009). A randomized controlled study on effects of ibuprofen on cognitive progression of Alzheimer's disease. *Aging Clin. Exp. Res.* 21, 102–110. doi: 10.1007/bf03325217

Patterson, S. L. (2015). Immune dysregulation and cognitive vulnerability in the aging brain: Interactions of microglia, IL-1beta, BDNF and synaptic plasticity. *Neuropharmacology* 96, 11–18. doi: 10.1016/j.neuropharm.2014.12.020

Peineau, S., Taghibiglou, C., Bradley, C., Wong, T. P., Liu, L., Lu, J., et al. (2007). LTP inhibits LTD in the hippocampus via regulation of GSK3beta. *Neuron* 53, 703–717. doi: 10.1016/j.neuron.2007.01.029

Peng, S., Wuu, J., Mufson, E. J., and Fahnestock, M. (2005). Precursor form of brain-derived neurotrophic factor and mature brain-derived neurotrophic factor are decreased in the pre-clinical stages of Alzheimer's disease. *J. Neurochem.* 93, 1412–1421. doi: 10.1111/j.1471-4159.2005.03135.x

Poggi, M., Bastelica, D., Gual, P., Iglesias, M. A., Gremeaux, T., Knauf, C., et al. (2007). C3H/HeJ mice carrying a toll-like receptor 4 mutation are protected against the development of insulin resistance in white adipose tissue in response to a high-fat diet. *Diabetologia* 50, 1267–1276. doi: 10.1007/s00125-007-0654-8

Pomilio, C., Gorojod, R. M., Riudavets, M., Vinuesa, A., Presa, J., Gregosa, A., et al. (2020). Microglial autophagy is impaired by prolonged exposure to beta-amyloid peptides: evidence from experimental models and Alzheimer's disease patients. *Geroscience* 42, 613–632. doi: 10.1007/s11357-020-00161-9

Puder, J. J., and Munsch, S. (2010). Psychological correlates of childhood obesity. *Int.J.Obes.(Lond)* 34(Suppl. 2), S37–S43.

Qi, Y., Klyubin, I., Cuello, A. C., and Rowan, M. J. (2018). NLRP3-dependent synaptic plasticity deficit in an Alzheimer's disease amyloidosis model in vivo. *Neurobiol. Dis.* 114, 24–30. doi: 10.1016/j.nbd.2018.02.016

Qiu, W. Q., and Folstein, M. F. (2006). Insulin, insulin-degrading enzyme and amyloid-beta peptide in Alzheimer's disease: review and hypothesis. *Neurobiol. Aging* 27, 190–198. doi: 10.1016/j.neurobiolaging.2005.01.004

Quinn, J. F., Raman, R., Thomas, R. G., Yurko-Mauro, K., Nelson, E. B., Van Dyck, C., et al. (2010). Docosahexaenoic acid supplementation and cognitive decline in Alzheimer disease: a randomized trial. *JAMA* 304, 1903–1911. doi: 10.1001/jama.2010.1510

Rajasekar, N., Nath, C., Hanif, K., and Shukla, R. (2017a). Intranasal Insulin Administration Ameliorates Streptozotocin (ICV)-Induced Insulin Receptor Dysfunction, Neuroinflammation, Amyloidogenesis, and Memory Impairment in Rats. *Mol. Neurobiol.* 54, 6507–6522. doi: 10.1007/s12035-016-0169-8

Rajasekar, N., Nath, C., Hanif, K., and Shukla, R. (2017b). Intranasal insulin improves cerebral blood flow, Nrf-2 expression and BDNF in STZ (ICV)-induced memory impaired rats. *Life Sci.* 173, 1–10. doi: 10.1016/j.lfs.2016.09.020

Rao, P., and Knaus, E. E. (2008). Evolution of nonsteroidal anti-inflammatory drugs (NSAIDs): cyclooxygenase (COX) inhibition and beyond. *J. Pharm. Pharm. Sci* 11, 81s–110s.

Reed, B., Villeneuve, S., Mack, W., Decarli, C., Chui, H. C., and Jagust, W. (2014). Associations between serum cholesterol levels and cerebral amyloidosis. *JAMA Neurol* 71, 195–200. doi: 10.1001/jamaneurol.2013.5390

Reger, M. A., Henderson, S. T., Hale, C., Cholerton, B., Baker, L. D., Watson, G. S., et al. (2004). Effects of beta-hydroxybutyrate on cognition in memory-impaired adults. *Neurobiol. Aging* 25, 311–314. doi: 10.1016/s0197-4580(03)00087-3

Reger, M. A., Watson, G. S., Green, P. S., Baker, L. D., Cholerton, B., Fishel, M. A., et al. (2008). Intranasal insulin administration dose-dependently modulates verbal memory and plasma amyloid-beta in memory-impaired older adults. *J. Alzheimers. Dis.* 13, 323–331. doi: 10.3233/jad-2008-13309

Reich, D., Gallucci, G., Tong, M., and De La Monte, S. M. (2018). Therapeutic Advantages of Dual Targeting of PPAR-delta and PPAR-gamma in an Experimental Model of Sporadic Alzheimer's Disease. *J Parkinsons Dis Alzheimers Dis* 5.

Reitz, C. (2013). Dyslipidemia and the risk of Alzheimer's disease. *Curr. Atheroscler. Rep* 15, 307.

Rhea, E. M., Nirkhe, S., Nguyen, S., Pemberton, S., Bammler, T. K., Beyer, R., et al. (2019). Molecular Mechanisms of Intranasal Insulin in SAMP8 Mice. *J. Alzheimers. Dis.* 71, 1361–1373. doi: 10.3233/jad-190707

Ridker, P. M., Rifai, N., Stampfer, M. J., and Hennekens, C. H. (2000). Plasma concentration of interleukin-6 and the risk of future myocardial infarction among apparently healthy men. *Circulation* 101, 1767–1772. doi: 10.1161/01.cir.101.15.1767

Risner, M. E., Saunders, A. M., Altman, J. F., Ormandy, G. C., Craft, S., Foley, I. M., et al. (2006). Efficacy of rosiglitazone in a genetically defined population with mild-to-moderate Alzheimer's disease. *Pharmacogenomics J.* 6, 246–254. doi: 10.1038/sj.tpj.6500369

Rockenstein, E., Torrance, M., Adame, A., Mante, M., Bar-On, P., Rose, J. B., et al. (2007). Neuroprotective effects of regulators of the glycogen synthase kinase-3beta signaling pathway in a transgenic model of Alzheimer's disease are associated with reduced amyloid precursor protein phosphorylation. *J. Neurosci.* 27, 1981–1991. doi: 10.1523/jneurosci.4321-06.2007

Rogers, J., Kirby, L. C., Hempelman, S. R., Berry, D. L., Mcgeer, P. L., Kaszniak, A. W., et al. (1993). Clinical trial of indomethacin in Alzheimer's disease. *Neurology* 43, 1609–1611.

Ronan, L., Alexander-Bloch, A., and Fletcher, P. C. (2019). Childhood Obesity, Cortical Structure, and Executive Function in Healthy Children. *Cereb Cortex.*

Ruegsegger, G. N., Vanderboom, P. M., Dasari, S., Klaus, K. A., Kabiraj, P., Mccarthy, C. B., et al. (2019). Exercise and metformin counteract altered mitochondrial function in the insulin-resistant brain. *JCI Insight* 4.

Ryan, C. M., Freed, M. I., Rood, J. A., Cobitz, A. R., Waterhouse, B. R., and Strachan, M. W. (2006). Improving metabolic control leads to better working memory in adults with type 2 diabetes. *Diabetes Care* 29, 345–351. doi: 10.2337/diacare.29.02.06.dc05-1626

Ryan, S. M., and Kelly, A. M. (2016). Exercise as a pro-cognitive, pro-neurogenic and anti-inflammatory intervention in transgenic mouse models of Alzheimer's disease. *Ageing Res. Rev.* 27, 77–92. doi: 10.1016/j.arr.2016.03.007

Sah, S. K., Lee, C., Jang, J. H., and Park, G. H. (2017). Effect of high-fat diet on cognitive impairment in triple-transgenic mice model of Alzheimer's disease. *Biochem. Biophys. Res. Commun.* 493, 731–736. doi: 10.1016/j.bbrc.2017.08.122

Saini, R. K., Rengasamy, K. R. R., Mahomoodally, F. M., and Keum, Y. S. (2020). Protective effects of lycopene in cancer, cardiovascular, and neurodegenerative

diseases: An update on epidemiological and mechanistic perspectives. *Pharmacol. Res.* 155, 104730. doi: 10.1016/j.phrs.2020.104730

Saiz-Vazquez, O., Puente-Martinez, A., Ubillos-Landa, S., Pacheco-Bonrostro, J., and Santabarbara, J. (2020). Cholesterol and Alzheimer's Disease Risk: A Meta-Meta-Analysis. *Brain Sci* 10.

Salameh, T. S., Bullock, K. M., Hujoel, I. A., Niehoff, M. L., Wolden-Hanson, T., Kim, J., et al. (2015). Central Nervous System Delivery of Intranasal Insulin: Mechanisms of Uptake and Effects on Cognition. *J. Alzheimers. Dis.* 47, 715–728. doi: 10.3233/jad-150307

Salameh, T. S., Mortell, W. G., Logsdon, A. F., Butterfield, D. A., and Banks, W. A. (2019). Disruption of the hippocampal and hypothalamic blood-brain barrier in a diet-induced obese model of type II diabetes: prevention and treatment by the mitochondrial carbonic anhydrase inhibitor, topiramate. *Fluids Barriers CNS* 16, 1.

Samant, N. P., and Gupta, G. L. (2021). Novel therapeutic strategies for Alzheimer's disease targeting brain cholesterol homeostasis. *Eur. J. Neurosci.* 53, 673–686. doi: 10.1111/ejn.14949

Sanguinetti, E., Guzzardi, M. A., Panetta, D., Tripodi, M., De Sena, V., Quaglierini, M., et al. (2019). Combined Effect of Fatty Diet and Cognitive Decline on Brain Metabolism, Food Intake, Body Weight, and Counteraction by Intranasal Insulin Therapy in 3xTg Mice. *Front Cell Neurosci* 13, 188.

Sato, T., Hanyu, H., Hirao, K., Kanetaka, H., Sakurai, H., and Iwamoto, T. (2011). Efficacy of PPAR-gamma agonist pioglitazone in mild Alzheimer disease. *Neurobiol. Aging* 32, 1626–1633. doi: 10.1016/j.neurobiolaging.2009.10.009

Scheff, S. W., Price, D. A., Ansari, M. A., Roberts, K. N., Schmitt, F. A., Ikonomovic, M. D., et al. (2015). Synaptic change in the posterior cingulate gyrus in the progression of Alzheimer's disease. *J. Alzheimers. Dis.* 43, 1073–1090. doi: 10.3233/jad-141518

Scheff, S. W., Price, D. A., Schmitt, F. A., and Mufson, E. J. (2006). Hippocampal synaptic loss in early Alzheimer's disease and mild cognitive impairment. *Neurobiol. Aging* 27, 1372–1384. doi: 10.1016/j.neurobiolaging.2005.09.012

Schmid, V., Kullmann, S., Gfrorer, W., Hund, V., Hallschmid, M., Lipp, H. P., et al. (2018). Safety of intranasal human insulin: A review. *Diabetes. Obes. Metab* 20, 1563–1577. doi: 10.1111/dom.13279

Searcy, J. L., Phelps, J. T., Pancani, T., Kadish, I., Popovic, J., Anderson, K. L., et al. (2012). Long-term pioglitazone treatment improves learning and attenuates pathological markers in a mouse model of Alzheimer's disease. *J. Alzheimers. Dis.* 30, 943–961. doi: 10.3233/jad-2012-111661

Selemon, L. D. (2013). A role for synaptic plasticity in the adolescent development of executive function. *Transl Psychiatry* 3, e238. doi: 10.1038/tp.2013.7

Shellington, E. M., Reichert, S. M., Heath, M., Gill, D. P., Shigematsu, R., and Petrella, R. J. (2018). Results From a Feasibility Study of Square-Stepping Exercise in Older Adults With Type 2 Diabetes and Self-Reported Cognitive Complaints to Improve Global Cognitive Functioning. *Can J Diabetes* 42.

Sheng, J. G., Bora, S. H., Xu, G., Borchelt, D. R., Price, D. L., and Koliatsos, V. E. (2003). Lipopolysaccharide-induced-neuroinflammation increases intracellular accumulation of amyloid precursor protein and amyloid beta peptide in APPswe transgenic mice. *Neurobiol. Dis.* 14, 133–145. doi: 10.1016/s0969-9961(03)00069-x

Shinto, L., Quinn, J., Montine, T., Dodge, H. H., Woodward, W., Baldauf-Wagner, S., et al. (2014). A randomized placebo-controlled pilot trial of omega-3 fatty acids and alpha lipoic acid in Alzheimer's disease. *J. Alzheimers. Dis.* 38, 111–120. doi: 10.3233/jad-130722

Sobol, N. A., Dall, C. H., Hogh, P., Hoffmann, K., Frederiksen, K. S., Vogel, A., et al. (2018). Change in Fitness and the Relation to Change in Cognition and Neuropsychiatric Symptoms After Aerobic Exercise in Patients with Mild Alzheimer's Disease. *J. Alzheimers. Dis.* 65, 137–145. doi: 10.3233/jad-180253

Sochocka, M., Donskow-Lysoniewska, K., Diniz, B. S., Kurpas, D., Brzozowska, E., and Leszek, J. (2019). The Gut Microbiome Alterations and Inflammation-Driven Pathogenesis of Alzheimer's Disease-a Critical Review. *Mol. Neurobiol.* 56, 1841–1851. doi: 10.1007/s12035-018-1188-4

Solas, M., Milagro, F. I., Ramirez, M. J., and Martinez, J. A. (2017). Inflammation and gut-brain axis link obesity to cognitive dysfunction: plausible pharmacological interventions. *Curr. Opin. Pharmacol* 37, 87–92. doi: 10.1016/j.coph.2017.10.005

Solmaz, V., Cinar, B. P., Yigitturk, G., Cavusoglu, T., Taskiran, D., and Erbas, O. (2015). Exenatide reduces TNF-alpha expression and improves hippocampal neuron numbers and memory in streptozotocin treated rats. *Eur. J. Pharmacol* 765, 482–487. doi: 10.1016/j.ejphar.2015.09.024

Solomon, A., Kivipelto, M., Wolozin, B., Zhou, J., and Whitmer, R. A. (2009). Midlife serum cholesterol and increased risk of Alzheimer's and vascular dementia three decades later. *Dement. Geriatr. Cogn. Disord* 28, 75–80. doi: 10.1159/000231980

Sparks, D. L., Scheff, S. W., Hunsaker, J. C. III, Liu, H., Landers, T., and Gross, D. R. (1994). Induction of Alzheimer-like beta-amyloid immunoreactivity in the brains of rabbits with dietary cholesterol. *Exp. Neurol.* 126, 88–94. doi: 10.1006/exnr.1994.1044

Spilman, P., Podlutskaya, N., Hart, M. J., Debnath, J., Gorostiza, O., Bredesen, D., et al. (2010). Inhibition of mTOR by rapamycin abolishes cognitive deficits and reduces amyloid-beta levels in a mouse model of Alzheimer's disease. *PLoS.One.* 5, e9979. doi: 10.1371/journal.pone.0009979

Stavoe, A. K. H., and Holzbaur, E. L. F. (2020). Neuronal autophagy declines substantially with age and is rescued by overexpression of WIPI2. *Autophagy* 16, 371–372. doi: 10.1080/15548627.2019.1695401

Stebbings, K. A., Choi, H. W., Ravindra, A., and Llano, D. A. (2016). The impact of aging, hearing loss, and body weight on mouse hippocampal redox state, measured in brain slices using fluorescence imaging. *Neurobiol. Aging* 42, 101–109. doi: 10.1016/j.neurobiolaging.2016.03.006

Steen, E., Terry, B. M., Rivera, E. J., Cannon, J. L., Neely, T. R., Tavares, R., et al. (2005). Impaired insulin and insulin-like growth factor expression and signaling mechanisms in Alzheimer's disease–is this type 3 diabetes? *J Alzheimers Dis* 7, 63–80. doi: 10.3233/jad-2005-7107

Stewart, C. R., Stuart, L. M., Wilkinson, K., Van Gils, J. M., Deng, J., Halle, A., et al. (2010). CD36 ligands promote sterile inflammation through assembly of a Toll-like receptor 4 and 6 heterodimer. *Nat. Immunol.* 11, 155–161. doi: 10.1038/ni.1836

Stohr, O., Schilbach, K., Moll, L., Hettich, M. M., Freude, S., Wunderlich, F. T., et al. (2013). Insulin receptor signaling mediates APP processing and beta-amyloid accumulation without altering survival in a transgenic mouse model of Alzheimer's disease. *Age (Dordr)* 35, 83–101. doi: 10.1007/s11357-011-9333-2

Stranahan, A. M., Arumugam, T. V., Cutler, R. G., Lee, K., Egan, J. M., and Mattson, M. P. (2008). Diabetes impairs hippocampal function through glucocorticoid-mediated effects on new and mature neurons. *Nat.Neurosci.* 11, 309–317. doi: 10.1038/nn2055

Subramanian, J., Savage, J. C., and Tremblay, M. E. (2020). Synaptic Loss in Alzheimer's Disease: Mechanistic Insights Provided by Two-Photon in vivo Imaging of Transgenic Mouse Models. *Front Cell Neurosci* 14, 592607.

Tai, L. M., Koster, K. P., Luo, J., Lee, S. H., Wang, Y. T., Collins, N. C., et al. (2014). Amyloid-beta pathology and APOE genotype modulate retinoid X receptor agonist activity in vivo. *J. Biol. Chem.* 289, 30538–30555. doi: 10.1074/jbc.m114.600833

Tamtaji, O. R., Heidari-Soureshjani, R., Mirhosseini, N., Kouchaki, E., Bahmani, F., Aghadavod, E., et al. (2019). Probiotic and selenium co-supplementation, and the effects on clinical, metabolic and genetic status in Alzheimer's disease: A randomized, double-blind, controlled trial. *Clin. Nutr.* 38, 2569–2575. doi: 10.1016/j.clnu.2018.11.034

Tanokashira, D., Kurata, E., Fukuokaya, W., Kawabe, K., Kashiwada, M., Takeuchi, H., et al. (2018). Metformin treatment ameliorates diabetes-associated decline in hippocampal neurogenesis and memory via phosphorylation of insulin receptor substrate 1. *FEBS Open Bio* 8, 1104–1118. doi: 10.1002/2211-5463.12436

Taylor, M. K., Sullivan, D. K., Mahnken, J. D., Burns, J. M., and Swerdlow, R. H. (2018). Feasibility and efficacy data from a ketogenic diet intervention in Alzheimer's disease. *Alzheimers Dement (N Y)* 4, 28–36. doi: 10.1016/j.trci.2017.11.002

Theriault, P., Elali, A., and Rivest, S. (2016). High fat diet exacerbates Alzheimer's disease-related pathology in APPswe/PS1 mice. *Oncotarget* 7, 67808–67827.

Tobin, M. K., Musaraca, K., Disouky, A., Shetti, A., Bheri, A., Honer, W. G., et al. (2019). Human Hippocampal Neurogenesis Persists in Aged Adults and Alzheimer's Disease Patients. *Cell Stem Cell.*

Toda, T., and Gage, F. H. (2017). Review: adult neurogenesis contributes to hippocampal plasticity. *Cell Tissue Res.*

Tong, L., Prieto, G. A., Kramar, E. A., Smith, E. D., Cribbs, D. H., Lynch, G., et al. (2012). Brain-derived neurotrophic factor-dependent synaptic plasticity

is suppressed by interleukin-1beta via p38 mitogen-activated protein kinase. *J. Neurosci.* 32, 17714–17724.

Tremmel, M., Gerdtham, U. G., Nilsson, P. M., and Saha, S. (2017). Economic Burden of Obesity: A Systematic Literature Review. *Int J Environ Res Public Health* 14.

Tu, S., Okamoto, S., Lipton, S. A., and Xu, H. (2014). Oligomeric Abeta-induced synaptic dysfunction in Alzheimer's disease. *Mol Neurodegener* 9, 48.

Turnbaugh, P. J., Ley, R. E., Mahowald, M. A., Magrini, V., Mardis, E. R., and Gordon, J. I. (2006). An obesity-associated gut microbiome with increased capacity for energy harvest. *Nature* 444, 1027–1031.

Uddin, M. S., Mamun, A. A., Labu, Z. K., Hidalgo-Lanussa, O., Barreto, G. E., and Ashraf, G. M. (2019). Autophagic dysfunction in Alzheimer's disease: Cellular and molecular mechanistic approaches to halt Alzheimer's pathogenesis. *J. Cell. Physiol.* 234, 8094–8112.

Van der Auwera, I., Wera, S., Van Leuven, F., and Henderson, S. T. (2005). A ketogenic diet reduces amyloid beta 40 and 42 in a mouse model of Alzheimer's disease. *Nutr Metab (Lond)* 2, 28.

van der Kant, R., Langness, V. F., Herrera, C. M., Williams, D. A., Fong, L. K., Leestemaker, Y., et al. (2019). Cholesterol Metabolism Is a Druggable Axis that Independently Regulates Tau and Amyloid-beta in iPSC-Derived Alzheimer's Disease Neurons. *Cell Stem Cell* 24.

van Duinkerken, E., and Ryan, C. M. (2019). Diabetes mellitus in the young and the old: Effects on cognitive functioning across the life span. *Neurobiol. Dis.* 134, 104608.

Varga, T., Czimmerer, Z., and Nagy, L. (2011). PPARs are a unique set of fatty acid regulated transcription factors controlling both lipid metabolism and inflammation. *Biochim. Biophys. Acta* 1812, 1007–1022.

Velloso, L. A., Folli, F., and Saad, M. J. (2015). TLR4 at the Crossroads of Nutrients, Gut Microbiota, and Metabolic Inflammation. *Endocr.Rev.* 36, 245–271.

Vidal-Puig, A., Jimenez-Linan, M., Lowell, B. B., Hamann, A., Hu, E., Spiegelman, B., et al. (1996). Regulation of PPAR gamma gene expression by nutrition and obesity in rodents. *J. Clin. Invest.* 97, 2553–2561.

Vinuesa, A., Bentivegna, M., Calfa, G., Filipello, F., Pomilio, C., Bonaventura, M. M., et al. (2019). Early Exposure to a High-Fat Diet Impacts on Hippocampal Plasticity: Implication of Microglia-Derived Exosome-like Extracellular Vesicles. *Mol. Neurobiol.* 56, 5075–5094.

Vinuesa, A., Pomilio, C., Menafra, M., Bonaventura, M. M., Garay, L., Mercogliano, M. F., et al. (2016). Juvenile exposure to a high fat diet promotes behavioral and limbic alterations in the absence of obesity. *Psychoneuroendocrinology* 72, 22–33.

Vogt, N. M., Kerby, R. L., Dill-Mcfarland, K. A., Harding, S. J., Merluzzi, A. P., Johnson, S. C., et al. (2017). Gut microbiome alterations in Alzheimer's disease. *Sci Rep* 7, 13537.

Wang, B., and Tontonoz, P. (2018). Liver X receptors in lipid signalling and membrane homeostasis. *Nat Rev Endocrinol* 14, 452–463.

Wang, Q., Hu, J., Liu, Y., Li, J., Liu, B., Li, M., et al. (2019). Aerobic Exercise Improves Synaptic-Related Proteins of Diabetic Rats by Inhibiting FOXO1/NF-kappaB/NLRP3 Inflammatory Signaling Pathway and Ameliorating PI3K/Akt Insulin Signaling Pathway. *J. Mol. Neurosci.* 69, 28–38.

Wang, T. (2015). TNF-alpha G308A polymorphism and the susceptibility to Alzheimer's disease: an updated meta-analysis. *Arch. Med. Res.* 46:24.

Wang, T., Fu, F. H., Han, B., Zhang, L. M., and Zhang, X. M. (2011). Long-term but not short-term aspirin treatment attenuates diabetes-associated learning and memory decline in mice. *Exp. Clin. Endocrinol. Diabetes* 119, 36–40.

Wang, Z., Dong, B., Hu, J., Adegbija, O., and Arnold, L. W. (2016). Exploring the non-linear association between BMI and mortality in adults with and without diabetes: the US National Health Interview Survey. *Diabet. Med.* 33, 1691–1699.

Warden, A., Truitt, J., Merriman, M., Ponomareva, O., Jameson, K., Ferguson, L. B., et al. (2016). Localization of PPAR isotypes in the adult mouse and human brain. *Sci Rep* 6, 27618.

Watson, G. S., Cholerton, B. A., Reger, M. A., Baker, L. D., Plymate, S. R., Asthana, S., et al. (2005). Preserved cognition in patients with early Alzheimer disease and amnestic mild cognitive impairment during treatment with rosiglitazone: a preliminary study. *Am. J. Geriatr. Psychiatry* 13, 950–958.

Wei, L., Yao, M., Zhao, Z., Jiang, H., and Ge, S. (2018). High-fat diet aggravates postoperative cognitive dysfunction in aged mice. *BMC Anesthesiol* 18, 20.

Who. (2018). *Obesity and overweight [Online]*. Available: http://www.who.int/mediacentre/factsheets/fs311/en/[Accessed] (accessed January 10, 2021).

Who. (2020). *https://www.who.int/news-room/fact-sheets/detail/dementia*. WHO. (accessed January 10, 2021).

Wilcox, G. (2005). Insulin and insulin resistance. *Clin Biochem Rev* 26, 19–39.

Wilhelmi de Toledo, F., Grundler, F., Bergouignan, A., Drinda, S., and Michalsen, A. (2019). Safety, health improvement and well-being during a 4 to 21-day fasting period in an observational study including 1422 subjects. *PLoS ONE* 14, e0209353.

Xue, Q. S., Sparks, D. L., and Streit, W. J. (2007). Microglial activation in the hippocampus of hypercholesterolemic rabbits occurs independent of increased amyloid production. *J Neuroinflammation* 4, 20.

Yan, Q., Zhang, J., Liu, H., Babu-Khan, S., Vassar, R., Biere, A. L., et al. (2003). Anti-inflammatory drug therapy alters beta-amyloid processing and deposition in an animal model of Alzheimer's disease. *J. Neurosci.* 23, 7504–7509.

Ying, W., Fu, W., Lee, Y. S., and Olefsky, J. M. (2020). The role of macrophages in obesity-associated islet inflammation and beta-cell abnormalities. *Nat Rev Endocrinol* 16, 81–90.

Yoon, D. H., Lee, J. Y., and Song, W. (2018). Effects of Resistance Exercise Training on Cognitive Function and Physical Performance in Cognitive Frailty: A Randomized Controlled Trial. *J. Nutr. Health Aging* 22, 944–951.

Zatta, P., Zambenedetti, P., Stella, M. P., and Licastro, F. (2002). Astrocytosis, microgliosis, metallothionein-I-II and amyloid expression in high cholesterol-fed rabbits. *J. Alzheimers. Dis.* 4, 1–9.

Zhang-Gandhi, C. X., and Drew, P. D. (2007). Liver X receptor and retinoid X receptor agonists inhibit inflammatory responses of microglia and astrocytes. *J. Neuroimmunol.* 183, 50–59.

Zhang, L., Tang, W., Chao, F. L., Zhou, C. N., Jiang, L., Zhang, Y., et al. (2020). Four-month treadmill exercise prevents the decline in spatial learning and memory abilities and the loss of spinophilin-immunoreactive puncta in the hippocampus of APP/PS1 transgenic mice. *Neurobiol. Dis.* 136, 104723.

Zhang, N., Liang, H., Farese, R. V., Li, J., Musi, N., and Hussey, S. E. (2015). Pharmacological TLR4 Inhibition Protects against Acute and Chronic Fat-Induced Insulin Resistance in Rats. *PLoS ONE* 10, e0132575.

Zhang, Z. H., Wen, L., Wu, Q. Y., Chen, C., Zheng, R., Liu, Q., et al. (2017). Long-Term Dietary Supplementation with Selenium-Enriched Yeast Improves Cognitive Impairment, Reverses Synaptic Deficits, and Mitigates Tau Pathology in a Triple Transgenic Mouse Model of Alzheimer's Disease. *J. Agric. Food Chem.* 65, 4970–4979.

Zhou, G., Myers, R., Li, Y., Chen, Y., Shen, X., Fenyk-Melody, J., et al. (2001). Role of AMP-activated protein kinase in mechanism of metformin action. *J. Clin. Invest.* 108, 1167–1174.

Conflict of Interest: The authors declare that the research was conducted in the absence of any commercial or financial relationships that could be construed as a potential conflict of interest.

Copyright © 2021 Vinuesa, Pomilio, Gregosa, Bentivegna, Presa, Bellotto, Saravia and Beauquis. This is an open-access article distributed under the terms of the Creative Commons Attribution License (CC BY). The use, distribution or reproduction in other forums is permitted, provided the original author(s) and the copyright owner(s) are credited and that the original publication in this journal is cited, in accordance with accepted academic practice. No use, distribution or reproduction is permitted which does not comply with these terms.

frontiers in Pharmacology

REVIEW
published: 28 April 2021
doi: 10.3389/fphar.2021.655052

CNS-Draining Meningeal Lymphatic Vasculature: Roles, Conundrums and Future Challenges

*Sofia Pereira das Neves, Nickoleta Delivanoglou and Sandro Da Mesquita**

Department of Neuroscience, Mayo Clinic, Jacksonville, FL, United States

A genuine and functional lymphatic vascular system is found in the meninges that sheath the central nervous system (CNS). This unexpected (re)discovery led to a reevaluation of CNS fluid and solute drainage mechanisms, neuroimmune interactions and the involvement of meningeal lymphatics in the initiation and progression of neurological disorders. In this manuscript, we provide an overview of the development, morphology and unique functional features of meningeal lymphatics. An outline of the different factors that affect meningeal lymphatic function, such as growth factor signaling and aging, and their impact on the continuous drainage of brain-derived molecules and meningeal immune cells into the cervical lymph nodes is also provided. We also highlight the most recent discoveries about the roles of the CNS-draining lymphatic vasculature in different pathologies that have a strong neuroinflammatory component, including brain trauma, tumors, and aging-associated neurodegenerative diseases like Alzheimer's and Parkinson's. Lastly, we provide a critical appraisal of the conundrums, challenges and exciting questions involving the meningeal lymphatic system that ought to be investigated in years to come.

Keywords: meninges, lymphatic vessels, central nervous system, drainage, cerebrospinal fluid, aging, disease, neuroinflammation

OPEN ACCESS

Edited by:
Mariela Fernanda Perez, National University of Cordoba, Argentina

Reviewed by:
Per Svenningsson, Karolinska Institutet (KI), Sweden
Anna Maria Pittaluga, University of Genoa, Italy

****Correspondence:***
Sandro Da Mesquita
damesquita@mayo.edu

Specialty section:
This article was submitted to Neuropharmacology, a section of the journal Frontiers in Pharmacology

Received: *18 January 2021*
Accepted: *13 April 2021*
Published: *28 April 2021*

Citation:
das Neves SP, Delivanoglou N and Da Mesquita S (2021) CNS-Draining Meningeal Lymphatic Vasculature: Roles, Conundrums and Future Challenges. Front. Pharmacol. 12:655052. doi: 10.3389/fphar.2021.655052

INTRODUCTION: THE LYMPHATIC SYSTEM

The lymphatic vasculature is an important component of the circulatory system that was initially described back in the 17th and 18th centuries, by the pioneering works of Gasparo Aselli, Olaus Rudbeck, Thomas Bartholin and Paolo Mascagni (Natale et al., 2017; Sandrone et al., 2019). The lymphatic system mediates the drainage of interstitial fluid (ISF) and regulates immune cell trafficking and surveillance in the vast majority of mammalian tissues including the intestine, lungs, heart, liver, diaphragm, skin, eye and even in the meninges that enclose the central nervous system (CNS) (Escobedo and Oliver, 2016; Petrova and Koh, 2018; Oliver et al., 2020; Petrova and Koh, 2020). The lymphatic vessels (LVs) are composed by lymphatic endothelial cells (LECs) that primordially arise by transdifferentiation from the endothelium of the cardinal vein during embryonic development (Francois et al., 2008; Nicenboim et al., 2015; Stone and Stainier, 2019). Commitment to the LEC lineage is dictated by vascular endothelial growth factor C (VEGF-C) signaling through vascular endothelial growth factor receptor 3 (VEGFR3) (Oh et al., 1997; Mäkinen et al., 2001; Mandriota et al., 2001). This signaling pathway induces the downstream activation of the transcription factor SOX18 and expression of the genes encoding for prospero-related homeobox 1 (PROX1), lymphatic vessel endothelial hyaluronan receptor-1 (LYVE-1), podoplanin (PDPN) and C–C motif chemokine ligand (CCL) 21 (Gunn et al., 1998; Banerji et al., 1999; Breiteneder-Geleff

et al., 1999; Wigle and Oliver, 1999; Francois et al., 2008). In turn, the transcription factor PROX1 acts synergistically with the nuclear factor chicken ovalbumin upstream promoter transcription factor II (COUP-TFII) to enhance the expression of LEC-associated genes, namely Flt4 (the gene encoding VEGFR3), and suppress the expression of genes mediating the commitment to the blood endothelial cell lineage (Lee et al., 2009; Sabine et al., 2012). Signaling pathways involving bone morphogenetic protein 2 (BMP2), RAF1/MEK/ERK or Phospholipase C-γ (PLC-γ) have also been implicated in LEC lineage commitment and modulation of LV formation and function (Mancini and Toker, 2009; Norrmén et al., 2009; Coso et al., 2012; Deng et al., 2013; Dunworth et al., 2014). In particular, PLC-γ regulates CLEC2-PDPN signaling, and PLC-γ2 deficiency leads to lymphatic malformation, aberrant uncoupling of the lymphatic and blood vasculature and backflow of venous blood into the lymphatic vasculature (Sebzda et al., 2006; Ichise et al., 2009; Ichise et al., 2016). During embryonic stages, differentiated LECs organize to form the so-called lymph sacs, which subsequently foster the sprouting and development of the lymphatic capillaries (Lee and Suami, 2020) that attach to the extracellular matrix, by interaction with anchoring filaments (Tammela and Alitalo, 2010). Further sprouting, pruning and cellular specialization refine the lymphatic system in a well-organized network that, together with the capillaries, consists of larger vessels (pre-collecting and collecting lymphatics containing specialized valves) and lymph nodes (LNs). Although most of the peripheral lymphatic vasculature forms during embryonic development, lymphatic sprouting and lymphangiogenesis can also take place after birth and in adulthood (Oliver et al., 2020; Petrova and Koh, 2020). Recent experimental evidence points to two main mechanisms of post-developmental lymphangiogenesis: proliferation of LECs (from pre-existing lymphatics) and cellular transdifferentiation. Bone marrow-derived cells, myeloid precursors, blood-forming hemogenic endothelial cells (from the dermal blood capillary bed) and heart-associated progenitor cells are amongst the cell types that can efficiently transdifferentiate into LECs (Mahadevan et al., 2014; Klotz et al., 2015; Martinez-Corral et al., 2015; Stanczuk et al., 2015; Pichol-Thievend et al., 2018; Maruyama et al., 2019; Lioux et al., 2020).

Lymphatic capillaries, also named initial LVs, are thin-walled and blind-ended vessels formed by a monolayer of LECs that may respond to higher levels of VEGF-C to initiate lymphangiogenesis (Pfeiffer et al., 2008; Lohela et al., 2009). Initial LVs have small button-like junctions, a discontinuous basement membrane and lack pericytes and smooth muscle cells (SMCs) (Dejana et al., 2009). The button-like junctions and anchoring filaments present in initial LVs constitute the primary lymphatic valves that enable the entry of macromolecules and immune cells (Dejana et al., 2009; Tammela and Alitalo, 2010). Initial LVs converge into pre-collecting and then collecting LVs, which are bigger in caliber and are surrounded by contractile SMCs. Collecting LVs are almost impermeable structures composed by tight and continuous zipper-like junctions and secondary intraluminal valves that prevent lymph backflow and promote unidirectional drainage (Petrova and Koh, 2020). LECs that form the collecting lymphatics express specific markers like FAT4, Ras interacting protein 1 (RASIP1) and CCL27, alongside other proteins that modulate secondary valve development and function, like Forkhead box protein C2 (FOXC2), Ephrin type-B 2, GATA-binding factor 2 (GATA2), PLC-γ and nuclear factor of activated T cells 1 (NFATc1) (Norrmén et al., 2009; Sabine et al., 2012; Brouillard et al., 2014; Kazenwadel et al., 2015; Liu et al., 2018; Betterman et al., 2020). The low-pressure unidirectional transportation of lymph fluid, cells and macromolecules is also facilitated by skeletal muscle contraction, arterial vasomotion, respiration (Bazigou and Makinen, 2013) and by mechanical forces like fluid pressure and shear stress (Tzima et al., 2005). Lymph drained from different peripheral organs circulates through the lymphatic vascular network and is ultimately drained back into the venous blood circulatory system via the thoracic duct (Oliver et al., 2020).

The lymphatic vasculature collects and transports various types of antigens and immune cells (such as T and antigen-presenting cells) from tissues into their respective draining LNs, thus contributing to immune surveillance and resolution of inflammation (Huggenberger et al., 2011; Onder et al., 2017; Oliver et al., 2020; Petrova and Koh, 2020). The initial and collecting LVs secrete CCL21 and CCL27, respectively, which bind to their distinct receptors C–C motif chemokine receptor (CCR) 7 and CCR10 expressed by different immune cell types, including activated dendritic cells (DCs), T and B cells. In response to CCL21 or CCL27 gradients, immune cells are recruited to the vicinity of LVs and initiate their migration into the LNs (Forster et al., 2008; Wick et al., 2008; Ulvmar et al., 2014). At the LNs, recruited and resident immune cell populations engage and orchestrate immune responses that may culminate in the activation, proliferation and migration of antigen-specific T and B cells into the blood circulation and homing into affected tissues. Alternatively, the process of lymphatic trafficking, egress and immune cell activation at the draining LNs can also be regulated by other proteins expressed by LECs, namely sphingosine-1-phosphate (S1P), colony-stimulating factor–1 (CSF1), vascular cell adhesion molecule 1 (VCAM-1) and intercellular adhesion molecule 1 (ICAM-1) (Pham et al., 2010; Huggenberger et al., 2011; Teijeira et al., 2017; Petrova and Koh, 2018; Mondor et al., 2019).

Severe lymphatic vasculature malfunction can seriously compromise the drainage of ISF and lead to the development of lymphedema. Lymphedema is a disabling and potentially life-threatening pathological condition characterized by tissue edema and swelling, exacerbated buildup of adipose tissue, compromised wound healing capacity and a dysfunctional immune system that often leads to recurrent infections (Rockson, 2001; Oliver et al., 2020). Primary lymphedema is hereditary and results from genetic anomalies that lead to deficient levels of proteins that regulate lymphangiogenesis and lymphatic function, including VEGFR3, FOXC2, SOX18, collagen and calcium binding EGF domains 1 (CCBE1), ADAM metallopeptidase with thrombospondin type 1 motif 3 (ADAMTS3) and GATA2 (Fang et al., 2000; Irrthum et al., 2000; Irrthum et al., 2003; Alders et al., 2009; Kazenwadel et al., 2012; Brouillard et al., 2017; Jones and Mansour, 2017; Oliver et al., 2020). Secondary

lymphedema results from damage to the lymphatic system that can be caused either from infections, such as filariasis, or certain therapeutic interventions, like surgical resection of LNs or tumors (Rockson, 2001; Pfarr et al., 2009; Oliver et al., 2020).

In 2015, two seminal studies have shown that the lymphatic system reaches even the border meningeal tissues of the CNS (Aspelund et al., 2015; Louveau et al., 2015). This recent (re) discovery of meningeal lymphatics led to a better understanding about the drainage of brain and spinal cord fluids and solutes (Antila et al., 2017; Louveau et al., 2018; Jacob et al., 2019) and provided a new vascular system that might be easily harnessed to treat brain insults and combat neurodegenerative diseases such as Alzheimer's and Parkinson's. In the following sections of this manuscript, we will provide an overview of the structural and functional roles of meningeal lymphatics in health and disease and propose hypotheses to be tested in future studies addressing the meningeal lymphatic system.

DEVELOPMENT, CYTOARCHITECTURE AND MORPHOLOGY OF MENINGEAL LYMPHATICS

Despite the early, but inconclusive, reports about the existence of a lymphatic-like system involved in cerebrospinal fluid (CSF) drainage to peripheral LNs (Brierley and Field, 1948; Bradbury and Cole, 1980; Bradbury et al., 1981; Szentistvanyi et al., 1984; Erlich et al., 1986; Andres et al., 1987; Yamada et al., 1991; Kida et al., 1993; Boulton et al., 1996; Killer et al., 1999; Silver et al., 1999; Gausas et al., 2007), the cytoarchitecture and functional features of the lymphatic vasculature present in the CNS meninges of both rodents and humans have only recently been systematically characterized (Aspelund et al., 2015; Louveau et al., 2015; Absinta et al., 2017; Jung et al., 2017; Da Mesquita et al., 2018b; Visanji et al., 2018).

In mice, meningeal LVs develop postnatally and become fully mature around postnatal day 28 (Antila et al., 2017), contrarily to most peripheral lymphatic vasculature that develops during embryonic stages, beginning at embryonic days 9–10 [peripheral lymphatic development was recently reviewed in detail by others (Gutierrez-Miranda and Yaniv, 2020)]. The experimental data available so far suggests that meningeal LECs originate from venous precursor cells, which are somewhat distinct from the ones that give rise to skin and intestinal lymphatics (Martinez-Corral et al., 2015; Stanczuk et al., 2015; Antila et al., 2017), in a process that is VEGFR3-dependent (Aspelund et al., 2015). In fact, loss-of-function studies have shown that both the development and maintenance of adult meningeal LVs are dependent on VEGF-C signaling through VEGFR3, but not on VEGF-D signaling (Antila et al., 2017). However, a more recent study has shown that mice lacking PLC-γ2 also present a structurally and functionally impaired meningeal lymphatic system, thus suggesting that meningeal lymphatic development might not be exclusively dependent on VEGFR3 signaling (Bálint et al., 2020). Primordial meningeal LECs stem from and around the veins at the skull foramina and later extend from the basal into the lateral and dorsal meninges along the major arteries (pterygopalatine and middle meningeal arteries) and venous sinuses (Aspelund et al., 2015; Antila et al., 2017; Izen et al., 2018; Ahn et al., 2019). In adult mice, the meningeal initial LVs are found lining the rostral rhinal vein, superior sagittal sinus, confluence of sinuses, transverse sinus, pterygopalatine artery and middle meningeal artery (**Figure 1**) (Aspelund et al., 2015; Louveau et al., 2015; Louveau et al., 2018; Ahn et al., 2019). The LECs that form the meningeal initial LVs also express the specific markers PROX1, LYVE-1, VEGFR3, PDPN and CCL21, but lack integrin α-9 which is involved in valve formation and is characteristically expressed in the meningeal collecting LVs (Antila et al., 2017; Louveau et al., 2018; Ahn et al., 2019). Initial LVs from the dorsal meninges converge to larger collecting-like lymphatics at the basal dural meninges that have tighter zipper-like junctional patterns, integrin α-9-expressing valves, but lack SMCs, thus resulting in a lymphatic network that extends throughout the brain meningeal dura layer (Aspelund et al., 2015; Louveau et al., 2018; Ahn et al., 2019). The collecting-like LVs are mostly found in the meninges attached to the lateral and basal parts of the skull, lining the petrosquamosal and sigmoid sinuses. Meningeal collecting-like LVs extend along the jugular vein and exit the skull through the foramina and merge into peripheral collecting LVs, which are wrapped by SMCs and drain primarily to the deep cervical LNs (CLNs) and later to the superficial CLNs (**Figure 1**) (Aspelund et al., 2015; Antila et al., 2017; Louveau et al., 2018; Ahn et al., 2019).

The vertebral meningeal LVs that wrap the spinal cord also develop postnatally, through a VEGF-C–VEGFR3-dependent stemming process, which starts at the spinal canal and gives rise to mature LVs at the vertebrae and intervertebral spaces from the cervical, thoracic and lumbar regions (Antila et al., 2017; Louveau et al., 2018; Jacob et al., 2019). Despite presenting distinct organizations and morphologies, the brain and spinal cord meningeal LVs are connected around the foramen magnum and at the cisterna magna (Antila et al., 2017; Jacob et al., 2019). Careful anatomical examinations involving Prox1 reporter mice and staining for different LEC-specific markers has shown that the architectural organization of the vertebral meningeal LVs is segmented, meaning that each vertebral disc is sheathed by two dorsal and two ventral semicircular lymphatic branches that are interconnected by thinner and elongated LVs (Jacob et al., 2019). Moreover, the vertebral meningeal LVs are in direct contact with nerves and ganglia, exit at the intervertebral foramina to connect to peripheral lymphatics and can drain into cervical, thoracic and lumbar LNs (Villaro et al., 1987; Miura et al., 1998; Holzmann et al., 2015; Ma et al., 2019a; Jacob et al., 2019).

Unlike the primordial non-lumenized LV-like structures (formed by mural LECs) found in the zebrafish meninges (Bower et al., 2017), the meningeal lymphatic vasculature found in rodents, non-human primates and humans shows quite similar marker expression, morphologies and topographies (Louveau et al., 2015; Absinta et al., 2017; Visanji et al., 2018). Despite recent reports showing VEGFR3-expressing LECs imbedded in the leptomeninges (Shibata-Germanos et al., 2020), and lymphatic processes reaching the pia mater (Cai et al., 2019), the current understanding is that the

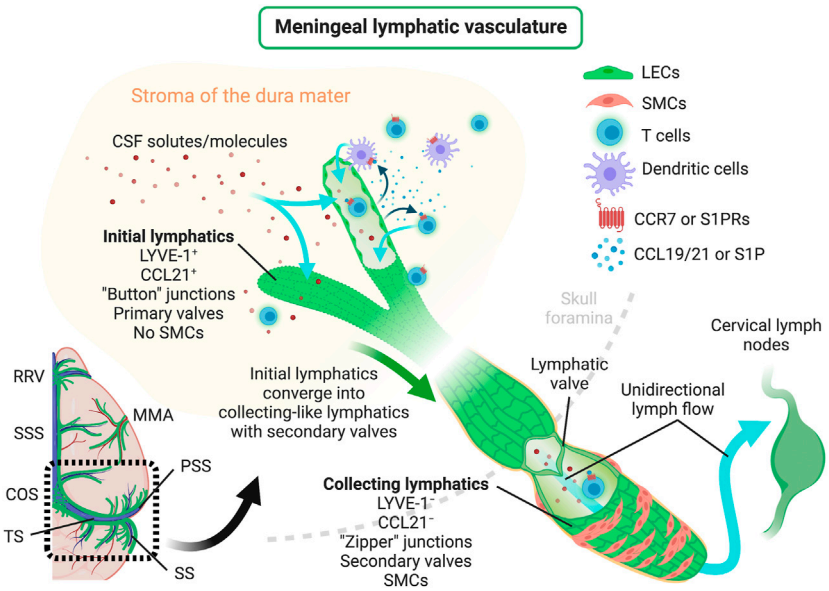

FIGURE 1 | Scheme depicting the structure of meningeal lymphatic vessels, lymphatic drainage of CSF solutes/molecules, mechanisms regulating the trafficking of immune cells through meningeal lymphatics and the unidirectional lymphatic flow into the brain draining CLNs. CCL19/21, C–C motif chemokine ligand 19/21; CCR7, C–C motif chemokine receptor 7; COS, confluence of sinuses; CSF, cerebrospinal fluid; LECs, lymphatic endothelial cells; LYVE-1, lymphatic vessel endothelial hyaluronan receptor-1; MMA, middle meningeal artery; PSS, petrosquamosal sinus; RRV, rostral rhinal vein; S1P, sphingosine-1-phosphate; S1PRs, sphingosine-1-phosphate receptors; SMCs, smooth muscle cells; SS, sigmoid sinus; SSS, superior sagittal sinus; TS, transverse sinus. Created with BioRender.com.

mature meningeal LVs are anatomically confined to the dura mater layer under homeostatic conditions (Louveau et al., 2015; Antila et al., 2017; Louveau et al., 2018; Jacob et al., 2019). However, this is still controversial and more in-depth studies are required to fully understand the anatomy of the mammalian meningeal lymphatic vasculature.

Noticeably, aging affects meningeal lymphatic morphology and function (Da Mesquita et al., 2018b), but spares the lymphatics found in the diaphragm, skin, ear and trachea (Ahn et al., 2019). In the next sections we will focus more on the aging-associated changes in the meningeal lymphatic system and their impact in diseases that affect the CNS.

MENINGEAL LYMPHATIC DRAINAGE AND BRAIN PHYSIOLOGY IN ADULTHOOD AND AGING

The existence of a *bona fide* meningeal lymphatic system led to a reassessment of CNS drainage routes and mechanisms. Outflow of fluids (and solutes) from the mammalian CNS is thought to occur via 3 main pathways: 1) the arachnoid granulations and villi at the venous sinuses in the meningeal dura mater (Weller, 1998), 2) the peripheral lymphatics in the vicinity of the cribriform plate (Bradbury and Westrop, 1983; Furukawa et al., 2008) and 3) the meningeal lymphatic vasculature (Aspelund et al., 2015; Louveau et al., 2015). Nevertheless, recent static and dynamic imaging studies strongly suggest that the major route of CSF outflow is via meningeal LVs rather than the nasal lymphatics or dural venous sinuses (Ma et al., 2017; Ahn et al., 2019; Kutomi and Takeda, 2020; Melin et al., 2020). In fact, the process of CSF drainage into the deep and superficial CLNs is dependent on the integrity of the meningeal lymphatic vascular network and was reduced: 1) upon photodynamic ablation of meningeal lymphatics, 2) in Prox1 heterozygous mice, which present mispatterned and leaky LVs (Harvey et al., 2005), and 3) upon surgical ligation of afferent lymphatics of the deep CLNs (Da Mesquita et al., 2018b; Louveau et al., 2018). However, reduction of CSF outflow into the deep CLNs did not significantly affect the drainage into the superficial CLNs, suggesting that alternative routes of lymphatic drainage might exist and should be explored in future studies (Louveau et al., 2018). The involvement of the dorsal meningeal initial lymphatics in CSF outflow is also somewhat debatable, mostly due to their small diameter, simple morphology and lack of intraluminal valves (Ahn et al., 2019). However, the dorsal initial lymphatics and the larger collecting-like basal lymphatics are part of the same meningeal lymphatic network—one where the initial lymphatics converge into collecting-like and then collecting LVs that exit the skull and are connected to the deep CLNs (Aspelund et al., 2015). In fact, several independent studies support the essential role of both the dorsal initial and basal collecting-like meningeal lymphatics in the drainage of brain-associated fluids, solutes and cells (Da Mesquita et al., 2018b; Louveau et al., 2018; Ahn et al., 2019; Liu X. et al., 2020; Hu et al., 2020; Song et al., 2020).

The meningeal lymphatic vasculature does not contact directly with the brain parenchyma under physiological conditions (Da Mesquita et al., 2018a). In the brain, fluid circulation, exchange and recycling are mediated by the glymphatic system, which consists of a perivascular route delimitated by the astrocytic end

feet (Iliff et al., 2012; Jessen et al., 2015). This brain perivascular pathway was initially described by Rennels and colleagues (Rennels et al., 1985), but only fully characterized and termed "glymphatic system" latter on via state-of-the-art imaging and functional studies (Iliff et al., 2012; Iliff et al., 2013a; Xie et al., 2013). Besides being involved in the clearance of solutes and metabolites from brain parenchyma back into the subarachnoid spaces, the glymphatic system also participates in the regulation of water, ion and cholesterol homeostasis (Jessen et al., 2015). Moreover, glymphatic function is known to be dependent on aquaporin 4 (AQP4) expression at the astrocytic endfeet (Iliff et al., 2012), as well as on body posture and respiratory and vasomotor pulsations (Klose et al., 2000; Iliff et al., 2013b; Lee et al., 2015). Molecular clearance through the glymphatic pathway in mice is increased during sleep (or under anesthesia) and decreased when the animals are awake (Xie et al., 2013; Hablitz et al., 2020). This feature is attributed, at least in part, to increased ISF volume (Berridge and Waterhouse, 2003) and increased AQP4 polarization to vascular astrocytic endfeet during sleep states (Hablitz et al., 2020).

Interestingly, the influx and efflux of CSF macromolecules through the glymphatic system was significantly impaired in adult mice with dysfunctional meningeal lymphatics as a result of photodynamic ablation of meningeal lymphatics, surgical ligation of the lymphatics afferent to the deep CLNs or Prox1 haplodeficiency (Da Mesquita et al., 2018b). These observations led to the conclusion that, although physically detached, the glymphatic and meningeal lymphatic systems are functionally connected (Da Mesquita et al., 2018a; Da Mesquita et al., 2018b). However, contrarily to glymphatic influx/efflux, meningeal lymphatic drainage of CSF content seems to be increased when mice are awake (Ma et al., 2019b; Hablitz et al., 2020), through a mechanism that is under circadian control, but does not dependend on the light/dark cycle (Hablitz et al., 2020). However, it is still unclear whether changes in the sleeping pattern impact on meningeal lymphatic function.

Meningeal lymphatics modulate the drainage of immune cells from the CNS meninges (Louveau et al., 2018; Hsu et al., 2019). Recent studies indicate that this process is mediated, at least in part, by CCR7 signaling (**Figure 1**), since the migration of T cells and DCs from the meningeal compartment into the deep CLNs was significantly reduced in Ccr7-null mice compared to wild type controls (Louveau et al., 2018). Yet, the chemoattractant S1P has also been implicated in immune cell trafficking through lymphatics (Czeloth et al., 2005; Rathinasamy et al., 2010) and it is still unclear whether the beneficial effects of S1P receptor modulators in the context of CNS autoimmunity, like fingolimod, [reviewed elsewhere (Chun and Hartung, 2010)] are achieved by blocking lymphatic drainage of leukocytes at the CNS meninges. Likewise, it is well established that the activation of peripheral LVs by proinflammatory cytokines, such as tumor necrosis factor (TNF), can induce the upregulation of leukocyte adhesion molecules, such as ICAM-1, VCAM-1 and E-selectin, that affect immune cell drainage and egress into LNs (Johnson et al., 2006). However, there is little evidence about the consequences of adhesion molecule overexpression in the activated meningeal lymphatic vasculature. In sum, the described evidence underlines the close involvement of the meningeal lymphatic system in the modulation of immune cell trafficking and the mechanisms that, if therapeutically targeted, might influence CNS immune cell drainage and activation.

Developing imaging tools has proven to be critical for the better understanding of meningeal lymphatic function in the human CNS. Different magnetic resonance imaging (MRI) protocols have been recently established to characterize the anatomy and function of meningeal LVs in humans. Some of these imaging techniques seem to allow the simultaneous measurement of CSF drainage into the CLNs, as well as the circulation of CSF/ISF solutes through the glymphatic pathway, under physiological and pathological conditions (Absinta et al., 2017; Ringstad et al., 2017; Taoka et al., 2017; Eide et al., 2018; Zhou W. et al., 2020; Zhou Y. et al., 2020; Ringstad and Eide, 2020; Yang et al., 2020; Ding et al., 2021). Alongside MRI, optical coherence tomography (OCT) has also been used to image meningeal LVs in animal models (Semyachkina-Glushkovskaya et al., 2017). However, this OCT protocol involved a transient step of blood-brain barrier (BBB) disruption, which means that, although promissing for longitudinal monitoring of lymphatic function (Gong et al., 2016), this technique would have to be revised in order to make it appropriate for the visualization of meningeal lymphatics in humans. The development or perfection of imaging techniques is critical to draw a comprehensive map of the meningeal lymphatic network in different mammalian species, and its contribution for waste clearance and immune cell trafficking in the CNS (Raper et al., 2016; Da Mesquita et al., 2018a).

Aging leads to a progressive impairment in glymphatic function that is accompanied by a decrease in dorsal meningeal LV diameter and coverage and, consequently, in reduced CSF outflow and macromolecule drainage into the deep CLNs (Kress et al., 2014; Ma et al., 2017; Da Mesquita et al., 2018b). The meningeal collecting-like LVs of older animals presented a lymphedematous phenotype characterized by increased size, higher number of branches, a dysmorphic distribution of type IV collagen and fewer lymphatic valves (Ahn et al., 2019). Interestingly, a similar decreased function of both the meningeal lymphatic and glymphatic systems was recently described in aged humans (Zhou Y. et al., 2020). Altogether, these findings suggest that a significant reduction of CNS lymphatic vascular drainage with aging is accompanied by deficits in CSF production (May et al., 1990; Liu G. et al., 2020) and fluid re-circulation through glymphatics (Kress et al., 2014; Zhou Y. et al., 2020). Of notice, boosting meningeal lymphatic function by inducing VEGF-C overexpression enhanced the cognitive performance of aged mice (Da Mesquita et al., 2018b). The beneficial effect of VEGF-C was abrogated in old mice that were also subjected to surgical ligation of the CSF-draining lymphatics afferent to the deep CLNs, which clearly showed that enhanced meningeal lymphatic drainage was responsible for the observed improvement in cognitive behavior (Da Mesquita et al., 2018b).

As we have described so far, the meningeal lymphatic vasculature is continuously draining the CNS, interacts with

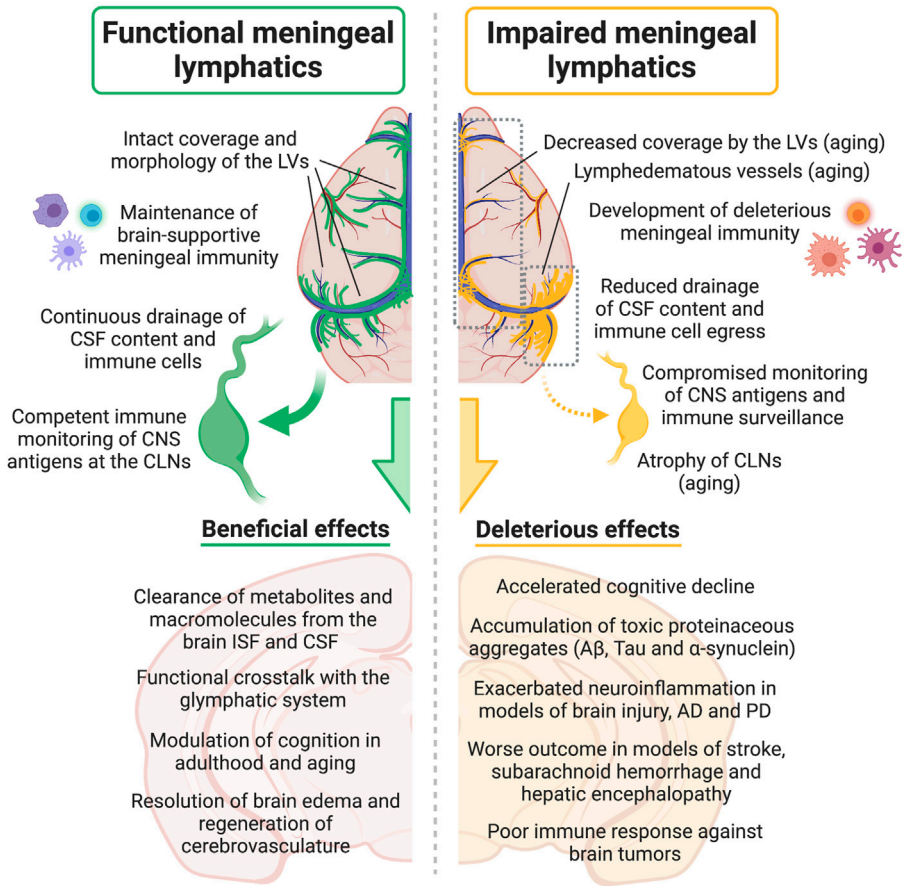

FIGURE 2 | Effects of meningeal lymphatic (dys)function on CSF drainage, immune cell trafficking into the cervical lymph nodes, meningeal immunity, CNS immune surveillance, neuroinflammation and other neural processes, either under physiological conditions or in disease models. Aβ, amyloid beta; AD, Alzheimer's disease; CNS, central nervous system; CSF, cerebrospinal fluid; CLNs, cervical lymph nodes; ISF, interstitial fluid; LVs, lymphatic vessels; PD, Parkinson's disease. Created with BioRender.com.

other mechanisms of brain cleansing and is severely affected by aging. We will next outline important experimental observations that support the close involvement of the meningeal lymphatic system in different neuropathological conditions that are closely linked with accumulation of toxic metabolic waste in the brain and persistent neuroinflammation. Additionally, we will discuss the possibilities of modulating meningeal lymphatic drainage to treat neurological disorders that preferentially afflict the elderly population.

ROLE OF MENINGEAL LYMPHATIC (DYS)FUNCTION IN NEUROLOGICAL DISORDERS

Aside from its role in modulating CNS drainage and homeostasis, the meningeal lymphatic vasculature is intrinsically involved in the pathophysiology of different neurodegenerative diseases. As we will describe in the following sections, recent studies have shown that dampened cleansing of molecules prone to aggregation and reduced immune cell egress into the draining CLNs, as a result of dysfunctional CNS lymphatic drainage, can have a significant impact on disease outcome (**Figure 2**).

Alzheimer's Disease

The accumulation of extracellular amyloid plaques rich in aggregated amyloid beta (Aβ) peptides is a pathological hallmark of Alzheimer's disease (AD) (Ittner and Gotz, 2011). Impairments in Aβ clearance mechanisms contribute to its accumulation, aggregation into toxic oligomeric intermediates and seeding into larger amyloid plaques (Wisniewski and Goni, 2014). Toxic Aβ species can be removed from the brain interstitium by several mechanisms, including degradation by enzymes (Qiu et al., 1998; Farris et al., 2003; Hernandez-Guillamon et al., 2015), phagocytosis by microglia and astrocytes (Weldon et al., 1998; Jones et al., 2013), receptor-mediated excretion across the BBB (Shibata et al., 2000; Silverberg et al., 2010), and perivascular efflux into CSF-filled compartments (namely the subarachnoid space) via the glymphatic system (Iliff et al., 2012). Importantly, Aβ accumulation can induce synaptic deficits (Terry et al., 1991; Mucke et al., 2000; Tsai et al., 2004), alterations in neuronal activity (Palop et al., 2007; Frazzini et al.,

2016), neuronal network dysfunction (Kowalski et al., 2001; Palop et al., 2007; Ben-Nejma et al., 2019), and behavioral deficits, such as cognitive impairment (Henderson et al., 1989; Grady et al., 2008).

Increased levels of Aβ peptides in the CSF are detected early-on in AD patients and precede the increased Aβ plaque deposition in the brain parenchyma (Bateman et al., 2012). Interestingly, studies involving postmortem tissue from AD patients and AD transgenic mice have shown that increased levels of Aβ can be detected in the meningeal layers (Joachim et al., 1988; Da Mesquita et al., 2018b), namely in the dura mater adjacent to the superior sagittal sinus (Da Mesquita et al., 2018b), and in the CLNs (Pappolla et al., 2014). Altogether these observations show that Aβ peptides have access to anatomical locations harboring the meningeal LVs, which can then promote their drainage into the periphery (Da Mesquita et al., 2018b). This prompted for the assessment of meningeal lymphatic function in AD transgenic mouse models that recapitulate cerebral amyloidosis. Although meningeal lymphatic function was found to be intact at younger ages in both J20 and 5xFAD transgenic mice (Da Mesquita et al., 2018b), altered lymphatic drainage was observed at older ages in 5xFAD (Kwon et al., 2019) and APP/PS1 mice (Wang et al., 2019). These discrepant observations might be explained by the combined effects of aging and Aβ toxicity on the meningeal lymphatic system, a subject that warrants further investigation (Da Mesquita et al., 2018b; Kwon et al., 2019). Induction of early meningeal lymphatic dysfunction by photodynamic ablation in adult J20 and 5xFAD mice resulted in exacerbated Aβ pathology in the meninges and brain (Da Mesquita et al., 2018b). Likewise, reduction of meningeal lymphatic output by ligation of the LVs afferent to the deep CLNs had detrimental effects in the levels of forebrain soluble $A\beta_{1\text{-}40}$ and $A\beta_{1\text{-}42}$, Aβ deposition and gliosis in APP/PS1 mice (Wang et al., 2019). Importantly, reducing meningeal lymphatic ouflow led to spatial learning deficits in adult wild type mice (Da Mesquita et al., 2018b) and worsened short-term working memory in APP/PS1 mice (Wang et al., 2019).

Recent studies have also tested the effects of boosting the function of the meningeal lymphatics in mouse models of AD. Intracisternal injection of recombinant human VEGF-C promoted dural lymphangiogenesis in 9-month-old APP/PS1 mice, reducing the levels of soluble $A\beta_{1-40}$ and $A\beta_{1-42}$ in the brain and CSF, and improving cognitive performance (Wen et al., 2018). In a different study, delivery of a viral vector expressing mouse VEGF-C into the cisterna magna of J20 animals at 6–7 months of age did not improve the Aβ levels in the CSF, amyloid deposition in the hippocampus, or cognitive performance (Da Mesquita et al., 2018b). These discordant results might be explained by the different degrees of meningeal lymphatic vessel function or by the distinct kinetics of brain Aβ production and plaque development in APP/PS1 and J20 mice (Mucke et al., 2000; Jankowsky et al., 2004). The different methods and regimens of VEGF-C delivery employed in each study (Da Mesquita et al., 2018b; Wen et al., 2018) might also explain the different outcomes. More experimental evidence is needed to better understand if and how VEGF-C treatment can be beneficial to treat AD-associated brain pathology and symptoms.

Besides the extracellular deposition of Aβ plaques, another AD pathological hallmark is the presence of intracellular neurofibrillary tangles, which are composed by hyperphosphorylated forms of the microtubule-associated protein Tau (Ittner and Gotz, 2011). The exact mechanisms that lead to the formation and propagation of neurofibrillary tangles in AD remain elusive. A recent study has shown that Tau clearance from the CNS was impaired in the K14-VEGFR3-Ig genetic mouse model (Patel et al., 2019), which lacks a functional meningeal lymphatic vasculature due to impaired VEGF-C/D–VEGFR3 signaling (Aspelund et al., 2015; Patel et al., 2019). The authors showed that injection of fluorescently conjugated recombinant monomeric Tau into the hippocampus of K14-VEGFR3-Ig mice resulted in increased Tau retention in the brain at 48- and 72-h post-injection, when compared to control mice with intact meningeal lymphatics (Patel et al., 2019). In accordance, K14-VEGFR3-Ig mice also showed a delayed appearance of Tau in the blood (Patel et al., 2019), again highlighting the important role of the meningeal lymphatic system in brain-derived antigen outflow.

Altogether, there is a growing body of evidence supporting the notion that an impaired meningeal lymphatic drainage in AD could promote both Aβ and Tau accumulation in the brain, affecting disease severity and aggravating cognitive decline.

Parkinson's Disease

The accumulation of toxic forms of α-synuclein in Parkinson's disease (PD) is closely linked with secondary pathological cascades that underlie the onset of clinical symptoms. One of the models used to study familial PD is the A53T transgenic mice that express the mutated A53T form of human α-synuclein (Giasson et al., 2002). Intracellular and extracellular aggregation of α-synuclein in the substantia nigra was significantly exacerbated in A53T mice after surgical ligation of the lymphatics draining into the deep CLNs (Zou et al., 2019). Increased α-synuclein aggregation after lymphatic ligation was accompanied by higher astrocytic activation, increased levels of proinflammatory cytokines, prominent loss of dopaminergic neurons and increased motor impairment, suggesting that decreased meningeal lymphatic drainage might affect different pathological features in the context of PD (Zou et al., 2019). Interestingly, A53T animals with ligated lymphatics also presented a decreased clearance of other macromolecules from the brain, namely of different toxic Tau species (Zou et al., 2019). Impairing the drainage of brain fluids and molecules into the deep CLNs in a PD model of α-synuclein fibril's toxicity (induced by injecting α-synuclein fibrils into the brain) resulted in a higher accumulation and propagation of phosphorylated α-synuclein in the brain (Ding et al., 2021). Meningeal LVs have been recently implicated in the pathophysiology of human idiopathic PD. Using an MRI technique to measure meningeal lymphatic parameters, the authors were able to show that patients with idiopathic PD exhibited significantly reduced flow through the meningeal LVs along the superior sagittal sinus and sigmoid sinus, as well as a notable delay in the perfusion of deep CLNs by

CSF-derived tracers, compared to atypical Parkinsonian patients. In fact, it was possible to accurately differentiate idiopathic PD and atypical Parkinsonian patients, with acceptable sensitivity and specificity, just by their profile of meningeal lymphatic outflow (Ding et al., 2021). Even though idiopathic PD and multiple system atrophy (one type of atypical Parkinsonian disorder) are both α-synucleinopathies, they are characterized by different species of misfolded α-synuclein (Shahnawaz et al., 2020), which highlights the need to understand whether the presence of distinct pathological α-synuclein aggregates in the CNS can have different effects on the meningeal lymphatic system. It will also be essential to explore if the modulation of meningeal lymphatic function (decreasing or increasing its drainage capacity) affects the neuroimmune response and behavior performance in PD (Joers et al., 2017; Butkovich et al., 2020). Additional experiments are also needed in order to understand if enhancing meningeal lymphatic drainage in PD might prove to be efficacious in alleviating not only brain α-synuclein pathology and neuroinflammation but also PD-related clinical symptoms, including motor deficits, sensory abnormalities, sleep disturbances, autonomic dysfunction, impaired gut motility, dysbiosis and fatigue (Pfeiffer, 2016; Chapelet et al., 2019; Prigent et al., 2019; Butkovich et al., 2020; Aho et al., 2021).

CNS Autoimmune Disease

Multiple sclerosis (MS) is the most common autoimmune demyelinating disease of the CNS, whose main pathological mechanisms and therapies have been discovered with the aid of the experimental autoimmune encephalomyelitis (EAE) mouse model (Steinman and Zamvil, 2005). Induction of chronic EAE in mice did not result in significant alterations in meningeal lymphatic morphology or CSF drainage into the deep CLNs at an early stage of the disease (Louveau et al., 2018). However, peripheral lymphangiogenesis was observed in the cribriform plate at a later stage of chronic EAE (Louveau et al., 2018; Hsu et al., 2019), which suggested that a pathological peripheral lymphatic remodeling could be affecting disease severity in this model (Louveau et al., 2018; Hsu et al., 2019). Analysis of the brain meninges of EAE mice revealed a higher number of T cells inside and around the meningeal LVs after the appearance of clinical symptoms, when compared to healthy controls (Louveau et al., 2018). Accordingly, a decreased number of T cells in the deep CLNs was observed in a spontaneous EAE model, immediately before the appearance of clinical manifestations, suggesting that activation of antigen-specific T cells in these draining LNs might precede CNS T cell infiltration (Furtado et al., 2008). These observations prompted for a better assessment of the roles of the peripheral nasal lymphatics and the meningeal lymphatics in the initiation and progression of disease in the EAE model (Louveau et al., 2016; Louveau et al., 2018). Surprisingly, dampening meningeal immune cell drainage into the deep CLNs, either by meningeal lymphatic vessel ablation (Louveau et al., 2018) or surgical resection of the deep CLNs (Furtado et al., 2008; Louveau et al., 2018), improved EAE clinical symptoms. Conversely, ablation of the nasal lymphatics near the cribriform plate reduced T cell drainage into the superficial CLNs, but did not affect EAE development or progression (Louveau et al., 2018). These observations suggested that the nasal lymphatic drainage route might have a minor role in this disease model and that the deep CLNs seem to be a key site of encephalitogenic T cell generation (Louveau et al., 2018). Transcriptomic analysis of myelin oligodendrocyte glycoprotein (MOG)-specific T cells isolated from deep CLNs of mice with dysfunctional meningeal LVs reveled a lessened encephalitogenic profile, when compared to EAE mice with intact meningeal lymphatics, which might explain the observed differences in clinical scores (Louveau et al., 2018). However, it is important to emphasize that resection of the deep CLNs at an advanced symptomatic stage of EAE resulted in decreased number of myelin basic protein (MBP)-specific T cells infiltrating the CNS, but was not sufficient to improve the animals clinical score (Furtado et al., 2008). Likewise, neither meningeal lymphatic ablation nor resection of the deep CLNs were able to prevent the appearance of clinical symptoms in the EAE model (Furtado et al., 2008; Louveau et al., 2018), suggesting that other routes of immune cell drainage and reactivation might be involved in disease onset and progression.

The lymphangiogenic factor VEGF-C has also been associated to altered disease outcome in EAE models. Overexpression of VEGF-C (Park et al., 2013; Hsu et al., 2019) and its receptor VEGFR3 (Park et al., 2013) occurs in the spinal cord (Park et al., 2013) and brain (Hsu et al., 2019) of EAE mice, compared to controls. Inhibition of VEGFR3 signaling, by peripheral injection of the tyrosine kinase inhibitor MAZ51, delayed EAE onset and decreased disease severity, by reducing demyelination and infiltration of cluster of differentiation (CD) 4 T cells in the spinal cord (Hsu et al., 2019). It is still debatable whether this beneficial effect was achieved through the modulation of the meningeal lymphatics, the peripheral nasal lymphatics, or both systems (Louveau et al., 2018; Hsu et al., 2019). Nevertheless, similarly to what was observed upon deep CLN's resection, treatment with MAZ51 at more advanced stages of EAE was not able to improve the clinical score (Hsu et al., 2019), which again implies that meningeal lymphatic drainage might play an important role in early stages of CNS autoimmune disease development, but a minor role in a later phase of disease.

Brain Tumors

Primary brain tumors (like gliomas) rarely spread into peripheral tissues (Mondin et al., 2010; Lun et al., 2011), a phenomenon that might be explained, in part, by the lack of LVs in close proximity to tumor cells within the brain parenchyma (Mondin et al., 2010; Da Mesquita et al., 2018a). Additionally, it was recently reported that the subdural and striatal injection of glioma or melanoma cells in mice induced dorsal meningeal lymphatic remodeling (Hu et al., 2020) and that glioma-bearing mice show impaired CSF outflow through meningeal LVs (Ma et al., 2019c). The abnormal redirection of CSF flow towards the spinal cord and altered turnover of brain fluid around the tumor environment (Shibahara et al., 2019) might be a consequence of decreased meningeal lymphatic CSF outflow and impaired glymphatics, which can be favoring the accumulation of toxic proteins,

cytokines and chemokines that enable tumor growth (Da Mesquita et al., 2018a). On the other hand, decreased CSF outflow may reduce the transport of tumor-derived antigens to the draining LNs, thus compromising the activation and proliferation of anti-tumor T cells (Alves de Lima et al., 2020). Interestingly, two recent studies have implicated the meningeal lymphatic system in the development of a protective immune response against tumor cells in the brain (Hu et al., 2020; Song et al., 2020). Enhancement of meningeal lymphatic drainage capacity by VEGF-C promoted the drainage of brain tumor cells into the deep CLNs and boosted anti-programmed cell death protein 1 (PD-1)/anti-cytotoxic T lymphocyte antigen 4 (CTLA-4)-mediated immunotherapy against intracranial tumors, without interfering with tumor angiogenesis or growth (Hu et al., 2020; Song et al., 2020). Importantly, the near-complete rejection of brain tumors by prophylactic VEGF-C overexpression was absent in mice with impaired lymphatic drainage into the deep CLNs (Song et al., 2020) or upon blockade of CCR7 signaling by CCL21, which directly implicates meningeal lymphatic drainage in these therapeutic approaches.

Brain Injury and Hemorrhage

Modulation of meningeal lymphatic drainage was shown to affect the outcome of brain injuries, such as traumatic brain injury (TBI), subarachnoid hemorrhage and stroke. Induction of TBI in mice resulted in a substantial decrease in meningeal lymphatic drainage as early as two hours post-injury, which was only fully restored two months later (Bolte et al., 2020). In accordance, CSF flow was altered in TBI (Johanson et al., 2011), and intracranial pressure was markedly increased at two hours post-injury (Bolte et al., 2020). Photodynamic ablation of meningeal lymphatics prior to TBI exacerbated the neuroinflammatory response, including the overexpression of complement pathway genes, and aggravated the cognitive deficits triggered by the injury. On the other hand, improving meningeal lymphatic function in old mice by viral-mediated VEGF-C overexpression decreased neuroinflammation induced by TBI (Bolte et al., 2020).

Increased meningeal T cell numbers were observed in a mouse model of subarachnoid hemorrhage, which could be attributed to an impairment in the draining capacity of meningeal LVs (Pu et al., 2019). Surgical resection of the deep CLNs in a rat model of subarachnoid hemorrhage further reduced the regional cerebral blood flow and led to worsened intracranial pressure, brain edema, oxidative stress and motor impairment (Sun et al., 2006; Sun et al., 2011). Exacerbated neuroinflammation and impaired cognitive performance were also observed in a mouse model of subarachnoid hemorrhage upon photodynamic ablation of meningeal lymphatics or injection with MAZ51 (Chen J. et al., 2020). Likewise, ligation of the collecting lymphatics draining into the deep CLNs resulted in worsened outcome in a model of subdural hematomas (Liu X. et al., 2020).

Increased VEGF-C levels were observed in the CSF and brain parenchyma of two different animal models of stroke (Gu et al., 2001; Esposito et al., 2019), pointing to a potentially augmented VEGFR3 signaling in lymphatic vasculature (Esposito et al., 2019). However, different stroke models have resulted in somewhat contradictory observations in terms of meningeal lymphatic remodeling and role. Meningeal lymphangiogenesis was observed in a photothrombosis-induced focal stroke model, but not in a stroke model induced by transient middle cerebral artery occlusion (MCAO) (Yanev et al., 2020). While it was initially reported that surgical blockade of lymphatic drainage into the CLNs led to increased infarction volume in a model of MCAO (Si et al., 2006), a more recent report has shown a conflicting reduction in infarction volume upon MCAO and resection of the superficial CLNs or MAZ51 treatment (Esposito et al., 2019). In addition, defective lymphatic function by *Vegfr3* haplodeficiency resulted in larger infarct volumes after MCAO, but not after photothrombosis-induced stroke (Yanev et al., 2020). Interestingly, an elegant study using different zebrafish models of brain thrombosis has described a transient formation and extension of lumenized LVs from the meninges into the injured brain parenchyma (Chen et al., 2019). These lymphatics were involved in fluid drainage, reduction of cerebral edema, and regressed shortly after cerebrovascular regeneration so that the brain parenchyma could return to its homeostatic lymphatic-free status (Chen et al., 2019). It remains to be investigated if the same mechanisms of transient meningeal lymphangiogenesis occur, or can be induced, in the mammalian injured CNS and whether this process supports the resolution of neuroinflammation and restoration of neuro-glio-vascular function upon injury, hemorrhage or stroke.

Hepatic Encephalopathy

Hepatic encephalopathy is a neurological complication that results from cirrhosis and causes cognitive, psychiatric and motor impairment (Weissenborn, 2019). Aberrant neuroinflammation is a common feature observed in animal models of hepatic encephalopathy (Liu R. et al., 2020; Izquierdo-Altarejos et al., 2020). Rats subjected to bile duct ligation, a hepatic encephalopathy disease model, presented increase meningeal lymphangiogenesis that was further stimulated by increasing VEGF-C levels in the CSF (Hsu et al., 2020). Interestingly, boosting meningeal lymphangiogenesis led to a down-regulation of proinflammatory genes, attenuated microglial activation in the brain cortex, and improved motor function (Hsu et al., 2020). Collectively, these results suggest that a faster resolution of brain inflammation through enhanced meningeal lymphatic drainage could improve hepatic encephalopathy.

MENINGEAL LYMPHATICS IN BRAIN HEALTH AND DISEASE: FUTURE CHALLENGES

The seminal (re)discovery of the meningeal lymphatic vasculature (Aspelund et al., 2015; Louveau et al., 2015) opened the door for an array of novel experimental data that have contributed to advance our knowledge about the mechanisms governing CNS lymphatic drainage. However, every significant step towards a more in-depth understanding of the meningeal lymphatic system in health and disease

(**Figure 2**), has been accompanied by fresh, interesting and puzzling questions. We will now summarize some open questions and hypothesis, which have been fueled by recent experimental evidence about the meningeal lymphatic system, brain aging and neurological disorders.

Aging has a profound impact on the meningeal lymphatics (Da Mesquita et al., 2018b; Ahn et al., 2019). However, the effect of aging is not exclusive to the CNS or its lymphatic vasculature, but systemic, affecting the blood composition and many peripheral tissues (Villeda et al., 2011; Chen M. B. et al., 2020; Schaum et al., 2020). The meningeal dural lymphatics are located right next to the fenestrated venous sinuses, which are quite permissive to the exchange of both molecules and cells between the blood and the stroma of the meninges (Balin et al., 1986; Alves de Lima et al., 2020). This means that an aged systemic milieu (Villeda et al., 2011; Chen M. B. et al., 2020; Schaum et al., 2020) characterized by altered levels of plasma solutes and proteins, as well as circulating immune cells, alongside a hypothetical loss of blood-meningeal integrity with aging (Rustenhoven et al., 2021) might take a significant toll on the meningeal lymphatic system.

While the cellular and molecular culprits of age-related meningeal lymphatic dysfunction remain unclear, the data gathered so far implicates the VEGF-C–VEGFR3 signaling pathway as a mechanism that can be therapeutically exploited to rescue meningeal lymphatic drainage in the aged CNS (Da Mesquita et al., 2018b). However, we know very little about the cellular sources of meningeal VEGF-C, or how aging impacts on VEGF-C production and maturation in the meningeal compartment. In fact, the same premises apply for other growth factors, cytokines or signaling pathways that have the ability to shape meningeal LEC function, namely VEGF-D (Achen et al., 1998), TNF and interleukin (IL)-1β (Schwager and Detmar, 2019), and altered growth factor signaling by WNT, BMP2 or through neuropilin 2 (Yuan et al., 2002; Dunworth et al., 2014; Cha et al., 2018). Moreover, it will be worth testing whether the morphological and functional changes in meningeal lymphatics with aging result from a dysregulated expression of the transcription factors FOXC2 and GATA2 due to changes in shear stress or extracellular matrix composition at the dural layer (Sabine et al., 2015; Sweet et al., 2015; Da Mesquita et al., 2018b; Rustenhoven et al., 2021). The loss of initial lymphatics in the meninges might also be explained by a reduced renewal capacity. Future studies should focus on the regenerative capacity of the meningeal lymphatic system in adulthood and aging, with a special emphasis on the cellular progenitors that can give rise to LECs [extensively reviewed in (Gutierrez-Miranda and Yaniv, 2020)] in the meningeal compartment. A loss of particular types of meningeal LEC's progenitors with aging may account for the change in meningeal lymphatic coverage and morphology, either in "normal" aging or in certain diseases of the CNS.

As previously highlighted in this review, defects in meningeal lymphatic output result in dampened glymphatic function (Da Mesquita et al., 2018b) and, consequently, in reduced excretion of brain molecular waste products into the subarachnoid CSF. This phenomenon could explain, at least in part, the accumulation of toxic Aβ, Tau or α-synuclein species in the brains of different models of neurodegenerative disorders (Da Mesquita et al., 2018b; Patel et al., 2019; Wang et al., 2019; Zou et al., 2019). However, the exact mechanisms governing the interactions between the meningeal lymphatics and the cellular components of the glymphatic perivascular route (astrocytes, perivascular macrophages, pericytes, SMCs, or blood endothelial cells, just to name a few) are still unknown [reviewed in (Da Mesquita et al., 2018a)]. The anatomical segregation between the meningeal lymphatic vasculature and the brain parenchymal cells (supposedly separated by a restricting blood-meningeal barrier), makes it even more challenging to pinpoint the molecular mediators underlying the crosstalk between the meningeal lymphatic system, brain phagocytes and the neurovascular unit (that shares cellular types with the glymphatic system), three important players in brain cleansing (Da Mesquita et al., 2018a; Sweeney et al., 2018a; Shi and Holtzman, 2018; Alves de Lima et al., 2020). Deciphering which specific brain cell types are more susceptible to reduced meningeal lymphatic function (and when it happens) might prove to be a herculean task, specially taking into consideration the wide effects of meningeal lymphatic dysfunction on fluid/macromolecule perivascular circulation throughout the whole brain (Da Mesquita et al., 2018b). One possible starting point will be to focus on processes that are closely involved in regulating the levels of Aβ and Tau aggregates in the brain, including the molecular transport mechanisms across the BBB (Sweeney et al., 2018b), or even glial and neuronal activation. Hypothetically, a decrease in meningeal lymphatic function could indirectly impact on the circadian levels of Aβ and Tau in the brain's ISF and CSF by shaping neuronal excitation and/or inhibition (Hong et al., 2011; Yamada et al., 2011). Alternatively, the meningeal lymphatics could be involved in the regulation of the sleep-awake cycle, which has a profound influence on brain processes that regulate the levels of extracellular toxic Aβ and Tau species in fluids and can affect their accumulation and aggregation in the brain (Iliff et al., 2012; Roh et al., 2012; Xie et al., 2013; Holth et al., 2019).

The neuroimmune system is a major player in brain aging and certain neurological disorders. However, it is still debatable whether meningeal lymphatic dysfunction is contributing to the changes observed in CNS immunity with aging. Reduced immune cell egress through lymphatics can be contributing to the higher frequency of T cells and altered macrophage and DC phenotypes observed in the aged meninges and brain (Mrdjen et al., 2018). Alongside the T cell pool expansion, there is an increased T cell clonality in the aged CNS, namely in the choroid plexus and at the vicinity of the brain ventricles and neurogenic niches, that was associated with deleterious changes in neuroinflammation and neurogenesis (Baruch et al., 2013; Dulken et al., 2019). Interestingly, changes in the response by T cells were also observed in human neurodegenerative diseases. Increased reactivity to α-synuclein peptides by peripheral helper and cytotoxic T cells from PD patients was detected immediately after the diagnosis of motor symptoms (Sulzer et al., 2017; Lindestam Arlehamn et al., 2020). Along the same line, clonally expanded CD4 and CD8 T cells specific to two Epstein–Barr virus antigens were found in the CSF of AD patients (Gate et al., 2020). The next step will be to perform

functional experiments in order to better understand whether these changes in T cell clonality impact disease severity or outcome. Importantly, future studies should also investigate what drives the phenomena of increased T cell clonality and reactivity in neurological diseases: we postulate that altered lymphatic drainage of CNS-derived antigens (Aβ, Tau, α-synuclein or persistent virus) and/or reduced immune cell egress (of T cells or antigen presenting cells) through meningeal lymphatics into the CLNs with aging (**Figure 2**), might contribute to the above-mentioned changes in CNS adaptive immunity. It is also possible that the aging-induced loss of initial LVs at the meningeal dural layer and at the CNS-draining CLNs results in decreased levels of certain chemokines, such as CCL19, CCL21 and CSF1, that are crucial for proper immune cell egress and surveillance of the CNS (Louveau et al., 2016; Mondor et al., 2019). Accordingly, improving meningeal lymphatic function in the aged or diseased CNS might represent a promising therapeutic method to revert an atypical immune response and resolve deleterious neuroinflammation. Treating aged mice with VEGF-C resulted in better cognitive performance as a direct consequence of improved lymphatic drainage into the deep CLNs (Da Mesquita et al., 2018b). It will be informative to experimentally assess whether the beneficial effects of VEGF-C were achieved by improved drainage of CSF solutes alone, by a fine-tuning of meningeal/brain immunity, or if both components were equally improved in old mice and contributed to better brain function.

Recent studies have linked defects in meningeal lymphatic drainage to exacerbated gliosis and overexpression of innate immune genes in models of TBI, brain α-synucleinopathy and hepatic encephalopathy (Zou et al., 2019; Bolte et al., 2020; Hsu et al., 2020). The next step will be to decipher the exact mechanisms through which meningeal lymphatics can shape the brain innate immune response. Brain resident innate myeloid cells, namely microglia and perivascular macrophages, play very important roles in response to traumatic insults and in disorders of different etiologies-for instance in EAE, AD and brain tumor models-showing in some cases disease-specific activation profiles (Keren-Shaul et al., 2017; Muller et al., 2017; Ajami et al., 2018; Kang et al., 2018). The fact that the meningeal lymphatic system has been closely implicated in the pathophysiology of similar models of disease (Da Mesquita et al., 2018b; Louveau et al., 2018; Hu et al., 2020; Song et al., 2020), emphasizes the need of exploring the possible connections (direct or indirect) between altered meningeal lymphatic function and abnormal brain innate myeloid cell activation.

All of the above-mentioned premises and hypothesis around meningeal lymphatics remain to be tested and might have major implications for the basic understanding of the pathophysiology of CNS autoimmune diseases and tumors, AD, PD and other neurological diseases. In sum, we are still a long way from knowing all the mechanisms governing meningeal lymphatic maturation, morphology and drainage, and if meningeal lymphatic function can be harnessed to achieve effective therapeutic outcomes in the aged and/or unhealthy CNS.

AUTHOR CONTRIBUTIONS

SN participated in the definition and writing of all the sections of the manuscript; ND wrote specific sections of the manuscript; SM defined the manuscript theme and sections, made the figures and supervised the writing of the manuscript.

ACKNOWLEDGMENTS

The authors would like to thank the members of the Department of Neuroscience at the Mayo Clinic for their support and valuable comments.

REFERENCES

Absinta, M., Ha, S.-K., Nair, G., Sati, P., Luciano, N. J., Palisoc, M., et al. (2017). Human and Nonhuman Primate Meninges Harbor Lymphatic Vessels that Can Be Visualized Noninvasively by MRI. *Elife* 6. doi:10.7554/eLife.29738

Achen, M. G., Jeltsch, M., Kukk, E., Makinen, T., Vitali, A., Wilks, A. F., et al. (1998). Vascular Endothelial Growth Factor D (VEGF-D) Is a Ligand for the Tyrosine Kinases VEGF Receptor 2 (Flk1) and VEGF Receptor 3 (Flt4). *Proc. Natl. Acad. Sci.* 95 (2), 548–553. doi:10.1073/pnas.95.2.548

Ahn, J. H., Cho, H., Kim, J.-H., Kim, S. H., Ham, J.-S., Park, I., et al. (2019). Meningeal Lymphatic Vessels at the Skull Base Drain Cerebrospinal Fluid. *Nature* 572 (7767), 62–66. doi:10.1038/s41586-019-1419-5

Aho, V. T. E., Houser, M. C., Pereira, P. A. B., Chang, J., Rudi, K., Paulin, L., et al. (2021). Relationships of Gut Microbiota, Short-Chain Fatty Acids, Inflammation, and the Gut Barrier in Parkinson's Disease. *Mol. Neurodegeneration* 16 (1), 6. doi:10.1186/s13024-021-00427-6

Ajami, B., Samusik, N., Wieghofer, P., Ho, P. P., Crotti, A., Bjornson, Z., et al. (2018). Single-cell Mass Cytometry Reveals Distinct Populations of Brain Myeloid Cells in Mouse Neuroinflammation and Neurodegeneration Models. *Nat. Neurosci.* 21 (4), 541–551. doi:10.1038/s41593-018-0100-x

Alders, M., Hogan, B. M., Gjini, E., Salehi, F., Al-Gazali, L., Hennekam, E. A., et al. (2009). Mutations in CCBE1 Cause Generalized Lymph Vessel Dysplasia in Humans. *Nat. Genet.* 41 (12), 1272–1274. doi:10.1038/ng.484

Alves de Lima, K., Rustenhoven, J., and Kipnis, J. (2020). Meningeal Immunity and its Function in Maintenance of the Central Nervous System in Health and Disease. *Annu. Rev. Immunol.* 38, 597–620. doi:10.1146/annurev-immunol-102319-103410

Andres, K. H., Düring, M., Muszynski, K., and Schmidt, R. F. (1987). Nerve Fibres and Their Terminals of the Dura Mater Encephali of the Rat. *Anat. Embryol.* 175 (3), 289–301. doi:10.1007/bf00309843

Antila, S., Karaman, S., Nurmi, H., Airavaara, M., Voutilainen, M. H., Mathivet, T., et al. (2017). Development and Plasticity of Meningeal Lymphatic Vessels. *J. Exp. Med.* 214 (12), 3645–3667. doi:10.1084/jem.20170391

Aspelund, A., Antila, S., Proulx, S. T., Karlsen, T. V., Karaman, S., Detmar, M., et al. (2015). A Dural Lymphatic Vascular System that Drains Brain Interstitial Fluid and Macromolecules. *J. Exp. Med.* 212 (7), 991–999. doi:10.1084/jem.20142290

Balin, B. J., Broadwell, R. D., Salcman, M., and el-Kalliny, M. (1986). Avenues for Entry of Peripherally Administered Protein to the Central Nervous System in Mouse, Rat, and Squirrel Monkey. *J. Comp. Neurol.* 251 (2), 260–280. doi:10.1002/cne.902510209

Bálint, L., Ocskay, Z., Deák, B. A., Jakus, Z., and Jakus, Z. (2020). Lymph Flow Induces the Postnatal Formation of Mature and Functional Meningeal Lymphatic Vessels. *Front. Immunol.* 10 (3043), 3043. doi:10.3389/fimmu.2019.03043

Banerji, S., Ni, J., Wang, S.-X., Clasper, S., Su, J., Tammi, R., et al. (1999). LYVE-1, a New Homologue of the CD44 Glycoprotein, Is a Lymph-specific Receptor for Hyaluronan. *J. Cel Biol* 144 (4), 789–801. doi:10.1083/jcb.144.4.789

Baruch, K., Ron-Harel, N., Gal, H., Deczkowska, A., Shifrut, E., Ndifon, W., et al. (2013). CNS-specific Immunity at the Choroid Plexus Shifts toward Destructive Th2 Inflammation in Brain Aging. *Proc. Natl. Acad. Sci.* 110 (6), 2264–2269. doi:10.1073/pnas.1211270110

Bateman, R. J., Xiong, C., Benzinger, T. L. S., Fagan, A. M., Goate, A., Fox, N. C., et al. (2012). Clinical and Biomarker Changes in Dominantly Inherited Alzheimer's Disease. *N. Engl. J. Med.* 367 (9), 795–804. doi:10.1056/NEJMoa1202753

Bazigou, E., and Makinen, T. (2013). Flow Control in Our Vessels: Vascular Valves Make Sure There Is No Way Back. *Cell. Mol. Life Sci.* 70 (6), 1055–1066. doi:10.1007/s00018-012-1110-6

Ben-Nejma, I. R. H., Keliris, A. J., Daans, J., Ponsaerts, P., Verhoye, M., Van der Linden, A., et al. (2019). Increased Soluble Amyloid-Beta Causes Early Aberrant Brain Network Hypersynchronisation in a Mature-Onset Mouse Model of Amyloidosis. *Acta Neuropathol. Commun.* 7 (1), 180. doi:10.1186/s40478-019-0810-7

Berridge, C. W., and Waterhouse, B. D. (2003). The Locus Coeruleus-Noradrenergic System: Modulation of Behavioral State and State-dependent Cognitive Processes. *Brain Res. Rev.* 42 (1), 33–84. doi:10.1016/s0165-0173(03)00143-7

Betterman, K. L., Sutton, D. L., Secker, G. A., Kazenwadel, J., Oszmiana, A., Lim, L., et al. (2020). Atypical Cadherin FAT4 Orchestrates Lymphatic Endothelial Cell Polarity in Response to Flow. *J. Clin. Invest.* 130 (6), 3315–3328. doi:10.1172/JCI99027

Bolte, A. C., Dutta, A. B., Hurt, M. E., Smirnov, I., Kovacs, M. A., McKee, C. A., et al. (2020). Meningeal Lymphatic Dysfunction Exacerbates Traumatic Brain Injury Pathogenesis. *Nat. Commun.* 11 (1), 4524. doi:10.1038/s41467-020-18113-4

Boulton, M., Yonung, A., Hay, J., Armstrong, D., Flessner, M., Schwartz, M., et al. (1996). Drainage of CSF through Lymphatic Pathways and Arachnoid Villi in Sheep: Measurement Of125l-Albumin Clearance. *Neuropathol. Appl. Neurobiol.* 22 (4), 325–333. doi:10.1111/j.1365-2990.1996.tb01111.x

Bower, N. I., Koltowska, K., Pichol-Thievend, C., Virshup, I., Paterson, S., Lagendijk, A. K., et al. (2017). Mural Lymphatic Endothelial Cells Regulate Meningeal Angiogenesis in the Zebrafish. *Nat. Neurosci.* 20 (6), 774–783. doi:10.1038/nn.4558

Bradbury, M. W., and Cole, D. F. (1980). The Role of the Lymphatic System in Drainage of Cerebrospinal Fluid and Aqueous Humour. *J. Physiol.* 299, 353–365. doi:10.1113/jphysiol.1980.sp013129

Bradbury, M. W., Cserr, H. F., and Westrop, R. J. (1981). Drainage of Cerebral Interstitial Fluid into Deep Cervical Lymph of the Rabbit. *Am. J. Physiology-Renal Physiol.* 240 (4), F329–F336. doi:10.1152/ajprenal.1981.240.4.F329

Bradbury, M. W., and Westrop, R. J. (1983). Factors Influencing Exit of Substances from Cerebrospinal Fluid into Deep Cervical Lymph of the Rabbit. *J. Physiol.* 339, 519–534. doi:10.1113/jphysiol.1983.sp014731

Breiteneder-Geleff, S., Soleiman, A., Kowalski, H., Horvat, R., Amann, G., Kriehuber, E., et al. (1999). Angiosarcomas Express Mixed Endothelial Phenotypes of Blood and Lymphatic Capillaries. *Am. J. Pathol.* 154 (2), 385–394. doi:10.1016/S0002-9440(10)65285-6

Brierley, J. B., and Field, E. J. (1948). The Connexions of the Spinal Sub-arachnoid Space with the Lymphatic System. *J. Anat.* 82 (3), 153–166.

Brouillard, P., Boon, L., and Vikkula, M. (2014). Genetics of Lymphatic Anomalies. *J. Clin. Invest.* 124 (3), 898–904. doi:10.1172/JCI71614

Brouillard, P., Dupont, L., Helaers, R., Coulie, R., Tiller, G. E., Peeden, J., et al. (2017). Loss of ADAMTS3 Activity Causes Hennekam Lymphangiectasia-Lymphedema Syndrome 3. *Hum. Mol. Genet.* 26 (21), 4095–4104. doi:10.1093/hmg/ddx297

Butkovich, L. M., Houser, M. C., Chalermpalanupap, T., Porter-Stransky, K. A., Iannitelli, A. F., Boles, J. S., et al. (2020). Transgenic Mice Expressing Human α-Synuclein in Noradrenergic Neurons Develop Locus Ceruleus Pathology and Nonmotor Features of Parkinson's Disease. *J. Neurosci.* 40 (39), 7559–7576. doi:10.1523/JNEUROSCI.1468-19.2020

Cai, R., Pan, C., Ghasemigharagoz, A., Todorov, M. I., Förstera, B., Zhao, S., et al. (2019). Panoptic Imaging of Transparent Mice Reveals Whole-Body Neuronal Projections and Skull-Meninges Connections. *Nat. Neurosci.* 22 (2), 317–327. doi:10.1038/s41593-018-0301-3

Cha, B., Geng, X., Mahamud, M. R., Zhang, J. Y., Chen, L., Kim, W., et al. (2018). Complementary Wnt Sources Regulate Lymphatic Vascular Development via PROX1-dependent Wnt/β-Catenin Signaling. *Cel Rep.* 25 (3), 571–584. doi:10.1016/j.celrep.2018.09.049

Chapelet, G., Leclair-Visonneau, L., Clairembault, T., Neunlist, M., and Derkinderen, P. (2019). Can the Gut Be the Missing Piece in Uncovering PD Pathogenesis?. *Parkinsonism Relat. Disord.* 59, 26–31. doi:10.1016/j.parkreldis.2018.11.014

Chen, J., He, J., Ni, R., Yang, Q., Zhang, Y., and Luo, L. (2019). Cerebrovascular Injuries Induce Lymphatic Invasion into Brain Parenchyma to Guide Vascular Regeneration in Zebrafish. *Develop. Cel* 49 (5), 697–710. doi:10.1016/j.devcel.2019.03.022

Chen, J., Wang, L., Xu, H., Xing, L., Zhuang, Z., Zheng, Y., et al. (2020a). Meningeal Lymphatics Clear Erythrocytes that Arise from Subarachnoid Hemorrhage. *Nat. Commun.* 11 (1), 3159. doi:10.1038/s41467-020-16851-z

Chen, M. B., Yang, A. C., Yousef, H., Lee, D., Chen, W., Schaum, N., et al. (2020b). Brain Endothelial Cells Are Exquisite Sensors of Age-Related Circulatory Cues. *Cel Rep.* 30 (13), 4418–4432. doi:10.1016/j.celrep.2020.03.012

Chun, J., and Hartung, H.-P. (2010). Mechanism of Action of Oral Fingolimod (FTY720) in Multiple Sclerosis. *Clin. Neuropharmacol.* 33 (2), 91–101. doi:10.1097/WNF.0b013e3181cbf825

Coso, S., Zeng, Y., Opeskin, K., and Williams, E. D. (2012). Vascular Endothelial Growth Factor Receptor-3 Directly Interacts with Phosphatidylinositol 3-kinase to Regulate Lymphangiogenesis. *PloS one* 7 (6), e39558. doi:10.1371/journal.pone.0039558

Czeloth, N., Bernhardt, G., Hofmann, F., Genth, H., and Förster, R. (2005). Sphingosine-1-phosphate Mediates Migration of Mature Dendritic Cells. *J. Immunol.* 175 (5), 2960–2967. doi:10.4049/jimmunol.175.5.2960

Da Mesquita, S., Fu, Z., and Kipnis, J. (2018a). The Meningeal Lymphatic System: A New Player in Neurophysiology. *Neuron* 100 (2), 375–388. doi:10.1016/j.neuron.2018.09.022

Da Mesquita, S., Louveau, A., Vaccari, A., Smirnov, I., Cornelison, R. C., Kingsmore, K. M., et al. (2018b). Functional Aspects of Meningeal Lymphatics in Ageing and Alzheimer's Disease. *Nature* 560 (7717), 185–191. doi:10.1038/s41586-018-0368-8

Dejana, E., Tournier-Lasserve, E., and Weinstein, B. M. (2009). The Control of Vascular Integrity by Endothelial Cell Junctions: Molecular Basis and Pathological Implications. *Develop. Cel.* 16 (2), 209–221. doi:10.1016/j.devcel.2009.01.004

Deng, Y., Atri, D., Eichmann, A., and Simons, M. (2013). Endothelial ERK Signaling Controls Lymphatic Fate Specification. *J. Clin. Invest.* 123 (3), 1202–1215. doi:10.1172/JCI63034

Ding, X.-B., Wang, X.-X., Xia, D.-H., Liu, H., Tian, H.-Y., Fu, Y., et al. (2021). Impaired Meningeal Lymphatic Drainage in Patients with Idiopathic Parkinson's Disease. *Nat. Med.* 27 (3), 411–418. doi:10.1038/s41591-020-01198-1

Dulken, B. W., Buckley, M. T., Navarro Negredo, P., Saligrama, N., Cayrol, R., Leeman, D. S., et al. (2019). Single-cell Analysis Reveals T Cell Infiltration in Old Neurogenic Niches. *Nature* 571 (7764), 205–210. doi:10.1038/s41586-019-1362-5

Dunworth, W. P., Cardona-Costa, J., Bozkulak, E. C., Kim, J.-D., Meadows, S., Fischer, J. C., et al. (2014). Bone Morphogenetic Protein 2 Signaling Negatively Modulates Lymphatic Development in Vertebrate Embryos. *Circ. Res.* 114 (1), 56–66. doi:10.1161/CIRCRESAHA.114.302452

Eide, P. K., Vatnehol, S. A. S., Emblem, K. E., and Ringstad, G. (2018). Magnetic Resonance Imaging Provides Evidence of Glymphatic Drainage from Human Brain to Cervical Lymph Nodes. *Sci. Rep.* 8 (1), 7194. doi:10.1038/s41598-018-25666-4

Erlich, S. S., McComb, J. G., Hyman, S., and Weiss, M. H. (1986). Ultrastructural Morphology of the Olfactory Pathway for Cerebrospinal Fluid Drainage in the Rabbit. *J. Neurosurg.* 64 (3), 466–473. doi:10.3171/jns.1986.64.3.0466

Escobedo, N., and Oliver, G. (2016). Lymphangiogenesis: Origin, Specification, and Cell Fate Determination. *Annu. Rev. Cel Dev. Biol.* 32, 677–691. doi:10.1146/annurev-cellbio-111315-124944

Esposito, E., Ahn, B. J., Shi, J., Nakamura, Y., Park, J. H., Mandeville, E. T., et al. (2019). Brain-to-cervical Lymph Node Signaling after Stroke. *Nat. Commun.* 10 (1), 5306. doi:10.1038/s41467-019-13324-w

Fang, J., Dagenais, S. L., Erickson, R. P., Arlt, M. F., Glynn, M. W., Gorski, J. L., et al. (2000). Mutations in FOXC2 (MFH-1), a Forkhead Family Transcription Factor, Are Responsible for the Hereditary Lymphedema-Distichiasis Syndrome. *Am. J. Hum. Genet.* 67 (6), 1382–1388. doi:10.1086/316915

Farris, W., Mansourian, S., Chang, Y., Lindsley, L., Eckman, E. A., Frosch, M. P., et al. (2003). Insulin-degrading Enzyme Regulates the Levels of Insulin, Amyloid -protein, and the -amyloid Precursor Protein Intracellular Domain In Vivo. *Proc. Natl. Acad. Sci.* 100 (7), 4162–4167. doi:10.1073/pnas.0230450100

Förster, R., Davalos-Misslitz, A. C., and Rot, A. (2008). CCR7 and its Ligands: Balancing Immunity and Tolerance. *Nat. Rev. Immunol.* 8 (5), 362–371. doi:10.1038/nri2297

François, M., Caprini, A., Hosking, B., Orsenigo, F., Wilhelm, D., Browne, C., et al. (2008). Sox18 Induces Development of the Lymphatic Vasculature in Mice. *Nature* 456 (7222), 643–647. doi:10.1038/nature07391

Frazzini, V., Guarnieri, S., Bomba, M., Navarra, R., Morabito, C., Mariggiò, M. A., et al. (2016). Altered Kv2.1 Functioning Promotes Increased Excitability in Hippocampal Neurons of an Alzheimer's Disease Mouse Model. *Cell Death Dis* 7, e2100. doi:10.1038/cddis.2016.18

Furtado, G. C., Marcondes, M. C. G., Latkowski, J.-A., Tsai, J., Wensky, A., and Lafaille, J. J. (2008). Swift Entry of Myelin-specific T Lymphocytes into the Central Nervous System in Spontaneous Autoimmune Encephalomyelitis. *J. Immunol.* 181 (7), 4648–4655. doi:10.4049/jimmunol.181.7.4648

Furukawa, M., Shimoda, H., Kajiwara, T., Kato, S., and Yanagisawa, S. (2008). Topographic Study on Nerve-Associated Lymphatic Vessels in the Murine Craniofacial Region by Immunohistochemistry and Electron Microscopy. *Biomed. Res.* 29 (6), 289–296. doi:10.2220/biomedres.29.289

Gate, D., Saligrama, N., Leventhal, O., Yang, A. C., Unger, M. S., Middeldorp, J., et al. (2020). Clonally Expanded CD8 T Cells Patrol the Cerebrospinal Fluid in Alzheimer's Disease. *Nature* 577 (7790), 399–404. doi:10.1038/s41586-019-1895-7

Gausas, R. E., Daly, T., and Fogt, F. (2007). D2-40 Expression Demonstrates Lymphatic Vessel Characteristics in the Dural Portion of the Optic Nerve Sheath. *Ophthalmic Plast. Reconstr. Surg.* 23 (1), 32–36. doi:10.1097/01.iop.0000249431.04116.a8

Giasson, B. I., Duda, J. E., Quinn, S. M., Zhang, B., Trojanowski, J. Q., and Lee, V. M.-Y. (2002). Neuronal α-Synucleinopathy with Severe Movement Disorder in Mice Expressing A53T Human α-Synuclein. *Neuron* 34 (4), 521–533. doi:10.1016/s0896-6273(02)00682-7

Gong, P., Es'haghian, S., Harms, K.-A., Murray, A., Rea, S., Wood, F. M., et al. (2016). *In vivo* label-free Lymphangiography of Cutaneous Lymphatic Vessels in Human Burn Scars Using Optical Coherence Tomography. *Biomed. Opt. Express* 7 (12), 4886–4898. doi:10.1364/BOE.7.004886

Grady, C. L., Haxby, J. V., Horwitz, B., Sundaram, M., Berg, G., Schapiro, M., et al. (2008). Longitudinal Study of the Early Neuropsychological and Cerebral Metabolic Changes in Dementia of the Alzheimer Type. *J. Clin. Exp. Neuropsychol.* 10 (5), 576–596. doi:10.1080/01688638808402796

Gu, W., Brännström, T., Jiang, W., Bergh, A., and Wester, P. (2001). Vascular Endothelial Growth Factor-A and -C Protein Up-Regulation and Early Angiogenesis in a Rat Photothrombotic Ring Stroke Model with Spontaneous Reperfusion. *Acta Neuropathol.* 102 (3), 216–226. doi:10.1007/s004010100370

Gunn, M. D., Tangemann, K., Tam, C., Cyster, J. G., Rosen, S. D., and Williams, L. T. (1998). A Chemokine Expressed in Lymphoid High Endothelial Venules Promotes the Adhesion and Chemotaxis of Naive T Lymphocytes. *Proc. Natl. Acad. Sci.* 95 (1), 258–263. doi:10.1073/pnas.95.1.258

Gutierrez-Miranda, L., and Yaniv, K. (2020). Cellular Origins of the Lymphatic Endothelium: Implications for Cancer Lymphangiogenesis. *Front. Physiol.* 11, 577584. doi:10.3389/fphys.2020.577584

Hablitz, L. M., Plá, V., Giannetto, M., Vinitsky, H. S., Stæger, F. F., Metcalfe, T., et al. (2020). Circadian Control of Brain Glymphatic and Lymphatic Fluid Flow. *Nat. Commun.* 11 (1), 4411. doi:10.1038/s41467-020-18115-2

Harvey, N. L., Srinivasan, R. S., Dillard, M. E., Johnson, N. C., Witte, M. H., Boyd, K., et al. (2005). Lymphatic Vascular Defects Promoted by Prox1 Haploinsufficiency Cause Adult-Onset Obesity. *Nat. Genet.* 37 (10), 1072–1081. doi:10.1038/ng1642

Henderson, V. W., Mack, W., and Williams, B. W. (1989). Spatial Disorientation in Alzheimer's Disease. *Arch. Neurol.* 46 (4), 391–394. doi:10.1001/archneur.1989.00520400045018

Hernandez-Guillamon, M., Mawhirt, S., Blais, S., Montaner, J., Neubert, T. A., Rostagno, A., et al. (2015). Sequential Amyloid-β Degradation by the Matrix Metalloproteases MMP-2 and MMP-9. *J. Biol. Chem.* 290 (24), 15078–15091. doi:10.1074/jbc.M114.610931

Holth, J. K., Fritschi, S. K., Wang, C., Pedersen, N. P., Cirrito, J. R., Mahan, T. E., et al. (2019). The Sleep-Wake Cycle Regulates Brain Interstitial Fluid Tau in Mice and CSF Tau in Humans. *Science* 363 (6429), 880–884. doi:10.1126/science.aav2546

Holzmann, J., Hennchen, M., and Rohrer, H. (2015). Prox1 Identifies Proliferating Neuroblasts and Nascent Neurons during Neurogenesis in Sympathetic Ganglia. *Devel Neurobio.* 75 (12), 1352–1367. doi:10.1002/dneu.22289

Hong, S., Quintero-Monzon, O., Ostaszewski, B. L., Podlisny, D. R., Cavanaugh, W. T., Yang, T., et al. (2011). Dynamic Analysis of Amyloid -Protein in Behaving Mice Reveals Opposing Changes in ISF versus Parenchymal A during Age-Related Plaque Formation. *J. Neurosci.* 31 (44), 15861–15869. doi:10.1523/JNEUROSCI.3272-11.2011

Hsu, M., Rayasam, A., Kijak, J. A., Choi, Y. H., Harding, J. S., Marcus, S. A., et al. (2019). Neuroinflammation-induced Lymphangiogenesis Near the Cribriform Plate Contributes to Drainage of CNS-Derived Antigens and Immune Cells. *Nat. Commun.* 10 (1), 229. doi:10.1038/s41467-018-08163-0

Hsu, S.-J., Zhang, C., Jeong, J., Lee, S.-i., McConnell, M., Utsumi, T., et al. (2021). Enhanced Meningeal Lymphatic Drainage Ameliorates Neuroinflammation and Hepatic Encephalopathy in Cirrhotic Rats. *Gastroenterology* 160 (4), 1315–1329. doi:10.1053/j.gastro.2020.11.036

Hu, X., Deng, Q., Ma, L., Li, Q., Chen, Y., Liao, Y., et al. (2020). Meningeal Lymphatic Vessels Regulate Brain Tumor Drainage and Immunity. *Cell Res* 30 (3), 229–243. doi:10.1038/s41422-020-0287-8

Huggenberger, R., Siddiqui, S. S., Brander, D., Ullmann, S., Zimmermann, K., Antsiferova, M., et al. (2011). An Important Role of Lymphatic Vessel Activation in Limiting Acute Inflammation. *Blood* 117 (17), 4667–4678. doi:10.1182/blood-2010-10-316356

Ichise, H., Ichise, T., Ohtani, O., and Yoshida, N. (2009). Phospholipase C 2 Is Necessary for Separation of Blood and Lymphatic Vasculature in Mice. *Development* 136 (2), 191–195. doi:10.1242/dev.025353

Ichise, H., Ichise, T., and Yoshida, N. (2016). Phospholipase Cγ2 Is Required for Luminal Expansion of the Epididymal Duct during Postnatal Development in Mice. *PLoS One* 11 (3), e0150521. doi:10.1371/journal.pone.0150521

Iliff, J. J., Lee, H., Yu, M., Feng, T., Logan, J., Nedergaard, M., et al. (2013a). Brain-wide Pathway for Waste Clearance Captured by Contrast-Enhanced MRI. *J. Clin. Invest.* 123 (3), 1299–1309. doi:10.1172/JCI67677

Iliff, J. J., Wang, M., Liao, Y., Plogg, B. A., Peng, W., Gundersen, G. A., et al. (2012). A Paravascular Pathway Facilitates CSF Flow through the Brain Parenchyma and the Clearance of Interstitial Solutes, Including Amyloid. *Sci. Translational Med.* 4 (147), 147ra111. doi:10.1126/scitranslmed.3003748

Iliff, J. J., Wang, M., Zeppenfeld, D. M., Venkataraman, A., Plog, B. A., Liao, Y., et al. (2013b). Cerebral Arterial Pulsation Drives Paravascular CSF-Interstitial Fluid Exchange in the Murine Brain. *J. Neurosci.* 33 (46), 18190–18199. doi:10.1523/JNEUROSCI.1592-13.2013

Irrthum, A., Devriendt, K., Chitayat, D., Matthijs, G., Glade, C., Steijlen, P. M., et al. (2003). Mutations in the Transcription Factor Gene SOX18 Underlie Recessive and Dominant Forms of Hypotrichosis-Lymphedema-Telangiectasia. *Am. J. Hum. Genet.* 72 (6), 1470–1478. doi:10.1086/375614

Irrthum, A., Karkkainen, M. J., Devriendt, K., Alitalo, K., and Vikkula, M. (2000). Congenital Hereditary Lymphedema Caused by a Mutation that Inactivates VEGFR3 Tyrosine Kinase. *Am. J. Hum. Genet.* 67 (2), 295–301. doi:10.1086/303019

Ittner, L. M., and Götz, J. (2011). Amyloid-β and tau - a toxic pas de deux in Alzheimer's disease. *Nat. Rev. Neurosci.* 12 (2), 67–72. doi:10.1038/nrn2967

Izen, R. M., Yamazaki, T., Nishinaka-Arai, Y., Hong, Y.-K., and Mukouyama, Y.-S. (2018). Postnatal Development of Lymphatic Vasculature in the Brain Meninges. *Dev. Dyn.* 247 (5), 741–753. doi:10.1002/dvdy.24624

Izquierdo-Altarejos, P., Cabrera-Pastor, A., Gonzalez-King, H., Montoliu, C., and Felipo, V. (2020). Extracellular Vesicles from Hyperammonemic Rats Induce

Neuroinflammation and Motor Incoordination in Control Rats. *Cells* 9 (3), 572. doi:10.3390/cells9030572

Jacob, L., Boisserand, L. S. B., Geraldo, L. H. M., de Brito Neto, J., Mathivet, T., Antila, S., et al. (2019). Anatomy and Function of the Vertebral Column Lymphatic Network in Mice. *Nat. Commun.* 10 (1), 4594. doi:10.1038/s41467-019-12568-w

Jankowsky, J. L., Fadale, D. J., Anderson, J., Xu, G. M., Gonzales, V., Jenkins, N. A., et al. (2004). Mutant Presenilins Specifically Elevate the Levels of the 42 Residue β-amyloid Peptide In Vivo: Evidence for Augmentation of a 42-specific γ Secretase. *Hum. Mol. Genet.* 13 (2), 159–170. doi:10.1093/hmg/ddh019

Jessen, N. A., Munk, A. S. F., Lundgaard, I., and Nedergaard, M. (2015). The Glymphatic System: A Beginner's Guide. *Neurochem. Res.* 40 (12), 2583–2599. doi:10.1007/s11064-015-1581-6

Joachim, C. L., Duffy, L. K., Morris, J. H., and Selkoe, D. J. (1988). Protein Chemical and Immunocytochemical Studies of Meningovascular β-amyloid Protein in Alzheimer's Disease and Normal Aging. *Brain Res.* 474 (1), 100–111. doi:10.1016/0006-8993(88)90673-7

Joers, V., Tansey, M. G., Mulas, G., and Carta, A. R. (2017). Microglial Phenotypes in Parkinson's Disease and Animal Models of the Disease. *Prog. Neurobiol.* 155, 57–75. doi:10.1016/j.pneurobio.2016.04.006

Johanson, C., Stopa, E., Baird, A., and Sharma, H. (2011). Traumatic Brain Injury and Recovery Mechanisms: Peptide Modulation of Periventricular Neurogenic Regions by the Choroid Plexus-CSF Nexus. *J. Neural Transm.* 118 (1), 115–133. doi:10.1007/s00702-010-0498-0

Johnson, L. A., Clasper, S., Holt, A. P., Lalor, P. F., Baban, D., and Jackson, D. G. (2006). An Inflammation-Induced Mechanism for Leukocyte Transmigration across Lymphatic Vessel Endothelium. *J. Exp. Med.* 203 (12), 2763–2777. doi:10.1084/jem.20051759

Jones, G. E., and Mansour, S. (2017). An Approach to Familial Lymphoedema. *Clin. Med.* 17 (6), 552–557. doi:10.7861/clinmedicine.17-6-552

Jones, R. S., Minogue, A. M., Connor, T. J., and Lynch, M. A. (2013). Amyloid-β-Induced Astrocytic Phagocytosis Is Mediated by CD36, CD47 and RAGE. *J. Neuroimmune Pharmacol.* 8 (1), 301–311. doi:10.1007/s11481-012-9427-3

Jung, E., Gardner, D., Choi, D., Park, E., Jin Seong, Y., Yang, S., et al. (2017). Development and Characterization of A Novel Prox1-EGFP Lymphatic and Schlemm's Canal Reporter Rat. *Sci. Rep.* 7 (1), 5577. doi:10.1038/s41598-017-06031-3

Kang, S. S., Ebbert, M. T. W., Baker, K. E., Cook, C., Wang, X., Sens, J. P., et al. (2018). Microglial Translational Profiling Reveals a Convergent APOE Pathway from Aging, Amyloid, and Tau. *J. Exp. Med.* 215 (9), 2235–2245. doi:10.1084/jem.20180653

Kazenwadel, J., Betterman, K. L., Chong, C.-E., Stokes, P. H., Lee, Y. K., Secker, G. A., et al. (2015). GATA2 Is Required for Lymphatic Vessel Valve Development and Maintenance. *J. Clin. Invest.* 125 (8), 2979–2994. doi:10.1172/JCI78888

Kazenwadel, J., Secker, G. A., Liu, Y. J., Rosenfeld, J. A., Wildin, R. S., Cuellar-Rodriguez, J., et al. (2012). Loss-of-function Germline GATA2 Mutations in Patients with MDS/AML or MonoMAC Syndrome and Primary Lymphedema Reveal a Key Role for GATA2 in the Lymphatic Vasculature. *Blood* 119 (5), 1283–1291. doi:10.1182/blood-2011-08-374363

Keren-Shaul, H., Spinrad, A., Weiner, A., Matcovitch-Natan, O., Dvir-Szternfeld, R., Ulland, T. K., et al. (2017). A Unique Microglia Type Associated with Restricting Development of Alzheimer's Disease. *Cell* 169 (7), 1276–1290. doi:10.1016/j.cell.2017.05.018

Kida, S., Pantazis, A., and Weller, R. O. (1993). CSF Drains Directly from the Subarachnoid Space into Nasal Lymphatics in the Rat. Anatomy, Histology and Immunological Significance. *Neuropathol. Appl. Neurobiol.* 19 (6), 480–488. doi:10.1111/j.1365-2990.1993.tb00476.x

Killer, H. E., Laeng, H. R., and Groscurth, P. (1999). Lymphatic Capillaries in the Meninges of the Human Optic Nerve. *J. Neuro-Ophthalmology* 19 (4), 222–228. doi:10.1097/00041327-199912000-00002

Klose, U., Strik, C., Kiefer, C., and Grodd, W. (2000). Detection of a Relation between Respiration and CSF Pulsation with an Echoplanar Technique. *J. Magn. Reson. Imaging* 11 (4), 438–444. doi:10.1002/(sici)1522-2586(200004)11:4<438::aid-jmri12>3.0.co;2-o

Klotz, L., Norman, S., Vieira, J. M., Masters, M., Rohling, M., Dubé, K. N., et al. (2015). Cardiac Lymphatics Are Heterogeneous in Origin and Respond to Injury. *Nature* 522 (7554), 62–67. doi:10.1038/nature14483

Kowalski, J. W., Gawel, M., Pfeffer, A., and Barcikowska, M. (2001). The Diagnostic Value of EEG in Alzheimer Disease. *J. Clin. Neurophysiol.* 18 (6), 570–575. doi:10.1097/00004691-200111000-00008

Kress, B. T., Iliff, J. J., Xia, M., Wang, M., Wei, H. S., Zeppenfeld, D., et al. (2014). Impairment of Paravascular Clearance Pathways in the Aging Brain. *Ann. Neurol.* 76 (6), 845–861. doi:10.1002/ana.24271

Kutomi, O., and Takeda, S. (2020). Identification of Lymphatic Endothelium in Cranial Arachnoid Granulation-like Dural Gap. *Microscopy (Oxf)* 69 (6), 391–400. doi:10.1093/jmicro/dfaa038

Kwon, S., Moreno-Gonzalez, I., Taylor-Presse, K., Edwards Iii, G., Gamez, N., Calderon, O., et al. (2019). Impaired Peripheral Lymphatic Function and Cerebrospinal Fluid Outflow in a Mouse Model of Alzheimer's Disease. *Jad* 69 (2), 585–593. doi:10.3233/JAD-190013

Lee, B. B., and Suami, H. (2020). "Ontogeny and Phylogeny of Lymphatics: Embryological Aspect," in *Lymphatic Structure and Function in Health and Disease*. Editors F. N.E. Gavins and J. S. Alexander (Cambridge, MA: Academic Press), 5–17. doi:10.1016/b978-0-12-815645-2.00002-2

Lee, H., Xie, L., Yu, M., Kang, H., Feng, T., Deane, R., et al. (2015). The Effect of Body Posture on Brain Glymphatic Transport. *J. Neurosci.* 35 (31), 11034–11044. doi:10.1523/JNEUROSCI.1625-15.2015

Lee, S., Kang, J., Yoo, J., Ganesan, S. K., Cook, S. C., Aguilar, B., et al. (2009). Prox1 Physically and Functionally Interacts with COUP-TFII to Specify Lymphatic Endothelial Cell Fate. *Blood* 113 (8), 1856–1859. doi:10.1182/blood-2008-03-145789

Lindestam Arlehamn, C. S., Dhanwani, R., Pham, J., Kuan, R., Frazier, A., Rezende Dutra, J., et al. (2020). α-Synuclein-specific T Cell Reactivity Is Associated with Preclinical and Early Parkinson's Disease. *Nat. Commun.* 11 (1), 1875. doi:10.1038/s41467-020-15626-w

Lioux, G., Liu, X., Temiño, S., Oxendine, M., Ayala, E., Ortega, S., et al. (2020). A Second Heart Field-Derived Vasculogenic Niche Contributes to Cardiac Lymphatics. *Develop. Cel.* 52 (3), 350–363. doi:10.1016/j.devcel.2019.12.006

Liu, G., Mestre, H., Sweeney, A. M., Sun, Q., Weikop, P., Du, T., et al. (2020a). Direct Measurement of Cerebrospinal Fluid Production in Mice. *Cel Rep.* 33 (12), 108524. doi:10.1016/j.celrep.2020.108524

Liu, R., Kang, J. D., Sartor, R. B., Sikaroodi, M., Fagan, A., Gavis, E. A., et al. (2020b). Neuroinflammation in Murine Cirrhosis Is Dependent on the Gut Microbiome and Is Attenuated by Fecal Transplant. *Hepatology* 71 (2), 611–626. doi:10.1002/hep.30827

Liu, X., Gao, C., Yuan, J., Xiang, T., Gong, Z., Luo, H., et al. (2020c). Subdural Haematomas Drain into the Extracranial Lymphatic System through the Meningeal Lymphatic Vessels. *Acta Neuropathol. Commun.* 8 (1), 16. doi:10.1186/s40478-020-0888-y

Liu, X., Gu, X., Ma, W., Oxendine, M., Gil, H. J., Davis, G. E., et al. (2018). Rasip1 Controls Lymphatic Vessel Lumen Maintenance by Regulating Endothelial Cell Junctions. *Development* 145 (17), dev165092. doi:10.1242/dev.165092

Lohela, M., Bry, M., Tammela, T., and Alitalo, K. (2009). VEGFs and Receptors Involved in Angiogenesis versus Lymphangiogenesis. *Curr. Opin. Cel Biol.* 21 (2), 154–165. doi:10.1016/j.ceb.2008.12.012

Louveau, A., Da Mesquita, S., and Kipnis, J. (2016). Lymphatics in Neurological Disorders: A Neuro-Lympho-Vascular Component of Multiple Sclerosis and Alzheimer's Disease?. *Neuron* 91 (5), 957–973. doi:10.1016/j.neuron.2016.08.027

Louveau, A., Herz, J., Alme, M. N., Salvador, A. F., Dong, M. Q., Viar, K. E., et al. (2018). CNS Lymphatic Drainage and Neuroinflammation Are Regulated by Meningeal Lymphatic Vasculature. *Nat. Neurosci.* 21 (10), 1380–1391. doi:10.1038/s41593-018-0227-9

Louveau, A., Smirnov, I., Keyes, T. J., Eccles, J. D., Rouhani, S. J., Peske, J. D., et al. (2015). Structural and Functional Features of Central Nervous System Lymphatic Vessels. *Nature* 523 (7560), 337–341. doi:10.1038/nature14432

Lun, M., Lok, E., Gautam, S., Wu, E., and Wong, E. T. (2011). The Natural History of Extracranial Metastasis from Glioblastoma Multiforme. *J. Neurooncol.* 105 (2), 261–273. doi:10.1007/s11060-011-0575-8

Ma, Q., Decker, Y., Müller, A., Ineichen, B. V., and Proulx, S. T. (2019a). Clearance of Cerebrospinal Fluid from the Sacral Spine through Lymphatic Vessels. *J. Exp. Med.* 216 (11), 2492–2502. doi:10.1084/jem.20190351

Ma, Q., Ineichen, B. V., Detmar, M., and Proulx, S. T. (2017). Outflow of Cerebrospinal Fluid Is Predominantly through Lymphatic Vessels and Is

Reduced in Aged Mice. *Nat. Commun.* 8 (1), 1434. doi:10.1038/s41467-017-01484-6

Ma, Q., Ries, M., Decker, Y., Müller, A., Riner, C., Bücker, A., et al. (2019b). Rapid Lymphatic Efflux Limits Cerebrospinal Fluid Flow to the Brain. *Acta Neuropathol.* 137 (1), 151–165. doi:10.1007/s00401-018-1916-x

Ma, Q., Schlegel, F., Bachmann, S. B., Schneider, H., Decker, Y., Rudin, M., et al. (2019c). Lymphatic Outflow of Cerebrospinal Fluid Is Reduced in Glioma. *Sci. Rep.* 9 (1), 14815. doi:10.1038/s41598-019-51373-9

Mahadevan, A., Welsh, I. C., Sivakumar, A., Gludish, D. W., Shilvock, A. R., Noden, D. M., et al. (2014). The Left-Right Pitx2 Pathway Drives Organ-specific Arterial and Lymphatic Development in the Intestine. *Develop. Cel.* 31 (6), 690–706. doi:10.1016/j.devcel.2014.11.002

Mäkinen, T., Jussila, L., Veikkola, T., Karpanen, T., Kettunen, M. I., Pulkkanen, K. J., et al. (2001). Inhibition of Lymphangiogenesis with Resulting Lymphedema in Transgenic Mice Expressing Soluble VEGF Receptor-3. *Nat. Med.* 7 (2), 199–205. doi:10.1038/84651

Mancini, M., and Toker, A. (2009). NFAT Proteins: Emerging Roles in Cancer Progression. *Nat. Rev. Cancer* 9 (11), 810–820. doi:10.1038/nrc2735

Mandriota, S. J., Jussila, L., Jeltsch, M., Compagni, A., Baetens, D., Prevo, R., et al. (2001). Vascular Endothelial Growth Factor-C-Mediated Lymphangiogenesis Promotes Tumour Metastasis. *EMBO J.* 20 (4), 672–682. doi:10.1093/emboj/20.4.672

Martinez-Corral, I., Ulvmar, M. H., Stanczuk, L., Tatin, F., Kizhatil, K., John, S. W. M., et al. (2015). Nonvenous Origin of Dermal Lymphatic Vasculature. *Circ. Res.* 116 (10), 1649–1654. doi:10.1161/CIRCRESAHA.116.306170

Maruyama, K., Miyagawa-Tomita, S., Mizukami, K., Matsuzaki, F., and Kurihara, H. (2019). Isl1-expressing Non-venous Cell Lineage Contributes to Cardiac Lymphatic Vessel Development. *Develop. Biol.* 452 (2), 134–143. doi:10.1016/j.ydbio.2019.05.002

May, C., Kaye, J. A., Atack, J. R., Schapiro, M. B., Friedland, R. P., and Rapoport, S. I. (1990). Cerebrospinal Fluid Production Is Reduced in Healthy Aging. *Neurology* 40 (3 Pt 1), 500. doi:10.1212/wnl.40.3_part_1.500

Melin, E., Eide, P. K., and Ringstad, G. (2020). *In vivo* assessment of Cerebrospinal Fluid Efflux to Nasal Mucosa in Humans. *Sci. Rep.* 10 (1), 14974. doi:10.1038/s41598-020-72031-5

Miura, M., Kato, S., and Lüdinghausen, M. v. (1998). Lymphatic Drainage of the Cerebrospinal Fluid from Monkey Spinal Meninges with Special Reference to the Distribution of the Epidural Lymphatics. *Arch. Histology Cytol.* 61 (3), 277–286. doi:10.1679/aohc.61.277

Mondin, V., Ferlito, A., Devaney, K. O., Woolgar, J. A., and Rinaldo, A. (2010). A Survey of Metastatic Central Nervous System Tumors to Cervical Lymph Nodes. *Eur. Arch. Otorhinolaryngol.* 267 (11), 1657–1666. doi:10.1007/s00405-010-1357-1

Mondor, I., Baratin, M., Lagueyrie, M., Saro, L., Henri, S., Gentek, R., et al. (2019). Lymphatic Endothelial Cells Are Essential Components of the Subcapsular Sinus Macrophage Niche. *Immunity* 50 (6), 1453–1466. doi:10.1016/j.immuni.2019.04.002

Mrdjen, D., Pavlovic, A., Hartmann, F. J., Schreiner, B., Utz, S. G., Leung, B. P., et al. (2018). High-dimensional Single-Cell Mapping of Central Nervous System Immune Cells Reveals Distinct Myeloid Subsets in Health, Aging, and Disease. *Immunity* 48 (3), 599. doi:10.1016/j.immuni.2018.02.014

Mucke, L., Masliah, E., Yu, G.-Q., Mallory, M., Rockenstein, E. M., Tatsuno, G., et al. (2000). High-Level Neuronal Expression of Aβ1-42in Wild-type Human Amyloid Protein Precursor Transgenic Mice: Synaptotoxicity without Plaque Formation. *J. Neurosci.* 20 (11), 4050–4058. doi:10.1523/JNEUROSCI.20-11-04050.2000

Müller, S., Kohanbash, G., Liu, S. J., Alvarado, B., Carrera, D., Bhaduri, A., et al. (2017). Single-cell Profiling of Human Gliomas Reveals Macrophage Ontogeny as a Basis for Regional Differences in Macrophage Activation in the Tumor Microenvironment. *Genome Biol.* 18 (1), 234. doi:10.1186/s13059-017-1362-4

Natale, G., Bocci, G., and Ribatti, D. (2017). Scholars and Scientists in the History of the Lymphatic System. *J. Anat.* 231 (3), 417–429. doi:10.1111/joa.12644

Nicenboim, J., Malkinson, G., Lupo, T., Asaf, L., Sela, Y., Mayseless, O., et al. (2015). Lymphatic Vessels Arise from Specialized Angioblasts within a Venous Niche. *Nature* 522 (7554), 56–61. doi:10.1038/nature14425

Norrmén, C., Ivanov, K. I., Cheng, J., Zangger, N., Delorenzi, M., Jaquet, M., et al. (2009). FOXC2 Controls Formation and Maturation of Lymphatic Collecting Vessels through Cooperation with NFATc1. *J. Cel Biol* 185 (3), 439–457. doi:10.1083/jcb.200901104

Oh, S.-J., Jeltsch, M. M., Birkenhäger, R., McCarthy, J. E. G., Weich, H. A., Christ, B., et al. (1997). VEGF and VEGF-C: Specific Induction of Angiogenesis and Lymphangiogenesis in the Differentiated Avian Chorioallantoic Membrane. *Develop. Biol.* 188 (1), 96–109. doi:10.1006/dbio.1997.8639

Oliver, G., Kipnis, J., Randolph, G. J., and Harvey, N. L. (2020). The Lymphatic Vasculature in the 21st Century: Novel Functional Roles in Homeostasis and Disease. *Cell* 182 (2), 270–296. doi:10.1016/j.cell.2020.06.039

Onder, L., Mörbe, U., Pikor, N., Novkovic, M., Cheng, H.-W., Hehlgans, T., et al. (2017). Lymphatic Endothelial Cells Control Initiation of Lymph Node Organogenesis. *Immunity* 47 (1), 80–92. doi:10.1016/j.immuni.2017.05.008

Palop, J. J., Chin, J., Roberson, E. D., Wang, J., Thwin, M. T., Bien-Ly, N., et al. (2007). Aberrant Excitatory Neuronal Activity and Compensatory Remodeling of Inhibitory Hippocampal Circuits in Mouse Models of Alzheimer's Disease. *Neuron* 55 (5), 697–711. doi:10.1016/j.neuron.2007.07.025

Pappolla, M., Sambamurti, K., Vidal, R., Pacheco-Quinto, J., Poeggeler, B., and Matsubara, E. (2014). Evidence for Lymphatic Aβ Clearance in Alzheimer's Transgenic Mice. *Neurobiol. Dis.* 71, 215–219. doi:10.1016/j.nbd.2014.07.012

Park, J.-M., Shin, Y.-J., Cho, J. M., Choi, J.-Y., Jeun, S.-S., Cha, J.-H., et al. (2013). Upregulation of Vascular Endothelial Growth Factor Receptor-3 in the Spinal Cord of Lewis Rats with Experimental Autoimmune Encephalomyelitis. *J. Histochem. Cytochem.* 61 (1), 31–44. doi:10.1369/0022155412462975

Patel, T. K., Habimana-Griffin, L., Gao, X., Xu, B., Achilefu, S., Alitalo, K., et al. (2019). Dural Lymphatics Regulate Clearance of Extracellular Tau from the CNS. *Mol. Neurodegeneration* 14 (1), 11. doi:10.1186/s13024-019-0312-x

Petrova, T. V., and Koh, G. Y. (2020). Biological Functions of Lymphatic Vessels. *Science* 369 (6500), eaax4063. doi:10.1126/science.aax4063

Petrova, T. V., and Koh, G. Y. (2018). Organ-specific Lymphatic Vasculature: From Development to Pathophysiology. *J. Exp. Med.* 215 (1), 35–49. doi:10.1084/jem.20171868

Pfarr, K. M., Debrah, A. Y., Specht, S., and Hoerauf, A. (2009). Filariasis and Lymphoedema. *Parasite Immunol.* 31 (11), 664–672. doi:10.1111/j.1365-3024.2009.01133.x

Pfeiffer, F., Kumar, V., Butz, S., Vestweber, D., Imhof, B. A., Stein, J. V., et al. (2008). Distinct Molecular Composition of Blood and Lymphatic Vascular Endothelial Cell Junctions Establishes Specific Functional Barriers within the Peripheral Lymph Node. *Eur. J. Immunol.* 38 (8), 2142–2155. doi:10.1002/eji.200838140

Pfeiffer, R. F. (2016). Non-motor Symptoms in Parkinson's Disease. *Parkinsonism Relat. Disord.* 22 (Suppl. 1), S119–S122. doi:10.1016/j.parkreldis.2015.09.004

Pham, T. H. M., Baluk, P., Xu, Y., Grigorova, I., Bankovich, A. J., Pappu, R., et al. (2010). Lymphatic Endothelial Cell Sphingosine Kinase Activity Is Required for Lymphocyte Egress and Lymphatic Patterning. *J. Exp. Med.* 207 (1), 17–27. doi:10.1084/jem.20091619

Pichol-Thievend, C., Betterman, K. L., Liu, X., Ma, W., Skoczylas, R., Lesieur, E., et al. (2018). A Blood Capillary Plexus-Derived Population of Progenitor Cells Contributes to Genesis of the Dermal Lymphatic Vasculature during Embryonic Development. *Development* 145 (10), dev160184. doi:10.1242/dev.160184

Prigent, A., Gonzales, J., Durand, T., Le Berre-Scoul, C., Rolli-Derkinderen, M., Neunlist, M., et al. (2019). Acute Inflammation Down-Regulates Alpha-Synuclein Expression in Enteric Neurons. *J. Neurochem.* 148 (6), 746–760. doi:10.1111/jnc.14656

Pu, T., Zou, W., Feng, W., Zhang, Y., Wang, L., Wang, H., et al. (2019). Persistent Malfunction of Glymphatic and Meningeal Lymphatic Drainage in a Mouse Model of Subarachnoid Hemorrhage. *Exp. Neurobiol.* 28 (1), 104–118. doi:10.5607/en.2019.28.1.104

Qiu, W. Q., Walsh, D. M., Ye, Z., Vekrellis, K., Zhang, J., Podlisny, M. B., et al. (1998). Insulin-degrading Enzyme Regulates Extracellular Levels of Amyloid β-Protein by Degradation. *J. Biol. Chem.* 273 (49), 32730–32738. doi:10.1074/jbc.273.49.32730

Raper, D., Louveau, A., and Kipnis, J. (2016). How Do Meningeal Lymphatic Vessels Drain the CNS?. *Trends Neurosciences* 39 (9), 581–586. doi:10.1016/j.tins.2016.07.001

Rathinasamy, A., Czeloth, N., Pabst, O., Förster, R., and Bernhardt, G. (2010). The Origin and Maturity of Dendritic Cells Determine the Pattern of Sphingosine 1-

phosphate Receptors Expressed and Required for Efficient Migration. *J. Immunol.* 185 (7), 4072–4081. doi:10.4049/jimmunol.1000568

Rennels, M. L., Gregory, T. F., Blaumanis, O. R., Fujimoto, K., and Grady, P. A. (1985). Evidence for a 'paravascular' Fluid Circulation in the Mammalian Central Nervous System, provided by the Rapid Distribution of Tracer Protein throughout the Brain from the Subarachnoid Space. *Brain Res.* 326 (1), 47–63. doi:10.1016/0006-8993(85)91383-6

Ringstad, G., and Eide, P. K. (2020). Cerebrospinal Fluid Tracer Efflux to Parasagittal Dura in Humans. *Nat. Commun.* 11 (1), 354. doi:10.1038/s41467-019-14195-x

Ringstad, G., Vatnehol, S. A. S., and Eide, P. K. (2017). Glymphatic MRI in Idiopathic Normal Pressure Hydrocephalus. *Brain* 140 (10), 2691–2705. doi:10.1093/brain/awx191

Rockson, S. G. (2001). Lymphedema. *Am. J. Med.* 110 (4), 288–295. doi:10.1016/s0002-9343(00)00727-0

Roh, J. H., Huang, Y., Bero, A. W., Kasten, T., Stewart, F. R., Bateman, R. J., et al. (2012). Disruption of the Sleep-Wake Cycle and Diurnal Fluctuation of -Amyloid in Mice with Alzheimer's Disease Pathology. *Sci. Translational Med.* 4 (150), 150ra122. doi:10.1126/scitranslmed.3004291

Rustenhoven, J., Drieu, A., Mamuladze, T., de Lima, K. A., Dykstra, T., Wall, M., et al. (2021). Functional Characterization of the Dural Sinuses as a Neuroimmune Interface. *Cell* 184 (4), 1000–1016. doi:10.1016/j.cell.2020.12.040

Sabine, A., Agalarov, Y., Maby-El Hajjami, H., Jaquet, M., Hägerling, R., Pollmann, C., et al. (2012). Mechanotransduction, PROX1, and FOXC2 Cooperate to Control Connexin37 and Calcineurin during Lymphatic-Valve Formation. *Develop. Cel.* 22 (2), 430–445. doi:10.1016/j.devcel.2011.12.020

Sabine, A., Bovay, E., Demir, C. S., Kimura, W., Jaquet, M., Agalarov, Y., et al. (2015). FOXC2 and Fluid Shear Stress Stabilize Postnatal Lymphatic Vasculature. *J. Clin. Invest.* 125 (10), 3861–3877. doi:10.1172/JCI80454

Sandrone, S., Moreno-Zambrano, D., Kipnis, J., and van Gijn, J. (2019). A (Delayed) History of the Brain Lymphatic System. *Nat. Med.* 25 (4), 538–540. doi:10.1038/s41591-019-0417-3

Schaum, N., Lehallier, B., Lehallier, B., Hahn, O., Pálovics, R., Hosseinzadeh, S., et al. (2020). Ageing Hallmarks Exhibit Organ-specific Temporal Signatures. *Nature* 583 (7817), 596–602. doi:10.1038/s41586-020-2499-y

Schwager, S., and Detmar, M. (2019). Inflammation and Lymphatic Function. *Front. Immunol.* 10, 308. doi:10.3389/fimmu.2019.00308

Sebzda, E., Hibbard, C., Sweeney, S., Abtahian, F., Bezman, N., Clemens, G., et al. (2006). Syk and Slp-76 Mutant Mice Reveal a Cell-Autonomous Hematopoietic Cell Contribution to Vascular Development. *Develop. Cel.* 11 (3), 349–361. doi:10.1016/j.devcel.2006.07.007

Semyachkina-Glushkovskaya, O., Abdurashitov, A., Dubrovsky, A., Bragin, D., Bragina, O., Shushunova, N., et al. (2017). Application of Optical Coherence Tomography for In Vivo Monitoring of the Meningeal Lymphatic Vessels during Opening of Blood-Brain Barrier: Mechanisms of Brain Clearing. *J. Biomed. Opt.* 22 (12), 1–9. doi:10.1117/1.JBO.22.12.121719

Shahnawaz, M., Mukherjee, A., Pritzkow, S., Mendez, N., Rabadia, P., Liu, X., et al. (2020). Discriminating α-synuclein Strains in Parkinson's Disease and Multiple System Atrophy. *Nature* 578 (7794), 273–277. doi:10.1038/s41586-020-1984-7

Shi, Y., and Holtzman, D. M. (2018). Interplay between Innate Immunity and Alzheimer Disease: APOE and TREM2 in the Spotlight. *Nat. Rev. Immunol.* 18 (12), 759–772. doi:10.1038/s41577-018-0051-1

Shibahara, I., Saito, R., Osada, Y., Kanamori, M., Sonoda, Y., Kumabe, T., et al. (2019). Incidence of Initial Spinal Metastasis in Glioblastoma Patients and the Importance of Spinal Screening Using MRI. *J. Neurooncol.* 141 (2), 337–345. doi:10.1007/s11060-018-03036-4

Shibata, M., Yamada, S., Kumar, S. R., Calero, M., Bading, J., Frangione, B., et al. (2000). Clearance of Alzheimer's Amyloid-β1-40 Peptide from Brain by LDL Receptor-Related Protein-1 at the Blood-Brain Barrier. *J. Clin. Invest.* 106 (12), 1489–1499. doi:10.1172/JCI10498

Shibata-Germanos, S., Goodman, J. R., Grieg, A., Trivedi, C. A., Benson, B. C., Foti, S. C., et al. (2020). Structural and Functional Conservation of Non-lumenized Lymphatic Endothelial Cells in the Mammalian Leptomeninges. *Acta Neuropathol.* 139 (2), 383–401. doi:10.1007/s00401-019-02091-z

Si, J., Chen, L., and Xia, Z. (2006). Effects of Cervical-Lymphatic Blockade on Brain Edema and Infarction Volume in Cerebral Ischemic Rats. *Chin. J. Physiol.* 49 (5), 258–265.

Silver, I., Li, B., Szalai, J., and Johnston, M. (1999). Relationship between Intracranial Pressure and Cervical Lymphatic Pressure and Flow Rates in Sheep. *Am. J. Physiology-Regulatory, Integr. Comp. Physiol.* 277 (6), R1712–R1717. doi:10.1152/ajpregu.1999.277.6.R1712

Silverberg, G. D., Messier, A. A., Miller, M. C., Machan, J. T., Majmudar, S. S., Stopa, E. G., et al. (2010). Amyloid Efflux Transporter Expression at the Blood-Brain Barrier Declines in Normal Aging. *J. Neuropathol. Exp. Neurol.* 69 (10), 1034–1043. doi:10.1097/NEN.0b013e3181f46e25

Song, E., Mao, T., Dong, H., Boisserand, L. S. B., Antila, S., Bosenberg, M., et al. (2020). VEGF-C-driven Lymphatic Drainage Enables Immunosurveillance of Brain Tumours. *Nature* 577 (7792), 689–694. doi:10.1038/s41586-019-1912-x

Stanczuk, L., Martinez-Corral, I., Ulvmar, M. H., Zhang, Y., Laviña, B., Fruttiger, M., et al. (2015). cKit Lineage Hemogenic Endothelium-Derived Cells Contribute to Mesenteric Lymphatic Vessels. *Cel Rep.* 10 (10), 1708–1721. doi:10.1016/j.celrep.2015.02.026

Steinman, L., and Zamvil, S. S. (2005). Virtues and Pitfalls of EAE for the Development of Therapies for Multiple Sclerosis. *Trends Immunol.* 26 (11), 565–571. doi:10.1016/j.it.2005.08.014

Stone, O. A., and Stainier, D. Y. R. (2019). Paraxial Mesoderm Is the Major Source of Lymphatic Endothelium. *Develop. Cel* 50 (2), 247–255. doi:10.1016/j.devcel.2019.04.034

Sulzer, D., Alcalay, R. N., Garretti, F., Cote, L., Kanter, E., Agin-Liebes, J., et al. (2017). T Cells from Patients with Parkinson's Disease Recognize α-synuclein Peptides. *Nature* 546 (7660), 656–661. doi:10.1038/nature22815

Sun, B.-l., Xie, F.-m., Yang, M.-f., Cao, M.-z., Yuan, H., Wang, H.-t., et al. (2011). Blocking Cerebral Lymphatic Drainage Deteriorates Cerebral Oxidative Injury in Rats with Subarachnoid Hemorrhage. *Acta Neurochir Suppl.* 110 (Pt 2), 49–53. doi:10.1007/978-3-7091-0356-2_10

Sun, B. L., Xia, Z. L., Wang, J. R., Yuan, H., Li, W. X., Chen, Y. S., et al. (2006). Effects of Blockade of Cerebral Lymphatic Drainage on Regional Cerebral Blood Flow and Brain Edema after Subarachnoid Hemorrhage. *Clin. Hemorheol. Microcirc.* 34 (1-2), 227–232.

Sweeney, M. D., Kisler, K., Montagne, A., Toga, A. W., and Zlokovic, B. V. (2018a). The Role of Brain Vasculature in Neurodegenerative Disorders. *Nat. Neurosci.* 21 (10), 1318–1331. doi:10.1038/s41593-018-0234-x

Sweeney, M. D., Sagare, A. P., and Zlokovic, B. V. (2018b). Blood-brain Barrier Breakdown in Alzheimer Disease and Other Neurodegenerative Disorders. *Nat. Rev. Neurol.* 14 (3), 133–150. doi:10.1038/nrneurol.2017.188

Sweet, D. T., Jiménez, J. M., Chang, J., Hess, P. R., Mericko-Ishizuka, P., Fu, J., et al. (2015). Lymph Flow Regulates Collecting Lymphatic Vessel Maturation In Vivo. *J. Clin. Invest.* 125 (8), 2995–3007. doi:10.1172/JCI79386

Szentistvanyi, I., Patlak, C. S., Ellis, R. A., and Cserr, H. F. (1984). Drainage of Interstitial Fluid from Different Regions of Rat Brain. *Am. J. Physiology-Renal Physiol.* 246 (6 Pt 2), F835–F844. doi:10.1152/ajprenal.1984.246.6.F835

Tammela, T., and Alitalo, K. (2010). Lymphangiogenesis: Molecular Mechanisms and Future Promise. *Cell* 140 (4), 460–476. doi:10.1016/j.cell.2010.01.045

Taoka, T., Masutani, Y., Kawai, H., Nakane, T., Matsuoka, K., Yasuno, F., et al. (2017). Evaluation of Glymphatic System Activity with the Diffusion MR Technique: Diffusion Tensor Image Analysis along the Perivascular Space (DTI-ALPS) in Alzheimer's Disease Cases. *Jpn. J. Radiol.* 35 (4), 172–178. doi:10.1007/s11604-017-0617-z

Teijeira, A., Hunter, M. C., Russo, E., Proulx, S. T., Frei, T., Debes, G. F., et al. (2017). T Cell Migration from Inflamed Skin to Draining Lymph Nodes Requires Intralymphatic Crawling Supported by ICAM-1/LFA-1 Interactions. *Cel Rep.* 18 (4), 857–865. doi:10.1016/j.celrep.2016.12.078

Terry, R. D., Masliah, E., Salmon, D. P., Butters, N., DeTeresa, R., Hill, R., et al. (1991). Physical Basis of Cognitive Alterations in Alzheimer's Disease: Synapse Loss Is the Major Correlate of Cognitive Impairment. *Ann. Neurol.* 30 (4), 572–580. doi:10.1002/ana.410300410

Tsai, J., Grutzendler, J., Duff, K., and Gan, W.-B. (2004). Fibrillar Amyloid Deposition Leads to Local Synaptic Abnormalities and Breakage of Neuronal Branches. *Nat. Neurosci.* 7 (11), 1181–1183. doi:10.1038/nn1335

Tzima, E., Irani-Tehrani, M., Kiosses, W. B., Dejana, E., Schultz, D. A., Engelhardt, B., et al. (2005). A Mechanosensory Complex that Mediates the Endothelial Cell Response to Fluid Shear Stress. *Nature* 437 (7057), 426–431. doi:10.1038/nature03952

Ulvmar, M. H., Werth, K., Braun, A., Kelay, P., Hub, E., Eller, K., et al. (2014). The Atypical Chemokine Receptor CCRL1 Shapes Functional CCL21 Gradients in Lymph Nodes. *Nat. Immunol.* 15 (7), 623–630. doi:10.1038/ni.2889

Villaro, A. C., Sesma, M. P., and Vazquez, J. J. (1987). Innervation of Mouse Lymph Nodes: Nerve Endings on Muscular Vessels and Reticular Cells. *Am. J. Anat.* 179 (2), 175–185. doi:10.1002/aja.1001790210

Villeda, S. A., Luo, J., Mosher, K. I., Zou, B., Britschgi, M., Bieri, G., et al. (2011). The Ageing Systemic Milieu Negatively Regulates Neurogenesis and Cognitive Function. *Nature* 477 (7362), 90–94. doi:10.1038/nature10357

Visanji, N. P., Lang, A. E., and Munoz, D. G. (2018). Lymphatic Vasculature in Human Dural Superior Sagittal Sinus: Implications for Neurodegenerative Proteinopathies. *Neurosci. Lett.* 665, 18–21. doi:10.1016/j.neulet.2017.11.001

Wang, L., Zhang, Y., Zhao, Y., Marshall, C., Wu, T., and Xiao, M. (2019). Deep Cervical Lymph Node Ligation Aggravates AD-like Pathology of APP/PS1 Mice. *Brain Pathol.* 29 (2), 176–192. doi:10.1111/bpa.12656

Weissenborn, K. (2019). Hepatic Encephalopathy: Definition, Clinical Grading and Diagnostic Principles. *Drugs* 79 (Suppl. 1), 5–9. doi:10.1007/s40265-018-1018-z

Weldon, D. T., Rogers, S. D., Ghilardi, J. R., Finke, M. P., Cleary, J. P., O'Hare, E., et al. (1998). Fibrillar β-Amyloid Induces Microglial Phagocytosis, Expression of Inducible Nitric Oxide Synthase, and Loss of a Select Population of Neurons in the Rat CNSIn Vivo. *J. Neurosci.* 18 (6), 2161–2173. doi:10.1523/JNEUROSCI.18-06-02161.1998

Weller, R. O. (1998). Pathology of Cerebrospinal Fluid and Interstitial Fluid of the CNS: Significance for Alzheimer Disease, Prion Disorders and Multiple Sclerosis. *J. Neuropathol. Exp. Neurol.* 57 (10), 885–894. doi:10.1097/00005072-199810000-00001

Wen, Y. R., Yang, J. H., Wang, X., and Yao, Z. B. (2018). Induced Dural Lymphangiogenesis Facilities Soluble Amyloid-Beta Clearance from Brain in a Transgenic Mouse Model of Alzheimer's Disease. *Neural Regen. Res.* 13 (4), 709–716. doi:10.4103/1673-5374.230299

Wick, N., Haluza, D., Gurnhofer, E., Raab, I., Kasimir, M.-T., Prinz, M., et al. (2008). Lymphatic Precollectors Contain a Novel, Specialized Subpopulation of Podoplaninlow, CCL27-Expressing Lymphatic Endothelial Cells. *Am. J. Pathol.* 173 (4), 1202–1209. doi:10.2353/ajpath.2008.080101

Wigle, J. T., and Oliver, G. (1999). Prox1 Function Is Required for the Development of the Murine Lymphatic System. *Cell* 98 (6), 769–778. doi:10.1016/s0092-8674(00)81511-1

Wisniewski, T., and Goñi, F. (2014). Immunotherapy for Alzheimer's Disease. *Biochem. Pharmacol.* 88 (4), 499–507. doi:10.1016/j.bcp.2013.12.020

Xie, L., Kang, H., Xu, Q., Chen, M. J., Liao, Y., Thiyagarajan, M., et al. (2013). Sleep Drives Metabolite Clearance from the Adult Brain. *Science* 342 (6156), 373–377. doi:10.1126/science.1241224

Yamada, K., Cirrito, J. R., Stewart, F. R., Jiang, H., Finn, M. B., Holmes, B. B., et al. (2011). *In vivo* microdialysis Reveals Age-dependent Decrease of Brain Interstitial Fluid Tau Levels in P301S Human Tau Transgenic Mice. *J. Neurosci.* 31 (37), 13110–13117. doi:10.1523/JNEUROSCI.2569-11.2011

Yamada, S., DePasquale, M., Patlak, C. S., and Cserr, H. F. (1991). Albumin Outflow into Deep Cervical Lymph from Different Regions of Rabbit Brain. *Am. J. Physiology-Heart Circulatory Physiol.* 261 (4 Pt 2), H1197–H1204. doi:10.1152/ajpheart.1991.261.4.H1197

Yanev, P., Poinsatte, K., Hominick, D., Khurana, N., Zuurbier, K. R., Berndt, M., et al. (2020). Impaired Meningeal Lymphatic Vessel Development Worsens Stroke Outcome. *J. Cereb. Blood Flow Metab.* 40 (2), 263–275. doi:10.1177/0271678X18822921

Yang, G., Deng, N., Liu, Y., Gu, Y., and Yao, X. (2020). Evaluation of Glymphatic System Using Diffusion MR Technique in T2DM Cases. *Front. Hum. Neurosci.* 14, 300. doi:10.3389/fnhum.2020.00300

Yuan, L., Moyon, D., Pardanaud, L., Breant, C., Karkkainen, M. J., Alitalo, K., et al. (2002). Abnormal Lymphatic Vessel Development in Neuropilin 2 Mutant Mice. *Development* 129 (20), 4797–4806.

Zhou, W., Shen, B., Shen, W.-q., Chen, H., Zheng, Y.-f., and Fei, J.-j. (2020a). Dysfunction of the Glymphatic System Might Be Related to Iron Deposition in the Normal Aging Brain. *Front. Aging Neurosci.* 12, 559603. doi:10.3389/fnagi.2020.559603

Zhou, Y., Cai, J., Zhang, W., Gong, X., Yan, S., Zhang, K., et al. (2020b). Impairment of the Glymphatic Pathway and Putative Meningeal Lymphatic Vessels in the Aging Human. *Ann. Neurol.* 87 (3), 357–369. doi:10.1002/ana.25670

Zou, W., Pu, T., Feng, W., Lu, M., Zheng, Y., Du, R., et al. (2019). Blocking Meningeal Lymphatic Drainage Aggravates Parkinson's Disease-like Pathology in Mice Overexpressing Mutated α-synuclein. *Transl Neurodegener* 8, 7. doi:10.1186/s40035-019-0147-y

Conflict of Interest: SM is holding patents and patent applications related to the novel findings described in original manuscripts that are mentioned in this review article.

The remaining authors declare that the research was conducted in the absence of any commercial or financial relationships that could be construed as a potential conflict of interest.

Copyright © 2021 das Neves, Delivanoglou and Da Mesquita. This is an open-access article distributed under the terms of the Creative Commons Attribution License (CC BY). The use, distribution or reproduction in other forums is permitted, provided the original author(s) and the copyright owner(s) are credited and that the original publication in this journal is cited, in accordance with accepted academic practice. No use, distribution or reproduction is permitted which does not comply with these terms.

frontiers in Pharmacology

ORIGINAL RESEARCH
published: 03 May 2021
doi: 10.3389/fphar.2021.647747

Amphetamine Induces Oxidative Stress, Glial Activation and Transient Angiogenesis in Prefrontal Cortex via AT_1-R

Osvaldo M. Basmadjian[1†], Victoria B. Occhieppo[1†], Natalia A. Marchese[2,3†], M. Jazmin Silvero C.[4†], María Cecilia Becerra[4†], Gustavo Baiardi[5,6†] and Claudia Bregonzio[1†]*

[1]*Departamento de Farmacología, Facultad de Ciencias Químicas, Instituto de Farmacología Experimental Córdoba (IFEC-CONICET), Universidad Nacional de Córdoba, Córdoba, Argentina,* [2]*Centro de Investigaciones en Química Biológica de Córdoba (CIQUIBIC), CONICET, Facultad de Ciencias Químicas, Universidad Nacional de Córdoba, Córdoba, Argentina,* [3]*Departamento de Química Biológica "Ranwel Caputto", Facultad de Ciencias Químicas, Universidad Nacional de Córdoba, Córdoba, Argentina,* [4]*Instituto Multidisciplinario de Biología Vegetal (IMBIV-CONICET) Departamento de Ciencias Farmacéuticas, Facultad de Ciencias Químicas, Universidad Nacional de Córdoba, Córdoba, Argentina,* [5]*Laboratorio de Neurofarmacología, (IIBYT-CONICET), Universidad Nacional de Córdoba, Córdoba, Argentina,* [6]*Facultad de Ciencias Químicas, Universidad Católica de Córdoba, Córdoba, Argentina*

Background: Amphetamine (AMPH) alters neurons, glia and microvessels, which affects neurovascular unit coupling, leading to disruption in brain functions such as attention and working memory. Oxidative stress plays a crucial role in these alterations. The angiotensin type I receptors (AT_1-R) mediate deleterious effects, such as oxidative/inflammatory responses, endothelial dysfunction, neuronal oxidative damage, alterations that overlap with those observed from AMPH exposure.

Aims: The aim of this study was to evaluate the AT_1-R role in AMPH-induced oxidative stress and glial and vascular alterations in the prefrontal cortex (PFC). Furthermore, we aimed to evaluate the involvement of AT_1-R in the AMPH-induced short-term memory and working memory deficit.

Methods: Male Wistar rats were repeatedly administered with the AT_1-R blocker candesartan (CAND) and AMPH. Acute oxidative stress in the PFC was evaluated immediately after the last AMPH administration by determining lipid and protein peroxidation. After 21 off-drug days, long-lasting alterations in the glia, microvessel architecture and to cognitive tasks were evaluated by GFAP, CD11b and von Willebrand immunostaining and by short-term and working memory assessment.

Results: AMPH induced acute oxidative stress, long-lasting glial reactivity in the PFC and a working memory deficit that were prevented by AT_1-R blockade pretreatment. Moreover, AMPH induces transient angiogenesis in PFC via AT_1-R. AMPH did not affect short-term memory.

Conclusion: Our results support the protective role of AT_1-R blockade in AMPH-induced oxidative stress, transient angiogenesis and long-lasting glial activation, preserving working memory performance.

Keywords: AT1 receptor, oxidative stress, angiogeneis, amphetamine, glia, working memory, short-term memory, prefrontal cortex

OPEN ACCESS

Edited by:
Vanessa Costhek Abilio, Federal University of São Paulo, Brazil

Reviewed by:
Ricardo Alexandre Leitao, University of Coimbra, Portugal
Erika E. Nishi, Federal University of São Paulo, Brazil

****Correspondence:***
Claudia Bregonzio
claubregonzio@unc.edu.ar

†ORCID:
Osvaldo M. Basmadjian
orcid.org/0000-0003-2354-6164
Victoria B. Occhieppo
orcid.org/0000-0002-9325-3458
Natalia A. Marchese
orcid.org/0000-0003-3636-9910
M. Jazmin Silvero C.
orcid.org/0000-0003-1585-2989
María Cecilia Becerra
orcid.org/0000-0003-2853-4437
Gustavo Baiardi
orcid.org/0000-0003-4329-4398
Claudia Bregonzio
orcid.org/0000-0003-3542-2177

Specialty section:
This article was submitted to Neuropharmacology, a section of the journal Frontiers in Pharmacology

Received: *30 December 2020*
Accepted: *30 March 2021*
Published: *03 May 2021*

Citation:
Basmadjian OM, Occhieppo VB, Marchese NA, Silvero C. MJ, Becerra MC, Baiardi G and Bregonzio C (2021) Amphetamine Induces Oxidative Stress, Glial Activation and Transient Angiogenesis in Prefrontal Cortex via AT_1-R. Front. Pharmacol. 12:647747. doi: 10.3389/fphar.2021.647747

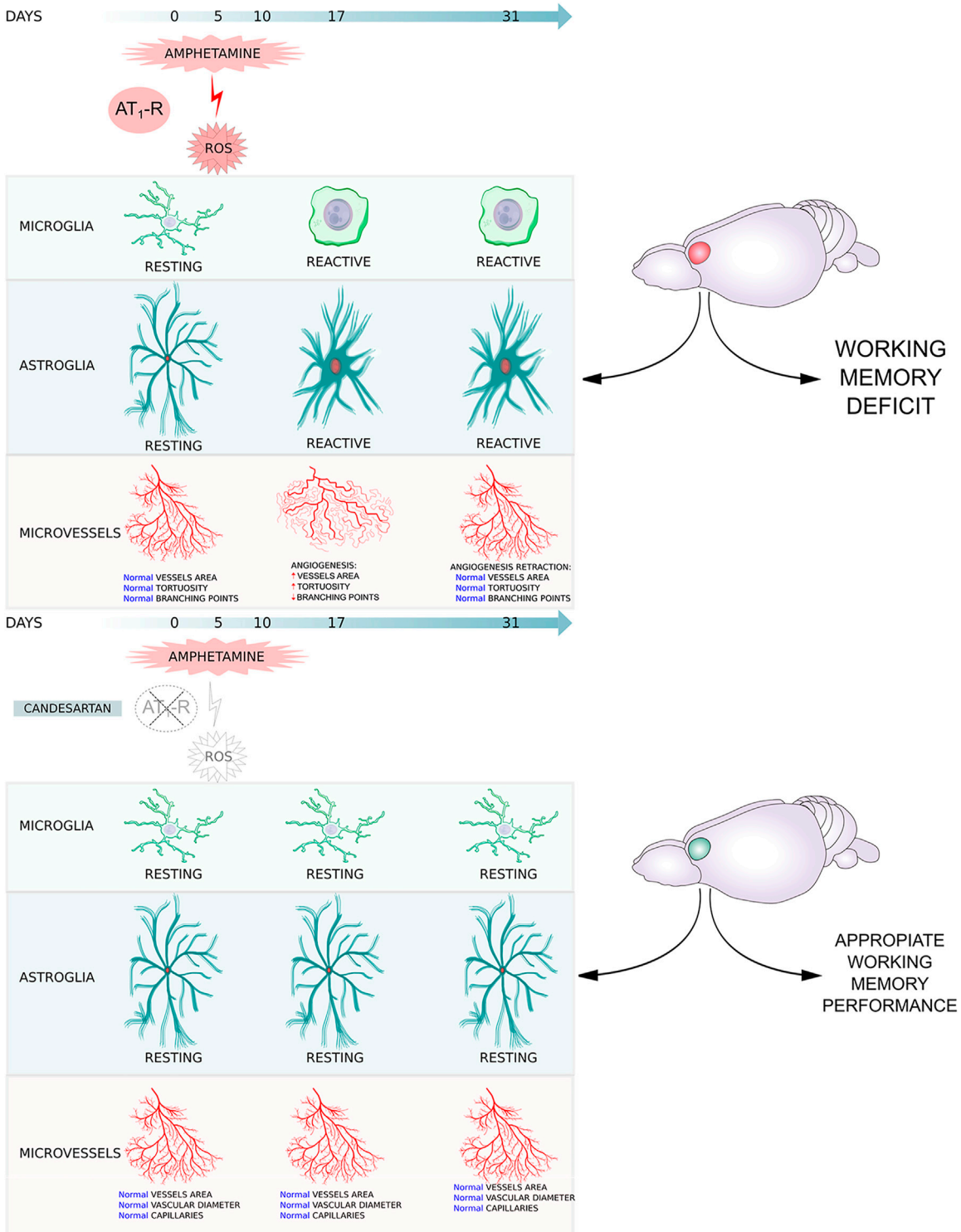

GRAPHICAL ABSTRACT |

INTRODUCTION

The psychostimulant properties of amphetamine (AMPH) make it useful for the treatment of some psychiatric diseases such as attention deficit hyperactivity disorder and narcolepsy; however, it has a high potential for abuse. AMPH and methamphetamine, after opioids, are the major contributors to the global disease burden attributable to drug use disorders (United Nations, 2017). In addition to its acute psychostimulant effects, AMPH exposure is also associated with a broad range of long-lasting changes in all components of the neurovascular unit. Neuronal, glial and vessel functioning are altered, losing suitable coupling between neuronal activity and nutrient delivery (Kalivas, 2007; Carvalho et al., 2012; Paz et al., 2013; Paz et al., 2014; Occhieppo et al., 2017; Schrantee et al., 2017).

Oxidative stress plays a crucial role in AMPH-induced neurotoxicity and glial activation (Moratalla et al., 2017). Thus, AMPH-induced mitochondrial dysfunction and dopamine oxidation lead to increased production of reactive oxygen species (ROS) (Moratalla et al., 2017; Tung et al., 2017). Reactive nitrogen species production is also induced by the increase of Ca^{2+} influx and oxide nitric synthase activity (Brown and Yamamoto, 2003). In consequence, these reactive compounds oxidize and alter the functioning of several cellular elements, including lipids, proteins and nucleic acids. AMPH-induced oxidative damage may subsequently induce microglial activation (Shaerzadeh et al., 2018). The excessive activation of these cells appears to contribute to some neurotoxic effects of AMPH, such as dopamine nerve endings degeneration (LaVoie et al., 2004). Microglial activation is also typically followed by astroglial activation, which contributes to increased levels of proinflammatory cytokines (Loftis and Janoswsky, 2014; Shaerzadeh et al., 2018). In rodents, amphetamines-induced glial reactivity and neuroinflammation are usually observed in brain areas that have dopaminergic endings such as striatum, hippocampus, thalamus and parietal cortex (Shaerzadeh et al., 2018). Interestingly, microglial hypertrophy is pronounced in the mice hippocampus exposed to amphetamines, while little changes are observed in this brain area in rats (Shaerzadeh et al., 2018). In contrast, brain areas with dopaminergic neuron bodies, such as ventral tegmental area and substantia nigra, show a low sensitivity to the amphetamines-induced microglial activation (Shaerzadeh et al., 2018). Thus, there is compelling evidence indicating decreased neuronal integrity and compromised glial reactivity in the prefrontal cortex (PFC) of human AMPH users and of rats exposed to AMPH (Sailasuta et al., 2010; Mackey et al., 2014; Shaerzadeh et al., 2018). In fact, in rodents and humans, AMPH exposure is usually associated with altered performance in cognitive tasks that are highly dependent on PFC functioning, such as attention and working memory (Potvin et al., 2018; Mizoguchi and Yamada, 2019).

AMPH-induced pro-inflammatory effects extend to brain microvasculature. Indeed, 24 h after non-toxic doses of AMPH, it was observed an increase in pro-inflammatory markers, oxidative stress, and heat shock protein expression in meninges-associated vasculature in rodents (Thomas et al., 2009; Thomas et al., 2010). Likewise, our previous results show a sensitized inflammatory response in brain microvessels 7 days after AMPH withdrawal (Marchese et al., 2020). Moreover, these alterations were accompanied by an angiogenic response in the prelimbic PFC (PL-PFC) and somatosensory cortex, evidenced as an increase in the area occupied by microvessels (Occhieppo et al., 2017; Marchese et al., 2020). The microvessels microarchitecture was also altered, showing fewer branching points and more tortuosity without changes in the diameter.

The renin-angiotensin system (RAS) was initially described as a peripheral humoral system, involved in blood pressure and hydro-electrolyte regulation (Peach 1977). Nowadays, it is recognized as a ubiquitous pleiotropic system, with all of its components synthesized within the central nervous system (von Bohlen and Halbach and Albrecht, 2006). Angiotensin II (Ang II), the main active peptide of the RAS, modulates a wide range of the central nervous system (CNS) functions by its AT_1-R. Brain AT_1-R has been reported to play a role in blood pressure and fluid homeostasis regulation, stress responses, depression and cognition, among others (Epstein et al., 1970; Jensen et al., 1992; Raghavendra et al., 2001; Bali and Jaggi 2013). Dopamine-innervated areas express high AT_1-R density, where they positively modulate dopamine synthesis, tonic, and evoked release (Hoebel et al., 1994; Brown et al., 1996; Paz et al., 2014). In this sense, in previous studies we found that AT_1-R modulate DA hyperreactivity induced by a single exposure of AMPH in caudate-putamen and nucleus accumbens (Paz et al., 2011). In addition, the previous AT_1-R blockade prevented the AMPH-induced locomotor sensitization and reversed the psychostimulant-induced locomotor sensitization when these receptors where locally antagonized in the caudate-putamen (Paz et al., 2011; Paz et al., 2014).

Moreover, the presence of AT_1-R has been described in all the components of the neurovascular unit (Yang et al., 1999; Zhou et al., 2006; Garrido-Gil et al., 2017). AT_1-R are constitutively expressed in astrocytes and their activation induces increased intracellular Ca^{2+} with the subsequent induction of early gene transcription (Delaney et al., 2008). These receptors regulate astroglial and microglial reactivity, inducing ROS production and pro-inflammatory cytokine release in the presence of lipopolysaccharides (Bhat et al., 2016). In brain microvessels, the activation of AT_1-R is associated with imbalance in vascular tone regulators together with vascular leakage and inflammatory cell recruitment (Yamakawa et al., 2003; Ando et al., 2004; Zhou et al., 2005).

AT_1-R blockers are currently used in the antihypertensive treatment and have a low incidence of adverse effects, even in elderly patients and they do not alter blood pressure in normotensive patients (Mimran and Ribstein, 1999; Israili, 2000; Shen et al., 2012). Among the several AT_1-R blockers available, candesartan (CAND) shows the tightest and longest-lasting binding to AT_1-R (Unger, 2000). Moreover, it was found that among losartan, irbesartan, telmisartan, CAND was the most effective angiotensin receptor blocker in crossing the blood-brain barrier (Unger, 2003). These reasons and the fact that AT_1-R activation/stimulation has overlapping effects with AMPH in the neurovascular unit components, make AT_1-R blockers a potential pharmacological tool to modulate some deleterious effects

induced by AMPH. The aim of this study was therefore to evaluate the AT_1-R role in AMPH-induced oxidative stress and the associated glial and vascular alterations in the PFC. Working and short-term memory were assessed as a functional outcome of PFC performance.

MATERIALS AND METHODS

Animals

Adult male Wistar rats (250–320 g), from the Department of Pharmacology vivarium (Facultad de Ciencias Químicas, Universidad Nacional de Córdoba, Argentina), were randomly housed in groups of three, one week before the beginning of the experimental protocol. The animals were maintained under controlled environmental conditions (20–24°C, 12 h light/dark cycle with lights on at 7 a.m.) with ad libitum access to food and water.

All procedures were approved by the Animal Care and Use Committee of the Facultad de Ciencias Químicas, Universidad Nacional de Córdoba, Argentina (Res. No. 270/18), in accordance with the NIH Guide for the Care and Use of Laboratory Animals.

Drugs

The selective AT_1-R antagonist, candesartan cilexetil (CAND, Laboratorios Phoenix, Buenos Aires, Argentina) was dissolved in 0.1 N $NaHCO_3$ (vehicle, VEH). The selected dose (3 mg/kg) is in the intermediate doses range (1–5 mg/kg) used in rodents studies (Callera et al., 2016) and was selected from previous work from our laboratory (Paz et al., 2013; Marchese et al., 2016; Occhieppo et al., 2017; Marchese et al., 2020) and taking into account the observed neuroprotective effect at that dose (Lu et al., 2005). d-AMPH sulfate was dissolved in 0.9% NaCl (saline, SAL) immediately before use. The dose (2.5 mg/kg) was selected considering previous studies from our laboratory (Marchese et al., 2016; Marchese et al. 2017; Marchese et al. 2020) and other studies that showed oxidative stress and neuroinflammatory effects induced by AMPH at similar doses (Dean et al., 2011; Gubert et al., 2016; Valvassori et al., 2019).

Animals were administered with the drugs in a different room from that they were housing and from where the behavioral experiments were performed.

Experimental Design

Experimental Protocol 1: AT_1-R Involvement in AMPH-Induced Oxidative Stress

From days 1 to 5, the animals received an oral dose of VEH/CAND (3 mg/kg) by gavage, using a feeding needle. From day 6 to 10, they received an oral dose of VEH/CAND immediately followed by an injection of SAL/AMPH (2.5 mg/kg, i. p.). Four experimental groups were formed: VEH-SAL, VEH AMPH, CAND-SAL and CAND-AMPH (**Figure 1A**). On day 10, the drug injection schedule was adapted to measure oxidative stress (see the oxidative stress protocols below).

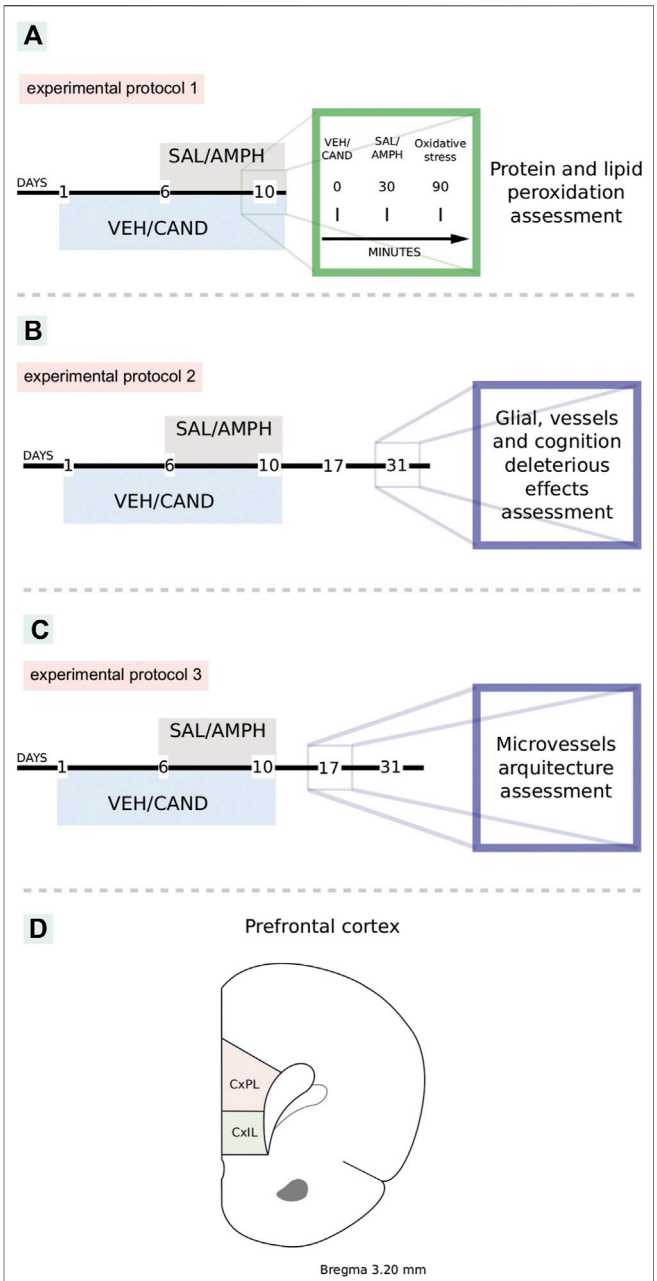

FIGURE 1 | Schematic representation of experimental protocols. VEH: vehicle, CAND: candesartan, SAL: saline, AMPH: amphetamine. Protocol 1: to study the effects of amphetamine and AT1-R blockade in oxidative stress **(A)**. Protocol 2: to study the effects of amphetamine and candesartan on memory, glial reactivity and angioplasticity after 21 days of withdrawal **(B)**. Protocol 3: to study the effects of amphetamine and candesartan on angioplasticity after 7 days of withdrawal **(C)**. Schematic representation of prelimbic and infralimbic subdivisions of the rat prefrontal cortex **(D)**. CxPL: prelimbic prefrontal cortex, CxIL: infralimbic prefrontal cortex.

Experimental Protocol 2: AT_1-R Involvement in Amphetamine-Induced Glial Reactivity and Angioplasticity 21 days After Withdrawal

From days 1 to 10, the animals received VEH/CAND (3 mg/kg) by gavage using a feeding needle and from days 6 to 10 after

VEH/CAND administration they were injected with SAL/AMPH (2.5 mg/kg, i. p.). They then remained undisturbed in their home cages for a drug-free period of 21 days until the experiment. Four experimental groups were formed: VEH-SAL, VEH-AMPH, CAND-SAL, and CAND-AMPH (**Figure 1B**).

Experimental Protocol 3: AT_1-R Involvement in Amphetamine-Induced Angioplasticity 7 days After Withdrawal

From days 1 to 10, the animals received VEH/CAND (3 mg/kg) by gavage using a feeding needle and from days 6 to 10 after VEH/CAND administration they were injected with SAL/AMPH (2.5 mg/kg, i. p.). They then remained undisturbed in their home cages for a drug-free period of 7 days until the experiment. Four experimental groups were formed: VEH-SAL, VEH-AMPH, CAND-SAL and CAND-AMPH (**Figure 1C**).

Oxidative Stress Assessment by Measurement of Protein and Lipid Peroxidation

On day 10 of experimental protocol 1, the animals received an oral dose of VEH/CAND (3 mg/kg) and 60 min later an injection of SAL/AMPH (2.5 mg/kg), according to their corresponding experimental group. Thirty minutes after the SAL/AMPH injection, the animals were sacrificed by decapitation and PFC was extracted including IL and PL subdivision.

Advanced Oxidation Protein Product Quantification

The initial total protein content was detected colorimetrically by Bradford reagent at an absorbance of 595 nm. The subsequent quantification of advanced oxidation protein products (AOPP) was also based on spectrophotometric detection, following Witko-Sarsat et al. (Witko-Sarsat et al., 1996). Briefly, 100 µl of PFC homogenate dilution, 100 µl of chloramine T (ChT, 0–100 µM) for calibration and 200 µl of PBS as blank were applied on a microtiter plate. Then, 10 µl of 1.16 M potassium iodide and 20 µl of glacial acetic acid were added to each well and absorbance at 340 nm was immediately read.

ChT was used as standard for the calibration curve. The concentration of AOPP was expressed as the equivalent of ChT units (µM) per milligram of proteins. All samples were analyzed in duplicate.

Lipid Peroxidation

Lipid oxidation was determined following a procedure similar to B. Avci et al. optimized for these samples (Avci et al., 2012). Briefly, 250 µl of trichloroacetic acid and 250 µl of thiobarbituric acid were added to 100 µl of non-diluted homogenate. Immediately, the samples were kept in boiling water for 10 min. Centrifugation at 129 g was performed for 10 min after cooling to clear the supernatant from denaturalized proteins. Absorbance was immediately measured at 532 nm. Thiobarbituric acid reactive substances were quantified using an extinction coefficient of $1.56 \times 10^5\ M^{-1}\ cm^{-1}$ and expressed as nanomoles of malondialdehyde (MDA) per milligram of proteins. Tissue proteins were estimated using Bradford reagent. All samples were analyzed in duplicate.

Immunohistochemistry of GFAP, CD11b and von Willebrand Factor

Astrogliosis and microgliosis were assessed by immunolabeling with the mouse monoclonal anti-glial fibrillary acidic protein antibody (GFAP, Sigma-Aldrich, MO, United States) and CD11b (Millipore, CA, United States), respectively. To evaluate the vascular network, endothelial cells were immunolabeled with the rabbit anti-von Willebrand factor (VWF, Dako Denmark A/S).

The animals were anesthetized with urethane (100 mg/kg i.p.) and transcardially perfused with 100 ml of saline and heparin (200 µl/L), followed by 200 ml of 4% paraformaldehyde in 0.1 M PBS (pH 7.4). The brains were removed and stored at 4°C in a 30% sucrose solution. Coronal sections of 20 µm (GFAP and CD11b immunohistochemistry) and 40 µm (VWF immunohistochemistry) were cut using a freezing microtome (Leica CM1510S) and collected in 0.01 M PBS (pH 7.4). Then, the endogenous peroxidase was blocked by incubation in a mixture of 10% H_2O_2 and 10% methanol for 2 h, followed by incubation with 10% normal goat serum (NGS; Natocor, Córdoba, Argentina) in 0.1 M PBS for 2 h to block nonspecific binding sites. The free-floating sections were incubated overnight at room temperature with mouse monoclonal GFAP (1:1,000), CD11b (1:1,000) and VWF (1:200). The next day, the sections were rinsed with 0.01 M PBS, and GFAP- and CD11b-labeled sections were incubated with biotin-labeled goat anti-mouse secondary antibody (Jackson Immunoresearch, Laboratories Inc., PA, United States) diluted 1:3,000 in 2% NGS-0.1M PBS and VWF-labeled sections were incubated with biotin-labeled anti-rabbit secondary antibody (Vector Laboratories, CA, United States) diluted 1:500 in 2% NGS-0.1M PBS. Later, they were incubated with avidin-biotin-peroxidase complex diluted 1:500 in 2% NGS-0.1M PBS (ABC-Vector Laboratories, CA, United States) for 2 h each, at room temperature. The peroxidase label was detected with diaminobenzidine hydrochloride (0.5 mg/ml, Sigma-Aldrich, MO, United States) and hydrogen peroxide; the solution was intensified with 1% cobalt chloride and 1% nickel ammonium sulfate. Finally, the free-floating sections were mounted on gelatinized slides, air-dried overnight, dehydrated, cleared in xylene, and placed under a coverslip with DPX mounting medium (Flucka Analytical).

Image Processing

The images were obtained using a Leica DM4000B microscope equipped with Leica FW4000 and a DFC Leica digital camera attached to a contrast enhancement device, and digitized images were stored in a computer. All the images were obtained with identical exposure times, gain and offsets, and saved in TIFF format (1392 × 1040 pixels). The images were processed using

ImageJ software (Schindelin et al., 2012). The analyses were made blinded to the experimental groups.

Image quantification was performed in the infralimbic (IL-PFC) and prelimbic (PL-PFC) areas (Bregma: 3.20 mm), which were identified and delimited according to the Paxinos and Watson atlas 2009 (both subregions are schematized in **Figure 1D**). The measurements were taken bilaterally in two sections and the final value was obtained as the average of the four sections counted.

Astrocyte Reactivity by GFAP Immunostaining

GFAP-stained sections were taken at 400x magnification and the area occupied by astrocytes was quantified fixing a threshold of 140–180 and expressed as the proportion of total area, evaluated in percentages.

Microglia Reactivity by CD11b Immunostaining

CD11b-stained sections were taken at 400x magnification and the area occupied by microglia was quantified fixing a threshold of 130–150 and expressed as the proportion of total area, evaluated in percentages.

Skeleton Analysis of Glial Cells

Glial morphology was assessed following a procedure adapted from Morrison et al. (Morrison and Filosa, 2013). Photomicrographs were pre-processed by the following workflow process: background subtraction, selection of the regions of interest with the multi-point tool, appling the morphological reconstruction tool of the MorpholibJ plugin (Legland et al., 2016), binarize the image by threshold selection and skeletonize the binary images. The AnalizeSkeleton plugin of ImageJ software (Arganda-Carreras et al., 2010) was applied and the total number of branches and branches average length was calculated. The number of branches was normalized dividing by the total number of pixels.

Vascular Network by von Willebrand Factor Immunostaining

The cortical microvessel architecture was analyzed by VWF immunohistochemistry using the vessel analysis plugin of ImageJ software (Elfarnawany, 2015), adapted from previous reports (Tata and Anderson 2002; Beauquis et al., 2010; Marchese et al., 2017; Marchese et al., 2020; Occhieppo et al., 2020). The parameters assessed were:

- Percentage of vessel area.
- Number of branching points in 0.01 mm^2 of VWF positive area.
- Vessel tortuosity (ratio between the real distance of adjacent branching points and their Euclidean distance—the shortest distance between them). The latter parameter takes values from 1 to infinite, where higher values indicate a more sinuous structure.

Behavior

Y-Maze Test

Working memory was assessed by the Y-maze test adapted from previous reports (Ahmad-Molaei et al., 2018; Famitafreshi and Karimian, 2018; Islam et al., 2019; Marchese et al., 2020). Briefly, the animals were placed at the center of a Y-shaped maze, with three equal arms (50 × 10 cm × 39 cm, at angles of 120°) and left to explore freely for 8 min (**Figure 2A**). The trial was monitored through a video camera positioned above the Y-maze and the number of spontaneous alternations and arms entries was counted. An arm entry was defined when four paws were within the arm. Spontaneous alternation was defined as three consecutive choices of three different arms. The results were expressed as the ratio between spontaneous alternation and the total possible alternations (number of entries minus 2). In this behavioral task, a lower alternation percentage is considered as a working memory deficit. Animals that displayed a 2 min period of immobility between arms were excluded from the final analysis.

Novel Object Recognition Test

Short-term memory was evaluated by the novel recognition test adapted from previous works (Baker and Kim, 2002; Arias-Cavieres et al., 2017; Ahmad-Molaei et al., 2018). Briefly, the animals were placed in an empty open arena (60 × 60 × 40 cm) in a different room from where they were housed. All the rats were tested between 9 a.m. and 6 p.m., under dim light, in a quiet room. The day before the experiment, the animals were habituated individually in the testing apparatus for 5 min, in two sessions 2 h apart. At the sample session on the experimental day, the animals were placed in the open arena, which had two identical objects aligned with a random wall of the arena, at a distance of 10 cm, and they were allowed to freely explore for 5 min (**Figure 2B**). In the test session 2 h later, the animals were placed in the same arena, but one object of the sample session had been replaced by a new one that had a different shape and texture (**Figure 2C**). Trials were monitored through a video camera positioned above each arena and the time spent in contact with the objects was quantified in both sessions. The results were expressed as the preference index (PI) of the new object (test session) and PI of the most explored object (sample session), calculated as follows:

$$PI = \frac{\text{novelobjectexploration}}{\text{totalobjectexploration}}\left(\frac{s}{s}\right).$$

A PI greater than 0.5 in the test session shows a preference for the new object and therefore recognition of the sample session objects. A PI near to 0.5 in the sample session shows no bias in the training session.

Two identical sets of different objects were used made of glass and plastic with variations in shape and texture.

Statistical Analysis

The data were analyzed using two-way ANOVA and reported as means ± SEM. The analysis considered VEH/CAND as a treatment factor and SAL/AMPH as a drug factor. If interaction was observed, multiple comparisons were made using the Tukey post-test. A value of $p < 0.05$ was considered significant. The analyses were performed using Graphpad Prism® 8.03 software.

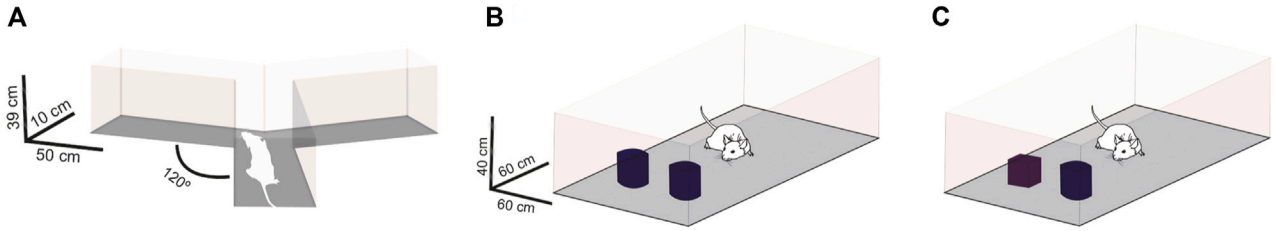

FIGURE 2 | Schematic representation of working memory and short-term memory assessment. Working memory assessment by Y-maze test **(A)**. Sample session of novel object recognition test **(B)**. Test session of novel object recognition test **(C)**.

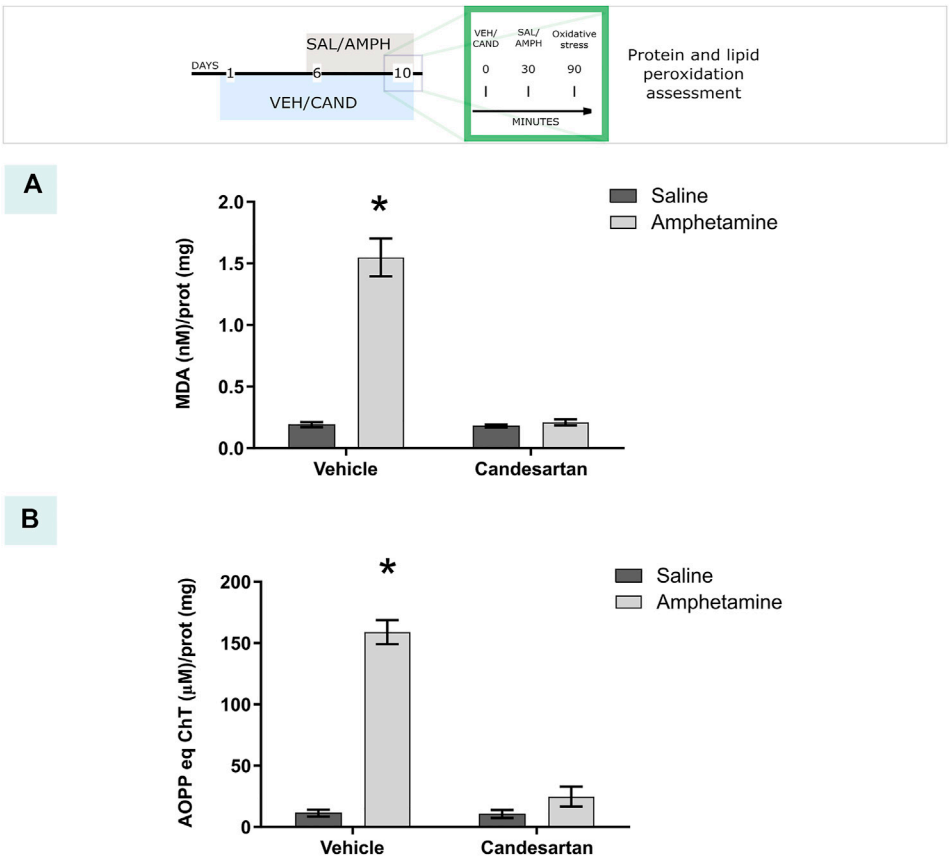

FIGURE 3 | AT_1-R blockade prevents amphetamine-induced oxidative stress. The graphs show the MDA and AOPP quantification as measurements of lipid and protein peroxidation, respectively, in the PFC for the four experimental groups of protocol 1. MDA quantification **(A)**. Equivalents of chloramine T quantification **(B)**. Values are the mean ± SEM; $n = 4$. *different from the rest of the groups ($p < 0.05$).

RESULTS

AT_1-R Blockade Prevents Amphetamine-Induced Oxidative Stress

Acute AMPH exposure induced an extensive oxidative stress, evaluated as lipid and protein peroxidation, which was totally blunted by the AT_1-R blockade pretreatment (**Figure 3**, experimental protocol 1).

The two-way ANOVA results of protein peroxidation showed a significant effect of treatment, drug and drug * treatment interaction factors ($F_{(1,\ 12)} = 145.9$, $p < 0.01$; $F_{(1,\ 12)} = 101.4$, $p < 0.01$; $F_{(1,\ 12)} = 99.29$, $p < 0.01$ respectively). Tukey Post Hoc comparison indicates a significant increase of protein peroxidation in the PFC in VEH-AMPH group when was compared with the rest of the groups ($p < 0.01$) and no significant differences in the comparison between the control groups (VEH-SAL and CAND-SAL; $p > 0.99$) and control groups with CAND-AMPH ($p = 0.51$ and $p = 0.47$, respectively, **Figure 3A**).

The two-way ANOVA results of lipid peroxidation showed a significant effect of treatment, drug and drug * treatment

interaction factors ($F_{(1, 12)} = 78.15$, $p < 0.01$; $F_{(1, 12)} = 74.09$, $p < 0.01$; $F_{(1, 12)} = 71.75$, $p < 0.01$ respectively). Tukey Post Hoc comparison indicates a significant increase of lipid peroxidation in the PFC in VEH-AMPH group when was compared with the rest of the groups ($p < 0.01$) and no significant differences in the comparison between the control groups (VEH-SAL and CAND-SAL; $p > 0.99$) and control groups with CAND-AMPH ($p > 0.99$ and $p > 0.99$, respectively, **Figure 3B**).

Amphetamine-Induced Gliosis in the Prelimbic Prefrontal Cortex Involves AT_1-R

Glial reactivity (astrogliosis and microgliosis) was observed after AMPH exposure in the PL-PFC, but not in the IL-PFC. These alterations were prevented by AT_1-R blockade pretreatment (**Figures 4B,C**). In PL-PFC, AMPH exposure increased the ramification of microglia and this alteration was prevented by the AT_1-R blockade. No changes in microglia ramification were observed in IL-PFC or in astroglia ramification in PL and IL-PFC after the treatments. The average branches length was similar among groups in microglia and astroglia in both brain regions.

The two-way ANOVA results of GFAP immunostaining in PL-PFC showed a significant effect of treatment and drug * treatment interaction factors ($F_{(1, 28)} = 4.29$, $p = 0.048$; $F_{(1, 28)} = 6.12$, $p = 0.020$; respectively) and no significant effect of drug factor ($F_{(1, 28)} = 3.15$, $p = 0.087$). Tukey Post Hoc comparison indicates a significant increase of GFAP occupied area in the PL-PFC in VEH-AMPH group when was compared with the VEH-SAL and CAND-AMPH groups ($p = 0.041$ and $p = 0.022$, respectively) and no significant differences in the comparison between the control groups (VEH-SAL and CAND-SAL; $p > 0.99$) and control groups with CAND-AMPH ($p > 0.99$ and $p = 0.95$, respectively; **Figure 4B**, left panel).

The two-way ANOVA results of CD11b immunostaining in PL-PFC showed a significant effect of drug and drug * treatment interaction factors ($F_{(1, 28)} = 7.25$, $p = 0.012$; $F_{(1, 28)} = 4.38$, $p = 0.046$; respectively) and no significant effect of treatment factor ($F_{(1, 28)} = 1.83$, $p = 0.187$). Tukey Post Hoc comparison indicates a significant increase of CD11b occupied area in the PL-PFC in VEH-AMPH group compared with the VEH-SAL and CAND-SAL groups ($p = 0.015$ and $p = 0.048$, respectively) and no significant differences in the comparison between control groups (VEH-SAL and CAND-SAL; $p = 0.94$) and VEH-AMPH and CAND-AMPH groups ($p = 0.126$; **Figure 4C**, left panel).

The two-way ANOVA results of GFAP immunostaining in IL-PFC showed no significant effect of drug, treatment and drug * treatment interaction factors ($F_{(1, 25)} = 0.03$, p = 0.849: $F_{(1, 25)} = 0.34$, p = 0.563; $F_{(1, 25)} = 0.50$, p = 0.486; respectively; **Figure 4B** right panel). The two-way ANOVA results of CD11b immunostaining in IL-PFC showed a significant effect of drug ($F_{(1, 21)} = 6.57$, p = 0.018) and no significant effects of treatment and drug*treatment interaction factors ($F_{(1, 21)} = 0.38$, p = 0.542: $F_{(1, 21)} = 0.97$, p = 0.335; respectively; **Figure 4C** right panel).

The two-way ANOVA results of microglia ramification in PL-PFC showed a significant effect of treatment and drug * treatment interaction factors ($F_{(1, 28)} = 11.70$, $p = 0.002$; $F_{(1, 28)} = 4.63$, $p = 0.040$; respectively) and no significant effect of drug factor ($F_{(1, 28)} = 3.19$, $p = 0.085$). Tukey Post Hoc comparison indicates a significant increase of microglia ramification in the PL-PFC in VEH-AMPH group compared with the CAND-SAL and CAND-AMPH groups ($p = 0.007$ and $p = 0.005$, respectively) and no significant differences in the comparison between control groups (VEH-SAL and CAND-SAL; $p = 0.771$) and VEH-AMPH and VEH-SAL groups ($p = 0.056$; **Figure 4F**, left panel).

The two-way ANOVA of microglia ramification in IL-PFC and astroglia ramification in both brain areas and average branches length of microglia and astroglia in both areas showed no significant effects in drug, treatment and drug * treatment interaction factors. These results are summarized in **Table 1** and in **Figures 4D–G**.

Amphetamine Induces Transient Angiogenesis in the Prefrontal Cortex

In IL-PFC, after 7 days of withdrawal, it was found an increase of microvessels tortuosity induced by AMPH exposure, that was prevented by AT_1-R blockade and no changes were observed in branching points microvessels (**Figure 5B**). On the contrary, after 21 days of withdrawal, it was observed no changes in microvessels tortuosity and an increase of branching points induced by AMPH in this brain area (this alteration was prevented by AT_1-R blockade, **Figure 5C**). No changes were observed in all microvessels parameters analyzed in PL-PFC after 21 days of withdrawal (**Table 2**).

The two-way ANOVA results of microvessels tortuosity in IL-PFC after 7 days of withdrawal showed a significant effect of drug, treatment and drug*treatment interaction factors ($F_{(1, 27)} = 9.22$, $p = 0.005$; $F_{(1, 27)} = 15.17$, $p < 0.001$; $F_{(1, 27)} = 4.67$, $p = 0.040$; respectively; **Figure 5B** right panel). Tukey Post Hoc comparison indicates a significant increase of microvessels tortuosity in the IL-PFC of VEH-AMPH group compared with the VEH-SAL, CAND-SAL and CAND-AMPH groups ($p = 0.005$, $p < 0.001$, and $p = 0.001$, respectively) and no significant differences in the comparison between control groups (VEH-SAL and CAND-SAL; $p = 0.604$) and CAND-SAL and CAND-AMPH groups ($p = 0.929$; **Figure 5B**, right panel). The two-way ANOVA results of microvessels branching points in IL-PFC after 7 days of withdrawal showed no significant effect of drug, treatment and drug * treatment interaction factors ($F_{(1, 27)} = 2.59$, $p = 0.119$; $F_{(1, 27)} = 0.09$, $p = 0.760$; $F_{(1, 27)} = 1.92$, $p = 0.178$; respectively; **Figure 5B** left panel).

The two-way ANOVA results of tortuosity in IL-PFC after 21 days of withdrawal showed no significant effects in drug ($F_{(1, 18)} = 0.27$, $p = 0.601$), treatment ($F_{(1, 18)} = 1.08$, $p = 0.313$) and drug * treatment interaction factors ($F_{(1, 18)} = 0.64$, $p = 0.432$; **Figure 5C** right panel). The two-way ANOVA results of branching points microvessels in IL-PFC after 21 days of withdrawal showed a significant effects of drug, treatment of drug * treatment interaction factors ($F_{(1, 18)} = 4.77$, $p = 0.042$; $F_{(1, 18)} = 14.54$, $p = 0.001$; $F_{(1, 18)} = 9.08$, $p = 0.007$; respectively; **Figure 5C** left panel). Tukey Post Hoc comparison indicates a significant increase of branching points in the IL-PFC of VEH-AMPH group compared with the VEH-SAL, CAND-SAL and CAND-AMPH groups ($p = 0.008$, $p = 0.004$ and $p < 0.001$, respectively) and no significant differences in the comparison between control groups (VEH-SAL and CAND-SAL; $p = 0.942$) and CAND-SAL and CAND-AMPH groups ($p = 0.935$; **Figure 5C**).

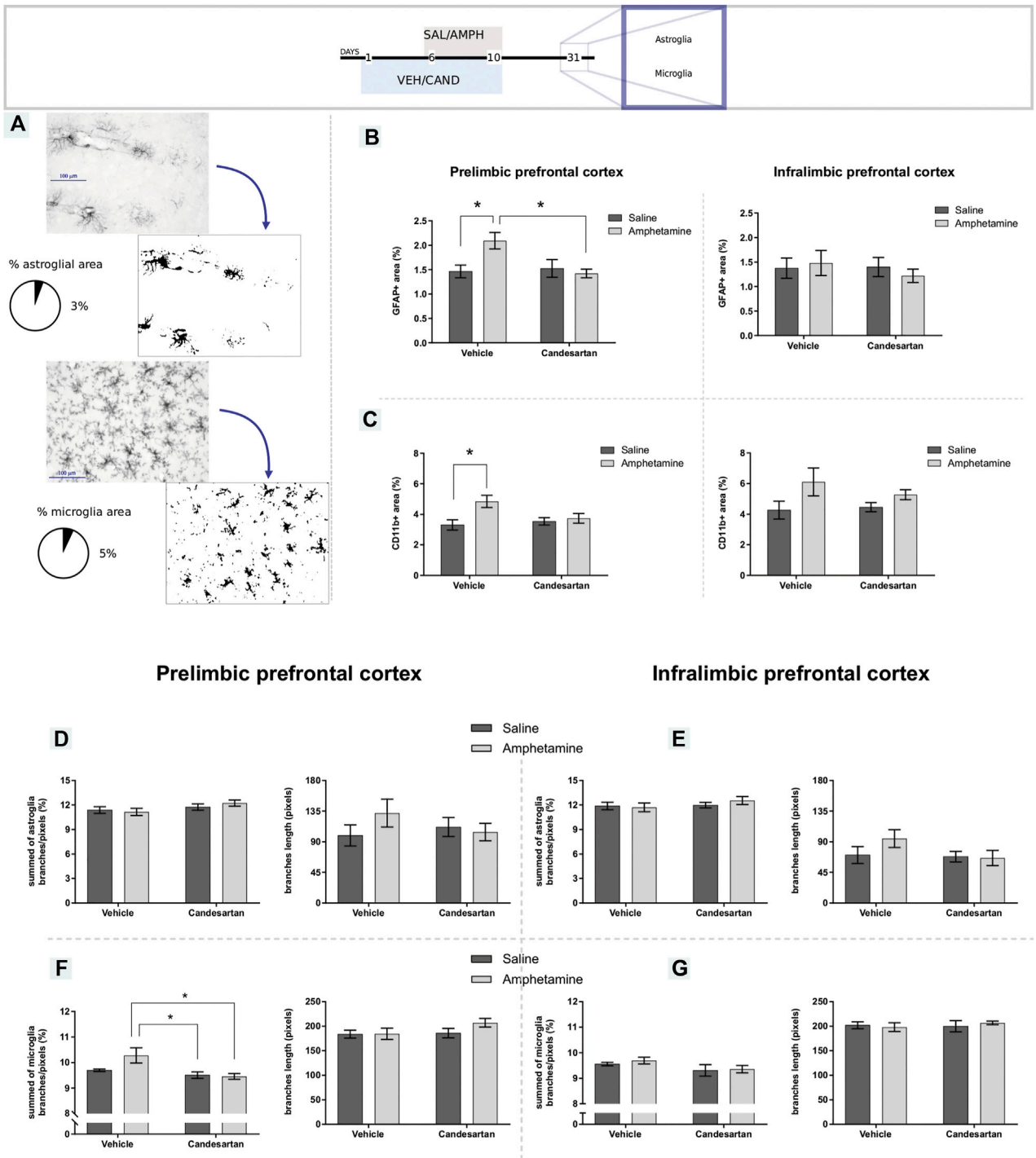

FIGURE 4 | Amphetamine induces gliosis selectively in the prelimbic prefrontal cortex by AT_1-R. The graphs show GFAP and CD11b expression and glial morphology in the PL- and IL-PFC as a measure of astrogliosis and microgliosis, respectively, for the four experimental groups of protocol 3. Schematic representation of GFAP and CD11b immunostaining assessment **(A)**. GFAP immunoreactive area in the PL- and IL-PFC **(B)**, left and right panel, respectively. CD11b positive area in the PL- and IL-PFC **(C)**, left and right panel, respectively. Summed of astroglia branches and average branches length in PL-PFC **(D)**, left and right panel, respectively. Summed of astroglia branches and average branches length in IL-PFC **(E)**, left and right panel, respectively. Summed of microglia branches and average branches length in PL-PFC **(F)**, left and right panel, respectively. Summed of microglia branches and average branches length in IL-.PFC **(G)**, left and right panel, respectively. Values are the mean ± SEM; $n = 6–9$. *different from VEH-SAL and CAND-AMPH ($p < 0.05$; **Figure 4A**) or different from VEH-SAL ($p < 0.05$; **Figure 4B**) or CAND-SAL and CAND-AMPH ($p < 0.05$; **Figure 4F** panel left).

TABLE 1 | Statistical results of glial morphological changes in PL and IL-PFC.

Prelimbic prefrontal cortex						
2-Way ANOVA	**Microglia branches lenght (pixels)**		**Summed of astroglia branches/pixels (%)**		**Astroglia branches lenght (pixels)**	
drug * treatment interaction	$F_{(1, 28)} = 1.154$	$p = 0.292$	$F_{(1, 27)} = 0.764$	$p = 0.390$	$F_{(1, 27)} = 1.692$	$p = 0.204$
Treatment	$F_{(1, 28)} = 1.702$	$P = 0.203$	$F_{(1, 27)} = 3.161$	$p = 0.087$	$F_{(1, 27)} = 0.257$	$P = 0.616$
Drug	$F_{(1, 28)} = 1.317$	$p = 0.261$	$F_{(1, 27)} = 0.089$	$p = 0.768$	$F_{(1, 27)} = 0.678$	$p = 0.418$

Infralimbic prefrontal cortex								
2-Way ANOVA	**Summed of microglia branches/pixels (%)**		**Microglia branches lenght (*p*ixels)**		**Summed of astroglia branches/*p*ixels (%)**		**Astroglia branches lenght (*p*ixels)**	
drug * treatment interaction	$F_{(1, 19)} = 0.067$	$p = 0.799$	$F_{(1, 21)} = 0.398$	$p = 0.535$	$F_{(1, 27)} = 0.614$	$p = 0.440$	$F_{(1, 27)} = 1.343$	$p = 0.257$
treatment	$F_{(1, 19)} = 3.337$	$p = 0.084$	$F_{(1, 21)} = 0.154$	$p = 0.699$	$F_{(1, 27)} = 1.027$	$p = 0.320$	$F_{(1, 27)} = 1.893$	$p = 0.180$
drug	$F_{(1, 19)} = 0.326$	$p = 0.575$	$F_{(1, 21)} = 0.029$	$p = 0.865$	$F_{(1, 27)} = 0.178$	$p = 0.676$	$F_{(1, 27)} = 0.957$	$p = 0.337$

The two-way ANOVA results of microvessels occupied area, branching points and tortuosity in PL-PFC after 21 days of withdrawal showed no significant effect of drug, treatment and drug * treatment interaction factors (**Table 2**).

Amphetamine-Induced Spatial Working Memory Deficit Involves AT_1-R

Previous exposure to AMPH induced a spatial working memory deficit, assessed after 21 days of withdrawal in the Y-maze paradigm (**Figure 6A**; experimental protocol 3). This deficit was not observed with the CAND pretreatment (**Figure 6A**; experimental protocol 3).

The two-way ANOVA results of spatial working memory assessment (Y-maze test) showed a significant effect of drug, treatment and drug * treatment interaction factors ($F_{(1, 39)} = 12.51$, $p = 0.001$; $F_{(1, 39)} = 5.11$, $p = 0.029$; $F_{(1, 39)} = 5.50$, $p = 0.024$; respectively; **Figure 6A**). Tukey Post Hoc comparison indicates a significant lower percentage of spontaneous alternations of VEH-AMPH group compared with the VEH-SAL, CAND-SAL and CAND-AMPH groups ($p < 0.001$, $p = 0.001$ and $p = 0.013$, respectively) and no significant differences in the comparison between control groups (VEH-SAL and CAND-SAL; $p > 0.999$) and CAND-SAL and CAND-AMPH groups ($p = 0.838$; **Figure 6A**).

An additional analysis of the total activity during the behavioral test was performed to discard motor differences among the four experimental groups (inset graph in **Figure 6A**). There were no differences in total number of entries to the Y-maze arms among drug, treatment and drug*treatment interaction factors ($F_{(1, 39)} = 0.02$, $p = 0.886$, $F_{(1, 39)} = 2.90$, $p = 0.096$, $F_{(1, 39)} = 0.02$, $p = 0.886$; respectively; inset **Figure 6A**).

Amphetamine Does Not Alter Short-Term Recognition Memory

AMPH exposure did not alter short-term recognition memory assessed in the novel object recognition (NOR) paradigm (**Figure 6B**; Experimental protocol 3). In the test session, the animals from the four experimental groups showed a greater preference for the new object, with a PI for the novel object greater than 0.5 (which shows recognition of the objects of the sample session) with no differences among the groups in drug, treatment and treatment*drug interaction factors ($F_{(1, 26)} = 0.07$, $p = 0.796$; $F_{(1, 26)} = 0.53$ $p = 0.474$; $F_{(1, 26)} < 0.01$, $p = 0.965$; respectively). Additionally, the PI of the sample test was around 0.5 for the four experimental groups with no differences in treatment and drug*treatment interaction factors ($F_{(1, 26)} = 0.13$ $p = 0.725$; $F_{(1, 26)} = 0.35$, $p = 0.558$; respectively; inset graph in **Figure 6B**). A significant effect of drug factor was observed ($F_{(1, 26)} = 11.30$, $p = 0.002$).

DISCUSSION

This work shows that AT_1-R blockade prevents AMPH-induced oxidative stress, evaluated as lipid and protein peroxidation. Our findings also support an AT_1-R role in the AMPH-induced transient angiogenesis in PFC and long-lasting astroglial and microglial reactivity (evaluated after 21 off-drug days) in the PL-PFC. Furthermore, we showed that AMPH, via AT_1-R, induced an enduring working memory deficit without short-term memory deleterious effects.

Several sources of brain insults induce oxidative stress via AT_1-R. Goel et al. and Salmani et al. showed that brain oxidative stress induced by central or peripheral LPS injection is modulated by AT_1-R, preventing its development by previous CAND or losartan oral administration (Goel et al., 2018; Salmani et al., 2020). Moreover, it has been shown that CAND at low doses (0.1 and 0.3 mg/kg) attenuate ischemic brain damage and inhibit the associated oxidative stress (Hamai et al., 2006). Moreover, Bild et al. showed that central angiotensin II injection (*via* i.c.v.) induced oxidative stress, which is prevented by central injection of AT_1-R blockers or angiotensin-converting enzyme inhibitors (Bild et al., 2013). In line with the present results, Xu et al. showed that methamphetamine induces oxidative stress and the associated neurotoxicity by AT_1-R, via phospholipase C β1 (Xu et al., 2021). As oxidative stress plays a crucial role in the amphetamines-induced neurotoxicity (Moratalla et al., 2017), the above and the present results suggest that AT_1-R may be involved in neurotoxicity effects of others amphetamines derivatives such as 3,4-methylenedioxymethamphetamine. The above described may result from AT_1-R regulation of mitochondria functioning

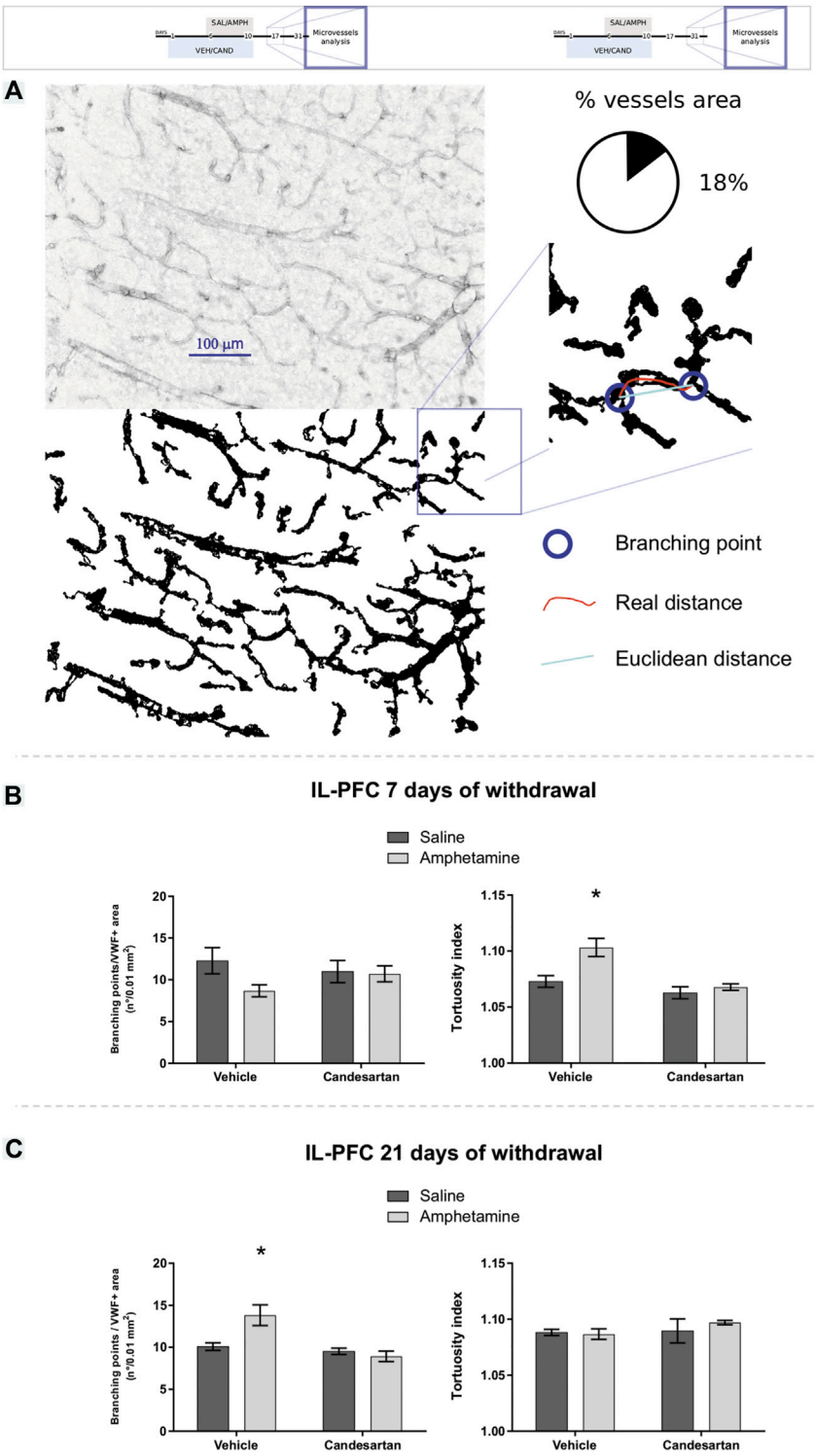

FIGURE 5 | Amphetamine induces transient angiogenesis in the prefrontal cortex. The graphs show VWF expression in the PL-PFC and IL-PFC as a measure of angioplasticity for the four experimental groups of experimental protocols 2 and 3. Schematic representation of the VWF immunostaining assessment **(A)**. The number of branching points and vascular tortuosity in IL-PFC after 7 days of withdrawal (experimental protocol 2) **(B)**, left and right panel, respectively. The number of branching points and vascular tortuosity in IL-PFC after 21 days of withdrawal (experimental protocol 3) **(C)**, left and right panel, respectively. Values are the mean ± SEM; n = 5–8. *different from VEH-SAL and CAND-AMPH ($p < 0.05$).

TABLE 2 | Statistical results of vascular morphological changes in PL-PFC.

	Prelimbic prefrontal cortex					
2-Way ANOVA	**Branching points/area**		**Tortuosity index**		**vWF occupied area %**	
VEH - SAL	5.76 ± 0.64		1.068 ± 0.004		7.27 ± 1.12	
VEH - AMPH	7.39 ± 1.60		1.077 ± 0.006		10.57 ± 2.08	
CAND - SAL	5.64 ± 1.46		1.080 ± 0.003		7.91 ± 0.98	
CAND - AMPH	4.26 ± 0.80		1.074 ± 0.002		7.84 ± 0.64	
drug*treatment interaction	$F_{(1, 19)} = 1.681$	$p = 0.210$	$F_{(1, 19)} = 3.455$	$p = 0.079$	$F_{(1, 19)} = 1.862$	$P = 0.188$
Treatment	$F_{(1, 19)} = 1.956$	$p = 0.178$	$F_{(1, 19)} = 1.272$	$p = 0.273$	$F_{(1, 19)} = 0.722$	$P = 0.406$
Drug	$F_{(1, 19)} = 0.012$	$p = 0.913$	$F_{(1, 19)} = 0.043$	$p = 0.838$	$F_{(1, 19)} = 1.714$	$P = 0.206$

(the main source of ROS). Recently, Valenzuela et al. showed that AT_1-R are present in this organelle and that their activation increases superoxide production by inducing NADPH oxidase complex activity (Valenzuela et al., 2016). Ang II also enhances cytoplasmic Ca^{2+}, which further activates NADPH oxidase complex activity (Prusty et al., 2017). The resulting oxidative damage may trigger the glial activation in PL-PFC observed 21 days after the last AMPH exposure. Furthermore, the prevention of glial reactivity via AT_1-R may be a direct effect, since these receptors are present in both cell types (Garrido-Gil et al., 2017). The increased CD11b positive area induced by AMPH exposure, through AT_1-R, in PL-PFC could result from the observed increase in microglia ramification. Morrison and Filosa reported a similar phenomenom, where ischemic stroke induced an increase of CD11b expression only in brain areas where an hyper-ramification microglia was presented (Morrison and Filosa, 2013). On the contrary, since no morphological changes were observed in astroglia, the increased GFAP positive area could be related with others processes such as increased number of GFAP positive cells or an increased tortuosity in their ramifications.

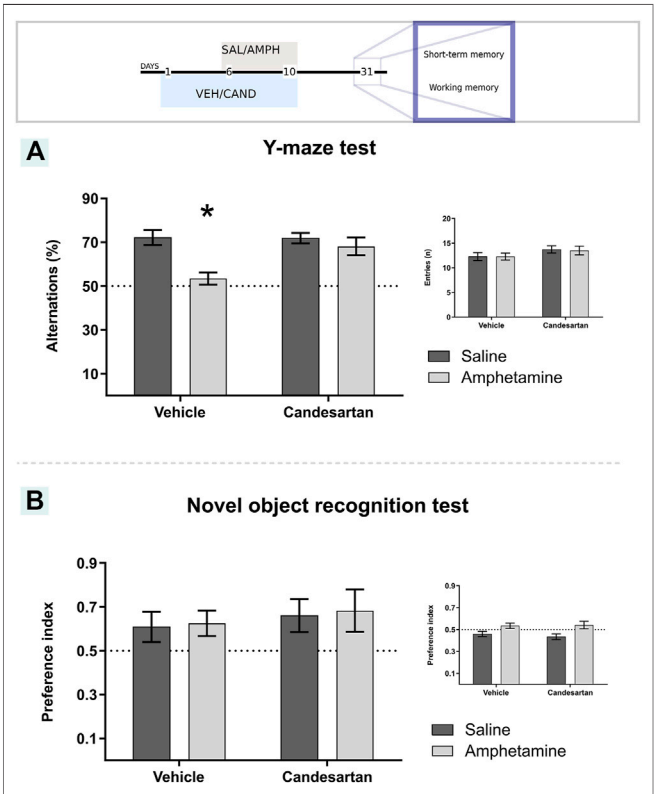

FIGURE 6 | Candesartan prevented amphetamine-induced working memory deficit and amphetamine did not induce changes in short-memory recognition performance. The graph shows working memory performance assessed by the Y-maze paradigm **(A)**. The main graph shows the percentage of spontaneous alternations in a Y-maze arena for the four experimental groups of protocol 3. Inset graph shows the number of entries to each arm in the Y-maze test. Values are the mean ± SEM, *different from the rest of the groups ($p < 0.05$); n = 10-11. The graph shows short-term memory performance evaluated as the time exploring each object in the one trial recognition task **(B)**. The results were expressed as the preference index for the four experimental groups in the test session of protocol 3. The inset figure shows the preference index for the sample session. Values are the mean ± SEM; n = 7-8.

It was shown that AT_1-R blockade exerts protective effects over gliosis and the release of pro-inflammatory compounds in several animal models of neuroinflammation (Pang et al., 2012; Labandeira-Garcia et al., 2017; Trigiani et al., 2018; Gong et al., 2019; Subudhi et al., 2019). Besides the inhibition of AT_1-R signaling, the anti-inflammatory effects of AT_1-R blockers could be also related to the shifting of Ang II effects towards AT_2 receptors (Gebre et al., 2018). In this regard, Bhat et al. showed that LPS increase AT_1-R and decrease AT_2-R expression in both *in vitro* and *in vivo* studies and the CAND prevention of the LPS-induced inflammation in both models is abolished when CAND is co-administered with an AT_2-R blocker (PD_{123319}) (Bhat et al., 2016). Even though CAND is accepted as a weak partial gamma receptor agonist (in contrast with others AT_1-R antagonists such as telmisartan and irbesartan) (Michel et al., 2013), the described modulation of glial reactivity by CAND could be related to the modulation of these receptors, as it was described in an animal model of traumatic brain injury (Villapol et al., 2012).

Despite their substantial functional differences, the IL- and the PL-PFC are often considered as a single brain region (ventral medial PFC) (Vertes, 2004). While IL-PFC functioning is involved with visceral/autonomic activity, the PL-PFC is linked with cognitive processes such as attention and working memory (Vertes, 2004). The PL-PFC seems to be particularly sensitive to AMPH damage since no glial changes were observed in the IL-PFC. These results are in line with our previous work showing AT_1-R participation in PFC microglial and astroglial reactivity

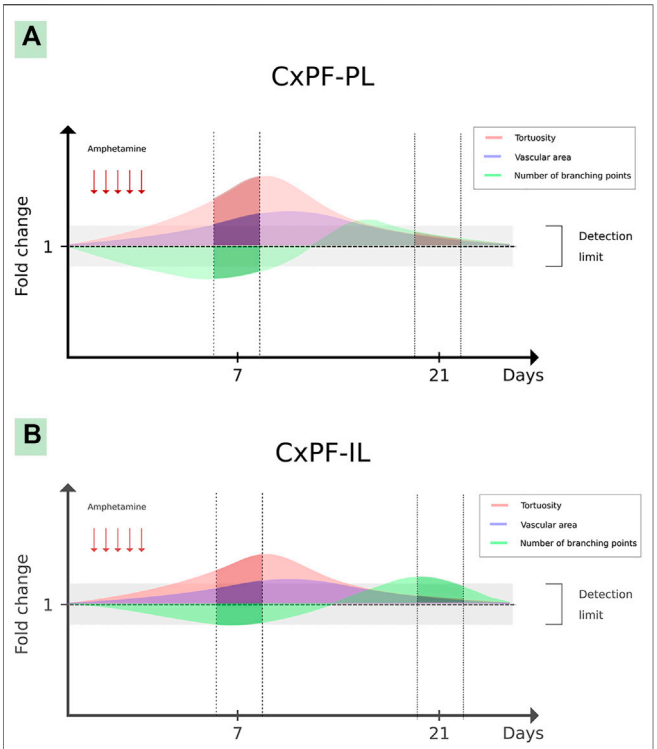

FIGURE 7 | Hypothetical transient angiogenesis induced by amphetamine in the prefrontal cortex. The graph shows hypothetical angiogenic changes induced by amphetamine in the PL-PFC **(A)** and IL-PFC **(B)** subdivisions. The darker lines show the described vascular microarchitecture changes in both brain structures (in days 7 and 21 after the last amphetamine exposure), meanwhile the translucent lines show hypothetical changes in the gaps among these periods.

7 days after AMPH withdrawal. In agreement with our previous studies, these results showed no AMPH-induced alteration in IL-PFC glial reactivity (Marchese et al., 2020). Bull et al. reported a similar astrocyte response, showing increased GFAP expression in the PL-PFC but not in the IL-PFC subdivision, after alcohol withdrawal (Bull et al., 2015). The differences between these brain regions may thus extend to AMPH toxicity. The selectiveness of the AMPH damage for discrete brain regions may explain the alteration of working memory but not of short-term memory observed in this work. It is well known that working memory depend on an integrated activity between PL-PFC and hippocampus (Spellman et al., 2015), while short-term memory mainly depends on the hippocampus and sub-regions of the medial temporal lobe such as the entorhinal and perirhinal cortex (Cohen and Stackman, 2015). In previous work, we observed an altered working memory performance together with astrogliosis and microgliosis in PL-PFC without glial alterations in dentate gyrus of hippocampus after 7 days of AMPH withdrawal, using the same psychostimulant exposure protocol (Marchese et al., 2020). Although, in the present work the glial reactivity was not evaluated after 21 days of withdrawal in hippocampus, the above results suggest that AMPH induces working memory independently of glial hippocampus alterations and co-occur with PL-PFC gliosis.

The AMPH-induced disturbance in the PL-PFC that leads to microglial and astroglial activation may also induce dysfunction in this brain area, leading to working memory deficit. Moreover, sustained glial activation may induce a neuroinflammatory scenario and contribute to PL-PFC dysfunction, in a self-perpetuating loop of damage-glial activation-neuroinflammation. In this regard, de Souza Gomez et al. reported that CAND prevents the working memory deficit and the oxidative imbalance induced by AMPH in mice assessed after a short withdrawal period (2 h) in the Y-maze paradigm (de Souza Gomes et al., 2015). In line with the present results, Che et al. and Arroyo-Garcia et al. reported no significant effects of AMPH exposure in short-term memory performance assessed in novel object recognition after prolonged withdrawal (more than 10 days) (Che et al., 2013; Arroyo-García et al., 2020). Despite that, all experimental groups showed a greater preference for the new object in the test session, the significant lower PI of control groups in the sample session could be a bias factor, affecting the test session performance in these experimental groups.

In previous studies, we showed that after 7 days withdrawal, AMPH induces angiogenesis in the PL-PFC via AT_1-R (Marchese et al., 2020). Interestingly, in the present work, we found no changes in PL-PFC microvessels area 21 days after AMPH withdrawal, indicating that vessel pruning took place after day 7 of withdrawal. Furthermore, other microvessel features such as branching points and tortuosity were also normalized 21 days after withdrawal. Considering that microvascular architecture were normalized after 21 days of withdrawal and working memory remained altered; the angiogenic changes observed in previous work after 7 days of AMPH withdrawal in PL-PFC (Marchese et al., 2020) would appear as a compensatory mechanism of hypoxia and/or inflammatory state induced by the psychostimulant and would not contribute to AMPH-induced working memory deficit. Moreover, the above results suggest that AMPH induces an angiogenic scenario via AT_1-R that gradually returns to normal in absence of the psychostimulant. Similar results were observed when rodents were exposed to prolonged hypoxia, showing increased angiogenesis that was later normalized in a normoxic environment (LaManna 2012). It has been shown that AT_1-R are involved in neovascularization in differents animals models of angiogenesis. In this sense, Miyajima et al. reported that the AT_1-R blockade by CAND prevents the neovascularization in a mouse renal cancer lung metastasis, preventing the increase in the CD34 and VEGF expresion in the tumor (Miyajima et al., 2002). Moreover, Kurosaka et al. showed a reduced angiogenesis (reduced CD31-positive microvessels) in AT_1-R knockout mice and in mice treated with the AT_1-R antagonist TCV-116 in a mouse model of wound healing (Kurosaka et al., 2009). Proangiogenic role of AT_1-R was also reported in an angiogenesis Matrigel model in mice, where the AT1-R blockade by CAND prevents the angiogenesis induction by the Matrigel injection measured by the CD31

positive cells count (Tamarat et al., 2002). Furthermore, Chu et al., using a similar AMPH protocol (2 mg/kg i.p. for four days), reported an increase of hypothalamic HIF-1, the main mediator of angiogenesis (Chu et al., 2019). Therefore, AMPH may induce angiogenic signals, even under normoxic conditions, leading to the transient angiogenesis observed.

The extensive AMPH-induced oxidative stress via AT_1-R, observed in the present work, may play an important role in angiogenic signaling because ROS are potential inducers of HIF-1 up-regulation. It has been found that ROS induces HIF-1 stabilization via prolyl-hydroxylase inactivation and HIF-1 transcription and transactivation (Belaidi et al., 2016; Kirtonia et al., 2020). In IL-PFC, AMPH induced an increased vascular tortuosity, via AT_1-R, together with no changes in branching points at day 7 of withdrawal. In line with these results, in a previous work we observed an AMPH-induced increase of vascular tortuosity in PL-PFC together with less branching points and an increased microvessels occupied area (Marchese et al., 2020). On the contrary, in the present work at day 21 of withdrawal, AMPH induced an increased number of branching points together with no changes in vascular tortuosity and microvessels occupied area (data not shown) in IL-PFC, whereas tortuosity, branching and microvessels occupied area were normalized in PL-PFC. From the above and taking into account that tortuosity is considered as an early step of neovascularization (Scott et al., 2014), we hypothesize that AMPH induces angiogenesis in both subdivisions of PFC but with a different time course and magnitude. As microvascular parameters were evaluated only in two time-points (7 and 21 after the last AMPH exposure), it is important to highlight that a more detailed analysis is needed to fully describe the time-course of angiogenic changes (onset, peak and disappearance) triggered by AMPH. The hypothetical transient angiogenesis described is schematized in **Figure 7**.

Taking into account that in the present work CAND was orally administered and the evidence showing that it crosses the blood-brain barrier (Michel et al., 2013), the CAND prevention of the AMPH alterations could result from central or peripheral AT_1-R antagonism or a combination of both effects.

Although, the present results show the AT_1-R involvement in the AMPH-induced working memory deficit, oxidative stress, gliosis and angiogenesis; the prevention effectiveness of these alterations by the AT_1-R blockade could depend on several factors such as dose, dosing regimen and extension of AMPH exposure. Therefore, studies with higher AMPH doses, different dosing regimens or with prolonged exposure to the psychostimulant would be useful to extend further the knowledge about AT_1-R role in the AMPH-induced alterations.

CONCLUSION

Overall, our results support a protective role of AT_1-R blockade in AMPH-induced oxidative stress and the subsequent long-lasting glial activation and transient angiogenesis, preserving working memory performance. CAND and several AT_1-R antagonists are currently used for hypertension treatment, with a low frequency of side effects, and they do not alter blood pressure in normotensive patients. Although more studies are necessary to characterize further the effectiveness of AT_1-R blockers in DA-imbalance-related pathologies.

DATA AVAILABILITY STATEMENT

The authors confirm that all data underlying the findings will be fully available at https://rdu.unc.edu.ar/ (Repositorio Digital de la Universidad Nacional de Córdoba).

ETHICS STATEMENT

The animal study was reviewed and approved by the Animal Care and Use Committee of Facultad de Ciencias Químicas, Universidad Nacional de Córdoba, Argentina (Res. No. 270/18).

AUTHOR CONTRIBUTIONS

OB, VO, NM, and MC performed the experiments. OB performed statistical analyses. MB, GB, and CB participated in behavioral tests planning and data interpretation. OB and CB wrote the manuscript and VO, NM, MC, and MB revised the manuscript.

FUNDING

This study was supported by grants from Foncyt BID PICT 2016 N°0403 and Secyt-UNC 2018 to CB and Secyt_-UNC 2018 to MB. MC, MB, GB and CB are career members of CONICET.

ACKNOWLEDGMENTS

The authors are grateful to Joss Heywood for his assistance in manuscript language revisionand to Alberto L. Oliveros, Lorena Mercado and Estela Salde for their laboratory technical assistance and Javier A. Reparaz, Yanina Altamirano and Nicolás Jaime for their technical assistance at the vivarium.

REFERENCES

Ahmad-Molaei, L., Hassanian-Moghaddam, H., Farnaghi, F., Tomaz, C., and Haghparast, A. (2018). Delay-Dependent Impairments in Memory and Motor Functions after Acute Methadone Overdose in Rats. *Front. Pharmacol.* 9. doi:10.3389/fphar.2018.01023

Ando, H., Jezova, M., Zhou, J., and Saavedra, J. M. (2004). Angiotensin II AT1Receptor Blockade Decreases Brain Artery Inflammation in a Stress-Prone Rat Strain. *Ann. N. Y. Acad. Sci.* 1018, 345–350. doi:10.1196/annals.1296.043

Arganda-Carreras, I., Fernández-González, R., Muñoz-Barrutia, A., and Ortiz-De-Solorzano, C. (2010). 3D reconstruction of histological sections: Application to mammary gland tissue. *Microsc. Res. Tech.* 73 (11), 1019–1029. doi:10.1002/jemt.20829

Arias-Cavieres, A., Adasme, T., Sánchez, G., Muñoz, P., and Hidalgo, C. (2017). Aging Impairs Hippocampal- Dependent Recognition Memory and LTP and Prevents the Associated RyR Up-regulation. *Front. Aging Neurosci.* 9, 111. doi:10.3389/fnagi.2017.00111

Arroyo-García, L. E., Tendilla-Beltrán, H., Vázquez-Roque, R. A., Jurado-Tapia, E. E., Díaz, A., Aguilar-Alonso, P., et al. (2020). Amphetamine sensitization alters hippocampal neuronal morphology and memory and learning behaviors. *Mol. Psychiatry*. 1–11. doi:10.1038/s41380-020-0809-2

Avci, B., Akar, A., Bilgici, B., and Tunçel, Ö. K. (2012). Oxidative stress induced by 1.8 GHz radio frequency electromagnetic radiation and effects of garlic extract in rats. *Int. J. Radiat. Biol.* 88, 799–805. doi:10.3109/09553002.2012.711504

Baker, K. B., and Kim, J. J. (2002). Effects of Stress and Hippocampal NMDA Receptor Antagonism on Recognition Memory in Rats. *Learn. Mem.* 9, 58–65. doi:10.1101/lm.46102

Bali, A., and Jaggi, A. S. (2013). Angiotensin as stress mediator: role of its receptor and interrelationships among other stress mediators and receptors. *Pharmacol. Res.* 76, 49–57. doi:10.1016/j.phrs.2013.07.004

Beauquis, J., Homo-Delarche, F., Giroix, M-H., Ehses, J., Coulaud, J., Roig, P., et al. (2010). Hippocampal neurovascular and hypothalamic-pituitary-adrenal axis alterations in spontaneously type 2 diabetic GK rats. *Exp. Neurol.* 222, 125–134. doi:10.1016/j.expneurol.2009.12.022

Belaidi, E., Morand, J., Gras, E., Pépin, J-L., and Godin-Ribuot, D. (2016). Targeting the ROS-HIF-1-endothelin axis as a therapeutic approach for the treatment of obstructive sleep apnea-related cardiovascular complications. *Pharmacol. Ther.* 168, 1–11. doi:10.1016/j.pharmthera.2016.07.010

Bhat, S. A., Goel, R., Shukla, R., and Hanif, K. (2016). Angiotensin Receptor Blockade Modulates NFκB and STAT3 Signaling and Inhibits Glial Activation and Neuroinflammation Better than Angiotensin-Converting Enzyme Inhibition. *Mol. Neurobiol.* 53, 6950–6967. doi:10.1007/s12035-015-9584-5

Bild, W., Hritcu, L., Stefanescu, C., and Ciobica, A. (2013). Inhibition of central angiotensin II enhances memory function and reduces oxidative stress status in rat hippocampus. *Prog. Neuro-Psychopharmacology Biol. Psychiatry* 43, 79–88. doi:10.1016/j.pnpbp.2012.12.009

Brown, J. M., and Yamamoto, B. K. (2003). Effects of amphetamines on mitochondrial function: Role of free radicals and oxidative stress. *Pharmacol. Ther.* 99, 45–53. doi:10.1016/s0163-7258(03)00052-4

Brown, D. C., Steward, L. J., Ge, J., and Barnes, N. M. (1996). Ability of angiotensin II to modulate striatal dopamine release via the AT1 receptor in vitro and in vivo. *Br. J. Pharmacol.* 118, 414–420. doi:10.1111/j.1476-5381.1996.tb15418.x

Bull, C., Syed, W. A., Minter, S. C., and Bowers, M. S. (2015). Differential response of glial fibrillary acidic protein-positive astrocytes in the rat prefrontal cortex following ethanol self-administration. *Alcohol. Clin. Exp. Res.* 39, 650–658. doi:10.1111/acer.12683

Callera, G. E., Antunes, T. T., Correa, J. W., Moorman, D., Gutsol, A., He, Y., et al. (2016). Differential renal effects of candesartan at high and ultra-high doses in diabetic mice-potential role of the ACE2/AT2R/Mas axis. *Biosci. Rep.* 36. doi:10.1042/bsr20160344

Carvalho, M., Carmo, H., Costa, V. M., Capela, J. P., Pontes, H., Remião, F., et al. (2012). Toxicity of amphetamines: An update. *Arch. Toxicol.* 86. doi:10.1007/s00204-012-0815-5

Che, Y., Cui, Y-H., Tan, H., Andreazza, A. C., Young, L. T., and Wang, J-F. (2013). Abstinence from repeated amphetamine treatment induces depressive-like behaviors and oxidative damage in rat brain. *Psychopharmacology* 227, 605–614. doi:10.1007/s00213-013-2993-0

Chu, S-C., Chen, P-N., Yu, C-H., Hsieh, Y-S., and Kuo, D-Y. (2019). Role of hypoxia-inducible factor-1α in regulating oxidative stress and hypothalamic neuropeptides-mediated appetite control. *Brain Res.* 1721, 146329. doi:10.1016/j.brainres.2019.146329

Cohen, S. J., and Stackman Jr., R. W., Jr. (2015). Assessing rodent hippocampal involvement in the novel object recognition task. a review. *Behav. Brain Res.* 285, 105–117. doi:10.1016/j.bbr.2014.08.002

de Souza Gomes, J. A., de Souza, G. C., Berk, M., Cavalcante, L. M., de Sousa, F. C. F., Budni, J., et al. (2015). Antimanic-like activity of candesartan in mice: Possible involvement of antioxidant, anti-inflammatory and neurotrophic mechanisms. *Eur. Neuropsychopharmacol.* 25. doi:10.1016/j.euroneuro.2015.08.005

Dean, O. M., van den Buuse, M., Berk, M., Copolov, D. L., Mavros, C., and Bush, A. I. (2011). N-acetyl cysteine restores brain glutathione loss in combined 2-cyclohexene-1-one and d-amphetamine-treated rats: relevance to schizophrenia and bipolar disorder. *Neurosci. Lett.* 499, 149–153. doi:10.1016/j.neulet.2011.05.027

Delaney, J., Chiarello, R., Villar, D., Kandalam, U., Castejon, A. M., and Clark, M. A. (2008). Regulation of c-fos, c-jun and c-myc gene expression by angiotensin II in primary cultured rat astrocytes: role of ERK1/2 MAP kinases. *Neurochem. Res.* 33, 545–550. doi:10.1007/s11064-007-9474-y

Elfarnawany, M. H. (2015). Signal processing methods for quantitative power doppler microvascular angiography. Available at: https://ir.lib.uwo.ca/etd/3106 (Accessed December 30, 2020).

Epstein, A. N., Fitzsimons, J. T., and Rolls, B. J. (1970). Drinking induced by injection of angiotensin into the brain of the rat. *J. Physiol.* 210, 457–474. doi:10.1113/jphysiol.1970.sp009220

Famitafreshi, H., and Karimian, M. (2018). Assessment of improvement in oxidative stress indices with resocialization in memory retrieval in Y-Maze in male rats. *J. Exp. Neurosci.* 12, 1179069518820323. doi:10.1177/1179069518820323

Garrido-Gil, P., Rodriguez-Perez, A. I., Fernandez-Rodriguez, P., Lanciego, J. L., and Labandeira-Garcia, J. L. (2017). Expression of angiotensinogen and receptors for angiotensin and prorenin in the rat and monkey striatal neurons and glial cells. *Brain Struct. Funct.* 222, 2559–2571. doi:10.1007/s00429-016-1357-z

Gebre, A. K., Altaye, B. M., Atey, T. M., Tuem, K. B., and Berhe, D. F. (2018). Targeting renin–angiotensin system against alzheimer's Disease. *Front. Pharmacol.* 9. doi:10.3389/fphar.2018.00440

Goel, R., Bhat, S. A., Hanif, K., Nath, C., and Shukla, R. (2018). Angiotensin II receptor blockers attenuate lipopolysaccharide-induced memory impairment by modulation of NF-κB-Mediated BDNF/CREB expression and apoptosis in spontaneously hypertensive rats. *Mol. Neurobiol.* 55, 1725–1739. doi:10.1007/s12035-017-0450-5

Gong, X., Hu, H., Qiao, Y., Xu, P., Yang, M., Dang, R., et al. (2019). The Involvement of Renin-Angiotensin System in Lipopolysaccharide-Induced Behavioral Changes, Neuroinflammation, and Disturbed Insulin Signaling. *Front. Pharmacol.* 10. doi:10.3389/fphar.2019.00318

Gubert, C., Fries, G. R., Pfaffenseller, B., Ferrari, P., Coutinho-Silva, R., Morrone, F. B., et al. (2016). Role of P2X7 receptor in an animal model of mania induced by D-amphetamine. *Mol. Neurobiol.* 53, 611–620. doi:10.1007/s12035-014-9031-z

Hamai, M., Iwai, M., Ide, A., Tomochika, H., Tomono, Y., Mogi, M., et al. (2006). Comparison of inhibitory action of candesartan and enalapril on brain ischemia through inhibition of oxidative stress. *Neuropharmacology* 51, 822–828. doi:10.1016/j.neuropharm.2006.05.029

Hoebel, B. G., Rada, P., Mark, G. P., and Hernandez, L. (1994). The power of integrative peptides to reinforce behavior by releasing dopamine. *Ann. NY Acad. Sci.* 739, 36–41. doi:10.1111/j.1749-6632.1994.tb19805.x

Islam, R., Matsuzaki, K., Sumiyoshi, E., Hossain, M. E., Hashimoto, M., Katakura, M., et al. (2019). Theobromine improves working memory by activating the CaMKII/CREB/BDNF pathway in rats. *Nutrients* 11, 888. doi:10.3390/nu11040888

Israili, Z. (2000). Clinical pharmacokinetics of angiotensin II (AT1) receptor blockers in hypertension. *J. Hum. Hypertens.* 14, S73–S86. doi:10.1038/sj.jhh.1000991

Jensen, L. L., Harding, J. W., and Wright, J. W. (1992). Role of paraventricular nucleus in control of blood pressure and drinking in rats. *Am. J. Physiology-Renal Physiol.* 262, F1068–F1075. doi:10.1152/ajprenal.1992.262.6.f1068

Kalivas, P. W. (2007). Cocaine and amphetamine-like psychostimulants: neurocircuitry and glutamate neuroplasticity. *Dialogues Clin. Neurosci.* 9, 389–397. doi:10.31887/DCNS.2007.9.4/pkalivas

Kirtonia, A., Sethi, G., and Garg, M. (2020). The multifaceted role of reactive oxygen species in tumorigenesis. *Cell. Mol. Life Sci.* 77, 4459–4483. doi:10.1007/s00018-020-03536-5

Kurosaka, M., Suzuki, T., Hosono, K., Kamata, Y., Fukamizu, A., Kitasato, H., et al. (2009). Reduced angiogenesis and delay in wound healing in angiotensin II type

1a receptor-deficient mice. *Biomed. Pharmacother.* 63 (9), 627–634. doi:10.1016/j.biopha.2009.01.001

Labandeira-Garcia, J. L., Rodríguez-Perez, A. I., Garrido-Gil, P., Rodriguez-Pallares, J., Lanciego, J. L., and Guerra, M. J. (2017). Brain renin-angiotensin system and microglial polarization: implications for aging and neurodegeneration. *Front. Aging Neurosci.* 9. doi:10.3389/fnagi.2017.00129

LaManna, J. C. (2012). Angioplasticity and cerebrovascular remodeling. *Adv. Exp. Med. Biol.* 737, 13–17. doi:10.1007/978-1-4614-1566-4_2

LaVoie, M. J., Card, J. P., and Hastings, T. G. (2004). Microglial activation precedes dopamine terminal pathology in methamphetamine-induced neurotoxicity. *Exp. Neurol.* 187, 47–57. doi:10.1016/j.expneurol.2004.01.010

Legland, D., Arganda-Carreras, I., and Andrey, P. (2016). MorphoLibJ: integrated library and plugins for mathematical morphology with imageJ. *Bioinformatics* 15 (22), 3532–3534. doi:10.1093/bioinformatics/btw413

Loftis, J. M., and Janowsky, A. (2014). Neuroimmune basis of methamphetamine toxicity. *Int. Rev. Neurobiol.* 118, 165–197. doi:10.1016/b978-0-12-801284-0.00007-5

Lu, Q., Zhu, Y-Z., and Wong, P. T-H. (2005). Neuroprotective effects of candesartan against cerebral ischemia in spontaneously hypertensive rats. *NeuroReport* 16, 1963–1967. doi:10.1097/01.wnr.0000187636.13147.cd

Mackey, S., Stewart, J. L., Connolly, C. G., Tapert, S. F., and Paulus, M. P. (2014). A voxel-based morphometry study of young occasional users of amphetamine-type stimulants and cocaine. *Drug and Alcohol Dependence* 135, 104–111. doi:10.1016/j.drugalcdep.2013.11.018

Marchese, N. A., Artur de laVillarmois, E., Basmadjian, O. M., Perez, M. F., Baiardi, G., and Bregonzio, C. (2016). Brain Angiotensin II AT1 receptors are involved in the acute and long-term amphetamine-induced neurocognitive alterations. *Psychopharmacology* 233, 795–807. doi:10.1007/s00213-015-4153-1

Marchese, N. A., Rodriguez, I. D., Basmadjian, O. M., Baiardi, G., and Bregonzio, C. (2017). Neurovascular unit alteration in somatosensory cortex and enhancement of thermal nociception induced by amphetamine involves central AT1 receptor activation. *Eur. J. Neurosci.* 45, 1586–1593. doi:10.1111/ejn.13594

Marchese, N. A., Occhieppo, V. B., Basmadjian, O. M., Casarsa, B. S., Baiardi, G., and Bregonzio, C. (2020). Angiotensin II modulates amphetamine-induced glial and brain vascular responses, and attention deficit via angiotensin type 1 receptor: Evidence from brain regional sensitivity to amphetamine. *Eur. J. Neurosci.* 51, 1026–1041. doi:10.1111/ejn.14605

Michel, M. C., Foster, C., Brunner, H. R., and Liu, L. (2013). A systematic comparison of the properties of clinically used angiotensin II type 1 receptor antagonists. *Pharmacol. Rev.* 65, 809–848. doi:10.1124/pr.112.007278

Mimran, A., and Ribstein, J. (1999). Angiotensin receptor blockers: pharmacology and clinical significance. *J. Am. Soc. Nephrol.* 10 (Suppl. 12), S273–S277.

Miyajima, A., Kosaka, T., Asano, T., Asano, T., Seta, K., Kawai, T., et al. (2002). Angiotensin II type I antagonist prevents pulmonary metastasis of murine renal cancer by inhibiting tumor angiogenesis. *Cancer Res.* 62 (15), 4176–4179.

Mizoguchi, H., and Yamada, K. (2019). Methamphetamine use causes cognitive impairment and altered decision-making. *Neurochem. Int.* 124. doi:10.1016/j.neuint.2018.12.019

Moratalla, R., Khairnar, A., Simola, N., Granado, N., García-Montes, J. R., Porceddu, P. F., et al. (2017). Amphetamine-related drugs neurotoxicity in humans and in experimental animals: Main mechanisms. *Prog. Neurobiol.* 155, 149–170. doi:10.1016/j.pneurobio.2015.09.011

Morrison, H. W., and Filosa, J. A. (2013). A quantitative spatiotemporal analysis of microglia morphology during ischemic stroke and reperfusion. *J. Neuroinflammation* 10, 4. doi:10.1186/1742-2094-10-4

Occhieppo, V. B., Marchese, N. A., Rodríguez, I. D., Basmadjian, O. M., Baiardi, G., and Bregonzio, C. (2017). Neurovascular unit alteration in somatosensory cortex and enhancement of thermal nociception induced by amphetamine involves central AT1receptor activation. *Eur. J. Neurosci.* 45, 1586–1593. doi:10.1111/ejn.13594

Occhieppo, V. B., Basmadjian, O. M., Marchese, N. A., Jazmin Silvero C., M., Rodríguez, A., Armonelli, S., et al. (2020). AT1-R is involved in the development of long-lasting, region-dependent and oxidative stress-independent astrocyte morphological alterations induced by ketamine. *Eur. J. Neurosci. N/a* doi:10.1111/ejn.14756

Pang, T., Wang, J., Benicky, J., Sánchez-Lemus, E., and Saavedra, J. M. (2012). Telmisartan directly ameliorates the neuronal inflammatory response to IL-1β partly through the JNK/c-Jun and NADPH oxidase pathways. *J. Neuroinflammation.* 9, 102. doi:10.1186/1742-2094-9-102

Paz, M. C., Assis, M. A., Cabrera, R. J., Cancela, L. M., and Bregonzio, C. (2011). The AT₁ angiotensin II receptor blockade attenuates the development of amphetamine-induced behavioral sensitization in a two-injection protocol. *Synapse* 65, 505–512. doi:10.1002/syn.20868

Paz, M. C., Marchese, N. A., Cancela, L. M., and Bregonzio, C. (2013). Angiotensin II AT₁ receptors are involved in neuronal activation induced by amphetamine in a two-injection protocol. *Biomed. Res. Int.* 2013, 534817. doi:10.1155/2013/534817

Paz, M. C., Marchese, N. A., Stroppa, M. M., Gerez de Burgos, N. M., Imboden, H., Baiardi, G., et al. (2014). Involvement of the brain renin-angiotensin system (RAS) in the neuroadaptive responses induced by amphetamine in a two-injection protocol. *Behav. Brain Res.* 272, 314–323. doi:10.1016/j.bbr.2014.07.021

Peach, M. J. (1977). Renin-angiotensin system: biochemistry and mechanisms of action. *Physiol. Rev.* 57, 313–370. doi:10.1152/physrev.1977.57.2.313

Potvin, S., Pelletier, J., Grot, S., Hébert, C., Barr, A., and Lecomte, T. (2018). Cognitive deficits in individuals with methamphetamine use disorder: A meta-analysis. *Addict. Behav.* 80. doi:10.1016/j.addbeh.2018.01.021

Prusty, S., Sahu, P., and Subudi, B. B. (2017). Angiotensin mediated oxidative stress and neuroprotective potential of antioxidants and AT1 receptor blockers. *MRMC.* 17, 518–528. doi:10.2174/1389557516666161025094539

Raghavendra, V., Chopra, K., and Kulkarni, S. K. (2001). Comparative studies on the memory- enhancing actions of captopril and losartan in mice using inhibitory shock avoidance paradigm. *Neuropeptides* 35, 65–69. doi:10.1054/npep.2000.0845

Sailasuta, N., Abulseoud, O., Harris, K. C., and Ross, B. D. (2010). Glial dysfunction in abstinent methamphetamine abusers. *J. Cereb. Blood Flow Metab.* 30, 950–960. doi:10.1038/jcbfm.2009.261

Salmani, H., Hosseini, M., Baghcheghi, Y., Moradi-Marjaneh, R., and Mokhtari-Zaer, A. (2020). Losartan modulates brain inflammation and improves mood disorders and memory impairment induced by innate immune activation: The role of PPAR-γ activation. *Cytokine* 125, 154860. doi:10.1016/j.cyto.2019.154860

Schindelin, J., Arganda-Carreras, I., Frise, E., Kaynig, V., Longair, M., Pietzsch, T., et al. (2012). Fiji: an open-source platform for biological-image analysis. *Nat Methods* 9 (7), 676–682. doi:10.1038/nmeth.2019

Schrantee, A., Tremoleda, J. L., Wylezinska-Arridge, M., Bouet, V., Hesseling, P., Meerhoff, G. F., et al. (2017). Repeated dexamphetamine treatment alters the dopaminergic system and increases the phMRI response to methylphenidate. *PLoS One.* 12, e0172776. doi:10.1371/journal.pone.0172776

Scott, A., Powner, M. B., and Fruttiger, M. (2014). Quantification of vascular tortuosity as an early outcome measure in oxygen induced retinopathy (OIR). *Exp. Eye Res.* 120, 55–60. doi:10.1016/j.exer.2013.12.020

Shaerzadeh, F., Streit, W. J., Heysieattalab, S., and Khoshbouei, H. (2018). Methamphetamine neurotoxicity, microglia, and neuroinflammation. *J. Neuroinflammation.* 15, 341. doi:10.1186/s12974-018-1385-0

Shen, P-C., He, L-Q., Yang, X-J., and Cao, H-X. (2012). Renal protection of losartan 50 mg in normotensive Chinese patients with nondiabetic chronic kidney disease. *J. Investig. Med.* 60, 1041–1047. doi:10.2310/jim.0b013e31826741d2

Spellman, T., Rigotti, M., Ahmari, S. E., Fusi, S., Gogos, J. A., and Gordon, J. A. (2015). Hippocampal-prefrontal input supports spatial encoding in working memory. *Nature* 522, 309–314. doi:10.1038/nature14445

Subudhi, S., Merino-Serrais, P., Di Grande, A., Dussmann, H., Prehn, J. H. M., Ní Chonghaile, T., et al. (2019). The anti-inflammatory compound candesartan cilexetil improves neurological outcomes in a mouse model of neonatal hypoxia. *Front. Immunol.* 10. doi:10.3389/fimmu.2019.01752

Tamarat, R., Silvestre, J-S., Durie, M., and Levy, B. I. (2002). Angiotensin II angiogenic effect in vivo involves vascular endothelial growth factor- and inflammation-related pathways. *Lab. Invest.* 82 (6), 747–756. doi:10.1097/01.lab.0000017372.76297.eb

Tata, D. A., and Anderson, B. J. (2002). A new method for the investigation of capillary structure. *J. Neurosci. Methods* 113, 199–206. doi:10.1016/s0165-0270(01)00494-0

Thomas, M., George, N. I., Patterson, T. A., and Bowyer, J. F. (2009). Amphetamine and environmentally induced hyperthermia differentially alter the expression of genes regulating vascular tone and angiogenesis in the meninges and associated vasculature. *Synapse* 63, 881–894. doi:10.1002/syn.20661

Thomas, M., George, N. I., Saini, U. T., Patterson, T. A., Hanig, J. P., and Bowyer, J. F. (2010). Endoplasmic reticulum stress responses differ in meninges and associated vasculature, striatum, and parietal cortex after a neurotoxic amphetamine exposure. *Synapse* 64, 579–593. doi:10.1002/syn.20763

Trigiani, L. J., Royea, J., Lacalle-Aurioles, M., Tong, X.-K., and Hamel, E. (2018). Pleiotropic Benefits of the Angiotensin Receptor Blocker Candesartan in a Mouse Model of Alzheimer Disease. *Hypertension* 72, 1217–1226. doi:10.1161/hypertensionaha.118.11775

Tung, C-S., Chang, S-T., Huang, C-L., and Huang, N-K. (2017). The neurotoxic mechanisms of amphetamine: step by step for striatal dopamine depletion. *Neurosci. Lett.* 639, 185–191. doi:10.1016/j.neulet.2017.01.002

Unger, T. (2000). Differences among angiotensin II type 1 receptor blockers: characteristics of candesartan cilexetil. *Blood Press.* 9, 14–18. doi:10.1080/080370500439164

Unger, T. (2003). Inhibiting angiotensin receptors in the brain: possible therapeutic implications. *Curr. Med. Res. Opin.* 19, 449–451. doi:10.1185/030079903125001974

United Nations (2017). *World drug report 2017*. Viena, Austria: United Nations Office on Drugs and Crime

Valenzuela, R., Costa-Besada, M. A., Iglesias-Gonzalez, J., Perez-Costas, E., Villar-Cheda, B., Garrido-Gil, P., et al. (2016). Mitochondrial angiotensin receptors in dopaminergic neurons. Role in cell protection and aging-related vulnerability to neurodegeneration. *Cell Death Dis.* 7, e2427. doi:10.1038/cddis.2016.327

Valvassori, S. S., Dal-Pont, G. C., Tonin, P. T., Varela, R. B., Ferreira, C. L., Gava, F. F., et al. (2019). Coadministration of lithium and celecoxib attenuates the behavioral alterations and inflammatory processes induced by amphetamine in an animal model of mania. *Pharmacol. Biochem. Behav.* 183, 56–63. doi:10.1016/j.pbb.2019.05.009

Vertes, R. P. (2004). Differential projections of the infralimbic and prelimbic cortex in the rat. *Synapse* 51, 32–58. doi:10.1002/syn.10279

Villapol, S., Yaszemski, A. K., Logan, T. T., Sánchez-Lemus, E., Saavedra, J. M., and Symes, A. J. (2012). Candesartan, an angiotensin II AT1-Receptor blocker and PPAR-γ agonist, reduces lesion volume and improves motor and memory function after traumatic brain injury in mice. *Neuropsychopharmacol* 37, 2817–2829. doi:10.1038/npp.2012.152

von Bohlen und Halbach, O., and Albrecht, D. (2006). The CNS renin-angiotensin system. *Cell Tissue Res.* 326, 599–616. doi:10.1007/s00441-006-0190-8

Witko-Sarsat, V., Friedlander, M., Capeillère-Blandin, C., Nguyen-Khoa, T., Nguyen, A. T., Zingraff, J., et al. (1996). Advanced oxidation protein products as a novel marker of oxidative stress in uremia. *Kidney Int.* 49, 1304–1313. doi:10.1038/ki.1996.186

Xu, X., Fan, R., Ruan, Y., Xu, M., He, J., Cao, M., et al. (2021). Inhibition of PLCβ1 signaling pathway regulates methamphetamine self-administration and neurotoxicity in rats. *Food Chem. Toxicol.* 149, 111970. doi:10.1016/j.fct.2021.111970

Yamakawa, H., Jezova, M., Ando, H., and Saavedra, J. M. (2003). Normalization of endothelial and inducible nitric oxide synthase expression in brain microvessels of spontaneously hypertensive rats by angiotensin II AT1 receptor inhibition. *J. Cereb. Blood Flow Metab.* 23, 371–380. doi:10.1097/01.wcb.0000047369.05600.03

Yang, G., Gray, T. S., Sigmund, C. D., and Cassell, M. D. (1999). The angiotensinogen gene is expressed in both astrocytes and neurons in murine central nervous system. *Brain Res.* 817, 123–131. doi:10.1016/s0006-8993(98)01236-0

Zhou, J., Ando, H., Macova, M., Dou, J., and Saavedra, J. M. (2005). Angiotensin II AT1 Receptor Blockade Abolishes Brain Microvascular Inflammation and Heat Shock Protein Responses in Hypertensive Rats. *J. Cereb. Blood Flow Metab.* 25, 878–886. doi:10.1038/sj.jcbfm.9600082

Zhou, J., Pavel, J., Macova, M., Yu, Z-X., Imboden, H., Ge, J. M., et al. (2006). AT 1 receptor blockade regulates the local angiotensin II system in cerebral microvessels from spontaneously hypertensive rats. *Stroke* 37, 1271–1276. doi:10.1161/01.str.0000217404.64352.d7

Conflict of Interest: The authors declare that the research was conducted in the absence of any commercial or financial relationships that could be construed as a potential conflict of interest.

Copyright © 2021 Basmadjian, Occhieppo, Marchese, Silvero C., Becerra, Baiardi and Bregonzio. This is an open-access article distributed under the terms of the Creative Commons Attribution License (CC BY). The use, distribution or reproduction in other forums is permitted, provided the original author(s) and the copyright owner(s) are credited and that the original publication in this journal is cited, in accordance with accepted academic practice. No use, distribution or reproduction is permitted which does not comply with these terms.

frontiers in Pharmacology

ORIGINAL RESEARCH
published: 07 May 2021
doi: 10.3389/fphar.2021.612981

Anti-Inflammatory Effects of Dimethyl Fumarate in Microglia via an Autophagy Dependent Pathway

Young-Sun Lee[1,2], *Deepak Prasad Gupta*[1], *Sung Hee Park*[1], *Hyun-Jeong Yang*[3] *and Gyun Jee Song*[1,2]*

[1]Department of Medical Science, College of Medicine, Catholic Kwandong University, Gangneung, Korea, [2]Translational Brain Research Center, International St. Mary's Hospital, Catholic Kwandong University, Incheon, Korea, [3]Department of Integrative Biosciences, University of Brain Education, Cheonan, Korea

Dimethyl fumarate (DMF), which has been approved by the Food and Drug Administration for the treatment of relapsing-remitting multiple sclerosis, is considered to exert anti-inflammatory and antioxidant effects. Microglia maintain homeostasis in the central nervous system and play a key role in neuroinflammation, while autophagy controls numerous fundamental biological processes, including pathogen removal, cytokine production, and clearance of toxic aggregates. However, the role of DMF in autophagy induction and the relationship of this effect with its anti-inflammatory functions in microglia are not well known. In the present study, we investigated whether DMF inhibited neuroinflammation and induced autophagy in microglia. First, we confirmed the anti-neuroinflammatory effect of DMF in mice with streptozotocin-induced diabetic neuropathy. Next, we used *in vitro* models including microglial cell lines and primary microglial cells to examine the anti-inflammatory and neuroprotective effects of DMF. We found that DMF significantly inhibited nitric oxide and proinflammatory cytokine production in lipopolysaccharide-stimulated microglia and induced the switch of microglia to the M2 state. In addition, DMF treatment increased the expression levels of autophagy markers including microtubule-associated protein light chain 3 (LC3) and autophagy-related protein 7 (ATG7) and the formation of LC3 puncta in microglia. The anti-inflammatory effect of DMF in microglia was significantly reduced by pretreatment with autophagy inhibitors. These data suggest that DMF leads to the induction of autophagy in microglia and that its anti-inflammatory effects are partially mediated through an autophagy-dependent pathway.

Keywords: neuroinflammation, autophagy, microglia, DMF, anti-inflammation

OPEN ACCESS

Edited by:
Flavia Eugenia Saravia, Universidad de Buenos Aires, Argentina

Reviewed by:
Jannette Rodriguez-Pallares, University of Santiago de Compostela, Spain
Alejandro Villarreal, University of Freiburg, Germany

***Correspondence:**
Gyun Jee Song
gyunjeesong@gmail.com

Specialty section:
This article was submitted to Neuropharmacology, a section of the journal Frontiers in Pharmacology

Received: *01 October 2020*
Accepted: *19 April 2021*
Published: *07 May 2021*

Citation:
Lee Y-S, Gupta DP, Park SH, Yang H-J and Song GJ (2021) Anti-Inflammatory Effects of Dimethyl Fumarate in Microglia via an Autophagy Dependent Pathway. Front. Pharmacol. 12:612981. doi: 10.3389/fphar.2021.612981

INTRODUCTION

Microglia, innate immune cells that play protective roles against invading pathogens in the central nervous system (CNS) (Afridi et al., 2020; Xu et al., 2020), comprise approximately 10% of all cells in the healthy mammalian brain (Augusto-Oliveira et al., 2019). Microglial activation is observed during viral or bacterial infection, neurodegenerative diseases such as Alzheimer's disease, and traumatic brain injury (Mariani and Kielian, 2009; Donat et al., 2017; Edison, 2020; Severini et al., 2021); activated microglia can be further subdivided into classical (M1) and alternative (M2) microglia (Jiang et al., 2020). The presence of interferon-gamma and lipopolysaccharide (LPS) switches microglia to the M1 state, wherein they express and/or release interferon-gamma, tumor

necrosis factor-alpha (TNF-α), interleukin (IL) 1β, IL-6, IL-12, IL-23, and inducible nitric oxide (NO) synthase (iNOS); microglia in the M1 state have been linked to reduced phagocytic ability. On the other hand, IL-4, IL-10, and IL-13 induce the microglial switch to the M2 state, wherein they release anti-inflammatory cytokines such as IL-4, IL-10, IL-13, and transforming growth factor-beta and increase the expression levels of arginase-1, brain-derived neurotrophic factor, and Ym1; the M2 microglia are recognized for their increased neuroprotective capacity. Thus, M1 and M2 microglia are involved in pathogenic and neuroprotective responses, respectively (Song et al., 2016; Song and Suk, 2017; Gupta et al., 2020).

Autophagy removes unnecessary or dysfunctional proteins and damaged organelles via the lysosomal machinery. Autophagy is critical for the maintenance of neuronal function and is considered to provide neuroprotection in neurodegenerative disorders. Proper regulation of autophagy is associated with beneficial outcomes in neurodegenerative diseases (Nixon, 2013; Cho et al., 2020). Although the interaction between autophagy and inflammation is complicated and controversial, neuroinflammation is implicated in autophagic dysfunction. For example, recent studies have reported neuroprotective as well as anti-neuroinflammatory effects of several autophagic modulators such as rapamycin, metformin, and resveratrol (Sarkar et al., 2009; Thellung et al., 2019).

Dimethyl fumarate (DMF) is a potent anti-inflammatory mediator which has been used for the treatment of psoriasis for many years (Altmeyer et al., 1994). Importantly, DMF has also been approved by the US Food and Drug Administration as an orally bioavailable compound for the treatment of multiple sclerosis (Hoefnagel et al., 2003; Fox et al., 2012; Gold et al., 2012; Xu et al., 2015). DMF reduces proinflammatory responses by inhibiting the NF-κB signaling pathway. In addition, DMF provides neuroprotection against α-synuclein toxicity via the activation of autophagy in a mouse model of Parkinson's disease (Lastres-Becker et al., 2016). However, there is limited information on the interaction between the anti-inflammatory effect and autophagy activation in DMF-treated microglia. Therefore, we investigated whether DMF induced autophagy in microglia and if DMF-induced autophagy had an impact on the inflammatory activation of microglia.

MATERIALS AND METHODS

Animals

C57BL/6 mice were obtained from Orient Bio (Gyeonggi, Korea) and maintained in specific pathogen-free conditions under a 12 h light:12 h dark light period in the animal facility of Gachon University. All animal experiments were performed under a protocol approved by the Institutional Animal Care and Use Committee at the Gachon University. Eight-week-old male C57BL/6 mice were injected with streptozotocin (STZ) (100 mg/kg intraperitoneal [i.p.], Sigma-Aldrich, Saint-Louis, MO) or PBS, as a vehicle control, after overnight fasting. The tail blood of mice was monitored for the development of hyperglycemia using a glucometer. After confirming that the blood glucose level was over 300 mg/dl for three consecutive days, the mice were injected with DMF (45 mg/kg, i.p.) or PBS, as a control, once a day for four weeks based on the previously published information (Yao et al., 2016; Hayashi et al., 2017).

Cells

HAPI (highly aggressively proliferating immortalized) cells, a rat microglial cell line, were cultured in Dulbecco's Modified Eagle medium (DMEM) supplemented with 10% fetal bovine serum (FBS) and 100 U/mL penicillin/streptomycin. BV-2 cells, an immortalized murine microglial cell line, were maintained in DMEM supplemented with 5% FBS and 100 U/mL penicillin/streptomycin. Primary mixed glial cells (MGC) were prepared from neonatal C57BL/6 mice on postnatal days 1–3, as previously described (Gupta et al., 2020), with minor modifications. The cell suspensions obtained from brain tissue dissection were cultured with DMEM supplemented with 10% FBS and 100 U/mL penicillin/streptomycin for three weeks, with medium changed every three days. After three weeks, the MGC were harvested, centrifuged, and replated in 96-well (4×10^4/well), 24-well (5×10^4/well), or 12-well (2×10^5/well) plates. For primary microglia isolation from MGC, confluent MGC were treated with mild trypsin (20–25%) for 20 min at 37°C, which resulted in the detachment of an intact layer of cells comprising virtually all astrocytes, leaving undisturbed a population of microglia on the plate. The purity of primary microglial culture was 96.9 ± 0.409%, which was determined by Iba-1immunostaining (**Supplementary Figure S1**). After washing with phosphate-buffered saline (PBS), the microglia were treated with trypsin (100%) for 5 min at 37°C. The cells were harvested, and the centrifuged cells were replated onto 24 well plates (5×10^4/well) containing poly-D-lysine-coated glass coverslips (diameter, 12 mm) (Saura et al., 2003).

Measurement of Nitric Oxide Production and Cell Viability

Cell culture medium was harvested after treatment with or without LPS (100 ng/ml) in the presence or absence of DMF. NO production was analyzed by the colorimetric Griess assay to determine the concentration of nitrite, a stable NO metabolite. The absorbance was detected at 540 nm by a microplate reader. Cell viability was determined by the MTT [3-(4, 5-dimethylthiazol-2-yl)-2, 5 diphenyl tetrazolium bromide] assay, and the sample absorbance was detected at 570 nm.

Real-Time Quantitative Polymerase Chain Reaction and Reverse Transcription-Polymerase Chain Reaction

Total RNA was isolated using Trizol® reagent (Invitrogen, Carlsbad, CA), and cDNA was synthesized using the Moloney murine leukemia virus reverse transcriptase (Promega) and oligo (dT) primers. Real-time quantitative PCR (RT-qPCR) was performed using a 7900HT fast real-time PCR system (Applied Biosystems, Carlsbad, CA) using the following

conditions: 95°C for 5 min, followed by 40 cycles at 95°C for 15 s and 60°C for 1 min. As an internal control, cyclophilin mRNA was amplified. The sequences of primer pairs are provided in **Supplementary Table S1**. Relative copy numbers were determined using the threshold crossing point (Ct) in combination with the ΔΔCt values, calculated by the 7900HT fast real-time PCR software. Traditional reverse transcription-PCR was performed with specific primer sets (**Supplementary Table S1**) at annealing temperatures of 57–60°C for 24–29 cycles using a T100 Thermal Cycler (Bio-Rad, Richmond, CA). After PCR, 10 μL of each PCR product was electrophoresed on a 2% agarose gel. DNA fragments were detected under ultraviolet light following ethidium bromide staining.

Western Blot Analysis

Total cell lysates were prepared using ice-cold lysis buffer (150 mM NaCl, 50 mM Tris, 1% Nonidet P-40 and 0.1% sodium dodecyl sulfate). The lysates were separated on sodium dodecyl sulfate-polyacrylamide gels and transferred to polyvinylidene difluoride membranes (Bio-Rad, CA). The membranes were blocked with 5% skim milk for 1 h and incubated with mouse anti-arginase-1 (1:1,000 dilution; BD Biosciences, NJ), rabbit anti-microtubule-associated protein light chain 3 (LC3; 1:1,000 dilution; MBL, Woburn, MA), or mouse anti-β actin (1:5,000 dilution; Sigma-Aldrich) antibody overnight at 4°C. Next, the membranes were incubated with appropriate horseradish peroxidase-conjugated secondary antibodies (1:2000 dilution) for 1 h at room temperature. The blots were visualized with a chemiluminescence detection kit (SuperSignal™ West Femto; Thermo Fisher, Franklin, MA).

Phagocytosis Assay

Phagocytosis assay was performed with Fluorescent zymosan Bioparticles from *Saccharomyces cerevisiae* (pH-sensitive pHrodo™ Red dye conjugates; Life Technologies, Carlsbad, USA). In brief, primary microglial cells were seeded at a density of 5×10^4 cells/well in 24-well plates and cultured for 48 h in DMEM supplemented with 10% FBS, followed by treatment with 10 μM DMF for 24 h. And then, cells incubated in serum-free medium containing fluorescently labeled zymosan particles (10 μg/ml) for 2 h at 37°C (Grozdanov et al., 2014). The cells were washed three times with PBS and fixed with 4% paraformaldehyde. Fluorescent images were captured using a laser scanning confocal fluorescent microscope (Nikon ECLIPSE 80*i*; Nikon, Japan).

Immunofluorescent Staining

Immunofluorescent staining of spinal cord sections and fixed cells in culture were performed as previously reported (Song et al., 2019). Briefly, tissue sections or cells fixed with 4% paraformaldehyde were blocked with 1% bovine serum albumin or normal serum in 0.3% Triton X-100 for 60 min at room temperature. The samples were next incubated with rabbit anti-glial fibrillary acidic protein (GFAP; 1:500, DAKO, Glostrup, Denmark), goat anti-Iba-1 (1:200, Novus, CO), or rabbit anti-LC3 (1:500, MBL) antibody in PBS containing 1% BSA at 4°C overnight. The samples were washed three times with 0.3% Triton X-100 in 0.1 M PBS, followed by incubation with FITC- or Cy3-conjugated secondary antibodies (1:200 for tissue sections and 1:500 for fixed cells) for 60 min at room temperature. Fluorescent images were captured using the Nikon ECLIPSE 80*i* laser scanning confocal fluorescent microscope. For the analysis of the immunofluorescence staining, the spinal cord images were outlined the size for the standardized reason of interest (ROI) by ImageJ. The threshold was adjusted and standardized for each image. The mean intensity of the fluorescence in pixels was measured. The percentage of area was calculated by dividing the pixel number of the protein expression with the total unfiltered pixel number in the ROI. For the analysis of LC3 puncta area in HAPI cells, the area of a single cell was marked and the LC3 punctate area was measured using ImageJ. The number of zymosan particles or LC3 puncta was analyzed using particle analyzer in ImageJ (Fiji, version 1.53c, National Institutes of Health, United States) (**Supplementary Figure S2**).

Statistical Analysis

Data were presented as means ± standard error of the mean (SEM) from three or more independent experiments. The normality of values had been checked then used parametric or non-parametric test. Statistical significance was analyzed by paired or unpaired Student's *t*-test for comparison of two groups and one-way or two-way ANOVA followed by multiple comparison test for multiple groups. A P value of <0.05 was considered to indicate statistical significance.

RESULTS

Dimethyl Fumarate Reduces Gliosis in the Spinal Cord of Streptozotocin (STZ)-Treated Diabetic Neuropathy Mice

STZ-induced diabetic neuropathy is a well-defined mouse model of neuroinflammation and reactive microglial activation (Wodarski et al., 2009; Talbot et al., 2010; Ellis and Bennett, 2013). To investigate whether DMF administration inhibited the hyperactivation of microglia and astrocytes, we measured the levels of Iba-1 and GFAP in the spinal cord of mice with STZ-induced diabetic neuropathy. The relative Iba-1 intensity was significantly higher in the STZ-treated mice than in the untreated control mice ($P < 0.05$) as shown in **Figures 1B,C**. The number and the area of Iba-1 positive cells also significantly increased in the STZ-treated mice than in the control mice, however the DMF treatment significantly lowered the intensity, number and area of Iba-1 positive cells in the spinal cord compared to STZ-treated mice ($P < 0.05$) (**Figures 1C–E**). Similarly, we found astrogliosis in STZ-treated mice (**Figures 1F–H**). STZ-induced astrogliosis was significantly reduced by DMF treatment as analyzed by the reduced intensity and the area of GFAP-positive cells. Notably we found hyper-ramified and amoeboid shaped microglia in STZ-treated mice. In contrast, the microglia morphology in DMF-treated mice showed small cell bodies and thin processes as in control group. These results suggested that DMF suppressed the

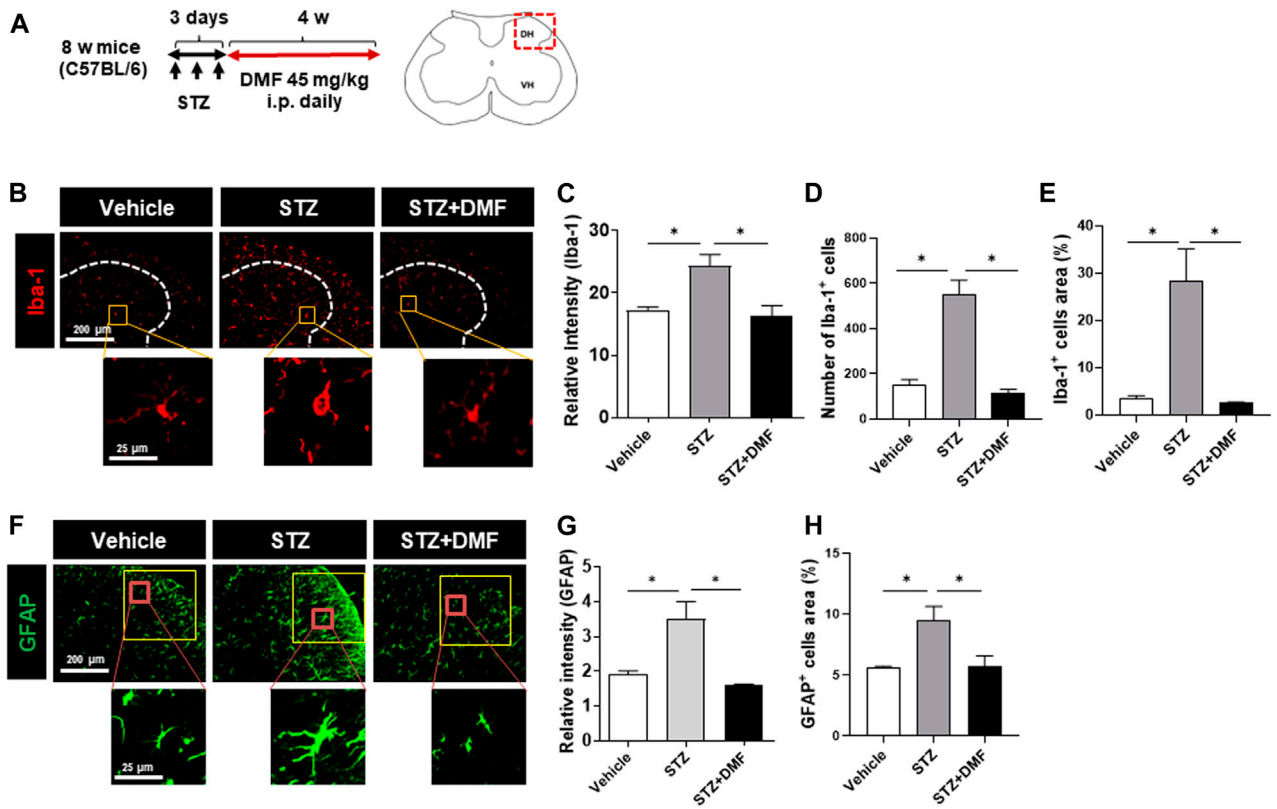

FIGURE 1 | Dimethyl fumarate reduces gliosis in the spinal cord of mice with STZ-treated diabetic neuropathy **(A)** C57BL/6 mice were injected with STZ (100 mg/kg, i.p.). After 3 days, the mice that developed diabetes were administered dimethyl fumarate (DMF, 45 mg/kg i.p.) once a day for four weeks. At the end of treatments, spinal cord sections were prepared and stained with anti-Iba-1 **(B–E)** or anti-glial fibrillary acidic protein (GFAP) antibody **(F–H)**. White dotted lines represent the dorsal horn of the spinal cord. Representative Iba-1$^+$ microglia are shown in the magnified images. The quantified relative fluorescence intensity for Iba-1$^+$ cells **(C)**, number of Iba-1$^+$ cells **(D)**, and the area of Iba-1$^+$ cells in the spinal cord **(E)** were analyzed. Representative GFAP$^+$ astrocytes are shown in the magnified images **(F)**. The quantified relative fluorescence intensity for GFAP$^+$ cells **(G)** and the area of GFAP$^+$ cells in the spinal cord **(H)** were analyzed (n = 3 mice/group, 3 images/mouse). Data are presented as means ± standard error of the mean (SEM). *P < 0.05 compared with STZ-treated mice from ANOVA, Tukey's multiple comparison test.

activation of microglia and astrocytes in the spinal cord of mice with STZ-induced diabetic neuropathy.

Dimethyl Fumarate Downregulates the Inflammatory Activation of Microglia

To investigate whether DMF has anti-inflammatory effects in microglia, we measured NO production in HAPI cells after DMF treatment. As shown in **Figure 2A**, the production of NO was significantly increased by LPS treatment for 24 h; however, the DMF co-treatment led to a dose-dependent reduction in NO production in HAPI cells, without any change in cell viability (**Figures 2A,B**). In addition, we determined the expression levels of the inflammatory cytokine TNF-α and IL-6 in HAPI cells after DMF treatment (**Figures 2C,D**). The mRNA levels of *TNF-α* and *IL-6* in HAPI cells, which were significantly increased with 6 h LPS (100 ng/ml) treatment, were significantly reduced in cells treated with 4 μM DMF. We also utilized the immortalized mouse microglial cell line BV-2 to confirm the anti-inflammatory effect of DMF in another microglial cell line. As shown in **Supplementary Figure S3**, the production of NO and the *IL-1β*, *TNF-α*, and *IL-6* mRNA levels, which were increased by LPS (100 ng/ml) treatment after 24 h, were reduced by 4 μM DMF co-treatment in BV-2 cells.

Dimethyl Fumarate Induces M2 Polarization and Phagocytosis in Microglia

Based on the results showing that DMF treatment induced an anti-inflammatory response in microglia, we next determined whether DMF induced M2 polarization by examining changes in arginase-1 expression, one of the best characterized markers of M2 polarization, in HAPI cells. As shown in **Figures 3A,B**, the level of arginase-1 protein was significantly increased by 24 h treatment with DMF and LPS compared to 24 h treatment with LPS alone in HAPI cells. While M1 microglia exhibit impaired phagocytic ability, M2 microglia have been demonstrated to maintain efficient phagocytosis (Akhmetzyanova et al., 2019). Thus, we next evaluated the phagocytic ability of primary microglia and BV-2 cells treated with DMF. We found that

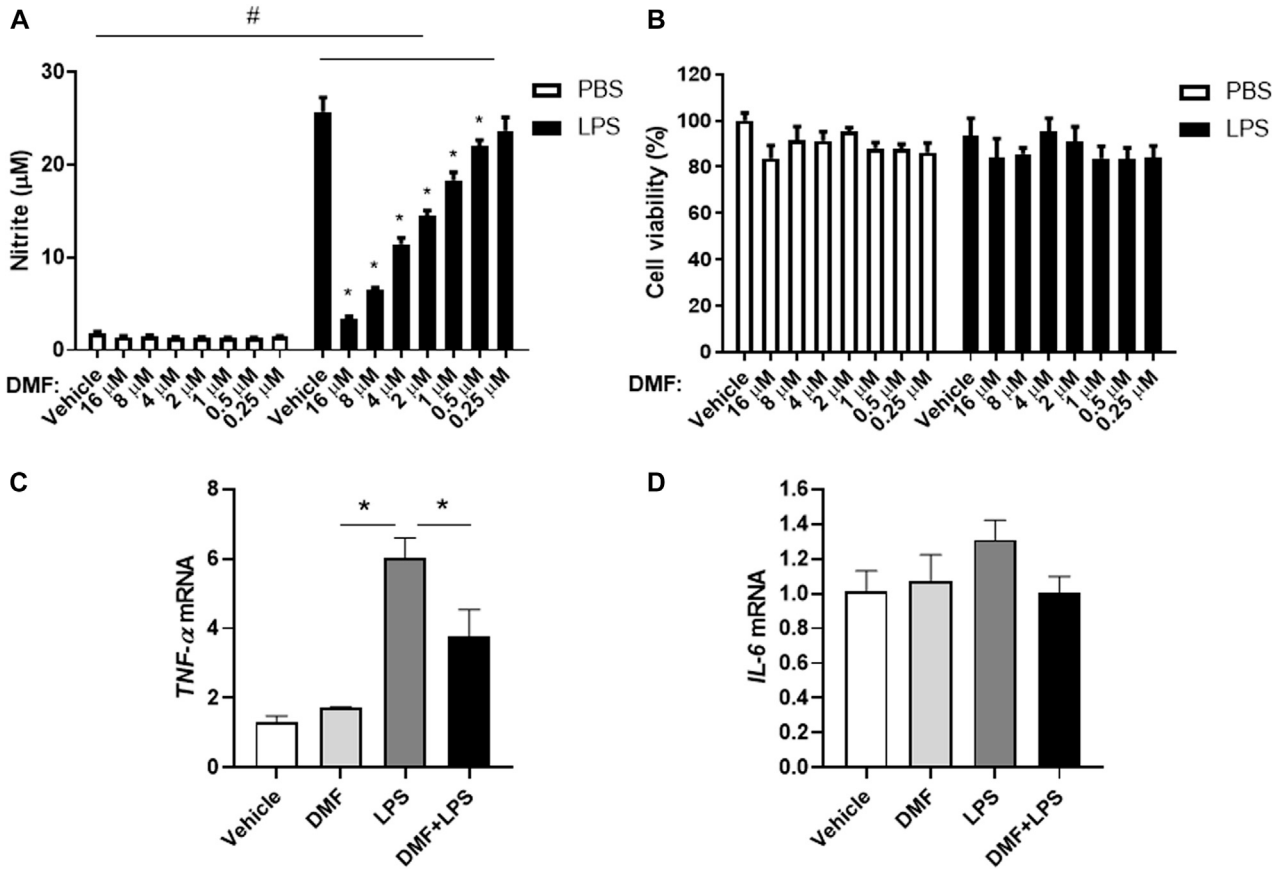

FIGURE 2 | DMF reduces inflammation in microglia. HAPI cells were seeded at 4×10^4 cells/well in a 96-well plate and incubated overnight. Cells were then treated with indicated concentration of DMF with or without LPS. After 24 h, nitric oxide (NO) production was measured by the Griess assay **(A)**, and cell viability was measured by the MTT assay **(B)**.**(C, D)** HAPI cells were seeded at 1×10^6 cells/well in a 6-well plate and incubated overnight. Cells were then treated with 4 μM DMF with or without LPS (100 ng/ml). After 6 h, the mRNA expression levels of tumor necrosis factor-alpha (*TNF-α*) **(C)** and interleukin- 6 (*IL-6*) **(D)** was determined by real-time quantitative polymerase chain reaction (RT-qPCR). Fold changes were calculated as the ratio of expression level in the LPS-only treated group. $n = 3$ independent experiments/group. Data are presented as means ± SEM. $^*P < 0.05$ compared with LPS-only treated group, $\#P < 0.05$ compared with vehicle-only treated group from two-way ANOVA with multiple comparison test.

the phagocytic ability was significantly improved by 16 h treatment with DMF and LPS compared to 16 h treatment with LPS only treated BV-2 cells (**Figures 3C,D**). In addition, the phagocytosis of fluorescently labeled zymosan particles was significantly higher in the DMF-treated primary microglia compared with the vehicle-treated control primary microglia (**Figures 3E,F**), suggesting that DMF induced M2 polarization in microglia.

Dimethyl Fumarate Induces Autophagy in Microglia

Autophagy is a physiological catabolic process which removes unnecessary or dysfunction proteins, and defective autophagy is associated with neuroinflammation. Thus, we next investigated whether DMF induced autophagy in microglia. LC3, which is used as a marker to monitor autophagy, is associated with the formation of autophagosomes and autolysosomes (Wang et al., 2013). To detect autophagy induction in DMF-treated cells, we measured the higher molecular-weight LC3-I and the lower molecular-weight LC3-II by Western blot analysis. As shown in **Figure 4A**, the expression level of LC3-II was increased at 3 h after DMF treatment in HAPI cells. In addition, the expression of LC3-II was significantly increased by 24-h treatment with DMF compared to vehicle control and showed a tendency of induction in the treatment with DMF and LPS compared with LPS alone in HAPI cells (**Figures 4B,C**). The measurement of LC3 puncta in HAPI cells by immunofluorescence revealed that the area of LC3 puncta per cell was significantly increased in DMF-treated HAPI cells (**Figures 4D,E**). The mRNA level of *Atg7*, an essential regulator of autophagosome assembly as one of the autophagy-related genes, was also increased after DMF treatment in HAPI cells (**Figure 4F**). We also found that the number of LC3 puncta per cell and the *Atg7* mRNA level was significantly increased in MGC treated with DMF (**Figures 4G,H,I**). These results suggest that DMF induced autophagy in microglia.

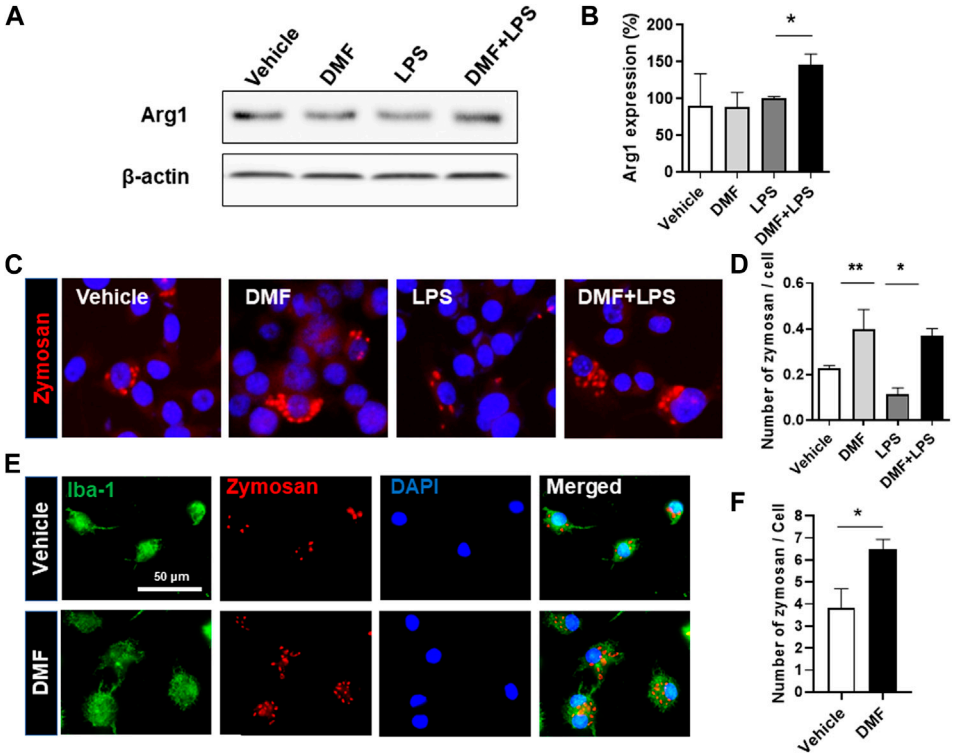

FIGURE 3 | DMF induces the neuroprotective M2 phenotype and phagocytosis in microglia **(A, B)** HAPI cells were seeded at 2.5×10^5 cells/well in a 6-well plate and incubated overnight. Cells were then treated with LPS (100 ng/ml) or DMF (4 μM) plus LPS (100 ng/ml) for 24 h. The expression of arginase-1 protein (Arg1) was determined by Western blot analysis **(B)** Histogram shows the densitometric analysis of Western blots. β-actin was used as the loading control and data were normalized to total β-actin. $n = 3$ independent experiments/group **(C, D)** BV-2 cells were seeded at 5×10^4 cells/well in a 24-well plate and incubated overnight. BV-2 cells were then treated with DMF (4 μM) with or without LPS (100 ng/ml) for 16 h, followed by the addition of opsonized zymosan-red particles into BV-2 cells and then incubated for another 4 h. The phagocytosed zymosan particles were counted and expressed as the number of zymosan particles per cell. A total of 463 control cells, 1117 DMF-treated cells, 990 LPS-treated cells, and 636 DMF + LPS-treated cells were analyzed. Results are representative of two independent experiments. Data are presented as means ± SEM. $^*P < 0.05$, $^{**}P < 0.01$ compared with LPS-treated mice from ANOVA, Tukey's multiple comparison test **(E,F)** Primary microglia were seeded at 5×10^4 cells/well in a 24-well plate and incubated overnight. The primary microglia were then treated with DMF (4 μM) for 48 h, followed by the addition of opsonized zymosan-red particles into the primary microglia and then incubated for another 2 h. The primary microglia were stained with the anti-Iba-1 antibody. The phagocytosed zymosan particles were counted and expressed as the number of zymosan particles per Ib1-1 positive microglial cell. A total of 157 control cells and 154 DMF-treated cells were analyzed. $n = 3$ independent experiments/group. Data are presented as means ± SEM. $^*P < 0.05$ from Student's t-test between indicated two groups.

Dimethyl Fumarate Induces Anti-inflammatory Response in Microglia via an Autophagy-dependent Pathway

Based on our finding that DMF induced autophagy in microglia, we next determined whether DMF-induced autophagy regulated the anti-inflammatory response in microglia by pretreatment of cultures with bafilomycin A1 (Mauvezin and Neufeld, 2015; Redmann et al., 2017) or SBI-0206965 (Martin et al., 2018; Wang et al., 2020), both potent inhibitors of cellular autophagy, for 1 h followed by treatment with DMF for 6 h. As expected, the mRNA levels of the anti-inflammatory cytokines *TNF-α* and *IL-6*, which were significantly increased by LPS treatment, were reduced by DMF treatment. Importantly, bafilomycin A1 and SBI-0206965 completely abrogated the DMF-induced reduction in proinflammatory cytokine production in primary MGC (**Figures 5A,B**). Additionally, we found that the NO production was significantly inhibited by DMF in LPS-treated MGC; this effect was abolished by pretreatment with the autophagy inhibitors (**Figures 5C,E**). The cell viability was not different in cells treated with bafilomycin A1 or SBI-0206965 and untreated control cells (**Figures 5D,F**). In addition, we used the specific NF-κB signaling inhibitor Bay 11–7082, given that DMF has been reported to reduce proinflammatory response through the NF-κB pathway. As shown in **Figures 5E,F**, Bay 11–7082 completely abrogated the DMF-induced reduction in NO production in primary MGC. These results suggested that not only the NF-κB pathway but also autophagy was involved in DMF-induced anti-inflammatory response in LPS-induced inflammatory response in MGC. In addition, we elucidated whether the DMF-induced phagocytosis was reduced by autophagy inhibition by pretreating cells with the autophagy inhibitor SBI-0206965 for 1 h before treatment with DMF for 24 h. As shown in **Figures 6A,B**, the significant increase in phagocytosis by DMF in primary microglia was ameliorated

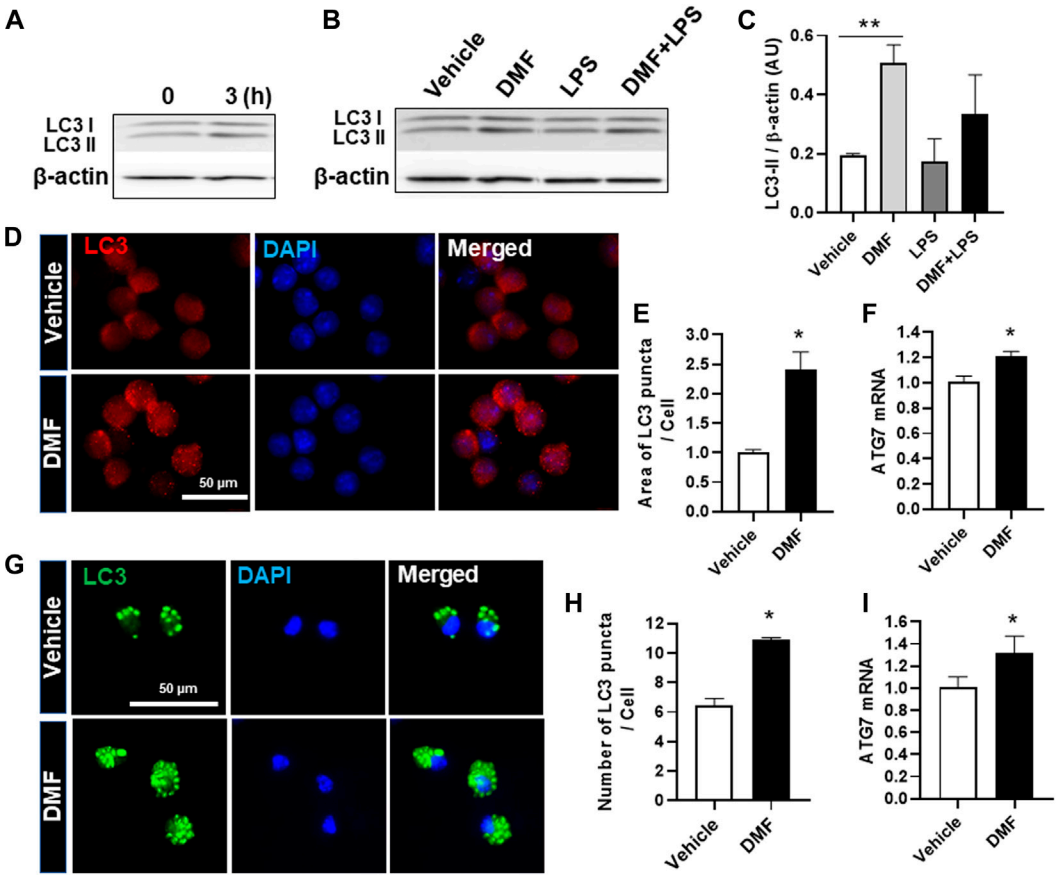

FIGURE 4 | DMF increases autophagy in microglia. HAPI cells were seeded at 2.5 × 10^5 cells/well in a 6-well plate and incubated overnight **(A)** Cells were then treated with DMF (4 μM) for 3 h **(B)** Cells were treated with LPS (100 ng/ml) or DMF (4 μM) plus LPS (100 ng/ml) for 24 h. The protein levels of LC3-I and LC3-II were determined by Western blot analysis. β-actin was used as the loading control. *n* = 3 independent experiments/group **(C)** Histogram shows the densitometric analysis of Western blots. β-actin was used as the loading control and data were normalized to total β-actin **(D)** HAPI cells were seeded at 2 × 10^4 cells/well in a 24-well plate and incubated overnight. Cells were then treated with DMF (4 μM) for 24 h and stained with the anti-LC3 antibody **(E)** The punctate area was determined from at least 3 independent images (Vehicle: 29 cells and DMF: 26 cells) using ImageJ and was expressed as the ratio of vehicle controls **(F)** HAPI cells were seeded at 1 × 10^6 cells/well in a 6-well plate and incubated overnight. Cells were then treated with DMF (4 μM) for 6 h. The mRNA expression levels of *Atg7* was determined by RT-qPCR. Fold changes were calculated as the ratio of expression level in untreated control cells **(G)** Primary microglia isolated from MGC were seeded at 5 × 10^4 cells/well in a 24-well plate and incubated overnight. Cells were then treated with DMF (10 μM) for 24 h, followed by staining with the anti-LC3 antibody **(H)** The number of LC3 puncta per cell was counted. A total of 27 control cells and 38 DMF-treated cells were analyzed **(I)** MGC were seeded at 2 × 10^5cells/well in a 12-well plate and incubated overnight. Cells were then treated with DMF (10 μM) for 6 h. The mRNA expression levels of *Atg7* was analyzed by RT-qPCR. Fold changes were calculated as the ratio of expression level in untreated control cells. *n* = 3 independent experiments/group. Data are presented as means ± SEM. **P* < 0.05 from Student's *t*-test for indicated two groups. ***P* < 0.01 compared with vehicle from ANOVA, Tukey's multiple comparison test.

by SBI-0206965 pretreatment. These results suggest that DMF-induced autophagy-mediated an anti-inflammatory response in microglia.

DISCUSSION

Neuroinflammation is a well-known pathophysiological process in many neurodegenerative diseases (Song and Suk, 2017; Stephenson et al., 2018). The crosstalk between neurons and glial cells regulates many physiological and pathological processes (Jha et al., 2018; Zhang et al., 2018; Linnerbauer et al., 2020). Microglia are important players in neuroinflammation as a major immune cell type in the CNS. Studies previously demonstrated that DMF treatment inhibited inflammation by reducing the synthesis of the proinflammatory mediators iNOS, TNF-α, IL-1β, and IL-6 in microglia (Paraiso et al., 2018). In the present study, we also found that DMF suppressed NO production and the mRNA levels of *TNF-α* and *IL-6* in microglial cell lines such as HAPI and BV-2 as well as in primary MGC. M1 microglia exacerbate neuroinflammation, whereas M2 microglia promote tissue repair and provide an anti-inflammatory response (Tang and Le, 2016; Song and Suk, 2017). Intriguingly, M2 microglia exhibit a high level of phagocytosis in the CNS (Cherry et al., 2015). Thus, we determined whether DMF promoted microglial polarization toward the M2 phenotype by investigating the expression of arginase-1 protein as a prototypic M2 marker in mice (Roszer, 2015). Arginase-1-positive microglia have been

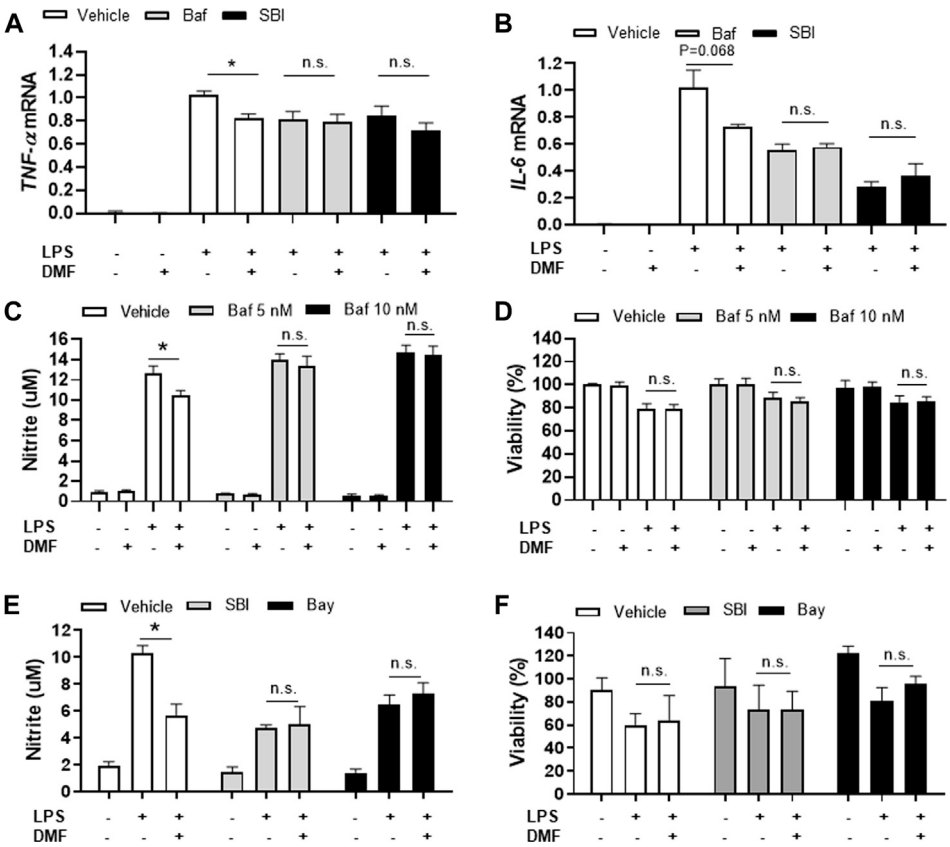

FIGURE 5 | DMF induces anti-inflammatory responses in MGC via an autophagy-dependent pathway **(A, B)** MGC were seeded at 2×10^5 cells/well in a 12-well plate and incubated overnight. Cells were then pretreated with bafilomycin (10 nM, Baf) or SBI-0206965 (5 μM, SBI) for 1 h, followed by treatment with DMF (4 μM) and LPS (1 μg/ml). After 6 h, the mRNA expression levels of *TNF-α* **(A)** and *IL-6* mRNA **(B)** were measured by RT-qPCR. Fold changes were calculated as the ratio of expression level in LPS-treated cells **(C, D)** MGC were seeded at 3×10^4 cells/well in a 96-well plate and incubated overnight. Cells were then pretreated with bafilomycin (5 (gray) or 10 (black)nM) for 1 h, followed by the addition of DMF (4 μM) and LPS (1 μg/ml). After 48 h, NO production was measured by the Griess assay **(C)** and cell viability was measured by the MTT assay **(D) (E, F)** MGC were seeded at 3×10^4 cells/well in a 96-well plate and incubated overnight. Cells were then pretreated with SBI-0206965 (5 μM, gray) or Bay 11–7082 (2.5 μM, Bay, black) for 1 h, followed by treatment with DMF (4 μM) and LPS (1 μg/ml). After 48 h, NO production **(E)** and cell viability **(F)** were measured. $n = 3$ independent experiments/group. Data are presented as means ± SEM. $^*P < 0.05$ compared with LPS treated group, n.s., not significant ($P > 0.05$).

shown to reduce Aβ plaque number during neuroinflammation in the CNS (Cherry et al., 2015). In the present study, we found that DMF treatment led to a significant increase in arginase-1 protein levels in microglia and induced phagocytosis in primary MGC and BV-2 cells. Phagocytosis is a critical process for maintaining homeostasis in CNS. Thus, understanding how to put the brake on M1 polarization and promote M2 polarization in the CNS may lead to the development of novel therapeutic approaches for targeting neurodegenerative disease. These results suggest that DMF might improve Aβ plaque clearance in the brain and spinal cord and reduce pathology via increased phagocytosis.

Recent findings in diabetic neuropathy demonstrate that glial cells, particularly microglia and astrocytes, are an important source of inflammatory mediators fundamentally involved in the pathogenesis of inflammation and neurodegeneration. Thus, we utilized the mouse model of STZ-induced diabetic neuropathy, in which the spinal cord exhibits microglial reactivation as a sign of neuroinflammation (Kiguchi et al., 2017; Song et al., 2019). In the present study, we found that the spinal dorsal horn showed hypertrophic morphology in mice with STZ-induced diabetic neuropathy, accompanied with an increase in the number of microglia and astrocytes, based on the expression levels of microglial and astrocytic phenotypic markers. These findings are in line with other studies in monkeys with type 2 diabetes and *db/db* mice (Liao et al., 2011; Kiguchi et al., 2017). The suppression of microglial accumulation and activation in the spinal cord are associated with the inhibition of neuropathic pain. In the present study, we found that DMF treatment suppressed gliosis in the spinal cord of mice with STZ-induced diabetic neuropathy, indicating that DMF might be useful for the management of diabetic neuropathy based on its neuroprotective effects. In addition, diabetes-related neurodegeneration is considered to be multifactorial, including hyperglycemia (Jing et al., 2013). Glucose toxicity in the brain has been shown to induce

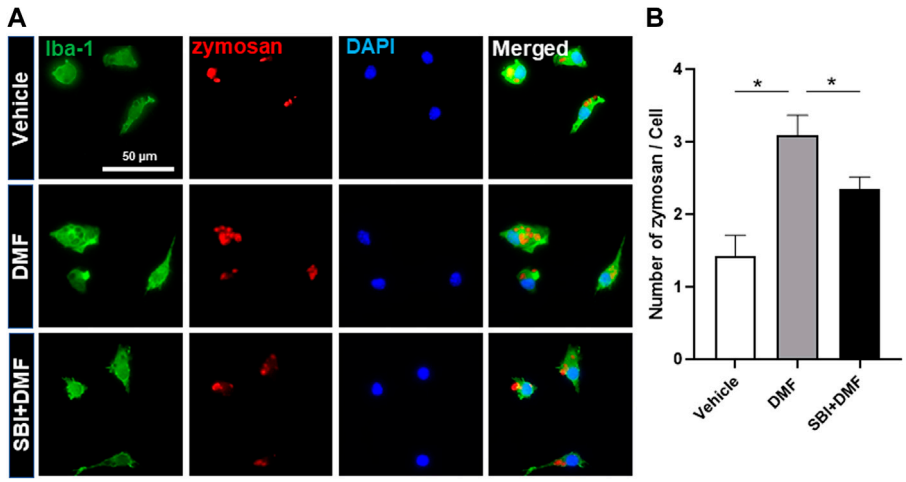

FIGURE 6 | DMF increases phagocytosis via an autophagy-dependent pathway in microglia **(A, B)** Primary microglia were seeded 5×10^4 cells/well in a 24-well plate and incubated overnight. Cells were then pretreated with SBI-0206965 (5 μM) for 1 h, followed by the addition of DMF (10 μM). After 24 h, opsonized zymosan-red particles were added into the cultures which were incubated for 2 h. The primary microglia were stained with the anti-Iba-1 antibody. The phagocytosed zymosan particles were counted and expressed as the number of zymosan particles per cell. The analysis included 78 control cells, 96 cells treated with DMF, and 110 cells treated with DMF plus SBI-0206965. n = 3 independent experiments/group. Data are presented as means ± SEM. $^*P < 0.05$ from ANOVA.

inflammation (Peiro et al., 2016); therefore, we also investigated whether the DMF-induced anti-inflammatory response was due to decreased blood sugar in DMF-treated mice with diabetic neuropathy. The mice with STZ-induced diabetic neuropathy exhibited hyperglycemia compared with the vehicle-administered mice; however, the blood glucose levels did not significantly changed following DMF treatment in the STZ-treated mice (data not shown). These findings indicate that the DMF exerts anti-inflammatory effects in the spinal cord without reducing the blood glucose level in mice with STZ-induced diabetic neuropathy.

Autophagy is essential for the removal of unnecessary cellular constituents and dysfunctional components. Autophagic dysfunction and inflammation are key players in the development of neurodegeneration (Su et al., 2016; Plaza-Zabala et al., 2017). Upregulation of autophagy promotes microglial polarization toward the M2 phenotype by the suppression of M1 markers, including iNOS/NO, TNF-α, and IL-6, and the induction of M2 markers, including arginase-1, Ym1/2, and IL-10. (Jin et al., 2018; Cho et al., 2020). In addition, TNF-α, an important proinflammatory cytokine, inhibits autophagy by impairing autophagic flux through the AKT/mammalian target of the rapamycin signaling pathway in microglia. In the present study, we found that DMF reduced NO production and the expression levels of genes associated with the M1 phenotype, including *TNF-α* and *IL-6*; DMF also induced arginase-1 expression and phagocytosis in microglia, both associated with the M2 phenotype. Thus, we determined whether DMF-induced anti-inflammatory response in microglia was mediated by the upregulation of autophagy and found that DMF induced autophagy in microglia is based on increased expression of LC3, the number and area of LC3 puncta, and *Atg7* mRNA expression level. The formation of autophagosomes is controlled by several ATG proteins such as ATG7 (Strohm and Behrends, 2020). Therefore, we hypothesized that DMF-induced autophagy might play a role in DMF-mediated anti-inflammatory response in microglia. We indeed found that the autophagy inhibitors bafilomycin A1 and SBI-0206965 inhibited the DMF-induced anti-inflammatory response microglia. These results suggest that DMF reduces inflammation via autophagy induction in microglia, which may be beneficial for neuroprotection and treatment of neuroinflammation. However, the role of autophagy in DMF treated microglia is still unclear. Therefore, the mechanism by which DMF induces autophagy in microglia and the level to which it is involved in DMF-induced anti-inflammatory effects in CNS needs to be understood to enable its development as a target of therapeutic approaches for neurodegeneration diseases. In addition, the role of DMF-induced autophagy in neurons or glial cell types, including microglia, astrocytes, and oligodendrocyte, should be investigated in future studies.

In summary, we demonstrated that DMF inhibited reactive microglial activation in the spinal cord and reduced proinflammatory response in microglia via the upregulation of autophagy. These results suggest that the therapeutic potential role of DMF in neurodegenerative diseases may partially involve the induction of autophagy in microglia.

DATA AVAILABILITY STATEMENT

The original contributions presented in the study are included in the article/**Supplementary Material**, further inquiries can be directed to the corresponding author.

ETHICS STATEMENT

The animal study was reviewed and approved by the Institutional Animal Care and Use Committee at the Gachon University.

AUTHOR CONTRIBUTIONS

YS-L performed experiments, data analysis and wrote the manuscript, DG and SP performed experiments and data analysis, H-JY performed data analysis and reviewed manuscript, GS designed the study, analyzed data, and wrote the manuscript. All authors contributed to the article and approved the submitted version.

FUNDING

This study was supported by a grant from the Basic Science Research Program through the National Research Foundation (2016R1D1A1B01009186). YS-L was supported by the National Research Foundation (NRF-2018R1D1A1B07048223).

ACKNOWLEDGMENTS

We thank Jeong-Woo Sohn (University of Catholic Kwandong University) for statistical support for this study.

SUPPLEMENTARY MATERIAL

The Supplementary Material for this article can be found online at: https://www.frontiersin.org/articles/10.3389/fphar.2021.612981/full#supplementary-material

REFERENCES

Afridi, R., Kim, J. H., Rahman, M. H., and Suk, K. (2020). Metabolic Regulation of Glial Phenotypes: Implications in Neuron-Glia Interactions and Neurological Disorders. *Front Cel Neurosci*. 14, 20. doi:10.3389/fncel.2020.00020

Akhmetzyanova, E., Kletenkov, K., Mukhamedshina, Y., and Rizvanov, A. (2019). Different Approaches to Modulation of Microglia Phenotypes After Spinal Cord Injury. *Front. Syst. Neurosci.* 13, 37. doi:10.3389/fnsys.2019.00037

Altmeyer, P. J., Mattlies, U., Pawlak, F., Hoffmann, K., Frosch, P. J., Ruppert, P., et al. (1994). Antipsoriatic Effect of Fumaric Acid Derivatives. *J Am Acad Dermatol.* 30, 977–981. doi:10.1016/s0190-9622(94)70121-0

Barth, M., Arrifano, G. P., Lopes-Araujo, A., Santos-Sacramento, L., Takeda, P. Y., Anthony, D. C., et al. (2019). What Do Microglia Really Do in Healthy Adult Brain? *Cells*. 8, 1293. doi:10.3390/cells8101293

Cherry, J. D., Olschowka, J. A., and O'banion, M. K. (2015). Arginase 1+ Microglia Reduce Abeta Plaque Deposition during IL-1beta-dependent Neuroinflammation. *J. Neuroinflammation.* 12, 203. doi:10.1186/s12974-015-0411-8

Cho, K. S., Lee, J. H., Cho, J., Cha, G.-H., and Song, G. J. (2020). Autophagy Modulators and Neuroinflammation. *Curr Med Chem.* 27, 955–982. doi:10.2174/0929867325666181031144605

Donat, C. K., Scott, G., Gentleman, S. M., and Sastre, M. (2017). Microglial Activation in Traumatic Brain Injury. *Front. Aging Neurosci.* 9, 208. doi:10.3389/fnagi.2017.00208

Edison, P. (2020). Neuroinflammation, Microglial Activation, and Glucose Metabolism in Neurodegenerative Diseases. *Int. Rev. Neurobiol.* 154, 325–344. doi:10.1016/bs.irn.2020.03.017

Ellis, A., and Bennett, D. L. H. (2013). Neuroinflammation and the Generation of Neuropathic Pain. *Br J Anaesth*. 111, 26–37. doi:10.1093/bja/aet128

Fox, R. J., Miller, D. H., Phillips, J. T., Hutchinson, M., Havrdova, E., Kita, M., et al. (2012). Placebo-controlled Phase 3 Study of Oral BG-12 or Glatiramer in Multiple Sclerosis. *N. Engl. J. Med.* 367, 1087–1097. doi:10.1056/nejmoa1206328

Gold, R., Kappos, L., Arnold, D. L., Bar-Or, A., Giovannoni, G., Selmaj, K., et al. (2012). Placebo-controlled Phase 3 Study of Oral BG-12 for Relapsing Multiple Sclerosis. *N. Engl. J. Med.* 367, 1098–1107. doi:10.1056/nejmoa1114287

Grozdanov, V., Bliederhaeuser, C., Ruf, W. P., Roth, V., Fundel-Clemens, K., Zondler, L., et al. (2014). Inflammatory Dysregulation of Blood Monocytes in Parkinson's Disease Patients. *Acta Neuropathol.* 128, 651–663. doi:10.1007/s00401-014-1345-4

Gupta, D. P., Park, S. H., Yang, H. J., Suk, K., and Song, G. J. (2020). Neuroprotective and Anti-Neuroinflammatory Effects of a Poisonous Plant *Croton* Tiglium Linn. *Extract. Toxins (Basel)*. 12. doi:10.3390/toxins12040261

Hayashi, G., Jasoliya, M., Sahdeo, S., Saccà, F., Pane, C., Filla, A., et al. (2017). Dimethyl Fumarate Mediates Nrf2-dependent Mitochondrial Biogenesis in Mice and Humans. *Hum. Mol. Genet.* 26, 2864–2873. doi:10.1093/hmg/ddx167

Hoefnagel, J. J., Thio, H. B., Willemze, R., and Bouwes Bavinck, J. N. (2003). Long-term Safety Aspects of Systemic Therapy with Fumaric Acid Esters in Severe Psoriasis. *Br. J. Dermatol.* 149, 363–369. doi:10.1046/j.1365-2133.2003.05433.x

Jha, M. K., Kim, J.-H., Song, G. J., Lee, W.-H., Lee, I.-K., Lee, H.-W., et al. (2018). Functional Dissection of Astrocyte-Secreted Proteins: Implications in Brain Health and Diseases. *Prog Neurobiol.* 162, 37–69. doi:10.1016/j.pneurobio.2017.12.003

Jiang, C. T., Wu, W. F., Deng, Y. H., and Ge, J. W. (2020). Modulators of Microglia Activation and Polarization in Ischemic Stroke (Review). *Mol. Med. Rep.* 21, 2006–2018. doi:10.3892/mmr.2020.11003

Jin, M. M., Wang, F., Qi, D., Liu, W. W., Gu, C., Mao, C. J., et al. (2018). A Critical Role of Autophagy in Regulating Microglia Polarization in Neurodegeneration. *Front. Aging Neurosci.* 10, 378. doi:10.3389/fnagi.2018.00378

Jing, Y.-H., Chen, K.-H., Kuo, P.-C., Pao, C.-C., and Chen, J.-K. (2013). Neurodegeneration in Streptozotocin-Induced Diabetic Rats Is Attenuated by Treatment with Resveratrol. *Neuroendocrinology*. 98, 116–127. doi:10.1159/000350435

Kiguchi, N., Ding, H., Peters, C. M., Kock, N. D., Kishioka, S., Cline, J. M., et al. (2017). Altered Expression of Glial Markers, Chemokines, and Opioid Receptors in the Spinal Cord of Type 2 Diabetic Monkeys. *Biochim Biophys Acta Mol Basis Dis*. 1863, 274–283. doi:10.1016/j.bbadis.2016.10.007

Lastres-Becker, I., García-Yagüe, A. J., Scannevin, R. H., Casarejos, M. J., Kügler, S., Rábano, A., et al. (2016). Repurposing the NRF2 Activator Dimethyl Fumarate as Therapy Against Synucleinopathy in Parkinson's Disease. *Antioxid Redox Signal.* 25, 61–77. doi:10.1089/ars.2015.6549

Liao, Y.-H., Zhang, G.-H., Jia, D., Wang, P., Qian, N.-S., He, F., et al. (2011). Spinal Astrocytic Activation Contributes to Mechanical Allodynia in a Mouse Model of Type 2 Diabetes. *Brain Research*. 1368, 324–335. doi:10.1016/j.brainres.2010.10.044

Linnerbauer, M., Wheeler, M. A., and Quintana, F. J. (2020). Astrocyte Crosstalk in CNS Inflammation. *Neuron*. 108 (4), 608–622. doi:10.1016/j.neuron.2020.08.012

Mariani, M. M., and Kielian, T. (2009). Microglia in Infectious Diseases of the Central Nervous System. *J. Neuroimmune Pharmacol.* 4, 448–461. doi:10.1007/s11481-009-9170-6

Martin, K. R., Celano, S. L., Solitro, A. R., Gunaydin, H., Scott, M., O'hagan, R. C., et al. (2018). A Potent and Selective ULK1 Inhibitor Suppresses Autophagy and Sensitizes *Cancer* Cells to Nutrient Stress. *iScience.* 8, 74–84. doi:10.1016/j.isci.2018.09.012

Mauvezin, C., and Neufeld, T. P. (2015). Bafilomycin A1 Disrupts Autophagic Flux by Inhibiting Both V-ATPase-dependent Acidification and Ca-p60a/serca-dependent Autophagosome-Lysosome Fusion. *Autophagy*. 11, 1437–1438. doi:10.1080/15548627.2015.1066957

Nixon, R. A. (2013). The Role of Autophagy in Neurodegenerative Disease. *Nat. Med.* 19, 983–997. doi:10.1038/nm.3232

Paraiso, H. C., Kuo, P. C., Curfman, E. T., Moon, H. J., Sweazey, R. D., Yen, J. H., et al. (2018). Dimethyl Fumarate Attenuates Reactive Microglia and Long-Term Memory Deficits Following Systemic Immune Challenge. *J. Neuroinflammation*. 15, 100. doi:10.1186/s12974-018-1125-5

Peiro, C., Romacho, T., Azcutia, V., Villalobos, L., Fernandez, E., Bolanos, J. P., et al. (2016). Inflammation, Glucose, and Vascular Cell Damage: the Role of the Pentose Phosphate Pathway. *Cardiovasc. Diabetol.* 15, 82. doi:10.1186/s12933-016-0397-2

Plaza-Zabala, A., Sierra-Torre, V., and Sierra, A. (2017). Autophagy and Microglia: Novel Partners in Neurodegeneration and Aging. *Int. J. Mol. Sci.* 18. doi:10.3390/ijms18030598

Redmann, M., Benavides, G. A., Berryhill, T. F., Wani, W. Y., Ouyang, X., Johnson, M. S., et al. (2017). Inhibition of Autophagy with Bafilomycin and Chloroquine Decreases Mitochondrial Quality and Bioenergetic Function in Primary Neurons. *Redox Biology*. 11, 73–81. doi:10.1016/j.redox.2016.11.004

Roszer, T. (2015). Understanding the Mysterious M2 Macrophage through Activation Markers and Effector Mechanisms. *Mediators Inflamm.* 2015, 816460. doi:10.1155/2015/816460

Sarkar, S., Ravikumar, B., Floto, R. A., and Rubinsztein, D. C. (2009). Rapamycin and mTOR-independent Autophagy Inducers Ameliorate Toxicity of Polyglutamine-Expanded Huntingtin and Related Proteinopathies. *Cell Death Differ*. 16, 46–56. doi:10.1038/cdd.2008.110

Saura, J., Tusell, J. M., and Serratosa, J. (2003). High-yield Isolation of Murine Microglia by Mild Trypsinization. *Glia* 44, 183–189. doi:10.1002/glia.10274

Severini, C., Barbato, C., Di Certo, M. G., Gabanella, F., Petrella, C., Di Stadio, A., et al. (2021). Alzheimer's Disease: New Concepts on the Role of Autoimmunity and of NLRP3 Inflammasome in the Pathogenesis of the Disease. *Curr. Neuropharmacol.* 19, 498–512. doi:10.2174/1570159X18666200621204546

Song, G. J., Nam, Y., Jo, M., Jung, M., Koo, J. Y., Cho, W., et al. (2016). A Novel Small-Molecule Agonist of PPAR-γ Potentiates an Anti-inflammatory M2 Glial Phenotype. *Neuropharmacology*. 109, 159–169. doi:10.1016/j.neuropharm.2016.06.009

Song, G. J., Rahman, M. H., Jha, M. K., Gupta, D. P., Park, S. H., Kim, J. H., et al. (2019). A Bcr-Abl Inhibitor GNF-2 Attenuates Inflammatory Activation of Glia and Chronic Pain. *Front. Pharmacol.* 10, 543. doi:10.3389/fphar.2019.00543

Song, G. J., and Suk, K. (2017). Pharmacological Modulation of Functional Phenotypes of Microglia in Neurodegenerative Diseases. *Front. Aging Neurosci.* 9, 139. doi:10.3389/fnagi.2017.00139

Stephenson, J., Nutma, E., Van Der Valk, P., and Amor, S. (2018). Inflammation in CNS Neurodegenerative Diseases. *Immunology*. 154, 204–219. doi:10.1111/imm.12922

Strohm, L., and Behrends, C. (2020). Glia-specific Autophagy Dysfunction in ALS. *Seminars in Cel Develop. Biology*. 99, 172–182. doi:10.1016/j.semcdb.2019.05.024

Su, P., Zhang, J., Wang, D., Zhao, F., Cao, Z., Aschner, M., et al. (2016). The Role of Autophagy in Modulation of Neuroinflammation in Microglia. *Neuroscience*. 319, 155–167. doi:10.1016/j.neuroscience.2016.01.035

Talbot, S., Chahmi, E., Dias, J., and Couture, R. (2010). Key Role for Spinal Dorsal Horn Microglial Kinin B1 Receptor in Early Diabetic Pain Neuropathy. *J Neuroinflammation*. 7, 36. doi:10.1186/1742-2094-7-36

Tang, Y., and Le, W. (2016). Differential Roles of M1 and M2 Microglia in Neurodegenerative Diseases. *Mol. Neurobiol.* 53, 1181–1194. doi:10.1007/s12035-014-9070-5

Thellung, S., Corsaro, A., Nizzari, M., Barbieri, F., and Florio, T. (2019). Autophagy Activator Drugs: A New Opportunity in Neuroprotection from Misfolded Protein Toxicity. *Int. J. Mol. Sci.* 20, 901. doi:10.3390/ijms20040901

Wang, B., Dong, G., Zhang, Q., Yan, F., Li, Z., Li, C., et al. (2020). The Inhibitor of Autophagy SBI-0206965 Aggravates Atherosclerosis through Decreasing Myeloid-Derived Suppressor Cells. *Exp. Ther. Med.* 19, 1370–1378. doi:10.3892/etm.2019.8317

Wang, L., Chen, M., Yang, J., and Zhang, Z. (2013). LC3 Fluorescent Puncta in Autophagosomes or in Protein Aggregates Can Be Distinguished by FRAP Analysis in Living Cells. *Autophagy*. 9, 756–769. doi:10.4161/auto.23814

Wodarski, R., Clark, A. K., Grist, J., Marchand, F., and Malcangio, M. (2009). Gabapentin Reverses Microglial Activation in the Spinal Cord of Streptozotocin-Induced Diabetic Rats. *Eur. J. Pain*. 13, 807–811. doi:10.1016/j.ejpain.2008.09.010

Xu, S., Lu, J., Shao, A., Zhang, J. H., and Zhang, J. (2020). Glial Cells: Role of the Immune Response in Ischemic Stroke. *Front. Immunol.* 11, 294. doi:10.3389/fimmu.2020.00294

Xu, Z., Zhang, F., Sun, F., Gu, K., Dong, S., and He, D. (2015). *Dimethyl Fumarate for Multiple Sclerosis*. Cochrane Database Syst. Rev. Oxford, U.K.; Vista, CA : Update Software, 22, CD011076, doi:10.1002/14651858.CD011076

Yao, Y., Miao, W., Liu, Z., Han, W., Shi, K., Shen, Y., et al. (2016). Dimethyl Fumarate and Monomethyl Fumarate Promote Post-Ischemic Recovery in Mice. *Transl. Stroke Res.* 7, 535–547. doi:10.1007/s12975-016-0496-0

Zhang, L., Xu, J., Gao, J., Wu, Y., Yin, M., and Zhao, W. (2018). CD200-, CX3CL1-, and TREM2-Mediated Neuron-Microglia Interactions and Their Involvements in Alzheimer's Disease. *Rev. Neurosci.* 29, 837–848. doi:10.1515/revneuro-2017-0084

Conflict of Interest: The authors declare that the research was conducted in the absence of any commercial or financial relationships that could be construed as a potential conflict of interest.

Copyright © 2021 Lee, Gupta, Park, Yang and Song. This is an open-access article distributed under the terms of the Creative Commons Attribution License (CC BY). The use, distribution or reproduction in other forums is permitted, provided the original author(s) and the copyright owner(s) are credited and that the original publication in this journal is cited, in accordance with accepted academic practice. No use, distribution or reproduction is permitted which does not comply with these terms.

frontiers in Pharmacology

ORIGINAL RESEARCH
published: 11 May 2021
doi: 10.3389/fphar.2021.661304

Maternal Nicotine Exposure Alters Hippocampal Microglia Polarization and Promotes Anti-inflammatory Signaling in Juvenile Offspring in Mice

Li Zhou[1], Xinrong Tao[1,2,3,4], Gang Pang[5], Min Mu[1,2,3,4], Qixian Sun[1], Fei Liu[1], Yuting Hu[1], Huihui Tao[1,2,3,4], Bing Li[1] and Keyi Xu[1,2,3,4]*

[1]Center for Medical Research, School of Medicine, Anhui University of Science and Technology, Huainan, China, [2]Key Laboratory of Industrial Dust Control and Occupational Health, Ministry of Education, Anhui University of Science and Technology, Huainan, China, [3]Key Laboratory of Industrial Dust Deep Reduction and Occupational Health and Safety, Anhui Higher Education Institutes, Anhui University of Science and Technology, Huainan, China, [4]Engineering Laboratory of Occupational Safety and Health, Anhui Province, Anhui University of Science and Technology, Huainan, China, [5]College of Basic Medical Science, Anhui Medical University, Hefei, China

Accumulating evidence reveal that maternal smoking or perinatal nicotine replacement therapy impairs hippocampal neurogenesis, neural development, and cognitive behaviors in the offspring. Microglia is a source of non-neural regulation of neuronal development and postnatal neurogenesis. In this study, we explored the impact of nicotine on the microglia during the development of hippocampus. Developmental nicotine exposure in a mouse model was conducted by supplementing nicotine in the drinking water to mother mice during gestation and lactation period. We found that juvenile offspring with maternal nicotine exposure presented physical and neurobehavioral development delay and an increase in anxiety-like behavior in the open field test on postnatal day (PND) 20. To further detect possible developmental neurotoxic effects of nicotine in offspring and underlying mechanism, whole genome microarray analysis of the expression profile of the hippocampus was performed on postnatal day 20. Significant alterations in the expression of genes related to inflammatory, neurotransmitter, and synapsis were observed in the hippocampus after maternal nicotine exposure, as compared to the vehicle control. Concurrently, an increase in microglial markers and the presence of M2 polarity state in the hippocampus of the nicotine offspring were observed by histological analysis and confocal z-stacking scanning. The M2 microglial polarization state was further confirmed with *in vitro* primary microglia culture by cytokine array, and double-positive expression of BDNF/Iba1 in microglia by immunohistochemical staining in the juvenile offspring hippocampus was visualized. We also found that nicotine offspring showed an increase of neurite length in the molecular layer and CA1 by Tuj1 staining, as well as an increase in the expression of synapse associated protein, PSD95, but the expression of NeuroD1 in CA1 and CA3 reduced. In summary, maternal nicotine exposure dysregulates immune-related genes expression by skewing the polarity of M2 microglia in the hippocampus, which may cause abnormal cognitive and behavioral performance in the offspring.

Keywords: maternal nicotine exposure, hippocampus, microglia, mouse, Offspring

OPEN ACCESS

Edited by:
Mariela Fernanda Perez, National University of Cordoba, Argentina

Reviewed by:
Luca Ferraro, University of Ferrara, Italy
Cheng Jiang, Yale University, United States

***Correspondence:**
Xinrong Tao
xrtao1116@hotmail.com

Specialty section:
This article was submitted to Neuropharmacology, a section of the journal Frontiers in Pharmacology

Received: *30 January 2021*
Accepted: *26 April 2021*
Published: *11 May 2021*

Citation:
Zhou L, Tao X, Pang G, Mu M, Sun Q, Liu F, Hu Y, Tao H, Li B and Xu K (2021) Maternal Nicotine Exposure Alters Hippocampal Microglia Polarization and Promotes Anti-inflammatory Signaling in Juvenile Offspring in Mice. Front. Pharmacol. 12:661304. doi: 10.3389/fphar.2021.661304

INTRODUCTION

Tobacco smoking, nicotine replacement therapy (NRT), e-cigarettes, as well as other nicotine exposure remain a major public health issue across the world (Guerby et al., 2020), and the trend of nicotine usage and exposure continues increasing over the past decades (Dai and Leventhal, 2019; Kapaya et al., 2019). Recent epidemiological studies have shown that 13.8% of pregnant women and 20.1% of non-pregnant reproductive age women smoke (Lopez et al., 2018), and female smoker population has been reported to be more difficult to quit smoking when compared with male smokes (Leventhal et al., 2007). NRT is used to reduce the nicotine withdrawal symptoms experienced by women before, during, and after pregnancy.

Some studies show that NRT is a safer alternative to tobacco smoking for pregnant women despite the lack of information on the toxicological effects of nicotine on the developing fetus (Mark et al., 2015; Mead et al., 2019). Nicotine in lactate can be absorbed by offspring through placenta and lactate and causes behavioral irritation and anxiety in the offspring (Karimiankakolaki et al., 2019). Nicotine exposure during pregnancy is associated with numerous fetal consequences including pre-mature birth, low birth weight, and Sudden Infant Death Syndrome (Salihu and Wilson, 2007; Knopik et al., 2016b; King et al., 2018; Buck et al., 2019), as well as neurodevelopmental disorders, such as attention deficit hyperactivity disorder, autism, and schizophrenia in developing children (Knopik et al., 2016a; Niemela et al., 2016; Golding et al., 2017; He et al., 2017; Quinn et al., 2017; Huang et al., 2018; Marceau et al., 2018). These observations demonstrate that the offspring are vulnerable to nicotine. Therefore, understanding the unique effects of nicotine use on offspring is critical for treating and preventing the adverse consequences that follow.

Previous studies have indicated that the effects of maternal nicotine exposure on offspring are intricated. Being altricial species, both humans and rodents undergo a pre and postnatal series of highly regulated, sequential changes to cell specialization, known as critical periods in central nervous system (CNS) development (Morgane et al., 1993). Exposure to nicotine, particularly when occurs during critical developmental periods, can adversely affect brain, immune system (Yan et al., 2020), and other systems throughout the body (Chen et al., 2020; Jamshed et al., 2020; Jian et al., 2020; McAlinden et al., 2020; Miranda et al., 2020). Chronic nicotine exposure *in utero* could alter neuronal cytoarchitecture, nicotinic acetylcholine receptor (nAChR) expression, and function of neurotransmitter systems (Lv et al., 2008; Gold et al., 2009). Activation of nAChRs by nicotine could induce developmental problems in premature stage, such as cholinergic-mediated signaling, which initiates neuronal transformation from replication to differentiation (Smith et al., 2010). Further, activation of nAChRs by nicotine impairs the development of neurotransmitter systems, especially dopamine (DA) (Azam et al., 2007; Zhang et al., 2020), norepinephrine (NE) (Sterley et al., 2014), and serotonin (5-HT) (Lee et al., 2018). In addition to alternations in nAChR expression and neurotransmitter system function, a recent study suggests that nicotine exposure during early development stage alters neurotrophins and neuroinflammation (Zelikoff et al., 2018a).

During early stage of postnatal development, the CNS is sensitive to external stimuli and internal neurotrophins, including nerve growth factor (NGF) and brain-derived neurotrophic factor (BDNF), which modulate brain plasticity to adapt to the environment (Berry et al., 2012). Several studies have reported the effects of maternal nicotine exposure on BDNF levels in different brain areas (Buck et al., 2019). Besides neurons, BDNF receptor is also expressed in M2 microglia (Ding et al., 2020). To date, only a paucity of research explored the relationship between nicotine and BDNF, and no study has yet elucidated the exact effect of maternal nicotine exposure on microglia BDNF of juvenile offspring.

Microglia are the resident innate immune cells of the CNS and exert functions of host defense and maintenance of normal tissue homeostasis, along with the support of neuronal development and processes in the healthy brain. The abnormality of microglial activation plays a critical role in neurodegenerative disease (Maleszewska et al., 2020; Nasi et al., 2020). Inflammatory mediators influence the brain during development. Neurodevelopmental disorders such as autism spectrum disorders, cognitive impairment, cerebral palsy, epilepsy, and schizophrenia are associated with early inflammation (Jiang et al., 2018). Nicotine has been shown to directly and indirectly mediated neuroinflammation (Sallam et al., 2019; Han et al., 2020), which can lead to neurodevelopmental disorders and lasting effects. However, activation of microglia during development due to nicotine exposure could have profound developmental consequences. Nicotine attenuated neuronal loss and decreased the expression of microglial activation markers of the hippocampal CA1 region in the eclampsia-like rat, which improved fetal outcomes (Li et al., 2016). Nicotine reduced neurogenesis and altered microglial profiles in the hippocampal DG (dentate gyrus) in an early postnatal period (Nakayama et al., 2019).

This study aimed to assess the *in vivo* effect of nicotine on neurodevelopment in juvenile offspring exposed to nicotine during critical early life stages. We identified the signature of mRNA in the hippocampus of offspring after maternal nicotine exposure to evaluate the hippocampal transcriptome alterations. The expression of inflammatory genes, as well as neurotransmitters and synaptic-associated genes, were changed. In this study, we for the first time reported that maternal nicotine exposure promoted M2-like microglial polarization to influence the hippocampal immune microenvironment in the offspring. We also found that maternal nicotine exposure promoted elongation of axons and increased the expression levels of synapse-related proteins (PSD95) in the hippocampus of offspring, but decreased the expression of a single transcription factor, NeuroD1. In conclusion, maternal nicotine exposure promotes the polarization of hippocampal microglia to M2 and alters inflammatory factors in the offspring, which may further modulate the morphology and function of neurons in the hippocampus, leading to developmental defects.

MATERIALS AND METHODS

Animals

Adult C57BL/6 mice were purchased from the Changzhou Cavion Experimental Animal Co, Ltd. (license number SCXY (Su) 20110003). The mice were housed in a room maintained on a standard 12 h light-dark cycle (lights on at 07:00 AM), with constant temperature and humidity (24 ± 2°C and 50%, respectively), and with free access to food and water. All procedures and operations were performed in strict accordance with the guidelines as described in the National Institutes of Health Guide for the Care and Use of Laboratory Animals (NIH Publication No. 8023, revised 1978) and were approved by the Institutional Animal Care and Use Committee at Anhui University of Science and Technology.

Maternal Nicotine Exposure

Adult C57BL/6 female mice (n = 12) were given nicotine (Sigma, N-3876; 200 μg/ml) in drinking water containing 1% saccharin (Shyuanye; 128–44–9) starting from 2 weeks premating until the offspring were weaned. The female control mice (n = 9) received drinking water containing 1% saccharin. 2 weeks after drinking nicotine solution, all female mice were paired with male mice at a 3:1 ratio until they gave birth. The offspring of either sex were used on postnatal day 20 (PND 20), but included an equal number of male and female mice and were distributed randomly for subsequent experiments (**Supplementary Table 1**).

Physical and Neurobehavioral Development

The birth weight of the offspring was weighed separately, 2~3 mice were selected at random from each cage for subsequent experiments. Eye opening was based on the degree of binocular opening that was equal to or greater than 1/2 of normal palpebral fissure. The olfactory reflex test started on PND 11 for consecutive days by placing the offspring in the center of a box with a clean absorbent cotton on one side and an odorous absorbent cotton on the other side to evaluate whether the offspring could distinguish the smell of the cage and reach the side of the absorbent cotton with the smell. Auditory startle test started on PND 11 for consecutive days, the offspring were placed in a cage alone and a metal block 15 cm away from the offspring was struck. The positive reactions include body suddenly curl, arch, and two consecutive positive stimulus responses were defined as the standard.

Open-Field Test

Open-field test was performed at PND 20. Locomotor activity was recorded and analyzed *via* an overhead video camera interfaced with behavioral tracking software EthoVision® XT 5.1 (Noldus Information Technology, Netherlands). The experiment was accomplished in a peaceful environment, and mice were acclimated to the behavioral recording room for 3 days, 60 min a day. Then mice were softly placed in the center of an open-field Plexiglas clear chamber (30 × 30 × 35 cm) and allowed to move freely for 5 min. The zone of the chamber was divided into the peripheral zone (area within 7.5 cm away from the edge) and the central zone (the rest area). Behavior test was carried out between 14:00 and 18:00, and all chambers were cleaned fully with 10% alcohol between trials to remove odor residue. The basal exploration activity was assessed by the total distance traveled (cm) and immobility (s), and anxiety-like behaviors were measured by the duration in the center area.

Histological Staining

Hippocampal Tissue Preparation

After opening the skull and cautious removal of adjacent, non-neural tissue, isolated total hippocampal tissue including dorsal and ventral was collected into a container and cooled on ice, then shift into ice-cold protein extraction buffer for western blot analysis or Trizol reagent for RT-qPCR analysis. The rest mice were deeply anesthetized and perfused transcardially with cold phosphate-buffered saline (PBS) followed by 4% paraformaldehyde (PFA) in 0.1 M PBS. Isolated brains were transferred into 4% paraformaldehyde in PBS (pH 7.4) for histological analysis.

Nissl Staining

The brains of mice were dissected and fixed in 4% paraformaldehyde for 24 h. A 4 mm-thick coronal section, including the bilateral hippocampus, was excised from the brains. The sections were fixed in 4% paraformaldehyde for another 24 h, dehydrated in alcohol, cleared with xylene, and embedded in paraffin. The paraffin-embedded brain sections were sliced at 5 μm thickness and Nissl-stained with 1% thionin, then observing the morphology of neural cells and damage of pyramidal neurons in the hippocampus of the two groups. While glia was counted separately in each field; glia cells were readily distinguished from neurons by their size, nuclear shape, cytoplasm, location, and characteristic staining (Roy et al., 2002).

Immunohistochemistry Staining

Double-labeling immunohistochemistry and colocalization analysis for microglia-derived BDNF were performed using dual staining of BDNF and Iba1. Paraffin-embedded hippocampal sections were prepared as described above. 5 μm-thickness hippocampal slices were stained against BDNF and Iba1. In brief, brain slices were baked at 60°C for 6 h, and the slides were deparaffinized in xylene and hydrated in gradient alcohol, and then rinsed in dd-H2O. Antigen retrieval was performed by incubation in 10 mM sodium citrate buffer via steam for 30 min. Endogenous peroxidase in the tissue was blocked by incubation with 3% H2O2 in dark for 10 min. Tissues were blocked for 1 h in 3% BSA-containing PBST and then incubated with primary antibodies at 4°C overnight. After rewarming for 40 min, then the sections were rinsed and incubated with secondary antibodies, donkey anti-goat IgG H&L, and donkey anti-rabbit IgG H&L for 40 min at room temperature. Lastly, the slices were stained with AP substrate (Vector Laboratories, SK-5100) for 10 min and then stained with DAB substrate (NJJCBio, W026-1-1) for 10 min and counterstained with hematoxylin. Slices were mounted and covered with a permanent mounting medium (Vector Laboratories, H-5000). Images were acquired with a BX50 microscope (Olympus, Tokyo, Japan).

TABLE 1 | Antibodies used in this study.

Antigen	Host	Dilution ratio	Company
Iba1	Rabbit	1:500 (IF)	Wako, 019–19,741
Iba1	Rabbit	1:1,000 (WB)	Abcam, ab178846
Iba1	Goat	1:300(IHC)	Novus bio, NB100–1028
BDNF	Rabbit	1:500(WB)	ABclonal, A16299
BDNF	Rabbit	1:300(IHC)	Abcam, ab108319
Tuj1	Rabbit	1:500	Abcam, ab18207
GAPDH	Rabbit	1:10,000	Proteintech, 10494-1-AP
GAD1	Rabbit	1:800	Proteintech, 10408-1-AP
PSD95	Rabbit	1:800	Proteintech, 20665-1-AP
NeuroD1	Mouse	1:500	Abcam, ab60704
Goat anti-rabbit IgG H&L	Goat	1:1,000	Abcam, ab6721
Donkey anti-goat IgG H&L	Donkey	1:1,000	Abcam, ab6885
Donkey anti-rabbit IgG H&L	Donkey	1:1,000	Abcam, ab6803-AP
Goat anti-rabbit IgG H&L	Goat	1:1,000	Life technology, A-11008
Goat anti-mouse IgG H&L	Goat	1:1,000	Life technology, A-28175
Goat anti-rabbit IgG H&L	Goat	1:1,000	Life technology, A-11037

For Tuj1 staining, slices were incubated with the anti-Tuj1 antibody at 4°C overnight. The second antibody was goat anti-rabbit IgG H&L, and then stained with DAB substrate for 10 min and counterstained with hematoxylin for 30 s. The stained slides were immersed in a graded series of ethanol and then, xylene to dehydration and transparency of tissues. Finally, slices were sealed with neutral gum and acquired images.

Immunofluorescence Staining

Harvested brains were further fixed with 4% PFA, soaked in 30% sucrose solution before embedding in OCT media. The hippocampal brains were then cut into 30 μm coronal frozen sections. Every 12th section was collected and processed. Slides were permeabilized with 0.1% Triton X-100 in PBS (PBST). After PBST washing, the slices were blocked with 5% goat serum (Beyotime Biotechnology, C0265) for 1 h before being incubated in anti-Iba1 antibody at 4°C overnight. After PBST washing, slices were incubated with Goat anti-Rabbit IgG H&L for 1 h at room temperature. Nucleus was counterstained with DAPI (1:2000; Beyotime Biotechnology, 1002). Slices were mounted with Antifade Mounting Medium (Beyotime Biotechnology, P0126) and stored at 4°C in dark. Images were acquired with an Olympus FV3000 laser scanning confocal microscope (Olympus, Waltham, United States), and a z-step size of 2 um. Z-stacks ranged from 24 to 26 um in thickness.

For Iba1 and NeuroD1 Double staining, slices were incubated with anti-Iba1 antibody and anti-NeuroD1 antibody at 4°C overnight. The second antibody was Goat anti-mouse IgG H&L and Goat anti-rabbit IgG H&L. Subsequent steps were performed as above. Primary and secondary antibodies were all listed in **Table 1**.

RNA Isolation, cDNA Synthesis, and Real-Time Quantitative PCR

Total RNA was isolated from the hippocampus using Trizol extraction method according to the manufacturer's instructions (Invitrogen). For cDNA synthesis, 5x All-In-One RT MasterMix (abm, Jiangsu, China) was used following the manufacturer's instructions using the PCR instrument (Hema9600). Real-time polymerase chain reaction was next performed on a QuantStudio three Real-Time PCR System (Thermo Fisher Scientific, United States) for the detection of BDNF, CXCL10, JUNB, IL-1β, IL-4, and the endogenous control GAPDH. For one amplification reaction, 5 μl of GoTaq® qPCR Master Mix (Promega, Madison, WI, United States), 0.4 μl of primer (10 μM), 1 μl of cDNA, 0.1 μl of CXR, and 3.5 μl of DNase-free water were mixed for detection. All qPCR primers were designed using Primer3 software and verified using the BLAST-like alignment tool. The oligonucleotides used for qPCR are listed in **Table 2**. The expression levels of the targeted genes were normalized to that of the endogenous control GAPDH by QuantStudioTM Design&Analysis Software (v1.3.1) based on the $2-\Delta\Delta Ct$ formula.

Microarray and Computational Analysis

The hippocampal RNA was analyzed using Arraystar RNA Flash Labeling Kit. After RNA labeling and hybridization, slides were scanned by Agilent DNA Microarray Scanner. Raw data were normalized and analyzed using GeneSpring GX v12.1 software (Agilent Technologies, Santa Clara, CA). Differentially expressed mRNA between two groups were identified through p value (cut–off: 0.05) and FC (cut–off: 1.5) sifting. Pathway and gene ontology (GO) analysis were applied to determine the roles of these differentially expressed mRNAs on biological pathways or GO terms. Hierarchical clustering and combined analysis were performed using in-house scripts (Kangcheng Biotechnology Company). The microarray data were deposited in Gene Expression Omnibus (GEO accession: GSE166311).

Primary Microglia Cultures and Cytokine Measurement by Protein Array

Primary Microglial Culture

Primary cultures of mice mixed glial cells (microglia and astrocytes) were obtained as described previously (Schildge et al., 2013) with a few modifications. Briefly, whole brain

TABLE 2 | The primer sequences used for real-time quantitative polymerase chain reaction analyses.

Gene	Forward sequence (5′-3′)	Reverse sequence (3′-5′)
GAPDH	GTGGGTGCAGCGAACTTTAT	CACTGAGCATCTCCCTCACA
BDNF	GCCTTTGGAGCCTCCTCTAC	TCAGTTGGCCTTTGGATACC
CXCL10	CCCACGTGTTGAGATCATTG	GAGGCTCTCTGCTGTCCATC
CCL12	GGTATTGGCTGGACCAGATG	CAAGGATGAAGGTTT GAGACG
JUNB	ACGGAGGGAGAGAAAAGCTC	AAGGCTGTTCCATTTTCGTG
IL-1β	TGGACCTTCCAGGATGAGGACA	GTTCATCTCGGAGCCTGT AGTG
IL-4	AACGAGGTCACAGGAGAAGG	TCTGCAGCTCCATGAGAACA

isolates were extracted from neonatal C57BL/6 mice pups aged 2–4 days and transferred into a new dish with 5 ml L-15 solution (Leibowitz L-15 + 0.1% BSA +1% Pen/Strep, Gibco) on ice. Mixed glial cultures were prepared from cerebral cortices. cortices were gently pipetted up and down 10 times and mechanically dissociated before cortical tissues were treated with 0.05% trypsin for 30 min at 37°C. Trypsinization was stopped by 10% fetal bovine serum (FBS). Mixed glia cells in the supernatant were collected and cultured in high glucose DMEM supplemented with 10% FBS, 1% penicillin/streptomycin, and 2 mM of L-glutamine (D-10 medium). Cells were cultured in a humidified incubator at 37°C (5% carbon dioxide). The culture medium was half-replaced every 4–6 days. Mixed glia cells became confluence after 14–21 days in culture medium. Loosely attached primary cultures of microglia were prepared after shaking at 100 rpm (Dragon Lab, #SK-D 1807-E, China) for 2 h at 37°C. The cell pellets were re-suspended and re-plated with D-10 medium for the following experiment.

Evaluation of Cytokines Collected From Cell Culture Supernatant

Primary microglia were re-plated into a 12-well plate. Blank served as the unstimulated control for each time point, lipopolysaccharide (LPS)-stimulated primary microglia as the pro-inflammatory control (LPS group), nicotine group, and LPS plus nicotine group were set up in this experiment. Microglia were stimulated with LPS, nicotine, or LPS plus nicotine at the final concentration of 10 μg/ml LPS, 10 μmol nicotine, 10 μg/ml LPS plus 10 μmol nicotine. Microglia cells were incubated with LPS for 24 h in LPS group. LPS plus nicotine group were pretreated with LPS for 30 min before application of nicotine for analyzing anti-inflammatory effects of nicotine. Medium were collected at 12/24 h, respectively. Then, Supernatants were obtained by centrifugation at 1200 rpm for 10 min at 4°C, and stored at −80°C until they were used for cytokine assay. Cytokines in the supernatant samples were detected using Quantibody® Mouse cytokine array 1 (Ray Biotech, United States) according to the manufacturer's instructions. In brief, the signals (green fluorescence, Cy3 channel, 532 nm excitation, and 542 nm emission) were captured using an InnoScan 300 Microarray Scanner (Innopsys, France). Quantitative data analysis was performed using Ray Biotech mouse Cytokines Array l software (GSM-CYT-1 Q-Analyzer).

Western Blot

The total protein of hippocampus was homogenized with RIPA lysis buffer (P0013B, Beyotime Biotechnology, Shanghai, China) containing PMSF, and phosphatase inhibitor on ice following incubation for 30 min at 4°C. Hippocampal lysates were centrifuged at 10,000 ×g for 10 min at 4°C. Supernatant was collected and the protein concentration was determined by a Bicinchoninic acid Protein Assay kit (P0009, Beyotime, Shanghai, China). The loading buffer was used to adjust the protein concentration and 40 μg protein was loaded and separated by 10% sodium SDS–PAGE (Beyotime Biotechnology) before being transferred to a PVDF membrane (Millipore). After 1 h BSA blocking, membranes were incubated with rabbit anti-Iba1 antibody, rabbit anti-BDNF antibody, rabbit anti-PSD95 antibody, anti-GAD1 antibody, and rabbit anti-GAPDH. After being incubated with the second antibody Goat Anti-Rabbit IgG H&L (HRP), membranes were washed with TBST 3 min for 5 times. The protein bands were visualization with chemiluminescent HRP substrate (P90720, Millipore Corporation, Burlington, MA) and detected by Molecular Imager ChemiDoc™ XRS + analysis system (BioRad Co., Hercules, CA). ImageJ was used for quantitative Western Blot analysis. All experiments were repeated four times.

STATISTICAL ANALYSIS

All data were plotted and analyzed using GraphPad Prism (6.01). The results were represented as the mean ± standard error means (SEM). A two-way analysis of variance (ANOVA) for the difference among three or more groups. A two-way repeated measures ANOVA for the difference of body weight were performed using SPSS software package (IBM). The difference among the two groups were analyzed using unpaired Student's t-tests as appropriate. A probability level of p value <0.05 was considered statistically significant.

RESULTS

Maternal Nicotine Exposure Altered Physical and Neurobehavioral Development in the Juvenile Offspring

Maternal nicotine exposure and tests in the offspring were performed according to the experimental paradigm showed in **Figures 1A,B**. Birth weight was measured from PND0-20. Maternal nicotine exposure causes low-birth weight (t = 2.6, p = 0.0107, vehicle: n = 44, nicotine: n = 60; **Figure 1C**, upper panel). Ten mice from five litters with similar birth time in each group (n = 2 mice/litter) were separately weighted at PND0, 4, 8, 12, 16, and 20. A two-way repeated measures ANOVA on body weight revealed a significant main effect of time ($F(4, 36) = 496.523$, $p < 0.001$, $n = 10$) and time × group interaction ($F(4, 36) = 4.041$, $p = 0.008$, $n = 10$), but no difference in group ($F(1,9) = 0.626$, $p = 0.449$, $n = 10$; **Figure 1C**, lower panel). The birth weight was significantly reduced in the nicotine group. The physical and neurobehavior development during lactation in the two groups were evaluated every day from

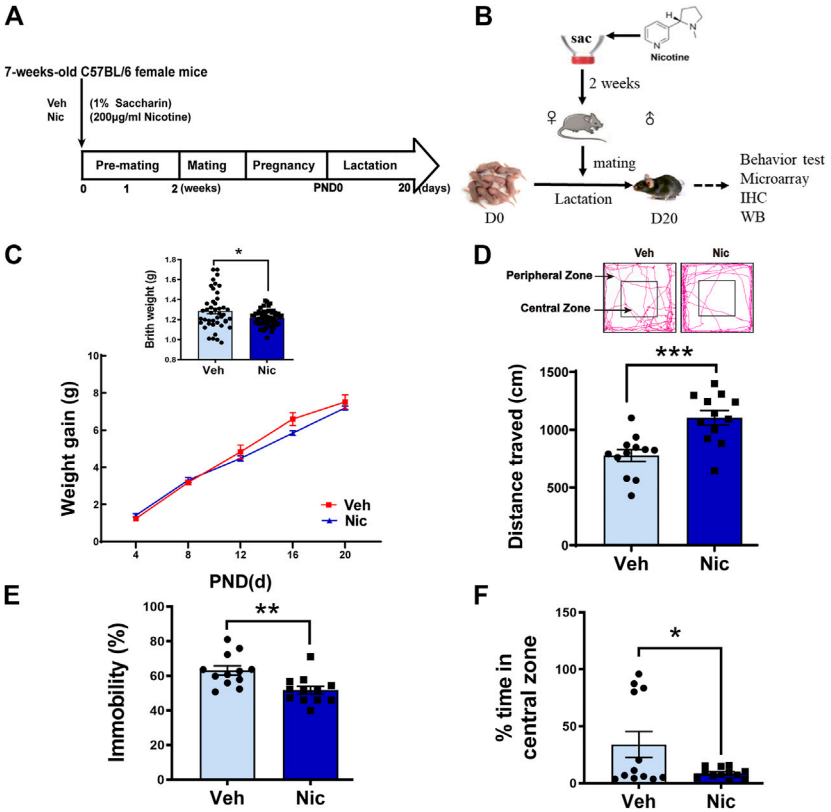

FIGURE 1 | Maternal nicotine exposure altered the offspring's physical development and exploration behavior. The experimental paradigm of maternal nicotine exposure **(A)** and tests in the offspring **(B)** were showed. Mice were terminated on PND20, and brain tissues were collected for further experiments after behavior tests were completed. **(C)** Birth weight and body weight gain throughout development were recorded. Open field test revealed that maternal nicotine exposure significantly increased the total distance traveled **(D)** of the offspring, but visibly reduced the immobility time **(E)**, and exploration time in the center zone **(F)**, as compared to the vehicle control (lower panel). The representative track diagram of open field test was showed (upper panel); $^{*}p < 0.05$, $^{**}p < 0.01$, $^{***}p < 0.001$, all data are means ± SEM.

PND0-20. Nicotine offspring showed significantly developmental retardation relative to those in vehicle mice: eye-opening (Veh: 12.79 ± 0.11, Nic: 15.17 ± 0.13; $t = 13.65$, $p < 0.0001$, vehicle: $n = 14$, nicotine: $n = 17$), auditory startle (Veh: 11.50 ± 0.20, Nic: 12.75 ± 0.31; $t = 3.498$, $p = 0.0023$, vehicle: $n = 14$, nicotine: $n = 8$), and olfactory reflex (Veh: 11.14 ± 0.10, Nic:12.05 ± 0.16; $t = 4.65$, $p < 0.0001$, vehicle: $n = 14$, nicotine: $n = 17$; **Table 3**). Open field test revealed that maternal nicotine exposure increased total distance traveled ($t = 4.018$, $p = 0.0006$, $n = 12$; **Figure 1D**), and significantly reduced the immobility time ($t = 3.231$, $p = 0.0038$, $n = 12$; **Figure 1E**), and exploration time in the center on PND 20 in offspring, as compared to the vehicle offspring ($t = 2.198$, $p = 0.0388$, $n = 12$; **Figure 1F**). These data indicate that maternal nicotine exposure leads to weight loss, neurodevelopmental delay, and reduce exploration behavior in their offspring.

Maternal Nicotine Exposure Increased Number of Microglial Cells in the Hippocampus of Juvenile Offspring

Nissl staining showed the whole hippocampal sample (low magnification, ×40) in the coronal plane from the vehicle and nicotine group (two pictures on the left-most side). DG, CA1, and CA3 subfield was indicated by the black frame (**Figure 2A**). Maternal nicotine exposure significantly increased the number of neuroglia (arrowheads) in CA1 ($t = 4.511$, $p = 0.0107$, $n = 3$) and CA3 ($t = 3.712$, $p = 0.0206$, $n = 3$; **Figure 2B**), but not in DG ($t = 0.172$, $p = 0.8722$, $n = 3$). Additionally, the expression of microglia marker Iba1 in the hippocampus was tested by immunofluorescent staining (**Figure 2C**). The expression intensity and the number of Iba1 positive cells were analyzed and counted using ImageJ, independently. The fluorescence intensity ($t = 3.408$, $p = 0.0271$, $n = 3$; **Figure 2D**) and count of Iba1+ cells in CA1 ($t = 3.396$, $p = 0.0274$, $n = 3$; **Figure 2E**) increased dramatically in juvenile nicotine group, but the number of Iba1+ microglia cells in DG or CA3 was not statistically significant (**Figure 2E**).

Microarray Analysis Identified Differentially Expressed Genes in the Hippocampus of the Juvenile Nicotine Offspring

Although the mechanisms of neuron-microglia signaling in regulating brain function *in vivo* have been well studied, the

TABLE 3 | Physiological development index in each different group.

Observation	Vehicle (n = 14)	Nicotine (n = 8–17)	Effect
Smell pups (%)			
PND11	85%	18%	
PND12	100%	76%	P < 0.001****
PND13	100%	100%	
Hearing pups (%)			
PND11	64%	0.0	
PND12	86%	50%	$p = 0.002$**
PND13	100%	75%	
PND14	100%	100%	
Eye opening pups (%)			
PND11	0.0	0.0	
PND12	21%	0.0	
PND13	100%	0.0	P < 0.0001****
PND14	100%	5%	
PND15	100%	82%	
PND16	100%	100%	

cellular and molecular mechanism of its action in the nicotine-exposed hippocampus during the development is still unclear. To investigate the influence of maternal nicotine exposure on microglia-mediated inflammatory response and neuronal function in the gene expression profile of hippocampus, microarray analysis was performed in 20 days hippocampus. The Agilent Feature Extraction Software was used to identify differentially expressed mRNA in nicotine and vehicle offspring. The threshold of volcano plot filtering used to screen the differentially expressed mRNAs was a fold change ≥1.5.

In the mRNA expression profiling data, 295 differently expressed mRNAs in the hippocampus of the nicotine offspring have been identified (**Figure 3A**). Compared to vehicle offspring, 132 mRNAs were significantly upregulated, and 163 mRNAs were obviously downregulated in nicotine offspring, respectively. Then we performed ontologic pathway enrichment analysis for the differently expressed genes enriched with attention to GO biological processes. We found that the most enriched GOs targeted by the upregulated and downregulated transcripts were involved in a variety of functions including metabolism, cellular process, biological regulation, signal transduction, cell communication, response to stimulus, and multicellular organismal regulation (**Figure 3B**).

The KEGG database was used to investigate the pathways in which the differentially expressed genes are involved. The 10 most enriched pathways (top 5 up-regulated and top 5 down-regulated pathways) in KEGG pathway annotations are shown in **Figure 3C**. Specifically, the upregulated pathways included drug metabolism-other enzyme, MAPK signaling pathway, neurotrophin signaling pathway, amyotrophic lateral sclerosis (ALS), and Ras signaling pathway. The downregulated pathways involved cytokine-cytokine receptor interaction, fluid shear stress and atherosclerosis, TNF signaling pathway, chemokine signaling pathway, and Th1 and Th2 cell differentiation.

To validate the results of the mRNA microarray assay, quantitative RT-PCR analysis was performed. The experiment demonstrated that CXCL10, CCL12, and JUNB, which relate to the TNF signaling pathway, were down-regulated significantly by nicotine. Yet, maternal nicotine exposure upregulates BDNF expression in the juvenile offspring hippocampus. These data were mostly consistent with the results of the microarray analysis.

To gain insight into the inflammatory response modulated by nicotine in the hippocampal microenvironment, the expression levels of IL-4 and IL-1β were examined by quantitative RT-PCR (**Figure 3G**). Our data indicated that nicotine leaded to an increase in IL-4 (anti-inflammatory cytokine) ($t = 3.892$, $p = 0.0177$, $n = 3$) and a decrease in IL-1β (inflammatory cytokine) ($t = 3.485$, $p = 0.0252$, $n = 3$). These data suggested that maternal nicotine exposure mainly led to anti-inflammatory responses in the hippocampus of juvenile offspring.

Prenatal Nicotine Exposure Induced Significant Changes in Transcripts for Many Anti-Inflammatory Genes, as well as Those Related to Neurotransmitter and Synaptic-Associated Genes in Offspring

Selected transcripts associated with inflammatory response were shown (**Figure 3D**). Nicotine exposure significantly increased the expression of inflammatory-associated transcripts Fgr, A2m, Alox5ap, Phka1, and Il13ra2, while decreased expression of the inflammatory chemokine CXCL10, CCL12, CCL17, CXCR5. Selected representative genes, CXCL10, CCL12, JUNB, BDNF, were confirmed with RT-qPCR (**Figure 3F**). Taken together, these data show that nicotine exposure has contrasting effects on immune-associated transcripts. Transcripts associated with synaptic and neurotransmitter function were also shown (**Figure 3E**). Nicotine dramatically suppressed the expression of transient gene Arc in the juvenile offspring, which is implicated in several types of synaptic plasticity, including synaptic scaling, long-term potentiation, and long-term depression. On the other hand, nicotine significantly increased the transient gene

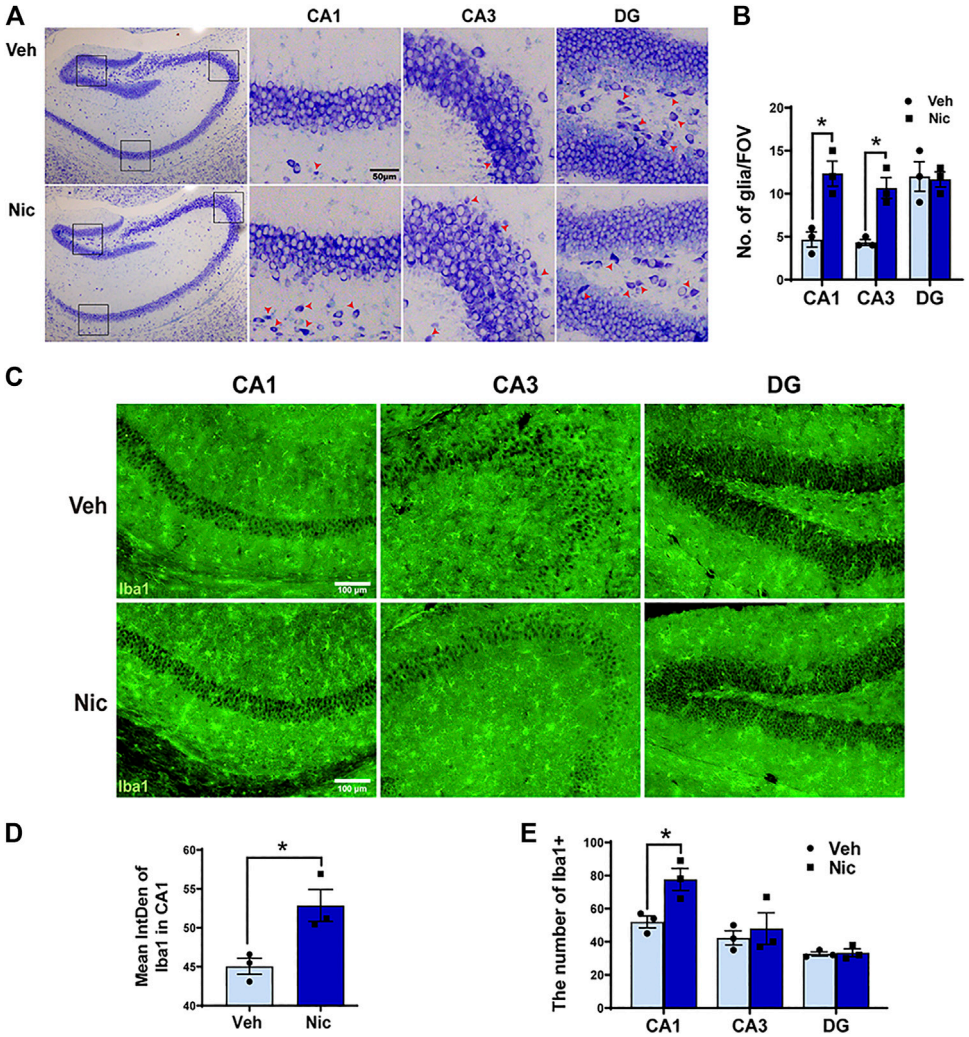

FIGURE 2 | Maternal nicotine exposure increased the number of neuroglia microglia, but not pyramidal neurons in the hippocampus of pups. (A) Photomicrograph showed the whole hippocampal sample in the coronal plane (two pictures on the left-most side). DG, CA1, and CA3 subfield are indicated by the black frame in the left-most image. Maternal nicotine exposure increased neuroglia (arrowhead) in DG, CA1, and CA3. **(B)** Neuroglial cells were quantified in the hippocampus. **(C)** Iba1-positive cells in the offspring' hippocampi were analyzed by immunofluorescence staining using floated section. The hippocampus of 20 day old offspring from the maternal nicotine-exposed group has more microglia cells (green) than the vehicle control. Representative images were shown. The quantification of immunofluorescence staining by ImageJ showed that the expression **(D)** and number **(E)** of Iba1 + cells increased obviously in the nicotine group. Scale bar: 50 μm (A); 100 μm (B); *$p < 0.05$, all data are means ± SEM.

BDNF. BDNF protein plays a critical role for the survival of neural cells after brain injury.

Nicotine Suppresses LPS-Induced Release of Inflammatory Cytokines in Primary Microglia Cells

To further validate the anti-inflammatory effects of nicotine, we used lipopolysaccharide (LPS)-stimulated primary microglia cultures to assess the anti-inflammatory effect of nicotine. Primary microglia were isolated and purified from postnatal day 2–4 mice cerebral cortices (**Figure 4A**). The purity of primary microglia was identified using immunofluorescent staining, and CD11b + or Iba1+ cells were marked as microglia (**Figure 4B**). Inflammatory response in microglia was evaluated by commercial cytokine arrays. Cytokine (**Figure 4C**) expression levels were represented by heat maps. LPS group up-regulated pro-inflammatory factors and down-regulated anti-inflammatory factors compared with blank control. Nicotine attenuated the elevated expression of pro-inflammatory factors (TNFα, IL-6, IL-10, KC, et al.), and the decreased expression of anti-inflammatory factors (IL-4, IL12, IL13, et al.) induced by LPS at 24 h, but had little influence at 12 h. Taken together, it indicates that nicotine exerts anti-inflammatory effects in LPS-induced inflammatory response. To validate the *in vivo* nicotine exposure in mice, we

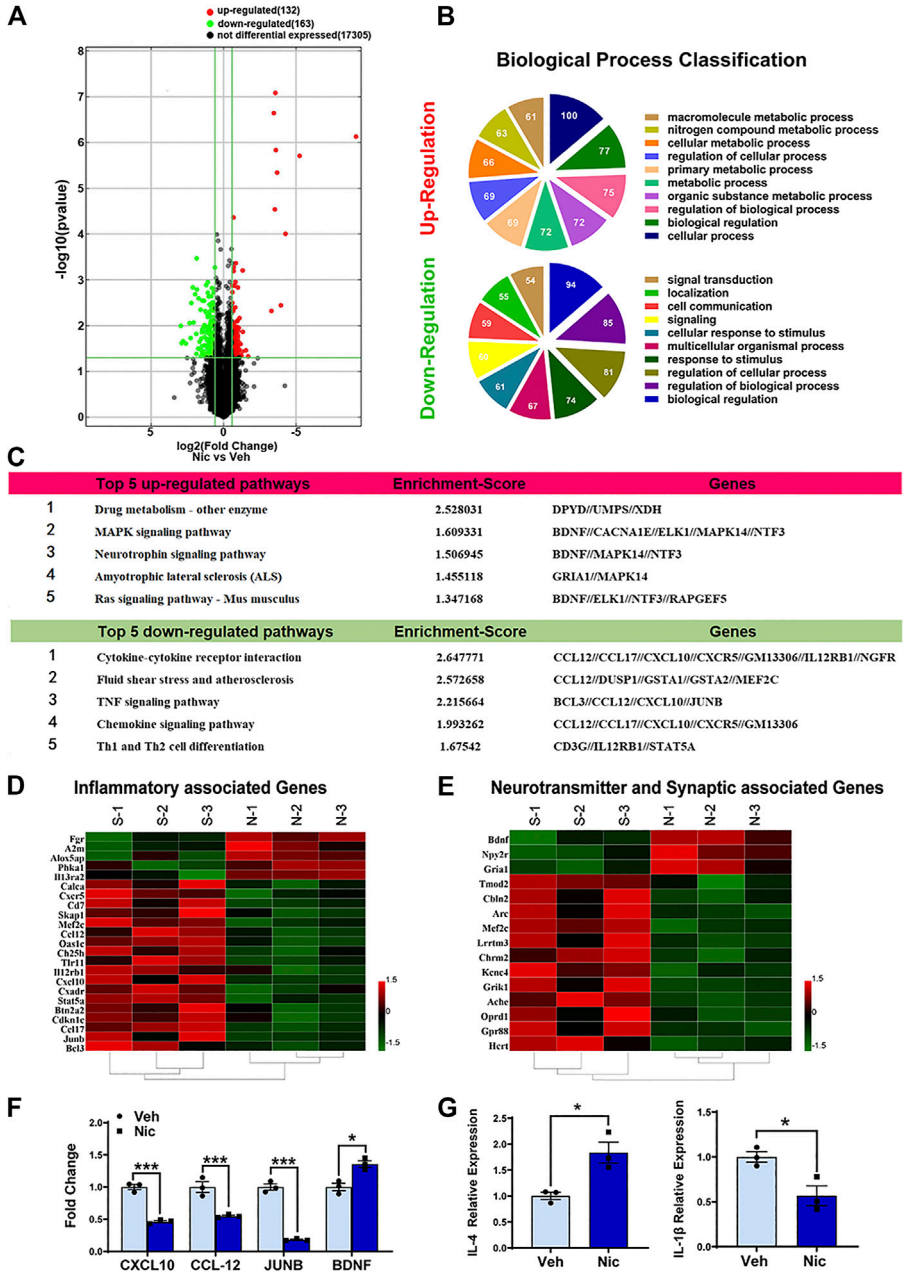

FIGURE 3 | Bioinformatic analysis of the expression profiles in 20 day old offspring' hippocampus. (A) The distribution of mRNA profiles was illustrated by volcano plots. There are 295 differentially expressed genes. "Red" indicates high relative expression, and "green" indicates low relative expression. **(B)** The pie chart showed the top 10 significant enrichment terms represented by the biological process. Larger sectors represent more significant enrichment. Varieties of biological functions were expressed differently after maternal nicotine exposure in the hippocampus of the PND20 mice, as compared to the vehicle control. **(C)** The top five upregulated and downregulated pathways in which hippocampus differentially expressed genes involved were listed. Hierarchical clustering heatmaps of inflammatory genes **(D)**, neurotransmitter, and synaptic associated genes **(E)** were generated using HEML software. **(F)** Confirmation of the microarray results, the expression of TNF and neurotrophin signaling pathway-related genes were validated by quantitative real-time PCR. **(G)** The representative genes of different inflammatory responses, IL-4 and IL-1β, were detected by quantitative real-time PCR. The columns represent the log-transformed median fold changes in expression relative to the vehicle group. *$p < 0.05$, all data are means ± SEM.

compared nicotine treatment relative to the blank with *in vitro* assay. Concentrations of cytokines (**Figure 4D**) in the group of nicotine treatment relative to the blank at 24 h were analyzed and shown in the bar graph. Nicotine down-regulated the pro-inflammatory factors and up-regulated the anti-inflammatory factors. These data suggest that nicotine promoted anti-inflammatory response by inhibiting the secretion of pro-inflammatory cytokines in microglia.

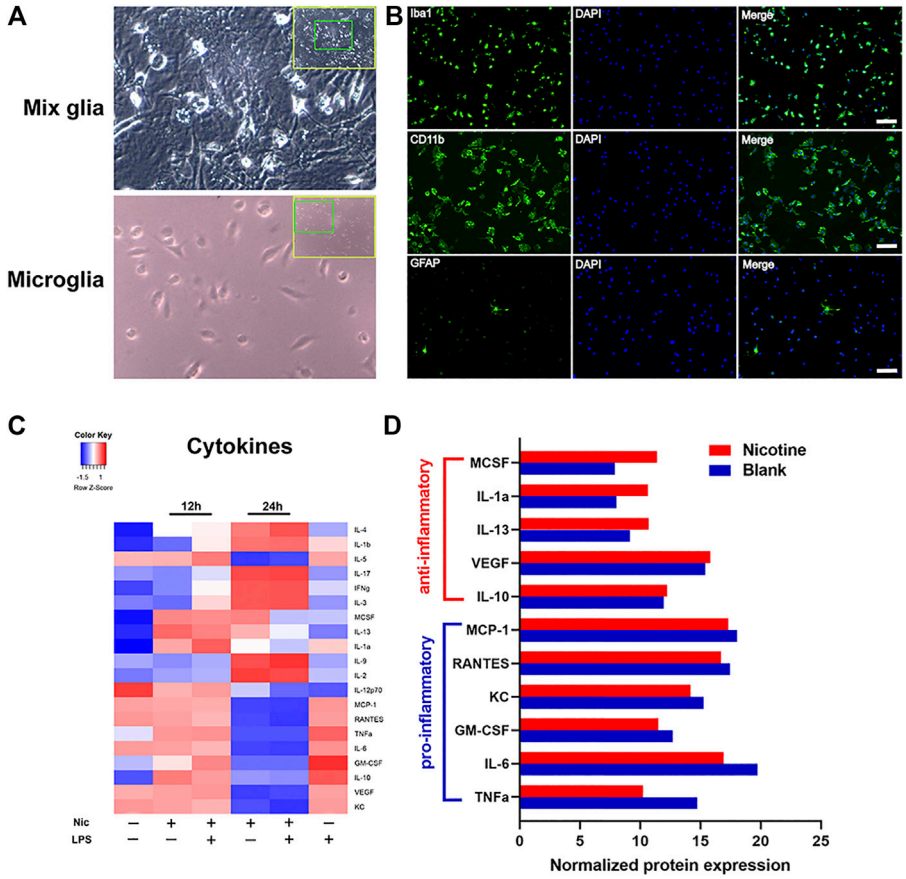

FIGURE 4 | Nicotine exposure suppressed inflammatory cytokine revealed by protein array. Primary microglia were isolated from postnatal day 2–4 mouse brain **(A)** and were identified by immunofluorescent staining with Iba1, CD11b, and GFAP antibody. Purified microglia were shown in **(B)**. GFAP positive astrocytes were found scarcely in the culture while the vast majority of cells were positive for Iba1 and CD11b staining. Unstimulated primary microglia were served as blank for each time point. LPS (10 μg/ml)-stimulated cells (LPS group), nicotine (10 μmol)-treated cells (nicotine group), and LPS (10 μg/ml) plus nicotine (10 μmol)-treated cells (LPS plus nicotine group) were used. Cells were pretreated with LPS 30 min before adding nicotine. Microglia cells incubated with LPS for 24 h were used as the pro-inflammatory control. Supernatant were collected at 12 and 24 h after treatment. Each group had duplicated wells. Pro-inflammatory and anti-inflammatory responses in microglia were evaluated by a commercial cytokine array. Cytokines expression levels were severally determined using a 20-array. Heat map representing cytokine concentrations was shown **(C)**. Quantitative analysis of cytokines secreted from primary microglia were presented in the graph **(D)**. Each group was duplicated, and the mean of the respective cytokine is represented in the heat map and the bar graph.

Maternal Nicotine Exposure Skewed the Polarity of Microglia to the M2 Phenotype in Juvenile Offspring

We next investigated whether nicotine promotes the expression of M2 microglia by examining their morphology. The hippocampus Iba1 + staining was shown (**Figure 5A**). The nicotine offspring presented an increase in the number of hippocampal Iba1+ cells fluorescent staining (t = 3.517, p = 0.0056, n = 6; **Figure 5B**) as compared to vehicle offspring. The hippocampus microglial cells of the vehicle offspring have a ramified shape with extensively branched processes. The cells of the nicotine offspring developed ameboid morphology characterized by cell body enlargement, decreased cell branching (t = 3.46, p = 0.0061, n = 6; **Figure 5C**) and shortened cell process lengths (t = 5.025, p = 0.0005, n = 6; **Figure 5D**). Taken together, these data demonstrate that nicotine promotes M2 microglial morphology in the hippocampus. To further determine the up-expression of hippocampal microglia-specific protein, the microglia-specific Iba1 protein was tested by western blot (**Figure 5E**). Consistently, an increase in Iba1 protein level was observed in the nicotine offspring (t = 2.549, p = 0.0289, n = 6; **Figure 5F**) as compared to that in vehicle control mice.

Nicotine Promoted Expression of BDNF in Hippocampal Microglia

To further characterize nicotine-induced changes to microglia, we measured the expression of Iba1 and BDNF by immunohistochemical staining. Iba1-positive cells were labeled with DAB (brown), and BDNF-positive cells were labeled with AP (red). There were more Iba1 + cells and BDNF + cells in the nicotine group (**Supplementary Figure S2**). Then we used double-labeling immunohistochemistry to detect the

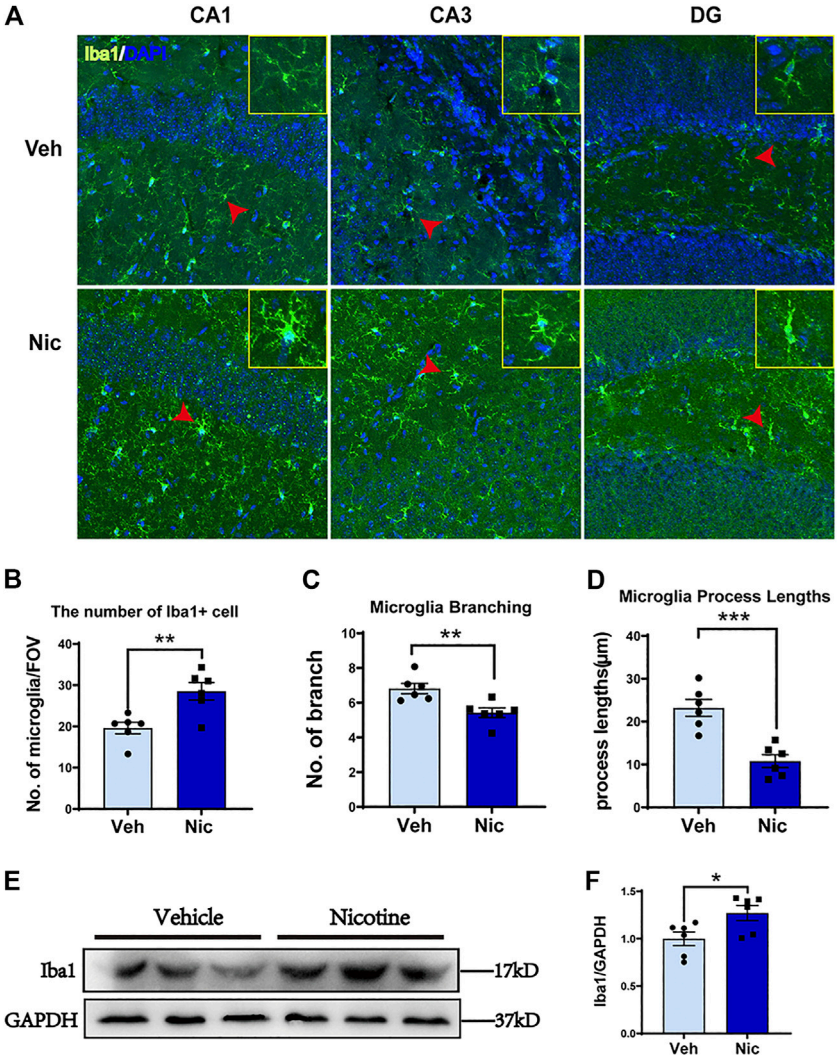

FIGURE 5 | Nicotine exposure increased the number of Iba1 positive microglial cells and promoted M2-like microglial polarization in the nicotine-exposed offspring's hippocampus. The morphology of microglia was detected by immunofluorescence staining. Representative images of the Iba1 expression in CA1, CA3, and DG were shown **(A)**. Olympus FV3000 Confocal Microscopy was used to get a Z-stack for 3-D reconstruction, and images showed that microglia cells changed their morphology from branching (in the control) to amoebic (in the nicotine-exposed group) in the offspring hippocampus. Nicotine exposure increased hippocampus microglial number **(B)**, but decreased microglial branching **(C)** and microglial process lengths **(D)**. CA1, CA3, and DG areas were used to generate the date presented in B-D. A point represented a calculated average of each measurement. **(E, F)** Iba1 protein level was increased in nicotine offspring revealed by western blot, as compared to vehicle offspring. *$p < 0.05$; **$p < 0.01$; ***$p < 0.001$; ****$p < 0.0001$. Scale bar = 50 μm all data are means ± SEM.

expression of microglia-derived BDNF. Magnification (×100) of representative the hippocampal coronal sections from the vehicle and nicotine group were shown, respectively, (**Figure 6A**, left). There were more Iba1+/BDNF− cells (colored with brown, pointed with blue arrowhead) and Iba1−/BDNF + cells (labeled with red, pointed with red arrow) in the hippocampus of the nicotine group. A large fraction of microglial cells were colocalized with BDNF (stained with red and brown) in CA1, CA3, and DG in nicotine offspring as pointed with yellow arrowhead and zoomed in the upper right frame of each image (**Figure 6A**). These data suggest that nicotine induced an increase in hippocampal microglia, mainly M2 state microglia, characterized by the production of BDNF. To further confirm the upregulation of BDNF, the BDNF protein in hippocampal tissue was tested by western blotting (**Figure 6B**). Consistently, an increase in BDNF protein level was observed in nicotine offspring ($t = 3.238$, $p = 0.0177$, $n = 4$) as compared to that in vehicle control mice (**Figure 6C**).

Maternal Nicotine Exposure Promoted Expressions of Neuronal Markers and Synaptic-Associated Protein in Offspring

To further determine whether nicotine influences neurons, we stained the neuron marker Tuj1 by immunohistochemical staining. Tuj1, neuron-specific class III β-tubulin in the

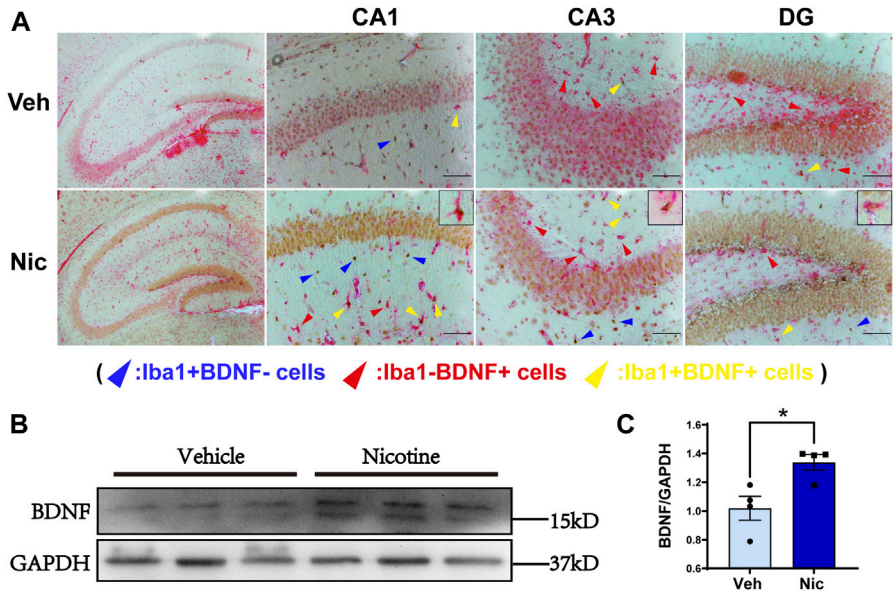

FIGURE 6 | Maternal nicotine increased the number of microglia Iba1 and BDNF double-positive staining cells. Low magnification (×100) of the hippocampal coronal sections of vehicle offspring and nicotine offspring (**A**, left) at postnatal day 20, respectively. Iba1-positive cells were marked with DAB (brown) and BDNF-positive cells were marked with AP (red). Increased number of Iba1-positive, BDNF-positive, and Iba1-positive BDNF-positive cells were observed in DG, CA1, CA3. The yellow arrowhead represents Iba1-positive BDNF-positive, the red arrowhead represents Iba1-negative BDNF-positive, and the blue arrowhead represents Iba1-positive BDNF-negative **(A)**. BDNF protein level was distinctly increased in nicotine offspring, as compared to vehicle offspring **(B, C)**. $^{**}p < 0.01$; Scale bar: 100 μm (A, B); 50 μm (C). all data are means ± SEM.

specific differentiation of neuronal cell types was labeled by immunohistochemical staining. One of the notable advantages of using immunohistochemistry to detect Tuj1 is its ability to show axon and terminal detail. Maternal nicotine exposure enhanced elongation of axons in ML (molecular layer), DG and CA1, but had no effect on axonal prolongation in CA3 (**Figure 7A**). The expression of NeuroD1, a potential regulator for terminal differentiation, neuronal maturation, and survival in the hippocampus, was tested by immunofluorescent staining (**Figure 7B**). The expression intensity of NeuroD1 positive cells were analyzed using ImageJ. Inversely, the fluorescence intensity of NeuroD1 decreased distinctly in the hippocampus ($t = 5.536$, $p = 0.0052$, $n = 3$) (**Figure 7C**), mainly including the intensities in CA1 ($t = 7.367$, $p = 0.0018$, $n = 3$) (**Figure 7D**) and CA3 ($t = 3.096$, $p = 0.0364$, $n = 3$) (**Figure 7E**), in nicotine group; The control group has greater NeuroD1 intensity in DG ($t = 1.676$, $p = 0.1691$, $n = 3$) compared to the nicotine group, but has no statistically significant difference. (**Figure 7F**). Then we examined synapse-associated proteins (GAD1 and PSD95) in the hippocampus by western blotting (**Figure 7G**). An increase in synaptic-associated protein level was observed in both PSD95 ($t = 3.232$, $p = 0.0179$, $n = 4$) and GAD1 ($t = 2.191$, $p = 0.071$, $n = 4$) (**Figure 7H**) in nicotine offspring as compared to that in vehicle control mice. These data indicated that nicotine induces the synaptic elongation except CA3 region, and promotes the expression of PSD95, there is no statistically significant difference in GAD1 levels between the control and nicotine group, but there is a trend of increase in GAD1 levels in the nicotine group.

DISCUSSION

Developmental nicotine exposure is associated with much neuronal dysplasia in offspring. Microglia play an important role throughout the development of the brain. However, it is not clear what role microglia plays in the hippocampal impairment caused by developmental nicotine exposure, and what is the effect of nicotine on the differentiation of neural stem cells in the hippocampus. This study is intended to establish a mouse model of maternal nicotine exposure and to explore nicotine-associated impairments on the polarization of hippocampal microglia, neurogenic differentiation, and behavior in juvenile offspring by using a variety of experimental methods. Firstly, our data showed that maternal nicotine exposure leads to offspring neurodevelopment delay and anxiety. Secondly, in the nicotine group, anti-inflammatory factors were up-regulated and proinflammatory factors were down-regulated, which is confirmed by *in vitro* experiment showing that nicotine promotes the secretion of anti-inflammatory cytokines in primary microglia. Thirdly, Maternal nicotine exposure induced the polarization of hippocampal microglia to M2, up-regulated BDNF, increase BDNF + microglia cells, but down-regulated NeuroD1. These data suggest that maternal exposure to nicotine polarized hippocampal microglia toward M2 and secreted BDNF, and microglia *via* anti-inflammatory cytokines and abnormal regulation of hippocampal neural progenitor cell differentiation can influence developmental disorders in offspring.

Nicotine is the major toxic substance in tobacco that causes mental and physical dependence. Oral nicotine administration *via*

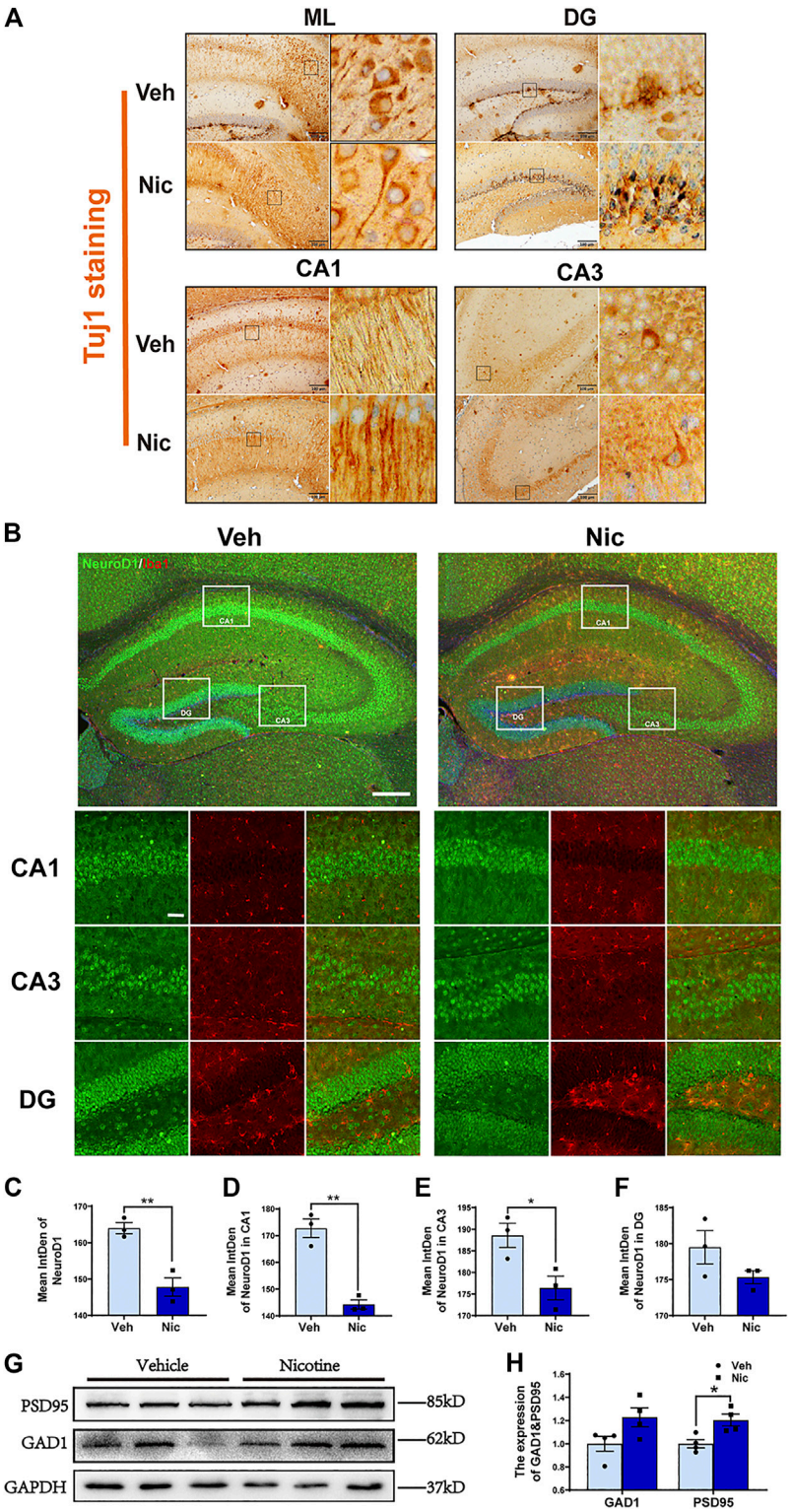

FIGURE 7 | Maternal nicotine exposure promoted elongation of axons and expression of the synaptic-associated protein in offspring. (A) Maternal nicotine exposure promoted elongation of axons in ML, DG and CA1, but did not affect on axonal prolongation in CA3. **(B)** NeuroD1-positive cells in the offspring' hippocampi were analyzed by immunofluorescence staining. Representative images were shown. **(C)** The quantification of fluorescence intensity by ImageJ showed that the immunofluorescence intensity of NeuroD1 decreased obviously in the hippocampus of the nicotine group, including in CA1 **(D)** and CA3 **(E)** not in DG **(F)**. **(G)** Western blot analysis of the activation of PSD95 and GAD1 in the hippocampus of the offspring. **(H)** PSD95 protein level was increased in nicotine offspring as compared to vehicle offspring. There is no difference in GAD1 between nicotine and vehicle treatment. *$p < 0.05$, **$p < 0.01$; Scale bar:200 μm (A); 200 μm (low power lens), 50 μm (high power lens) (B). all data are means ± SEM.

drinking water has been used in various experiments, such as addiction, withdrawal, and toxicity. The 200 μg/ml nicotine in drinking can produce 100–200 ng/ml blood plasma cotinine, which is equal to the plasma cotinine level of a moderate smoker (Lawson et al., 1998; Mojica et al., 2018). Moreover, the nicotine level in breast milk is even higher than that in the blood, and nicotine in breast milk can be absorbed through the placenta and lactation angiogenesis and cause anxiety-like behavior in offspring (Matta et al., 2007; Karimiankakolaki et al., 2019). Smoking or nicotine exposure during pregnancy is associated with low birth weight (Knopik et al., 2016b; Zeng et al., 2020), which is consistent with the findings of our study. However, during development, the weight gain does not show significant differences between nicotine offspring and vehicle ones. These differences may be a result of fetal tissue hypoxia, intrauterine growth restriction before birth, but the adverse intrauterine environment disappeared without an obvious discrepancy in body weight following birth. Nicotine exposure during pregnancy could lead to adverse effects on neurobehavioral in offspring, such as increased anxiety, depression-like behavior, postnatal hyperactivity, cognitive impairment, severe mental illness disorders et al. (Alkam et al., 2013; Quinn et al., 2017). Similarly, delayed development of eye-opening, auditory startle, and olfactory reflex after birth, as well as anxiety-like behavior presented in the OFT on PND 20 in nicotine juvenile offspring greatly support developmental neurotoxicity of nicotine. Four mice in the vehicle group spent over ~80% of their time during OFT in the center zone, this might result from individual differences.

We acknowledge that the gender-specific difference in nicotine's effects on the brain and behavior during the perinatal period has been reported previously in mice (Zhang et al., 2018; Martin et al., 2020). However, when analyzing spontaneous locomotor, hippocampal RNA expression, and neuroinflammation, and the neuronal marker, and focusing on postnatal day 20 when mice were not sexually mature, we did not perform gender-difference analysis upon nicotine's effect. Firstly because, sex hormones in the male and female hippocampus fluctuated from P0 to P21 (Zuloaga et al., 2014) and increased from as early as embryonic period day 11(E11), and up until postnatal day 21(P21) (Franklin et al., 2019). Secondly, the study of Single-cell RNA Sequencing of microglia revealed nine unique clusters of microglial at three major developmental ages of mice, E14.5, P4/P5, and P100, but does not find any differences in the transcriptomes among males and females mice (Hammond et al., 2019). In this experiment, subjects in each group contain an equal number of males and females, which would not largely impact chronic developmental nicotine exposure on microglia phenotype and function in this study.

To date, microarrays have been extensively used to examine changes in gene expression. Very few studies examine changes of gene expression in the hippocampus induced by nicotine using microarray. We provided the first evidence that a large number of mRNAs related to inflammatory cytokines and chemokines were differentially expressed in developing hippocampus following maternal nicotine exposure. Nicotine juvenile offspring express a different inflammatory-associated transcriptional profile in the hippocampus, as indicated by a decrease in expression of pro-inflammatory chemokines/cytokines and an increased expression of anti-inflammatory chemokines/cytokines. A balance of the pro- and anti-inflammatory response is needed to maintain homeostasis of the CNS. Pro-inflammatory chemokine, such as IFN-γ-induced protein 10 (IP-10, also known as CXCL10), as a classical pro-inflammatory M1 marker (Lescoat et al., 2020), was greatly downregulated following nicotine exposure (Shaykhiev et al., 2009). Anti-inflammatory cytokine IL-4, a multifunctional cytokine, was upregulated in the hippocampus of nicotine offspring and has been reported involved in the regulation of inflammatory responses of the CNS (Zhao et al., 2015). IL-4 in the hippocampus drove M2 microglia to promote neurogenesis, which attenuated depressive-like behaviors (Zhang et al., 2021). Together, these data suggest that nicotine suppresses the M1 response or even tilt the phenotype toward M2.

With chemokines and cytokines alteration, nicotine also alters expression levels of transcripts regulating neurotransmitter release and synaptic function. There are several up-regulated genes within the hippocampus, such as BDNF, NPY2R, and Gria1, and downregulated genes such as Arc, which are well known in the neural plasticity and pathogenesis of central nervous disease and abnormal behavior. In line with this, recent studies also report that increased BDNF expression in the hippocampus is associated with anxiolytic effects (Ma et al., 2017; Onodera et al., 2020). Neurotransmitter receptors on microglia (Lee, 2013) can be activated, and in return modulate pro- and anti-inflammatory function. BDNF, a main member of the neurotrophin family, regulates many neuronal functions including cell differentiation, cell survival, neurotransmission release, and synaptic plasticity. Nicotine exposure enhances the expression of BDNF both *in vivo* and *in vitro* (Lang et al., 2007; Guo et al., 2020). Similarly, BDNF was significantly upregulated in the hippocampus of nicotine offspring, and colocalized with M2-like microglia showed in our data.

Maternal nicotine exposure promotes M2-like polarization of microglia in juvenile offspring. M2-like polarization of microglia cells express and secrete BDNF, attenuate localized inflammation, actively involved in self-tissue repair and coping with adverse intrauterine consequences of offspring after long-term chronic nicotine exposure (Damborsky and Winzer-Serhan, 2012). Moreover, BDNF has been shown to support microglial activation *in vivo* (Jiang et al., 2011), which could lead to microgliosis and amplification of neuroinflammation. Nicotine exposure during pregnancy can impair immune response. Microglia are macrophage-like resident immune cells of the CNS combating infection, clearing cellular debris, and maintaining tissue homeostasis. When the immune system is challenged and microglia are activated, the activated microglia have the potential to function in either a neurodegenerative or a neuroprotective way (Ueno et al., 2013). Some latest investigations suggest that microglia can be activated into a classic activated state (M1 state) or selectively activated state (M2 state) (Ju et al., 2015; Wehrspaun et al., 2015). In the M1 state, activated microglial cells produce proinflammatory cytokines, which are considered to be detrimental; In contrast, activated microglial cells of the M2 state secrete anti-inflammatory cytokines and neurotrophins, including IL-4, BDNF, and glial cell-derived neurotrophic factor (GDNF), which are regarded to be beneficial. The increase in Iba1+/BDNF+ cells within the hippocampus was examined by immunohistochemical staining in our study which confirms that nicotine exposure skews the polarity of microglia to the

M2 phenotype, All together these data show that nicotine exposure induces microglia to convert to M2-type cells.

Microglia activation affects both the structural and functional properties of neurons. In response to injury, neurons could produce adhesion molecules and trophic factors that recruit and activate microglial cells and astrocytes (Ramesh et al., 2013). Microglia have been revealed to be active participants in complex neurodevelopmental programs such as neurogenesis and synaptic pruning, in which they interact with neurons and glia to provide nutritional support, respond to cytokine (Cowan and Petri, 2018). Synaptic pruning is a part of the normal developmental process of the brain, occurring at frequent levels in the first weeks after birth. Microglia constantly scan neurons by extending and contracting processes, all the while signaling with neurons and actively maintaining the health of synapses (Zelikoff et al., 2018b). However, the present study and previous studies (Andoh et al., 2020; Iovino et al., 2020) showed that disruption of synaptic pruning by abnormally activated microglia may contribute to cognitive impairment, neurodegenerative diseases, and anxiety-like behavior.

Maternal nicotine exposure affects the maturity and difference of neurons. Neurite outgrowth is a basic process for neurobehavior that involves neuronal differentiation and migration during brain development, which is essential for the communication of the nervous system (Vernes et al., 2011). *In vitro* experiment on brain organic chip model showed that the group treated with low-dose nicotine increased neurite length, suggesting that nicotine at a low concentration triggers a neuronal outgrowth. In contrast, the group treated with high-dose nicotine reduced neurite length, which indicated a disturbed neurite outgrowth (Wang et al., 2018). Tuj1 is a marker of immature neurons, differentiation, and migration, which was revealed to exist in immature neuronal cell bodies, dendrites, axons, and axon terminals (Moon et al., 2019). Likewise, in our study, maternal nicotine exposure increases Tuj1 positive neurite length in ML and CA1. NeuroD1 is principally expressed in the nervous system late in development and is, therefore, more likely to be involved in terminal differentiation, neuronal maturation, and survival (Gaudillière et al., 2004). Furthermore, NeuroD1 was capable of reprogramming neuroglia into functional neurons, which may provide a potential therapeutic approach to restore lost neuronal function in the injured or diseased brain. Therefore, we hypothesized that maternal nicotine exposure was able to stimulate the extension of immature neuronal neurite and over-expression of synapse-associated proteins, but inhibited neuronal maturation and survival by reducing the expression of NeuroD1.

Pharmacological modulation of functional phenotypes of microglia has shown to be a promising cell-based regenerative strategy for neurological diseases (Papa et al., 2016; Song and Suk, 2017). Particular attention is given to utilizing M2 microglial polarization as a potential therapeutic option during the recovery phase (Cherry et al., 2014; Yao and Zu, 2020). For instance, M2-like microglia preserve myelin homeostasis after white matter integrity (WMI) in traumatic brain injury (Wang et al., 2015). M2 microglia obtained by IL-4 stimulation, used for cell transplantation therapy for spinal cord injury, have significantly higher scores for spinal cord injury when compared with systemic administration of IL-4 (Kobashi et al., 2020). IL4-driven microglia phenotypic shift modulated hippocampal neurogenesis and stress in a BDNF-dependent manner (Zhang et al., 2021). The protective mechanisms exerted by M2 microglia to treat CNS injury have also been discussed in recent review articles (Tang and Le, 2016; Du et al., 2017). The treatment polarizing microglia subpopulation toward different phenotypes at different stages of injury might account for future study because microglia polarization has pros and cons (Hu et al., 2015). Based on our finding, M2 microglia-induced therapy in combination with BDNF can be a potential therapeutic strategy for the treatment of neurodevelopmental disorders caused by early life nicotine exposure.

The present study is the first to explore the effects of maternal nicotine exposure on the hippocampal transcriptome and the polarized status of hippocampal microglia in juvenile offspring, as well as the potential roles BDNF playing in the process. The anti-inflammation cytokine and chemokine from microglia induced in the hippocampus of nicotine offspring maybe a kind of protective traumatic stress response. Microglia play a key role in maternal nicotine exposure affecting neurodevelopment in juvenile offspring which would be an interesting study in the future.

DATA AVAILABILITY STATEMENT

The datasets presented in this study can be found in online repositories. The names of the repository/repositories and accession number(s) can be found in the article/**Supplementary Material**.

ETHICS STATEMENT

The animal study was reviewed and approved by the Anhui University of Science and Technology.

AUTHOR CONTRIBUTIONS

XT and GP conceived and designed this experiment. LZ, QS, FL, YH, BL, and KX performed the experiment, collected data, and drafted this article. MM and HT analyzed the data.

FUNDING

This work was supported by the National Natural Science Foundation in China, (81471161), Top Talent Project of Anhui Department of Education (gxbjZD16), Natural Science Foundation of Anhui Province (1808085MH247), and Graduate Student Innovation Fund (2019CX 2069).

SUPPLEMENTARY MATERIAL

The Supplementary Material for this article can be found online at: https://www.frontiersin.org/articles/10.3389/fphar.2021.661304/full#supplementary-material

REFERENCES

Alkam, T., Kim, H.-C., Mamiya, T., Yamada, K., Hiramatsu, M., and Nabeshima, T. (2013). Evaluation of Cognitive Behaviors in Young Offspring of C57BL/6J Mice after Gestational Nicotine Exposure during Different Time-Windows. *Psychopharmacology* 230 (3), 451–463. doi:10.1007/s00213-013-3175-9

Andoh, M., Ikegaya, Y., and Koyama, R. (2020). Microglia in Animal Models of Autism Spectrum Disorders. *Prog. Mol. Biol. translational Sci.* 173, 239–273. doi:10.1016/bs.pmbts.2020.04.012

Azam, L., Chen, Y., and Leslie, F. M. (2007). Developmental Regulation of Nicotinic Acetylcholine Receptors within Midbrain Dopamine Neurons. *Neuroscience* 144 (4), 1347–1360. doi:10.1016/j.neuroscience.2006.11.011

Berry, A., Bindocci, E., and Alleva, E. (2012). NGF, Brain and Behavioral Plasticity. *Neural plasticity* 2012, 1–9. doi:10.1155/2012/784040

Buck, J. M., O'Neill, H. C., and Stitzel, J. A. (2019). Developmental Nicotine Exposure Elicits Multigenerational Disequilibria in proBDNF Proteolysis and Glucocorticoid Signaling in the Frontal Cortices, Striata, and Hippocampi of Adolescent Mice. *Biochem. Pharmacol.* 168, 438–451. doi:10.1016/j.bcp.2019.08.003

Chen, H.-j., Li, G.-l., Zhang, W.-x., Fan, J., Hu, L., Zhang, L., et al. (2020). Maternal Nicotine Exposure during Pregnancy and Lactation Induces Brown Adipose Tissue Whitening in Female Offspring. *Toxicol. Appl. Pharmacol.* 409, 115298. doi:10.1016/j.taap.2020.115298

Cherry, J. D., Olschowka, J. A., and O'Banion, M. (2014). Neuroinflammation and M2 Microglia: the Good, the Bad, and the Inflamed. *J. neuroinflammation* 11, 98. doi:10.1186/1742-2094-11-98

Cowan, M., and Petri, W. A. (2018). Microglia: Immune Regulators of Neurodevelopment. *Front. Immunol.* 9, 2576. doi:10.3389/fimmu.2018.02576

Dai, H., and Leventhal, A. M. (2019). Prevalence of E-Cigarette Use Among Adults in the United States, 2014-2018, *JAMA* 322(18), 1824–1827. doi:10.1001/jama.2019.15331

Damborsky, J. C., and Winzer-Serhan, U. H. (2012). Effects of Sex and Chronic Neonatal Nicotine Treatment on Na2+/K+/Cl− Co-transporter 1, K+/Cl− Co-transporter 2, Brain-Derived Neurotrophic Factor, NMDA Receptor Subunit 2A and NMDA Receptor Subunit 2B mRNA Expression in the Postnatal Rat hippocampus. *Neuroscience* 225, 105–117. doi:10.1016/j.neuroscience.2012.09.002

Ding, H., Chen, J., Su, M., Lin, Z., Zhan, H., Yang, F., et al. (2020). BDNF Promotes Activation of Astrocytes and Microglia Contributing to Neuroinflammation and Mechanical Allodynia in Cyclophosphamide-Induced Cystitis. *J. Neuroinflammation* 17 (1), 19. doi:10.1186/s12974-020-1704-0

Du, L., Zhang, Y., Chen, Y., Zhu, J., Yang, Y., and Zhang, H.-L. (2017). Role of Microglia in Neurological Disorders and Their Potentials as a Therapeutic Target. *Mol. Neurobiol.* 54 (10), 7567–7584. doi:10.1007/s12035-016-0245-0

Franklin, M., Armoskus, C., Taniguchi, S., Moder, C., Trang, K., Santacruz, M., et al. (2019). Androgenic Regulation of Sexually Dimorphic Expression of RNA Binding Motif Protein 48 in the Developing Mouse Cortex and hippocampus. *Int. J. Dev. Neurosci.* 78, 33–44. doi:10.1016/j.ijdevneu.2019.07.011

Gaudillière, B., Konishi, Y., de la Iglesia, N., Yao, G.-l., and Bonni, A. (2004). A CaMKII-NeuroD Signaling Pathway Specifies Dendritic Morphogenesis. *Neuron* 41 (2), 229–241. doi:10.1016/s0896-6273(03)00841-9

Gold, A. B., Keller, A. B., and Perry, D. C. (2009). Prenatal Exposure of Rats to Nicotine Causes Persistent Alterations of Nicotinic Cholinergic Receptors. *Brain Res.* 1250, 88–100. doi:10.1016/j.brainres.2008.10.076

Golding, J., Ellis, G., Gregory, S., Birmingham, K., Iles-Caven, Y., Rai, D., et al. (2017). Grand-maternal Smoking in Pregnancy and Grandchild's Autistic Traits and Diagnosed Autism. *Sci. Rep.* 7, 46179. doi:10.1038/srep46179

Guerby, P., Garabedian, C., Berveiller, P., Legendre, G., Grangé, G., and Berlin, I. (2020). Tobacco and Nicotine Cessation during Pregnancy. *Obstet. Gynecol.* 136 (2), 428–429. doi:10.1097/AOG.0000000000004033

Guo, L., Zhang, Y., Lv, Q., and Zhang, Z. (2020). Nicotine Induces P2X4 Receptor, Interleukin-1 Beta, and Brain-Derived Neurotrophic Factor Expression in BV2 Microglia Cells. *Neuroreport* 31 (18), 1249–1255. doi:10.1097/wnr.0000000000001546

Hammond, T. R., Dufort, C., Dissing-Olesen, L., Giera, S., Young, A., Wysoker, A., et al. (2019). Single-Cell RNA Sequencing of Microglia throughout the Mouse Lifespan and in the Injured Brain Reveals Complex Cell-State Changes. *Immunity* 50 (1), 253–271. e256. doi:10.1016/j.immuni.2018.11.004

Han, X., Zhou, N., Hu, H., Li, X., and Liu, H. (2020). Nicotine Alleviates Cortical Neuronal Injury by Suppressing Neuroinflammation and Upregulating Neuronal PI3K-AKT Signaling in an Eclampsia-like Seizure Model. *Neurotox Res.* 38, 665–681. doi:10.1007/s12640-020-00265-2

He, X., Lu, J., Dong, W., Jiao, Z., Zhang, C., Yu, Y., et al. (2017). Prenatal Nicotine Exposure Induces HPA Axis-Hypersensitivity in Offspring Rats via the Intrauterine Programming of Up-Regulation of Hippocampal GAD67. *Arch. Toxicol.* 91 (12), 3927–3943. doi:10.1007/s00204-017-1996-8

Hu, X., Leak, R. K., Shi, Y., Suenaga, J., Gao, Y., Zheng, P., et al. (2015). Microglial and Macrophage Polarization-New Prospects for Brain Repair. *Nat. Rev. Neurol.* 11 (1), 56–64. doi:10.1038/nrneurol.2014.207

Huang, L., Wang, Y., Zhang, L., Zheng, Z., Zhu, T., Qu, Y., et al. (2018). Maternal Smoking and Attention-Deficit/Hyperactivity Disorder in Offspring: A Meta-Analysis. *Pediatrics* 141 (1), e20172465. doi:10.1542/peds.2017-2465

Iovino, L., Tremblay, M. E., and Civiero, L. (2020). Glutamate-induced Excitotoxicity in Parkinson's Disease: The Role of Glial Cells. *J. Pharmacol. Sci.* 144, 151–164. doi:10.1016/j.jphs.2020.07.011

Jamshed, L., Perono, G. A., Jamshed, S., and Holloway, A. C. (2020). Early Life Exposure to Nicotine: Postnatal Metabolic, Neurobehavioral and Respiratory Outcomes and the Development of Childhood Cancers. *Toxicol. Sci. : official J. Soc. Toxicol.* 178, 3–15. doi:10.1093/toxsci/kfaa127

Jian, J., Zhang, P., Li, Y., Liu, B., Zhang, Y., Zhang, L., et al. (2020). Reprogramming of miR-181a/DNA Methylation Patterns Contribute to the Maternal Nicotine Exposure-Induced Fetal Programming of Cardiac Ischemia-Sensitive Phenotype in Postnatal Life. *Theranostics* 10 (25), 11820–11836. doi:10.7150/thno.48297

Jiang, N. M., Cowan, M., Moonah, S. N., and Petri, W. A. (2018). The Impact of Systemic Inflammation on Neurodevelopment. *Trends Molecular Medicine* 24 (9), 794–804. doi:10.1016/j.molmed.2018.06.008

Jiang, Y., Wei, N., Lu, T., Zhu, J., Xu, G., and Liu, X. (2011). Intranasal Brain-Derived Neurotrophic Factor Protects Brain from Ischemic Insult via Modulating Local Inflammation in Rats. *Neuroscience* 172, 398–405. doi:10.1016/j.neuroscience.2010.10.054

Ju, L., Zeng, H., Chen, Y., Wu, Y., Wang, B., and Xu, Q. (2015). Dual Polarization of Microglia Isolated from Mixed Glial Cell Cultures. *J. Neurosci. Res.* 93 (9), 1345–1352. doi:10.1002/jnr.23563

Kapaya, M., D'Angelo, D. V., Tong, V. T., England, L., Ruffo, N., Cox, S., et al. (2019). Use of Electronic Vapor Products before, during, and after Pregnancy Among Women with a Recent Live Birth - Oklahoma and Texas, 2015. *MMWR Morb. Mortal. Wkly. Rep.* 68 (8), 189–194. doi:10.15585/mmwr.mm6808a1

Karimiankakolaki, Z., Mazloomy Mahmoodabad, S. S., Kazemi, A., and Fallahzadeh, H. (2019). Designing an Educational Intervention on Second-Hand Smoke in Smoker Men on the Exposure of Pregnant Wives: a Protocol for a Randomized Controlled Trial. *Reprod. Health* 16 (1), 11. doi:10.1186/s12978-019-0673-1

King, E., Campbell, A., Belger, A., and Grewen, K. (2018). Prenatal Nicotine Exposure Disrupts Infant Neural Markers of Orienting. *Nicotine Tob. Res.* 20 (7), 897–902. doi:10.1093/ntr/ntx177

Knopik, V. S., Marceau, K., Bidwell, L. C., Palmer, R. H. C., Smith, T. F., Todorov, A., et al. (2016a). Smoking during Pregnancy and ADHD Risk: A Genetically Informed, Multiple-Rater Approach. *Am. J. Med. Genet.* 171 (7), 971–981. doi:10.1002/ajmg.b.32421

Knopik, V. S., Marceau, K., Palmer, R. H. C., Smith, T. F., and Heath, A. C. (2016b). Maternal Smoking during Pregnancy and Offspring Birth Weight: A Genetically-Informed Approach Comparing Multiple Raters. *Behav. Genet.* 46 (3), 353–364. doi:10.1007/s10519-015-9750-6

Kobashi, S., Terashima, T., Katagi, M., Nakae, Y., Okano, J., Suzuki, Y., et al. (2020). Transplantation of M2-Deviated Microglia Promotes Recovery of Motor Function after Spinal Cord Injury in Mice. *Mol. Ther.* 28 (1), 254–265. doi:10.1016/j.ymthe.2019.09.004

Lang, U. E., Sander, T., Lohoff, F. W., Hellweg, R., Bajbouj, M., Winterer, G., et al. (2007). Association of the Met66 Allele of Brain-Derived Neurotrophic Factor (BDNF) with Smoking. *Psychopharmacology* 190 (4), 433–439. doi:10.1007/s00213-006-0647-1

Lawson, G. M., Hurt, R. D., Dale, L. C., Offord, K. P., Croghan, I. T., Schroeder, D. R., et al. (1998). Application of Serum Nicotine and Plasma Cotinine

Concentrations to Assessment of Nicotine Replacement in Light, Moderate, and Heavy Smokers Undergoing Transdermal Therapy. *J. Clin. Pharmacol.* 38 (6), 502–509. doi:10.1002/j.1552-4604.1998.tb05787.x

Lee, M. (2013). Neurotransmitters and Microglial-Mediated Neuroinflammation. *Cpps* 14 (1), 21–32. doi:10.2174/1389203711314010005

Lee, S. Y., Sirieix, C. M., Nattie, E., and Li, A. (2018). Pre- and Early Postnatal Nicotine Exposure Exacerbates Autoresuscitation Failure in Serotonin-Deficient Rat Neonates. *J. Physiol.* 596 (23), 5977–5991. doi:10.1113/jp275885

Lescoat, A., Lelong, M., Jeljeli, M., Piquet-Pellorce, C., Morzadec, C., Ballerie, A., et al. (2020). Combined Anti-fibrotic and Anti-inflammatory Properties of JAK-Inhibitors on Macrophages In Vitro and In Vivo: Perspectives for Scleroderma-Associated Interstitial Lung Disease. *Biochem. Pharmacol.* 178, 114103. doi:10.1016/j.bcp.2020.114103

Leventhal, A. M., Waters, A. J., Boyd, S., Moolchan, E. T., Lerman, C., and Pickworth, W. B. (2007). Gender Differences in Acute Tobacco Withdrawal: Effects on Subjective, Cognitive, and Physiological Measures. *Exp. Clin. Psychopharmacol.* 15 (1), 21–36. doi:10.1037/1064-1297.15.1.21

Li, X., Han, X., Bao, J., Liu, Y., Ye, A., Thakur, M., et al. (2016). Nicotine Increases Eclampsia-like Seizure Threshold and Attenuates Microglial Activity in Rat hippocampus through the α7 Nicotinic Acetylcholine Receptor. *Brain Res.* 1642, 487–496. doi:10.1016/j.brainres.2016.04.043

Lopez, A. A., Redner, R., Kurti, A. N., Keith, D. R., Villanti, A. C., Stanton, C. A., et al. (2018). Tobacco and Nicotine Delivery Product Use in a U.S. National Sample of Women of Reproductive Age. *Prev. Med.* 117, 61–68. doi:10.1016/j.ypmed.2018.03.001

Lv, J., Mao, C., Zhu, L., Zhang, H., Pengpeng, H., Xu, F., et al. (2008). The Effect of Prenatal Nicotine on Expression of Nicotine Receptor Subunits in the Fetal Brain. *Neurotoxicology* 29 (4), 722–726. doi:10.1016/j.neuro.2008.04.015

Ma, J., Wang, F., Yang, J., Dong, Y., Su, G., Zhang, K., et al. (2017). Xiaochaihutang Attenuates Depressive/anxiety-like Behaviors of Social Isolation-Reared Mice by Regulating Monoaminergic System, Neurogenesis and BDNF Expression. *J. ethnopharmacology* 208, 94–104. doi:10.1016/j.jep.2017.07.005

Maleszewska, M., Steranka, A., Smiech, M., Kaza, B., Pilanc, P., Dabrowski, M., et al. (2020). Sequential Changes in Histone Modifications Shape Transcriptional Responses Underlying Microglia Polarization by Glioma. *Glia* 69, 109–123. doi:10.1002/glia.23887

Marceau, K., Cinnamon Bidwell, L., Karoly, H. C., Evans, A. S., Todorov, A. A., Palmer, R. H., et al. (2018). Within-Family Effects of Smoking during Pregnancy on ADHD: the Importance of Phenotype. *J. Abnorm Child. Psychol.* 46 (4), 685–699. doi:10.1007/s10802-017-0320-7

Mark, K. S., Farquhar, B., Chisolm, M. S., Coleman-Cowger, V. H., and Terplan, M. (2015). Knowledge, Attitudes, and Practice of Electronic Cigarette Use Among Pregnant Women. *J. Addict. Med.* 9 (4), 266–272. doi:10.1097/adm.0000000000000128

Martin, M. M., McCarthy, D. M., Schatschneider, C., Trupiano, M. X., Jones, S. K., Kalluri, A., et al. (2020). Effects of Developmental Nicotine Exposure on Frontal Cortical GABA-To-Non-GABA Neuron Ratio and Novelty-Seeking Behavior. *Cereb. Cortex* 30 (3), 1830–1842. doi:10.1093/cercor/bhz207

Matta, S. G., Balfour, D. J., Benowitz, N. L., Boyd, R. T., Buccafusco, J. J., Caggiula, A. R., et al. (2007). Guidelines on Nicotine Dose Selection for In Vivo Research. *Psychopharmacology* 190 (3), 269–319. doi:10.1007/s00213-006-0441-0

McAlinden, K., Naidu, V., Sohal, S., and Sharma, P. (2020). In Utero Exposure to Nicotine Containing Electronic Cigarettes Increases the Risk of Allergic Asthma in Female Offspring. *Am. J. Physiol. Lung Cell. Mol. Physiol.* doi:10.1152/ajplung.00230.2019

Mead, E. L., Cruz-Cano, R., Groom, A., Hart, J. L., Walker, K. L., Giachello, A. L., et al. (2019). Responses to Cigarette Health Warning Labels, Harm Perceptions and Knowledge in a National Sample of Pregnant and Non-pregnant Women of Reproductive Age. *Addict. behaviors* 90, 10–13. doi:10.1016/j.addbeh.2018.10.013

Miranda, R. A., de Moura, E. G., Soares, P. N., Peixoto, T. C., Lopes, B. P., de Andrade, C. B. V., et al. (2020). Thyroid Redox Imbalance in Adult Wistar Rats that Were Exposed to Nicotine during Breastfeeding. *Sci. Rep.* 10 (1), 15646. doi:10.1038/s41598-020-72725-w

Mojica, C., Bai, Y., and Lotfipour, S. (2018). Maternal Nicotine Exposure Effects on Adolescent Learning and Memory Are Abolished in Alpha(α)2* Nicotinic Acetylcholine Receptor-Null Mutant Mice. *Neuropharmacology* 135, 529–535. doi:10.1016/j.neuropharm.2018.04.010

Moon, H. Y., Javadi, S., Stremlau, M., Yoon, K. J., Becker, B., Kang, S.-U., et al. (2019). Conditioned Media from AICAR-Treated Skeletal Muscle Cells Increases Neuronal Differentiation of Adult Neural Progenitor Cells. *Neuropharmacology* 145, 123–130. doi:10.1016/j.neuropharm.2018.10.041

Morgane, P. J., Austin-LaFrance, R., Bronzino, J., Tonkiss, J., Díaz-Cintra, S., Cintra, L., et al. (1993). Prenatal Malnutrition and Development of the Brain. *Neurosci. Biobehavioral Rev.* 17 (1), 91–128. doi:10.1016/s0149-7634(05)80234-9

Nakayama, A., Yoshida, M., Kagawa, N., and Nagao, T. (2019). The Neonicotinoids Acetamiprid and Imidacloprid Impair Neurogenesis and Alter the Microglial Profile in the Hippocampal Dentate Gyrus of Mouse Neonates. *J. Appl. Toxicol.* 39 (6), 877–887. doi:10.1002/jat.3776

Nasi, M., De Gaetano, A., Bianchini, E., De Biasi, S., Gibellini, L., Neroni, A., et al. (2020). Mitochondrial Damage-Associated Molecular Patterns Stimulate Reactive Oxygen Species Production in Human Microglia. *Mol. Cell Neurosci.* 108, 103538. doi:10.1016/j.mcn.2020.103538

Niemelä, S., Sourander, A., Surcel, H.-M., Hinkka-Yli-Salomäki, S., McKeague, I. W., Cheslack-Postava, K., et al. (2016). Prenatal Nicotine Exposure and Risk of Schizophrenia Among Offspring in a National Birth Cohort. *Ajp* 173 (8), 799–806. doi:10.1176/appi.ajp.2016.15060800

Onodera, J., Nagata, H., Nakashima, A., Ikegaya, Y., and Koyama, R. (2020). Neuronal Brain-derived Neurotrophic Factor Manipulates Microglial Dynamics. *Glia* 69, 890–904. doi:10.1002/glia.23934

Papa, S., Caron, I., Rossi, F., and Veglianese, P. (2016). Modulators of Microglia: a Patent Review. *Expert Opin. Ther. patents* 26 (4), 427–437. doi:10.1517/13543776.2016.1135901

Quinn, P. D., Rickert, M. E., Weibull, C. E., Johansson, A. L. V., Lichtenstein, P., Almqvist, C., et al. (2017). Association between Maternal Smoking during Pregnancy and Severe Mental Illness in Offspring. *JAMA Psychiatry* 74 (6), 589–596. doi:10.1001/jamapsychiatry.2017.0456

Ramesh, G., MacLean, A. G., and Philipp, M. T. (2013). Cytokines and Chemokines at the Crossroads of Neuroinflammation, Neurodegeneration, and Neuropathic Pain. *Mediators Inflamm.* 2013, 480739. doi:10.1155/2013/480739

Roy, T. S., Seidler, F. J., and Slotkin, T. A. (2002). Prenatal Nicotine Exposure Evokes Alterations of Cell Structure in hippocampus and Somatosensory Cortex. *J. Pharmacol. Exp. Ther.* 300 (1), 124–133. doi:10.1124/jpet.300.1.124

Salihu, H. M., and Wilson, R. E. (2007). Epidemiology of Prenatal Smoking and Perinatal Outcomes. *Early Hum. Dev.* 83 (11), 713–720. doi:10.1016/j.earlhumdev.2007.08.002

Sallam, M. Y., El-Gowilly, S. M., Fouda, M. A., Abd-Alhaseeb, M. M., and El-Mas, M. M. (2019). Brainstem Cholinergic Pathways Diminish Cardiovascular and Neuroinflammatory Actions of Endotoxemia in Rats: Role of NFκB/α7/α4β2AChRs Signaling. *Neuropharmacology* 157, 107683. doi:10.1016/j.neuropharm.2019.107683

Schildge, S., Bohrer, C., Beck, K., and Schachtrup, C. (2013). Isolation and Culture of Mouse Cortical Astrocytes. *JoVE* 71, 50079. doi:10.3791/50079

Shaykhiev, R., Krause, A., Salit, J., Strulovici-Barel, Y., Harvey, B.-G., O'Connor, T. P., et al. (2009). Smoking-dependent Reprogramming of Alveolar Macrophage Polarization: Implication for Pathogenesis of Chronic Obstructive Pulmonary Disease. *J. Immunol.* 183 (4), 2867–2883. doi:10.4049/jimmunol.0900473

Smith, A. M., Dwoskin, L. P., and Pauly, J. R. (2010). Early Exposure to Nicotine during Critical Periods of Brain Development: Mechanisms and Consequences. *J. Pediatr. Biochem.* 1 (2), 125–141. doi:10.3233/jpb-2010-0012

Song, G. J., and Suk, K. (2017). Pharmacological Modulation of Functional Phenotypes of Microglia in Neurodegenerative Diseases. *Front. Aging Neurosci.* 9, 139. doi:10.3389/fnagi.2017.00139

Sterley, T.-L., Howells, F. M., and Russell, V. A. (2014). Nicotine-stimulated Release of [3H]norepinephrine Is Reduced in the hippocampus of an Animal Model of Attention-Deficit/hyperactivity Disorder, the Spontaneously Hypertensive Rat. *Brain Res.* 1572, 1–10. doi:10.1016/j.brainres.2014.05.005

Tang, Y., and Le, W. (2016). Differential Roles of M1 and M2 Microglia in Neurodegenerative Diseases. *Mol. Neurobiol.* 53 (2), 1181–1194. doi:10.1007/s12035-014-9070-5

Ueno, M., Fujita, Y., Tanaka, T., Nakamura, Y., Kikuta, J., Ishii, M., et al. (2013). Layer V Cortical Neurons Require Microglial Support for Survival during Postnatal Development. *Nat. Neurosci.* 16 (5), 543–551. doi:10.1038/nn.3358

Vernes, S. C., Oliver, P. L., Spiteri, E., Lockstone, H. E., Puliyadi, R., Taylor, J. M., et al. (2011). Foxp2 Regulates Gene Networks Implicated in Neurite Outgrowth in the Developing Brain. *Plos Genet.* 7 (7), e1002145. doi:10.1371/journal.pgen.1002145

Wang, G., Shi, Y., Jiang, X., Leak, R. K., Hu, X., Wu, Y., et al. (2015). HDAC Inhibition Prevents White Matter Injury by Modulating Microglia/macrophage Polarization through the GSK3β/PTEN/Akt axis. *Proc. Natl. Acad. Sci. USA* 112 (9), 2853–2858. doi:10.1073/pnas.1501441112

Wang, Y., Wang, L., Zhu, Y., and Qin, J. (2018). Human Brain Organoid-On-A-Chip to Model Prenatal Nicotine Exposure. *Lab. Chip* 18 (6), 851–860. doi:10.1039/c7lc01084b

Wehrspaun, C. C., Haerty, W., and Ponting, C. P. (2015). Microglia Recapitulate a Hematopoietic Master Regulator Network in the Aging Human Frontal Cortex. *Neurobiol. Aging* 36 (8), 2443.e9–2443.e20. doi:10.1016/j.neurobiolaging.2015.04.008

Yan, H.-y., Wen, X., Chen, L.-z., Feng, Y.-t., Liu, H.-x., Qu, W., et al. (2021). Augmented Autophagy Suppresses Thymocytes Development via Bcl10/p-P65 Pathway in Prenatal Nicotine Exposed Fetal Mice. *Ecotoxicology Environ. Saf.* 207, 111272. doi:10.1016/j.ecoenv.2020.111272

Yao, K., and Zu, H.-b. (2020). Microglial Polarization: Novel Therapeutic Mechanism against Alzheimer's Disease. *Inflammopharmacol* 28 (1), 95–110. doi:10.1007/s10787-019-00613-5

Zelikoff, J. T., Parmalee, N. L., Corbett, K., Gordon, T., Klein, C. B., and Aschner, M. (2018a). Microglia Activation and Gene Expression Alteration of Neurotrophins in the *Hippocampus* Following Early-Life Exposure to E-Cigarette Aerosols in a Murine Model. *Toxicol. Sci. : official J. Soc. Toxicol.* 162 (1), 276–286. doi:10.1093/toxsci/kfx257

Zelikoff, J. T., Parmalee, N. L., Corbett, K., Gordon, T., Klein, C. B., and Aschner, M. (2018b). Microglia Activation and Gene Expression Alteration of Neurotrophins in the *Hippocampus* Following Early-Life Exposure to E-Cigarette Aerosols in a Murine Model. *Toxicol. Sci.* 162 (1), 276–286. doi:10.1093/toxsci/kfx257

Zeng, Z., Meyer, K. F., Lkhagvadorj, K., Kooistra, W., Reinders-Luinge, M., Xu, X., et al. (2020). Prenatal Smoke Effect on Mouse offspringIgf1promoter Methylation from Fetal Stage to Adulthood Is Organ and Sex Specific. *Am. J. Physiology-Lung Cell Mol. Physiol.* 318 (3), L549–L561. doi:10.1152/ajplung.00293.2019

Zhang, J., Rong, P., Zhang, L., He, H., Zhou, T., Fan, Y., et al. (2021). IL4-driven Microglia Modulate Stress Resilience through BDNF-dependent Neurogenesis. *Sci. Adv.* 7 (12), eabb9888. doi:10.1126/sciadv.abb9888

Zhang, L., Spencer, T. J., Biederman, J., and Bhide, P. G. (2018). Attention and Working Memory Deficits in a Perinatal Nicotine Exposure Mouse Model. *PLoS One* 13 (5), e0198064. doi:10.1371/journal.pone.0198064

Zhang, M., Zhang, D., Dai, J., Cao, Y., Xu, W., He, G., et al. (2020). Paternal Nicotine Exposure Induces Hyperactivity in Next-Generation via Down-Regulating the Expression of DAT. *Toxicology* 431, 152367. doi:10.1016/j.tox.2020.152367

Zhao, X., Wang, H., Sun, G., Zhang, J., Edwards, N. J., and Aronowski, J. (2015). Neuronal Interleukin-4 as a Modulator of Microglial Pathways and Ischemic Brain Damage. *J. Neurosci.* 35 (32), 11281–11291. doi:10.1523/jneurosci.1685-15.2015

Zuloaga, D. G., Zuloaga, K. L., Hinds, L. R., Carbone, D. L., and Handa, R. J. (2014). Estrogen Receptor β Expression in the Mouse Forebrain: Age and Sex Differences. *J. Comp. Neurol.* 522 (2), 358–371. doi:10.1002/cne.23400

Conflict of Interest: The authors declare that the research was conducted in the absence of any commercial or financial relationships that could be construed as a potential conflict of interest.

Copyright © 2021 Zhou, Tao, Pang, Mu, Sun, Liu, Hu, Tao, Li and Xu. This is an open-access article distributed under the terms of the Creative Commons Attribution License (CC BY). The use, distribution or reproduction in other forums is permitted, provided the original author(s) and the copyright owner(s) are credited and that the original publication in this journal is cited, in accordance with accepted academic practice. No use, distribution or reproduction is permitted which does not comply with these terms.

frontiers in Pharmacology

REVIEW
published: 12 May 2021
doi: 10.3389/fphar.2021.674325

Neuroinflammation as a Therapeutic Target for Mitigating the Long-Term Consequences of Acute Organophosphate Intoxication

*Peter M. Andrew and Pamela J. Lein**

Department of Molecular Biosciences, School of Veterinary Medicine, University of California, Davis, CA, United States

Acute intoxication with organophosphates (OPs) can cause a potentially fatal cholinergic crisis characterized by peripheral parasympathomimetic symptoms and seizures that rapidly progress to *status epilepticus* (SE). While current therapeutic countermeasures for acute OP intoxication significantly improve the chances of survival when administered promptly, they are insufficient for protecting individuals from chronic neurologic outcomes such as cognitive deficits, affective disorders, and acquired epilepsy. Neuroinflammation is posited to contribute to the pathogenesis of these long-term neurologic sequelae. In this review, we summarize what is currently known regarding the progression of neuroinflammatory responses after acute OP intoxication, drawing parallels to other models of SE. We also discuss studies in which neuroinflammation was targeted following OP-induced SE, and explain possible reasons why such therapeutic interventions have inconsistently and only partially improved long-term outcomes. Finally, we suggest future directions for the development of therapeutic strategies that target neuroinflammation to mitigate the neurologic sequelae of acute OP intoxication.

Keywords: acquired epilepsy, astrocytes, cognitive impairment, functional polarization, microglia, glial cell activation

OPEN ACCESS

Edited by:
Maria Graciela Castro, University of Michigan, United States

Reviewed by:
Robert C Wykes, University College London, United Kingdom
Bin Gu, The Ohio State University, United States

****Correspondence:***
Pamela J. Lein
pjlein@ucdavis.edu

Specialty section:
This article was submitted to Neuropharmacology, a section of the journal Frontiers in Pharmacology

Received: *01 March 2021*
Accepted: *30 April 2021*
Published: *12 May 2021*

Citation:
Andrew PM and Lein PJ (2021) Neuroinflammation as a Therapeutic Target for Mitigating the Long-Term Consequences of Acute Organophosphate Intoxication. Front. Pharmacol. 12:674325. doi: 10.3389/fphar.2021.674325

INTRODUCTION

Organophosphates (OPs) are a group of compounds originally synthesized in the 1930s as insecticides. Throughout the 20th century, OPs were widely used to control insects in residential and agricultural settings. While their residential use has been increasingly restricted in the United States and European Union over the past several decades due to human health concerns, they remain the most widely used class of insecticides worldwide with particularly heavy use in developing countries (Voorhees et al., 2016). In the United States and most European countries, poisoning with OP pesticides is largely the result of occupational or accidental exposures; however, globally, suicidal self-poisoning with OPs annually accounts for over 200,000 deaths and significantly greater morbidity (Mew et al., 2017). Unfortunately, this lethal acute toxicity led to the weaponization of OPs as nerve agents during World War II (Costa 2018). OP nerve agents remain credible chemical threats as evidenced by their use as chemical weapons in the Syrian civil wars, and a number of high-profile terrorist attacks and assassination events, notably, the Tokyo subway and Matsumoto sarin gas attacks and the assassination of Kim Jong-Nam in Kuala Lumpur (Jett and Spriggs 2020).

Evidence from both human and animal studies establishes neurotoxicity as the primary endpoint of concern following acute intoxication with OPs. The canonical mechanism of OP neurotoxicity is inhibition of the enzyme acetylcholinesterase (Costa 2018), which normally functions to terminate cholinergic transmission throughout the central and peripheral nervous systems. Acute inhibition of acetylcholinesterase activity by > 60–80% can lead to a clinical toxidrome referred to as cholinergic crisis. This toxidrome is characterized by peripheral parasympathetic symptoms, depression of central control of respiration, seizures that can rapidly progress to *status epilepticus* (SE) and death (Eddleston et al., 2008; Hulse et al., 2014). The standard of care treatment for OP-induced cholinergic crisis, which can be fatal if not treated, includes atropine to block peripheral muscarinic receptors, oxime to reactivate acetylcholinesterase, and benzodiazepines to reduce seizure activity (Bird et al., 2003; Eddleston et al., 2008). However, if treatment is not initiated within minutes after the onset of clinical symptoms, survivors of acute OP poisoning often face significant long-term morbidity, including cognitive dysfunction, affective disorders or spontaneous recurrent seizures (SRS) that typically manifest in the weeks to months after the initial exposure (Roldan-Tapia et al., 2006; Dassanayake et al., 2007, 2008; Chen 2012; De Araujo Furtado et al., 2012; Pereira et al., 2014; Figueiredo et al., 2018). Therefore, new therapeutic strategies are needed to mitigate the long-term effects of acute OP intoxication, particularly in cases where initial treatment is delayed. However, efforts to develop more effective therapeutic approaches have been stymied by the lack of data regarding the pathogenic mechanisms underlying the chronic effects associated with acute OP intoxication.

Neuroinflammation has been proposed to be a key pathogenic mechanism underlying the chronic neurologic consequences of acute OP poisoning (Guignet and Lein 2019). Neuroinflammation refers to the immune-mediated, microglial and astrocyte-propagated responses organized within the nervous system in response to injury in the brain or systemic inflammation (Kraft and Harry 2011; Viviani et al., 2014). This hypothesis derives in part from increasing evidence over the past decade demonstrating that acute OP intoxication triggers robust neuroinflammatory responses that develop within hours and can persist for weeks to months post-exposure, preceding and/or coinciding with the onset of long-term effects. This hypothesis is further supported by clinical and experimental data implicating neuroinflammation in the pathogenesis of cognitive impairment, affective disorders and epilepsy in models other than acute OP intoxication. However, data causally linking neuroinflammation to the chronic neurologic consequences of acute OP intoxication are sparse, and the few studies that have tested therapeutic interventions that mitigate neuroinflammation in experimental models of acute OP intoxication have not consistently reported improved neurological outcomes. Here, we provide an overview of the evidence demonstrating that acute OP intoxication causes chronic neurologic outcomes, review the experimental evidence implicating neuroinflammation as a mechanism linking acute OP neurotoxicity to these long-term health effects, and discuss critical data gaps that need to be addressed to better understand the diagnostic and therapeutic implications of OP-induced neuroinflammation.

EVIDENCE OF CHRONIC NEUROLOGIC SEQUELAE OF ACUTE OP INTOXICATION

Clinical evidence suggests that survivors of acute OP intoxication may suffer long-term neurologic effects after initial effects have subsided (Chen 2012; Figueiredo et al., 2018). In a recent systematic review of the evidence for long-term effects after acute exposure to intoxicating levels of sarin nerve agent, the authors concluded that acute poisoning with sarin is known to be a neurological hazard to humans during the first 7 days following exposure and suspected to be a hazard in the weeks to years after exposure (Jett et al., 2020). Long-term effects identified in humans acutely intoxicated with sarin included reduced cholinesterase activity, visual and ocular effects, impaired learning and memory, and structural changes in the brain (Jett et al., 2020). Experimental animal models confirm that acute intoxication with sarin and other OPs is associated with chronic adverse outcomes, including persistent neuropathology, cognitive deficits and electroencephalographic abnormalities, including SRS (De Araujo Furtado et al., 2012; Pereira et al., 2014). As in humans, these neurologic sequelae develop weeks to months following recovery from the initial cholinergic crisis and are resistant to current medical countermeasures (Shih et al., 2003; Deshpande et al., 2014; Shrot et al., 2014; Kuruba et al., 2018; Wu et al., 2018; Supasai et al., 2020). Below we provide a brief review of the data demonstrating chronic effects of acute OP intoxication.

Behavioral and Psychiatric Abnormalities Following Acute OP Intoxication

The Tokyo subway and Matsumoto sarin gas attacks in the 1990s provide the most comprehensive clinical dataset demonstrating correlations between acute OP poisoning and subsequent neurologic abnormalities. Individuals exposed to sarin during the Tokyo subway attack experienced psychomotor and memory deficits that persisted for years after the chemical attack with more highly exposed individuals exhibiting more severe cognitive deficiencies (Nishiwaki et al., 2001; Miyaki et al., 2005). Humans acutely poisoned with OP pesticides exhibit neurologic consequences similar to those observed in humans intoxicated with sarin. Some of the earliest reports of humans poisoned with OP pesticides describe memory deficits, decreased attention and alertness (Metcalf and Holmes 1969). Later studies confirmed that acute intoxication with OP pesticides was associated with impaired attention and memory as well as deficits in higher cognitive functions, such as mental abstraction (Savage et al., 1988; Rosenstock et al., 1991; Steenland et al., 1994; Stallones and Beseler 2002; Roldan-Tapia et al., 2006). Impaired performance on simple tasks like reading comprehension (Stallones and Beseler 2002), underscores the significant negative impacts of acute OP intoxication on survivors' quality of life.

There is substantial human evidence linking repeated occupational exposures to OP pesticides and nerve agents at levels that do not cause cholinergic crisis with increased risk of psychiatric disorders, particularly depression and anxiety-related mood disorders (Levin et al., 1976; Stephens et al., 1995; Bazylewicz-Walczak et al., 1999; Mackenzie Ross et al., 2010), and with Gulf War Syndrome, a complex set of symptoms seen in Gulf War veterans that includes depression, anxiety, and memory loss (Golomb 2008). Fewer studies have evaluated the effects of acute OP intoxication on affect, but those that have indicated that acute OP poisoning also increased risk for affective disorders (Ohtani et al., 2004; Yanagisawa et al., 2006). In survivors of the Matsumoto sarin attack examined 5 years post-exposure, the incidence of psychological issues, including depressive mood, was significantly increased relative to age-matched control subjects living in the same city at the time of the attack but not exposed to sarin (Yanagisawa et al., 2006). It is challenging to dissociate the subjective experience of trauma from the effects of OP exposure on affective changes. The human data support an increased risk for post-traumatic stress disorder (PTSD) in survivors of both the Tokyo subway and Matsumoto attacks (Ohtani et al., 2004; Yanagisawa et al., 2006). However, exposed individuals displayed several psychiatric symptoms not typically associated with PTSD (Ohtani et al., 2004), suggesting a role for OP intoxication in altering affect independent of traumatic psychological experience. Consistent with this interpretation, agricultural workers acutely poisoned with OP pesticides are at a significantly increased risk for depression, anxiety and mood disorders (Stallones and Beseler 2002; Roldan-Tapia et al., 2006; Beseler et al., 2008; Wesseling et al., 2010). Moreover, a positive association has been demonstrated between the number of acute intoxication events and both the incidence of depression- and anxiety-related symptomatology and risk for suicidal ideation (Wesseling et al., 2010).

Observations from experimental animal models largely parallel the human condition. For example, rats (Filliat et al., 1999) or mice (Filliat et al., 2007) acutely intoxicated with the OP nerve agent soman exhibited marked deficits in spatial learning that correlated with neuropathology in the CA1 region of the hippocampus, a brain region integral to cognitive and mnemonic processes. While impaired cognitive function persisted at 90 days after exposure to soman, the neuropathologic effects in the hippocampus were largely resolved by this time (Filliat et al., 2007). These observations suggest that the chronic effects of acute OP intoxication on cognition and memory are not dependent on sustained neuropathologic changes in the hippocampus, implying the contribution of additional pathogenic processes. Similarly, acute intoxication with OP pesticides had long-term effects on cognitive function in animal models. In rat models of acute intoxication with diisopropylfluorophosphate (DFP), deficits in spatial learning and memory were observed within 1 month after exposure (Brewer et al., 2013), while impairments in fear conditioning manifested about 1 month post-exposure and persisted to at least 2 months post-exposure (Flannery et al., 2016; Guignet et al., 2020). Likewise, rats acutely intoxicated with paraoxon, the oxon metabolite of parathion, exhibited pronounced deficits in the novel object recognition task that persisted up to 14 weeks post-exposure (Deshpande et al., 2014).

A number of animal studies indicate that acute OP intoxication changes behaviors thought to have face validity to human affective disorders. Rats acutely intoxicated with the OP pesticide DFP (Wright et al., 2010) or paraoxon (Deshpande et al., 2014) exhibited increased immobility time in the forced swim test, a measure of despair-like depressive behavior. Paraoxon-intoxicated rats also displayed anhedonia in the sucrose preference test (Deshpande et al., 2014), another indicator of depressive-like behavior. Acute soman intoxication produced a robust and persistent anxiogenic phenotype in mice (Coubard et al., 2008) and rats (Prager et al., 2014). Similarly, rats acutely intoxicated with paraoxon exhibited increased anxiety-like behavior up to 14 weeks following exposure (Deshpande et al., 2014). Conversely, acute intoxication with DFP produced an anxiolytic effect in rats (Guignet et al., 2020). This latter observation is consistent with reports from rat models of acute sarin intoxication, in which rats demonstrated a persistent anxiolytic effect for up to 6 months post exposure (Grauer et al., 2008). While additional investigation is necessary to resolve the exact nature of the link between acute OP intoxication and affective behavior, both human and animal evidence strongly suggest that acute OP intoxication has long-term impacts on affect.

Electroencephalographic Abnormalities in the Brain

Early studies of agricultural and industrial workers acutely intoxicated with OP pesticides or nerve agents identified subtle, yet persistent alterations in electroencephalographic (EEG) activity (Metcalf and Holmes 1969; Duffy et al., 1979). These studies, however, included individuals exposed on multiple occasions, making it difficult to determine whether a single acute intoxication event caused long-term EEG abnormalities. Nonetheless, studies of survivors of the Tokyo subway sarin attack indicated that at 1 year post-intoxication, these individuals had abnormalities in baseline EEG activity (Murata et al., 1997; Yanagisawa et al., 2006) and abnormal EEG responses to auditory and visual stimuli (Murata et al., 1997).

Experimental animal data confirm and expand these human data. SRS have been demonstrated in animals following acute intoxication with OP nerve agents or pesticides (De Araujo Furtado et al., 2010; Putra et al., 2019; Guignet et al., 2020). Rats acutely intoxicated with soman (De Araujo Furtado et al., 2010) or DFP (Guignet et al., 2020) similarly presented with a latent period of relatively normal EEG activity after the OP-induced SE that evolved into SRS within weeks following exposure. Further investigation is needed to comprehensively characterize SRS following acute OP intoxication; for example, investigators have yet to identify the factors that influence duration of the latency period, as well as the regional distribution of epileptic foci during acute OP-induced SE and during SRS. Nonetheless, parallels between the development of SRS in animal models of acute OP intoxication and the acquisition of injury-induced epilepsy in human patients

suggests acute OP intoxication can trigger epileptogenic processes in human survivors.

NEUROINFLAMMATION AS A MECHANISM CONTRIBUTING TO THE NEUROLOGIC SEQUELAE OF ACUTE OP INTOXICATION

Research to identify pathogenic mechanisms underlying the long-term neurologic consequences of acute OP intoxication have historically focused on mechanisms responsible for sustaining seizure activity. Seizure activity has been considered the primary driver of not only immediate, but also long-term neuropathology and neurologic outcomes (McDonough and Shih 1997) because of extensive experimental data demonstrating a direct correlation between seizure duration and the extent of brain damage (Lallement et al., 1994; McDonough et al., 1995; Flannery et al., 2016). Consequently, it has been hypothesized that seizure termination is an effective therapeutic strategy for mitigating the neurologic sequelae of acute OP intoxication. However, clinical (Roldan-Tapia et al., 2006; Dassanayake et al., 2007, 2008; Chen 2012; De Araujo Furtado et al., 2012; Pereira et al., 2014; Figueiredo et al., 2018) and experimental (Shih et al., 2003; Deshpande et al., 2014; Shrot et al., 2014; Kuruba et al., 2018; Wu et al., 2018; Supasai et al., 2020) data indicate that survivors of acute OP intoxication have increased risk of developing chronic neurologic effects even if they receive effective anti-seizure treatment. Additionally, a subset of rats not experiencing significant seizure activity after acute DFP intoxication at a dose that triggered sustained SE in the majority of animals had significant neuropathology, albeit the neuropathologic lesions were delayed in onset and resolved earlier than similar lesions in the majority of DFP-intoxicated animals (Gonzalez et al., 2020). Thus, while seizure severity and/or duration are significant determinants of the extent of long-term brain damage following acute OP intoxication, additional pathogenic mechanisms independent of seizure activity seem to be involved.

Neuroinflammation has emerged as a potential pathogenic mechanism contributing to the chronic neurologic consequences of acute OP intoxication. Similar to peripheral inflammatory responses, neuroinflammation is often critical to functional recovery (Yang and Zhou 2019). However, aberrant or prolonged activation of neuroinflammatory pathways is characteristic of a number of neurologic disorders, and chronic neuroinflammation is often associated with disease progression (Skaper et al., 2018; Kwon and Koh 2020). As a result, significant research effort is currently focused on understanding the role of neuroinflammation in seizures in general, and more specifically, in OP-induced SE. While a strong association between seizures and neuroinflammation has been documented in humans with seizure disorders and experimental animal models of seizures triggered by factors other than OPs (Aronica and Crino 2011; Vezzani and Viviani 2015; Rana and Musto 2018; Vezzani et al., 2019), evidence implicating neuroinflammation as a pathogenic mechanism linking acute OP intoxication to long-term neurologic consequences is more nascent.

Neuroinflammation Following Acute OP Intoxication

An increasing body of experimental evidence indicates that acute OP intoxication triggers robust neuroinflammatory responses that evolve over the course of hours to months following exposure (Banks and Lein 2012; Guignet and Lein 2019). In rat and mouse models of acute intoxication with OP nerve agents or OP pesticides, astrocytes responded with transcriptional and translational upregulation of GFAP within hours of SE (Baille-Le Crom et al., 1995; Damodaran et al., 2002; Liu et al., 2012; Rojas et al., 2015; Rojas et al., 2018). By 24 h, GFAP immunoreactivity leveled off (Zimmer et al., 1997; Collombet et al., 2005; Collombet et al., 2007; Liu et al., 2012); however, a second increase in GFAP immunoreactivity emerged within 3–7 days and persisted up to 3 months after the initial exposure (Collombet et al., 2005; Collombet et al., 2007; Angoa-Pérez et al., 2010; Liu et al., 2012; Siso et al., 2017; Putra et al., 2019; Guignet et al., 2020).

Microglial responses to acute OP intoxication tend to manifest more slowly than astrocytic responses and differ between animal models. Following acute intoxication with OP nerve agents, microglia progressively adopted the classic ameboid morphology of activated phagocytic microglia within 2–3 days and clustered around regions of severe tissue damage (Zimmer et al., 1997; Collombet et al., 2005). In a mouse model of soman intoxication, this type of microglial response was largely diminished by 8 days post exposure (Collombet et al., 2005). In contrast, in a rat model of acute intoxication with the OP pesticide DFP, at 1 day post-exposure, ionized calcium binding adaptor molecule 1 (IBA1) was not significantly upregulated compared to vehicle control animals, and microglia were largely ramified (Flannery et al., 2016; Siso et al., 2017). However, by 2–3 days post-DFP exposure, IBA1 immunolabeling was significantly elevated and microglia had transitioned to an active ameboid morphology (Rojas et al., 2015; Flannery et al., 2016; Siso et al., 2017). IBA1 immunoreactivity continued to increase up to 7 days post-DFP exposure and elevated IBA1 immunolabeling persisted up to 2 months (Siso et al., 2017; Guignet et al., 2020). Thus, microglial responses may vary by agent (soman vs. DFP) and species (mouse vs. rat) as has been reported for other experimental situations (Colton et al., 1996; Colton 2009; Lam et al., 2017).

Acute OP intoxication also elicited pronounced shifts in the expression of inflammatory mediators. Soman upregulated transcription of the proinflammatory cytokines interleukin 1-beta (IL-1β), IL-6 and TNFα, as well as several immune cell adhesion molecules within 6 h of exposure (Svensson et al., 2001; Williams et al., 2003; Dillman et al., 2009). Some data suggested that the transcriptional upregulation persisted up to 7 days post-exposure (Dhote et al., 2007). An initial increase in protein levels

of proinflammatory cytokines was seen as early as 2 h following exposure to OP nerve agents, but returned to baseline after 48 h (Chapman et al., 2006; Johnson and Kan 2010; Johnson et al., 2011). There was some evidence of a second, more enduring upregulation of proinflammatory cytokines, with one study reporting elevated levels of IL-1β, IL-6 and TNFα peptides in the rat cortex 1 month following acute intoxication with sarin (Chapman et al., 2006).

Experimental investigations of the effects of acute intoxication with OP pesticides on inflammatory mediators have yielded mixed findings. Chemokine mRNA and protein expression was largely upregulated within 1 day after DFP exposure and altered expression patterns persisted through 28 days post-exposure (Liang et al., 2018; Rojas et al., 2018; Hobson et al., 2019). However, both increased and decreased levels of pro- and anti-inflammatory cytokine mRNA and protein have been reported in rats following acute DFP intoxication (Li et al., 2015; Liang et al., 2018; Rojas et al., 2018; Hobson et al., 2019). These shifts in cytokine expression were evident within 1 day post-exposure and persisted for up to 2 weeks (Hobson et al., 2019). Additional investigation is needed to more comprehensively characterize the spatiotemporal changes in chemokines and cytokines following acute OP pesticide intoxication.

Levels of COX-2 mRNA and protein were significantly upregulated within hours of acute OP intoxication and remained elevated up to 1 week following exposure (Angoa-Pérez et al., 2010; Rojas et al., 2015; Rojas et al., 2018). PGE2 levels in the brains of rats acutely intoxicated with sarin were significantly elevated within 2 days following exposure, but returned to baseline by 6 days post-exposure (Grauer et al., 2008). A second increase in PGE2 levels was observed at 1 month following sarin intoxication that persisted for up to 6 months post-exposure (Chapman et al., 2006; Grauer et al., 2008; Chapman et al., 2015). Recently, significant shifts in the profile of other inflammatory lipids have been reported in the brain of rats following acute DFP intoxication (Yang et al., 2019). In this model, numerous proinflammatory lipid mediators were found to be upregulated in a region-specific manner between 1 and 7 days following DFP intoxication, while levels of anti-inflammatory lipids were diminished over this same time period (Yang et al., 2019).

While much of the evidence demonstrating neuroinflammatory responses triggered by acute OP intoxication comes from experimental animal models (see below), there are data suggesting a similar neuroinflammatory response may happen in humans. For example, expression of proinflammatory genes was upregulated in human astrocytes exposed to the OP pesticide chlorpyrifos *in vitro* (Mense et al., 2006). Patients with OP-associated Gulf War Illness were found to have elevated brain expression of translocator protein (TSPO), a biomarker of neuroinflammation (Guilarte 2019), by PET imaging (Alshelh et al., 2020). These studies suggest the possibility that OPs induce inflammatory pathways independent of seizure activity, as has been shown in a rat model of acute DFP intoxication (Gonzalez et al., 2020). Whether acute OP-induced SE induces neuroinflammation in humans has yet to be investigated.

IS NEUROINFLAMMATION CAUSALLY LINKED TO THE LONG-TERM NEUROLOGIC CONSEQUENCES ASSOCIATED WITH ACUTE OP INTOXICATION?

As described in *Neuroinflammation as a Mechanism Contributing to the Neurologic Sequelae of Acute OP Intoxication*, there is substantial experimental evidence documenting that acute OP intoxication triggers robust neuroinflammation prior to and/or coincident with the onset of long-term neurologic effects, and increased neuroinflammation can persist for weeks to months. Whether neuroinflammation is a cause of the chronic neurologic consequences associated with acute OP intoxication remains debatable. The strongest support for this hypothesis comes from studies probing a causal role for neuroinflammation in the pathogenesis of cognitive dysfunction and epileptogenesis triggered by factors other than acute OP intoxication. For example, delayed onset of cognitive deficits and SRS are observed in experimental animal models of pilocarpine- and kainate-induced SE (Müller et al., 2009; Rattka et al., 2013), and research with these models support a contribution of neuroinflammatory processes to chronic neurologic sequelae. Similarly, a body of research ties SE-associated neuroinflammation to the development of subsequent neurobehavioral impairment. In particular, pharmacological suppression of microglial activation (Sun et al., 2015; Liu et al., 2017; Oliveira et al., 2018), modulation of cytokine levels (Somera-Molina et al., 2009; Li et al., 2017), or inhibition of mTOR signaling (Brewster et al., 2013; Schartz et al., 2016) is coincident with improved cognitive behavior across species and SE models. Additionally, there are reports that suppression of eicosanoid signaling in the context of SE attenuates cognitive deficits (Levin et al., 1976; Gobbo and O'Mara 2004). Other studies, however, suggest that COX inhibition does not attenuate SE-associated cognitive impairment (Kunz et al., 2005; Polascheck et al., 2010). It has been proposed that such conflicting data may reflect differences in pharmacological specificity for COX isoforms (Rojas et al., 2014) or that efficacy is critically tied to the timing of COX2 upregulation following SE (Jiang et al., 2015).

Across SE models, substantial evidence suggests a connection between neuroinflammation and epileptogenic processes (Rana and Musto 2018; Vezzani et al., 2019). In particular, pro-inflammatory cytokines have been causally linked to ictogenic processes *via* well-characterized molecular mechanisms (Vezzani et al., 2008; Vezzani et al., 2019). Pharmacological inhibition of COX signaling throughout experimentation attenuates the incidence, frequency, and duration of SRS following SE (Jung et al., 2006; Ma et al., 2012). However, targeted pharmacologic inhibition of COX2 during the latent period following SE

TABLE 1 | Effects of anti-inflammatory therapeutics in OP models.

OP model	Pretreatments	Therapeutic class	Therapeutic agent	Dosing regimen	Outcome	References
Rat—Sarin (108 ug/kg, i.m.)	None	NSAID	Indomethacin Ibuprofen	10 mg/kg, at onset of convulsions	↑ seizure severity	Chapman et al. (2019)
Rat—Sarin (108 ug/kg, i.m.)	None	Steroid	Methylprednisolone Dexamethasone	20 mg/kg, at onset of convulsions	↑ seizure severity	Chapman et al. (2019)
Rat—Sarin (108 ug/kg, i.m.)	None	Steroid	Methylprednisolone Dexamethasone	20 mg/kg ip at 4, 20 hr after sarin	No improvement in clinical seizure severity or PGE2 levels at 24 and 48 h.	Chapman et al. (2019)
Rat—Sarin (108ug/kg, i.m.)	None	COX-2 Inhibitor	Nimesulide	6 mg/kg at 4, 20 h after sarin	↓ TNFa, PGE2, IL1B, and IL6 expression at 8 and 24 h; No improvement to neuropathology.	Chapman et al. (2019)
Rat—Sarin (108 ug/kg, i.m.)	None	COX inhibitor	Ibuprofen	10 mg/kg at 4, 20 h after sarin	↓ IL6 expression at 24 h; No improvement to neuropathology.	Chapman et al. (2019)
Rat—Sarin (108 ug/kg, i.m.)	None	Phospholipase A2 Inhibitor	Quinacrine	5 mg/kg at 4, 20 h after sarin	↓ IL1B and IL6 expression at 24 h; No improvement to neuropathology.	Chapman et al. (2019)
Rat—Sarin (108 ug/kg, i.m.)	None	PGE Analogue	Ilomedin Prostin Misoprostol	Immediately after sarin, again at 2 hr after sarin	↓ TNFa, IL1B, and IL6 expression at 24 h; Prostin and misoprostol ↓ TSPO expression at 24 h; At 7 d, all-or-none reduction in TSPO.	Chapman et al. (2019)
Rat—Soman (154 ug/kg, s.c.)	30 m asoxime chloride (125 mg/kg, i.m.)	Antioxidant	AEOL10150	7 mg/kg, s.c. 1, 5, or 15 min after SE onset, repeated every 4 h	↓ oxidative stress, microglial activation, neurodegeneration, and proinflammatory cytokine expression at 24 h.	Liang et al., (2019)
Rat—Soman (180 ug/kg, s.c.)	30 m asoxime chloride (125 mg/kg, i.m.)	Immune modulator	Poly-YE	1 mg/kg, s.c. 24 h post intoxication	↓ neurodegeneration and microglial activation in the piriform cortex at 28 d; No significant improvements in Barnes Maze performance.	Finkelstein et al. (2012)
Rat—DFP (9.5 mg/kg, i.p.)	30 m with pyridostigmine bromide (0.1 mg/kg, s.c.), 10 m with atropine methylbromide (20 mg/kg, s.c.)	EP2 receptor antagonist	TG6-10–1	5 mg/kg, i.p. i) 1 h prior to DFP; ii) two injections (4 and 21 h after SE-onset); iii) six injections (80–150 min, 5–6 h, 9–21 h, 31–42 h, and 48 hr after SE-onset)	Treatment iii) ↓ delayed mortality, ↑ weight gain, ↓ transcription of cytokines/chemokines, ↓ IBA1 mRNA and immunolabeling, ↓ FJB in CA1 at 4 d.	Rojas et al. (2015)
Rat—DFP (9.5 mg/kg, i.p.)	30 m with pyridostigmine bromide (0.1 mg/kg, s.c.), 10 m with atropine methylbromide (20 mg/kg, s.c.)	EP2 receptor antagonist	TG6-10–1	5 mg/kg, i.p. i) 1 h prior to DFP; ii) three injections (1.5, 6, 21 h after SE-onset); iii) six injections (1.5, 6, 21, 30, 45–47, and 52–55 h after SE-onset)	Treatment iii) improved discrimination in the NOR at 4 w post intoxication.	Rojas et al. (2016)
Rat—DFP (4 mg/kg, s.c.)	None	iNOS inhibitor	1400 W	20 mg/kg every 12 h for 3 d	↓ GFAP and IBA1 cells at 7 d; ↓ incidence, duration, and frequency of SRS over 12 w; ↓ reactive astrogliosis and microgliosis at 12 w.	Putra et al. (2019)
Rat—DFP (4.5 mg/kg, s.c.)	30 m pyridostigmine (0.1 mg/kg, i.m.)	Antioxidant	AEOL10150	5 mg/kg s.c. 5 min into SE, repeated every 4 h	↓ proinflammatory mediators at 24 h.	Liang et al. (2018)
Rat—DFP (5 mg/kg, i.p.)	None	Immune modulator	Naltrexone	5 mg/kg starting 1 h post intoxication, repeated daily.	Reduced learning deficits over 4 w post intoxication.	Brewer et al. (2013)

(Continued on following page)

TABLE 1 | (*Continued*) Effects of anti-inflammatory therapeutics in OP models.

OP model	Pretreatments	Therapeutic class	Therapeutic agent	Dosing regimen	Outcome	References
Rat—DFP (9 mg/kg, i.p.)	30 m pyridostigmine bromide (0.1 mg/kg, i.m.), 10 m atropine methylnitrate (20 mg/kg, i.m.)	Growth factor	Neuregulin-1 (NRG-1)	3.2 ug/kg, internal carotid artery i) 5 min pretreatment; ii) post-treatment 1 hr after DFP intoxication; iii) post-treatment 4 h after DFP intoxication	Treatment i) at 24 h ↓ neurodegeneration and oxidative stress; ↓ shifts in microglia activation; ↓ expression of proinflammatory cytokines; Treatment ii) ↓ neurodegeneration at 24 h.	Li et al. (2012); Li et al. (2015)
Rat—DFP (4 mg/kg, s.c.)	None	Antioxidant	Diapocynin (DPO)	300 mg/kg, p.o., six doses, 12 h intervals beginning 2 h post-DFP	Mitigates motor deficits at 18 d; ↓ astrogliosis, neurodegeneration, and inflammatory cytokine expression at 6 w.	Putra et al. (2020)
Rat—Paraoxon (0.45 mg/kg, i.m.)	None	Immune modulator	Poly-YE	1 mg/kg, s.c. 24 h post intoxication	↓ neurodegeneration in the piriform cortex and amygdala at 28 d; ↓ microglial activation and ↑ BDNF in the piriform cortex at 28 d.	Finkelstein et al. (2012)

DFP, diisopropylfluorophosphate; TMB4, trimedoxime bromide; MDZ, midazolam; AMN, atropine methyl nitrate; AS, atropine sulfate; 2-PAM, pralidoxime; SE, status epilepticus; ↑, increase; ↓, decrease; FJB, Fluoro-Jade B; NOR, novel object recognition.

provides only modest, if any, benefit in mitigating SRS across SE models (Holtman et al., 2010; Polascheck et al., 2010), suggesting that COX2 inhibition may attenuate acute seizure activity but has minimal efficacy in blocking epileptogenesis. Alternative anti-inflammatory strategies, including pharmacological inhibition of microglial activation (Wang et al., 2015), mTOR inhibition (Zeng et al., 2009), and spingosine-1-phosphate analog-mediated immunosuppression (Gao et al., 2012; Pitsch et al., 2019) have also been shown to attenuate the frequency or severity of SRS following SE.

A Role for Neuroinflammation in the Long-Term Neurologic Effects of Acute OP Intoxication

As described in *Neuroinflammation as a Mechanism Contributing to the Neurologic Sequelae of Acute OP Intoxication*, there is substantial evidence detailing the extent and persistence of neuroinflammation following acute OP intoxication. These observations support the hypothesis that neuroinflammation may contribute to the chronic neurologic consequences of acute OP intoxication. However, only a few studies have directly tested this possibility by experimentally manipulating neuroinflammatory responses to probe their involvement in the neurologic outcomes of OP-induced SE (**Table 1**). The majority of studies evaluating the mechanistic role of neuroinflammation in the long-term effects of acute OP intoxication have focused on assessing the effects of blocking neuroinflammation on neuropathologic outcomes. Therapeutic strategies that inhibit prostaglandin signaling reduced histopathologic and biochemical indices of neurodegeneration and neuroinflammation in the rat brain within days of acute DFP intoxication (Rojas et al., 2015; Chapman et al., 2019). Similarly, neuregulin-1, an anti-inflammatory growth factor, reduced DFP-induced neurodegeneration and neuroinflammation when administered to rats following DFP exposure (Li et al., 2012; Li et al., 2015). Indirect targeting of inflammation *via* inhibition of oxidative stress, a process closely linked to neuroinflammation (Eastman et al., 2020), also suppressed neuroinflammation and neurodegeneration in a rat model of DFP-induced SE (Liang et al., 2018; Liang et al., 2019; Putra et al., 2019; Putra et al., 2020).

Few studies have evaluated the role of neuroinflammation in the development of long-term neurologic outcomes associated with acute OP intoxication, and those that have provide conflicting results. Pharmacologic antagonism of the PGE2 receptor (EP2) following DFP-induced SE significantly reduced neuroinflammation and neurodegeneration in the rat brain (Rojas et al., 2015). This treatment also attenuated chronic deficits in learning and memory tasks but did not mitigate OP-associated changes in anxiety-like behavior or delayed mortality (Rojas et al., 2016). Similarly, reduced production of reactive oxygen species (ROS) *via* inhibition of inducible nitric oxide synthase (iNOS) mitigated DFP-induced neuroinflammation, evidenced as significantly decreased activation of microglia and astrocytes, and decreased expression of proinflammatory cytokines coincident with a lower incidence, frequency, and intensity of SRS (Putra et al., 2019). However, reduced neuroinflammation does not always coincide with functional improvements. For example, enhancing regulatory T cell activity following acute soman or paraoxon intoxication reduced microglial activation and neurodegeneration at

28 days post-exposure in the rat amygdala and piriform cortex, but did not improve performance on the Barnes maze (Finkelstein et al., 2012). Administration of the antioxidant diapocynin following acute DFP intoxication lowered proinflammatory cytokine expression and astrogliosis, but did not mitigate learning and memory deficits in the Morris water maze in rats acutely intoxicated with DFP (Putra et al., 2020).

There is indirect evidence of a causal association between neuroinflammation and functional deficits downstream of OP-induced SE. Rats administered the anesthetic urethane following acute DFP intoxication had greater reduction in neuroinflammation and development of SRS compared to rats given diazepam after DFP (Rojas et al., 2018). Urethane also provided more complete seizure control than diazepam, making it is impossible to determine the extent to which reduced neuroinflammation is responsible for SRS suppression (Rojas et al., 2018). Similarly, daily administration of naltrexone, an opioid receptor antagonist with anti-inflammatory properties (Younger et al., 2014), following DFP-induced SE improved performance of DFP intoxicated rats in the Morris water maze (Brewer et al., 2013). However, whether decreased inflammation was responsible for the improved cognition is not known because inflammation was not directly measured (Brewer et al., 2013). While these studies support the hypothesis that neuroinflammation is associated with functional deficits following OP-induced SE, they do not confirm a causal relationship.

While it has yet to be definitively demonstrated that neuroinflammation mediates the long-term neurologic effects of acute OP intoxication, current evidence suggests neuroinflammation likely contributes to at least a subset of these neurologic sequelae. Additional research efforts are needed to directly investigate the role of neuroinflammation in OP-associated outcomes. The OP research community can look to analogous studies in non-OP SE models for guidance.

THE COMPLEXITIES OF NEUROINFLAMMATION AS A THERAPEUTIC TARGET

The complex relationship between neuroinflammation and the development of long-term outcomes following SE continues to stymie therapeutic advancement. There are sufficient clinical data demonstrating that inflammatory processes exacerbate or perpetuate established epilepsy. Indeed, suppression of inflammatory pathways is efficacious in the treatment of some refractory epilepsies (Vezzani and Granata 2005). Yet the role of neuroinflammation during acute SE and the latent epileptogenic period remains ambiguous. As described above, extensive data depicts both neuroprotective and neurotoxic roles of the neuroinflammatory response, but the relative contributions of these different responses to functional outcomes of SRS and cognitive/behavioral impairment remain obscure. However, evaluation of the available data suggests several possible explanations for these seemingly discrepant findings.

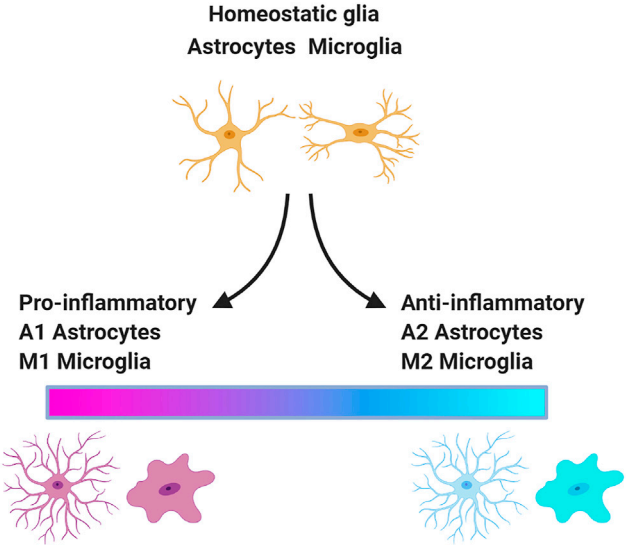

FIGURE 1 | Upon insult, microglia and astrocytes can adopt a variety of phenotypes associated with different functions. This schematic presents one model of the functional polarization of microglia and astrocytes following acute OP intoxication illustrating a continuum from the extreme pro-inflammatory to anti-inflammatory state. There is some evidence of phenotypic diversity of microglia and astrocytes in animal models of acute OP intoxication (Maupu et al., 2021). Figure created with BioRender.com.

The Heterogeneous Functional Nature of the Neuroinflammatory Response

The neuroinflammatory response involves the coordinated function of numerous cellular mediators and soluble molecules. To date, SE research has generally taken a blunt approach to targeting inflammatory processes by providing therapeutics with broad anti-inflammatory activity. While there are instances in which such strategies provide therapeutic benefit (Ma et al., 2012), it may be advantageous to use more nuanced approaches. For example, COX inhibitors target a key enzyme in prostaglandin synthesis to alter the production of many different eicosanoids, which have differing effects on recovery following brain insult (Lopez-Vales and David 2019). COX inhibition decreases synthesis of PGE2, which is associated with pro-ictogenic activity in pentylenetetrazole (PTZ)-induced seizures in rats (Oliveira et al., 2008) and neurodegeneration in a mouse model of pilocarpine-induced SE (Jiang et al., 2012). However, COX inhibition also decreases synthesis of PF2α, which exerts antiseizure effects in a mouse model of kainate-induced SE (Kim et al., 2008), and PGD2, which attenuates PTZ-induced seizures in mice (Kaushik

et al., 2014). Thus, non-specific inhibition of COX activity impacts prostaglandin signaling associated with both protective and deleterious effects following chemical-induced SE. Inhibition of these functionally divergent signaling pathways could account for some of the seemingly disparate effects of COX inhibition on neurological outcomes following SE. More directed treatments, such as those selectively targeting PGE2 signaling, have more consistently produced beneficial effects on outcomes following SE (Jiang et al., 2012; Rojas et al., 2015; Rojas et al., 2016).

Similarly, neuroinflammation encompasses heterogeneous activational states of microglia and astrocytes. Many investigations that measure microglia and astrocyte activation as biomarkers of neuroinflammation equate astrocyte and microglia hypertrophy with neurotoxic outcomes; however, the morphology of microglia and astrocytes is not a reliable indicator of functional status. Activation-associated changes to their morphology have been linked to diverse functional phenotypes (**Figure 1**), including both neurotoxic and neuroprotective activities (Olah et al., 2011; Liddelow and Barres 2017; Adams and Gallo 2018). As the field moves forward, it will be critical to consider the functional heterogeneity among microglia and astrocytes exhibiting morphologies classically associated with activation.

Single-cell transcriptomic approaches can be effectively employed to identify functional subsets of microglia and myeloid cells in the CNS *via* their unique transcriptional profiles (Liddelow et al., 2017; Jordão et al., 2019; Masuda et al., 2019). Microglial subtypes are induced in a context-dependent manner with distinct transcriptional footprints associated with specific CNS conditions, including homeostasis vs. brain damage or disease (Jordão et al., 2019; Masuda et al., 2019). Similarly, subtypes of reactive astrocytes are recognized across various homeostatic and disease states (Pestana et al., 2020). The functional polarization of microglia and astrocytes (**Figure 1**) has not been comprehensively investigated in experimental models of acute OP intoxication. The debate surrounding the M1/M2 and A1/A2 paradigm must be acknowledged (Ransohoff 2016; Escartin et al., 2021), but characterizing the functional polarization of microglia and astrocytes following OP-induced SE would provide critical insight regarding the role of microglia and astrocytes in mediating the neurologic sequelae of acute OP intoxication. This in turn would inform therapeutic strategies to preserve the neuroprotective actions of microglia and astrocytes while blocking their injurious effects.

Temporal Changes in the Neuroinflammatory Response

The inconsistent therapeutic efficacy of approaches that block neuroinflammation following OP-induced SE may be due to the neuroinflammatory response changing with time post-exposure. The role of inflammatory mediators following chemical-induced SE varies across the phases of acute SE, the latent period of epileptogenesis, and chronic epilepsy. In experimental animal models of chemical-induced SE, administration of anti-inflammatory therapeutics prior to SE induction exacerbated both acute seizure activity and subsequent neuroinflammation and did not decrease neurodegeneration (Gobbo and O'Mara 2004; Takemiya et al., 2006; Koo et al., 2018; Chapman et al., 2019). Conversely, supplementation with proinflammatory PGE2 analogs at the time of sarin exposure attenuated neuroinflammation triggered by SE (Chapman et al., 2019). Such data suggest that during the very acute phases of SE, neuroinflammatory processes decrease seizure severity and subsequent neuroinflammation. Delayed administration of a COX2 inhibitor several hours after SE decreased the neuroinflammatory response to acute sarin intoxication (Chapman et al., 2019) and attenuated neurodegeneration following kainate-induced SE (Gobbo and O'Mara 2004; Takemiya et al., 2006). These observations indicate that timing of pharmacologic inhibition of neuroinflammation is critically important and the therapeutic window likely varies depending on the therapeutic target and the model of chemical-induced SE.

Recent studies also hint to a similar impact of time post-SE with regards to the role of microglia. The depletion of microglia prior to pilocarpine- or kainate-induced SE exacerbated acute seizure activity (Liu et al., 2020; Wu et al., 2020), demonstrating that microglia serve a critical protective role during the acute phase of chemical-induced SE, and may reflect microglial regulation of excitatory neurotransmission during SE (Liu et al., 2020). The neuroprotective role of microglia during acute injury is also observed in other models of CNS insult not related to seizures (Rice et al., 2015; Szalay et al., 2016; Jin et al., 2017), suggesting involvement of acute protection beyond regulation of excitatory neurotransmission.

The role of microglia with increasing time after chemical-induced SE is largely undefined. Only one investigation thus far has evaluated the effects of microglial depletion post-SE on the development of SRS (Wu et al., 2020). Microglial depletion beginning 20 days after kainate-induced SE aggravated the frequency, intensity, and duration of SRS in mice (Wu et al., 2020). While the authors report that SRS developed within 28 days post-exposure in their mouse model of kainate-induced SE, they did not evaluate the time course of SRS development. Thus, it is possible that exacerbation of chronic SRS could reflect the absence of microglia and their protective function during acute SRS events. In other words, if microglia are depleted at a time when animals have already developed SRS, then microglia depletion may aggravate seizure activity as it does during the acute SE phase. In order to resolve this question, further studies are required in which microglia are depleted during the latent epileptogenic phase. The relevance of this approach is suggested by studies demonstrating that the delayed depletion of microglia in other neuroinflammatory models hastened functional recovery and promoted resolution of neuroinflammation (Rice et al., 2015; Rice et al., 2017; Lloyd et al., 2019).

While less frequently considered, a similar role has been proposed for astrocytes following SE in a rat model of acute sarin intoxication (Lazar et al., 2016). Experimental findings suggest that initial astrocytic responses are neuroprotective, whereas a second "wave" of activation in the first few days

post-SE promotes acute neurodegeneration (Lazar et al., 2016). Consistent with these observations, a recent functional characterization of astrocytic responses in a mouse model of acute DFP intoxication suggested that neurotoxic "A1" astrocytes emerge several days post-SE (Maupu et al., 2021). Specific functional subsets of astrocytes have not been targeted by therapeutic intervention; therefore, the relative contributions of A1 vs. A2 astrocytes to the neurologic sequelae of SE induced by OPs or other chemicals remain in question.

Proposed Model of the Temporal Changes in the Functional Role of Neuroinflammation Following Acute OP Intoxication

The neuroprotective vs. neurotoxic roles of neuroinflammation may continue to evolve in the weeks and months following acute OP intoxication (Collombet 2011; Banks and Lein 2012). Collombet posits that astrocyte-derived neurotrophic factors released during a late wave of astrocyte activation support neuronal cell survival and promote proliferation of neural progenitors (Collombet 2011). The proposed "beneficial" role of delayed astrocyte activation derives from two experimental observations: 1) astrocytes secreted a number of factors with well-defined neuroprotective and neurogenic functions (e.g., BDNF, VEGF); and 2) delayed neurodegeneration following soman-induced SE correlated temporally with diminished astrocyte activation. The Collombet model, however, is based upon data from a mouse model of acute soman intoxication in which there was minimal microglial activation in the weeks following acute OP intoxication (Collombet et al., 2005). More recent data from rat models of acute DFP intoxication showed rapid activation of both microglia and astrocytes that persisted for weeks following the initial insult (Flannery et al., 2016; Siso et al., 2017; Putra et al., 2019; Guignet et al., 2020). Together, these observations suggest that the spatiotemporal profile of neuroinflammation likely varies depending on the context in which SE is triggered.

As discussed above, there is evidence showing that the functional role of microglia shifts over the course of the neuroinflammatory response following acute brain injury in a variety of neurologic diseases not related to seizures (Rice et al., 2015; Szalay et al., 2016; Jin et al., 2017; Rice et al., 2017; Lloyd et al., 2019). These data suggest that the functional profile of microglia similarly changes with time following acute OP intoxication. Consistent with this possibility, temporal shifts in microglial phenotype are observed in non-OP models of SE (Benson et al., 2015), and evidence from a mouse model of acute DFP intoxication hints at similar changes in microglial phenotype during the first several days following DFP-induced SE (Maupu et al., 2021). More research is needed to fully characterize the spatiotemporal profile of microglial polarization over more extended periods of time after acute OP intoxication and to determine the effects of interventions targeting functional subsets of microglia on long-term neurologic consequences.

Microglia are known to regulate astrocytic polarization (Liddelow et al., 2017), suggesting the neuroprotective vs. neurotoxic potential of astrocytes may be related to changes in microglia polarization (Liddelow and Barres 2017). Thus, in situations with robust and potentially shifting profiles of microglial activation, it is likely that the functional polarization of microglia critically influences the functional polarization of astrocytes, and ultimately, the general direction of the neuroinflammatory response following acute OP intoxication. Indeed, there is evidence that neurotoxic C3-positive astrocyte polarization develops by 3 days after kainate- or DFP-induced SE (Wei et al., 2020; Maupu et al., 2021) and remains elevated at 6 weeks post intoxication (Putra et al., 2020). Importantly, this astrocytic polarization was dependent on microglial function (Wei et al., 2020), suggesting that microglia promoted the delayed development of neurotoxic astrocytes following acute OP intoxication.

We propose a model of the relationship between neuroinflammation and functional outcomes over time following OP-induced SE (**Figure 2**) in which acute neuroinflammatory responses are beneficial, while sustained neuroinflammatory responses are detrimental (Yang and Zhou 2019). The model illustrated in **Figure 2** divides the neuroinflammatory response broadly into "beneficial" and "detrimental" responses; however, the composition of each component undoubtedly shifts over time. For example, the classical microglial response may be beneficial in the short-term but detrimental in chronic situations. Regardless, the overall trend remains the same; a response that is initially beneficial becomes detrimental over time. As an intentional simplification, this design does not distinguish between the individual contributions of the diverse mediators involved in the neuroinflammatory response, leaving room for the incorporation of discrete cell populations or inflammatory processes into the classifications of "beneficial" or "detrimental." The currently available therapeutic data are generally consistent with this model. Thus, administration of an anti-inflammatory treatment prior to, during or shortly after SE is most frequently associated with more severe or longer seizure activity and/or more extensive neuropathology (Baik et al., 1999; Kunz and Oliw 2001; Holtman et al., 2010; Duffy et al., 2014; Radu et al., 2017; Chapman et al., 2019). Conversely, delayed administration of an anti-inflammatory during the hours and/or days following termination of SE tended to more reliably improve long-term outcomes (Kunz et al., 2005; Jiang et al., 2013; Jiang et al., 2015; Radu et al., 2017).

While rigorous experimentation is needed to validate our proposed model of the functional role of neuroinflammation following acute OP intoxication, it advocates for the evaluation of current anti-inflammatory therapeutics at more delayed times after SE induced by acute OP intoxication and other triggers. It should be noted that this proposed scheme is compatible with the Collombet framework (Collombet 2011) in that astrogliosis in the absence of robust and persistent "M1" microglial responses could be beneficial. However, emerging data suggests that persistent microglial activation contributes to adverse astrocytic activation and ultimately a detrimental neuroinflammatory response. It is

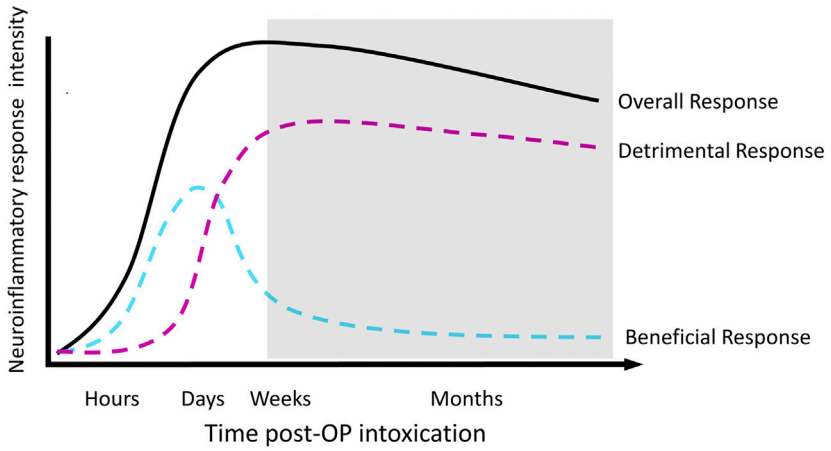

FIGURE 2 | Proposed temporal profile of the neuroinflammatory response to acute OP intoxication. The shaded area depicts the development of chronic neurological sequelae.

likely that among the multiplicity of actors involved in the SE-induced neuroinflammatory response, many have time-dependent neuroprotective vs. neurotoxic roles. To better understand the functional role of neuroinflammation following acute OP intoxication, it is critical that the field more accurately defines the time-dependent functional profile of independent neuroinflammatory components. In the near future, these studies will need to be conducted using animal models; however, with increasing interest in developing radioligands for positron emission tomography (PET) that selectively recognize functional subsets of microglia and astrocytes, it may be possible to translate preclinical data to the clinical setting.

CONCLUSION

Research on acute OP intoxication has made significant advances in characterizing the long-term effects of OP-induced SE. Despite these advances, limited progress has been made in developing therapeutics that meaningfully improve long-term neurologic effects. Neuroinflammation is emerging as a potentially critical determinant of SE-associated neurologic consequences. Substantial evidence indicates that the spatiotemporal profile of neuroinflammation is consistent with a proposed role in the various neurologic sequelae linked to acute OP intoxication; however, therapeutic interventions targeting neuroinflammation in experimental animal models of chemical-induced SE have been equivocal. This likely reflects differences in the timing of therapeutic interventions relative to shifts in the functional profile of microglia and astrocytes as a function of time post-exposure. Increased understanding of the spatiotemporal profiles of functional polarization of microglia and astrocytes coupled with increasing availability of biomarkers for distinguishing their different functional states will enable more targeted therapeutic strategies and optimal therapeutic windows that preserve the protective functions and attenuate the neurotoxic effects of microglia and astrocytes.

AUTHOR CONTRIBUTIONS

PA and PL conceptualized the manuscript. PA summarized the literature and drafted the manuscript. PA and PL revised and edited the manuscript.

FUNDING

This work was supported by the CounterACT Program, National Institutes of Health Office of the Director and the National Institute of Neurological Disorders and Stroke (Grant number U54 NS079202). PA was supported by predoctoral fellowships from the University of California, Davis, School of Veterinary Medicine and the ARCS Foundation.

ACKNOWLEDGMENTS

We thank Suzette Smiley-Jewell (UC Davis CounterACT Center) for her assistance in editing this manuscript.

SUPPLEMENTARY MATERIAL

The Supplementary Material for this article can be found online at: https://www.frontiersin.org/articles/10.3389/fphar.2021.674325/full#supplementary-material

REFERENCES

Adams, K. L., and Gallo, V. (2018). The Diversity and Disparity of the Glial Scar. *Nat. Neurosci.* 21 (1), 9–15. doi:10.1038/s41593-017-0033-9

Alshelh, Z., Albrecht, D. S., Bergan, C., Akeju, O., Clauw, D. J., Conboy, L., et al. (2020). *In-vivo* Imaging of Neuroinflammation in Veterans with Gulf War Illness. *Brain Behav. Immun.* 87, 498–507. doi:10.1016/j.bbi.2020.01.020

Angoa-Pérez, M., Kreipke, C. W., Van Shura, K. E., Thomas, D. M., Van Shura, K. E., Lyman, M., et al. (2010). Soman Increases Neuronal COX-2 Levels: Possible Link between Seizures and Protracted Neuronal Damage. *NeuroToxicology* 31 (6), 738–746. doi:10.1016/J.NEURO.2010.06.007

Aronica, E., and Crino, P. B. (2011). Inflammation in Epilepsy: Clinical Observations. *Epilepsia* 52 (Suppl. 3), 26–32. doi:10.1111/j.1528-1167.2011.03033.x

Baik, E. J., Kim, E. J., Lee, S. H., and Moon, C. (1999). Cyclooxygenase-2 Selective Inhibitors Aggravate Kainic Acid Induced Seizure and Neuronal Cell Death in the hippocampus. *Brain Res.* 843 (1-2), 118–129. doi:10.1016/s0006-8993(99)01797-7

Baille-Le Crom, V., Collombet, J. M., Carpentier, P., Brochier, G., Burckhart, M. F., Foquin, A., et al. (1995). Early Regional Changes of GFAP mRNA in Rat hippocampus and Dentate Gyrus during Soman-Induced Seizures. *Neuroreport* 7 (1), 365–369. doi:10.1097/00001756-199512290-00086

Banks, C. N., and Lein, P. J. (2012). A Review of Experimental Evidence Linking Neurotoxic Organophosphorus Compounds and Inflammation. *Neurotoxicology* 33 (3), 575–584. doi:10.1016/j.neuro.2012.02.002

Bazylewicz-Walczak, B., Majczakowa, W., and Szymczak, M. (1999). Behavioral Effects of Occupational Exposure to Organophosphorous Pesticides in Female Greenhouse Planting Workers. *Neurotoxicology* 20 (5), 819–826.

Benson, M. J., Manzanero, S., and Borges, K. (2015). Complex Alterations in Microglial M1/M2 Markers during the Development of Epilepsy in Two Mouse Models. *Epilepsia* 56 (6), 895–905. doi:10.1111/epi.12960

Beseler, C. L., Stallones, L., Hoppin, J. A., Alavanja, M. C. R., Alavanja, M. C. R., Blair, A., et al. (2008). Depression and Pesticide Exposures Among Private Pesticide Applicators Enrolled in the Agricultural Health Study. *Environ. Health Perspect.* 116 (12), 1713–1719. doi:10.1289/ehp.11091

Bird, S. B., Gaspari, R. J., and Dickson, E. W. (2003). Early Death Due to Severe Organophosphate Poisoning Is a Centrally Mediated Process. *Acad. Emerg. Med* 10 (4), 295–298. doi:10.1111/j.1553-2712.2003.tb01338.x

Brewer, K. L., Troendle, M. M., Pekman, L., and Meggs, W. J. (2013). Naltrexone Prevents Delayed Encephalopathy in Rats Poisoned with the Sarin Analogue Diisopropylflurophosphate. *Am. J. Emerg. Med.* 31 (4), 676–679. doi:10.1016/j.ajem.2012.12.003

Brewster, A. L., Lugo, J. N., Patil, V. V., Lee, W. L., Qian, Y., Vanegas, F., et al. (2013). Rapamycin Reverses Status Epilepticus-Induced Memory Deficits and Dendritic Damage. *PLoS ONE* 8 (3), e57808. doi:10.1371/journal.pone.0057808

Chapman, S., Grauer, E., Gez, R., Egoz, I., and Lazar, S. (2019). Time Dependent Dual Effect of Anti-inflammatory Treatments on Sarin-Induced Brain Inflammation: Suggested Role of Prostaglandins. *NeuroToxicology* 74, 19–27. doi:10.1016/J.NEURO.2019.05.006

Chapman, S., Kadar, T., and Gilat, E. (2006). Seizure Duration Following Sarin Exposure Affects Neuro-Inflammatory Markers in the Rat Brain. *NeuroToxicology* 27 (2), 277–283. doi:10.1016/J.NEURO.2005.11.009

Chapman, S., Yaakov, G., Egoz, I., Rabinovitz, I., Raveh, L., Kadar, T., et al. (2015). Sarin-induced Brain Damage in Rats Is Attenuated by Delayed Administration of Midazolam. *NeuroToxicology* 49, 132–138. doi:10.1016/j.neuro.2015.05.001

Chen, Y. (2012). Organophosphate-induced Brain Damage: Mechanisms, Neuropsychiatric and Neurological Consequences, and Potential Therapeutic Strategies. *Neurotoxicology* 33 (3), 391–400. doi:10.1016/j.neuro.2012.03.011

Collombet, J.-M., Four, E., Bernabé, D., Masqueliez, C., Burckhart, M.-F., Baille, V., et al. (2005). Soman Poisoning Increases Neural Progenitor Proliferation and Induces Long-Term Glial Activation in Mouse Brain. *Toxicology* 208 (3), 319–334. doi:10.1016/J.TOX.2004.11.036

Collombet, J.-M., Four, E., Fauquette, W., Burckhart, M.-F., Masqueliez, C., Bernabé, D., et al. (2007). Soman Poisoning Induces Delayed Astrogliotic Scar and Angiogenesis in Damaged Mouse Brain Areas. *NeuroToxicology* 28 (1), 38–48. doi:10.1016/J.NEURO.2006.07.011

Collombet, J.-M. (2011). Nerve Agent Intoxication: Recent Neuropathophysiological Findings and Subsequent Impact on Medical Management Prospects. *Toxicol. Appl. Pharmacol.* 255 (3), 229–241. doi:10.1016/J.TAAP.2011.07.003

Colton, C. A. (2009). Heterogeneity of Microglial Activation in the Innate Immune Response in the Brain. *J. Neuroimmune Pharmacol.* 4 (4), 399–418. doi:10.1007/s11481-009-9164-4

Colton, C., Wilt, S., Gilbert, D., Chernyshev, O., Snell, J., and Dubois-Dalcq, M. (1996). Species Differences in the Generation of Reactive Oxygen Species by Microglia. *Mol. Chem. Neuropathol.* 28 (1-3), 15–20. doi:10.1007/BF02815200

Costa, L. G. (2018). Organophosphorus Compounds at 80: Some Old and New Issues. *Toxicol. Sci.* 162 (1), 24–35. doi:10.1093/toxsci/kfx266

Coubard, S., Béracochéa, D., Collombet, J.-M., Philippin, J.-N., Krazem, A., Liscia, P., et al. (2008). Long-term Consequences of Soman Poisoning in Mice. *Behav. Brain Res.* 191 (1), 95–103. doi:10.1016/j.bbr.2008.03.027

Damodaran, T. V., Bilska, M. A., Rahman, A. A., and Abou-Donia, M. B. (2002). Sarin Causes Early Differential Alteration and Persistent Overexpression in mRNAs Coding for Glial Fibrillary Acidic Protein (GFAP) and Vimentin Genes in the Central Nervous System of Rats. *Neurochem. Res.* 27 (5), 407–415. doi:10.1023/A:1015508132137

Dassanayake, T., Weerasinghe, V., Dangahadeniya, U., Kularatne, K., Dawson, A., Karalliedde, L., et al. (2007). Cognitive Processing of Visual Stimuli in Patients with Organophosphate Insecticide Poisoning. *Neurology* 68 (23), 2027–2030. doi:10.1212/01.wnl.0000264423.12123.f0

Dassanayake, T., Weerasinghe, V., Dangahadeniya, U., Kularatne, K., Dawson, A., Karalliedde, L., et al. (2008). Long-term Event-Related Potential Changes Following Organophosphorus Insecticide Poisoning. *Clin. Neurophysiol.* 119 (1), 144–150. doi:10.1016/j.clinph.2007.09.134

De Araujo Furtado, M., Lumley, L. A., Robison, C., Tong, L. C., Lichtenstein, S., and Yourick, D. L. (2010). Spontaneous Recurrent Seizures after Status Epilepticus Induced by Soman in Sprague-Dawley Rats. *Epilepsia* 51 (8), 1503–1510. doi:10.1111/j.1528-1167.2009.02478.x

De Araujo Furtado, M., Rossetti, F., Chanda, S., and Yourick, D. (2012). Exposure to Nerve Agents: from Status Epilepticus to Neuroinflammation, Brain Damage, Neurogenesis and Epilepsy. *Neurotoxicology* 33 (6), 1476–1490. doi:10.1016/j.neuro.2012.09.001

Deshpande, L. S., Phillips, K., Huang, B., and DeLorenzo, R. J. (2014). Chronic Behavioral and Cognitive Deficits in a Rat Survival Model of Paraoxon Toxicity. *NeuroToxicology* 44, 352–357. doi:10.1016/j.neuro.2014.08.008

Dhote, F., Peinnequin, A., Carpentier, P., Baille, V., Delacour, C., Foquin, A., et al. (2007). Prolonged Inflammatory Gene Response Following Soman-Induced Seizures in Mice. *Toxicology* 238 (2-3), 166–176. doi:10.1016/j.tox.2007.05.032

Dillman, J. F., Phillips, C. S., Kniffin, D. M., Tompkins, C. P., Hamilton, T. A., and Kan, R. K. (2009). Gene Expression Profiling of Rat hippocampus Following Exposure to the Acetylcholinesterase Inhibitor Soman. *Chem. Res. Toxicol.* 22 (4), 633–638. doi:10.1021/tx800466v

Duffy, B. A., Chun, K. P., Ma, D., Lythgoe, M. F., and Scott, R. C. (2014). Dexamethasone Exacerbates Cerebral Edema and Brain Injury Following Lithium-Pilocarpine Induced Status Epilepticus. *Neurobiol. Dis.* 63, 229–236. doi:10.1016/j.nbd.2013.12.001

Duffy, F. H., Burchfiel, J. L., Burchfiel, P. H., Gaon, M., and Sim, V. M. (1979). Long-term Effects of an Organophosphate upon the Human Electroencephalogram. *Toxicol. Appl. Pharmacol.* 47 (1), 161–176. doi:10.1016/0041-008X(79)90083-8

Eastman, C. L., D'Ambrosio, R., and Ganesh, T. (2020). Modulating Neuroinflammation and Oxidative Stress to Prevent Epilepsy and Improve Outcomes after Traumatic Brain Injury. *Neuropharmacology* 172, 107907. doi:10.1016/j.neuropharm.2019.107907

Eddleston, M., Buckley, N. A., Eyer, P., and Dawson, A. H. (2008). Management of Acute Organophosphorus Pesticide Poisoning. *The Lancet* 371 (9612), 597–607. doi:10.1016/S0140-6736(07)61202-1

Escartin, C., Galea, E., Lakatos, A., O'Callaghan, J. P., Petzold, G. C., Serrano-Pozo, A., et al. (2021). Reactive Astrocyte Nomenclature, Definitions, and Future Directions. *Nat. Neurosci.* 24, 312–325. doi:10.1038/s41593-020-00783-4

Figueiredo, T. H., Apland, J. P., Braga, M. F. M., and Marini, A. M. (2018). Acute and Long-Term Consequences of Exposure to Organophosphate Nerve Agents in Humans. *Epilepsia* 59 (Suppl. 2), 92–99. doi:10.1111/epi.14500

Filliat, P., Baubichon, D., Burckhart, M. F., Pernot-Marino, I., Foquin, A., Masqueliez, C., et al. (1999). Memory Impairment after Soman Intoxication in Rat: Correlation with Central Neuropathology. Improvement with Anticholinergic and Antiglutamatergic Therapeutics. *Neurotoxicology* 20, 535–549.

Filliat, P., Coubard, S., Pierard, C., Liscia, P., Beracochea, D., Four, E., et al. (2007). Long-term Behavioral Consequences of Soman Poisoning in Mice. *NeuroToxicology* 28, 508–519. doi:10.1016/j.neuro.2006.11.004

Finkelstein, A., Kunis, G., Berkutzki, T., Ronen, A., Krivoy, A., Yoles, E., et al. (2012). Immunomodulation by Poly-YE Reduces Organophosphate-Induced Brain Damage. *Brain Behav. Immun.* 26 (1), 159–169. doi:10.1016/J.BBI.2011.09.002

Flannery, B. M., Bruun, D. A., Rowland, D. J., Banks, C. N., Austin, A. T., Kukis, D. L., et al. (2016). Persistent Neuroinflammation and Cognitive Impairment in a Rat Model of Acute Diisopropylfluorophosphate Intoxication. *J. Neuroinflammation* 13 (1), 267. doi:10.1186/s12974-016-0744-y

Gao, F., Liu, Y., Li, X., Wang, Y., Wei, D., and Jiang, W. (2012). Fingolimod (FTY720) Inhibits Neuroinflammation and Attenuates Spontaneous Convulsions in Lithium-Pilocarpine Induced Status Epilepticus in Rat Model. *Pharmacol. Biochem. Behav.* 103 (2), 187–196. doi:10.1016/J.PBB.2012.08.025

Gobbo, O. L., and O'Mara, S. M. (2004). Post-treatment, but Not Pre-treatment, with the Selective Cyclooxygenase-2 Inhibitor Celecoxib Markedly Enhances Functional Recovery from Kainic Acid-Induced Neurodegeneration. *Neuroscience* 125 (2), 317–327. doi:10.1016/j.neuroscience.2004.01.045

Golomb, B. A. (2008). Acetylcholinesterase Inhibitors and Gulf War Illnesses. *Proc. Natl. Acad. Sci.* 105 (11), 4295–4300. doi:10.1073/pnas.0711986105

González, E. A., Rindy, A. C., Guignet, M. A., Calsbeek, J. J., Bruun, D. A., Dhir, A., et al. (2020). The Chemical Convulsant Diisopropylfluorophosphate (DFP) Causes Persistent Neuropathology in Adult Male Rats Independent of Seizure Activity. *Arch. Toxicol.* 94 (6), 2149–2162. doi:10.1007/s00204-020-02747-w

Grauer, E., Chapman, S., Rabinovitz, I., Raveh, L., Weissman, B.-A., Kadar, T., et al. (2008). Single Whole-Body Exposure to Sarin Vapor in Rats: Long-Term Neuronal and Behavioral Deficits. *Toxicol. Appl. Pharmacol.* 227 (2), 265–274. doi:10.1016/J.TAAP.2007.11.006

Guignet, M., Dhakal, K., Flannery, B. M., Hobson, B. A., Zolkowska, D., Dhir, A., et al. (2020). Persistent Behavior Deficits, Neuroinflammation, and Oxidative Stress in a Rat Model of Acute Organophosphate Intoxication. *Neurobiol. Dis.* 133, 104431. doi:10.1016/J.NBD.2019.03.019

Guignet, M., and Lein, P. J. (2019). "Neuroinflammation in Organophosphate-Induced Neurotoxicity," in *Advances in Neurotoxicology: Role of Inflammation in Environmental Neurotoxicity*. Editors M. Aschner and L. G. Costa (Cambridge, MA: Academic Press), 35–79. doi:10.1016/bs.ant.2018.10.003

Guilarte, T. R. (2019). TSPO in Diverse CNS Pathologies and Psychiatric Disease: A Critical Review and a Way Forward. *Pharmacol. Ther.* 194, 44–58. doi:10.1016/j.pharmthera.2018.09.003

Hobson, B. A., Rowland, D. J., Sisó, S., Guignet, M. A., Harmany, Z. T., Bandara, S. B., et al. (2019). TSPO PET Using [18F]PBR111 Reveals Persistent Neuroinflammation Following Acute Diisopropylfluorophosphate Intoxication in the Rat. *Toxicol. Sci.* 170 (2), 330–344. doi:10.1093/toxsci/kfz096

Holtman, L., van Vliet, E. A., Edelbroek, P. M., Aronica, E., and Gorter, J. A. (2010). Cox-2 Inhibition Can Lead to Adverse Effects in a Rat Model for Temporal Lobe Epilepsy. *Epilepsy Res.* 91 (1), 49–56. doi:10.1016/j.eplepsyres.2010.06.011

Hulse, E. J., Davies, J. O. J., Simpson, A. J., Sciuto, A. M., and Eddleston, M. (2014). Respiratory Complications of Organophosphorus Nerve Agent and Insecticide Poisoning. Implications for Respiratory and Critical Care. *Am. J. Respir. Crit. Care Med.* 190 (12), 1342–1354. doi:10.1164/rccm.201406-1150CI

Jett, D. A., Sibrizzi, C. A., Blain, R. B., Hartman, P. A., Lein, P. J., Taylor, K. W., et al. (2020). A National Toxicology Program Systematic Review of the Evidence for Long-Term Effects after Acute Exposure to Sarin Nerve Agent. *Crit. Rev. Toxicol.* 50 (6), 474–490. doi:10.1080/10408444.2020.1787330

Jett, D. A., and Spriggs, S. M. (2020). Translational Research on Chemical Nerve Agents. *Neurobiol. Dis.* 133, 104335. doi:10.1016/j.nbd.2018.11.020

Jiang, J., Ganesh, T., Du, Y., Quan, Y., Serrano, G., Qui, M., et al. (2012). Small Molecule Antagonist Reveals Seizure-Induced Mediation of Neuronal Injury by Prostaglandin E2 Receptor Subtype EP2. *Proc. Natl. Acad. Sci.* 109 (8), 3149–3154. doi:10.1073/pnas.1120195109

Jiang, J., Quan, Y., Ganesh, T., Pouliot, W. A., Dudek, F. E., and Dingledine, R. (2013). Inhibition of the Prostaglandin Receptor EP2 Following Status Epilepticus Reduces Delayed Mortality and Brain Inflammation. *Proc. Natl. Acad. Sci. USA* 110 (9), 3591–3596. doi:10.1073/pnas.1218498110

Jiang, J., Yang, M.-s., Quan, Y., Gueorguieva, P., Ganesh, T., and Dingledine, R. (2015). Therapeutic Window for Cyclooxygenase-2 Related Anti-inflammatory Therapy after Status Epilepticus. *Neurobiol. Dis.* 76, 126–136. doi:10.1016/j.nbd.2014.12.032

Jin, W.-N., Shi, S. X.-Y., Li, Z., Li, M., Wood, K., Gonzales, R. J., et al. (2017). Depletion of Microglia Exacerbates Postischemic Inflammation and Brain Injury. *J. Cereb. Blood Flow Metab.* 37 (6), 2224–2236. doi:10.1177/0271678X17694185

Johnson, E. A., Dao, T. L., Guignet, M. A., Geddes, C. E., Koemeter-Cox, A. I., and Kan, R. K. (2011). Increased Expression of the Chemokines CXCL1 and MIP-1α by Resident Brain Cells Precedes Neutrophil Infiltration in the Brain Following Prolonged Soman-Induced Status Epilepticus in Rats. *J. Neuroinflammation* 8 (1), 41. doi:10.1186/1742-2094-8-41

Johnson, E. A., and Kan, R. K. (2010). The Acute Phase Response and Soman-Induced Status Epilepticus: Temporal, Regional and Cellular Changes in Rat Brain Cytokine Concentrations. *J. Neuroinflammation* 7 (1), 40–49. doi:10.1186/1742-2094-7-40

Jordão, M. J. C., Sankowski, R., Brendecke, S. M., SagarLocatelli, G., Tai, Y.-H., et al. (2019). Single-cell Profiling Identifies Myeloid Cell Subsets with Distinct Fates during Neuroinflammation. *Science* 363 (6425), eaat7554. doi:10.1126/science.aat7554

Jung, K.-H., Chu, K., Lee, S.-T., Kim, J., Sinn, D.-I., Kim, J.-M., et al. (2006). Cyclooxygenase-2 Inhibitor, Celecoxib, Inhibits the Altered Hippocampal Neurogenesis with Attenuation of Spontaneous Recurrent Seizures Following Pilocarpine-Induced Status Epilepticus. *Neurobiol. Dis.* 23 (2), 237–246. doi:10.1016/j.nbd.2006.02.016

Kaushik, M. K., Aritake, K., Kamauchi, S., Hayaishi, O., Huang, Z.-L., Lazarus, M., et al. (2014). Prostaglandin D2 Is Crucial for Seizure Suppression and Postictal Sleep. *Exp. Neurol.* 253, 82–90. doi:10.1016/j.expneurol.2013.12.002

Kim, H.-J., Chung, J.-I., Lee, S. H., Jung, Y.-S., Moon, C.-H., and Baik, E. J. (2008). Involvement of Endogenous Prostaglandin F2α on Kainic Acid-Induced Seizure Activity through FP Receptor: The Mechanism of Proconvulsant Effects of COX-2 Inhibitors. *Brain Res.* 1193, 153–161. doi:10.1016/j.brainres.2007.12.017

Koo, B.-B., Michalovicz, L. T., Calderazzo, S., Kelly, K. A., Sullivan, K., Killiany, R. J., et al. (2018). Corticosterone Potentiates DFP-Induced Neuroinflammation and Affects High-Order Diffusion Imaging in a Rat Model of Gulf War Illness. *Brain Behav. Immun.* 67, 42–46. doi:10.1016/J.BBI.2017.08.003

Kraft, A. D., and Harry, G. J. (2011). Features of Microglia and Neuroinflammation Relevant to Environmental Exposure and Neurotoxicity. *Int. J. Environ. Res. Public Health* 8 (7), 2980–3018. doi:10.3390/ijerph8072980

Kunz, T., and Oliw, E. H. (2001). Nimesulide Aggravates Kainic Acid-Induced Seizures in the Rat. *Pharmacol. Toxicol.* 88 (5), 271–276. doi:10.1034/j.1600-0773.2001.d01-116.x

Kunz, T., Marklund, N., Hillered, L., and Oliw, E. H. (2005). Assessment of the Effects of the Cyclooxygenase-2 Inhibitor Rofecoxib on Visuospatial Learning and Hippocampal Cell Death Following Kainate-Induced Seizures in the Rat. *Cogn. Brain Res.* 25 (3), 826–832. doi:10.1016/j.cogbrainres.2005.09.017

Kuruba, R., Wu, X., and Reddy, D. S. (2018). Benzodiazepine-refractory Status Epilepticus, Neuroinflammation, and Interneuron Neurodegeneration after Acute Organophosphate Intoxication. *Biochim. Biophys. Acta Mol. Basis Dis.* 1864 (9 Pt B), 2845–2858. doi:10.1016/j.bbadis.2018.05.016

Kwon, H. S., and Koh, S.-H. (2020). Neuroinflammation in Neurodegenerative Disorders: the Roles of Microglia and Astrocytes. *Transl Neurodegener* 9 (1), 42. doi:10.1186/s40035-020-00221-2

Lallement, G., Pernot-Marino, I., Baubichon, D., Burckhart, M.-F., Carpentier, P., and Blanchet, G. (1994). Modulation of Somaninduced Neuropathology with an Anticonvulsant Regimen. *Neuroreport* 5 (17), 2265–2268. doi:10.1097/00001756-199411000-00015

Lam, D., Lively, S., and Schlichter, L. C. (2017). Responses of Rat and Mouse Primary Microglia to Pro- and Anti-inflammatory Stimuli: Molecular Profiles, K+ Channels and Migration. *J. Neuroinflammation* 14 (1), 1–30. doi:10.1186/s12974-017-0941-3

Lazar, S., Egoz, I., Brandeis, R., Chapman, S., Bloch-Shilderman, E., and Grauer, E. (2016). Propagation of Damage in the Rat Brain Following Sarin Exposure: Differential Progression of Early Processes. *Toxicol. Appl. Pharmacol.* 310, 87–97. doi:10.1016/J.TAAP.2016.09.008

Levin, H. S., Rodnitzky, R. L., and Mick, D. L. (1976). Anxiety Associated with Exposure to Organophosphate Compounds. *Arch. Gen. Psychiatry* 33 (2), 225–228. doi:10.1001/archpsyc.1976.01770020061010

Li, T., Zhai, X., Jiang, J., Song, X., Han, W., Ma, J., et al. (2017). Intraperitoneal Injection of IL-4/IFN-γ Modulates the Proportions of Microglial Phenotypes and Improves Epilepsy Outcomes in a Pilocarpine Model of Acquired Epilepsy. *Brain Res.* 1657, 120–129. doi:10.1016/j.brainres.2016.12.006

Li, Y., Lein, P. J., Ford, G. D., Liu, C., Stovall, K. C., White, T. E., et al. (2015). Neuregulin-1 Inhibits Neuroinflammatory Responses in a Rat Model of Organophosphate-Nerve Agent-Induced Delayed Neuronal Injury. *J. Neuroinflammation* 12 (1), 64. doi:10.1186/s12974-015-0283-y

Li, Y., Lein, P. J., Liu, C., Bruun, D. A., Giulivi, C., Ford, G. D., et al. (2012). Neuregulin-1 Is Neuroprotective in a Rat Model of Organophosphate-Induced Delayed Neuronal Injury. *Toxicol. Appl. Pharmacol.* 262 (2), 194–204. doi:10.1016/J.TAAP.2012.05.001

Liang, L.-P., Pearson-Smith, J. N., Huang, J., Day, B. J., and Patel, M. (2019). Neuroprotective Effects of a Catalytic Antioxidant in a Rat Nerve Agent Model. *Redox Biol.* 20, 275–284. doi:10.1016/j.redox.2018.10.010

Liang, L.-P., Pearson-Smith, J. N., Huang, J., McElroy, P., Day, B. J., and Patel, M. (2018). Neuroprotective Effects of AEOL10150 in a Rat Organophosphate Model. *Toxicol. Sci.* 162 (2), 611–621. doi:10.1093/toxsci/kfx283

Liddelow, S. A., and Barres, B. A. (2017). Reactive Astrocytes: Production, Function, and Therapeutic Potential. *Immunity* 46 (6), 957–967. doi:10.1016/j.immuni.2017.06.006

Liddelow, S. A., Guttenplan, K. A., Clarke, L. E., Bennett, F. C., Bohlen, C. J., Schirmer, L., et al. (2017). Neurotoxic Reactive Astrocytes Are Induced by Activated Microglia. *Nature* 541 (7638), 481–487. doi:10.1038/nature21029

Liu, C., Li, Y., Lein, P. J., and Ford, B. D. (2012). Spatiotemporal Patterns of GFAP Upregulation in Rat Brain Following Acute Intoxication with Diisopropylfluorophosphate (DFP). *Curr. Neurobiol.* 3 (2), 90–97.

Liu, H.-j., Lai, X., Xu, Y., Miao, J.-k., Li, C., Liu, J.-y., et al. (2017). α-Asarone Attenuates Cognitive Deficit in a Pilocarpine-Induced Status Epilepticus Rat Model via a Decrease in the Nuclear Factor-Kb Activation and Reduction in Microglia Neuroinflammation. *Front. Neurol.* 8 (DEC), 661. doi:10.3389/fneur.2017.00661

Liu, M., Jiang, L., Wen, M., Ke, Y., Tong, X., Huang, W., et al. (2020). Microglia Depletion Exacerbates Acute Seizures and Hippocampal Neuronal Degeneration in Mouse Models of Epilepsy. *Am. J. Physiol. Cel Physiol* 319, C605–C610. doi:10.1152/ajpcell.00205.2020

Lloyd, A. F., Davies, C. L., Holloway, R. K., Labrak, Y., Ireland, G., Carradori, D., et al. (2019). Central Nervous System Regeneration Is Driven by Microglia Necroptosis and Repopulation. *Nat. Neurosci.* 22 (7), 1046–1052. doi:10.1038/s41593-019-0418-z

López-Vales, R., and David, S. (2019). Bioactive Lipids in Inflammation after Central Nervous System Injury. *Adv. Exp. Med. Biol.* 1127, 181–194. doi:10.1007/978-3-030-11488-6_12

Ma, L., Cui, X.-L., Wang, Y., Li, X.-W., Yang, F., Wei, D., et al. (2012). Aspirin Attenuates Spontaneous Recurrent Seizures and Inhibits Hippocampal Neuronal Loss, Mossy Fiber Sprouting and Aberrant Neurogenesis Following Pilocarpine-Induced Status Epilepticus in Rats. *Brain Res.* 1469, 103–113. doi:10.1016/j.brainres.2012.05.058

Mackenzie Ross, S. J., Brewin, C. R., Curran, H. V., Furlong, C. E., Abraham-Smith, K. M., and Harrison, V. (2010). Neuropsychological and Psychiatric Functioning in Sheep Farmers Exposed to Low Levels of Organophosphate Pesticides. *Neurotoxicol Teratol* 32 (4), 452–459. doi:10.1016/j.ntt.2010.03.004

Masuda, T., Sankowski, R., Staszewski, O., Böttcher, C., Amann, L., Sagar, et al. (2019). Spatial and Temporal Heterogeneity of Mouse and Human Microglia at Single-Cell Resolution. *Nature* 566 (7744), 388–392. doi:10.1038/s41586-019-0924-x

Maupu, C., Enderlin, J., Igert, A., Oger, M., Auvin, S., Hassan-Abdi, R., et al. (2021). Diisopropylfluorophosphate-induced Status Epilepticus Drives Complex Glial Cell Phenotypes in Adult Male Mice. *Neurobiol. Dis.* 152, 105276. doi:10.1016/j.nbd.2021.105276

McDonough, J. H., Jr., Dochterman, L. W., Smith, C. D., and Shih, T. M. (1995). Protection against Nerve Agent-Induced Neuropathology, but Not Cardiac Pathology, Is Associated with the Anticonvulsant Action of Drug Treatment. *Neurotoxicology* 16 (1), 123–132.

McDonough, J. H., and Shih., T.-M. (1997). Neuropharmacological Mechanisms of Nerve Agent-Induced Seizure and Neuropathology 1 1The Animals Used in Studies Performed in, or Sponsored by, This Institute Were Handled in Accordance with the Principles Stated in the Guide for the Care and Use of Laboratory Animals, Proposed by the Committee on Care and Use of Laboratory Animals of the Institute of Laboratory Animal Resources, National Research Council, DHHA, National Institute of Health Publication #85-23, 1985, and the Animal Welfare Act of 1966, as Amended. The Opinions, or Assertions Contained Herein Are the Private Views of the Authors, and Are Not to Be Construed as Reflecting the Views of the Department of the Army or the Department of Defense. *Neurosci. Biobehavioral Rev.* 21 (5), 559–579. doi:10.1016/S0149-7634(96)00050-4

Mense, S. M., Sengupta, A., Lan, C., Zhou, M., Bentsman, G., Volsky, D. J., et al. (2006). The Common Insecticides Cyfluthrin and Chlorpyrifos Alter the Expression of a Subset of Genes with Diverse Functions in Primary Human Astrocytes. *Toxicol. Sci.* 93 (1), 125–135. doi:10.1093/toxsci/kfl046

Metcalf, D. R., and Holmes, J. H. (1969). Eeg, Psychological, and Neurological Alterations in Humans with Organophosphorus Exposure. *Ann. NY Acad. Sci.* 160, 357–365. doi:10.1111/j.1749-6632.1969.tb15857.x

Mew, E. J., Padmanathan, P., Konradsen, F., Eddleston, M., Chang, S.-S., Phillips, M. R., et al. (2017). The Global Burden of Fatal Self-Poisoning with Pesticides 2006-15: Systematic Review. *J. Affective Disord.* 219, 93–104. doi:10.1016/j.jad.2017.05.002

Miyaki, K., Nishiwaki, Y., Maekawa, K., Ogawa, Y., Asukai, N., Yoshimura, K., et al. (2005). Effects of Sarin on the Nervous System of Subway Workers Seven Years after the Tokyo Subway Sarin Attack. *Jrnl Occup. Health* 47 (4), 299–304. doi:10.1539/joh.47.299

Müller, C. J., Gröticke, I., Bankstahl, M., and Löscher, W. (2009). Behavioral and Cognitive Alterations, Spontaneous Seizures, and Neuropathology Developing after a Pilocarpine-Induced Status Epilepticus in C57BL/6 Mice. *Exp. Neurol.* 219 (1), 284–297. doi:10.1016/j.expneurol.2009.05.035

Murata, K., Araki, S., Yokoyama, K., Okumura, T., Ishimatsu, S., Takasu, N., et al. (1997). Asymptomatic Sequelae to Acute Sarin Poisoning in the Central and Autonomic Nervous System 6 Months after the Tokyo Subway Attack. *J. Neurol.* 244 (10), 601–606. doi:10.1007/s004150050153

Nishiwaki, Y., Maekawa, K., Ogawa, Y., Asukai, N., Minami, M., and Omae, K. (2001). Effects of Sarin on the Nervous System in Rescue Team Staff Members and Police Officers 3 Years after the Tokyo Subway Sarin Attack. *Environ. Health Perspect.* 109 (11), 1169–1173. doi:10.1289/ehp.011091169

Ohtani, T., Iwanami, A., Kasai, K., Yamasue, H., Kato, T., Sasaki, T., et al. (2004). Post-traumatic Stress Disorder Symptoms in Victims of Tokyo Subway Attack: a 5-year Follow-Up Study. *Psychiatry Clin. Neurosci.* 58 (6), 624–629. doi:10.1111/j.1440-1819.2004.01313.x

Olah, M., Biber, K., Vinet, J., and Boddeke, H. W. G. M. (2011). Microglia Phenotype Diversity. *CNS Neurol. Disord. Drug Targets* 10 (1), 108–118. doi:10.2174/187152711794488575

Oliveira, C. V. d., Grigoletto, J., Canzian, J. M., Duarte, M. M. M. F., Duarte, T., Furian, A. F., et al. (2018). Effect of Atorvastatin on Behavioral Alterations and Neuroinflammation during Epileptogenesis. *Epilepsy Behav.* 78, 109–117. doi:10.1016/j.yebeh.2017.10.021

Oliveira, M. S., Furian, A. F., Rambo, L. M., Ribeiro, L. R., Royes, L. F. F., Ferreira, J., et al. (2008). Modulation of Pentylenetetrazol-Induced Seizures by Prostaglandin E2 Receptors. *Neuroscience* 152 (4), 1110–1118. doi:10.1016/j.neuroscience.2008.01.005

Pereira, E. F. R., Aracava, Y., DeTolla, L. J., Beecham, E. J., Basinger, G. W., Wakayama, E. J., et al. (2014). Animal Models that Best Reproduce the Clinical Manifestations of Human Intoxication with Organophosphorus Compounds. *J. Pharmacol. Exp. Ther.* 350 (2), 313–321. doi:10.1124/jpet.114.214932

Pestana, F., Edwards-Faret, G., Belgard, T. G., Martirosyan, A., and Holt, M. G. (2020). No Longer Underappreciated: The Emerging Concept of Astrocyte Heterogeneity in Neuroscience. *Brain Sci.* 10 (3), 168. doi:10.3390/brainsci10030168

Pitsch, J., Kuehn, J. C., Gnatkovsky, V., Müller, J. A., van Loo, K. M. J., de Curtis, M., et al. (2019). Anti-epileptogenic and Anti-convulsive Effects of Fingolimod

in Experimental Temporal Lobe Epilepsy. *Mol. Neurobiol.* 56 (3), 1825–1840. doi:10.1007/s12035-018-1181-y

Polascheck, N., Bankstahl, M., and Löscher, W. (2010). The COX-2 Inhibitor Parecoxib Is Neuroprotective but Not Antiepileptogenic in the Pilocarpine Model of Temporal Lobe Epilepsy. *Exp. Neurol.* 224 (1), 219–233. doi:10.1016/j.expneurol.2010.03.014

Prager, E. M., Aroniadou-Anderjaska, V., Almeida-Suhett, C. P., Figueiredo, T. H., Apland, J. P., Rossetti, F., et al. (2014). The Recovery of Acetylcholinesterase Activity and the Progression of Neuropathological and Pathophysiological Alterations in the Rat Basolateral Amygdala after Soman-Induced Status Epilepticus: Relation to Anxiety-like Behavior. *Neuropharmacology* 81, 64–74. doi:10.1016/j.neuropharm.2014.01.035

Putra, M., Gage, M., Sharma, S., Gardner, C., Gasser, G., Anantharam, V., et al. (2020). Diapocynin, an NADPH Oxidase Inhibitor, Counteracts Diisopropylfluorophosphate-induced Long-term Neurotoxicity in the Rat Model. *Ann. N.Y. Acad. Sci.* 1479 (1), 75–93. doi:10.1111/nyas.14314

Putra, M., Sharma, S., Gage, M., Gasser, G., Hinojo-Perez, A., Olson, A., et al. (2020). Inducible Nitric Oxide Synthase Inhibitor, 1400W, Mitigates DFP-Induced Long-Term Neurotoxicity in the Rat Model. *Neurobiol. Dis.* 133, 104443. doi:10.1016/J.NBD.2019.03.031

Radu, B. M., Epureanu, F. B., Radu, M., Fabene, P. F., and Bertini, G. (2017). Nonsteroidal Anti-inflammatory Drugs in Clinical and Experimental Epilepsy. *Epilepsy Res.* 131, 15–27. doi:10.1016/j.eplepsyres.2017.02.003

Rana, A., and Musto, A. E. (2018). The Role of Inflammation in the Development of Epilepsy. *J. Neuroinflammation* 15 (1), 144. doi:10.1186/s12974-018-1192-7

Ransohoff, R. M. (2016). A Polarizing Question: Do M1 and M2 Microglia Exist?. *Nat. Neurosci.* 19 (8), 987–991. doi:10.1038/nn.4338

Rattka, M., Brandt, C., and Löscher, W. (2013). The Intrahippocampal Kainate Model of Temporal Lobe Epilepsy Revisited: Epileptogenesis, Behavioral and Cognitive Alterations, Pharmacological Response, and Hippoccampal Damage in Epileptic Rats. *Epilepsy Res.* 103 (2-3), 135–152. doi:10.1016/j.eplepsyres.2012.09.015

Rice, R. A., Pham, J., Lee, R. J., Najafi, A. R., West, B. L., and Green, K. N. (2017). Microglial Repopulation Resolves Inflammation and Promotes Brain Recovery after Injury. *Glia* 65 (6), 931–944. doi:10.1002/glia.23135

Rice, R. A., Spangenberg, E. E., Yamate-Morgan, H., Lee, R. J., Arora, R. P. S., Hernandez, M. X., et al. (2015). Elimination of Microglia Improves Functional Outcomes Following Extensive Neuronal Loss in the hippocampus. *J. Neurosci.* 35 (27), 9977–9989. doi:10.1523/JNEUROSCI.0336-15.2015

Rojas, A., Ganesh, T., Lelutiu, N., Gueorguieva, P., and Dingledine, R. (2015). Inhibition of the Prostaglandin EP2 Receptor Is Neuroprotective and Accelerates Functional Recovery in a Rat Model of Organophosphorus Induced Status Epilepticus. *Neuropharmacology* 93, 15–27. doi:10.1016/J.NEUROPHARM.2015.01.017

Rojas, A., Ganesh, T., Manji, Z., O'Neill, T., and Dingledine, R. (2016). Inhibition of the Prostaglandin E2 Receptor EP2 Prevents Status Epilepticus-Induced Deficits in the Novel Object Recognition Task in Rats. *Neuropharmacology* 110 (Pt A), 419–430. doi:10.1016/j.neuropharm.2016.07.028

Rojas, A., Jiang, J., Ganesh, T., Yang, M.-S., Lelutiu, N., Gueorguieva, P., et al. (2014). Cyclooxygenase-2 in Epilepsy. *Epilepsia* 55 (1), 17–25. doi:10.1111/epi.12461

Rojas, A., Wang, W., Glover, A., Manji, Z., Fu, Y., and Dingledine, R. (2018). Beneficial Outcome of Urethane Treatment Following Status Epilepticus in a Rat Organophosphorus Toxicity Model. *eNeuro* 5 (2), ENEURO.0070–18.2018. doi:10.1523/ENEURO.0070-18.2018

Roldan-Tapia, L., Nieto-Escamez, F. A., del Aguila, E. M., Laynez, F., Parron, T., and Sanchez-Santed, F. (2006). Neuropsychological Sequelae from Acute Poisoning and Long-Term Exposure to Carbamate and Organophosphate Pesticides. *Neurotoxicology and Teratology* 28 (6), 694–703. doi:10.1016/j.ntt.2006.07.004

Rosenstock, L., Keifer, M., Daniell, W. E., McConnell, R., and Claypoole, K. (1991). Chronic Central Nervous System Effects of Acute Organophosphate Pesticide Intoxication. *The Lancet* 338 (8761), 223–227. doi:10.1016/0140-6736(91)90356-T

Savage, E. P., Keefe, T. J., Mounce, L. M., Heaton, R. K., Lewis, J. A., and Burcar, P. J. (1988). Chronic Neurological Sequelae of Acute Organophosphate Pesticide Poisoning. *Arch. Environ. Health* 43 (1), 38–45. doi:10.1080/00039896.1988.9934372

Schartz, N. D., Herr, S. A., Madsen, L., Butts, S. J., Torres, C., Mendez, L. B., et al. (2016). Spatiotemporal Profile of Map2 and Microglial Changes in the Hippocampal CA1 Region Following Pilocarpine-Induced Status Epilepticus. *Sci. Rep.* 6, 1–12. doi:10.1038/srep24988

Shih, T.-M., Duniho, S. M., and McDonough, J. H. (2003). Control of Nerve Agent-Induced Seizures Is Critical for Neuroprotection and Survival☆ ☆The Animals Used in These Studies Were Handled in Accordance with the Principles Stated in the Guide for the Care and Use of Laboratory Animals, Proposed by the Committee to Revise the Care and Use of Laboratory Animals of the Institute of Laboratory Animal Resources, National Research Council, and Published by National Academy Press, 1996, and the Animal Welfare Act of 1966, as Amended. The Opinions or Assertions Contained Herein Are the Private Views of the Authors, and Are Not to Be Construed as Reflecting the Views of the Department of the Army or the Department of Defense. *Toxicol. Appl. Pharmacol.* 188 (2), 69–80. doi:10.1016/s0041-008x(03)00019-x

Shrot, S., Ramaty, E., Biala, Y., Bar-Klein, G., Daninos, M., Kamintsky, L., et al. (2014). Prevention of Organophosphate-Induced Chronic Epilepsy by Early Benzodiazepine Treatment. *Toxicology* 323, 19–25. doi:10.1016/j.tox.2014.05.010

Sisó, S., Hobson, B. A., Harvey, D. J., Bruun, D. A., Rowland, D. J., Garbow, J. R., et al. (2017). Editor's Highlight: Spatiotemporal Progression and Remission of Lesions in the Rat Brain Following Acute Intoxication with Diisopropylfluorophosphate. *Toxicol. Sci.* 157 (2), 330–341. doi:10.1093/toxsci/kfx048

Skaper, S. D., Facci, L., Zusso, M., and Giusti, P. (2018). An Inflammation-Centric View of Neurological Disease: Beyond the Neuron. *Front. Cel. Neurosci.* 12, 72. doi:10.3389/fncel.2018.00072

Somera-Molina, K. C., Nair, S., Van Eldik, L. J., Watterson, D. M., and Wainwright, M. S. (2009). Enhanced Microglial Activation and Proinflammatory Cytokine Upregulation Are Linked to Increased Susceptibility to Seizures and Neurologic Injury in a 'two-Hit' Seizure Model. *Brain Res.* 1282, 162–172. doi:10.1016/j.brainres.2009.05.073

Stallones, L., and Beseler, C. (2002). Pesticide Poisoning and Depressive Symptoms Among Farm Residents. *Ann. Epidemiol.* 12 (6), 389–394. doi:10.1016/s1047-2797(01)00298-8

Steenland, K., Jenkins, B., Ames, R. G., O'Malley, M., Chrislip, D., and Russo, J. (1994). Chronic Neurological Sequelae to Organophosphate Pesticide Poisoning. *Am. J. Public Health* 84 (5), 731–736. doi:10.2105/AJPH.84.5.731

Stephens, R., Spurgeon, A., Calvert, I. A., Beach, J., Levy, L. S., Harrington, J. M., et al. (1995). Neuropsychological Effects of Long-Term Exposure to Organophosphates in Sheep Dip. *The Lancet* 345 (8958), 1135–1139. doi:10.1016/S0140-6736(9590976-1

Sun, H., Wu, H. Q., Yu, X., Zhang, G. L., Zhang, R., Zhan, S. Q., et al. (2015). Angiotensin II and its Receptor in Activated Microglia Enhanced Neuronal Loss and Cognitive Impairment Following Pilocarpine-Induced Status Epilepticus. *Mol. Cell Neurosci.* 65, 58–67. doi:10.1016/j.mcn.2015.02.014

Supasai, S., Gonzalez, E. A., Rowland, D. J., Hobson, B., Bruun, D. A., Guignet, M. A., et al. (2020). Acute Administration of Diazepam or Midazolam Minimally Alters Long-Term Neuropathological Effects in the Rat Brain Following Acute Intoxication with Diisopropylfluorophosphate. *Eur. J. Pharmacol.* 886, 173538. doi:10.1016/j.ejphar.2020.173538

Svensson, I., Waara, L., Johansson, L., Bucht, A., and Cassel, G. (2001). Soman-Induced Interleukin-1β mRNA and Protein in Rat Brain. *NeuroToxicology* 22 (3), 355–362. doi:10.1016/S0161-813X(01)00022-5

Szalay, G., Martinecz, B., Lénárt, N., Környei, Z., Orsolits, B., Judák, L., et al. (2016). Microglia Protect against Brain Injury and Their Selective Elimination Dysregulates Neuronal Network Activity after Stroke. *Nat. Commun.* 7 (1), 1–13. doi:10.1038/ncomms11499

Takemiya, T., Maehara, M., Matsumura, K., Yasuda, S., Sugiura, H., and Yamagata, K. (2006). Prostaglandin E2 Produced by Late Induced COX-2 Stimulates Hippocampal Neuron Loss after Seizure in the CA3 Region. *Neurosci. Res.* 56 (1), 103–110. doi:10.1016/j.neures.2006.06.003

Vezzani, A., Balosso, S., and Ravizza, T. (2008). The Role of Cytokines in the Pathophysiology of Epilepsy. *Brain Behav. Immun.* 22 (6), 797–803. doi:10.1016/j.bbi.2008.03.009

Vezzani, A., Balosso, S., and Ravizza, T. (2019). Neuroinflammatory Pathways as Treatment Targets and Biomarkers in Epilepsy. *Nat. Rev. Neurol.* 15 (8), 459–472. doi:10.1038/s41582-019-0217-x

Vezzani, A., and Granata, T. (2005). Brain Inflammation in Epilepsy: Experimental and Clinical Evidence. *Epilepsia* 46 (11), 1724–1743. doi:10.1111/j.1528-1167.2005.00298.x

Vezzani, A., and Viviani, B. (2015). Neuromodulatory Properties of Inflammatory Cytokines and Their Impact on Neuronal Excitability. *Neuropharmacology* 96 (Pt A), 70–82. doi:10.1016/J.NEUROPHARM.2014.10.027

Viviani, B., Boraso, M., Marchetti, N., and Marinovich, M. (2014). Perspectives on Neuroinflammation and Excitotoxicity: a Neurotoxic Conspiracy? *Neurotoxicology* 43, 10–20. doi:10.1016/j.neuro.2014.03.004

Voorhees, J. R., Rohlman, D. S., Lein, P. J., and Pieper, A. A. (2016). Neurotoxicity in Preclinical Models of Occupational Exposure to Organophosphorus Compounds. *Front. Neurosci.* 10, 590. doi:10.3389/fnins.2016.00590

Wang, N., Mi, X., Gao, B., Gu, J., Wang, W., Zhang, Y., et al. (2015). Minocycline Inhibits Brain Inflammation and Attenuates Spontaneous Recurrent Seizures Following Pilocarpine-Induced Status Epilepticus. *Neuroscience* 287, 144–156. doi:10.1016/j.neuroscience.2014.12.021

Wei, Y., Chen, T., Bosco, D. B., Xie, M., Zheng, J., Dheer, A., et al. (2020). The Complement C3-C3aR Pathway Mediates Microglia-Astrocyte Interaction Following Status Epilepticus. *Glia* 69, 1155. doi:10.1002/glia.23955

Wesseling, C., De Joode, B. V. W., Keifer, M., London, L., Mergler, D., and Stallones, L. (2010). Symptoms of Psychological Distress and Suicidal Ideation Among Banana Workers with a History of Poisoning by Organophosphate or N-Methyl Carbamate Pesticides. *Occup. Environ. Med.* 67 (11), 778–784. doi:10.1136/oem.2009.047266

Williams, A. J., Berti, R., Yao, C., Price, R. A., Velarde, L. C., Koplovitz, I., et al. (2003). Central Neuro-Inflammatory Gene Response Following Soman Exposure in the Rat. *Neurosci. Lett.* 349 (3), 147–150. doi:10.1016/S0304-3940(03)00818-8

Wright, L. K. M., Liu, J., Nallapaneni, A., and Pope, C. N. (2010). Behavioral Sequelae Following Acute Diisopropylfluorophosphate Intoxication in Rats: Comparative Effects of Atropine and Cannabinomimetics. *Neurotoxicology and Teratology* 32 (3), 329–335. doi:10.1016/j.ntt.2009.12.006

Wu, W., Li, Y., Wei, Y., Bosco, D. B., Xie, M., Zhao, M. G., et al. (2020). Microglial Depletion Aggravates the Severity of Acute and Chronic Seizures in Mice. *Brain Behav. Immun.* 89, 245–255. doi:10.1016/j.bbi.2020.06.028

Wu, X., Kuruba, R., and Reddy, D. S. (2018). Midazolam-Resistant Seizures and Brain Injury after Acute Intoxication of Diisopropylfluorophosphate, an Organophosphate Pesticide and Surrogate for Nerve Agents. *J. Pharmacol. Exp. Ther.* 367 (2), 302–321. doi:10.1124/jpet.117.247106

Yanagisawa, N., Morita, H., and Nakajima, T. (2006). Sarin Experiences in Japan: Acute Toxicity and Long-Term Effects. *J. Neurol. Sci.* 249, 76–85. doi:10.1016/j.jns.2006.06.007

Yang, J., Bruun, D. A., Wang, C., Wan, D., McReynolds, C. B., Kenny, P., et al. (2019). Lipidomes of Brain from Rats Acutely Intoxicated with Diisopropylfluorophosphate Identifies Potential Therapeutic Targets. *Toxicol. Appl. Pharmacol.* 382, 114749. doi:10.1016/j.taap.2019.114749

Yang, Q. Q., and Zhou, J. W. (2019). Neuroinflammation in the Central Nervous System: Symphony of Glial Cells. *Glia* 67 (6), 1017–1035. doi:10.1002/glia.23571

Younger, J., Parkitny, L., and McLain, D. (2014). The Use of Low-Dose Naltrexone (LDN) as a Novel Anti-inflammatory Treatment for Chronic Pain. *Clin. Rheumatol.* 33 (4), 451–459. doi:10.1007/s10067-014-2517-2

Zeng, L. H., Rensing, N. R., and Wong, M. (2009). The Mammalian Target of Rapamycin Signaling Pathway Mediates Epileptogenesis in a Model of Temporal Lobe Epilepsy. *J. Neurosci.* 29 (21), 6964–6972. doi:10.1523/JNEUROSCI.0066-09.2009

Zimmer, L. A., Ennis, M., and Shipley, M. T. (1997). Soman-induced Seizures Rapidly Activate Astrocytes and Microglia in Discrete Brain Regions. *J. Comp. Neurol.* 378 (4), 482–492. doi:10.1002/(SICI)1096-9861(19970224)378:4<482::AID-CNE4>3.0.CO;2-Z

Conflict of Interest: The authors declare that the research was conducted in the absence of any commercial or financial relationships that could be construed as a potential conflict of interest.

Copyright © 2021 Andrew and Lein. This is an open-access article distributed under the terms of the Creative Commons Attribution License (CC BY). The use, distribution or reproduction in other forums is permitted, provided the original author(s) and the copyright owner(s) are credited and that the original publication in this journal is cited, in accordance with accepted academic practice. No use, distribution or reproduction is permitted which does not comply with these terms.

frontiers in Neuroscience

REVIEW
published: 17 May 2021
doi: 10.3389/fnins.2021.663650

Methylene Blue Application to Lessen Pain: Its Analgesic Effect and Mechanism

Seung Won Lee[1] *and Hee Chul Han*[2]*

[1] *Good Doctor Research Institute, College of Medicine, Korea University, Seoul, South Korea,* [2] *Department of Physiology, College of Medicine and Neuroscience Research Institute, Korea University, Seoul, South Korea*

Methylene blue (MB) is a cationic thiazine dye, widely used as a biological stain and chemical indicator. Growing evidence have revealed that MB functions to restore abnormal vasodilation and notably it is implicated even in pain relief. Physicians began to inject MB into degenerated disks to relieve pain in patients with chronic discogenic low back pain (CDLBP), and some of them achieved remarkable outcomes. For osteoarthritis and colitis, MB abates inflammation by suppressing nitric oxide production, and ultimately relieves pain. However, despite this clinical efficacy, MB has not attracted much public attention in terms of pain relief. Accordingly, this review focuses on how MB lessens pain, noting three major actions of this dye: anti-inflammation, sodium current reduction, and denervation. Moreover, we showed controversies over the efficacy of MB on CDLBP and raised also toxicity issues to look into the limitation of MB application. This analysis is the first attempt to illustrate its analgesic effects, which may offer a novel insight into MB as a pain-relief dye.

Keywords: methylene blue, pain, anti-inflammation, sodium current, denervation

OPEN ACCESS

Edited by:
Claudia Bregonzio,
CCT CONICET Córdoba, Argentina

Reviewed by:
Cristiane Salum,
Federal University of ABC, Brazil
Sulev Kõks,
University of Tartu, Estonia

***Correspondence:**
Hee Chul Han
heehan@korea.ac.kr

Specialty section:
This article was submitted to Neuropharmacology, a section of the journal Frontiers in Neuroscience

Received: *03 February 2021*
Accepted: *16 April 2021*
Published: *17 May 2021*

Citation:
Lee SW and Han HC (2021) Methylene Blue Application to Lessen Pain: Its Analgesic Effect and Mechanism. Front. Neurosci. 15:663650. doi: 10.3389/fnins.2021.663650

INTRODUCTION

In 1876, German chemist Heinrich Caro synthesized methylene blue (MB) for the first time in history, which was basically applied for textiles as an aniline dye. Around the same time, it was found that MB is capable of staining cells by binding to their structures, in addition, sometimes inactivating bacteria. This discovery prepared the innovative ground for biological or medical studies related to MB. Numerous scientists applied it to a variety of animal and bacterial studies, importantly Paul Ehrlich introduced it to humans in 1891 as an anti-malarial agent. Indeed, this dye has been introduced to treat different diseases even including dementia, cancer, and depression (Wainwright and Crossley, 2002; Schirmer et al., 2003; Schirmer et al., 2011).

In the present day, MB is primarily known for a vasoconstrictor. It downregulates basically nitric oxide (NO), which is responsible for relaxing vascular smooth muscle, and leads to vasoconstriction (Wolin et al., 1990; Pan et al., 2019). However, under pathological conditions, NO is overexpressed and then contributes to inflammation as a pro-inflammatory mediator (Luo and Cizkova, 2000; Lundberg et al., 2008; Leiper and Nandi, 2011). Of note, MB suppresses the iNOS/NO-mediated inflammatory signaling by directly downregulating inducible NO synthase (iNOS) (Cohen et al., 2000). In addition, P2X receptor family, long non-coding RNA (lncRNA), and inflammasome are also involved in MB-mediated anti-inflammation (Ahn et al., 2017; Li et al., 2018; Zheng and Li, 2019). Accordingly, MB application can be an important strategy to reduce inflammation and pain.

In general, voltage-gated sodium channels (VGSCs) play an important role in evoking action potentials (APs) and, when activated, they consequently contribute to exciting neurons and thus facilitating communication with other ones. Interestingly, MB decreased significantly I_{NA} (voltage-gated sodium currents) in hippocampal CA1 neurons and, more importantly, attenuated markedly neural firing rates in the afferent nerve fibers (Zhang et al., 2010; Lee et al., 2021), which implies that MB may impede pain transmission by dampening neuronal excitability elicited by VGSCs.

In addition, MB may contribute to pain reduction by hindering or damaging nerve connection to tissues, which is referred to as denervation. Indeed, it can make affected nerve fibers or neurons incapable of sensing pain. Peng et al. (2007) conducted intradiscal MB injection in patients with chronic discogenic low back pain (CDLBP) to relieve pain for the first time. Most of patients showed encouraging results and this improvement lasted at least one year. Moreover, in a case, there were no noticeable side effects and complications in those patients even after prolonged follow-ups (Peng et al., 2010). However, as opposed to expectations, these outstanding outcomes faced a lot of challenges. We will deal with the controversies around the results in the relevant section.

Despite these remarkable reports, MB has not drawn much attention from the public specifically concerning pain. Thus, in this review, we will show MB-driven analgesic effects and their possible mechanisms along with the relevant experimental evidence and clinical cases. Finally, we will provide a novel insight into MB as a pain reliever.

MB AND ANTI-INFLAMMATION

Blockade of NOS/NO-Mediated Inflammatory Signaling

Inflammation is tightly correlated with pain as a critical cause. It directly or indirectly induces nociceptive responses and in many cases underlies pain or pain-related diseases (Zhang H. et al., 2016; Harth and Nielson, 2019; Matsuda et al., 2019). It is well known that MB decreases NO formation by directly suppressing endothelial NOS (eNOS) expression, and blocks also the conversion of guanosine triphosphate (GTP) to cyclic guanosine monophosphate (cGMP) by suppressing soluble guanylate cyclase (sGC) expression in vascular smooth muscles, which in turn leads to vasoconstriction (**Figure 1A**; Wolin et al., 1990; Pan et al., 2019).

The MB-Induced Interruption of iNOS/NO-NF-κB Signaling

Based on this pathway, MB weakens inflammation since NO plays a crucial role in the pathogenesis of inflammation as a pro-inflammatory mediator. This dye inhibits iNOS/NO pathway to affect nuclear factor kappa-light-chain-enhancer of activated B cells (NF-κB) activation. Silent information regulator 1 (Sirt1), which is a deacetylase and have a protective role under stress conditions, inactivates NF-κB and tumor protein p53 (p53) by deacetylating them. In contrast, iNOS/NO activates these two transcription factors by inactivating Sirt1 via S-nitrosylation (Nakazawa et al., 2017). NF-κB activation facilitates inflammatory cytokine expression, importantly, upregulates iNOS to enhance inflammatory signaling (Nakazawa et al., 2017; Jiang et al., 2020), and p53 activation induces cell death (Aubrey et al., 2018). However, MB prevents these events by downregulating iNOS in multiple inflammatory milieus. It directly inhibits iNOS expression and also attenuates the binding of NF-κB to iNOS promoter, thus resulting in the blockade of iNOS/NO-NF-κB signaling (**Figure 1B**; Huang et al., 2015).

Specifically, in human cartilage explants, MB decreased NO accumulation and iNOS expression in a dose dependent manner, and upregulated transforming growth factor beta (TGF-β) receptors, known as an important factor for cartilage matrix synthesis. As a result, it prevented the degradation of cartilage matrix and proteoglycan (Cohen et al., 2000). In ulcerative colitis rats, MB decreased remarkably NO production and inflammatory cytokine (IL-1β, IL-6, and TNF-α) levels. Functionally, with the alleviated tissue injury and edema in the submucosa, there was a significant improvement in intestinal permeability after MB application (Dinc et al., 2015). Accordingly, these studies demonstrated that MB has a critical role in negatively modulating NOS expression and NO production and ultimately is able to induce functional improvement in the inflamed tissues.

During nerve injury, Toll-like receptor 4 (TLR4) initiates neuroimmune activation in the nervous system. Notably, TLR4 activates NF-κB by mediating its nuclear localization, which in turn promotes pro-inflammatory cytokine expression and ultimately leads to inflammatory hyperalgesia (Lacagnina et al., 2018; Yadav and Surolia, 2019). Tanga et al. demonstrated for the first time that upon nerve injury (L5 nerve transection), behavioral hypersensitivity is induced via TLR4/NF-κB pathway, suggesting that TLR4 activation is a critical cause of the pathogenesis of neuropathic and chronic pain (Tanga et al., 2005). In this context, targeting TLR4/NF-κB pathway can be recommended as a decisive therapeutic strategy to relieve nerve injury–induced neuroinflammation and pain (Yadav and Surolia, 2019; Ye et al., 2020).

Interestingly, TLR4 is much involved in iNOS activation (Deng et al., 2015). This implies that MB may participate in suppressing the development and maintenance of neuropathic pain by downregulating directly iNOS and weakening NF-κB activation as previously described. A clinical study showed that systemic MB administration improved 10 patients with chronic refractory neuropathic pain, which was assumably due to the MB-mediated blockade of iNOS/NO pathway (Miclescu et al., 2015).

The MB-Induced Interruption of nNOS/cGMP/PKG Signaling

Lastly, neuronal NOS (nNOS), predominantly found in neurons, is also responsible for NO production and engaged in NO-mediated pathway (Kourosh-Arami et al., 2020). This enzyme has been much investigated specifically concerning chronic and inflammatory pain. In particular, nNOS has a critical role in the development of chronic and neuropathic pain upon nerve

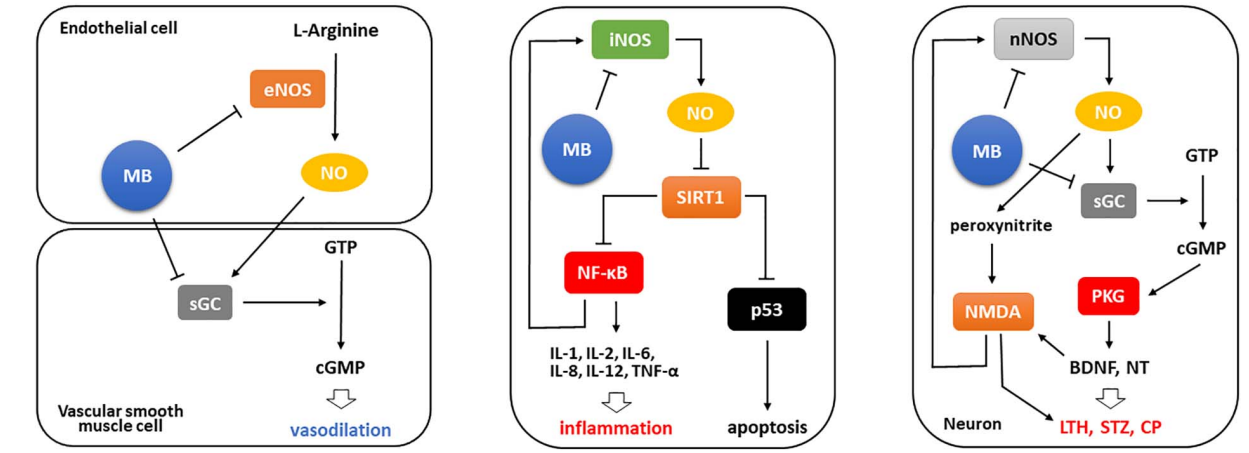

FIGURE 1 | MB is involved in anti-inflammation by suppressing iNOS/NO-NF-κB pathway. **(A)** Basically, MB downregulates both eNOS and sGC that are major factors converting GTP to cGMP, ultimately leading to vasoconstriction. **(B)** Upon tissue injury, iNOS functions as a strong inflammatory mediator in different types of cells. It inhibits Sirt1 activation by NO-mediated S-nitrosylation, which in turn activates NF-κB and p53 to facilitate inflammatory cytokine expression and apoptosis, respectively. Of note, NF-κB activation intensifies these events by activating iNOS/NO-NF-κB pathway. Conversely, MB directly abates iNOS expression and moreover decreases the binding of NF-κB to iNOS promoter, which consequently interrupts this inflammatory signaling. **(C)** Meanwhile, NMDA receptors are activated during nerve injury and induces Ca^{2+} influx, which then results in the excessive expression of nNOS and markedly activates nNOS/NO signaling. The increased NO production stimulates NMDA receptors and triggers NO/cGMP/PKG cascade, which promotes the subsequent BNDF upregulation and neurotransmitter release and ultimately induces long-term hyperexcitability and central sensitization. Notably, BDNF and peroxynitrite potentiate NMDA receptors, which stimulate nNOS expression again. However, MB weakens these responses by inhibiting nNOS and sGC activation, thus may prevent the development of persistent pain.LTH, long-term hyperexcitability; STZ, sensitization; NT, neurotransmitter; CP, chronic pain.

injury (Kim et al., 2011), while iNOS is partially related to it (Rocha et al., 2020). Interestingly, a study demonstrated that spinal nNOS, not eNOS and iNOS, is significantly upregulated after inflammatory pain induction and contributes to central sensitization (Chu et al., 2005). In this respect, nNOS has been highlighted as a target to dampen pain in both inflammatory and non-inflammatory milieus (Mukherjee et al., 2014; Demir et al., 2019). Moreover, it was found that NO/cGMP-mediated pathway, a downstream target of nNOS, is crucial for the development and maintenance of pain (Li et al., 2020), and cGMP protein kinase (PKG) is considered as a potent generator in this event since leading to long-term hyperexcitability and pain sensitization in neurons by inducing neurotransmitter release and upregulating brain-derived neurotrophic factor (BDNF) (Lewin and Walters, 1999; Sung et al., 2017; Wang et al., 2021). Furthermore, BDNF released during nerve injury and peroxynitrite activated via nNOS/NO signaling potentiate N-methyl-D-aspartate (NMDA) receptors, which then induces long-term hyperexcitability and upregulates nNOS, respectively (Pall, 2002; Chen et al., 2014; **Figure 1C**).

Importantly, MB is able to downregulate both nNOS and sGC, resulting in the inhibition of nNOS/NO-mediated signaling. Rey-Funes et al. (2016) demonstrated that MB protects retinal damage in rats with ischemic proliferative retinopathy, which is associated with local inflammation in the ischemic retina. MB suppressed the expression levels of nNOS and proangiogenic factors such as matrix metalloproteinase (MMP)-2 and MMP-9 and upregulated pigment epithelium-derived factor (PEDF), ultimately leading to the reduction of inner retinal thickness, gliosis, and retinal angiogenesis.

Inhibited NOS Activation Potentiates Opioidergic Effects

Opioids are substances with similar effects to those of morphine and used primarily for lessening pain. Basically, opioids act by binding to opioid receptors (ORs), which show analgesia by reducing cyclic adenosine monophosphate (cAMP) and causing the resultant decrease in the excitatory ion channels (Quirion et al., 2020; Sun et al., 2020; Kaski et al., 2021).

However, a number of issues concerning their addiction and adverse effects have been raised. In effect, morphine application may induce inflammatory cytokine expression such as IL-1β, IL-6, and TNF-α, ultimately contributing to inflammation and neurotoxic events. Importantly, it was found that reduced nNOS activation not only enhances the antinociception of morphine but also inhibits the morphine-induced neurotoxicity by downregulating inflammatory mediators (Machelska et al., 1997; Osmanlıoğlu et al., 2020). In this regard, MB may also contribute to these events as a potent NOS inhibitor. A clinical report showed that oral MB administration relieved oral mucositis-related intractable pain and more importantly reduced significantly morphine requirement in the relevant patients (Roldan et al., 2017).

There are some links between TLR4, OR, and cholecystokinin (CCK). CCK, an important neurohormone, plays a variety

of roles in the nervous system and notably engaged in pain reduction mainly via CCK-B receptors (Roca-Lapirot et al., 2019; Keppel Hesselink, 2020). Interestingly, this peptide functions to inhibit OR activity and thus reduces the morphine-induced antinociception (Torres-López et al., 2007; Yang et al., 2018). Meanwhile, upon nerve injury, *Tlr4* genes are significantly expressed in the midbrain and medulla of CCK-B receptor knockout mice compared to those of wild type, implying that CCK is involved in innate immunity (Kõks et al., 2008). This result is supported by recent studies that CCK has a pivotal role in anti-inflammation by decreasing inflammatory mediators (Funakoshi et al., 2019; Saia et al., 2020). It has not yet been confirmed that MB is related to these links. However, it is believed that MB possibly shows a synergistic effect with morphine and CCK, thus enhancing anti-inflammatory and analgesic effects.

Downregulation of P2XR and lncRNA

MB-Mediated P2XR Downregulation Induces Anti-inflammation and Pain Relief

Purinergic P2X receptor subtypes have been highlighted as a nociceptor that causes inflammation and pain. These receptors are characterized by ligand-gated ionotropic channels activated in response to the binding of adenosine 5′-triphosphate (ATP), exhibiting a non-selective cationic permeability such as K^+, Na^+, and Ca^{2+} that can contribute to opening voltage-gated channels on neurons by depolarizing membrane potential and activate a diversity of intracellular Ca^{2+}-dependent signaling pathways (Surprenant and North, 2009; Schmid and Evans, 2019). In particular, P2 × 3 and P2 × 2/3 receptors among the subunits are distributed in the dorsal root ganglion (DRG) and the central terminal of primary afferent fibers, mainly small-diameter unmyelinated C-fibers, and play a critical role in pain transmission in the periphery (North, 2004; Bernier et al., 2018; Stephan et al., 2018). Interestingly, MB is highly correlated with this P2X receptor-mediated events.

Li et al. showed that MB alleviated inflammation and pain in osteoarthritis (OA) rabbits by negatively modulating P2 × 3 receptors. In this study, after intra-articular MB administration, weight distribution in the hind paw was significantly restored and the swelling ratio in the inflamed knees also markedly declined. Inflammatory cytokine levels (TNF-α, IL-1β, IL-6, and IL-8) were also remarkably reduced in the articular cartilage with a significant decrease in P2 × 3 receptor expression. Moreover, this event was reversed by P2 × 3 overexpression (Li et al., 2018).

Decreased lncRNA Contributes to Anti-inflammation

Meanwhile, lncRNA has been highlighted as a new player in gene regulation. Previous studies revealed that increased lncRNA is a critical cause of neuropathic pain, and interacts with P2XRs to initiate and maintain pain (Zhao et al., 2013; Li et al., 2017). Also, it is much implicated in inflammatory events (Chen et al., 2019).

Interestingly, MB may contribute to anti-inflammation and pain relief by downregulating this lncRNA. Zheng and Li demonstrated that MB negatively regulates a long non-coding RNA (lncRNA), specifically a chondrocyte inflammation–associated lncRNA (CILinc02), overexpressed in osteoarthritic cartilage tissues and cultured OA cells, and decreased inflammatory cytokine levels (IL-1, IL-6, and IL-17). Of note, MB suppressed even chondrocyte degradation. Conversely, CILinc02 overexpression resulted in inflammation and apoptosis (Zheng and Li, 2019).

Inhibition of Inflammasome Formation and Activation

Inflammasome is an intracellular multiprotein complex that functions to process cytokine precursors into their mature forms and induce an inflammatory form of programmed cell death termed pyroptosis, which, ultimately, has a crucial role in providing host defense against harmful intruders (Matsuda et al., 2019).

Upon stimulation, inflammasome initiates the expression of cytosolic sensing proteins, called a priming step, which include nucleotide-binding oligomerization domain (NOD), leucine-rich repeat (LRR), pyrin domain-containing protein 3 (NLRP3), NLR family caspase recruitment domain (CARD)-containing protein 4 (NLRC4), absent in melanoma 2 (AIM2), and cytokine precursors. And inflammasome requires the second phase triggered by pathogen- and danger-associated molecular patterns, an activation step, to assemble a cytosolic sensor, an adaptor [apoptosis-associated speck-like protein containing a CARD (APC)], and an effector (pro-caspase-1) into inflammasome complex, and to secrete IL-1β and IL-18 (Kanneganti, 2015; Rathinam and Fitzgerald, 2016; Swanson et al., 2019; Yang et al., 2019).

Interestingly, it was found that MB inhibits inflammasome activation by interrupting both steps. Ahn et al. elucidated the relation between MB and inflammasome for the first time, demonstrating that MB suppresses both canonical and non-canonical processes by decreasing dose-dependently the expression of NLRP3, pro-IL-1β and caspase-1, as well as reactive oxygen species (ROS) production (Ahn et al., 2017).

Similarly, neuroinflammation triggered by spinal cord injury (SCI) was alleviated by the MB-mediated inhibition of NLRP3 and NLRC4 inflammasome formation in microglia. In SCI animals, following MB administration, their locomotive activities were ameliorated and inflammatory cytokine levels (IL-1β, IL-6, and TNF-α) were also diminished (Lin et al., 2017). Overall MB-mediated anti-inflammation pathways are summarized in **Table 1**.

MB AND SODIUM CURRENT REDUCTION

Early Studies for MB and I_{NA}

It is an old story that MB is involved in the reduction of excitatory synaptic currents. In earlier periods, Armstrong, Croop, and Starkus conducted pioneering experiments to explore the inactivation of sodium channels and their electrophysiological profiles using an artificial inactivation model established by administering MB into squid giant axons. The dyes blocked efficiently both the I_g (gate current) and I_{NA}, as well as

simulated the channel inactivation even after pronase, an agent of eliminating normal inactivation, treatment (Armstrong and Croop, 1982). Similarly, a subsequent study showed that MB weakened sodium currents in both normal and pronase-treated crayfish giant axons (Starkus et al., 1984). In the two studies, MB was believed to be a gate-immobilizing open-pore blocker rather than an inactivation enhancer, since directly blocking sodium pores rather than promoting or speeding the inactivation process (**Figure 2**; Armstrong and Croop, 1982; Starkus et al., 1984).

Altered VGSC-Dependent Currents and Neural Firing Rates

Zhang et al. (2010) explored the effect of MB on sodium currents and found that MB alters VGSC-mediated electrophysiological events. MB application diminished the peak amplitude of I_{NA} up to 45% at 100 μM, number of repetitive firings, and V_{max} (AP upstroke velocity) in rat hippocampal slices. In addition, it accelerated I_{NA} inactivation and even retarded the shift from inactivation to recovery state.

Importantly, Lee et al. (2021) performed the first *in vivo* experiments to investigate the link between MB-mediated neural firing patterns and pain reduction in rats using *in vivo* single nerve recordings and behavioral studies. This study showed dramatic results that neural firing rates significantly decreased in a dose-dependent manner after MB administration and, notably, this event lasted longer than that of lidocaine, showing anesthetic-like firing patterns. Ultimately, MB improved pain behaviors in rodents. These results demonstrate that MB abates pain by markedly suppressing neural excitability (Lee et al., 2021).

Silenced Excitable Neurons as a Critical Cause of Pain Relief

Exciting neurons is the most fundamental step to convey signals and to relay or cause several subsequent responses. Moreover, VGSCs are directly engaged in AP generation and affect the

TABLE 1 | MB-mediated multiple anti-inflammation pathways.

Pathways	Changes in key elements	Final results	References
MB-NOS/NO	iNOS expression ↓ NO production ↓ TGF-β receptor expression ↑	cartilage matrix and proteoglycan degradation ↓ (in cultured human cartilage explants)	Cohen et al., 2000
	iNOS expression ↓ NO production ↓ IL-1β, IL-6, TNF-α expression ↓	tissue injury and edema ↓ (in rats with acetic acid-induced colitis)	Dinc et al., 2015
	iNOS expression ↓ NO production ↓	NF-κB binding to iNOS promoter ↓ (in mouse organs and cultured cells)	Huang et al., 2015
	nNOS expression ↓ MMP-2, MMP-3 expression ↓ PEDF expression ↑	inner retinal thickness ↓ gliosis ↓ retinal angiogenesis ↓ (in retinopathy rats)	Rey-Funes et al., 2016
MB-P2 × 3	P2 × 3R expression ↓ IL-1β, IL-6, IL-8, TNF-α expression ↓	swelling ratio in the inflamed knee ↓ weight distribution in hind paws ↑ (in OA rabbits)	Li et al., 2018
MB-lncRNA	CILinc02 expression ↓ IL-1, IL-6, and IL-17 expression ↓	chondrocyte degradation ↓ inflammation ↓ (in human cartilage tissues and primary cells)	Zheng and Li, 2019
MB-inflammasome	NLRP3, pro-IL-1β expression ↓ IL-1β, IL-18, caspase-1 expression ↓ mitochondrial ROS production ↓	inflammasome activation ↓ (in bone marrow-derived macrophages)	Ahn et al., 2017
	NLRP3 expression ↓ ROS production ↓ IL-1β, IL-6, IL-18, TNF-α expression ↓	NLRP3 and NLRC4 inflammasome formation ↓ neuroinflammation ↓ locomotive function ↑ (in cultured microglia and spinal cord injured rats)	Lin et al., 2017

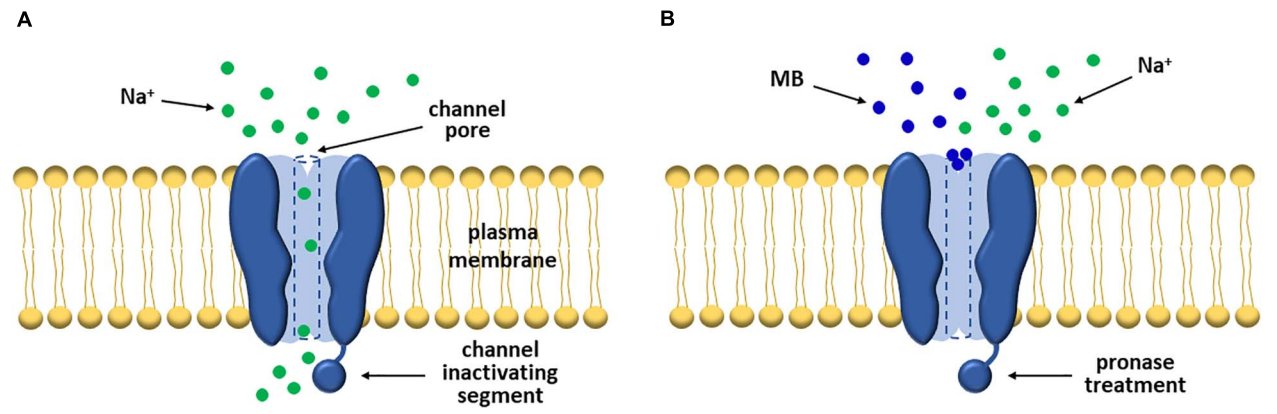

FIGURE 2 | MB significantly attenuates sodium currents by blocking VGSCs. **(A)** In general, VGSCs allow sodium ions to flow into the cell in the activated state. **(B)** However, early researchers found that the gate and sodium currents of the channels were markedly suppressed post-MB treatment. And notably, this event was maintained even after pronase treatment. Thus, they interpreted this event as MB functions as a pore blocker rather than an inactivation enhancer.

resultant reactions including signal propagation, opening other channels, vesicle release, cell-to-cell communication, and other related responses (Kruger and Isom, 2016; Wang et al., 2017). Accordingly, it is natural to postulate that VGSCs and AP generation play a crucial role even in pain transmission (Dubin and Patapoutian, 2010; Bennett et al., 2019). Interestingly, multiple evidence demonstrates that MB silences excitable cells (or nerves) by significantly attenuating I_{NA} and AP production, which ultimately leads to pain relief (Armstrong and Croop, 1982; Starkus et al., 1984, 1993; Zhang et al., 2010; Lee et al., 2021). Therefore, these two crucial electrophysiological activities, weakened sodium currents and decreased neural firing rates, are possible causes that can elucidate how MB contributes to pain relief.

MB AND DENERVATION

Early Cases for MB Application

Denervation is defined as loss or interruption of nerve connection to an organ, which thereby may contribute to pain relief by making nerves shut off sensory transmission. In history, MB began to rear its head for denervation firstly to treat itch. In 1968, Professor Rygick in the Moscow University reported for the first time an effect of MB on chronic pruritus ani (PA), characterized by severe itching in the perianal area, noting that patients with chronic PA was significantly improved after subcutaneous MB administration (Rygick, 1968). In 1979, Wollock and Dintsman inspired by Rygick's work conducted also an intervention to treat intractable PA locally administering MB into the perianal skin and produced remarkable results that eight out of nine patients were completely improved post-MB treatment. Importantly, Eusebio et al. conducted an electron microscopic investigation aimed at the perianal skin of intractable PA patients treated with subcutaneous MB and no distinct nerve endings were detected in the samples even after a long-term (7 years) follow-up. Thus, they interpreted that this improvement was attributed to death of nerve endings connected to the perianal skin, that is, denervation (Eusebio et al., 1990). Most recently, PA patients treated with MB showed satisfactory scores at 6-week, as well as 3-year, follow-ups. The recurrence rate was low (7.5%) even three years after MB treatment. In the study, MB was also considered as a critical agent to sever nerve endings (Kim et al., 2019).

Intradiscal MB Injection and Debates

The Novel Intervention to Treat Chronic Pain

Similar to the itching cases, MB was applied to inflamed intervertebral disks (IVDs) in CDLBP patients. In 2007, Peng et al. (2007) reported encouraging outcomes in the treatment of CDLBP using a minimal invasive method, intradiscal MB injection. They believed that MB has a capacity to mitigate pain in the patients by blocking nerve conduction or destroying nerve endings around the painful disks that may be vascularized and extensively innervated owing to disk degeneration. This was a first prospective clinical trial conducted for examining the pain-relieving effect of MB in human subjects. In this study, MB was administered into the affected disks of CDLBP patients using a discographic needle (1 ml of 1% MB), then pain intensity and disability of the patients were measured by visual analog scale (VAS) and oswestry disability index (ODI). As a result, most patients were evidently or completely improved and there were no side effects or complications during long-term follow-up periods (12-23 months) (Peng et al., 2007). After four years, Peng et al. (2010) conducted a randomized placebo-controlled trial in 72 eligible participants, who accepted intradiscal MB injection or placebo treatment. For numerical rating scale (NRS) and ODI scores, there were dramatic or obvious improvements in most patients treated with MB. Of note, these events lasted even to the subsequent follow-up visits at 12 and 25 months.

Controversies and Refutations for Intradiscal MB Application

However, their outcomes were immediately challenged and debated over a more fundamental issue. Bogduk (2010) explained that cultural factors may affect the manner in which patients report their outcomes, and Chinese patients may report their physical conditions more favorably to physicians or assessors than United States or British patients do. Another commentary was about the safety of MB. MB has a potent neurotoxic effect and can be leaked to the spinal canal through annular tears during intradiscal administration since discogenic pain is associated with annular tears (Levine and Richeimer, 2011). Lastly, a researcher argued that there is no LBP treatment that can immunize against new LBP episodes, emphasizing that discography accelerates disk degeneration after years (Schiltenwolf et al., 2011).

In 2019, an article directly refuted the previous results of Peng et al. (2010) designing a study protocol almost identical to their previous study to verify their outcomes (Kallewaard et al., 2019). As a result, there were no significant differences between MB plus lidocaine treatment group and placebo plus lidocaine group after NRS, ODI, quality of life (QOL), and VAS measurement. They concluded that the outcomes of the previous study were not able to be reproduced (Kallewaard et al., 2019).

Short-Term Effect of Intradiscal MB Application on Chronic Low Back Pain

Over years after Peng et al. (2010), there have been multiple attempts to perform intradiscal MB injection in CDLBP patients. Kim et al. revealed that following intradiscal MB injection, there was a significant decrease in VAS (1, 3, and 6 months) and ODI (one and three months) scores in 20 CDLBP patients, but, one year after intervention, such outcomes were reproduced only in five patients (Kim et al., 2012). Accordingly, the patients showed short-term improvement (three or six months) after intervention. Gupta et al. showed a relatively low success rate (13%) in eight CDLBP patients after a single intradiscal MB injection (Gupta et al., 2012). Levi et al. revealed that there were very limited benefits in the VAS and ODI scores in 16 CDLBP patients. Only a few patients (25% or less) met the criteria for success at the follow-up periods (Levi et al., 2014). Lastly, Zhang X. et al. (2016) reported the short-term clinical outcomes in CDLBP patients. Their NRS and ODI scores were significantly decreased at 1- to 6-month follow-ups. Imaging experiments showed that the mean

apparent diffusion coefficient (ADC) and T2 values significantly increased at 6- and 12-month, but not 3-month, follow-ups.

Collectively, it was found that MB is effective in CDLBP patients at least in a short period (until 3 or 6 months after treatment), which is also supported by the most recent review report (Deng et al., 2021). Similarly, radiofrequency (RF) denervation also resulted in short-term improvement (4 weeks or 6 months) in patients with chronic LBP (Leclaire et al., 2001; Nath et al., 2008; Al-Najjim et al., 2018). In addition, epidermal nerve fibers were regenerated in healthy humans about 100 days after capsaicin-induced denervation (Polydefkis et al., 2004). Regarding knee osteoarthritis, RF denervation contributed to pain reduction in patients with inflamed knee joints and their joint function was ameliorated. This improvement lasted 6 and 3 months, respectively (Wang R. et al., 2019). Based on these results, it is believed that denervating effects do not exceed 6 months. Accordingly, the short-term improvement observed in CDLBP patients is interpreted reasonable. Overall results of the studies were summarized in **Table 2**.

MB AND TOXICITY ISSUES

Serotonin Toxicity

The Contribution of MB to Serotonin Toxicity as a Potent MAO Inhibitor

In the last 20 years, it has been reported that depressive or anxiety patients taking serotonergic medications experienced ST, also referred to as serotonin syndrome, after MB administration. The investigators and medical doctors have believed that the toxicity is deeply linked with the synergism of MB and the medications, and that such patients may be more vulnerable to ST (Ng et al., 2008; Ng and Cameron, 2010; Kapadia et al., 2016; Wolvetang et al., 2016).

ST is characterized by the excessive accumulation of serotonin into the body, which, ultimately, leads to neuromuscular hyperexcitability by the excessive serotonergic agonism of the central and peripheral nervous system, whose clinical findings include agitation, tremor, inducible and ocular clonus, diaphoresis, hyperreflexia, hypertonia, and hyperthermia (over 38°C) (Boyer and Shannon, 2005). A great number of case reports showed that these events occurred predominantly in mental patients who had been taking serotonergic antidepressant medications including fluoxetine [a selective serotonin reuptake inhibitor (SSRI)] (Martindale and Stedeford, 2003; Kapadia et al., 2016), paroxetine, a SSRI (Bach et al., 2004; Mihai et al., 2007; Ng et al., 2008; Shanmugam et al., 2008; Schwiebert et al., 2009; Wolvetang et al., 2016), venlafaxine [a selective serotonin and norepinephrine reuptake inhibitor (SSNRI)] (Majithia and Stearns, 2006), citalopram, a SSRI (Mathew et al., 2006; Pollack et al., 2009), duloxetine, a SSNRI (Rowley et al., 2009), and clomipramine [a serotonin reuptake inhibitor (SRI)] (Khan et al., 2007), and have been commonly interpreted to be attributed to the reaction of MB as a potent monoamine oxidase A (MAO-A) inhibitor (Gillman, 2011; Top et al., 2014). In effect, MAO has a part in the degradation process of a diversity of monoamines such as serotonin, epinephrine, norepinephrine, dopamine, and histamine (Yeung et al., 2019; Floris et al., 2020). In this regard, MB augments serotonin levels in the synaptic cleft by suppressing the activity of MAO, which, furthermore, may lead to ST along with the use of SRIs, SSRIs, and SSNRIs due to over-enhanced serotonergic transmission (Zuschlag et al., 2018).

The Risk of Intravenous MB Application in Patients Taking Serotonergic Medications

Previous studies showed that ST was precipitated after intravenous MB administration predominantly at doses of 5-7.5 mg/kg except for the case of a 65-year-old woman (1.75 mg/kg) (Mihai et al., 2007; Ng et al., 2008). More importantly, Gillman reported that even a low dose of MB (0.75 mg/kg) administered via the intravenous route may reach peak plasma concentration and cause CNS toxicity (or ST) in those being treated with the medications facilitating serotonergic transmission (Schwiebert et al., 2009; Gillman, 2011). The drug safety update, a newsletter issued by the Medicines and Healthcare products Regulatory Agency (MHRA), also informed that patients who have recently treated with serotonergic antidepressants should avoid intravenous MB and be closely observed if administered with MB, and that intravenous MB can be approved only for patients with drug-induced methemoglobinemia at a dose of 1–2 mg/kg (MHRA, 2009). Oral administration of MB is not likely to cause ST since the MB concentration in blood and brain was significantly higher after intravenous, compared to oral, administration (Peter et al., 2000; Top et al., 2014). Therefore, we need to avoid intravenous route and consider about proper dosage to prevent this toxicity event.

TABLE 2 | Overall results of intradiscal MB Injection in CDLBP Patients.

Case report	Number of patients	Measurements	Duration of pain relief	Success rate
Peng et al., 2007	24	VAS, ODI	23 mo	87% at 3, 6, and 12 (or more) mo
Peng et al., 2010	36 (MB) 36 (placebo)	NRS, ODI	24 mo	89% at 6, 12, and 24 mo
Kim et al., 2012	20	VAS, ODI	12 mo	55% and 20% at 3 and 12 mo
Gupta et al., 2012	8	retrospective analysis	12 mo	13% at 12 mo
Levi et al., 2014	16	VAS, ODI	6 mo	25%, 21%, and 25% at 1, 2, and 6 mo, respectively
Zhang X. et al., 2016	33	NRS, ODI	12 mo	81, 75, 63 and 54% at 1, 3, 6, and 12 mo, respectively
Kallewaard et al., 2019	40 (MB) 41 (placebo)	NRS, PGIC, VAS, ODI, QoL	6 mo	15(12)%, 25(20)%, and 35(25)% at 6 wk, 3 mo, and 6 mo in NRS (PGIC), respectively

PGIC, patent global impression of change; wk, week(s); mo, month(s).

Other Issues

A previous study demonstrated that MB deteriorated the dendritic arbor of isolated neurons and was engaged in cell death in a dose-dependent manner (no neurotoxic effects at concentrations of 0.25 μM or less) (Vutskits et al., 2008). More recently, it was found that MB has a detrimental effect on the viability of nucleus pulposus and annulus fibrosus cells. But MB at lower doses had little effect on both (Wang X. et al., 2019; Zhang et al., 2019). Thus, these results imply that high-dose MB may impair them, thus we need to consider about proper dosage in the clinical setting.

DISCUSSION

In the present review, we illustrated MB-driven analgesic effects and their possible mechanisms based on key clinical and experimental studies. In effect, MB is much closely involved in pain relief via the following major actions: anti-inflammation, sodium current reduction, and denervation (**Figure 3**).

First of all, MB is deeply related to anti-inflammation. Notably, it triggers a variety of anti-inflammatory pathways and functions to decrease the expression level of pro-inflammatory cytokines in a variety of ways, including inhibition of iNOS/NO signaling, downregulation of P2XR and lncRNA, and interruption of priming and activation steps required for inflammasome complex formation and activation. Ultimately, these anti-inflammatory responses contribute to restoring inflamed tissues and lessening pain (**Table 1**; Vutskits et al., 2008; Dinc et al., 2015; Ahn et al., 2017; Li et al., 2018; Zheng and Li, 2019). In addition, MB reduces the amplitude of I_{NA}, accelerates the I_{NA} inactivation, delays the shift from inactivation to recovery state in neurons, and importantly decreases neural firing rates, which can therefore alleviate pain by impeding VGSC-mediated neuronal excitability (Zhang et al., 2010; Lee et al., 2021). Lastly, MB is involved in denervation. MB has been believed to have a neurolytic effect and thus to destroy dermal nerve endings for years. Of note, this effect was confirmed by an electron microscopic experiment (Eusebio et al., 1990; Etter and Myers, 2002). In clinical cases, CDLBP patients were improved for at least 3 or 6 months after intradiscal MB injection and RF denervation (Kim et al., 2012; Maas et al., 2015; Zhang X. et al., 2016; Al-Najjim et al., 2018).

However, there are toxicity problems with MB application. Patients being treated with serotonergic medications are likely to suffer ST after intravenous MB administration (mainly at doses of 5-7.5 mg/kg) due to the synergistic effect of MB and the medications. In addition, MB is able to damage cultured neurons (Vutskits et al., 2008) and NP and AF cells in a dose-dependent manner (Wang X. et al., 2019; Zhang et al., 2019). Therefore, we should find proper dose levels and administration routes to protect MB-induced adverse events.

MB is a blue dye that had been used at first for textile manufacturing. Similarly, at the present day, it is applied as a dye to mark and visualize a certain tissue or region in the

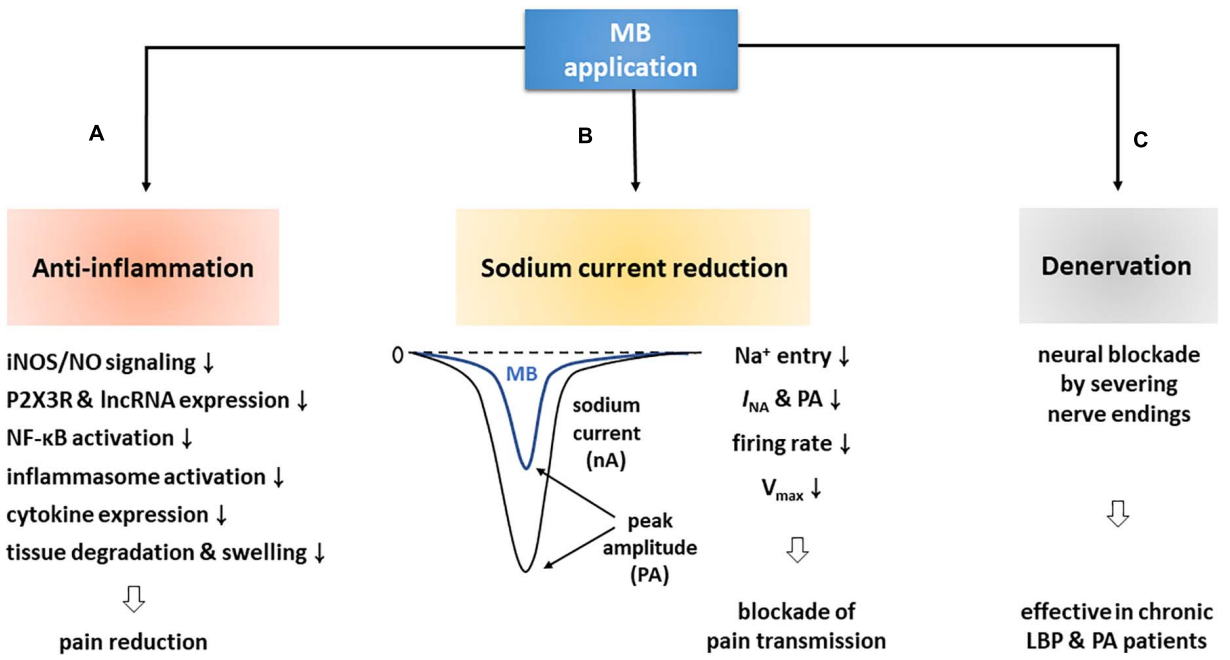

FIGURE 3 | MB contributes to pain reduction via three major routes. **(A)** First of all, MB is deeply involved in anti-inflammation. MB application blocks iNOS/NO signaling by downregulating iNOS, and suppresses P2 × 3R and lncRNA expression, NF-κB activation, and inflammasome formation, which thereby decreases inflammatory cytokine levels. These events are ultimately followed by pain reduction with the prevention of tissue degradation and swelling. **(B)** In addition, MB application attenuates neuronal excitability by decreasing I_{NA} and firing rates. These altered electrophysiological properties may contribute to pain relief by blocking synaptic transmission. **(C)** Lastly, MB application improved chronic PA and LBP. An electron microscopic experiment demonstrated that such efficacy was due to the death of nerve endings.

clinical and experimental settings. However, astonishingly, MB has been also used in biological and medical studies for a long time. Importantly, this review highlighted the relation between MB and pain reduction and made an effort to inform the relevant mechanisms. MB is engaged in pain reduction via diverse routes, but there is a still lack of scientific evidence. There are still a lot of blanks to be filled in the anti-inflammatory pathways and remain possible links to be uncovered between MB and pain-related receptors.

Modern medicine lies in the positivist tradition, which implies that medicine must be based on a solid foundation and the foundation can be constructed by the faithful observation of life phenomena (Cabanis, 1803). In addition, the certainty of medical facts can be guaranteed by that of experimental science such as experimental certainty and logical certainty. The former can be obtained by senses of observant subjects, the latter by intellectual action of humans (Bouillaud, 1836). With regard to the relation between MB and pain control, a solid foundation has not been established yet, although MB intercalates into critical signal pathways to reduce inflammation and pain. Thus, we need still further investigations to build the foundation and reach the certainty of medical facts.

Lessening pain is one of the salient issues in the medical profession, which may also determine our QoL. A great number of medications have been explored and are now applied to patients to relieve pain. Given the actions of MB in pathological or inflammatory milieus, this review offers a strong possibility that this dye may be developed as a new therapeutic agent for pain patients.

AUTHOR CONTRIBUTIONS

First of all, HH and SL set up the concept of this study, were involved in its overall design, and wrote this manuscript. Moreover, SL put a lot of effort into acquiring and analyzing the relevant articles and data, and made tables and figures to illustrate more clearly methylene blue-mediated events and mechanisms. Both authors contributed to completing this manuscript.

FUNDING

This research was supported by Basic Science Research Program through the National Research Foundation of Korea (NRF) funded by the Ministry of Education (grant number: NRF-2019R1I1A1A01063196) and supported by BMI Korea Inc. (grant no: Q1829241). BMI Korea Inc. (http://www.bmikr.co.kr), which funded partially this study, is a biotech company and mainly involved in the research and production of medicines and medical instruments. This company always supports basic medical sciences for universities and other institutes. However, this company has never been involved in the study design, collection, analysis, interpretation of data, the writing of this article, or the decision to submit it for publication.

REFERENCES

Ahn, H., Kang, S. G., Yoon, S. I., Ko, H. J., Kim, P. H., Hong, E. J., et al. (2017). Methylene blue inhibits NLRP3, NLRC4, AIM2, and non-canonical inflammasome activation. *Sci. Rep.* 7:12409.

Al-Najjim, M., Shah, R., Rahuma, M., and Gabbar, O. A. (2018). Lumbar facet joint injection in treating low back pain: radiofrequency denervation versus SHAM procedure. Systematic review. *J. Orthop.* 15, 1–8. doi: 10.1016/j.jor.2017.10.001

Armstrong, C. M., and Croop, R. S. (1982). Simulation of Na channel inactivation by thiazine dyes. *J Gen Physiol* 80, 641–662. doi: 10.1085/jgp.80.5.641

Aubrey, B. J., Kelly, G. L., Janic, A., Herold, M. J., and Strasser, A. (2018). How does p53 induce apoptosis and how does this relate to p53-mediated tumour suppression? *Cell Death Differ.* 25, 104–113. doi: 10.1038/cdd.2017.169

Bach, K. K., Lindsay, F. W., Berg, L. S., and Howard, R. S. (2004). Prolonged postoperative disorientation after methylene blue infusion during parathyroidectomy. *Anesth Analg* 99, 1573–1574. doi: 10.1213/01.ane.0000134860.73875.cf

Bennett, D. L., Clark, A. J., Huang, J., Waxman, S. G., and Dib-Hajj, S. D. (2019). The role of voltage-gated sodium channels in pain signaling. *Physiol. Rev,* 99, 1079–1151. doi: 10.1152/physrev.00052.2017

Bernier, L. P., Ase, A. R., and Seguela, P. (2018). P2X receptor channels in chronic pain pathways. *Br. J. Pharmacol.* 175, 2219–2230. doi: 10.1111/bph.13957

Bogduk, N. (2010). A cure for back pain? *Pain* 149, 7–8. doi: 10.1016/j.pain.2009.05.022

Bouillaud, J. (1836). *Essai sur la Philosophie Médicale et sur les Généralités de la Clinique Médicale*. Oxford: Université d'Oxford. De Just Rouvier et E. Le Bouvier.

Boyer, E. W., and Shannon, M. (2005). The serotonin syndrome. *N. Engl. J. Med.* 352, 1112–1120.

Cabanis, P. J. G. (1803). *Du Degré de Certitude de la Médecine*. Paris: Crapelet.

Chen, J., Ao, L., and Yang, J. (2019). Long non-coding RNAs in diseases related to inflammation and immunity. *Ann. Transl. Med.* 7:494. doi: 10.21037/atm.2019.08.37

Chen, W., Walwyn, W., Ennes, H. S., Kim, H., Mcroberts, J. A., and Marvizón, J. C. (2014). BDNF released during neuropathic pain potentiates NMDA receptors in primary afferent terminals. *Eur. J. Neurosci.* 39, 1439–1454. doi: 10.1111/ejn.12516

Chu, Y.-C., Guan, Y., Skinner, J., Raja, S. N., Johns, R. A., and Tao, Y.-X. (2005). Effect of genetic knockout or pharmacologic inhibition of neuronal nitric oxide synthase on complete Freund's adjuvant-induced persistent pain. *Pain* 119, 113–123. doi: 10.1016/j.pain.2005.09.024

Cohen, N., Robinson, D., Ben-Ezzer, J., Hemo, Y., Hasharoni, A., Wolmann, Y., et al. (2000). Reduced NO accumulation in arthrotic cartilage by exposure to methylene blue. *Acta Orthop. Scand.* 71, 630–636. doi: 10.1080/000164700317362299

Demir, I. E., Heinrich, T., Carty, D. G., Saricaoglu, ØC., Klauss, S., Teller, S., et al. (2019). Targeting nNOS ameliorates the severe neuropathic pain due to chronic pancreatitis. *EBioMedicine* 46, 431–443. doi: 10.1016/j.ebiom.2019.07.055

Deng, M., Huang, H., Ma, Y. G., Zhou, Y., Chen, Q., and Xie, P. (2021). Intradiskal injection of methylene blue for discogenic back pain: a meta-analysis of randomized controlled trials. *J. Neurol. Surg. A Cent Eur. Neurosurg.* 82, 161–165. doi: 10.1055/s-0040-1721015

Deng, S., Yu, K., Zhang, B., Yao, Y., Wang, Z., Zhang, J., et al. (2015). Toll-like receptor 4 promotes NO synthesis by upregulating GCHI expression under oxidative stress conditions in sheep Monocytes/Macrophages. *Oxid. Med. Cell.Longev.* 2015:359315.

Dinc, S., Caydere, M., Akgul, G., Yenidogan, E., Hucumenoglu, S., and Rajesh, M. (2015). Methylene Blue inhibits the inflammatory process of the acetic acid-induced colitis in the rat colonic mucosa. *Int. Surg.* 100, 1364–1374. doi: 10.9738/intsurg-d-15-00118.1

Dubin, A. E., and Patapoutian, A. (2010). Nociceptors: the sensors of the pain pathway. *J. Clin. Invest.* 120, 3760–3772. doi: 10.1172/jci42843

Etter, L., and Myers, S. A. (2002). Pruritus in systemic disease: mechanisms and management. *Dermatol. Clin.* 20, 459–472. doi: 10.1016/s0733-8635(02)00011-6

Eusebio, E. B., Graham, J., and Mody, N. (1990). Treatment of intractable pruritus ani. *Dis Colon Rectum.* 33, 770–772. doi: 10.1007/bf02052324

Floris, G., Cadeddu, R., and Bortolato, M. (2020). "The effects of serotonin degradation on psychopathology: role of monoamine oxidase," in *Handbook of the Behavioral Neurobiology of Serotonin*, eds C. P. Müller and K. A. Cunningham (Cambridge, MA: Academic Press), 267–278. doi: 10.1016/b978-0-444-64125-0.00014-1

Funakoshi, A., Tatsuno, K., Shimauchi, T., Fujiyama, T., Ito, T., and Tokura, Y. (2019). Cholecystokinin downregulates psoriatic inflammation by its possible self-regulatory effect on epidermal keratinocytes. *J. Immunol.* 202:2609. doi: 10.4049/jimmunol.1801426

Gillman, P. K. (2011). CNS toxicity involving methylene blue: the exemplar for understanding and predicting drug interactions that precipitate serotonin toxicity. *J. Psychopharmacol.* 25, 429–436. doi: 10.1177/0269881109359098

Gupta, G., Radhakrishna, M., Chankowsky, J., and Asenjo, J. F. (2012). Methylene blue in the treatment of discogenic low back pain. *Pain Physician* 15, 333–338. doi: 10.36076/ppj.2012/15/333

Harth, M., and Nielson, W. R. (2019). Pain and affective distress in arthritis: relationship to immunity and inflammation. *Expert Rev. Clin. Immunol.* 15, 541–552. doi: 10.1080/1744666x.2019.1573675

Huang, C., Tong, L., Lu, X., Wang, J., Yao, W., Jiang, B., et al. (2015). Methylene blue attenuates iNOS induction through suppression of transcriptional factor binding amid iNOS mRNA transcription. *J. Cell Biochem.* 116, 1730–1740. doi: 10.1002/jcb.25132

Jiang, M., Wang, H., Liu, Z., Lin, L., Wang, L., Xie, M., et al. (2020). Endoplasmic reticulum stress-dependent activation of iNOS/NO-NF-κB signaling and NLRP3 inflammasome contributes to endothelial inflammation and apoptosis associated with microgravity. *FASEB J.* 34, 10835–10849. doi: 10.1096/fj.202000734r

Kallewaard, J. W., Wintraecken, V. M., Geurts, J. W., Willems, P. C., Van Santbrink, H., Terwiel, C. T. M., et al. (2019). A multicenter randomized controlled trial on the efficacy of intradiscal methylene blue injection for chronic discogenic low back pain: the IMBI study. *Pain* 160, 945–953. doi: 10.1097/j.pain.0000000000001475

Kanneganti, T. D. (2015). The inflammasome: firing up innate immunity. *Immunol. Rev.* 265, 1–5. doi: 10.1111/imr.12297

Kapadia, K., Cheung, F., Lee, W., Thalappillil, R., Florence, F. B., and Kim, J. (2016). Methylene blue causing serotonin syndrome following cystocele repair. *Urol. Case Rep.* 9, 15–17. doi: 10.1016/j.eucr.2016.07.012

Kaski, S. W., White, A. N., Gross, J. D., and Siderovski, D. P. (2021). Potential for kappa-opioid receptor agonists to engineer nonaddictive analgesics: a narrative review. *Anesth. Anal.* 132, 406–419. doi: 10.1213/ane.0000000000005309

Keppel Hesselink, J. M. (2020). Rediscovery of ceruletide, a CCK agonist, as an analgesic drug. *J. Pain Res.* 13, 123–130. doi: 10.2147/jpr.s232714

Khan, M. A., North, A. P., and Chadwick, D. R. (2007). Prolonged postoperative altered mental status after methylene blue infusion during parathyroidectomy: a case report and review of the literature. *Ann. R. Coll. Surg. Engl.* 89, W9–W11.

Kim, J. H., Kim, D. H., and Lee, Y. P. (2019). Long-term follow-up of intradermal injection of methylene blue for intractable, idiopathic pruritus ani. *Tech. Coloproctol.* 23, 143–149. doi: 10.1007/s10151-019-01934-x

Kim, K. H., Kim, J. I., Han, J. A., Choe, M. A., and Ahn, J. H. (2011). Upregulation of neuronal nitric oxide synthase in the periphery promotes pain hypersensitivity after peripheral nerve injury. *Neuroscience* 190, 367–378. doi: 10.1016/j.neuroscience.2011.05.064

Kim, S. H., Ahn, S. H., Cho, Y. W., and Lee, D. G. (2012). Effect of intradiscal methylene blue injection for the chronic discogenic low back pain: one year prospective follow-up study. *Ann. Rehabil. Med.* 36, 657–664. doi: 10.5535/arm.2012.36.5.657

Kõks, S., Fernandes, C., Kurrikoff, K., Vasar, E., and Schalkwyk, L. C. (2008). Gene expression profiling reveals upregulation of Tlr4 receptors in Cckb receptor deficient mice. *Behav. Brain Res.* 188, 62–70. doi: 10.1016/j.bbr.2007.10.020

Kourosh-Arami, M., Hosseini, N., Mohsenzadegan, M., Komaki, A., and Joghataei, M. T. (2020). Neurophysiologic implications of neuronal nitric oxide synthase. *Rev. Neurosci.* 31, 617–636. doi: 10.1515/revneuro-2019-0111

Kruger, L. C., and Isom, L. L. (2016). Voltage-Gated Na+ Channels: not just for conduction. *Cold Spring Harbor Perspect. Biol.* 8:a029264. doi: 10.1101/cshperspect.a029264

Lacagnina, M. J., Watkins, L. R., and Grace, P. M. (2018). Toll-like receptors and their role in persistent pain. *Pharmacol. Ther.* 184, 145–158. doi: 10.1016/j.pharmthera.2017.10.006

Leclaire, R., Fortin, L., Lambert, R., Bergeron, Y. M., and Rossignol, M. (2001). Radiofrequency facet joint denervation in the treatment of low back pain: a placebo-controlled clinical trial to assess efficacy. *Spine* 26, 1411–1416. discussion 1417, doi: 10.1097/00007632-200107010-00003

Lee, S. W., Moon, S. W., Park, J. S., Suh, H. R., and Han, H. C. (2021). Methylene blue induces an analgesic effect by significantly decreasing neural firing rates and improves pain behaviors in rats. *Biochem. Biophys. Res. Commun.* 541, 36–42. doi: 10.1016/j.bbrc.2021.01.008

Leiper, J., and Nandi, M. (2011). The therapeutic potential of targeting endogenous inhibitors of nitric oxide synthesis. *Nat. Rev. Drug Discov.* 10, 277–291. doi: 10.1038/nrd3358

Levi, D. S., Horn, S., and Walko, E. (2014). Intradiskal methylene blue treatment for diskogenic low back pain. *PM R* 6, 1030–1037. doi: 10.1016/j.pmrj.2014.04.008

Levine, R., and Richeimer, S. H. (2011). Spinal methylene blue is hazardous. *PAIN* 152, 952–953. doi: 10.1016/j.pain.2011.01.009

Lewin, M. R., and Walters, E. T. (1999). Cyclic GMP pathway is critical for inducing long–term sensitization of nociceptive sensory neurons. *Nat. Neurosci.* 2, 18–23. doi: 10.1038/4520

Li, G., Jiang, H., Zheng, C., Zhu, G., Xu, Y., Sheng, X., et al. (2017). Long noncoding RNA MRAK009713 is a novel regulator of neuropathic pain in rats. *PAIN* 158, 2042–2052. doi: 10.1097/j.pain.0000000000001013

Li, H., Liu, S., Wang, Z., Zhang, Y., and Wang, K. (2020). Hydrogen sulfide attenuates diabetic neuropathic pain through NO/cGMP/PKG pathway and μ-opioid receptor. *Exp. Biol. Med.* 245, 823–834. doi: 10.1177/1535370220918193

Li, X., Tang, C., Wang, J., Guo, P., Wang, C., Wang, Y., et al. (2018). Methylene blue relieves the development of osteoarthritis by upregulating lncRNA MEG3. *Exp. Ther. Med.* 15, 3856–3864.

Lin, Z. H., Wang, S. Y., Chen, L. L., Zhuang, J. Y., Ke, Q. F., Xiao, D. R., et al. (2017). Methylene blue mitigates acute neuroinflammation after spinal cord injury through inhibiting nlrp3 inflammasome activation in microglia. *Front. Cell Neurosci.* 11:391. doi: 10.3389/fncel.2017.00391

Lundberg, J. O., Weitzberg, E., and Gladwin, M. T. (2008). The nitrate-nitrite-nitric oxide pathway in physiology and therapeutics. *Nat. Rev. Drug Discov.* 7, 156–167. doi: 10.1038/nrd2466

Luo, Z. D., and Cizkova, D. (2000). The role of nitric oxide in nociception. *Curr. Rev. Pain* 4, 459–466. doi: 10.1007/s11916-000-0070-y

Maas, E. T., Ostelo, R. W., Niemisto, L., Jousimaa, J., Hurri, H., Malmivaara, A., et al. (2015). Radiofrequency denervation for chronic low back pain. *Cochrane Database Syst. Rev.* CD008572.

Machelska, H., Labuz, D., Przewłocki, R., and Przewłocka, B. (1997). Inhibition of nitric oxide synthase enhances antinociception mediated by mu, delta and kappa opioid receptors in acute and prolonged pain in the rat spinal cord. *J. Pharmacol. Exp. Ther.* 282, 977–984.

Majithia, A., and Stearns, M. P. (2006). Methylene blue toxicity following infusion to localize parathyroid adenoma. *J. Laryngol. Otol.* 120, 138–140. doi: 10.1017/s0022215105005098

Martindale, S. J., and Stedeford, J. C. (2003). Neurological sequelae following methylene blue injection for parathyroidectomy. *Anaesthesia* 58, 1041–1042. doi: 10.1046/j.1365-2044.2003.03415_23.x

Mathew, S., Linhartova, L., and Raghuraman, G. (2006). Hyperpyrexia and prolonged postoperative disorientation following methylene blue infusion during parathyroidectomy. *Anaesthesia* 61, 580–583. doi: 10.1111/j.1365-2044.2006.04619.x

Matsuda, M., Huh, Y., and Ji, R. R. (2019). Roles of inflammation, neurogenic inflammation, and neuroinflammation in pain. *J. Anesth.* 33, 131–139. doi: 10.1007/s00540-018-2579-4

MHRA, (2009). *Methylthioninium Chloride (methylene blue): Update on Central Nervous System (CNS) Toxicity*. London: Medicines and Healthcare products Regulatory Agency, 2.

Miclescu, A. A., Svahn, M., and Gordh, T. E. (2015). Evaluation of the protein biomarkers and the analgesic response to systemic methylene blue in patients with refractory neuropathic pain: a double-blind, controlled study. *J. Pain Res.* 8, 387–397. doi: 10.2147/jpr.s84685

Mihai, R., Mitchell, E. W., and Warwick, J. (2007). Dose-response and postoperative confusion following methylene blue infusion during parathyroidectomy. *Can. J. Anaesth.* 54, 79–81. doi: 10.1007/bf03021907

Mukherjee, P., Cinelli, M. A., Kang, S., and Silverman, R. B. (2014). Development of nitric oxide synthase inhibitors for neurodegeneration and neuropathic pain. *Chem. Soc. Rev.* 43, 6814–6838. doi: 10.1039/c3cs60467e

Nakazawa, H., Chang, K., Shinozaki, S., Yasukawa, T., Ishimaru, K., Yasuhara, S., et al. (2017). iNOS as a driver of inflammation and apoptosis in mouse skeletal muscle after burn injury: possible involvement of sirt1 s-nitrosylation-mediated acetylation of p65 NF-κB and p53. *PLoS One* 12:e0170391. doi: 10.1371/journal.pone.0170391

Nath, S., Nath, C. A., and Pettersson, K. (2008). Percutaneous lumbar zygapophysial (Facet) joint neurotomy using radiofrequency current, in the management of chronic low back pain: a randomized double-blind trial. *Spine* 33, 1291–1297. doi: 10.1097/brs.0b013e31817329f0

Ng, B. K. W., and Cameron, A. J. D. (2010). The role of methylene blue in serotonin syndrome: a systematic review. *Psychosomatics* 51, 194–200. doi: 10.1016/s0033-3182(10)70685-x

Ng, B. K. W., Cameron, A. J. D., Liang, R., and Rahman, H. (2008). Serotonin syndrome following methylene blue infusion during parathyroidectomy: a case report and literature review. *Can. J. Anesth.* 55, 36–41. doi: 10.1007/bf03017595

North, R. A. (2004). P2X3 receptors and peripheral pain mechanisms. *J. Physiol.* 554, 301–308.

Osmanlıoğlu, H. Ø, Yıldırım, M. K., Akyuva, Y., Yıldızhan, K., and Nazıroğlu, M. (2020). Morphine induces apoptosis, inflammation, and mitochondrial oxidative stress via activation of TRPM2 Channel and nitric oxide signaling pathways in the hippocampus. *Mol. Neurobiol.* 57, 3376–3389. doi: 10.1007/s12035-020-01975-6

Pall, M. L. (2002). NMDA sensitization and stimulation by peroxynitrite, nitric oxide, and organic solvents as the mechanism of chemical sensitivity in multiple chemical sensitivity. *Faseb J.* 16, 1407–1417. doi: 10.1096/fj.01-0861hyp

Pan, P. F., Wang, Y., Li, X. P., Yang, C. B., Zhong, H., Du, X. X., et al. (2019). Effects of methylene blue on the nitric oxide-soluble guanylate cyclase-cyclic guanylyl monophosphate pathway and cytokine levels in rats with sepsis. *Int. J. Clin. Exp. Med.* 12, 12203–12211.

Peng, B., Pang, X., Wu, Y., Zhao, C., and Song, X. (2010). A randomized placebo-controlled trial of intradiscal methylene blue injection for the treatment of chronic discogenic low back pain. *Pain* 149, 124–129. doi: 10.1016/j.pain.2010.01.021

Peng, B., Zhang, Y., Hou, S., Wu, W., and Fu, X. (2007). Intradiscal methylene blue injection for the treatment of chronic discogenic low back pain. *Eur. Spine J.* 16, 33–38. doi: 10.1007/s00586-006-0076-1

Peter, C., Hongwan, D., Küpfer, A., and Lauterburg, B. H. (2000). Pharmacokinetics and organ distribution of intravenous and oral methylene blue. *Eur. J. Clin. Pharmacol.* 56, 247–250. doi: 10.1007/s002280000124

Pollack, G., Pollack, A., Delfiner, J., and Fernandez, J. (2009). Parathyroid surgery and methylene blue: a review with guidelines for safe intraoperative use. *Laryngosc.* 119, 1941–1946. doi: 10.1002/lary.20581

Polydefkis, M., Hauer, P., Sheth, S., Sirdofsky, M., Griffin, J. W., and Mcarthur, J. C. (2004). The time course of epidermal nerve fibre regeneration: studies in normal controls and in people with diabetes, with and without neuropathy. *Brain* 127, 1606–1615. doi: 10.1093/brain/awh175

Quirion, B., Bergeron, F., Blais, V., and Gendron, L. (2020). The delta-opioid receptor; a target for the treatment of pain. *Front. Mol. Neurosci.* 13:52. doi: 10.3389/fnmol.2020.00052

Rathinam, V. A., and Fitzgerald, K. A. (2016). Inflammasome complexes: emerging mechanisms and effector functions. *Cell* 165, 792–800. doi: 10.1016/j.cell.2016.03.046

Rey-Funes, M., Larrayoz, I. M., Fernández, J. C., Contartese, D. S., Rolón, F., Inserra, P. I. F., et al. (2016). Methylene blue prevents retinal damage in an experimental model of ischemic proliferative retinopathy. *Am. J. Physiol. Regul. Integr. Comp. Physiol.* 310, R1011–R1019.

Roca-Lapirot, O., Fossat, P., Ma, S., Egron, K., Trigilio, G., López-González, M. J., et al. (2019). Acquisition of analgesic properties by the cholecystokinin (CCK)/CCK2 receptor system within the amygdala in a persistent inflammatory pain condition. *Pain* 160, 345–357. doi: 10.1097/j.pain.0000000000001408

Rocha, P. A., Ferreira, A. F. B., Da Silva, J. T., Alves, A. S., Martins, D. O., Britto, L. R. G., et al. (2020). Effects of selective inhibition of nNOS and iNOS on neuropathic pain in rats. *Mol. Cell. Neurosci.* 105:103497. doi: 10.1016/j.mcn.2020.103497

Roldan, C. J., Nouri, K., Chai, T., and Huh, B. (2017). Methylene blue for the treatment of intractable pain associated with oral mucositis. *Pain Pract.* 17, 1115–1121. doi: 10.1111/papr.12566

Rowley, M., Riutort, K., Shapiro, D., Casler, J., Festic, E., and Freeman, W. D. (2009). Methylene blue-associated serotonin syndrome: a 'Green' encephalopathy after parathyroidectomy. *Neurocrit. Care* 11, 88–93. doi: 10.1007/s12028-009-9206-z

Rygick, A. N. (1968). *Atlas of the Operations on the Rectum and Colon*. Moscow: Meduch Posovie.

Saia, R. S., Ribeiro, A. B., and Giusti, H. (2020). Cholecystokinin modulates the mucosal inflammatory response and prevents the lipopolysaccharide-induced intestinal epithelial barrier dysfunction. *Shock* 53, 242–251. doi: 10.1097/shk.0000000000001355

Schiltenwolf, M., Fischer, C., and Kunz, P. (2011). How perfect studies may be? Comment on Peng et al. A randomized placebo-controlled trial of intradiscal methylene blue injection for the treatment of chronic discogenic low back pain. Pain 2010;149:124-9. *Pain* 152:954. author reply 954-955, doi: 10.1016/j.pain.2011.01.008

Schirmer, R. H., Coulibaly, B., Stich, A., Scheiwein, M., Merkle, H., Eubel, J., et al. (2003). Methylene blue as an antimalarial agent. *Redox Rep.* 8, 272–275. doi: 10.1179/135100003225002899

Schirmer, R. H., Adler, H., Pickhardt, M., and Mandelkow, E. (2011). Lest we forget you–methylene blue. *Neurobiol. Aging* 32:2325.e7–16. doi: 10.1016/j.neurobiolaging.2010.12.012

Schmid, R., and Evans, R. J. (2019). ATP-Gated P2X receptor channels: molecular insights into functional roles. *Annu. Rev. Physiol.* 81, 43–62. doi: 10.1146/annurev-physiol-020518-114259

Schwiebert, C., Irving, C., and Gillman, P. K. (2009). Small doses of methylene blue, previously considered safe, can precipitate serotonin toxicity. *Anaesthesia* 64, 924–924. doi: 10.1111/j.1365-2044.2009.06029.x

Shanmugam, G., Kent, B., Alsaiwadi, T., and Baskett, R. (2008). Serotonin syndrome following cardiac surgery. *Interact. Cardiovasc. Thorac. Surg.* 7, 656–657. doi: 10.1510/icvts.2007.173104

Starkus, J. G., Heggeness, S. T., and Rayner, M. D. (1984). Kinetic analysis of sodium channel block by internal methylene blue in pronased crayfish giant axons. *Biophys. J.* 46, 205–218. doi: 10.1016/s0006-3495(84)84014-x

Starkus, J. G., Rayner, M. D., Fleig, A., and Ruben, P. C. (1993). Fast and slow inactivation of sodium channels: effects of photodynamic modification by methylene blue. *Biophys. J.* 65, 715–726. doi: 10.1016/s0006-3495(93)81098-1

Stephan, G., Huang, L., Tang, Y., Vilotti, S., Fabbretti, E., Yu, Y., et al. (2018). The ASIC3/P2X3 cognate receptor is a pain-relevant and ligand-gated cationic channel. *Nat. Commun.* 9:1354.

Sun, J., Chen, S.-R., and Pan, H.-L. (2020). μ-Opioid receptors in primary sensory neurons are involved in supraspinal opioid analgesia. *Brain Res.* 1729:146623. doi: 10.1016/j.brainres.2019.146623

Sung, Y.-J., Sofoluke, N., Nkamany, M., Deng, S., Xie, Y., Greenwood, J., et al. (2017). A novel inhibitor of active protein kinase G attenuates chronic inflammatory and osteoarthritic pain. *Pain* 158, 822–832. doi: 10.1097/j.pain.0000000000000832

Surprenant, A., and North, R. A. (2009). Signaling at purinergic P2X receptors. *Annu. Rev. Physiol.* 71, 333–359. doi: 10.1146/annurev.physiol.70.113006.100630

Swanson, K. V., Deng, M., and Ting, J. P. (2019). The NLRP3 inflammasome: molecular activation and regulation to therapeutics. *Nat. Rev. Immunol.* 19, 477–489. doi: 10.1038/s41577-019-0165-0

Tanga, F. Y., Nutile-Mcmenemy, N., and Deleo, J. A. (2005). The CNS role of Toll-like receptor 4 in innate neuroimmunity and painful neuropathy. *Proc. Natl. Acad. Sci. U.S.A.* 102, 5856–5861. doi: 10.1073/pnas.0501634102

Top, W. M., Gillman, P. K., De Langen, C. J., and Kooy, A. (2014). Fatal methylene blue associated serotonin toxicity. *Neth. J. Med.* 72, 179–181.

Torres-López, J. E., Juárez-Rojop, I. E., Granados-Soto, V., Diaz-Zagoya, J. C., Flores-Murrieta, F. J., Ortíz-López, J. U., et al. (2007). Peripheral participation of cholecystokinin in the morphine-induced peripheral antinociceptive effect in non-diabetic and diabetic rats. *Neuropharmacology* 52, 788–795. doi: 10.1016/j.neuropharm.2006.09.015

Vutskits, L., Briner, A., Klauser, P., Gascon, E., Dayer, A. G., Kiss, J. Z., et al. (2008). Adverse effects of methylene blue on the central nervous system. *Anesthesiology* 108, 684–692. doi: 10.1097/aln.0b013e3181684be4

Wainwright, M., and Crossley, K. B. (2002). Methylene Blue–a therapeutic dye for all seasons? *J. Chemother.* 14, 431–443. doi: 10.1179/joc.2002.14.5.431

Wang, F., Ma, S.-B., Tian, Z.-C., Cui, Y.-T., Cong, X.-Y., Wu, W.-B., et al. (2021). Nociceptor-localized cGMP-dependent protein kinase I is a critical generator for central sensitization and neuropathic pain. *PAIN* 162, 135–151. doi: 10.1097/j.pain.0000000000002013

Wang, J., Ou, S.-W., and Wang, Y.-J. (2017). Distribution and function of voltage-gated sodium channels in the nervous system. *Channels* 11, 534–554. doi: 10.1080/19336950.2017.1380758

Wang, R., Ma, C., Han, Y., Tan, M., and Lu, L. (2019). Effectiveness of denervation therapy on pain and joint function for patients with refractory knee osteoarthritis: a systematic review and meta-analysis. *Pain Physician* 22, 341–352. doi: 10.36076/ppj/2019.22.341

Wang, X., Zhang, S., Xie, Z., Chen, L., Yang, B., and Wu, X. (2019). deleterious effects of methylene blue on rat nucleus pulposus cell in vitro: changes in cell viability and secretory phenotype in exposed cells. *J. Neurol. Surg. A Cent. Eur. Neurosurg.* 80, 174–179. doi: 10.1055/s-0038-1670638

Wolin, M. S., Cherry, P. D., Rodenburg, J. M., Messina, E. J., and Kaley, G. (1990). Methylene blue inhibits vasodilation of skeletal muscle arterioles to acetylcholine and nitric oxide via the extracellular generation of superoxide anion. *J. Pharmacol. Exp. Ther.* 254, 872–876.

Wolvetang, T., Janse, R., and Ter Horst, M. (2016). Serotonin syndrome after methylene blue administration during cardiac surgery: a case report and review. *J. Cardiothorac. Vasc. Anesth.* 30, 1042–1045. doi: 10.1053/j.jvca.2015.11.019

Yadav, S., and Surolia, A. (2019). Lysozyme elicits pain during nerve injury by neuronal Toll-like receptor 4 activation and has therapeutic potential in neuropathic pain. *Sci. Transl. Med.* 11:eaav4176. doi: 10.1126/scitranslmed.aav4176

Yang, Y., Li, Q., He, Q.-H., Han, J.-S., Su, L., and Wan, Y. (2018). Heteromerization of μ-opioid receptor and cholecystokinin B receptor through the third transmembrane domain of the μ-opioid receptor contributes to the anti-opioid effects of cholecystokinin octapeptide. *Exp. Mol. Med.* 50, 1–16. doi: 10.1038/s12276-018-0090-5

Yang, Y., Wang, H., Kouadir, M., Song, H., and Shi, F. (2019). Recent advances in the mechanisms of NLRP3 inflammasome activation and its inhibitors. *Cell Death Dis.* 10:128.

Ye, Y., Wang, Y., Yang, Y., and Tao, L. (2020). Aloperine suppresses LPS-induced macrophage activation through inhibiting the TLR4/NF-κB pathway. *Inflammation Res.* 69, 375–383. doi: 10.1007/s00011-019-01313-0

Yeung, A. W. K., Georgieva, M. G., Atanasov, A. G., and Tzvetkov, N. T. (2019). Monoamine oxidases (MAOs) as privileged molecular targets in neuroscience: research literature analysis. *Front. Mol. Neurosci.* 12:143. doi: 10.3389/fnmol.2019.00143

Zhang, H., Li, F., Li, W. W., Stary, C., Clark, J. D., Xu, S., et al. (2016). The inflammasome as a target for pain therapy. *Br. J. Anaesth.* 117, 693–707. doi: 10.1093/bja/aew376

Zhang, X., Hao, J., Hu, Z., and Yang, H. (2016). Clinical evaluation and magnetic resonance imaging assessment of intradiscal methylene blue injection for the treatment of discogenic low back pain. *Pain Physician* 19, E1189–E1195.

Zhang, L., Liu, Y., Huang, Z., Nan, L., Wang, F., Zhou, S., et al. (2019). Toxicity effects of methylene blue on rat intervertebral disc annulus fibrosus cells. *Pain Physician* 22, 155–164. doi: 10.36076/ppj/2019.22.155

Zhang, Y., Zhao, J., Zhang, T., and Yang, Z. (2010). In vitro assessment of the effect of methylene blue on voltage-gated sodium channels and action potentials in rat hippocampal CA1 pyramidal neurons. *Neurotoxicology* 31, 724–729. doi: 10.1016/j.neuro.2010.07.001

Zhao, X., Tang, Z., Zhang, H., Atianjoh, F. E., Zhao, J.-Y., Liang, L., et al. (2013). A long noncoding RNA contributes to neuropathic pain by silencing Kcna2 in primary afferent neurons. *Nat. Neurosci.* 16, 1024–1031. doi: 10.1038/nn.3438

Zheng, J., and Li, Q. (2019). Methylene blue regulates inflammatory response in osteoarthritis by noncoding long chain RNA CILinc02. *J. Cell Biochem.* 120, 3331–3338. doi: 10.1002/jcb.27602

Zuschlag, Z. D., Warren, M. W., and Schultz, S. K. (2018). Serotonin toxicity and urinary analgesics: a case report and systematic literature review of methylene blue-induced serotonin syndrome. *Psychosomatics* 59, 539–546. doi: 10.1016/j.psym.2018.06.012

Conflict of Interest: The authors declare that the research was conducted in the absence of any commercial or financial relationships that could be construed as a potential conflict of interest.

Copyright © 2021 Lee and Han. This is an open-access article distributed under the terms of the Creative Commons Attribution License (CC BY). The use, distribution or reproduction in other forums is permitted, provided the original author(s) and the copyright owner(s) are credited and that the original publication in this journal is cited, in accordance with accepted academic practice. No use, distribution or reproduction is permitted which does not comply with these terms.

frontiers in Neuroscience

ORIGINAL RESEARCH
published: 02 June 2021
doi: 10.3389/fnins.2021.596976

Discovery of a Highly Conserved Peptide in the Iron Transporter Melanotransferrin that Traverses an Intact Blood Brain Barrier and Localizes in Neural Cells

Chaahat S. B. Singh[1,2,3,4,5†], Brett A. Eyford[1,2,3,4†], Thomas Abraham[6†], Lonna Munro[1,2,3,4], Kyung Bok Choi[1,2,3,4], Mark Okon[7], Timothy Z. Vitalis[8], Reinhard Gabathuler[8,9], Chieh-Ju Lu[1,2,3,4], Cheryl G. Pfeifer[1,2,3,4], Mei Mei Tian[8] and Wilfred A. Jefferies[1,2,3,4,5,10,11,12]*

[1] Michael Smith Laboratories, University of British Columbia, Vancouver, BC, Canada, [2] The Vancouver Prostate Centre, Vancouver General Hospital, Vancouver, BC, Canada, [3] Centre for Blood Research, University of British Columbia, Vancouver, BC, Canada, [4] The Djavad Mowafaghian Centre for Brain Health, University of British Columbia, Vancouver, BC, Canada, [5] Department of Medical Genetics, University of British Columbia, Vancouver, BC, Canada, [6] Department of Neural and Behavioral Sciences and Microscopy Imaging Core Lab, Pennsylvania State College of Medicine, Hershey, PA, United States, [7] Department of Chemistry, University of British Columbia, Vancouver, BC, Canada, [8] Bioasis Technologies Inc., Guilford, CT, United States, [9] King's College London, London, United Kingdom, [10] Department of Urologic Sciences, University of British Columbia, Vancouver, BC, Canada, [11] Department of Microbiology and Immunology, University of British Columbia, Vancouver, BC, Canada, [12] Department of Zoology, University of British Columbia, Vancouver, BC, Canada

OPEN ACCESS

Edited by:
Flavia Eugenia Saravia, Universidad de Buenos Aires, Argentina

Reviewed by:
Santiago J. Ballaz, Yachay Tech University, Ecuador
Florencia Labombarda, CONICET Instituto de Biología y Medicina Experimental (IBYME), Argentina

***Correspondence:**
Wilfred A. Jefferies
wilf@msl.ubc.ca

† These authors have contributed equally to this work and share first authorship

Specialty section:
This article was submitted to Neuropharmacology, a section of the journal Frontiers in Neuroscience

Received: *20 August 2020*
Accepted: *01 April 2021*
Published: *02 June 2021*

Citation:
Singh CSB, Eyford BA, Abraham T, Munro L, Choi KB, Okon M, Vitalis TZ, Gabathuler R, Lu C-J, Pfeifer CG, Tian MM and Jefferies WA (2021) Discovery of a Highly Conserved Peptide in the Iron Transporter Melanotransferrin that Traverses an Intact Blood Brain Barrier and Localizes in Neural Cells. Front. Neurosci. 15:596976. doi: 10.3389/fnins.2021.596976

The blood-brain barrier (BBB) hinders the distribution of therapeutics intended for treatment of diseases of the brain. Our previous studies demonstrated that that a soluble form of melanotransferrin (MTf; Uniprot P08582; also known as p97, MFI2, and CD228), a mammalian iron-transport protein, is an effective carrier for delivery of drug conjugates across the BBB into the brain and was the first BBB targeting delivery system to demonstrate therapeutic efficacy within the brain. Here, we performed a screen to identify peptides from MTf capable of traversing the BBB. We identified a highly conserved 12-amino acid peptide, termed MTfp, that retains the ability to cross the intact BBB undigested, distribute throughout the parenchyma, and enter endosomes and lysosomes within neurons, astrocytes and microglia in the brain. This peptide may provide a platform for the transport of therapeutics to the CNS, and thereby offers new avenues for potential treatments of neuropathologies that are currently refractory to existing therapies.

Keywords: blood-brain barrer, MTfp, drug delivery and targeting, peptide transport, neuronal targeting, microglial targeting, glial targeting, melanotransferrin

INTRODUCTION

Many neurological diseases of the central nervous system (CNS) remain untreatable because the blood-brain barrier (BBB) excludes efficacious drugs from entering the brain (Rapoport, 2000; Cressant et al., 2004; Pardridge, 2007a; Banks, 2016). Methods developed to enhance the delivery of drugs to treat diseases in the brain often fail to provide significant improvements to long-term survival (Braasch et al., 2004; Kleinschnitz et al., 2010; Radermacher et al., 2013).

Several studies describe examples of antibodies conjugated to drugs that can cross the BBB as a result of their interaction with specific receptors (Jefferies et al., 1984), that suggests that drugs conjugated to the natural, endogenous ligands for these specific receptors may be of value in the ferrying therapeutic cargo to the brain (Boado et al., 2007). In order to address this, we have investigated the expression and distribution of ligands and receptor molecules on brain capillary endothelium (Food et al., 1994; Rothenberger et al., 1996; Demeule et al., 2002; Moroo et al., 2003), with the goal that these may provide novel routes of entry into the brain.

Melanotransferrin (MTf, Uniprot P08582; also known as p97, MFI2 and CD228) is an iron-binding glycoprotein belonging to the transferrin (Tf) family of molecules. MTf shares a 40% protein sequence identity with human lactoferrin and Tf (Rose et al., 1986), and is highly conserved across various species (McNagny et al., 1996). MTf is one of the oldest members in this family of proteins, dating back to more than 670 million years, and may have split from serum Tf soon after the duplication of the N and C terminal lobes, suggesting an indispensable role for MTf in iron metabolism (Lambert et al., 2005). In many species, from insects to mammals, alternative RNA splicing yields both secreted, soluble form (sMTf) and glycosylphosphatidylinositol (GPI)-anchored forms of MTf (gpiMTf) (Kennard et al., 1995; Moroo et al., 2003; Yang et al., 2004). Using isothermal titration calorimetry and differential scanning calorimetry (Creagh et al., 2005), we determined that, unlike Tf, MTf binds only one molecule of iron with an apparent binding affinity constant of 4.4×10^{17} M^{-1}, which is an affinity intermediate between the binding constants of iron to the N- and C-lobes of Tf measured under the same conditions, suggesting that MTf may successfully compete for iron *in vivo* (Rose et al., 1986; Lin et al., 1994; Kennard et al., 1995; Demeule et al., 2002; Moroo et al., 2003). The three dimensional structure of MTf has only recently been determined (Hayashi et al., 2021), and while it is useful to draw comparisons with available crystal structure data for Tf (in both its apo and holo states), it is clear that MTf and Tf have notable structural differences, most notably MTf exists as a soluble and membrane-bound form, while Tf is only found in a soluble form (Baker et al., 1992; Alemany et al., 1993; Food et al., 1994). The gpiMTf form can transport iron into mammalian cells (Kennard et al., 1995), while sMTf is able to efficiently cross the BBB and deliver iron to the CNS (Moroo et al., 2003). The latter result is particularly noteworthy as no other Tf family member has been reported to possess significant BBB transcytotic function (Kennard et al., 1995; Demeule et al., 2002; Moroo et al., 2003; Thom et al., 2018a). A broadly-specific receptor (low-density lipoprotein receptor-related protein) is capable of binding plasminogen-MTf complexes and appears to act as a receptor for MTf (Demeule et al., 2003).

We previously created a recombinant soluble form of MTf (Yang et al., 2004) analogous to sMTf that is an effective carrier for delivery of drug conjugates across the BBB into the brain (Demeule et al., 2002; Moroo et al., 2003; Karkan et al., 2008). This form of sMTf is actively transported across the BBB, by receptor mediated transcytosis at rates 10–15 times higher than those obtained with either serum transferrin (Tf) or lactoferrin (Lf) (Demeule et al., 2002). In addition, therapeutics conjugated to sMTf, can be shuttled across the BBB and were among the first BBB targeting delivery system to demonstrate therapeutic efficacy within the brain. For example, mice suffering from otherwise inaccessible brain tumors were treated with sMTf-drug or sMTf-antibody conjugates resulting in reduction of tumor growth (Karkan et al., 2008; Gabathuler et al., 2013; Nounou et al., 2016). Thus, sMTf is established as an endogenous protein with clear potential as a BBB drug delivery vehicle, however, MTf is relatively large (738 residue, ∼80 kDa) (Rose et al., 1986) and this may limit its versatility as a "trojan horse" in brain delivery.

The variability in conformation, glycosylation, anchoring and metal binding, presents potential complications to the use of MTf as a robust, reproducible, clinically useful drug delivery vehicle. Therefore, to improve upon the utility of sMTf as a drug-delivery vector, we fragmented the sMTf protein in order to identify peptides that retains the capability of carrying molecular cargo across the BBB. Here we report the identification of a fully functional, 12 amino acid derived from sMTf termed MTfp, that penetrates the brain after peripheral injection. We have previously reported that MTfp is capable of delivering a protein-based interleukin 1 receptor antagonist across the BBB and effectively ameliorates neuropathic pain in a preclinical model (Thom et al., 2018b). Furthermore we recently reported MTfp can act as a nanomule to deliver NOX4-specific siRNA to the brain that attenuate ischemic stroke (Eyford et al., 2021). Here we present comprehensive documentation on the discovery MTfp using a combination of bioinformatics and structural protein studies, its efficacy of transport into the brain of live animals, and its localization within intracellular compartments in microglia, neurons, and astrocytes within the brain parenchymal cells using microscopy.

MATERIALS AND METHODS

Animal Experiments

All protocols and procedures involving the care and use of animals in these studies reviewed and approved by the University of British Columbia Animal Care Committee, which operates under the Canadian Council for Animal Care. All studies involving live animals complied with ARRIVE guidelines (Percie du Sert et al., 2020).

Purification and Fragmentation of MTf

Recombinant human sMTf was expressed and purified at the University of British Columbia, as described previously (Hegedus et al., 1999; Yang et al., 2004). To perform trypsin digestion, 200 μL of MTf (10 mg/mL) were diluted in 1 mL of 0.15 M Tris, 6 M guanidine, 10 mM dithiothreitol, pH 9. The sample was heated at 60°C for 15 min and cooled to room temperature. The solution was further diluted with 1.8 mL of 0.15 M Tris, pH 9. Forty μg of sequencing grade modified trypsin (Cat. #V5111, Promega) were dissolved in 400 μL of 0.15 M Tris and added to the reaction mixture (1:50 trypsin to MTf ratio). The sample was incubated at 37°C for 20 h, lyophilized and

stored at −20°C. The digest was dissolved in 5 mL of 0.1% formic acid and the tryptic peptide mixture was cleaned using Sep-Pack C8 cartridges (Cat. #WAT036775, Waters). The tryptic peptides were lyophilized and stored at −20°C until transcytosis assays were performed.

Mass Spectrometry for Peptide Identification

Peptide identification was performed by MRM Proteomics (Victoria, BC). Lyophilized supernatants from the *in vitro* BBB experiments were rehydrated with 2% acetonitrile, 0.1% formic acid. The samples were resolved by liquid chromatography at 0.4 mL/min, over 43 min, using an Agilent Eclipse Plus C18 (150 × 2.1 mm, 1.8 μm) column. The eluates were analyzed on an Agilent 6490 QQQ mass spectrometer in positive mode, controlled by Agilent's MassHunter Workstation software (version B.04.01). All acquisition methods used the following parameters: 3,500 V capillary voltage, 250°C sheath gas temperature at 11 L/min sheath gas flow. The electron multiplier had a 400 V offset, the nebulizer was set to 30 p.s.i., and the first and third quadrupoles were set to unit resolution. A default fragmentor voltage and cell accelerator voltage of 380 and 5 V, respectively. The maximum cycle time was 352.5 ms. All data was processed using Agilent Quantitation software (v.B.04.01) with automatic peak detection and smoothing Gaussian width of 5. All integrated peaks were manually inspected to ensure correct peak detection and integration. For accuracy, peaks with intensity less than 50 counts and/or intra-ion pair retention time difference greater than 0.02 min were not quantitated. Quantitation was achieved by spiking a predetermined, optimized mixture of stable isotope standard peptides into the relevant experiment: YYDYSGAFR = 500 fmol/μL; DSSHAFTLDELR = 2 pmol/μL; ADVTEWR = 100 fmol/μL; VPAHAVVVR = 200 fmol/μL; ADTDGGLIFR = 200 fmol/μL. The Uniprot file human MTF used for identification was P08582[1] and the peptide peak lists were submitted to a Mascot 2.3 server against the Uniprot-Swissprot database. The peak areas were calculated for the top three peptides for each protein detected with high confidence.

In vitro BBB Model and Transcytosis Assays

Work involving peptide transcytosis through the *in vitro* BBB model was performed by Cellial Technologies (Lens France). The *in vitro* model of the BBB consists of primary bovine brain capillary endothelial cells grown to confluence on collagen coated; polycarbonate transwell inserts (0.4 μm pore size, 24 mm diameter, Cat. #3412, Corning) and supported by primary rat glial cells. Under these conditions, endothelial cells retain endothelial markers (factor VIII –related antigen, non-thrombogenic surface, production of prostacyclin, angiotensin converting enzyme activity) and characteristics of the BBB (presence of tight junctions and P-glycoprotein, paucity of pinocytotic vesicles, monoamine oxidase activity, γ-glutamyl transpeptidase activity and 500–800 Ω/cm^2 electrical resistance) (Meresse et al., 1989; Dehouck et al., 1990; Fenart et al., 1998).

[1]https://www.uniprot.org/uniprot/P08582

Primary cultures of glial cells were isolated from newborn rat cerebral cortex (Booher and Sensenbrenner, 1972). After the meninges had been cleaned off, the brain tissue was forced gently through a nylon sieve. DMEM supplemented with 10% (v/v) fetal bovine serum, 2 mM glutamine and 50 μg/mL of gentamicin was used for the dissociation of cerebral tissue and development of glial cells. The glial cells were plated at a concentration of 1.25 × 10^5 cells/mL in six-well plates and incubated at 37°C in 5% CO_2. The medium was changed twice a week. Three weeks after seeding, cultures of glial cells become stabilized.

Primary bovine brain capillary endothelial cells were cultured on gelatin-coated Petri dishes in DMEM supplemented with 10% (v/v) calf serum, 10% (v/v) horse serum, 2 mM glutamine and 50 μg/mL gentamicin. One ng/mL of basic fibroblast growth factor was then added every other day. Under these conditions, endothelial cells form a confluent monolayer in 12 days. Transwell inserts were coated, on the upper side, with rat-tail collagen prepared according to the method of Bornstein (Bornstein, 1958). Confluent endothelial cells were trypsinized and plated on the upper side of the filters at a density of 4 × 10^5 cells per insert.

Lucifer Yellow (LY), at 20 μM, was used as a paracellular marker allowing the evaluation of the integrity of the BBB. Ringer-HEPES buffer (150 mM NaCl; 5.2 mM KCl; 2.2 mM CaCl2; 0.2 mM MgCl2•6$H_2$0; 6 mM $NaHCO_3$; 5 mM HEPES; 2.8 mM glucose) was added to the lower compartment (abluminal side) of a six-well plate (3 mL per well). One mL Ringer-HEPES buffer containing the trypsin-digested MTf or synthetic peptide (0.25 mg/mL), in co-incubation with LY, was placed in the upper compartment (luminal side). Incubations were performed on a rocking platform at 37°C for 2 h. Experiments were performed in triplicate with filters containing a confluent monolayer of endothelial cells or in triplicate with empty filters coated only with collagen. At the end of the incubation period, aliquots of abluminal and luminal liquid were collected. Detection of LY fluorescence was performed using a fluorescence counter (Fluoroskan Ascent, Thermolab Systems) to ensure BBB integrity. Supernatants from the luminal and abluminal compartments were lyophilized and stored at −80°C until peptide analysis by mass spectrometry.

Synthesis of MTfp Conjugates

MTfp (DSSHAFTLDELRYC), reversed MTfp (revMTfp; RLEDLTFAHSSDYC), and the positive control for BBB transport, RVGp (YTIWMPENPRPGTPCDIFTNSRGKRASNGYC) were synthesized by Anaspec (Fremont, United States) and conjugated to Cy5. Each peptide was synthesized with addition "YC" residues on the C terminus to facilitate fluorescent labeling. After the reaction, the crude reaction mixture was purified using semi-preparative reverse phase C18 chromatography. The fractions containing the blue-colored product were collected, pooled, lyophilized and stored at −80°C.

3D Fluorescence Microscopy Imaging

Three sets of 3D fluorescence microscopy experiments were performed. The first set measured the BBB penetration of Cy5 tagged MTfp using DeltaVision Elite integrated with Huygens

TABLE 1 | Soluble melanotransferrin tryptic peptides at 3 micron pore size.

Tryptic Peptide Sequence (SEQ ID NO:)	Ablum 120:Area	Lum 120:Area	Ablum 120 conf	IonScore Ablum 120	Exp Value Ablum 120	Lum 120conf	IonScore Lum 120	Exp Value Lum 120
LFSHEGSSFQMFSSEAYGQK (SEQ ID NO:55)	1.28E+09	4.55E+09	High	115	2.50E-11	High	130	8.40E-13
HTTVFDNTNGHNSEPWAAELR (SEQ ID NO:56)	1.28E+09	1.05E+10	High	106	2.80E-10	High	103	5.80E-10
HTTVFDNTNGHNSEPWAAELR (SEQ ID NO:56)	7.04E+09	1.92E+10	High	101	9.50E-10	High	109	1.40E-10
AVSDYFGGSCVPGAGETSYSESLCR (SEQ ID NO:57)	5.49E+08	5.51E+09	High	101	2.80E-10	High	125	1.20E-12
NYPSSLCALCVGDEQGR (SEQ ID NO:58)	7.34E+07	6.15E+08	High	100	6.60E-10	High	111	6.40E-11
TLPSWGQALLSQDFELLCR (SEQ ID NO:59)	2.25E+06	1.94E+09	High	94	5.10E-09	High	133	6.80E-13
AQDLFGDDHNKNGFK (SEQ ID NO:15)	9.09E+08	5.40E+08	High	87	2.40E-08	High	72	7.10E-07
CLAEGAGDVAFVK (SEQ ID NO:60)	2.20E+09	4.38E+09	High	87	3.10E-08	High	92	7.90E-09
MFDSSNYHGQDLLFK (SEQ ID NO:61)	9.62E+08	2.06E+09	High	86	2.50E-08	High	81	7.20E-08
ADTDGGLIFR (SEQ ID NO:10)	1.59E+10	1.11E+10	High	82	8.50E-08	High	82	9.10E-08
LFSHEGSSFQMFSSEAYGQK (SEQ ID NO:55)	1.94E+08	1.06E+09	High	81	5.50E-08	High	104	3.20E-10
MFDSSNYHGQDLLFK (SEQ ID NO:61)	5.67E+09	1.73E+10	High	79	1.40E-07	High	79	1.50E-07
MFDSSNYHGQDLLFK (SEQ ID NO:61)	3.22E+07	1.01E+08	High	79	1.10E-07	High	77	1.60E-07
CGDMAVAFR (SEQ ID NO:II)	3.58E+09	7.79E+09	High	76	1.50E-07	High	79	7.30E-08
GDSSGEGVCDKSPLER (SEQ ID NO:6)	1.93E+09	5.08E+08	High	74	3.10E-07	High	82	4.20E-08
AQDLFGDDHNKNGFK (SEQ ID NO:15)	4.27E+08	7.66E+07	High	74	3.80E-07	Medium	28	1.50E-02
CGDMAVAFR (SEQ ID NO:II)	4.54E+08	2.20E+08	High	71	3.40E-07	High	79	5.50E-08
LFSHEGSSFQMFSSEAYGQKDLLFK (SEQ ID NO:62)	1.30E+07	8.27E+07	High	70	1.40E-06	High	33	6.00E-03
RDSSHAFTLDELR (SEQ ID NO:63)	1.66E+09	5.02E+09	High	68	2.70E-06	High	80	1.60E-07
AQDLFGDDHNK (SEQ ID NO:64)	3.69E+09	1.08E+09	High	63	4.50E-06	High	55	2.60E-05
LSVMGCDVLK (SEQ ID NO:65)	2.43E+09	1.07E+10	High	62	9.70E-06	High	53	8.40E-05
SEDYELLCPNGAR (SEQ ID NO:14)	2.52E+08	1.25E+08	High	62	3.90E-06	High	49	8.00E-05
EAGIQPSLLCVR (SEQ ID NO:66)	8.66E+08	1.99E+09	High	60	1.20E-05	High	59	1.40E-05
SSHVTIDTLKGVK (SEQ ID NO:4)	1.12E+08	4.73E+07	High	60	8.50E-06	High	57	1.30E-05
WCATSDPEQHK (SEQ ID NO:2)	1.01E+09	1.37E+08	High	59	5.00E-06	High	57	7.90E-06
HTTVFDNTNGHNSEPWAAELR (SEQ ID NO:56)	0.00E+00	2.95E+07	High	55	2.90E-05	High	51	6.20E-05
LSVMGCDVLK (SEQ ID NO:65)	4.85E+08	3.08E+09	High	55	4.70E-05	High	53	8.10E-05

(Continued)

TABLE 1 | Continued

Tryptic Peptide Sequence (SEQ ID NO:)	Ablum 120:Area	Lum 120:Area	Ablum 120 conf	IonScore Ablum 120	Exp Value Ablum 120	Lum 120conf	IonScore Lum 120	Exp Value Lum 120
DSSHAFTLDELR (SEQ ID NO:13)	5.87E+09	1.03E+10	High	54	5.20E-05	High	59	1.70E-05
LCRGDSSGEGVCDK (SEQ ID NO:5)	2.64E+05	2.17E+05	High	52	2.90E-05	High	47	9.70E-05
SSHVTIDTLK (SEQ ID NO:67)	3.37E+09	1.74E+09	High	48	1.90E-04	High	43	6.80E-04
LKPEIQCVSAK (SEQ ID NO:12)	4.39E+09	1.00E+09	High	46	3.00E-04	High	45	4.20E-04
VPAHAVVVR (SEQ ID NO:9)	1.24E+08	3.48E+07	High	45	6.S0E-05	High	40	2.00E-04
ADVTEWR (SEQ ID NO:8)	1.05E+10	9.31E+08	High	44	4.80E-04	High	48	2.30E-04
RSSHVTIDTLK (SEQ ID NO:3)	1.64E+08	9.53E+07	High	43	6.90E-04	High	45	4.lOE-04
SEDYELLCPNGAR (SEQ ID NO:14)	2.10E+09	2.51E+08	High	42	4.80E-04	High	60	7.40E-06
WCVLSTPEIQK (SEQ ID NO:68)	1.09E+07	0.00E+00	Medium	37	4.20E-03			
YYDYSGAFR (SEQ ID NO:7)	6.41E+09	1.00E+09	Medium	31	3.80E-03	High	51	3.70E-05
GLLCDPNR (SEQ ID NO:69)	1.65E+09	1.97E+08	Medium	30	8.60E-03	Medium	29	1.20E-02
DSSHAFTLDELRGK (SEQ ID NO:70)	1.99E+07	0.00E+00	Low	26	5.20E-02			
GLLCDPNRLPPYLR (SEQ ID NO:71)	6.75E+09	2.32E+10	Low	25	3.20E-02	Low	19	1.40E-01
EHGLKPVVGEVYDQEVGTSYYAVAVVRR (SEQ ID NO:72)	1. 70E+07	0.00E+00	Low	22	5.30E-02			
GLLCDPNRLPPYLR (SEQ ID NO:71)	1.09E+07	2.00E+08	Low	18	2.00E-01	Medium	26	3.lOE-02
CVGNSQERYYGYR (SEQ ID NO:73)	4.94E+06	0.00E+00	Low	18	1.30E-01			
CLVENAGDVAFVR (SEQ ID NO:74)	1.30E+08	5.49E+08	Low	16	4.lOE-01	High	72	1.20E-06
DSTS ELVPIATQTYEA WLGHEYLHAM K (SEQ ID NO:75)	1.55E+07	3.56E+08	Low	15	4.lOE-01	Low	11	1.00E+00
DSTS ELVPIATQTYEA WLGHEYLHAM K (SEQ ID NO:75)	0.00E+00	0.00E+00	Low	12	7.80E-01			
TLPSWGQALLSQDFELLCR (SEQ ID NO:59)	0.00E+00	0.00E+00				High	111	1.00E-10
LFSHEGSSFQMFSSEAYGQK (SEQ ID NO:55)	0.00E+00	0.00E+00				High	79	1.20E-07
IQAEQVDAVTLSGEDIYTAGK (SEQ ID NO:76)	0.00E+00	3.48E+06				High	75	4.30E-07
HSTVLENTDGK (SEQ ID NO:77)	0.00E+00	2.10E+07				High	66	2.70E-06
TVGWNVPVGYLVESGR (SEQ ID NO:78)	0.00E+00	9.38E+07				High	62	8.40E-06
LLNEGQR (SEQ ID NO:79)	0.00E+00	1.71E+07				High	43	4.30E-04
LFSHEGSSFQMFSSEAYGQKDLLFK (SEQ ID NO:80)	0.00E+00	0.00E+00				High	40	1.20E-03
ADTDGGLIFRLLNEGQR (SEQ ID NO:81)	0.00E+00	3.69E+07				High	40	1.50E-03
HTTVFDNTNGHNSEPWAAELR (SEQ ID NO:56)	0.00E+00	0.00E+00				High	38	1.20E-03

Deconvolution Software (GE, United States). As an extension of this, a set of sections were prepared to assess the cellular localization of the Cy-5 tagged MTfp in the CNS. The second set of experiments addressed the localization of Cy-5 tagged MTfp in various cell types and subcellular objects using the Leica SP8 X system (Leica, Germany).

TABLE 2 | Tryptic peptides of sMTf cross an *in vitro* BBB.

Peptide	Abundance in trypsin digest (fmol)	Luminal abundance (T = 120, fmol)	Abluminal abundance (T = 120, fmol)	Abluminal vs. luminal (%)	Abluminal vs. total (%)
DSSHAFTLDELRI	2.05E+04	1.62E+04	3.90E+02	2.41	1.90
ADTDGGLIFR	9.69E+04	7.19E+04	1.55E+03	2.16	1.60
VPAHAVWR	5.25E+03	3.20E+03	7.96E+01	2.49	1.52
ADVTEWR	6.09E+04	3.79E+04	5.02E+02	1.32	0.82
YYDYSGAFR	2.26E+04	8.43E+03	1.13E+01	0.13	0.05

Molar abundances are normalized against compartment volumes. Fraction of peptide found in the abluminal compartment compared to the initial concentration is used as the measure of transcytosis efficiency. The discrepancy between Initial concentration and abluminal concentration plus luminal concentration is likely explained by a combination of peptide degradation and adhesion to the collagen matrix or cellular monolayer.

To show that MTfp can cross the BBB, PBS, RVGp-Cy5, revMTfp-Cy5 and MTfp-Cy5 were injected IV into 6–8 week-old, female CD-1 mice (0.5 mM in PBS, 0.1 mL/mouse). Briefly, CD-1 female mice (19.4–25.6 g body weight on day of dosing, 3 per group) were injected once with PBS or one of the peptides. Two hours post injection, mice received a second IV injection of tomato lectin conjugated to FITC (100 μg/mouse, 0.1 mL). Ten minutes later, the animals were terminally anesthetized with an IP injection of 0.2 mL ketamine (200 mg/kg) and Rhompun (20 mg/kg). The bloodstream was flushed by intracardiac perfusion for 10 min at a flow rate of 1 mL/min with heparinized saline (0.9% NaCl, 100 U/mL heparin).

The brains were removed and fixed with 4% paraformaldehyde overnight and then transferred into PBS+0.01% sodium azide and stored at 4°C. The brains were embedded in 4% agarose, fixed onto the microtome stage and sectioned (20 μm) at 4°C. The sections were stained with DAPI and then mounted on microscopic slides. Glass coverslips were mounted on the sections using Prolong Gold antifade reagent. In another experiment, to assess the localization of the peptide in the CNS, brains from mice injected with either PBS or Cy5-MTfp followed by FITC- tomato lectin. The brains were collected and processed as stated above. These were then incubated with antibodies targeted against neurons (NeuN; ab177487), microglia (TMEM; ab209064), astrocytes (GFAP; ab7260), lysosomes (LAMP-1; sc-19992-AF546) and endosomes (EEA-1; sc-137130), secondary antibody staining was done for unconjugated primary antibodies with Alexa fluor 680 goat anti-mouse IgG (cat# A21058), Alexa fluor 680 goat anti-rabbit IgG (Cat #A21076) and then counter-stained with DAPI, cover slipped, imaged and quantitatively analyzed to determine the extent of localization of various cell types and subcellular objects with MTfp.

The microscopy experiments, which quantitatively assessed the cellular location of MTfp within the brain, were performed using Leica SP8 X system (Leica, Germany). 3D confocal images were acquired with a Leica AOBS SP8 laser scanning confocal microscope (Leica, Heidelberg, Germany) using a high-resolution Leica 63X/1.4 or 40X/1.3 Plan-Apochromat oil immersion objective lens. Excitations were performed using either diode or tunable white light laser sources. All images and spectral data (except DAPI) were generated using the highly sensitive HyD detectors (with gated option) in de-scanned mode. The backscattered emission signals from the sample were delivered through the tunable filter (AOBS), the detection pinhole, spectral dispersion prism, and finally to the PMT/HyD detectors. For 3D image data set acquisition, the excitation beam was first focused at the maximum signal intensity focal position within the brain tissue sample and the appropriate HyD gain levels were then selected to obtain the pixel intensities within range of 0–255 (8-bit images) using a color gradient function. The beginning and end of the 3D stack were set based on the signal level degradation. Series of 2D images for a selected 3D stack volume were then acquired with 1,024 × 1,024 pixels. The 3D stack images with optical section thickness (z-axis) of approximately 0.3 μm were captured from tissue volumes.

Spectral measurements to confirm the presence of Cy5 signal in the brain parenchyma were also performed using 32-channel Nikon Spectral Detector integrated with Nikon A1 MP+ Multi- Photon Microscope system (Nikon Instruments, New York). The laser used to produce the fluorescence emission from Cy5 was a mode-locked femto-second Spectra-Physics InSight DS femtosecond single-box laser system with automated dispersion compensation tunable between 680 and 1,300 nm (Spectra-Physics, Mountain View, CA). The laser output was attenuated using AOTF and the average power was consistently maintained below the damage threshold of the samples. The power attenuated laser was directed to a Nikon scan head coupled with Nikon upright microscope system (Nikon Instruments, New York). The laser beam was then focused on the specimen through a high numerical aperture, low magnification, long working distance, water immersion objective, CFI75 Apo Water 25X/1.1 LWD 2.0 mm WD. The backscattered emission from the sample was collected through the same objective lens. Nikon NIS Element Software was used for the image acquisition.

For each tissue volume reported here, z-section images were compiled and finally the 3D image restoration was performed using VOLOCITY software (Perkin Elmar, United Kingdom). The volume estimation was performed on the 3D image data sets recorded from four or more cortical area of brain tissue samples. Algorithms were developed to automate the quantification of the test materials and blood capillaries, and to accurately quantify test materials localized in blood capillaries vs. brain parenchyma. In these procedures, a noise removal filter (kernel size of 3 × 3) was used to remove the noise associated with the images. To define the boundary between the objects (for instance, blood capillaries)

and the background, the lower threshold level in the histogram was set to exclude all possible background voxel values. The sum of all the voxels above this threshold level is determined to be the volume. Fields from each experimental group were pooled.

Statistics

For Microscopy Images

ANOVA was used to assess the volume fractions (for instance, MTfp-Cy5) in the brain parenchyma (Prism 6, Graphpad, La Jolla, United States). The level of significance was $p < 0.05$ for the ANOVA and the *p*-values were corrected for multiple comparisons in the *post-hoc* analysis.

Nuclear Magnetic Resonance

All experiments were performed in a Bruker Ascend 850 MHz magnet at the University of British Columbia. Data were processed and analyzed using the programs TopSpin (BRUKER Ltd.) and Sparky (Goddard and Kneller) respectively. Proton correlation (COSY), total correlation (TOCSY), nuclear Overhauser effect (NOESY) spectroscopy as well as proton-carbon heteronuclear single quantum correlation (HSQC) and heteronuclear multiple bond correlation (HMBC) spectroscopy were performed on synthetic, 5 mM DSSHAFTLDELR peptide in 25 mM sodium phosphate buffer (pH 6.5) with 5% D_2O at 10, 20, 30, and 37°C. Spectral assignment was performed manually and chemical shift data were assessed by MICS (Motif Identification from Chemical Shifts) software (Shen and Bax, 2012).

Virtual Crystal

The crystal structure of MTf was only determined recently (Hayashi et al., 2021), after the present study was completed. *In silico* homology models were generated using the Robetta structure server (Baker_Lab) (data not shown) and compared to published crystals structures of human Tf (Wally et al., 2006; Wally and Buchanan, 2007).

RESULTS

Identification of MTfp

In order to identify a fragment of sMTf, that retains the ability to cross the BBB, purified, recombinant human sMTf was digested with either hydroxylamine (NH_2OH), cyanogen bromide (CNBr) or trypsin. The resulting fragments were placed on the luminal side of an *in vitro* bovine BBB model and, after 2 h, the presence of MTf fragments on the abluminal side was assessed by SDS-PAGE (NH_2OH and CNBr) and mass spectrometry (all digestions). No fragments from the CNBr or NH_2OH digests were found on the abluminal side of the BBB model (data not shown). However, 50 potential tryptic peptides were tested (**Table 1**), and five were identified in the abluminal medium of the *in vitro* BBB model: DSSHAFTLDELR; ADTDGGLIFR; VPAHAVVVR; ADVTEWR; and YYDYSGAFR. To determine relative transport efficiencies, these five peptides were synthesized and retested individually in the same BBB model system. Quantitation of transcytosis was achieved by spiking known concentrations of stable isotope labeled peptides prior to mass spectrometry. The most efficiently transcytosed peptide (DSSHAFTLDELR, MTf460-471, now known as MTfp, or commercially as $xB^{3\,TM}$ peptide) was selected as the most promising candidate for use as a BBB transport vector (**Table 2**). MTfp transit across the BBB *in vivo* was tested in mice by injecting a MTfp-Cy5 conjugate intravenously (IV), followed by visualization and quantification by 3D deconvolution fluorescence microscopy (**Figure 1** and **Supplementary Table 1**). Approximately two times greater fractional fluorescence was measured in the brain parenchyma of MTfp-Cy5 injected wild type (WT) mice when compared to control mice injected with PBS or reversed MTfp-Cy5 (revMTfp-Cy5). Interestingly, MTfp penetrated the BBB with efficiency statistically similar to that of a larger, known brain-targeting peptide derived from a rabies virus glycoprotein (RVGp). Next, the MTfp was shown to colocalize in neurons, microglia and astrocytes in the CNS. As shown in **Figure 2**, we demonstrated that 90% of the neurons expressing NeuN co-labeled with MTfp; 70% of astrocytes expressing GFAP co-labeled with MTfp; and 80% of microglia expressing TMEM co-labeled with MTfp. The subcellular markers investigated show that 40% of the MTfp is found in the lysosomes and approximately 20% is found in the early endosomes. This data demonstrates for the first time that MTfp injected IV, is widely dispersed in the brain and it is taken up into intracellular organelles.

Structural Studies of MTfp

Structural studies were carried out to identify unique features of MTfp that enable it to retain the ability of the parent molecule to cross the BBB and also differentiate it from its phylogenetic cousins such as Tf and Lf, which do not efficiently cross the BBB. MTfp (DSSHAFTLDELR) is well-conserved through evolution (**Table 3**). There is perfect sequence identity among most primates and strong conservation among many other mammals. Divergence is typically restricted to the first five residues (DSSHA). Although the primary amino acid sequence of MTfp and the analogous Tf peptide (Tfp) are different, their location on their respective proteins and their secondary structures are predicted to be nearly identical. Both are displayed as surface-exposed amphipathic turns/loops between beta-strands. The hydrophobic residues of MTfp (Phe_{465}, Leu_{467}, and Leu_{470}) are oriented toward the core of the protein, analogous to hydrophobic residues in Tfp, while the remaining residues appear to be solvent-exposed. In its protein context, both MTfp and Tfp are generally unstructured but anchoring by the hydrophobic residues seems to impart a slight helical character in the conserved C-terminal region (FTLDELR). Based on secondary structure comparison, it appears that the key differences between MTfp and Tfp are MTf $His_{463,}$ which is absent in the shorter, 11 amino acid peptide of Tfp and the substitution of an asparagine in Tfp for glutamate in MTfp at position 469 in the putative helical region. It is likely that the polar orientation and slight helical conformation of MTfp are important for MTfp's receptor

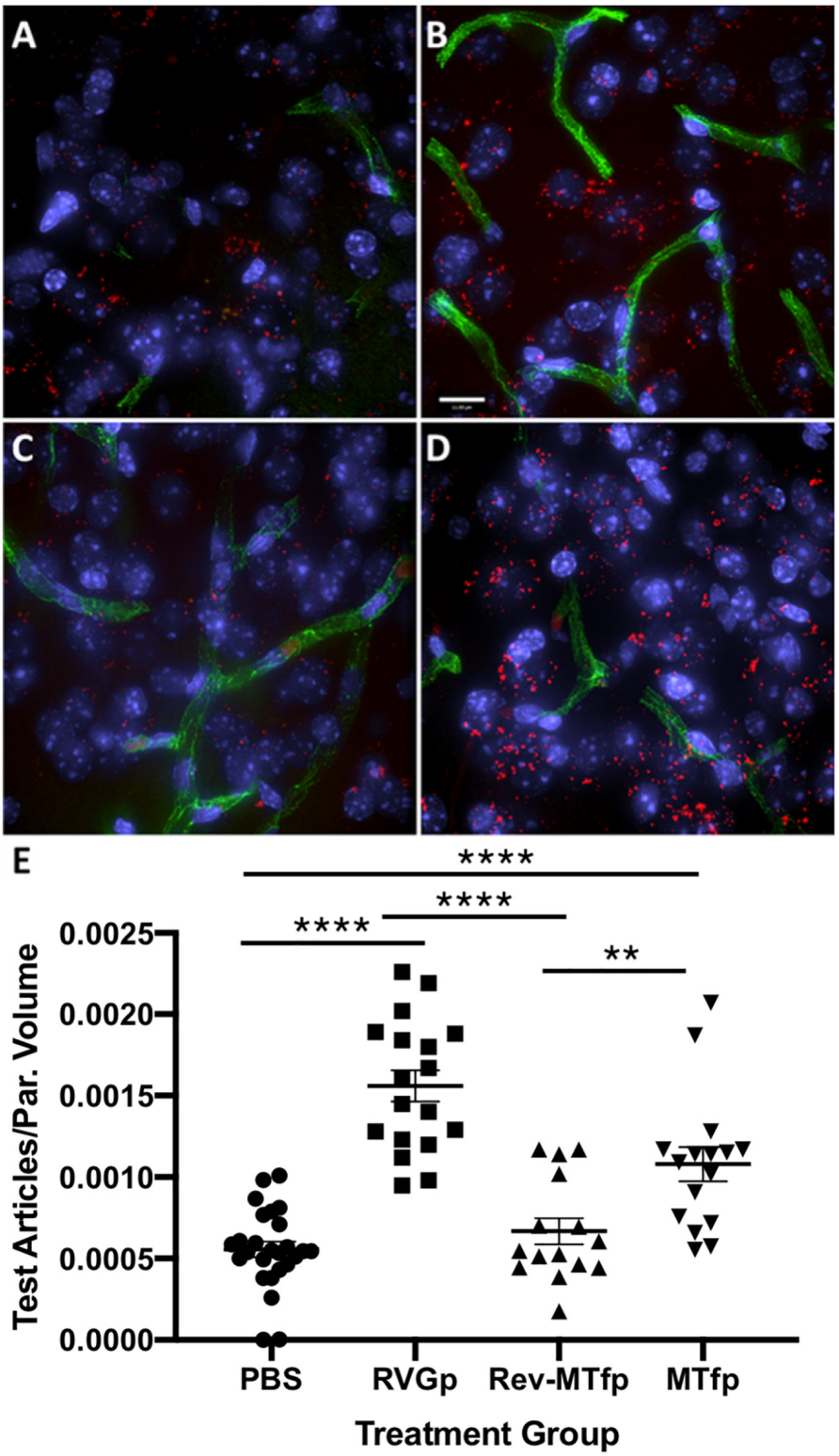

FIGURE 1 | Representative deconvolved images showing localization of MTfp in the brains of mice. Cell nuclei are blue (DAPI) and capillaries are green (FITC). **(A)** Fluorescence (red) in the brain for a mouse treated with PBS (i.e., background fluorescence), **(B)** Cy5 fluorescence in the brain after IV injection with RVGp-Cy5, **(C)** Cy5 fluorescence in the brain after IV injection of revMTfp-Cy5, **(D)** Cy5 fluorescence in the brain after IV injection of MTfp-Cy5, **(E)** brain distribution of Cy5 in wild type mice, where values indicate total volume of Cy5 fluorescence in each tissue normalized to tissue volume (VTA_{BPV} in **Supplementary Table 1**). Data are shown as individual points with the error bars indicating means ± SEM (n = 3, 3 sections/animal and 4–11 fields of view per section). $^{**}p < 0.01$, $^{****}p < 0.0001$.

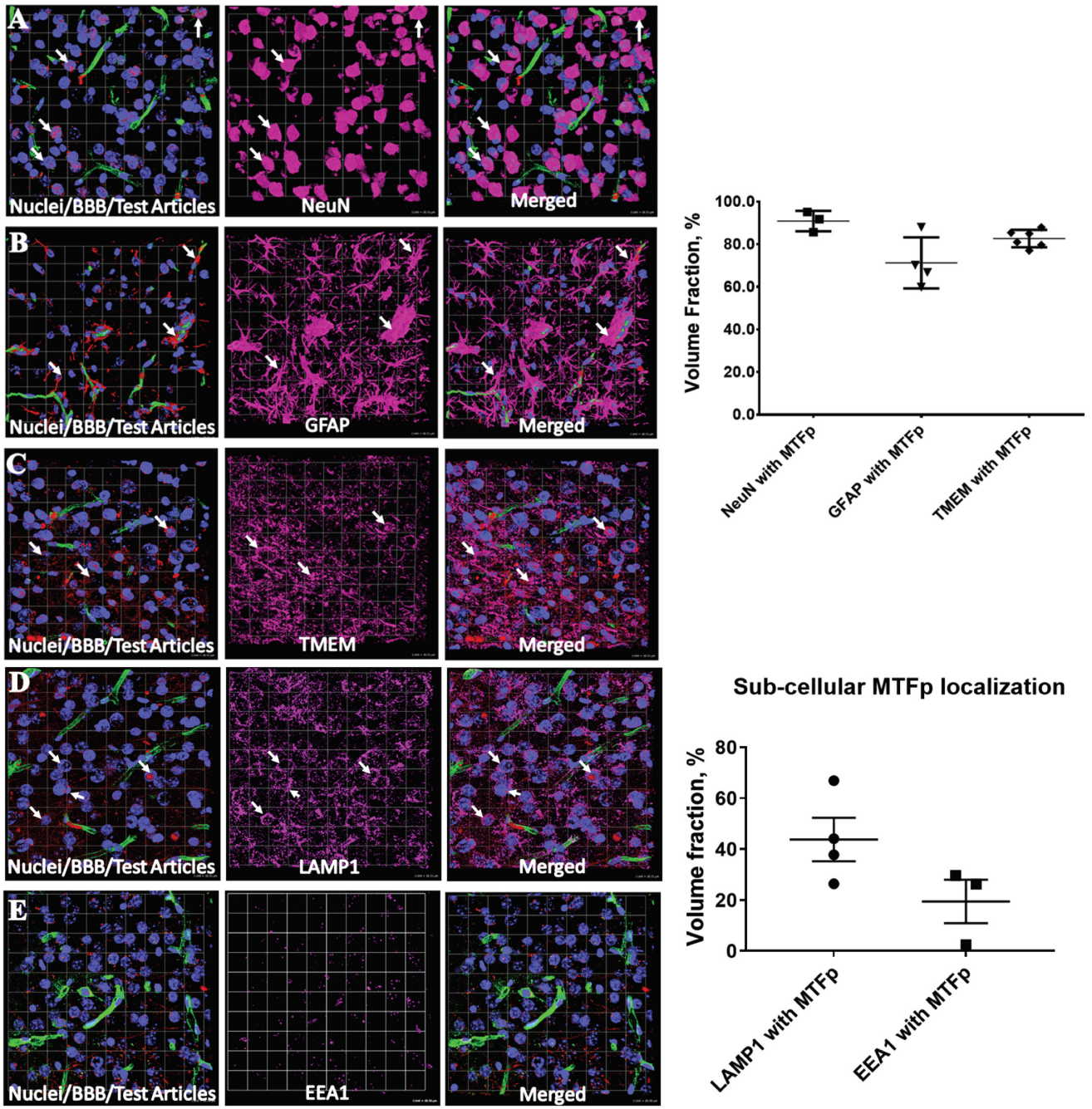

FIGURE 2 | Representative 3D confocal images showing localization of various cell types and subcellular objects with MTfp in the mouse brain sections. Cell nuclei are in blue color (DAPI) and BBBs are in green color (FITC). (**A–C)** Cellular localization of MTFp and **(A–E)** subcellular localization of MTFp. **(A)** Localization of neuronal marker NeuN (Pink) with MTfp (Red), **(B)** localization of Astrocytes marker GFAP (Pink) with MTfp (Red), **(C)** localization of Microglia marker TMEM (Pink) with MTfp (Red), **(D)** localization of Lysosomal marker LAMP1 (Pink) with MTfp (Red), **(E)** localization of Endosomal marker EEA1 (Pink) with MTfp (Red). White arrows indicate co-localization of MTfp (red) and cells (pink). The graphs represent the extent of localization of various cell types and subcellular objects with MTfp in the CNS as a percentage of fluorescence volume fraction. Each animal is presented as an individual data point in the graph with the error bars indicating mean ± SEM.

binding capability. In the MTf protein context, this polarity would be maintained by repulsion between adjacent acidic residues and hydrophobic interactions with the core of the protein. However, these stabilizing hydrophobic interactions are absent when MTfp exists as a peptide in solution. It is possible that an entropic cost, needed to orient the free peptide into an appropriate receptor- binding conformation, may reduce receptor affinity and thus rates of transcytosis.

TABLE 3 | Phylogenetic comparisons of MTfp homologues.

Common name	Species	Protein name	Accession #	Identity (%)	Sequence
Human	*Homo Sapien*	Melanotransferrin	NP_005920.2	100	DSSHAFTLDELR
Squirrel monkey	*Saimiri boliviensis boliviensis*	Melanotransferrin	XP_003926465.1	100	DSSHAFTLDELR
Bonobo	*Pan paniscus*	Melanotransferrin	XP_003806495.1	100	DSSHAFTLDELR
Chimpanzee	*Pan troglodytes*	Melanotransferrin	XP_003310242.2	100	DSSHAFTLDELR
Crab-eating macaque	*Macaca fascicularis*	hypothetical protein	EHH61865.1	100	DSSHAFTLDELR
Gibbon	*Nomascus leucogenys*	Melanotransferrin	XP_004089765.1	100	DSSHAFTLDELR
Baboon	*Papio anubis*	Melanotransferrin	XP_003895366.1	100	DSSHAFTLDELR
Rhesus macaque	*Macaca mulatta*	hypothetical protein	XP_001096034.2	100	DSSHAFTLDELR
Western lowland gorilla	*Gorilla gorilla gorilla*	Melanotransferrin	XP_004038326.1	100	DSSHAFTLDELR
Marmoset	*Callithrix jacchus*	Melanotransferrin	XP_005545367.1	100	DSSHAFTLDELR
Jerboa	*Jaculus jaculus*	Melanotransferrin	XP_004654417.1	92	DSSDAFTLDELR
Galago	*Otolemur garnettii*	Melanotransferrin	XP_003792792.1	92	DSSHSFTLDELR
Orangutan	*Pongo abelii*	Melanotransferrin	XP_002814515.1	92	DSSDAFTLDELR
Ground squirrel	*Ictidomys tridecemlineatus*	Melanotransferrin	XP_005341032.1	92	DSSYAFTLDELR
Rhinoceros	*Ceratotherium simum simum*	Melanotransferrin	XP_004424596.1	92	NSSHAFTLDELR
Alpaca	*Vicugna pacos*	Melanotransferrin	XP_006200994.1	83	NSSYAFTLDELR
Pika	*Ochotona princeps*	Melanotransferrin	XP_004578302.1	83	DSSYAFPLDELR
Flying fox	*Pteropus alecto*	Melanotransferrin	ELK17609.1	83	NSSYAFTLDELR
Bottlenose dolphin	*Tursiops truncatus*	Melanotransferrin	XP_004327245.1	83	NSSYAFTLDELR
Treeshrew	*Tupaia chinensis*	Melanotransferrin	XP_006156877.1	83	DSTHAFTVDELR
Chirrup	*Pantholops hodgsonii*	Melanotransferrin	XP_005966619.1	83	NSSYAFTLDELR
Domestic cat	*Felis catus*	Melanotransferrin	XP_003991825.1	83	NSSYAFTLDELR
Domestic cattle	*Bos taurus*	Melanotransferrin	NP_001179241.1	83	NSSYAFTLDELR
Domestic ferret	*Mustela putorius furo*	Melanotransferrin	XP_004806840.1	83	NSSYAFTLDELR
Giant panda	*Ailuropoda Melanoleuca*	Melanotransferrin	XP_002916802.1	83	NSSYAFTLDELR
Goat	*Capra hircus*	Melanotransferrin	XP_005675137.1	83	NSSYAFTLDELR
Mouse	*Mus musculus*	Melanotransferrin	NP_038928.1	83	DSSYSFTLDELR
Orca	*Orcinus orca*	Melanotransferrin	XP_004278827.1	83	NSSNAFTLDELR
Chinchilla	*Chinchilla lanigera*	Melanotransferrin	XP_005383209.1	83	DSSSAFTLNELR
Armadillo	*Dasypus novemcinctus*	Melanotransferrin	XP_004465950.1	83	DSSYAFTLDELW
Brown rat	*Rattus norvegicus*	Melanotransferrin	NP_001099342.1	83	DSSYSFTLDELR
Walrus	*Odobenus rosmarus divergens*	Melanotransferrin	XP_004391934.1	83	NSSSAFTLDELR
Prairie vole	*Microtus ochrogaster*	Melanotransferrin	XP_005344882.1	83	DSSYSFTLDELR
Domestic sheep	*Ovis aries*	Melanotransferrin	XP_004003067.1	83	NSSYAFTLDELR
Weddell seal	*Leptonychotes weddellii*	Melanotransferrin	XP_006742939.1	83	NSSYAFTLDELR
Bactrian camel	*Camelus ferus*	Melanotransferrin	XP_006179034.1	83	NSSYAFTLDELR
Wild boar	*Sus scrofa*	Melanotransferrin	XP_001926353.5	83	NSSYAFTLDELR
Yak	*Bos mutus*	Melanotransferrin	XP_005897887.1	83	NSSYAFTLDELR
African savanna elephant	*Loxodonta africana*	Melanotransferrin	XP_003412850.1	75	NSSYAFTMDELR
Chinese hamster	*Cricetulus griseus*	Melanotransferrin	ERE76419.1	75	DRSYSFTLDELR
Rabbit	*Oryctolagus cuniculus*	Melanotransferrin	NP_001075461.1	75	DSAYAFTVDELR
Degu	*Octodon degus*	Melanotransferrin	XP_004644626.1	75	DSSSAFNLNELR
Domestic dog	*Canis lupus familiaris*	Melanotransferrin	XP_005639711.1	75	NSSDAFSLDELR
Domestic guinea pig	*Cavia porcellus*	Melanotransferrin	XP_003477010.2	75	DSSSAFSLNELR
Shrew	*Sorex araneus*	Melanotransferrin	XP_004603294.1	75	NSSDAFSLDELR
Manatee	*Trichechus manatus latirostris*	Melanotransferrin	XP_004373762.1	75	NSSYAFTMDELR
Golden hamster	*Mesocricetus auratus*	Melanotransferrin	XP_005071744.1	75	DRSYSFTLDELR
Opossum	*Monodelphis domestica*	Melanotransferrin	XP_001381165.2	75	NSSYSFTLDELR
Horse	*Equus caballus*	Melanotransferrin	XP_005601955.1	75	NSSYAFTVDELR
Madagascar hedgehog	*Echinops telfairi*	Melanotransferrin	XP_004712393.1	75	NSSYAFTVDELR
Star-nosed mole	*Condylura cristata*	Melanotransferrin	XP_004675477.1	75	NSSYAFSLDELR
Human	*Homo Sapien*	Transferrin	AAB22049.1	33	SASD_LTWDNLK
Human	*Homo Sapien*	Lactoferrin	AAA59511.1	17	SDTSLTWNSVK

Amino acids which differ from the human MTfp sequence are labelled in red.

However, we have shown that MTfp is capable of transcytosis, comparable to intact sMTf.

Since this is the first known example of a peptide, derived from a larger plasma protein, being able to cross the BBB, we chose to assess the molecular dynamics of this peptide in solution over a range of temperatures (10, 20, 30, and 37°C) by proton-carbon heteronuclear multiple bond correlation spectroscopy (HMBC) and proton-proton Nuclear Overhauser Effect Spectroscopy (NOESY) nuclear magnetic resonance (NMR). As expected, based on chemical shift data from the HMBC experiments, at all temperatures, MTfp is calculated to be an unstructured coil (data not shown). However, at cooler temperatures (10 and 20°C), amide to amide NOESY signals, consistent with a helical conformation, were also observed (**Figure 3**).

DISCUSSION

Widely hailed approaches for the delivery of therapeutics to the brain often successfully demonstrate transport of the carrier or localization in an area of the brain after the BBB is disrupted by pathogenesis or by design but few, if any actually treat a CNS disease when the BBB remains intact. Different strategies have included delivery of micro-encapsulated drugs and radical methods to transiently increase the permeability of the BBB, allowing diffusion of injected drugs from the periphery into the brain (McAllister et al., 2000; Rapoport, 2000; Kinoshita et al., 2006; Pardridge, 2007a; Carpentier et al., 2016; Tsou et al., 2017). The latter approach has the additional toxicity caused by uncontrolled entry of the blood constituents into the brain and vice-versa. Traditionally, drug design has had

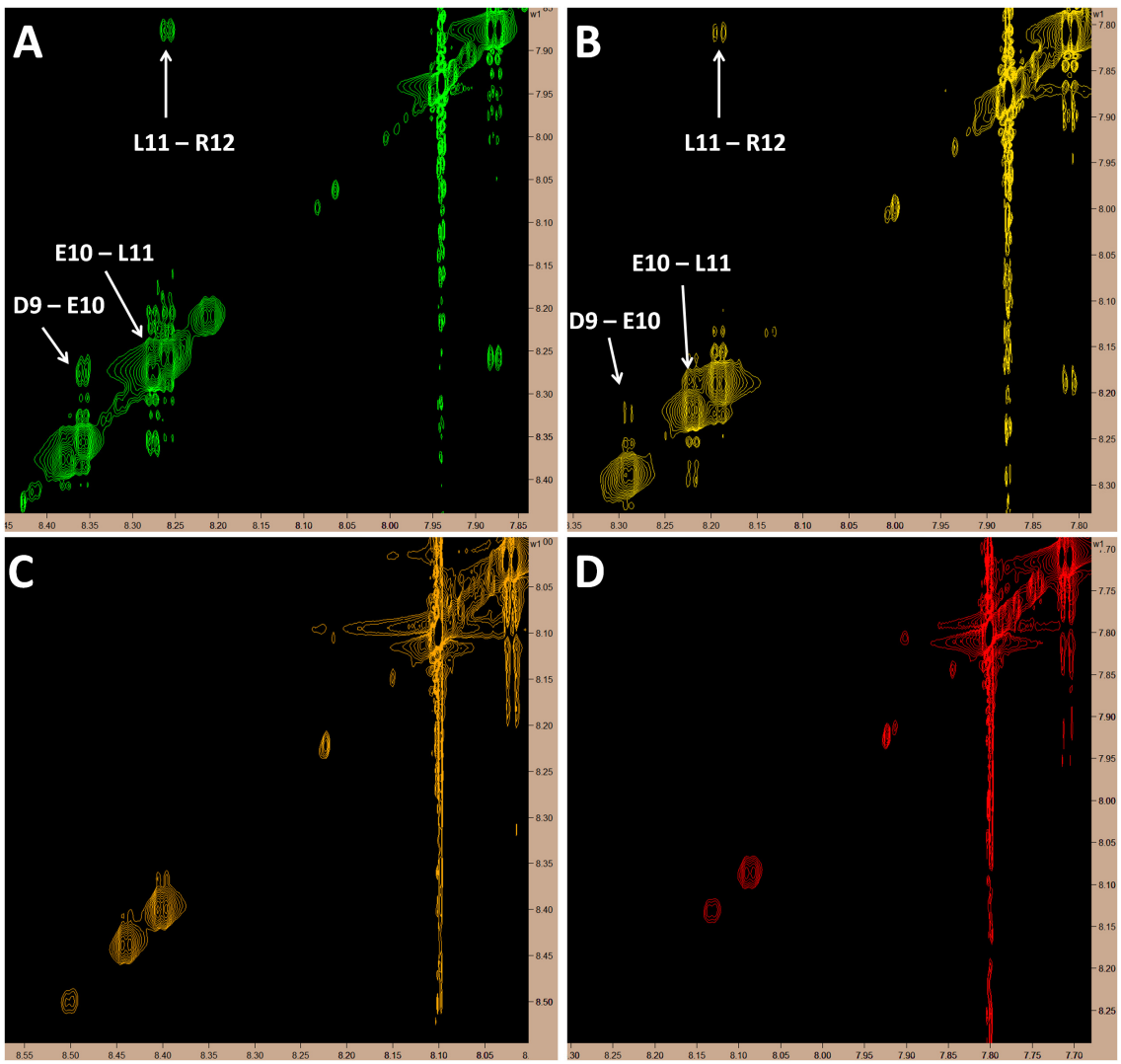

FIGURE 3 | Proton NMR showing amide to amide proximity. Cross-peak signals suggestive of a helical structure in the C-terminus of MTfp can be seen at 10 and 20°C but all signals in this region fade as temperature rises; possibly due to proton exchange with solvent. All images represent 5 mM MTfp in 25 mM sodium phosphate buffer at pH 7 with 5% D_2O. **(A)** 10°C. **(B)** 20°C. **(C)** 30°C. **(D)** 37°C.

to consider factors such as lipid solubility, charge, molecular weight and antiport action (Ohnishi et al., 1995; Patel and Patel, 2017). Drugs conjugated to small hydrophobic peptides and proteins (Pardridge, 2007a,b; Banks, 2015) or antibodies able to bind to receptors expressed on the luminal surface of the BBB (Jefferies et al., 1984; Coloma et al., 2000; Zuchero et al., 2016), have been studied. For example, MRC OX26, an antibody made against the transferrin receptor (Jefferies et al., 1984) has been used to deliver drugs to tumors in the periphery (Kratz et al., 1998) and in the brain (Lee et al., 2000; Sonoda et al., 2018). Although delivery to the brain is sometimes achievable, its use is limited due to saturation of the receptor, low dissociation rate of the antibody on the abluminal side of the BBB and consequential recycling of the receptor back to the blood (Moos and Morgan, 2001). Hyper-immunity against the carrier may also limit repeated treatments with the same drug conjugates (Tovey and Lallemand, 2011; Carrasco-Triguero et al., 2019). In addition, many of the targeted receptors are widely expressed in other tissues resulting in potential toxicity (Kratz et al., 1998). Thus, novel approaches are required to increase the survival of patients with CNS tumors and other currently untreatable brain diseases such as lysosomal storage diseases.

We have previously shown that the soluble form of mammalian iron-binding protein melanotransferrin is able to deliver small anti-cancer agents to the brain and reduce the growth of tumors therein resulting in extending the survival of the treated animals. However, there are limitations in using sMTf and other large protein carriers. These include; heterogeneity in post-translational modifications, variability in the site of cargo chemical conjugation and the adoption of different structural conformations upon conjugation that may alter the targeting moiety or the action of the drug. The other major problem is that approaches using chemical conjugates are not scalable and batch production requires standards of equivalency that are cost and time prohibitive.

In the context of the present study, the variability in conformation, glycosylation, anchoring and metal binding, presents potential complications to the use of sMTf as a robust, reproducible, clinically useful drug delivery vehicle. Therefore, to improve upon the utility of sMTf as a drug-delivery vector, we fragmented the protein in order to identify the minimally active region that retains the capability of carrying molecular cargo across the BBB. We report the identification of a 12 amino acid peptide (MTfp; DSSHAFTLDELR), derived from melanotransferrin protein, that retains the ability crosses the BBB *in vitro* and *in vivo*. Interestingly, MTfp penetrated the BBB with efficiency similar to that of a larger, known brain-targeting peptide derived from a rabies virus glycoprotein (RVGp) (Kumar et al., 2007; Alvarez-Erviti et al., 2011). Using a novel stable isotopic liquid chromatography mass spectrometry methodology to measure the transport of MTfp into the brain, we have reported elsewhere the initial rate of entry as 2.1 nM/min (Singh et al., 2020). Structural studies were then carried out to identify unique features of MTfp that enable it to retain the ability to cross the BBB and also differentiate it from its phylogenetic cousins such as Tf and Lf, which do not efficiently cross the BBB. MTfp (DSSHAFTLDELR) is well-conserved through evolution (**Table 3**). There is perfect sequence identity among most primates and strong conservation among many other mammals. Divergence is typically restricted to the first five residues (DSSHA). When there is a substitution, the altered amino acid is often physiochemically similar and therefore, potentially benign. The lack of variability in the C-terminal portion of MTfp suggests that this region is most important for receptor binding. This supposition is supported by the facts that human MTfp was identified by transcytosis across a model of the bovine BBB and *in vivo* transcytosis is observed in mice. Both bovine and murine MTfp homologues differ from the human version by two amino acids; both near the N terminus (**Table 3**). MTfp shows significantly reduced sequence identity with analogous peptides from the close MTf relatives, Tf or Lf (**Table 3**), this feature potentially explaining the unique ability of MTf for BBB transcytosis compared to other members of the transferrin family. The three dimensional structure of MTf, co-crystallized with the Fab portion of the anti-MTf antibody SC57.32, was only recently determined (Hayashi et al., 2021). This crystal structure confirms our analysis that the DSSHAFTLDELR peptide is not only exposed on the surface, but that it extends outward from the structure and forms part of the epitope for the antibody used in the crystallization. This implies DSSHAFTLDELR would be available as a suitable docking region for receptors.

Furthermore, we present preliminary evidence that MTfp is able to adopt a helical conformation (**Figure 3**). Secondary structure is unusual in such a small peptide; however, our experimental data suggests that MTfp has the propensity to adopt a transient helical character, possibly driven by repulsion between the neighboring acidic residues. Perhaps this tendency toward a helix, similar to its conformation while part of sMTf, reduces the energetic cost of peptide-receptor binding and contributes to the peptide's unique transcytosis potential.

Designing efficient "vectors" (antibodies, protein carriers, viruses, nanoparticles) to navigate and deliver therapeutics across the BBB, in a controlled and non-invasive manner, remains one of the key goals of drug development for brain diseases. Drug design for CNS diseases is constrained by factors such as lipid solubility, charge, molecular weight, and the antiport action of specific transporters. Many methods developed to enhance the delivery of drugs to treat brain diseases have failed to provide significant improvements to long-term survival. Drugs conjugated to small hydrophobic peptides, proteins, or antibodies are able to bind to receptors expressed on the luminal surface of the BBB, however, without accumulation in the brain the resulting efficacious consequences on disease are often severely lacking. Unfortunately, these approaches are often limited due to saturation of the receptors, low dissociation rate on the abluminal side of the BBB, and recycling of the receptor back to the lumen. In addition, many targeted receptors are widely expressed in tissues other than the brain, resulting in potential toxicity and reduced transport to the brain because of competition in

peripheral tissues. The data on the identification of a MTf-derived 12 amino acid peptide that retains its ability to cross the BBB and enter the intracellular compartment of resident neurons, astrocytes and microglia may begin to address many of these existing limitations.

DATA AVAILABILITY STATEMENT

The original contributions presented in the study are included in the article/**Supplementary Material**, further inquiries can be directed to the corresponding author/s.

ETHICS STATEMENT

The animal study was reviewed and approved by the University of British Columbia, Animal Care Committee, under the guidelines of the Canadian Council for Animal Care.

AUTHOR CONTRIBUTIONS

BAE, CSBS, and WAJ wrote the manuscript. WAJ conceived the project and conducted the analysis leading to the identification of MTfp. All authors contributed to the manuscript, revised it, and approved the final version.

FUNDING

WAJ was provided funding through donations to the Sullivan Urology Foundation at Vancouver General Hospital and by grants from the Canadian Institutes for Health Research (MOP-133635), the Natural Sciences and Engineering Research Council of Canada (CRDPJ 452456-13), the W. Garfield Weston Foundation, and a University of British Columbia, industrial partnership agreement with Bioasis Technologies Inc. (BTI). TA was supported by NIH Grants 1S10OD010756-01A1 and 1S10OD018124-01A1. BAE was supported by Postdoctoral Fellowships from the Michael Smith Foundation for Health Research, the Centre for Blood Research at the University of British Columbia, and the Pacific Alzheimer's Foundation. CSBS was supported by an Alzheimer's Drug Discovery Foundation Outstanding Young Investigator Scholarship, a William and Dorothy Gilbert Graduate Scholarship in Biomedical Sciences at the University of British Columbia, and a scholarship from the Centre for Blood Research Graduate Student Award at the University of British Columbia.

ACKNOWLEDGMENTS

We thank Lawrence McIntosh from the University of British Columbia, Department of Chemistry for access to the NMR equipment, consultation on the NMR experiments, and data analysis; Terry Pearson from the University of Victoria, Department of Biochemistry for his comments on the manuscript; and Wade Edris for his technical assistance with confocal and deconvolution microscopy imaging. We also thank MRM Proteomics, Cellial Technologies, and Ava McHugh for their professional services. This manuscript is originally part of a larger study that has been released as a pre-print at bioR*x*iv (Eyford et al., 2019).

SUPPLEMENTARY MATERIAL

The Supplementary Material for this article can be found online at: https://www.frontiersin.org/articles/10.3389/fnins.2021.596976/full#supplementary-material

REFERENCES

Alemany, R., Vila, M. R., Franci, C., Egea, G., Real, F. X., and Thomson, T. M. (1993). Glycosyl phosphatidylinositol membrane anchoring of melanotransferrin (p97): apical compartmentalization in intestinal epithelial cells. *J. Cell Sci.* 104, 1155–1162.

Alvarez-Erviti, L., Seow, Y., Yin, H., Betts, C., Lakhal, S., and Wood, M. J. (2011). Delivery of siRNA to the mouse brain by systemic injection of targeted exosomes. *Nat. Biotechnol.* 29, 341–345. doi: 10.1038/nbt.1807

Baker, E. N., Baker, H. M., Smith, C. A., Stebbins, M. R., Kahn, M., Hellstrom, K. E., et al. (1992). Human melanotransferrin (p97) has only one functional iron-binding site. *FEBS Lett.* 298, 215–218.

Baker_Lab Robetta is a Protein Structure Prediction Service that is Continually Evaluated Through CAMEO. Seattle, WA: Baker_Lab. (accessed 2015).

Banks, W. A. (2015). Peptides and the blood-brain barrier. *Peptides* 72, 16–19.

Banks, W. A. (2016). From blood-brain barrier to blood-brain interface: new opportunities for CNS drug delivery. *Nat. Rev. Drug Discov.* 15, 275–292.

Boado, R. J., Zhang, Y., Zhang, Y., Xia, C. F., and Pardridge, W. M. (2007). Fusion antibody for Alzheimer's disease with bidirectional transport across the blood-brain barrier and abeta fibril disaggregation. *Bioconjug. Chem.* 18, 447–455. doi: 10.1021/bc060349x

Booher, J., and Sensenbrenner, M. (1972). Growth and cultivation of dissociated neurons and glial cells from embryonic chick, rat and human brain in flask cultures. *Neurobiology* 2, 97–105.

Bornstein, M. B. (1958). Reconstituted rattail collagen used as substrate for tissue cultures on coverslips in Maximow slides and roller tubes. *Lab. Invest.* 7, 134–137.

Braasch, D. A., Paroo, Z., Constantinescu, A., Ren, G., Oz, O. K., Mason, R. P., et al. (2004). Biodistribution of phosphodiester and phosphorothioate siRNA. *Bioorg. Med. Chem. Lett.* 14, 1139–1143. doi: 10.1016/j.bmcl.2003.12.074

Carpentier, A., Canney, M., Vignot, A., Reina, V., Beccaria, K., Horodyckid, C., et al. (2016). Clinical trial of blood-brain barrier disruption by pulsed ultrasound. *Sci. Transl. Med.* 8:343re2. doi: 10.1126/scitranslmed.aaf6086

Carrasco-Triguero, M., Dere, R. C., Milojic-Blair, M., Saad, O. M., Nazzal, D., Hong, K., et al. (2019). Immunogenicity of antibody-drug conjugates: observations across 8 molecules in 11 clinical trials. *Bioanalysis* 11, 1555–1568. doi: 10.4155/bio-2018-0259

Coloma, M. J., Lee, H. J., Kurihara, A., Landaw, E. M., Boado, R. J., Morrison, S. L., et al. (2000). Transport across the primate blood-brain barrier of a genetically engineered chimeric monoclonal antibody to the human insulin receptor. *Pharm. Res.* 17, 266–274.

Creagh, A. L., Tiong, J. W., Tian, M. M., Haynes, C. A., and Jefferies, W. A. (2005). Calorimetric studies of melanotransferrin (p97) and its interaction with iron. *J. Biol. Chem.* 280, 15735–15741. doi: 10.1074/jbc.m414650200

Cressant, A., Desmaris, N., Verot, L., Brejot, T., Froissart, R., Vanier, M. T., et al. (2004). Improved behavior and neuropathology in the mouse model of Sanfilippo type IIIB disease after adeno-associated virus-mediated gene transfer

in the striatum. *J. Neurosci.* 24, 10229–10239. doi: 10.1523/jneurosci.3558-04.2004

Dehouck, M. P., Meresse, S., Delorme, P., Fruchart, J. C., and Cecchelli, R. (1990). An easier, reproducible, and mass-production method to study the blood-brain barrier in vitro. *J. Neurochem.* 54, 1798–1801. doi: 10.1111/j.1471-4159.1990.tb01236.x

Demeule, M., Bertrand, Y., Michaud-Levesque, J., Jodoin, J., Rolland, Y., Gabathuler, R., et al. (2003). Regulation of plasminogen activation: a role for melanotransferrin (p97) in cell migration. *Blood* 102, 1723–1731. doi: 10.1182/blood-2003-01-0166

Demeule, M., Poirier, J., Jodoin, J., Bertrand, Y., Desrosiers, R. R., Dagenais, C., et al. (2002). High transcytosis of melanotransferrin (P97) across the blood-brain barrier. *J. Neurochem.* 83, 924–933. doiNODOI doi: 10.1046/j.1471-4159.2002.01201.x

Eyford, B. A., Singh, C. S. B., Abraham, T., Munro, L., Choi, K. B., Hildebrandt, R., et al. (2019). A nanomule peptide-siRNA conjugate that traverses the intact blood brain barrier and attenuates stroke. *BioRxiv* [Preprint] doi: 10.1101/871186 BioRxiv: 871186

Eyford, B. A., Singh, C. S. B., Abraham, T., Munro, L., Choi, K. B., Hildebrandt, R., et al. (2021) A nanomule peptide carrier delivers siRNA across the intact blood-brain barrier to attenuate ischemic stroke. *Front. Mol. Biosci.* 8:611367. doi: 10.3389/fmolb.2021.611367

Fenart, L., Buee-Scherrer, V., Descamps, L., Duhem, C., Poullain, M. G., Cecchelli, R., et al. (1998). Inhibition of P-glycoprotein: rapid assessment of its implication in blood-brain barrier integrity and drug transport to the brain by an in vitro model of the blood-brain barrier. *Pharm. Res.* 15, 993–1000.

Food, M. R., Rothenberger, S., Gabathuler, R., Haidl, I. D., Reid, G., and Jefferies, W. A. (1994). Transport and expression in human melanomas of a transferrin-like glycosylphosphatidylinositol-anchored protein. *J. Biol. Chem.* 269, 3034–3040. doi: 10.1016/s0021-9258(17)42043-6

Gabathuler, R., Vitalis, T. Z., Nounou, M. I., Iqbal, U., Moreno, M., Adkins, C. E., et al. (2013). "Abstract A247: BT2111, a new anticancer agent composed of trastuzumab and transcend a vector for brain delivery for the treatment of metastatic Her2+ breast cancer," in *Paper Presented At: AACR-NCI-EORTC International Conference: Molecular Targets and Cancer Therapeutics* (Boston, MA: Moelcular Cancer Therapeutics).

Goddard, T. D., and Kneller, D. G.. (). *SPARKY 3*. San Francisco, CA: University of California. (accessed 2015).

Hayashi, K., Longenecker, K. L., Liu, Y. L., Faust, B., Prashar, A., Hampl, J., et al. (2021). Complex of human Melanotransferrin and SC57.32 Fab fragment reveals novel interdomain arrangement with ferric N-lobe and open C-lobe. *Sci. Rep.* 11:566. doi: 10.1038/s41598-020-79090-8

Hegedus, D. D., Pfeifer, T. A., Theilmann, D. A., Kennard, M. L., Gabathuler, R., Jefferies, W. A., et al. (1999). Differences in the expression and localization of human melanotransferrin in lepidopteran and dipteran insect cell lines. *Protein Expr. Purif.* 15, 296–307.

Jefferies, W. A., Brandon, M. R., Hunt, S. V., Williams, A. F., Gatter, K. C., and Mason, D. Y. (1984). Transferrin receptor on endothelium of brain capillaries. *Nature* 312, 162–163. doi: 10.1038/312162a0

Karkan, D., Pfeifer, C., Vitalis, T. Z., Arthur, G., Ujiie, M., Chen, Q., et al. (2008). A unique carrier for delivery of therapeutic compounds beyond the blood-brain barrier. *PLoS One* 3:e2469. doi: 10.1371/journal.pone.0002469

Kennard, M. L., Richardson, D. R., Gabathuler, R., Ponka, P., and Jefferies, W. A. (1995). A novel iron uptake mechanism mediated by GPI-anchored human p97. *EMBO J.* 14:4178. doi: 10.1002/j.1460-2075.1995.tb00091.x

Kinoshita, M., McDannold, N., Jolesz, F. A., and Hynynen, K. (2006). Noninvasive localized delivery of Herceptin to the mouse brain by MRI-guided focused ultrasound-induced blood-brain barrier disruption. *Proc. Natl. Acad. Sci. U.S.A.* 103, 11719–11723. doi: 10.1073/pnas.0604318103

Kleinschnitz, C., Grund, H., Wingler, K., Armitage, M. E., Jones, E., Mittal, M., et al. (2010). Post-stroke inhibition of induced NADPH oxidase type 4 prevents oxidative stress and neurodegeneration. *PLoS Biol.* 8:e1000479. doi: 10.1371/journal.pbio.1000479

Kratz, F., Beyer, U., Roth, T., Tarasova, N., Collery, P., Lechenault, F., et al. (1998). Transferrin conjugates of doxorubicin: synthesis, characterization, cellular uptake, and in vitro efficacy. *J. Pharm. Sci.* 87, 338–346. doi: 10.1021/js970246a

Kumar, P., Wu, H., McBride, J. L., Jung, K. E., Kim, M. H., Davidson, B. L., et al. (2007). Transvascular delivery of small interfering RNA to the central nervous system. *Nature* 448, 39–43. doi: 10.1038/nature05901

Lambert, L. A., Perri, H., Halbrooks, P. J., and Mason, A. B. (2005). Evolution of the transferrin family: conservation of residues associated with iron and anion binding. *Comp. Biochem. Physiol. B Biochem. Mol. Biol.* 142, 129–141. doi: 10.1016/j.cbpb.2005.07.007

Lee, H. J., Engelhardt, B., Lesley, J., Bickel, U., and Pardridge, W. M. (2000). Targeting rat anti-mouse transferrin receptor monoclonal antibodies through blood-brain barrier in mouse. *J. Pharmacol. Exp. Ther.* 292, 1048–1052.

Lin, L. N., Mason, A. B., Woodworth, R. C., and Brandts, J. F. (1994). Calorimetric studies of serum transferrin and ovotransferrin. Estimates of domain interactions, and study of the kinetic complexities of ferric ion binding. *Biochemistry* 33, 1881–1888. doi: 10.1021/bi00173a035

McAllister, L. D., Doolittle, N. D., Guastadisegni, P. E., Kraemer, D. F., Lacy, C. A., Crossen, J. R., et al. (2000). Cognitive outcomes and long-term follow-up results after enhanced chemotherapy delivery for primary central nervous system lymphoma. *Neurosurgery* 46, 51–60. discussion 60-51, doi: 10.1093/neurosurgery/46.1.51

McNagny, K. M., Rossi, F., Smith, G., and Graf, T. (1996). The eosinophil-specific cell surface antigen, EOS47, is a chicken homologue of the oncofetal antigen melanotransferrin. *Blood* 87, 1343–1352. doi: 10.1182/blood.v87.4.1343.bloodjournal8741343

Meresse, S., Dehouck, M. P., Delorme, P., Bensaid, M., Tauber, J. P., Delbart, C., et al. (1989). Bovine brain endothelial cells express tight junctions and monoamine oxidase activity in long-term culture. *J. Neurochem.* 53, 1363–1371. doi: 10.1111/j.1471-4159.1989.tb08526.x

Moos, T., and Morgan, E. H. (2001). Restricted transport of anti-transferrin receptor antibody (OX26) through the blood-brain barrier in the rat. *J. Neurochem.* 79, 119–129. doi: 10.1046/j.1471-4159.2001.00541.x

Moroo, I., Ujiie, M., Walker, B. L., Tiong, J. W. C., Vitalis, T. Z., Karkan, D., et al. (2003). Identification of a novel route of iron transcytosis across the mammalian blood-brain barrier. *Microcirculation* 10, 457–462. doi: 10.1038/sj.mn.7800213

Nounou, M. I., Adkins, C. E., Rubinchik, E., Terrell-Hall, T. B., Afroz, M., Vitalis, T., et al. (2016). Anti-cancer antibody trastuzumab-melanotransferrin conjugate (BT2111) for the treatment of metastatic HER2+ breast cancer tumors in the brain: an in-vivo study. *Pharm. Res.* 33, 2930–2942. doi: 10.1007/s11095-016-2015-0

Ohnishi, T., Tamai, I., Sakanaka, K., Sakata, A., Yamashima, T., Yamashita, J., et al. (1995). In vivo and in vitro evidence for ATP-dependency of P-glycoprotein-mediated efflux of doxorubicin at the blood-brain barrier. *Biochem. Pharmacol.* 49, 1541–1544. doi: 10.1016/0006-2952(95)00082-b

Pardridge, W. M. (2007a). Blood-brain barrier delivery of protein and non-viral gene therapeutics with molecular Trojan horses. *J. Control Release* 8, 345–348. doi: 10.1016/j.jconrel.2007.04.001

Pardridge, W. M. (2007b). Brain drug development and brain drug targeting. *Pharm. Res.* 24, 1729–1732.

Patel, M. M., and Patel, B. M. (2017). Crossing the blood-brain barrier: recent advances in drug delivery to the brain. *CNS Drugs* 31, 109–133. doi: 10.1007/s40263-016-0405-9

Percie du Sert, N., Ahluwalia, A., Alam, S., Avey, M. T., Baker, M., Browne, W. J., et al. (2020). Reporting animal research: explanation and elaboration for the ARRIVE guidelines 2.0. *PLoS Biol* 18:e3000411. doi: 10.1371/journal.pbio.3000411

Radermacher, K. A., Wingler, K., Langhauser, F., Altenhofer, S., Kleikers, P., Hermans, J. J., et al. (2013). Neuroprotection after stroke by targeting NOX4 as a source of oxidative stress. *Antioxid. Redox Signal.* 18, 1418–1427. doi: 10.1089/ars.2012.4797

Rapoport, S. I. (2000). Osmotic opening of the blood-brain barrier: principles, mechanism, and therapeutic applications. *Cell Mol. Neurobiol.* 20, 217–230.

Rose, T. M., Plowman, G. D., Teplow, D. B., Dreyer, W. J., Hellstrom, K. E., and Brown, J. P. (1986). Primary structure of the human melanoma-associated antigen p97 (melanotransferrin) deduced from the mRNA sequence. *Proc. Natl. Acad. Sci. U.S.A* 83, 1261–1265. doi: 10.1073/pnas.83.5.1261

Rothenberger, S., Food, M. R., Gabathuler, R., Kennard, M. L., Yamada, T., Yasuhara, O., et al. (1996). Coincident expression and distribution of

melanotransferrin and transferrin receptor in human brain capillary endothelium. *Brain Res.* 712, 117–121. doi: 10.1016/0006-8993(96)88505-2

Shen, Y., and Bax, A. (2012). Identification of helix capping and b-turn motifs from NMR chemical shifts. *J. Biomol. NMR* 52, 211–232. doi: 10.1007/s10858-012-9602-0

Singh, C. S. B., Gordon, J. A., Adomat, H., Guns, E. S. T., Lu, C. J., Pfeifer, C. G., et al. (2020). A stable isotopic liquid chromatography mass spectrometry method to measure the transport of peptides to the brain. *J. Biol. Chem.*

Sonoda, H., Morimoto, H., Yoden, E., Koshimura, Y., Kinoshita, M., Golovina, G., et al. (2018). A blood-brain-barrier-penetrating anti-human transferrin receptor antibody fusion protein for neuronopathic mucopolysaccharidosis II. *Mol. Ther.* 26, 1366–1374. doi: 10.1016/j.ymthe.2018.02.032

Thom, G., Burrell, M., Haqqani, A. S., Yogi, A., Lessard, E., Brunette, E., et al. (2018a). Enhanced delivery of galanin conjugates to the brain through bioengineering of the anti-transferrin receptor antibody OX26. *Mol. Pharm.* 15, 1420–1431. doi: 10.1021/acs.molpharmaceut.7b00937

Thom, G., Tian, M. M., Hatcher, J. P., Rodrigo, N., Burrell, M., Gurrell, I., et al. (2018b). A peptide derived from melanotransferrin delivers a protein-based interleukin 1 receptor antagonist across the BBB and ameliorates neuropathic pain in a preclinical model. *J. Cereb. Blood Flow Metab.* 39, 2074–2088. doi: 10.1177/0271678x18772998

Tovey, M. G., and Lallemand, C. (2011). Immunogenicity and other problems associated with the use of biopharmaceuticals. *Ther. Adv. Drug Saf.* 2, 113–128. doi: 10.1177/2042098611406318

Tsou, Y. H., Zhang, X. Q., Zhu, H., Syed, S., and Xu, X. (2017). Drug delivery to the brain across the blood-brain barrier using nanomaterials. *Small* 13:1701921. doi: 10.1002/smll.201701921

Wally, J., and Buchanan, S. K. (2007). A structural comparison of human serum transferrin and human lactoferrin. *Biometals* 20, 249–262. doi: 10.1007/s10534-006-9062-7

Wally, J., Halbrooks, P. J., Vonrhein, C., Rould, M. A., Everse, S. J., Mason, A. B., et al. (2006). The crystal structure of iron-free human serum transferrin provides insight into inter-lobe communication and receptor binding. *J. Biol. Chem.* 281, 24934–24944. doi: 10.1074/jbc.m604592200

Yang, J., Tiong, J., Kennard, M., and Jefferies, W. A. (2004). Deletion of the GPI pre-anchor sequence in human p97–a general approach for generating the soluble form of GPI-linked proteins. *Protein Expr. Purif.* 34, 28–48. doi: 10.1016/j.pep.2003.09.007

Zuchero, Y. J., Chen, X., Bien-Ly, N., Bumbaca, D., Tong, R. K., Gao, X., et al. (2016). Discovery of novel blood-brain barrier targets to enhance brain uptake of therapeutic antibodies. *Neuron* 89, 70–82. doi: 10.1016/j.neuron.2015.11.024

Conflict of Interest: Bioasis Technologies Inc., (BTI) is a University of British Columbia start-up company. TZV, RG, and MMT were employees and equity holders in BTI at the time this work was undertaken. WAJ was the founding scientist and an equity holder in BTI at the time this work was undertaken. The funding sources had no influence in the study design, data collection, analysis or interpretation of data, in the writing of the manuscript or on the decision to submit for publication.

The remaining authors declare that the research was conducted in the absence of any commercial or financial relationships that could be construed as a potential conflict of interest.

Copyright © 2021 Singh, Eyford, Abraham, Munro, Choi, Okon, Vitalis, Gabathuler, Lu, Pfeifer, Tian and Jefferies. This is an open-access article distributed under the terms of the Creative Commons Attribution License (CC BY). The use, distribution or reproduction in other forums is permitted, provided the original author(s) and the copyright owner(s) are credited and that the original publication in this journal is cited, in accordance with accepted academic practice. No use, distribution or reproduction is permitted which does not comply with these terms.

frontiers in Pharmacology

ORIGINAL RESEARCH
published: 21 June 2021
doi: 10.3389/fphar.2021.672392

Early IGF-1 Gene Therapy Prevented Oxidative Stress and Cognitive Deficits Induced by Traumatic Brain Injury

*Agustín. J. Montivero[1], Marisa. S. Ghersi[1], M. Jazmín Silvero C[2], Emilce Artur de la Villarmois[1], Johanna Catalan-Figueroa[1,3], Macarena Herrera[1], María Cecilia Becerra[2], Claudia. B. Hereñú[1] and Mariela. F. Pérez[1]**

[1]Instituto de Farmacología Experimental de Córdoba (IFEC-CONICET), Departamento de Farmacología, Facultad de Ciencias Químicas, Universidad Nacional de, Córdoba, Argentina, [2]Instituto Multidisciplinario de Biología Vegetal (IMBIV-CONICET), Departamento de Ciencias Farmacéuticas, Facultad de Ciencias Químicas, Universidad Nacional de, Córdoba, Argentina, [3]Escuela de Química y Farmacia, Facultad de Medicina, Universidad Católica del Maule, Talca, Chile

Traumatic Brain Injury (TBI) remains a leading cause of morbidity and mortality in adults under 40 years old. Once primary injury occurs after TBI, neuroinflammation and oxidative stress (OS) are triggered, contributing to the development of many TBI-induced neurological deficits, and reducing the probability of critical trauma patients´ survival. Regardless the research investment on the development of anti-inflammatory and neuroprotective treatments, most pre-clinical studies have failed to report significant effects, probably because of the limited blood brain barrier permeability of no-steroidal or steroidal anti-inflammatory drugs. Lately, neurotrophic factors, such as the insulin-like growth factor 1 (IGF-1), are considered attractive therapeutic alternatives for diverse neurological pathologies, as they are neuromodulators linked to neuroprotection and anti-inflammatory effects. Considering this background, the aim of the present investigation is to test early IGF-1 gene therapy in both OS markers and cognitive deficits induced by TBI. Male Wistar rats were injected *via* Cisterna Magna with recombinant adenoviral vectors containing the IGF-1 gene cDNA 15 min post-TBI. Animals were sacrificed after 60 min, 24 h or 7 days to study the advanced oxidation protein products (AOPP) and malondialdehyde (MDA) levels, to recognize the protein oxidation damage and lipid peroxidation respectively, in the TBI neighboring brain areas. Cognitive deficits were assessed by evaluating working memory 7 days after TBI. The results reported significant increases of AOPP and MDA levels at 60 min, 24 h, and 7 days after TBI in the prefrontal cortex, motor cortex and *hippocampus*. In addition, at day 7, TBI also reduced working memory performance. Interestingly, AOPP, and MDA levels in the studied brain areas were significantly reduced after IGF-1 gene therapy that in turn prevented cognitive deficits, restoring TBI-animals working memory performance to similar values regarding control. In conclusion, early IGF-1 gene therapy could be considered a novel therapeutic approach to targeting neuroinflammation as well as to preventing some behavioral deficits related to TBI.

Keywords: traumatic brain injury, neuroinflammation, secondary injury, cognitive deficits, IGF-1 gene therapy

OPEN ACCESS

Edited by:
Carlos Spuch, Instituto de Investigación Sanitaria Galicia Sur (IISGS), Spain

Reviewed by:
Tejaswini Doifode, Carilion Clinic, United States
Rosalia Crupi, University of Messina, Italy

****Correspondence:***
Mariela. F. Pérez
mfperez@unc.edu.ar

Specialty section:
This article was submitted to Neuropharmacology, a section of the journal Frontiers in Pharmacology

Received: *25 February 2021*
Accepted: *08 June 2021*
Published: *21 June 2021*

Citation:
Montivero AJ, Ghersi MS, Silvero C MJ, Artur de la Villarmois E, Catalan-Figueroa J, Herrera M, Becerra MC, Hereñú CB and Pérez MF (2021) Early IGF-1 Gene Therapy Prevented Oxidative Stress and Cognitive Deficits Induced by Traumatic Brain Injury. Front. Pharmacol. 12:672392. doi: 10.3389/fphar.2021.672392

INTRODUCTION

Traumatic brain injury (TBI) is the consequence of an external mechanical force applied to the cranium and its content. This event may cause temporary or permanent disabilities on TBI survivors because of its consequences at physical, cognitive or psychological levels (Niedzwecki et al., 2008; Steyerberg et al., 2008; Stocchetti and Zanier, 2016; Wolfe et al., 2018). The TBI's severity can be classified as mild (mTBI), moderate or severe taking into account the clinical presentation of a patient's neurologic signs and symptoms (Kay et al., 1993; Katz and Alexander, 1994; Ponsford et al., 2016). Furthermore, TBI is considered a worldwide increasingly critical health problem, according to recent studies in the United States, revealing that the number of "TBI-related emergency department visits, hospitalizations, and deaths increased by 53%" from 2006 to 2014 (Centers for Disease Contr, 2019).

Injuries related to TBI can be classified into primary and secondary. The first ones, occur at the moment of trauma and can be manifested as focal injuries (e.g. skull fractures, intracranial hematomas, lacerations, concussions, penetrating wounds), or diffuse injuries (as in diffuse axonal injury) (Alain and Wang, 2008; Katerji et al., 2019). The secondary injuries appear immediately after trauma and may last for long periods (Nortje and Menon, 2004; Pearn et al., 2017). They are frequently associated with ischemia, brain edema, and neuroinflammation, and may take place in a period from days to weeks, or even months, triggering a complex cascade of intracellular signaling, which include ATP depletion, mitochondrial dysfunction, oxidative stress (OS), and cytoskeleton damage (Montivero et al., 2021). In turn, those events induce the production of toxic and pro-inflammatory mediators, such as prostaglandins, oxidative metabolites, chemokines, and proinflammatory cytokines, which can lead to lipid peroxidation, protein oxidation, enhanced blood brain barrier (BBB) disruption and brain edema to finally induce neuronal dysfunction or death (Krishnamurthy et al., 2016; Pearn et al., 2017).

It has been described that secondary injury mechanisms, as outlined above, may contribute to the cognitive deficits observed even long-term after injury. Individuals suffering from TBI of any severity could experience a cluster of symptoms for a prolonged period of time (Kushner, 1998; Ryan and Warden, 2003; McMahon et al., 2014; Stocchetti and Zanier, 2016), commonly recognized as post-concussive syndrome (PCS) (Alexander, 1995; Ryan and Warden, 2003; Stocchetti and Zanier, 2016; Montivero et al., 2021). The PCS includes a variety of symptoms ranging from cognitive symptoms (speech changes, attention loss, dysfunction in executive function and memory, or mental slowing, among others) Kaplan et al. (2018); physical and somatic symptoms (hearing and visual disturbances, sensitivity to light or sound, pain, headaches, dizziness, nausea, fatigue, sleep disruption, and even seizures) (Lozano et al., 2015; Webster et al., 2017; Kaplan et al., 2018; Wolfe et al., 2018) and emotional/behavioral symptoms (executive dysfunction, anxiety, irritability, depression, and attention deficit) (Arciniegas et al., 2005; Bryan, 2013; Paterno et al., 2017). Regretfully, it is difficult to identify those individuals at risk for PCS with the standard clinical assessment used. Nevertheless, since the working memory is one of the cognitive functions primarily affected by TBI, its clinical evaluation, including functional magnetic resonance imaging performed within the first week of injury, may contribute to predicting the patients´ outcome (Christodoulou et al., 2001; Ricker et al., 2001; Hillary et al., 2011; Wylie et al., 2015; Montivero et al., 2021).

Unfortunately, there are no available pharmacological therapies to prevent or reverse early secondary events in order to reduce long-term disabilities described in TBI patients (Paterno et al., 2017). Several neurotrophins synthesis can be locally stimulated in the brain after TBI, among them, insulin like growth factor-1 (IGF-1) (Madathil et al., 2010; Schober et al., 2010). However, TBI-induced increments in IGF-1 and IGF-1-related signaling molecules seem to be transient and probably are not enough to provide neuroprotection or stimulate sub-acute repair or regenerative mechanisms. Early studies in TBI patients have shown a reduction in serum IGF-1 levels (Agha et al., 2004; Popovic et al., 2004; Wagner et al., 2010; Zgaljardic et al., 2011; Olivecrona et al., 2013), even after mTBI Robles et al. (2009), Wagner et al. (2010), while other investigations have reported that there were either no changes Bondanelli et al. (2002) or a long-term increase in serum IGF-1 levels after injury (Wildburger et al., 2001). These differences can be due to the diverse patient population included in those studies, as well as different trauma types, gender, injury severity, patient age, and brain regions affected (Madathil et al., 2015). Nonetheless, low IGF-1 serum levels have been implicated in the development of cognitive dysfunction Trejo et al. (2004), Koopmans et al. (2006) and were positively correlated with cognitive impairment in TBI survivors tested up to a year post injury (Madathil et al., 2015). Thus, it is plausible to consider that low plasma IGF-1 levels may contribute to the primary causes of cognitive disorders after TBI (Madathil et al., 2015). However, even though early IGF-1 administration promotes regenerative events such as neurogenesis and angiogenesis in a TBI animal model Whitaker-Lea and Valadka (2017), its therapeutic potential after TBI has not yet been assessed. It should be emphasized, that different clinical trials have shown acceptable tolerability of systemic IGF-1 therapy in moderate to severe TBI patients, as well as enhanced metabolic outcome in comparison to placebo-treated patients (Hatton et al., 1997; Madathil et al., 2015). Furthermore, systemic growth hormone administration produced increments in IGF-1 levels, inducing a tendency to improve the functional outcomes in treated patients (Dubiel et al., 2018).

Considering all the evidence aforementioned, and the fact that IGF-1 gene therapy targets brain cells *in vivo* Hereñú et al. (2009) and can decrease behavioral functional impairments in aged rats (Nishida et al., 2011; Pardo et al., 2017), the aim of the present study is to evaluate the effectiveness of early IGF-1 gene therapy in the treatment of TBI for preventing OS as well as improving cognitive deficits.

MATERIAL AND METHODS

Ethics

All procedures were carried out in accordance with the Guide for the Care and Use of Laboratory Animals as adopted and

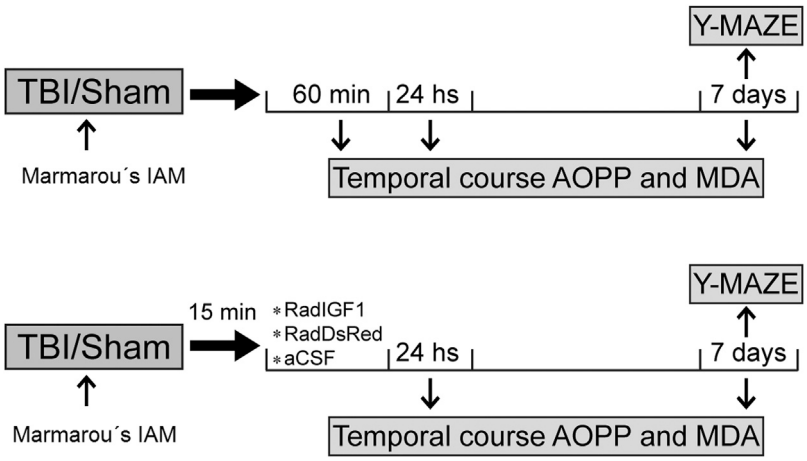

FIGURE 1 | Experimental design. Chart illustrating our experimental design including Marmarou's impact acceleration model (Marmarou´s IAM), viral vectors administration, temporal course of protein (AOPP) and lipids (MDA) peroxidation, and neurobehavioral assesements (Y-Maze test).

promulgated by the National Institutes of Health and the EU (Eighth Edition, 2011) and approved by the Animal Care and Use Committee, Facultad de Ciencias Químicas (Res. Dec. 1194/2017 and 2336/2019), Universidad Nacional de Córdoba. In this study, a total of 97 male Wistar rats (270–310 gr) were obtained from the Department of Pharmacology-IFEC-CONICET vivarium (Facultad de Ciencias Químicas, Universidad Nacional de Córdoba, Argentina) and were housed in groups of 3, in plastic boxes with metallic gridded tops, using sawdust as bedding material, in a temperature and humidity controlled conditions under a 12-h light/dark cycle (lights on at 7 am). Food and water were freely available. Experiments were made minimizing the number of animals used and their suffering.

Animal Model of TBI

In order to mimic human diffuse TBI caused by falls or motor vehicle accidents, we used the Marmarou's impact acceleration model (Marmarou´s IAM) that recreates global impact on the brain (Foda and Marmarou, 1994; Marmarou et al., 1994; Silva et al., 2011; Xiong et al., 2013). For this purpose, animals were anesthetized (Ketamine 55 mg/kg/xylazine 11 mg/kg) and subjected to a controlled TBI, described elsewhere (Marmarou et al., 1994; Silva et al., 2011). Briefly, the "trauma device" consists of 1 m removable aluminum tube, attached to a wooden platform, which allows a controlled impact when dropping a 45 gr brass sphere onto a stainless steel disc located above the animal head, causing a 0.45J impact when it is dropped from the mentioned height. Under anesthesia, animals were placed on the platform covered with a foam bed, with their heads located under an extreme of the tube, approximately midline between Lambda and Bregma. The stainless steel disc was located between the animal's head and the tube, in order to prevent skull fractures. Then, they were subjected to the impact by dropping the sphere from the aluminum tube top. In the control group (Sham) the animals were anesthetized and placed on the trauma device platform, but they did not received impact.

Once animals received the impact (TBI group) or its mimic (Sham group) they were divided into groups to perform the experiments as it was shown in **Figure 1**: Temporal course of OS and behavior after TBI and the effects of early IGF-1 gene therapy in OS and behavior.

Temporal Course of Advanced Oxidation Protein Products and Malondialdehyde Quantification after TBI

Sixteen animals were subjected to the protocol described in 2.2 (TBI or Sham) and divided into four groups (Sham; TBI 60 min; TBI 24 h, and TBI 7 days) in order to evaluate AOPP and MDA concentrations at different time points after TBI (60 min, 24 h, and 7 days). After the times indicated, animals were sacrificed by guillotine, their brains were removed and Prefrontal Cortex (PFC), Motor Cortex (MC) and *Hippocampus* (HIP) were dissected.

Tissue samples were then homogenized with phosphate buffer saline (PBS) 0.1 M and centrifugated for 10 min at 4°C and 12,000g. The supernatant was diluted 1/30 for HIP and 1/20 for PFC and MC in PBS 0.1 M. AOPP and MDA determinations were made as it was previously described with modifications (Occhieppo et al., 2020). Briefly, AOPP determinations were performed accordingly to Katerji et al. (2019) and 200 µL of the diluted sample, chloramine T (0–100 µmol/L) for calibration or PBS 0.1 M pH 7 as blank, were applied in different microtiter plate wells. Then, 10 µL of 1.16 M potassium iodide and 20 µL of acetic acid (glacial) were added to each well and absorbance was immediately read at 340 nm. The AOPP concentration was expressed in chloramine units (µmol/L) per milligram of proteins.

For MDA determinations, 250 µL of trichloroacetic acid and 250 µL of thiobarbituric acid were added to 500 µL of diluted sample. Immediately after, samples were kept in boiling water for 10 min. Then, they were centrifugated at 1,000 rpm for 10 min, and after cooling to clear the supernatant from denaturalized proteins, absorbance was measured at 532 nm. Thiobarbituric

acid-reactive substances were quantified using an extinction coefficient of $1.56 \times 105\ M^{-1}cm^{-1}$ and expressed as nanomole of malondialdehyde (MDA) per milligram of proteins. In both AOPP and MDA determinations, tissue proteins were determined by using the Bradford reagent (Occhieppo et al., 2020).

IGF-1 Gene Therapy after TBI

Viral Vectors

For animal treatment we employed recombinant adenoviral vectors (RAd) previously constructed as carriers to deliver either the therapeutic cDNA of IGF-1 gene (RadIGF1) or the red fluorescent protein from Discosoma sp DsRed (RadDsRed), as control virus (Hereñú et al., 2007). The viral dose [10^{10} plaque forming units (pfu) of the appropriate vector] was suspended in 30 μL artificial cerebrospinal fluid (aCSF- in mM: NaCl 124, KCl 2.5, $NaHCO_3$ 26, $MgCl_2$ 2, $CaCl_2$ 2, and glucose 10; pH 7.4; 310 mosM/Kg) and administered directly into the subarachnoid space *via* Cisterna Magna. Once administered, adenoviral vectors were distributed by the cerebrospinal fluid and the ependymal cells were infected. The expression of DsRed was verified in transversal brain slices from animals subjected to TBI that received RadDsRed (see protocol below). DsRed fluorescence was more abundant in posterior brain slices near the injection site (**Figure 4A**) rather than anterior brain slices (**Figures 4B,C**).

Experimental Protocol

Effect of IGF-1 Gene Therapy in AOPP and MDA after TBI

In order to test effectiveness of CNS IGF-1 over-expression on OS markers reversion, 32 animals were randomly assigned to either Sham or TBI, which received a single administration (30 μL) of aCSF or viral suspension respectively. The procedure was carried out as previously described (Nishida et al., 2020). Briefly, 15 min after the TBI protocol, and still under anesthesia, animals' heads were shaved and cleaned with 70% ethanol in order to expose the area of injection (Cisterna Magna). They were then placed on a stereotactic apparatus in hyperflexion prone position, in order to expand the Cisterna Magna. A 29G needle fitted to a 1 ml syringe was used to deliver viral administration. Entry into the Cisterna Magna was verified by drawing out 30 μL clear cerebrospinal fluid, which was replaced by 30 μL of viral suspension or aCSF. For the 24 h time point, TBI animals received either RadIGF1 suspension (TBI RadIGF1 group) or aCSF (TBI group); while for the 7 days time point TBI animals received RadIGF1 suspension (TBI RadIGF1 group), RadDsRed suspension (TBI RadDsRed group) or aCSF (TBI group). Sham groups were simultaneously tested at both time points, but they received 30 μL of aCSF without receiving TBI. After treatment, animals were kept undisturbed in their homeboxes until their sacrifice.

Effect of IGF-1 Gene Therapy in Working Memory after TBI

In order to test the efficacy of IGF-1 gene therapy in reversing cognitive deficits induced by TBI, forty-nine animals were randomly assigned to Sham or TBI. Treatment was performed as indicated in the previous paragraph, for the 7 days time point. Then, animals were placed back in their homeboxes and after 7 days they were tested in the Y-Maze task as it is described below. We obtained four groups depending on treatment: Sham, TBI; TBI RadDsRed, and TBI RadIGF1.

Y-Maze Test

The Y-maze task allows the assessment of working memory by measuring the number of spontaneous alternations. This can be assessed by allowing mice to freely explore all the three arms of the maze. This behavior is driven by the innate curiosity of rodents to explore previously unvisited areas. The apparatus is made of three arms (50 cm long, 10 cm wide, and 20 cm high) of water-proof wood, elevated to a height of 50 cm above the floor. The test was conducted as it was described elsewhere with modifications (Xiong et al., 2013). Briefly, rats were placed at the end of arm #1 facing the center and they could choose between arm #2 and arm #3. Entry into an arm was defined as placement of the four paws into the arm and an alternation was defined as triplet of consecutive entries to different arms. The test lasted 8 min. Animals that did not reach the inclusion criteria (at least five entries and/or 2 min without a new movement or entry) were excluded. The number of total entries was also quantified as an indicator of locomotor activity.

Statistical Analyses

Results of positive control (TBI) and experimental animals (TBI + treatment) were normalized to negative controls (Sham). The delta method was used for dispersion graphic display Polli et al. (1997), since it allows weighing how much the dispersion of each set of variables affects their means ratio dispersion. If normal data distribution was confirmed by Shapiro-Wilk test, the Student's t-test was used when two independent groups were compared. For more than two group comparisons, data were analyzed by one-way ANOVA, followed by Tukey's Honest Significant Difference test. On the other hand, data with non-normal distribution were analyzed by using Mann-Whitney test, or Kruskal-Wallis followed by Nemenyi test. A 95% confidence level was considered for all analyses.

For OS markers determinations and behavior performed 7 days after TBI, experiments were designed as independent groups and analyzed by using one-way ANOVA in order to reduce the number of animals used. It can be noted that the group administered with the control virus (RadDsRed) was only included in this time point or the same reasons.

RESULTS

TBI-Induced Increments in Oxidative Stress Markers Last up to 7 days Post Trauma

It has been recently shown that controlled cortical impact (another animal model of TBI) induced early and significant increases in lipid ROS and MDA levels, which returned to baseline seven days after TBI (Xie et al., 2019). In our model we observed a similar pattern of AOPP and MDA increments; nevertheless, even though we observed a decrease in OS levels after 7 days of TBI, they did not return to baseline. **Figures 2A–C** shows that the AOPP concentration in trauma adjacent regions or immediately below was significantly elevated at 60 min,

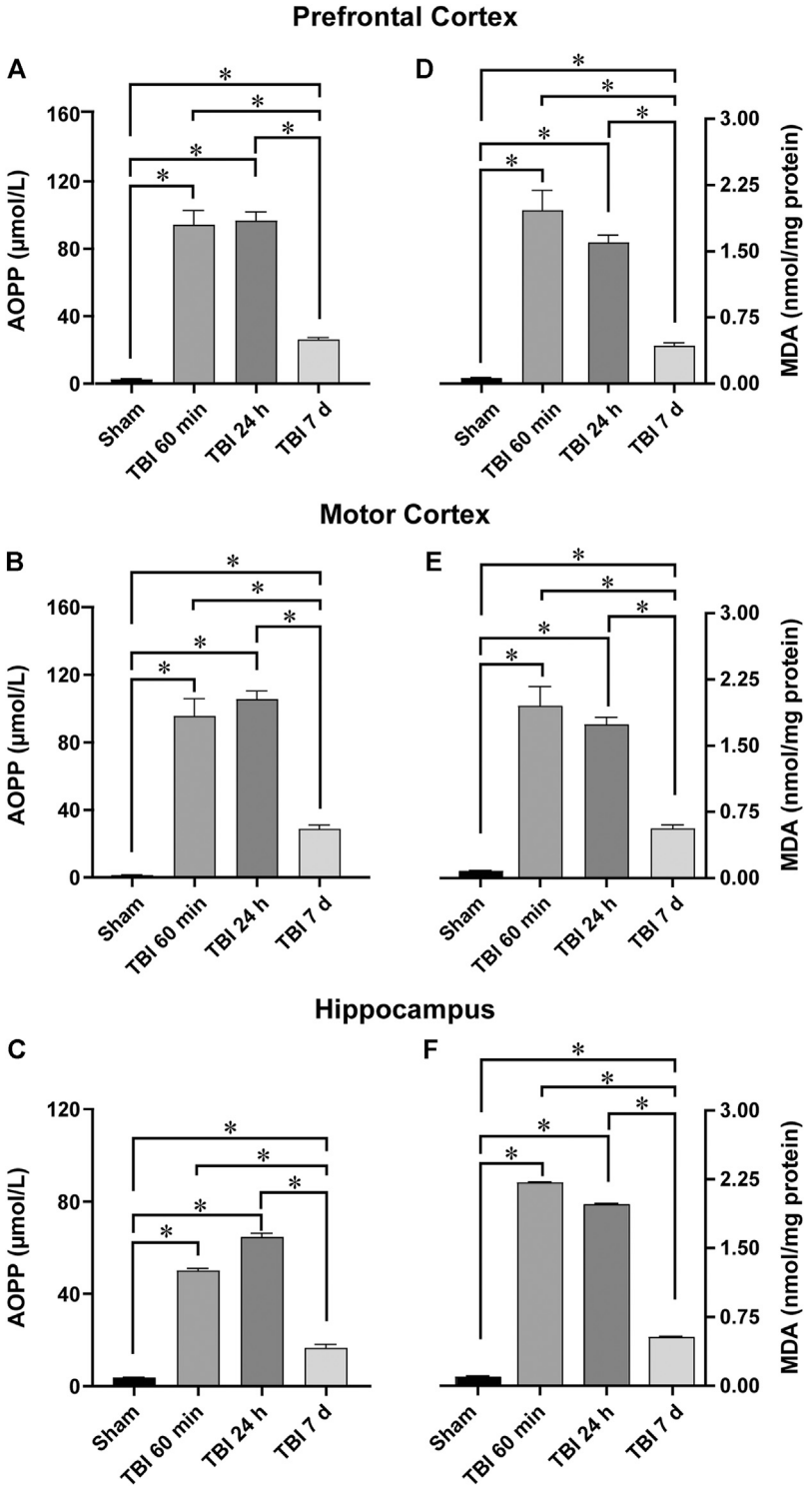

FIGURE 2 | TBI induces a persistent increment in OS biomarkers. The graphs show the AOPP and MDA quantification as measurements of lipid and protein peroxidation, respectively, in brain areas neighboring the trauma area, such as **(A)** and **(D)** Prefrontal cortex; **(B)** and **(E)** Motor cortex; and **(C)** and **(F)** *Hippocampus*. Bars represent the mean ± SEM; $n = 4$. *Indicates significant difference ($p < 0.05$).

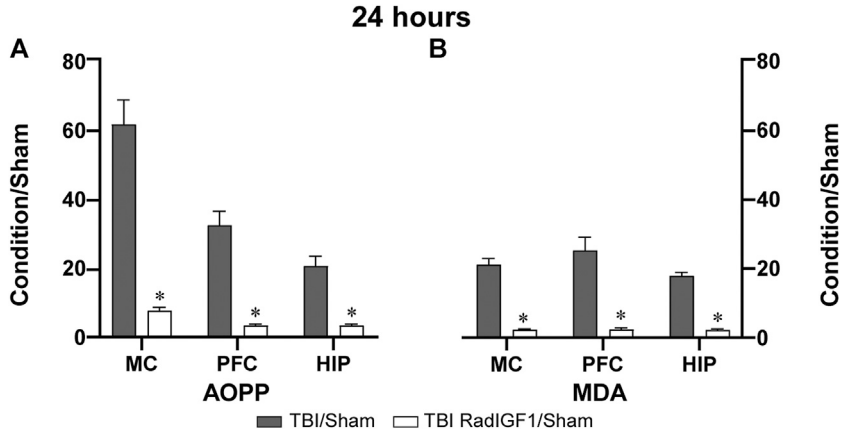

FIGURE 3 | Early IGF-1 treatment reduced TBI- induced OS biomarkers 24 h after injury. The graph shows the AOPP **(A)** and MDA **(B)** quantification as measurements of protein and lipid peroxidation, respectively, in brain areas neighboring the trauma area, such as Motor cortex (MC), Prefrontal cortex (PFC), and hippocampus (HIP). Results of positive control (TBI) and treated animals (TBI RadIGF1), referred as "condition" in the *Y* axes, were normalized to negative controls (Sham). Bars represent the mean ± SEM; n = 4–6. *Different from TBI/Sham in each brain structure ($p < 0.05$).

reaching a maximum 24 h after TBI, when compared to Sham condition. Main effects were observed in PFC [F (3, 10) = 168.6; $p < 0.0001$] (**Figure 2A**), MC (**Figure 2B**) [F (3, 10) = 176.9; $p < 0.0001$], and HIP (**Figure 2C**) [F (3, 10) = 492.9; $p < 0.0001$]. The post-hoc test indicated that all groups of animals submitted to TBI were significantly different from Sham group ($p < 0,05$). Furthermore, the 7 days group was also significantly different from 60 min to 24 h groups ($p < 0.05$), indicating that there is a trend to reduce AOPP levels on day 7 after TBI, even though they are still increased when compared to Sham group in all the brain structures studied.

In the case of MDA levels, the same AOPP pattern of increment/reduction was observed. **Figures 2D–F** shows the inverted U-shaped pattern in MDA concentrations with main effect in PFC (**Figure 2D**) [F (3, 10) = 132.6; $p < 0.0001$], MC (**Figure 2E**) [F (3, 10) = 148.9; $p < 0.0001$] and HIP (**Figure 2F**) [F (3, 10) = 23,278; $p < 0.0001$]. Tukey's post-hoc test indicated that groups from all time points were significantly higher than the Sham group ($p < 0,05$), and the 7 days group was significantly lower than 60 min and 24 h groups in all brain structures investigated ($p < 0.05$).

Early IGF-1 Gene Therapy Prevented Increments in Oxidative Stress Markers at 24 h and 7 days Induced by TBI

24 h after TBI, AOPP concentrations in different brain structures were determined in animals that received gene therapy 15 min after the head trauma (**Figure 3A**). This treatment significantly reduced the AOPP mean ratios of treated condition (TBI RadIGF1/Sham) when compared with the "untreated condition" (TBI/Sham) in MC (t = 69.92; $p < 0.000000001$), HIP (t = 36.29; $p < 0.0001$) and PFC (U = 0; $p < 0.05$). Over expression of IGF-1, also impacted on MDA levels measured 24 h after TBI (**Figure 3B**). The mean ratios of the "treated condition" (TBI RadIGF1/Sham) were significantly reduced when compared to no treatment condition (TBI/Sham) in MC (t = 57.2; $p < 0.00001$), PFC (t = 85.35; $p < 0.000000001$), and HIP (t = 58.54; $p < 0.000000001$). These results indicate that early gene therapy prevented the peak in the AOPP and MDA levels observed 24 h after TBI.

In other groups of animals, the effect of early gene therapy 7 days after TBI over AOPP and MDA concentrations was studied (**Figure 4**). The following treatments were applied to animals submitted to TBI: i) control group: viral vectors containing cDNA of red fluorescent protein from Discosoma sp DsRed (RadDsRed); and ii) experimental group: viral vectors containing the therapeutic cDNA of IGF-1 gene (RadIGF1) as treatment. A main effect was observed in AOPP mean ratios of different conditions in MC [F (2, 11) = 54.98; $p < 0.00001$], PFC [F (2, 11) = 179.6; $p < 0.0000001$] and HIP [F (2, 11) = 44.26; $p < 0.0001$] (**Figure 4D**). In all brain structures, TBI/Sham group and control group (TBI RadDsRed/Sham group) means ratio were elevated 50% or more in comparison to the experimental group's means ratio (TBI RadIGF1/Sham group), the post-hoc test indicated that AOPP mean ratios of experimental group were significantly different from AOPP mean ratios of untreated conditions (TBI/Sham) and from AOPP mean ratios of control treatment conditions ($p < 0.05$). Furthermore, no differences were found between AOPP mean rations of TBI/Sham and TBI RadDsRed/Sham groups. These results indicate that early gene therapy was able to prevent the sustained increment in AOPP concentrations observed up to 7 days after TBI, and this effect was due to IGF-1 over-expression and not because of viral vectors administration.

Figure 4B shows significant main effects in MDA mean ratios 7 days after TBI and treatments in MC [F (2, 11) = 133.34; $p < 0.000001$], PFC [F (2, 11) = 1468.37; $p < 0.000000001$] and HIP [F (2, 11) = 607.17; $p < 0.00000001$]. The post-hoc test in all brain structures indicated that MDA means ratio of TBI RadIGF1/

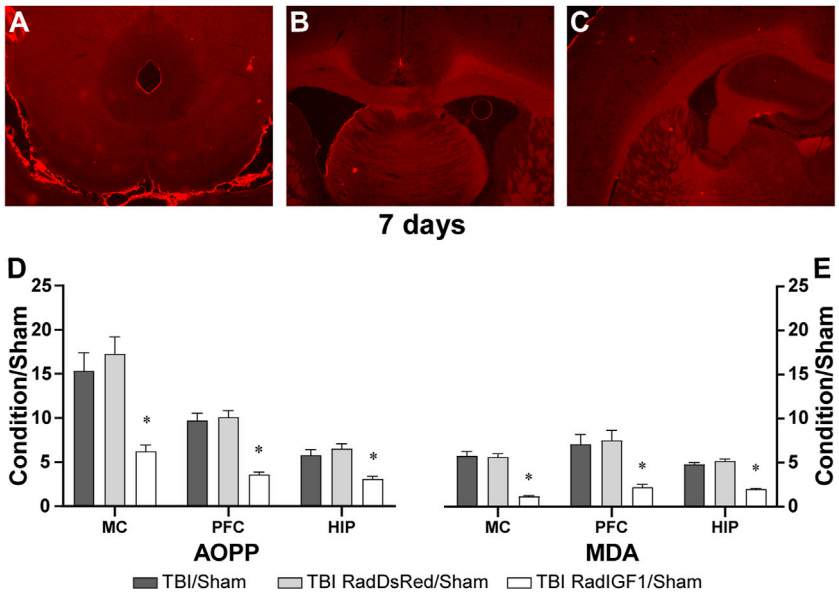

FIGURE 4 | Early IGF-1 treatment prevented TBI- induced OS biomarkers 7 days after injury. Microscopic photographs of brain areas showing expression of fluorescent DsRed Protein. DsRed fluorescence is more abundant in posterior brain slices, near the injection site **(A)** rather than anterior brain slices **(B–C)**. The graph shows the AOPP **(D)** and MDA **(E)** quantification as measurements of protein and lipid peroxidation, respectively, in brain areas neighboring the trauma area, such as Motor cortex (MC), Prefrontal cortex (PFC), and hippocampus (HIP). Results of positive control (TBI) and treated animals (TBI + treatment), referred as "condition" in the *Y* axes, were normalized to negative controls (Sham). Bars represent the mean ± SEM; $n = 4–6$. *Different from TBI/Sham and TBI RadDsRed/Sham in each brain structure ($p < 0.05$).

Sham were significantly different regarding TBI/Sham group and TBIRadDsRed/Sham groups. Furthermore, no differences were found between MDA mean rations of both TBI/Sham and TBI RadDsRed/Sham groups. As it was described before, these results indicated that early IGF-1 over-expression after TBI was able to prevent the sustained increase observed in lipids peroxidation as a consequence of trauma.

Early IGF-1 Gene Therapy Prevented Cognitive Deficits Observed 7 days after TBI

As it was described before, working memory is one of the cognitive domains primarily affected by TBI that could predict patient's outcome (Ricker et al., 2001; Wylie et al., 2015; Montivero et al., 2021). In preclinical studies, an individual with normal working memory will remember the arms of the Y-maze that it has already visited and will show a tendency to enter the less recently visited arm. The correct performance requires interaction across several different regions of the brain, such as the HP and PFC (Kraeuter et al., 2019). In the present work we observed, under our experimental conditions, a deficit in this domain in the TBI group (**Figure 5A**) since a significant reduction was observed in spontaneous alterations in the TBI group compared to Sham (t = 2,825; p = 0,0083). No significant differences were detected in the number of arm entries (t = 1,623; p = 0,1147) (**Figure 5B**), indicating that the reduction in spontaneous alterations was not consequence of a reduced locomotor activity.

In this experiment, the following treatments were applied to animals submitted to TBI: i) control group: viral vectors containing cDNA of red fluorescent protein from Discosoma sp DsRed (RadDsRed); and ii) experimental group: viral vectors containing the therapeutic cDNA of IGF-1 gene (RadIGF1) as treatment. The percentage of alternances and number of entries were expressed as ratios between treatments and Sham (**Figures 5C,D** respectively). A significant main effect in the mean ratio of the percentage of spontaneous alterations was observed between TBI/Sham, TBI RadDsRed/Sham and TBI RadIGF1/Sham groups [F (2, 31) = 5,051; p = 0,0131] (**Figure 5C**). The post-hoc test indicated that mean ratio of TBI RadIGF1/Sham group was significantly higher compared to the TBI/Sham group mean ratio. If we look at the TBI RadIGF-1/Sham group mean in **Figure 5C**, we can observe that it is close to 1, because spontaneous alterations of experimental group were similar to Sham, indicating a prevention of the deficits observed in the TBI in the animals that received the early IGF-1 gene therapy (**Figure 5C**). Furthermore, Tukey's test showed no significant differences between TBI/Sham and TBI RadDsRed/Sham groups, showing that the control treatment did not have impact on spontaneous alternations in the Y-maze test (**Figure 5C**). Once again, locomotor activity was not affected by treatments, since no main effect in the number of arm entries mean ratio was found between groups [F (3, 46) = 1.649; p = 0,1911] (**Figure 5D**).

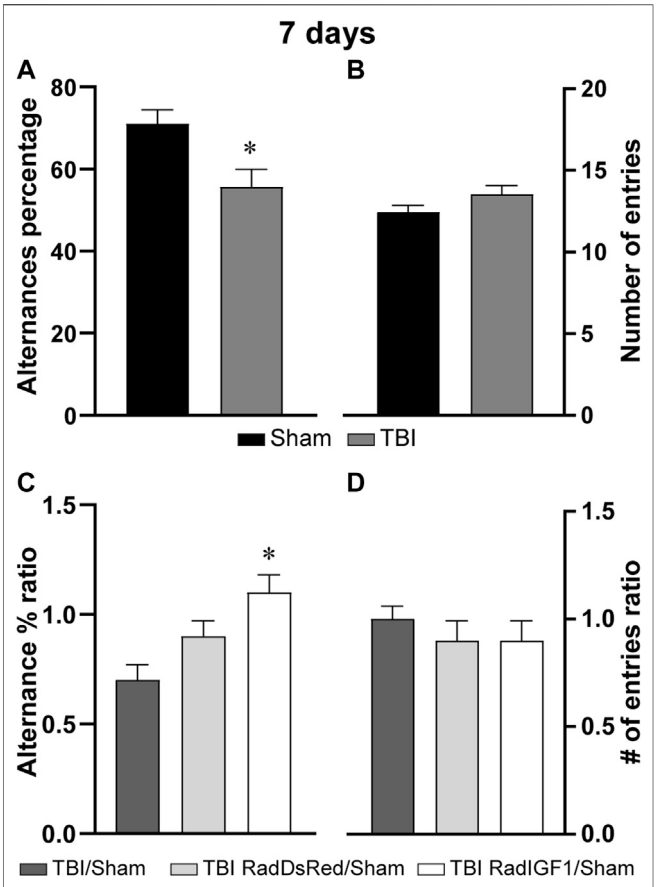

FIGURE 5 | Early IGF-1 treatment prevented TBI-induced working memory deficit observed 7 days after injury. The graphs show working memory performance assessed by the Y-maze paradigm. Graphs **(A)** and **(B)** show the percentage of spontaneous alternations and percentage of spontaneous alternations in a Y-maze arena, respectively, in Sham and TBI groups. Graphs **(C)** and **(D)** represent the percentage of spontaneous alternations or number of entries ratio respectively, between TBI or TBI + treatment groups and Sham group (TBI/Sham, TBI RadDsRed/Sham, and TBI RadIGF1/Sham). Bars represent the mean ± SEM, n = 10–11. *Different from TBI/Sham (p = 0,0095).

DISCUSSION

In this work, we showed that mTBI increases some OS markers as a result of secondary injury. These markers were observed early after TBI (60 min), reaching their highest levels at 24 h in all brain structures analyzed. In addition, even though AOPP and MDA products were significantly reduced on day 7 after TBI, they did not return to basal levels. These results are in line with studies that point out neuroinflammation as a key player in brain damage severity and patients' outcome after any kind of TBI. For instance, recognized neuroinflammation serum protein markers, such as Glial Fibrillary Acidic Protein (GFAP) and S100B, have demonstrated to have a correlation to both severity and outcome in TBI (Pelinka et al., 2004; Luoto et al., 2017). Furthermore, the more severe the TBI is, the less successful outcome is observed in patients and animal models. Many severe TBI models have shown important brain damage and correlate neuroinflammation with memory disorders (Farbood et al., 2015; Zhang et al., 2017). Thus, with our model, we have shown that even mTBI can lead to memory impairment as a sign of PCS. The observed deficits in working memory 7 days after TBI, related to impaired cognitive function, were probably the result of the early neuroinflammatory cascade triggered by secondary injury mechanisms. Working memory performance depends on the PFC integrity (Riggall and Postle, 2012; Lara and Wallis, 2015). Interestingly, we have observed an increase of OS markers in this brain structure that remains elevated over a 7-days period after TBI, compared to Sham animals. This could be explained as the result of microglia hyperactivation, as it occurs in the pathogenesis of many CNS diseases Pekny and Pekna (2016), and/or changes in cerebral blood perfusion (Babior, 2000; Block et al., 2006; Block and Hong, 2007), which in turn may affect neuronal excitability that finally shape the disrupted working memory performance observed.

Although increasing knowledge about injury mechanisms of TBI has led to a better understanding of its complex pathogenesis, pharmacological strategies focused on ameliorating them are yet missing. To date in clinical practice, medical management of TBI is tailored according to the severity of each case considering the Glasgow scale. In moderate to severe cases the treatment aim is to keep a normal intracranial pressure (ICP) in order to maintain an adequate cerebral blood pressure (CCP), which is an indicator of brain perfusion. The pharmacological armamentarium consists in sedation, neuromuscular blocking, and hyperosmolar agents that contribute to decreasing ICP (Carney et al., 2017). On the other hand, mTBI has a different approach because most of the time the ICP remains within normal ranges, thus the treatment is mainly focused on headaches management and the control of PCS- related symptoms. In these cases, painkillers are the most used medication with only evidence of improving pain, but not decreasing the symptoms duration nor improving cognitive deficits. TBI-related mood disorders can be improved by using antidepressants and psychostimulants, and yet not dealing adequately with memory deficits. Unfortunately, none of them can interfere with the neuroinflammatory cascade that could be the main cause of the sequelae after severe or mTBI (Whyte et al., 2002; Comper et al., 2005; Wheaton et al., 2011; Huang et al., 2016). In the present study we propose an early IGF-1 gene therapy, considering previous reports regarding its neuroprotective and anti-inflammatory effects (Zheng et al., 2000; Carlson and Saatman, 2018; Serhan et al., 2019). In fact, a small clinical trial showed improvement in neurological outcome in severe TBI patients, when intravenous IGF-1 was administered for several days, without effect in those with mTBI (Hatton et al., 1997). Our results indicate that locally administered IGF-1 gene therapy a few minutes after TBI, significantly reduces recognized OS markers, such as the protein and lipid (AOPP and MDA concentrations respectively) peroxidation increments observed at 24 h and impairs its long-term maintenance, also by reducing their levels 7 days after TBI. It is worth noting that this effect is specifically due to IGF-1 over-expression and not only by viruses' administration since control viruses (RadDsRed) did

not reduce AOPP nor MDA levels 7 days after TBI. With this experimental approach, we were able to express the Red protein in brain areas neighboring to the virus administration site (see **Figure 4A**), and since the effects were observed in frontal brain areas such as PFC and MC, the newly produced IGF-1 could be actively transported through the choroid plexus and translocated to the cerebrospinal fluid to finally reach different areas of the nervous tissue, as it was recently reported (Nishida et al., 2020). Nevertheless, further studies need to be performed to reveal changes in other players involved in the OS balance: antioxidants enzymes such as superoxide dismutase, catalase, and glutathione peroxidase, as well as accumulation of oxidation products of the proteins and lipids, like protein carbonyl and 4-hydroxynonenal (Impellizzeri et al., 2019; Siracusa et al., 2020).

The PFC plays an important role in execution of behavioral tasks that require spatial working memory, and a direct PFC-HIP pathway allows the encoding of salient spatial signals during task execution (Deakin et al., 2012). In fact, lesion- or drug-induced disturbances in HIP function certainly affect spatial working memory performance (Dillon et al., 2008; Tian et al., 2017; Ayabe et al., 2019). In the present study, we found persistent increases in OS markers in these two relevant brain structures that may affect the PFC-HIP bidirectional control required to observe spontaneous alternations. Early IGF-1 gene therapy was able to prevent the behavioral deficits observed in TBI rats after 7 days of injury. Only the group treated with vectors carrying the cDNA of IGF-1 gene showed a percentage of spontaneous arm alternations similar to the control group (Sham), while the TBI or TBI expressing Red protein groups did not show differences from each other and had lower performance rate than the controls in Y-maze spontaneous alternations. All together, these results could indicate that normal working memory can be preserved long-term after injury if critical initial secondary injury mechanisms were prevented in brain structures critical to this cognitive function. This novel therapeutic approach could be beneficial from IGF-1 peripheral administration for many reasons: first, local over-expression can be maintained even after a month from a single administration (Falomir-Lockhart et al., 2019); second, local over-expression may reduce systemic effects compared to peripheral administrations which may need massive doses in order to reach therapeutic CNS IGF-1 concentrations and lastly no doubts about treatment patient's adherence, since administration must be performed during hospitalization, in a temporal window that guarantees the pharmacological effect.

In conclusion, results presented in this work indicate that brain focalized IGF-1 over-expression could be an effective therapeutic approach targeting neuroinflammation and also improving the cognitive deficits observed after TBI.

DATA AVAILABILITY STATEMENT

The original contributions presented in the study are included in the article/supplementary material, further inquiries can be directed to the corresponding author.

ETHICS STATEMENT

The animal study was reviewed and approved by the Animal Care and Use Committee, Facultad de Ciencias Químicas (Res. Dec. 1194/2017 and 2336/2019), Universidad Nacional de Córdoba.

AUTHOR CONTRIBUTIONS

MP designed, supervised the study and wrote the manuscript. AM and MG in collaboration with EA performed experimental protocols regarding TBI protocols, treatments and behavioural tests and collaborate with OS determinations and statistical analysis. JC-F performed the statistical analyses and figures. JS performed OS determinations under supervision of CH. CH developed and produced viral vectors. MH processed tissue and obtained images of red fluorescent protein expression from animals treated with RAdDsRed viruses. Authors reviewed content and approved the final version of the manuscript for publication.

FUNDING

This study was supported by the grants from CONSOLIDAR SECyT-UNC 2018 and PRIMAR SECyT-UNC 2019 to Pérez, IFEC-CONICET Institutional grant 2019, and CONSOLIDAR SECyT-UNC 2018 to Becerra.

ACKNOWLEDGMENTS

The authors are grateful to Alberto L. Oliveros, Estela Salde, and Lorena Mercado for their technical laboratory assistance and to Jessica Mendelson for her assistance in English editing.

REFERENCES

Agha, A., Rogers, B., Sherlock, M., O'Kelly, P., Tormey, W., Phillips, J., et al. (2004). Anterior Pituitary Dysfunction in Survivors of Traumatic Brain Injury. *J. Clin. Endocrinol. Metab.* 89 (10), 4929–4936. doi:10.1210/jc.2004-0511

Alain, B. B., and Wang, Y. J. (2008). Cushing's Ulcer in Traumatic Brain Injury. *Chin. J. Traumatol.* 11 (2), 114–119. doi:10.1016/s1008-1275(08)60024-3

Alexander, M. P. (1995). Mild Traumatic Brain Injury: Pathophysiology, Natural History, and Clinical Management. *Neurology*. 45 (7), 1253–1260. doi:10.1212/wnl.45.7.1253

Arciniegas, D. B., Anderson, C. A., Topkoff, J., and McAllister, T. W. (2005). Mild Traumatic Brain Injury: a Neuropsychiatric Approach to Diagnosis, Evaluation, and Treatment. *Neuropsychiatr. Dis. Treat.* 1 (4), 311–327.

Ayabe, T., Ano, Y., Ohya, R., Kitaoka, S., and Furuyashiki, T. (2019). The Lacto-Tetrapeptide Gly-Thr-Trp-Tyr, β-Lactolin, Improves Spatial Memory

Functions via Dopamine Release and D1 Receptor Activation in the Hippocampus. *Nutrients*. 11 (10). doi:10.3390/nu11102469

Babior, B. M. (2000). Phagocytes and Oxidative Stress. *Am. J. Med.* 109 (1), 33–44. doi:10.1016/s0002-9343(00)00481-2

Block, M. L., and Hong, J-S. (2007). Chronic Microglial Activation and Progressive Dopaminergic Neurotoxicity. *Biochem. Soc. Trans.* 35 (Pt 5), 1127–1132. doi:10.1042/bst0351127

Block, M. L., Li, G., Qin, L., Wu, X., Pei, Z., Wang, T., et al. (2006). Potent Regulation of Microglia-derived Oxidative Stress and Dopaminergic Neuron Survival: Substance P vs. Dynorphin. *FASEB j.* 20 (2), 251–258. doi:10.1096/fj.05-4553com

Bondanelli, M., Ambrosio, M. R., Margutti, A., Boldrini, P., Basaglia, N., Franceschetti, P., et al. (2002). Evidence for Integrity of the Growth Hormone/insulin-like Growth Factor-1 axis in Patients with Severe Head Trauma during Rehabilitation. *Metabolism*. 51 (10), 1363–1369. doi:10.1053/meta.2002.34714

Bryan, C. J. (2013). Multiple Traumatic Brain Injury and Concussive Symptoms Among Deployed Military Personnel. *Brain Inj.* 27 (12), 1333–1337. doi:10.3109/02699052.2013.823651

Carlson, S. W., and Saatman, K. E. (2018). Central Infusion of Insulin-like Growth Factor-1 Increases Hippocampal Neurogenesis and Improves Neurobehavioral Function after Traumatic Brain Injury. *J. Neurotrauma*. 35 (13), 1467–1480. doi:10.1089/neu.2017.5374

Carney, N., Totten, A. M., O'Reilly, C., Ullman, J. S., Hawryluk, G. W. J., Bell, M. J., et al. (2017). Guidelines for the Management of Severe Traumatic Brain Injury, Fourth Edition. *Neurosurgery*. 80 (1), 6–15. doi:10.1227/neu.0000000000001432

Centers for Disease Control and Prevention (2019). *Surveillance Report of Traumatic Brain Injury-Related Emergency Department Visits, Hospitalizations, and Deaths-United States, 2014*. Washington, D.C: Centers Dis Control Prev US Dep Heal Hum Serv, 24. Available at: www.cdc.gov/TraumaticBrainInjury

Christodoulou, C., DeLuca, J., Ricker, J. H., Madigan, N. K., Bly, B. M., Lange, G., et al. (2001). Functional Magnetic Resonance Imaging of Working Memory Impairment after Traumatic Brain Injury. *J. Neurol. Neurosurg. Psychiatry*. 71 (2), 161–168. doi:10.1136/jnnp.71.2.161

Comper, P., Bisschop, S. M., Carnide, N., and Tricco, A. (2005). A Systematic Review of Treatments for Mild Traumatic Brain Injury. *Brain Inj.* 19 (11), 863–880. doi:10.1080/02699050400025042

Deakin, I. H., Nissen, W., Law, A. J., Lane, T., Kanso, R., Schwab, M. H., et al. (2012). Transgenic Overexpression of the Type I Isoform of Neuregulin 1 Affects Working Memory and Hippocampal Oscillations but Not Long-Term Potentiation. *Cereb. Cortex*. 22 (7), 1520–1529. doi:10.1093/cercor/bhr223

Dillon, G. M., Qu, X., Marcus, J. N., and Dodart, J.-C. (2008). Excitotoxic Lesions Restricted to the Dorsal CA1 Field of the hippocampus Impair Spatial Memory and Extinction Learning in C57BL/6 Mice. *Neurobiol. Learn. Mem.* 90 (2), 426–433. doi:10.1016/j.nlm.2008.05.008

Dubiel, R., Callender, L., Dunklin, C., Harper, C., Bennett, M., Kreber, L., et al. (2018). Phase 2 Randomized, Placebo-Controlled Clinical Trial of Recombinant Human Growth Hormone (rhGH) during Rehabilitation from Traumatic Brain Injury. *Front. Endocrinol. (Lausanne)*. 9, 520. doi:10.3389/fendo.2018.00520

Farbood, Y., Sarkaki, A., Dianat, M., Khodadadi, A., Haddad, M. K., and Mashhadizadeh, S. (2015). Ellagic Acid Prevents Cognitive and Hippocampal Long-Term Potentiation Deficits and Brain Inflammation in Rat with Traumatic Brain Injury. *Life Sci.* 124, 120–127. doi:10.1016/j.lfs.2015.01.013

Falomir-Lockhart, E., Dolcetti, F. J. C., García-Segura, L. M., Hereñú, C. B., and Bellini, M. J. (2019). IGF1 Gene Therapy Modifies Microglia in the Striatum of Senile Rats. *Front. Aging Neurosci.* 11, 48. doi:10.3389/fnagi.2019.00048

Foda, M. A., and Marmarou, A. (1994). A New Model of Diffuse Brain Injury in Rats. Part II: Morphological Characterization. *J. Neurosurg.* 80 (2), 301–313. doi:10.3171/jns.1994.80.2.0301

Hatton, J., Rapp, R. P., Kudsk, K. A., Brown, R. O., Luer, M. S., Bukar, J. G., et al. (1997). Intravenous Insulin-like Growth Factor-I (IGF-I) in Moderate-To-Severe Head Injury: a Phase II Safety and Efficacy Trial. *Foc.* 2 (5), E9. doi:10.3171/foc.1997.2.5.9

Hereñú, C. B., Cristina, C., Rimoldi, O. J., Becú-Villalobos, D., Cambiaggi, V., Portiansky, E. L., et al. (2007). Restorative Effect of Insulin-like Growth Factor-I Gene Therapy in the Hypothalamus of Senile Rats with Dopaminergic Dysfunction. *Gene Ther.* 14 (3), 237–245. doi:10.1038/sj.gt.3302870

Hereñú, C. B., Sonntag, W. E., Morel, G. R., Portiansky, E. L., and Goya, R. G. (2009). The Ependymal Route for Insulin-like Growth Factor-1 Gene Therapy in the Brain. *Neuroscience*. 163 (1), 442–447. doi:10.1016/j.neuroscience.2009.06.024

Hillary, F. G., Medaglia, J. D., Gates, K., Molenaar, P. C., Slocomb, J., Peechatka, A., et al. (2011). Examining Working Memory Task Acquisition in a Disrupted Neural Network. *Brain*. 134 (Pt 5), 1555–1570. doi:10.1093/brain/awr043

Huang, C.-H., Huang, C.-C., Sun, C.-K., Lin, G.-H., and Hou, W.-H. (2016). Methylphenidate on Cognitive Improvement in Patients with Traumatic Brain Injury: A Meta-Analysis. *Curr Neuropharmacol.* 14 (3), 272–281. doi:10.2174/1570159x13666150514233033

Impellizzeri, D., Peritore, A. F., Cordaro, M., Gugliandolo, E., Siracusa, R., Crupi, R., et al. (2019). The Neuroprotective Effects of Micronized PEA (PEA-m) Formulation on Diabetic Peripheral Neuropathy in Mice. *FASEB j.* 33 (10), 11364–11380. doi:10.1096/fj.201900538r

Kaplan, G. B., Leite-Morris, K. A., Wang, L., Rumbika, K. K., Heinrichs, S. C., Zeng, X., et al. (2018). Pathophysiological Bases of Comorbidity: Traumatic Brain Injury and Post-Traumatic Stress Disorder. *J. Neurotrauma*. 35 (2), 210–225. doi:10.1089/neu.2016.4953

Katerji, M., Filippova, M., and Duerksen-Hughes, P. (2019). Approaches and Methods to Measure Oxidative Stress in Clinical Samples: Research Applications in the Cancer Field. *Oxid Med. Cel Longev.* 2019, 1–29. doi:10.1155/2019/1279250

Katz, D. I., and Alexander, M. P. (1994). Traumatic Brain Injury. *Arch. Neurol.* 51 (7), 661–670. doi:10.1001/archneur.1994.00540190041013

Kay, T., Harrington, D. E., and Adams, R. (1993). American Congress of Rehabilitation Medicine, Head Injury Interdisciplinary Special Interest Group. Definition of Mild Traumatic Brain Injury. *J. Head Trauma Rehabil. [Internet]*. 8 (3), 86–87. doi:10.1097/00001199-199309000-00009

Koopmans, G. C., Brans, M., Gómez-Pinilla, F., Duis, S., Gispen, W. H., Torres-Aleman, I., et al. (2006). Circulating Insulin-like Growth Factor I and Functional Recovery from Spinal Cord Injury under Enriched Housing Conditions. *Eur. J. Neurosci.* 23 (4), 1035–1046. doi:10.1111/j.1460-9568.2006.04627.x

Kraeuter, A.-K., Guest, P. C., and Sarnyai, Z. (2019). The Y-Maze for Assessment of Spatial Working and Reference Memory in Mice. *Methods Mol. Biol.* 1916, 105–111. doi:10.1007/978-1-4939-8994-2_10

Krishnamurthy, K., and Laskowitz, D. T. (2016). "Cellular and Molecular Mechanisms of Secondary Neuronal Injury Following Traumatic Brain Injury,". Editors D Laskowitz and G Grant (Boca Raton (FL))

Kushner, D. (1998). Mild Traumatic Brain Injury. *Arch. Intern. Med.* 158 (15), 1617–1624. doi:10.1001/archinte.158.15.1617

Lara, A. H., and Wallis, J. D. (2015). The Role of Prefrontal Cortex in Working Memory: A Mini Review. *Front. Syst. Neurosci.* 9, 173. doi:10.3389/fnsys.2015.00173

Lozano, D., Gonzales-Portillo, G. S., Acosta, S., de la Pena, I., Tajiri, N., Kaneko, Y., et al. (2015). Neuroinflammatory Responses to Traumatic Brain Injury: Etiology, Clinical Consequences, and Therapeutic Opportunities. *Neuropsychiatr. Dis. Treat.* 11, 97–106. doi:10.2147/NDT.S65815

Luoto, T. M., Raj, R., Posti, J. P., Gardner, A. J., Panenka, W. J., and Iverson, G. L. (2017). A Systematic Review of the Usefulness of Glial Fibrillary Acidic Protein for Predicting Acute Intracranial Lesions Following Head Trauma. *Front. Neurol.* 8, 652. doi:10.3389/fneur.2017.00652

Madathil, S. K., Evans, H. N., and Saatman, K. E. (2010). Temporal and Regional Changes in IGF-1/IGF-1R Signaling in the Mouse Brain after Traumatic Brain Injury. *J. Neurotrauma*. 27 (1), 95–107. doi:10.1089/neu.2009.1002

Madathil, S. K., and Saatman, K. E. (2015). "IGF-1/IGF-R Signaling in Traumatic Brain Injury: Impact on Cell Survival, Neurogenesis, and Behavioral Outcome,". Editor F. H Kobeissy (Boca Raton (FL)

Marmarou, A., Foda, M. A., Brink, W. v. d., Campbell, J., Kita, H., and Demetriadou, K. (1994). A New Model of Diffuse Brain Injury in Rats. *J. Neurosurg.* 80 (2), 291–300. doi:10.3171/jns.1994.80.2.0291

McMahon, P. J., Hricik, A., Yue, J. K., Puccio, A. M., Inoue, T., Lingsma, H. F., et al. (2014). Symptomatology and Functional Outcome in Mild Traumatic Brain Injury: Results from the Prospective TRACK-TBI Study. *J. Neurotrauma*. 31 (1), 26–33. doi:10.1089/neu.2013.2984

Montivero, A. J., Ghersi, M. S., Catalán-Figueroa, J., Culasso, A. F., and Hereñú, C. B. (2021). "Beyond Acute Traumatic Brain Injury: Molecular Implications of Associated Neuroinflammation in Higher-Order Cognitive Processes," in *Psychiatry and Neuroscience Update*. Editors P.Á. Gargiulo and H.L. Mesones Arroyo (No Title: Springer C)

Niedzwecki, C. M., Marwitz, J. H., Ketchum, J. M., Cifu, D. X., Dillard, C. M., and Monasterio, E. A. (2008). Traumatic Brain Injury. *J. Head Trauma Rehabil.* 23 (4), 209–219. doi:10.1097/01.htr.0000327253.61751.29

Nishida, F., Morel, G. R., Hereñú, C. B., Schwerdt, J. I., Goya, R. G., and Portiansky, E. L. (2011). Restorative Effect of Intracerebroventricular Insulin-like Growth Factor-I Gene Therapy on Motor Performance in Aging Rats. *Neuroscience*. 177, 195–206. doi:10.1016/j.neuroscience.2011.01.013

Nishida, F., Zanuzzi, C. N., Sisti, M. S., Falomir Lockhart, E., Camiña, A. E., Hereñú, C. B., et al. (2020). Intracisternal IGF-1 Gene Therapy Abrogates Kainic Acid-induced Excitotoxic Damage of the Rat Spinal Cord. *Eur. J. Neurosci.* 52 (5), 3339–3352. doi:10.1111/ejn.14876

Nortje, J., and Menon, D. K. (2004). Traumatic Brain Injury: Physiology, Mechanisms, and Outcome. *Curr. Opin. Neurol.* 17 (6), 711–718. doi:10.1097/00019052-200412000-00011

Occhieppo, V. B., Basmadjian, O. M., Marchese, N. A., Silvero, C. M. J., Rodríguez, A., Armonelli, S., et al. (2020). AT(1) -R Is Involved in the Development of Long-Lasting, Region-dependent and Oxidative Stress-independent Astrocyte Morphological Alterations Induced by Ketamine. *Eur. J. Neurosci.* doi:10.1111/ejn.14756

Olivecrona, Z., Dahlqvist, P., and Koskinen, L-O. D. (2013). Acute Neuro-Endocrine Profile and Prediction of Outcome after Severe Brain Injury. *Scand. J. Trauma Resusc Emerg. Med.* 21, 33. doi:10.1186/1757-7241-21-33

Pardo, J., Abba, M. C., Lacunza, E., Ogundele, O. M., Paiva, I., Morel, G. R., et al. (2017). IGF-I Gene Therapy in Aging Rats Modulates Hippocampal Genes Relevant to Memory Function. *Journals Gerontol. Ser. A. [Internet]*. 73 (4), 459–467. doi:10.1093/gerona/glx125

Paterno, R., Folweiler, K. A., and Cohen, A. S. (2017). Pathophysiology and Treatment of Memory Dysfunction after Traumatic Brain Injury. *Curr. Neurol. Neurosci. Rep.* 17 (7), 52. doi:10.1007/s11910-017-0762-x

Pearn, M. L., Niesman, I. R., Egawa, J., Sawada, A., Almenar-Queralt, A., Shah, S. B., et al. (2017). Pathophysiology Associated with Traumatic Brain Injury: Current Treatments and Potential Novel Therapeutics. *Cell Mol Neurobiol*. 37 (4), 571–585. doi:10.1007/s10571-016-0400-1

Pekny, M., and Pekna, M. (2016). Reactive Gliosis in the Pathogenesis of CNS Diseases. *Biochim. Biophys. Acta (Bba) - Mol. Basis Dis.* 1862 (3), 483–491. doi:10.1016/j.bbadis.2015.11.014

Pelinka, L. E., Kroepfl, A., Leixnering, M., Buchinger, W., Raabe, A., and Redl, H. (2004). GFAP versus S100B in Serum after Traumatic Brain Injury: Relationship to Brain Damage and Outcome. *J. Neurotrauma*. 21 (11), 1553–1561. doi:10.1089/neu.2004.21.1553

Polli, J. E., Rekhi, G. S., Augsburger, L. L., and Shah, V. P. (1997). Methods to Compare Dissolution Profiles and a Rationale for Wide Dissolution Specifications for Metoprolol Tartrate Tablets. *J. Pharm. Sci.* 86 (6), 690–700. doi:10.1021/js960473x

Ponsford, J. L., Spitz, G., and McKenzie, D. (2016). Using Post-Traumatic Amnesia to Predict Outcome after Traumatic Brain Injury. *J. Neurotrauma*. 33 (11), 997–1004. doi:10.1089/neu.2015.4025

Popovic, V., Pekic, S., Pavlovic, D., Maric, N., Jasovic-Gasic, M., Djurovic, B., et al. (2004). Hypopituitarism as a Consequence of Traumatic Brain Injury (TBI) and its Possible Relation with Cognitive Disabilities and Mental Distress. *J. Endocrinol. Invest.* 27 (11), 1048–1054. doi:10.1007/bf03345308

Ricker, J. H., Hillary, F. G., and DeLuca, J. (2001). Functionally Activated Brain Imaging (O-15 PET and fMRI) in the Study of Learning and Memory after Traumatic Brain Injury. *J. Head Trauma Rehabil.* 16 (2), 191–205. doi:10.1097/00001199-200104000-00007

Riggall, A. C., and Postle, B. R. (2012). The Relationship between Working Memory Storage and Elevated Activity as Measured with Functional Magnetic Resonance Imaging. *J. Neurosci.* 32 (38), 12990–12998. doi:10.1523/jneurosci.1892-12.2012

Robles, J. F., Navarro, J. E. V., Maglinao, M. L. D., Matawaran, B. J. A-S. A., Andag-Silva, A. A., Mercado-Asis, L. B., et al. (2009). Traumatic Injury to the Brain and Endocrine Evaluation of the Anterior Pituitary a Year after the Event (The TRIBE Study). *Int. J. Endocrinol. Metab.* 7, 72–81.

Ryan, L. M., and Warden, D. L. (2003). Post Concussion Syndrome. *Int. Rev. Psychiatry* 15 (4), 310–316. doi:10.1080/09540260310001606692

Schober, M. E., Block, B., Beachy, J. C., Statler, K. D., Giza, C. C., and Lane, R. H. (2010). Early and Sustained Increase in the Expression of Hippocampal IGF-1, but Not EPO, in a Developmental Rodent Model of Traumatic Brain Injury. *J. Neurotrauma*. 27 (11), 2011–2020. doi:10.1089/neu.2009.1226

Serhan, A., Boddeke, E., and Kooijman, R. (2019). Insulin-Like Growth Factor-1 Is Neuroprotective in Aged Rats with Ischemic Stroke. *Front. Aging Neurosci.* 11, 349. doi:10.3389/fnagi.2019.00349

Silva, D. d. S., Brito, J. N. P. d. O., Ibiapina, J. O., Lima, M. F. M. B., Medeiros, A. R. G. d. V., Queiroz, B. H. C. e., et al. (2011). Traumatic Brain Injury: Clinical and Pathological Parameters in an Experimental Weightdrop Model. *Acta Cir. Bras.* 26 (2), 94–100. doi:10.1590/s0102-86502011000200004

Siracusa, R., Scuto, M., Fusco, R., Trovato, A., Ontario, M. L., Crea, R., et al. (2020). Anti-inflammatory and Anti-oxidant Activity of Hidrox(®) in Rotenone-Induced Parkinson's Disease in Mice. *Antioxidants (Basel, Switzerland)*. 9 (9), 824. doi:10.3390/antiox9090824

Steyerberg, E. W., Mushkudiani, N., Perel, P., Butcher, I., Lu, J., McHugh, G. S., et al. (2008). Predicting Outcome after Traumatic Brain Injury: Development and International Validation of Prognostic Scores Based on Admission Characteristics. *Plos Med.* 5 (8), 1251–1261. doi:10.1371/journal.pmed.0050165

Stocchetti, N., and Zanier, E. R. (2016). Chronic Impact of Traumatic Brain Injury on Outcome and Quality of Life: a Narrative Review. *Crit. Care*. 20 (1), 148. doi:10.1186/s13054-016-1318-1

Tian, J., Geng, F., Gao, F., Chen, Y.-H., Liu, J.-H., Wu, J.-L., et al. (2017). Down-Regulation of Neuregulin1/ErbB4 Signaling in the Hippocampus Is Critical for Learning and Memory. *Mol. Neurobiol.* 54 (6), 3976–3987. doi:10.1007/s12035-016-9956-5

Trejo, J. L., Carro, E., Lopez-Lopez, C., and Torres-Aleman, I. (2004). Role of Serum Insulin-like Growth Factor I in Mammalian Brain Aging. *Growth Horm. IGF Res.* 14 (Suppl. A), 39–43. doi:10.1016/j.ghir.2004.03.010

Wagner, J., Dusick, J. R., McArthur, D. L., Cohan, P., Wang, C., Swerdloff, R., et al. (2010). Acute Gonadotroph and Somatotroph Hormonal Suppression after Traumatic Brain Injury. *J. Neurotrauma*. 27 (6), 1007–1019. doi:10.1089/neu.2009.1092

Webster, K. M., Sun, M., Crack, P., O'Brien, T. J., Shultz, S. R., and Semple, B. D. (2017). Inflammation in Epileptogenesis after Traumatic Brain Injury. *J. Neuroinflammation*. 14 (1), 10. doi:10.1186/s12974-016-0786-1

Wheaton, P., Mathias, J. L., and Vink, R. (2011). Impact of Pharmacological Treatments on Cognitive and Behavioral Outcome in the Postacute Stages of Adult Traumatic Brain Injury. *J. Clin. Psychopharmacol.* 31 (6), 745–757. doi:10.1097/jcp.0b013e318235f4ac

Whitaker-Lea, W. A., and Valadka, A. B. (2017). Acute Management of Moderate-Severe Traumatic Brain Injury. *Phys. Med. Rehabil. Clin. North America*. 28 (2), 227–243. doi:10.1016/j.pmr.2016.12.002

Whyte, J., Vaccaro, M., Grieb-Neff, P., and Hart, T. (2002). Psychostimulant Use in the Rehabilitation of Individuals with Traumatic Brain Injury. *J. Head Trauma Rehabil.* 17 (4), 284–299. doi:10.1097/00001199-200208000-00003

Wildburger, R., Zarkovic, N., Leb, G., Borovic, S., Zarkovic, K., and Tatzber, F. (2001). Post-traumatic Changes in Insulin-like Growth Factor Type 1 and Growth Hormone in Patients with Bone Fractures and Traumatic Brain Injury. *Wien Klin Wochenschr* 113 (3–4), 119–126.

Wolfe, L. F., Sahni, A. S., and Attarian, H. (2018). Sleep Disorders in Traumatic Brain Injury. *NeuroRehabilitation*. 43 (3), 257–266. doi:10.3233/nre-182583

Wylie, G. R., Freeman, K., Thomas, A., Shpaner, M., OKeefe, M., Watts, R., et al. (2015). Cognitive Improvement after Mild Traumatic Brain Injury Measured with Functional Neuroimaging during the Acute Period. *PLoS One*. 10 (5), e0126110. doi:10.1371/journal.pone.0126110

Xie, B. S., Wang, Y. Q., Lin, Y., Mao, Q., Feng, J. F., Gao, G. Y., et al. (2019). Inhibition of Ferroptosis Attenuates Tissue Damage and Improves Long-term Outcomes after Traumatic Brain Injury in Mice. *CNS Neurosci. Ther.* 25 (4), 465–475. doi:10.1111/cns.13069

Xiong, Y., Mahmood, A., and Chopp, M. (2013). Animal Models of Traumatic Brain Injury. *Nat. Rev. Neurosci.* 14 (2), 128–142. doi:10.1038/nrn3407

Zgaljardic, D. J., Guttikonda, S., Grady, J. J., Gilkison, C. R., Mossberg, K. A., High Jr, W. M., et al. (2011). Serum IGF-1 Concentrations in a Sample of Patients with Traumatic Brain Injury as a Diagnostic Marker of Growth Hormone Secretory Response to Glucagon Stimulation Testing. *Clin. Endocrinol. (Oxf).* 74 (3), 365–369. doi:10.1111/j.1365-2265.2010.03935.x

Zhang, Y., Zhang, Z. G., Chopp, M., Meng, Y., Zhang, L., Mahmood, A., et al. (2017). Treatment of Traumatic Brain Injury in Rats with N-Acetyl-Seryl-Aspartyl-Lysyl-Proline. *J Neurosurg.* 126 (3), 782–795. doi:10.3171/2016.3.jns152699

Zheng, W.-H., Kar, S., Doré, S., and Quirion, R. (2000). Insulin-like Growth Factor-1 (IGF-1): a Neuroprotective Trophic Factor Acting via the Akt Kinase Pathway. *J. Neural Transm. Suppl.* 8 (60), 261–272. doi:10.1007/978-3-7091-6301-6_17

Conflict of Interest: The authors declare that the research was conducted in the absence of any commercial or financial relationships that could be construed as a potential conflict of interest.

Copyright © 2021 Montivero, Ghersi, Silvero C, Artur de la Villarmois, Catalan-Figueroa, Herrera, Becerra, Hereñú and Pérez. This is an open-access article distributed under the terms of the Creative Commons Attribution License (CC BY). The use, distribution or reproduction in other forums is permitted, provided the original author(s) and the copyright owner(s) are credited and that the original publication in this journal is cited, in accordance with accepted academic practice. No use, distribution or reproduction is permitted which does not comply with these terms.

frontiers in Pharmacology

ORIGINAL RESEARCH
published: 21 June 2021
doi: 10.3389/fphar.2021.689346

Pathological Neuroinflammatory Conversion of Reactive Astrocytes Is Induced by Microglia and Involves Chromatin Remodeling

Alejandro Villarreal[1]*, *Camila Vidos*[1], *Matías Monteverde Busso*[1,2], *María Belén Cieri*[1,2] and *Alberto Javier Ramos*[1,2]*

[1]Laboratorio de Neuropatología Molecular, Instituto de Biología Celular y Neurociencia "Prof. E. De Robertis" UBA-CONICET, Facultad de Medicina, Universidad de Buenos Aires, Buenos Aires, Argentina, [2]Primera Unidad Académica de Histología, Embriología, Biología Celular y Genética, Facultad de Medicina, Universidad de Buenos Aires, Buenos Aires, Argentina

Following brain injury or in neurodegenerative diseases, astrocytes become reactive and may suffer pathological remodeling, features of which are the loss of their homeostatic functions and a pro-inflammatory gain of function that facilitates neurodegeneration. Pharmacological intervention to modulate this astroglial response and neuroinflammation is an interesting new therapeutic research strategy, but it still requires a deeper understanding of the underlying cellular and molecular mechanisms of the phenomenon. Based on the known microglial–astroglial interaction, the prominent role of the nuclear factor kappa B (NF-κB) pathway in mediating astroglial pathological pro-inflammatory gain of function, and its ability to recruit chromatin-remodeling enzymes, we first explored the microglial role in the initiation of astroglial pro-inflammatory conversion and then monitored the progression of epigenetic changes in the astrocytic chromatin. Different configurations of primary glial culture were used to modulate microglia–astrocyte crosstalk while inducing pro-inflammatory gain of function by lipopolysaccharide (LPS) exposure. *In vivo*, brain ischemia by cortical devascularization (pial disruption) was performed to verify the presence of epigenetic marks in reactive astrocytes. Our results showed that 1) microglia is required to initiate the pathological conversion of astrocytes by triggering the NF-κB signaling pathway; 2) this interaction is mediated by soluble factors and induces stable astroglial phenotypic changes; 3) the pathological conversion promotes chromatin remodeling with stable increase in H3K9K14ac, temporary increase in H3K27ac, and temporary reduction in heterochromatin mark H3K9me3; and 4) *in vivo* reactive astrocytes show increased H3K27ac mark in the neuroinflammatory milieu from the ischemic penumbra. Our findings indicate that

OPEN ACCESS

Edited by:
Flavia Eugenia Saravia, Universidad de Buenos Aires, Argentina

Reviewed by:
Mercedes Lasaga, University of Buenos Aires, Argentina
Rocío Ruiz, Sevilla University, Spain

***Correspondence:**
Alejandro Villarreal
avillarreal.med@gmail.com
Alberto Javier Ramos
ajramos.fmed@gmail.com

Specialty section:
This article was submitted to Neuropharmacology, a section of the journal Frontiers in Pharmacology

Received: *31 March 2021*
Accepted: *25 May 2021*
Published: *21 June 2021*

Citation:
Villarreal A, Vidos C, Monteverde Busso M, Cieri MB and Ramos AJ (2021) Pathological Neuroinflammatory Conversion of Reactive Astrocytes Is Induced by Microglia and Involves Chromatin Remodeling. Front. Pharmacol. 12:689346. doi: 10.3389/fphar.2021.689346

Abbreviations: 5-FU, 5-fluorouracyl; BSA, bovine serum albumin; CNS, central nervous system; DAMP, damage-associated molecular pattern; DMEM, Dulbecco's modified Eagle medium; GFAP, glial fibrillary acidic protein; IL-1β, interleukin 1-beta; IL-1α, interleukin 1-alpha; Iba-1, ionized calcium binding adaptor molecule 1; NF-κB, nuclear factor kappa B; PRR, pattern recognition receptor; CM, conditioned medium; TLR4, toll like receptor 4; VPA, valproic acid; AEC, astrocyte-enriched culture; GMC, glial mixed culture; HATs, histone acetyltransferases; HDACs, histone deacetylases; TNFα, tumor necrosis factor alpha; C1q, complement component 1q; LPS, lipopolysaccharide; H3, histone 3; H3K9K14ac, acetylation of histone 3 at lysins 9 and 14 (activating mark); H3K27ac, acetylation of histone 3 at lysin 27 (activating mark); and H3K9me3, trimethylation of histone 3 at lysin 9 (repressive mark).

astroglial pathological pro-inflammatory gain of function is associated with profound changes in the configuration of astrocytic chromatin, which in turn are initiated by microglia-derived cues. These results open a new avenue in the study of potential pharmacological interventions that modify the initiation and stabilization of astroglial pathological remodeling, which would be useful in acute and chronic CNS injury. Epigenetic changes represent a plausible pharmacological target to interfere with the stabilization of the pathological astroglial phenotype.

Keywords: neuroinflammation, reactive astrogliosis, epigenetics, NF-κB, microglia–astrocyte crosstalk

INTRODUCTION

Astrocytes are the main players in maintaining brain homeostasis, having cellular pathways that allow them to protect neurons from glutamate excitotoxicity, extracellular ion disbalances, ammonium accumulation, and reactive oxygen species, as has been extensively reviewed (Sofroniew and Vinters, 2010; Clarke and Barres, 2013; Pekny et al., 2016; Santello et al., 2019). Furthermore, astrocytes provide structural and metabolic support to neurons, modulate synapses, and take part in the blood–brain barrier, among several other beneficial functions on the healthy central nervous system (CNS).

Under pathological conditions such as traumatic brain injury and brain ischemia or in neurodegenerative diseases, astrocytes participate in a cellular response to damage known as reactive gliosis, along with microglia and other cell types. In particular, astrocytes suffer temporal and spatial gradual morphological alterations together with profound transcriptomic changes (Sofroniew, 2009; Sofroniew, 2015; Anderson et al., 2016). Morphological and molecular studies indicate that astrocyte response is heterogeneous across CNS regions and even within regions (Anderson et al., 2014; Ramos, 2016; Bribian et al., 2018; Matias et al., 2019).

Reactive astrogliosis is part of the nervous tissue response to injury, which is triggered as an attempt to control damage and promote regeneration (Barres, 2008; Cregg et al., 2014; Sofroniew, 2015). However, sustained pro-inflammatory signals may lead to astroglial pathological remodeling with a pro-inflammatory gain of function that exacerbates neuronal death (Liu et al., 2011, 2020; Lian et al., 2016; Kirkley et al., 2017; Liddelow et al., 2017; Verkhratsky et al., 2019; Matejuk and Ransohoff, 2020). Initiation of the reactive astrocyte pathological remodeling has been partially explained by previous work from our group and others. We have shown that DAMP (damage-associated molecular pattern) or PAMP (pathogen-associated molecular pattern) exposure induce astroglial pro-inflammatory and neurotoxic phenotype remodeling in a PRR (pattern recognition receptor)- and NF-κB–dependent manner (Angelo et al., 2014, 2014; Lian et al., 2015; Rosciszewski et al., 2017). However, the dynamics of the activation of these processes and the requirements of non–cell autonomous (i.e., extrinsic) components have not yet been fully addressed.

Once engaged in the pro-inflammatory gain of function, reactive astrocytes show a very stable phenotype (Ramos et al., 2004; Díaz-Amarilla et al., 2011; Sofroniew, 2015; Pekny et al., 2016; Villarreal et al., 2016). This intriguing stable phenotype is likely to be sustained by extrinsic (non–cell autonomous) or intrinsic (cell autonomous) mechanisms. Extrinsic mechanisms involve the constitutive release of soluble cues from neighbor cells such as microglia or other immunocompetent cell partners, which sustain a pro-inflammatory astrocyte microenvironment. On the other hand, the intrinsic mechanisms may involve long-term changes in gene expression, and thus, epigenetic mechanisms are the candidates for stabilization of the pro-inflammatory astroglial phenotype.

Specifically, it has been reported that NF-κB interacts with chromatin remodelers such as p300 acetyltransferase, recruiting them to specific regulatory regions and increasing local histone acetylation and transcription of pro-inflammatory genes (Berghe et al., 1999; Mukherjee et al., 2013). In general, histone acetylation correlates with active transcription. The enzymes responsible for adding acetyl groups are widely known as histone acetyl transferases (HATs). Their counterparts, responsible for removing acetyl groups, are named histone deacetylases (HDACs). The balance between the activities of these enzymes determines the levels of acetylated histones and active transcription. HDACs have already been investigated as possible targets to modulate inflammation (Grunstein, 1997; Marmorstein and Zhou, 2014; Tessarz and Kouzarides, 2014; Voss and Thomas, 2018). However, the molecular mechanisms regulated by these enzymes in neural cells, and specifically in astrocytes, are still far from being fully understood. Here, we explored global changes of histone acetylation in reactive astrocytes and their role in the stabilization of the pro-inflammatory astrocytic gain of function.

MATERIAL AND METHODS

Materials

Antibodies were purchased from Dako (rabbit polyclonal anti-GFAP, cat# Z0334), Abcam (goat polyclonal anti–Iba-1, cat# ab5076), Chemicon-Millipore (mouse monoclonal anti-Actin, cat# MAB1501), Sigma (mouse monoclonal anti-GFAP, cat# G3893), Santa Cruz (mouse monoclonal anti-p65, cat# sc-8008 and mouse monoclonal anti-H3K9K14ac, cat# sc518011), and Diagenode (H3K27AC, cat# C15410174 and H3K9me3, cat# C15410193, which were a kind gift from Prof. Dr Tanja Vogel,

Institute for Anatomy and Cell Biology, Dept. of Molecular Embryology, University of Freiburg, Germany). Fluorescent secondary antibodies (Alexa Fluor 594 and 488) and peroxidase-conjugated secondary antibodies raised in donkey were purchased from Jackson Immunoresearch (United States).

Cell culture reagents were obtained from Invitrogen Life Technologies (Carlsbad, United States). Fetal calf serum (FCS) was purchased from Natocor (Córdoba, Argentina). Poly-L-lysine, DAPI (4′,6-diamidino-2-phenylindole), and other chemicals were purchased from Sigma (United States).

Primary Cultures of Glial Cells

Primary cultures were obtained from postnatal day 2–3 cerebral cortex of mice as already described (Rosciszewski et al., 2019), with minor changes. Briefly, cortices from both hemispheres were dissected under a microscope and mechanically dissociated using tweezers and by pipetting up and down with a decreasing micropipette tip diameter. The supernatant was transferred to a new tube and centrifuged at 1000 rpm for 5 min to pellet the cells. The clear supernatant was removed, and the cells were resuspended in Dulbecco's Modified Eagle Medium (DMEM) supplemented with 10% fetal calf serum, 2 mm L-glutamine, and 100 μg/ml penicillin/streptomycin (complete medium). The cells were plated in flasks and incubated at 37°C in a 5% CO_2 atmosphere until confluence was reached, which typically takes one week. Medium change was conducted one day after plating and then after 2 or 3 days. After reaching confluence, flasks were treated according to each culture configuration. Untreated flasks lead to glial mixed cultures (GMC), which were split into poly-lysine–coated multiwell plates or single-well plates.

To obtain astrocyte-enriched culture (AEC), microglial depletion was achieved by 48 h of shaking under dark conditions, replacing the medium every 24 h. To eliminate proliferating microglia, 5-fluorouracyl (5-FU) was added to the medium and incubated for an additional 24 h. After 5-FU exposure, the astrocytes were washed 3 times with complete medium and incubated at least 24 h before splitting (Angelo et al., 2014).

Reconstituted glial cultures were performed with microglia collected from the supernatant 24 and 48 h after shaking under dark conditions. Cells were centrifuged, resuspended in fresh complete medium, and immediately added on the top of a monolayer of AEC. For experiments in which microglia-conditioned medium was required, microglia obtained as explained before was plated on poly-lysine–coated multiwell plates. Under every condition, the cells were incubated for at least 24 h before treatments.

LPS Treatment

Cells from GMC, AEC, microglia-reconstituted AEC, and isolated microglia were replated at least 24 h before treatment. Two hours before treatment, complete medium was replaced with reduced-serum DMEM (2% FCS). LPS was added to each well at a final concentration of 25 ng/ml. This concentration was selected after dose-response studies that determined that GMC exposed to 25 ng/ml of LPS for 3 h promotes astroglial pro-inflammatory gain of function and neuronal death (Rosciszewski et al., 2019).

Using this protocol with 2% FCS, the untreated cells (namely, Ctrl) show a percentage of nuclear p65 in astrocytes that is below 0.5%. Microglia-conditioned medium was obtained by extracting medium after 1 h of exposure and immediately transferring it to wells containing AEC. Microglia was switched to complete medium until the end of the experiment and processed to confirm p65 nuclear translocation.

Cortical Devascularization (Pial Disruption) Model of Ischemia

Adult male Wistar rats (300–350 g) were obtained from the Animal Facility of the National Atomic Energy Commission (Comisión Nacional de Energía Atómica, CNEA, Argentina). The animals were housed in a controlled environment (12/12-h light/dark cycle and controlled humidity and temperature, with free access to standard laboratory rat food and water) under the permanent supervision of professional staff. The animals were anesthetized with ketamine/xylazine (90/10 mg/kg i.p.) and subjected to a unilateral cortical devascularization (CD) as previously described (Herrera and Cuello, 1992; Villarreal et al., 2011; Villarreal et al., 2016), (**Figure 6E**). Briefly, the rats were placed in a stereotaxic apparatus, and a small surface of the skull between the coronal suture and the bregma line was removed to expose the underlying vasculature. A 27-gauge needle was used to cut the overlying dura and tear it away from the underlying pia. A sterile cotton swab was then used to tear back the pia and to disrupt the pial blood vessels overlaying the exposed cortex. Immediately, small sterile cotton pieces embedded in sterile saline solution were laid on the cortical surface until all bleeding ceased (usually less than 50 s). All cotton pieces were removed, and the incision in the overlying skin was then closed, using the temporal muscle and the attached fascia to cover the lesion site. After surgery, the animals were housed individually to allow recovery for 4 days. During the surgery and the whole awakening period, body temperature was maintained by means of a heating pad. Animal care for this experimental protocol was in accordance with NIH guidelines for the care and use of laboratory animals, the Guidelines for the Use of Animals in Neuroscience Research by the Society for Neuroscience, and the ARRIVE guidelines and was approved by the CICUAL Committee of the School of Medicine, University of Buenos Aires.

Immunofluorescent Staining

For *in vitro* analysis, cells were fixed using a solution of 4% paraformaldehyde plus 4% sucrose in PBS (pH 7.2) for 15 min at room temperature at specific time points after the onset of treatments (Villarreal et al., 2014, 2016; Rosciszewski et al., 2019). After 15 min of fixation, the cells were washed three times with PBS and kept at 4°C. Before antibody incubation, fixated cells were permeabilized with 0.1% Triton-X in PBS for 15 min, followed by 30 min of incubation with blocking solution (5% normal horse serum in PBS). The cells were then incubated overnight with specific primary antibodies diluted in blocking solution. In specific experiments, microglia was detected using Tomato Lectin (TL) –FITC conjugate (Sigma), which was

incubated together with the antibodies at a dilution of 1/1,000. After removal of primary antibodies, the cells were washed three times with PBS, followed by 4 h of incubation with fluorescent secondary antibodies. The cells were then washed three more times in PBS, incubated for 5 min with DAPI in PBS, and washed three more times with PBS.

For *in vivo* histological analysis, 4 days post-lesion (DPL), the animals were deeply anesthetized with ketamine/xylazine (90/10 mg/kg, i.p.) and perfused through the left ventricle as described (Aviles-Reyes et al., 2010). Brains were cryoprotected and snap-frozen, and coronal brain sections with a thickness of 25 μm were obtained using a cryostat (Leica). Free-floating sections were kept in a cryoprotective solution (30% glycerol and 20% ethylene glycol in 0.05 M phosphate buffer) at −20°C until use and processed in the free-floating state as previously described (Aviles-Reyes et al., 2010; Angelo et al., 2014). Primary and secondary antibodies were diluted in a solution with 3% normal horse serum and 0.3% Triton X-100 in PBS. Isotypic specific secondary antibodies labeled with Alexa 488 or 594 were used, and nuclear counterstaining was carried out with DAPI (0.1 μg/ml).

Microscopy and Image Analysis and Processing

Imaging was conducted using an Olympus IX-81 microscope equipped with a DP71 camera (Olympus, Japan). *In vitro*, from each well, several images with a primary magnification of 20x were obtained and analyzed by a different person blinded to the treatment. All treatments and biological replicates of single experiments were imaged and documented in the same microscopy session. *In vivo*, for each animal, we obtained at least two images from the contralateral (CONTRA) and lesioned (ipsilateral, IPSI) hemispheres at a primary magnification of 20x and analyzed around 300 nuclei per image. Two 20x images cover most of the lesion caused by the cortical injury. Astrocytes and microglia were identified by their $GFAP^+$ immunostaining, while microglia was identified by the $Iba\text{-}1^+$ immunoreactivity.

Morphological analysis and cell counting (percentages of cells that are positive for a specific marker or protein) were conducted using Fiji (NIH, Schindelin et al., 2012). Images were merged, and cell counting was done using the Cell Counter plugin with channels Red, Green, and Blue overlapped.

Similarly, analysis of mean fluorescence intensity (MFI) for histone marks (typically, the red channel) was done in Fiji (Schindelin et al., 2012) with all channels overlapped to identify cell types. For each histone mark in astrocytes, a first region of interest (ROI) was delimited inside the DAPI-stained nucleus (nROI) of a GFAP-positive cell and a second one was delimited outside (oROI) to detect background signals. The mean fluorescence intensity of each single nucleus was calculated as nROI-oROI. In this way, we extracted a specific background signal in each analyzed nucleus. All nuclear measurements (>100 nuclei/image) from one image were averaged, and then, the means of at least three images were averaged to obtain the mean of a biological replicate. *In vivo*, the levels of histone modification were measured as they were *in vitro*, with the difference that *in vivo*, we also measured all the nuclei in a field independently of GFAP expression (Total). Since a specific histone modification could be changing in all cell types, we used this parameter to calculate a clean relative ratio of change in astrocytes due to the ischemic injury: Astrocyte/Total = [Astrocyte histone modification in ipsilateral (IPSI)/Total histone modification in ipsilateral (IPS)]/[Astrocyte histone modification in contralateral (CONTRA)/Total histone modification in CONTRA].

To estimate NF-κB activation, the percentage of a specific cell type with nuclear p65 ($p65^{nuc}$) was calculated as the number of specific cell types (GFAP or Iba-1) with $p65^{nuc}$ divided by the total number of specific cell types and multiplied by 100. The percentage of specific astrocytic or microglial morphological subtypes was calculated as the number of cells of a specific subtype divided by the total number of cells (GFAP or Iba-1) and multiplied by 100. The percentage of astrocytes and microglia was calculated as the number of cells immunoreactive for GFAP or Iba-1 divided by the total nuclei (DAPI) and multiplied by 100.

For figure preparation, images were processed (including size bar and labeling) using Fiji (Schindelin et al., 2012) and Inkscape (https://inkscape.org/). Bar size is indicated in each figure.

Semiquantitative PCR

Cells plated and treated in 10-cm-diameter plates were collected using a fenol–chloroform base extraction protocol, with Prep-Zol (Inbio Highway, Tandil, Argentina) as the reagent and following the manufacturer's indications. Total mRNA was converted into cDNA using a Genbiotech MMLV RT kit with oligo dTs (Genbiotech). PCR assays were performed using specific primers (Invitrogen): lL1β F: GAAAGACGGCACACCCACC, R: AAACCGCTTTTCCATCTTCTTCT; C3 F: AGCTTCAGG GTCCCAGCTAC, R: GCTGGAATCTTGATGGAGACGC; actin F: CACCACTTTCTACAATGAGC, R: CGGTCAGGA TCTTCATGAGG; and TBP F: ACCGTGAAT CTTGGCTGTA, R: CCGTGGCTCTCTTATTCTCA. PCR amplicons were run in a 1.5% agarose gel using TAE buffer and imaged using a VersaDoc 4,000 imaging system (Bio-Rad, United States). Each experiment included negative controls in which PCR reactions were performed in the absence of reverse transcriptase (Villarreal et al., 2014; Rosciszewski et al., 2017). Detailed PCR protocols are available from the authors under request.

Images were inverted and analyzed by NIH Fiji analysis for gels, where the optic density (OD) for each band is calculated. The value obtained for every band is first normalized to its housekeeping gene (actin or TBP). Then, the normalized value corresponding to the LPS treatment of each biological replicate was normalized to its control (untreated): LPS–Ctrl. Using one-sample t-test, we compared each normalized value to 0 (Ctrl=0).

Statistical Analysis

While conducting glial primary culture, individual animals were processed separately, and cultures coming from different animals were considered different biological replicates (n). Values are plotted as mean and SEM.

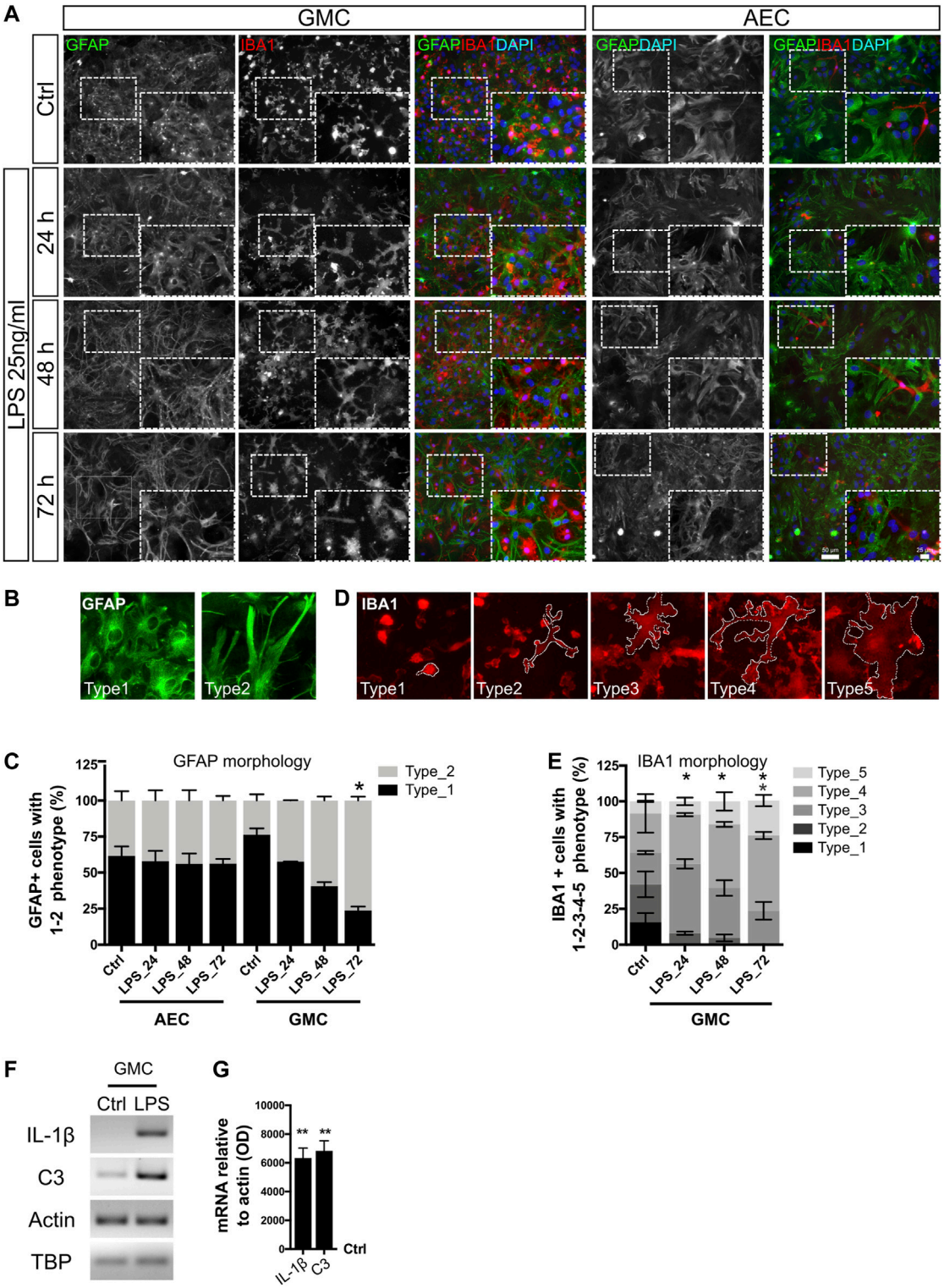

FIGURE 1 | Phenotypic conversion of astrocytes and microglia in response to LPS. **(A)** Astrocyte-enriched cultures (AECs) and glial mixed cultures (GMCs) were incubated with LPS during the indicated time points in reduced-serum medium. To address cell morphology in response to LPS, we performed double immunofluorescence staining for GFAP and Iba-1 to distinguish astrocytes and microglia, respectively. **(B)** Representative images of the morphological classification of GFAP$^+$ astrocytes *in vitro*. Type 1 astrocytes are polygonal-shaped astrocytes with few projections and type 2 astrocytes present highly stellated and elongated morphology. **(C)** Abundance of GFAP$^+$ astroglial cell types for AEC or GMC at the analyzed time points. Bars show the mean percentage of three to four biological

(*Continued*)

FIGURE 1 | replicates with the standard error of the mean (SEM). Each time point was compared to the respective control (no LPS) using the nonparametric Kruskal–Wallis test with the statistical significance represented as $^{*}p < 0.05$; $n = 3$. **(D)** Representative images of the morphological classification of Iba-1^{+} microgliocytes in five cell types, going from small bright and roundish microglial cells (type 1) to filamentous morphology (types 2–4) and ameboid flattened morphology (type 5) after LPS exposure. Dashed lines represent the cytoplasm limits of each microglial phenotype. **(E)** Distribution of microglial phenotypes in GMC exposed to LPS. Bars show the mean percentage of three biological replicates with the standard error of the mean (SEM). Each time point was compared to the respective control (no LPS) using the nonparametric Kruskal–Wallis test with the statistical significance represented as $^{*}p < 0.05$; $n = 3$. **(F)** Representative bands for the indicated mRNAs are shown from GMC exposed for 20 h to LPS. Actin and TBP were used as housekeeping genes. **(G)** Graph showing relative changes of mRNAs after normalization to actin. LPS condition was compared to its control (no LPS) using one-sample *t*-test with the statistical significance represented as $^{**}p < 0.01$, $n = 4$.

Typically, cultures obtained from one animal were split into different wells or plates to conduct different treatments. The "n" number used in each experiment, which is specified in each figure legend, was never below three, and most experiments were repeated at least twice. In some experiments such as fluorescence measurements, the means from each condition were normalized to the control in order to obtain ratios (mean treated/mean control). In such cases, the control takes a value of one. In other experiments, such as PCR approaches and nuclear p65 analysis, the mean from the control conditions was subtracted from the treatment means to obtain the difference as a magnitude of change (mean treated–mean control). In such cases, the control takes a value of 0. In any case, each condition was compared to the untreated control using one-sample *t*-test against the hypothetical mean of one or 0, depending on the normalization. To compare between two conditions, a two-tailed Student's t-test was conducted. For comparing non-normalized percentages, we used the nonparametric Kruskal–Wallis test. In all cases, a p value below 0.05 ($p < 0.05$) was considered as the parameter of significance. Statistical analysis and graph plotting were conducted using Prism GraphPad software.

RESULTS

Phenotypic Conversion of Astrocytes and Microglia in Response to LPS Exposure

We initially addressed the morphological changes of astrocytes and microglia at different time points after LPS stimulus (24, 48, and 72 h) (**Figure 1A**). Astrocytes in GMC respond to LPS with phenotypic changes toward a more stretched and filamentous morphology. **Figure 1A** shows the typical morphological changes that were initiated after 24 h of LPS exposure but became statistically significant after 48 and 72 h. We conducted the experiments in glial mixed culture (GMC) containing 20% microglia and in astroglia-enriched cultures (AECs) containing less than 1% microglia. For quantitative studies, GFAP^{+} astrocytes were classified into two morphological phenotypes: the type 1 astrocytes were polygonal-shaped with few evident projections; while the type 2 astrocytes were highly stellated and elongated astrocytes (**Figure 1B**). **Figure 1C** and **Supplementary Figure S1A** show the increased abundance of the type 2 phenotype at different time points after LPS stimulus in GMC but not in microglia-depleted AEC.

In GMC cultures, microglia also responded to LPS with morphological changes, as evidenced by an increased proportion of ameboid (Caldeira et al., 2014) and large-size cells. To quantify the changes in the microglial phenotype, a morphological classification of five phenotypes was used (**Figure 1D**). Small bright and roundish microglial cells were observed under control conditions, and a 24 h LPS exposure induced rapid cytoplasmic remodeling of rounded microglia to adopt a highly filamentous phenotype (**Figures 1A,E** and **Supplementary Figure S1B**). Notably, LPS did not induce a statistically significant change in the total cell number, nor in the proportion between astrocytes, microglia, and the total cell number in GMC or AEC (**Supplementary Figures S1C–E**).

In all cases for AEC, the abundance of microglial cells was below 1%. Most imaged fields did not show any microglial cells, and some others showed very low counts (up to four cells). No evident phenotypic changes were observed in the very few Iba-1^{+} cells that remained in AEC, even under LPS exposure. However, microglial morphologies did not enter the classification used in GMC, showing already different basal morphological control conditions. These findings might suggest not only a microglial to astroglial interaction as described by Liddelow et al. (2017) but also a bidirectional communication between astrocytes and microglia to achieve morphological changes in response to LPS, probably through the release of soluble mediators such as C3, as already suggested (Lian et al., 2016).

We conclude that the astroglial phenotype changes dramatically in response to LPS only in the presence of microglia. Such changes start 24 h after exposure and gradually increase until 72 h after exposure. We then asked whether such a morphological phenotype correlates with the expression of genes related to the pro-inflammatory gain of function. mRNA analysis of pro-inflammatory genes showed an increase in the expression of IL-1β and C3, both markers of reactive and pro-inflammatory astroglia (**Figures 1F,G**). Taken together, astrocytes from GMC become reactive in response to LPS in the presence of microglia, showing features of a pathological remodeling with pro-inflammatory gain of function. The activation of C3 expression is not surprising in light of the finding that the C3 promoter has putative NF-κB binding sites (Lian et al., 2015). Furthermore, astrocytic C3 released to the extracellular space signals to neurons and microglia, mediating death and activation, respectively (Lian et al., 2015; Lian et al., 2016). In agreement, we have already reported that LPS (25 ng/ml)-treated GMC becomes neurotoxic to primary cortical neurons (Rosciszewski et al., 2019). Surprisingly, astrocytes in AEC showed a minor morphological response to LPS but a prominent increase in IL-1β expression, as assessed by RT-PCR. These results reinforce the idea that only a minor proportion of microgliocytes (less than 1%) are enough to provide the TLR4 receptor to subsequently induce the activation of neighboring astrocytes in the culture.

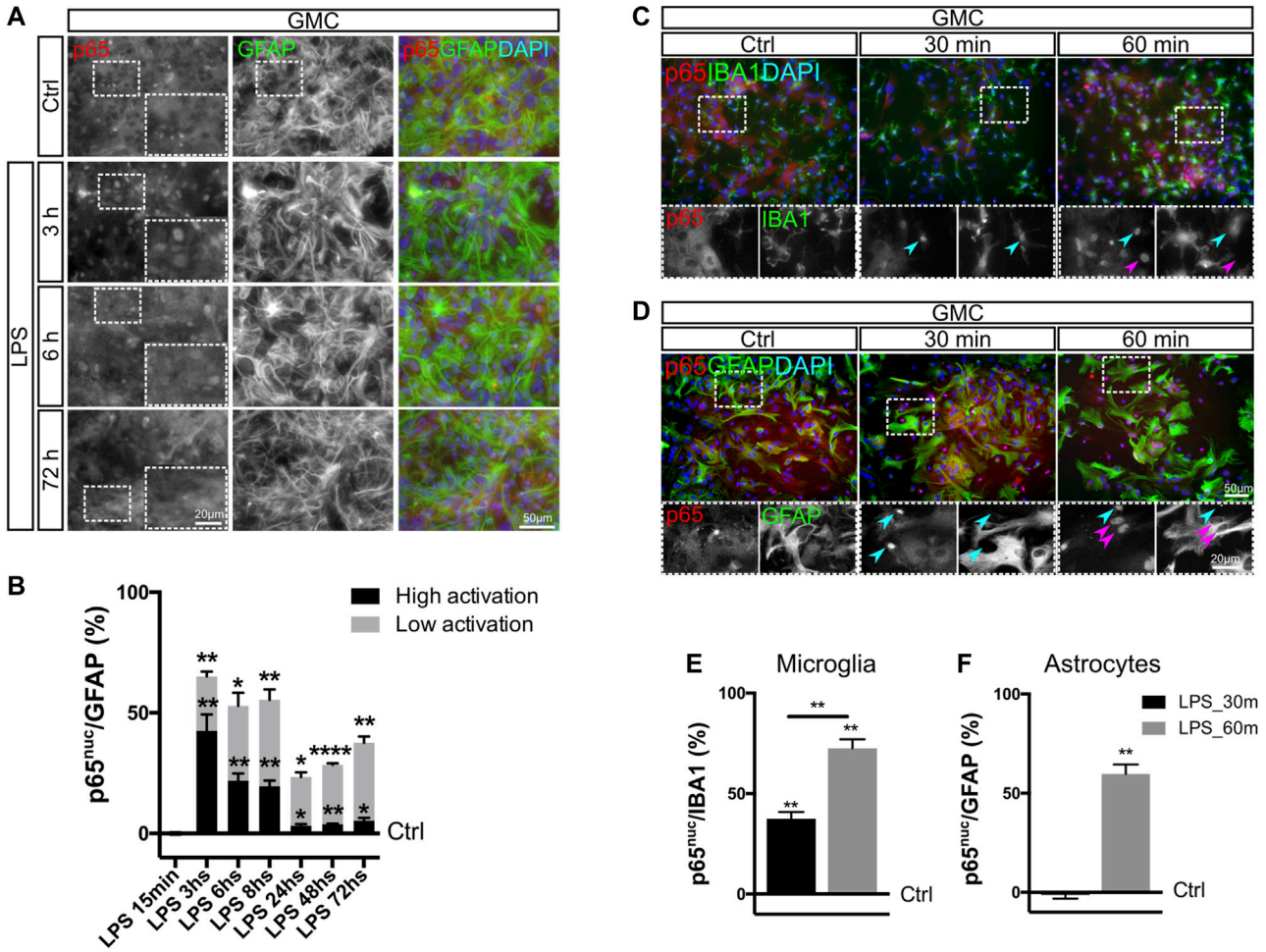

FIGURE 2 | NF-κB activation in microglia occurs faster than in astrocytes. **(A)** Glial mixed cultures (GMCs) were incubated with LPS during the indicated time points in reduced-serum medium. To analyze NF-κB activation in astrocytes in response to LPS, we performed double immunofluorescence staining for GFAP and p65, determining the nuclear p65 localization ($p65^{nuc}$). **(B)** Graph showing the proportion of $GFAP^{+}/p65^{nuc}$ cells from the total GFAP-positive cells after subtracting the percentage of $GFAP^{+}/p65^{nuc}$ under control conditions (Ctrl = 0). Bars show the mean percentage of three to four biological replicates with the SEM. Low activation corresponds to $GFAP^{+}$ astrocytes, in which $p65^{nuc}$ and cytoplasmic p65 ($p65^{cyt}$) staining was homogeneous. High activation corresponds to $GFAP^{+}$ astrocytes with distinguishable $p65^{nuc}$ staining. Each time point was compared to the respective control (no LPS) using one-sample *t*-test with the statistical significance represented as $^{*}p < 0.05$, $^{**}p < 0.01$, or $^{****}p < 0.0001$; $n = 3$–4. **(C, D)** Glial mixed cultures (GMCs) were incubated with LPS during the indicated time points in reduced-serum medium. To address $p65^{nuc}$ in microglia and astrocytes in response to LPS, we performed double immunofluorescence staining for Iba-1 and p65 **(C)** or GFAP and p65 **(D),** respectively. **(E)** Graph showing the proportion of $Iba\text{-}1^{+}/p65^{nuc}$–positive cells from the total Iba-1–positive cells after subtracting the percentage of $Iba\text{-}1^{+}/p65^{nuc}$ under control conditions (Ctrl = 0). Each time point was compared to the respective control (no LPS) using one-sample *t*-test with the statistical significance represented as $^{**}p < 0.01$; n = 3. Comparison between treatments (time points) was conducted using Student's t-test with the statistical significance represented as $^{**}p < 0.01$; $n = 3$. **(F)** Graph showing the percentage of $GFAP^{+}/p65^{nuc}$-positive cells from the total GFAP-positive cells after subtracting the percentage of $GFAP^{+}/p65^{nuc}$ from the control (Ctrl=0). Each time point was compared to the respective control (no LPS) using one-sample *t*-test with the statistical significance represented as $^{**}p < 0.01$; $n = 3$.

Long-Lasting NF-κB Activation in Astrocytes

It has been previously shown by us and others that the NF-κB pathway mediates astrocytic pro-inflammatory gain of function (Lian et al., 2015; Rosciszewski et al., 2019). However, NF-κB activation is usually studied only during a short time period after stimulation. We next explored in detail the profile of NF-κB pathway activation in astrocytes and microglia following LPS exposure.

Keeping in mind that astrocytic phenotypic changes are still visualized after 72 h of LPS exposure, we then asked whether NF-κB was still active at that time point. For that purpose, we assessed the nuclear localization of the p65 subunit as a parameter of NF-κB activation (Villarreal et al., 2014) in GMC exposed to LPS. Using a reduced-serum medium allowed us to initiate these experiments with a low basal NF-κB activity, with less than 0.5% of astrocytes showing nuclear p65 ($p65^{nuc}$) under control conditions and most cells having a clear negative nuclear staining (**Figures 2A,D**).

When analyzing cells with active NF-κB, we defined two levels of staining: *high activation*, corresponding to clear nuclear staining, and *low activation*, corresponding to homogeneous

nuclear and cytoplasmic staining (non-negative nuclei) (**Supplementary Figure S2B**). Independently of the level of activation, graphs also indicate the total percentage of astrocytes with $p65^{nuc}$ staining. The analysis of the time-course experiments showed that nuclear staining in astrocytes remains negative for 30 min (**Supplementary Figure S2A**) and becomes positive at 1 h of LPS exposure (**Figures 2A,B**). Specifically, we have observed that NF-κB in astrocytes shows an initial pattern of high activation (3–8 h), which is then replaced by a pattern of low but persistent activation at 24, 48, and 72 h (**Figure 2B**). We conclude that LPS exposure induces a long-lasting NF-κB activation in astrocytes when a significant amount of microglial cells is present in the culture.

NF-κB Activation in Microglia Precedes NF-κB Activation in Astrocytes

Liddelow and colleagues (2017) demonstrated in a model of *in vivo* neonatal LPS injection that astrocyte conversion to the neurotoxic phenotype, which includes C3 expression, is microglia-dependent, suggesting that microglia are first responders to the pro-inflammatory stimulus. We explored if this response includes a faster NF-κB activation in microglia by following the dynamics of NF-κB activation in astrocytes and microglia from GMC. Using double immunofluorescent staining for Iba-1/$p65^{nuc}$ and GFAP/$p65^{nuc}$ at 30 and 60 min after LPS stimulus in microglia and astrocytes, respectively, we observed that microglia were fast responders to LPS, with $p65^{nuc}$ staining significantly increasing already after 30 min of LPS exposure, while astrocytes required at least 60 min to reach a similar response (**Figures 2C–F**).

We concluded that NF-κB pathway activation after LPS exposure in mixed glial culture occurs sequentially, initially in microglia and then in astrocytes. This result is in line with previous findings showing that LPS-induced astroglial pro-inflammatory gain of function depends on the initial TLR4-mediated microglia activation (Liddelow et al., 2017). Taken together, our results indicate that the initial activation of microglia includes NF-κB activation and might represent a key step in crosstalk initiation following a pro-inflammatory stimulus.

Microglia Abundance Determines Initial NF-κB Activation in Astrocytes

We noticed in our experimental model using AEC that LPS-induced NF-κB activation in astrocytes at 1 h is lower than that for astrocytes in GMC. This may suggest that at least for this initial time point, p65 nuclear translocation depends on the presence of microglia. We then asked whether the increasing microglia abundance in AEC cultures could modulate NF-κB activation. With this aim, we reconstituted AEC cultures by adding primary microglia, achieving an increase in the mean abundance of Iba-1 positive cells in 5% steps (going from 5 to 10%) (**Supplementary Figures S3A,B**). Using this paradigm, we observed that this 5% increase in microglia abundance promoted a 40% increase in the amount of astrocytes showing active NF-κB at 60 min after LPS exposure, as assessed by $p65^{nuc}$ staining (**Figures 3A,B**). It is interesting to note that the addition of microglia did not accelerate the astroglial response to LPS at 30 min but increased the amount of astrocytes showing a significant NF-κB activation at 60 min (**Figure 3B**). Detailed images of these reconstituted glial cultures showed an initial NF-κB activation in astrocytes acquiring a *cluster-like* staining (**Supplementary Figure S3C**).

We compiled data from four different experiments and plotted the ratio of astrocytes with nuclear p65 staining ($GFAP^+/p65^{nuc}$) 60 min after LPS exposure vs. abundance of Iba-1^+ microglia in culture and observed a clear positive correlation between both variables. As shown in **Figure 3C**, when the microglia abundance is lower than 1%, the proportion of $GFAP^+/p65^{nuc}$ cells is close to 0.5%. Increasing the microglial abundance to 5% microglia leads to a mean of 20% $GFAP^+/p65^{nuc}$ and 10% leads to above 50% of $GFAP^+/p65^{nuc}$ astrocytes. The 20% microglia corresponds to the abundance in GMC, and this level increases NF-κB activation up to a mean of 60% $GFAP^+/p65^{nuc}$ (**Figure 3C**).

We conclude that the abundance of microglia in the culture conditions the strength of the initial NF-κB activation in astrocytes, but it does not affect the speed of the initial NF-κB activation. It is worth noticing that *in vivo*, the number of microglial cells may remain constant for a short period of time, but then, microglial clone expansion may, in turn, affect astroglial reactivity.

NF-κB Initial Activation in Astrocytes Depends on Microglial Soluble Factors

In GMC, microglia and astrocytes are in direct physical contact. We next address whether physical contact between microglia and astrocytes was necessary to trigger the initial p65 nuclear translocation induced by LPS exposure. With this aim, we exposed purified microglia to LPS for 60 min and collected the conditioned medium. Microglia activation was confirmed by immunofluorescent double staining for Tomato Lectin/$p65^{nuc}$ (**Figure 3D**). We then exposed microglia-depleted AEC to microglia-conditioned medium and analyzed the NF-κB activation by quantifying the $GFAP^+/p65^{nuc}$ cells after 30 and 60 min of incubation. We observed a significant increase in the $GFAP^+/p65^{nuc}$ cells at both time points, it being higher at 60 min for astrocytes exposed to microglia-conditioned medium (**Figures 3E,F**). Although at 30 min the response was very low (below 3% on average), it was consistent across the biological replicates, again showing this intriguing delay in NF-κB activation in astrocytes. It is important to notice that these AECs are depleted from microglia, and consequently, they do not respond to LPS in terms of nuclear p65 (**Supplementary Figures S3D,E**).

We concluded that the initial NF-κB activation is triggered by soluble factors released from the microglia and does not require physical contact between astrocytes and microglia.

Chromatin Remodeling in Astrocytes is Microglia-Dependent

After engaging in cellular crosstalk with LPS-treated microglia, astrocytes change their phenotype toward a reactive and pro-

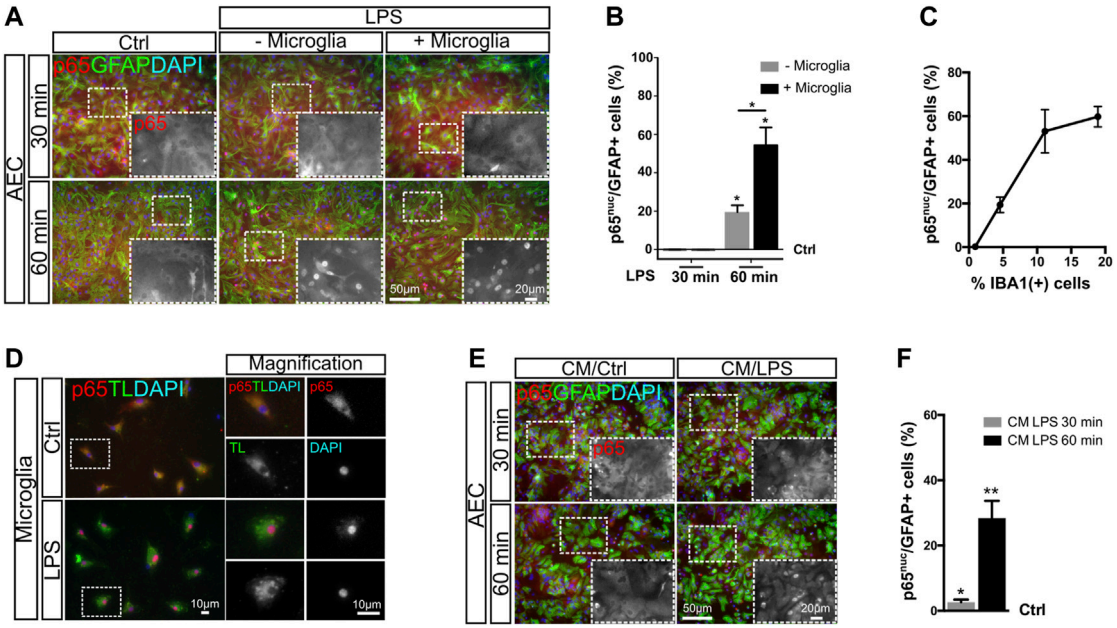

FIGURE 3 | NF-κB initial activation in astrocytes depends on microglial soluble factors. **(A)** Astrocyte-enriched cultures (AECs) or microglia-reconstituted AEC (+microglia) were incubated with LPS during the indicated time points in reduced-serum medium. To analyze NF-κB activation in astrocytes in response to LPS, we performed double immunofluorescence staining for GFAP and p65, determining the nuclear p65 localization ($p65^{nuc}$). **(B)** Graph showing the percentage of $GFAP^+/p65^{nuc}$-positive cells from the total GFAP-positive cells after subtracting the percentage of $GFAP^+/p65^{nuc}$ from the control (Ctrl = 0). Each time point was compared to the respective control (no LPS) using one-sample *t*-test with the statistical significance represented as $^*p < 0.05$; $n = 3$. Comparisons between treatments were conducted using Student's t-test with the statistical significance represented as $^*p < 0.05$; $n = 3$. **(C)** Graph showing the proportion of $GFAP^+/p65^{nuc}$-positive cells plotted against the abundance of Iba-1^+ cells from different experiments. Each dot corresponds to a different experiment and represents the mean of 3 different cultures. **(D)** Isolated microglia was incubated for 1 h with LPS in reduced-serum medium to obtain microglia-conditioned medium. To analyze NF-κB activation in isolated microglia in response to LPS, we performed double staining for FITC–tomato lectin and p65, determining the nuclear p65 localization ($p65^{nuc}$). **(E)** Astrocyte-enriched cultures (AECs) with 1 h LPS-stimulated microglia-conditioned medium during the indicated time points. To analyze NF-κB activation in astrocytes in response to LPS, we performed double immunofluorescence staining for GFAP and p65, determining the nuclear p65 localization ($p65^{nuc}$). **(F)** Graph showing the percentage of $GFAP^+/p65^{nuc}$-positive cells from the total GFAP-positive cells in CM-exposed astrocytes after subtracting the percentage of $GFAP^+/p65^{nuc}$ from the control (Ctrl=0). Each time point was compared to the respective control (no LPS) using one-sample *t*-test with the statistical significance represented as $^*p < 0.05$, $^{**}p < 0.01$; $n = 6$.

inflammatory state. This was evidenced by morphological changes, activation of NF-κB, and expression of pro-inflammatory genes. Such a phenotype remains stable for at least 72 h after LPS exposure, a time point after the initial peak of NF-κB activation (**Figures 1**, **2**). NF-κB is known to promote histone acetylation (Berghe et al., 1999; Mukherjee et al., 2013), and it is widely accepted that histone acetylation promotes an active state of the chromatin. Given that astrocyte phenotypic changes correlate with major changes in gene expression, we then asked whether this is reflected in global changes of histone acetylation. We also asked if those possible changes were, as are NF-κB activation and phenotype conversion, microglia-dependent.

With this aim, we treated AEC and GMC with LPS and monitored histone 3 acetylation (H3Ac) intensity in astrocytes by conducting double immunofluorescent staining for GFAP and H3K9K14ac. Notably, we observed a significant increase in H3K9K14ac intensity after 24 h in astrocytes only in the presence of microglia (**Figures 4A,B**). Furthermore, the increase in H3K9K14ac intensity in astrocytes remained for at least 72 h (**Figures 4C,D**).

It should be highlighted that the LPS-mediated increased H3K9K14ac fluorescence intensity appears to be highly heterogeneous within the astroglial population, with a subpopulation of astrocytes shifting toward an increase in H3K9K14ac intensity. Overall, our results indicate an increase in global histone acetylation in LPS-induced reactive astrocytes. Interestingly, H3K9K14ac has been previously associated with p65 occupancy at regulatory regions (Federman et al., 2013).

Next, we studied H3K27ac mark, which has been linked to p300 acetyltransferase activity (Weinert et al., 2018). This enzyme is a known interaction partner of the p65 NF-κB subunit in the regulation of pro-inflammatory genes (Berghe et al., 1999). We therefore analyzed the levels of H3K27ac in astrocyte nuclei after LPS exposure and observed that the global intensity of H3K27ac slightly increased after 24 h (**Figures 5A,B**). Increased transcriptional activity is usually accompanied by decreased repressive marks such as H3K9me3, a mark for heterochromatin (Becker et al., 2016). Using the same experimental approach, we addressed H3K9me3 intensity in astrocytes by conducting double immunofluorescent stainings for GFAP and H3K9me3. Interestingly, we observed a transient but significant decrease in

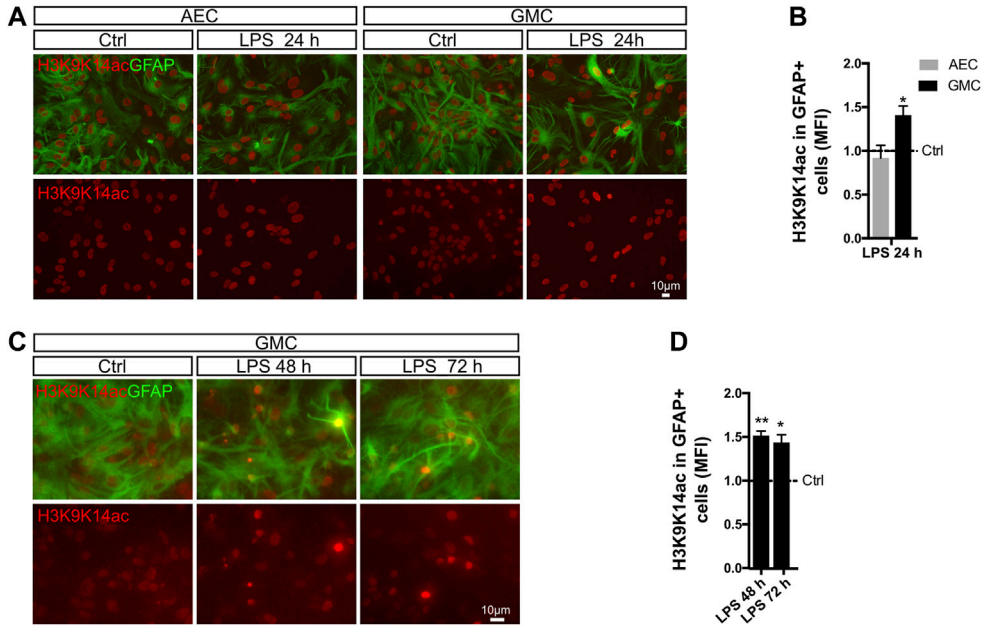

FIGURE 4 | Histone acetylation in astrocytes is microglia-dependent. **(A)** Astrocyte-enriched cultures (AECs) or glial mixed cultures (GMCs) were incubated with LPS for 24 h in reduced-serum medium. To address changes in the global levels of histone 3 acetylation in astrocytes in response to LPS, we performed double immunofluorescence staining for GFAP and acetylated lysins 9 and 14 of histone 3 (H3K9K14ac). **(B)** Graph showing the mean fluorescence intensity (MFI) for H3K9K14ac in the nuclei of GFAP-positive cells after normalizing to the control (Ctrl = 1). Each time point was compared to the respective control (no LPS) using one-sample *t*-test with the statistical significance represented as $^{*}p < 0.05$. $n = 3$–6. **(C)** Glial mixed cultures (GMCs) were incubated with LPS during the indicated time points in reduced-serum medium. To address changes in the global levels of histone 3 acetylation in astrocytes in response to LPS, we performed double immunofluorescence staining for GFAP and acetylated lysins 9 and 14 of histone 3 (H3K9K14ac). **(D)** Graph showing the mean fluorescence intensity (MFI) for H3K9K14ac in the nuclei of GFAP-positive cells after normalizing to the control (Ctrl = 1). Each time point was compared to the respective control (no LPS) using one-sample *t*-test with the statistical significance represented as $^{*}p < 0.05$, $^{**}p < 0.01$; $n = 3$.

the levels of H3K9me3 intensity after 48 h in astrocytes from GMC, which recovered control values by 72 h (**Figures 5C,D**).

We conclude that exposure to LPS triggers global long-term changes in H3Ac and temporal changes in H3K27ac and H3K9me3 in astrocytes when microglia is available. A global increase in histone acetylation together with dynamic changes of specific epigenetic marks might indicate actual chromatin reconfiguration in astrocytes that are engaged in a pro-inflammatory gain of function after LPS exposure.

Brain Injury Promotes Chromatin Remodeling in Reactive Astrocytes

Long-lasting astroglial phenotypical remodeling is a hallmark of focal brain injury. Focal brain ischemia in rodents reproduces several features of human ischemic brains, with extended reactive gliosis and a prominent ischemic core surrounded by penumbra (Aviles-Reyes et al., 2010; Villarreal et al., 2011, 2016). Reactive astrogliosis rapidly occurs, and NF-κB activation has been evidenced in the tissue surrounding the ischemic core, giving rise to the pro-inflammatory gain of function in a subset of the astroglial population (Rosciszewski et al., 2017) that is notably stable even when cultured *ex vivo* (Villarreal et al., 2016). Based on these reports and the present findings, we explored if the chromatin remodeling events that we described *in vitro* for mixed glial cultures were also present *in vivo* in an experimental model of brain ischemia by cortical devascularization. For that purpose, we subjected animals to the pial disruption model that produces a cortical devascularizing lesion (Aviles-Reyes et al., 2010; Villarreal et al., 2011; Villarreal et al., 2016). As shown in **Figure 6**, we observed at 4 days post-lesion that there were an increased abundance of the epigenetic mark H3K27ac and a decrease in H3K9me3 mark, specifically in $GFAP^{+}$ astrocytes from the ischemic penumbra, in all analyzed animals when compared to the uninjured hemisphere (**Figures 6A–C**). We also analyzed the histone modification intensity in all nuclei and found, for both marks, a slight decrease in abundance (**Figure 6C**). We then calculated the net amount of change in histone modification in $GFAP^{+}$ cells by normalizing this value to total intensity. Results showed that H3K27ac in astrocytes was significantly increased, while H3K9me3 did not change (**Figure 6D**). This suggests that the H3K27ac increase is astrocyte-specific and is a penumbra-associated phenomenon *in vivo* (**Figure 6E**).

We conclude that chromatin remodeling events are a common feature that reactive astrocytes exhibit, both *in vitro* and *in vivo*.

DISCUSSION

Reactive astrogliosis is a generic response of astrocytes triggered by different types of CNS injuries. After decades of conflicting

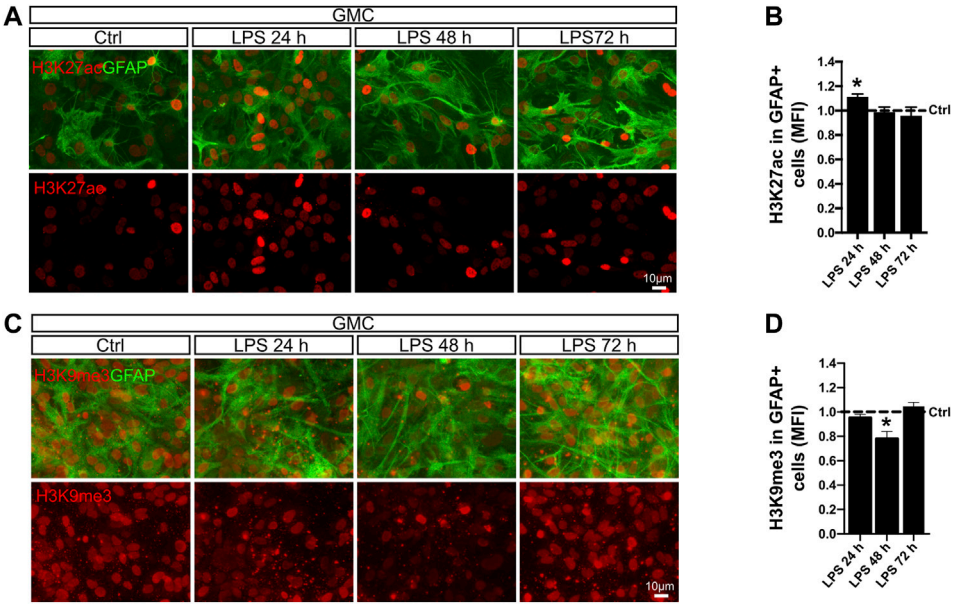

FIGURE 5 | LPS promotes global chromatin remodeling in astrocytes in a time-dependent manner. **(A)** Glial mixed cultures (GMCs) were incubated with LPS during the indicated time points in reduced-serum medium. To address changes in histone 3 acetylation at lysin 27 (H3K27ac) in astrocytes in response to LPS, we performed double immunofluorescence staining for GFAP and H3K27ac. **(B)** Graph showing the mean fluorescence intensity (MFI) for H3K27ac in the nuclei of GFAP-positive cells after normalizing to the control (Ctrl = 1). Each time point was compared to the respective control (no LPS) using one-sample *t*-test with the statistical significance represented as $^*p < 0.05$; $n = 3$. **(C)** Glial mixed cultures (GMCs) were incubated with LPS during the indicated time points in reduced-serum medium. To address changes in trimethylated histone 3 lysin 9 (H3K9me3), immunofluorescence staining for GFAP and H3K9me3 was performed. **(D)** Graph showing the mean fluorescence intensity (MFI) for H3K9K9me3 in the nuclei of GFAP-positive cells after normalizing to the control (Ctrl = 1). Each time point was compared to the respective control (no LPS) using one-sample t-test with the statistical significance represented as $^*p < 0.05$, $n = 4$.

reports attributing beneficial or detrimental effects, results from the last decade obtained using transcriptomic approaches have shown that reactive gliosis is a complex phenomenon that involves astroglial remodeling and deleterious effects occurring when astrocytes lose their homeostatic features and/or suffer a pro-inflammatory gain of function (Zamanian et al., 2012; Anderson et al., 2016; Escartin et al., 2021). Once initiated by diffuse or focal injury, reactive astrogliosis becomes stable over time with glial scar formation (Sofroniew, 2009; Orr and Gensel, 2018) or *ex vivo* cultures of reactive astrocytes being exquisite examples of such stability (Díaz-Amarilla et al., 2011; Villarreal et al., 2016).

The prominent role of NF-κB in reactive astrogliosis and specifically in astroglial pro-inflammatory gain of function pointed us toward studying the potential chromatin remodeling effects downstream of NF-κB activation. Given the fact that large transcriptomic changes were reported for reactive astrocytes, we here explored, in a global manner, the levels of astrocytic acetylated histone 3 at lysins 9 and 14, which were already linked to NF-κB pathway activation (Federman et al., 2013). We found that astroglial H3K9K14ac levels are elevated after LPS exposure and remain increased for several days only in the presence of microglia. Similarly, H3K27ac showed an acute increase in astrocytes by 24 h after LPS exposure. These results are of significant interest to the current work, since H3K27ac mark is added by acetyltransferase p300, which is in turn a very well-known interaction partner of NF-κB in active regulatory regions (Weinert et al., 2018). It is likely that these activating marks allow the transcription of genes involved in reactive astrogliosis. Interestingly, our present *in vivo* results have shown that these pathways are also active in a model of brain ischemia by pial disruption.

NF-κB–dependent chromatin remodeling is associated with histone acetylation at active transcriptional sites. In addition, H3K9me3, a mark for heterochromatin and transcription silencing (Becker et al., 2016), resulted in temporarily decreased reactive astrocytes being remodeled to the pro-inflammatory gain of function by LPS exposure. Overall, we hypothesize that the increases in activating marks together with a decrease in repressive marks in the same regions allow stable chromatin reconfiguration in reactive astrocytes. Furthermore, homeostatic genes or genes that are not involved in reactive phenotypes are likely to be repressed. This means that while some regions become part of active transcription, others may become repressed. This may explain the fact that the observed changes (H3K27ac and H3K9me3) are temporal, when addressed globally. Future experiments will address such changes on a genome-wide basis at a single-gene resolution.

Interestingly, the presently reported findings, highly indicative of astroglial chromatin remodeling, are paralleled with the expression of pro-inflammatory genes that have been shown to be detrimental for neuronal survival (Rosciszewski et al., 2019). Chromatin remodeling is likely to be occurring in astrocytes during the process of pathological remodeling that

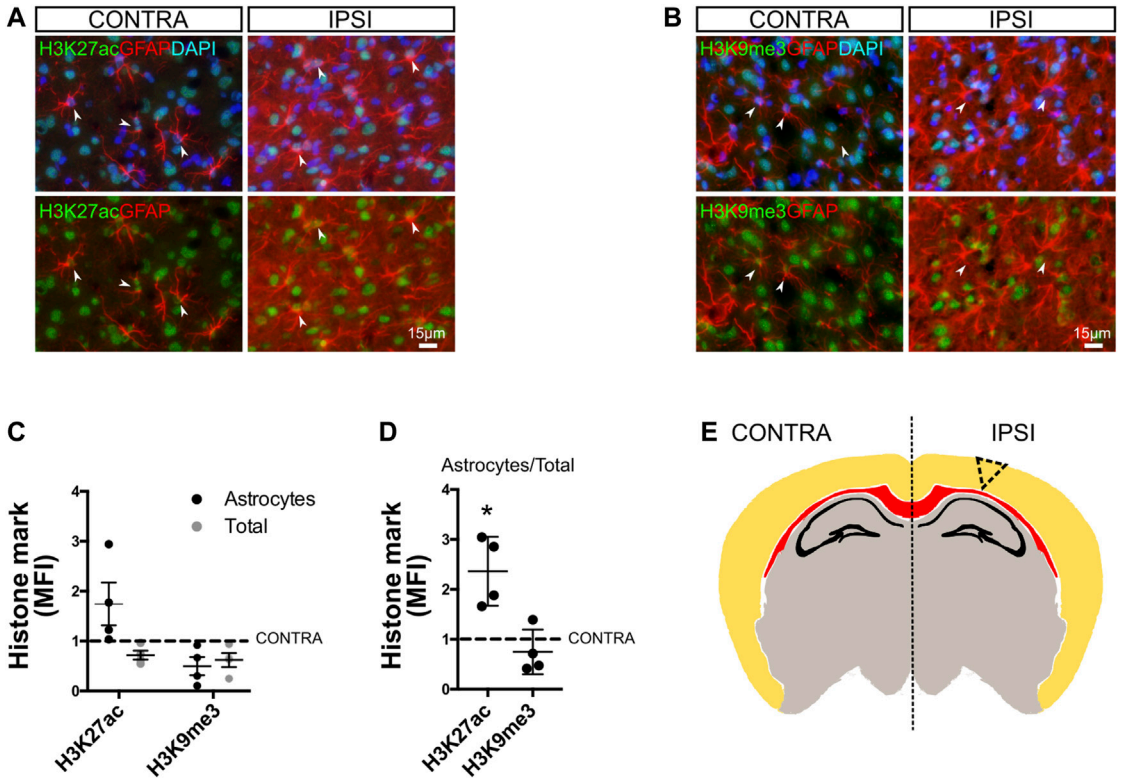

FIGURE 6 | Chromatin remodeling in reactive astrocytes after cortical ischemic injury *in vivo*. **(A)** Brain sections from animals subjected to cortical devascularization were processed for immunofluorescence staining. To address changes in the global levels of H3K27ac in astrocytes in response to damage, we performed double immunofluorescence staining for GFAP and H3K27ac. Images show representative fields of the contralateral (CONTRA) hemisphere and the ipsilateral (IPSI) hemisphere with and without nuclear DAPI counterstaining. The arrowheads indicate representative astrocytes with visible nuclei. Here, GFAP intensity was enhanced using FIJI software to visualize cells, and intensity is not representative of the reactivity state. **(B)** Similar to A, we performed double immunofluorescence staining for GFAP and H3K9me3. **(C)** Graph showing the mean fluorescence intensity (MFI) for H3K27ac and H3K9me3 in the nuclei of GFAP-positive cells (black dots = astrocytes) or in other cell types nuclei (gray dots = total) after normalizing to the control (Ctrl = 1). **(D)** Graph showing the mean fluorescence intensity (MFI) for H3K27ac and H3K9me3 in the nuclei of GFAP-positive cells relative to the total nuclei and after normalizing to the control (Ctrl = 1). Average from the hemisphere of one animal was compared to the respective contralateral hemisphere (CONTRA) using one-sample t-test with the statistical significance represented as $^*p < 0.05$, n = 4. **(E)** Schematic representation of a coronal section from a murine brain indicating the site of the cortical lesion (triangle dotted lines). The corpus callosum is shown in red and the hippocampal pyramidal cell layer and dentate gyrus are shown in black.

leads to the pro-inflammatory gain of function induced by LPS exposure (**Figure 7**).

Our results also provide new evidence with regard to microglia–astrocyte crosstalk under inflammatory conditions induced by exposure to a powerful pro-inflammatory molecule such as bacterial LPS. First, we show that NF-κB activation in microglia precedes NF-κB activation in astrocytes. It has been stated that microglia mediates astroglial pro-inflammatory conversion, leading to the idea of temporal causality between the responses of both cell types (Liddelow et al., 2017). However, to the best of our knowledge, this was never shown in terms of NF-κB activation. Our present results provide an interesting insight in terms of the temporal activation of the NF-κB pathway in the different glial cell types. Obvious candidates for this initial fast microglial response are the pattern recognition receptors (PRRs) of the toll-like receptor family, specifically TLR4, which is the prototypical LPS receptor expressed in microglia. We further described that astrocyte initial NF-κB activation, and not just activation strength, is microglia-dependent. Direct contact between microglia and astrocytes might have a role in astrocyte initial activation; however, our results suggest that microglia signaling to astrocytes under these conditions is mediated by soluble factors, which is in agreement with previous results produced by Liddelow et al. (2017). As expected, the concentration threshold of soluble factors probably depends on the amount of microglia in culture; thus, the astroglial response is more intense when increasing the microglial cell number. Moreover, the fact that astrocytes respond to conditioned medium already at 30 min suggests that the required 60 min period in GMC is crucial for the release of soluble factors from the microglia. Taken together, our results indicate that astrocytes might not be able to initially respond to LPS in the absence of microglial soluble factors, but after the initial stimulation, cell-autonomous mechanisms prevail, and astrocytes follow the reactive gliosis gene expression program. The identity of the soluble factors released by microglia was partially revealed in previous works that determined that IL-1α, TNFα, and C1q are involved in

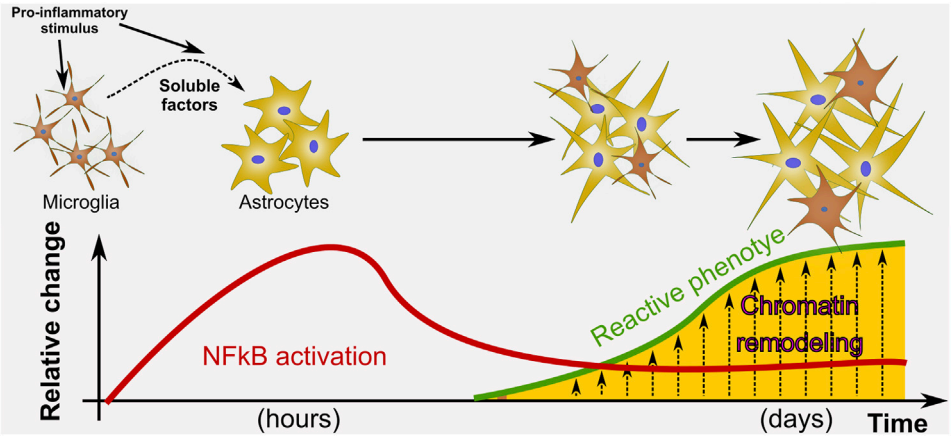

FIGURE 7 | Proposed model of astrocyte phenotype conversion. We propose a model in which a pro-inflammatory stimulus such as LPS activates NF-κB in astrocytes and promotes pathological remodeling of reactive astrocytes with pro-inflammatory gain of function only when microglia is present. In our *in vitro* paradigm, cell-to-cell communication to activate NF-κB nuclear translocation does not depend on physical contact with microglia but on the release of soluble factors. We propose that after NF-κB initial activation, the astrocyte reactive phenotype is sustained by epigenetic changes at the chromatin level.

microglia-dependent astrocytic activation in rodent glia or in human induced pluripotent stem cell–derived astrocytes (Liddelow et al., 2017; Santos et al., 2017). However, it still remains to be determined if these cytokines are able to activate the full downstream epigenetic remodeling presently described following the pro-inflammatory gain of function induced by LPS. Our group will address this topic in future studies.

Although most of the attention has been focused on microglial to astroglial communication, astrocytes are also able to signal to microglia, propagating the inflammatory response in time and space. Particularly, pro-inflammatory astrocytes show increased C3 expression, which is released to the extracellular space (Liddelow et al., 2017), C3 being another NF-κB–dependent gene and having microglia C3R on its membrane (Lian et al., 2015). In agreement, we found that LPS-exposed astrocytes induced C3 gene expression and that microglial cells from GMC but not from AEC showed profound morphological alterations following LPS exposure. This might be indicating that microglia also require astrocyte activation in order to become pro-inflammatory.

Histone acetylation is a promising pharmacological target to modulate gene transcription of cells in pathological contexts, and great advances have been made in the cancer research field, producing a large number of compounds that can be repurposed for developing new treatment strategies (Hontecillas-Prieto et al., 2020). The use of HDAC inhibitors has been generically proposed to modulate the neuroinflammatory response (Chuang et al., 2009; Durham et al., 2017; Yang et al., 2017; Neal and Richardson, 2018); however, even if HDAC inhibition results in a global anti-inflammatory effect, a more detailed analysis clearly depicting the effects in the different cell types of the neurovascular unit is still pending. Additionally, molecular targets are not always clearly defined for these drugs, since modifications of HDAC non-histone targets are also being modulated by these approaches (Glozak et al., 2005; Singh et al., 2010). Furthermore, commonly used HDAC inhibitors like VPA are also known to have several non-HDAC targets (Soria-Castro et al., 2019). This last issue has led to the design of novel and improved HDAC inhibitors (Yang et al., 2017; Ziemka-Nalecz et al., 2018).

In summary, our results show that NF-κB activation in microglia precedes NF-κB engagement in astrocytes when cells are exposed to LPS. Microglia abundance is relevant for initial NF-κB activation in astrocytes, and soluble factors seem to be essential for this crosstalk. Microglia is also required for promoting chromatin remodeling events in astrocytes that are concomitant with increased pro-inflammatory cytokine expression and neurotoxic effects, both features of the pathological remodeling with pro-inflammatory gain of function. *In vivo* experimental ischemia also shows the activation of this downstream NF-κB signaling pathway and chromatin remodeling events in reactive astrocytes from the ischemic penumbra. Taken together, these results strongly suggest that microglia is not only required for astrocyte initial activation and acquisition of a pro-inflammatory phenotype but also for sustaining astrocyte phenotypic pathological remodeling with pro-inflammatory gain of function through mechanisms of chromatin remodeling. The identification of this new potential pharmacological target to control pathological astroglial remodeling opens a new avenue for future therapeutic research in CNS diseases where the detrimental role of astrocytic pro-inflammatory conversion has been evidenced.

DATA AVAILABILITY STATEMENT

The original contributions presented in the study are included in the article/**Supplementary Material**; further inquiries can be directed to the corresponding authors.

ETHICS STATEMENT

The animal study was reviewed and approved by the CICUAL Committee of the School of Medicine, University of Buenos Aires.

AUTHOR CONTRIBUTIONS

AR and AV conceived the project, designed the experiments, analyzed the data, interpreted and discussed results, and wrote the manuscript. AV, CV, MB, and MC designed the experiments, carried out the experimental work and analysis, discussed the results, and revised the manuscript.

FUNDING

ISN-CAEN_2020. Educational Grants, Category B (AV). AP-Biotech_2019 (AV). PICT-2018-0920 (AV); PICT 2017-2203 (AJR); UBACYT (AJR); PIP CONICET 479 (AJR). CV is an undergrad fellow of UBACYT. MC is a doctoral fellow of UBACYT; AV and AR are researchers from CONICET.

ACKNOWLEDGMENTS

We thank Biot. Andrea Pecile and Marianella Ceol for the animal care, Lic. Nerina Villalba for her assistance with the IX-83 microscope, and Bioq. Carla Bonavita for proofreading the manuscript.

SUPPLEMENTARY MATERIAL

The Supplementary Material for this article can be found online at: https://www.frontiersin.org/articles/10.3389/fphar.2021.689346/full#supplementary-material

REFERENCES

Anderson, M. A., Ao, Y., and Sofroniew, M. V. (2014). Heterogeneity of Reactive Astrocytes. *Neurosci. Lett.* 565, 23–29. doi:10.1016/j.neulet.2013.12.030

Anderson, M. A., Burda, J. E., Ren, Y., Ao, Y., O'Shea, T. M., Kawaguchi, R., et al. (2016). Astrocyte Scar Formation Aids central Nervous System Axon Regeneration. *Nature* 532, 195–200. doi:10.1038/nature17623

Angelo, M. F., Aguirre, A., Avilés Reyes, R. X., Villarreal, A., Lukin, J., Melendez, M., et al. (2014). The Proinflammatory RAGE/NF-κB Pathway Is Involved in Neuronal Damage and Reactive Gliosis in a Model of Sleep Apnea by Intermittent Hypoxia. *PLoS ONE* 9, e107901, doi:10.1371/journal.pone.0107901

Aviles-Reyes, R. X., Angelo, M. F., Villarreal, A., Rios, H., Lazarowski, A., and Ramos, A. J. (2010). Intermittent Hypoxia during Sleep Induces Reactive Gliosis and Limited Neuronal Death in Rats: Implications for Sleep Apnea. *J. Neurochem.* 112, 854–869. doi:10.1111/j.1471-4159.2009.06535.x

Barres, B. A. (2008). The Mystery and Magic of Glia: A Perspective on Their Roles in Health and Disease. *Neuron* 60, 430–440. doi:10.1016/j.neuron.2008.10.013

Becker, J. S., Nicetto, D., and Zaret, K. S. (2016). H3K9me3-Dependent Heterochromatin: Barrier to Cell Fate Changes. *Trends Genet.* 32, 29–41. doi:10.1016/j.tig.2015.11.001

Berghe, W. V., De Bosscher, K., Boone, E., Plaisance, S., and Haegeman, G. (1999). The Nuclear Factor-Kb Engages CBP/p300 and Histone Acetyltransferase Activity for Transcriptional Activation of the Interleukin-6 Gene Promoter. *J. Biol. Chem.* 274, 32091–32098. doi:10.1074/jbc.274.45.32091

Bribian, A., Pérez-Cerdá, F., Matute, C., and López-Mascaraque, L. (2018). Clonal Glial Response in a Multiple Sclerosis Mouse Model. *Front. Cel. Neurosci.* 12. doi:10.3389/fncel.2018.00375

Caldeira, C. u., Oliveira, A. F., Cunha, C., Vaz, A. R., FalcÃ£o, A. S., Fernandes, A., et al. (2014). Microglia Change from a Reactive to an Age-like Phenotype with the Time in Culture. *Front. Cel. Neurosci.* 8, 152. doi:10.3389/fncel.2014.00152

Chuang, D.-M., Leng, Y., Marinova, Z., Kim, H.-J., and Chiu, C.-T. (2009). Multiple Roles of HDAC Inhibition in Neurodegenerative Conditions. *Trends Neurosciences* 32, 591–601. doi:10.1016/j.tins.2009.06.002

Clarke, L. E., and Barres, B. A. (2013). Emerging Roles of Astrocytes in Neural Circuit Development. *Nat. Rev. Neurosci.* 14, 311–321. doi:10.1038/nrn3484

Cregg, J. M., DePaul, M. A., Filous, A. R., Lang, B. T., Tran, A., and Silver, J. (2014). Functional Regeneration beyond the Glial Scar. *Exp. Neurol.* 253, 197–207. doi:10.1016/j.expneurol.2013.12.024

Díaz-Amarilla, P., Olivera-Bravo, S., Trias, E., Cragnolini, A., Martínez-Palma, L., Cassina, P., et al. (2011). Phenotypically Aberrant Astrocytes that Promote Motoneuron Damage in a Model of Inherited Amyotrophic Lateral Sclerosis. *Proc. Natl. Acad. Sci.* 108, 18126–18131. doi:10.1073/pnas.1110689108

Durham, B. S., Grigg, R., and Wood, I. C. (2017). Inhibition of Histone Deacetylase 1 or 2 Reduces Induced Cytokine Expression in Microglia through a Protein Synthesis Independent Mechanism. *J. Neurochem.* 143, 214–224. doi:10.1111/jnc.14144

Escartin, C., Galea, E., Lakatos, A., O'Callaghan, J. P., Petzold, G. C., Serrano-Pozo, A., et al. (2021). Reactive Astrocyte Nomenclature, Definitions, and Future Directions. *Nat. Neurosci.*, 24, 1–14. doi:10.1038/s41593-020-00783-4

Federman, N., de la Fuente, V., Zalcman, G., Corbi, N., Onori, A., Passananti, C., et al. (2013). Nuclear Factor B-dependent Histone Acetylation Is Specifically Involved in Persistent Forms of Memory. *J. Neurosci.* 33, 7603–7614. doi:10.1523/JNEUROSCI.4181-12.2013

Glozak, M. A., Sengupta, N., Zhang, X., and Seto, E. (2005). Acetylation and Deacetylation of Non-histone Proteins. *Gene* 363, 15–23. doi:10.1016/j.gene.2005.09.010

Grunstein, M. (1997). Histone Acetylation in Chromatin Structure and Transcription. *Nature* 389, 349–352. doi:10.1038/38664

Herrera, D. G., and Cuello, A. C. (1992). Glial Fibrillary Acidic Protein Immunoreactivity Following Cortical Devascularizing Lesion. *Neuroscience* 49, 781–791. doi:10.1016/0306-4522(92)90356-7

Hontecillas-Prieto, L., Flores-Campos, R., Silver, A., de Álava, E., Hajji, N., and García-Domínguez, D. J. (2020). Synergistic Enhancement of Cancer Therapy Using HDAC Inhibitors: Opportunity for Clinical Trials. *Front. Genet.* 11. doi:10.3389/fgene.2020.578011

Kirkley, K. S., Popichak, K. A., Afzali, M. F., Legare, M. E., and Tjalkens, R. B. (2017). Microglia Amplify Inflammatory Activation of Astrocytes in Manganese Neurotoxicity. *J. Neuroinflammation* 14, 99. doi:10.1186/s12974-017-0871-0

Lian, H., Litvinchuk, A., Chiang, A. C.-A., Aithmitti, N., Jankowsky, J. L., and Zheng, H. (2016). Astrocyte-Microglia Cross Talk through Complement Activation Modulates Amyloid Pathology in Mouse Models of Alzheimer's Disease. *J. Neurosci.* 36, 577–589. doi:10.1523/JNEUROSCI.2117-15.2016

Lian, H., Yang, L., Cole, A., Sun, L., Chiang, A. C.-A., Fowler, S. W., et al. (2015). Nfκb-Activated Astroglial Release of Complement C3 Compromises Neuronal Morphology and Function Associated with Alzheimer's Disease. *Neuron* 85, 101–115. doi:10.1016/j.neuron.2014.11.018

Liddelow, S. A., Guttenplan, K. A., Clarke, L. E., Bennett, F. C., Bohlen, C. J., Schirmer, L., et al. (2017). Neurotoxic Reactive Astrocytes Are Induced by Activated Microglia. *Nature* 541, 481–487. doi:10.1038/nature21029

Liu, L.-r., Liu, J.-c., Bao, J.-s., Bai, Q.-q., and Wang, G.-q. (2020). Interaction of Microglia and Astrocytes in the Neurovascular Unit. *Front. Immunol.* 11. doi:10.3389/fimmu.2020.01024

Liu, W., Tang, Y., and Feng, J. (2011). Cross Talk between Activation of Microglia and Astrocytes in Pathological Conditions in the central Nervous System. *Life Sci.* 89, 141–146. doi:10.1016/j.lfs.2011.05.011

Marmorstein, R., and Zhou, M.-M. (2014). Writers and Readers of Histone Acetylation: Structure, Mechanism, and Inhibition. *Cold Spring Harbor Perspect. Biol.* 6, a018762. doi:10.1101/cshperspect.a018762

Matejuk, A., and Ransohoff, R. M. (2020). Crosstalk between Astrocytes and Microglia: An Overview. *Front. Immunol.* 11. doi:10.3389/fimmu.2020.01416

Matias, I., Morgado, J., and Gomes, F. C. A. (2019). Astrocyte Heterogeneity: Impact to Brain Aging and Disease. *Front. Aging Neurosci.* 11. doi:10.3389/fnagi.2019.00059

Mukherjee, S. P., Behar, M., Birnbaum, H. A., Hoffmann, A., Wright, P. E., and Ghosh, G. (2013). Analysis of the RelA:CBP/p300 Interaction Reveals its Involvement in NF-Kb-Driven Transcription. *Plos Biol.* 11, e1001647. doi:10.1371/journal.pbio.1001647

Neal, M., and Richardson, J. R. (2018). Epigenetic Regulation of Astrocyte Function in Neuroinflammation and Neurodegeneration. *Biochim. Biophys. Acta (Bba) - Mol. Basis Dis.* 1864, 432–443. doi:10.1016/j.bbadis.2017.11.004

Orr, M. B., and Gensel, J. C. (2018). Spinal Cord Injury Scarring and Inflammation: Therapies Targeting Glial and Inflammatory Responses. *Neurotherapeutics* 15, 541–553. doi:10.1007/s13311-018-0631-6

Pekny, M., Pekna, M., Messing, A., Steinhäuser, C., Lee, J.-M., Parpura, V., et al. (2016). Astrocytes: a central Element in Neurological Diseases. *Acta Neuropathol.* 131, 323–345. doi:10.1007/s00401-015-1513-1

Ramos, A. (2016). Astroglial Heterogeneity: Merely a Neurobiological Question? or an Opportunity for Neuroprotection and Regeneration after Brain Injury? *Neural Regen. Res.* 11, 1739–1741. doi:10.4103/1673-5374.194709

Ramos, A. J., Rubio, M. D., Defagot, C., Hischberg, L., Villar, M. J., and Brusco, A. (2004). The 5HT1A Receptor Agonist, 8-OH-DPAT, Protects Neurons and Reduces Astroglial Reaction after Ischemic Damage Caused by Cortical Devascularization. *Brain Res.* 1030, 201–220. doi:10.1016/j.brainres.2004.10.019

Rosciszewski, G., Cadena, V., Auzmendi, J., Cieri, M. B., Lukin, J., Rossi, A. R., et al. (2019). Detrimental Effects of HMGB-1 Require Microglial-Astroglial Interaction: Implications for the Status Epilepticus -Induced Neuroinflammation. *Front. Cel. Neurosci.* 13, 380. doi:10.3389/fncel.2019.00380

Rosciszewski, G., Cadena, V., Murta, V., Lukin, J., Villarreal, A., Roger, T., et al. (2017). Toll-Like Receptor 4 (TLR4) and Triggering Receptor Expressed on Myeloid Cells-2 (TREM-2) Activation Balance Astrocyte Polarization into a Proinflammatory Phenotype. *Mol. Neurobiol.* 55(5), 3875-3888. doi:10.1007/s12035-017-0618-z

Santello, M., Toni, N., and Volterra, A. (2019). Astrocyte Function from Information Processing to Cognition and Cognitive Impairment. *Nat. Neurosci.* 22, 154–166. doi:10.1038/s41593-018-0325-8

Santos, R., Vadodaria, K. C., Jaeger, B. N., Mei, A., Lefcochilos-Fogelquist, S., Mendes, A. P. D., et al. (2017). Differentiation of Inflammation-Responsive Astrocytes from Glial Progenitors Generated from Human Induced Pluripotent Stem Cells. *Stem Cel Rep.* 8, 1757–1769. doi:10.1016/j.stemcr.2017.05.011

Schindelin, J., Arganda-Carreras, I., Frise, E., Kaynig, V., Longair, M., Pietzsch, T., et al. (2012). Fiji: an Open-Source Platform for Biological-Image Analysis. *Nat. Methods* 9, 676–682. doi:10.1038/nmeth.2019

Singh, B. N., Zhang, G., Hwa, Y. L., Li, J., Dowdy, S. C., and Jiang, S.-W. (2010). Nonhistone Protein Acetylation as Cancer Therapy Targets. *Expert Rev. Anticancer Ther.* 10, 935–954. doi:10.1586/era.10.62

Sofroniew, M. V. (2015). Astrogliosis. *Cold Spring Harb Perspect. Biol.* 7, a020420. doi:10.1101/cshperspect.a020420

Sofroniew, M. V. (2009). Molecular Dissection of Reactive Astrogliosis and Glial Scar Formation. *Trends Neurosciences* 32, 638–647. doi:10.1016/j.tins.2009.08.002

Sofroniew, M. V., and Vinters, H. V. (2010). Astrocytes: Biology and Pathology. *Acta Neuropathol.* 119, 7–35. doi:10.1007/s00401-009-0619-8

Soria-Castro, R., Schcolnik-Cabrera, A., Rodríguez-López, G., Campillo-Navarro, M., Puebla-Osorio, N., Estrada-Parra, S., et al. (2019). Exploring the Drug Repurposing Versatility of Valproic Acid as a Multifunctional Regulator of Innate and Adaptive Immune Cells. *J. Immunol. Res.* 2019, 1–24. doi:10.1155/2019/9678098

Tessarz, P., and Kouzarides, T. (2014). Histone Core Modifications Regulating Nucleosome Structure and Dynamics. *Nat. Rev. Mol. Cel Biol* 15, 703–708. doi:10.1038/nrm3890

Verkhratsky, A., Ho, M. S., Vardjan, N., Zorec, R., and Parpura, V. (2019). General Pathophysiology of Astroglia. *Adv. Exp. Med. Biol.* 1175, 149–179. doi:10.1007/978-981-13-9913-8_7

Villarreal, A., Aviles Reyes, R. X., Angelo, M. F., Reines, A. G., and Ramos, A. J. (2011). S100B Alters Neuronal Survival and Dendrite Extension via RAGE-Mediated NF-Kb Signaling. *J. Neurochem.* 117, 321–332. doi:10.1111/j.1471-4159.2011.07207.x

Villarreal, A., Rosciszewski, G., Murta, V., Cadena, V., Usach, V., Dodes-Traian, M. M., et al. (2016). Isolation and Characterization of Ischemia-Derived Astrocytes (IDAs) with Ability to Transactivate Quiescent Astrocytes. *Front. Cel. Neurosci.* 10, 139. doi:10.3389/fncel.2016.00139

Villarreal, A., Seoane, R., González Torres, A., Rosciszewski, G., Angelo, M. F., Rossi, A., et al. (2014). S100B Protein Activates a RAGE-dependent Autocrine Loop in Astrocytes: Implications for its Role in the Propagation of Reactive Gliosis. *J. Neurochem.* 131, 190–205. doi:10.1111/jnc.12790

Voss, A. K., and Thomas, T. (2018). Histone Lysine and Genomic Targets of Histone Acetyltransferases in Mammals. *Bioessays* 40, 1800078, doi:10.1002/bies.201800078

Weinert, B. T., Narita, T., Satpathy, S., Srinivasan, B., Hansen, B. K., Schölz, C., et al. (2018). Time-Resolved Analysis Reveals Rapid Dynamics and Broad Scope of the CBP/p300 Acetylome. *Cell* 174, 231–244. doi:10.1016/j.cell.2018.04.033

Yang, S.-S., Zhang, R., Wang, G., and Zhang, Y.-F. (2017). The Development Prospection of HDAC Inhibitors as a Potential Therapeutic Direction in Alzheimer's Disease. *Transl Neurodegener* 6, 19. doi:10.1186/s40035-017-0089-1

Zamanian, J. L., Xu, L., Foo, L. C., Nouri, N., Zhou, L., Giffard, R. G., et al. (2012). Genomic Analysis of Reactive Astrogliosis. *J. Neurosci.* 32, 6391–6410. doi:10.1523/JNEUROSCI.6221-11.2012

Ziemka-Nalecz, M., Jaworska, J., Sypecka, J., and Zalewska, T. (2018). Histone Deacetylase Inhibitors: A Therapeutic Key in Neurological Disorders? *J. Neuropathol. Exp. Neurol.* 77, 855–870. doi:10.1093/jnen/nly073

Conflict of Interest: The authors declare that the research was conducted in the absence of any commercial or financial relationships that could be construed as a potential conflict of interest.

Copyright © 2021 Villarreal, Vidos, Monteverde Busso, Cieri and Ramos. This is an open-access article distributed under the terms of the Creative Commons Attribution License (CC BY). The use, distribution or reproduction in other forums is permitted, provided the original author(s) and the copyright owner(s) are credited and that the original publication in this journal is cited, in accordance with accepted academic practice. No use, distribution or reproduction is permitted which does not comply with these terms.

frontiers in Cellular Neuroscience

REVIEW
published: 21 June 2021
doi: 10.3389/fncel.2021.654284

Connecting Neuroinflammation and Neurodegeneration in Multiple Sclerosis: Are Oligodendrocyte Precursor Cells a Nexus of Disease?

Morgan W. Psenicka[1], *Brandon C. Smith*[1,2], *Rachel A. Tinkey*[1,3] *and Jessica L. Williams*[1,4]*

[1] Department of Neurosciences, Lerner Research Institute, Cleveland Clinic, Cleveland, OH, United States, [2] Department of Biological, Geological, and Environmental Sciences, Cleveland State University, Cleveland, OH, United States, [3] School of Biomedical Sciences, Kent State University, Kent, OH, United States, [4] Brain Health Research Institute, Kent State University, Kent, OH, United States

The pathology in neurodegenerative diseases is often accompanied by inflammation. It is well-known that many cells within the central nervous system (CNS) also contribute to ongoing neuroinflammation, which can promote neurodegeneration. Multiple sclerosis (MS) is both an inflammatory and neurodegenerative disease in which there is a complex interplay between resident CNS cells to mediate myelin and axonal damage, and this communication network can vary depending on the subtype and chronicity of disease. Oligodendrocytes, the myelinating cell of the CNS, and their precursors, oligodendrocyte precursor cells (OPCs), are often thought of as the targets of autoimmune pathology during MS and in several animal models of MS; however, there is emerging evidence that OPCs actively contribute to inflammation that directly and indirectly contributes to neurodegeneration. Here we discuss several contributors to MS disease progression starting with lesion pathology and murine models amenable to studying particular aspects of disease. We then review how OPCs themselves can play an active role in promoting neuroinflammation and neurodegeneration, and how other resident CNS cells including microglia, astrocytes, and neurons can impact OPC function. Further, we outline the very complex and pleiotropic role(s) of several inflammatory cytokines and other secreted factors classically described as solely deleterious during MS and its animal models, but in fact, have many neuroprotective functions and promote a return to homeostasis, in part via modulation of OPC function. Finally, since MS affects patients from the onset of disease throughout their lifespan, we discuss the impact of aging on OPC function and CNS recovery. It is becoming clear that OPCs are not simply a bystander during MS progression and uncovering the active roles they play during different stages of disease will help uncover potential new avenues for therapeutic intervention.

Keywords: multiple sclerosis, neuroinflammation, oligodendrocyte precursor cell, neurodegeneration, glia, animal models, remyelination

OPEN ACCESS

Edited by:
Jason R. Plemel,
University of Alberta, Canada

Reviewed by:
Gonçalo Castelo-Branco,
Karolinska Institutet (KI), Sweden
Maryna Baydyuk,
Georgetown University, United States

***Correspondence:**
Jessica L. Williams
williaj39@ccf.org

Specialty section:
This article was submitted to Non-Neuronal Cells, a section of the journal Frontiers in Cellular Neuroscience

Received: *22 January 2021*
Accepted: *20 May 2021*
Published: *21 June 2021*

Citation:
Psenicka MW, Smith BC, Tinkey RA and Williams JL (2021) Connecting Neuroinflammation and Neurodegeneration in Multiple Sclerosis: Are Oligodendrocyte Precursor Cells a Nexus of Disease? Front. Cell. Neurosci. 15:654284. doi: 10.3389/fncel.2021.654284

INTRODUCTION

Multiple sclerosis (MS) is an inflammatory and neurodegenerative disease of the central nervous system (CNS) characterized by loss of myelin, oligodendrocytes, and axons (Chang et al., 2000, 2002). The global prevalence of MS has increased over the last several years and is highest in North America and Europe (Belbasis et al., 2015). MS represents a large personal and socioeconomical burden. The average age of onset is 30 and 25 years after diagnosis, nearly 50% of MS patients will require permanent use of a wheelchair (Dendrou et al., 2015). Most patients (85%) exhibit the relapsing-remitting form of MS (RRMS), in which disease begins with episodes of neurological dysfunction followed by partial or complete remission, and later progresses to secondary progressive MS (SPMS) with fewer remissions and increasing clinical deterioration (Thompson et al., 1991; Compston and Coles, 2008; Hurwitz, 2009). Some patients (15%) have a third subtype of MS, primary progressive (PPMS), and experience unremitting, progressive loss of neurological function from the onset of disease (Confavreux et al., 2000; Miller and Leary, 2007; Hurwitz, 2009; McCarthy and Weinberg, 2015). Neurological disability in RRMS is due to immune-mediated demyelination, while SPMS and PPMS is dominated by neurodegenerative processes (Miller and Leary, 2007). Thus, it is not surprising that the 12 FDA-approved immunomodulatory therapies have demonstrated efficacy for RRMS, while a single approved therapy may be beneficial for SPMS or PPMS, although long-term studies are still required (Noseworthy et al., 2000; Leary and Thompson, 2003; Wingerchuk and Carter, 2014; Feinstein et al., 2015; Montalban et al., 2017). It is also acknowledged that while the standard therapies for treating MS reduce relapses in RRMS patients (Haghikia et al., 2013; Feinstein et al., 2015), they do not halt neurodegeneration and disability continues, becoming permanent. Investigating the potential link between neuroinflammatory and neurodegenerative processes during autoimmunity may uncover a source of novel therapeutic potential for MS patients.

MS is a neurodegenerative and inflammatory disease mediated by autoreactive immune cells that initiate myelin and axon injury in a progressive manner, which leads to sustained motor and sensory function loss (Trapp et al., 1998; Noseworthy et al., 2000; Trapp and Nave, 2008). Following myelin destruction during the pathogenesis of MS, axons are left exposed, inefficient, and susceptible to degeneration. During remyelination, damaged axons reacquire a myelin sheath and recover lost function (Franklin, 2002). Clinically, this process occurs early on and requires the generation of new oligodendrocytes (OLs) (Keirstead and Blakemore, 1997), the myelinating cell of the CNS, from oligodendrocyte precursor cells (OPCs) (Watanabe et al., 2002). Although there is also evidence to suggest that mature OLs too can participate in remyelination of MS lesions (Duncan et al., 2018). Importantly, in the harsh lesion environment, remyelination does occur (Prineas et al., 1993). However, while there are OPCs found in and around MS lesions (Chang et al., 2002), remyelination efficiency wanes with patient age and as lesions and the disease become more chronic (Franklin, 2002; Frischer et al., 2015; Gruchot et al., 2019). OPCs are typically more sensitive to growth factors produced by resident CNS cells compared to mature myelinating OLs, which are largely unresponsive to identical factors, although the molecular mechanisms responsible for this dichotomy remain poorly understood (Moore et al., 2015). Functionally, the maturation of OPCs to OLs is vital to regain homeostasis as this conversion provides critical structural, metabolic, and trophic support to neuronal axons (Funfschilling et al., 2012; Lee et al., 2012; Duncan et al., 2021). However, within the MS lesion environment, there are several factors that can suppress proper OPC function, preventing successful remyelination and, thus, potentially contributing to neurodegeneration and dampening clinical improvement (Compston and Coles, 2002; Franklin, 2002; Gruchot et al., 2019).

The extracellular milieu in which OPCs reside can heavily influence their ability to migrate, proliferate, and/or mature into myelinating OLs. Within the MS lesion, there are a variety of both resident CNS cells and infiltrating peripheral immune cells, although the type and amount of each cell population varies depending on the lesion type (Bo et al., 1994; Bruck et al., 1994, 1995; Trapp et al., 1998). While the etiology of MS is largely unknown, it is well-established that subsets of infiltrating T cells heavily contribute to pathology with the help of peripheral monocytes, macrophages, and the CNS resident innate immune cells, microglia. While there are multiple routes of entry, a primary method of gaining access to the CNS by peripheral leukocytes is to breach the endothelial (and pericyte) layer of the blood-brain barrier (BBB). There, they are able to then penetrate the glia limitans and the astrocyte endfeet of the neurovascular unit, responding to localizing cues and upregulating adhesion molecules via the release of inflammatory mediators (Lopes Pinheiro et al., 2016; Prinz and Priller, 2017; Williams et al., 2020). In addition to this intricate, pathological interplay among cells of the periphery and CNS, there is significant heterogeneity among the cell populations that contribute to this complex neuroinflammatory lesion environment. While several T cell subsets are known to perpetuate inflammation in MS and in many experimental models of MS, particularly in acute phases of disease, mice that lack $CD4^+$ and $CD8^+$ T cells have significant deficits in remyelination (Bieber et al., 2003), highlighting the complicated nature of neuro-immune interactions ongoing in MS. Beyond the complexities of peripheral immune cell contributions to pathology and repair, microglia and astrocytes exhibit an exceptional amount of genetic, morphological, and functional heterogeneity depending on microenvironmental cues (Masuda et al., 2020; Escartin et al., 2021), which can significantly influence how OPCs function as glia are highly communicative with other glia (Peferoen et al., 2014; Liu et al., 2020; Nutma et al., 2020) as well as with neurons (Stogsdill and Eroglu, 2017). Here, we will discuss the underlying pathological neuroinflammatory processes and factors that contribute to neurodegeneration and MS progression, focusing on the role of glial intercellular communication, the microenvironment, and OPCs.

MULTIPLE SCLEROSIS LESIONS

Between 1862 and 1865, colleagues Jean Martin Charcot and Alfred Vulpian identified a form of spinal MS. Then, in April of 1866, Charcot macroscopically described nearly identical sclerotic lesions in both the brain and spinal cord during an autopsy. He later presented microscopic characteristics of these lesions, identifying a sharp boarder between the lesion and normal-appearing tissue with a transition zone, and a lesion center consisting of "greasy droplets" that resembled myelin and a description of axonal degeneration (Zalc, 2018). In more recent years, the characterization of MS lesions has been extensively described (Lassmann et al., 1998; Trapp et al., 1998, 2018; Kuhlmann et al., 2017), although new knowledge regarding the lesion environment is continually being uncovered. While lesions are found in both white and gray matter, they are predominantly localized to white matter tracts and are typically categorized into active, chronic active, and inactive, with lesions often transitioning between types (Trapp et al., 1998; Kuhlmann et al., 2017). Myelocortical lesions were also recently described in the gray matter of a subset of MS patients and may indicate that neuron degeneration can occur independently of cerebral white matter demyelination (Trapp and Ontaneda, 2018). Understanding the pathophysiology underlying these various lesion types may hint at the potential link between neuroinflammation and neurodegeneration and uncover possible interventions to prevent permanent disability in MS patients.

Active lesions are characterized as having a significant amount of peripheral immune cell infiltration, often including a substantial population of $CD8^+$ T cells, $CD20^+$ B cells, and macrophages, along with some $CD4^+$ T cells (Correale and Villa, 2010; Disanto et al., 2012; Machado-Santos et al., 2018). These lesions also have involvement from CNS resident cells including reactive astrocytes and activated microglia throughout the lesion, with a high concentration of microglia ringing the lesion edge (Frischer et al., 2015). Active lesions are highly inflammatory, largely due to the quantity of infiltrating cells producing a myriad of cytokines and other inflammatory factors (Cannella and Raine, 1995; Kutzelnigg et al., 2005; Frischer et al., 2009), which contribute to demyelination and eventual axonal loss (Trapp et al., 1998). However, despite the inflammatory nature of active lesions, oligodendrocytes often reappear during early stages of remyelination in acute MS, contributing to partial or complete recovery (Lassmann, 1983; Prineas et al., 1993; Raine and Wu, 1993; Lucchinetti et al., 1999, 2000; Barkhof et al., 2003; Patrikios et al., 2006). RRMS is typically associated with predominately active lesions and recovering/remyelinating plaques (Harris et al., 1991; Thompson et al., 1991). In patients with RRMS, axon signal conduction tends to be reduced within active lesions, which can lead to a very heterogenous profile of symptoms, depending on the CNS region in which the lesion is located (Kutzelnigg et al., 2005; Campbell et al., 2012; Heß et al., 2020). During RRMS and in early SPMS and PPMS, the majority of lesions are active and chronic active. However, in more chronic stages of MS, the proportion of lesions begin to shift more toward inactive (Luchetti et al., 2018).

Chronic active lesions are often referred to as slowly expanding or smoldering lesions and are characterized by fewer infiltrating cells, further accumulation of microglia on lesion edges, with fewer microglia located in the center of the lesion compared to active lesions (Dal-Bianco et al., 2017; Absinta et al., 2018; Calvi et al., 2020). While demyelination still occurs in chronic active lesions, particularly along the lesion edge, there is a significant reduction in the rate of demyelination. This is accompanied by a reduction in remyelination relative to active lesions (Absinta et al., 2019; Wang et al., 2019; Elliott et al., 2020), with the center of the lesion remaining demyelinated and unlikely to remyelinate (Calvi et al., 2020; Elliott et al., 2020; Heß et al., 2020). In the center of chronic active lesions, reactive astrocytes proliferate and form a dense network of overlapping astrocytes with few axons, referred to as the glial scar (Voskuhl et al., 2009; Sofroniew and Vinters, 2010; Jonkman et al., 2015; Kuhlmann et al., 2017). In a recent *in vivo* cohort study, chronic active lesions were detected by magnetic resonance imaging using their characteristic rims and were associated with an aggressive disease course and poorer clinical outcomes (Absinta et al., 2019). Inactive lesions are associated with prolonged disease duration, and unlike active and chronic active lesions, are characterized by a lack of infiltrating cells and microglia, as well as a stark loss of axons and near complete depletion of mature oligodendrocytes, leading to their static nature (Brück et al., 1996; Correale and Villa, 2010; Jonkman et al., 2015; Kuhlmann et al., 2017). However, analogous to chronic active lesions, gliotic scars consisting of astrocytes are still present (Kornek et al., 2000; Peterson et al., 2001).

Active, chronic active, and inactive lesions occur simultaneously in MS patients but tend to shift in predominance depending on disease chronicity (Brück et al., 1996; Kornek et al., 2000; Frischer et al., 2015; Jonkman et al., 2015; Kuhlmann et al., 2017; Heß et al., 2020). Lesions tend to progress from active to chronic active to inactive as an individual lesion progresses, with some exceptions (Harris et al., 1991; Thompson et al., 1991; Kuhlmann et al., 2017; Absinta et al., 2018). The most notable exceptions are active lesions, which can completely or partially remyelinate rather than progressing onto chronic active depending on lesion severity (Frischer et al., 2015; Jonkman et al., 2015). Additionally, inactive and later stage chronic active lesions can be reactivated to a more active lesion phenotype (Thompson et al., 1991; Kuhlmann et al., 2017; Absinta et al., 2018), suggesting that inactive lesions may be reinfiltrated by a new wave of macrophages/microglia. Interestingly, macrophages occupying active and chronic active lesions often contain lipids, presumably from ingesting myelin debris, and are immunomodulatory rather than inflammatory in nature (Boven et al., 2006). This heterogenous mix of lesion types, and thus cellular composition, may partially account for the inefficacy of currently approved immunomodulatory drugs in treating SPMS and PPMS patients, as the role of inflammation can vastly differ between lesion types (Bates, 2011; Ciotti and Cross, 2018). Limiting inflammation in active lesions is certainly beneficial; however, in lesions lacking significant inflammation, the impact of immune modulation is likely minimal, or may even have potentially negative consequences, in chronic active and inactive

lesions. To this point, remyelination most frequently occurs around the borders of lesions where inflammation is most pronounced (Brück et al., 1996; Jonkman et al., 2015; Wang et al., 2019; Calvi et al., 2020); and, many animal studies have revealed a critical role for immune components in CNS remyelination and repair, particularly during chronic stages of disease. To better understand the complex nature of the CNS environment during MS, several murine models have been developed and are critical in uncovering novel therapeutic modalities and elucidating multiple aspects of disease.

MURINE MODELS OF MS

Progressively sophisticated animal models of human neurological pathology are continuously being developed and improved. These models make it feasible to examine complex cellular interactions within the CNS and their contributions to neuroinflammation and disease progression (Kipp et al., 2017). While no animal model perfectly recapitulates observed MS pathology, there are components of any given model which are useful, replicating different clinical, immunological, and histological aspects of human disease. Genetic manipulations using the Cre/*lox* and other systems in combination with some murine models of MS are valuable tools in elucidating specific molecular pathways important for MS pathology and repair.

Experimental Autoimmune Encephalomyelitis (EAE)

EAE is the most commonly used animal model for MS, sharing many features of the human disease, with the inflammatory components being of particular interest (Borjini et al., 2016). The classical EAE phenotype, characterized by ascending flaccid paralysis and preferential immune infiltration of the spinal cord, has been widely utilized since its characterization in the 1930s (Croxford et al., 2011). Ascending paralysis correlates with peripheral immune infiltration and inflammation in the lumbar region of the spinal cord, which becomes progressively more inflamed throughout the acute phase of disease (Miller et al., 2010). Clinical signs, most notably, an abnormal gait, tail paralysis, and hindlimb paralysis, are scored using a standard system. In general, the EAE model yields high disease incidence with a consistent and robust disease course that is very replicable (Stromnes and Goverman, 2006), and though not fully understood, is nonetheless well-characterized. Shared aspects of EAE and MS pathology include the targeted destruction of myelin accompanied by axonal degradation, which results in multiple disseminated lesions, predominantly located in perivascular spaces (Kornek et al., 2000). Likewise, both EAE and MS share common temporal characteristics, evidenced by inflammatory lesion development, followed by demyelination, gliosis, decreased frequency of lesion-associated mononuclear cell infiltrates, and limited remyelination (Storch et al., 1998). However, EAE is induced via external immunization while MS occurs spontaneously (Stromnes and Goverman, 2006). As such, EAE can represent many inflammatory characteristics of MS including peripheral immune cell priming, followed by CNS infiltration, and subsequent CNS resident cell responses (Baxter, 2007). Model heterogeneity exists within EAE, with various antigenic targets and murine strains being used. The most common immunizing antigens include myelin-associated glycoprotein, myelin basic protein, oligodendrocytic basic protein, myelin oligodendrocyte glycoprotein (MOG), and proteolipid protein (PLP). The target of choice is dependent on the genetic background of the strain being used. EAE is most commonly induced in rodents, which have an easily and consistently replicable disease induction, with mice used preferentially over rats in the last few decades (Miller et al., 2010; Croxford et al., 2011).

EAE is primarily considered a $CD4^+$ T cell-mediated disease (Van Kaer et al., 2019), although the particular role of various $CD4^+$ T helper cell subsets and, to an extent, $CD8^+$ cytotoxic T cells are also well-appreciated (Sun et al., 2001; Sonobe et al., 2007). However, like MS, EAE has a complex immune profile in which natural killer T cells (Jahng et al., 2001; Singh et al., 2001; Denney et al., 2012), $\gamma\delta$T cells (Blink and Miller, 2009), mucosal invariant cells (Pál et al., 2001; Mars et al., 2002; Croxford et al., 2006), and B cells (Matsushita et al., 2008; Pöllinger et al., 2009; Pierson et al., 2014; Harp et al., 2015) each contribute to pathology. Further, other adaptive and innate leukocytes can have differing roles, imposing either regulatory or pathogenic functions depending on the disease state, which have alternate contributions to EAE pathogenesis (Mcginley et al., 2018; Van Kaer et al., 2019).

There are two primary methods commonly used to induce EAE: active immunization using a myelin antigen with adjuvants (typically complete Freund's adjuvant and pertussis toxin) and passive induction via adoptive transfer of activated, myelin-specific T cells from an immune-primed donor into a naïve recipient without the use of adjuvants (Stromnes and Goverman, 2006). Actively induced EAE in the C57Bl/6 mouse strain is typically a biphasic model, with an induction phase and an effector phase (Miller et al., 2010). During induction, similar to early lesions in RRMS, focal vascular disruptions and increased BBB permeability precede microglial activation and peripheral leukocyte infiltration (Alvarez et al., 2015; Barkauskas et al., 2015). Next, myelin-specific T cells extravasate across the endothelial layer and into the CNS and initiate pro-inflammatory signaling cascades to promote the recruitment of B cells (Furtado et al., 2008; Matsushita et al., 2008), innate immune cell infiltration, and T cell reactivation (Pierson et al., 2014). These primed T helper cells secrete a number of cytokines, including interferon (IFN)γ and tumor necrosis factor (TNF)α, which activate microglia and peripheral macrophages (Ponomarev et al., 2005; Ajami et al., 2011). Of note, OPCs are also responsive to (Rodgers et al., 2015) and secrete cytokines (Moore et al., 2015) and accumulate perivascularly, contributing to BBB compromise during EAE (Girolamo et al., 2019). Further, this inflammatory cytokine cascade leads to increased phagocytic activity by activated mononuclear cells and enhanced cytotoxic effects of cytokines secreted by $CD4^+$ T cells and monocytes, enhancing the demyelination of axons, eventual axonal transection, and neuronal cell death (Miller et al., 2010). Even as the acute inflammatory response fades

and levels of cellular infiltrates decreases, axons continue to degenerate. In C57Bl/6J mice immunized with the myelin peptide MOG_{35-55}, axonal density was reduced within lesions at early and chronic time points and significant axonal loss was observed in both the gray matter and normal-appearing white matter, which was associated with clinical impairment (Herrero-Herranz et al., 2008). Similarly, axonal pathology is a hallmark of MS and a substantial contributor to irreversible clinical disability (Trapp et al., 1998). Passive EAE via adoptive transfer of activated, myelin-specific T cells into naïve hosts can be used to study the effector phase without introducing potentially confounding effects of the adjuvants used for active immunization (Brocke et al., 1996; Stromnes and Goverman, 2006). Additionally, compared to active EAE, passive EAE is highly synchronous and consistent. Although a limitation of passive EAE is limited microglial activation, the absence of sustained demyelination and variable axonal injury, it is extremely useful for the study of immune control mechanisms, T cell-mediated neuroinflammation induction, and immune cell-specific mechanisms of tissue injury (Kipp et al., 2012; Lassmann and Bradl, 2017).

There are several variations of EAE aside from the C57Bl/6 model used to study various aspects of MS pathology. Other commonly used models include SJL/J mice immunized against the myelin peptide $PLP_{139-151}$ (Tuohy et al., 1989). This model has a number of similarities with the C57Bl/6 EAE model in terms of pathology; however, an advantage to the SJL/J model is that mice develop a progressive relapsing-remitting disease course (Whitham et al., 1991; Miller and Karpus, 2007). Relapsing-remitting EAE can be induced via active immunization or by transfer of activated PLP-specific T cells, the latter of which is associated with epitope spreading (McRae et al., 1995) or the development of immunity to secondary endogenous antigens following initial immune priming to a self-antigen (Vanderlugt and Miller, 1996). While this model suffers from the lack of genetic deletion strategies, it is useful for testing novel treatment strategies with respect to additional clinical parameters including reductions in relapse rate. Finally, some models of EAE yield an alternative clinical presentation, referred to as atypical EAE, which often display ataxia, head tilting, and axial rotation associated with parenchymal hindbrain inflammation (Simmons et al., 2013). This is most often seen in animals with a disruption in IFNγ signaling (Wensky et al., 2005; Lees et al., 2008; Liu et al., 2015). Some models present with a mixed phenotype developing both atypical and classical signs (Pierson et al., 2012), mimicking the heterogenous regional localization of MS lesions in patients.

Viral Encephalomyelitis

Several viruses initiate chronic infections in the murine CNS, serving as useful models for the study of axonal damage and inflammatory-induced demyelination. Two well-characterized demyelinating viral models involve encephalomyelitis induced by the RNA viruses Theiler's murine encephalomyelitis virus (TMEV), a member of the non-enveloped *Picornaviridae* family, and mouse hepatitis virus (MHV), a member of the enveloped *Coronaviridae* family (Miller et al., 2001; Stohlman and Hinton, 2001; Bergmann et al., 2006; Mecha et al., 2013).

TMEV

Similar to EAE, the pathology of TMEV-induced encephalomyelitis is dependent on the dose administered, the viral strain, and the genetic background of the mouse. There are highly neurovirulent strains, such as GDVII and FA, which induce an acute, often fatal encephalitis (DePaula-Silva et al., 2017; Savarin and Bergmann, 2017; Libbey and Fujinami, 2021). There are also attenuated variants of TMEV, including BeAn and the Daniel's strain (DA). Infecting the CNS of susceptible SJL/J mice with an attenuated strain generates a biphasic CNS pathology, while infection of C57Bl/6J induces an acute infection, which is rapidly cleared (Zoecklein et al., 2003; Richards et al., 2011). Therefore, TMEV intracerebral infection of SJL/J mice is the most commonly used MS animal model as it produces acute encephalomyelitis followed by a chronic demyelinating phase, primarily in the spinal cord. The chronic demyelinating stage is called TMEV-induced demyelinating disease (TMEV-IDD) (Bröer et al., 2016). Unlike other models, TMEV-IDD lacks substantial remyelination due to its progressive nature, so it does not easily mirror a relapsing-remitting phenotype (Ulrich et al., 2008). Thus, TMEV most effectively models MS types with hallmark chronic, progressive immune-mediated demyelination with remyelination failure as TMEV-IDD animals show a continuous increase in motor disability which coincides with increases in white matter damage (Sun et al., 2015; Leitzen et al., 2019). The number of OPCs within TMEV-IDD lesions is transiently higher than homeostatic levels. $GFAP^+$ cells are likewise present in elevated numbers in spinal cord lesions. Interestingly, lesion-associated $NG2^+$ OPCs can co-express GFAP or CNPase suggesting potential alternative routes of OPC differentiation, which may affect remyelination capacity (Ulrich et al., 2008). Both the BeAn and DA strains can induce TMEV-IDD, but there are strain-related differences in pathology. BeAn infection in susceptible SJL/J mice develop clinical signs similar to those observed in EAE, including irregular gait and hind limb paralysis. DA-infected mice develop the same clinical features, but not until 140–180 days post-infection (Oleszak et al., 2004).

Following the acute phase of TMEV-DA infection, viral replication persists at low levels in macrophages and microglia (Clatch et al., 1990; Qi and Dal Canto, 1996; Jelachich and Lipton, 1999) and to a lesser extent in astrocytes and OLs (Zheng et al., 2001). There is immune infiltration in the hindbrain subcortical gray matter but little to no white matter infiltration throughout the acute phase (Oleszak et al., 2004). During the chronic phase, depending on viral dosage and host age, susceptible SJL/J mice develop MS-like chronic neuroinflammation which presents as functional motor deficits. TMEV-DA-induced lesions mimic features of MS cortical lesions in that chronic demyelinating white matter has extensive peripheral leukocyte infiltrates, the majority of which are $CD4^+$ (Palma et al., 1999; Mohindru et al., 2006) and $CD8^+$ T cells (Begolka et al., 2001; Lyman et al., 2004), though some monocytes/macrophages (Mack et al., 2003) and comparably few B cells are also present (Gilli et al.,

2015). In particular, PLP-reactive $CD4^+$ Th1 cells have been implicated in the perpetuation of disease (Katz-Levy et al., 2000) and epitope spreading (Miller et al., 1997; Mcmahon et al., 2005) has been demonstrated to strengthen myelin antigenic responses at 2–4 weeks (McCarthy et al., 2012; DePaula-Silva et al., 2017). This leads to extensive white matter damage and axonal loss in TMEV-infected mice, particularly in the thoracic and cervical spinal cord, as early as 7 days post-infection (Leitzen et al., 2019). Over the following weeks, damaged axons are surrounded by locally activated macrophages/microglia without peripheral T cell recruitment or demyelination, which does not occur until the chronic phase. Interestingly, areas of axonal damage corresponded to chronic demyelination late in infection (Tsunoda and Fujinami, 2010), which may mirror aspects of MS where neuronal death precedes demyelination and T cell involvement.

MHV

Studies employing MHV-induced demyelination have largely focused on two neurotropic strains: the mildly neurovirulent and hepatotropic MHV-A59 strain and a neuroattenuated variant of the lethal JHM strain, designated 2.2-V-1 (Fleming et al., 1986; Bergmann et al., 2006; Templeton et al., 2008; Bender and Weiss, 2010; Bender et al., 2010). Following intracerebral inoculation, CNS cells become acutely infected. After infection, chronic demyelination occurs. Clinical signs such as hind limb paralysis correlate with neuroinflammation and white matter damage (Savarin and Bergmann, 2017). The virus infects and replicates within ependymocytes, microglia, astrocytes, and OLs, comparatively sparing neurons (Wang et al., 1992). Control of virus in astrocytes and microglia/macrophages is perforin-mediated (Lin et al., 1997; Bergmann et al., 2004), while IFNγ controls viral replication within OLs (Parra et al., 1999; Bergmann et al., 2004). The MHV-A59 strain infects neurons and glial cells and induces a mild encephalitis (Lavi et al., 1999; Phillips et al., 2002), whereas the JHM v2.2-1 variant is more gliatropic (Lin et al., 1997; Bergmann et al., 2004), largely sparing neurons, and causes a more severe encephalitis which progresses to hind limb paralysis from which the majority of mice recover (Rempel et al., 2004; Bender and Weiss, 2010). Despite the distinct cellular tropisms, both virus strains spread from the brain to the spinal cord and infectious virus is generally controlled within 10–14 days. Of note, viral RNA persists in spinal cords for several months, up to a year post-infection in the case of MHV-JHM v2.2-1 (Savarin and Bergmann, 2017). Demyelination is prominent in spinal cord white matter 14 to 30 days post-infection, after initial virus control, depending on the MHV strain and age at infection. A caveat is that many MHV-A59 studies are carried out in 4–5 week-old mice, whereas MHV-JHM v2.2-1 studies administer virus to 6–7 week-old mice preempting direct comparisons (Lavi et al., 1984; Fleming et al., 1987; Jordan et al., 1989; Templeton and Perlman, 2007). Both infections cause the upregulation of numerous chemokines and cytokines to enhance recruitment of various leukocytes including neutrophils, monocytes, natural killer cells, $CD4^+$ and $CD8^+$ T cells as well as various B cell subsets in a regulated, temporal pattern, yet the magnitude of inflammatory mediators as well as leukocyte subsets is dependent on the virus variant (Williamson et al., 1991; Bergmann et al., 2001; Liu and Lane, 2001; Tschen et al., 2002). $CD8^+$ T cells, with the help of $CD4^+$ T cells, are the main effector cells in viral control (Phares et al., 2012). Despite a potent T cell mediated response, upregulation of inhibitory ligands, like programmed death-ligand 1, counteract exuberant effector function to limit pathology potentially contributing to persistence (Phares et al., 2010; Puntambekar et al., 2011). Demyelination is immune-mediated as immunodeficient (SCID and RAG-deficient) mice do not develop overt demyelination (Houtman and Fleming, 1996; Wu and Perlman, 1999) and both virus-specific $CD4^+$ and $CD8^+$ T cells alone can mediate demyelination (Bergmann et al., 2004; Stohlman et al., 2008). Moreover, microglia and macrophages have been shown to mediate demyelination (Savarin et al., 2016). This overt demyelination lends itself to elegant remyelination studies as chemokines like CXCR2 are highly upregulated and are critical to OPC-mediated repair (Marro et al., 2019; Skinner and Lane, 2020). Despite an overall reduction in T cells during viral persistence, new lesions are continuously formed as shown by lipid laden myeloid cells (Wu et al., 2000; Liu et al., 2001; Rempel et al., 2004), consistent with MS lesions.

Chemical or Toxin-Induced Demyelination Models

Chemical and toxin-mediated demyelination models largely lack the immune component relevant to EAE, TMEV, and MHV. Inflammatory models indeed more closely resemble MS pathology in many ways, but are more complex and are less consistent in terms of demyelination chronology and lesion localization, extent, and characteristics. Inflammation-independent models are nonetheless useful for in-depth analyses of CNS resident cells engaged in the de- and remyelination process and are often employed to investigate therapeutics which limit demyelination or stimulate remyelination (Procaccini et al., 2015). Gliotoxic agents ethidium bromide (EtBr) and lysolecithin induce focal demyelination at their injection site, while the systemically administered copper chelator cuprizone (CPZ) induces reversible white and gray matter demyelination throughout the brain (Blakemore and Franklin, 2008; Bai et al., 2016; Lubetzki et al., 2020).

EtBr and Lysolecithin

The EtBr model has seen extensive use in rats and remains preferentially a rat model, though it has recently been used in mice, revealing subtle differences in pathology between the two rodents. EtBr is a DNA intercalator and its toxicity preferentially impacts astrocytes by restricting their ability to release trophic factors leading to associated OLs to die, along with the affected astrocytes, while largely sparing neurons. The death of these glia in and around the injection site results in localized demyelination (Torre-Fuentes et al., 2020). Immunoreactive $GFAP^+$ astrocytes are then recruited, but remain confined to the lesion perimeter. EtBr injection into murine ventral spinal cord white matter induces hind limb motor deficits, similar to those seen in other models, which can persist with accompanying $CD45^+$ infiltrating

immune cells and axonal loss in chronic stages (Kuypers et al., 2013). While EtBr has been used in mice, the studies outlining its use are limited. Lysolecithin is more commonly used and as a result has been more thoroughly characterized.

Lysolecithin is a phospholipase A2 activator, which, much like EtBr, induces a highly reproducible focal demyelination in CNS white matter (Procaccini et al., 2015). The toxin acts as a detergent-like agent directly deteriorating myelin sheaths by solubilizing the lipid membrane, effectively destroying myelin while sparing other cells and cellular components. As a result, OPCs are spared and lysolecithin-induced lesions remyelinate faster than most other demyelination models (Bjelobaba et al., 2018), with nearly all axons encased in myelin sheaths by day 23 post-injection (Jeffery and Blakemore, 1995), offering a consistent, timely, and reproducible method for studying OPCs in the context of de- and remyelination events. Interestingly, while demyelination has been described as being T and B cell-independent, CD4- and CD8-deficient mice had significantly reduced remyelination at the injection site compared to controls, indicating T cells may be involved in myelin repair and proper OPC function (Bieber et al., 2003). Unlike EtBr and CPZ, lysolecithin is not considered to be fully immune-independent, acting as a chemoattractant to monocytes and initiating a limited focal inflammatory response (Torre-Fuentes et al., 2020) and remyelination that is accompanied by significant astrogliosis (Jeffery and Blakemore, 1995). While useful, EtBr and lysolecithin are technically demanding models and de- and remyelination is restricted to the site of injection.

Cuprizone

CPZ, a low molecular weight copper chelator, is systemically administered to mice typically by incorporating it into standard chow. Copper is an enzymatic cofactor necessary for many metabolic functions, including ATP production, and while its exact mechanism of action is unknown, it is generally accepted that the chelation of copper is highly disruptive to the robust cellular metabolism of OLs (Praet et al., 2014). Within myelinating OLs, it can cause the formation of cellular megamitochondria, ATP shortages, reactive oxygen species build up, and endoplasmic reticulum stress, all of which OLs are particularly vulnerable to due to their highly intensive metabolism required for myelin production. Additionally, disruption of oxygen scavenging by CPZ can be exacerbated and catalyzed via the Fenton reaction by the high amount of sequestered iron within cells, producing more reactive oxygen species (Praet et al., 2014). T cell suppression occurs during demyelination, which allows the effects of CPZ to be discriminated from particular immune compartments. Demyelination in both the gray and white matter of the brain are highly reproducible, synchronous, and anatomically distinct during the time mice are fed CPZ-embedded chow (Matsushima and Morell, 2001; Torre-Fuentes et al., 2020) unlike the demyelination that is seen in EAE or in virally-induced demyelination. Withdrawal of the CPZ diet also allows consistent remyelination. This feature enables precise timing and elucidation of specific mechanisms, particularly those active in CNS glia, during de- and remyelination. While peripheral immune cell infiltration is limited in this model, $CXCR2^+$ neutrophils are thought to be critical for demyelination (Liu et al., 2010). CPZ is therefore ideal for the study of de- and remyelination with a focus on resident CNS cells and perhaps an ideal model for studying a "two-hit" mechanism, relevant in MS pathology.

Like many models for MS, there are differences in CPZ-induced pathology depending on the CPZ dosage and mouse strain used. Using 0.2% CPZ chow in 8–10 week-old C57Bl/6J mice is the most commonly used and well-characterized models. In C57Bl/6 mice, 0.2% CPZ induced reliable and complete demyelination of the caudal corpus callosum and superior cerebellar peduncle without significant weight loss or liver toxicity (Hiremath et al., 1998). The typical timeframe of CPZ exposure is 5–6 weeks, with early demyelination occurring as early as 3 weeks with a significant presence of $NG2^+$ OPCs and microglia within the corpus callosum (Hiremath et al., 1998; Mason et al., 2000; Williams et al., 2014). This is accompanied by significant gliosis, largely due to proliferating astrocytes. These astrocytes are thought to contribute to damaged myelin clearance via recruitment of microglia as ablation of $GFAP^+$ astrocytes during CPZ intoxication resulted in decreased microglial activation, excess myelin debris, impaired OPC proliferation, and a delay in remyelination (Skripuletz et al., 2013). Microglia and astrocytes also significantly upregulate interleukin (IL)-1β, which is thought to induce the release of insulin-like growth factor (IGF)-1 during CPZ demyelination (Mason et al., 2001; Matsushima and Morell, 2001), suggesting a role for these glia in a return to homeostasis. A clear perk of the CPZ model of demyelination is that remyelination occurs rapidly and spontaneously following the cessation of CPZ treatment with sequential myelin proteins expressed as early as 1 week post-CPZ cessation (Lindner et al., 2008). Importantly, chronic exposure to CPZ (12–16 weeks) results in axonal damage, even with concurrent remyelination. Although, remyelination using this chronic paradigm is delayed by 2-fold compared to mice fed CPZ for 6 weeks (Lindner et al., 2009). Although remyelination occurs in MS lesions, it is often inhibited, particularly in chronic disease stages; thus, this model represents a plausible way to elucidate potential mechanisms of remyelination failure in MS.

Other variations of the CPZ model include combining components of EAE induction to establish MS-like lesions in the brain. In most iterations of EAE, there is little to no immune cell infiltration in the cerebrum; however, immunization of C57Bl/6 mice fed CPZ with MOG_{35-55} resulted in significant lesions, characterized by T cell accumulation and axonal damage in the demyelinated corpus callosum, which were detectable by magnetic resonance imaging (Boretius et al., 2012). Another variation of this combined approach utilizes mice pre-treated with CPZ for 3 weeks, followed by standard chow for 2 weeks to establish focal lesions. Mice were then immunized with the MOG_{35-55} peptide, which induced significant forebrain lesions within white matter tracts and cortical and subcortical gray matter. Further, in addition to demyelination, these lesions exhibited discontinuation of the glia limitans, infiltration of neutrophils and granulocytes, and focal axonal damage (Scheld et al., 2016; Ruther et al., 2017). Combining passive transfer

EAE with CPZ demyelination revealed that adoptive transfer of myelin-reactive T cells into CPZ-fed mice had significant immune cell infiltration and preservation of demyelinated axons, though these axons were reduced in diameter (Baxi et al., 2015). Other models using CPZ include inducing biochemical modifications to myelin to produce a secondary immune response, which resulted in myelin-reactive splenocytes and MS-like lesions (Caprariello et al., 2018). These models are important as they reflect a "neurodegeneration first" model in which brain-intrinsic pathology triggers the peripheral immune response.

OPCs IN NEUROINFLAMMATION AND NEURODEGENERATION

A vital role for OPCs has been well-described with respect to remyelination in MS lesions and in several experimental models (Franklin and Ffrench-Constant, 2008; Chang et al., 2012; Staugaitis et al., 2012; Hughes et al., 2013; Young et al., 2013; Kremer et al., 2015). It has also recently been shown that heterogeneity exists between OLs during MS, which may contribute to disease progression (Jakel et al., 2019) or could be a result of OPC plasticity to repair damage (Foerster et al., 2019). However, there is also evidence of additional non-remyelinating functions of OPCs that may actively contribute to the development of neuroinflammation. Initial demyelinating insults stimulate recruitment of OPCs into early lesion sites and induce proliferation (Boyd et al., 2013; Takahashi et al., 2013). While this cellular expansion can lead to the replenishment of OLs through activation of regenerative genes such as *Olig2* and *Sox2* (Zhao et al., 2015; Tiane et al., 2019), a deficiency in the ability of OPCs to differentiate into OLs contributes to demyelination and axonal damage within lesions, leading to neurodegeneration (Chang et al., 2002; Boyd et al., 2013; Gruchot et al., 2019). Inflammation has been identified as a key factor in the suppression of OPC differentiation, as differential expression of surface receptors allows OPCs to have a very broad and diverse response to cytokine stimulation (Schmitz and Chew, 2008; Moore et al., 2015). While activation of inflammatory pathways in OPCs is associated with cytotoxicity as well as stunted differentiation and maturation (Moore et al., 2015), it also leaves them primed to modulate immune function.

Under homeostatic conditions, OPCs express low levels of inflammatory genes, which are normally seen in microglia, that are critical for environmental surveillance and movement to areas of demyelination (Fernandez-Castaneda and Gaultier, 2016; Voronova et al., 2017). In a disease state such as MS, expression of these genes can be significantly upregulated, potentially contributing to participation of OPCs in neuroinflammation, and further myelin and axon damage. Single-cell RNA sequencing of OPCs isolated from spinal cord tissue of mice with EAE revealed transcriptomic splicing that yielded upregulated disease-associated transcripts. Major histocompatibility (MHC) class I and II genes were highly expressed in EAE-derived OPCs compared to those in control mice, which was mediated by secretion of IFNγ by invading leukocytes (**Figure 1**). Furthermore, OPCs from EAE mice had increased phagocytic capacity as well as an ability to promote proliferation of and cytokine production from $CD4^+$ memory and effector T cells via MHC II antigen presentation. Importantly, OPCs stimulated with IFNγ and/or MOG_{35-55} were not able to induce proliferation of naïve $CD4^+$ T cells (Falcao et al., 2018), suggesting that priming of T cells first by professional antigen presenting cells is necessary for T cell interactions with antigen presented by OL lineage cells.

Similar relationships between OPCs and $CD8^+$ T cells have been demonstrated using the CPZ model of demyelination. Adoptive transfer of myelin reactive T cells following CPZ treatment revealed that exposure to IFNγ upregulates MHC I antigen presentation machinery and immunoproteasome subunits in OPCs, promoting TNFα and IFNγ expression by $CD8^+$ T cells. Perforin and granzyme secretion were also stimulated, promoting OPC-targeted cell death in the corpus callosum *in vivo* (**Figure 1**). Further, analysis of postmortem MS tissue revealed abundant expression of the immunoproteasome gene *PSMB8* in $SOX10^+$ OL lineage cells specifically in demyelinated white matter lesions (Kirby et al., 2019). This suggests that immunoproteasome upregulation in OPCs may impair remyelination 2-fold: by active destruction of OPCs and shifting OPCs toward an immune-reactive state, contributing to chronic neurodegeneration observed in progressive MS patients (Basler et al., 2014; Kirby et al., 2019). Activation of immunomodulatory function in relation to antigen presentation by OPCs is also linked to extracellular receptors involved in phagocytosis and cytokine production, such as lipoprotein receptor-related protein 1. Further, specific deletion in OLs and OPCs led to a reduction of both infiltrating cells and MHC I expression by OPCs in EAE and in CPZ (Fernández-Castañeda et al., 2020). Together, these studies suggest that OPCs are active contributors to ongoing inflammation by direct stimulation of autoreactive T cells via myelin antigen presentation during MS and in several models of demyelination.

In addition to antigen presentation molecules, OPCs have also been shown to produce select inflammatory cytokines and chemokines in areas of demyelination. Gene expression analysis of OPCs from control and CPZ-treated mice demonstrated increased expression of IL-1β in activated $PDGFR\alpha^+$ OPCs from demyelinated regions (Moyon et al., 2015; **Figure 1**). IL-1β is a strong inducer of the innate immune response and has been detected within lesions and in the cerebrospinal fluid (CSF) of MS patients (Dujmovic et al., 2009; Burm et al., 2016). Further, OPCs were found to be a prominent producer of IL-17 during EAE as deletion of the upstream signaling molecule Act1 specifically in $NG2^+$ cells drastically reduced EAE severity. Importantly, the same was not true for other CNS cells including neurons, mature OLs, and astrocytes (Kang et al., 2013). Of note, this reduction in EAE severity due to decreased OPC-derived IL-17 was likely not a direct effect on OPCs themselves since it was later found that IL-17A caused OPCs to exit the cell cycle and differentiate (Rodgers et al., 2015). In addition to the secretion of cytokines, chemokines involved in immune cell recruitment were also expressed by OPCs derived from the brains of mice treated with CPZ. These chemokines also included monocyte and microglia localizing cues like CCL2, which was significantly upregulated

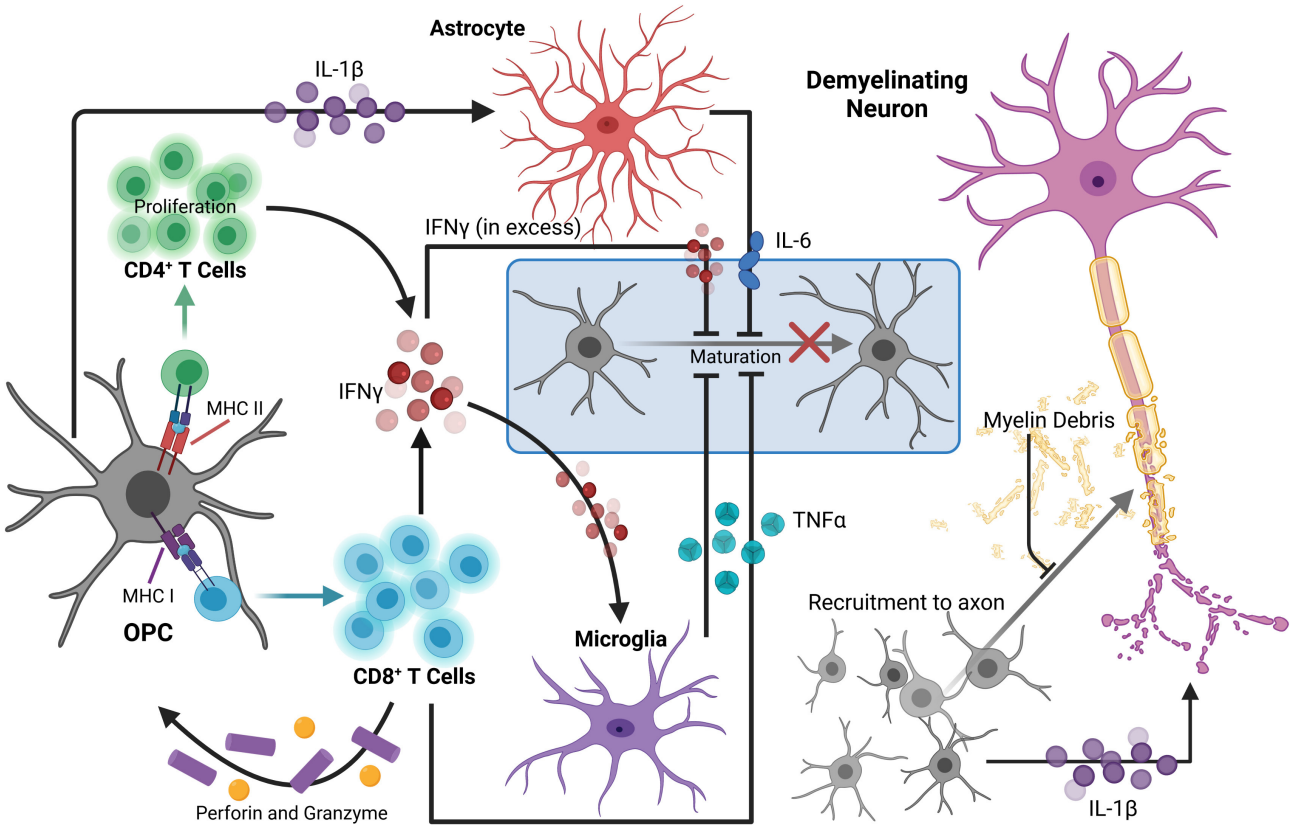

FIGURE 1 | OPCs contribute to the perpetuation of inflammation, leading to enhanced neurodegeneration in MS. During neuroinflammation, IFNγ can upregulate both MHC I and II antigen presentation molecules on OPCs to promote functional antigen presentation to $CD4^+$ and $CD8^+$ T cells, respectively. The antigen-MHC I complex can then induce TNFα and IFNγ expression by $CD8^+$ T cells, as well as perforin and granzyme secretion, which can contribute to localized OPC cell death. OPCs also promote proliferation of and cytokine production by $CD4^+$ memory and effector T cells via MHC II antigen presentation. TNFα produced by microglia in response to IFNγ signaling by T lymphocytes can also impair OPC differentiation. Excess extracellular IFNγ is associated with inhibition of OPC maturation and oligodendrocyte cell death. OPC expression of IL-1β is also increased by IFNγ signaling, and stimulates IL-6 production by astrocytes, which can directly reduce OPC differentiation capacity. IL-1β produced by OPCs may also contribute to neuronal cytotoxicity directly by enhancing cytotoxic glutamatergic synaptic transmission. Myelin debris from degenerating myelin sheathes repel OPCs, inhibiting recruitment and maturation. Taken together, in a neuroinflammatory state, there are many barriers limiting axonal support, repair, and remyelination by OL lineage cells that are perpetuated by OPCs themselves. Created with BioRender.com.

by $Olig1^+$ cells within active, demyelinating lesions and along the borders of chronic lesions (Moyon et al., 2015). Taken together, the upregulation of genes associated with chemotaxis as well as modulation of inflammatory responses demonstrates a more direct role for OPCs in neuroinflammation through active participation in immune cell recruitment.

Another way OPCs are known to contribute to neuroinflammatory processes is through their dynamic interactions with the CNS vasculature. Active lesion analysis of MS patient tissue showed OPC clustering around vessels, indicating impaired perivascular migration. Grouping of OPCs at these sites was found to result from abnormal Wnt signaling that prevented detachment of OPCs from vessels. This was demonstrated in several *in vivo* models and caused improper astrocytic endfeet interactions with the vasculature and altered integrity of endothelial tight junctions via release of Wif1, which reduced claudin-5 expression. The inability of OPCs to detach from CNS vasculature led to a deficiency in OPC recruitment to demyelinated areas as well as disruption of the BBB (Niu et al., 2019). OPCs have also been shown to mediate opening of the BBB just prior to demyelination in white matter injuries through upregulation of matrix metalloproteinase (MMP)9 in response to IL-1β (Seo et al., 2013). MMP9 mediates proteolysis of the basal lamina and tight junction proteins, which can contribute to BBB permeability and ultimately result in an influx of peripheral immune cells, further contributing to demyelination and chronic neuroinflammation (Mirshafiey et al., 2014).

Sustained inflammatory activity by OPCs may also contribute to neurodegeneration as a deviation toward this phenotype contributes to a dysregulation in myelin production, which critically impacts axonal survival and proper axon conduction (Lubetzki and Stankoff, 2014; Seidl, 2014). Specifically, OPCs in an immune reactive state have a reduced ability to differentiate, reducing their capacity to remyelinate lesioned areas due to a decline in newly formed OLs. Cytokine production by OPCs, such as the production of IL-1β, may impact differentiation

to OLs, as it is known to stimulate a number of cytotoxic cytokines from activated immune cells and glia, including IL-6 by astrocytes, which can inhibit OL maturation (Schonrock et al., 2000; Moore et al., 2015; Petkovic et al., 2016; **Figure 1**). TNFα produced by microglia in response to IFNγ signaling by T lymphocytes can also impair OPC maturation through processes such as mitochondrial dysfunction or cytotoxicity (Kim et al., 2011; Bonora et al., 2014). Likewise, excess extracellular IFNγ during acute inflammatory conditions has been associated with inhibition of OPC maturation and induction of OL cell death during MS (Vartanian et al., 1995; Falcao et al., 2018; Kirby et al., 2019; **Figure 1**). Furthermore, chronic MS lesions typically contain immature OPCs suggesting that OPCs are prevented from differentiating, rather than lost, and this may be a primary contributor to remyelination failure in some neurodegenerative diseases, including MS (Chang et al., 2002; Kuhlmann et al., 2008).

Finally, OPCs can contribute to neurodegeneration by directly or indirectly impacting neuron survival and function via cytokine signaling. IL-1β produced by OPCs may contribute to neuronal cytotoxicity as excessive IL-1β has been shown to enhance cytotoxic glutamatergic synaptic transmission, which results in p53-mediated apoptosis (Rossi et al., 2014a) (**Figure 1**). Additionally, stimulation of cytokine production from $CD4^+$ and $CD8^+$ T cells by OPC antigen presentation can negatively impact neuronal health. Notably, IFNγ has been heavily implicated in MS pathology, as it is known to promote Th1 responses (Olsson, 1992; Fletcher et al., 2010), but it may also impact neurons directly by enhancing glutamate toxicity through dysregulation of α-amino-3-hydroxy-5-methyl-4-isoxazolepropionic (AMPA) receptors, which results in calcium influx, nitric oxide (NO) production, and a decrease in mitochondrial function (Mizuno et al., 2008). Moreover, release of TNFα from T cells and other immune cells can also affect glutamatergic transmission in neurons by promoting sustained AMPA receptor activity. This sustained activity results in dendritic spine loss and alterations in synaptic activity, which also contributes to neurodegeneration (Centonze et al., 2009). As a result, the prevention of OPC immune reactivity presents an interesting avenue for the reduction of neuroinflammation and neurodegeneration, and may lead to novel treatment options for MS patients.

OPC INFLUENCERS DURING NEUROINFLAMMATION AND NEURODEGENERATION

Many of the factors that influence OPC function during neuroinflammation are downstream of the cytokines IFNγ, TNFα, and IL-1β (**Table 1**). While the inflammatory effects of these cytokines actively contribute to microglial-led degeneration (Brück et al., 1996; Pang et al., 2010; Domingues et al., 2016; Cignarella et al., 2020), these same factors are necessary not only for effective myelin debris clearance (Lampron et al., 2015), but also for providing many of the factors responsible for the migration of OPCs and fostering their maturation (Nicholas et al., 2002; Pasquini et al., 2011; Vogel et al., 2013). Many of these factors are secreted by other CNS resident cells including, but not exclusive to, microglia, astrocytes, and neurons (**Table 1**).

Cytokines

IFNγ is known to drive acute autoimmune neuroinflammation by activating antigen presenting cells, promoting the differentiation of Th1 cells, and regulating peripheral immune cell infiltration into the CNS (Lees et al., 2008; Fletcher et al., 2010). Astrocytes treated with IFNγ can promote the proliferation and differentiation of myelin-specific Th1 cells (Dong and Benveniste, 2001) and upregulate localizing cues to direct CNS immune cell entry during acute EAE (Rosenman et al., 1995; Williams et al., 2020). While the most characterized effects of IFNγ during acute disease are primarily pathogenic, the role of IFNγ signaling during chronic stages of MS and in models of neuroinflammation, when the presence of the peripheral immune cells are reduced, remain incompletely understood. In fact, there is mounting evidence to suggest that IFNγ also has protective functions, particularly during chronic disease (Furlan et al., 2001; Sosa et al., 2015; Sun et al., 2017a; Smith et al., 2020). Further, some discrepancy exists regarding the effects of IFNγ on OPCs, likely due to differences in dosage and/or model system. For example, *in vitro*, low levels of IFNγ, while non-apoptoic, were demonstrated to inhibit OPC cell cycle exit, which bolstered the population of immature OPCs and reduced maturation into $O1^+$ OLs (Chew et al., 2005). A later study also reported that even lower doses of IFNγ were not toxic to OPCs, but that IFNγ treatment led to a downregulation of the immature OPC marker platelet-derived growth factor receptor (PDGFR)α and the proliferative marker Ki-67, causing OPCs to reversibly exit the cell cycle (Tanner et al., 2011), which is necessary for maturation. Further, after sustained exposure to non-toxic, low-dose IFNγ, induced pluripotent stem cells from peripheral blood mononuclear cells from progressive MS patients differentiated into OL lineage cells had reduced differentiation (Morales Pantoja et al., 2020; Starost et al., 2020). This highlights the complexity of IFNγ signaling and need for further studies to elucidate its many roles during neuroinflammation and neurodegeneration.

TNFα is another pleiotropic cytokine with multiple disparate cellular responses including apoptosis, cell survival, and proliferation, and its function is receptor- and cell-context dependent (Locksley et al., 2001). In MS patients, TNFα expression was higher in lesions compared to non-inflammatory neurological disease controls and is detectible in the CSF (Cannella and Raine, 1995; Burman et al., 2014). However, following injection of TNFα into uninjured brains, OPCs did not upregulate NG2 expression, suggesting that exogenous TNFα alone does not activate OPCs *in vivo* (Rhodes et al., 2006). Although TNFα receptor (TNFR)1 is expressed by OPCs and is known to mediate neurotoxic functions (Su et al., 2011), TNFR2 signaling largely correlates with CNS repair and immune modulation either via activation in cells of the OL lineage themselves (Madsen et al., 2020) or in astrocytes or microglia, leading to downstream mediators of OL maturation and myelination (Patel et al., 2012; Fischer et al., 2014; Gao et al., 2017). Indeed, clinical trials using lenercept, an inhibitor

TABLE 1 | CNS-derived factors that modulate OPC function.

Factor	Type	Upstream Signal	Source	OPC Effect	Promote (+)/Inhibit (–)	References
CCL2	Chemokine	IL-1β	Astrocytes	Migration	+	Glabinski et al., 1996; Wang et al., 2014; Moyon et al., 2015
CCL3	Chemokine	IFNγ	Astrocytes Microglia	Migration	–	Couturier et al., 2016; Shen et al., 2021
CCL11	Chemokine	IFNγ TNFα	Astrocytes Microglia	Migration Proliferation Maturation	+/–	Maysami et al., 2006a; Ding et al., 2015; Parajuli et al., 2015
CXCL1	Chemokine	IL-1β	Astrocytes Microglia	Migration Proliferation	+	Robinson et al., 1998; Tsai et al., 2002; Omari et al., 2005; Karim et al., 2019; Michael et al., 2020
CXCL10	Chemokine	IFNγ	Astrocytes Microglia	Maturation	–	Luster et al., 1985; Vanguri and Farber, 1994; Xia et al., 2000; Tirotta et al., 2011; Moore et al., 2015
CXCL12	Chemokine	IL-1β TNFα	Astrocytes	Migration Proliferation Maturation	+	Maysami et al., 2006b; Patel et al., 2010; Cruz-Orengo et al., 2011; Luo et al., 2016
IFNγ	Cytokine	Other	Microglia	Proliferation Maturation	+/–	Chew et al., 2005; Lin et al., 2006; Tanner et al., 2011; Hindinger et al., 2012
IL-1β	Cytokine	Other	Astrocytes Microglia	Migration Proliferation Maturation	+/–	Vela et al., 2002; Wang et al., 2015; Zhou et al., 2017
IL-6	Cytokine	IL-1β	Astrocytes Microglia	Maturation	+/–	Schonrock et al., 2000; Moore et al., 2015; Petkovic et al., 2016
IL-11	Cytokine	IL-1β	Astrocytes	Proliferation Maturation	+	Zhang et al., 2006; Gurfein et al., 2009
LIF	Cytokine	IFNγ	Astrocytes	Maturation	+/–	Butzkueven et al., 2002; Stark et al., 2004; Ishibashi et al., 2006
TNFα	Cytokine	IFNγ	Microglia	Proliferation	+/–	Patel and Klein, 2011; Welser-Alves and Milner, 2013
Anosmin-1	ECM	Other	Astrocytes	Migration	–	Bribián et al., 2008
CSPGs (family)	ECM	IL-1β	Astrocytes	Migration Maturation	–	Anderson et al., 2016; Sun et al., 2017b
Fibronectin	ECM	Other	Astrocytes Microglia	Migration Maturation	+/–	Stoffels et al., 2013
Hyaluronan	ECM	Other	Astrocytes	Maturation	–	Back et al., 2005; Nair et al., 2008
Laminin	ECM	Other	Astrocytes	Proliferation Maturation	+	Chun et al., 2003
Tenascin-C	ECM	IFNγ	Astrocytes	Migration Proliferation	+/–	Garcion et al., 2001; Ogawa et al., 2005
Tenascin-R	ECM	Other	Astrocytes	Maturation	+	Czopka et al., 2009; Okuda et al., 2014
Vitronectin	ECM	Other	Astrocytes	Proliferation	+	Milner et al., 1999; Baron et al., 2002
BDNF	Growth Factor	TNFα	Astrocytes Microglia	Proliferation Maturation	+	Ferrini and De Koninck, 2013; Miyamoto et al., 2015

(Continued)

TABLE 1 | Continued

Factor	Type	Upstream Signal	Source	OPC Effect	Promote (+)/Inhibit (–)	References
CNTF	Growth Factor	Other	Astrocytes	Maturation	+	Dallner et al., 2002; Talbott et al., 2007
FGF2	Growth Factor	IL-1β	Astrocytes Microglia	Migration Proliferation	+	Clemente et al., 2011
IGF-1	Growth Factor	IL-1β IFNγ	Astrocytes Microglia	Proliferation Maturation	+	Mason et al., 2001; Lin et al., 2005; Butovsky et al., 2006
IGF-2	Growth Factor	IFNγ	Microglia	Maturation	+	Nicholas et al., 2002
NT3	Growth Factor	Other	Astrocytes	Proliferation	+	Wong et al., 2013
PDGF-AA	Growth Factor	TNFα	Astrocytes	Migration Proliferation	–	Silberstein et al., 1996; Fruttiger et al., 1999; Baron et al., 2000, 2002; Frost et al., 2003
VEGFA	Growth Factor	IL-1β IFNγ	Astrocytes	Migration	+	Hayakawa et al., 2011; Argaw et al., 2012
Triiodothyronine	Hormone	Other	Astrocytes	Maturation	+	Dugas et al., 2012; Dezonne et al., 2013
Prostaglandin E_2	Lipid	IL-1β	Astrocytes Microglia	Maturation	–	Marusic et al., 2005; Shiow et al., 2017
Adenosine	Neurotransmitter	Other	Neuron	Proliferation Maturation	+	Stevens et al., 2002; Safarzadeh et al., 2016
ATP	Neurotransmitter	IFNγ	Astrocytes Neurons	Migration Maturation	+/–	Verderio and Matteoli, 2001; Agresti et al., 2005; Hamilton et al., 2010
GABA	Neurotransmitter	IL-1β	Neuron	Migration	+	Lin and Bergles, 2004; Tong et al., 2009
Glutamate	Neurotransmitter	IL-1β	Astrocytes Neuron	Migration Maturation	+	Haberlandt et al., 2011; Zonouzi et al., 2011; Li et al., 2013; Xiao et al., 2013
BMP2, 4, 6, and 7	Protein	IFNγ	Astrocytes Neurons	Maturation	–	Ara et al., 2008; Miyagi et al., 2012
Galactin-3	Protein	Other	Astrocytes Microglia	Maturation	+	Pasquini et al., 2011; Itabashi et al., 2018; Thomas and Pasquini, 2018; Ramírez Hernández et al., 2020
Semaphorin 3A	Protein	Other	Astrocytes Microglia	Migration	–	Spassky et al., 2002; Syed et al., 2011; Yamaguchi et al., 2012
Semaphorin 3F	Protein	Other	Astrocytes Microglia	Migration	+	Spassky et al., 2002
Semaphorin 4D	Protein	Other	Astrocytes Microglia	Migration	–	Spassky et al., 2002; Yamaguchi et al., 2012
TIMP-1	Protein	IL-1β	Astrocytes	Maturation	+	Crocker et al., 2006; Welser-Alves et al., 2011; Nicaise et al., 2019b
Wnt (family)	Protein	IL-1β TNFα	Astrocytes Neurons	Maturation	+/–	Fancy et al., 2009; Feigenson et al., 2009; Edara et al., 2020; Guérit et al., 2021
Retinoic Acid	Morphogen	Other	Astrocytes	Proliferation Maturation	+	van Neerven et al., 2010; Shearer et al., 2012; Morrison et al., 2020

of TNFR1 action, resulted in increased frequency, duration, and severity of MS relapses (1999).

IL-1 signaling has also been implicated in both MS pathogenesis and repair and has many roles within the CNS. It is thought to have many functions in the promotion of the inflammatory response as mice deficient in IL-1 receptors are protected from the development of neuroinflammation and EAE (Matsuki et al., 2006). Further, IL-1β in particular, is found to be highly concentrated in MS lesions, and is likewise increased in the CSF of MS patients (Cannella and Raine, 1995; Rossi et al., 2014b). Conversely, IL-1β was necessary for remyelination after CPZ-induced demyelination of the corpus callosum, as IL-1β-deficient animals had reduced IGF-1 production, delaying OPC maturation (Mason et al., 2001). Despite its role in promoting growth factor production necessary for CNS repair, like TNFα, IL-1β is thought to be a risk factor in MS (De Jong et al., 2002). Given the many targets of IFNγ, TNFα, and IL-1β, their prominent roles in cell-cell communication within the CNS, and variations in their expression over the course of acute and chronic neuroinflammatory disease, these cytokines remain relevant targets of MS research.

Cell Types

Microglia

Microglia are considered the resident macrophage of the CNS. They originate from early yolk sac progenitors (Ginhoux et al., 2010; Kierdorf et al., 2013; Gomez Perdiguero et al., 2015) and are critical for proper CNS development, maintaining homeostasis, and mounting an inflammatory response in the event of a pathogenic insult (Butovsky and Weiner, 2018). Microglia are self-renewing via stable turnover throughout the lifespan and are maintained without the contribution of peripheral monocytes under homeostatic conditions (Askew et al., 2017). It is well-established that microglia heavily impact neuronal function, refining synapse connectivity and providing trophic support (Paolicelli et al., 2011; Schafer et al., 2012). They also have sophisticated communication networks with other glia including astrocytes and OPCs (Domingues et al., 2016; Linnerbauer et al., 2020). Like all glial subtypes, microglia exhibit a high degree of heterogeneity and plasticity (Bottcher et al., 2019; Masuda et al., 2020), are heavily influenced by the microenvironment, and can significantly contribute to neuroinflammation and CNS recovery (Gosselin et al., 2014; Lavin et al., 2014; Voet et al., 2019).

OPCs have differing responses to the various inflammatory states of microglia, partially due to a difference in trophic factors expressed by specific activation states (Pang et al., 2000, 2010; Domingues et al., 2016; Hagemeyer et al., 2017; **Figure 2**). Classically activated microglia are highly inflammatory and tend to inhibit OPC differentiation (Kigerl et al., 2009) as well as induce pro-apoptotic signals via excessive TNFα signaling. Comparatively, steady-state microglia aid OPCs primarily via the secretion of various trophic factors (Hanisch and Kettenmann, 2007; Hagemeyer et al., 2017), which are typically aimed at maintaining homeostasis and facilitating OPC proliferation (**Table 1**). As such, these quiescent microglia tend to secrete IGF-2 and galectin-2, which prompt OPC proliferation and prime OPCs for other differentiation signals (Nicholas et al., 2001, 2002; Pasquini et al., 2011; Hoyos et al., 2014; **Figure 2**). Likewise, alternatively activated microglia also express many of the same trophic factors secreted by both steady-state and highly inflammatory microglia, but in more moderate amounts (Domingues et al., 2016; Cignarella et al., 2020; Wang et al., 2020). These alternatively activated microglia express more galectin-2 than steady-state microglia, which further promote OPCs differentiation (Nicholas et al., 2002; Pasquini et al., 2011; Hoyos et al., 2014). Additionally, they produce moderate amounts of TNFα and NO, which did not exert cytotoxic effects and promoted OPC differentiation (Nicholas et al., 2002; De Jager et al., 2009; Karamita et al., 2017). Of note, while steady-state, classically activated, and alternatively activated microglia are well-studied, disease settings present a host of intermediate and unique activation states that lead to responses that are widely varied (Brück et al., 1996; Miron et al., 2013; Domingues et al., 2016; Wang et al., 2020).

In addition to the secretion of various inflammatory and/or tissue protective factors, microglia significantly alter the microenvironment through their phagocytic functions. During MS, microglia are the primary contributors to the clearance of myelin debris (Davalos et al., 2005; Lampron et al., 2015; Lloyd and Miron, 2019; Cignarella et al., 2020). Without myelin debris removal, proper remyelination by OPCs is significantly hindered, regardless of the remyelination-promoting factors present (Lampron et al., 2015; Cignarella et al., 2020; **Figure 1**). Myelin debris also contributes to inflammation and can activate microglia (Williams et al., 1994; Vogel et al., 2013). Within chronic-active lesions, the lesion edge houses a majority of the myelin debris, which promotes the formation of the microglial ring and enhances inflammatory activation (Frischer et al., 2015; Kuhlmann et al., 2017). Excessive activation of microglia can further damage OLs, contributing to the slowly expanding nature of chronic-active lesions (Dal-Bianco et al., 2017; Calvi et al., 2020). During active clearance, microglia also send inhibitory signals that block OPC migration and differentiation (Williams et al., 1994; Vogel et al., 2013; Lampron et al., 2015). As myelin debris is cleared, inflammation is typically reduced and OPCs lose the inhibitory signals from the highly activated microglia ringing the lesion (Williams et al., 1994; Vogel et al., 2013; Dal-Bianco et al., 2017; Calvi et al., 2020). However, at this point in neurodegeneration, neurons have largely died and the glial scar has begun forming (Brück et al., 1996; Voskuhl et al., 2009; Kuhlmann et al., 2017), creating new barriers for OPC differentiation.

Astrocytes

Astrocytes have numerous essential roles in nearly all aspects of CNS function and to meet the complex needs of their surroundings, astrocytes are highly heterogenous. During homeostatic conditions, astrocytes provide many neurotropic factors, promoting the survival and growth of surrounding neurons and glia (Escartin et al., 2021; **Figure 2**). However, we and others have shown that during inflammatory events, such as in MS and EAE, astrocytes are highly responsive to cytokines and inflammatory mediators (Zhang and Barres, 2010; Daniels et al., 2017; John Lin et al., 2017; Smith et al., 2020; Williams et al.,

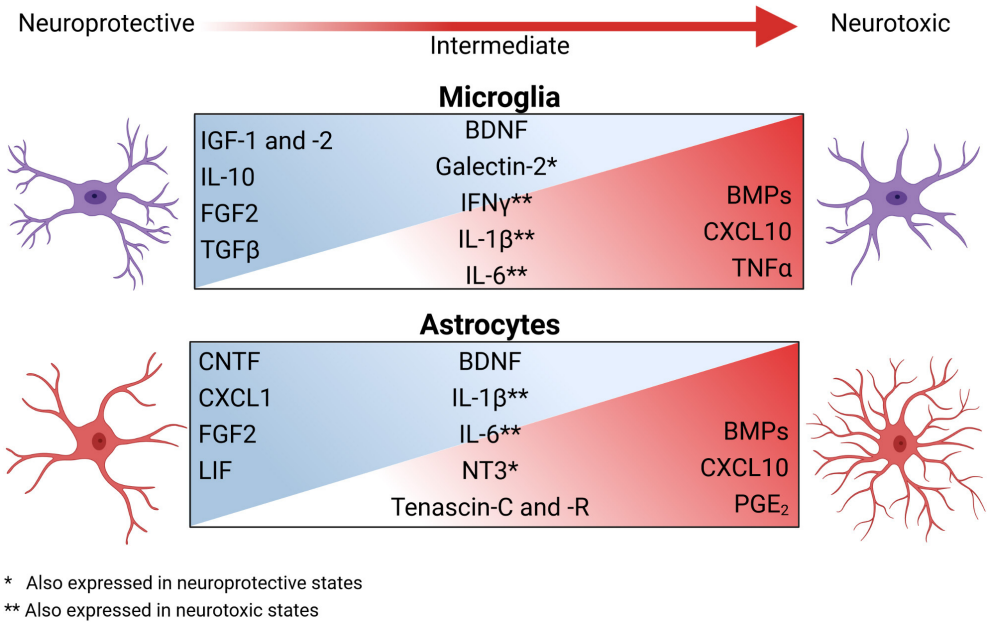

FIGURE 2 | The secretory profiles of glia change across the spectrum of reactive phenotypes and have broad impacts on OPC function during neuroinflammation and neurodegeneration. During homeostasis, astrocytes and microglia interact with other CNS resident cells to help maintain a homeostatic environment via the secretion of trophic factors. During neuroinflammation, the microenvironment changes both cellularly and molecularly to shift the activation state of these glia, inducing a spectrum of glial secretory profiles. Factors secreted during this shift include growth factors, cytokines, survival signals, and ECM modulators. Classically activated microglia and astrocytes are highly inflammatory and significantly contribute to microenvironmental neurotoxicity and inhibit OPCs by secreting bone morphogenic proteins (BMPs), chemokines, cytokines, and prostaglandin E2 (PGE_2). As inflammation resolves, the reactive state of microglia and astrocytes again promote the reparative properties of OPCs. Created with BioRender.com.

2020). This diverse astrocytic response is critical in healthy tissue preservation and reducing prolonged CNS exposure to cytotoxic mediators. Indeed, ablation of astrocytes following several types of CNS injury led to sustained inflammation, impaired BBB repair, and increased neurodegeneration (Bush et al., 1999; Faulkner et al., 2004; Gao et al., 2005; Sofroniew, 2005; Myer et al., 2006; Voskuhl et al., 2009; Arai and Lo, 2010; Hayakawa et al., 2014; Anderson et al., 2016; Liddelow and Barres, 2017).

Reactive astrocytes act in concert with other CNS cells to sustain the neuroinflammatory response necessary for the resolution of pathogenic threats to the CNS. As is the case with microglia, OPCs respond differently to varying activation states of astrocytes (Su et al., 2011; Voskuhl et al., 2019; Willis et al., 2020). As concluded recently, the binary division of reactive astrocytes into neurotoxic and neuroprotective is far too limited to capture the diverse astrocytic subsets (Escartin et al., 2021). Astrocytes can heavily influence OPC function via their effect on the microenvironment (Kiray et al., 2016) and by modulating the extracellular matrix (ECM) (Risau and Wolburg, 1990; Sixt et al., 2001). Traditionally, the ECM is described as a scaffolding on which OPCs traffic to reach demyelinated areas in need of repair (Hu et al., 2009). More recently, the ECM deposited by astrocytes was also shown to provide directional cues to OPCs and specific signals to initiate differentiation (Lau et al., 2013; Wang et al., 2017). Modulatory components of the ECM that can affect the ability of OPCs to migrate, proliferate, or differentiate include fibronectin, anosmin-1, laminin, hyaluronan, and several members of the chondroitin sulfate proteoglycan (CSPG) family, along with many other ECM modifiers (Benarroch, 2015; **Table 1**). Of note, inflammatory astrocytes tend to express the ECM proteins tenascin C and R, which inhibit migration of OPCs while simultaneously promoting OPC differentiation (Frik et al., 2018; **Table 1**). While it is thought that the timing and level of astrocyte activation significantly influences the migration and differentiation of OPCs via modulation of the ECM, the exact role of the differing astrocytic subtypes on modification of the ECM is complex and an area of active research, which was recently reviewed in detail (Ghorbani and Yong, 2021).

Astrocytes modify the microenvironment beyond modulating the ECM. The most neurotoxic astrocytes cause cellular damage (Liddelow et al., 2017); however, not only do more neuroprotective astrocytes promote a more trophic environment, recent evidence shows that intermediates between these subtypes can mediate a wider variety of beneficial effects (Teo and Bourne, 2018; Bhatia et al., 2019; **Figure 2**). A spectrum of reactive astrocyte states are implicated in OPC migration, proliferation, and differentiation (Nutma et al., 2020; Wheeler et al., 2020; Escartin et al., 2021) and produce some inflammatory factors, which are necessary for myelin debris removal and a return to a stable microenvironment (Erta et al., 2012; Traiffort et al., 2020). For example, leukemia inhibitor factor (LIF), fibroblast growth factor (FGF)2, and ciliary neurotropic factor (CNTF) are expressed by astrocytes that are categorized as non-reactive, neuroprotective, and/or in an intermediate reactive

state (Aloisi et al., 1994; Müller et al., 2007; Delgado-Rivera et al., 2009; **Figure 2**). Further, astrocytes may contribute to a return to tissue homeostasis via IFNγ-mediated upregulation of the immunoproteasome to degrade oxidatively damaged proteins and clear oxygen radicals at sites of inflammation (Smith et al., 2020). As with ECM-modifying factors, the microenvironment established by astrocytes is a balance of timing and level of response (Ponath et al., 2018). One prime example of the breakdown of this balance is the formation of the glial scar. The glial scar forms in chronic lesions in response to severe damage and consists primarily of reactive astrocytes (Dal-Bianco et al., 2017; Kuhlmann et al., 2017; Adams and Gallo, 2018). Traditionally, the glial scar is viewed as a double-edged sword, in that it limits the initial damage but precludes regeneration as reviewed by Adams and Gallo (2018). However, other evidence suggests that the glial scar releases trophic factors responsible for neuronal growth and OPC proliferation, migration, and survival including brain-derived neurotrophic factor (BDNF) and neurotrophin (NT)3 (Anderson et al., 2016; Haindl et al., 2019; **Figure 2**; **Table 1**). However, while axons within glial scars in other models remyelinate (Bradbury and Burnside, 2019), those in MS lesions are less likely to, particularly in lesions surrounded by an inflammatory border (Dal-Bianco et al., 2017; Kuhlmann et al., 2017). These lesions that progress from chronic active to the inactive quiescent state have very little if any remyelination due to the inability of OPCs to migrate (Kornek et al., 2000; Li et al., 2016).

Neurons

Neuronal communication with OPCs via neurotransmitters is altered in MS and in MS models. Early studies suggested glutamate signaling may block OPC proliferation (Gallo et al., 1996; Yuan et al., 1998); however, using lysolecithin, it was later found that demyelinated axons formed functional glutamatergic synapses with OPCs that migrated from the subventricular zone. As OPCs matured into OLs, glutamatergic signaling was lost, indicating a potential role for glutamate in the migration of OPCs to lesioned areas (Etxeberria et al., 2010). Another neurotransmitter, gamma-aminobutyric acid (GABA), while excitatory during development, is the primary inhibitory neurotransmitter in the mammalian CNS. OPCs express the GABA-A receptor and endogenous GABA may also affect OPC migration by inhibiting AMPA receptor-mediated glutamatergic signaling (Lin and Bergles, 2004). Additionally, GABA promoted OPC migration in rat brain slice cultures (Tong et al., 2009) and neuronal GABA signaling is impaired in EAE, particularly in the striatum (Rossi et al., 2011), along with excessive glutamate activity (Centonze et al., 2009). There are several indications that neurotransmitters play an important role in the function of OPCs during neuroinflammation; however, the precise mechanisms that may enhance or prevent neurodegeneration are yet to be fully elucidated.

In response to neuronal action potentials, OPCs upregulate adenosine receptors, which are largely beneficial. Adenosine is known to inhibit OPC proliferation and stimulate cell cycle exit via A1 adenosine receptors (A_1ARs), allowing OPCs to differentiate into myelinating OLs (Stevens et al., 2002). Activation of A_1ARs on OPCs was later shown to also promote migration (Othman et al., 2003). During EAE, A_1AR-deficient mice had worsened axonal injury, demyelination, as well as upregulation of pro-inflammatory factors by microglia/macrophages resulting in enhanced OL death (Tsutsui et al., 2004). Conversely, stimulation of A_{2A} receptors inhibits OPC maturation, which is in contrast to the oligodendrogenesis promoting effects of A_{1A}Rs (Coppi et al., 2013). Since OPCs form synapses with neurons during development and are electrically active (Káradóttir et al., 2008), it is believed that restoration of normal electrical activity in neurons could aid in remyelination and recovery from demyelinating insults. A study using lysolecithin-induced lesions showed that demyelinated axons were still able to propagate action potentials, which promoted OPC differentiation and remyelination within the lesion. This corresponded to an activity-dependent increase in the OPC pool in mice that received repeated neuronal electrical stimulation (Ortiz et al., 2019). While there is dysregulation of neuron-OPC crosstalk during ongoing neuroinflammation, the primary source of the secreted OPC-modulating factors are lymphocytes, microglia/macrophages, and astrocytes. Although neurons rely on myelin and mature OL support for proper functioning, they are nonetheless an important contributor to neuroinflammatory pathology and are critical to OPC-mediated CNS repair.

EFFECTS OF AGING ON OPCs

Aging is a significant risk factor for most neurodegenerative disorders (Minden et al., 2004; Hou et al., 2019), and is correlated with a more progressive disease course in patients diagnosed with MS over the age of 40 (Scalfari et al., 2011). With advancing age, MS disease progression tends to shift toward a less inflammatory, neurodegenerative state, as only one-third of patients continue with RRMS past the age of 75 (Tutuncu et al., 2013; Scalfari et al., 2014). The potential for clinical recovery is reduced with age and can ultimately contribute to neurodegeneration (Sanai et al., 2016). Specifically, as both patient age and disease duration increase, demyelination becomes more infrequent due to a decrease in acute inflammatory events; however, the capacity of OPCs to remyelinate damaged neurons also becomes impaired (Bramow et al., 2010; Ruckh et al., 2012). Previously demyelinated axons risk long-term exposure to chronic inflammation and can become irreversibly damaged as a result (Kornek et al., 2000).

Age-related remyelination failure has been linked to suppression of OPC differentiation as large pools of undifferentiated OL lineage cells were present in chronically demyelinated MS lesions in post-mortem tissue (Boyd et al., 2013). It has also been shown that functionally, OPCs become regionally heterogenous with age, suggesting that particular areas of the CNS may be at greater risk for long-term damage (Spitzer et al., 2019). Rat OPC cultures harvested from young (2–3 months) and aged (20–24 months) cohorts *in vitro* showed that the aged OPCs had a reduced capacity for differentiation.

They also lacked proliferative growth factors, as roughly 20% expressed mature OL markers compared to 60% by OPCs from younger animals. Moreover, treatment of aged OPCs with maturation stimulating factors failed to increase the population of mature OLs efficiently, requiring weeks of additional time to fully mature compared to young OPCs, suggesting that aging induces intrinsic changes within OPCs that restrict their response to extracellular differentiation signals (Neumann et al., 2019). In another study, *in situ* hybridization analysis of OPCs in young (8–10 weeks) and aged (>1 year) rats undergoing EtBr-mediated demyelination revealed that OPCs in aged animals were recruited to the lesion site more slowly. Transcript levels of the OPC markers *Pdgfra* and *MyT1* were comparatively retained in aged rats and mature OL markers of *Mbp* and *Gtx* were delayed, indicative of impaired differentiation (Sim et al., 2002).

The intrinsic changes associated with both OPC differentiation and recruitment may be linked to cellular senescence, or the cessation of the cell cycle and a deviation from normal cell function toward an inflammatory state (Gorgoulis et al., 2019). Considered a hallmark of normal aging, cellular senescence is induced by a variety of stress signals related to DNA damage such as oxidative stress and release of inflammatory cytokines, all of which are associated with MS pathology (Haider et al., 2011; Elkjaer et al., 2019). In addition, cells that are senescent maintain the ability to release these factors, promoting cellular senescence in neighboring cells through paracrine signaling and generating pools of senescent cells that accumulate over time (Dimri et al., 1995; Ressler et al., 2006; Acosta et al., 2013). Aged OPCs have elevated levels of DNA damage as well as increased mRNA transcript levels of cellular senescence markers including *Cdkn2a* (Neumann et al., 2019). Upregulation of additional markers, such as senescence-associated beta-galactosidase, on $SOX2^{+}$ OPCs resulted in inhibited differentiation suggesting that functional inhibition of OPC recruitment and differentiation may be partially explained by a shift toward a senescent phenotype (Nicaise et al., 2019a). Cellular senescence is not confined to cells with stem-like properties; it has also been documented in glial cells (Kritsilis et al., 2018), and may further affect the capacity of OPCs to mature and facilitate repair of damaged axons. Specifically, transcript analysis of astrocytes from young and aged rats showed an upregulation of genes associated with both senescence and inflammation such as *Mmp3*, *p53*, and *p21* in older astrocytes compared to those from younger rats. Similarly, there was a decrease in aged cells undergoing the G2 and S phases of the cell cycle, which was accompanied by an increase in cells associated with the G1 phase, demonstrating inhibited astrocytic proliferation (Willis et al., 2020).

Astrocytes are crucial for maintaining CNS microenvironments conducive to homeostasis and proper OPC function (Liedtke et al., 1996; Gadea et al., 2009; Kiray et al., 2016). One way astrocytes regulate the microenvironment is through release of extracellular vesicles. These vesicles are not exempt from age-related cellular effects, as vesicles purified from aged astrocytes had a reduced ability to support OPC differentiation (Willis et al., 2020), suggesting that age-induced senescence of other CNS resident cells may contribute to deficient remyelination in chronic MS lesions and can affect the remyelinating capacity of OPCs specifically. Another critical extrinsic microenvironmental cue that modulates OPC function is the mechanical stiffness of the progenitor niche. In an elegant study by Segel et al., interrogation of the OPC microenvironment revealed increased stiffness with age, which caused a loss of function of OPCs. This was reversed using scaffolds to mimic the "young" microenvironment, suggesting tissue stiffness is a critical regulator of aged OPCs (Segel et al., 2019a,b). Notably, apelin-APJ signaling in OL lineage cells increases the capacity for maturation, and a decrease in signaling has been implicated as a key factor in age-related remyelination impairment. Recently, activity of the APJ pathway has been shown to be significantly downregulated with age, as the primary ligand, apelin, is decreased in the plasma of older mice and correlates with APJ deficiency-induced hypomyelination in neonatal mice during development. Furthermore, mice induced with EAE as well as with toxin-mediated demyelination showed increased remyelination with activation of the APJ pathway *in vivo*, while also promoting transcript signatures of mature OLs in human OPCs (Ito et al., 2021). Stimulation of pro-differentiation pathways may be a viable treatment option to reverse the effects of aging on remyelination capacity and assist in reducing neurodegeneration in progressive stages of MS.

CONCLUDING REMARKS

While it is clear that resident CNS cells contribute to ongoing inflammation during MS, the complexity of the signaling events in various cells types, the interactions between those cells, and the role these processes have in neurodegeneration are only beginning to be understood. This intricate cellular and molecular symphony can also vary widely depending on the subtype of MS, the stage of disease, and the age of the patient. Since remyelination failure is a significant roadblock in the treatment of MS (Franklin, 2002; Gruchot et al., 2019; Galloway et al., 2020), many early studies have focused on promoting OPC maturation to promote remyelination and prevent axon degeneration. Additionally, using multiple animal models of MS that recapitulate several aspects of the human disease, OPCs were shown to not only prevent neurodegeneration by participating in remyelination, but disease-specific OPCs were also identified and have the ability to present antigen to T cells, exacerbating neuroinflammation (Falcao et al., 2018; Kirby et al., 2019; **Figure 1**). Therefore, while elucidating the obstacles impeding remyelination is certainly critical to improve treatment options for MS patients and initiate recovery, more recent evidence suggests that OPCs have a much more versatile role in neuroinflammation and neurodegeneration, offering additional OPC-specific therapeutic targets.

In addition to factors intrinsic to OPC function during neuroinflammation and neurodegeneration in MS, there are a multitude of factors that impact the MS lesion

microenvironment that critically regulate OPC migration, proliferation, and maturation (**Figure 2**; **Table 1**). Primary contributors to the inflammatory milieu are cytokines, which can be secreted from infiltrating peripheral leukocytes as well as other glia including microglia and astrocytes. Inflammatory cytokines like IFNγ, TNFα, and IL-1β are well-described in the literature as perpetuating inflammation by activation of infiltrated immune cells and surrounding glia and inducing cell death and damage to OLs, leading to demyelination and eventual neurodegeneration, particularly in early disease phases like RRMS. However, depending on the concentration, the responding cell type, and the receptors through which they signal, these same cytokines can have a variety of neuroprotective effects. Further, the activation state of neighboring microglia and astrocytes can strongly influence how OPCs respond to demyelinating insults by altering the ECM or the profile of trophic factors that they secrete (**Figure 2**), positioning OPCs at the center of many neuroinflammatory and neurodegenerative processes.

AUTHOR CONTRIBUTIONS

JW generated the concept design. MP, BS, RT, and JW wrote and edited this manuscript. MP created the figures. MP, BS, and RT created the table. All authors contributed to the article and approved the submitted version.

FUNDING

This work was supported by the National Institute of Neurological Disorders and Stroke (NINDS) research grant R01 NS119178 awarded to JW.

ACKNOWLEDGMENTS

The authors thank Dr. Cornelia Bergmann for offering her expertise and for thoughtful and thorough editing of the viral encephalomyelitis section and acknowledge Dr. Maksim Sinyuk for his contributions to the genesis of this review.

REFERENCES

(1999). TNF neutralization in MS: results of a randomized, placebo-controlled multicenter study. The Lenercept Multiple Sclerosis Study Group and The University of British Columbia MS/MRI Analysis Group. *Neurology* 53, 457–465. doi: 10.1212/WNL.53.3.457

Absinta, M., Sati, P., Fechner, A., Schindler, M. K., Nair, G., and Reich, D. S. (2018). Identification of chronic active multiple sclerosis lesions on 3T MRI. *Am. J. Neuroradiol.* 39, 1233–1238. doi: 10.3174/ajnr.A5660

Absinta, M., Sati, P., Masuzzo, F., Nair, G., Sethi, V., Kolb, H., et al. (2019). Association of chronic active multiple sclerosis lesions with disability *in vivo*. *JAMA Neurol.* 76, 1474–1483. doi: 10.1001/jamaneurol.2019.2399

Acosta, J. C., Banito, A., Wuestefeld, T., Georgilis, A., Janich, P., Morton, J. P., et al. (2013). A complex secretory program orchestrated by the inflammasome controls paracrine senescence. *Nat. Cell. Biol.* 15, 978–990. doi: 10.1038/ncb2784

Adams, K. L., and Gallo, V. (2018). The diversity and disparity of the glial scar. *Nat. Neurosci.* 21, 9–15. doi: 10.1038/s41593-017-0033-9

Agresti, C., Meomartini, M. E., Amadio, S., Ambrosini, E., Volonté C., Aloisi, F., et al. (2005). ATP regulates oligodendrocyte progenitor migration, proliferation, and differentiation: involvement of metabotropic P2 receptors. *Brain. Res. Rev.* 48, 157–165. doi: 10.1016/j.brainresrev.2004.12.005

Ajami, B., Bennett, J. L., Krieger, C., Mcnagny, K. M., and Rossi, F. M. V. (2011). Infiltrating monocytes trigger EAE progression, but do not contribute to the resident microglia pool. *Nat. Neurosci.* 14, 1142–1149. doi: 10.1038/nn.2887

Aloisi, F., Rosa, S., Testa, U., Bonsi, P., Russo, G., Peschle, C., et al. (1994). Regulation of leukemia inhibitory factor synthesis in cultured human astrocytes. *J. Immunol.* 152, 5022–5031.

Alvarez, J. I., Saint-Laurent, O., Godschalk, A., Terouz, S., Briels, C., Larouche, S., et al. (2015). Focal disturbances in the blood–brain barrier are associated with formation of neuroinflammatory lesions. *Neurobiol. Dis.* 74, 14–24. doi: 10.1016/j.nbd.2014.09.016

Anderson, M. A., Burda, J. E., Ren, Y., Ao, Y., O'shea, T. M., Kawaguchi, R., et al. (2016). Astrocyte scar formation aids central nervous system axon regeneration. *Nature* 532, 195–200. doi: 10.1038/nature17623

Ara, J., See, J., Mamontov, P., Hahn, A., Bannerman, P., Pleasure, D., et al. (2008). Bone morphogenetic proteins 4, 6, and 7 are up-regulated in mouse spinal cord during experimental autoimmune encephalomyelitis. *J. Neurosci. Res.* 86, 125–135. doi: 10.1002/jnr.21462

Arai, K., and Lo, E. H. (2010). Astrocytes protect oligodendrocyte precursor cells via MEK/ERK and PI3K/Akt signaling. *J. Neurosci. Res.* 88, 758–763. doi: 10.1002/jnr.22256

Argaw, A. T., Asp, L., Zhang, J., Navrazhina, K., Pham, T., Mariani, J. N., et al. (2012). Astrocyte-derived VEGF-A drives blood-brain barrier disruption in CNS inflammatory disease. *J. Clin. Invest.* 122, 2454–2468. doi: 10.1172/JCI60842

Askew, K., Li, K., Olmos-Alonso, A., Garcia-Moreno, F., Liang, Y., Richardson, P., et al. (2017). Coupled proliferation and apoptosis maintain the rapid turnover of microglia in the adult brain. *Cell. Rep.* 18, 391–405. doi: 10.1016/j.celrep.2016.12.041

Back, S. A., Tuohy, T. M., Chen, H., Wallingford, N., Craig, A., Struve, J., et al. (2005). Hyaluronan accumulates in demyelinated lesions and inhibits oligodendrocyte progenitor maturation. *Nat. Med.* 11, 966–972. doi: 10.1038/nm1279

Bai, C. B., Sun, S., Roholt, A., Benson, E., Edberg, D., Medicetty, S., et al. (2016). A mouse model for testing remyelinating therapies. *Exp. Neurol.* 283, 330–340. doi: 10.1016/j.expneurol.2016.06.033

Barkauskas, D. S., Dixon Dorand, R., Myers, J. T., Evans, T. A., Barkauskas, K. J., Askew, D., et al. (2015). Focal transient CNS vessel leak provides a tissue niche for sequential immune cell accumulation during the asymptomatic phase of EAE induction. *Exp. Neurol.* 266, 74–85. doi: 10.1016/j.expneurol.2015.02.018

Barkhof, F., Brück, W., De Groot, C. J. A., Bergers, E., Hulshof, S., Geurts, J., et al. (2003). Remyelinated lesions in multiple sclerosis: magnetic resonance image appearance. *Arch. Neurol.* 60, 1073–1081. doi: 10.1001/archneur.60.8.1073

Baron, W., Metz, B., Bansal, R., Hoekstra, D., and de Vries, H. (2000). PDGF and FGF-2 signaling in oligodendrocyte progenitor cells: regulation of proliferation and differentiation by multiple intracellular signaling pathways. *Mol. Cell. Neurosci.* 15, 314–329. doi: 10.1006/mcne.1999.0827

Baron, W., Shattil, S. J., and Ffrench-Constant, C. (2002). The oligodendrocyte precursor mitogen PDGF stimulates proliferation by activation of αvβ3 integrins. *EMBO J.* 21, 1957–1966. doi: 10.1093/emboj/21.8.1957

Basler, M., Mundt, S., Muchamuel, T., Moll, C., Jiang, J., Groettrup, M., et al. (2014). Inhibition of the immunoproteasome ameliorates experimental autoimmune encephalomyelitis. *EMBO. Mol. Med.* 6, 226–238. doi: 10.1002/emmm.201303543

Bates, D. (2011). Treatment effects of immunomodulatory therapies at different stages of multiple sclerosis in short-term trials. *Neurology* 76:S14. doi: 10.1212/WNL.0b013e3182050388

Baxi, E. G., Debruin, J., Tosi, D. M., Grishkan, I. V., Smith, M. D., Kirby, L. A., et al. (2015). Transfer of myelin-reactive th17 cells impairs endogenous remyelination in the central nervous system of cuprizone-fed mice. *J. Neurosci.* 35, 8626–8639. doi: 10.1523/JNEUROSCI.3817-14.2015

Baxter, A. G. (2007). The origin and application of experimental autoimmune encephalomyelitis. *Nat. Rev. Immunol.* 7, 904–912. doi: 10.1038/nri2190

Begolka, W. S., Haynes, L. M., Olson, J. K., Padilla, J., Neville, K. L., Dal Canto, M., et al. (2001). CD8-deficient SJL mice display enhanced susceptibility to Theiler's virus infection and increased demyelinating pathology. *J. Neurovirol.* 7, 409–420. doi: 10.1080/135502801753170264

Belbasis, L., Bellou, V., Evangelou, E., Ioannidis, J. P., and Tzoulaki, I. (2015). Environmental risk factors and multiple sclerosis: an umbrella review of systematic reviews and meta-analyses. *Lancet Neurol.* 14, 263–273. doi: 10.1016/S1474-4422(14)70267-4

Benarroch, E. E. (2015). Extracellular matrix in the CNS. *Neurology* 85:1417. doi: 10.1212/WNL.0000000000002044

Bender, S. J., Phillips, J. M., Scott, E. P., and Weiss, S. R. (2010). Murine coronavirus receptors are differentially expressed in the central nervous system and play virus strain-dependent roles in neuronal spread. *J. Virol.* 84, 11030–11044. doi: 10.1128/JVI.02688-09

Bender, S. J., and Weiss, S. R. (2010). Pathogenesis of murine coronavirus in the central nervous system. *J. Neuroimmune Pharmacol.* 5, 336–354. doi: 10.1007/s11481-010-9202-2

Bergmann, C. C., Lane, T. E., and Stohlman, S. A. (2006). Coronavirus infection of the central nervous system: host–virus stand-off. *Nat. Rev. Microbiol.* 4, 121–132. doi: 10.1038/nrmicro1343

Bergmann, C. C., Parra, B., Hinton, D. R., Ramakrishna, C., Dowdell, K. C., Stohlman, S., et al. (2004). Perforin and gamma interferon-mediated control of coronavirus central nervous system infection by CD8 T cells in the absence of CD4 T cells. *J. Virol.* 78, 1739–1750. doi: 10.1128/JVI.78.4.1739-1750.2004

Bergmann, C. C., Ramakrishna, C., Kornacki, M., and Stohlman, S. (2001). Impaired T cell immunity in B cell-deficient mice following viral central nervous system infection. *J. Immunol.* 167, 1575–1583. doi: 10.4049/jimmunol.167.3.1575

Bhatia, T. N., Pant, D. B., Eckhoff, E. A., Gongaware, R. N., Do, T., Hutchison, D. F., et al. (2019). Astrocytes do not forfeit their neuroprotective roles after surviving intense oxidative stress. *Front. Mol. Neurosci.* 12:87. doi: 10.3389/fnmol.2019.00087

Bieber, A. J., Kerr, S., and Rodriguez, M. (2003). Efficient central nervous system remyelination requires T cells. *Ann. Neurol.* 53, 680–684. doi: 10.1002/ana.10578

Bjelobaba, I., Begovic-Kupresanin, V., Pekovic, S., and Lavrnja, I. J. (2018). Animal models of multiple sclerosis: focus on experimental autoimmune encephalomyelitis. *J. Neurosci. Res.* 96, 1021–1042. doi: 10.1002/jnr.24224

Blakemore, W. F., and Franklin, R. J. (2008). Remyelination in experimental models of toxin-induced demyelination. *Curr. Top. Microbiol. Immunol.* 318, 193–212. doi: 10.1007/978-3-540-73677-6_8

Blink, S. E., and Miller, S. D. (2009). The contribution of γδ T cells to the pathogenesis of EAE and MS. *Curr. Mol. Med.* 9, 15–22. doi: 10.2174/156652409787314516

Bo, L., Mork, S., Kong, P. A., Nyland, H., Pardo, C. A., and Trapp, B. D. (1994). Detection of MHC class II-antigens on macrophages and microglia, but not on astrocytes and endothelia in active multiple sclerosis lesions. *J. Neuroimmunol.* 51, 135–146. doi: 10.1016/0165-5728(94)90075-2

Bonora, M., De Marchi, E., Patergnani, S., Suski, J. M., Celsi, F., Bononi, A., et al. (2014). Tumor necrosis factor-α impairs oligodendroglial differentiation through a mitochondria-dependent process. *Cell. Death. Differ.* 21, 1198–1208. doi: 10.1038/cdd.2014.35

Boretius, S., Escher, A., Dallenga, T., Wrzos, C., Tammer, R., Brück, W., et al. (2012). Assessment of lesion pathology in a new animal model of MS by multiparametric MRI and DTI. *Neuroimage* 59, 2678–2688. doi: 10.1016/j.neuroimage.2011.08.051

Borjini, N., Fernández, M., Giardino, L., and Calzà, L. (2016). Cytokine and chemokine alterations in tissue, CSF, and plasma in early presymptomatic phase of experimental allergic encephalomyelitis (EAE), in a rat model of multiple sclerosis. *J. Neuroinflamm.* 13:291. doi: 10.1186/s12974-016-0757-6

Bottcher, C., Schlickeiser, S., Sneeboer, M. A. M., Kunkel, D., Knop, A., et al. (2019). Human microglia regional heterogeneity and phenotypes determined by multiplexed single-cell mass cytometry. *Nat. Neurosci.* 22, 78–90. doi: 10.1038/s41593-018-0290-2

Boven, L. A., Van Meurs, M., Van Zwam, M., Wierenga-Wolf, A., Hintzen, R. Q., Boot, R. G., et al. (2006). Myelin-laden macrophages are anti-inflammatory, consistent with foam cells in multiple sclerosis. *Brain* 129, 517–526. doi: 10.1093/brain/awh707

Boyd, A., Zhang, H., and Williams, A. (2013). Insufficient OPC migration into demyelinated lesions is a cause of poor remyelination in MS and mouse models. *Acta Neuropathol.* 125, 841–859. doi: 10.1007/s00401-013-1112-y

Bradbury, E. J., and Burnside, E. R. (2019). Moving beyond the glial scar for spinal cord repair. *Nat. Commun.* 10:3879. doi: 10.1038/s41467-019-11707-7

Bramow, S., Frischer, J. M., Lassmann, H., Koch-Henriksen, N., Lucchinetti, C. F., Sørensen, P. S., et al. (2010). Demyelination versus remyelination in progressive multiple sclerosis. *Brain* 133, 2983–2998. doi: 10.1093/brain/awq250

Bribián, A., Esteban, P. F., Clemente, D., Soussi-Yanicostas, N., Thomas, J. L., Zalc, B., et al. (2008). A novel role for anosmin-1 in the adhesion and migration of oligodendrocyte precursors. *Dev. Neurobiol.* 68, 1503–1516. doi: 10.1002/dneu.20678

Brocke, S., Quigley, L., Mcfarland, H. F., and Steinman, L. (1996). Isolation and characterization of autoreactive T cells in experimental autoimmune encephalomyelitis of the mouse. *Methods* 9, 458–462. doi: 10.1006/meth.1996.0053

Bröer, S., Käufer, C., Haist, V., Li, L., Gerhauser, I., Anjum, M., et al. (2016). Brain inflammation, neurodegeneration and seizure development following picornavirus infection markedly differ among virus and mouse strains and substrains. *Exp. Neurol.* 279, 57–74. doi: 10.1016/j.expneurol.2016.02.011

Bruck, W., Porada, P., Poser, S., Rieckmann, P., Hanefeld, F., Kretzschmar, H. A., et al. (1995). Monocyte/macrophage differentiation in early multiple sclerosis lesions. *Ann. Neurol.* 38, 788–796. doi: 10.1002/ana.410380514

Bruck, W., Schmied, M., Suchanek, G., Bruck, Y., Breitschopf, H., Poser, S., et al. (1994). Oligodendrocytes in the early course of multiple sclerosis. *Ann. Neurol.* 35, 65–73. doi: 10.1002/ana.410350111

Brück, W., Sommermeier, N., Bergmann, M., Zettl, U., Goebel, H. H., Kretzschmar, H. A., et al. (1996). CHAPTER 14 - macrophages in multiple sclerosis. *Immunobiology* 195, 588–600. doi: 10.1016/S0171-2985(96)80024-6

Burm, S. M., Peferoen, L. A., Zuiderwijk-Sick, E. A., Haanstra, K. G., T., Hart, B. A., et al. (2016). Expression of IL-1β in rhesus EAE and MS lesions is mainly induced in the CNS itself. *J. Neuroinflamm.* 13:138. doi: 10.1186/s12974-016-0605-8

Burman, J., Svensson, E., Fransson, M., Loskog, A. S., Zetterberg, H., Raininko, R., et al. (2014). The cerebrospinal fluid cytokine signature of multiple sclerosis: a homogenous response that does not conform to the Th1/Th2/Th17 convention. *J. Neuroimmunol.* 277, 153–159. doi: 10.1016/j.jneuroim.2014.10.005

Bush, T. G., Puvanachandra, N., Horner, C. H., Polito, A., Ostenfeld, T., Svendsen, C. N., et al. (1999). Leukocyte infiltration, neuronal degeneration, and neurite outgrowth after ablation of scar-forming, reactive astrocytes in adult transgenic mice. *Neuron* 23, 297–308. doi: 10.1016/S0896-6273(00)80781-3

Butovsky, O., and Weiner, H. L. (2018). Microglial signatures and their role in health and disease. *Nat. Rev. Neurosci.* 19, 622–635. doi: 10.1038/s41583-018-0057-5

Butovsky, O., Ziv, Y., Schwartz, A., Landa, G., Talpalar, A. E., Pluchino, S., et al. (2006). Microglia activated by IL-4 or IFN-γ differentially induce neurogenesis and oligodendrogenesis from adult stem/progenitor cells. *Mol. Cell. Neurosci.* 31, 149–160. doi: 10.1016/j.mcn.2005.10.006

Butzkueven, H., Zhang, J.-G., Soilu-Hanninen, M., Hochrein, H., Chionh, F., Shipham, K. A., et al. (2002). LIF receptor signaling limits immune-mediated demyelination by enhancing oligodendrocyte survival. *Nat. Med.* 8, 613–619. doi: 10.1038/nm0602-613

Calvi, A., Haider, L., Prados, F., Tur, C., Chard, D., and Barkhof, F. (2020). *In vivo* imaging of chronic active lesions in multiple sclerosis. *Mult. Scler.* 1–8. doi: 10.1177/1352458520958589

Campbell, Z., Sahm, D., Donohue, K., Jamison, J., Davis, M., Pellicano, C., et al. (2012). Characterizing contrast-enhancing and re-enhancing lesions in multiple sclerosis. *Neurology* 78, 1493–1499. doi: 10.1212/WNL.0b013e3182553bd2

Cannella, B., and Raine, C. S. (1995). The adhesion molecule and cytokine profile of multiple sclerosis lesions. *Ann. Neurol.* 37, 424–435. doi: 10.1002/ana.410370404

Caprariello, A. V., Rogers, J. A., Morgan, M. L., Hoghooghi, V., Plemel, J. R., Koebel, A., et al. (2018). Biochemically altered myelin triggers autoimmune demyelination. *Proc. Natl. Acad. Sci. U.S.A.* 115, 5528–5533. doi: 10.1073/pnas.1721115115

Centonze, D., Muzio, L., Rossi, S., Cavasinni, F., De Chiara, V., Bergami, A., et al. (2009). Inflammation triggers synaptic alteration and degeneration

in experimental autoimmune encephalomyelitis. *J. Neurosci.* 29, 3442–3452. doi: 10.1523/JNEUROSCI.5804-08.2009

Chang, A., Nishiyama, A., Peterson, J., Prineas, J., and Trapp, B. D. (2000). NG2-positive oligodendrocyte progenitor cells in adult human brain and multiple sclerosis lesions. *J. Neurosci.* 20, 6404–6412. doi: 10.1523/JNEUROSCI.20-17-06404.2000

Chang, A., Staugaitis, S. M., Dutta, R., Batt, C. E., Easley, K. E., Chomyk, A. M., et al. (2012). Cortical remyelination: a new target for repair therapies in multiple sclerosis. *Ann. Neurol.* 72, 918–926. doi: 10.1002/ana.23693

Chang, A., Tourtellotte, W. W., Rudick, R., and Trapp, B. D. (2002). Premyelinating oligodendrocytes in chronic lesions of multiple sclerosis. *N. Engl. J. Med.* 346, 165–173. doi: 10.1056/NEJMoa010994

Chew, L. J., King, W. C., Kennedy, A., and Gallo, V. (2005). Interferon-gamma inhibits cell cycle exit in differentiating oligodendrocyte progenitor cells. *Glia* 52, 127–143. doi: 10.1002/glia.20232

Chun, S. J., Rasband, M. N., Sidman, R. L., Habib, A. A., and Vartanian, T. (2003). Integrin-linked kinase is required for laminin-2-induced oligodendrocyte cell spreading and CNS myelination. *J. Cell. Biol.* 163, 397–408. doi: 10.1083/jcb.200304154

Cignarella, F., Filipello, F., Bollman, B., Cantoni, C., Locca, A., Mikesell, R., et al. (2020). TREM2 activation on microglia promotes myelin debris clearance and remyelination in a model of multiple sclerosis. *Acta Neuropathol.* 140, 513–534. doi: 10.1007/s00401-020-02193-z

Ciotti, J. R., and Cross, A. H. (2018). Disease-modifying treatment in progressive multiple sclerosis. *Curr. Treat. Opt. Neurol.* 20:12. doi: 10.1007/s11940-018-0496-3

Clatch, R. J., Miller, S. D., Metzner, R., Dal Canto, M. C., and Lipton, H. L. (1990). Monocytes/macrophages isolated from the mouse central nervous system contain infectious Theiler's murine encephalomyelitis virus (TMEV). *Virology* 176, 244–254. doi: 10.1016/0042-6822(90)90249-Q

Clemente, D., Ortega, M. C., Arenzana, F. J., and de Castro, F. (2011). FGF-2 and Anosmin-1 are selectively expressed in different types of multiple sclerosis lesions. *J. Neurosci.* 31, 14899–14909. doi: 10.1523/JNEUROSCI.1158-11.2011

Compston, A., and Coles, A. (2002). Multiple sclerosis. *Lancet* 359, 1221–1231. doi: 10.1016/S0140-6736(02)08220-X

Compston, A., and Coles, A. (2008). Multiple sclerosis. *Lancet* 372, 1502–1517. doi: 10.1016/S0140-6736(08)61620-7

Confavreux, C., Vukusic, S., Moreau, T., and Adeleine, P. (2000). Relapses and progression of disability in multiple sclerosis. *N. Engl. J. Med.* 343, 1430–1438. doi: 10.1056/NEJM200011163432001

Coppi, E., Cellai, L., Maraula, G., Pugliese, A. M., and Pedata, F. (2013). Adenosine A(2)A receptors inhibit delayed rectifier potassium currents and cell differentiation in primary purified oligodendrocyte cultures. *Neuropharmacology* 73, 301–310. doi: 10.1016/j.neuropharm.2013.05.035

Correale, J., and Villa, A. (2010). Role of CD8+ CD25+ Foxp3+ regulatory T cells in multiple sclerosis. *Ann. Neurol.* 67, 625–638. doi: 10.1002/ana.21944

Couturier, J., Stancu, I.-C., Schakman, O., Pierrot, N., Huaux, F., Kienlen-Campard, P., et al. (2016). Activation of phagocytic activity in astrocytes by reduced expression of the inflammasome component ASC and its implication in a mouse model of Alzheimer disease. *J. Neuroinflamm.* 13:20. doi: 10.1186/s12974-016-0477-y

Crocker, S. J., Milner, R., Pham-Mitchell, N., and Campbell, I. L. (2006). Cell and agonist-specific regulation of genes for matrix metalloproteinases and their tissue inhibitors by primary glial cells. *J. Neurochem.* 98, 812–823. doi: 10.1111/j.1471-4159.2006.03927.x

Croxford, A. L., Kurschus, F. C., and Waisman, A. (2011). Mouse models for multiple sclerosis: historical facts and future implications. *Biochim. Biophys. Acta* 1812, 177–183. doi: 10.1016/j.bbadis.2010.06.010

Croxford, J. L., Miyake, S., Huang, Y.-Y., Shimamura, M., and Yamamura, T. (2006). Invariant Vα19i T cells regulate autoimmune inflammation. *Nat. Immunol.* 7, 987–994. doi: 10.1038/ni1370

Cruz-Orengo, L., Holman, D. W., Dorsey, D., Zhou, L., Zhang, P., Wright, M., et al. (2011). CXCR7 influences leukocyte entry into the CNS parenchyma by controlling abluminal CXCL12 abundance during autoimmunity. *J. Exp. Med.* 208, 327–339. doi: 10.1084/jem.20102010

Czopka, T., Von Holst, A., Schmidt, G., Ffrench-Constant, C., and Faissner, A. (2009). Tenascin C and tenascin R similarly prevent the formation of myelin membranes in a RhoA-dependent manner, but antagonistically regulate the expression of myelin basic protein via a separate pathway. *Glia* 57, 1790–1801. doi: 10.1002/glia.20891

Dal-Bianco, A., Grabner, G., Kronnerwetter, C., Weber, M., Höftberger, R., Berger, T., et al. (2017). Slow expansion of multiple sclerosis iron rim lesions: pathology and 7 T magnetic resonance imaging. *Acta Neuropathol.* 133, 25–42. doi: 10.1007/s00401-016-1636-z

Dallner, C., Woods, A. G., Deller, T., Kirsch, M., and Hofmann, H.-D. (2002). CNTF and CNTF receptor alpha are constitutively expressed by astrocytes in the mouse brain. *Glia* 37, 374–378. doi: 10.1002/glia.10048

Daniels, B. P., Jujjavarapu, H., Durrant, D. M., Williams, J. L., Green, R. R., White, J. P., et al. (2017). Regional astrocyte IFN signaling restricts pathogenesis during neurotropic viral infection. *J. Clin. Invest.* 127, 843–856. doi: 10.1172/JCI88720

Davalos, D., Grutzendler, J., Yang, G., Kim, J. V., Zuo, Y., Jung, S., et al. (2005). ATP mediates rapid microglial response to local brain injury *in vivo*. *Nat. Neurosci.* 8, 752–758. doi: 10.1038/nn1472

De Jager, P. L., Jia, X., Wang, J., De Bakker, P. I., Ottoboni, L., Aggarwal, N. T., et al. (2009). Meta-analysis of genome scans and replication identify CD6, IRF8 and TNFRSF1A as new multiple sclerosis susceptibility loci. *Nat. Genet.* 41, 776–782. doi: 10.1038/ng.401

De Jong, B. A., Huizinga, T. W., Bollen, E. L., Uitdehaag, B. M., Bosma, G. P., Van Buchem, M. A., et al. (2002). Production of IL-1beta and IL-1Ra as risk factors for susceptibility and progression of relapse-onset multiple sclerosis. *J. Neuroimmunol.* 126, 172–179. doi: 10.1016/S0165-5728(02)00056-5

Delgado-Rivera, R., Harris, S. L., Ahmed, I., Babu, A. N., Patel, R. P., Ayres, V., et al. (2009). Increased FGF-2 secretion and ability to support neurite outgrowth by astrocytes cultured on polyamide nanofibrillar matrices. *Matrix Biol.* 28, 137–147. doi: 10.1016/j.matbio.2009.02.001

Dendrou, C. A., Fugger, L., and Friese, M. A. (2015). Immunopathology of multiple sclerosis. *Nat. Rev. Immunol.* 15, 545–558. doi: 10.1038/nri3871

Denney, L., Kok, W. L., Cole, S. L., Sanderson, S., Mcmichael, A. J., and Ho, L.-P. (2012). Activation of invariant NKT cells in early phase of experimental autoimmune encephalomyelitis results in differentiation of Ly6Chi inflammatory monocyte to M2 macrophages and improved outcome. *J. Immunol.* 189, 551–557. doi: 10.4049/jimmunol.1103608

DePaula-Silva, A. B., Hanak, T. J., Libbey, J. E., and Fujinami, R. S. (2017). Theiler's murine encephalomyelitis virus infection of SJL/J and C57BL/6J mice: models for multiple sclerosis and epilepsy. *J. Neuroimmunol.* 308, 30–42. doi: 10.1016/j.jneuroim.2017.02.012

Dezonne, R. S., Stipursky, J., Araujo, A. P. B., Nones, J., Pavão, M. S. G., Porcionatto, M., et al. (2013). Thyroid hormone treated astrocytes induce maturation of cerebral cortical neurons through modulation of proteoglycan levels. *Front. Cell. Neurosci.* 7, 125–125. doi: 10.3389/fncel.2013.00125

Dimri, G. P., Lee, X., Basile, G., Acosta, M., Scott, G., Roskelley, C., et al. (1995). A biomarker that identifies senescent human cells in culture and in aging skin *in vivo*. *Proc. Natl. Acad. Sci. U.S.A.* 92, 9363–9367. doi: 10.1073/pnas.92.20.9363

Ding, X., Yan, Y., Li, X., Li, K., Ciric, B., Yang, J., et al. (2015). Silencing IFN-γ binding/signaling in astrocytes versus microglia leads to opposite effects on central nervous system autoimmunity. *J. Immunol.* 194, 4251–4264. doi: 10.4049/jimmunol.1303321

Disanto, G., Morahan, J. M., Barnett, M. H., Giovannoni, G., and Ramagopalan, S. V. (2012). The evidence for a role of B cells in multiple sclerosis. *Neurology* 78, 823–832. doi: 10.1212/WNL.0b013e318249f6f0

Domingues, H. S., Portugal, C. C., Socodato, R., and Relvas, J. B. (2016). Oligodendrocyte, astrocyte, and microglia crosstalk in myelin development, damage, and repair. *Front. Cell. Dev. Biol.* 4:71. doi: 10.3389/fcell.2016.00071

Dong, Y., and Benveniste, E. N. (2001). Immune function of astrocytes. *Glia* 36, 180–190. doi: 10.1002/glia.1107

Dugas, J. C., Ibrahim, A., and Barres, B. A. (2012). The T3-induced gene KLF9 regulates oligodendrocyte differentiation and myelin regeneration. *Mol. Cell. Neurosci.* 50, 45–57. doi: 10.1016/j.mcn.2012.03.007

Dujmovic, I., Mangano, K., Pekmezovic, T., Quattrocchi, C., Mesaros, S., Stojsavljevic, N., et al. (2009). The analysis of IL-1 beta and its naturally occurring inhibitors in multiple sclerosis: the elevation of IL-1 receptor antagonist and IL-1 receptor type II after steroid therapy. *J. Neuroimmunol.* 207, 101–106. doi: 10.1016/j.jneuroim.2008.11.004

Duncan, G. J., Simkins, T. J., and Emery, B. (2021). Neuron-oligodendrocyte interactions in the structure and integrity of axons. *Front. Cell. Dev. Biol.* 9:653101. doi: 10.3389/fcell.2021.653101

Duncan, I. D., Radcliff, A. B., Heidari, M., Kidd, G., August, B. K., and Wierenga, L. A. (2018). The adult oligodendrocyte can participate in remyelination. *Proc. Natl. Acad. Sci. U.S.A.* 115, E11807–E11816. doi: 10.1073/pnas.1808064115

Edara, V. V., Nooka, S., Proulx, J., Stacy, S., Ghorpade, A., and Borgmann, K. (2020). β-Catenin regulates wound healing and IL-6 expression in activated human astrocytes. *Biomedicines* 8:479. doi: 10.3390/biomedicines8110479

Elkjaer, M. L., Frisch, T., Reynolds, R., Kacprowski, T., Burton, M., Kruse, T. A., et al. (2019). Molecular signature of different lesion types in the brain white matter of patients with progressive multiple sclerosis. *Acta Neuropathol. Commun.* 7:205. doi: 10.1186/s40478-019-0855-7

Elliott, C., Arnold, D. L., Chen, H., Ke, C., Zhu, L., Chang, I., et al. (2020). Patterning chronic active demyelination in slowly expanding/evolving white matter MS lesions. *Am. J. Neuroradiol.* 41, 1584–1591. doi: 10.3174/ajnr.A6742

Erta, M., Quintana, A., and Hidalgo, J. (2012). Interleukin-6, a major cytokine in the central nervous system. *Int. J. Biol. Sci.* 8, 1254–1266. doi: 10.7150/ijbs.4679

Escartin, C., Galea, E., Lakatos, A., O'callaghan, J. P., Petzold, G. C., Serrano-Pozo, A., et al. (2021). Reactive astrocyte nomenclature, definitions, and future directions. *Nat. Neurosci.* 24, 312–325. doi: 10.1038/s41593-020-00783-4

Etxeberria, A., Mangin, J.-M., Aguirre, A., and Gallo, V. J. (2010). Adult-born SVZ progenitors receive transient synapses during remyelination in corpus callosum. *Nat. Neurosci.* 13, 287–289. doi: 10.1038/nn.2500

Falcao, A. M., Van Bruggen, D., Marques, S., Meijer, M., Jakel, S., Agirre, E., et al. (2018). Disease-specific oligodendrocyte lineage cells arise in multiple sclerosis. *Nat. Med.* 24, 1837–1844. doi: 10.1038/s41591-018-0236-y

Fancy, S. P., Baranzini, S. E., Zhao, C., Yuk, D. I., Irvine, K. A., Kaing, S., et al. (2009). Dysregulation of the Wnt pathway inhibits timely myelination and remyelination in the mammalian CNS. *Genes Dev.* 23, 1571–1585. doi: 10.1101/gad.1806309

Faulkner, J. R., Herrmann, J. E., Woo, M. J., Tansey, K. E., Doan, N. B., and Sofroniew, M. V. (2004). Reactive astrocytes protect tissue and preserve function after spinal cord injury. *J. Neurosci.* 24, 2143–2155. doi: 10.1523/JNEUROSCI.3547-03.2004

Feigenson, K., Reid, M., See, J., Crenshaw, E. B., and Grinspan, J. B. (2009). Wnt signaling is sufficient to perturb oligodendrocyte maturation. *Mol. Cell. Neurosci.* 42, 255–265. doi: 10.1016/j.mcn.2009.07.010

Feinstein, A., Freeman, J., and Lo, A. C. (2015). Treatment of progressive multiple sclerosis: what works, what does not, and what is needed. *Lancet Neurol.* 14, 194–207. doi: 10.1016/S1474-4422(14)70231-5

Fernández-Castañeda, A., Chappell, M. S., Rosen, D. A., Seki, S. M., Beiter, R. M., Johanson, D. M., et al. (2020). The active contribution of OPCs to neuroinflammation is mediated by LRP1. *Acta Neuropathol.* 139, 365–382. doi: 10.1007/s00401-019-02073-1

Fernandez-Castaneda, A., and Gaultier, A. (2016). Adult oligodendrocyte progenitor cells - multifaceted regulators of the CNS in health and disease. *Brain Behav. Immun.* 57, 1–7. doi: 10.1016/j.bbi.2016.01.005

Ferrini, F., and De Koninck, Y. (2013). Microglia control neuronal network excitability via BDNF signalling. *Neural Plast* 2013:429815. doi: 10.1155/2013/429815

Fischer, R., Wajant, H., Kontermann, R., Pfizenmaier, K., and Maier, O. (2014). Astrocyte-specific activation of TNFR2 promotes oligodendrocyte maturation by secretion of leukemia inhibitory factor. *Glia* 62, 272–283. doi: 10.1002/glia.22605

Fleming, J., Trousdale, M., Bradbury, J., Stohlman, S., and Weiner, L. J. (1987). Experimental demyelination induced by coronavirus JHM (MHV-4): molecular identification of a viral determinant of paralytic disease. *Microb. Pathog.* 3, 9–20. doi: 10.1016/0882-4010(87)90033-7

Fleming, J. O., Trousdale, M. D., El-Zaatari, F. A., Stohlman, S. A., and Weiner, L. P. (1986). Pathogenicity of antigenic variants of murine coronavirus JHM selected with monoclonal antibodies. *J. Virol.* 58, 869–875. doi: 10.1128/jvi.58.3.869-875.1986

Fletcher, J. M., Lalor, S. J., Sweeney, C. M., Tubridy, N., and Mills, K. H. (2010). T cells in multiple sclerosis and experimental autoimmune encephalomyelitis. *Clin. Exp. Immunol.* 162, 1–11. doi: 10.1111/j.1365-2249.2010.04143.x

Foerster, S., Hill, M. F. E., and Franklin, R. J. M. (2019). Diversity in the oligodendrocyte lineage: plasticity or heterogeneity? *Glia* 67, 1797–1805. doi: 10.1002/glia.23607

Franklin, R. J. (2002). Why does remyelination fail in multiple sclerosis? *Nat. Rev. Neurosci.* 3, 705–714. doi: 10.1038/nrn917

Franklin, R. J., and Ffrench-Constant, C. (2008). Remyelination in the CNS: from biology to therapy. *Nat. Rev. Neurosci.* 9, 839–855. doi: 10.1038/nrn2480

Frik, J., Merl-Pham, J., Plesnila, N., Mattugini, N., Kjell, J., Kraska, J., et al. (2018). Cross-talk between monocyte invasion and astrocyte proliferation regulates scarring in brain injury. *EMBO Rep.* 19:e45294. doi: 10.15252/embr.201745294

Frischer, J. M., Bramow, S., Dal-Bianco, A., Lucchinetti, C. F., Rauschka, H., Schmidbauer, M., et al. (2009). The relation between inflammation and neurodegeneration in multiple sclerosis brains. *Brain* 132, 1175–1189. doi: 10.1093/brain/awp070

Frischer, J. M., Weigand, S. D., Guo, Y., Kale, N., Parisi, J. E., Pirko, I., et al. (2015). Clinical and pathological insights into the dynamic nature of the white matter multiple sclerosis plaque. *Ann. Neurol.* 78, 710–721. doi: 10.1002/ana.24497

Frost, E. E., Nielsen, J. A., Le, T. Q., and Armstrong, R. C. (2003). PDGF and FGF2 regulate oligodendrocyte progenitor responses to demyelination. *J. Neurobiol.* 54, 457–472. doi: 10.1002/neu.10158

Fruttiger, M., Karlsson, L., Hall, A. C., Abramsson, A., Calver, A. R., Bostrom, H., et al. (1999). Defective oligodendrocyte development and severe hypomyelination in PDGF-A knockout mice. *Development* 126:457. doi: 10.1242/dev.126.3.457

Funfschilling, U., Supplie, L. M., Mahad, D., Boretius, S., Saab, A. S., Edgar, J., et al. (2012). Glycolytic oligodendrocytes maintain myelin and long-term axonal integrity. *Nature* 485, 517–521. doi: 10.1038/nature11007

Furlan, R., Brambilla, E., Ruffini, F., Poliani, P. L., Bergami, A., Marconi, P. C., et al. (2001). Intrathecal delivery of IFN-γ protects C57BL/6 mice from chronic-progressive experimental autoimmune encephalomyelitis by increasing apoptosis of central nervous system-infiltrating lymphocytes. *J. Immunol.* 167, 1821–1829. doi: 10.4049/jimmunol.167.3.1821

Furtado, G. C., Marcondes, M. C. G., Latkowski, J.-A., Tsai, J., Wensky, A., and Lafaille, J. J. (2008). Swift entry of myelin-specific T lymphocytes into the central nervous system in spontaneous autoimmune encephalomyelitis. *J. Immunol.* 181, 4648–4655. doi: 10.4049/jimmunol.181.7.4648

Gadea, A., Aguirre, A., Haydar, T. F., and Gallo, V. (2009). Endothelin-1 regulates oligodendrocyte development. *J. Neurosci.* 29, 10047–10062. doi: 10.1523/JNEUROSCI.0822-09.2009

Gallo, V., Zhou, J. M., Mcbain, C. J., Wright, P., Knutson, P. L., and Armstrong, R. C. (1996). Oligodendrocyte progenitor cell proliferation and lineage progression are regulated by glutamate receptor-mediated K+ channel block. *J. Immunol.* 16, 2659–2670. doi: 10.1523/JNEUROSCI.16-08-02659.1996

Galloway, D. A., Gowing, E., Setayeshgar, S., and Kothary, R. (2020). Inhibitory milieu at the multiple sclerosis lesion site and the challenges for remyelination. *Glia* 68, 859–877. doi: 10.1002/glia.23711

Gao, H., Danzi, M. C., Choi, C. S., Taherian, M., Dalby-Hansen, C., Ellman, D. G., et al. (2017). Opposing functions of microglial and macrophagic TNFR2 in the pathogenesis of experimental autoimmune encephalomyelitis. *Cell Rep.* 18, 198–212. doi: 10.1016/j.celrep.2016.11.083

Gao, Q., Li, Y., and Chopp, M. (2005). Bone marrow stromal cells increase astrocyte survival via upregulation of phosphoinositide 3-kinase/threonine protein kinase and mitogen-activated protein kinase kinase/extracellular signal-regulated kinase pathways and stimulate astrocyte trophic factor gene expression after anaerobic insult. *Neuroscience* 136, 123–134. doi: 10.1016/j.neuroscience.2005.06.091

Garcion, E., Faissner, A., and ffrench-Constant, C. (2001). Knockout mice reveal a contribution of the extracellular matrix molecule tenascin-C to neural precursor proliferation and migration. *Development* 128, 2485–2496. doi: 10.1242/dev.128.13.2485

Ghorbani, S., and Yong, V. W. (2021). The extracellular matrix as modifier of neuroinflammation and remyelination in multiple sclerosis. *Brain* 36:awab043. doi: 10.1093/brain/awab059

Gilli, F., Li, L., Campbell, S. J., Anthony, D. C., and Pachner, A. R. (2015). The effect of B-cell depletion in the Theiler's model of multiple sclerosis. *J. Neurol. Sci.* 359, 40–47. doi: 10.1016/j.jns.2015.10.012

Ginhoux, F., Greter, M., Leboeuf, M., Nandi, S., See, P., Gokhan, S., et al. (2010). Fate mapping analysis reveals that adult microglia derive from primitive macrophages. *Science* 330, 841–845. doi: 10.1126/science.1194637

Girolamo, F., Errede, M., Longo, G., Annese, T., Alias, C., Ferrara, G., et al. (2019). Defining the role of NG2-expressing cells in experimental models of multiple sclerosis. A biofunctional analysis of the neurovascular unit in wild type and NG2 null mice. *PLoS ONE* 14:e0213508. doi: 10.1371/journal.pone.0213508

Glabinski, A. R., Balasingam, V., Tani, M., Kunkel, S. L., Strieter, R. M., Yong, V. W., et al. (1996). Chemokine monocyte chemoattractant protein-1 is expressed by astrocytes after mechanical injury to the brain. *J. Immunol.* 156, 4363–4368.

Gomez Perdiguero, E., Klapproth, K., Schulz, C., Busch, K., Azzoni, E., Crozet, L., et al. (2015). Tissue-resident macrophages originate from yolk-sac-derived erythro-myeloid progenitors. *Nature* 518, 547–551. doi: 10.1038/nature13989

Gorgoulis, V., Adams, P. D., Alimonti, A., Bennett, D. C., Bischof, O., Bishop, C., et al. (2019). Cellular senescence: defining a path forward. *Cell* 179, 813–827. doi: 10.1016/j.cell.2019.10.005

Gosselin, D., Link, V. M., Romanoski, C. E., Fonseca, G. J., Eichenfield, D. Z., Spann, N. J., et al. (2014). Environment drives selection and function of enhancers controlling tissue-specific macrophage identities. *Cell* 159, 1327–1340. doi: 10.1016/j.cell.2014.11.023

Gruchot, J., Weyers, V., Gottle, P., Forster, M., Hartung, H. P., Kury, P., et al. (2019). The molecular basis for remyelination failure in multiple sclerosis. *Cells* 8:825. doi: 10.3390/cells8080825

Guérit, S., Fidan, E., Macas, J., Czupalla, C. J., Figueiredo, R., Vijikumar, A., et al. (2021). Astrocyte-derived Wnt growth factors are required for endothelial blood-brain barrier maintenance. *Prog. Neurobiol.* 199:101937. doi: 10.1016/j.pneurobio.2020.101937

Gurfein, B. T., Zhang, Y., López, C. B., Argaw, A. T., Zameer, A., Moran, T. M., et al. (2009). IL-11 regulates autoimmune demyelination. *J. Immunol.* 183, 4229–4240. doi: 10.4049/jimmunol.0900622

Haberlandt, C., Derouiche, A., Wyczynski, A., Haseleu, J., Pohle, J., Karram, K., et al. (2011). Gray matter NG2 cells display multiple Ca2+-signaling pathways and highly motile processes. *PLoS ONE* 6:e17575. doi: 10.1371/journal.pone.0017575

Hagemeyer, N., Hanft, K. M., Akriditou, M. A., Unger, N., Park, E. S., Stanley, E. R., et al. (2017). Microglia contribute to normal myelinogenesis and to oligodendrocyte progenitor maintenance during adulthood. *Acta. Neuropathol.* 134, 441–458. doi: 10.1007/s00401-017-1747-1

Haghikia, A., Hohlfeld, R., Gold, R., and Fugger, L. (2013). Therapies for multiple sclerosis: translational achievements and outstanding needs. *Trends Mol. Med.* 19, 309–319. doi: 10.1016/j.molmed.2013.03.004

Haider, L., Fischer, M. T., Frischer, J. M., Bauer, J., Hoftberger, R., Botond, G., et al. (2011). Oxidative damage in multiple sclerosis lesions. *Brain* 134, 1914–1924. doi: 10.1093/brain/awr128

Haindl, M. T., Köck, U., Zeitelhofer-Adzemovic, M., Fazekas, F., and Hochmeister, S. (2019). The formation of a glial scar does not prohibit remyelination in an animal model of multiple sclerosis. *Glia* 67, 467–481. doi: 10.1002/glia.23556

Hamilton, N., Vayro, S., Wigley, R., and Butt, A. M. (2010). Axons and astrocytes release ATP and glutamate to evoke calcium signals in NG2-glia. *Glia* 58, 66–79. doi: 10.1002/glia.20902

Hanisch, U.-K., and Kettenmann, H. (2007). Microglia: active sensor and versatile effector cells in the normal and pathologic brain. *Nat. Neurosci.* 10, 1387–1394. doi: 10.1038/nn1997

Harp, C. R. P., Archambault, A. S., Sim, J., Ferris, S. T., Mikesell, R. J., Koni, P. A., et al. (2015). B cell antigen presentation is sufficient to drive neuroinflammation in an animal model of multiple sclerosis. *J. Immunol.* 194, 5077–5084. doi: 10.4049/jimmunol.1402236

Harris, J. O., Frank, J. A., Patronas, N., Mcfarlin, D. E., and Mcfarland, H. F. (1991). Serial gadolinium-enhanced magnetic resonance imaging scans in patients with early, relapsing-remitting multiple sclerosis: implications for clinical trials and natural history. *Ann. Neurol.* 29, 548–555. doi: 10.1002/ana.410290515

Hayakawa, K., Pham, L. D., Arai, K., and Lo, E. H. (2014). Reactive astrocytes promote adhesive interactions between brain endothelium and endothelial progenitor cells via HMGB1 and beta-2 integrin signaling. *Stem Cell Res.* 12, 531–538. doi: 10.1016/j.scr.2013.12.008

Hayakawa, K., Pham, L. D., Som, A. T., Lee, B. J., Guo, S., Lo, E. H., et al. (2011). Vascular endothelial growth factor regulates the migration of oligodendrocyte precursor cells. *J. Neurosci.* 31, 10666–10670. doi: 10.1523/JNEUROSCI.1944-11.2011

Herrero-Herranz, E., Pardo, L. A., Gold, R., and Linker, R. A. (2008). Pattern of axonal injury in murine myelin oligodendrocyte glycoprotein induced experimental autoimmune encephalomyelitis: implications for multiple sclerosis. *Neurobiol. Dis.* 30, 162–173. doi: 10.1016/j.nbd.2008.01.001

Heß, K., Starost, L., Kieran, N. W., Thomas, C., Vincenten, M. C. J., Antel, J., et al. (2020). Lesion stage-dependent causes for impaired remyelination in MS. *Acta Neuropathol.* 140, 359–375. doi: 10.1007/s00401-020-02189-9

Hindinger, C., Bergmann, C. C., Hinton, D. R., Phares, T. W., Parra, G. I., Hussain, S., et al. (2012). IFN-γ signaling to astrocytes protects from autoimmune mediated neurological disability. *PLoS ONE* 7:e42088. doi: 10.1371/journal.pone.0042088

Hiremath, M. M., Saito, Y., Knapp, G. W., Ting, J. P., Suzuki, K., and Matsushima, G. K. (1998). Microglial/macrophage accumulation during cuprizone-induced demyelination in C57BL/6 mice. *J. Neuroimmunol.* 92, 38–49. doi: 10.1016/S0165-5728(98)00168-4

Hou, Y., Dan, X., Babbar, M., Wei, Y., Hasselbalch, S. G., Croteau, D. L., et al. (2019). Ageing as a risk factor for neurodegenerative disease. *Nat. Rev. Neurol.* 15, 565–581. doi: 10.1038/s41582-019-0244-7

Houtman, J. J., and Fleming, J. O. (1996). Dissociation of demyelination and viral clearance in congenitally immunodeficient mice infected with murine coronavirus JHM. *J. Neurovirol.* 2, 101–110. doi: 10.3109/13550289609146543

Hoyos, H. C., Rinaldi, M., Mendez-Huergo, S. P., Marder, M., Rabinovich, G. A., Pasquini, J. M., et al. (2014). Galectin-3 controls the response of microglial cells to limit cuprizone-induced demyelination. *Neurobiol. Dis.* 62, 441–455. doi: 10.1016/j.nbd.2013.10.023

Hu, J., Deng, L., Wang, X., and Xu, X. M. (2009). Effects of extracellular matrix molecules on the growth properties of oligodendrocyte progenitor cells *in vitro*. *J. Neurosci. Res.* 87, 2854–2862. doi: 10.1002/jnr.22111

Hughes, E. G., Kang, S. H., Fukaya, M., and Bergles, D. E. (2013). Oligodendrocyte progenitors balance growth with self-repulsion to achieve homeostasis in the adult brain. *Nat. Neurosci.* 16, 668–676. doi: 10.1038/nn.3390

Hurwitz, B. J. (2009). The diagnosis of multiple sclerosis and the clinical subtypes. *Ann. Indian Acad. Neurol.* 12, 226–230. doi: 10.4103/0972-2327.58276

Ishibashi, T., Dakin, K. A., Stevens, B., Lee, P. R., Kozlov, S. V., Stewart, C. L., et al. (2006). Astrocytes promote myelination in response to electrical impulses. *Neuron* 49, 823–832. doi: 10.1016/j.neuron.2006.02.006

Itabashi, T., Arima, Y., Kamimura, D., Higuchi, K., Bando, Y., Takahashi-Iwanaga, H., et al. (2018). Cell- and stage-specific localization of galectin-3, a β-galactoside-binding lectin, in a mouse model of experimental autoimmune encephalomyelitis. *Neurochem. Int.* 118, 176–184. doi: 10.1016/j.neuint.2018.06.007

Ito, M., Muramatsu, R., Kato, Y., Sharma, B., Uyeda, A., Tanabe, S., et al. (2021). Age-dependent decline in remyelination capacity is mediated by apelin–APJ signaling. *Nat. Aging* 1, 284–294. doi: 10.1038/s43587-021-00041-7

Jahng, A. W., Maricic, I., Pedersen, B., Burdin, N., Naidenko, O., Kronenberg, M., et al. (2001). Activation of natural killer T cells potentiates or prevents experimental autoimmune encephalomyelitis. *J. Exp. Med.* 194, 1789–1799. doi: 10.1084/jem.194.12.1789

Jakel, S., Agirre, E., Mendanha Falcao, A., Van Bruggen, D., Lee, K. W., Knuesel, I., et al. (2019). Altered human oligodendrocyte heterogeneity in multiple sclerosis. *Nature* 566, 543–547. doi: 10.1038/s41586-019-0903-2

Jeffery, N. D., and Blakemore, W. F. (1995). Remyelination of mouse spinal cord axons demyelinated by local injection of lysolecithin. *J. Neurocytol.* 24, 775–781. doi: 10.1007/BF01191213

Jelachich, M. L., and Lipton, H. L. (1999). Restricted Theilerandapos's murine encephalomyelitis virus infection in murine macrophages induces apoptosis. *J. Gen. Virol.* 80, 1701–1705. doi: 10.1099/0022-1317-80-7-1701

John Lin, C. C., Yu, K., Hatcher, A., Huang, T. W., Lee, H. K., Carlson, J., et al. (2017). Identification of diverse astrocyte populations and their malignant analogs. *Nat. Neurosci.* 20, 396–405. doi: 10.1038/nn.4493

Jonkman, L. E., Soriano, A. L., Amor, S., Barkhof, F., Van Der Valk, P., Vrenken, H., et al. (2015). Can MS lesion stages be distinguished with MRI? A postmortem MRI and histopathology study. *J. Neurol.* 262, 1074–1080. doi: 10.1007/s00415-015-7689-4

Jordan, C. A., Friedrich Jr, V. L., Godfraind, C., Cardellechio, C. B., Holmes, K. V., and Dubois-Dalcq, M. J. G. (1989). Expression of viral and myelin gene transcripts in a murine CNS demyelinating disease caused by a coronavirus. *Glia* 2, 318–329. doi: 10.1002/glia.440020505

Kang, Z., Wang, C., Zepp, J., Wu, L., Sun, K., Zhao, J., et al. (2013). Act1 mediates IL-17-induced EAE pathogenesis selectively in NG2+ glial cells. *Nat. Neurosci.* 16, 1401–1408. doi: 10.1038/nn.3505

Káradóttir, R., Hamilton, N. B., Bakiri, Y., and Attwell, D. (2008). Spiking and nonspiking classes of oligodendrocyte precursor glia in CNS white matter. *Nat. Neurosci.* 11, 450–456. doi: 10.1038/nn2060

Karamita, M., Barnum, C., Möbius, W., Tansey, M. G., Szymkowski, D. E., Lassmann, H., et al. (2017). Therapeutic inhibition of soluble brain TNF promotes remyelination by increasing myelin phagocytosis by microglia. *JCI Insight* 2:e87455. doi: 10.1172/jci.insight.87455

Karim, H., Kim, S. H., Lauderdale, K., Lapato, A. S., Atkinson, K., Yasui, N., et al. (2019). Analogues of ERβ ligand chloroindazole exert immunomodulatory and remyelinating effects in a mouse model of multiple sclerosis. *Sci. Rep.* 9:503. doi: 10.1038/s41598-018-37420-x

Katz-Levy, Y., Neville, K. L., Padilla, J., Rahbe, S., Begolka, W. S., Girvin, A. M., et al. (2000). Temporal development of autoreactive Th1 responses and endogenous presentation of self myelin epitopes by central nervous system-resident APCs in Theiler's virus-infected mice. *J. Immunol.* 165, 5304–5314. doi: 10.4049/jimmunol.165.9.5304

Keirstead, H. S., and Blakemore, W. F. (1997). Identification of post-mitotic oligodendrocytes incapable of remyelination within the demyelinated adult spinal cord. *J. Neuropathol. Exp. Neurol.* 56, 1191–1201. doi: 10.1097/00005072-199711000-00003

Kierdorf, K., Erny, D., Goldmann, T., Sander, V., Schulz, C., Perdiguero, E. G., et al. (2013). Microglia emerge from erythromyeloid precursors via Pu.1- and Irf8-dependent pathways. *Nat. Neurosci.* 16, 273–280. doi: 10.1038/nn.3318

Kigerl, K. A., Gensel, J. C., Ankeny, D. P., Alexander, J. K., Donnelly, D. J., and Popovich, P. G. (2009). Identification of two distinct macrophage subsets with divergent effects causing either neurotoxicity or regeneration in the injured mouse spinal cord. *J. Neurosci.* 29:13435. doi: 10.1523/JNEUROSCI.3257-09.2009

Kim, S., Steelman, A. J., Koito, H., and Li, J. (2011). Astrocytes promote TNF-mediated toxicity to oligodendrocyte precursors. *J. Neurochem.* 116, 53–66. doi: 10.1111/j.1471-4159.2010.07084.x

Kipp, M., Nyamoya, S., Hochstrasser, T., and Amor, S. (2017). Multiple sclerosis animal models: a clinical and histopathological perspective. *Brain Pathol.* 27, 123–137. doi: 10.1111/bpa.12454

Kipp, M., Van Der Star, B., Vogel, D. Y. S., Puentes, F., Van Der Valk, P., Baker, D., et al. (2012). Experimental *in vivo* and *in vitro* models of multiple sclerosis: EAE and beyond. *Mult. Scler. Relat. Disord.* 1, 15–28. doi: 10.1016/j.msard.2011.09.002

Kiray, H., Lindsay, S. L., Hosseinzadeh, S., and Barnett, S. C. (2016). The multifaceted role of astrocytes in regulating myelination. *Exp. Neurol.* 283, 541–549. doi: 10.1016/j.expneurol.2016.03.009

Kirby, L., Jin, J., Cardona, J. G., Smith, M. D., Martin, K. A., Wang, J., et al. (2019). Oligodendrocyte precursor cells present antigen and are cytotoxic targets in inflammatory demyelination. *Nat. Commun* 10:3887. doi: 10.1038/s41467-019-11638-3

Kornek, B., Storch, M. K., Weissert, R., Wallstroem, E., Stefferl, A., Olsson, T., et al. (2000). Multiple sclerosis and chronic autoimmune encephalomyelitis: a comparative quantitative study of axonal injury in active, inactive, and remyelinated lesions. *Am. J. Pathol.* 157, 267–276. doi: 10.1016/S0002-9440(10)64537-3

Kremer, D., Kury, P., and Dutta, R. (2015). Promoting remyelination in multiple sclerosis: current drugs and future prospects. *Mult. Scler.* 21, 541–549. doi: 10.1177/1352458514566419

Kritsilis, M., S, V.R., Koutsoudaki, P. N., Evangelou, K., Gorgoulis, V. G., and Papadopoulos, D. (2018). Ageing, cellular senescence and neurodegenerative disease. *Int. J. Mol. Sci.* 19:2937. doi: 10.3390/ijms19102937

Kuhlmann, T., Ludwin, S., Prat, A., Antel, J., Brück, W., and Lassmann, H. (2017). An updated histological classification system for multiple sclerosis lesions. *Acta Neuropathol.* 133, 13–24. doi: 10.1007/s00401-016-1653-y

Kuhlmann, T., Miron, V., Cui, Q., Wegner, C., Antel, J., and Brück, W. (2008). Differentiation block of oligodendroglial progenitor cells as a cause for remyelination failure in chronic multiple sclerosis. *Brain* 131, 1749–1758. doi: 10.1093/brain/awn096

Kutzelnigg, A., Lucchinetti, C. F., Stadelmann, C., Brück, W., Rauschka, H., Bergmann, M., et al. (2005). Cortical demyelination and diffuse white matter injury in multiple sclerosis. *Brain* 128, 2705–2712. doi: 10.1093/brain/awh641

Kuypers, N. J., James, K. T., Enzmann, G. U., Magnuson, D. S. K., and Whittemore, S. R. (2013). Functional consequences of ethidium bromide demyelination of the mouse ventral spinal cord. *Exp. Neurol.* 247, 615–622. doi: 10.1016/j.expneurol.2013.02.014

Lampron, A., Larochelle, A., Laflamme, N., Préfontaine, P., Plante, M.-M., Sánchez, M. G., et al. (2015). Inefficient clearance of myelin debris by microglia impairs remyelinating processes. *J. Exp. Med.* 212, 481–495. doi: 10.1084/jem.20141656

Lassmann, H. (1983). Comparative neuropathology of chronic experimental allergic encephalomyelitis and multiple sclerosis. *Schriftenr. Neurol.* 25, 1–135. doi: 10.1007/978-3-642-45558-2

Lassmann, H., and Bradl, M. (2017). Multiple sclerosis: experimental models and reality. *Acta Neuropathol.* 133, 223–244. doi: 10.1007/s00401-016-1631-4

Lassmann, H., Raine, C. S., Antel, J., and Prineas, J. W. (1998). Immunopathology of multiple sclerosis: report on an international meeting held at the Institute of Neurology of the University of Vienna. *J. Neuroimmunol.* 86, 213–217. doi: 10.1016/S0165-5728(98)00031-9

Lau, L. W., Cua, R., Keough, M. B., Haylock-Jacobs, S., and Yong, V. W. (2013). Pathophysiology of the brain extracellular matrix: a new target for remyelination. *Nat. Rev. Neurosci.* 14, 722–729. doi: 10.1038/nrn3550

Lavi, E., Gilden, D. H., Wroblewska, Z., Rorke, L. B., and Weiss, S. R. (1984). Experimental demyelination produced by the A59 strain of mouse hepatitis virus. *Neurology* 34, 597–597. doi: 10.1212/WNL.34.5.597

Lavi, E., Sarma, J. D., and Weiss, S. R. (1999). Cellular reservoirs for coronavirus infection of the brain in β2-microglobulin knockout mice. *Pathobiology* 67, 75–83. doi: 10.1159/000028054

Lavin, Y., Winter, D., Blecher-Gonen, R., David, E., Keren-Shaul, H., Merad, M., et al. (2014). Tissue-resident macrophage enhancer landscapes are shaped by the local microenvironment. *Cell* 159, 1312–1326. doi: 10.1016/j.cell.2014.11.018

Leary, S. M., and Thompson, A. J. (2003). Interferon beta-1a in primary progressive multiple sclerosis. *J. Neurol. Sci.* 206, 215–216. doi: 10.1016/S0022-510X(02)00350-7

Lee, Y., Morrison, B. M., Li, Y., Lengacher, S., Farah, M. H., Hoffman, P. N., et al. (2012). Oligodendroglia metabolically support axons and contribute to neurodegeneration. *Nature* 487, 443–448. doi: 10.1038/nature11314

Lees, J. R., Golumbek, P. T., Sim, J., Dorsey, D., and Russell, J. H. (2008). Regional CNS responses to IFN-gamma determine lesion localization patterns during EAE pathogenesis. *J. Exp. Med.* 205, 2633–2642. doi: 10.1084/jem.20080155

Leitzen, E., Jin, W., Herder, V., Beineke, A., Elmarabet, S. A., Baumgärtner, W., et al. (2019). Comparison of reported spinal cord lesions in progressive multiple sclerosis with theiler's murine encephalomyelitis virus induced demyelinating disease. *J. Mol. Sci.* 20:989. doi: 10.3390/ijms20040989

Li, C., Xiao, L., Liu, X., Yang, W., Shen, W., Hu, C., et al. (2013). A functional role of NMDA receptor in regulating the differentiation of oligodendrocyte precursor cells and remyelination. *Glia* 61, 732–749. doi: 10.1002/glia.22469

Li, J., Zhang, L., Chu, Y., Namaka, M., Deng, B., Kong, J., et al. (2016). Astrocytes in oligodendrocyte lineage development and white matter pathology. *Front. Cell. Neurosci.* 10:119. doi: 10.3389/fncel.2016.00119

Libbey, J. E., and Fujinami, R. S. (2021). Viral mouse models used to study multiple sclerosis: past and present. *Arch. Virol.* 166, 1015–1033. doi: 10.1007/s00705-021-04968-5

Liddelow, S. A., and Barres, B. A. (2017). Reactive astrocytes: production, function, and therapeutic potential. *Immunity* 46, 957–967. doi: 10.1016/j.immuni.2017.06.006

Liddelow, S. A., Guttenplan, K. A., Clarke, L. E., Bennett, F. C., Bohlen, C. J., Schirmer, L., et al. (2017). Neurotoxic reactive astrocytes are induced by activated microglia. *Nature* 541, 481–487. doi: 10.1038/nature21029

Liedtke, W., Edelmann, W., Bieri, P. L., Chiu, F. C., Cowan, N. J., Kucherlapati, R., et al. (1996). GFAP is necessary for the integrity of CNS white matter architecture and long-term maintenance of myelination. *Neuron* 17, 607–615. doi: 10.1016/S0896-6273(00)80194-4

Lin, M. T., Stohlman, S. A., and Hinton, D. R. (1997). Mouse hepatitis virus is cleared from the central nervous systems of mice lacking perforin-mediated cytolysis. *J. Virol.* 71, 383–391. doi: 10.1128/JVI.71.1.383-391.1997

Lin, S., Fan, L.-W., Pang, Y., Rhodes, P. G., Mitchell, H. J., and Cai, Z. (2005). IGF-1 protects oligodendrocyte progenitor cells and improves neurological functions

following cerebral hypoxia–ischemia in the neonatal rat. *Brain Res.* 1063, 15–26. doi: 10.1016/j.brainres.2005.09.042

Lin, S. C., and Bergles, D. E. (2004). Synaptic signaling between GABAergic interneurons and oligodendrocyte precursor cells in the hippocampus. *Nat. Neurosci.* 7, 24–32. doi: 10.1038/nn1162

Lin, W., Kemper, A., Dupree, J. L., Harding, H. P., Ron, D., and Popko, B. (2006). Interferon-γ inhibits central nervous system remyelination through a process modulated by endoplasmic reticulum stress. *Brain* 129, 1306–1318. doi: 10.1093/brain/awl044

Lindner, M., Fokuhl, J., Linsmeier, F., Trebst, C., and Stangel, M. (2009). Chronic toxic demyelination in the central nervous system leads to axonal damage despite remyelination. *Neurosci. Lett.* 453, 120–125. doi: 10.1016/j.neulet.2009.02.004

Lindner, M., Heine, S., Haastert, K., Garde, N., Fokuhl, J., Linsmeier, F., et al. (2008). Sequential myelin protein expression during remyelination reveals fast and efficient repair after central nervous system demyelination. *Neuropathol. Appl. Neurobiol.* 34, 105–114. doi: 10.1111/j.1365-2990.2007.00879.x

Linnerbauer, M., Wheeler, M. A., and Quintana, F. J. (2020). Astrocyte crosstalk in CNS inflammation. *Neuron* 108, 608–622. doi: 10.1016/j.neuron.2020.08.012

Liu, L., Belkadi, A., Darnall, L., Hu, T., Drescher, C., Cotleur, A. C., et al. (2010). CXCR2-positive neutrophils are essential for cuprizone-induced demyelination: relevance to multiple sclerosis. *Nat. Neurosci.* 13, 319–326. doi: 10.1038/nn.2491

Liu, L. R., Liu, J. C., Bao, J. S., Bai, Q. Q., and Wang, G. Q. (2020). Interaction of microglia and astrocytes in the neurovascular unit. *Front. Immunol.* 11:1024. doi: 10.3389/fimmu.2020.01024

Liu, M. T., Keirstead, H. S., and Lane, T. E. (2001). Neutralization of the chemokine CXCL10 reduces inflammatory cell invasion and demyelination and improves neurological function in a viral model of multiple sclerosis. *J. Immunol.* 167, 4091–4097. doi: 10.4049/jimmunol.167.7.4091

Liu, M. T., and Lane, T. E. (2001). Chemokine expression and viral infection of the central nervous system: regulation of host defense and neuropathology. *Immunol. Res.* 24, 111–119. doi: 10.1385/IR:24:2:111

Liu, Y., Holdbrooks, A. T., Meares, G. P., Buckley, J. A., Benveniste, E. N., and Qin, H. J. (2015). Preferential recruitment of neutrophils into the cerebellum and brainstem contributes to the atypical experimental autoimmune encephalomyelitis phenotype. *J. Immunol.* 195, 841–852. doi: 10.4049/jimmunol.1403063

Lloyd, A. F., and Miron, V. E. (2019). The pro-remyelination properties of microglia in the central nervous system. *Nat. Rev. Neurol.* 15, 447–458. doi: 10.1038/s41582-019-0184-2

Locksley, R. M., Killeen, N., and Lenardo, M. J. (2001). The TNF and TNF receptor superfamilies: integrating mammalian biology. *Cell* 104, 487–501. doi: 10.1016/S0092-8674(01)00237-9

Lopes Pinheiro, M. A., Kooij, G., Mizee, M. R., Kamermans, A., Enzmann, G., Lyck, R., et al. (2016). Immune cell trafficking across the barriers of the central nervous system in multiple sclerosis and stroke. *Biochim. Biophys. Acta* 1862, 461–471. doi: 10.1016/j.bbadis.2015.10.018

Lubetzki, C., and Stankoff, B. (2014). Demyelination in multiple sclerosis. *Handb. Clin. Neurol.* 122, 89–99. doi: 10.1016/B978-0-444-52001-2.00004-2

Lubetzki, C., Zalc, B., Williams, A., Stadelmann, C., and Stankoff, B. (2020). Remyelination in multiple sclerosis: from basic science to clinical translation. *Lancet Neurol.* 19, 678–688. doi: 10.1016/S1474-4422(20)30140-X

Lucchinetti, C., Bruck, W., Parisi, J., Scheithauer, B., Rodriguez, M., and Lassmann, H. (1999). A quantitative analysis of oligodendrocytes in multiple sclerosis lesions. A study of 113 cases. *Brain* 122(Pt. 12), 2279–2295. doi: 10.1093/brain/122.12.2279

Lucchinetti, C., Bruck, W., Parisi, J., Scheithauer, B., Rodriguez, M., and Lassmann, H. (2000). Heterogeneity of multiple sclerosis lesions: implications for the pathogenesis of demyelination. *Ann. Neurol.* 47, 707–717. doi: 10.1002/1531-8249(200006)47:6andlt;707::AID-ANA3andgt;3.0.CO;2-Q

Luchetti, S., Fransen, N. L., Van Eden, C. G., Ramaglia, V., Mason, M., and Huitinga, I. (2018). Progressive multiple sclerosis patients show substantial lesion activity that correlates with clinical disease severity and sex: a retrospective autopsy cohort analysis. *Acta Neuropathol.* 135, 511–528. doi: 10.1007/s00401-018-1818-y

Luo, X., Tai, W. L., Sun, L., Pan, Z., Xia, Z., Chung, S. K., et al. (2016). Crosstalk between astrocytic CXCL12 and microglial CXCR4 contributes to the development of neuropathic pain. *Mol. Pain* 12:1744806916636385. doi: 10.1177/1744806916636385

Luster, A. D., Unkeless, J. C., and Ravetch, J. V. (1985). Gamma-interferon transcriptionally regulates an early-response gene containing homology to platelet proteins. *Nature* 315, 672–676. doi: 10.1038/315672a0

Lyman, M. A., Myoung, J., Mohindru, M., and Kim, B. S. (2004). Quantitative, not qualitative, differences in CD8+ T cell responses to Theiler's murine encephalomyelitis virus between resistant C57BL/6 and susceptible SJL/J mice. *Eur. J. Immunol.* 34, 2730–2739. doi: 10.1002/eji.200324811

Machado-Santos, J., Saji, E., Tröscher, A. R., Paunovic, M., Liblau, R., Gabriely, G., et al. (2018). The compartmentalized inflammatory response in the multiple sclerosis brain is composed of tissue-resident CD8+ T lymphocytes and B cells. *Brain* 141, 2066–2082. doi: 10.1093/brain/awy151

Mack, C. L., Vanderlugt-Castaneda, C. L., Neville, K. L., and Miller, S. D. (2003). Microglia are activated to become competent antigen presenting and effector cells in the inflammatory environment of the Theiler's virus model of multiple sclerosis. *J. Neuroimmunol.* 144, 68–79. doi: 10.1016/j.jneuroim.2003.08.032

Madsen, P. M., Desu, H. L., De Rivero Vaccari, J. P., Florimon, Y., Ellman, D. G., Keane, R. W., et al. (2020). Oligodendrocytes modulate the immune-inflammatory response in EAE via TNFR2 signaling. *Brain Behav. Immun.* 84, 132–146. doi: 10.1016/j.bbi.2019.11.017

Marro, B. S., Skinner, D. D., Cheng, Y., Grist, J. J., Dickey, L. L., Eckman, E., et al. (2019). Disrupted CXCR2 signaling in oligodendroglia lineage cells enhances myelin repair in a viral model of multiple sclerosis. *J. Virol.* 93:e00240-19. doi: 10.1128/JVI.00240-19

Mars, L. T., Laloux, V., Goude, K., Desbois, S., Saoudi, A., Van Kaer, L., et al. (2002). Cutting edge: Vα14-Jα281 NKT cells naturally regulate experimental autoimmune encephalomyelitis in nonobese diabetic mice. *J. Immunol.* 168, 6007–6011. doi: 10.4049/jimmunol.168.12.6007

Marusic, S., Leach, M. W., Pelker, J. W., Azoitei, M. L., Uozumi, N., Cui, J., et al. (2005). Cytosolic phospholipase A2 alpha-deficient mice are resistant to experimental autoimmune encephalomyelitis. *J. Exp. Med.* 202, 841–851. doi: 10.1084/jem.20050665

Mason, J. L., Jones, J. J., Taniike, M., Morell, P., Suzuki, K., and Matsushima, G. K. (2000). Mature oligodendrocyte apoptosis precedes IGF-1 production and oligodendrocyte progenitor accumulation and differentiation during demyelination/remyelination. *J. Neurosci. Res.* 61, 251–262. doi: 10.1002/1097-4547(20000801)61:3<251::AID-JNR3>3.0.CO;2-W

Mason, J. L., Suzuki, K., Chaplin, D. D., and Matsushima, G. K. (2001). Interleukin-1beta promotes repair of the CNS. *J. Neurosci.* 21, 7046–7052. doi: 10.1523/JNEUROSCI.21-18-07046.2001

Masuda, T., Sankowski, R., Staszewski, O., and Prinz, M. (2020). Microglia heterogeneity in the single-cell era. *Cell Rep.* 30, 1271–1281. doi: 10.1016/j.celrep.2020.01.010

Matsuki, T., Nakae, S., Sudo, K., Horai, R., and Iwakura, Y. J. (2006). Abnormal T cell activation caused by the imbalance of the IL-1/IL-1R antagonist system is responsible for the development of experimental autoimmune encephalomyelitis. *Int. Immunol.* 18, 399–407. doi: 10.1093/intimm/dxh379

Matsushima, G. K., and Morell, P. (2001). The neurotoxicant, cuprizone, as a model to study demyelination and remyelination in the central nervous system. *Brain Pathol.* 11, 107–116. doi: 10.1111/j.1750-3639.2001.tb00385.x

Matsushita, T., Yanaba, K., Bouaziz, J. D., Fujimoto, M., and Tedder, T. F. (2008). Regulatory B cells inhibit EAE initiation in mice while other B cells promote disease progression. *J. Clin. Invest.* 118, 3420–3430. doi: 10.1172/JCI36030

Maysami, S., Nguyen, D., Zobel, F., Heine, S., Höpfner, M., and Stangel, M. (2006a). Oligodendrocyte precursor cells express a functional chemokine receptor CCR3: Implications for myelination. *J. Neuroimmunol.* 178, 17–23. doi: 10.1016/j.jneuroim.2006.05.021

Maysami, S., Nguyen, D., Zobel, F., Pitz, C., Heine, S., Höpfner, M., et al. (2006b). Modulation of rat oligodendrocyte precursor cells by the chemokine CXCL12. *Neuroreport* 17, 1187–1190. doi: 10.1097/01.wnr.0000227985.92551.9a

McCarthy, D. P., Richards, M. H., and Miller, S. D. (2012). Mouse models of multiple sclerosis: experimental autoimmune encephalomyelitis and Theiler's virus-induced demyelinating disease. *Methods Mol. Biol.* 900, 381–401. doi: 10.1007/978-1-60761-720-4_19

McCarthy, M. K., and Weinberg, J. B. (2015). The immunoproteasome and viral infection: a complex regulator of inflammation. *Front. Microbiol.* 6:21. doi: 10.3389/fmicb.2015.00021

Mcginley, A. M., Edwards, S. C., Raverdeau, M., and Mills, K. H. G. (2018). Th17 cells, γδ T cells and their interplay in EAE and multiple sclerosis. *J. Autoimmun.* 87, 97–108. doi: 10.1016/j.jaut.2018.01.001

Mcmahon, E. J., Bailey, S. L., Castenada, C. V., Waldner, H., and Miller, S. D. (2005). Epitope spreading initiates in the CNS in two mouse models of multiple sclerosis. *Nat. Med.* 11, 335–339. doi: 10.1038/nm1202

McRae, B. L., Vanderlugt, C. L., Dal Canto, M. C., and Miller, S. D. (1995). Functional evidence for epitope spreading in the relapsing pathology of experimental autoimmune encephalomyelitis. *J. Exp. Med.* 182, 75–85. doi: 10.1084/jem.182.1.75

Mecha, M., Carrillo-Salinas, F. J., Mestre, L., Feliú, A., and Guaza, C. (2013). Viral models of multiple sclerosis: neurodegeneration and demyelination in mice infected with Theiler's virus. *Prog. Neurobiol.* 101–102, 46–64. doi: 10.1016/j.pneurobio.2012.11.003

Michael, B. D., Bricio-Moreno, L., Sorensen, E. W., Miyabe, Y., Lian, J., Solomon, T., et al. (2020). Astrocyte- and neuron-derived CXCL1 drives neutrophil transmigration and blood-brain barrier permeability in viral encephalitis. *Cell Rep.* 32:108150. doi: 10.1016/j.celrep.2020.108150

Miller, D. H., and Leary, S. M. (2007). Primary-progressive multiple sclerosis. *Lancet Neurol.* 6, 903–912. doi: 10.1016/S1474-4422(07)70243-0

Miller, S. D., and Karpus, W. J. (2007). Experimental autoimmune encephalomyelitis in the mouse. *Curr. Protoc. Immunol.* doi: 10.1002/0471142735.im1501s77

Miller, S. D., Karpus, W. J., and Davidson, T. S. (2010). Experimental autoimmune encephalomyelitis in the mouse. *Curr. Protoc. Immunol.* 88, 15.11.11–15.11.20. doi: 10.1002/0471142735.im1501s88

Miller, S. D., Olson, J. K., and Croxford, J. L. (2001). Multiple pathways to induction of virus-induced autoimmune demyelination: lessons from Theiler's virus infection. *J. Autoimmun.* 16, 219–227. doi: 10.1006/jaut.2000.0489

Miller, S. D., Vanderlugt, C. L., Begolka, W. S., Pao, W., Yauch, R. L., Neville, K. L., et al. (1997). Persistent infection with Theiler's virus leads to CNS autoimmunity via epitope spreading. *Nat. Med.* 3, 1133–1136. doi: 10.1038/nm1097-1133

Milner, R., Huang, X., Wu, J., Nishimura, S., Pytela, R., Sheppard, D., et al. (1999). Distinct roles for astrocyte alphavbeta5 and alphavbeta8 integrins in adhesion and migration. *J. Cell Sci.* 112:4271. doi: 10.1242/jcs.112.23.4271

Minden, S. L., Frankel, D., Hadden, L. S., Srinath, K. P., and Perloff, J. N. (2004). Disability in elderly people with multiple sclerosis: an analysis of baseline data from the Sonya Slifka Longitudinal Multiple Sclerosis Study. *NeuroRehabilitation* 19, 55–67. doi: 10.3233/NRE-2004-19107

Miron, V. E., Boyd, A., Zhao, J.-W., Yuen, T. J., Ruckh, J. M., Shadrach, J. L., et al. (2013). M2 microglia and macrophages drive oligodendrocyte differentiation during CNS remyelination. *Nat. Neurosci.* 16, 1211–1218. doi: 10.1038/nn.3469

Mirshafiey, A., Asghari, B., Ghalamfarsa, G., Jadidi-Niaragh, F., and Azizi, G. (2014). The significance of matrix metalloproteinases in the immunopathogenesis and treatment of multiple sclerosis. *Sultan Qaboos Univ. Med. J.* 14, e13–e25. doi: 10.12816/0003332

Miyagi, M., Mikawa, S., Sato, T., Hasegawa, T., Kobayashi, S., Matsuyama, Y., et al. (2012). BMP2, BMP4, noggin, BMPRIA, BMPRIB, and BMPRII are differentially expressed in the adult rat spinal cord. *Neuroscience.* 203, 12–26. doi: 10.1016/j.neuroscience.2011.12.022

Miyamoto, N., Maki, T., Shindo, A., Liang, A. C., Maeda, M., Egawa, N., et al. (2015). Astrocytes promote oligodendrogenesis after white matter damage via brain-derived neurotrophic factor. *J. Neurosci.* 35:14002. doi: 10.1523/JNEUROSCI.1592-15.2015

Mizuno, T., Zhang, G., Takeuchi, H., Kawanokuchi, J., Wang, J., Sonobe, Y., et al. (2008). Interferon-gamma directly induces neurotoxicity through a neuron specific, calcium-permeable complex of IFN-gamma receptor and AMPA GluR1 receptor. *Faseb. J.* 22, 1797–1806. doi: 10.1096/fj.07-099499

Mohindru, M., Kang, B., and Kim, B. S. (2006). Initial capsid-specific CD4+ T cell responses protect against Theiler's murine encephalomyelitisvirus-induced demyelinating disease. *Eur. J. Immunol.* 36, 2106–2115. doi: 10.1002/eji.200535785

Montalban, X., Hauser, S. L., Kappos, L., Arnold, D. L., Bar-Or, A., Comi, G., et al. (2017). Ocrelizumab versus placebo in primary progressive multiple sclerosis. *N. Engl. J. Med.* 376, 209–220. doi: 10.1056/NEJMoa1606468

Moore, C. S., Cui, Q. L., Warsi, N. M., Durafourt, B. A., Zorko, N., Owen, D. R., et al. (2015). Direct and indirect effects of immune and central nervous system-resident cells on human oligodendrocyte progenitor cell differentiation. *J. Immunol.* 194, 761–772. doi: 10.4049/jimmunol.1401156

Morales Pantoja, I. E., Smith, M. D., Rajbhandari, L., Cheng, L., Gao, Y., Mahairaki, V., et al. (2020). iPSCs from people with MS can differentiate into oligodendrocytes in a homeostatic but not an inflammatory milieu. *PLoS ONE* 15:e0233980. doi: 10.1371/journal.pone.0233980

Morrison, V. E., Smith, V. N., and Huang, J. K. (2020). Retinoic acid is required for oligodendrocyte precursor cell production and differentiation in the postnatal mouse corpus callosum. *eneuro* 7, 1–18. doi: 10.1523/ENEURO.0270-19.2019

Moyon, S., Dubessy, A. L., Aigrot, M. S., Trotter, M., Huang, J. K., Dauphinot, L., et al. (2015). Demyelination causes adult CNS progenitors to revert to an immature state and express immune cues that support their migration. *J. Neurosci.* 35, 4–20. doi: 10.1523/JNEUROSCI.0849-14.2015

Müller, A., Hauk, T. G., and Fischer, D. (2007). Astrocyte-derived CNTF switches mature RGCs to a regenerative state following inflammatory stimulation. *Brain* 130, 3308–3320. doi: 10.1093/brain/awm257

Myer, D. J., Gurkoff, G. G., Lee, S. M., Hovda, D. A., and Sofroniew, M. V. (2006). Essential protective roles of reactive astrocytes in traumatic brain injury. *Brain* 129, 2761–2772. doi: 10.1093/brain/awl165

Nair, A., Frederick, T. J., and Miller, S. D. (2008). Astrocytes in multiple sclerosis: a product of their environment. *Cell. Mol. Life. Sci.* 65, 2702–2720. doi: 10.1007/s00018-008-8059-5

Neumann, B., Baror, R., Zhao, C., Segel, M., Dietmann, S., Rawji, K. S., et al. (2019). Metformin restores CNS remyelination capacity by rejuvenating aged stem cells. *Cell Stem Cell* 25, 473–485.e478. doi: 10.1016/j.stem.2019.08.015

Nicaise, A. M., Johnson, K. M., Willis, C. M., Guzzo, R. M., and Crocker, S. J. (2019b). TIMP-1 promotes oligodendrocyte differentiation through receptor-mediated signaling. *Mol. Neurobiol.* 56, 3380–3392. doi: 10.1007/s12035-018-1310-7

Nicaise, A. M., Wagstaff, L. J., Willis, C. M., Paisie, C., Chandok, H., Robson, P., et al. (2019a). Cellular senescence in progenitor cells contributes to diminished remyelination potential in progressive multiple sclerosis. *Proc. Natl. Acad. Sci. U.S.A.* 116, 9030–9039. doi: 10.1073/pnas.1818348116

Nicholas, R. S., Stevens, S., Wing, M. G., and Compston, D. A. (2002). Microglia-derived IGF-2 prevents TNFalpha induced death of mature oligodendrocytes *in vitro*. *J. Neuroimmunol.* 124, 36–44. doi: 10.1016/S0165-5728(02)00011-5

Nicholas, R. S., Wing, M. G., and Compston, A. (2001). Nonactivated microglia promote oligodendrocyte precursor survival and maturation through the transcription factor NF-kappa B. *Eur. J. Neurosci.* 13, 959–967. doi: 10.1046/j.0953-816x.2001.01470.x

Niu, J., Tsai, H. H., Hoi, K. K., Huang, N., Yu, G., Kim, K., et al. (2019). Aberrant oligodendroglial-vascular interactions disrupt the blood-brain barrier, triggering CNS inflammation. *Nat. Neurosci.* 22, 709–718. doi: 10.1038/s41593-019-0369-4

Noseworthy, J. H., Lucchinetti, C., Rodriguez, M., and Weinshenker, B. G. (2000). Multiple sclerosis. *N. Engl. J. Med.* 343, 938–952. doi: 10.1056/NEJM200009283431307

Nutma, E., Van Gent, D., Amor, S., and Peferoen, L.,a.N. (2020). Astrocyte and oligodendrocyte cross-talk in the central nervous system. *Cells* 9:600. doi: 10.3390/cells9030600

Ogawa, K., Ito, M., Takeuchi, K., Nakada, A., Heishi, M., Suto, H., et al. (2005). Tenascin-C is upregulated in the skin lesions of patients with atopic dermatitis. *J. Dermatol. Sci.* 40, 35–41. doi: 10.1016/j.jdermsci.2005.06.001

Okuda, H., Tatsumi, K., Morita, S., Shibukawa, Y., Korekane, H., Horii-Hayashi, N., et al. (2014). Chondroitin sulfate proteoglycan tenascin-R regulates glutamate uptake by adult brain astrocytes. *J. Biol. Chem.* 289, 2620–2631. doi: 10.1074/jbc.M113.504787

Oleszak, E. L., Chang, J. R., Friedman, H., Katsetos, C. D., and Platsoucas, C. D. (2004). Theilerand's virus infection: a model for multiple sclerosis. *Clin. Microbiol. Rev.* 17:174. doi: 10.1128/CMR.17.1.174-207.2004

Olsson, T. (1992). Cytokines in neuroinflammatory disease: role of myelin autoreactive T cell production of interferon-gamma. *J. Neuroimmunol.* 40, 211–218. doi: 10.1016/0165-5728(92)90135-8

Omari, K. M., John, G. R., Sealfon, S. C., and Raine, C. S. (2005). CXC chemokine receptors on human oligodendrocytes: implications for multiple sclerosis. *Brain* 128, 1003–1015. doi: 10.1093/brain/awh479

Ortiz, F. C., Habermacher, C., Graciarena, M., Houry, P.-Y., Nishiyama, A., Nait Oumesmar, B., et al. (2019). Neuronal activity *in vivo* enhances functional myelin repair. *JCI Insight* 5:e123434. doi: 10.1172/jci.insight.123434

Othman, T., Yan, H., and Rivkees, S. (2003). Oligodendrocytes express functional A1 adenosine receptors that stimulate cellular migration. *Glia* 44, 166–172. doi: 10.1002/glia.10281

Pál, E., Tabira, T., Kawano, T., Taniguchi, M., Miyake, S., and Yamamura, T. J. (2001). Costimulation-dependent modulation of experimental autoimmune encephalomyelitis by ligand stimulation of Vα14 NK T cells. *J. Immunol.* 166, 662–668. doi: 10.4049/jimmunol.166.1.662

Palma, J. P., Yauch, R. L., Lang, S., and Kim, B. S. (1999). Potential role of CD4+ T cell-mediated apoptosis of activated astrocytes in Theiler's virus-induced demyelination. *J. Immunol.* 162, 6543–6551.

Pang, Y., Cai, Z., and Rhodes, P. G. (2000). Effects of lipopolysaccharide on oligodendrocyte progenitor cells are mediated by astrocytes and microglia. *J. Neurosci. Res.* 62, 510–520. doi: 10.1002/1097-4547(20001115)62:4andlt;510::AID-JNR5andgt;3.0.CO;2-F

Pang, Y., Campbell, L., Zheng, B., Fan, L., Cai, Z., and Rhodes, P. (2010). Lipopolysaccharide-activated microglia induce death of oligodendrocyte progenitor cells and impede their development. *Neuroscience* 166, 464–475. doi: 10.1016/j.neuroscience.2009.12.040

Paolicelli, R. C., Bolasco, G., Pagani, F., Maggi, L., Scianni, M., Panzanelli, P., et al. (2011). Synaptic pruning by microglia is necessary for normal brain development. *Science* 333, 1456–1458. doi: 10.1126/science.1202529

Parajuli, B., Horiuchi, H., Mizuno, T., Takeuchi, H., and Suzumura, A. (2015). CCL11 enhances excitotoxic neuronal death by producing reactive oxygen species in microglia. *Glia* 63, 2274–2284. doi: 10.1002/glia.22892

Parra, B., Hinton, D. R., Marten, N. W., Bergmann, C. C., Lin, M. T., Yang, C. S., et al. (1999). IFN-γ is required for viral clearance from central nervous system oligodendroglia. *J. Immunol.* 162, 1641–1647.

Pasquini, L. A., Millet, V., Hoyos, H. C., Giannoni, J. P., Croci, D. O., Marder, M., et al. (2011). Galectin-3 drives oligodendrocyte differentiation to control myelin integrity and function. *Cell Death Differ.* 18, 1746–1756. doi: 10.1038/cdd.2011.40

Patel, J. R., and Klein, R. S. (2011). Mediators of oligodendrocyte differentiation during remyelination. *FEBS. Lett.* 585, 3730–3737. doi: 10.1016/j.febslet.2011.04.037

Patel, J. R., McCandless, E. E., Dorsey, D., and Klein, R. S. (2010). CXCR4 promotes differentiation of oligodendrocyte progenitors and remyelination. *Proc. Natl. Acad. Sci. U.S.A.* 107, 11062–11067. doi: 10.1073/pnas.1006301107

Patel, J. R., Williams, J. L., Muccigrosso, M. M., Liu, L., Sun, T., Rubin, J. B., et al. (2012). Astrocyte TNFR2 is required for CXCL12-mediated regulation of oligodendrocyte progenitor proliferation and differentiation within the adult CNS. *Acta Neuropathol.* 124, 847–860. doi: 10.1007/s00401-012-1034-0

Patrikios, P., Stadelmann, C., Kutzelnigg, A., Rauschka, H., Schmidbauer, M., Laursen, H., et al. (2006). Remyelination is extensive in a subset of multiple sclerosis patients. *Brain* 129, 3165–3172. doi: 10.1093/brain/awl217

Peferoen, L., Kipp, M., Van Der Valk, P., Van Noort, J. M., and Amor, S. (2014). Oligodendrocyte-microglia cross-talk in the central nervous system. *Immunology* 141, 302–313. doi: 10.1111/imm.12163

Peterson, J. W., Bö, L., Mörk, S., Chang, A., and Trapp, B. D. (2001). Transected neurites, apoptotic neurons, and reduced inflammation in cortical multiple sclerosis lesions. *Ann. Neurol.* 50, 389–400. doi: 10.1002/ana.1123

Petkovic, F., Campbell, I. L., Gonzalez, B., and Castellano, B. (2016). Astrocyte-targeted production of interleukin-6 reduces astroglial and microglial activation in the cuprizone demyelination model: implications for myelin clearance and oligodendrocyte maturation. *Glia* 64, 2104–2119. doi: 10.1002/glia.23043

Phares, T. W., Stohlman, S. A., Hinton, D. R., Atkinson, R., and Bergmann, C. C. (2010). Enhanced antiviral T cell function in the absence of B7-H1 is insufficient to prevent persistence but exacerbates axonal bystander damage during viral encephalomyelitis. *J. Immunol.* 185, 5607–5618. doi: 10.4049/jimmunol.1001984

Phares, T. W., Stohlman, S. A., Hwang, M., Min, B., Hinton, D. R., and Bergmann, C. C. (2012). CD4 T cells promote CD8 T cell immunity at the priming and effector site during viral encephalitis. *J. Virol.* 86, 2416–2427. doi: 10.1128/JVI.06797-11

Phillips, J. J., Chua, M. M., Rall, G. F., and Weiss, S. R. (2002). Murine coronavirus spike glycoprotein mediates degree of viral spread, inflammation, and virus-induced immunopathology in the central nervous system. *Virology* 301, 109–120. doi: 10.1006/viro.2002.1551

Pierson, E., Simmons, S. B., Castelli, L., and Goverman, J. M. (2012). Mechanisms regulating regional localization of inflammation during CNS autoimmunity. *Immunol. Rev.* 248, 205–215. doi: 10.1111/j.1600-065X.2012.01126.x

Pierson, E. R., Stromnes, I. M., and Goverman, J. M. (2014). B cells promote induction of experimental autoimmune encephalomyelitis by facilitating reactivation of T cells in the central nervous system. *J. Immunol.* 192, 929–939. doi: 10.4049/jimmunol.1302171

Pöllinger, B., Krishnamoorthy, G., Berer, K., Lassmann, H., Bösl, M. R., Dunn, R., et al. (2009). Spontaneous relapsing-remitting EAE in the SJL/J mouse: MOG-reactive transgenic T cells recruit endogenous MOG-specific B cells. *J. Exp. Med.* 206, 1303–1316. doi: 10.1084/jem.20090299

Ponath, G., Park, C., and Pitt, D. (2018). The role of astrocytes in multiple sclerosis. *Front. Immunol.* 9:217. doi: 10.3389/fimmu.2018.00217

Ponomarev, E. D., Shriver, L. P., Maresz, K., and Dittel, B. N. (2005). Microglial cell activation and proliferation precedes the onset of CNS autoimmunity. *J. Neurosci. Res.* 81, 374–389. doi: 10.1002/jnr.20488

Praet, J., Guglielmetti, C., Berneman, Z., Van Der Linden, A., and Ponsaerts, P. (2014). Cellular and molecular neuropathology of the cuprizone mouse model: clinical relevance for multiple sclerosis. *Neurosci. Biobehav. Rev.* 47, 485–505. doi: 10.1016/j.neubiorev.2014.10.004

Prineas, J. W., Barnard, R. O., Kwon, E. E., Sharer, L. R., and Cho, E. S. (1993). Multiple sclerosis: remyelination of nascent lesions. *Ann. Neurol.* 33, 137–151. doi: 10.1002/ana.410330203

Prinz, M., and Priller, J. (2017). The role of peripheral immune cells in the CNS in steady state and disease. *Nat. Neurosci.* 20, 136–144. doi: 10.1038/nn.4475

Procaccini, C., De Rosa, V., Pucino, V., Formisano, L., and Matarese, G. (2015). Animal models of Multiple Sclerosis. *Eur. J. Pharmacol.* 759, 182–191. doi: 10.1016/j.ejphar.2015.03.042

Puntambekar, S. S., Bergmann, C. C., Savarin, C., Karp, C. L., Phares, T. W., Parra, G. I., et al. (2011). Shifting hierarchies of interleukin-10-producing T cell populations in the central nervous system during acute and persistent viral encephalomyelitis. *J. Virol.* 85, 6702–6713. doi: 10.1128/JVI.00200-11

Qi, Y., and Dal Canto, M. C. (1996). Effect of Theiler's murine encephalomyelitis virus and cytokines on cultured oligodendrocytes and astrocytes. 45, 364–374.

Raine, C. S., and Wu, E. (1993). Multiple sclerosis: remyelination in acute lesions. *J. Neuropathol. Exp. Neurol.* 52, 199–204. doi: 10.1097/00005072-199305000-00003

Ramírez Hernández, E., Sánchez-Maldonado, C., Mayoral Chávez, M. A., Hernández-Zimbrón, L. F., Patricio Martínez, A., Zenteno, E., et al. (2020). The therapeutic potential of galectin-1 and galectin-3 in the treatment of neurodegenerative diseases. *Expert Rev. Neurother.* 20, 439–448. doi: 10.1080/14737175.2020.1750955

Rempel, J. D., Murray, S. J., Meisner, J., and Buchmeier, M. J. (2004). Differential regulation of innate and adaptive immune responses in viral encephalitis. *Virology* 318, 381–392. doi: 10.1016/j.virol.2003.09.023

Ressler, S., Bartkova, J., Niederegger, H., Bartek, J., Scharffetter-Kochanek, K., Jansen-Dürr, P., et al. (2006). p16INK4A is a robust *in vivo* biomarker of cellular aging in human skin. *Aging Cell.* 5, 379–389. doi: 10.1111/j.1474-9726.2006.00231.x

Rhodes, K. E., Raivich, G., and Fawcett, J. W. (2006). The injury response of oligodendrocyte precursor cells is induced by platelets, macrophages and inflammation-associated cytokines. *Neuroscience* 140, 87–100. doi: 10.1016/j.neuroscience.2006.01.055

Richards, M. H., Getts, M. T., Podojil, J. R., Jin, Y.-H., Kim, B. S., and Miller, S. D. (2011). Virus expanded regulatory T cells control disease severity in the Theiler's virus mouse model of MS. *J. Autoimmun.* 36, 142–154. doi: 10.1016/j.jaut.2010.12.005

Risau, W., and Wolburg, H. (1990). Development of the blood-brain barrier. *Trends Neurosci.* 13, 174–178. doi: 10.1016/0166-2236(90)90043-A

Robinson, S., Tani, M., Strieter, R. M., Ransohoff, R. M., and Miller, R. H. (1998). The chemokine growth-regulated oncogene-alpha promotes spinal

cord oligodendrocyte precursor proliferation. *J. Neurosci.* 18, 10457–10463. doi: 10.1523/JNEUROSCI.18-24-10457.1998

Rodgers, J. M., Robinson, A. P., Rosler, E. S., Lariosa-Willingham, K., Persons, R. E., Dugas, J. C., et al. (2015). IL-17A activates ERK1/2 and enhances differentiation of oligodendrocyte progenitor cells. *Glia* 63, 768–779. doi: 10.1002/glia.22783

Rosenman, S. J., Shrikant, P., Dubb, L., Benveniste, E. N., and Ransohoff, R. M. (1995). Cytokine-induced expression of vascular cell adhesion molecule-1 (VCAM-1) by astrocytes and astrocytoma cell lines. *J. Immunol.* 154, 1888–1899.

Rossi, S., Motta, C., Studer, V., Macchiarulo, G., Volpe, E., Barbieri, F., et al. (2014a). Interleukin-1β causes excitotoxic neurodegeneration and multiple sclerosis disease progression by activating the apoptotic protein p53. *Mol. Neurodegen.* 9:56. doi: 10.1186/1750-1326-9-56

Rossi, S., Muzio, L., De Chiara, V., Grasselli, G., Musella, A., Musumeci, G., et al. (2011). Impaired striatal GABA transmission in experimental autoimmune encephalomyelitis. *Brain Behav. Immun.* 25, 947–956. doi: 10.1016/j.bbi.2010.10.004

Rossi, S., Studer, V., Motta, C., Germani, G., Macchiarulo, G., Buttari, F., et al. (2014b). Cerebrospinal fluid detection of interleukin-1β in phase of remission predicts disease progression in multiple sclerosis. *J. Neuroinflamm.* 11, 1–8. doi: 10.1186/1742-2094-11-32

Ruckh, J. M., Zhao, J. W., Shadrach, J. L., Van Wijngaarden, P., Rao, T. N., Wagers, A. J., et al. (2012). Rejuvenation of regeneration in the aging central nervous system. *Cell Stem Cell* 10, 96–103. doi: 10.1016/j.stem.2011.11.019

Ruther, B. J., Scheld, M., Dreymueller, D., Clarner, T., Kress, E., Brandenburg, L. O., et al. (2017). Combination of cuprizone and experimental autoimmune encephalomyelitis to study inflammatory brain lesion formation and progression. *Glia* 65, 1900–1913. doi: 10.1002/glia.23202

Safarzadeh, E., Jadidi-Niaragh, F., Motallebnezhad, M., and Yousefi, M. (2016). The role of adenosine and adenosine receptors in the immunopathogenesis of multiple sclerosis. *Inflamm. Res.* 65, 511–520. doi: 10.1007/s00011-016-0936-z

Sanai, S. A., Saini, V., Benedict, R. H., Zivadinov, R., Teter, B. E., Ramanathan, M., et al. (2016). Aging and multiple sclerosis. *Mult. Scler.* 22, 717–725. doi: 10.1177/1352458516634871

Savarin, C., and Bergmann, C. C. (2017). Viral-induced suppression of self-reactive T cells: lessons from neurotropic coronavirus-induced demyelination. *J. Neuroimmunol.* 308, 12–16. doi: 10.1016/j.jneuroim.2017.01.003

Savarin, C., Bergmann, C. C., Hinton, D. R., and Stohlman, S. A. (2016). Differential regulation of self-reactive CD4(+) T cells in cervical lymph nodes and central nervous system during viral encephalomyelitis. *Front. Immunol.* 7:370. doi: 10.3389/fimmu.2016.00370

Scalfari, A., Neuhaus, A., Daumer, M., Ebers, G. C., and Muraro, P. A. (2011). Age and disability accumulation in multiple sclerosis. *Neurology* 77, 1246–1252. doi: 10.1212/WNL.0b013e318230a17d

Scalfari, A., Neuhaus, A., Daumer, M., Muraro, P. A., and Ebers, G. C. (2014). Onset of secondary progressive phase and long-term evolution of multiple sclerosis. *J. Neurol. Neurosurg. Psychiatry* 85, 67–75. doi: 10.1136/jnnp-2012-304333

Schafer, D. P., Lehrman, E. K., Kautzman, A. G., Koyama, R., Mardinly, A. R., Yamasaki, R., et al. (2012). Microglia sculpt postnatal neural circuits in an activity and complement-dependent manner. *Neuron* 74, 691–705. doi: 10.1016/j.neuron.2012.03.026

Scheld, M., Rüther, B. J., Große-Veldmann, R., Ohl, K., Tenbrock, K., Dreymüller, D., et al. (2016). Neurodegeneration triggers peripheral immune cell recruitment into the forebrain. *J. Neurosci.* 36, 1410–1415. doi: 10.1523/JNEUROSCI.2456-15.2016

Schmitz, T., and Chew, L. J. (2008). Cytokines and myelination in the central nervous system. *ScientificWorldJournal* 8, 1119–1147. doi: 10.1100/tsw.2008.140

Schonrock, L. M., Gawlowski, G., and Bruck, W. (2000). Interleukin-6 expression in human multiple sclerosis lesions. *Neurosci. Lett.* 294, 45–48. doi: 10.1016/S0304-3940(00)01543-3

Segel, M., Neumann, B., Hill, M. F. E., Weber, I. P., Viscomi, C., Zhao, C., et al. (2019a). Author Correction: Niche stiffness underlies the ageing of central nervous system progenitor cells. *Nature* 573:E3. doi: 10.1038/s41586-019-1552-1

Segel, M., Neumann, B., Hill, M. F. E., Weber, I. P., Viscomi, C., Zhao, C., et al. (2019b). Niche stiffness underlies the ageing of central nervous system progenitor cells. *Nature* 573, 130–134. doi: 10.1038/s41586-019-1484-9

Seidl, A. H. (2014). Regulation of conduction time along axons. *Neuroscience* 276, 126–134. doi: 10.1016/j.neuroscience.2013.06.047

Seo, J. H., Miyamoto, N., Hayakawa, K., Pham, L. D., Maki, T., Ayata, C., et al. (2013). Oligodendrocyte precursors induce early blood-brain barrier opening after white matter injury. *J. Clin. Invest.* 123, 782–786. doi: 10.1172/JCI65863

Shearer, K. D., Fragoso, Y. D., Clagett-Dame, M., and McCaffery, P. J. (2012). Astrocytes as a regulated source of retinoic acid for the brain. *Glia* 60, 1964–1976. doi: 10.1002/glia.22412

Shen, K., Reichelt, M., Kyauk, R. V., Ngu, H., Shen, Y. A., Foreman, O., et al. (2021). Multiple sclerosis risk gene Mertk is required for microglial activation and subsequent remyelination. *Cell Rep.* 34:108835. doi: 10.1016/j.celrep.2021.108835

Shiow, L. R., Favrais, G., Schirmer, L., Schang, A.-L., Cipriani, S., Andres, C., et al. (2017). Reactive astrocyte COX2-PGE2 production inhibits oligodendrocyte maturation in neonatal white matter injury. *Glia* 65, 2024–2037. doi: 10.1002/glia.23212

Silberstein, F. C., De Simone, R., Levi, G., and Aloisi, F. (1996). Cytokine-regulated expression of platelet-derived growth factor gene and protein in cultured human astrocytes. *J. Neurochem.* 66, 1409–1417. doi: 10.1046/j.1471-4159.1996.66041409.x

Sim, F. J., Zhao, C., Penderis, J., and Franklin, R. J. (2002). The age-related decrease in CNS remyelination efficiency is attributable to an impairment of both oligodendrocyte progenitor recruitment and differentiation. *J. Neurosci.* 22, 2451–2459. doi: 10.1523/JNEUROSCI.22-07-02451.2002

Simmons, S. B., Pierson, E. R., Lee, S. Y., and Goverman, J. M. (2013). Modeling the heterogeneity of multiple sclerosis in animals. *Trends Immunol.* 34, 410–422. doi: 10.1016/j.it.2013.04.006

Singh, A. K., Wilson, M. T., Hong, S., Olivares-Villagómez, D., Du, C., Stanic, A. K., et al. (2001). Natural killer T cell activation protects mice against experimental autoimmune encephalomyelitis. *J. Exp. Med.* 194, 1801–1811. doi: 10.1084/jem.194.12.1801

Sixt, M., Engelhardt, B., Pausch, F., Hallmann, R., Wendler, O., and Sorokin, L. M. (2001). Endothelial cell laminin isoforms, laminins 8 and 10, play decisive roles in T cell recruitment across the blood-brain barrier in experimental autoimmune encephalomyelitis. *J. Cell. Biol.* 153, 933–946. doi: 10.1083/jcb.153.5.933

Skinner, D. D., and Lane, T. E. (2020). CXCR2 signaling and remyelination in preclinical models of demyelination. *DNA Cell. Biol.* 39, 3–7. doi: 10.1089/dna.2019.5182

Skripuletz, T., Hackstette, D., Bauer, K., Gudi, V., Pul, R., Voss, E., et al. (2013). Astrocytes regulate myelin clearance through recruitment of microglia during cuprizone-induced demyelination. *Brain* 136, 147–167. doi: 10.1093/brain/aws262

Smith, B. C., Sinyuk, M., Jenkins, J. E. III., Psenicka, M. W., and Williams, J. L. (2020). The impact of regional astrocyte interferon-gamma signaling during chronic autoimmunity: a novel role for the immunoproteasome. *J. Neuroinflamm.* 17:184. doi: 10.1186/s12974-020-01861-x

Sofroniew, M. V. (2005). Reactive astrocytes in neural repair and protection. *Neuroscientist* 11, 400–407. doi: 10.1177/1073858405278321

Sofroniew, M. V., and Vinters, H. V. (2010). Astrocytes: biology and pathology. *Acta Neuropathol.* 119, 7–35. doi: 10.1007/s00401-009-0619-8

Sonobe, Y., Jin, S., Wang, J., Kawanokuchi, J., Takeuchi, H., Mizuno, T., et al. (2007). Chronological changes of CD4+ and CD8+ T cell subsets in the experimental autoimmune encephalomyelitis, a mouse model of multiple sclerosis. *J. Exp. Med.* 213, 329–339. doi: 10.1620/tjem.213.329

Sosa, R. A., Murphey, C., Robinson, R. R., and Forsthuber, T. G. (2015). IFN-γ ameliorates autoimmune encephalomyelitis by limiting myelin lipid *peroxidation*. 112, E5038–E5047. doi: 10.1073/pnas.1505955112

Spassky, N., de Castro, F., Le Bras, B., Heydon, K., Quéraud-LeSaux, F., Bloch-Gallego, E., et al. (2002). Directional guidance of oligodendroglial migration by class 3 semaphorins and netrin-1. *J. Neurosci.* 22, 5992–6004. doi: 10.1523/JNEUROSCI.22-14-05992.2002

Spitzer, S. O., Sitnikov, S., Kamen, Y., Evans, K. A., Kronenberg-Versteeg, D., Dietmann, S., et al. (2019). oligodendrocyte progenitor cells become

regionally diverse and heterogeneous with age. *Neuron* 101, 459–471 e455. doi: 10.1016/j.neuron.2018.12.020

Stark, J. L., Lyons, J.-A., and Cross, A. H. (2004). Interferon-gamma produced by encephalitogenic cells induces suppressors of cytokine signaling in primary murine astrocytes. *J. Neuroimmunol.* 151, 195–200. doi: 10.1016/j.jneuroim.2004.03.005

Starost, L., Lindner, M., Herold, M., Xu, Y. K. T., Drexler, H. C. A., Hess, K., et al. (2020). Extrinsic immune cell-derived, but not intrinsic oligodendroglial factors contribute to oligodendroglial differentiation block in multiple sclerosis. *Acta Neuropathol.* 140, 715–736. doi: 10.1007/s00401-020-02217-8

Staugaitis, S. M., Chang, A., and Trapp, B. D. (2012). Cortical pathology in multiple sclerosis: experimental approaches to studies on the mechanisms of demyelination and remyelination. *Acta Neurol. Scand. Suppl.* 97–102. doi: 10.1111/ane.12041

Stevens, B., Porta, S., Haak, L. L., Gallo, V., and Fields, R. D. (2002). Adenosine: a neuron-glial transmitter promoting myelination in the CNS in response to action potentials. *Neuron* 36, 855–868. doi: 10.1016/S0896-6273(02)01067-X

Stoffels, J. M. J., de Jonge, J. C., Stancic, M., Nomden, A., van Strien, M. E., Ma, D., et al. (2013). Fibronectin aggregation in multiple sclerosis lesions impairs remyelination. *Brain* 136, 116–131. doi: 10.1093/brain/aws313

Stogsdill, J. A., and Eroglu, C. (2017). The interplay between neurons and glia in synapse development and plasticity. *Curr. Opin. Neurobiol.* 42, 1–8. doi: 10.1016/j.conb.2016.09.016

Stohlman, S. A., and Hinton, D. R. (2001). Viral induced demyelination. *Brain Pathol.* 11, 92–106. doi: 10.1111/j.1750-3639.2001.tb00384.x

Stohlman, S. A., Hinton, D. R., Parra, B., Atkinson, R., and Bergmann, C. C. (2008). CD4 T cells contribute to virus control and pathology following central nervous system infection with neurotropic mouse hepatitis virus. *J. Virol.* 82, 2130–2139. doi: 10.1128/JVI.01762-07

Storch, M. K., Stefferl, A., Brehm, U., Weissert, R., Wallström, E., Kerschensteiner, M., et al. (1998). Autoimmunity to myelin oligodendrocyte glycoprotein in rats mimics the spectrum of multiple sclerosis pathology. *Brain Pathol.* 8, 681–694. doi: 10.1111/j.1750-3639.1998.tb00194.x

Stromnes, I. M., and Goverman, J. M. (2006). Passive induction of experimental allergic encephalomyelitis. *Nat. Protoc.* 1, 1952–1960. doi: 10.1038/nprot.2006.284

Su, Z., Yuan, Y., Chen, J., Zhu, Y., Qiu, Y., Zhu, F., et al. (2011). Reactive astrocytes inhibit the survival and differentiation of oligodendrocyte precursor cells by secreted TNF-alpha. *J. Neurotrauma* 28, 1089–1100. doi: 10.1089/neu.2010.1597

Sun, D., Whitaker, J. N., Huang, Z., Liu, D., Coleclough, C., Wekerle, H., et al. (2001). Myelin antigen-specific CD8+ T cells are encephalitogenic and produce severe disease in C57BL/6 mice. *J. Immunol.* 166, 7579–7587. doi: 10.4049/jimmunol.166.12.7579

Sun, L., Li, Y., Jia, X., Wang, Q., Li, Y., Hu, M., et al. (2017a). Neuroprotection by IFN-γ via astrocyte-secreted IL-6 in acute neuroinflammation. *Oncotarget* 8:40065. doi: 10.18632/oncotarget.16990

Sun, Y., Deng, Y., Xiao, M., Hu, L., Li, Z., and Chen, C. (2017b). Chondroitin sulfate proteoglycans inhibit the migration and differentiation of oligodendrocyte precursor cells and its counteractive interaction with laminin. *Int. J. Mol. Med.* 40, 1657–1668. doi: 10.3892/ijmm.2017.3153

Sun, Y., Lehmbecker, A., Kalkuhl, A., Deschl, U., Sun, W., Rohn, K., et al. (2015). STAT 3 represents a molecular switch possibly inducing astroglial instead of oligodendroglial differentiation of oligodendroglial progenitor cells in Theiler's murine encephalomyelitis. *Neuropathol. Appl. Neurobiol.* 41, 347–370. doi: 10.1111/nan.12133

Syed, Y. A., Hand, E., Möbius, W., Zhao, C., Hofer, M., Nave, K. A., et al. (2011). Inhibition of CNS remyelination by the presence of semaphorin 3A. *J. Neurosci.* 31:3719. doi: 10.1523/JNEUROSCI.4930-10.2011

Takahashi, C., Muramatsu, R., Fujimura, H., Mochizuki, H., and Yamashita, T. (2013). Prostacyclin promotes oligodendrocyte precursor recruitment and remyelination after spinal cord demyelination. *Cell Death Dis.* 4:e795. doi: 10.1038/cddis.2013.335

Talbott, J. F., Cao, Q., Bertram, J., Nkansah, M., Benton, R. L., Lavik, E., et al. (2007). CNTF promotes the survival and differentiation of adult spinal cord-derived oligodendrocyte precursor cells in vitro but fails to promote remyelination *in vivo*. *Exp. Neurol.* 204, 485–489. doi: 10.1016/j.expneurol.2006.12.013

Tanner, D. C., Cherry, J. D., and Mayer-Proschel, M. (2011). Oligodendrocyte progenitors reversibly exit the cell cycle and give rise to astrocytes in response to interferon-gamma. *J. Neurosci.* 31, 6235–6246. doi: 10.1523/JNEUROSCI.5905-10.2011

Templeton, S. P., Kim, T. S., O'malley, K., and Perlman, S. (2008). Maturation and localization of macrophages and microglia during infection with a neurotropic murine coronavirus. *Brain Pathol.* 18, 40–51. doi: 10.1111/j.1750-3639.2007.00098.x

Templeton, S. P., and Perlman, S. J (2007). Pathogenesis of acute and chronic central nervous system infection with variants of mouse hepatitis virus, strain JHM. *Immunol. Res.* 39, 160–172. doi: 10.1007/s12026-007-0079-y

Teo, L., and Bourne, J. (2018). Current opinion on a role of the astrocytes in neuroprotection. *Neural Regen. Res.* 13, 797–798. doi: 10.4103/1673-5374.232466

Thomas, L., and Pasquini, L. A. (2018). Galectin-3-mediated glial crosstalk drives oligodendrocyte differentiation and (re)myelination. *Front. Cell. Neurosci.* 12:297. doi: 10.3389/fncel.2018.00297

Thompson, A. J., Kermode, A. G., Wicks, D., Macmanus, D. G., Kendall, B. E., Kingsley, D. P., et al. (1991). Major differences in the dynamics of primary and secondary progressive multiple sclerosis. *Ann. Neurol.* 29, 53–62. doi: 10.1002/ana.410290111

Tiane, A., Schepers, M., Rombaut, B., Hupperts, R., Prickaerts, J., Hellings, N., et al. (2019). From OPC to oligodendrocyte: an epigenetic journey. *Cells* 8:1236. doi: 10.3390/cells8101236

Tirotta, E., Ransohoff, R. M., and Lane, T. E. (2011). CXCR2 signaling protects oligodendrocyte progenitor cells from IFN-γ/CXCL10-mediated apoptosis. *Glia* 59, 1518–1528. doi: 10.1002/glia.21195

Tong, X.-P., Li, X.-Y., Zhou, B., Shen, W., Zhang, Z.-J., Xu, T.-L., et al. (2009). Ca2+ signaling evoked by activation of Na+ channels and Na+/Ca2+ exchangers is required for GABA-induced NG2 cell migration. *J. Cell. Biol.* 186, 113–128. doi: 10.1083/jcb.200811071

Torre-Fuentes, L., Moreno-Jiménez, L., Pytel, V., Matías-Guiu, J., Gómez-Pinedo, U., and Matías-Guiu, J. J. N. (2020). Experimental models of demyelination and remyelination. *Neurologia* 35, 32–39. doi: 10.1016/j.nrleng.2019.03.007

Traiffort, E., Kassoussi, A., Zahaf, A., and Laouarem, Y. (2020). Astrocytes and microglia as major players of myelin production in normal and pathological conditions. *Front. Cell. Neurosci.* 14, 79–79. doi: 10.3389/fncel.2020.00079

Trapp, B. D., and Nave, K. A. (2008). Multiple sclerosis: an immune or neurodegenerative disorder? *Annu. Rev. Neurosci.* 31, 247–269. doi: 10.1146/annurev.neuro.30.051606.094313

Trapp, B. D., and Ontaneda, D. (2018). Identifying a new subtype of multiple sclerosis. *Neurodegen. Dis. Manag.* 8, 367–369. doi: 10.2217/nmt-2018-0032

Trapp, B. D., Peterson, J., Ransohoff, R. M., Rudick, R., Mork, S., and Bo, L. (1998). Axonal transection in the lesions of multiple sclerosis. *N. Engl. J. Med.* 338, 278–285. doi: 10.1056/NEJM199801293380502

Trapp, B. D., Vignos, M., Dudman, J., Chang, A., Fisher, E., Staugaitis, S. M., et al. (2018). Cortical neuronal densities and cerebral white matter demyelination in multiple sclerosis: a retrospective study. *Lancet Neurol.* 17, 870–884. doi: 10.1016/S1474-4422(18)30245-X

Tsai, H. H., Frost, E., To, V., Robinson, S., Ffrench-Constant, C., Geertman, R., et al. (2002). The chemokine receptor CXCR2 controls positioning of oligodendrocyte precursors in developing spinal cord by arresting their migration. *Cell* 110, 373–383. doi: 10.1016/S0092-8674(02)00838-3

Tschen, S.-I., Bergmann, C. C., Ramakrishna, C., Morales, S., Atkinson, R., Stohlman, S., et al. (2002). Recruitment kinetics and composition of antibody-secreting cells within the central nervous system following viral encephalomyelitis. *J. Immunol.* 168, 2922–2929. doi: 10.4049/jimmunol.168.6.2922

Tsunoda, I., and Fujinami, R. S. (2010). Neuropathogenesis of Theiler's murine encephalomyelitis virus infection, an animal model for multiple sclerosis. *J. Neuroimmune Pharmacol.* 5, 355–369. doi: 10.1007/s11481-009-9179-x

Tsutsui, S., Schnermann, J., Noorbakhsh, F., Henry, S., Yong, V. W., Winston, B. W., et al. (2004). A1 adenosine receptor upregulation and activation attenuates neuroinflammation and demyelination in a model of multiple sclerosis. *J. Neurosci.* 24, 1521–1529. doi: 10.1523/JNEUROSCI.4271-03.2004

Tuohy, V. K., Lu, Z., Sobel, R. A., Laursen, R. A., and Lees, M. B. (1989). Identification of an encephalitogenic determinant of myelin proteolipid protein for SJL mice. *J. Immunol.* 142, 1523–1527.

Tutuncu, M., Tang, J., Zeid, N. A., Kale, N., Crusan, D. J., Atkinson, E. J., et al. (2013). Onset of progressive phase is an age-dependent clinical milestone in multiple sclerosis. *Mult. Scler.* 19, 188–198. doi: 10.1177/1352458512451510

Ulrich, R., Seeliger, F., Kreutzer, M., Germann, P. G., and Baumgartner, W. (2008). Limited remyelination in Theiler's murine encephalomyelitis due to insufficient oligodendroglial differentiation of nerve/glial antigen 2 (NG2)-positive putative oligodendroglial progenitor cells. *Neuropathol. Appl. Neurobiol.* 34, 603–620. doi: 10.1111/j.1365-2990.2008.00956.x

Van Kaer, L., Postoak, J. L., Wang, C., Yang, G., and Wu, L. (2019). Innate, innate-like and adaptive lymphocytes in the pathogenesis of MS and EAE. *Cell. Mol. Immunol.* 16, 531–539. doi: 10.1038/s41423-019-0221-5

van Neerven, S., Nemes, A., Imholz, P., Regen, T., Denecke, B., Johann, S., et al. (2010). Inflammatory cytokine release of astrocytes in vitro is reduced by all-trans retinoic acid. *J. Neuroimmunol.* 229, 169–179. doi: 10.1016/j.jneuroim.2010.08.005

Vanderlugt, C. J., and Miller, S. D. (1996). Epitope spreading. *Curr. Opin. Immunol.* 8, 831–836. doi: 10.1016/S0952-7915(96)80012-4

Vanguri, P., and Farber, J. M. (1994). IFN and virus-inducible expression of an immediate early gene, crg-2/IP-10, and a delayed gene, I-A alpha in astrocytes and microglia. *J. Immunol.* 152, 1411–1418.

Vartanian, T., Li, Y., Zhao, M., and Stefansson, K. (1995). Interferon-gamma-induced oligodendrocyte cell death: implications for the pathogenesis of multiple sclerosis. *Mol. Med.* 1, 732–743. doi: 10.1007/BF03401888

Vela, J. M., Molina-Holgado, E., Arévalo-Martín, A., Almazán, G., and Guaza, C. (2002). Interleukin-1 regulates proliferation and differentiation of oligodendrocyte progenitor cells. *Mol. Cell Neurosci.* 20, 489–502. doi: 10.1006/mcne.2002.1127

Verderio, C., and Matteoli, M. (2001). ATP mediates calcium signaling between astrocytes and microglial cells: modulation by IFN-γ. *J. Immunol.* 166, 6383–6391. doi: 10.4049/jimmunol.166.10.6383

Voet, S., Prinz, M., and Van Loo, G. (2019). Microglia in central nervous system inflammation and multiple sclerosis pathology. *Trends Mol. Med.* 25, 112–123. doi: 10.1016/j.molmed.2018.11.005

Vogel, D. Y. S., Vereyken, E. J. F., Glim, J. E., Heijnen, P. D., Moeton, M., van der Valk, P., et al. (2013). Macrophages in inflammatory multiple sclerosis lesions have an intermediate activation status. *J. Neuroinflamm*10:809. doi: 10.1186/1742-2094-10-35

Voronova, A., Yuzwa, S. A., Wang, B. S., Zahr, S., Syal, C., Wang, J., et al. (2017). Migrating interneurons secrete fractalkine to promote oligodendrocyte formation in the developing mammalian brain. *Neuron* 94, 500–516.e509. doi: 10.1016/j.neuron.2017.04.018

Voskuhl, R. R., Itoh, N., Tassoni, A., Matsukawa, M. A., Ren, E., Tse, V., et al. (2019). Gene expression in oligodendrocytes during remyelination reveals cholesterol homeostasis as a therapeutic target in multiple sclerosis. *Proc. Natl. Acad. Sci. U.S.A.* 116:10130. doi: 10.1073/pnas.1821306116

Voskuhl, R. R., Peterson, R. S., Song, B., Ao, Y., Morales, L. B., Tiwari-Woodruff, S., et al. (2009). Reactive astrocytes form scar-like perivascular barriers to leukocytes during adaptive immune inflammation of the CNS. *J. Neurosci.* 29, 11511–11522. doi: 10.1523/JNEUROSCI.1514-09.2009

Wang, C., Barnett, M. H., Yiannikas, C., Barton, J., Parratt, J., You, Y., et al. (2019). Lesion activity and chronic demyelination are the major determinants of brain atrophy in MS. *Neurol. Neuroimmunol. Neuroinflamm.* 6:e593. doi: 10.1212/NXI.0000000000000593

Wang, F. I., Hinton, D. R., Gilmore, W., Trousdale, M. D., and Fleming, J. O. (1992). Sequential infection of glial cells by the murine hepatitis virus JHM strain (MHV-4) leads to a characteristic distribution of demyelination. *Lab. Invest.* 66, 744–754.

Wang, H. F., Liu, X. K., Li, R., Zhang, P., Chu, Z., Wang, C. L., et al. (2017). Effect of glial cells on remyelination after spinal cord injury. *Neural Regen. Res.* 12, 1724–1732. doi: 10.4103/1673-5374.217354

Wang, J., He, X., Meng, H., Li, Y., Dmitriev, P., Tian, F., et al. (2020). Robust myelination of regenerated axons induced by combined manipulations of GPR17 and microglia. *Neuron* 108, 876–886.e874. doi: 10.1016/j.neuron.2020.09.016

Wang, W.-Y., Tan, M.-S., Yu, J.-T., and Tan, L. (2015). Role of pro-inflammatory cytokines released from microglia in Alzheimer's disease. *Ann. Transl. Med.* 3:36. doi: 10.3978/j.issn.2305-5839.2015.03.49

Wang, Y., Jin, S., Sonobe, Y., Cheng, Y., Horiuchi, H., Parajuli, B., et al. (2014). Interleukin-1β induces blood-brain barrier disruption by downregulating Sonic hedgehog in astrocytes. *PLoS ONE* 9:e110024. doi: 10.1371/journal.pone.0110024

Watanabe, M., Toyama, Y., and Nishiyama, A. (2002). Differentiation of proliferated NG2-positive glial progenitor cells in a remyelinating lesion. *J. Neurosci. Res.* 69, 826–836. doi: 10.1002/jnr.10338

Welser-Alves, J. V., Crocker, S. J., and Milner, R. (2011). A dual role for microglia in promoting tissue inhibitor of metalloproteinase (TIMP) expression in glial cells in response to neuroinflammatory stimuli. *J. Neuroinflamm.* 8:61. doi: 10.1186/1742-2094-8-61

Welser-Alves, J. V., and Milner, R. (2013). Microglia are the major source of TNF-α and TGF-β1 in postnatal glial cultures; regulation by cytokines, lipopolysaccharide, and vitronectin. *Neurochem. Int.* 63, 47–53. doi: 10.1016/j.neuint.2013.04.007

Wensky, A. K., Furtado, G. C., Marcondes, M. C. G., Chen, S., Manfra, D., Lira, S. A., et al. (2005). IFN-γ determines distinct clinical outcomes in autoimmune encephalomyelitis. *J. Immunol.* 174, 1416–1423. doi: 10.4049/jimmunol.174.3.1416

Wheeler, M. A., Clark, I. C., Tjon, E. C., Li, Z., Zandee, S. E. J., Couturier, C. P., et al. (2020). MAFG-driven astrocytes promote CNS inflammation. *Nature* 578, 593–599. doi: 10.1038/s41586-020-1999-0

Whitham, R. H., Bourdette, D. N., Hashim, G. A., Herndon, R. M., Ilg, R., Vandenbark, A., et al. (1991). Lymphocytes from SJL/J mice immunized with spinal cord respond selectively to a peptide of proteolipid protein and transfer relapsing demyelinating experimental autoimmune encephalomyelitis. *J. Immunol.* 146, 101–107.

Williams, J. L., Manivasagam, S., Smith, B. C., Sim, J., Vollmer, L. L., Daniels, B. P., et al. (2020). Astrocyte-T cell crosstalk regulates region-specific neuroinflammation. *Glia* 68, 1361–1374. doi: 10.1002/glia.23783

Williams, J. L., Patel, J. R., Daniels, B. P., and Klein, R. S. (2014). Targeting CXCR7/ACKR3 as a therapeutic strategy to promote remyelination in the adult central nervous system. *J. Exp. Med.* 211, 791–799. doi: 10.1084/jem.20131224

Williams, K., Ulvestad, E., Waage, A., Antel, J. P., and Mclaurin, J. (1994). Activation of adult human derived microglia by myelin phagocytosis *in vitro*. *J. Neurosci. Res.* 38, 433–443. doi: 10.1002/jnr.490380409

Williamson, J. S., Sykes, K. C., and Stohlman, S. (1991). Characterization of brain-infiltrating mononuclear cells during infection with mouse hepatitis virus strain JHM. *J. Neuroimmunol.* 32, 199–207. doi: 10.1016/0165-5728(91)90189-E

Willis, C. M., Nicaise, A. M., Bongarzone, E. R., Givogri, M., Reiter, C. R., Heintz, O., et al. (2020). Astrocyte support for oligodendrocyte differentiation can be conveyed via extracellular vesicles but diminishes with age. *Sci. Rep.* 10:828. doi: 10.1038/s41598-020-57663-x

Wingerchuk, D. M., and Carter, J. L. (2014). Multiple sclerosis: current and emerging disease-modifying therapies and treatment strategies. *Mayo Clin. Proc.* 89, 225–240. doi: 10.1016/j.mayocp.2013.11.002

Wong, A. W., Xiao, J., Kemper, D., Kilpatrick, T. J., and Murray, S. S. (2013). Oligodendroglial expression of TrkB independently regulates myelination and progenitor cell proliferation. *J. Neurosci.* 33:4947. doi: 10.1523/JNEUROSCI.3990-12.2013

Wu, G. F., Dandekar, A. A., Pewe, L., and Perlman, S. J. (2000). CD4 and CD8 T cells have redundant but not identical roles in virus-induced demyelination. *J. Immunol.* 165, 2278–2286. doi: 10.4049/jimmunol.165.4.2278

Wu, G. F., and Perlman, S. J. (1999). Macrophage infiltration, but not apoptosis, is correlated with immune-mediated demyelination following murine infection with a neurotropic coronavirus. *J. Virol.* 73, 8771–8780. doi: 10.1128/JVI.73.10.8771-8780.1999

Xia, M. Q., Bacskai, B. J., Knowles, R. B., Qin, S. X., and Hyman, B. T. (2000). Expression of the chemokine receptor CXCR3 on neurons and the elevated expression of its ligand IP-10 in reactive astrocytes: in vitro ERK1/2 activation and role in Alzheimer's disease. *J. Neuroimmunol.* 108, 227–235. doi: 10.1016/S0165-5728(00)00285-X

Xiao, L., Hu, C., Yang, W., Guo, D., Li, C., Shen, W., et al. (2013). NMDA receptor couples Rac1-GEF Tiam1 to direct oligodendrocyte precursor cell migration. *Glia* 61, 2078–2099. doi: 10.1002/glia.22578

Yamaguchi, W., Tamai, R., Kageura, M., Furuyama, T., and Inagaki, S. (2012). Sema4D as an inhibitory regulator in oligodendrocyte development. *Mol. Cell. Neurosci.* 49, 290–299. doi: 10.1016/j.mcn.2011.12.004

Young, K. M., Psachoulia, K., Tripathi, R. B., Dunn, S. J., Cossell, L., Attwell, D., et al. (2013). Oligodendrocyte dynamics in the healthy adult CNS: evidence for myelin remodeling. *Neuron* 77, 873–885. doi: 10.1016/j.neuron.2013.01.006

Yuan, X., Eisen, A. M., Mcbain, C. J., and Gallo, V. J. D. (1998). A role for glutamate and its receptors in the regulation of oligodendrocyte development in cerebellar tissue slices. *Development* 125, 2901–2914. doi: 10.1242/dev.125.15.2901

Zalc, B. (2018). One hundred and fifty years ago Charcot reported multiple sclerosis as a new neurological disease. *Brain* 141, 3482–3488. doi: 10.1093/brain/awy287

Zhang, Y., and Barres, B. A. (2010). Astrocyte heterogeneity: an underappreciated topic in neurobiology. *Curr. Opin. Neurobiol.* 20, 588–594. doi: 10.1016/j.conb.2010.06.005

Zhang, Y., Taveggia, C., Melendez-Vasquez, C., Einheber, S., Raine, C. S., Salzer, J. L., et al. (2006). Interleukin-11 potentiates oligodendrocyte survival and maturation, and myelin formation. *J. Neurosci.* 26, 12174–12185. doi: 10.1523/JNEUROSCI.2289-06.2006

Zhao, C., Ma, D., Zawadzka, M., Fancy, S. P., Elis-Williams, L., Bouvier, G., et al. (2015). Sox2 sustains recruitment of oligodendrocyte progenitor cells following CNS demyelination and primes them for differentiation during remyelination. *J. Neurosci.* 35, 11482–11499. doi: 10.1523/JNEUROSCI.3655-14.2015

Zheng, L., Calenoff, M. A., and Dal Canto, M. C. (2001). Astrocytes, not microglia, are the main cells responsible for viral persistence in Theiler's murine encephalomyelitis virus infection leading to demyelination. *J. Neuroimmunol.* 118, 256–267. doi: 10.1016/S0165-5728(01)00338-1

Zhou, Y., Zhang, J., Wang, L., Chen, Y., Wan, Y., He, Y., et al. (2017). Interleukin-1β impedes oligodendrocyte progenitor cell recruitment and white matter repair following chronic cerebral hypoperfusion. *Brain Behav. Immun.* 60, 93–105. doi: 10.1016/j.bbi.2016.09.024

Zoecklein, L. J., Pavelko, K. D., Gamez, J., Papke, L., Mcgavern, D. B., Ure, D. R., et al. (2003). Direct comparison of demyelinating disease induced by the Daniel's strain and bean strain of theiler's murine encephalomyelitis virus. *Brain Pathol.* 13, 291–308. doi: 10.1111/j.1750-3639.2003.tb00029.x

Zonouzi, M., Renzi, M., Farrant, M., and Cull-Candy, S. G. (2011). Bidirectional plasticity of calcium-permeable AMPA receptors in oligodendrocyte lineage cells. *Nat. Neurosci.* 14, 1430–1438. doi: 10.1038/nn.2942

Conflict of Interest: The authors declare that the research was conducted in the absence of any commercial or financial relationships that could be construed as a potential conflict of interest.

Copyright © 2021 Psenicka, Smith, Tinkey and Williams. This is an open-access article distributed under the terms of the Creative Commons Attribution License (CC BY). The use, distribution or reproduction in other forums is permitted, provided the original author(s) and the copyright owner(s) are credited and that the original publication in this journal is cited, in accordance with accepted academic practice. No use, distribution or reproduction is permitted which does not comply with these terms.

frontiers in Neuroscience

SYSTEMATIC REVIEW
published: 21 June 2021
doi: 10.3389/fnins.2021.618589

Effect of Ulinastatin on Early Postoperative Cognitive Dysfunction in Elderly Patients Undergoing Surgery: A Systemic Review and Meta-Analysis

Mei Duan[1†], *Fangyan Liu*[1†], *Huiqun Fu*[1], *Shuai Feng*[1], *Xue Wang*[2] *and Tianlong Wang*[1*]

[1] *Department of Anesthesiology, Xuanwu Hospital, Capital Medical University, Beijing, China,* [2] *Department of Library, Xuanwu Hospital, Capital Medical University, Beijing, China*

OPEN ACCESS

Edited by:
Claudia Bregonzio, CCT CONICET Córdoba, Argentina

Reviewed by:
Wen Ouyang, Third Xiangya Hospital of Central South University, China
Nasiara Karim, University of Malakand, Pakistan

***Correspondence:**
Tianlong Wang
w_tl5595@hotmail.com

[†] *These authors share first authorship*

Specialty section:
This article was submitted to Neuropharmacology, a section of the journal Frontiers in Neuroscience

Received: *17 October 2020*
Accepted: *11 May 2021*
Published: *21 June 2021*

Citation:
Duan M, Liu F, Fu H, Feng S, Wang X and Wang T (2021) Effect of Ulinastatin on Early Postoperative Cognitive Dysfunction in Elderly Patients Undergoing Surgery: A Systemic Review and Meta-Analysis. Front. Neurosci. 15:618589. doi: 10.3389/fnins.2021.618589

Background: Postoperative cognitive dysfunction (POCD) is associated with neuroinflammation by triggering the systemic inflammatory responses. Related studies have demonstrated that ulinastatin, which is a urinary trypsin inhibitor, inhibited the release of inflammatory mediators and improved postoperative cognitive function in elderly patients undergoing major surgery. However, there are controversial results put forwarded by some studies. This systemic review aimed to evaluate the effect of ulinastatin on POCD in elderly patients undergoing surgery.

Methods: We searched PubMed, Embase, Cochrane Library, Web of Science, and Ovid to find relevant randomized controlled trials (RCTs) of ulinastatin on POCD in elderly patients undergoing surgery. The primary outcomes included the incidence of POCD and the Mini-Mental State Examination (MMSE) scores. The secondary outcome was the levels of inflammatory cytokines such as tumor necrosis factor (TNF)-α, S100β, C-reactive protein (CRP), interleukin (IL)-6, and IL-10. RevMan 5.3 was used to conduct the meta-analysis.

Results: Ten RCTs were included finally. Compared with controls, ulinastatin significantly reduced the incidence of POCD [risk ratio (RR) = 0.29, 95% CI 0.21–0.41, test of RR = 1: $Z = 7.05$, $p < 0.00001$]. In addition, patients in the ulinastatin group have lower levels of TNF-α, S100β, CRP, and IL-6 and higher level of IL-10 in serum following surgery.

Conclusion: These findings suggested that ulinastatin can be used as an anti-inflammatory drug for POCD prevention in elderly patients undergoing surgery.

Systematic Review Registration Number: CRD42019137449.

Keywords: elderly patients, surgery, perioperative inflammation, postoperative cognitive dysfunction, ulinastatin, meta-analysis

INTRODUCTION

Postoperative cognitive dysfunction (POCD) is a central nervous system complication that occurs after surgery in the elderly and is characterized by mental confusion, anxiety, personality changes, and memory impairment. Elderly patients are at high risk of POCD. The occurrence of POCD is correlated with decreased quality of life and increased mortality, and there is a possibility of increased risk for developing dementia, such as Alzheimer's disease (AD) (Bekker et al., 2010; Browndyke et al., 2013; Berger et al., 2014).

Although the mechanism of POCD remains unclear, systemic inflammation and neuroinflammation are regarded as important pathologic processes of POCD (Berger et al., 2014, 2015). Moreover, inhibition of systemic inflammatory response during the early postoperative period improves postoperative cognitive function, reducing the incidence of POCD in the elderly (Zhang et al., 2018). Alarmins were released from the surgical trauma tissue injury or secreted by stimulated leukocytes and epithelial cells, such as high-mobility histone 1, neutrophils, and monocyte cytoplasmic proteins S100A8 and S100A9, as well as systemic endotoxemia, which in turn activate the inflammatory pathway, leading to the release of pro-inflammatory cytokines and anti-inflammatory cytokines, such as tumor necrosis factor (TNF)-α, interleukin (IL)-1β, IL-6, IL-10, and so on (Chan et al., 2012; Schietroma et al., 2013, 2016). After that, the peripheral inflammatory cytokines activate and compromise with the blood–brain barrier (BBB) integrity, allowing increased infiltration of inflammatory factors and macrophages into the brain (Fu et al., 2014), ultimately leading to the damage of neurological function (Leslie, 2017; Wei et al., 2019).

Ulinastatin is a urinary trypsin inhibitor (UTI) that is extracted from human urine, which subsequently can inhibit the enzyme activity and stable lysosomal membrane and effectively reduce the systemic inflammatory response (Atal and Atal, 2016). UTI is widely used in patients with pancreatitis, septicopyemia, disseminated intravascular coagulation, and shock (Inoue et al., 2009). And ulinastatin could inhibit the systemic inflammatory response by directly suppressing the activation of neutrophils and monocyte-macrophages and capture lipopolysaccharide (LPS) and bind to LPS receptors, further inhibiting the LPS-induced systemic inflammatory response (Ma et al., 2016; Li X. F. et al., 2018).

Therefore, it has been speculated that the occurrence of POCD can be reduced by inhibiting inflammation and the release of plasma LPS and directly protecting the BBB after infusing ulinastatin. However, some studies suggested that preoperative prophylactic ulinastatin showed no improvement in the POCD. The discrepancy in these results might be due to the surgical stimuli experienced and the timing and dose of ulinastatin used.

To clarify these, a meta-analysis was conducted to examine the efficacy of ulinastatin for the prevention of early POCD in elderly patients, which assists in the future clinical decision-making process.

Abbreviations: POCD, postoperative cognitive dysfunction; AD, Alzheimer's disease; MMSE score, Mini-Mental State Examination score; UTI, urinary trypsin inhibitor; RCTs, randomized controlled trials; BBB, blood–brain barrier; DSM-5, Diagnostic and Statistical Manual for Mental Disorders, Fifth Edition; RR, related risk; ORs, odds ratios; 95% CI, 95% confidence interval; SMD, standard mean difference.

MATERIALS AND METHODS

Preferred Reporting Items for Systematic Reviews and Meta-Analyses (PRISMA) guidelines were followed in reporting this systematic review and meta-analysis (**Figure 1**) (Moher et al., 2009a). A review protocol was developed prior to conducting the study.

Inclusion and Exclusion Criteria

The eligible studies were adopted into this systematic review and meta-analysis following the patient, intervention, comparison, outcomes, and study design strategy (Moher et al., 2009b).

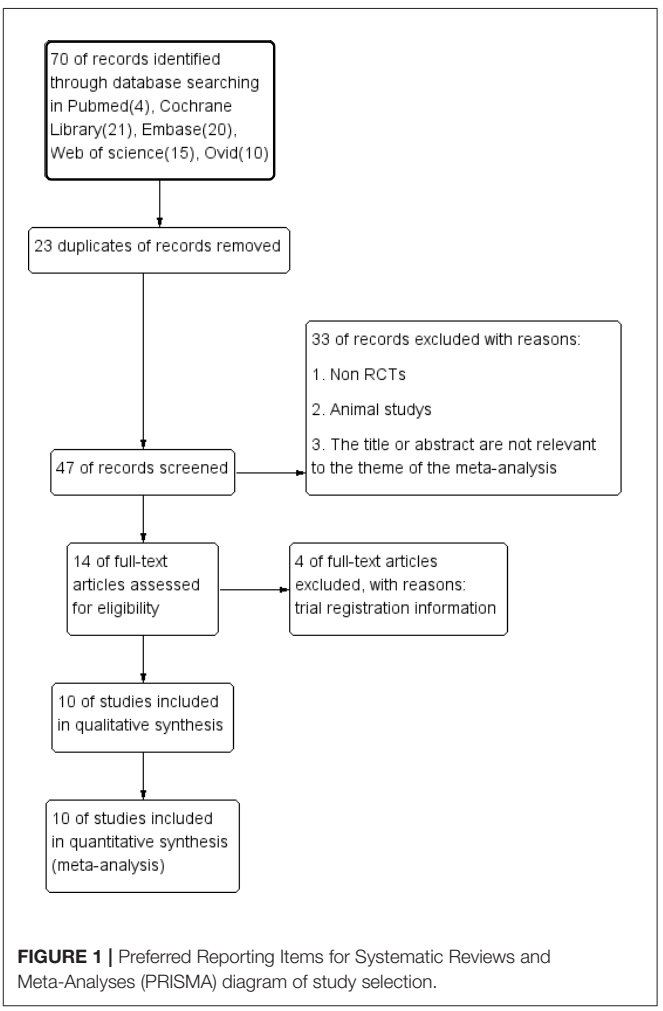

FIGURE 1 | Preferred Reporting Items for Systematic Reviews and Meta-Analyses (PRISMA) diagram of study selection.

Types of Studies
Inclusion: Only randomized controlled trials (RCTs) were included. Exclusion: Observational cohort and case-control studies, case reports, experimental studies, and reviews were excluded.

Types of Participants
Subjects enrolled in our systematic review were elderly patients (age ≥60 years) who were undergoing surgical operations, with no restriction of race and gender.

Types of Interventions
Patients in the ulinastatin group were treated with ulinastatin intravenously before and/or after surgery; the control group received placebo administration of normal saline, and the volume of normal saline must be the same as that of the administered ulinastatin.

Types of Outcome Measurement
The primary outcome measures included the incidence of POCD and the Mini-Mental State Examination (MMSE) score. And the secondary outcome measures were the level of TNF-α, S100β, C-reactive protein (CRP), IL-6, and IL-10 in the blood.

Search Strategy and Study Selection
We searched PubMed, Embase, Cochrane Library, Web of Science, and Ovid to find relevant RCTs. The search strategy was drafted by an experienced librarian and searched by a combination of medical subject headings and free words. The explicit search strategy used herein was presented in **Supplementary File 1**. In addition, the literature data that identified the registration test but not published were also searched. The test data were obtained by contacting the appropriate author if necessary.

In addition, each study should have the research site, publication year, and a clear definition of the sample size. At least one outcome indicator, such as odds ratio (OR) or risk ratio (RR), and its 95% confidence interval (CI) should be provided by the study. Detailed description of the intervention group and the control group as well as POCD diagnostic criteria should be clearly stated.

Exclusion criteria were as follows: duplicate articles, review articles, animal experiments, and articles that did not meet the research objectives. Furthermore, the articles that have design defects and poor quality, with incomplete data and unclear outcome, and that cannot provide and convert into OR or RR and its 95% CI, and whose statistical method is incorrect and cannot be corrected were excluded from the meta-analysis.

Literature Screening, Data Extraction, and Quality Assessment
Two researchers independently screened the literature, extracted the data, and evaluated the methodological quality of the studies identified. We evaluated the methodological quality of 10 RCTs identified by Cochrane risk bias assessment (Higgins et al., 2011). The evaluation contents included random sequence generation, allocation concealment, blinding of investigators and participants, blinding of outcome assessment, incomplete outcome data, selective reporting, and other biases. Any disagreements between the two researchers were solved by discussion or by consulting a third party to reach a consensus. **Table 1** showed the extracted contents from 10 RCTs, and the outcome of quality assessment was presented in **Figure 2**.

Grading of Recommendations, Assessment, Development, and Evaluations (GRADE) methods were used to evaluate the quality of evidence for each outcome, classified as very low, low, moderate, or high (Balshem et al., 2011). It was evaluated using GRADEPro software 3.6 (GRADE Working Group).

Statistical Analysis
We used RevMan 5.3 to conduct this meta-analysis. For dichotomous data, RRs with 95% CIs were used to express the effect sizes, while mean difference (MD) and 95% CIs were used for continuous data.

Firstly, we conducted a heterogeneity test (significance level, $\alpha = 0.10$) to evaluate the extent of heterogeneity in combination with the I^2-test (Higgins et al., 2003). A fixed-effects model or a random-effects model was selected based on the results of I^2-test. A fixed-effects model was used to conduct the meta-analysis if no heterogeneity ($p > 0.1$ and $I^2 < 50\%$) was observed among the studies. If significant heterogeneity ($p \leq 0.1$ or $I^2 \geq 50\%$) was observed, then a random-effects model was used for the meta-analysis. The Z-test was used to determine the significance of the pooled effect size, and a $p < 0.05$ was considered statistically significant. In addition, if there was significant heterogeneity among the studies, subgroup or sensitivity analysis should be conducted.

Publication bias was assessed using the funnel plots, Egger's regression test (Egger et al., 1997), and Begg's adjusted rank correlation (Begg and Mazumdar, 1994), which was conducted with the Stata software (Stata Corp., TX, USA; version 15.0).

RESULTS

Literature Search Results
Initially, 70 relevant studies were identified in total. Of these, 23 duplicates and 33 records deviating from inclusion criteria were excluded. In addition, four trial registration data were excluded. Finally, 10 RCTs were included in the meta-analysis after reviewing the full text of each article and then were evaluated with the RCT Quality Assessment Scale. The results of the literature screening process according to PRISMA are shown in **Figure 1**.

Basic Features and Quality Assessment of Included Studies
The characteristics of the included studies are presented in **Table 1**. We applied Cochrane risk bias assessment in the quality evaluation of the included studies, and most studies were at low risk of bias as shown in **Figure 2**.

TABLE 1 | Characteristic of the included studies.

Study	Study design	Population	Intervention and control	Outcomes
Ge et al. (2011) China	RCT	ASA I–II, age ≥65 and ≤83 years, hip joint replacement under combined spinal-epidural anesthesia U: 80 patients, 72.8 ± 7.5 C: 80 patients, 75.0 ± 9.2	U: intravenous injection of ulinastatin 10,000 U/kg before skin incision, and 5,000 U/kg after surgery on days 1–3 C: an equivalent amount of normal saline	Incidence of POCD
Ge et al. (2015) China	RCT	ASA I–III, age ≥60 and ≤75 years, coronary artery bypass grafting surgery under general anesthesia U1: 31 patients, 69.1 ± 4.8 U2: 30 patients, 68.9 ± 4.7 C: 32 patients, 67.7 ± 5.4	U1 and U2: the 16,000 U/kg or 8,000 U/kg ulinastatin injection was diluted to 60 ml with 0.59% sodium chloride solution, and intravenous infusion was continued at a rate of 20 ml/h before induction of anesthesia C: The control group was given the same volume of 0.59% chlorine by the same method	Incidence of POCD, IL-6, IL-10, TNF-α, S100β
Kang et al. (2010) China	RCT	ASA I–II, age ≥65 and ≤83 years, hip joint replacement under combined spinal-epidural anesthesia U: 40 patients, 75.0 ± 7.8 C: 40 patients, 72.8 ± 7.3	U: intravenous injection of ulinastatin with 10,000 U/kg before skin incision, and 5,000 U/kg after surgery on days 1–3 C: an equivalent amount of normal saline	Incidence of POCD, S100β
Li et al. (2016) China	RCT	ASA II–III, CPB valvular replacement surgery under general anesthesia U: 30 patients C: 30 patients	U: the observation group was pumped into 12,000 U/kg UTI through vein after anesthesia induction, and given 6,000 U/kg UTI from vitro pipeline 5 rain before the end of CPB C: the control group was given the same amount of saline solution	Incidence of POCD, IL-6, IL-10, TNF-α, S100β, NE, SOD, MDA
Pan et al. (2016) China	RCT	ASA I–II, age ≥65 and ≤85 years, laparoscopic colorectal cancer surgery under general anesthesia U: 41 patients, 72.4 ± 7.5 C: 41 patients, 73.9 ± 8.4	U: 2 KU/kg ulinastatin before induction of anesthesia, followed by 1 KU/(kg·h) intravenous pumping until the end of surgery C: the same volume of normal saline	Incidence of POCD, MMSE score on the day of surgery and postoperative day 1/3, TNF-α, IL-6, TGF-β, IL-4
Shan et al. (2015) China	RCT	ASA I–II, age ≥65 years, hip fracture surgery under combined spinal-epidural anesthesia U: 21 patients, 78.0 ± 2.0 C: 27 patients, 75.0 ± 1.0	U: intravenous injection of ulinastatin with 5 000 U/kg before skin incision and at the moment of the end of operation C: the same volume of normal saline	Incidence of POCD, MMSE score on the day of surgery and postoperative day 1/3/7, CRP
Wang et al. (2017) China	RCT	ASA I–II, age ≥60 years, TNM II–III patients after one lung ventilation surgery under intravenous general anesthesia and receiving neoadjuvant chemotherapy U: 38 patients, 66.0 ± 6.0 C: 37 patients, 67.0 ± 5.0	U: ulinastatin 10,000 U/kg diluted to 100 ml with normal saline and infused intravenously over a period of 20 min before anesthesia induction and 5,000 U/kg after surgery on days 1–3 C: an equivalent amount of normal saline	Incidence of POCD, MMSE score on postoperative day 7, IL-6, IL-10, CRP, S100β
Lili et al. (2013) China	Double-blind trial RCT	ASA I–II, age ≥65 years, abdominal surgery under intravenous general anesthesia U: 40 patients, 75.6 ± 7.2 C: 40 patients, 74.1 ± 8.1	U: ulinastatin 10,000 U/kg diluted to 100 ml with normal saline and infused intravenously over a period of 30 min before surgical incision and 5,000 U/kg after surgery on days 1–3 C: an equivalent amount of normal saline	Incidence of POCD, IL-6, TNF-α, CRP, S100β
Yang et al. (2017) China	RCT	ASA I–II, age ≥65 years, laparoscopic gastrectomy surgery under general anesthesia U: 50 patients, 70.6 ± 6.7 C: 40 patients, 69.5 ± 5.3	U: patients in the combination group were first injected with ulinastatin 10,000 U/kg within 15–20 min. Then, dexmedetomidine was administered in the same manner as the control group, and the administration was stopped 30 min before the end of the operation C: before the induction of anesthesia, the control group was given a loading dose of dexmedetomidine 0.5 μg/kg, after 15 min of infusion, the pump was continuously pumped at 0.3 μg/kg·h, and the infusion was stopped 30 min before the end of the operation	Incidence of POCD, MMSE score on the day of surgery and postoperative day 1/7, IL-6, S100β, TNF-α

(Continued)

TABLE 1 | Continued

Study	Study design	Population	Intervention and control	Outcomes
Zhang et al. (2018) China	Double-blind trial RCT	ASA I–II, age ≥65 and ≤85 years, spine surgery under intravenous general anesthesia U: 30 patients, 72.8 ± 5.3 C: 30 patients, 71.3 ± 5.0	U: intravenous infusion of ulinastatin 10,000 U/kg following anesthesia induction and before surgical incision, and 5,000 U/kg on post-operative days 1 and 2 C: an equivalent amount of normal saline	Incidence of POCD, MoCA score on postoperative day 7, IL-6, CRP, LPS, MMP-9

SOD, Superoxide Dismutase; MDA, Malondialdehyde; MMSE, Mini-Mental State Examination; TGF-β, Transforming Growth Factor-β; MoCA, Montreal Cognitive Assessment; MMP-9, Matrix Metalloprotein-9.

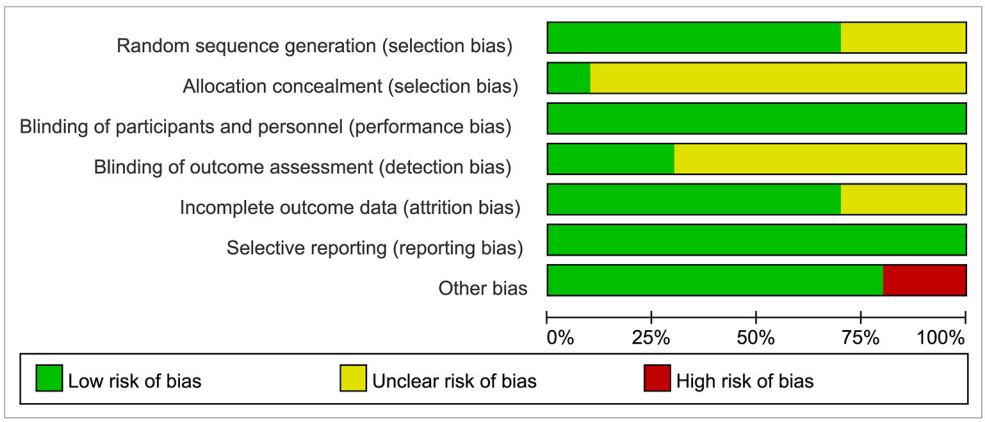

FIGURE 2 | Risk of bias graph: review authors' judgments about each risk of bias item presented as percentages across all included studies.

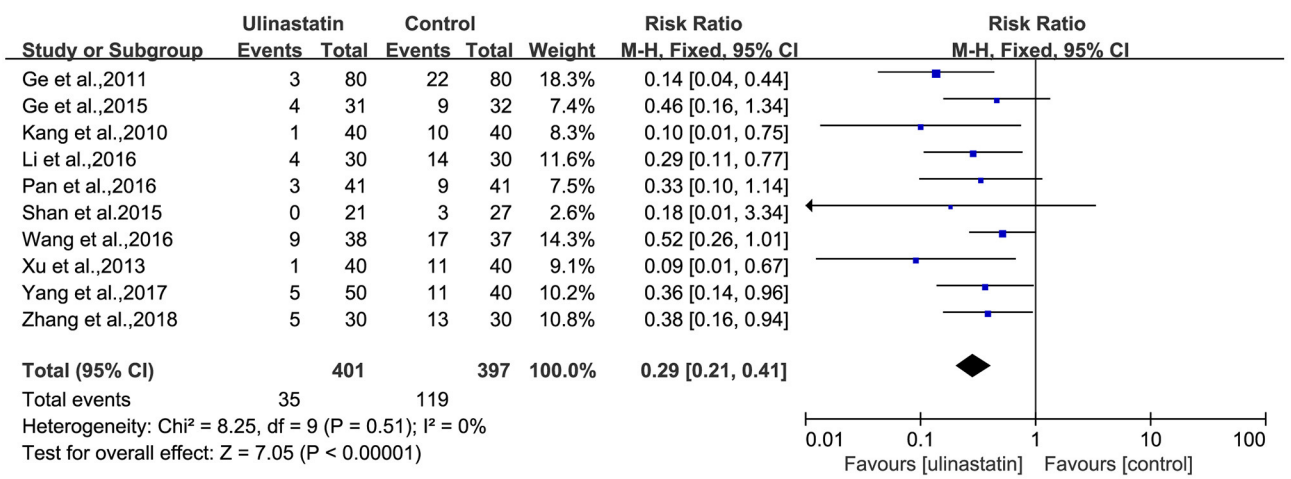

FIGURE 3 | Forest plot: Meta-analysis and pooled risk ratio (RR) of the effect of ulinastatin on postoperative cognitive dysfunction (POCD).

Meta-Analysis Results

Incidence of Postoperative Cognitive Dysfunction

There was no substantial heterogeneity among the studies ($p = 0.51$, $I^2 = 0\%$; **Figure 3**). Therefore, a fixed-effects model was applied in this meta-analysis, and the results presented by the forest map showed that the incidence of POCD in the ulinastatin group was significantly lower than that in the control group (RR = 0.29, 95% CI 0.21–0.41, test of RR = 1: $Z = 7.05$, $p < 0.00001$; **Figure 3**). To verify the stability of the effects of the interventions, a sensitivity analysis was conducted where each study was eliminated to determine the variation in results. The results showed that there was no significant difference between the results obtained after the knockout and the total combined values (RR = 0.290, 95% CI 0.206–0.409; **Supplementary File 2**).

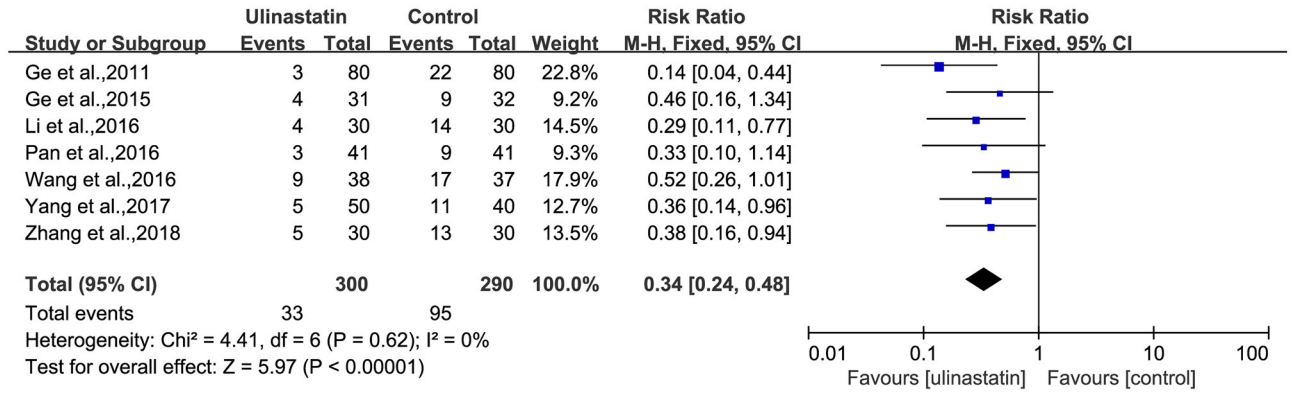

FIGURE 4 | Forest plot: Meta-analysis and pooled risk ratio (RR) of the effect of ulinastatin on postoperative cognitive dysfunction (POCD) after removing three articles with publication biases.

The GRADE quality of evidence for POCD rate was judged to be moderate. The funnel plot of POCD was a little asymmetrical (**Supplementary File 3**). The Egger's regression asymmetry test ($p = 0.011$) and the Begg's adjusted rank correlation test ($p = 0.049$) showed evidence of publication bias regarding POCD rates. Therefore, we removed Xu, Shan, and Kang, which had obvious publication biases. And we analyzed the forest plot for POCD rates again, and the result showed that there was still a lower POCD rate in the ulinastatin group than that that in the control group, the same as before removing (RR = 0.34, 95% CI 0.24–0.48, test of RR = 1: $Z = 5.97$, $p < 0.00001$; **Figure 4**). The influence analysis of individual studies on the pooled RR is presented that the benefit effect of ulinastatin on POCD is stable (RR = 0.336, 95% CI 0.235–0.481; **Supplementary File 4**). The GRADE quality of evidence for POCD rate was judged to be high after removing three articles with publication biases. And the funnel plot of POCD after removing the three articles with publication bias was nearly symmetrical (**Supplementary File 5**). The Egger's regression asymmetry test ($p = 0.087$) and the Begg's adjusted rank correlation test ($p = 0.133$) showed no publication bias regarding POCD rates.

Postoperative Mini-Mental State Examination Score

Three RCTs reported the MMSE score on day 1 after surgery. Three RCTs reported the MMSE score on day 3 after surgery, and three RCTs reported the MMSE score on day 7 after surgery.

A substantial heterogeneity was observed among the three subgroups ($p < 0.00001$, $I^2 = 81\%$; **Figure 5**) and in each group ($p = 0.34$, $p = 0.51$, $p = 0.19$; $I^2 = 7\%$, $I^2 = 0\%$, $I^2 = 40\%$; **Figure 5**). Then, the random-effects model was used in the meta-analysis, and the outcomes presented showed significant differences about MMSE scores after surgery between the ulinastatin group and the control group. It was obvious that the MMSE score after surgery in the ulinastatin group was higher than that in the control group (MD = 1.89, 95% CI 1.34–2.44, test of RR = 1: $Z = 6.69$, $p < 0.00001$; **Figure 5**). The GRADE quality of evidence for the MMSE score was judged to be high. The funnel plot of the MMSE score at postoperative day was symmetrical, indicating no publication bias among the 10 RCTs (**Supplementary File 6**). The Egger's regression asymmetry test ($p = 0.061$, $p = 0.253$, $p = 0.104$) and the Begg's adjusted rank correlation test ($p = 1.000$, $p = 0.296$, $p = 0.296$) showed no publication bias regarding MMSE scores at postoperative days 1, 3, and 7, respectively.

The Level of Inflammatory Factors

The relevant inflammatory factors were also measured among the 10 RCTs included. From the results of these inflammatory factors, we found no difference in the preoperative inflammatory factor levels between the ulinastatin group and the control group. The levels of TNF-α, S100β, and IL-6 were significantly increased after surgery (**Supplementary File 7**). Furthermore, the control group had significantly higher levels than those in the ulinastatin group, and the difference was statistically significant (test of RR = 1 : Z = 3.42, 3.49, 5.52, $P < 0.05$; **Figures 6–8**). Also the CRP levels were elevated postoperatively in the two groups and was higher in the ulinastatin group than that in the control group, but showing no significant difference (test of RR =1: $Z = 1.78$, $p = 0.08$; **Figure 9**). Inversely, the level of IL-10 was higher postoperatively in the ulinastatin group than that in the control group (test of RR = 1: $Z = 1.96$, $p = 0.05$; **Figure 10**). In a word, these findings suggest that ulinastatin can attenuate the development of POCD and improve the MMSE scores after surgery, which is most likely through a reduction of TNF-α, S100β protein, pro-inflammatory IL-6, and CRP and an increase of anti-inflammatory IL-10 levels.

DISCUSSION

This article systematically analyzed the protective effects of ulinastatin in the treatment of patients with early POCD. Ten RCTs were included in this meta-analysis. Based on the findings of this study, ulinastatin effectively reduced the incidence of early POCD by inhibiting the release of pro-inflammatory

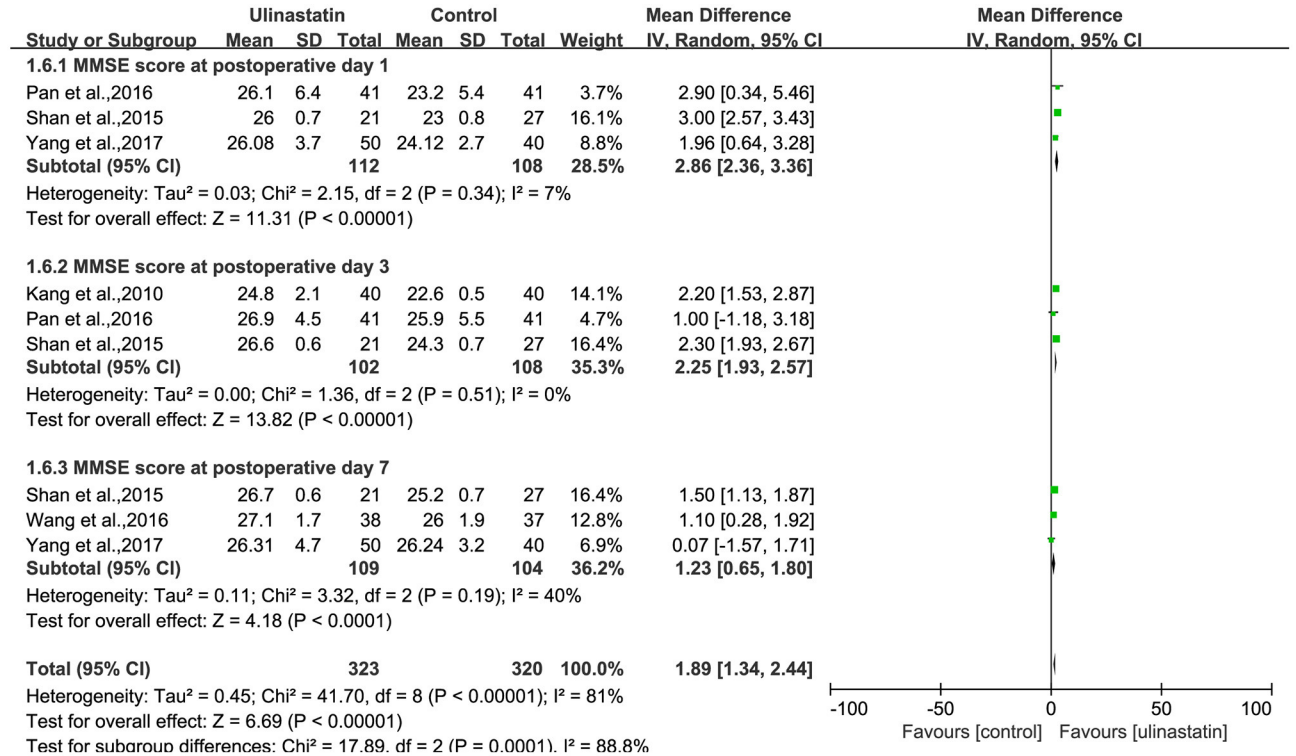

FIGURE 5 | Forest plot: Comparing the Mini-Mental State Examination (MMSE) scores of patients receiving ulinastatin vs. control divided by postoperative days 1, 3, 7.

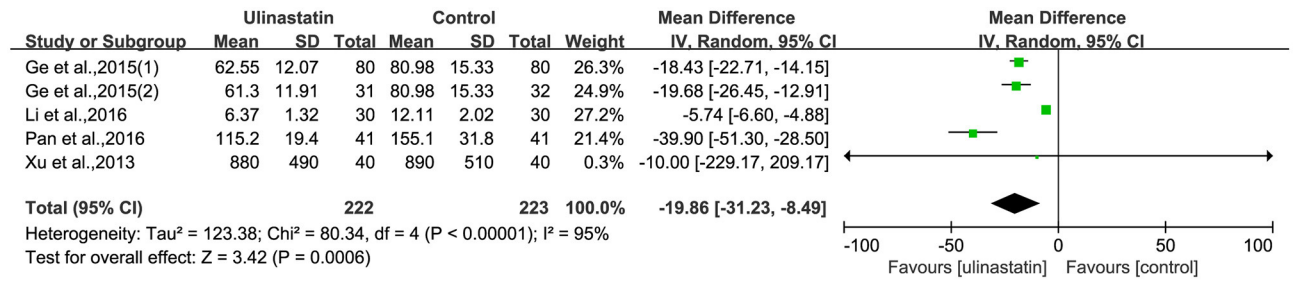

FIGURE 6 | Forest plot: Comparing plasma tumor necrosis factor (TNF)-α of patients receiving ulinastatin vs. control.

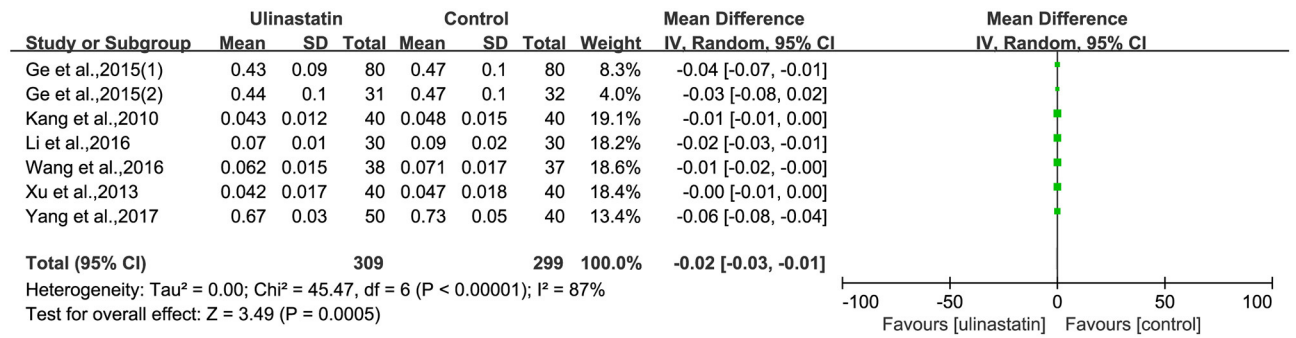

FIGURE 7 | Forest plot: Comparing plasma S100β of patients receiving ulinastatin vs. control.

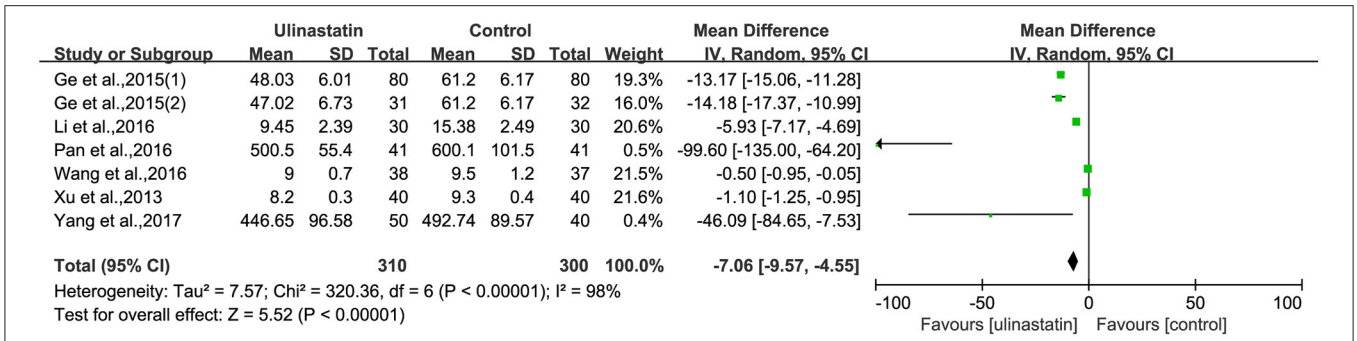

FIGURE 8 | Forest plot: Comparing plasma interleukin (IL)-6 of patients receiving ulinastatin vs. control.

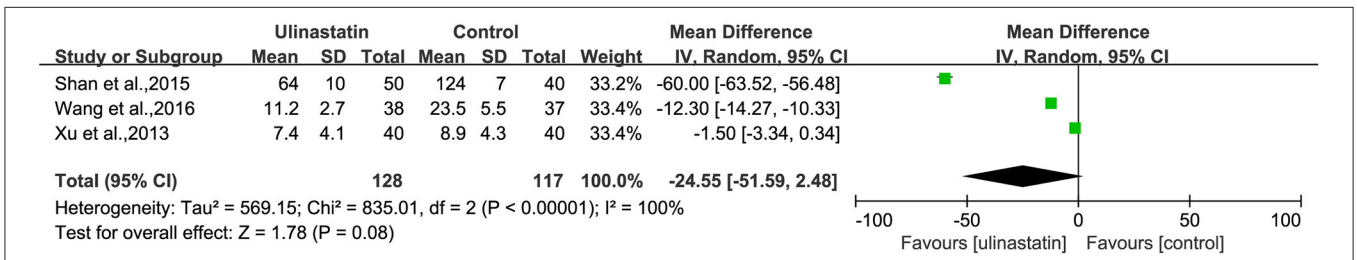

FIGURE 9 | Forest plot: Comparing plasma C-reactive protein (CRP) of patients receiving ulinastatin vs. control.

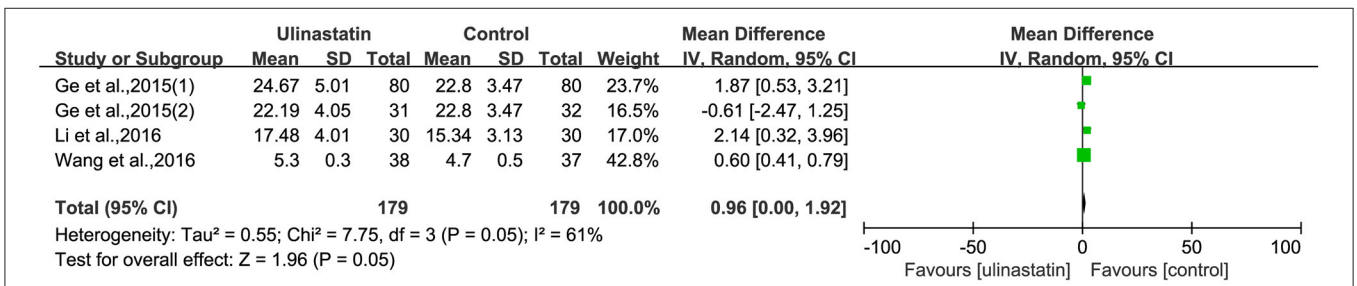

FIGURE 10 | Forest plot: Comparing plasma interleukin (IL)-10 of patients receiving ulinastatin vs. control.

cytokines and promoting the upregulation of anti-inflammatory cytokine IL-10.

TNF-α and IL-6 are pro-inflammatory cytokines that are associated with cognitive impairment (Liu et al., 2018). A variety of rodent surgical models show that pro-inflammatory cytokines are both upregulated in peripheral tissue and central nervous system (Terrando et al., 2010; Fidalgo et al., 2011). In human studies, the serum and cerebrospinal fluid of patients with postoperative cognitive impairment also showed an increase in pro-inflammatory cytokines, which had nothing to do with the type of operation (Buvanendran et al., 2006; Hirsch et al., 2016), which has been confirmed by a meta-analysis (Peng et al., 2013). Tissue trauma after an operation releases IL-1β and TNF-α and further promotes the increase of IL-6 cytokine, which is related to the degree of tissue trauma (Mannick et al., 2001; Menger and Vollmar, 2004). Pro-inflammatory factor IL-6 is considered to be an independent predictor of postoperative cognitive impairment (Dong et al., 2016), and perioperative inflammatory factors are closely related to the occurrence of postoperative cognitive impairment in elderly patients (Li et al., 2012). Our included studies illustrated that the levels of serum TNF-α and IL-6 were significantly increased after surgery, and ulinastatin may attenuate POCD by inhibiting the release of TNF-α and IL-6.

Moreover, ulinastatin was proven to upregulate anti-inflammatory factor IL-10 (Lili et al., 2013), which was associated with improvement of postoperative cognitive function (Lili et al., 2013; Wang et al., 2017). Ulinastatin can decrease the levels of pro-inflammatory cytokines TNF-α, CRP, and IL-6 by activating phosphoinositide 3-kinase (PI3K)/Akt/Nrf2 pathway and promote the release of anti-inflammatory cytokine IL-10 by inhibiting c-Jun N-terminal kinase (JNK)/nuclear factor (NF)-κB pathway (Li S. T. et al., 2018). Relevant findings demonstrate that ulinastatin can attenuate the elevation of S100β protein levels and the incidence of POCD, most likely by the mechanism

of reducing serum IL-6 and CRP levels and increasing IL-10 levels (Lili et al., 2013). These were also consistent with our study.

Though the meta-analysis result of the plasma CRP was not significantly different between the ulinastatin and the control group, possibly on account of less cases, relevant studies showed that the plasma CRP at postoperative day 3 was more likely to promote the occurrence of POCD (Zhang et al., 2015). Hudetz et al. (2011) stated that IL-6 and CRP were significantly elevated in plasma of patients with postoperative memory impairment. The above evidence indicated that systemic inflammation was regarded as an important pathologic process of POCD (Berger et al., 2014, 2015), and ulinastatin plays a critical role in the inhibition of early POCD.

The BBB integrity compromised by the peripheral inflammatory cytokines may allow inflammatory factors and macrophages into the brain directly (Fu et al., 2014) or cause the release of molecules, further reflecting neuronal damage (Thelin et al., 2017). Serum S100β is one of these molecules and is an acidic calcium-binding protein that is first found in astrocytes and Schwann cells (Linstedt et al., 2002). S100β is usually elevated in the blood and cerebrospinal fluid following nervous system damage during BBB impairment, which has been considered as a biomarker of cognitive impairment (Linstedt et al., 2002; Li et al., 2012). Ulinastatin was found lowering the concentration of plasma S100β in the first 2 days after an operation (Kang et al., 2010; Lili et al., 2013). Ulinastatin might downregulate the level of S100β in blood through impeding the inflammatory cascades and lowering the level of pro-inflammatory cytokines TNF-α, CRP, and IL-6 (Wang et al., 2017), further protecting the BBB integrity from peripheral inflammatory cytokines and decreasing neuronal damage. Our included studies showed that the levels of serum S100β were significantly increased after surgery. The concentration of postoperative serum S100β in the ulinastatin group was significantly lower than that in the control group. Furthermore, the incidence of POCD in the ulinastatin group was lower than that in the control group. These results demonstrated that ulinastatin may attenuate POCD by inhibiting the generation of S100β.

Systemic inflammatory response has been proven to be induced by gut microbiome-driving LPS with surgery-induced intestinal barrier dysfunction (Rhee, 2014; Schietroma et al., 2016). According to a trial that was included in our study, the level of serum LPS showed an association with the incidence of POCD (Zhang et al., 2018). LPS protein complex with toll-like receptor-4 activating the cellular NF-κB signaling pathway led to the increase of pro-inflammatory cytokines in the blood and in the brain (Li et al., 2004; Brun et al., 2007). The intraperitoneal injection of LPS triggered systemic inflammation and neuroinflammation, consequently inducing the cognitive function in aged rats (Kan et al., 2016). Zhang et al. (2018) found that the serum LPS and the occurrence of POCD were lower in the ulinastatin group than those in the control group. Studies showed that ulinastatin also inhibited the inflammatory cascade triggered by LPS in the blood. Furthermore, ulinastatin reduced the intestinal protease content, slowed down the digestion of intestinal tissue by protease, and reduced the damage of intestinal mucosa during ischemia, thereby protecting the intestinal barrier function. This article did not cover this, and so more rigorous research is needed to confirm this.

However, Li et al. (2013) suggested that ulinastatin could not improve cognitive function in aged rats. The intensity of systemic inflammatory response varied with the types of surgery, and this might be the reason for the differential effects of ulinastatin on early POCD from various types of surgeries. It was probably insufficient for the inhibition of initiation and degree of inflammatory response. In addition, it might also be related to the underlying inflammatory state and cognition of different age groups. In a word, there are confounding factors that affected the function of ulinastatin, and the dose of ulinastatin administered during the perioperative period remains to be considered.

There are some limitations in this study. Firstly, the lack of gray literature may lead to publication biases. Secondly, the timing and dose of ulinastatin were not consistent in the included studies, possibly affecting the results of the analysis. In addition, it was recommended that the diagnostic criteria for POCD should be aligned with the clinical diagnostic criteria of neurocognitive disorders such as those that have already been used in the Diagnostic and Statistical Manual for Mental Disorders, Fifth Edition (DSM-5). Furthermore, POCD has been defined in previous research studies to describe an objectively measurable decline in cognitive function at varying intervals after anesthesia and surgery, i.e., up to 3–12 months after surgery (Evered et al., 2018). In our study, POCD was diagnosed by MMSE scores in short-term after surgery in the included studies. Therefore, the effect of ulinastatin on surgery-induced POCD should be evaluated according to the recommended diagnostic criteria of POCD from The Nomenclature Consensus Working Group.

In summary, the prophylactic use of ulinastatin can effectively reduce the incidence of early cognitive impairment after surgery in elderly patients by reducing inflammation. However, due to certain limitations of the quality and quantity of the included studies, the results of this study should be considered with more caution, and more high-quality, large-sample RCTs are needed to verify the results.

CONCLUSIONS

This systematic review and meta-analysis of available evidence suggested that the application of ulinastatin reduced the incidence of early POCD and improved the MMSE score by attenuating the elevated serum levels of TNF-α, S100β protein, and IL-6 and increasing serum IL-10 levels. Nevertheless, high-quality RCTs that are adequately powered are needed to address the shortcomings of this study.

DATA AVAILABILITY STATEMENT

All data generated or analyzed during this study are included in this published article.

AUTHOR CONTRIBUTIONS

MD and FL designed and conceived the study, participated in the acquisition, analysis and interpretation of data,

and drafted the manuscript. SF and XW participated in the analysis and interpretation of data and contributed to the manuscript. TW and HF conceived the study, participated in its design and coordination, and helped to draft the manuscript. All authors read and approved the final manuscript.

FUNDING

This study was supported by the Beijing Municipal Administration of Hospitals Clinical Medicine Development of Special Funding Support under Grant No. ZYLX201818.

ACKNOWLEDGMENTS

The authors thank Xuanwu hospital library management workers and statistics professional who contributed a lot to the article.

SUPPLEMENTARY MATERIAL

The Supplementary Material for this article can be found online at: https://www.frontiersin.org/articles/10.3389/fnins.2021.618589/full#supplementary-material

Supplementary File 1 | The search strategy formula about the Meta-Analysis.

Supplementary File 2 | Sensitivity analysis graph: evaluating the stability of the effect of ulinastatin on POCD.

Supplementary File 3 | Funnel plot about the incidence of POCD among included studies.

Supplementary File 4 | Sensitivity analysis graph: evaluating the stability of the effect of ulinastatin on POCD after removing three articles with publication bias.

Supplementary File 5 | Funnel plot about the incidence of POCD after removing three articles with publication bias.

Supplementary File 6 | Funnel plot about the MMSE score among included studies.

Supplementary File 7 | Changes in inflammatory factors reported by included studies.

REFERENCES

Atal, S. S., and Atal, S. (2016). Ulinastatin - a newer potential therapeutic option for multiple organ dysfunction syndrome. *J. Basic Clin. Physiol. Pharmacol.* 27, 91–99. doi: 10.1515/jbcpp-2015-0003

Balshem, H., Helfand, M., Schünemann, H. J., Oxman, A. D., Kunz, R., Brozek, J., et al. (2011). GRADE guidelines: 3. Rating the quality of evidence. *J. Clin. Epidemiol.* 64, 401–406. doi: 10.1016/j.jclinepi.2010.07.015

Begg, C. B., and Mazumdar, M. (1994). Operating characteristics of a rank correlation test for publication bias. *Biometrics* 50, 1088–1101. doi: 10.2307/2533446

Bekker, A., Lee, C., de Santi, S., Pirraglia, E., Zaslavsky, A., and Farber, S., et al. (2010). Does mild cognitive impairment increase the risk of developing postoperative cognitive dysfunction? *Am. J. Surg.* 199, 782–788. doi: 10.1016/j.amjsurg.2009.07.042

Berger, M., Nadler, J. W., Browndyke, J., Terrando, N., Ponnusamy, V., Cohen, H. J., et al. (2015). Postoperative cognitive dysfunction: minding the gaps in our knowledge of a common postoperative complication in the elderly. *Anesthesiol. Clin.* 33, 517–550. doi: 10.1016/j.anclin.2015.05.008

Berger, M. M. P., Burke, J. M. P., Eckenhoff, R. M., and Mathew, J. M. (2014). Alzheimer's disease, anesthesia, and surgery: a clinically focused review. *J. Cardiothoracic Vasc. Anesthesia* 28, 1609–1623. doi: 10.1053/j.jvca.2014.04.014

Browndyke, J. N., Giovanello, K., Petrella, J., Hayden, K., Chiba-Falek, O., Tucker, K. A., et al. (2013). Phenotypic regional functional imaging patterns during memory encoding in mild cognitive impairment and Alzheimer's disease. *Alzheimers Dement* 9, 284–294. doi: 10.1016/j.jalz.2011.12.006

Brun, P., Castagliuolo, I., Leo, V. D., Buda, A., Pinzani, M., Palu, G., et al. (2007). Increased intestinal permeability in obese mice: new evidence in the pathogenesis of nonalcoholic steatohepatitis. *Am. J. Physiol. Gastrointestinal Liver Physiol.* 292, G518–G525. doi: 10.1152/ajpgi.00024.2006

Buvanendran, A., Kroin, J. S., Berger, R. A., Hallab, N. J., Saha, C., Negrescu, C., et al. (2006). Upregulation of prostaglandin E2 and interleukins in the central nervous system and peripheral tissue during and after surgery in humans. *Anesthesiology* 104, 403–410. doi: 10.1097/00000542-200603000-00005

Chan, J. K., Roth, J., Oppenheim, J. J., Tracey, K. J., Vogl, T., Feldmann, M., et al. (2012). Alarmins: awaiting a clinical response. *J. Clin. Invest.* 122, 2711–2719. doi: 10.1172/JCI62423

Dong, Y., Xu, Z., Huang, L., Zhang, Y., and Xie, Z. (2016). Peripheral surgical wounding may induce cognitive impairment through interlukin-6-dependent mechanisms in aged mice. *Med. Gas Res.* 6, 180–186. doi: 10.4103/2045-9912.196899

Egger, M., Davey, S. G., Schneider, M., and Minder, C. (1997). Bias in meta-analysis detected by a simple, graphical test. *BMJ* 315, 629–634. doi: 10.1136/bmj.315.7109.629

Evered, L., Silbert, B., Knopman, D. S., Scott, D. A., DeKosky, S. T., Rasmussen, L. S., et al. (2018). Recommendations for the nomenclature of cognitive change associated with anaesthesia and surgery-−2018. *Br. J. Anaesthesia* 121, 1005–1012. doi: 10.1016/j.bja.2017.11.087

Fidalgo, A. R., Cibelli, M., White, J. P., Nagy, I., Maze, M., and Ma, D. (2011). Systemic inflammation enhances surgery-induced cognitive dysfunction in mice. *Neurosci. Lett.* 498, 63–66. doi: 10.1016/j.neulet.2011.04.063

Fu, H. Q., Yang, T., Xiao, W., Fan, L., Wu, Y., Terrando, N., et al. (2014). Prolonged neuroinflammation after lipopolysaccharide exposure in aged rats. *PLoS ONE* 9:e106331. doi: 10.1371/journal.pone.0106331

Ge, Y. L., Shi, H. W., Zhu, W. F., Ma, Z. L., Wei, H. Y., Gu, X. P., et al. (2015). Effects of ulinastatin on cognitive function in patients with coronary artery bypass grafting. *Zhejiang Da Xue Xue Bao Yi Xue Ban* 44, 532–538.

Ge, Y. Y., Xu, Y., Cheng, J. Q., Chen, J. M., Xu, R. M., and Jiang, Y. D. (2011). Case-control study on the effect of ulinastatin on postoperative complications in elderly patients undergoing hip joint replacement. *Zhongguo Gu Shang* 24, 459–462.

Higgins, J. P. T., Altman, D. G., Gotzsche, P. C., Juni, P., Moher, D., Oxman, A. D., et al. (2011). The Cochrane Collaboration's tool for assessing risk of bias in randomised trials. *BMJ* 343:d5928. doi: 10.1136/bmj.d5928

Higgins, J. P. T., Thompson, S. G., Deeks, J. J., and Altman, D. G. (2003). Measuring inconsistency in meta-analyses. *BMJ* 327, 557–560. doi: 10.1136/bmj.327.7414.557

Hirsch, J., Vacas, S., Terrando, N., Yuan, M., Sands, L. P., Kramer, J., et al. (2016). Perioperative cerebrospinal fluid and plasma inflammatory markers after orthopedic surgery. *J. Neuroinflamm.* 13:211. doi: 10.1186/s12974-016-0681-9

Hudetz, J. A., Gandhi, S. D., Iqbal, Z., Patterson, K. M., and Pagel, P. S. (2011). Elevated postoperative inflammatory biomarkers are associated with short- and medium-term cognitive dysfunction after coronary artery surgery. *J. Anesthesia* 25, 1–9. doi: 10.1007/s00540-010-1042-y

Inoue, K., Takano, H., Sato, H., Yanagisawa, R., and Yoshikawa, T. (2009). Protective role of urinary trypsin inhibitor in lung expression of proinflammatory cytokines accompanied by lethal liver injury in mice. *Immunopharmacol. Immunotoxicol.* 31, 446–450. doi: 10.1080/08923970902769646

Kan, M. H., Yang, T., Fu, H. Q., Fan, L., Wu, Y., Terrando, N., et al. (2016). Pyrrolidine dithiocarbamate prevents neuroinflammation and cognitive dysfunction after endotoxemia in rats. *Front. Aging Neurosci.* 8:175. doi: 10.3389/fnagi.2016.00175

Kang, Y. M., Ge, Y. Y., Cheng, J. Q., Chen, Y. B., Yuan, N., Zhao, L. J., et al. (2010). Effect of ulinastatin on post-operative cognition disorders in elderly patients undergoing hip joint replacement. *Zhongguo Gu Shang* 23, 355–358.

Leslie, M. (2017). The post-op brain. *Science* 356, 898–900. doi: 10.1126/science.356.6341.898

Li, G., Sun, S., Cao, X., Zhong, J., and Tong, E. (2004). LPS-induced degeneration of dopaminergic neurons of Substantia nigra in rats. *J. Huazhong Univ. Sci. Technol. Med. Sci.* 24: 83–86. doi: 10.1007/BF02830714

Li, M., Yong-Zhe, L., Ya-Qun, M., Sheng-Suo, Z., Li-Tao, Z., and Ning-Ling, P. (2013). Ulinastatin alleviates neuroinflammation but fails to improve cognitive function in aged rats following partial hepatectomy. *Neurochem. Res.* 38, 1070–1077. doi: 10.1007/s11064-013-1018-z

Li, S., Feng, L., Li, L., Yue, J., and He, Y. (2016). Influence of ulinastatin on inflammatory factors and cognitive function in patients with cardiac surgery under cardiopulmonary bypass. *Progress Modern Biomed.* 16, 1930–1933. doi: 10.13241/j.cnki.pmb.2016.10.033

Li, S. T., Dai, Q., Zhang, S. X., Liu, Y. J., Yu, Q. Q., Tan, F., et al. (2018). Ulinastatin attenuates LPS-induced inflammation in mouse macrophage RAW264.7 cells by inhibiting the JNK/NF-kappaB signaling pathway and activating the PI3K/Akt/Nrf2 pathway. *Acta Pharmacol. Sin.* 39, 1294–1304. doi: 10.1038/aps.2017.143

Li, X. F., Zhang, X. J., Zhang, C., Wang, L. N., Li, Y. R., Zhang, Y., et al. (2018). Ulinastatin protects brain against cerebral ischemia/reperfusion injury through inhibiting MMP-9 and alleviating loss of ZO-1 and occludin proteins in mice. *Exp. Neurol.* 302, 68–74. doi: 10.1016/j.expneurol.2017.12.016

Li, Y. C., Xi, C. H., An, Y. F., Dong, W. H., and Zhou, M. (2012). Perioperative inflammatory response and protein S-100beta concentrations - relationship with post-operative cognitive dysfunction in elderly patients. *Acta Anaesthesiol. Scand.* 56, 595–600. doi: 10.1111/j.1399-6576.2011.02616.x

Lili, X., Zhiyong, H., and Jianjun, S. (2013). A preliminary study of the effects of ulinastatin on early postoperative cognition function in patients undergoing abdominal surgery. *Neurosci Lett.* 541, 15–19. doi: 10.1016/j.neulet.2013.02.008

Linstedt, U., Meyer, O., Kropp, P., Berkau, A., Tapp, E., and Zenz, M. (2002). Serum concentration of S-100 protein in assessment of cognitive dysfunction after general anesthesia in different types of surgery. *Acta Anaesthesiol. Scand.* 46, 384–389. doi: 10.1034/j.1399-6576.2002.460409.x

Liu, X., Yu, Y., and Zhu, S. (2018). Correction: inflammatory markers in postoperative delirium (POD) and cognitive dysfunction (POCD): a meta-analysis of observational studies. *PLoS ONE* 13:e209284. doi: 10.1371/journal.pone.0209284

Ma, L., Zhang, H., Liu, Y. Z., Yin, Y. L., Ma, Y. Q., and Zhang, S. S. (2016). Ulinastatin decreases permeability of blood–brain barrier by inhibiting expression of MMP-9 and t-PA in postoperative aged rats. *Int. J. Neurosci.* 126, 463–468. doi: 10.3109/00207454.2015.1025394

Mannick, J. A., Rodrick, M. L., and Lederer, J. A. (2001). The immunologic response to injury. *J. Am. Coll. Surg.* 193, 237–244. doi: 10.1016/S1072-7515(01)01011-0

Menger, M. D., and Vollmar, B. (2004). Surgical trauma: hyperinflammation versus immunosuppression? *Langenbecks Arch. Surg.* 389, 475–484. doi: 10.1007/s00423-004-0472-0

Moher, D., Liberati, A., Tetzlaff, J., and Altman, D. G. (2009a). Preferred reporting items for systematic reviews and meta-analyses: the PRISMA statement. *J. Clin. Epidemiol.* 62, 1006–1012. doi: 10.1016/j.jclinepi.2009.06.005

Moher, D., Liberati, A., Tetzlaff, J., and Altman, D. G. (2009b). Preferred reporting items for systematic reviews and meta-analyses: the PRISMA statement. *BMJ* 339:b2535. doi: 10.1136/bmj.b2535

Pan, C., Chen, Y., and Wu, Y. (2016). Dexmedetomidine combined with ulinastatin improves postoperative cognitive dysfunction in elderly patients after Iaparoscopic colorectal cancer surgery by regulating pro-inflammatory/anti-inflammatory system. *WCJD* 24, 166–172. doi: 10.11569/wcjd.v24.i17.2755

Peng, L., Xu, L., and Ouyang, W. (2013). Role of peripheral inflammatory markers in postoperative cognitive dysfunction (POCD): a meta-analysis. *PLoS ONE* 8:e79624. doi: 10.1371/journal.pone.0079624

Rhee, S. H. (2014). Lipopolysaccharide: basic biochemistry, intracellular signaling, and physiological impacts in the gut. *Intestinal Res.* 12, 90–95. doi: 10.5217/ir.2014.12.2.90

Schietroma, M., Pessia, B., Carlei, F., Cecilia, E., and Amicucci, G. (2016). Gut barrier function and systemic endotoxemia after laparotomy or laparoscopic resection for colon cancer: a prospective randomized study. *J. Minimal Access Surg.* 12, 254–259. doi: 10.4103/0972-9941.169982

Schietroma, M., Pessia, B., Carlei, F., Cecilia, E. M., and Amicucci, G. (2013). Intestinal permeability, systemic endotoxemia, and bacterial translocation after open or laparoscopic resection for colon cancer: a prospective randomized study. *Int. J. Colorectal Dis.* 28, 1651–1660. doi: 10.1007/s00384-013-1751-4

Shan, X., Zhang, X., Li, X., Xu, G., and Li, Z. (2015). Effect of ulinastatin on postoperative cognitive function in the elderly with fracture. *Zhonghua Yi Xue Za Zhi* 95, 1586–1589.

Terrando, N., Monaco, C., Ma, D., Foxwell, B. M., Feldmann, M., and Maze, M. (2010). Tumor necrosis factor-alpha triggers a cytokine cascade yielding postoperative cognitive decline. *Proc. Natl. Acad. Sci. U.S.A.* 107, 20518–20522. doi: 10.1073/pnas.1014557107

Thelin, E. P., Zeiler, F. A., Ercole, A., Mondello, S., Buki, A., and Bellander, B. M., et al. (2017). Serial sampling of serum protein biomarkers for monitoring human traumatic brain injury dynamics: a systematic review. *Front. Neurol.* 8:300. doi: 10.3389/fneur.2017.00300

Wang, K. Y., Yang, Q. Y., Tang, P., Li, H. X., Zhao, H. W., and Ren, X. B. (2017). Effects of ulinastatin on early postoperative cognitive function after one-lung ventilation surgery in elderly patients receiving neoadjuvant chemotherapy. *Metab. Brain Dis.* 32, 427–435. doi: 10.1007/s11011-016-9926-7

Wei, P., Yang, F., Zheng, Q., Tang, W., and Li, J. (2019). The potential role of the NLRP3 inflammasome activation as a link between mitochondria ROS generation and neuroinflammation in postoperative cognitive dysfunction. *Front. Cell Neurosci.* 13:73. doi: 10.3389/fncel.2019.00073

Yang, C., Wang, H., Song, Y., Li, Y., and Ma, L. (2017). Effects of dexmedetomidine combined with ulinastatinon the postoperative cognitive dysfunction in elderly patients with gastrointestinal tumor resection. *Progress in Modern Biomedcine* 17, 101–105. doi: 10.13241/j.cnki.pmb.2017.35.021

Zhang, M., Zhang, Y. H., Fu, H. Q., Zhang, Q. M., and Wang, T. L. (2018). Ulinastatin may significantly improve postoperative cognitive function of elderly patients undergoing spinal surgery by reducing the translocation of lipopolysaccharide and systemic inflammation. *Front. Pharmacol.* 9:1007. doi: 10.3389/fphar.2018.01007

Zhang, Y., Guo, X., Zhang, Q., Yan, G., and Wang, T. (2015). Serum CRP and urinary trypsin inhibitor implicate postoperative cognitive dysfunction especially in elderly patients. *Int. J. Neurosci.* 125, 501–506. doi: 10.3109/00207454.2014.949341

Conflict of Interest: The authors declare that the research was conducted in the absence of any commercial or financial relationships that could be construed as a potential conflict of interest.

The reviewer WO declared a past co-authorship with one of the authors TW to the handling editor.

Copyright © 2021 Duan, Liu, Fu, Feng, Wang and Wang. This is an open-access article distributed under the terms of the Creative Commons Attribution License (CC BY). The use, distribution or reproduction in other forums is permitted, provided the original author(s) and the copyright owner(s) are credited and that the original publication in this journal is cited, in accordance with accepted academic practice. No use, distribution or reproduction is permitted which does not comply with these terms.

frontiers in Pharmacology

ORIGINAL RESEARCH
published: 21 June 2021
doi: 10.3389/fphar.2021.599543

Baicalin Attenuates Oxygen–Glucose Deprivation/Reoxygenation–Induced Injury by Modulating the BDNF-TrkB/PI3K/Akt and MAPK/Erk1/2 Signaling Axes in Neuron–Astrocyte Cocultures

Changxiang Li[1†], Conglu Sui[2†], Wei Wang[1], Juntang Yan[1], Nan Deng[1], Xin Du[1], Fafeng Cheng[1], Xiaona Ma[2], Xueqian Wang[1]* and Qingguo Wang[1]**

[1]School of Traditional Chinese Medicine Department, Beijing University of Chinese Medicine, Beijing, China, [2]Third Affiliated Hospital, Beijing University of Chinese Medicine, Beijing, China

Background: Baicalin (BCL), a candidate drug for ischemic stroke, has been indicated to protect neurons by promoting brain-derived neurotrophic factor (BDNF). However, the cellular source of BDNF release promoted by baicalin and its detailed protective mechanism after ischemia/reperfusion remains to be studied. The aim of this study was to investigate the neuroprotective mechanisms of baicalin against oxygen–glucose deprivation/reoxygenation (OGD/R) in a neuron–astrocyte coculture system and to explore whether the BDNF-TrkB pathway is involved.

Methods and Results: A neuron–astrocyte coculture system was established to elucidate the role of astrocytes in neurons under OGD/R conditions. The results demonstrated that astrocytes became reactive astrocytes and released more BDNF in the coculture system to attenuate neuronal apoptosis and injury after OGD/R. BCL maintained the characteristics of reactive astrocytes and obviously increased the expression of cyclic AMP response element-binding protein (CREB) and the levels of BDNF in the coculture system after OGD/R. To further verify whether BDNF binding to its receptor tyrosine kinase receptor B (TrkB) was required for the neuroprotective effect of baicalin, we examined the effect of ANA-12, an antagonist of TrkB, on NA system injury, including oxidative stress, inflammation, and apoptosis induced by OGD/R. The results showed that treatment of NA systems with ANA-12 significantly attenuated the neuroprotection of BCL. The phosphatidylinositol 3-kinase (PI3K)/protein kinase B (Akt) and mitogen-activated protein kinase (MAPK)/extracellular signal-regulated kinase (ERK) pathways are two important downstream cascades of signaling pathways activated by BDNF binding to TrkB. We investigated the expressions of TrkB, PI3K, Akt, MAPK, and ERK. The results demonstrated that baicalin significantly increased the expressions of TrkB, PI3K/AKT, and MAPK/ERK.

Conclusion: The neuroprotective effects of baicalin against oxidative stress, inflammation, and apoptosis were improved by astrocytes, mainly mediated by increasing the release of BDNF and its associated receptor TrkB and downstream signaling regulators PI3K/Akt and MAPK/ERK1/2.

Keywords: ischemic stroke, baicalin, astrocyte, coculture, BDNF/TrkB pathway, apoptosis, inflammation

OPEN ACCESS

Edited by:
Mariela Fernanda Perez, National University of Córdoba, Argentina

Reviewed by:
Santiago Quiroga, National University of Córdoba, Argentina
Crhistian Luis Bender, Instituto de Farmacología Experimental de Córdoba (IFEC), Argentina
Lize Xiong, Fourth Military Medical University, China

***Correspondence:**
Xiaona Ma
fightandfight@yeah.net
Xueqian Wang
shirlyding@163.com
Qingguo Wang
wangqg8558@163.com

[†]These authors have contributed equally to this work

Specialty section:
This article was submitted to Neuropharmacology, a section of the journal Frontiers in Pharmacology

Received: *27 August 2020*
Accepted: *05 January 2021*
Published: *21 June 2021*

Citation:
Li C, Sui C, Wang W, Yan J, Deng N, Du X, Cheng F, Ma X, Wang X and Wang Q (2021) Baicalin Attenuates Oxygen–Glucose Deprivation/Reoxygenation–Induced Injury by Modulating the BDNF-TrkB/PI3K/Akt and MAPK/Erk1/2 Signaling Axes in Neuron–Astrocyte Cocultures. Front. Pharmacol. 12:599543. doi: 10.3389/fphar.2021.599543

INTRODUCTION

Stroke is a predominant cause of permanent disability and death worldwide (Katan and Luft 2018). Ischemic strokes (ISs) account for approximately 87% of all strokes (Dabrowska et al., 2019). Even after decades of research, recombinant tissue-type plasminogen activator (Rt-PA) is the only standard therapeutic drug approved by the FDA to treat ISs. Only a few patients (2–5%) can receive Rt-PA thrombolytic therapy because of the narrow time window (McDermott et al., 2019). Therefore, there is an increasing focus on developing neuroprotective agents.

In a great number of studies, neuroprotective agent development experiments only target neurons that lack contact with other types of brain cells and cannot reflect the characteristics of the *in vivo* brain. Other brain cells have critical specific signals and of execution cascades that can also promote neuronal recovery (Liu and Chopp 2016; Venkat et al., 2018; Sun et al., 2019). Moreover, all cell types in the brain may be destroyed after ISs, and the relative balance among them is broken (Dalkara et al., 2016; Liu and Chopp 2016; Venkat et al., 2018). Interactions between these cells regulate complex brain functions under pathological conditions and further aggravate brain damage (Venkat et al., 2018). Therefore, the development of neuroprotective agents aims to expand their effect from protecting pure neurons to protecting multiple types of cells and coordinating their interactions.

Cocultivation systems are increasingly used for cell–cell interactions and for studying drugs to protect neurons indirectly by targeting one type of cell after ischemia-reperfusion (Xue et al., 2013; Yamamizu et al., 2017; Bhalerao et al., 2020; Heymans et al., 2020). Astrocytes, a critical structural and functional part of the neurovascular unit, play an essential role in maintaining normal brain function and responses to ischemic lesions (Liu and Chopp 2016). After an ischemic stroke, astrocytes contribute to neurogenesis, synaptogenesis, and axonal remodeling, thereby promoting neurological recovery (Liu and Chopp 2016). The pivotal involvement of astrocytes designates them as excellent therapeutic targets to improve functional outcomes following a stroke (Sun et al., 2019). Astrocytes and neurons interact closely under physiological and pathological conditions after an IS (Liu and Chopp 2016). In this study, we established a relevant and convenient neuron–astrocyte coculture system to recapitulate this complex interaction.

Baicalin (BCL) is an effective drug candidate for the treatment of ISs. BCL, isolated from the root of *Scutellaria baicalensis* Georgi, is an important flavonoid compound as a potential neuroprotective agent (Kandhasamy et al., 2018). A number of *in vitro* and *in vivo* studies have demonstrated that BCL possessed various pharmacological mechanisms, including antioxidative stress, anti-excitotoxicity, antiapoptotic, and anti-inflammatory effects, inducing neuroregeneration and promoting the expression of neurotrophic factors (Zhu et al., 2012; Fafeng et al., 2013; Liang et al., 2017; Kandhasamy et al., 2018). Moreover, BCL exhibits a variety of beneficial effects in the central nervous system by protecting neurons, astrocytes, Schwann cells, brain microvascular endothelial cells, and the blood–brain barrier from ischemia-reperfusion injury (Shi et al., 2017; Wenpu et al., 2017; Kandhasamy et al., 2018; Song et al., 2020). In particular, a previous study indicated that treatment with BCL remarkably promoted the expression of BDNF in a global cerebral ischemia/reperfusion injury model (Cao et al., 2011).

BDNF, one of the most important neurotrophic factors, promotes neuronal survival and repairs brain damage following ischemia/reperfusion (Liu et al., 2020). A previous study showed that BDNF exerted neuroprotective effects against ischemic stress and inflammation, and decreases apoptosis. TrkB is an endogenous receptor of BDNF with high affinity. The intracellular domain of the tyrosine residue is autophosphorylated after BDNF binds to TrkB, resulting in ligand-induced dimerization of each receptor, which subsequently activates downstream cascades of signals from three signaling pathways activated by TrkB: the PI3K/Akt, MAPK/ERK, and PLCγ pathways (Liu et al., 2020). However, the precise protective mechanisms of BCL during cerebral ischemia/reperfusion through BDNF-TrkB remain to be studied.

Accumulating studies have suggested that BDNF is produced in neurons, but astrocytes are also an important source of BDNF in the brain. BDNF is released from astrocytes via exocytosis to regulate the function of neighboring neurons (Nobukazu et al., 2015; Hong et al., 2016). The coculture system of astrocytes and neurons is suitable for studying the effect of neuroprotective agents on neurons by promoting the release of BDNF from astrocytes (Quesseveur et al., 2013; Hong et al., 2016). Therefore, we established a coculture system of neurons and astrocytes to investigate the neuroprotective mechanisms of BCL against neuronal injury induced by OGD/R and to explore whether the BDNF-TrkB-PI3K/Akt and BDNF-TrkB-MAPK/ERK signaling pathways were involved.

MATERIALS AND METHODS

Animals

Newborn Sprague–Dawley (SD) rats of indicated days were purchased from Beijing Weitong Lihua Experimental Animal Technology (license no. SCXK 20160006, Beijing, China). Animal welfare and experimental procedures were carried out in accordance with the National Institutes of Health Guide for the Care and Use of Laboratory Animals and were approved by the Ethics Committee of Experimental Animals of Beijing University of Chinese Medicine (BUCM-3-2016040201-2003).

Isolation and Culture of Primary Neurons and Astrocytes

Primary neurons and astrocytes were obtained as in our previous study (Li et al., 2019a; Li et al., 2019b). Briefly, brains were dissected from 0- to 24-hour-old (neurons) and 2- to 3-day-old (astrocytes) SD rats. The brains were cut into halves, and the meninges were removed with tweezers. The cortices were dissected away, and much of the white matter was removed. The cortex was digested at 37°C for 20 min with 0.125% trypsin-

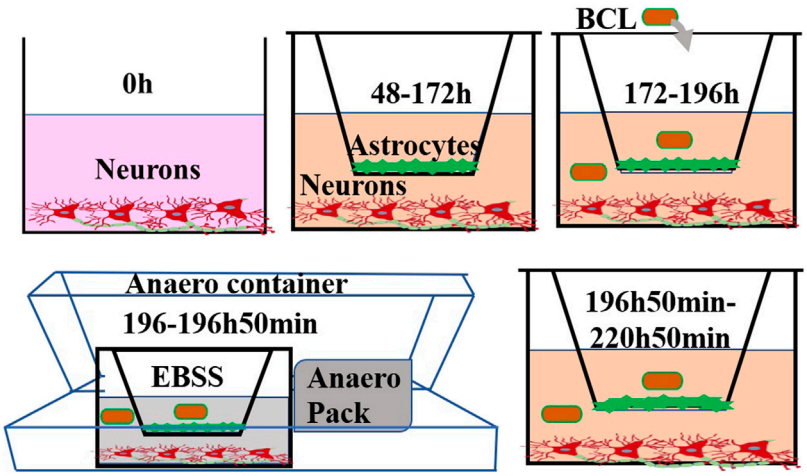

FIGURE 1 | Experimental steps of this study. Neurons were cultured at the bottom of a Transwell filter at 0 h. After 48 h, astrocytes were seeded on the upper side of the inserts. At 172 h, the experiments were performed. The cells were treated with BCL for 24 h prior to OGD/R. To mimic ischaemic conditions, cocultures were subjected to OGD for 50 min, and the cultures were returned to a normoxic incubator for 24 h. Structural and functional evaluations under pathophysiological conditions were undertaken at 220 h 50 min.

EDTA (Sigma-Aldrich, St. Louis, MO, United States). The digested cortical tissues were terminated and homogenized to single-cell suspensions with Dulbecco's modified Eagle's medium (DMEM)/F12 medium (Gibco-BRL, Grand Island, NY, United States) containing 10% FBS (Gibco-BRL). Then, the suspension was filtered through a 70-μm cell strainer and centrifuged at 800 rpm for 5 min. The precipitate of neurons was resuspended with Neurobasal-A medium (Gibco-BRL) containing 10% FBS, 2% B27 (Invitrogen; Thermo Fisher Scientific, Inc.), 0.25% GlutaMAX (Gibco-BRL), and 1% penicillin/streptomycin (P/S, Gibco-BRL). Cells were then seeded at a density of 1×10^6 cells/ml into 0.01% poly-l-lysine (PLL, Sigma-Aldrich) precoated dishes. The medium was changed to non-serum formula after seeding for 6–8 h. The precipitate of astrocytes was resuspended with DMEM/F12 (Gibco-BRL) containing 10% FBS (Gibco-BRL) and 1% P/S (Gibco-BRL). Then, 50% of the medium was replaced every two days.

Establishment of Neuron–Astrocyte Cocultures

Before starting the coculture, neurons were cultured on the bottom of a Transwell plate (Corning, 3460, 0.4 μm, New York, NY, United States), and the cultures were maintained in Neurobasal-A medium containing 2% B27, 0.25% GlutaMAX, and 1% P/S for at least 48 h. When the confluence gradually increased to 80%, astrocytes were used to establish the model. Astrocytes (2×10^5 cells/cm^2) were seeded into the matching well in the insert membrane in the Petri dish at 48 h. The time when the neurons were plated was defined as zero *in vitro*. At 172 h, the experiments were performed. The procedure for establishing the model is shown in **Figure 1**. The system for cocultivation according to the above method is defined as the NA system. Moreover, as controls, the cocultures were considered as the NA group, and neurons and astrocytes were cultured alone as the N group and A group, respectively.

Protective Effects of Baicalin on Astrocytes and Neurons Exposed to Oxygen–Glucose Deprivation/Reoxygenation

The protective effects of BCL against the OGD/R insult in the NA model were evaluated at the most appropriate dose in different cell types. The neurons and astrocytes were seeded in 96-well plates. The cells were treated with different concentrations of BCL (137.5, 68.75, 34.38, 17.19, 8.59, 4.30, 2.15, and 1.08 μg/ml) for 24 h before OGD/R. The medium was replaced with deoxygenated Earle's balanced salt solution without glucose with different concentrations of BCL. Subsequently, the cells were placed into the sealed Anaero container with an Anaero Pack (Mitsubishi, Tokyo, Japan) for 1 h. OGD was terminated by replacing Earle's balanced salt solution (EBSS) with the complete medium with different concentrations of BCL, and the cells were cultured under normoxic conditions at 37°C for 24 h. Control indicates no treatment throughout the OGD/R in a standard medium. The cell viability was set as 100% in the control group. The model indicates treatment with OGD (1 h)/R (24 h).

Oxygen–Glucose Deprivation/ Reoxygenation Insult on NA and Drug Administration

As shown in **Figure 1**, we used OGD/R in the *in vitro* NA model to mimic ischemic conditions. Briefly, the medium was replaced with deoxygenated EBSS (Leagene Biotech Co., Beijing, China) at 196 h. Then, the NA models were placed into a sealed Anaero container with an Anaero Pack (Mitsubishi, Tokyo, Japan) for 50 min to initiate OGD insult. OGD was terminated by complete medium, and the cocultures were cultured under normoxic

conditions at 37°C for 24 h to mimic reoxygenation. The cocultures with the above treatment were defined as the model group. The cocultures in the control group were incubated in DMEM/F12 with 20% FBS, 1% penicillin, and streptomycin without the above OGD/R treatment.

BCL was purchased from the National Institute for the Control of Pharmaceutical and Biological Products (Beijing, China). The BCL solution was prepared in glucose-free EBSS and DMEM/F12 containing 20% FBS and 1% P/S. The cultures were randomly divided into five groups: 1) control group, 2) OGD/R group, 3) BCL-L group (BCL: 8.59 μg/ml), 4) BCL-H group (BCL: 34.38 μg/ml), 5) BCL-H + ANA group (BCL + ANA12: 34.38 μg/ml+10 μM). The cells in the BCL-H group and BCL-L group were treated with BCL for 24 h prior to OGD/R and then under OGD conditions for 50 min. OGD was terminated, and the cells were cultured for an additional 24 h under normoxic conditions in the presence of BCL. The cocultures in the BCL-H and BCL-L groups were treated with BCL throughout the OGD/R process. The administration method of the BCL-H + ANA group was to add ANA-12 on the basis of BCL-H. Moreover, the N group, A group, and NA group treated with OGD/R were defined as the N + OGD/R group, A + OGD/R group, and NA + OGD/R group, respectively.

Immunofluorescence and Image Acquisition

Immunofluorescence staining of neurons and astrocytes was performed. The neurons and astrocytes were fixed with 4% paraformaldehyde for 15 min. Then, the cells were blocked and permeabilized for 1 h using a mixture of 0.1% Triton X-100 (Fisher Scientific) and 10% goat serum (Sigma) in PBS. Finally, the cells were incubated with primary antibodies against MAP2 (Abcam) and GFAP (Abcam) at 4°C overnight. Cells were incubated with secondary antibodies (Alexa Fluor 647-conjugated goat anti-chicken IgY, Abcam; FITC-conjugated goat anti-mouse IgG, Abcam) for 1 h. Images were captured by Olympus fluorescence microscopy after staining the nuclei with DAPI (4′,6-diamidino-2-phenylindole).

Flow Cytometric Analysis of Apoptosis

Analysis of apoptosis was carried out by flow cytometry using an Annexin V Apoptosis Detection Kit. Cells were digested with EDTA-free enzymes, harvested and washed twice with PBS, and then resuspended in 500 μL binding buffer. Next, the cells were stained with 5 μL Annexin V FITC and 5 μL PI (Kegen, Nanjing, Jiangsu Province, China), and the resuspended cells were incubated for 10 min in the dark. Finally, the cells were immediately examined on a FACSCalibur (BD Biosciences, Franklin, NJ, United States) flow cytometer, and the data were analyzed with Cell Quest software (BD Biosciences).

Assay of Inflammation and Oxidative Stress Activity

Interleukin-1β (IL-1β; Wuhan Liu he Biotechnology Co., Wuhan, China), interleukin-6 (IL-6; Wuhan Liu he Biotechnology Co.), and tumor necrosis factor-α (TNF-α; Proteintech) were assessed using ELISA kits according to the manufacturer's instructions. The optical density was measured at a wavelength of 450 nm using a microplate reader (Biotek, Winooski, Vermont, United States). Malondialdehyde (MDA; Jiancheng, Nanjing, China), superoxide dismutase (SOD; Jiancheng), and nitric oxide (NO; Jiancheng) were measured using commercial kits according to the manufacturer's instructions.

Assay of Brain-Derived Neurotrophic Factor by ELISA

The neurons cultured alone, astrocytes cultured alone, and neuron–astrocyte coculture system were treated with OGD/R. BCL was administered to the NA system after OGD/R. Their supernatants were harvested to determine the levels of the secreted BDNF. Additionally, cytoplasm contents in neurons or astrocytes in the NA + OGD/R group, NA + BCL-H + OGD/R group, and NA group were obtained using lysis buffer containing 50 mM Tris-HCl PH7.4, 2% SDS, 0.1 M NaCl, 1 mM EDTA, 1% Triton X-100, 0.5 μg/ml aprotinin, 1 mM sodium orthovanadate, and 1 mM PMSF. The levels of BDNF (Wuhan Liu he Biotechnology Co.) were measured by ELISA according to the manufacturer's instructions. The optical density was measured at a wavelength of 450 nm using a microplate reader (Biotek, Winooski, Vermont, United States).

Western Blot Analysis

The changes in protein levels were quantified using WB analysis. Cells were washed with PBS. Protein was obtained using the RIPA buffer (PPLYGEN, China) according to the manufacturer's instructions. The resuspended supernatant was quantified for the protein concentration using the BCA protein assay kit (KeyGen). Protein samples (30 mg per sample) were resolved using a 10% Tris/glycine SDS-PAGE gel and then transferred to a polyvinylidene difluoride membrane. Membranes were incubated in PBST containing 5% nonfat milk for 30 min. Following incubation with the primary antibodies in PBST/TBST containing 5% BSA that recognize anti–microtubule-associated protein-2 (MAP-2, Abcam), anti-cysteinyl aspartate-specific proteinase-3 (caspase-3, Proteintech), anti-cysteinyl aspartate-specific proteinase-9 (caspase-9, Proteintech), anti–B-cell lymphoma 2 (Bcl-2, Affinity), anti–Bcl-2 associated X protein (Bax, Proteintech), anti-TrkB (Affinity), anti–p-TrkB (Affinity), anti-CREB (Affinity), anti–p-CREB (Affinity), anti-PI3K (Affinity), anti–p-PI3K (Affinity), anti-Akt (Affinity), anti–p-Akt (Affinity), anti–mitogen-activated protein kinase (anti-MAPK (Affinity), anti–p-MAPK (Affinity), anti-extracellular signal-regulated kinase1/2 (anti-ERK1/2, Affinity), anti-CREB (Affinity), anti–p-ERK1/2 (Affinity), and anti-GAPDH at 4°C overnight, the blots were washed and then incubated with anti-rabbit IgG for 1 h at 25°C. After subsequent washes in TBST, immunolabeling was detected using enhanced chemiluminescence reagents (Perkin Elmer, Waltham, MA) and quantified by densitometry using an image analyzer (Bio-Rad, United States).

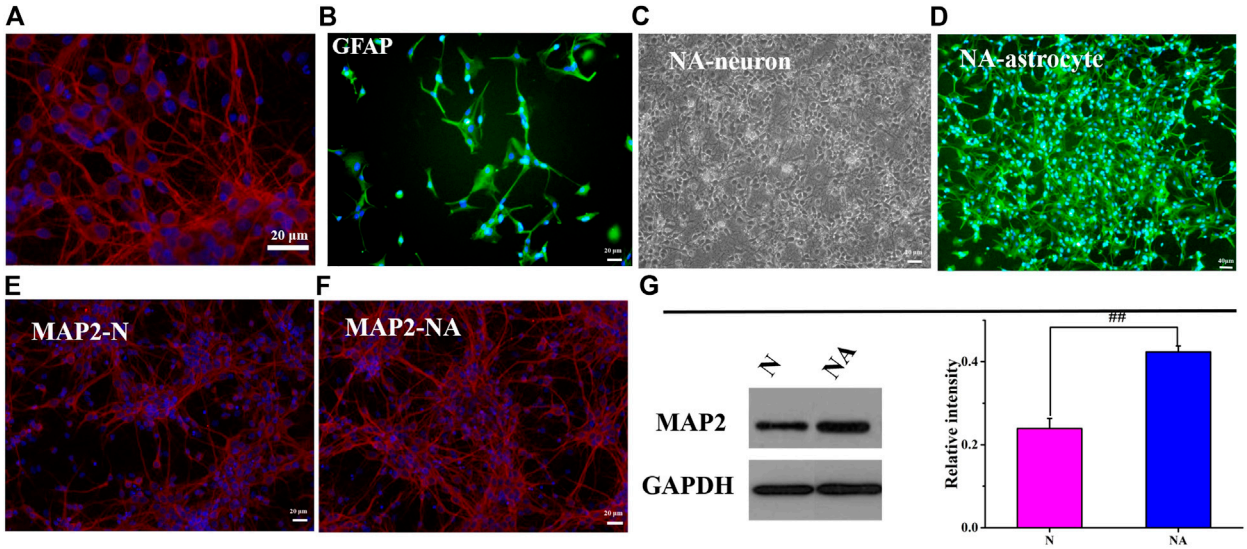

FIGURE 2 | Neuronal morphology in the N group and NA system. **(A)** Neurons were positive for MAP-2 (red). **(B)** Astrocytes were positive for GFAP (green). **(C)** The morphology of neurons in the coculture system. **(D)** The morphology of astrocytes in the coculture system. **(E)** MAP-2 (red) in the N group (N). **(F)** MAP-2 (red) in the NA group (NA). **(G)** The expression of MAP2 in the N group and NA group. ##$p < 0.01$, N vs. the NA group.

Statistical Analysis

All data are expressed as the mean ± standard deviation. Multiple comparisons were performed using one-way analysis of variance (ANOVA), and each group of data was subjected to the least significant difference (LSD) test using SPSS 20.0 (SPSS, Chicago, IL, United States). An unpaired two-tailed *t*-test was performed for comparisons between two groups. Values of $p < 0.05$ were considered to be significant, and $p < 0.01$ was considered to be highly significant.

RESULTS

Neuronal Morphology in N Group and NA Group

The purity of neurons and astrocytes was in line with that in a previous study (Li et al., 2019b; Li et al., 2019a) (**Figures 2A,B**). As shown in **Figures 2C,D**, we observed the growth conditions of neurons and astrocytes in the coculture system. To better observe the morphology of the neurons, we compared the morphology of neurons in the absence or presence of astrocytes at 172 h. MAP2 is a marker of neuron cell bodies, dendrites, and dendritic spines (Zhu et al., 2016). Accordingly, we performed immunofluorescence staining of MAP2 in neurons. As expected, neurons cocultured with astrocytes were significantly more mature than neurons cultured alone. As shown in **Figures 2E,F**, the number of neurons in the coculture system was greater than that in the monoculture system. Neuronal synapses were more fully extended, elongated, branched, and formed a distinct network with an increased number of branches in the coculture systems. Moreover, WB results showed that the MAP2 level was significantly higher ($p < 0.01$) in the NA system than that in the monoculture cocultured with astrocytes (**Figure 2G**). The results indicated that astrocytes had promoting effects on neurite outgrowth and neuronal network formation. The *in vitro* coculture system was a more reliable, scalable, and suitable tool to study accurately the aspects of astrocyte–neuron functional properties and interactions while being easily accessible for cell type–specific manipulations and observations.

The Damage of Neurons Exposed to Oxygen–Glucose Deprivation/Reoxygenation

We evaluated neuronal apoptosis and morphology in different culture systems after OGD to observe the effects of astrocytes on neurons (**Figures 3A–E**). The results showed that OGD/R induced significant neuronal apoptosis (**Figure 3A**). However, in comparison with cultures in the absence of astrocytes, the coculture system led to dramatically less neuronal apoptosis ($p < 0.01$) (**Figure 3A**). In the neuron system cultured alone, the neurons fell off, and the axons of the neurons were severely broken after OGD/R (**Figure 3C**). The morphology of neurons in the NA coculture system is better than that in the N group (**Figures 3C,E**). The results indicated that astrocytes exerted a beneficial protective effect on neurons after OGD/R.

Protective Effects of Baicalin on Astrocytes and Neurons Exposed to Oxygen–Glucose Deprivation/Reoxygenation

As shown in **Figure 4**, BCL was not toxic at the concentration of 8.59–68.75 μg/ml and showed significant protective effects in this study. We found that 34.38 μg/ml BCL was the optimal dose and showed a more significant protective effect than 8.59 μg/ml BCL ($p < 0.01$).

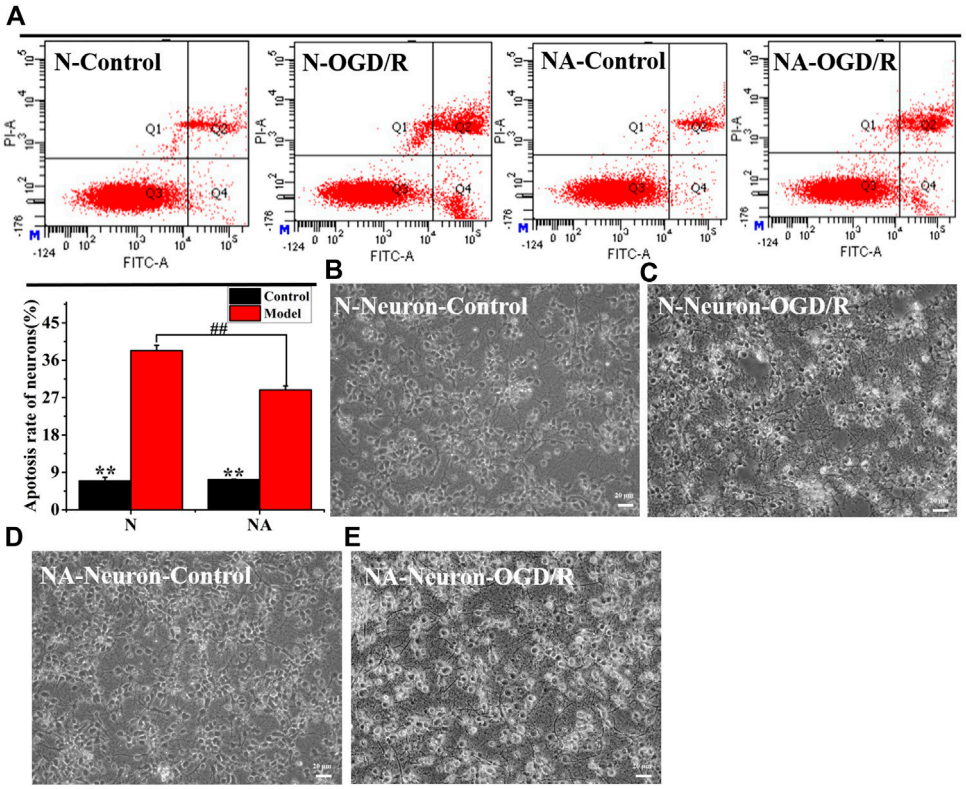

FIGURE 3 | Neuronal apoptosis and morphology in N and NA groups. **(A)** Neuron apoptosis in the N and NA groups. **(B)** Neuronal morphology in the N group. **(C)** Neuronal morphology in the N group after OGD/R. **(D)** Neuronal morphology in the NA group. **(E)** Neuronal morphology in the NA group after OGD/R. $^{**}p < 0.01$, vs. the model group; $\#\#p < 0.01$, N vs. the NA group.

Reactive Astrocytes and Brain-Derived Neurotrophic Factor Secretion after Oxygen–Glucose Deprivation/ Reoxygenation

A previous study showed that astrocytes are activated and they undergo important morphological changes to become reactive astrocytes after ischemia (Choudhury and Ding, 2016). In addition to the detrimental role during the early stage of ischemic onset, reactive astrocytes play a beneficial role in the brain (Liu and Chopp 2016). In view of the protective effect of astrocytes on neurons, we observed changes in astrocytes in the coculture system. Intermediate filament GFAP is a marker of astrocyte activation, which is essential for the cell structure and cell function of astrocytes (Choudhury and Ding, 2016). Previous studies have shown that astrocytes around the lesion were reactivated and that GFAP was dramatically upregulated in a time- and space-dependent manner after IS (Choudhury and Ding 2016). Our research results were in line with those of previous theories. We observed the morphological structure of astrocytes, which had a polygonal morphology, more synapses, and larger cell bodies after OGD/R using immunofluorescence by detecting the expression of GFAP, was very in line with the characteristics of reactive astrocytes (**Figure 5B**). Astrocytes expressed high levels of GFAP after OGD/R, while the number of astrocytes was not increased, which was different from the control astrocytes (**Figures 5A,B**). Activated reactive astrocytes protect neurons after stroke by producing a variety of neurotrophic factors, including nerve growth factor, basic fibroblast growth factor, BDNF, and glial cell–derived neurotrophic factor (Liu and Chopp 2016). BDNF, the most abundant neurotrophin in the mammalian CNS, exerts neuroprotective effects in ischemic stroke (Liu et al., 2020). Accumulating studies have suggested that BDNF was produced in neurons, but astrocytes were also an important source of BDNF in the brain (Hong et al., 2016). BDNF is released from astrocytes *via* exocytosis to regulate the function of neighboring neurons (Nobukazu et al., 2015; Hong et al., 2016). Based on this OGD/R model, very few studies have focused on the release of BDNF from neurons or astrocytes and the coculture system of neurons and astrocytes. Therefore, we detected the level of BDNF in the A group, N group, and NA group after OGD/R. Apart from neurons, astrocytes cultured alone can also produce BDNF after OGD/R. The levels of BDNF were higher in the NA system than those in neurons or astrocytes cultured alone ($p < 0.01$) (**Figure 5D**). Interestingly, the content of BDNF in the coculture system was higher than the sum of neurons and astrocytes cultured separately ($p < 0.01$). We further detected the content of BDNF in the cytoplasm of neurons and astrocytes

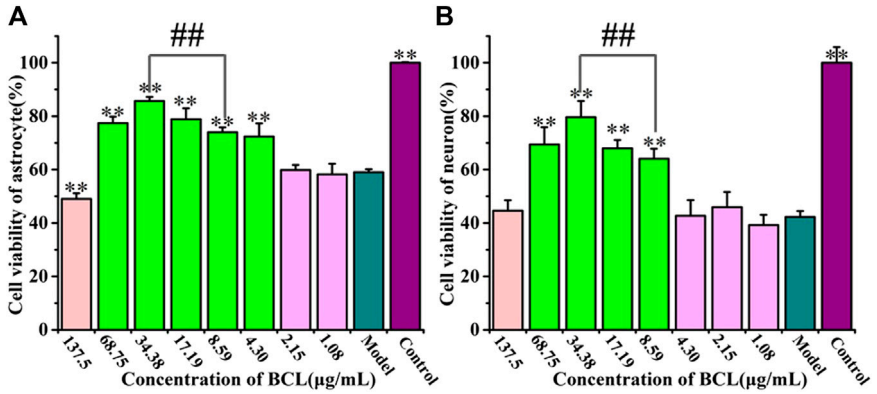

FIGURE 4 | Protective effects of baicalin on astrocytes and neurons after OGD/R. **(A)** Cell viability counts indicating the protective effects of BCL on astrocytes after OGD/R. **(B)** Cell viability counts showing the protective effects of BCL on neurons after OGD/R. $^{**}p < 0.01$, vs. the model group; $\#\#p < 0.01$, 34.38 μg/ml vs. 8.59 μg/ml.

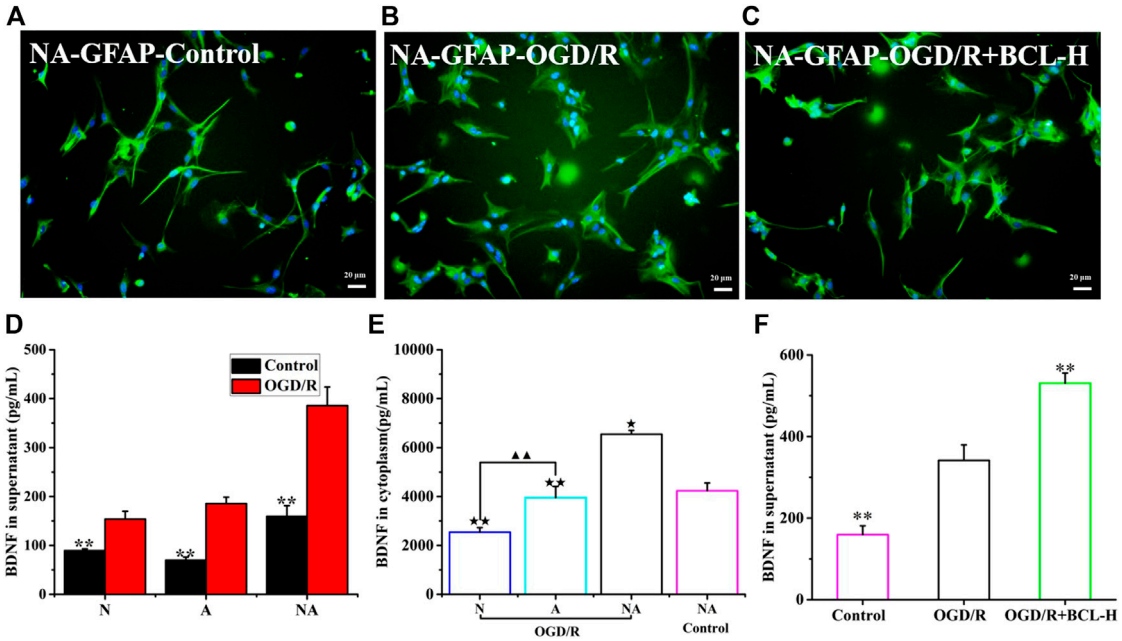

FIGURE 5 | Reactive astrocytes and BDNF secretion after OGD/R. **(A)** Morphology of astrocytes (GFAP) in the NA coculture system in the control group. **(B)** Morphology of astrocytes (GFAP) in the NA coculture system after OGD/R. **(C)** The effects of BCL on the morphology of astrocytes in the NA coculture system after OGD/R. **(D)** BDNF release in the N group, A group, and NA group after OGD/R. **(E)** The level of BDNF in neuronal cytoplasm (N), astrocyte cytoplasm (A), and NA system. **(F)** The effects of BCL on BDNF release in the NA group after OGD/R. ★★$p < 0.01$, ★$p < 0.05$ vs. NA + BCL-H + OGD/R group; ▲▲$p < 0.01$, N OGD/R group vs. A OGD/R group; $^{**}p < 0.01$, vs. OGD/R group.

in the NA culture system after OGD/R. We found that BDNF in the cytoplasm of astrocytes was significantly higher than that in neurons ($p < 0.01$) (**Figure 5E**). It is speculated that the reason is that the neurons were severely damaged and the astrocytes were in an activated state to become the important source of BDNF. To examine whether the activated state of astrocytes can be maintained by BCL, we measured the morphology of astrocytes treated with BCL after OGD/R. Without increasing the number of astrocytes, BCL maintained the activated state of astrocytes (**Figure 5C**). Moreover, we wanted to investigate whether BCL can affect the synthesis and secretion of BDNF. The results showed that BDNF was secreted more in the model group than in the control group ($p < 0.01$), and BCL treatment further promoted this progress (**Figure 5F**). To further observe the source of BDNF, we detected the content of BDNF in the cytoplasm. The results showed that BDNF was synthesized more in the A + OGD/R group than in the N + OGD/R group ($p < 0.01$) (**Figure 5E**).

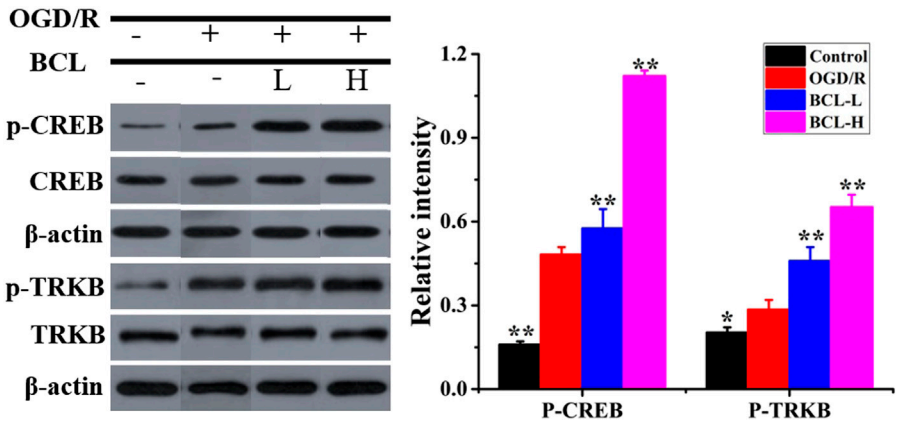

FIGURE 6 | Effects of BCL (34.38 μg/ml, 8.59 μg/ml) on the expression of CREB and TrkB in the NA system after OGD/R. Quantified results were normalized to β-actin expression. $^{**}p < 0.01$, $^{*}p < 0.01$, vs. OGD/R group.

The Effects of Baicalin on the Expression of TrkB and CREB in the NA System after Oxygen–Glucose Deprivation/Reoxygenation

Considering the promoting effect of BCL on the synthesis and secretion of BDNF, we examined whether BCL treatment could promote the expression of CREB, a transcription factor that increased BDNF expression (Bo et al., 2015). WB assays were performed for p-CREB with BCL treatment in the NA system after OGD/R. The data (**Figure 6**) showed that the expression of p-CREB in the OGD/R group was significantly higher than that in the control group ($p < 0.01$). BCL treatment upregulated the expression of p-CREB ($p < 0.01$). Activated CREB initiates the transcription of BDNF genes. Mature BDNF binds with higher-affinity Trk receptors to increase axonal growth, differentiation, morphology, neuronal survival, synaptic plasticity, and the resultant networks. Therefore, we examined the expression of TrkB. As shown in **Figure 6**, TrkB was expressed more in the model group than in the control group, and BCL treatment further promoted this progress ($p < 0.01$).

Baicalin Maintained the Morphology of Neurons and the Expression of MAP2 after Oxygen–Glucose Deprivation/Reoxygenation

MAP2, a neuron-specific cytoskeletal protein, is an independent criterion for defining axons that reflect neuronal morphology (Zhang et al., 2019). As shown in **Figures 7A,B**, MAP2 expression was significantly lower in the model group than that in the control group ($p < 0.01$), while the BCL group demonstrated higher MAP2 expression than that in the model group ($p < 0.01$). Compared with the model group, MAP2 expression was increased in the treatment groups ($p < 0.01$). In addition to WB, we performed microscopic imaging to observe the morphological changes in neurons. We found that neuronal axons were fully extended and formed a distinct network in the control group (**Figure 7C**). OGD/R-treated neurons displayed morphological collapse with significantly destructive dendrites and shedding of cells (**Figure 7D**). However, BCL treatment prevented the occurrence of morphological collapse upon OGD/R insult (**Figures 7E,F**). To confirm the hypothesis that the BDNF-TrkB pathway mediates the protective effect of BCL against OGD/R-induced injury, we next explored whether ANA12 reverses the protective effect of BCL against OGD/R-induced injury in neurons. Interestingly, inhibition of TrkB with ANA12 partially blocked the neuroprotective effects of BCL (**Figures 7A,B,G**). These results strongly suggested that BDNF-TrkB signaling played an essential role in BCL-mediated neuroprotective effects against OGD/R-induced damage.

Baicalin Attenuated Oxygen–Glucose Deprivation/Reoxygenation–Induced Apoptosis

WB was performed to confirm the effect of BCL in preventing OGD/R-induced apoptosis in neurons, and we found that OGD/R significantly induced neural apoptosis (**Figure 8**). However, relative to that of the OGD/R group, BCL treatment effectively attenuated OGD/R-induced apoptosis. Nevertheless, the apoptosis inhibitory effect of BCL in neurons can be attenuated by ANA12, a potent and selective TrkB antagonist that suppresses the activity of TrkB and its downstream signaling axis. As shown in **Figure 8**, Bcl-2 expression was significantly lower in the OGD/R group than that in the control group ($p < 0.01$), while the BCL group demonstrated higher Bcl-2 expression than that in the OGD/R group ($p < 0.01$). However, in contrast to Bcl-2 expression, Bax, caspase-3, and caspase-9 expressions

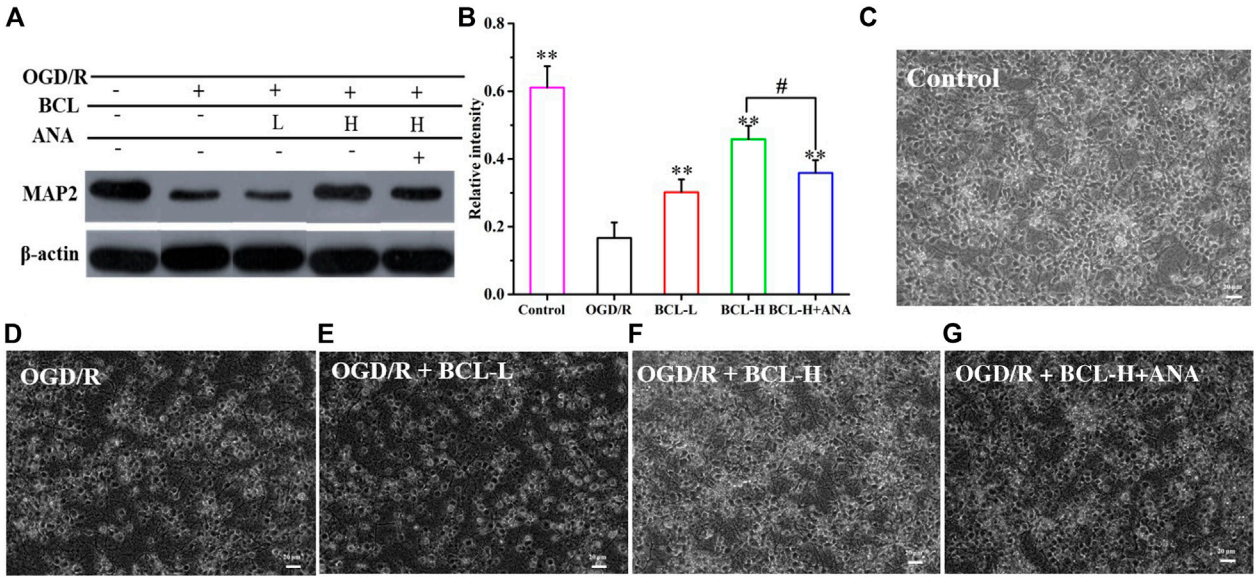

FIGURE 7 | Effects of BCL (34.38 μg/ml and 8.59 μg/ml) and TrkB antagonist on neurons in the NA system after OGD/R. **(A–B)** The effect of BCL on the expression of MAP2. **(C)** Neuronal morphology in the control group. **(D)** Neuronal morphology in the OGD/R group. **(E)** Neuronal morphology in the OGD/R + BCL-L group. **(F)** Neuronal morphology in the OGD/R + BCL-H group. **(G)** Neuronal morphology in the OGD/R + BCL-H + ANA group. Quantified results were normalized to β-actin expression. $^{**}p < 0.01$, vs. OGD/R group, $\#p < 0.05$, BCL-H group vs. BCL-H+ANA group.

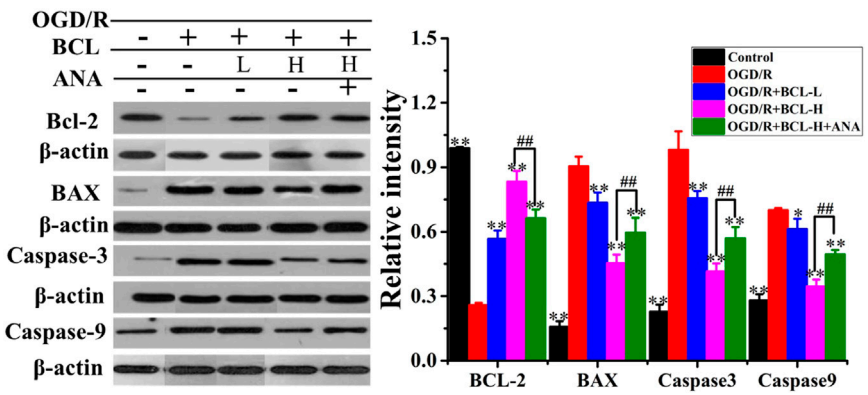

FIGURE 8 | Effect of BCL (34.38 μg/ml and 8.59 μg/ml) on apoptosis proteins after OGD/R. Quantified results were normalized to β-actin expression. $^{**}p < 0.01$, $^{*}p < 0.05$, vs. model group, $\#\#p < 0.01$, OGD/R + BCL-H group vs. OGD/R + BCL-H + ANA group.

were significantly higher in the model group than those in the control group ($p < 0.01$), while lower Bax, caspase-3, and caspase-9 expressions were observed in the treatment groups than those in the model group ($p < 0.01$). These effects of BCL on Bcl-2 expression were suppressed by treatment with ANA12; in contrast, Bax, caspase-3, and caspase-9 protein levels were increased ($p < 0.01$). From the aforementioned results, we concluded that BCL was effective in preventing OGD-induced apoptosis to protect neurons. BDNF-TrkB signaling was necessary for the neuroprotective actions of BCL on neurons in the OGD/R-treated NA coculture system. The neuroprotective actions of BCL in the NA coculture system were mediated at least in part by BDNF.

The Effects of Baicalin and ANA12 on Inflammation and Free Radicals after Oxygen–Glucose Deprivation/ Reoxygenation

The brain represents almost 20% of the body's oxygen consumption under normal physiological conditions, generating more free radicals than other organs. After the

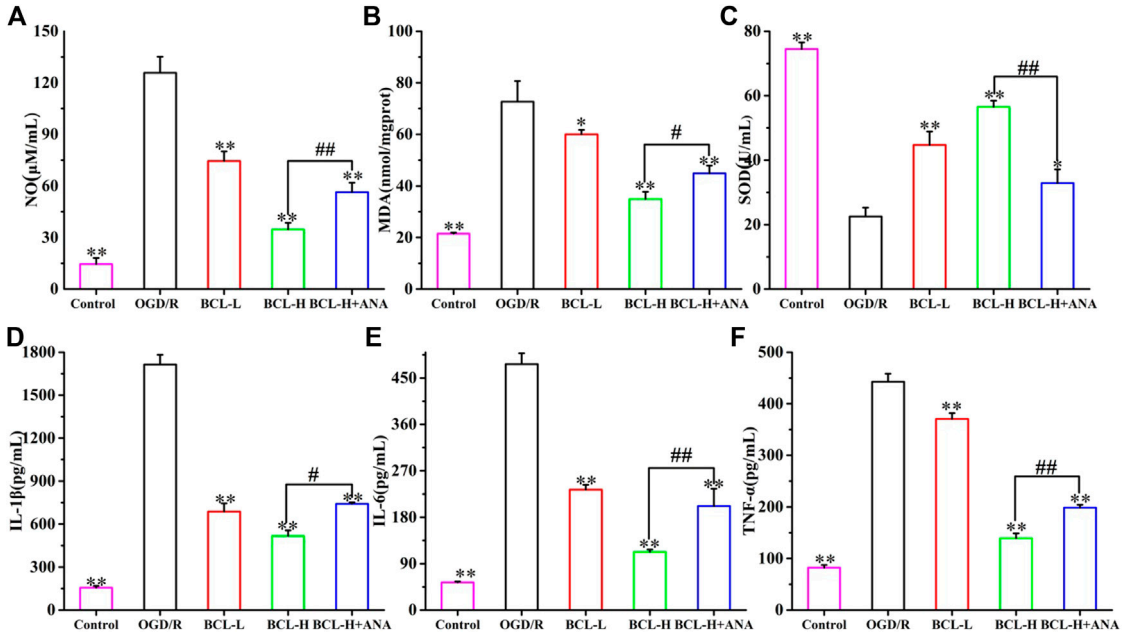

FIGURE 9 | Effect of BCL (34.38 μg/ml, 8.59 μg/ml) on inflammation and oxidative/nitrosative stress in the NA system after OGD/R. **(A)** The effect of BCL on NO in the NA system after OGD/R. **(B)** The effect of BCL on MDA in the NA system after OGD/R. **(C)** The effect of BCL on SOD in the NA system after OGD/R. **(D)** The effect of BCL on the IL-1β level in the NA system after OGD/R. **(E)** The effect of BCL on IL-6 in the NA system after OGD/R. **(F)** The effect of BCL on TNF-α in the NA system after OGD/R. $^{**}p < 0.01$, $^{*}p < 0.05$, vs. OGD/R group; $\#p < 0.05$, $\#\#p < 0.01$, BCL-H group vs. BCL-H+ANA group.

ischemia-reperfusion injury, the brain produces a large number of free radicals, mainly oxidative nitrosative stress, which plays an important role in the pathogenesis mechanism of IS (Sun et al., 2018). However, the characteristics of the brain are more vulnerable to free radical damage. Moreover, inflammation, a secondary injury mechanism following IS, plays an important role in the progression of IS. Inhibition of inflammation and oxidative/nitrosative stress can decrease brain injury and improve neurological outcomes (Yenari et al., 2014). The results of the present study are in line with the above theory. As shown in **Figures 9A–C**, compared with the control group, the expression of NO (**Figure 9A**) and MDA (**Figure 9B**) after OGD/R increased, and SOD (**Figure 9C**) significantly decreased ($p < 0.01$). However, the elevation of NO and MDA was significantly attenuated by BCL treatment. BCL treatment increased the expression level of SOD ($p < 0.01$). Furthermore, we evaluated the effect of BCL on the expression of IL-1β (**Figure 9D**) and IL-6 (**Figure 9E**) and TNF-α (**Figure 9F**). Compared with the control group, OGD/R treatment significantly increased the expression levels of TNF-α, IL-1β, and IL-6 ($p < 0.01$). Compared with that in the OGD/R group, BCL robustly reduced the release of inflammatory cytokines ($p < 0.01$). The results indicate that BCL has a dose-dependent effect against oxidative/nitrosative stress and inflammation. To verify further whether TrkB activation was required for the neuroprotective effect of BCL, we examined the effect of ANA12, an TrkB Receptor antagonists, on inflammation and free radicals induced by OGD/R. In the presence of ANA12, compared with those of the BCL-H group, the effects of BCL on oxidative/nitrosative stress and anti-inflammatory effects of BCL were significantly reduced (NO, SOD, IL-6, and TNF-α: $p < 0.01$; MDA and IL-1β: $p < 0.05$). These experiments demonstrated that BDNF-TrkB signaling was necessary for the neuroprotective actions of BCL in the OGD/R-treated NA coculture system. Our findings here indicated that the neuroprotective actions of BCL in the NA coculture system were mediated at least in part by BDNF.

The Effects of Baicalin and TrkB Receptor Antagonists on the Expression of PI3K and Akt in the NA System after Oxygen–Glucose Deprivation/Reoxygenation

The expression of BDNF and the moderate activity of its associated signaling axes, such as TrkB/PI3K/Akt and TrkB/MAPK/ERK1/2, are required for neuronal survival, neuron morphology, anti-inflammation, antioxidant stress, and antiapoptosis. Therefore, it is interesting to propose that BCL mediated neuroprotection is mediated by modulating BDNF/TrkB and their downstream signaling pathways. BDNF binding to high-affinity TrkB triggers its dimerization and autophosphorylation of intracellular tyrosine residues, leading to downstream PI3K/Akt signaling activation (Kowianski et al., 2018). The PI3K/Akt signaling pathway exerts multiple cellular functions, including antiapoptotic and pro-survival activities, enhancement of dendritic growth and

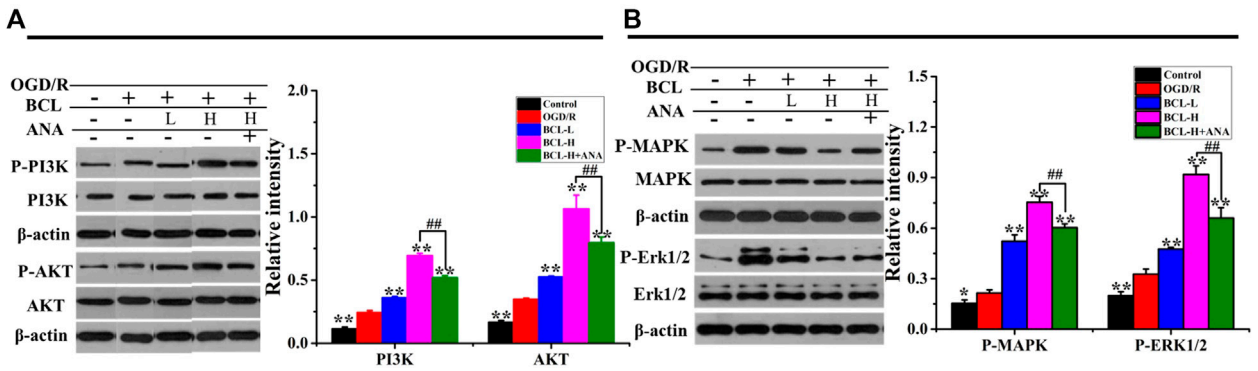

FIGURE 10 | Effects of BCL (34.38 μg/ml and 8.59 μg/ml) and ANA12 on the expression of PI3K, Akt, MAPK, and ERK in NA systems after OGD/R. **(A)** The effect of BCL on the expression of PI3K and Akt in the NA system after OGD/R. **(B)** The effect of BCL on the expression of MAPK and ERK in NA systems after OGD/R. Quantified results were normalized to β-actin expression. $^{**}p < 0.01$, vs. OGD/R group; $\#\#p < 0.01$, BCL-H group vs. BCL-H + ANA group.

branching, and long-term maintenance of synaptic plasticity (Yoshii and Constantine-Paton 2010; Kowianski et al., 2018; Liu et al., 2020). The MAPK/ERK signaling pathway plays a critical role in cell growth and differentiation, protein synthesis–dependent plasticity, neuronal survival, and neuronal differentiation promotion (Autry and Monteggia 2012; Kowianski et al., 2018). As shown in **Figure 10**, we found that the model group had significantly higher expressions of PI3K, Akt, MAPK, and ERK after OGD/R than the control group in the NA system ($p < 0.01$). BCL treatment significantly promoted the expression of PI3K, Akt, MAPK, and ERK ($p < 0.01$). Moreover, statistical analysis of the data indicated that the BCL-H group had significantly higher expressions of PI3K, Akt, MAPK, and ERK in the NA system after OGD/R than the BCL-H + ANA12 group ($p < 0.01$); that was, the effects of BCL were suppressed by pretreatment with ANA12.

DISCUSSION

Previous studies have often focused on the changes and plasticity of neurons in the recovery of neurological function after IS. However, other cells with complex specific signals and cascade reactions that affect neuronal recovery also need to be studied. Interestingly, the pharmacological agents tested to target neurons may also affect other neuronal functions. As a major constituent of the central nervous system, astrocytes constitute 50% of all the cells in the central nervous system and play essential roles in maintaining brain function (Filous and Silver 2016). In particular, astrocytes contribute to neurogenesis and synaptogenesis in normal brain function and axonal remodeling after IS (Liu and Chopp 2016). In light of the many actions of astrocytes on neurons, drugs targeting reactive astrocytes may effectively sustain neuronal function and hence survival after IS. Constructing an *in vitro* neuron and astrocyte coculture system can provide an advantageous platform for studying the interaction between astrocytes and neurons and the therapeutic effects of drugs on neurons through astrocytes. In line with a previous study, we found that astrocytes provided positive protection to neurons under normal and pathological conditions. In the presence of astrocytes, the neuronal phenotype was more neuroprotective effect of BCL the characteristics of brain tissue *in vivo*. After OGD/R, the morphology of neurons in the coculture system was better, and the apoptosis rate was lower. Astrocytes become reactive in response to pathological conditions following IS. Our research was consistent with previous research theories. Compared with the control group, the morphology of astrocytes conformed to the characteristics of reactive astrocytes, which had a polygonal morphology, larger cell bodies, and an increased number of synapses after OGD/R. A previous study showed that reactive astrocytes played an important role in neuroprotection and neurorestoration after IS.

The release of neurotrophic factors is an important reason for the protective effect of reactive astrocytes (Sofroniew 2005; Choudhury and Ding 2016). BDNF is released from astrocytes *via* exocytosis to regulate the function of neighboring neurons (Zhang et al., 2015; Hong et al., 2016; Shih et al., 2017). For the first time, our research focused on the release of BDNF from neurons or astrocytes in a neuron–astrocyte coculture system after OGD/R. The results showed that neurons and astrocytes can mutually promote the release of BDNF in the coculture system. Astrocytes become an important source of BDNF because astrocytes were in an activated state, while damaged neurons reduced the release of BDNF. As shown in **Figure 11**, BDNF released by reactive astrocytes in the coculture system were an important cause of anti-neuronal apoptosis and damage after OGD/R. BCL treatment can maintain the activated state of astrocytes and increase BDNF levels in the NA coculture system. BDNF expression is regulated by CREB. Deregulation of CREB indicates that a deficiency in neurotrophic factor synthesis

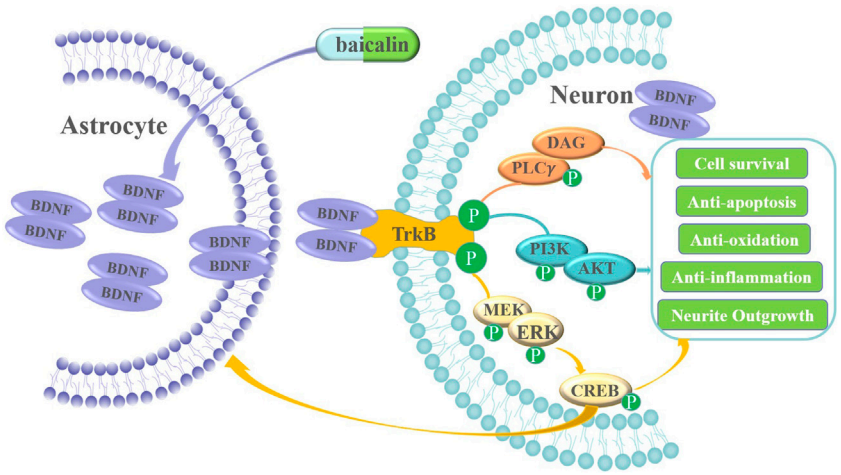

FIGURE 11 | Scheme of the neuroprotective mechanism of BCL after OGD/R.

and signaling underlies IS. BCL treatment can increase the expression of CREB, which further promotes the release of BDNF. BCL-promoted release of endogenous BDNF has important clinical significance. Previous studies focused on developing exogenous small-molecule mimetics of BDNF. However, because of the short serum half-life, poor bioavailability, extremely low BBB penetration, and limited diffusion within CNS tissue, exogenous BDNF has been proven to have certain problems clinically. Therefore, it is reasonable to enhance further the expression of BDNF from neurons and reactive astrocytes by pharmacological treatments.

Additionally, BCL treatment increased downstream activation of its cognate TrkB receptors, leading to the hypothesis that neuroprotection provided by BCL to the NA coculture system damaged by OGD/R is mediated by BDNF. It has been well established that BCL effectively exerts neuroprotective activity in *in vitro* and *in vivo* models, including antioxidant, antiapoptotic, anti-inflammatory, and anti-excitotoxicity effects; protection of the mitochondria; promotion of neuronal protective factor expression; and adult neurogenesis effects (Cao et al., 2011; Zhu et al., 2012; Fafeng et al., 2013; Liang et al., 2017; Kandhasamy et al., 2018). To test this hypothesis, we asked whether downstream activation of TrkB receptors by BDNF was required for neuroprotection by BCL. First, we took a pharmacological approach using an antagonist of high-affinity neurotrophin TrkB receptors, ANA12. The present study found that BCL could attenuate OGD/R-related pathological mechanisms, including free radicals, inflammation, and apoptosis, whose effects were decreased by ANA12. However, the protective effect of baicalin on the coculture system was not completely mediated by BDNF/TrkB, and it can also directly resist oxidative stress, inflammation, and apoptosis. Moreover, activation of three downstream targets of BDNF/TrkB signaling (p-ERK, p-CREB, and p-Akt) was increased in the NA coculture system by BCL treatment. ANA12 also decreased the effects of BCL on the expressions of p-ERK1/2, p-Akt, and p-CREB in the NA coculture system. The PI3K/Akt and MAPK/ERK1/2 cascades are pivotal signaling pathways that promote neuronal survival and plasticity to provide essential protective effects on neuronal activity after IS (Liu et al., 2020). Similarly, the activation of PI3K, Akt, MAPK, and ERK by BCL treatment was not completely blocked, and they can also be activated through other pathways. A large number of previous studies have proven that BCL plays a role in resisting oxidative stress, inflammation, and apoptosis through a large number of pathways, including TLR4/NF-κB, JAK2/STAT3, and PPARγ (Liang et al., 2017). Therefore, BDNF-TrkB/PI3K/AKT and BDNF-TrkB/MAPK/ERK were only part of the protective mechanism.

In summary, the present work identified astrocytes as an important source of BDNF after OGD/R. BCL upregulated the release of BDNF and the expression of proteins related to the BDNF-TrkB pathway in the neuron–astrocyte coculture system and that blockade of the BDNF-TrkB pathway reversed the protective effect of BCL against OGD/R-induced oxidative stress, inflammation, and apoptosis. These results suggest that the BDNF-TrkB pathway may be a newly contributory mechanism to the protective effects of BCL against OGD/R-induced injury paradigms. The present study could provide a potential clinical drug that can protect multiple mechanisms, protect multiple cells, and promote neuronal recovery through astrocytes.

DATA AVAILABILITY STATEMENT

The original contributions presented in the study are included in the article; further inquiries can be directed to the corresponding authors.

ETHICS STATEMENT

The animal study was reviewed and approved by the National Institutes of Health Guide for the Care and Use of Laboratory

Animals and was approved by the Ethics Committee of Experimental Animals of Beijing University of Chinese Medicine (BUCM-3-2016040201-2003).

AUTHOR CONTRIBUTIONS

Study concept and design: CL, JY, WW, FC, and QW; paper writing and language polishing: CL, XM, XW, and FC; experiment implementation: ND and XD. Revising the reviewers' comments: CS. All authors approved the final version of this paper.

FUNDING

This study was supported by the National Natural Science Foundation of China (Grant No. 81430102).

SUPPLEMENTARY MATERIAL

The Supplementary Material for this article can be found online at: https://www.frontiersin.org/articles/10.3389/fphar.2021.599543/full#supplementary-material

REFERENCES

Autry, A. E., and Monteggia, L. M. (2012). Brain-derived neurotrophic factor and neuropsychiatric disorders. *Pharmacol. Rev.* 64 (2), 238–258. doi:10.1124/pr.111.005108

Bhalerao, A., Sivandzade, F., Archie, S. R., Chowdhury, E. A., Noorani, B., and Cucullo, L. (2020). *In vitro* modeling of the neurovascular unit: advances in the field. *FBCNS* 17 (1), 22. doi:10.1186/s12987-020-00183-7

Bo, J., Fang, W., Si, Y., Peng, F., Deng, Z. F., Xiao, J. L., et al. (2015). SKF83959 produces antidepressant effects in a chronic social defeat stress model of depression through BDNF-TrkB pathway. *Int. J. Neuropsychopharmacol.* 6, pyu096. doi:10.1093/ijnp/pyu096

Cao, Y., Mao, X., Sun, C., Zheng, P., Gao, J., Wang, X., et al. (2011). Baicalin attenuates global cerebral ischemia/reperfusion injury in gerbils via anti-oxidative and anti-apoptotic pathways. *Brain Res. Bull.* 85 (6), 396–402. doi:10.1016/j.brainresbull.2011.05.002

Choudhury, G. R., and Ding, S. (2016). Reactive astrocytes and therapeutic potential in focal ischemic stroke. *Neurobiol. Dis.* 85, 234–244. doi:10.1016/j.nbd.2015.05.003

Dabrowska, S., Andrzejewska, A., Lukomska, B., and Janowski, M. (2019). Neuroinflammation as a target for treatment of stroke using mesenchymal stem cells and extracellular vesicles. *J. Neuroinflammation* 16 (1), 178. doi:10.1186/s12974-019-1571-8

Dalkara, T., Alarcon-Martinez, L., and Yemisci, M. (2016). "Role of pericytes in neurovascular unit and stroke,"in *Non-neuronal mechanisms of brain damage and repair after stroke*. (Berlin, Germany: Springer), 25–(43.)

Fafeng, C., Yi, L., Xianggen, Z., Wenting, S., Xueqian, W., Xiaoguang, S., et al. (2013). Baicalin's therapeutic time window of neuroprotection during transient focal cerebral ischemia and its antioxidative effects in vitro and in vivo. *Evid. Based Complement. Altern. Med.* 2013 (20), 120261. doi:10.1155/2013/120261

Filous, A. R., and Silver, J. (2016). Targeting astrocytes in CNS injury and disease: a translational research approach. *Prog. Neurobiol.* 144, 173–187. doi:10.1016/j.pneurobio.2016.03.009

Heymans, M., Figueiredo, R., Dehouck, L., Francisco, D., Sano, Y., Shimizu, F., et al. (2020). Contribution of brain pericytes in blood-brain barrier formation and maintenance: a transcriptomic study of cocultured human endothelial cells derived from hematopoietic stem cells. *FBCNS* 17 (1), 48. doi:10.1186/s12987-020-00208-1

Hong, Y., Zhao, T., Li, X. J., and Li, S. (2016). Mutant huntingtin impairs BDNF release from astrocytes by disrupting conversion of rab3a-GTP into rab3a-GDP. *J. Neurosci.* 36 (34), 8790. doi:10.1523/jneurosci.0168-16.2016

Kandhasamy, S., Ponnuvel, D., Minju, K., Se, P., and Songmun, K. (2018). Neuroprotective and cognitive enhancement potentials of baicalin: a review. *Brain Sci.* 8 (6), 104. doi:10.3390/brainsci8060104

Katan, M., and Luft, A. (2018). Global burden of stroke. *Semin. Neurol.* 38 (2), 208–211. doi:10.1055/s-0038-1649503

Kowianski, P., Lietzau, G., Czuba, E., Waskow, M., Steliga, A., and Morys, J. (2018). BDNF: a key factor with multipotent impact on brain signaling and synaptic plasticity. *Cell Mol. Neurobiol.* 38 (3), 579–593. doi:10.1007/s10571-017-0510-4

Li, C. X., Wang, X. Q., Cheng, F. F., Yan, X., and Wang, Q. G. (2019a). Hyodeoxycholic acid protects the neurovascular unit against oxygen-glucose deprivation and reoxygenation-induced injury *in vitro*. *Neural Regen. Res.* 14 (11), 1941. doi:10.4103/1673-5374.259617

Li, C., Wang, X., Cheng, F., Du, X., Yan, J., Zhai, C., et al. (2019b). Geniposide protects against hypoxia/reperfusion-induced blood-brain barrier impairment by increasing tight junction protein expression and decreasing inflammation, oxidative stress, and apoptosis in an *in vitro* system. *Eur. J. Pharmacol.* 854, 224–231. doi:10.1016/j.ejphar.2019.04.021

Liang, W., Huang, X., and Chen, W. (2017). The effects of baicalin and baicalein on cerebral ischemia: a review. *Aging Dis.* 8 (6), 850–867. doi:10.14336/ad.2017.0829

Liu, W., Wang, X., O'Connor, M., Wang, G., and Han, F. (2020). Brain-derived neurotrophic factor and its potential therapeutic role in stroke comorbidities. *Neural Plast.* 2020, 1969482. doi:10.1155/2020/1969482

Liu, Z., and Chopp, M. (2016). Astrocytes, therapeutic targets for neuroprotection and neurorestoration in ischemic stroke. *Prog. Neurobiol.* 144, 103–120. doi:10.1016/j.pneurobio.2015.09.008

McDermott, M., Skolarus, L. E., and Burke, J. F. (2019). A systematic review and meta-analysis of interventions to increase stroke thrombolysis. *BMC Neurol.* 19 (1), 86. doi:10.1186/s12883-019-1298-2

Nobukazu, M., Takakuni, M., Akihiro, S., Liang, A. C., Mitsuyo, M., Naohiro, E., et al. (2015). Astrocytes promote oligodendrogenesis after white matter damage via brain-derived neurotrophic factor. *J. Neurosci. Official J. Soc. Neurosci.* 35 (41), 14002–14008. doi:10.1523/JNEUROSCI.1592-15.2015

Quesseveur, G., David, D. J., Gaillard, M. C., Pla, P., Wu, M. V., Nguyen, H. T., et al. (2013). BDNF overexpression in mouse hippocampal astrocytes promotes local neurogenesis and elicits anxiolytic-like activities. *Transl. Psychiatry* 3 (4), e253. doi:10.1038/tp.2013.30

Shi, X., Fu, Y., Zhang, S. S., Hao, D., and Jin, C. (2017). Baicalin attenuates subarachnoid hemorrhagic brain injury by modulating blood-brain barrier disruption, inflammation, and oxidative damage in mice. *Oxidative Med. Cell Longevity* 2017, 1–9. doi:10.1155/2017/1401790

Shih, H. C., Kuan, Y. H., and Shyu, B. C. (2017). Targeting BDNF in the medial thalamus for the treatment of central poststroke pain in a rodent model. *Pain* 158 (7), 1302–1313. doi:10.1097/j.pain.0000000000000915

Sofroniew, M. V. (2005). Reactive astrocytes in neural repair and protection. *Neuroscientist* 11 (5), 400. doi:10.1177/1073858405278321

Song, X., Gong, Z., Liu, K., Kou, J., and Liu, K. (2020). Baicalin combats glutamate excitotoxicity via protecting glutamine synthetase from ROS-induced 20S proteasomal degradation. *Redox Biol.* 34, 101559. doi:10.1016/j.redox.2020.101559

Sun, L., Zhang, Y., Liu, E., Ma, Q., Anatol, M., Han, H., et al. (2019). The roles of astrocyte in the brain pathologies following ischemic stroke. *Brain Inj.* 33 (6), 712–716. doi:10.1080/02699052.2018.1531311

Sun, M. S., Jin, H., Sun, X., Huang, S., Zhang, F. L., Guo, Z. N., et al. (2018). Free radical damage in ischemia-reperfusion injury: an obstacle in acute ischemic stroke after revascularization therapy. *Oxidative Med. Cell Longevity* 2018 (2), 1–17. doi:10.1155/2018/3804979

Venkat, P., Shen, Y., Chopp, M., and Chen, J. (2018). Cell-based and pharmacological neurorestorative therapies for ischemic stroke. *Neuropharmacology* 134, 310–322. doi:10.1016/j.neuropharm.2017.08.036

Wenpu, Z., Huayu, W., Kun, Z., Peizhen, L., and Fuben, X. (2017). Baicalin promotes the viability of Schwann cells *in vitro* by regulating neurotrophic factors. *Exp. Ther. Med.* 14 (1), 507–514. doi:10.3892/etm.2017.4524

Xue, Q., Liu, Y., Qi, H., Ma, Q., Xu, L., Chen, W., et al. (2013). A novel brain neurovascular unit model with neurons, astrocytes and microvascular endothelial cells of rat. *Int. J. Biol. Sci.* 9 (2), 174–189. doi:10.7150/ijbs.5115

Yamamizu, K., Iwasaki, M., Takakubo, H., Sakamoto, T., Ikuno, T., Miyoshi, M., et al. (2017). InVitro modeling of blood-brain barrier with human iPSC-derived endothelial cells, pericytes, neurons, and astrocytes via notch signaling. *Stem Cel Rep.* 8 (3), 634–647. doi:10.1016/j.stemcr.2017.01.023

Yenari, M. A., Kawabori, M., and Kim, J. Y. (2014). Innate inflammatory responses in stroke: mechanisms and potential therapeutic targets. *Curr. Med. Chem.* 21 (18), 2076–2097. doi:10.2174/09298673216613228205146

Yoshii, A., and Constantine-Paton, M. (2010). Postsynaptic BDNF-TrkB signaling in synapse maturation, plasticity, and disease. *Dev. Neurobiol.* 70 (5), 304–322. doi:10.1002/dneu.20765

Zhang, M., Ergin, V., Lin, L., Stork, C., Chen, L., and Zheng, S. (2019). Axonogenesis is coordinated by neuron-specific alternative splicing programming and splicing regulator PTBP2. *Neuron* 101 (4), 690–706. doi:10.1016/j.neuron.2019.01.022

Zhang, Y., Lan, R., Wang, J., Li, X. Y., Zhu, D. N., Ma, Y. Z., et al. (2015). Acupuncture reduced apoptosis and up-regulated BDNF and GDNF expression in hippocampus following hypoxia-ischemia in neonatal rats. *J. Ethnopharmacol.* 172, 124–132. doi:10.1016/j.jep.2015.06.032

Zhu, H., Wang, Z., Xing, Y., Gao, Y., Ma, T., Lou, L., et al. (2012). Baicalin reduces the permeability of the blood–brain barrier during hypoxia *in vitro* by increasing the expression of tight junction proteins in brain microvascular endothelial cells. *J. Ethnopharmacol.* 141 (2), 714–720. doi:10.1016/j.jep.2011.08.063

Zhu, Y. B., Gao, W., Zhang, Y., Jia, F., Zhang, H. L., Liu, Y. Z., et al. (2016). Astrocyte-derived phosphatidic acid promotes dendritic branching. *entific Rep.* 6, 21096. doi:10.1038/srep21096

Conflict of Interest: The authors declare that the research was conducted in the absence of any commercial or financial relationships that could be construed as a potential conflict of interest.

Copyright © 2021 Li, Sui, Wang, Yan, Deng, Du, Cheng, Ma, Wang and Wang. This is an open-access article distributed under the terms of the Creative Commons Attribution License (CC BY). The use, distribution or reproduction in other forums is permitted, provided the original author(s) and the copyright owner(s) are credited and that the original publication in this journal is cited, in accordance with accepted academic practice. No use, distribution or reproduction is permitted which does not comply with these terms.

frontiers in Pharmacology

ORIGINAL RESEARCH
published: 15 July 2021
doi: 10.3389/fphar.2021.630003

A Computational Exploration of the Molecular Network Associated to Neuroinflammation in Alzheimer's Disease

Fatima El Idrissi[1,2], *Bernard Gressier*[1,2], *David Devos*[1,3] *and Karim Belarbi*[1,2]*

[1]*Univ. Lille, Inserm, CHU-Lille, Lille Neuroscience & Cognition, Lille, France,* [2]*Département de Pharmacologie de la Faculté de Pharmacie, Univ. Lille, Lille, France,* [3]*Département de Pharmacologie Médicale, I-SITE ULNE, LiCEND, Lille, France*

Neuroinflammation, as defined by the presence of classically activated microglia, is thought to play a key role in numerous neurodegenerative disorders such as Alzheimer's disease. While modulating neuroinflammation could prove beneficial against neurodegeneration, identifying its most relevant biological processes and pharmacological targets remains highly challenging. In the present study, we combined text-mining, functional enrichment and protein-level functional interaction analyses to 1) identify the proteins significantly associated to neuroinflammation in Alzheimer's disease over the scientific literature, 2) distinguish the key proteins most likely to control the neuroinflammatory processes significantly associated to Alzheimer's disease, 3) identify their regulatory microRNAs among those dysregulated in Alzheimer's disease and 4) assess their pharmacological targetability. 94 proteins were found to be significantly associated to neuroinflammation in Alzheimer's disease over the scientific literature and IL4, IL10 and IL13 signaling as well as TLR-mediated MyD88- and TRAF6-dependent responses were their most significantly enriched biological processes. IL10, TLR4, IL6, AKT1, CRP, IL4, CXCL8, TNF-alpha, ITGAM, CCL2 and NOS3 were identified as the most potent regulators of the functional interaction network formed by these immune processes. These key proteins were indexed to be regulated by 63 microRNAs dysregulated in Alzheimer's disease, 13 long non-coding RNAs and targetable by 55 small molecules and 8 protein-based therapeutics. In conclusion, our study identifies eleven key proteins with the highest ability to control neuroinflammatory processes significantly associated to Alzheimer's disease, as well as pharmacological compounds with single or pleiotropic actions acting on them. As such, it may facilitate the prioritization of diagnostic and target-engagement biomarkers as well as the development of effective therapeutic strategies against neuroinflammation in Alzheimer's disease.

Keywords: Alzheimer disease, cytokines, interleukins, microglia, neuroinflammation, toll-like receptors, tumor necrosis factor-alpha, neurodegenerative diseases

OPEN ACCESS

Edited by:
Claudia Bregonzio, CCT CONICET Córdoba, Argentina

Reviewed by:
Rodrigo Quiroga, National University of Cordoba, Argentina
Sudhanshu P. Raikwar, Barrow Neurological Institute (BNI), United States

***Correspondence:**
Karim Belarbi
karim.belarbi@inserm.fr

Specialty section:
This article was submitted to Neuropharmacology, a section of the journal Frontiers in Pharmacology

Received: *16 November 2020*
Accepted: *29 June 2021*
Published: *15 July 2021*

Citation:
El Idrissi F, Gressier B, Devos D and Belarbi K (2021) A Computational Exploration of the Molecular Network Associated to Neuroinflammation in Alzheimer's Disease. Front. Pharmacol. 12:630003. doi: 10.3389/fphar.2021.630003

INTRODUCTION

Despite extensive research there is still no cure for Alzheimer's disease, the commonest cause of dementia. Alzheimer's disease is characterized by neuronal loss in specific brain regions associated with the formation of amyloid-beta senile plaques and tau-immunoreactive neurofibrillary tangles (Polanco et al., 2018). Another hallmark of the disease is the presence of neuroinflammation as defined by the presence of classically activated microglial cells (Fan et al., 2017; Dani et al., 2018). Microglial cells are the resident immune cells of the central nervous system (Ransohoff and Cardona, 2010). While their activation is needed to defend the brain from injury, it has become clear that a sustained and uncontrolled inflammation could contribute to neurodegeneration, for instance leading to vascular dysfunction, mitochondrial dysfunction and oxidative stress (Sochocka et al., 2013; Orsucci et al., 2013).

Several lines of evidence support that better understanding the neuroinflammatory process in Alzheimer's disease could lead to the development of new diagnostic and therapeutic tools. Positron emission tomography showed that microglial activation is observed from the earliest stages of Alzheimer's disease and correlates both with amyloid deposition and tau aggregation (Dani et al., 2018). Moreover, exciting data demonstrated that the immune challenges could trigger and exacerbate tau and amyloid pathologies (Bhaskar et al., 2010; Krstic et al., 2012), possibly contributing to a pathological vicious circle that could favor regulated neuronal death. Genetic studies including genome-wide studies have also associated inflammation-related genes to the etiology of Alzheimer's disease (i.e. ABCA7, CLU, CR1, HLA-DRB1, HLA-DRB5, PICALM, and TREM2) (Lambert et al., 2009; Jun et al., 2010; Guerreiro et al., 2013; Lambert et al., 2013; Jansen et al., 2019), further supporting the concept of neuroinflammation as a pathogenic factor in Alzheimer's disease. To date, a major challenge is to identify the key processes and proteins linked to neuroinflammation in Alzheimer's disease. Available information reveals a complex picture with the implication of central and peripheral cell types and of a plethora of proteins including pro-inflammatory cytokines, anti-inflammatory cytokines, chemoattractant molecules, peripheral immune mediators as well as their receptors and downstream signaling targets (Itagaki et al., 1988; Togo et al., 2002; Monsonego et al., 2003). Mining useful information in these data for the development of diagnostic and therapeutic neuroprotective strategies remains highly challenging.

Integrated bioinformatics can help to explore complex biological pathways, by analyzing large amount of data and by performing analyses over many distinct datasets. In the present study, we used integrated bioinformatics to perform a systematic review of the proteins associated to neuroinflammation in Alzheimer's disease over the scientific literature and then to identify the most represented biological processes and the key candidate proteins to modulate them. We combined text-mining, Gene Ontology and Reactome functional enrichment analysis, protein-protein functional interaction analysis, non-coding RNA-target interaction analysis and drug–protein interaction analysis and identified eleven proteins with the highest ability to modulate neuroinflammatory processes in Alzheimer's disease. As such, our study provides data that could help to further explore the time-dependent role of the immune response in Alzheimer's disease and to prioritize the development of neuroinflammation-centered diagnostic or therapeutic tools against Alzheimer's disease.

MATERIALS AND METHODS

Protein Collection (Text-Mining)

A systematic review of the proteins relating to Alzheimer's disease neuroinflammation was collected using the pubmed2ensembl resource that has been developed as an extension to the BioMart system for mining the biological literature for genes (http://pubmed2ensembl.ls.manchester.ac.uk/) (Baran et al., 2011). The string 'neuroinflammation alzheimer' was used to retrieve the Ensembl Gene ID related both to neuroinflammation and Alzheimer's disease in the Homo sapiens (human) genome assembly GRCh37 from Genome Reference Consortium. We then used UniProtKB Retrieve/ID mapper (https://www.uniprot.org/) to retrieve the UniProtKB protein identifiers associated to these Ensembl Gene ID (UniProt, 2019). All the protein identifiers were imported into Cytoscape 3.7.2 for subsequent analysis.

Gene Set Enrichment

Gene Ontology (GO) enrichment of the collected proteins was first performed using the ClueGo + CluePedia Cytoscape plug-in, with annotation from GO Cellular Component, GO Molecular Function and GO Biological Process categories (Bindea et al., 2009). A p-value <0.05 was considered as the cutoff criterion. The most enriched annotations were then visualized using the ggplot2 package in R language (www.r-project.org). Functional enrichment analysis of the proteins was subsequently performed and visualized using the Reactome Pathway database (https://reactome.org) (Fabregat et al., 2017; Jassal et al., 2020). Proteins from the 10 most significantly enriched biological processes identified with Reactome were selected for subsequent analysis.

Protein-Protein Functional Interaction

The STRING protein query database (http://string-db.org) was used to construct a protein-protein functional interaction network in Cytoscape (Szklarczyk et al., 2019). The minimum required interaction score was set to 0.7 to retain only high-confidence functional interactions. We then used the CentiScaPe Cytoscape plug-in to calculate the node degree and betweenness centrality of each protein. The nodes that had a degree centrality and a betweenness centrality greater than or equal to the mean were identified as key proteins (e.g. more likely to modulate neuroinflammation) and retained for subsequent microRNA-target and drug-protein interaction analyses.

Integration of Regulatory MicroRNAs and Long Non-Coding RNAs (lncRNAs) in the Key Protein Network

The microRNA-target interactions were identified using the miRTarBase Homo sapiens 8.0 database that curates experimentally validated microRNA-target interactions and includes 502,652 microRNA target interactions (Huang et al., 2020). The lncRNA-target interactions were obtained from the LncRNA2Target 2.0 database, by retaining only interactions

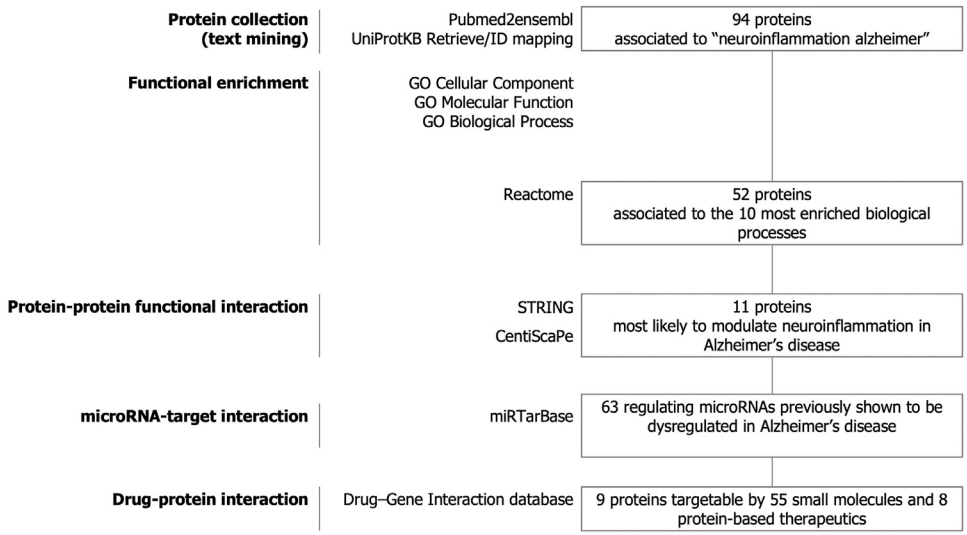

FIGURE 1 | Study design. Text-mining was used to support large-scale screening of the scientific literature to collect 94 proteins related to neuroinflammation in Alzheimer's disease. The entire dataset was analyzed for functional enrichment by using Gene Ontology (GO) cellular localization, molecular functions, biological pathways and by using the Reactome Pathway database and 52 proteins were associated to the 10 most significantly enriched pathways. Protein-protein functional interaction using STRING and CentisScaPe allowed us to identify 11 key proteins most likely to modulate neuroinflammation in Alzheimer's disease. Finally, non-coding RNA-target interaction and drug-gene interaction analysis showed that the key proteins were indexed to be targetable by a total of 63 microRNAs dysregulated in Alzheimer's disease and by 55 small molecules and 8 protein-based therapeutics.

inferred from the low-throughput experiments such as immunoprecipitation assays, RNA pull down assays, luciferase reporter assays, RT-qPCR or western blot (Cheng et al., 2019). Regulating microRNAs that are significantly dysregulated in the blood of Alzheimer's disease patients were selected based on the data published by Leidinger and coworkers (Additional file 1 of their electronic Supplementary Material; (Leidinger et al., 2013). The microRNA-target and lncRNA-target interactions and the microRNAs relative abundance in Alzheimer's disease (log2(fold change); (Leidinger et al., 2013) were mapped using the CyTargetLinker v4.1.0 Cytoscape application (Kutmon et al., 2018).

Drug-Gene Interaction Analysis

The Drug–Gene Interaction database 3.0 (DGIdb v3.0; http://www.dgidb.org/) was used to search for existing associations between drugs (e.g. small molecule compounds or immunotherapies) and essential proteins from our dataset (Cotto et al., 2018). The results of the search were visualized using Cytoscape so that information on protein targetability, drug-protein interaction, drug nature and drug FDA-approval could be easily apprehended.

RESULTS

Identification of Proteins Associated to Alzheimer's Neuroinflammation

The strategy of our study to identify key candidate proteins to modulate neuroinflammation in Alzheimer's disease is depicted in **Figure 1**. Text-mining using the pubmed2ensembl resource that links over 2,000,000 articles to nearly 150,000 genes (Baran et al., 2011) allowed us to systematically collect a list of 94 unique proteins related to neuroinflammation in Alzheimer's disease. The list of the 94 proteins with corresponding Gene symbols, Ensembl Gene and UniProtKB identifiers is provided in **Supplementary Table 1**.

Gene Ontology (GO) functional enrichment analyses were performed using ClueGo + CluePedia plug-in to explore the cellular localization, molecular functions and biological pathways associated to these proteins. All the collected genes had functional annotations in the selected ontologies. The Cellular Component annotations showed an important enrichment (e.g. over-representation) of the proteins located in the extracellular region, at the cell surface or periphery or at the synapse. The gene ontology enrichment analysis of Biological process annotations showed that the most enriched terms were *inflammatory response*, *positive regulation of cytokine production* and *response to lipopolysaccharide*. Finally, Molecular function annotations revealed an enrichment for proteins with *amyloid-beta or peptide binding* activities or *cytokine receptor binding activities*. Other enriched terms were related to arachidonic acid and fatty acid binding, to NADPH oxidoreductase activity or to ionotropic glutamate receptor activity. The top eight enriched terms of the Cellular Component, Biological Process and Molecular Function are shown in **Figure 2**. The proteins of our dataset that are annotated for the top eight enriched Molecular Function annotations are listed in **Figure 3**.

Together, our results show that the proteins associated to Alzheimer's disease neuroinflammation are primarily connected to amyloid beta as well as oxidative stress and lipid metabolism that are critically involved in the neuropathogenesis of Alzheimer's disease.

Selection of the Most Relevant Biological Processes

To identify the most relevant biological processes involved in neuroinflammation in Alzheimer's disease, we performed a

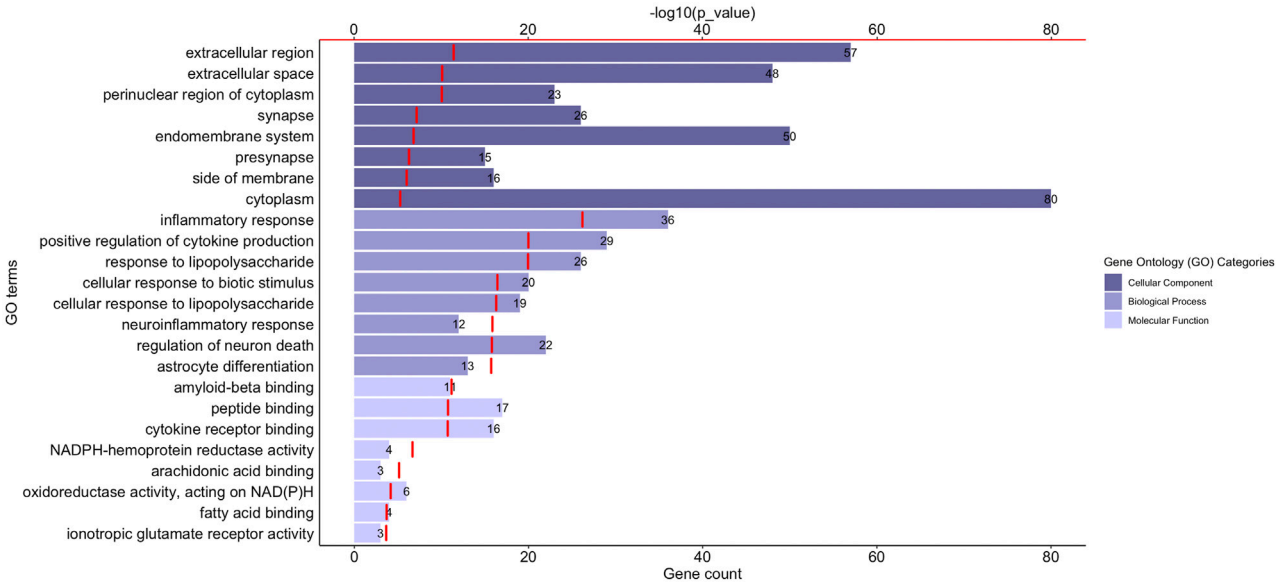

FIGURE 2 | Functional enrichment analysis of the proteins associated to neuroinflammation in Alzheimer's disease. The graph shows the top eight over-represented Gene Ontology (GO) cellular localization, GO molecular functions and GO biological pathways annotations (*Y*-axis), the number of proteins of our dataset included in each term (length of the histogram bars and number displayed next to each histogram bar, lower *X*-axis) and the –log10(*p*_value) levels (red segments, upper *X*-axis). *p*-value ≤ 0.05.

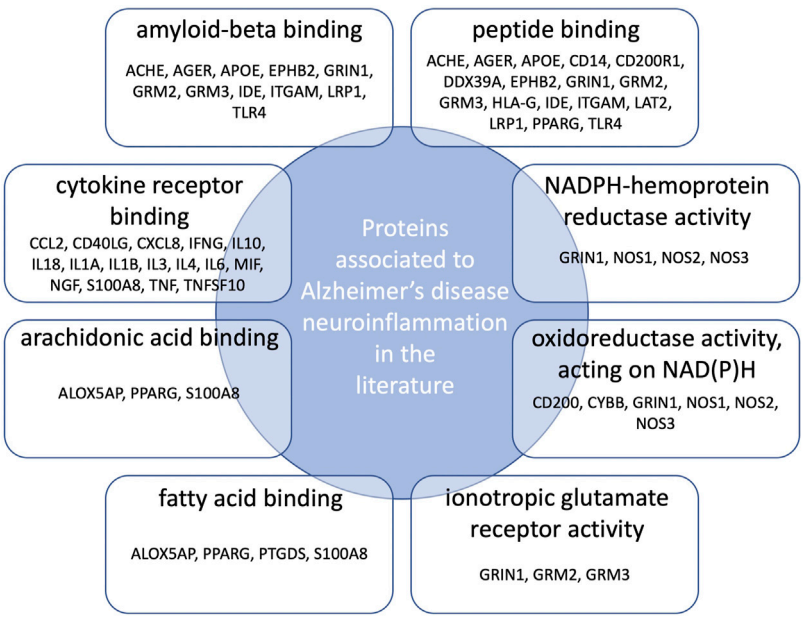

FIGURE 3 | Connections between proteins associated to neuroinflammation in Alzheimer's disease and the top eight over-represented molecular functions annotations. Protein names are those belonging both to our dataset and the enriched GO molecular functions annotations.

functional enrichment of the collected proteins by using the Reactome Pathway database. The 10 most relevant pathways sorted by *p*-value were *Interleukin-4 and Interleukin-13 signaling* ($p = 1.11 \times 10^{-16}$), *Signaling by Interleukins* ($p = 1.11 \times 10^{-16}$), *Interleukin-10 signaling* ($p = 5.77 \times 10^{-15}$), *Immune System* ($p = 9.30 \times 10^{-14}$), *Cytokine Signaling in Immune system* ($p = 5.70 \times 10^{-13}$), *Innate Immune System* ($p = 6.60 \times 10^{-8}$), *Toll-like Receptor Cascades* ($p = 8.11 \times 10^{-7}$), *TRAF6 mediated induction of NFkB and MAP kinases upon TLR7/8 or 9 activation* ($p = 1.00 \times 10^{-6}$), *MyD88 dependent cascade initiated*

TABLE 1 | Function enrichment results of proteins associated to neuroinflammation in Alzheimer's disease using the Reactome Pathway database. Count: enriched gene number in the category.

Term	Count	*p*-value
Interleukin-4 and Interleukin-13 signaling	17	1.11×10^{-16}
Signaling by interleukins	29	1.11×10^{-16}
Interleukin-10 signaling	12	5.77×10^{-15}
Immune system	53	9.30×10^{-14}
Cytokine signaling in immune system	33	5.70×10^{-13}
Innate immune system	29	6.60×10^{-8}
Toll-like receptor cascades	10	8.11×10^{-7}
TRAF6 mediated induction of NFkB and MAP kinases upon TLR7/8 or 9 activation	8	1.00×10^{-6}
MyD88 dependent cascade initiated on endosome	8	1.085×10^{-6}
Toll like receptor 7/8 (TLR7/8) cascade	8	1.085×10^{-6}

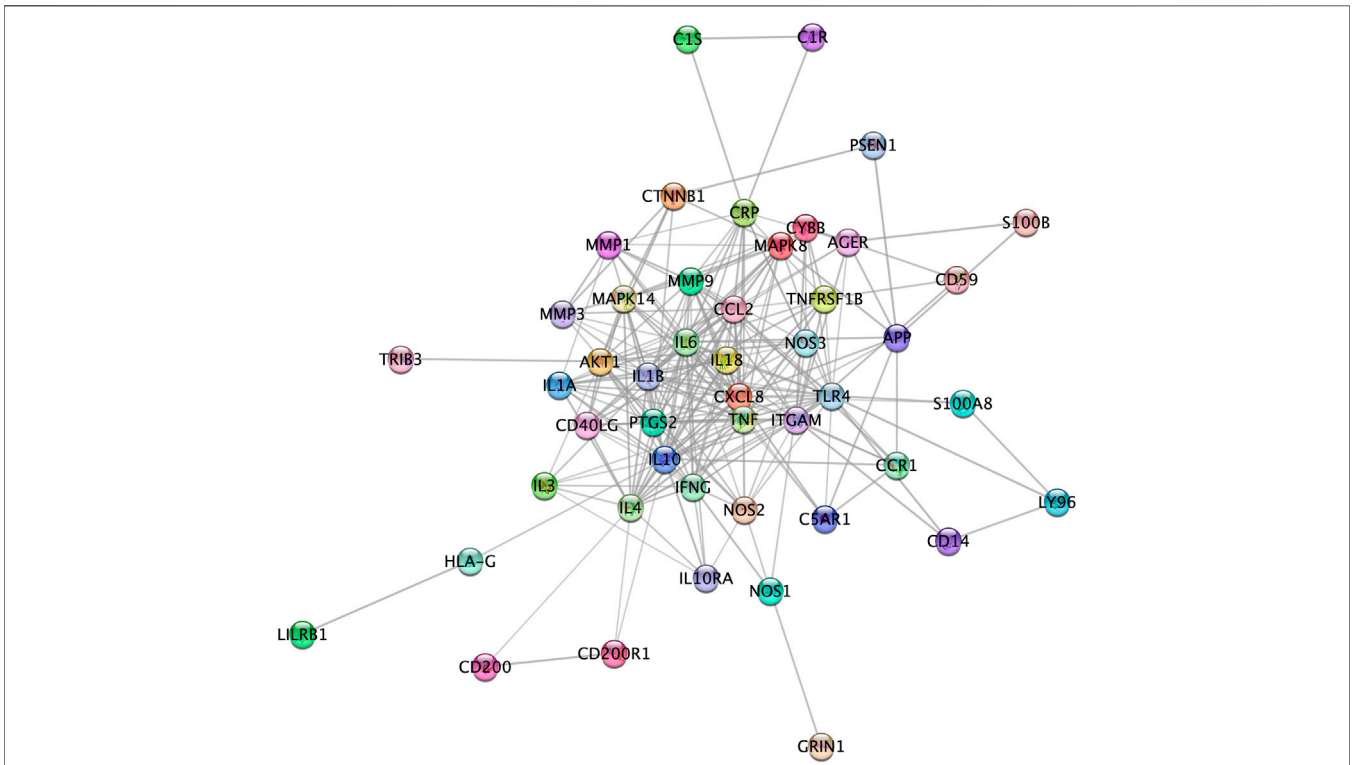

FIGURE 4 | High confidence protein-protein functional interaction network of proteins associated to the most relevant biological processes in neuroinflammation in Alzheimer's disease. Among the 52 proteins associated to the biological processes, 5 (CD4, CHGA, GIG25, LAT2 and MIF) did not show high confidence protein-protein functional interaction in the network and therefore are not represented here.

on endosome ($p = 1.085 \times 10^{-6}$) and *Toll Like Receptor 7/8 (TLR7/8) Cascade* ($p = 1.085 \times 10^{-6}$) (**Table 1**). 52 proteins from the 10 aforementioned most enriched pathways were retained for protein-protein functional interaction analysis.

Identification of High-Confidence Protein Functional Interactions

Figure 4 represents the protein-protein functional interaction network of the aforesaid proteins. In this representation, nodes represent proteins and edges represent functional interactions. There were 47 interconnected nodes (e.g. proteins) and 244 relationship pairs (e.g. functional interactions). Degree average value was 9.38 and betweenness average value was 47.69. We selected nodes with both higher than average degree (e.g. the measure of the total number of edges connected to the protein) and betweenness (e.g. an indicator of how important the protein is to the shortest paths through the network) as key proteins most likely to have the ability to modulate the aforementioned biological processes and thus neuroinflammation in Alzheimer's disease. The 11 proteins that met this selection criterion sorted by high to low betweenness value were:

TABLE 2 | Proteins with highest than average betweenness and degree in the protein-protein functional interaction network.

Protein name	UniProtKB ID	Betweenness	Degree
IL10	P22301	300,549477	24
TLR4	O00206	253,174429	24
IL6	P05231	208,838661	29
AKT1	P31749	204,665414	17
CRP	P02741	190,958865	15
IL4	P05112	127,805378	18
CXCL8	P10145	118,536469	22
TNF	P01375	116,879025	25
ITGAM	P11215	94,1162934	17
CCL2	P13500	70,1571213	22
NOS3	P29474	62,2581681	11

interleukin (IL)10, Toll-like receptor (TLR)4, IL6, AKT1, C-reactive protein (CRP), IL4, C-X-C motif chemokine ligand (CXCL)8, Tumor necrosis factor (TNF) alpha, integrin alpha M (ITGAM), C-C motif chemokine ligand (CCL)2 and nitric oxide synthase (NOS)3 (**Table 2**). These proteins should be considered as the most potent modulators of neuroinflammation in Alzheimer's disease and were next analyzed for microRNA- and drug-protein interaction.

Integration of Regulatory Non-Coding RNAs Into the Key Protein Network

Non-coding RNAs including microRNAs and lncRNAs play crucial roles in regulating gene expression and have emerged as key regulators of immune cell functions in innate and adaptive immunity. We first aimed to identify microRNAs both 1) regulating the key protein network as indexed in the experimentally validated gene–microRNA interaction database miRTarBase and 2) dysregulated in Alzheimer's disease blood samples, as reported by Leidiger and coworkers (Leidinger et al., 2013). This led to the identification of 63 dysregulated mature microRNAs including 22 with higher and 41 with lower expression levels in Alzheimer's disease (**Figure 5**). The corresponding list of mature microRNAs with protein targets is provided in **Supplementary Table 2**. We also integrated 13 lncRNAs known to regulate the key protein as indexed in the LncRNA2Target database (**Figure 5**). The corresponding list of lncRNAs with protein targets and bibliographic references is provided in **Supplementary Table 3**.

Drug–Protein Network Construction and Identification of Targetable Proteins

To assess to what extent the 11 proteins could be pharmacologically targeted, drug-proteins relationships were predicted using the Drug–Gene Interaction database 3.0. Among the 11 proteins, 9 were indexed to be targeted by a total of 63 drugs. The NOS3 protein had the most interactions with drugs ($n = 29$), followed by TNF alpha ($n = 19$), AKT1 ($n = 5$) and TLR4 ($n = 5$) and IL6 ($n = 4$). There was a total of 67 drug–protein relationships in the network. Drugs comprised 8 protein-based therapies of which 6 had a FDA-approval as well as 55 small compounds of which 10 had a FDA-approval. Drug-protein interactions can be visualized in **Figure 6**.

DISCUSSION

This study used text-mining and data-based bioinformatics to explore the protein network underlying neuroinflammatory processes in Alzheimer's disease. Text-mining has been recommended for large-scale screening (O'Mara-Eves et al., 2015) and can be used to identify key pathways and candidate genes for drug-discovery and Human health (Singhal et al., 2016; Lever et al., 2019; Pan et al., 2019). In our study, it allowed to collect 94 proteins significantly associated to neuroinflammation in Alzheimer's disease over the scientific literature (**Supplementary Table 1**). It is important to note that text-mining has biases due to the imbalance in research attention where some genes are highly investigated while others are ignored (Wang et al., 2015; Oprea et al., 2018). Therefore, the obtained list of proteins is not meant to be exhaustive and may particularly miss proteins still sparsely mentioned in the literature. As such our study may be considered as complementary to other studies such as genome-wide association studies for the further development of diagnostic and target-engagement biomarkers for drug discovery.

Gene Ontology enrichment analysis was used to get first insights into the profile of the 94 collected proteins (Bindea et al., 2009). Cellular localization annotations showed an overrepresentation of cellular compartments essential for communication (e.g. *extracellular space*, *synapse*, *presynaptic compartment* and *side of membranes*) consistent with the fact that an altered cerebral microenvironment and a dysregulated cell-to-cell crosstalk are critically involved in neuroinflammation (Schwartz and Deczkowska, 2016; Fabiani and Antollini, 2019). Most overrepresented molecular function annotations were *amyloid beta binding activity*—an activity presented by proteins such as ITGAM (also named CD11b) (Goodwin et al., 1997) and TLR4 (Liu et al., 2020)—as well as *cytokine receptor binding activity*, further linking the amyloid peptide to the innate immune response in Alzheimer's disease. Molecular function annotations also defined NADPH oxidation, *fatty acid* and *arachidonic acid binding* as well as *glutamate signaling* as significant functions, therefore connecting neuroinflammation to NADPH oxidases and arachidonic acid metabolism critically involved in the neuropathogenesis of Alzheimer's disease (Fricker et al., 2018; Tarafdar and Pula, 2018; Chen et al., 2020). Altogether, the Gene Ontology annotation enrichment helped to capture a coherent picture of neuroinflammation in Alzheimer's disease and its connections to relevant molecular functions and biological pathways.

Finding the biological processes that are mostly associated to neuroinflammation in Alzheimer's disease remains highly challenging. We aimed to address this challenge without *a priori* by analyzing the functional enrichment of our protein dataset using the Reactome Pathway database. Signaling of the anti-inflammatory cytokines IL4, IL10 and IL13 appeared as the most significantly enriched processes. These pathways have been

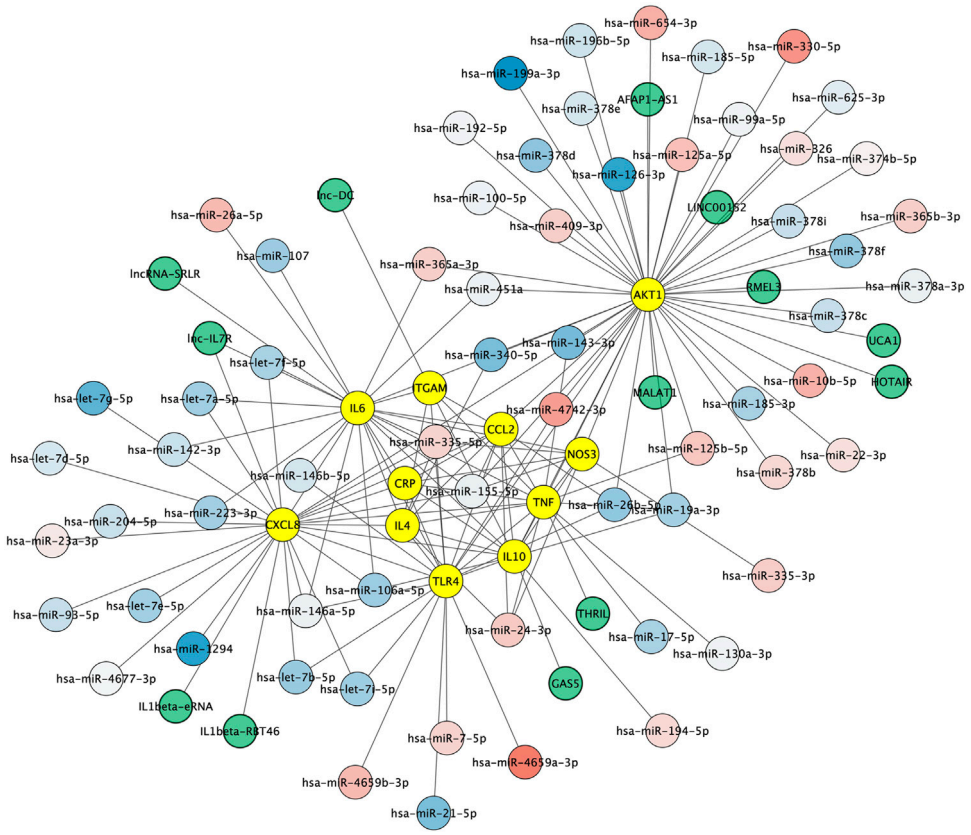

FIGURE 5 | Non-coding RNA-protein interaction network. Experimentally validated interactions between microRNAs dysregulated in Alzheimer (blue to red round shapes), lncRNAs (green round shapes) and key proteins in Alzheimer's disease neuroinflammation (yellow round shapes). Blue to red gradient denotes low to high relative abundance of microRNAs in Alzheimer's disease patient samples according to (Leidinger et al., 2013).

proposed to have protective role in Alzheimer's disease by inducing the clearance of amyloid-beta and the secretion of anti-inflammatory cytokines and neurotrophic factors (Szczepanik et al., 2001; Kawahara et al., 2012; Kiyota et al., 2012; Tang et al., 2019). On the opposite, IL4 and IL13 signaling could exacerbate oxidative stress by activating microglial NADPH oxidases and cyclooxygenase 2 (Park et al., 2009; Jeong et al., 2019). Likewise, TLR signaling as well as the MyD88 and the TNF receptor associated factor (TRAF)6 dependent molecular cascades (that both play an essential role in TLR-elicited intracellular signaling) were identified as important processes. Here again, both beneficial and detrimental roles were attributed to TLRs and for instance TLR7, TLR8 and TLR9 signaling could enhance microglial amyloid beta uptake in the early stage of Alzheimer's disease, but over time contribute to sustained neuroinflammation (Gambuzza et al., 2014). Taken together, our data highlight that the main processes associated to neuroinflammation in Alzheimer's disease have both beneficial as well as detrimental roles, and these may be time-dependent. As such, developing strategies to enhance their protective effects or to combat their pathological responses in a disease-stage manner could prove therapeutic potential for Alzheimer's disease.

Identifying the proteins critically involved in the regulation of the aforementioned processes required to detect key proteins based on the network topology. We found 11 proteins with higher than average degree and betweenness and thus with the highest ability to control the immune processes. These key proteins included the anti-inflammatory cytokines IL4 and IL10 and the pro-inflammatory cytokines TNF-alpha and IL6 that balance appears to be important for maintaining a less pathologic immune profile, as suggested by a recent study of Taipa and coworkers that found that a collection of both pro-inflammatory and anti-inflammatory cytokines were correlated with less cognitive decline in patients after one year (Taipa et al., 2019). Key proteins also included the neutrophil chemoattractant CXCL8 and CCL2 (also named monocyte chemoattractant protein (MCP)1) that exert their effects on target cells via the G protein-coupled receptors CXCL5/CXCL8 receptor (CXCR)1 and 2 and the C-C chemokine receptor (CCR)2, respectively (Zhang et al., 2013; Mamik and Ghorpade, 2016; Chou et al., 2018; Haarmann et al., 2019). Of note, both CXCL8 and CCL2 levels were found to be increased in the cerebrospinal fluid and brain tissue of Alzheimer's disease patients (Galimberti et al., 2006; Sokolova et al., 2009) and higher CCL2 levels in cerebrospinal fluid were associated with a faster rate of

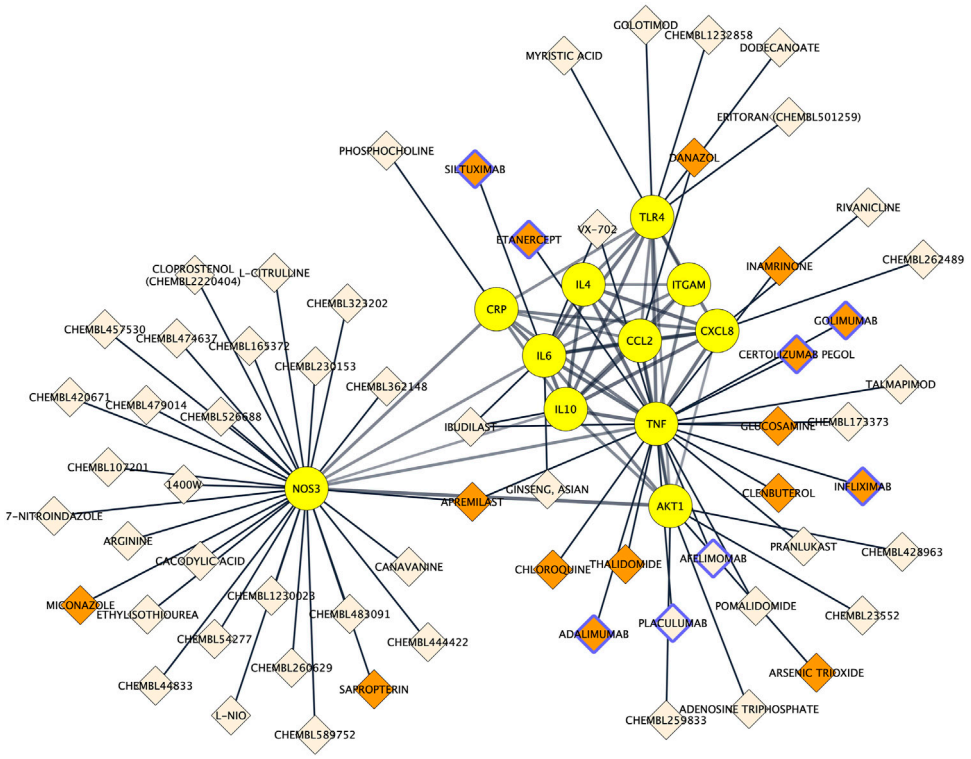

FIGURE 6 | Protein-drug interaction network. Existing associations between drugs (e.g. small molecule compounds or immunotherapies; diamond shapes) and key proteins in Alzheimer's disease neuroinflammation (yellow round shapes). FDA-approved drugs and non-FDA-approved drugs are respectively colored in orange and light beige. Protein-based therapies are bordered with purple.

cognitive decline during the early stages of the disease (Westin et al., 2012). Our study also pinpointed at TLR4 and ITGAM (also named CD11b, one protein subunit that forms macrophage antigen complex-1 (Mac-1) or complement receptor 3 (CR3)) that stimulation by amyloid beta leads to microglia activation, resulting in increased cytokine production and oxidative stress (Hong et al., 2016; Yang et al., 2020). Levels of natural CR3 ligands, such as complement fragments, ICAM-1, and fibrin, are also increased in Alzheimer's disease patients (van Oijen et al., 2005; Daborg et al., 2012; Janelidze et al., 2018). Of interest, the activation of CCR2 (Bakos et al., 2017), CXCR1 and CXCR2 (Lane et al., 2006), TLR4 (Fang et al., 2017) and ITGAM (Zhang et al., 2011) all trigger the phosphoinositide 3-kinase (PI3K)/Akt pathway that is perturbated in the brain of patients (Steen et al., 2005; Liu et al., 2011) and that downstream targets include the kinase AKT1, another key protein in our results. Also of interest, the activity of calcium-responsive NOS3, another key node in our study otherwise known as an important regulator of vascular function and of oxidative homeostasis, is also intertwined with that of AKT1 (Dossumbekova et al., 2008; Silva and Garvin, 2009). Finally, our study identified CRP that is increased in brain tissue from Alzheimer's disease patients (Wood et al., 1993; Iwamoto et al., 1994) and that should be considered not only as a marker but also as a driver of neuroinflammation, since CRP can bind to the complement factor 1q (C1q) and activate the classical complement cascade (Slevin et al., 2015; Braig et al., 2017). The identification of these 11 functionally interconnected proteins provides more specific biomarkers modulating neuroinflammatory processes in Alzheimer's disease. Furthermore, the identification of microRNAs regulating these proteins and known to be deregulated in Alzheimer's disease such as hsa-miR-26a-5p, hsa-miR-107, hsa-miR-26b-5p or hsa-let-7f-5p support their implication in Alzheimer's disease pathogenesis as well as their interest as potential peripheral biomarkers (Wang et al., 2008; Mendes-Silva et al., 2016; Guo et al., 2017; Swarbrick et al., 2019). Likewise, the identification of lncRNAs acting on targets such as CXCL8, TNF-alpha, IL6, IL10 or ITGAM support their role, still largely unexplored, as important regulators of the human innate immune response (Wang et al., 2014a; Cui et al., 2014; Ilott et al., 2014; Li et al., 2014; Li et al., 2017) (**Supplementary Table 3**).

Drug–protein interactions analysis revealed that 9 of the 11 key proteins could be targeted by a total of 55 small molecules and 8 protein-based therapeutics. The latter comprised FDA approved TNF-alpha antagonists (infliximab, etanercept, adalimumab, golimumab and certolizumab pegol) that were found to be associated with lower Alzheimer's disease risk in patients with rheumatoid arthritis and psoriasis (Zhou et al., 2020) and proved positive immune and cognitive outcomes in rodent models of Alzheimer's disease (Kim et al., 2016; Paouri et al., 2017; Park et al., 2019). They also included the IL6-targeting antibody siltuximab that was launched for the treatment of

multicentric Castleman but that has not been evaluated to date in the context of Alzheimer's disease, to our knowledge. Drug-protein interaction analysis also pictured small molecules such as thalidomide that reduces the production of TNF-alpha (Sampaio et al., 1991; Gabbita et al., 2012) and that more potent derivative 3,6-dithiothalidomide ameliorated cognition in a rat models of LPS-induced sustained microglia activation (Belarbi et al., 2012) and in a triple transgenic mouse model of Alzheimer's disease (Tweedie et al., 2012). Likewise, we identified glucosamine that was shown to inhibit in microglial cells lipopolysaccharide-induced TNF-alpha expression, Ca2+ influx and outward K+ currents, which are typically representative of microglial activation (Yi et al., 2005). Interestingly, our analysis also highlighted several phosphodiesterase inhibitors such as apremilast (phosphodiesterase 4 inhibitor) that interferes with NOS3 and cytokines production (Schett et al., 2010; Gulisano et al., 2018), inamrinone (phosphodiesterase 3 inhibitor) or ibudilast (a non-selective 3, 4, 10, 11 phosphodiesterase inhibitor). Of note, ibudilast is currently approved for use as an anti-inflammatory in Japan, improved amyloid beta-induced cognitive impairment in rodent (Wang et al., 2014b) and acts through TLR4 blockade (Schwenkgrub et al., 2017a), reduction of pro-inflammatory cytokines TNF-alpha, IL6 and IL1-beta (Wakita et al., 2003; Schwenkgrub et al., 2017b), up-regulation the anti-inflammatory cytokine IL4 and IL10 and various neurotrophic factors (Mizuno et al., 2004). Although these drug-protein association should overall be taken with caution, given that the drugs' effects on the network may depend on their dose and on the disease stage and severity, they may be useful to explore the neuroinflammatory cascade involved in Alzheimer's disease.

In conclusion, our study provides a review of proteins associated to neuroinflammation in Alzheimer's disease and identifies 11 interrelated key proteins with the highest ability to control neuroinflammatory processes in Alzheimer's disease. While some proteins such as TNF-alpha are largely evaluated, our data provide evidence to encourage further investigation on others such as CCL2, CXCL8, IL-10, TLR4, CRP or AKT1 that appears as a key component for translating extracellular information into downstream biological responses regulating microglia phenotype. Assessing these proteins could then help for the evaluation of disease-modifying properties, for example for assessing the impact of the recently FDA-approved aducanumab on neuroinflammation-related endpoints. A major challenge for future therapies will be to enhance the protective role or combat the pathological roles of immune processes such as IL4, IL10 and IL13 or TLR-mediated MyD88- and TRAF6- dependent signaling, and this will require to better understanding the time-dependent role of these processes in Alzheimer's disease. Our study prioritizes biomarkers and putative targets and identifies non-coding RNAs and pharmacological compounds with single or pleiotropic actions acting on them. As such, it may facilitate the way to novel diagnostic and therapeutic neuroprotective strategies for Alzheimer's disease.

DATA AVAILABILITY STATEMENT

The original contributions presented in the study are included in the article/**Supplementary Material**, further inquiries can be directed to the corresponding author.

AUTHOR CONTRIBUTIONS

FI contributed to the methodology and the execution of the study. DD and BG revised the manuscript providing expertise in pharmacology and clinical neurology. KB designed the study, contributed to the methodology and execution of the study, analyzed the data and wrote the manuscript.

FUNDING

This research was funded by Région Hauts-de-France (Projet Santé Environnement; KB), University of Lille and Centre National de la Recherche Scientifique (Projet Exploratoire Premier Soutien PEPS; KB), Lille FHU-VasCog (KB) and Campus France (KB).

SUPPLEMENTARY MATERIAL

The Supplementary Material for this article can be found online at: https://www.frontiersin.org/articles/10.3389/fphar.2021.630003/full#supplementary-material

REFERENCES

Bakos, E., Thaiss, C. A., Kramer, M. P., Cohen, S., Radomir, L., Orr, I., et al. (2017). CCR2 Regulates the Immune Response by Modulating the Interconversion and Function of Effector and Regulatory T Cells. *J. Immunol.* 198 (12), 4659–4671. doi:10.4049/jimmunol.1601458

Baran, J., Gerner, M., Haeussler, M., Nenadic, G., and Bergman, C. M. (2011). pubmed2ensembl: a Resource for Mining the Biological Literature on Genes. *PLoS One* 6 (9), e24716. doi:10.1371/journal.pone.0024716

Belarbi, K., Jopson, T., Tweedie, D., Arellano, C., Luo, W., Greig, N. H., et al. (2012). TNF-α Protein Synthesis Inhibitor Restores Neuronal Function and Reverses Cognitive Deficits Induced by Chronic Neuroinflammation. *J. Neuroinflammation* 9, 23. doi:10.1186/1742-2094-9-23

Bhaskar, K., Konerth, M., Kokiko-Cochran, O. N., Cardona, A., Ransohoff, R. M., and Lamb, B. T. (2010). Regulation of Tau Pathology by the Microglial Fractalkine Receptor. *Neuron* 68 (1), 19–31. doi:10.1016/j.neuron.2010.08.023

Bindea, G., Mlecnik, B., Hackl, H., Charoentong, P., Tosolini, M., Kirilovsky, A., et al. (2009). ClueGO: a Cytoscape Plug-In to Decipher Functionally Grouped Gene Ontology and Pathway Annotation Networks. *Bioinformatics* 25 (8), 1091–1093. doi:10.1093/bioinformatics/btp101

Braig, D., Nero, T. L., Koch, H.-G., Kaiser, B., Wang, X., Thiele, J. R., et al. (2017). Transitional Changes in the CRP Structure lead to the Exposure of Proinflammatory Binding Sites. *Nat. Commun.* 8, 14188. doi:10.1038/ncomms14188

Chen, F., Ghosh, A., Lin, J., Zhang, C., Pan, Y., Thakur, A., et al. (2020). 5-lipoxygenase Pathway and its Downstream Cysteinyl Leukotrienes as Potential Therapeutic Targets for Alzheimer's Disease. *Brain Behav. Immun.* 88, 844–855. doi:10.1016/j.bbi.2020.03.022

Cheng, L., Wang, P., Tian, R., Wang, S., Guo, Q., Luo, M., et al. (2019). LncRNA2Target v2.0: a Comprehensive Database for Target Genes of lncRNAs in Human and Mouse. *Nucleic Acids Res.* 47 (D1), D140–D144. doi:10.1093/nar/gky1051

Chou, A., Krukowski, K., Morganti, J., Riparip, L.-K., and Rosi, S. (2018). Persistent Infiltration and Impaired Response of Peripherally-Derived Monocytes after Traumatic Brain Injury in the Aged Brain. *Int. J. Mol. Sci.* 19 (6), 1616. doi:10.3390/ijms19061616

Cotto, K. C., Wagner, A. H., Feng, Y.-Y., Kiwala, S., Coffman, A. C., Spies, G., et al. (2018). DGIdb 3.0: a Redesign and Expansion of the Drug-Gene Interaction Database. *Nucleic Acids Res.* 46 (D1), D1068–D1073. doi:10.1093/nar/gkx1143

Cui, H., Xie, N., Tan, Z., Banerjee, S., Thannickal, V. J., Abraham, E., et al. (2014). The Human Long Noncoding RNA lnc-IL7R Regulates the Inflammatory Response. *Eur. J. Immunol.* 44 (7), 2085–2095. doi:10.1002/eji.201344126

Daborg, J., Andreasson, U., Pekna, M., Lautner, R., Hanse, E., Minthon, L., et al. (2012). Cerebrospinal Fluid Levels of Complement Proteins C3, C4 and CR1 in Alzheimer's Disease. *J. Neural Transm.* 119 (7), 789–797. doi:10.1007/s00702-012-0797-8

Dani, M., Wood, M., Mizoguchi, R., Fan, Z., Walker, Z., Morgan, R., et al. (2018). Microglial Activation Correlates *In Vivo* with Both Tau and Amyloid in Alzheimer's Disease. *Brain* 141 (9), 2740–2754. doi:10.1093/brain/awy188

Dossumbekova, A., Berdyshev, E. V., Gorshkova, I., Shao, Z., Li, C., Long, P., et al. (2008). Akt Activates NOS3 and Separately Restores Barrier Integrity in H2O2-Stressed Human Cardiac Microvascular Endothelium. *Am. J. Physiology-Heart Circulatory Physiol.* 295 (6), H2417–H2426. doi:10.1152/ajpheart.00501.2008

Fabiani, C., and Antollini, S. S. (2019). Alzheimer's Disease as a Membrane Disorder: Spatial Cross-Talk Among Beta-Amyloid Peptides, Nicotinic Acetylcholine Receptors and Lipid Rafts. *Front. Cel. Neurosci.* 13, 309. doi:10.3389/fncel.2019.00309

Fabregat, A., Sidiropoulos, K., Viteri, G., Forner, O., Marin-Garcia, P., Arnau, V., et al. (2017). Reactome Pathway Analysis: a High-Performance In-Memory Approach. *BMC Bioinformatics* 18 (1), 142. doi:10.1186/s12859-017-1559-2

Fan, Z., Brooks, D. J., Okello, A., and Edison, P. (2017). An Early and Late Peak in Microglial Activation in Alzheimer's Disease Trajectory. *Brain* 140 (3), aww349–803. doi:10.1093/brain/aww349

Fang, W., Bi, D., Zheng, R., Cai, N., Xu, H., Zhou, R., et al. (2017). Identification and Activation of TLR4-Mediated Signalling Pathways by Alginate-Derived Guluronate Oligosaccharide in RAW264.7 Macrophages. *Sci. Rep.* 7 (1), 1663. doi:10.1038/s41598-017-01868-0

Fricker, M., Tolkovsky, A. M., Borutaite, V., Coleman, M., and Brown, G. C. (2018). Neuronal Cell Death. *Physiol. Rev.* 98 (2), 813–880. doi:10.1152/physrev.0001110.1152/physrev.00011.2017

Gabbita, S. P., Srivastava, M. K., Eslami, P., Johnson, M. F., Kobritz, N. K., Tweedie, D., et al. (2012). Early Intervention with a Small Molecule Inhibitor for Tumor Nefosis Factor-α Prevents Cognitive Deficits in a Triple Transgenic Mouse Model of Alzheimer's Disease. *J. Neuroinflammation* 9, 99. doi:10.1186/1742-2094-9-99

Galimberti, D., Schoonenboom, N., Scheltens, P., Fenoglio, C., Bouwman, F., Venturelli, E., et al. (2006). Intrathecal Chemokine Synthesis in Mild Cognitive Impairment and Alzheimer Disease. *Arch. Neurol.* 63 (4), 538–543. doi:10.1001/archneur.63.4.538

Gambuzza, M., Sofo, V., Salmeri, F., Soraci, L., Marino, S., and Bramanti, P. (2014). Toll-like Receptors in Alzheimer's Disease: a Therapeutic Perspective. *Cnsnddt* 13 (9), 1542–1558. doi:10.2174/1871527313666140806124850

Goodwin, J. L., Kehrli, M. E., Jr., and Uemura, E. (1997). Integrin Mac-1 and Beta-Amyloid in Microglial Release of Nitric Oxide. *Brain Res.* 768 (1-2), 279–286. doi:10.1016/s0006-8993(97)00653-7

Guerreiro, R., Wojtas, A., Bras, J., Carrasquillo, M., Rogaeva, E., Majounie, E., et al. (2013). TREM2 Variants in Alzheimer's Disease. *N. Engl. J. Med.* 368 (2), 117–127. doi:10.1056/NEJMoa1211851

Gulisano, W., Tropea, M. R., Arancio, O., Palmeri, A., and Puzzo, D. (2018). Sub-efficacious Doses of Phosphodiesterase 4 and 5 Inhibitors Improve Memory in a Mouse Model of Alzheimer's Disease. *Neuropharmacology* 138, 151–159. doi:10.1016/j.neuropharm.2018.06.002

Guo, R., Fan, G., Zhang, J., Wu, C., Du, Y., Ye, H., et al. (2017). A 9-microRNA Signature in Serum Serves as a Noninvasive Biomarker in Early Diagnosis of Alzheimer's Disease. *Jad* 60 (4), 1365–1377. doi:10.3233/JAD-170343

Haarmann, A., Schuhmann, M., Silwedel, C., Monoranu, C.-M., Stoll, G., and Buttmann, M. (2019). Human Brain Endothelial CXCR2 Is Inflammation-Inducible and Mediates CXCL5- and CXCL8-Triggered Paraendothelial Barrier Breakdown. *Int. J. Mol. Sci.* 20 (3), 602. doi:10.3390/ijms20030602

Hong, S., Beja-Glasser, V. F., Nfonoyim, B. M., Frouin, A., Li, S., Ramakrishnan, S., et al. (2016). Complement and Microglia Mediate Early Synapse Loss in Alzheimer Mouse Models. *Science* 352 (6286), 712–716. doi:10.1126/science.aad8373

Huang, H.-Y., Lin, Y.-C. -D., Li, J., Huang, K.-Y., Shrestha, S., Hong, H.-C., et al. (2020). miRTarBase 2020: Updates to the Experimentally Validated microRNA-Target Interaction Database. *Nucleic Acids Res.* 48 (D1), D148–D54. doi:10.1093/nar/gkz896

Ilott, N. E., II, Heward, J. A., Roux, B., Tsitsiou, E., Fenwick, P. S., Lenzi, L., et al. (2014). Long Non-coding RNAs and Enhancer RNAs Regulate the Lipopolysaccharide-Induced Inflammatory Response in Human Monocytes. *Nat. Commun.* 5, 3979. doi:10.1038/ncomms4979

Itagaki, S., McGeer, P. L., and Akiyama, H. (1988). Presence of T-Cytotoxic Suppressor and Leucocyte Common Antigen Positive Cells in Alzheimer's Disease Brain Tissue. *Neurosci. Lett.* 91 (3), 259–264. doi:10.1016/0304-3940(88)90690-8

Iwamoto, N., Nishiyama, E., Ohwada, J., and Arai, H. (1994). Demonstration of CRP Immunoreactivity in Brains of Alzheimer's Disease: Immunohistochemical Study Using Formic Acid Pretreatment of Tissue Sections. *Neurosci. Lett.* 177 (1-2), 23–26. doi:10.1016/0304-3940(94)90035-3

Janelidze, S., Mattsson, N., Stomrud, E., Lindberg, O., Palmqvist, S., Zetterberg, H., et al. (2018). CSF Biomarkers of Neuroinflammation and Cerebrovascular Dysfunction in Early Alzheimer Disease. *Neurology* 91 (9), e867–e877. doi:10.1212/WNL.0000000000006082

Jansen, I. E., Savage, J. E., Watanabe, K., Bryois, J., Williams, D. M., Steinberg, S., et al. (2019). Genome-wide Meta-Analysis Identifies New Loci and Functional Pathways Influencing Alzheimer's Disease Risk. *Nat. Genet.* 51 (3), 404–413. doi:10.1038/s41588-018-0311-9

Jassal, B., Matthews, L., Viteri, G., Gong, C., Lorente, P., Fabregat, A., et al. (2020). The Reactome Pathway Knowledgebase. *Nucleic Acids Res.* 48 (D1), D498–D503. doi:10.1093/nar/gkz1031

Jeong, J. Y., Chung, Y. C., and Jin, B. K. (2019). Interleukin-4 and Interleukin-13 Exacerbate Neurotoxicity of Prothrombin Kringle-2 in Cortex *In Vivo* via Oxidative Stress. *Int. J. Mol. Sci.* 20 (8), 1927. doi:10.3390/ijms20081927

Jun, G., Naj, A. C., Beecham, G. W., Wang, L. S., Buros, J., Gallins, P. J., et al. (2010). Meta-analysis Confirms CR1, CLU, and PICALM as Alzheimer Disease Risk Loci and Reveals Interactions with APOE Genotypes. *Arch. Neurol.* 67 (12), 1473–1484. doi:10.1001/archneurol.2010.201

Kawahara, K., Suenobu, M., Yoshida, A., Koga, K., Hyodo, A., Ohtsuka, H., et al. (2012). Intracerebral Microinjection of Interleukin-4/interleukin-13 Reduces β-amyloid Accumulation in the Ipsilateral Side and Improves Cognitive Deficits in Young Amyloid Precursor Protein 23 Mice. *Neuroscience* 207, 243–260. doi:10.1016/j.neuroscience.2012.01.049

Kim, D. H., Choi, S.-M., Jho, J., Park, M.-S., Kang, J., Park, S. J., et al. (2016). Infliximab Ameliorates AD-Associated Object Recognition Memory Impairment. *Behav. Brain Res.* 311, 384–391. doi:10.1016/j.bbr.2016.06.001

Kiyota, T., Ingraham, K. L., Swan, R. J., Jacobsen, M. T., Andrews, S. J., and Ikezu, T. (2012). AAV Serotype 2/1-mediated Gene Delivery of Anti-inflammatory Interleukin-10 Enhances Neurogenesis and Cognitive Function in APP+PS1 Mice. *Gene Ther.* 19 (7), 724–733. doi:10.1038/gt.2011.126

Krstic, D., Madhusudan, A., Doehner, J., Vogel, P., Notter, T., Imhof, C., et al. (2012). Systemic Immune Challenges Trigger and Drive Alzheimer-like Neuropathology in Mice. *J. Neuroinflammation* 9, 151. doi:10.1186/1742-2094-9-151

Kutmon, M., Ehrhart, F., Willighagen, E. L., Evelo, C. T., and Coort, S. L. (2018). CyTargetLinker App Update: A Flexible Solution for Network Extension in Cytoscape. *F1000Res* 7, 743. doi:10.12688/f1000research.14613.2

Lambert, J.-C., Heath, S., Heath, S., Even, G., Campion, D., Sleegers, K., et al. (2009). Genome-wide Association Study Identifies Variants at CLU and CR1 Associated with Alzheimer's Disease. *Nat. Genet.* 41 (10), 1094–1099. doi:10.1038/ng.439

Lambert, J. C., Ibrahim-Verbaas, C. A., Harold, D., Naj, A. C., Sims, R., Bellenguez, C., et al. (2013). Meta-analysis of 74,046 Individuals Identifies 11 New Susceptibility Loci for Alzheimer's Disease. *Nat. Genet.* 45 (12), 1452–1458. doi:10.1038/ng.2802

Lane, H. C., Anand, A. R., and Ganju, R. K. (2006). Cbl and Akt Regulate CXCL8-Induced and CXCR1- and CXCR2-Mediated Chemotaxis. *Int. Immunol.* 18 (8), 1315–1325. doi:10.1093/intimm/dxl064

Leidinger, P., Backes, C., Deutscher, S., Schmitt, K., Mueller, S. C., Frese, K., et al. (2013). A Blood Based 12-miRNA Signature of Alzheimer Disease Patients. *Genome Biol.* 14 (7), R78. doi:10.1186/gb-2013-14-7-r78

Lever, J., Jones, M. R., Danos, A. M., Krysiak, K., Bonakdar, M., Grewal, J. K., et al. (2019). Text-mining Clinically Relevant Cancer Biomarkers for Curation into the CIViC Database. *Genome Med.* 11 (1), 78. doi:10.1186/s13073-019-0686-y

Li, Y., Li, Y., Huang, S., He, K., Zhao, M., Lin, H., et al. (2017). Long Non-coding RNA Growth Arrest Specific Transcript 5 Acts as a Tumour Suppressor in Colorectal Cancer by Inhibiting Interleukin-10 and Vascular Endothelial Growth Factor Expression. *Oncotarget* 8 (8), 13690–13702. doi:10.18632/oncotarget.14625

Li, Z., Chao, T.-C., Chang, K.-Y., Lin, N., Patil, V. S., Shimizu, C., et al. (2014). The Long Noncoding RNA THRIL Regulates TNF Expression through its Interaction with hnRNPL. *Proc. Natl. Acad. Sci.* 111 (3), 1002–1007. doi:10.1073/pnas.1313768111

Liu, Y., Dai, Y., Li, Q., Chen, C., Chen, H., Song, Y., et al. (2020). Beta-amyloid Activates NLRP3 Inflammasome via TLR4 in Mouse Microglia. *Neurosci. Lett.* 736, 135279. doi:10.1016/j.neulet.2020.135279

Liu, Y., Liu, F., Grundke-Iqbal, I., Iqbal, K., and Gong, C.-X. (2011). Deficient Brain Insulin Signalling Pathway in Alzheimer's Disease and Diabetes. *J. Pathol.* 225 (1), 54–62. doi:10.1002/path.2912

Mamik, M. K., and Ghorpade, A. (2016). CXCL8 as a Potential Therapeutic Target for HIV-Associated Neurocognitive Disorders. *Curr. Drug Targets* 17 (1), 111–121. doi:10.2174/1389450116666150626124544

Mendes-Silva, A. P., Pereira, K. S., Tolentino-Araujo, G. T., Nicolau, E. d. S., Silva-Ferreira, C. M., Teixeira, A. L., et al. (2016). Shared Biologic Pathways between Alzheimer Disease and Major Depression: A Systematic Review of MicroRNA Expression Studies. *Am. J. Geriatr. Psychiatry* 24 (10), 903–912. doi:10.1016/j.jagp.2016.07.017

Mizuno, T., Kurotani, T., Komatsu, Y., Kawanokuchi, J., Kato, H., Mitsuma, N., et al. (2004). Neuroprotective Role of Phosphodiesterase Inhibitor Ibudilast on Neuronal Cell Death Induced by Activated Microglia. *Neuropharmacology* 46 (3), 404–411. doi:10.1016/j.neuropharm.2003.09.009

Monsonego, A., Zota, V., Karni, A., Krieger, J. I., Bar-Or, A., Bitan, G., et al. (2003). Increased T Cell Reactivity to Amyloid β Protein in Older Humans and Patients with Alzheimer Disease. *J. Clin. Invest.* 112 (3), 415–422. doi:10.1172/JCI1810410.1172/jci200318104

O'Mara-Eves, A., Thomas, J., McNaught, J., Miwa, M., and Ananiadou, S. (2015). Using Text Mining for Study Identification in Systematic Reviews: a Systematic Review of Current Approaches. *Syst. Rev.* 4, 5. doi:10.1186/2046-4053-4-5

Oprea, T. I., Bologa, C. G., Brunak, S., Campbell, A., Gan, G. N., Gaulton, A., et al. (2018). Unexplored Therapeutic Opportunities in the Human Genome. *Nat. Rev. Drug Discov.* 17 (5), 317–332. doi:10.1038/nrd.2018.14

Orsucci, D., Mancuso, M., Caldarazzo Ienco, E., Simoncini, C., Siciliano, G., and Bonuccelli, U. (2013). Vascular Factors and Mitochondrial Dysfunction: a central Role in the Pathogenesis of Alzheimer's Disease. *Curr. Neurovasc. Res.* 10 (1), 76–80. doi:10.2174/156720213804805972

Pan, Y., Liu, J., and Qi, F. (2019). Identification of Key Candidate Genes and Molecular Pathways in white Fat browning: an Anti-obesity Drug Discovery Based on Computational Biology. *Hum. Genomics* 13 (1), 55. doi:10.1186/s40246-019-0239-x

Paouri, E., Tzara, O., Kartalou, G.-I., Zenelak, S., and Georgopoulos, S. (2017). Peripheral Tumor Necrosis Factor-Alpha (TNF-α) Modulates Amyloid Pathology by Regulating Blood-Derived Immune Cells and Glial Response in the Brain of AD/TNF Transgenic Mice. *J. Neurosci.* 37 (20), 5155–5171. doi:10.1523/JNEUROSCI.2484-16.2017

Park, J., Lee, S.-Y., Shon, J., Kim, K., Lee, H. J., Kim, K. A., et al. (2019). Adalimumab Improves Cognitive Impairment, Exerts Neuroprotective Effects and Attenuates Neuroinflammation in an Aβ1-40-Injected Mouse Model of Alzheimer's Disease. *Cytotherapy* 21 (6), 671–682. doi:10.1016/j.jcyt.2019.04.054

Park, K. W., Baik, H. H., and Jin, B. K. (2009). IL-13-induced Oxidative Stress via Microglial NADPH Oxidase Contributes to Death of Hippocampal Neurons *In Vivo*. *J. Immunol.* 183 (7), 4666–4674. doi:10.4049/jimmunol.0803392

Polanco, J. C., Li, C., Bodea, L.-G., Martinez-Marmol, R., Meunier, F. A., and Götz, J. (2018). Amyloid-β and Tau Complexity - towards Improved Biomarkers and Targeted Therapies. *Nat. Rev. Neurol.* 14 (1), 22–39. doi:10.1038/nrneurol.2017.162

Ransohoff, R. M., and Cardona, A. E. (2010). The Myeloid Cells of the central Nervous System Parenchyma. *Nature* 468 (7321), 253–262. doi:10.1038/nature09615

Sampaio, E. P., Sarno, E. N., Galilly, R., Cohn, Z. A., and Kaplan, G. (1991). Thalidomide Selectively Inhibits Tumor Necrosis Factor Alpha Production by Stimulated Human Monocytes. *J. Exp. Med.* 173 (3), 699–703. doi:10.1084/jem.173.3.699

Schett, G., Sloan, V. S., Stevens, R. M., and Schafer, P. (2010). Apremilast: a Novel PDE4 Inhibitor in the Treatment of Autoimmune and Inflammatory Diseases. *Ther. Adv. Musculoskelet.* 2 (5), 271–278. doi:10.1177/1759720X10381432

Schwartz, M., and Deczkowska, A. (2016). Neurological Disease as a Failure of Brain-Immune Crosstalk: The Multiple Faces of Neuroinflammation. *Trends Immunol.* 37 (10), 668–679. doi:10.1016/j.it.2016.08.001

Schwenkgrub, J., Zaremba, M., Mirowska-Guzel, D., and Kurkowska-Jastrzebska, I. (2017). Ibudilast: a Nonselective Phosphodiesterase Inhibitor in Brain Disorders. *Postepy Hig Med. Dosw (Online)* 71 (0), 137–148. doi:10.5604/01.3001.0010.3798

Schwenkgrub, J., Zaremba, M., Joniec-Maciejak, I., Cudna, A., Mirowska-Guzel, D., and Kurkowska-Jastrzębska, I. (2017). The Phosphodiesterase Inhibitor, Ibudilast, Attenuates Neuroinflammation in the MPTP Model of Parkinson's Disease. *PLoS One* 12 (7), e0182019. doi:10.1371/journal.pone.0182019

Silva, G. B., and Garvin, J. L. (2009). Akt1 Mediates Purinergic-dependent NOS3 Activation in Thick Ascending Limbs. *Am. J. Physiol.-Renal Physiol.* 297 (3), F646–F652. doi:10.1152/ajprenal.00270.2009

Singhal, A., Simmons, M., and Lu, Z. (2016). Text Mining Genotype-Phenotype Relationships from Biomedical Literature for Database Curation and Precision Medicine. *Plos Comput. Biol.* 12 (11), e1005017. doi:10.1371/journal.pcbi.1005017

Slevin, M., Matou, S., Zeinolabediny, Y., Corpas, R., Weston, R., Liu, D., et al. (2015). Monomeric C-Reactive Protein-A Key Molecule Driving Development of Alzheimer's Disease Associated with Brain Ischaemia? *Sci. Rep.* 5, 13281. doi:10.1038/srep13281

Sochocka, M., Koutsouraki, E., Gasiorowski, K., and Leszek, J. (2013). Vascular Oxidative Stress and Mitochondrial Failure in the Pathobiology of Alzheimer's Disease: a New Approach to Therapy. *CNS Neurol. Disord. Drug Targets* 12 (6), 870–881. doi:10.2174/18715273113129990072

Sokolova, A., Hill, M. D., Rahimi, F., Warden, L. A., Halliday, G. M., and Shepherd, C. E. (2009). Monocyte Chemoattractant Protein-1 Plays a Dominant Role in the Chronic Inflammation Observed in Alzheimer's Disease. *Brain Pathol.* 19 (3), 392–398. doi:10.1111/j.1750-3639.2008.00188.x

Steen, E., Terry, B. M., J. Rivera, E., Cannon, J. L., Neely, T. R., Tavares, R., et al. (2005). Impaired Insulin and Insulin-like Growth Factor Expression and Signaling Mechanisms in Alzheimer's Disease - Is This Type 3 Diabetes? *Jad* 7 (1), 63–80. doi:10.3233/jad-2005-7107

Swarbrick, S., Wragg, N., Ghosh, S., and Stolzing, A. (2019). Systematic Review of miRNA as Biomarkers in Alzheimer's Disease. *Mol. Neurobiol.* 56 (9), 6156–6167. doi:10.1007/s12035-019-1500-y

Szczepanik, A., Funes, S., Petko, W., and Ringheim, G. E. (2001). IL-4, IL-10 and IL-13 Modulate Aβ(1-42)-Induced Cytokine and Chemokine Production in Primary Murine Microglia and a Human Monocyte Cell Line. *J. Neuroimmunol* 113 (1), 49–62. doi:10.1016/s0165-5728(00)00404-5

Szklarczyk, D., Gable, A. L., Lyon, D., Junge, A., Wyder, S., Huerta-Cepas, J., et al. (2019). STRING V11: Protein-Protein Association Networks with Increased Coverage, Supporting Functional Discovery in Genome-wide Experimental Datasets. *Nucleic Acids Res.* 47 (D1), D607–D613. doi:10.1093/nar/gky1131

Taipa, R., das Neves, S. P., Sousa, A. L., Fernandes, J., Pinto, C., Correia, A. P., et al. (2019). Proinflammatory and Anti-inflammatory Cytokines in the CSF of Patients with Alzheimer's Disease and Their Correlation with Cognitive Decline. *Neurobiol. Aging* 76, 125–132. doi:10.1016/j.neurobiolaging.2018.12.019

Tang, R. H., Qi, R. Q., and Liu, H. Y. (2019). Interleukin-4 Affects Microglial Autophagic Flux. *Neural Regen. Res.* 14 (9), 1594–1602. doi:10.4103/1673-5374.25597510.4103/1673-5374.247422

Tarafdar, A., and Pula, G. (2018). The Role of NADPH Oxidases and Oxidative Stress in Neurodegenerative Disorders. *Int. J. Mol. Sci.* 19 (12), 3824. doi:10.3390/ijms19123824

Togo, T., Akiyama, H., Iseki, E., Kondo, H., Ikeda, K., Kato, M., et al. (2002). Occurrence of T Cells in the Brain of Alzheimer's Disease and Other Neurological Diseases. *J. Neuroimmunol* 124 (1-2), 83–92. doi:10.1016/s0165-5728(01)00496-9

Tweedie, D., Ferguson, R. A., Fishman, K., Frankola, K. A., Van Praag, H., Holloway, H. W., et al. (2012). Tumor Necrosis Factor-α Synthesis Inhibitor 3,6′-dithiothalidomide Attenuates Markers of Inflammation, Alzheimer Pathology and Behavioral Deficits in Animal Models of Neuroinflammation and Alzheimer's Disease. *J. Neuroinflammation* 9, 106. doi:10.1186/1742-2094-9-106

UniProt, C. (2019). UniProt: a Worldwide Hub of Protein Knowledge. *Nucleic Acids Res.* 47 (D1), D506–D515. doi:10.1093/nar/gky1049

van Oijen, M., Witteman, J. C., Hofman, A., Koudstaal, P. J., and Breteler, M. M. B. (2005). Fibrinogen Is Associated with an Increased Risk of Alzheimer Disease and Vascular Dementia. *Stroke* 36 (12), 2637–2641. doi:10.1161/01.STR.0000189721.31432.26

Wakita, H., Tomimoto, H., Akiguchi, I., Lin, J.-X., Ihara, M., Ohtani, R., et al. (2003). Ibudilast, a Phosphodiesterase Inhibitor, Protects against white Matter Damage under Chronic Cerebral Hypoperfusion in the Rat. *Brain Res.* 992 (1), 53–59. doi:10.1016/j.brainres.2003.08.028

Wang, H., Mei, Z. l., Zhong, K. L., Hu, M., Long, Y., Miao, M. X., et al. (2014). Pretreatment with Antiasthmatic Drug Ibudilast Ameliorates Aβ1-42-Induced Memory Impairment and Neurotoxicity in Mice. *Pharmacol. Biochem. Behav.* 124, 373–379. doi:10.1016/j.pbb.2014.07.006

Wang, P., Xue, Y., Han, Y., Lin, L., Wu, C., Xu, S., et al. (2014). The STAT3-Binding Long Noncoding RNA Lnc-DC Controls Human Dendritic Cell Differentiation. *Science* 344 (6181), 310–313. doi:10.1126/science.1251456

Wang, W.-X., Rajeev, B. W., Stromberg, A. J., Ren, N., Tang, G., Huang, Q., et al. (2008). The Expression of MicroRNA miR-107 Decreases Early in Alzheimer's Disease and May Accelerate Disease Progression through Regulation of -Site Amyloid Precursor Protein-Cleaving Enzyme 1. *J. Neurosci.* 28 (5), 1213–1223. doi:10.1523/JNEUROSCI.5065-07.2008

Wang, Z., Clark, N. R., and Ma'ayan, A. (2015). Dynamics of the Discovery Process of Protein-Protein Interactions from Low Content Studies. *BMC Syst. Biol.* 9, 26. doi:10.1186/s12918-015-0173-z

Westin, K., Buchhave, P., Nielsen, H., Minthon, L., Janciauskiene, S., and Hansson, O. (2012). CCL2 Is Associated with a Faster Rate of Cognitive Decline during Early Stages of Alzheimer's Disease. *PLoS One* 7 (1), e30525. doi:10.1371/journal.pone.0030525

Wood, J. A., Wood, P. L., Ryan, R., Graff-Radford, N. R., Pilapil, C., Robitaille, Y., et al. (1993). Cytokine Indices in Alzheimer's Temporal Cortex: No Changes in Mature IL-1β or IL-1RA but Increases in the Associated Acute Phase Proteins IL-6, α2-macroglobulin and C-Reactive Protein. *Brain Res.* 629 (2), 245–252. doi:10.1016/0006-8993(93)91327-o

Yang, J., Wise, L., and Fukuchi, K.-i. (2020). TLR4 Cross-Talk with NLRP3 Inflammasome and Complement Signaling Pathways in Alzheimer's Disease. *Front. Immunol.* 11, 724. doi:10.3389/fimmu.2020.00724

Yi, H. A., Yi, S. D., Jang, B. C., Song, D. K., Shin, D. H., Mun, K. C., et al. (2005). Inhibitory Effects of Glucosamine on Lipopolysaccharide-induced Activation in Microglial Cells. *Clin. Exp. Pharmacol. Physiol.* 32 (12), 1097–1103. doi:10.1111/j.1440-1681.2005.04305.x

Zhang, D., Hu, X., Qian, L., Chen, S.-H., Zhou, H., Wilson, B., et al. (2011). Microglial MAC1 Receptor and PI3K Are Essential in Mediating β-amyloid Peptide-Induced Microglial Activation and Subsequent Neurotoxicity. *J. Neuroinflammation* 8 (1), 3. doi:10.1186/1742-2094-8-3

Zhang, K., Tian, L., Liu, L., Feng, Y., Dong, Y.-B., Li, B., et al. (2013). CXCL1 Contributes to β-Amyloid-Induced Transendothelial Migration of Monocytes in Alzheimer's Disease. *PLoS One* 8 (8), e72744. doi:10.1371/journal.pone.0072744

Zhou, M., Xu, R., Kaelber, D. C., and Gurney, M. E. (2020). Tumor Necrosis Factor (TNF) Blocking Agents Are Associated with Lower Risk for Alzheimer's Disease in Patients with Rheumatoid Arthritis and Psoriasis. *PLoS One* 15 (3), e0229819. doi:10.1371/journal.pone.0229819

Conflict of Interest: The authors declare that the research was conducted in the absence of any commercial or financial relationships that could be construed as a potential conflict of interest.

Copyright © 2021 El Idrissi, Gressier, Devos and Belarbi. This is an open-access article distributed under the terms of the Creative Commons Attribution License (CC BY). The use, distribution or reproduction in other forums is permitted, provided the original author(s) and the copyright owner(s) are credited and that the original publication in this journal is cited, in accordance with accepted academic practice. No use, distribution or reproduction is permitted which does not comply with these terms.

frontiers in Pharmacology

ORIGINAL RESEARCH
published: 19 July 2021
doi: 10.3389/fphar.2021.694476

Glucagon-Like Peptide-1 Analog Exendin-4 Ameliorates Cocaine-Mediated Behavior by Inhibiting Toll-Like Receptor 4 Signaling in Mice

Changliang Zhu[1,2], Hong Tao[3], Shikuo Rong[4], Lifei Xiao[2], Xinxiao Li[2], Shucai Jiang[1], Baorui Guo[2], Lei Wang[2], Jiangwei Ding[2], Caibing Gao[1], Haigang Chang[1], Tao Sun[1,2] and Feng Wang[2,5]**

[1]Department of Neurosurgery, General Hospital of Ningxia Medical University, Yinchuan, China, [2]Ningxia Key Laboratory of Cerebro Cranial Disease, Incubation Base of National Key Laboratory, Ningxia Medical University, Yinchuan, China, [3]Department of Neurosurgery, The First Affiliated Hospital of Nanchang University, Nanchang, China, [4]Department of General Surgery, Chengdu Second Hospital, Chendu, China, [5]Department of Neurosurgery, The First Affiliated Hospital of Zhejiang University School of Medicine, Hangzhou, China

OPEN ACCESS

Edited by:
Mariela Fernanda Perez, National University of Cordoba, Argentina

Reviewed by:
Alejandra Pacchioni, National University of Rosario, Argentina
Zheng-Xiong Xi, National Institute on Drug Abuse (NIDA), United States

***Correspondence:**
Tao Sun
suntao_nxmu@163.com
Feng Wang
nxwwang@163.com

Specialty section:
This article was submitted to Neuropharmacology, a section of the journal Frontiers in Pharmacology

Received: 13 April 2021
Accepted: 28 June 2021
Published: 19 July 2021

Citation:
Zhu C, Tao H, Rong S, Xiao L, Li X, Jiang S, Guo B, Wang L, Ding J, Gao C, Chang H, Sun T and Wang F (2021) Glucagon-Like Peptide-1 Analog Exendin-4 Ameliorates Cocaine-Mediated Behavior by Inhibiting Toll-Like Receptor 4 Signaling in Mice. Front. Pharmacol. 12:694476. doi: 10.3389/fphar.2021.694476

Exendin-4 (Ex4), a long-lasting glucagon-like peptide-1 analog, was reported to exert favourable actions on inhibiting cocaine-associated rewarding and reinforcing effects of drug in animal models of addiction. However, the therapeutic potential of different dose of GLP-1 receptor agonist Ex4 in different behavioral paradigms and the underlying pharmacological mechanisms of action are incompletely understood. Herein, we firstly investigated the effects of Ex4 on cocaine-induced condition place preference (CPP) as well as extinction and reinstatement in male C57BL/6J mice. Additionally, we sought to elucidate the underlying pharmacological mechanism of these actions of Ex4. The paradigm of cocaine-induced CPP was established using 20 mg/kg cocaine or saline alternately during conditioning, while the reinstatement paradigm was modeled using 10 mg/kg cocaine on the reinstatement day. Different dose of Ex4 was administrated intraperitoneally either during conditioning or during extinction state or only on the test day. To elucidate the molecular mechanism underlying the potential effects of Ex4 on maladaptive behaviors of cocaine, the TLR4-related inflammation within the hippocampus was observed by immunofluorescence staining, and the expression levels of toll-like receptor 4 (TLR4), tumor necrosis factor (TNF)-α, and interleukin (IL)-1β were detected by Western blotting. As a consequence, systemic administration of different dose of Ex4 was sufficient to inhibit the acquisition and expression of cocaine-induced CPP, facilitate the extinction of cocaine-associated reward and attenuate reinstatement of cocaine-induced behavior. Furthermore, Ex4 treatment diminished expression levels of TLR4, TNF-α, and IL-1β, which were up-regulated by cocaine exposure. Altogether, our results indicated that Ex4 effectively ameliorated cocaine-induced behaviors likely through neurobiological mechanisms partly attributable to the inhibition of TLR4, TNF-α and IL-1β in mice. Consequently, our findings improved our

understanding of the efficacy of Ex4 for the amelioration of cocaine-induced behavior and suggested that Ex4 may be applied as a drug candidate for cocaine addiction.

Keywords: cocaine, condition place preference, extinction, reinstatement, exendin-4, neuroinflammation, toll-like receptor 4

INTRODUCTION

Addiction to drugs is an enormous health issue worldwide; approximately 19 million people worldwide were addicted to cocaine in 2018, corresponding to 0.4% of the global population aged 15–64 years (Niaz et al., 2020). Emerging surveys indicate that the proportion of cocaine consumption is climbing (Hughes et al., 2016). Cocaine addiction is a chronic brain disease characterized by high incidence of relapse to compulsive behavior following detoxification, regardless of catastrophic consequence (Leshner, 1997). However, the efficacy of available opioid receptor antagonists and therapeutic options for the treatment of cocaine use disorder has been shown to be limited (Jerlhag, 2019). Thus, there is a clear need to identify novel therapeutic drugs for the treatment of cocaine use disorder.

Glucagon-like peptide-1 (GLP-1) is commonly referred to as an incretin hormone and satiation factor secreted predominantly by enteroendocrine Lcells and preproglucagon neurons (Coller and Hutchinson, 2012; Hutchinson and Watkins, 2014), which exerts metabolic effects on energy homeostasis and food intake in preclinical studies (Holst, 2007; Barrera et al., 2011; Turton et al., 2016). GLP-1 is rapidly degraded by dipeptidyl peptidase-IV which is abundantly expressed in the central nervous system (Crews et al., 2017). GLP-1 is supposed to activate GLP-1 receptor (GLP-1R), a G-protein coupled receptor, to stimulate the secretion of insulin and block the secretion of glucagon in a nutrient-dependent way to achieve the goal of regulating glucose homeostasis (Holst, 2007). GLP-1 receptor is highly expressed throughout the whole brain including the hippocampus (Merchenthaler et al., 1999; Lathe, 2001; Hamilton and Lscher, 2009; Holst et al., 2011; Isacson et al., 2011; Richards et al., 2014), which is traditionally thought to be the main brain region of memory and learning (Bohbot and Corkin, 2007) and involved in substance use disorder (Meyers et al., 2003; Meyers et al., 2006; Olmo et al., 2006). These data indicate that GLP-1 is capable of interacting with and modulating hippocampus, which is part of mesolimbic reward system and implicated in addiction-like behavior (Kenny, 2011; Grill and Hayes, 2012; Williams and Elmquist, 2012; Hayes and Schmidt, 2016; Jerlhag, 2019). Nevertheless, the clinical utility of GLP-1 is limited due to its relatively short half-life. In contrast to GLP-1, its analogue exendin4 (Ex4) possesses a longer half-life (Gallwitz, 2004), and easily crosses the blood-brain barrier (Holscher, 2010). Therefore, Ex4 are widely applied for the treatment of type II diabetes and obesity (Drucker and Nauck, 2006; Hamilton and Lscher, 2009; Lovshin and Drucker, 2009; Eng et al., 2014; Richards et al., 2014; Pi-Sunyer et al., 2015; Andersen et al., 2018). In addition, Ex4 has also caused considerable interest in recent years because of the possible actions on ameliorating the maladaptive behavior of cocaine such as cocaine-induced CPP as well as locomotor activity, and self-administration (Hernandez and Schmidt, 2019). However, few studies have explored the underlying effects of GLP-1R agonist Ex4 on extinction as well as reinstatement and its possible molecular mechanisms to date.

Recently, GLP-1R agonists have received increasing attention due to its neuroprotective (Holst et al., 2011) and anti-inflammatory effects (Hattori et al., 2010; Campbell and Drucker 2013; Lee and Jun 2016; Géa et al., 2020). For instance, GLP-1R agonists reportedly inhibited oxidative stress and inflammatory mediators in animal model of diabetes (Wu et al., 2011). In addition, Ex4 has been confirmed to be effective in reducing indices of inflammation, including TLR4, tumor necrosis factor (TNF)-α, and interleukin (IL)-1β levels (Ajay et al., 2011). Moreover, GLP-1R agonists have been examined to have a profound impacts on cell proliferation, growth, survival, and repair in preclinincal study of neurodegenerative diseases (Gault and Hölscher 2018). For instance, the favorable effects of Ex4 has also been confirmed in treating many neurodegenerative diseases characterized by chronic neuroinflammation, such as Alzheimer's disease, Parkinson's disease, Huntington diseases, and amyotrophic lateral sclerosis (Li et al., 2009; Martin et al., 2009; Li et al., 2010; Yazhou et al., 2012). Interestingly, the neuroinflammation pertinent to the aberrant expression TLR4, IL-1β and TNF-α has also been validated to be heavily implicated in chronic cocaine consumption in growing studies (Sekine et al., 2008; Cearley et al., 2011; Clark et al., 2013; Hutchinson and Watkins, 2014; Northcutt, et al., 2015; Lacagnina et al., 2016). However, it remain unclear whether the suppressive ability of GLP-1R agonists Ex4 to mitigate neuroinflammation could be repurposed to ameliorate the cocaine-induced behavior in mice.

Indeed, neuroinflammation has been widely considered to be involved in many central nervous system (CNS) diseases (Block and Hong, 2005; Chen et al., 2006; Tansey et al., 2007). In search for new therapeutic drug targets for substance abuse, the neuroinflammation has been found to play a significant role in neural adaptations after chronic drugs exposure, and the anti-inflammatory ingredients may represent a novel and effective therapeutic approach for behavioral treatment of substance use disorders (Kohno et al., 2019). The primary pathway related to neuroinflammatory processes is triggered by pattern recognition receptors (PRR), including endogenous danger signals (DAMPs), and microbes or invading pathogens (MAMPs/PAMPs), which recognized the possible threats such as pathogen invasion or tissue damage. Toll like receptors (TLRs), the most common PRR, are mainly disturbed on microglia (Hanamsagar et al., 2012), which was expressed throughout brain with highest levels in hippocampus, basal ganglia, and substantia nigra (Lawson et al., 1990). Indeed, TLR4-mediated neuroinflammation has been shown to play a pivotal role in alcohol (June et al., 2015), morphine (Hutchinson 2012), and cocaine-associated

behaviors (Northcutt et al., 2015). Additionally, TLR4-mediated microglial activation promotes proinflammatory cytokine release including IL-1β and TNF-α (Brown et al., 2011) that were implicated in drug addiction (Correia et al., 2020). Therefore, neuroinflammation associated with TLR4, IL-1β, and TNF-α may play a pivotal role in substance abuse. For instance, these anti-inflammatory agents including naloxone Ibudilast and Minocycline have exerted promising actions in the treatment for substance use disorders (Garrido-Mesa et al., 2013; Ray et al., 2014; Northcutt, et al., 2015). Although these work have yielded intriguing outcomes, thus far, few studies has reported the effects of other anti-inflammatory agents on cocaine addiction (Correia et al., 2020). Consequently, we hypothesized that the favorable actions of GLP-1R agonists Ex4 as a novel anti-inflammatory agents on the amelioration of the maladaptive cocaine-induced behavior is exerted by suppressing TLR4-related neuroinflammation in mice.

To examine our hypothesis, we firstly evaluated the effects of Ex4 on modulating the acquisition and expression of cocaine-induced CPP as well as facilitating extinction and blocking reinstatement in animal model of cocaine-induced CPP. Finally, we attempted to explore the role of GLP-1R agonist Ex4 in reducing abnormal expression of TLR4, TNF-α, and IL-1β in hippocampus.

MATERIALS AND METHODS

Animals

Adult male C57BL/6J mice (18–22 g body weight) were provided by the Experimental Animal Center of Ningxia Medical University (China). All animals were housed in a specific pathogen-free environment under a 12-h light/dark cycle with lights on from 07:00 AM to 07:00 PM, a constant room temperature (20–25°C) and ambient humidity (50–60%), and free access to water and rodent food. In order to reduce the psychological stress induced by intraperitoneal injections, each mouse was kept in the testing room for 30 min on consecutive days before the beginning of each experiment. The experiment was initiated after acclimation for one week. The animal study was approved by the Ningxia Key Laboratory of Cerebrocranial Disease. All experimental procedures involving mice were implemented according to national, regional, and local laws and regulations, in accordance with the guidelines established by the Animal Research Ethics Committee of Ningxia Medical University. We took great care to minimize animal suffering and the number of animals used in this study.

Drugs and Antibodies

Cocaine-hydrochloride was obtained from China National Medicines Corporation Limited (Beijing, China) and was dissolved in sterile 0.9% physiological saline solution (0.9% NaCl) to a concentration of 4 mg/ml. The drug was freshly prepared for intraperitoneal (i.p.) administration at doses of 20 mg/kg body weight to induce the CPP paradigm or 10 mg/kg body weight to produce reinstatement of CPP. Saline was used as a vehicle solution. The GLP-1R agonist Ex4 was purchased from MedChemExpress (MCE, United States) and was diluted in 0.9% physiological saline solution at a concentration of 0.6 μg/ml. Ex4 was freshly prepared at 100.0, 30.0, 1.0, and 0.1 μg/kg body weight which has been shown to significantly decrease the rewarding effects of cocaine (Reddy et al., 2016.; Hernandez and Schmidt, 2019). Injections of Ex4 and cocaine-HCl were alternatively performed on the left or right side of the peritoneum. Ex4 was administered 1 h before repeated injections of cocaine (20 mg/kg, i.p.) or saline (5 ml/kg), and cocaine was administered immediately before the commencement of the trial. Although cocaine was injected only on the conditioning day, Ex4 was injected every day for 8 days. Primary antibodies, including anti-TLR4, anti-IL-1β, and anti-TNF-α antibodies, were purchased from Abcam (San Francisco, CA, United States). To evaluate the protein expression of TLR4 and components of pro-inflammatory (TNF-α and IL-1β) signaling pathways in the hippocampus, mice received 20 mg/kg of cocaine (Rodríguez-Arias et al., 2009; Araos et al., 2015). The cocaine-induced CPP paradigm was established to examine cocaine CPP extinction and reinstatement using 20 mg/kg (conditioning session) and 10 mg/kg (priming dose, reinstatement session). The dose for conditioning (20 mg/kg, i.p.) was chosen because it elicits strong CPP behavior (Meye et al., 2016; Ladrón de Guevara-Mirand et al., 2018). During the experiments, solutions and drugs were stored at 4°C, and antibodies were stored at −20°C.

Experimental Design and Procedures

In our experiment, cocaine (20 mg/kg) or an equal volume of saline (5 ml/kg) were administered by intraperitoneal injection on alternate days. There were four different phases in our study: 1) preconditioning phase; 2) conditioning (training/acquisition); 3) extinction, conducted 8 days after the test 2, when the CPP score was determined, followed by drug administration; and 4) reinstatement, which occurred 24 h after the last extinction and was used to investigate reinstatement of cocaine-induced CPP by cocaine priming (10 mg/kg body weight) on the challenge day. The tests of CPP score were performed on days 2, 10, 14, 19, and 20. Mice were sacrificed, and hippocampus tissues were collected after behavioral examinations for western blot analyses (n = 5 mice/group) or immunofluorescence staining (n = 3 mice/group). During the experiment, none of the mice died.

Conditioning Apparatus

The general procedure for the CPP was performed as previously described, with slight modifications (Meye et al., 2016). Briefly, the conditioning for CPP was performed using a shuttle apparatus consisting of two equally sized larger compartments (24 cm length × 14 cm width × 30 cm height) separated by a smaller compartment (7.0 cm length × 7.0 cm width × 30 cm height) with retractable guillotine doors; the larger compartment contained four black walls and a smooth black floor, the other compartment contained four white walls and a rough white floor covered with blue sandpaper. The two larger compartments had different visual and tactile cues. The gray central corridor contained twogray walls and a smooth floor leading into the corresponding compartment. The removable guillotine doors

separated the three compartments to prevent animals from crossing the chambers and were raised on test days. Tracking of the mice in the apparatus was performed using an infrared video camera suspended approximately 1 m above the test arena. The overhead infrared camera and computer were used to record the real-time positions of the mice and their movement throughout the three compartments. The time spent in each chamber and total distance traveled were recorded using a computerized video tracking system (video behavior analysis software Smart 3.0; Panlab, Spain; supported by RWD Life Science Co., Ltd., China).

Pre-Conditioning Stage (days 1–2)

On days 1–2, all mice were positioned in the middle area of the apparatus and permitted to freely explore all three compartments for 45 min prior to the commence of the experiment. Following habituation, the mice were again placed in the middle intersection of the chambers and allowed to explore freely for 20 min; their time spent in a white chamber (referred as non-preferred chamber) were recorded to set their basal preference. After completion of this test, biased mice with their time in any compartment more than 960 s or less than 240 s were excluded, and then these mice were randomly separated into four groups in response to the requirement of different experiments.

Conditioning Stage (days 3–10)

On days 3–10, cocaine conditioning was conducted with cocaine (20 mg/kg, i.p.) or saline (5 ml/kg, i.p.) for 8 days, including four drug sessions and four saline sessions. Animals On days 3, 5, 7, and 9, mice were administered cocaine and then instantly confined to the designed cocaine- or saline-paired compartments by closing the removable guillotine doors for 45 min after treatment. The white compartment of the CPP cage in this trial was defined as the cocaine-paired compartment. On days 4, 6, 8, and 10, mice were confined to the opposite compartment for the same amount of time following saline injection. In this phase, all animals were conditioned once a day. Place preference testing was performed after an 8-days conditioning period. During this test, the mice were habituated in the center corridor and freely moved throughout the apparatus for 20 min. After the mice completed the test, mice were sacrificed for analysis by western blotting or immunofluorescence staining. The remaining mice were returned to their cages. The CPP score was calculated as the time spent in the cocaine-paired chamber during the test of 20 min. CPP was considered to be achieved when the CPP score was significantly higher on CPP tests than baseline preference.

Condition Place Preference Extinction (days 11–19)

Following the acquisition and expression of cocaine-induced CPP, all animals were subjected to extinction training for eight days. During the extinction period, mice were not administered cocaine or Ex4 and were confined in the cocaine-paired compartment or saline-paired compartment for 45 min on alternate days. CPP testing of extinction was performed on day 19 to analyze the effects of treatment with Ex4 on extinction responses to cocaine-induced CPP after 8 days of extinction training. In this study, extinction was achieved when there was no significant difference in CPP scores compared to pretest. No drug treatments were performed on the test day. After the mice completed the test, these mice were returned to animal cages.

Reinstatement of Condition Place Preference (day 20)

Following eight days of extinction, mice who had been previously conditioned with cocaine and achieved extinction criterion were primed with a half dose of cocaine (10 mg/kg, i.p.). The reinstatement test was initiated to analyze the effects of Ex4 treatment on the reinstatement of the cocaine-elicited CPP. For the saline-conditioned control group, mice were primed with saline (5 ml/kg, i.p.).

Locomotor Activity

The general procedure used for locomotor activity was similar to a previously described procedure (Meye et al., 2016). Locomotor activity as total distance that each mice traveled in chambers during the 20 min was recorded while animals were subject to the behavioral testing session above.

Western Blotting Analysis

After completing the behavioral experiment, mice were euthanized by cervical dislocation, and their brains were immediately removed, flash-frozen in liquid nitrogen, and stored at −80°C. Western blotting was performed to determine the hippocampal expression levels of TLR4, TNF-α, and IL-1β proteins after drug addiction. Hippocampal tissue samples (~50 mg) were prepared, ground in a homogenizer, and extracted using a BCA Protein Extraction Kit (cat. no. KGP2100; KeyGEN Biotechnology Co., Ltd., Jiangsu, China). Protein samples from each group were then separated by sodium dodecyl sulfate-polyacrylamide gel electrophoresis and transferred to polyvinylidene difluoride membranes (Millipore, United States). The membranes were blocked with 5% skim milk powder for 2 h at room temperature and then incubated in primary antibodies targeting TLR4 (1:1,000; Abcam), TNF-α (1:1,000; Abcam), IL-1β (1:500; Bioworld Technology), and β-actin (1:2,000; Abcam) for more than 24 h at 4°C. Membranes were then washed three times for 5 min each in TBST and incubated with the corresponding secondary antibody (1:1,000) at room temperature for 2 h. Enhanced chemiluminescence reagent was used to detect proteins, and the ratio of the gray value of the target protein band to the gray level of the β-actin band was used to quantify the relative expression level of the target protein. Normalized methods were used for Western blot quantification in order to minimize the impact of variations of experimental error. At great length, the stained blot was imaged, line was drawn around the target protein (TLR4, TNF-α, and IL-1β) or β-actin in each lane, and then the grayscale values were measured using Image J software. The relative value of each of the target protein levels was expressed

as the gray values of each target protein divided by the corresponding β-actin. By this means, the relative gray values in different groups was calculated, and then it was divided by the saline group. Ultimately, the normalizing Western blot results of the protein in four groups was procured.

Immunofluorescence Staining

Following completion of behavioral tests, mice were euthanized by cervical dislocation, and their brains were immediately removed and flash-frozen in ice-cold isopentane. Next, 20-μm-thick slices were collected from the dorsal hippocampus, thaw-mounted on slides, and stored at −80°C until use. Specimens were dehydrated with sucrose, frozen, and then soaked in phosphate-buffered saline solution for 10 min. Tissue sections were then treated with 3% hydrogen peroxide and incubated with 3% bovine serum albumin, followed by incubation with anti-TLR4 antibodies (1:1,000) overnight at 4°C. After washing, the sections were incubated in secondary antibodies at room temperature for 1 h, and nuclei were stained with 4′,6-diamidino-2-phenylindole (Cat. no. ZLI-9557; ZSGB-BIO, Beijing, China). Images were captured with a Leica DM6 fluorescence microscope (Leica, Germany) and the fluorescence density among different groups was compared using Image J, which was similar to the literature (Jensen, 2013).

Statistical Analysis

GraphPad Prism 8.4.0 (GraphPad Software) and SPSS 23.0 were used for statistical analysis for all experiments. All data are presented as means ± standard errors of the means. The data from cocaine-induced CPP between pre-conditioning and post-conditioning was analyzed using paired t-test. One-way repeated measures analysis of variance (ANOVA) was also used to analyze the statistical significance of effects of Ex4 on cocaine-induced CPP and TLR4, TNF-α, IL-1β proteins in the hippocampus. *Post hoc* analyses of significant effects were conducted using the Tukey's, Dunnett's or Bonferroni test. For multiple groups comparison, two-way ANOVA with one repeated measurement was performed between-subjects factors of drug treatment and within-subjects factors of test session. Student's t-test was used for comparisons between independent groups. Differences with p values < 0.05 were considered statistically significant.

RESULTS

Effects of Ex4 Pretreatment on the Acquisition of Cocaine-Induced Condition Place Preference

We firstly examined the role of repeated pretreatment of Ex4 (100.0, 1.0, and 0.1 μg/kg) in the acquisition of cocaine-induced CPP. Each mouse was pretreated with saline (5 ml/kg) or Ex4 60 min before i.p. injection of cocaine or saline and was then treated with an i.p. injection of cocaine-HCl (20 mg/kg) or an equal volume of saline (5 ml/kg) during the cocaine conditioning period alternately every other day. The implemention of experimental timeline was described as in **Figure 1A**. Four out of 36 mice were excluded because they spent less than 240 s or more than 960 s in any chamber in the state of pretest. And then the remaining 32 mice were then randomly assigned to four independent groups: vehicle, Ex4 (100.0 μg/kg), Ex4 (1.0 μg/kg), and Ex4 (0.1 μg/kg) groups, and experienced eight-days CPP training. Vehicle (saline 1 ml/kg) and Ex4 (100.0, 1.0, and 0.1 μg/kg) were administered to animals in the vehicle and Ex4 treatment groups 1 h before injection of cocaine or saline. As shown in **Figure 1B**, a paired t-test showed that after experiencing 8-days of cocaine CPP training, cocaine induced a significant increase in CPP score in vehicle group compared to the baseline preference (t_7 = 6.636, $p < 0.001$). However, cocaine failed to produce the similar CPP response in the Ex4 groups at the dose of 10 μg/kg (t_7 = 1.748, $p > 0.05$), Ex4 1 μg/kg (t_7 = 1.527, $p > 0.05$), and Ex4 0.1 μg/kg (t_7 = 1.876, $p > 0.05$). Furthermore, a one-way ANOVA (repeated measures) showed that there was a statistical difference in time spent in the cocaine-paired chamber among these four groups [$F_{(3,31)}$ = 15.12, p = 0.0002, **Figure 1B**], and Dunnett's multiple comparisons *post hoc* analysis revealed that Ex4 at the dose of 10.0 μg/kg (p = 0.0035), 1.0 μg/kg (p = 0.0027), and 0.1 μg/kg (p = 0.0089) significantly decreased the CPP score in comparison with the vehicle group. Therefore, these results suggest that Ex4 pretreatment prevents the acquisition of cocaine-induced CPP.

Effects of a Single Injection of Ex4 on the Expression of Cocaine-Induced Condition Place Preference

We further investigated the impacts of a single infusion of Ex4 on the expression of cocaine-induced CPP. As shown in **Figure 3A**, the general procedure of this experiment protocol was similar to experiment one except that Ex4 was intraperitoneally injected at dose of 100.0, 1.0, and 0.1 μg/kg only on the CPP test day. In total, there are 4 mice were discarded because of original room bias. Subsequently, the remaining animals were separated into four independent groups and exposed to the next 8-days of cocaine-associated CPP training, and CPP test. As shown in **Figure 2B**, a paired t-test showed that cocaine induced a significant elevation in CPP score in the vehicle group when compared to the initial preference (t_7 = 4.709, p = 0.0022). However, cocaine had no significant effects in the Ex4 groups at the dose of 10 μg/kg (t_7 = 1.612, $p > 0.05$), Ex4 1 μg/kg (t_7 = 1.355, $p > 0.05$), and Ex4 0.1 μg/kg (t_7 = 1.759, $p > 0.05$). Furthermore, a one-way ANOVA (repeated measures) revealed a statistical difference in time spent in the cocaine-paired chamber among these groups [$F_{(3,31)}$ = 16.96, p = 0.0013, **Figure 2B**], and Dunnett's multiple comparisons *post hoc* analysis showed that Ex4 at the dose of 100.0 μg/kg (p = 0.0090), 1.0 μg/kg (p = 0.0086) and 0.1 μg/kg (p = 0.0046) produced significant reduction in the CPP score in comparison with the vehicle group. Thus, these results indicate that an acute single injection of Ex4 inhibits the expression of cocaine-induced CPP.

Effects of Repeated Injection of Ex4 on the Extinction and Reinstatement of Cocaine-Induced Condition Place Preference

We assessed the ability of post-extinction Ex4 to modulate the extinction and reinstatement of cocaine-induced CPP. The general

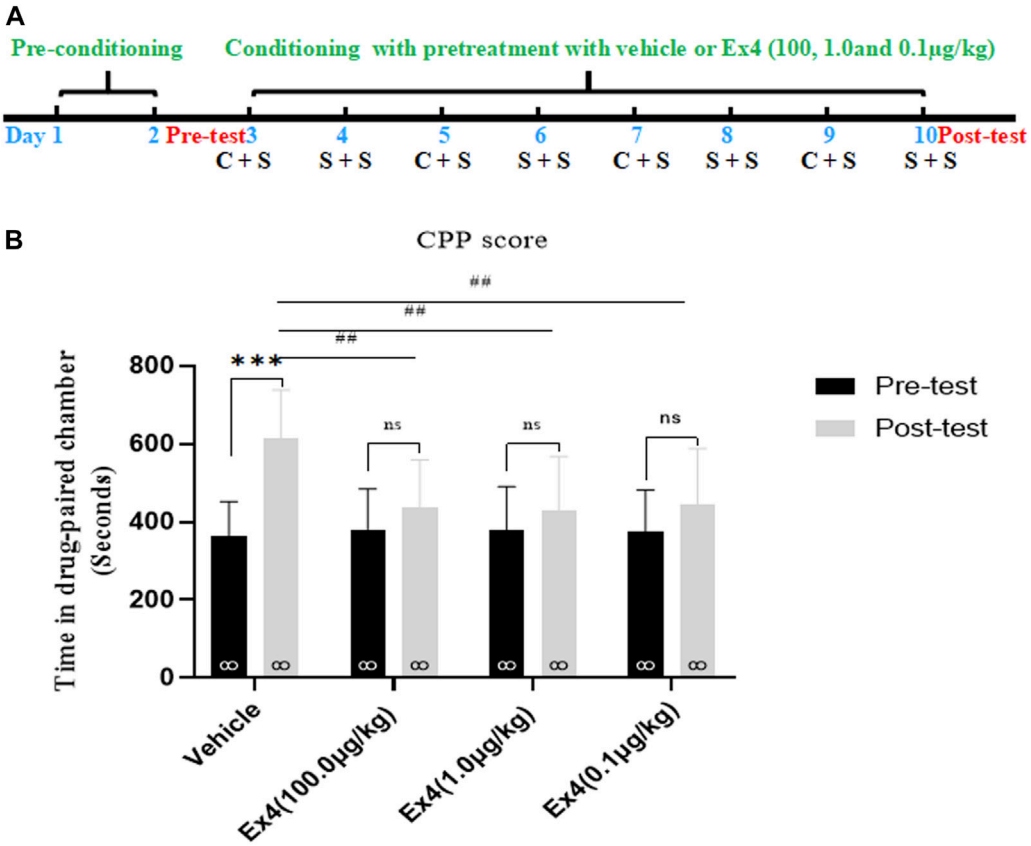

FIGURE 1 | Ex4's pretreatment prevents the acquisition of cocaine-induced CPP. **(A)** The experimental schedule for saline (S) as well as cocaine (C) and Ex4 treatments. **(B)** CPP scores following systemic treatment with vehicle and Ex4 (100, 1.0, and 0.1 μg/kg) during cocaine conditioning show that cocaine induced a significant CPP that was prevented by Ex4 pretreatment. *** represents $p < 0.001$ vs pretest, ns represents no significant difference, paired t-test. ## represents $p < 0.01$ vs vehicle, one-way ANOVA followed by a Dunnett's *post hoc* test. All data are presented as the mean ± SEM.

experimental flow as well as Ex4 and cocaine treatments were performed as shown in **Figure 2A**. In total, 21 mice were ruled out from this experiment. Animals were randomly separated into four groups and conditioned to cocaine (20 mg/kg, ip) on alternating days. After completion of 8-days of consecutive CPP training, a room preference for the cocaine-paired chamber was established in all groups when compared with the CPP responses in the preconditioning phase ($p < 0.001$ for vehicle, 100.0, 1.0, and 0.1 μg/kg Ex4 groups, Student's t-test **Figure 3B**). Subsequently, mice were daily treated with Ex4 (10.0, 1.0, and 0.1 μg/kg) or vehicle immediately after each extinction session. In test 1, the CPP was incompletely extinguished when compared with the CPP responses in the preconditioning state ($p = 0.0038$ for vehicle group, Student's t test **Figure 3B**). Additionally, one-way rmANOVA showed that there was a significant difference among four groups in the test 1 [$F_{(3,42)} = 3.547$, $p = 0.0230$, **Figure 3B**], and Dunnett's multiple comparisons *post hoc* analysis revealed that the CPP score was reduced by Ex4 at dose of 10.0 μg/kg ($p = 0.0320$), 1.0 μg/kg ($p = 0.0162$), and 0.1 μg/kg ($p = 0.0454$) compared to the vehicle group. These results illustrated that repeated administration of Ex4 strengthened the extinction. Different from test 1, the CPP was completely extinguished in test 2 when compared with the CPP responses in the preconditioning stage ($p > 0.05$ for vehicle, 100.0, 1.0, and 0.1 μg/kg Ex4 groups, Student's t test **Figure 3B**). Further, the effects of post-extinction Ex4 on the reinstatement of cocaine-CPP was observed. On the reinstatement day, priming with cocaine (10 mg/kg, ip) in the vehicle group produced a reinstatement of the cocaine-induced CPP ($t_{21} = 5.294$, $p < 0.001$, Student's t-test). One-way repeated measures ANOVA revealed a statistical difference in the CPP score among vehicle and Ex4 treatment groups [$F_{(3,32)} = 5.643$, $p = 0.0036$, one-way rmANOVA, **Figure 3B**], and Dunnett's multiple comparisons showed that the CPP response was significantly attenuated by the administration of Ex4 at dose of 10.0 μg/kg ($p = 0.0039$), 1.0 μg/kg ($p = 0.0044$), and 0.1 μg/kg ($p = 0.0348$), indicating that Ex4inhibited the reinstatement. Altogether, these results suggest that repeated injection of Ex4 during extinction promotes the extinction and attenuate the reinstatement of cocaine-induced CPP.

Effects of Single Injection of Ex4 on the Reinstatement of Cocaine-Induced Condition Place Preference

We next examined the actions of single administration of Ex4 on the reinstatement of cocaine-induced CPP. The general

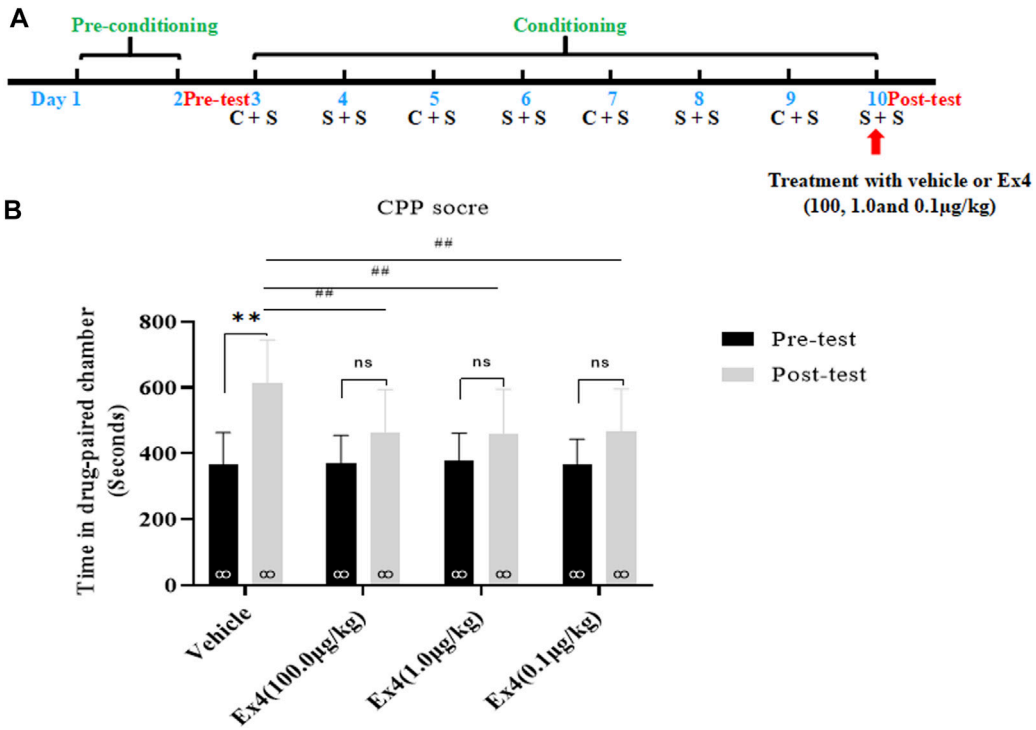

FIGURE 2 | Ex4's single treatment blocks expression of cocaine-induced CPP. **(A)** The experimental schedule for saline (S) as well as cocaine (C) and Ex4 treatments. **(B)** CPP scores following a single treatment withvehicle and Ex4 (100, 1.0, and 0.1 μg/kg) on the CPP test day show that cocaine induced a significant CPP that was blocked by systemic Ex4 treatment. ** represents $p < 0.01$ vs pretest, ns represents no significant difference, paired t-test. ## represents $p < 0.01$ vs vehicle, one-way ANOVA followed by a Dunnett's *post hoc* test. All data are presented as the mean ± SEM.

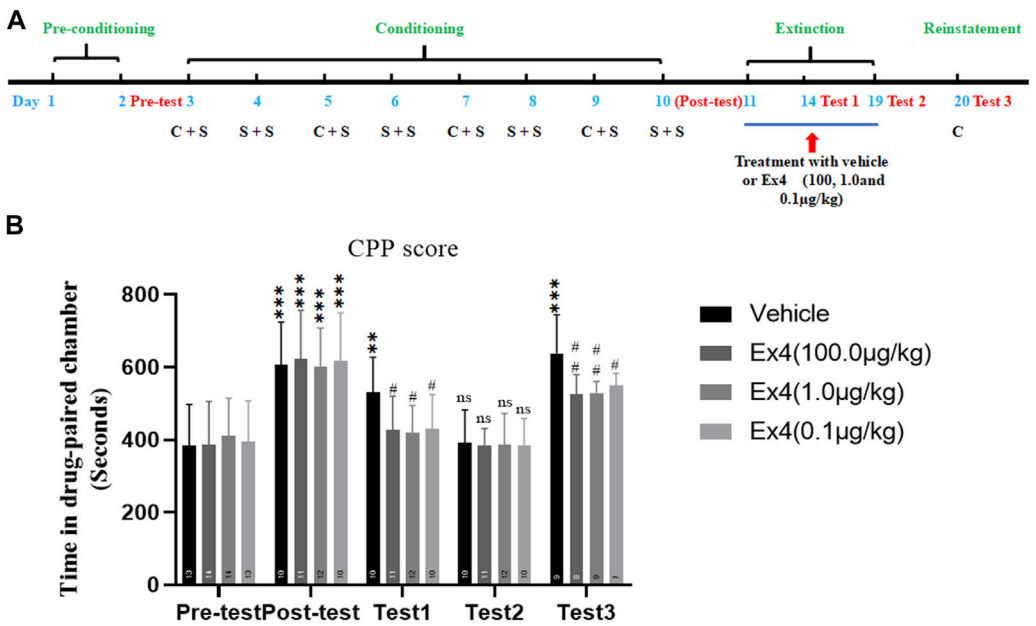

FIGURE 3 | Ex4's chronic treatment facilitates extinction and inhibits reinstatement of cocaine-induced CPP. **(A)** The experimental schedule for saline (S) as well as cocaine (C) and Ex4 treatments. **(B)** CPP scoresfollowing systemic treatment with vehicle and Ex4 (100, 1.0, and 0.1 μg/kg) during the extinction show thatpost-extinction Ex4 treatment facilitates extinction of CPP and inhibits cocaine-primed reinstatement comparedto the vehicle group. ** and *** represent $p < 0.01$ vs pretest and $p < 0.01$ vs pretest, ns represents no significantdifference, Student's t test. # and ## represent $p < 0.05$ vs vehicle and $p < 0.01$ vs vehicle, one-way ANOVA followed by a Dunnett's *post hoc* test. All data are presented as the mean ± SEM.

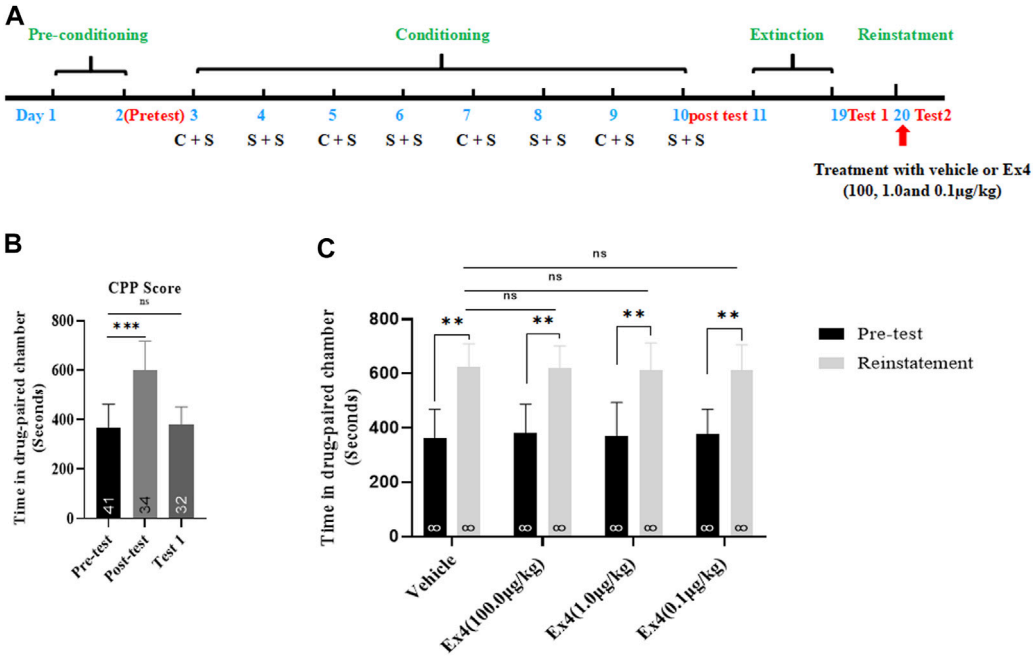

FIGURE 4 | Ex4's single treatment does not attenuate reinstatement of cocaine-induced CPP. **(A)** The experimental schedule for saline (S) as well as cocaine (C) and Ex4 treatments. **(B)** CPP scores following cocaine conditioning and extinction show that compared to the pretest cocaine treated mice ($n = 34$) induced asignificant CPP, which was extinguished by extinction training. *** represents $p < 0.001$ vs pretest, ns represents no significant difference, Student's t-test. **(C)** CPP scores following an acute single treatment with vehicle and Ex4 (100, 1.0, and 0.1 μg/kg) on the reinstatement day show that animals treated with Ex4 ($n = 8$) have no significant effects on preventing cocaine-triggered reinstatement compare to vehicle ($n = 8$). ** represents $p < 0.01$ vs pretest, paired t-test. ns represents no significant difference, one-way ANOVA followed by a Dunnett's *post hoc* test. All data are presented as the mean ± SEM.

experimental timeline was shown in **Figure 4A**. From preconditioning to extinction session, a total of 9 mice were excluded. As shown in **Figure 4B**, a Student's t-test showed that the overwhelm majority of animals exhibited a strong place preference for the cocaine-paired chamber after they were subject to the consecutive eight-days of CPP training ($t_{74} = 9.65$, $p < 0.001$). The extinction standard was achieved because there is no difference in CPP score between the test 1 and the pretest ($t_{72} = 0.5814$, $p = 0.5628$, Student's t-test, **Figure 4B**). Next, these animals were randomly divided into four independent groups and received vehicle or different dose of Ex4 (10.0, 1.0 and 0.1 μg/kg) on the challenge day to investigate the effects of single infusion of Ex4 on the cocaine-primed reinstatement of CPP. As a result, half dose of cocaine produced a significant place preference for the cocaine-paired chamber among all groups regardless of Ex4 treatment ($p = 0.0033$, $p = 0.0022$, $p = 0.0028$ and $p = 0.0025$ for vehicle, 100.0, 1.0 and 0.1 μg/kg Ex4, respectively, Paired t test, **Figure 4C**). Furthermore, as shown in **Figure 4C**, one-way rmANOVA showed that there was no significant induction among these groups when compared to the vehicle group [$F_{(3,31)} = 0.1448$, $p = 0.8364$], and Dunnett's multiple comparisons *post hoc* analysis also revealed that this CPP response can not be blocked by single administration of Ex4 at dose of 10.0 μg/kg ($p = 0.9277$), 1.0 μg/kg ($p = 0.9574$), and 0.1 μg/kg ($p = 0.8993$). Consequently, these results indicate that single infusion of Ex4 fails to attenuate the reinstatement of cocaine-induced CPP.

Effects of Ex4 Pretreatment on the Acquisition of the Cocaine-Induced Condition Place Preference and Aberrant Expression of TLR4, TNF-α, and IL1-β in the Hippocampus

The experimental schedule for Ex4 and cocaine treatments was described in **Figure 5A**. Six mice were ruled out from the present experiment. At the end of the pretest, mice were randomly divided into four groups including Sal + Sal (pretreatment with saline injection 1 h prior to saline administration), Coc + Sal (pretreatment with an equal volume of saline 1 h prior to cocaine administration), Sal + Ex4 (pretreatment with Ex4 1 h prior to saline administration), and Coc + Ex4 (pretreatment with the same dose of Ex4 as for the Sal + Ex4 group 1 h before cocaine administration), and then underwent the following eight days of cocaine-CPP training. As shown in **Figure 5B**, one-way rmANOVA showed that there was significant difference among these groups after a cocaine CPP training [$F_{(3,31)} = 8.990$, $p = 0.0062$]. In addition, Bonferroni *post hoc* analysis also revealed that cocaine produced a significant CPP compared to the Sal + Sal group ($p < 0.001$), and that this CPP response was attenuated by Ex4 pretreatment ($p = 0.0039$) compared to the Coc + Sal group. As shown by Bonferroni *post hoc* analysis, the CPP score in Ex4+Sal group does not differ from the Sal + Sal group ($p > 0.05$), suggesting that Ex4 treatment alone during CPP

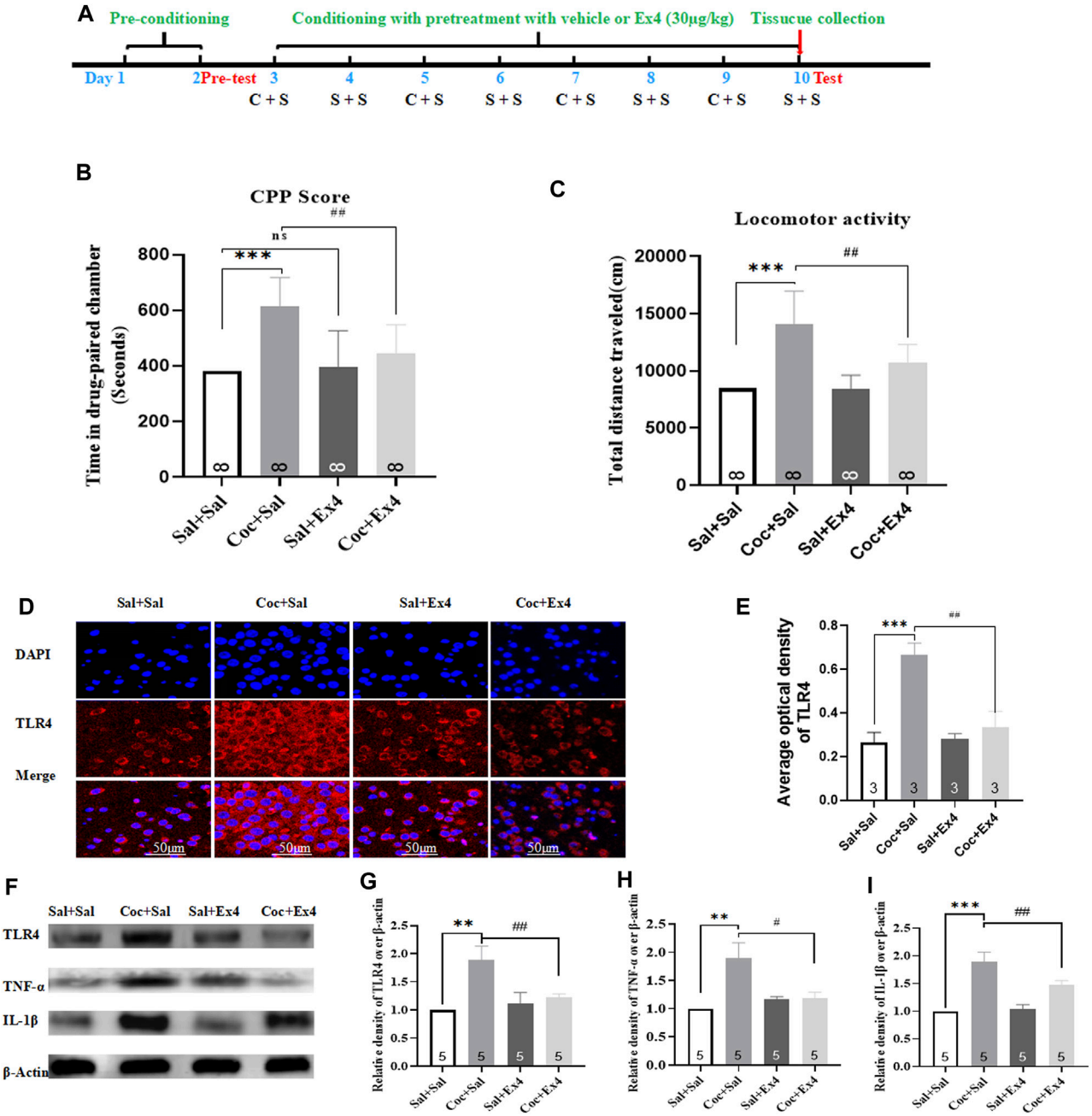

FIGURE 5 | Ex4's pretreatment inhibits the acquisition of cocaine-induced CPP and alleviates expression levels of TLR4, TNF-α and IL-1β. **(A)** The experimental schedule for saline (S) as well as cocaine (C) and exendin-4 treatment. **(B)** CPP scores following cocaine conditioning with systemic treatment with saline and Ex4 (30.0 μg/kg) show that compared to Sal+Sal group cocaine induced a significant CPP that was lessened by Ex4 treatment. *** represents $p < 0.001$ vs Sal+Sal, ## represent $p < 0.01$ vs Coc+Sal, ns represents no significant difference, one-way ANOVA followed by a Bonferroni's *post hoc* test. **(C)** Locomotor activity following cocaine conditioning with systemic pretreatment with saline and Ex4 (30.0 μg/kg) show that a hyperactivity induced by cocaine was reduced by Ex4 treatment. *** represents $p < 0.001$ vs Sal+Sal , ## represent $p < 0.01$ vs Coc+Sal, one-way ANOVA followed by a Bonferroni's *post hoc* test. **(D)** Representative images of immunofluorescent staining with TLR4 (red), and DAPI (blue) in the hippocampus from the different groups (scale bar = 50 μm). Systemic administration of Ex4 diminished fluorescence density of TLR4 up-regulated by cocaine exposure ($n = 3$ in each group). **(E)** Semiquantitative analysis of the relative density of TLR4 by densitometric analysis in different groups. *** represents $p < 0.001$ vs Sal+Sal, ## represent $p < 0.01$ vs Coc+Sal, one-way ANOVA followed by a Tukey's *post hoc* test. **(F)** Representative immunoblots of TLR4, TNF-α and IL-1β proteins in different groups ($n = 5$ in each group). **(G)** Semiquantitative analysis of the relative levels of TLR4 by densitometric analysis in different groups. *** represents $p < 0.001$ vs Sal+Sal , ## represent $p < 0.01$ vs Coc+Sal, one-way ANOVA followed by a Tukey's *post hoc* test. **(H)** Semiquantitativeanalysis of the relative levels of TNF-α by densitometric analysis in different groups. ** represents $p < 0.01$ vs Sal+Sal, # represent $p < 0.05$ vs Coc+Sal, one-way ANOVA followed by a Tukey's *post hoc* test. **(I)** Semiquantitative analysis of the relative levels of IL-1β by densitometric analysis in different groups. *** represents $p < 0.001$ vs Sal+Sal, ## represent $p < 0.01$ vs Coc+Sal, one-way ANOVA followed by a Tukey's posthoc test. All data are presented as the mean ± SEM. Sal indicates saline. Coc indicates cocaine. Ex4 indicates Exendin-4.

conditioning did not produce CPP paradigm compared to the Sal + Sal group. Similar to CPP response, Ex4 pretreatment had a statistically significant effect on the hyperactivity elicited by cocaine was observed [$F_{(3,31)}$ = 16.44, p = 0.0008, **Figure 5C**], and Bonferroni *post hoc* analysis indicated that cocaine increased the locomotion compared to the Sal + Sal group (p = 0.0004, **Figure 5C**) that was reduced by Ex4 compared to the Coc + Sal group (p = 0.0079). Overall, these findings showed that the strong CPP response and cocaine conditioned locomotion were attenuated by Ex4 pretreatment.

After the completion of test, all animals were sacrificed and the hippocampus tissues was harvested to detect the expressions levels of TLR4, TNF-α, and IL1-β using Western blot and immunofluorescence staining. The reason why we chose hippocampus is that it has been considered the center of the learning of associations between the environmental context and unconditioned stimuli in mammals (Bohbot and Corkin, 2007; Kim and Fanselow, 1992). Immunofluorescence staining demonstrated that neuronal lesions caused by cocaine re-exposure in the hippocampus were repaired by Ex4 treatment (**Figures 5D,E**). As depicted in **Figure 5E**, TLR4 was presented in the cytoplasm and repeated administration of cocaine produced different fluorescence density of TLR4 [$F_{(3,11)}$ = 254.0, p = 0.0032, one-way ANOVA], and Tukey's multiple comparisons test showed that higher density of TLR4 caused by cocaine was significantly reversed by Ex4 treatment (p = 0.0031). In line with the results of immunofluorescence staining, Western blotting also showed that there was a statistical difference in the relative expression of TLR4 among these groups [$F_{(3,19)}$ = 42.27, p = 0.0002, one-way ANOVA, **Figures 5F,G**], and Tukey's *post hoc* analysis revealed that the protein overexpression produced by cocaine was significantly decreased by Ex4 (p = 0.0097). Activation of TLR4 facilitates the release of pro-inflammatory cytokine such as IL-1β and TNFα (Brown et al., 2011). Similar to the results of TLR4, Tukey's multiple comparisons *post hoc* analysis indicated that cocaine produced the higher protein levels of TNF-α (p = 0.0057, one-way ANOVA, **Figure 5H**) and IL1-β (p = 0.0009, one-way ANOVA, **Figure 5I**). Interestingly, compared to the Coc + Sal group, Ex4 significantly alleviated the expression levels of TNF-α (p = 0.0326, one-way ANOVA followed by Tukey's multiple comparisons test, **Figure 5H**) and IL1-β (p = 0.0233, one-way rmANOVA followed by Tukey's multiple comparisons test; **Figure 5I**). Taken together, these results revealed that Ex4 pretreatment suppressed the indices of inflammation (TLR4, TNF-α, and IL1-β) within the hippocampus.

Effects of Ex4 on the Reinstatement of the Cocaine-Induced Condition Place Preference, Locomotor Activity, and Aberrant Expression of TLR4, TNF-α, and IL1-β

The timeline was depicted in **Figure 6A**. There are a total of eight animals were excluded because of CPP training failure. Afterward, the remaining 32 mice were randomly divided into two groups including Sal + Sal group (administrated with saline alone during conditioning) and Coc + Sal group (administrated with saline and Coc during conditioning). As shown in **Figure 6B**, most animals spent more time in the cocaine-paired chamber after cocaine CPP training (t_{55} = 9.631, p < 0.001, Student's t-test), revealing that mice treated with repetitive administration of cocaine (20 mg/kg) induced a significant CPP score (609.3 ± 92.3 s) when compared to the CPP responses in the pretest (381.6 ± 51.2 s). However, repeated administration of saline failed to induce a CPP (t_{54} = 0.067, p > 0.05, Student's t-test). Subsequently, all mice were subject to Ex4 or saline treatments daily administrated immediately after each extinction session and divided into four groups including Sal + Sal group, Coc + Sal group, Sal + Ex4 group and Coc + Ex4 group to assess the effects of Ex4 on the extinction and reinstatement of cocaine-induced CPP. The CPP response of the mice showed an significant difference among these groups [treatment: $F_{(1, 28)}$ = 7.933, p = 0.0088; test: $F_{(3,28)}$ = 5.299, p = 0.0051; interaction $F_{(3,28)}$ = 3.032, p = 0.0458; two-way rmANOVA, **Figure 6C**], and Bonferroni's multiple comparisons test indicated that the CPP score of the Coc + Sal group remains higher than the Sal + Sal group (p = 0.003). On one hand, these results suggested that administration of Ex4 had a significant effect on the extinction of CPP. On the other hand, these results also revealed that the CPP response was not completely extinguished in test 1. As shown in **Figure 6C**, however, on test 2, two-way rmANOVA followed by Bonferroni's multiple comparisons test revealed that animals among these groups had no difference in CPP score when compared to the Sal + Sal group (p > 0.05), indicating that they achieved extinction criteria. Similarly, there is a statistical difference in locomotor activity among there groups [treatment: $F_{(1, 28)}$ = 8.904, p = 0.0099; test: $F_{(3,28)}$ = 6.127, p = 0.0046; interaction $F_{(3,28)}$ = 6.265, p = 0.0013; two-way rmANOVA, **Figure 6D**]. Subsequently, we observed the effects of chronic Ex4 treatment on the cocaine-induced reinstatement of CPP. On the reinstatement test day, one-way rmANOVA showed that there was significant difference in CPP score among these groups after priming with half dose of cocaine [$F_{(3,31)}$ = 21.56, p < 0.001, **Figure 6E**], and Bonferroni *post hoc* analysis revealed that compared to the Sal + Sal group cocaine produced a significant CPP (p = 0.0008) that was attenuated by Ex4 treatment (p = 0.0081). Additionally, one-way rmANOVA also showed that there was significant difference among these groups after priming with half dose of cocaine [$F_{(3,31)}$ = 42.01, p < 0.001, **Figure 6F**], and Bonferroni *post hoc* analysis revealed that compared to the Sal + Sal group cocaine significantly increased locomotor activity (p = 0.0009) that was attenuated by Ex4 treatment (p = 0.0426). Overall, these results indicate that post-extinction Ex4 does not only inhibit the reinstatement of cocaine-CPP but also reduced the locomotion elicited by priming with cocaine on the reinstatement day.

Following the reinstatement test, the molecular mechanisms of these therapeutic actions of Ex4 were evaluated using Western blotting and immunofluorescence staining. As shown in **Figures 6G,H**, the Sal + Sal, Coc + Sal group, Sal + Ex4 and Coc + Ex4 groups displayed different fluorescence intensity [$F_{(3,11)}$ = 421.3, p = 0.0002, one-way ANOVA], and Tukey's multiple comparisons *post hoc* analysis showed that the fluorescence intensity of TLR4 which was enhanced by cocaine (p = 0.0003) was significantly attenuated by Ex4 (p = 0.0063). Similar to result of immunofluorescence staining, Western

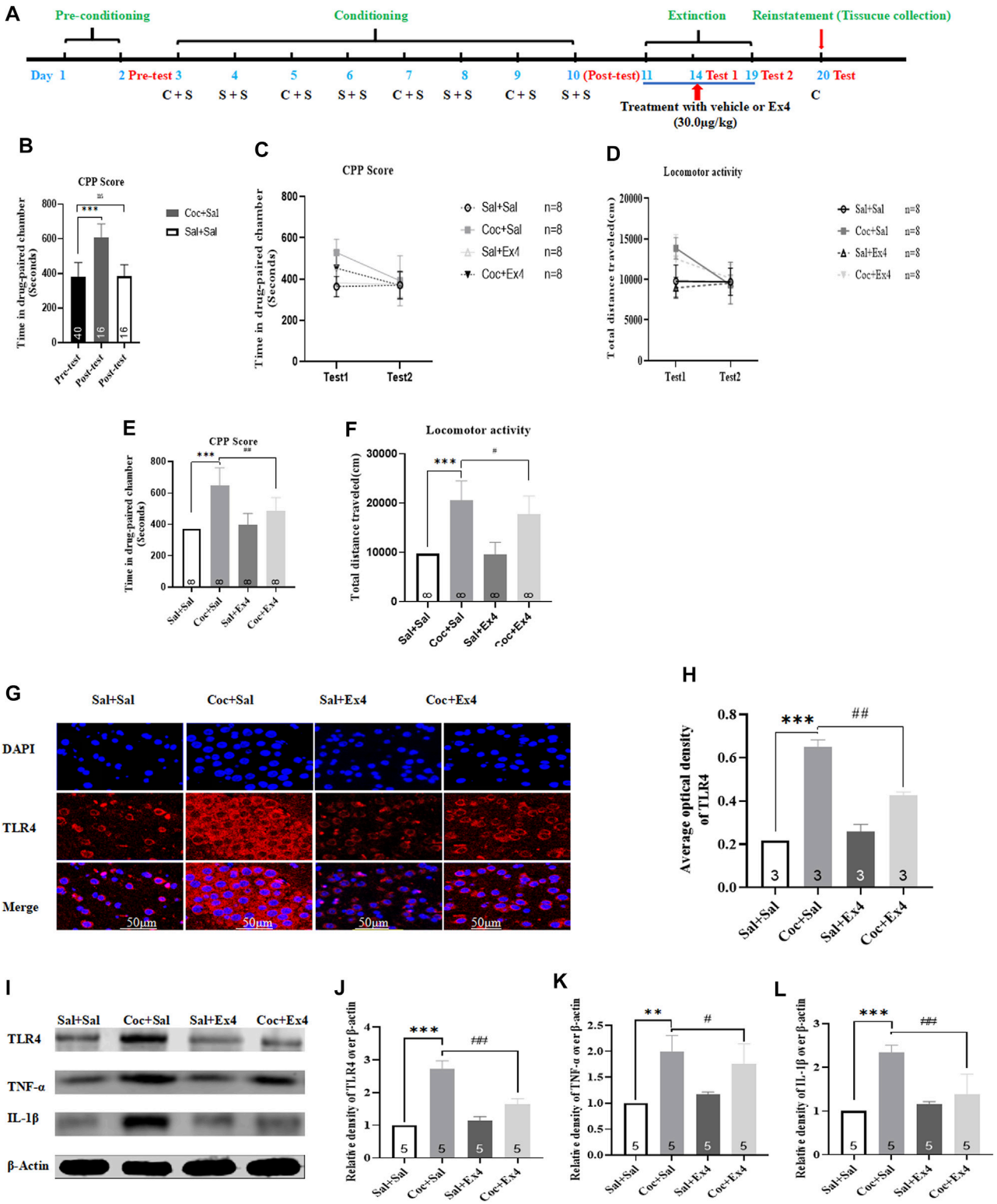

FIGURE 6 | Ex4's chronic treatment promotes extinction as well as suppresses reinstatement of cocaine-induced CPP and relieves expression levels of TLR4, TNF-α and IL-1β. **(A)** The complete experimental schedule for the behavioral procedure as well as saline (S), cocaine (C), and Ex4 treatment protocols. **(B)** CPP scores of the pre-test and post-test show that cocaine produced a significant CPP response after cocaine conditioning training. *** represents $p < 0.001$ vs pretest, Student's t test. **(C)** CPP scores following post-extinction Ex4 treatment vehicle and Ex4 (30 μg/kg) immediately after each extinction training show that Ex4 treated animals

(*Continued*)

FIGURE 6 | potentiates extinction of CPP compared to saline treated animals. N = 8 per group, *** represents $p < 0.001$ vs Sal+Sal, ns represents no significant difference, two-way ANOVA followed by a Bonferroni's *post hoc* test. **(D)** Locomotor activity following post-extinction treatment with saline and Ex4 (30.0 μg/kg) show that Ex4 treated animals reduces locomotion compared to saline treated animals. N = 8 per group, *** represents $p < 0.001$ vs Sal+Sal, ns represents no significant difference, two-way ANOVA followed by aBonferroni's *post hoc* test. (E) CPP scores after priming with half dose of cocaine show that Ex4 treated animals inhibits cocaine-primed reinstatement compared to saline treated animals. N = 8 per group, *** represents $p < 0.001$ vs Sal+Sal , ## represent $p < 0.01$ vs Coc+Sal, one-way ANOVA followed by a Bonferroni's *post hoc* test. **(F)** The results of locomotor activity show that Ex4 treatment inhibits cocaine-induced hyperactivity. N = 8 pergroup, *** represents $p < 0.001$ vs Sal+Sal, # represent $p < 0.05$ vs Coc+Sal, one-way ANOVA followed by a Bonferroni's *post hoc* test. **(G)** Representative images of immunofluorescent staining with TLR4 (red), andDAPI (blue) in the hippocampus from the different groups (scale bar = 50 μm). Post-extinction Ex4 diminishesfluorescence density of TLR4 up-regulated by cocaine priming ($n = 3$ in each group). **(H)** Semiquantitativeanalysis of the relative density of TLR4 by densitometric analysis in different groups. *** represents $p < 0.001$ vs Sal+Sal, ## represent $p < 0.01$ vs Coc+Sal, one-way ANOVA followed by a Tukey's *post hoc* test. **(I)** Representative immunoblots of TLR4, TNF-α and IL-1β proteins in different groups ($n = 5$ in each group). **(J)** Semiquantitative analysis of the relative levels of TLR4 by densitometric analysis in different groups. *** represents $p < 0.001$ vs Sal+Sal, ## represent $p < 0.01$ vs Coc+Sal, one-way ANOVA followed by a Tukey's *post hoc* test. **(K)** Semiquantitative analysis of the relative levels of TNF-α by densitometric analysis in differentgroups. ** represents $p < 0.01$ vs Sal+Sal, # represent $p < 0.05$ vs Coc+Sal, one-way ANOVA followed by a Tukey's *post hoc* test. **(L)** Semiquantitative analysis of the relative levels of IL-1β by densitometric analysis indifferent groups. *** represents $p < 0.001$ vs Sal+Sal, ## represent $p < 0.01$ vs Coc+Sal, one-way ANOVA followed by a Tukey's *post hoc* test. All data are presented as the mean ± SEM. Sal indicates saline. Cocindicates cocaine. Ex4 indicates Exendin-4.

blotting also revealed the different protein content of TLR4 among these groups [$F_{(3,19)} = 132.1$, $p < 0.0001$, one-way ANOVA, **Figures 6I,J**), and Tukey's multiple comparisons *post hoc* analysis showed that cocaine increased the protein level of TLR4 ($p = 0.0004$) that was significantly reduced via Ex4 treatment ($p = 0.0077$). Consistent with these results, Tukey's multiple comparisons test showed that the levels of TNF-α ($p = 0.0064$, one-way ANOVA, **Figure 6K**) and IL-1β ($p = 0.0002$, one-way ANOVA, **Figure 6L**) were significantly higher in Coc + Sal group than in Coc + Ex4 group. Similarly, Tukey's multiple comparisons *post hoc* analysis showed that treatment with Ex4 significantly relieved the expression levels of TNF-α ($p = 0.0351$, one-way ANOVA, **Figure 6K**) and IL1-β ($p = 0.0078$, one-way ANOVA, **Figure 6L**). In summary, these results indicates that Ex4 alleviates TLR4-associated inflammatory signaling.

DISCUSSION

In the current study, we demonstrated that the different dose of GLP-1R analog Ex4 (administrated daily during the cocaine conditioning) inhibited the acquisition and expression of cocaine-induced CPP. Moreover, we showed that repetitive Ex4 treatment (immediately after the each extinction session) did not only facilitate the extinction of cocaine-associated CPP but also attenuated reinstatement elicited by a single infusion of cocaine (10 mg/kg on the reinstatement day). Finally, we found the molecular mechanisms underlying these therapeutic effects of Ex4 on ameliorating these cocaine-mediated behaviors were closely associated with down-regulation of inflammatory cytokines in the hippocampus, including TLR4, TNF-α, and IL-1β. Consequently, these findings provide additional support for the potential role of glucagon-like peptide-1 agonist in the cocaine-mediated behavior amelioration.

The condition place preference (CPP) paradigm, based on classical Pavlovian conditioning, has traditionally been considered to be one of the most commonly behavioral models applied to study the rewarding properties of psychostimulants (Tzschentke, 1998; Bardo and Bevins, 2000). In the CPP paradigm, the addictive drug's rewarding effects functions as an unconditioned stimuli (United States), whereas the conditioned stimuli (CS) actions as a secondary stimuli which was acquired mainly by repeatedly pairing the rewarding properties of drugs with environmental stimuli in the process of cocaine conditioning. In line with previous work (Meye et al., 2016; Ladrón de Guevara-Mirand et al., 2018), we also found that systemic administration of cocaine (20 mg/kg) during conditioning phase is competent to produce a significant CPP paradigm for the overwhelming majority of animals. These indicate that although no cocaine was available on the CPP test day, the familiar drug-paired compartment was still preferred by mice. Further, these results also illustrate that the rewarding efficacy of cocaine well paired with the designed drug-paired compartment. Different from cocaine, however, Ex4 and saline were inadequate to induce a room preference or aversion, identical to previous work demonstrating that Ex4 itself did not produce a CPP (Egecioglu et al., 2013). Importantly, these cocaine-induced behavioral changes including CPP learned by mice in the previous drug-paired environment could be abolished by systemic Ex4 administration (Skibicka, 2013; Engel and Jerlhag, 2014; Hayes and Schmidt, 2016), fitting with the findings in our study demonstrating that single or repeated pretreatment with Ex4 significantly produced a significant reduction in the time spent in the cocaine-affiliated chamber on the CPP test day. Overall, repeated or single administration of Ex4 have a profound influence on the amelioration of addictive cocaine-mediated behaviors such as the acquisition and expression of CPP paradigm.

Extinction training is an active learning process that leads to a gradual decline in acquired response. It generates the new learning and memories that predict no more delivery of addictive drugs, through which the expression of initial memories of addictive drugs to control behavior was suppressed (Marlatt, 1990; Chesworth and Corbit, 2015), and thereby reducing the susceptibility of relapse (Heather and Bradley, 1990). However, extinction exposure alone proves insufficient (Marlatt, 1990). Additional studies have determined that extinction can be clearly promoted by pharmacological treatment (Botreau et al., 2006; Paolone et al., 2009). However, to our knowledge, few studies have investigated

the role of Ex4 in extinction of cocaine-related behavior to date. Thus, elucidating the potential effects of Ex4 on extinction of cocaine-induced CPP is another important purpose in the present study. As reported previously (Botreau et al., 2006; Paolone et al., 2009), our work found that mice treated with Ex4 appear to extinguish more quickly than mice treated with saline in the first three days of extinction training. Additionally, our findings further imply that the new learning and memories induced by combination between Ex4 and extinction training significantly suppress the initial memories of cocaine-related CPP, thereby enhancing the extinction.

The high incidence of relapse after abstinence is the primary hallmark of cocaine addiction (Leshner, 1997). However, the effects of available medication and treatment strategies on relapse is limited (O'Brien, 1997). Manipulating memory reconsolidation reportedly proposed as another more effective treatment option to decrease the relapse of cocaine addiction (Rich and Torregrossa, 2018). Using reinstatement paradigm model that has been viewed as the most commonly used animal model of relapse of cocaine-associated behavior (Schmidt et al., 2005), the therapeutic actions of Ex4 treatment on the reconsolidation and reinstatement of cocaine-related behavior were evaluated in the present study. We found that a significant CPP was acquired after a period of extinction and priming injection of a half dose of cocaine, indicating that simultaneous re-exposure to the context cues previously associated with cocaine abuse and cocaine itself precipitated a craving-induced relapse, and that the drug-triggered reinstatement paradigm has been successfully established as well. In addition, an acute single injection of cocaine (on the reinstatement day) markedly increased locomotion that was clearly affected by post-extinction Ex4. Similarly, in our work, post-extinction Ex4 treatment with combination of the extinction training received desirable actions on attenuating reinstatement of CPP through affecting the memory reconsolidation. However, single administration of Ex4 on reinstatement day failed to produce similar effects on extinction and reinstatement. The precise reason why single injection of Ex4 was unable to block relapse remain elusive. But the possible explanation is that single injection of Ex4, lack of combination of extinction training, was not sufficient to modulate memories reconsolidation. Consequently, the therapeutic efficacy of Ex4 on reinstatement and memory reconsolidation depends greatly on combination with extinction training. Regardless of the mechanisms underlying the inability of single administration of Ex4 on reinstatement of cocaine-CPP, our results are sufficient to illustrate that Ex4 exert far-reach effects on extinction and reinstatement of cocaine-mediated CPP.

Taken together, the CPP as well as extinction and reinstatement induced by cocaine were significantly affected using systemic administration of Ex4. These findings expanded on these studies showing that the important effects of systemic dose of GLP-1 receptor agonists on addiction-like behaviors in preclinical model of cocaine use disorder (Graham et al., 2013; Hernandez et al., 2018). However, little is known about the underlying mechanisms through which Ex4 ameliorates addictive behaviors associated with cocaine consumption.

Inflammation and Cocaine Addiction

A variety of work reveal an important role of neuroinflammation in many central nervous system (CNS) diseases (Block and Hong, 2005; Tansey et al., 2007; Chen et al., 2016) and that neuroinflammation was believed to contribute to the progression and maintenance of substance use disorders including cocaine (Hutchinson and Watkins, 2014; Northcutt et al., 2015; Lacagnina et al., 2016). The aberrant regulation of neuroimmune signaling caused by drug consumption may impair neuronal function, aggravate neurodegeneration, and promote neurotoxicity, which might result in drug-associated behaviors via activation of microglia (Lacagnina et al., 2016; Liu et al., 2016; Pocock and Kettenmann, 2007). Furthermore, the microglia activation also promoted the release of pro-inflammatory cytokines including IL-1β and TNF-α, and the generation of reactive oxygen and nitrogen species that cause further neuronal lesion (Beardsley and Hauser, 2014). In line with these data, we also observed that animals who acquired a strong CPP always showed the corresponding over-expression of TLR4, IL-1β, and TNF-α protein in the hippocampus. Further, these animals also showed a higher fluorescence density of TLR4 in the CA3 region of the hippocampus. Thus, it is conceivable that there the over-expression of TLR4, IL-1β, and TNF-α in the hippocampus is strongly associated with cocaine-related behavior, and suppressing these neuroinflammation may serve as a promising treatments for substance use disorders (Kohno et al., 2019).

Mechanisms Through Which GLP-1R Agonists Attenuate Cocaine Reward

Indeed, several potential anti-inflammatory pharmacotherapies with an ability to inhibit expression of IL-1β and TNF-α, such as Ibudilast (Ray et al., 2014) and Minocycline (Garrido-Mesa et al., 2013) have been shown to exert therapeutic actions on treatments for substance use disorders. Similarly, a recent clinical study showed that the anti-inflammatory agent naloxone, which targets IL-1β and TNF-α, can effectively attenuate dopamine release and thereby prevent the development of CPP in rats (Northcutt et al., 2015). We therefore hypothesized that anti-inflammatory components with the ability to suppress TLR4, IL-1β, and TNF-α signaling may repurposed as modulator of the dopamine release and cocaine-seeking behaviors (Correia et al., 2020). Intriguingly, accumulating studies have demonstrated that GLP-1R agonists Ex4 also possessed the anti-inflammatory properties (Hattori et al., 2010; Ajay et al., 2011; Campbell and Drucker, 2013; Lee and Jun 2016; Pinho-Ribeiro et al., 2017; Thangavel et al., 2017; Géa et al., 2020). For instance, TLR4 (Ajay et al., 2011), TNF-α and IL-1β (Pinho-Ribeiro et al., 2017; Thangavel et al., 2017) were effectively alleviated by Ex4 treatment. Our findings extend these data and identify that Ex4 did not only exert a significantly suppressive effects on the expression TLR4, TNF-α, and IL-1β in hippocampus but also ameliorated the cocaine-related maladaptive behaviors. In addition, we also found that Ex4 repaired neuronal damage caused by cocaine. Collectedly, Ex4 did not only alleviate the expression levels of TLR4, TNF-α, and IL-1β within hippocampus but also repaired the neuronal damage, thereby functioning as a novel anti-inflammatory agents.

Although we have shown that Ex4 ameliorates cocaine-mediated behavior via inhibiting the abnormal expression of TLR4, TNF-α and IL-1β in hippocampus, further studies are needed to investigate the possible direct targets of Ex4. Indeed, recent study have indicated that systemic administration of Ex4 is also distributed in other area of brain such as the accumbens core and shell, Ventral tegmental area (VTA) and Lateral septum (LS) (Hernandez and Schmidt, 2019). Additionally, these nucleus were reportedly associated with the rewarding effects of psychostimulant abuse (Schmidt and Pierce, 2010; Hernandez and Schmidt, 2019). For instance, previous study has demonstrated that peripheral administration of Ex4 inhibit the neurotransmitter dopamine release in the nucleus accumbens after cocaine exposure (Egecioglu et al., 2013; Sorensen et al., 2015). Accordingly, it is conceivable that the therapeutic actions of Ex4 on cocaine-related behaviors may be closely associated with other region of brain including the nucleus accumbens and inhibition of the dopamine release. In the further study, we intend to examine the effects of direct injection of Ex4 into the nucleus accumbens on the dopamine release and the potential mechanism. In addition, it is still unknown whether the over-expression of TNF-α, and IL-1β was directly attributable to the TLR4 activation or chronic cocaine exposure. Further studies are needed to assess whether Ex4 can exert neuroprotective effects for treating cocaine use disorder by blocking TLR3 and TLR2 signaling or through other factors. Moreover, sex differences in the efficacy of Ex4 for reducing cocaine-seeking behaviors were not explored in the current study, and additional research is needed to evaluate whether other anti-inflammatory agents have the same biological effects as Ex4 on other commonly abused drugs. Finally, although the molecular mechanisms of Ex4 were discussed, behavioral and pharmacological treatments should be further investigated in human clinical trials. In conclusion, we found that repeated administration of cocaine significantly augmented the time spent in cocaine-paired chamber, increased locomotor activity, and promoted the release of TLR4 and pro-inflammatory cytokines (IL-1β and TNF-α) in the hippocampus. Notably, most of these alterations caused by chronic cocaine exposure can be significantly blocked by Ex4 treatment through a mechanism involving reduced hippocampal TLR4, IL-1β and TNF-α signaling. On one hand, elucidating the mechanistic role of TLR4, IL-1β and TNF-α in cocaine-induced behavior is essential to ameliorate the understanding of progression and maintenance of cocaine addiction. On another hand, these findings offer innovative insights into the therapeutic effects of the widely available Ex4 on TLR4-associated neuroiflammation in an animal model of cocaine addiction. Therefore, GLP-1R agonist Ex4 might be a promising medication candidate for substance use disorder.

DATA AVAILABILITY STATEMENT

The original contributions presented in the study are included in the article, further inquiries can be directed to the corresponding authors.

ETHICS STATEMENT

The animal study was reviewed and approved by The animal study was reviewed and approved by Animal Research Ethics Committee of Ningxia Medical University.

AUTHOR CONTRIBUTIONS

TS and FW participated in the study design. SR, XL, LX, SJ, BG, LW, JD, CG, and HC took part in data collection, analysis of data, and preparation of the manuscript. All authors read and approved the final manuscript. TH designed the experiments. CZ designed the experiments and performed the experiments, analyzed data, made the figures, performed the statistical analysis, and wrote the manuscript and takes responsibility for the integrity of the data and the accuracy of the data analysis.

FUNDING

We gratefully acknowledged the following funding sources for this study: the National Natural Science Foundation of China (NSFC, 82060261 and 81660226) and the Key Research and Development Program of Ningxia (2018BFG02007).

ACKNOWLEDGMENTS

The authors thank Ningxia Key Laboratory of Cerebrocranial Disease (Ningxia Medical University, Yinchuan, China) for help with the whole experiments.

REFERENCES

Ajay, C., Husam, G., Mehul, V., Ling, S. C., Kelly, K., Sandeep, D., et al. (2011). Exenatide Exerts a Potent Antiinflammatory Effect. *J. Clin. Endocrinol. Metab.* 97, 198–207. doi:10.1210/jc.2011-1508

Andersen, A., Lund, A., Knop, F. K., and Vilsbøll, T. (2018). Glucagon-like Peptide 1 in Health and Disease. *Nat. Rev. Endocrinol.* 14, 390–403. doi:10.1038/s41574-018-0016-2

Araos, P., Pedraz, M., Serrano, A., Lucena, M., Barrios, V., García-Marchena, N., et al. (2015). Plasma Profile of Pro-inflammatory Cytokines and Chemokines in Cocaine Users under Outpatient Treatment: Influence of Cocaine Symptom Severity and Psychiatric Co-morbidity. *Addict. Biol.* 20, 756–772. doi:10.1111/adb.12156

Bardo, M. T., and Bevins, R. A. (2000). Conditioned Place Preference: what Does it Add to Our Preclinical Understanding of Drug Reward? *Psychopharmacology (Berl)* 153, 31–43. doi:10.1007/s002130000569

Barrera, J. G., Jones, K. R., Herman, J. P., D'Alessio, D. A., Woods, S. C., and Seeley, R. J. (2011). Hyperphagia and Increased Fat Accumulation in Two Models of Chronic CNS Glucagon-like Peptide-1 Loss of Function. *J. Neurosci.* 31, 3904–3913. doi:10.1523/JNEUROSCI.2212-10.2011

Beardsley, P. M., and Hauser, K. F. (2014). Glial Modulators as Potential Treatments of Psychostimulant Abuse. *Adv. Pharmacol.* 69, 1–69. doi:10.1016/B978-0-12-420118-7.00001-9

Block, M. L., and Hong, J. S. (2005). Microglia and Inflammation-Mediated Neurodegeneration: Multiple Triggers with a Common Mechanism. *Prog. Neurobiol.* 76, 77–98. doi:10.1016/j.pneurobio.2005.06.004

Bohbot, V. D., and Corkin, S. (2007). Posterior Parahippocampal Place Learning in H.M. *Hippocampus* 17, 863–872. doi:10.1002/hipo.20313

Botreau, F., Paolone, G., and Stewart, J. (2006). D-cycloserine Facilitates Extinction of a Cocaine-Induced Conditioned Place Preference. *Behav. Brain Res.* 172, 173–178. doi:10.1016/j.bbr.2006.05.012

Brown, J., Wang, H., Hajishengallis, G. N., and Martin, M. (2011). TLR-signaling Networks: an Integration of Adaptor Molecules, Kinases, and Cross-Talk. *J. Dent. Res.* 90, 417–427. doi:10.1177/0022034510381264

Campbell, J. E., and Drucker, D. J. (2013). Pharmacology, Physiology, and Mechanisms of Incretin Hormone Action. *Cell Metab.* 17, 819–837. doi:10.1016/j.cmet.2013.04.008

Cearley, C. N., Blindheim, K., Sorg, B. A., Krueger, J. M., and Churchill, L. (2011). Acute Cocaine Increases Interleukin-1β mRNA and Immunoreactive Cells in the Cortex and Nucleus Accumbens. *Neurochem. Res.* 36, 686–692. doi:10.1007/s11064-011-0410-9

Chen, R., Tilley, M. R., WeiZhou, H. F., Zhou, F., Zhou, F. M., Ching, S., et al. (2006). Abolished Cocaine Reward in Mice with a Cocaine-Insensitive Dopamine Transporter. *Proc. Natl. Acad. Sci. U S A.* 103, 9333–9338. doi:10.1073/pnas.0600905103

Chen, W. W., Zhang, X., and Huang, W. J. (2016). Role of Neuroinflammation in Neurodegenerative Diseases (Review). *Mol. Med. Rep.* 13, 3391–3396. doi:10.3892/mmr.2016.4948

Chesworth, R., and Corbit, L. H. (2017). Recent Developments in the Behavioural and Pharmacological Enhancement of Extinction of Drug Seeking. 22, 3–43. *Addict. Biol.* doi:10.1111/adb.12337

Clark, K. H., Wiley, C. A., and Bradberry, C. W. (2013). Psychostimulant Abuse and Neuroinflammation: Emerging Evidence of Their Interconnection. *Neurotox. Res.* 23, 174–188. doi:10.1007/s12640-012-9334-7

Coller, J. K., and Hutchinson, M. R. (2012). Implications of central Immune Signaling Caused by Drugs of Abuse: Mechanisms, Mediators and New Therapeutic Approaches for Prediction and Treatment of Drug Dependence. *Pharmacol. Ther.* 134, 219–245. doi:10.1016/j.pharmthera.2012.01.008.35

Correia, C., Romieu, P., Olmstead, M. C., and Befort, K. (2020). Can Cocaine-Induced Neuroinflammation Explain Maladaptive Cocaine-Associated Memories? *Neurosci. Biobehav. Rev.* 111, 69–83. doi:10.1016/j.neubiorev.2020.01.001

Crews, F. T., Walter, T. J., Coleman, L. G., and Vetreno, R. P. (2017). Toll-like Receptor Signaling and Stages of Addiction. *Psychopharmacology (Berl)* 234, 1483–1498. doi:10.1007/s00213-017-4560-636

Del Olmo, N., Higuera-Matas, A., Miguéns, M., García-Lecumberri, C., Borcel, E., Solís, J. M., et al. (2006). Hippocampal Synaptic Plasticity and Water Maze Learning in Cocaine Self-Administered Rats. *Ann. N. Y. Acad. Sci.* 1074, 427–437. doi:10.1196/annals.1369.043

Drucker, D. J., and Nauck, M. A. (2006). The Incretin System: Glucagon-like Peptide-1 Receptor Agonists and Dipeptidyl Peptidase-4 Inhibitors in Type 2 Diabetes. *Lancet* 368, 1696–1705. doi:10.1016/S0140-6736(06)69705-5

Egecioglu, E., Engel, J. A., and Jerlhag, E. (2013). The Glucagon-like Peptide 1 Analogue, Exendin-4, Attenuates the Rewarding Properties of Psychostimulant Drugs in Mice. *Plos. One.* 8, e69010. doi:10.1371/journal.pone.0069010

Eng, C., Kramer, C. K., Zinman, B., and Retnakaran, R. (2014). Glucagon-like Peptide-1 Receptor Agonist and Basal Insulin Combination Treatment for the Management of Type 2 Diabetes: a Systematic Review and Meta-Analysis. *Lancet* 384, 2228–2234. doi:10.1016/S0140-6736(14)61335-0

Engel, J. A., and Jerlhag, E. (2014). Role of Appetite-Regulating Peptides in the Pathophysiology of Addiction: Implications for Pharmacotherapy. *Cns. Drugs* 28, 875–886. doi:10.1007/s40263-014-0178-y

Géa, L. P., da Rosa, E. D., Panizzutti, B. S., de Aguiar, É. Z., de Oliveira, L. F., Ferrari, P., et al. 2020). Reduction of Hippocampal Il-6 Levels in Lps-Injected Rats Following Acute Exendin-4 Treatment. *Naunyn-schmiedeberg's Arch. Pharmacol.* 393 (Suppl. 1). 1303–1311. doi:10.1007/s00210-020-01867-5

Garrido-Mesa, N., Zarzuelo, A., and Gálvez, J. (2013). Minocycline: Far beyond an Antibiotic. *Br. J. Pharmacol.* 169, 337–352. doi:10.1111/bph.12139

Gault, V. A., and Hölscher, C. (2018). GLP-1 Receptor Agonists Show Neuroprotective Effects in Animal Models of Diabetes. *Peptides* 100, 101–107. doi:10.1016/j.peptides.2017.11.017

Graham, D. L., Erreger, K., Galli, A., and Stanwood, G. D. (2013). GLP-1 Analog Attenuates Cocaine Reward. *Mol. Psychiatry* 18, 961–962. doi:10.1038/mp.2012.141

Grill, H. J., and Hayes, M. R. (2012). Hindbrain Neurons as an Essential Hub in the Neuroanatomically Distributed Control of Energy Balance. *Cel. Metab.* 16, 296–309. doi:10.1016/j.cmet.2012.06.015

Hamilton, A., and Hölscher, C. (2009). Receptors for the Incretin Glucagon-like Peptide-1 Are Expressed on Neurons in the central Nervous System. *Neuroreport* 20, 1161–1166. doi:10.1097/WNR.0b013e32832fbf14

Hanamsagar, R., Hanke, M. L., and Kielian, T. (2012). Toll-like Receptor (TLR) and Inflammasome Actions in the central Nervous System. *Trends. Immunol.* 33, 333–342. doi:10.1016/j.it.2012.03.001

Hattori, Y., Jojima, T., Tomizawa, A., Satoh, H., Hattori, S., Kasai, K., et al. (2010). A Glucagon-like Peptide-1 (GLP-1) Analogue, Liraglutide, Upregulates Nitric Oxide Production and Exerts Anti-inflammatory Action in Endothelial Cells. *Diabetologia* 53, 2256–2263. doi:10.1007/s00125-010-1831-8

Hayes, M. R., and Schmidt, H. D. (2016). Glp-1 Influences Food and Drug Reward. *Curr. Opin. Behav. Sci.* 9, 66–70. doi:10.1016/j.cobeha.2016.02.005

Heather, N., and Bradley, B. P. (1990). Cue Exposure as a Practical Treatment for Addictive Disorders: Why Are We Waiting? *Addict. Behav.* 15, 335–337. doi:10.1016/0306-4603(90)90043-w

Hernandez, N. S., Ige, K. Y., Mietlicki-Baase, E. G., Molina-Castro, G. C., Turner, C. A., Hayes, M. R., et al. (2018). Glucagon-like Peptide-1 Receptor Activation in the Ventral Tegmental Area Attenuates Cocaine Seeking in Rats. *Neuropsychopharmacology* 43, 2000–2008. doi:10.1038/s41386-018-0010-3

Hernandez, N. S., and Schmidt, H. D. (2019). Central Glp-1 Receptors: Novel Molecular Targets for Cocaine Use Disorder. *Physiol. Behav.* 206, 93–105. doi:10.1016/j.physbeh.2019.03.026

Holscher, C. (2010). Incretin analogues that have been developed to treat type 2 diabetes hold promise as a novel treatment strategy for Alzheimer's disease. *Recent. Pat. CNS Drug Discov.* 5, 109–117. doi:10.2174/157488910791213130

Holst, J. J., Burcelin, R., and Nathanson, E. (2011). Neuroprotective Properties of GLP-1: Theoretical and Practical Applications. *Curr. Med. Res. Opin.* 27, 547–558. doi:10.1185/03007995.2010.549466

Holst, J. J. (2007). The Physiology of Glucagon-like Peptide 1. *Physiol. Rev.* 87, 1409–1439. doi:10.1152/physrev.00034.2006

Hughes, A., Williams, M. R., Lipari, R. N., and Van Horn, S. (2016). "State Estimates of Past Year Cocaine Use Among Young Adults: 2014 and 2015," in *Center for Behavioral Health Statistics and Quality, Substance Abuse and Mental Health Services Administration* (Rockville, MD: The CBHSQ Report).

Hutchinson, M. R., Northcutt, A. L., Hiranita, T., Wang, X., Lewis, S. S., Thomas, J., et al. (2012). Opioid Activation of Toll-like Receptor 4 Contributes to Drug Reinforcement. *J. Neurosci.* 32, 11187–11200. doi:10.1523/JNEUROSCI.0684-12.2012

Hutchinson, M. R., and Watkins, L. R. (2014). Why Is Neuroimmunopharmacology Crucial for the Future of Addiction Research?. *Neuropharmacology* 76 Pt B, 218–227. doi:10.1016/j.neuropharm.2013.05.039.37

Isacson, R., Nielsen, E., Dannaeus, K., Bertilsson, G., Patrone, C., Zachrisson, O., et al. (2011). The Glucagon-like Peptide 1 Receptor Agonist Exendin-4 Improves Reference Memory Performance and Decreases Immobility in the Forced Swim Test. *Eur. J. Pharmacol.* 650, 249–255. doi:10.1016/j.ejphar.2010.10.008

Jensen, E. C. (2013). Quantitative Analysis of Histological Staining and Fluorescence Using Imagej. *Anat. Rec. (Hoboken)* 296, 378–381. doi:10.1002/ar.22641

Jerlhag, E. (2019). Gut-brain axis and Addictive Disorders: a Review with Focus on Alcohol and Drugs of Abuse. *Pharmacol. Ther.* 196, 1–14. doi:10.1016/j.pharmthera.2018.11.005

June, H. L., Liu, J., Warnock, K. T., Bell, K. A., Balan, I., Bollino, D., et al. (2015). CRF-amplified Neuronal TLR4/MCP-1 Signaling Regulates Alcohol Self-Administration. *Neuropsychopharmacology* 40, 1549–1559. doi:10.1038/npp.2015.4

Kenny, P. J. (2011). Common Cellular and Molecular Mechanisms in Obesity and Drug Addiction. *Nat. Rev. Neurosci.* 12, 638–651. doi:10.1038/nrn3105

Kim, J. J., and Fanselow, M. S. (1992). Modality-specific Retrograde Amnesia of Fear. *Science* 256, 675–677. doi:10.1126/science.1585183

Kohno, M., Link, J., Dennis, L. E., Mccready, H., Huckans, M., Hoffman, W. F., et al. (2019). Neuroinflammation in Addiction: a Review of Neuroimaging Studies and Potential Immunotherapies. *Pharmacol. Biochem. Behav.* 179: 34–42. doi:10.1016/j.pbb.2019.01.007

Lacagnina, M. J., Rivera, P. D., and Bilbo, S. D. (2017). Glial and Neuroimmune Mechanisms as Critical Modulators of Drug Use and Abuse. *Neuropsychopharmacology* 42(1):156–177. doi:10.1038/npp.2016.121

Ladrón de Guevara-Miranda, D., Moreno-Fernández, R. D., Gil-Rodríguez, S., Rosell-Valle, C., Estivill-Torrús, G., Serrano, A., et al. (2018). Lysophosphatidic Acid-induced Increase in Adult Hippocampal Neurogenesis Facilitates the Forgetting of Cocaine-contextual Memory. *Addict. Biol.* 24(3):458–470. doi:10.1111/adb.12612

Lathe, R. (2001). Hormones and the hippocampus. *J. Endocrinol.* 169, 205–231. doi:10.1677/joe.0.1690205

Lawson, L. J., Perry, V. H., Dri, P., and Gordon, S. (1990). Heterogeneity in the Distribution and Morphology of Microglia in the normal Adult Mouse Brain. *Neuroscience* 39, 151–170. doi:10.1016/0306-4522(90)90229-W

Lee, Y. S., and Jun, H. S. (2016). Anti-Inflammatory Effects of GLP-1-Based Therapies beyond Glucose Control. *Mediators Inflamm.* 2016, 3094642–3094711. doi:10.1155/2016/3094642

Leshner, A. I. (1997). Addiction Is a Brain Disease, and it Matters. *Science* 278, 45–47. doi:10.1126/science.278.5335.45

Li, Y., Chigurupati, S., Holloway, H. W., Mughal, M., Tweedie, D., Bruestle, D. A., et al. (2012). Exendin-4 Ameliorates Motor Neuron Degeneration in Cellular and Animal Models of Amyotrophic Lateral Sclerosis. *Plos. ONE.* 7, e32008. doi:10.1371/journal.pone.0032008

Li, Y., Perry, T., Kindy, M. S., Harvey, B. K., Tweedie, D., Holloway, H. W., et al. (2009). Glp-1 Receptor Stimulation Preserves Primary Cortical and Dopaminergic Neurons in Cellular and Rodent Models of Stroke and Parkinsonism. *Proc. Natl. Acad. Sci. U S A.* 106, 1285–1290. doi:10.1073/pnas.0806720106

Li, Y., Duffy, K. B., Ottinger, M. A., Ray, B., Bailey, J. A., Holloway, H. W., et al. (2010). GLP-1 Receptor Stimulation Reduces Amyloid-β Peptide Accumulation and Cytotoxicity in Cellular and Animal Models of Alzheimer's Disease. *Jad* 19, 1205–1219. doi:10.3233/JAD-2010-1314

Liu, H., Leak, R. K., and Hu, X. (2016). Neurotransmitter receptors on microglia. *Stroke Vasc. Neurol.* 1, 52–58. doi:10.1136/svn-2016-000012

Lovshin, J. A., and Drucker, D. J. (2009). Incretin-based Therapies for Type 2 Diabetes Mellitus. *Nat. Rev. Endocrinol.* 5, 262–269. doi:10.1038/nrendo.2009.48

Marlatt, G. A. (1990). Cue Exposure and Relapse Prevention in the Treatment of Addictive Behaviors. *Addict. Behav.* 15, 395–399. doi:10.16/0306-4603(90)90048-3

Martin, B., Golden, E., Carlson, O. D., Pistell, P., Zhou, J., Kim, W., et al. (2009). Exendin-4 Improves Glycemic Control, Ameliorates Brain and Pancreatic Pathologies, and Extends Survival in a Mouse Model of Huntington's Disease. *Diabetes* 58, 318–328. doi:10.2337/db08-0799

Meier, J. J., Nauck, M. A., Kranz, D., Holst, J. J., Deacon, C. F., Gaeckler, D., et al. (2004). Secretion, Degradation, and Elimination of Glucagon-like Peptide 1 and Gastric Inhibitory Polypeptide in Patients with Chronic Renal Insufficiency and Healthy Control Subjects. *Diabetes* 53, 654–662. doi:10.2337/diabetes.53.3.654

Merchenthaler, I., Lane, M., and Shughrue, P. (1999). Distribution of Pre-pro-glucagon and Glucagon-like Peptide-1 Receptor Messenger RNAs in the Rat central Nervous System. *J. Comp. Neurol.* 403, 261–280. doi:10.1016/0306-4603(90)90048-39861(19990111)403:2<261::aid-cne8>3.0.co;2-52-5

Meye, F. J., Soiza-Reilly, M., Smit, T., Diana, M. A., Schwarz, M. K., and Mameli, M. (2016). Shifted Pallidal Co-release of GABA and Glutamate in Habenula Drives Cocaine Withdrawal and Relapse. *Nat. Neurosci.* 19(8):1019–1024. doi:10.1038/nn.4334

Meyers, R. A., Zavala, A. R., and Neisewander, J. L. (2003). Dorsal, but Not Ventral, Hippocampal Lesions Disrupt Cocaine Place Conditioning. *Neuroreport* 14, 2127–2131. doi:10.1097/00001756-200311140-00023

Meyers, R. A., Zavala, A. R., Speer, C. M., and Neisewander, J. L. (2006). Dorsal hippocampus Inhibition Disrupts Acquisition and Expression, but Not Consolidation, of Cocaine Conditioned Place Preference. *Behav. Neurosci.* 120, 401–412. doi:10.1037/0735-7044.120.2.401

Niaz, K., Haar, K., Carpentier, C., and Pietchman, T. (2020). World Drug Report 2020. Available at: www.unodc.org/wdr2020 (Accessed June 2020).

Northcutt, A. L., Hutchinson, M. R., Wang, X., Baratta, M. V., Hiranita, T., Cochran, T. A., et al. (2015). DAT Isn't All that: Cocaine Reward and Reinforcement Require Toll-like Receptor 4 Signaling. *Mol. Psychiatry* 20, 1525–1537. doi:10.1038/mp.2014.177

O'Brien, C. P. (1997). A Range of Research-Based Pharmacotherapies for Addiction. *Science* 278, 66–70. doi:10.1126/science.278.5335.66

Paolone, G., Botreau, F., and Stewart, J. (2009). The Facilitative Effects of D-Cycloserine on Extinction of a Cocaine-Induced Conditioned Place Preference Can Be Long Lasting and Resistant to Reinstatement. *Psychopharmacology (Berl)* 202 (1-3), 403–409. doi:10.1007/s00213-008-1280-y

Pi-Sunyer, X., Astrup, A., Fujioka, K., Greenway, F., Halpern, A., Krempf, M., et al. (2015). A Randomized, Controlled Trial of 3.0 Mg of Liraglutide in Weight Management. *N. Engl. J. Med.* 373, 11–22. doi:10.1056/NEJMoa1411892

Pinho-Ribeiro, F. A., Verri, W. A., and Chiu, I. M. (2017). Nociceptor Sensory Neuron-Immune Interactions in Pain and Inflammation. *Trends Immunolimmunol* 38, 5–19. doi:10.1016/j.it.2016.10.001

Pocock, J. M., and Kettenmann, H. (2007). Neurotransmitter receptors on microglia. *Trends Neurosci.* 30, 527–535. doi:10.1016/j.tins.2007.07.007

Ray, L. A., Roche, D. J., Heinzerling, K., and Shoptaw, S. (2014). Opportunities for the Development of Neuroimmune Therapies in Addiction. *Int. Rev. Neurobiol.* 118, 381–401. doi:10.1016/B978-0-12-801284-0.00012-9

Reddy, I. A., Pino, J. A., Weikop, P., Osses, N., Sørensen, G., Bering, T., et al. (2016). Glucagon-like Peptide 1 Receptor Activation Regulates Cocaine Actions and Dopamine Homeostasis in the Lateral Septum by Decreasing Arachidonic Acid Levels. *Transl. Psychiatry* 6, e809. doi:10.1038/tp.2016.86

Rich, M. T., and Torregrossa, M. M. (2018). Molecular and Synaptic Mechanisms Regulating Drug-Associated Memories: towards a Bidirectional Treatment Strategy. *Brain Res. Bull.* 141, 58–71. doi:10.1016/j.brainresbull.2017.09.003

Richards, P., Parker, H. E., Adriaenssens, A. E., Hodgson, J. M., Cork, S. C., Trapp, S., et al. (2014). Identification and Characterization of GLP-1 Receptor-Expressing Cells Using a New Transgenic Mouse Model. *Diabetes* 63, 1224–1233. doi:10.2337/db13-1440

Rodríguez-Arias, M., Castillo, A., Daza-Losada, M., Aguilar, M. A., and Miñarro, J. (2009). Effects of Extended Cocaine Conditioning in the Reinstatement of Place Preference. *Physiol. Behav.* 96, 620–630. doi:10.1016/j.physbeh.2008.12.011

Schmidt, H. D., Anderson, S., Famous, K., Kumaresan, V., and Pierce, R. (2005). Anatomy and pharmacology of cocaine priming-induced reinstatement of drug seeking. *Eur.J. Pharmacol.* 526, 65–76. doi:10.1016/j.ejphar.2005.09.068

Schmidt, H. D., and Pierce, R. C. (2010). Cocaine-induced Neuroadaptations in Glutamate Transmission: Potential Therapeutic Targets for Craving and Addiction. *Ann. N. Y. Acad. Sci.* 1187, 35–75. doi:10.1111/j.1749-6632.2009.05144.x

Sekine, Y., Ouchi, Y., Sugihara, G., Takei, N., Yoshikawa, E., Nakamura, K., et al. (2008). Methamphetamine Causes Microglial Activation in the Brains of Human Abusers. *J. Neurosci.* 28, 5756–5761. doi:10.1523/JNEUROSCI.1179-08.2008

Skibicka, K. P. (2013). The central Glp-1: Implications for Food and Drug Reward. *Front. Neurosci.* 7, 181. doi:10.3389/fnins.2013.00181

Sørensen, G., Reddy, I. A., Weikop, P., Graham, D. L., Stanwood, G. D., Wortwein, G., et al. (2015). The Glucagon-like Peptide 1 (GLP-1) Receptor Agonist Exendin-4 Reduces Cocaine Self-Administration in Mice. *Physiol. Behav.* 149, 262–268. doi:10.1016/j.physbeh.2015.06.013

Tansey, M. G., McCoy, M. K., and Frank-Cannon, T. C. (2007). Neuroinflammatory Mechanisms in Parkinson's Disease: Potential Environmental Triggers, Pathways, and Targets for Early Therapeutic Intervention. *Exp. Neurol.* 208, 1–25. doi:10.1016/j.expneurol.2007.07.004

Thangavel, R., Kempuraj, D., Zaheer, S., Raikwar, S., Ahmed, M. E., Selvakumar, G. P., et al. (2017). Glia Maturation Factor and Mitochondrial Uncoupling Proteins 2 and 4 Expression in the Temporal Cortex of Alzheimer's Disease Brain. *Front. Aging Neurosci.* 9, 150. doi:10.3389/fnagi.2017.00150

Turton, M. D., O'Shea, D., Gunn, I., Beak, S. A., Edwards, C. M. B., Meeran, K., et al. (1996). A Role for Glucagon-like Peptide-1 in the central Regulation of Feeding. *Nature* 379, 69–72. doi:10.1038/379069a0

Tzschentke, T. M. (1998). Measuring Reward with the Conditioned Place Preference Paradigm: a Comprehensive Review of Drug Effects, Recent Progress and New Issues. *Prog. Neurobiol.* 56, 613–672. doi:10.1016/S0301-0082(98)00060-4

Williams, K. W., and Elmquist, J. K. (2012). From Neuroanatomy to Behavior: central Integration of Peripheral Signals Regulating Feeding Behavior. *Nat. Neurosci.* 15, 1350–1355. doi:10.1038/nn.3217

Wu, J. D., Xu, X. H., Zhu, J., Ding, B., Du, T. X., Gao, G., et al. (2011). Effect of Exenatide on Inflammatory and Oxidative Stress Markers in Patients with Type 2 Diabetes Mellitus. *Diabetes Technol. Ther.* 13, 143–148. doi:10.1089/dia.2010.0048

Conflict of Interest: The authors declare that the research was conducted in the absence of any commercial or financial relationships that could be construed as a potential conflict of interest.

Copyright © 2021 Zhu, Tao, Rong, Xiao, Li, Jiang, Guo, Wang, Ding, Gao, Chang, Sun and Wang. This is an open-access article distributed under the terms of the Creative Commons Attribution License (CC BY). The use, distribution or reproduction in other forums is permitted, provided the original author(s) and the copyright owner(s) are credited and that the original publication in this journal is cited, in accordance with accepted academic practice. No use, distribution or reproduction is permitted which does not comply with these terms.

frontiers in Pharmacology

ORIGINAL RESEARCH
published: 05 August 2021
doi: 10.3389/fphar.2021.707859

Long-Lasting Changes in Glial Cells Isolated From Rats Subjected to the Valproic Acid Model of Autism Spectrum Disorder

Marianela Evelyn Traetta[1,2], *Nonthué Alejandra Uccelli*[1], *Sandra Cristina Zárate*[3,4], *Dante Gómez Cuautle*[1], *Alberto Javier Ramos*[1,3] *and Analía Reinés*[1,2]*

[1]*Instituto de Biología Celular y Neurociencia "Prof. E. De Robertis" (IBCN), CONICET - Universidad de Buenos Aires, Buenos Aires, Argentina,* [2]*Facultad de Farmacia y Bioquímica, Cátedra de Farmacología, Universidad de Buenos Aires, Buenos Aires, Argentina,* [3]*Facultad de Medicina, Departamento de Histología, Embriología, Biología Celular y Genética, Universidad de Buenos Aires, Buenos Aires, Argentina,* [4]*Instituto de Investigaciones Biomédicas (INBIOMED), CONICET - Universidad de Buenos Aires, Buenos Aires, Argentina*

Synaptic alterations concomitant with neuroinflammation have been described in patients and experimental models of autism spectrum disorder (ASD). However, the role of microglia and astroglia in relation to synaptic changes is poorly understood. Male Wistar rats prenatally exposed to valproic acid (VPA, 450 mg/kg, i.p.) or saline (control) at embryonic day 10.5 were used to study synapses, microglia, and astroglia in the prefrontal cortex (PFC) at postnatal days 3 and 35 (PND3 and PND35). Primary cultures of cortical neurons, microglia, and astroglia isolated from control and VPA animals were used to study each cell type individually, neuron-microglia and microglia-astroglia crosstalk. In the PFC of VPA rats, synaptic changes characterized by an increase in the number of excitatory synapses were evidenced at PND3 and persisted until PND35. At PND3, microglia and astroglia from VPA animals were morphologically similar to those of age-matched controls, whereas at PND35, reactive microgliosis and astrogliosis were observed in the PFC of VPA animals. Cortical neurons isolated from VPA rats mimicked *in vitro* the synaptic pattern seen *in vivo*. Cortical microglia and astroglia isolated from VPA animals exhibited reactive morphology, increased pro-inflammatory cytokines, and a compromised miRNA processing machinery. Microglia from VPA animals also showed resistance to a phagocytic challenge. In the presence of neurons from VPA animals, microglia isolated from VPA rats revealed a non-reactive morphology and promoted neurite outgrowth, while microglia from control animals displayed a reactive profile and promoted dendritic retraction. In microglia-astroglia co-cultures, microglia from VPA animals displayed a reactive profile and exacerbated astrocyte reactivity. Our study

OPEN ACCESS

Edited by:
Flavia Eugenia Saravia, Universidad de Buenos Aires, Argentina

Reviewed by:
Roberta Facchinetti, Sapienza University of Rome, Italy
Amiel Rosenkranz, Rosalind Franklin University of Medicine and Science, United States

***Correspondence:**
Analía Reinés
areines@ffyb.uba.ar

Specialty section:
This article was submitted to Neuropharmacology, a section of the journal Frontiers in Pharmacology

Received: *10 May 2021*
Accepted: *29 June 2021*
Published: *05 August 2021*

Citation:
Traetta ME, Uccelli NA, Zárate SC, Gómez Cuautle D, Ramos AJ and Reinés A (2021) Long-Lasting Changes in Glial Cells Isolated From Rats Subjected to the Valproic Acid Model of Autism Spectrum Disorder. Front. Pharmacol. 12:707859. doi: 10.3389/fphar.2021.707859

Abbreviations: ASD, autism spectrum disorder; ATP, adenosine triphosphate; DAPI, 4′,6-diamidino-2-phenylindole dihydrochloride; DIV, days *in vitro*; DMEM, Dulbecco's Modified Eagle medium; E, embryonic day; FCS, fetal calf serum; GAD-67, glutamic acid decarboxylase 67; GFAP, glial fibrillary acidic protein; Iba1, ionized calcium-binding adapter molecule 1; IF, immunofluorescence; IL1β, interleukin-1β; IL6, interleukin-6; LPS, lipopolysaccharide; MAP-2, microtubule-associated protein 2; miRNA, microRNA; PND, postnatal day; PSD-95, postsynaptic density protein-95; PFC, prefrontal cortex; RT-PCR, reverse transcription polymerase chain reaction; SD, standard deviation; ST, synaptosomes or synaptic terminals; SYN, synaptophysin; TEM, transmission electron microscopy; TNFα, tumor necrosis factor α; vGLUT-1, vesicular glutamate transporter 1; VPA, valproic acid.

indicates that cortical microglia from VPA animals are insensitive or adapted to neuronal cues expressed by neurons from VPA animals. Further, long-term *in vivo* microgliosis could be the result of altered microglia-astroglia crosstalk in VPA animals. Thus, our study highlights cortical microglia-astroglia communication as a new mechanism implicated in neuroinflammation in ASD; consequently, we propose that this crosstalk is a potential target for interventions in this disorder.

Keywords: neuroinflammation, microglia, astrocyte, synapse, autism

INTRODUCTION

Autism spectrum disorder (ASD) is a developmental condition characterized by social and communication deficits and restricted, repetitive patterns of behavior, interests, or activities (American Psychiatric Association, 2013). ASD neurobiology includes genetic and environmental factors (De Rubeis et al., 2014; Modabbernia et al., 2017). The genetic basis is complex, and alterations in epigenetic pathways have also been reported (De Rubeis et al., 2014; Geschwind and Flint, 2015). Several large-scale genetic studies have highlighted many genes as risk factors for ASD pathogenesis (Sebat et al., 2007; Anney et al., 2010; De Rubeis et al., 2014; Iossifov et al., 2014). Particularly, point mutations, gene deletions, and polymorphisms for several synaptic components such as cell adhesion molecules, scaffold proteins, and glutamate receptors have been documented (Betancur et al., 2009; Leblond et al., 2014; Hu et al., 2016). Moreover, dendritic alterations that might affect synapse formation and stability and altered spine density were observed in different brain areas in patients with ASD (Raymond et al., 1996; Hutsler and Zhang, 2010). Given that affected genes are linked to synaptic function and plasticity (Bourgeron, 2015; Lin et al., 2016) and structural dendritic and synaptic alterations were described in ASD, this disorder has been proposed to be a synaptopathy (Guang et al., 2018).

Neuroinflammation has been extensively documented in ASD, described as microgliosis and astrogliosis in different brain regions and increased expression of pro-inflammatory cytokines (Liao et al., 2020). Both astrocytes and microglia functions are critical for proper brain development: microglia promote synapse formation and refine circuits by pruning synapses (Stevens et al., 2007; Miyamoto et al., 2016), and astrocytes are critical in maintaining physiological homeostasis within the brain, playing important roles in synapse formation and supporting neuronal function (Araque and Navarrete, 2010; Allen and Eroglu, 2017). Both glial cells impact and react to the environment, making their contribution a valuable target to modulate (Zhang et al., 2010; Lenz and Nelson, 2018). Indeed, it is still a matter of debate whether glial alterations during development lead to ASD onset or neuroinflammation is a pathophysiological response to altered synaptic connectivity.

During neuroinflammation, microglia are the first glial cells to react by releasing cytokines that engage astrocytes, further intensifying neuroinflammation (Zhang et al., 2010; Kirkley et al., 2017; Liddelow et al., 2017; Auzmendi et al., 2020). Microglia rapidly adapt to the environment by changing their morphology: they shift from a ramified morphology to an amoeboid shape by retracting and thickening their processes and enlarging their soma (Kreutzberg, 1996; Matta et al., 2019). It is worth mentioning that prolonged dysregulated microglial activity has been implicated in brain neurotoxicity (Dheen et al., 2007). Astrocyte reactive gliosis is characterized by upregulation of intermediate filaments, particularly glial fibrillary acidic protein (GFAP) (Hol and Pekny, 2015) and morphological changes characterized by process extension and hypertrophy (Sofroniew and Vinters, 2010). There is also a bidirectional communication between microglia and astrocytes mediated by the increased secretion of signaling molecules and cytokines (Zhang et al., 2010; Matta et al., 2019; Matejuk and Ransohoff, 2020). For instance, reactive microglia release of IL1, IL6, and TNFα can trigger astrocyte reactivity (Zhang et al., 2010; Liddelow et al., 2017). In turn, reactive astrocytes release ATP and promote microglia activation (Coco et al., 2003; Bianco et al., 2005; Davalos et al., 2005).

Idiopathic ASD can be modeled in rats by prenatal exposure to valproic acid (VPA). This experimental model (VPA model) mimics the main behavioral and neuroanatomical alterations found in patients with ASD (Schneider and Przewłocki, 2005; Roullet et al., 2013; Nicolini and Fahnestock, 2018). Both neuronal and glial changes have been described in different brain regions in this model (Codagnone et al., 2015; Bronzuoli et al., 2018; Nicolini and Fahnestock, 2018; Traetta et al., 2021). Indeed, we have described changes in synaptic markers in key areas related to ASD behavioral deficits, such as the prefrontal cortex (PFC) and the hippocampus (Codagnone et al., 2015; Traetta et al., 2021). In particular, the PFC plays a key role in social behavior, decision-making, and emotional processing (Dixon et al., 2017; Chini and Hanganu-Opatz, 2021). In VPA animals, the PFC is characterized by synaptic changes shown as an increase in the synaptic marker synaptophysin (SYN) (Codagnone et al., 2015) and hyper-connectivity and hyper-plasticity (Rinaldi et al., 2008). It is worth mentioning that these synaptic changes are shown concomitantly with microgliosis and astrogliosis (Codagnone et al., 2015; Bronzuoli et al., 2018). Thus, this brain region is a key area to study the role of microglia and astroglia in ASD. Defining the contribution of these glial cells in the context of synaptic alterations may provide new targets for modulating neuroinflammation in ASD.

The present study explores the role of microgliosis and astrogliosis in relation to the synaptic changes in ASD. Therefore, we focused on cortical synapses, microglia, and

astroglia using the rat VPA model. We used an *in vivo* experimental design to shed light on the temporal association of cortical synaptic and glial changes and an *in vitro* approach to study neuronal, microglia, and astroglia individually and neuron-microglia and microglia-astroglia crosstalk. Our work shows that microglia and astroglia display long-lasting changes and a distinctive pro-inflammatory program *in vitro*, altering not only the cytokine profile but also miRNA processing machinery. While microglia from VPA animals are adapted to their neuronal substrate, microglia-astroglia crosstalk exacerbates reactivity. We provide evidence that cortical microglia are adapted to VPA-induced neuronal alterations and *in vivo* gliosis could result from altered microglia-astroglia crosstalk. Therefore, our study highlights the critical role of microglia-astroglia communication as a new mechanism underlying neuroinflammation in ASD and suggests this process as a new target for interventions.

MATERIALS AND METHODS

Animals

The VPA model was induced as previously described (Schneider and Przewłocki, 2005; Traetta et al., 2021). Wistar rats provided by Facultad de Ciencias Exactas y Naturales (Universidad de Buenos Aires) were housed in an air-conditioned room (20 ± 2°C) and maintained on a 12 h light/dark cycle with food and water *ad libitum*. They were mated overnight, and the day when spermatozoa were found in vaginal smears was considered embryonic day (E) 0. On E10.5, pregnant dams were given 450 mg/kg VPA intraperitoneally (sodium valproate, Parafarm, Droguería Saporiti S.A.C.I.F.I.A.) or saline solution. Experiments in this study were performed on male pups only: those prenatally exposed to VPA were VPA animals and those exposed to saline were control animals. Pups used for neuronal and glial cultures were born from different dams: each primary neuronal culture was obtained from 3 control and 3 VPA animals at postnatal day (PND) 1 and each primary glial culture from 4 control and 4 VPA animals at PND3. Male siblings were used for evaluating early postnatal development and juvenile behavior to validate the model (**Supplementary Materials and Methods**). At PND3 and PND35, 4–6 control and 4–6 VPA animals in each PND from 4 different saline and 4 VPA-injected dams were used for immunofluorescence assays; 4 animals (PND35) per group from 3 different saline and 3 VPA-injected dams were used for the electron microscopy study. All experiments were carried out following the Guide for the Care and Use of Laboratory Animals provided by the NIH (United States) and were approved by the Ethics Committee for the Care and Use of Laboratory Animals of the School of Pharmacy and Biochemistry at Universidad de Buenos Aires (Approval No. 180613–1 and 2320).

Primary Cortical Cultures

Primary cortical neuronal culture: cortical neuronal cultures were prepared from PND1 control and VPA animals as previously described (Reinés et al., 2012; Traetta et al., 2021). The entire cerebral cortex was used. Cells were plated at a density of 5×10^4 cells/cm^2 on poly-D-lysine (Sigma-Aldrich Co.) coated glass coverslips for immunofluorescence assays. They were maintained for up to 7 days *in vitro* (DIV) in a Neurobasal Medium supplemented with 2% v/v B27 and 0.5 mM glutamine (All from Gibco, Invitrogen Carlsbad, CA, United States).

Primary cortical glial cultures and treatments: primary mixed cortical glial cultures were prepared from control and VPA animals at PND3 as previously described (Rosciszewski et al., 2019; Zárate et al., 2019; Traetta et al., 2021). The entire cerebral cortex was used. Once cells reached confluence, they were subjected to shaking at 180 rpm for 24 h; microglia cells were detached and re-seeded on poly-D-lysine-coated glass coverslips at a density of 4×10^4 cells/cm^2 for treatments and immunofluorescence assays or at a density of 6×10^4 cells/cm^2 on plastic dishes for flow cytometry. They were kept up to 7 DIV in Dulbecco's Modified Eagle Medium (DMEM; Gibco, Invitrogen Carlsbad, CA, United States) supplemented with 50% v/v F12 (Gibco, Invitrogen Carlsbad, CA, United States), 10% v/v fetal calf serum (FCS; Natocor, Córdoba, Argentina), and 100 mg/ml penicillin-streptomycin (Gibco, Invitrogen Carlsbad, CA, United States). Cultures obtained with this procedure showed >98% Iba1 (+) microglia as previously described (Traetta et al., 2021). Microglial cultures from control and VPA animals were challenged with 20 ng/ml of lipopolysaccharide (LPS; *E. Coli* O26: B6 - L3755, Sigma-Aldrich Co.) for 24 h or cortical synaptosomes (ST, synaptic terminals) obtained from naïve adult male Wistar rats (Phillips et al., 2001) for 4 h as previously described (Traetta et al., 2021).

Cells still attached after the first 24 h shaking were subjected to a second 24 h shaking to detach remaining microglia and oligodendrocyte precursors. Then, cells were incubated with 0.625% v/v 5-fluorouracil (Gibco, Invitrogen Carlsbad, CA, United States) for 24 h and washed and incubated in DMEM supplemented with 10% v/v FCS and 100 mg/ml penicillin-streptomycin for an additional 2 DIV. Then, cells were trypsinized (Gibco, Invitrogen Carlsbad, CA, United States) and re-seeded on poly-D-lysine-coated glass coverslips at a density of 2.5×10^4 cells/cm^2 for treatments and immunofluorescence assays or on plastic dishes for flow cytometry. Astroglial-enriched cultures obtained with this procedure showed >93% GFAP (+) astrocytes, as reported in the literature (Villarreal et al., 2014; Zárate et al., 2019).

For mixed astroglial-microglial cultures, once cells reached confluence, they were tripsinized and re-seeded on poly-D-lysine coated glass coverslips at a density of 2.5×10^4 cells/cm^2 for treatments and immunofluorescence assays. They were kept in DMEM supplemented with 10% v/v FCS and 100 mg/ml penicillin-streptomycin for an additional 2 DIV. Mixed glial cultures showed 60% GFAP (+) astrocytes, as previously reported (Rosciszewski et al., 2019). Mixed glial cultures (DIV2) from control and VPA animals were also treated for 4 h with cortical synaptosomes (ST, synaptic terminals) obtained from naïve adult male Wistar rats (Chung et al., 2013).

Cortical neuron-microglia co-cultures: cortical neuronal and microglia cultures were performed as described above. Isolated

microglia obtained from mixed cultures of control and VPA animals were seeded at a density of 4×10^4 cells/cm^2 on cortical neurons (DIV4) from control or VPA animals, leading to 4 experimental groups: neurons and microglia from control animals, neurons and microglia from VPA animals, neurons from control animals and microglia from VPA animals, and neurons from VPA animals and microglia from control animals. The neuronal and microglial co-cultures were maintained in a Neurobasal Medium supplemented with 2% v/v B27 and 0.5 mM glutamine at 37°C and 5% CO_2 for 5 days. In addition, microglia and neurons from control and VPA animals were seeded on coverslips as basal conditions as described for primary cultures, but this time, they were kept in culture for the same time and under the same conditions as co-cultures.

Immunofluorescence

Tissue sections: control and VPA animals were fixed at PND3 and PND35 as previously detailed (Traetta et al., 2021). At PND3, animals were decapitated, and brains were fixed by immersion in 4% w/v paraformaldehyde in 0.1 M phosphate buffer at 4°C for 24 h. At PND35, animals were anesthetized (125 mg/kg ketamine hydrochloride and 10 mg/kg xylazine, i.p.), transcardially perfused with heparinized saline solution and fixed with 4% w/v paraformaldehyde in 0.1 M phosphate buffer. Brains (PND35) were post-fixed in the same fixative solution at 4°C for 3 h and brains from both PND3 and PND35 animals were equilibrated in 30% w/v sucrose in 0.1 M phosphate buffer before being stored at −70°C. Immunofluorescence technique was performed on 35 µm thick coronal slices of the prefrontal cortex (PFC) corresponding to plates 6–9 (from bregma 4.20 to 2.70) of the atlas of Paxinos and Watson (Paxinos and Watson, 1986) as previously described (Codagnone et al., 2015). Slices were permeabilized (0.5% v/v Triton X-100) and blocked (3% v/v normal horse serum). They were incubated with primary antibodies at 4°C for 48 h and with fluorescent secondary antibodies at room temperature for 1 h. The following primary antibodies were used: anti-synaptophysin (SYN; Millipore Cat# MAB329, RRID: AB_94,786) (1:3,000), anti-vGLUT-1 (Millipore Cat# AB5905, RRID: AB_2,301,751) (1:5,000), anti-glial fibrillary acidic protein (GFAP; Dako Cat# Z0334, RRID: AB_10,013,382) (1:2000), and anti-Iba1 (Wako Cat# 019–19,741, RRID: AB_839,504) (1:4,000) and were followed by fluorescent secondary antibodies (Jackson ImmunoResearch Laboratories, Inc.). Slices were mounted using Mowiol 4–88 (Sigma-Aldrich Co.). Each immunofluorescence assay consisted of 3 PFC serial sections of 4-6 control or VPA animals from 4 different saline and 4 VPA-injected dams.

Cell culture: cortical neurons (DIV7), microglia (DIV7), astrocytes (DIV2), mixed glial cultures (DIV2), and neuron-microglia co-cultures (DIV9) were fixed and processed for immunofluorescence as previously described (Reinés et al., 2012; Podestá et al., 2014). Time points for fixation correspond to fully differentiated cells in culture. Briefly, cells were fixed in 4% w/v paraformaldehyde/4% w/v sucrose in phosphate-buffered saline for 20 min. After permeabilization (0.1% v/v Triton X-100) and blockade (5% v/v normal horse serum), cells were subsequently incubated with primary antibodies overnight at 4°C and with fluorescent secondary antibodies for 1 h at room temperature. The following primary antibodies were used: anti-SYN (1:5,000), anti-microtubule-associated protein 2 (MAP-2; Sigma-Aldrich Cat# M4403, RRID: AB_477,193) (1:500), anti-PSD-95 (Thermo Fisher Scientific Cat# MA1-045, RRID: AB_325,399) (1:200), anti-GAD-67 (Millipore Cat# MAB5406, RRID: AB_2,278,725) (1: 1,000), anti-GFAP (1:2000), and anti-Iba1 (1:1,500), followed by fluorochrome-conjugated secondary antibodies (Jackson ImmunoResearch Laboratories, Inc.). 4′,6-Diamidino-2-phenylindole dihydrochloride (DAPI; Sigma-Aldrich Co.) (0.5 µg/ml) was used for the nucleus staining. Coverslips were mounted using Mowiol 4–88 (Sigma-Aldrich Co.). Assays were repeated 2–3 times, employing independent cultures.

Imaging and Analysis

Immunofluorescence images were captured by an epifluorescence Olympus IX81 microscope equipped with a CCD model DP71 digital camera (Olympus). Image analysis was performed with ImageJ (NIH) software. Quantification parameters were kept constant between groups for analysis, and no blinding method was applied. Final figures were created with Photoshop CS6. In the case of bright and contrast adjustments, they were equally applied to all groups.

***Tissue sections*:** two adjacent non-overlapping images were taken from each hemisphere to sample the medial PFC of animals at PND3 and PND35 according to the atlas of Paxinos and Watson (Paxinos and Watson, 1986). SYN, vGLUT-1, and GFAP immunolabeling were measured as positive immunoreactive areas relative to the total area of the field of view (relative immunoreactive area). To assess the immunoreactive area, we transformed images into grayscale and set a threshold capable of differentiating positive immunoreactive structures from the background. This threshold was kept constant between experimental groups, and the areas of positive structures were those that exceeded the threshold (Codagnone et al., 2015). Iba1 immunolabeling analysis included quantifying the relative immunoreactive area and assesing microglia morphology by classifying Iba1 (+), cells into ramified and unramified categories according to developmental stage (Ueno et al., 2013). At PND3, ramified microglia presented two or more branches, which in turn had more small branches, and unramified microglia were ameboid or showed one or two short, simple branches. At PND35, ramified microglia were considered when a cell presented small soma and more than two long and thin processes, whereas unramified microglia showed larger soma and few short and thick processes.

***Neuronal parameters in culture*:** the immunoreactive pattern generated by synaptic proteins (SYN, PSD-95, and GAD-67) was analyzed as previously detailed (Podestá et al., 2014; Traetta et al., 2021). Briefly, synaptic puncta were captured, setting a single threshold for all experimental groups to distinguish individual puncta from the background and to minimize the probability of including merged structures in the quantification and quantified defining a particle size according to each marker (0.15–0.6 µm^2 for SYN and PSD-95 and 0.4–1.2 µm^2 for GAD-67). The quantitative analysis included the total puncta number per

neuron indicative of synapse number, the average area occupied by a single punctum (individual puncta area), and the total area occupied by all puncta. Characterization of dendritic arborization consisted of assessing the dendritic tree area by subtracting the area of the soma from the total MAP-2 area, the length of the longest primary dendrite, the number of primary dendrites, and the number of secondary dendrites. Synapses relative to the dendritic tree were quantified as the SYN puncta number relative to a standardized dendrite length (30 μm).

Microglial morphological studies in culture: since microglia adopted different forms according to culture conditions, different parameters were assessed to study their morphology. Microglia [Iba1 (+) cells] morphology in culture and its changes based on the response to different stimuli (LPS or ST) were assessed by measuring the mean area and circularity per field (445 × 335 μm^2) using ImageJ (NIH) software as previously described (Traetta et al., 2021). These parameters reflect changes in either the extent of individual cell reactivity or the proportion of cells with a reactive profile. In the case of neuron-microglia co-cultures, microglia [Iba1 (+) cells] were classified into four different morphological types according to the number of branches and the size of the soma: cells with long and fine branches as type I, ameboid and large cells as type II, small with one or two very small branches as type III, and small, rounded and unbranched cells as type IV. In the case of mixed cortical glial cultures, microglia [Iba1 (+) cells] were classified into ramified (abundant long or short branches) or unramified (ameboid or bipolar) categories. Results of co-cultures and mixed glial cultures are expressed as mean values of the percentage of each morphology per field. Each field analyzed for neuron-microglia co-cultures corresponded to 445 × 335 μm^2 and each field for mixed glial cultures to 890 × 670 μm^2.

Astrocyte studies in culture: cortical astrocytes in astroglial-enriched and mixed cultures were classified according to their morphology as previously described (Acaz-Fonseca et al., 2019; Rosciszewski et al., 2019). Astrocytes [GFAP (+) cells] were considered polygonal if they lacked pronounced cytoplasmic protrusions, bipolar if they presented an elongated cell body or one long thin projection, or stellate if they had a smaller cell body and three or more long processes. Results are expressed as mean values of the percentage of each morphology per field (890 × 670 μm^2).

Transmission Electron Microscopy and Analysis

At PND35, control and VPA animals were fixed for electron microscopy as previously described (Traetta et al., 2021; Reinés et al., 2012). Briefly, they were anesthetized as detailed above and transcardially fixed with 4% w/v paraformaldehyde and 2.5% v/v glutaraldehyde in 0.1 M phosphate buffer. Sections were post-fixed in 0.05% w/v osmium tetroxide and dehydrated and embedded in Durcupan. The number of animals employed is in accordance with the literature (Kim et al., 2013; Xu et al., 2020). Sections of the medial PFC from 4 control and 4 VPA animals were contrasted with uranyl acetate and lead citrate as previously detailed (Traetta et al., 2021; Reinés et al., 2012) and photographed with a Zeiss 109 electron microscope equipped with a Gatan W10000 digital camera. Synapse number was assessed throughout 300 μm^2 of the medial PFC using the ImageJ (NIH) cell counter plugin and expressed as synapse number per μm^2. An average of 70 and 105 synapses per animal were found in control animals and the VPA group, respectively. The counting criterion was a pre-synapse with visible pre-synaptic vesicles and a prominent post-synaptic density indicative of an excitatory synapse morphology (Stewart et al., 2014).

Flow Cytometry and Analysis

Cultured cortical microglial cells (DIV7) and astrocytes (DIV2) isolated from control and VPA animals were harvested, fixed, and run on a Partec PAS III flow cytometer (Partec, GmbH, Münster, Germany), as previously described (Zárate et al., 2019; Traetta et al., 2021). Data analysis was performed with WinMDI 98 software. Based on the control group, we selected a representative region on a dot plot and then we used that same region to analyze the VPA group. Forward Scatter (FSC) and Side Scatter (SSC) mean values were used to determine relative cell size and internal complexity (granularity), respectively. Moreover, microglia and astrocytes from two independent cultures were evaluated separately. The high number of cells required per condition limited the repetitions of the experiments performed. A representative experiment of each cell type is shown.

Reverse Transcription Polymerase Chain Reaction Assays

RT-PCR assays were performed as previously described (Rosciszewski et al., 2018). RNA was isolated using the Quick-RNA™ Miniprep Kit (ZYMO Research, United States). The cDNA was generated using the MMLV-RT Kit (Genbiotech, Argentina) with Oligo(dT)18 Primers (Genbiotech, Argentina). PCR assays were performed using specific primers: TBP (Fwd: ACCGTGAAT CTTGGCTGTAA; Rev: CCGTGGCTCTCTTAT TCTCA; amplification product: 114 bp); IL1β: (Fwd: TCCATG AGCTTTGTACAAGG; Rev: GGTGCTGATGTACCAGTTGG; amplification product: 246 pb); TNFα: (Fwd: GTAGCCCACGTC GTAGCAAA; Rev: AAATGGCAAATCGGCTGACG; amplification product: 217 bp); IL6: (Fwd: CTCTCCGCAAGAGACTT CAG; Rev: TCTGACAGTGCA TCATCGCT; amplification product: 245 bp); Dicer: (Fwd: TTAACCTTTTGGTGTTTGATGAGTGT; Rev: GGACATGAT GGACAATTTTCACA; amplification product: 94 bp); Drosha: (Fwd: CAAAGGCAAGACGCACAG; Rev: CATAGGACGACA CGGCTTG; amplification product: 79 bp). TBP, IL1β, TNFα, IL6, and Drosha were amplified by 30 cycles and the annealing temperature was 60°C, while Dicer was amplified by 30 cycles and the annealing temperature was 62°C. PCR products were run in a 1.5% agarose gel and imaged using a Gel Doc EZ imager (Bio-Rad, United States). Each experiment included negative controls, in which MMLV-RT Kit reactions were performed in the absence of reverse transcriptase. Detailed RT and PCR protocols are

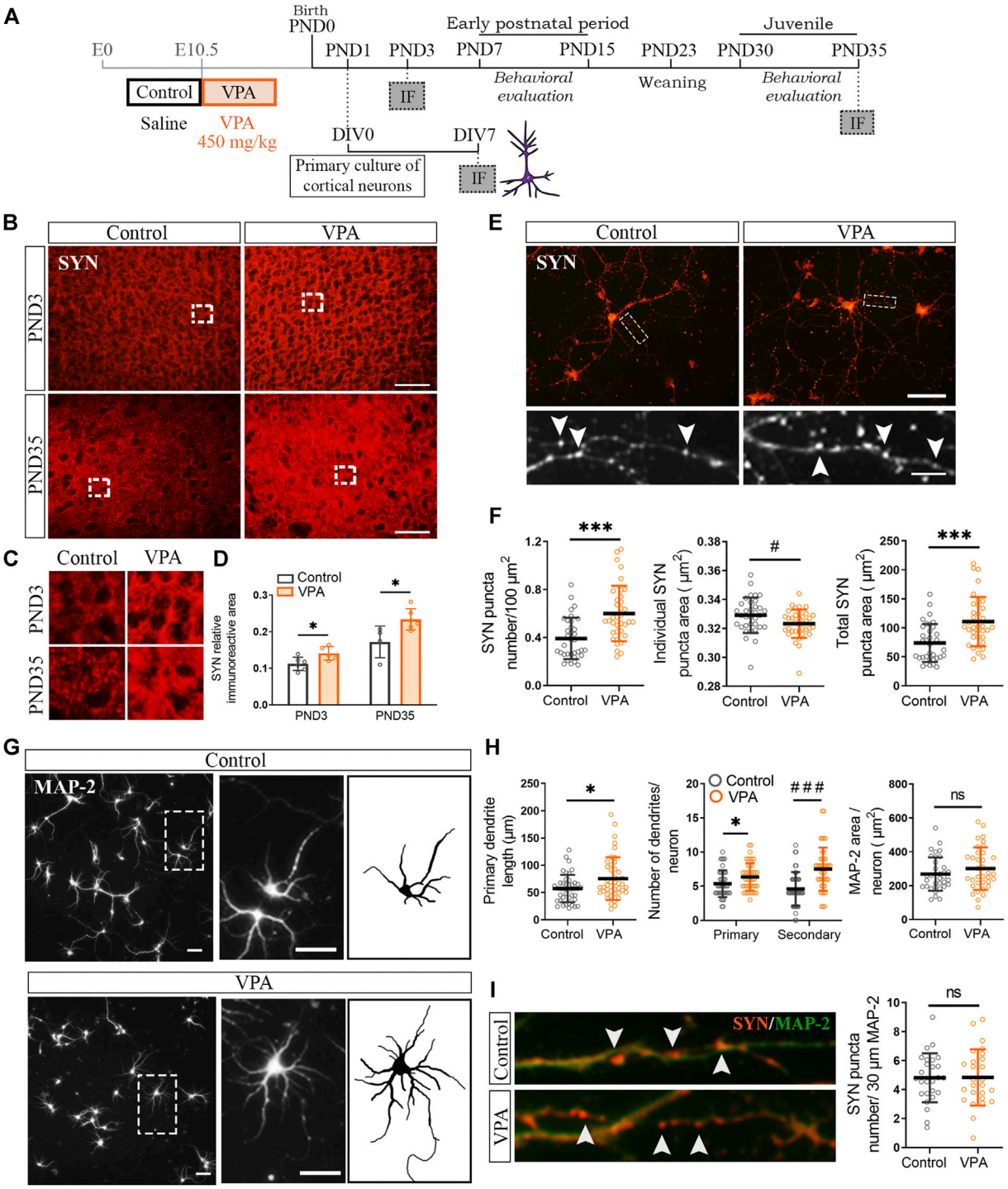

FIGURE 1 | Synaptic changes in the prefrontal cortex (PFC) of VPA rats were present at PND3 and were mimicked *in vitro*, in the absence of glia, by cortical neurons isolated from VPA rats. **(A)** Experimental groups were defined by prenatal VPA injection and pups were behaviorally evaluated. Primary cortical neuronal cultures were prepared from postnatal day (PND) 1 control and VPA pups, kept in culture until day *in vitro* (DIV) 7 and processed for immunofluorescence (IF). At PND3 and PND35, brains from control and VPA animals were processed for IF. **(B)** The PFC from control and VPA animals immunostained for synaptophysin (SYN) at PND3 and PND35. **(C)** Magnifications (×3) of SYN immunostaining revealed a punctate pattern. **(D)** Quantification showed an increase in SYN relative immunoreactive area in the PFC of VPA rats at PND3 and PND35. **(E)** Cortical neurons isolated from control and VPA animals immunostained for SYN. Magnification details SYN immunostaining pattern and arrowheads indicate individual puncta. **(F)** Neurons isolated from VPA animals showed an increase in SYN puncta number, a decrease in individual puncta size, and an increase in total SYN puncta area. **(G)** Cortical neurons isolated from control and VPA animals immunostained for MAP-2; a magnification of an individual neuron from each group and a scheme highlighting its dendritic arborization. **(H)** Quantification revealed longer primary dendrites and an increase in the number of

(*Continued*)

FIGURE 1 | primary and secondary dendrites in neurons from VPA animals. Total area of the dendritic tree did not differ between groups. **(I)** Photomicrographs display dendrites co-immunostained for SYN and MAP-2. Quantification revealed no statistically significant differences in SYN puncta number relative to the dendritic length between groups. Results are expressed as mean values (±SD). **(D)** Control, $n = 4–6$ animals; VPA, $n = 5–6$ animals. **(F,H)** Control, $n = 34–44$ neurons; VPA, $n = 34–44$ neurons from 2 independent cultures. **(I)** Control, $n = 26$ neurons; VPA, $n = 26$ neurons from 2 independent cultures). ns: non-significant, $^{*}p < 0.05$, $^{***}p < 0.001$ between groups by Student's *t*-test; $\#p < 0.05$, $\#\#\#p < 0.001$ between groups by Mann–Whitney *U* test. Scale bars: 50 μm **(B,E,G)**; 10 μm (inset **(E)**); the length of the photomicrographs in **I** corresponds to 30 μm.

available from authors upon request. Results shown correspond to 4 independent microglia or astroglial-enriched cultures at DIV7 and DIV2, respectively.

Statistical Analysis

Statistical analysis was performed using InfoStat software (Facultad de Ciencias Agropecuarias, Universidad Nacional de Córdoba, Argentina). Student's *t*-test or Mann–Whitney U test was applied when comparing two independent groups. The first was selected if the variables analyzed fulfilled the requirement of normality (Shapiro–Wilk test) and homogeneity of variances (F-test). In the case of comparing more than two groups, the Kruskal–Wallis test was performed. The analyses and levels of significance between groups are detailed in each figure legend. Values for T, W, H, n, degrees of freedom (df), and exact *p* values are shown in **Supplementary Tables S1, S2**. Statistical significance was set at $p < 0.05$.

RESULTS

Cultured Cortical Neurons Isolated From Valproic Acid Rats in the Absence of Glia Mimic the Synaptic Pattern Observed *In Vivo* in the Prefrontal Cortex

To address the temporal association of synapse and glial changes in the PFC of VPA rats, we first evaluated SYN immunostaining soon after birth in the neonatal period (PND3) and later during the juvenile postnatal period (PND35) (**Figure 1A**). Postnatal time points correspond to the postnatal day before the maturation deficits were evident in VPA animals [poor performance in the negative geotaxis test and delayed eye-opening (**Supplementary Figures S1A–C**)] and the juvenile period, once the social impairment was established in the VPA model (**Supplementary Figures S1A,D**). The PFC of VPA rats showed increased SYN immunostaining at PND3 and PND35 (**Figure 1B**), as confirmed by quantification (**Figure 1D**). SYN immunolabeling showed the typical synaptic pattern that corresponds to protein clusters (**Figure 1C**). These results indicate that cortical synaptic changes are already evident early during the neonatal period.

Since synaptic alterations observed *in vivo* can be due to either primary neuronal alterations and/or microglial/astroglial altered physiology, we evaluated synapse formation in the absence of glial cells. For that purpose, we cultured cortical neurons isolated from control and VPA animals at PND1 (**Figure 1A**). **Figure 1E** shows cortical neurons in culture immunostained for SYN. They display the typical punctate SYN immunostaining that corresponds to synaptic clusters. Primary cortical neurons isolated from VPA rats formed in culture (DIV7) a greater number of synapses than that in controls, as revealed by the increase in SYN puncta number and total SYN puncta area (**Figure 1F**). Cortical neurons isolated from VPA animals also showed a reduction in individual SYN puncta size indicative of smaller clusters of synaptic vesicles (**Figure 1F**). As synapse formation and dendritic arborization are tightly associated (Rollenhagen et al., 2013), we studied the dendritic tree of cortical neurons by MAP-2 immunostaining (**Figure 1G**). Cortical neurons isolated from VPA animals exhibited a more complex dendritic arbor characterized by longer primary dendrites and a greater number of primary and secondary dendrites (**Figure 1H**). However, these rendered no differences in dendritic tree area that might indicate dendrites of smaller caliber (**Figure 1H**). **Figure 1I** shows neurons co-labeled with SYN/MAP-2; quantification of SYN puncta number relative to dendritic length revealed the absence of statistically significant differences between groups. These results imply that *in vitro* and in the absence of glia, postnatal cortical neurons isolated from VPA rats mimic the *in vivo* increase in synapse number and that the higher complexity of dendritic arborization could account for such synapse increment.

The Greater Number of Excitatory Synapses Characterizes the Cortical Synaptic Profile of Valproic Acid Animals *In Vivo* and *In Vitro*

To determine the contribution of glutamatergic synapses to the increase in the number of synapses in the PFC of VPA animals, at PND3 and PND35, we evaluated the immunostaining for vesicular glutamate transporter (vGLUT-1) and electron microscopy, respectively (**Figures 2A–C**). The PFC of VPA rats showed increased vGLUT-1 immunolabeling at PND3 confirmed by quantification of the relative immunoreactive area (**Figure 2B**). At PND35, quantification of asymmetric synapses revealed a greater number of excitatory synapses in the PFC of VPA rats than that in the controls (**Figure 2C**). To study excitatory and inhibitory synapses in cortical neurons isolated from control and VPA animals cultured in the absence of glia, cells were immunostained for PSD-95 and GAD-67, respectively (**Figures 2A,D,F**). Both synaptic markers displayed the characteristic punctate immunostaining (**Figures 2D,F**, higher magnification). Cortical neurons from VPA animals formed a higher number of excitatory post-synapses in culture, as revealed by the increase in PSD-95 puncta number and total PSD-95 puncta area (**Figures 2D,E**); post-synapses were smaller as indicated by the reduction in individual PSD-95 puncta area (**Figure 2E**). These results parallel the alterations in SYN puncta (**Figures 1E,F**).

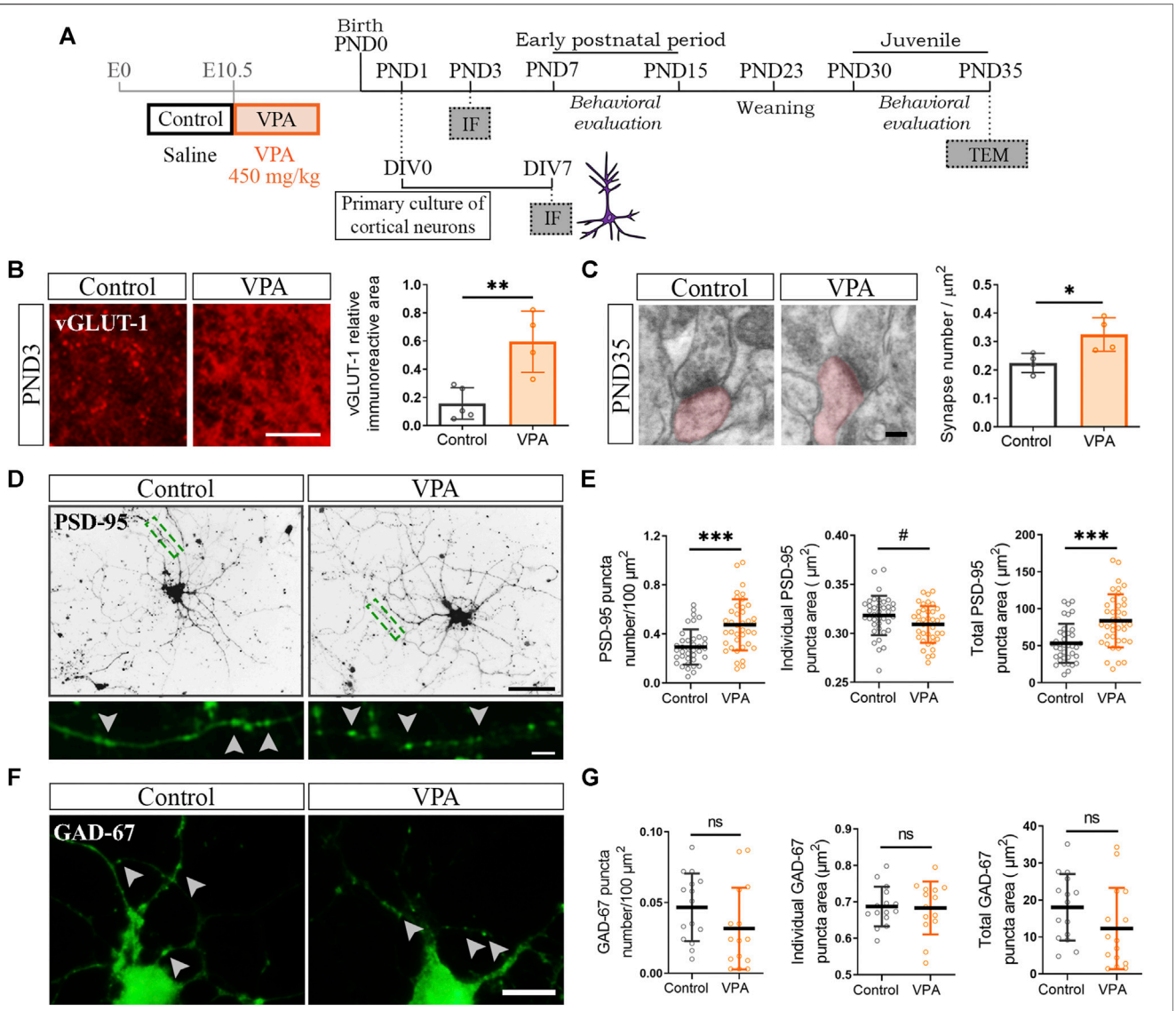

FIGURE 2 | Increased number of excitatory synapses in the prefrontal cortex (PFC) of VPA animals and in cultured cortical neurons isolated from VPA rats. **(A)** Once the VPA model was established, primary cortical neuronal cultures were prepared from PND1 control and VPA pups and processed at day *in vitro* (DIV) 7 for immunofluorescence (IF). The model was validated behaviorally. Brains from control and VPA animals were processed at PND3 for IF and at PND35 for transmission electron microscopy (TEM) analysis. **(B)** At PND3, the PFC of VPA animals displayed an increase in vesicular glutamate transporter 1 (vGLUT-1) relative immunoreactive area. **(C)** At PND35, the PFC of VPA animals exhibited a greater number of excitatory synapses (asymmetric) by TEM. **(D)** Cultured cortical neurons isolated from control and VPA animals immunostained for PSD-95. Magnification depicts a punctate immunostaining pattern. **(E)** Quantification showed an increase in PSD-95 puncta number, a reduced individual puncta size and an increase in total puncta area in neurons from VPA animals. **(F)** Cortical neurons isolated from control and VPA animals immunostained for GAD-67. Arrowheads indicate individual puncta. **(G)** No statistically significant differences were found between groups in any parameter quantified. Results are expressed as mean values (±SD). **(B,C)** Control, $n = 4$–5 animals; VPA, $n = 4$ animals. **(E)** Control, $n = 38$ neurons; VPA, $n = 39$ neurons from 2 independent cultures. **(G)** Control, $n = 15$ neurons; VPA, $n = 15$ neurons from 2 independent cultures. ns: non-significant, $^{*}p < 0.05$, $^{**}p < 0.01$, and $^{***}p < 0.001$ between groups by Student's *t*-test and $\#p < 0.05$ between groups by Mann–Whitney *U* Test (for individual GAD-67 puncta area). Scale bars: 50 µm **(D)**; 25 µm **(B)**; 10 µm **(F)**; 5 µm (inset **(D)**); 100 nm **(C)**.

Regarding GABAergic synapses, no statistically significant differences were found between neurons from control and VPA animals in either GAD-67 puncta number, total area, or individual GAD-67 puncta area (**Figures 2F,G**). These results show that the PFC of VPA rats exhibits an increase in excitatory synapses in both the neonatal and juvenile periods and that this synaptic pattern is reproduced *in vitro* in the absence of glial cells.

Cortical Microglia Isolated From Valproic Acid Animals Once Synaptic Changes Are Already Established Show *In Vitro* Long-Lasting Changes

Keeping in mind that synaptic changes are already evident in the neonatal period and persist into the juvenile stage in the PFC of

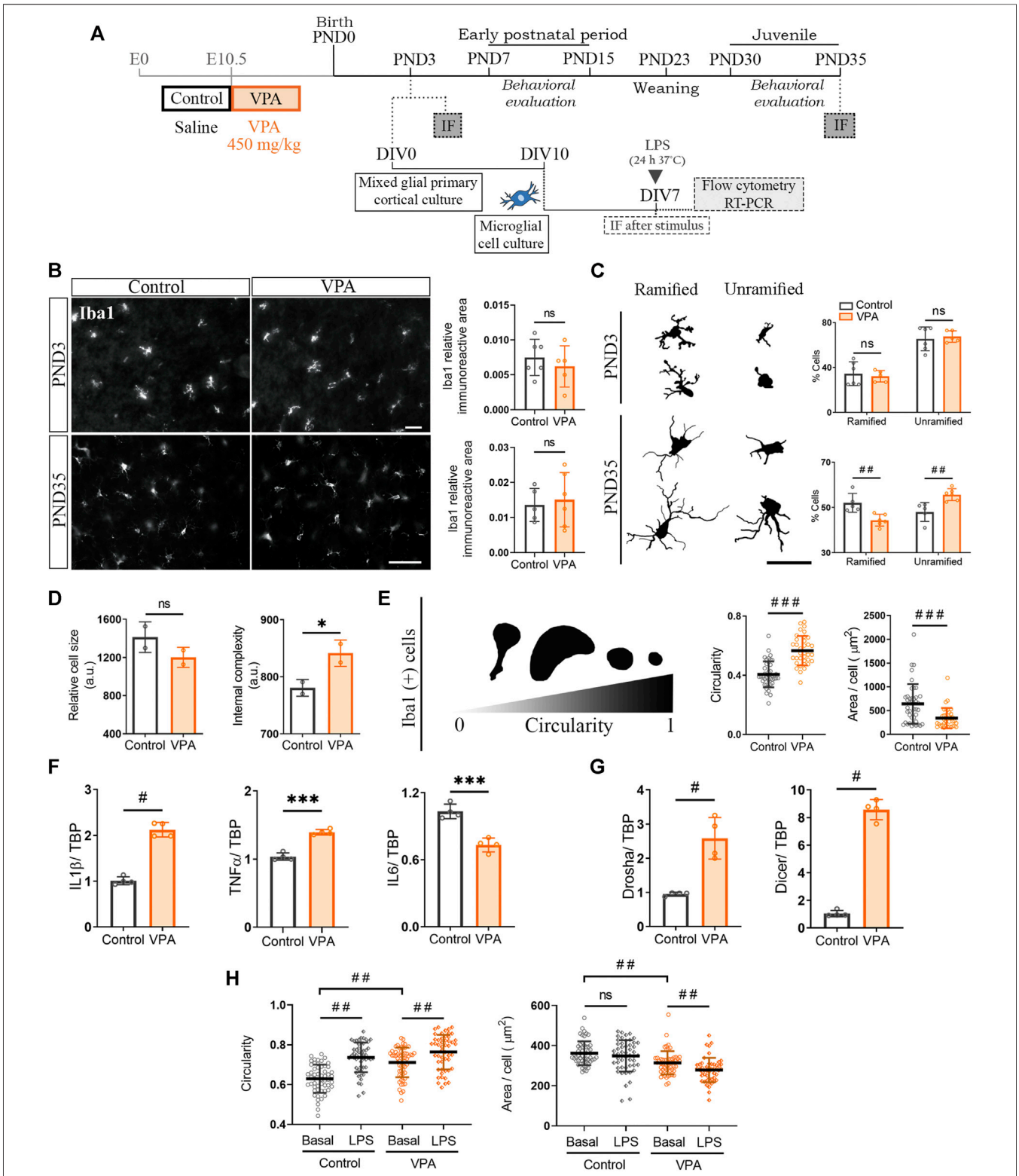

FIGURE 3 | Cultured cortical microglia isolated from VPA animals showed a pro-inflammatory profile which was absent *in vivo* at PND3 but present at PND35. **(A)** Primary mixed cortical glial cultures were prepared from postnatal day (PND) 3 control and VPA animals. At day *in vitro* (DIV) 10, microglia were detached, re-seeded, and grown for 7 days before analysis. Siblings were behaviorally evaluated. At PND3 and PND35, brains from control and VPA animals were processed for immunofluorescence (IF). **(B)** PFC of control and VPA animals immunostained for Iba1. At PND3 and PND35, no statistically significant differences were found in Iba1 relative immunoreactive area. **(C)** Schematic representation of microglial morphology at PND3 and PND35. At PND35 but not at PND3, the PFC of VPA rats

(*Continued*)

FIGURE 3 | evidenced an increase in the proportion of unramified Iba1 (+) cells concomitantly with a decrease of ramified cells. **(D)** Cultured microglia isolated from VPA animals showed preserved size but increased internal complexity when analyzed by flow cytometry. **(E)** Representation of microglia morphology in culture immunostained for Iba1 (DIV7) and its associated circularity. Microglia isolated from VPA animals displayed an increase in circularity and a smaller cell area. **(F)** Microglia isolated from VPA animals showed increased expression of IL1β and TNFα but lower IL6 RNA levels. **(G)** The expression of Drosha and Dicer was increased in microglia isolated from VPA rats. **(H)** After a 24 h LPS stimulus, microglia from both control and VPA animals showed greater circularity, but only microglia from VPA animals showed a smaller size compared with their basal condition. Results are expressed as mean values (±SD). **(B,C)** Control, n = 5–6 animals; VPA, n = 5–6 animals. **(D)** A representative experiment run by duplicate. **(E)** Control, n = 42 photomicrographs; VPA, n = 35 photomicrographs from 3 independent cultures; **(F,G)** 4 independent cultures; **(H)** n = 50–57 photomicrographs per group from 2 independent cultures. **(B–G)** ns: non-significant (for B,D); $^{*}p < 0.05$, and $^{***}p < 0.001$ between groups by Student's t-test (for C); $\#p < 0.05$, $\#\#p < 0.01$, and $\#\#\#p < 0.001$ between groups by Mann–Whitney U test; **(H)** $\#\#p < 0.01$ between groups by Kruskal–Wallis test. Scale bar: 50 μm.

VPA animals, we aimed to analyze microglial morphology early at PND3 and later at PND35 (**Figure 3A**). Initial quantification of the Iba1 immunostained area showed no statistically significant differences at either PND3 or PND35 between control and VPA animals (**Figure 3B**). Further meticulous morphology assessment of Iba1 (+) cells revealed a similar proportion of ramified and unramified microglia in control and VPA animals at PND3 (**Figure 3C**). However, as development proceeds, at PND35, the PFC of VPA rats showed a smaller percentage of ramified microglia and a higher proportion of unramified cells than those of control animals (**Figure 3C**). These results suggest that microglia show a normal profile at PND3 but turns into reactive microglia at PND35 *in vivo*.

To study microglial cells in the absence of neurons, we prepared primary microglial cultures from control and VPA rats at PND3 (**Figure 3A**). This time point is appropriate for culturing glial cells (McCarthy and de Vellis, 1980; Tamashiro et al., 2012); in this case, it coincides with the presence of early synaptic changes in the PFC of VPA animals (**Figure 1B**). Under basal conditions, cortical microglia isolated from VPA animals showed a tendency to be smaller and to have increased internal complexity (**Figure 3D**) consistent with the decreased cell area and increased circularity found by morphological evaluation of Iba1 (+) cells (**Figure 3E**). A greater internal complexity, greater circularity, and reduced cell area are characteristic parameters of reactive microglia (Ritzel et al., 2015; Lively and Schlichter, 2018). This reactive microglial morphology matched the pro-inflammatory cytokine profile found in microglia isolated from VPA animals (**Figure 3F**) (Lively and Schlichter, 2018; Hoogland et al., 2015). Since miRNA processing enzymes are involved in regulating inflammatory responses in microglia (Varol et al., 2017), we studied the expressions of Drosha and Dicer in microglia isolated from control and VPA rats. The expressions of Drosha and Dicer were increased in microglia isolated from VPA animals (**Figure 3G**). Since the absence of Dicer exacerbates the microglia pro-inflammatory response (Varol et al., 2017), these results may suggest that the microglial cytokine expression profile is regulated by both transcriptional and translational control mechanisms resulting in a mild pro-inflammatory profile. We then evaluated microglial response when exposed to the pro-inflammatory LPS stimulus. Cortical microglia from both control and VPA animals reacted by increasing cell circularity (**Figure 3H**). This result indicates that even when microglia from VPA animals show a reactive morphological profile under basal conditions, these cells are able to further respond to a pro-inflammatory stimulus and the experimental assay can evidence further increments in microglia reactivity.

Altogether, our results indicate that microglial cells isolated from VPA animals show long-lasting changes when fully differentiated in culture, characterized by a basal reactive profile but still with a preserved response to classical pro-inflammatory LPS. These results suggest that even though microglial alterations *in vivo* seem absent at PND3 and become statistically representative at PND35, isolated microglia at PND3 already show an altered, mild reactive profile when maintained in culture *in vitro*, which do support early microglia modifications at PND3.

Adaptive Response of Cortical Microglia to Neuronal Milieu in Valproic Acid Rats: Normal Morphological Profile, Preserved Neurite Outgrowth Stimulation, and Resistance to Phagocytic Stimuli

Considering that both neurons and microglia isolated from VPA animals mimic juvenile alterations once differentiated individually *in vitro*, but microglial changes are only evident in the PFC of juvenile VPA animals, we aimed to study how neurons and microglia from control and VPA rats interact *in vitro* in reconstituted cultures. Neuron-microglia interaction was studied in reconstituted co-cultures of primary cortical neurons and microglia isolated from control and VPA rats by evaluating microglial morphology and neuronal parameters (**Figure 4A**). Since microglial reactivity profile is associated with cell functionality (Walker et al., 2014; Fernández-Arjona et al., 2019), we first determined microglial response to different neuronal microenvironments by co-culturing microglia isolated from control and VPA animals with neurons from control or VPA rats and measuring cell morphology in cells immunostained for Iba1. Representative photomicrographs in **Figure 4B** show Iba1 (+) cell classification into four morphological categories that were used to study their response to neurons isolated from control or VPA rats. As shown in **Figure 4B**, microglial cells isolated from control rats revealed a quite different morphological profile when exposed to neurons isolated from VPA rats compared to those with neurons from controls (**Figure 4B**). Interestingly, microglia isolated from VPA animals showed the same profile when exposed to neurons from control and VPA rats. Indeed, this morphological profile was also similar to that shown by microglia from control animals exposed to neurons from control rats. Thus, we conclude that microglia derived from VPA animals are adapted to the molecular cues shown by

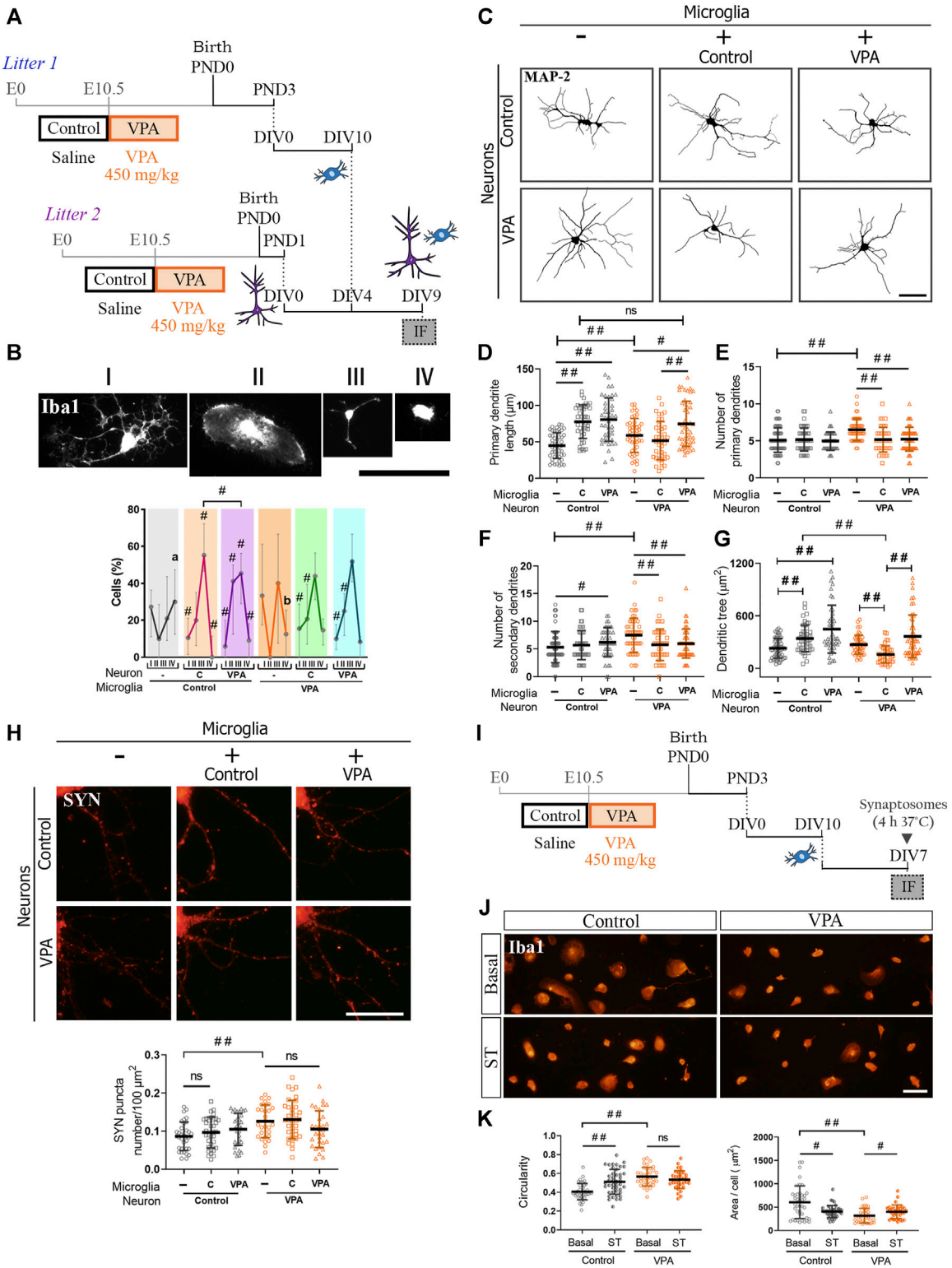

FIGURE 4 | Microglia from VPA animals showed resistance to phagocytic stimuli and, in the presence of neurons isolated from VPA rats, acquired a normal morphological profile and promoted neurite outgrowth. **(A)** Co-cultures were obtained by seeding cortical microglia on cortical neurons (DIV4). After 5 days in co-culture conditions, cells were processed for immunofluorescence (IF). **(B)** Representation of microglial morphology in co-cultures immunostained for Iba1 and its categorization (I–V). In the presence of neurons, microglia isolated from VPA rats showed a similar morphological profile regardless of neuronal substrate, which was similar to microglia from control rats in the presence of neurons from control animals. Microglia isolated from control rats evidenced a different profile when exposed to neurons

(*Continued*)

FIGURE 4 | from VPA animals. **(C)** Dendritic arbor of cortical neurons isolated from control and VPA animals in co-culture conditions and immunostained for MAP-2. **(D)** Except for neurons isolated from VPA animals exposed to microglia from control animals, an increase in the length of primary dendrites was observed in the other conditions. Microglia isolated from control or VPA animals reduced the number of **(E)** primary and **(F)** secondary dendrites of neurons isolated from VPA animals. **(G)** An increase or a trend toward an increase in dendritic tree area was concomitant to the dendritic outgrowth effect. Microglia isolated from control animals reduced the dendritic tree area of neurons from VPA rats. **(H)** Cortical neurons isolated from control and VPA animals immunostained for SYN in the absence and presence of microglia from control and VPA animals. Quantification revealed no statistically significant differences in SYN puncta number in the presence of microglia. **(I)** Primary microglia cultures were exposed to synaptic terminals (ST). **(J)** Microglial culture from control and VPA animals immunolabeled for Iba1 under basal conditions and after exposure to ST. **(K)** Microglia isolated from VPA animals showed greater circularity and a smaller cell area than those in the control group under basal conditions. After exposure to ST, microglia from control animals responded with an increase in circularity and a reduction in the cell area. Microglia from VPA animals responded with a slight increase in cell area. Results are expressed as **(B)** median with interquartile range (n = 24–27 photomicrographs per group from 2 independent co-cultures); **(D-H,K)** mean values (±SD): **(D–G)** 39–68 neurons per group from 2 independent co-cultures; **(H)** 29–35 neurons per group from 2 independent co-cultures; **(K)** 34–43 photomicrographs per group from 3 independent cultures). ns: non-significant; #$p < 0.05$; ##$p < 0.01$ between groups by Kruskal–Wallis test. In **(B),** # indicates difference from the microglial culture of that same precedence and different letters show differences between microglia experimental groups. Scale bars: 50 μm **(B,C,J)**; 25 μm **(H)**.

neurons derived from VPA animals. Microglial cells from VPA animals are adapted to their neuronal substrate, thus behaving as control microglia in the presence of control neurons.

Since microglia promote neurite outgrowth *in vitro* (Zhang and Fedoroff, 1996), we addressed microglial effects on dendritic arborization in neuron-microglia co-cultures (**Figure 4A**). **Figure 4C** shows representative photomicrographs of MAP-2 immunostaining in cortical neurons isolated from control and VPA rats and cultured in the absence or presence of microglia isolated from either experimental group. As expected, microglia from control animals promoted neurite outgrowth in neurons from control animals by inducing longer primary dendrites, leading to an increase in dendritic tree area (**Figures 4C,D,G**). Likewise, microglia isolated from VPA rats induced neurite outgrowth by increasing the length of primary dendrites in neurons isolated either from VPA or control animals (**Figures 4C,D**). Accordingly, a trend toward an increase or a significant increase in dendritic tree area was recorded in neurons from VPA and control animals, respectively (**Figure 4G**). Besides, microglia isolated from control or VPA animals decreased the number of primary and secondary dendrites in neurons from VPA animals but not in neurons from control animals (**Figures 4E,F**). Surprisingly, while microglia from VPA animals promoted dendritic outgrowth on any neuronal substrates, microglia isolated from control animals did not increase dendritic length and even reduced the dendritic tree area of neurons isolated from VPA rats (**Figures 4D,G**). These results indicate that microglia isolated from VPA animals induce similar dendritic effects on neurons from control or VPA animals and these resemble those induced by microglia from control animals on neurons isolated from control animals. Moreover, microglia from control animals induce distinctive effects on neurons isolated from VPA rats by eliciting opposing changes to those produced by microglia from VPA animals. Thus, microglia from VPA animals seem to be adapted to the neuronal milieu; consequently, they respond as normal microglia even on neurons exhibiting synaptic and dendritic changes.

As microglia also play a role in synapse formation and pruning (Paolicelli et al., 2011; Schafer et al., 2012; Miyamoto et al., 2016), we studied the effect of microglia isolated from control and VPA animals on SYN puncta number in neurons in these co-culture conditions from both experimental groups (**Figures 4A,H**). As previously shown in **Figure 1F**, neurons isolated from VPA animals showed an increase in SYN puncta number in the absence of microglia (**Figure 4H**). In our experimental conditions, microglia from control animals did not modify SYN puncta number in neurons from either control or VPA rats. Similarly, microglia from VPA rats did not affect SYN puncta number irrespective of the neuronal substrate. These results suggest that microglia from VPA animals have no counteracting effect on the increase in synapse number shown in neurons from VPA rats. Thus, we evaluated microglia response under a phagocytic stimulus induced by exposure to synaptic terminals (**Figures 4I,J**). To assess a general response, isolated cortical microglia from control and VPA animals were exposed to cortical synaptosomes purified from naïve rats and then immunostained for Iba1. Microglia isolated from control animals and exposed to synaptic terminals showed increased circularity and reduced cellular area (**Figure 4K**), both changes indicative of cell reactivity. Interestingly, microglia isolated from VPA animals did not show a statistically significant morphological response after exposure to synaptic terminals (**Figures 4J,K**), even when these cells increased their circularity in response to LPS (**Figure 3H**). These results indicate that cortical microglia isolated from VPA animals cannot alter synapse number when co-cultured with neurons and show resistance to the phagocytic stimulus by synaptosomes. Overall, results suggest that microglia isolated from VPA animals are less sensitive or adapted to their neuronal milieu, adopting a normal morphological profile, promoting neurite outgrowth, and showing a lack of response to phagocytic cues.

Cortical Astrocytes Isolated From Valproic Acid Rats Are Engaged in a Long-Lasting Pro-Inflammatory Program

Our results show that cortical microglia from VPA animals exhibit a normal morphological profile when exposed to neurons from VPA animals *in vitro*. However, these cells display a reactive morphology in the PFC of VPA rats at PND35 *in vivo*. Since astrocytes are known to modulate the microglial function (Matejuk and Ransohoff, 2020; Liddelow et al., 2020) and, in the PFC of VPA animals, these glial cells exhibit a reactive morphology at PND35 (Codagnone et al., 2015), we hypothesized that astroglia-microglia crosstalk could be

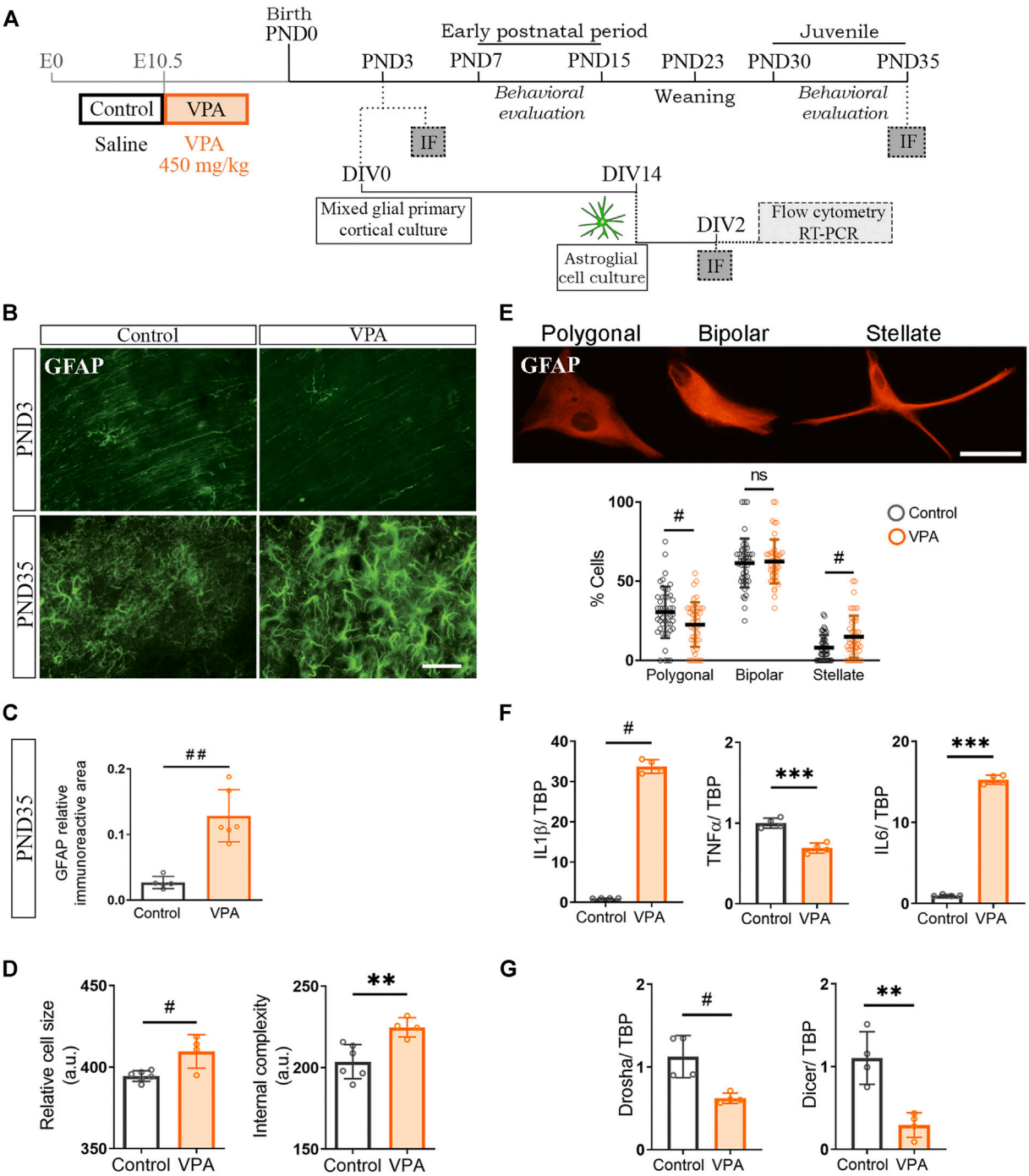

FIGURE 5 | Cultured cortical astroglia isolated from VPA animals showed an inflammatory profile that was revealed *in vivo* at PND35. **(A)** Mixed cortical glial cultures were prepared from postnatal day (PND) 3 control and VPA rats to obtain astroglial-enriched cultures, which were processed [day *in vitro* (DIV) 2] for flow cytometry, RT-PCR, and immunofluorescence. Siblings were behaviorally evaluated. At PND3 and 35, immunofluorescence (IF) was performed on brains from control and VPA animals. **(B)** The PFC of control and VPA rats immunostained for GFAP at PND3 and 35. At PND3, the immunostaining pattern corresponded to radial glia and at PND35 to astrogliosis in VPA animals. **(C)** Quantification at PND35 confirmed an increase in GFAP relative immunoreactive area in the PFC of VPA animals. **(D)** Cortical astrocytes in culture isolated from VPA animals showed an increase in cell size and internal complexity when analyzed by flow cytometry. **(E)** Representation of astrocyte morphology in culture immunostained for GFAP and its corresponding categorization. Astrocytes isolated from VPA animals displayed a reduction in the proportion of polygonal cells with a concomitant increase in stellate astrocytes. **(F)** Astrocytes isolated from VPA animals showed increased expression of IL1β and IL6 but lowered TNFα RNA levels. **(G)** The expression of Drosha and Dicer was diminished in astrocytes isolated from VPA rats. Results are expressed as mean values (±SD). **(C)** Control, $n = 5$ animals; VPA, $n = 6$ animals. **(D)** A representative experiment. **(E)** Control, $n = 47$ photomicrographs; VPA, $n = 47$ photomicrographs from 3 independent cultures. **(F,G)**: 4 independent cultures, $^{**}p < 0.01$, $^{***}p < 0.001$ between groups by Student's *t*-test and ns: non-significant; $\#p < 0.05$; $\#\#p < 0.01$ between groups by Mann–Whitney *U* test. Scale bar: 50 μm.

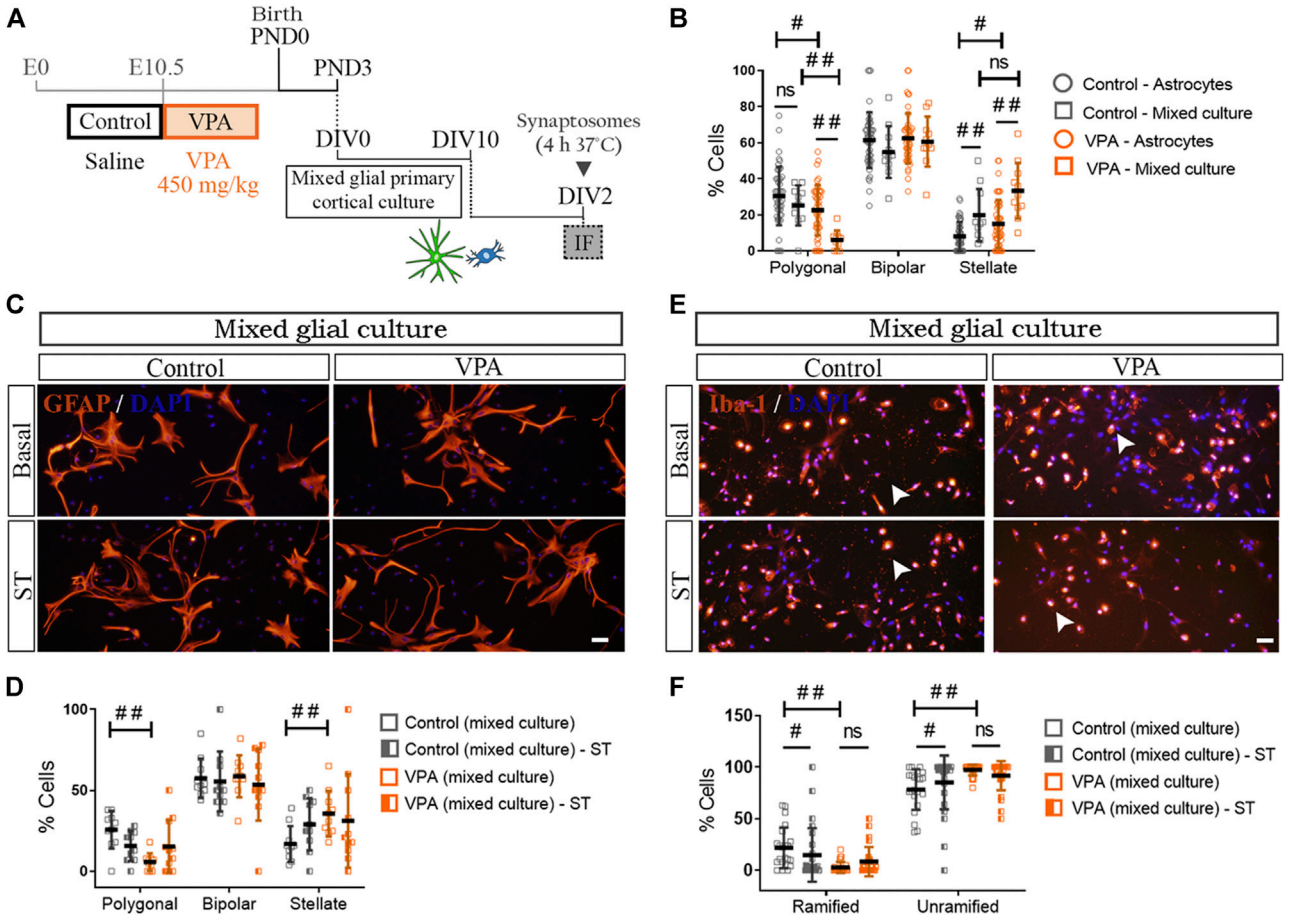

FIGURE 6 | Impact of astrocyte-microglia crosstalk on morphological profiles and responses to synaptic terminals of glial cells isolated from control and VPA animals. **(A)** Mixed cortical glial cultures isolated from control and VPA animals were exposed to synaptosomes (ST) (DIV2). **(B)** In mixed glial cultures from control animals, the presence of microglia increased the proportion of stellate astrocytes compared with astroglial-enriched cultures (astrocytes). In the VPA group, the presence of microglia increased stellate and decreased polygonal astrocytes when compared with astroglial-enriched cultures (astrocytes). **(C)** Mixed glial cultures from control and VPA animals under basal conditions and after exposure to cortical ST immunostained for GFAP and labeled with DAPI. **(D)** In mixed glial cultures, astrocyte morphology is not altered by exposure to ST in either control or VPA group. **(E)** Mixed glial cultures from control and VPA animals immunostained for Iba1 and labeled with DAPI under basal conditions and after exposure to cortical ST. **(F)** While in mixed glial cultures from control animals exposed to ST, microglia responded with a decrease in ramified cells and an increase in unramified cells, in mixed cultures isolated from VPA animals, microglia failed to respond. Results are expressed as mean values (±SD) **(B)**: 11 photomicrographs per group from two independent mixed cultures and 47 photomicrographs per group from three independent astroglial-enriched cultures. **(D,F)** 10–26 photomicrographs per group from 2 independent mixed cultures; ns: non-significant; #$p < 0.05$; ##$p < 0.01$ between groups by Kruskal–Wallis test. Scale bars: 50 µm.

responsible for the long-term reactive microgliosis *in vivo* in VPA animals. We first determined the temporal relationship of astroglial morphology with respect to synaptic changes by evaluating GFAP immunostaining in the PFC of control and VPA rats at PND3 and PND35 (**Figure 5A**). At PND3, the PFC of VPA rats showed a GFAP pattern compatible with immature glia (radial glia) and similar to age-matched control animals (Farhy-Tselnicker and Allen, 2018). At PND35, GFAP immunostaining was increased in the VPA group (**Figure 5B**) as confirmed by quantification of relative immunoreactive area (**Figure 5C**), which is indicative of astrogliosis (Hol and Pekny, 2015). These results suggest that cortical astrogliosis is evident after synaptic changes are established in the PFC (PND3). Then, to study astrocytes in the absence of neurons and microglia, we isolated cortical astrocytes from control and VPA animals (PND3) and grew them in culture (**Figure 5A**). Astrocytes isolated from the VPA group showed increased cell size and internal complexity assessed by flow cytometry (**Figure 5D**). Morphological evaluation of astrocytes in culture immunostained for GFAP revealed an increased proportion of stellate cells with a concomitant decrease in the proportion of polygonal astrocytes in the VPA group (**Figure 5E**). Stellate morphology, larger astrocytes, and higher internal complexity are parameters of increased cell reactivity (Rosciszewski et al., 2019; Acaz-Fonseca et al., 2019). In accordance with the reactive morphological profile, cortical astrocytes isolated from VPA rats exhibited a pro-inflammatory cytokine expression profile (**Figure 5F**). We next evaluated miRNA processing enzymes

and found that astrocytes isolated from VPA animals showed a reduced expression of Drosha and Dicer (**Figure 5G**). This alteration can be associated with a pro-inflammatory program since Dicer deficiency proved to lead to astrogliosis (Sun et al., 2019). Altogether, these results indicate that cortical astrocytes isolated from VPA animals show long-lasting changes that give rise to a reactive profile once fully differentiated *in vitro* and this parallels with astrogliosis observed in the PFC of VPA animals at PND35. Considering that major astrogliogenesis occurs after the neonatal period (Farhy-Tselnicker and Allen, 2018) and that astrocytes are crucial for modulating microglial function (Matejuk and Ransohoff, 2020), long-lasting changes in astrocytes could affect microglia and, thus, contribute to the microglial reactive profile seen in the PFC of VPA rats at PND35.

Distinctive Cortical Astrocyte-Microglia Crosstalk in Valproic Acid Rats

Our previous results suggest that long-lasting changes in cortical astrocytes isolated from VPA animals may affect the astroglial function and consequently astroglia-microglial crosstalk (Matejuk and Ransohoff, 2020). To address astrocyte-microglia bidirectional communication, we studied astrocyte morphology in mixed cortical glial cultures immunostained for GFAP (**Figures 6A**,**B**). In mixed glial cultures isolated from control animals, the presence of microglia increased the proportion of stellate cells without modifying the proportion of polygonal astrocytes [astroglial-enriched cultures (astrocytes) vs. mixed cultures] (**Figure 6B**). It should be noted that, as also shown in **Figure 5E**, astrocytes isolated from VPA animals exhibited an increased proportion of stellate astrocytes concomitantly with a reduction in the proportion of polygonal cells in astroglial-enriched cultures [astroglial-enriched cultures (astrocytes) vs. mixed cultures] (**Figure 6B**). In these astrocytes, the presence of microglia further increased the proportion of stellate cells with a concomitant reduction in the proportion of polygonal astrocytes (**Figure 6B**). **Figure 6D** shows quantification of astrocyte morphology in cortical mixed cultures from control and VPA animals exposed to synaptic terminals. In the presence of microglia, exposure to synaptic terminals did not promote morphological changes in astrocytes isolated from either control or VPA rats when compared with basal mixed culture conditions (**Figures 6C,D**). Thus, results indicate that the presence of microglia exacerbates the reactive morphological profile of astrocytes isolated from VPA rats toward an increase in stellate cells and a reduction in polygonal cells, indicative of astrocyte reactivity. Results suggest that cortical astroglia-microglia crosstalk in the VPA model results in greater astrocyte reactivity.

We then evaluated astrocyte-microglia crosstalk by assessing microglia morphology in Iba1 (+) cells from mixed cortical glial cultures (**Figures 6E,F**). In the presence of astrocytes, microglia from VPA animals showed increased basal reactivity as indicated by a lower proportion of ramified microglia and a higher proportion of unramified cells in comparison with mixed glial cultures from control rats (**Figure 6F**). It is worth mentioning that a similar microglia profile was found in microglia cultures from VPA animals (**Figure 3E**). In the presence of astrocytes, exposure to synaptic terminals induced a reduction in ramified cells concomitantly with an increase in the proportion of unramified microglia in the control group (**Figure 6F**) (Bohatschek et al., 2001). However, such an effect was not observed in microglial cells in mixed cultures from VPA animals (**Figure 6F**). It should be mentioned that microglia isolated from VPA rats were also insensitive to a phagocytic stimulus (**Figure 3F**). Results indicate that microglia display a reactive profile in the presence of astrocytes and that astrocyte-microglia crosstalk does not engage microglia in a phagocytic response.

DISCUSSION

This study provides evidence of long-lasting microglia and astroglia changes induced by prenatal exposure to VPA and suggests microglia-astroglia crosstalk as a key process implicated in neuroinflammation described for ASD. Our findings reveal that cortical microglia isolated from VPA animals are insensitive or adapted to synaptic changes and that microglia-astroglia crosstalk enables microglia pro-inflammatory profile and exacerbates astrogliosis without engaging microglia in response to phagocytic stimuli. In the present work, we used the VPA rat model since it mimics behavioral, anatomical, synaptic, and glial patterns described in ASD (Nicolini and Fahnestock, 2018) and studied synaptic and glial profiles in the PFC, a brain area associated with ASD impairments (Benekareddy et al., 2018; Chini and Hanganu-Opatz, 2021). Herein, we show that in the PFC of VPA animals, synaptic changes are evident in the neonatal period, but there is an absence of microgliosis. *In vitro*, cortical microglia isolated from VPA animals, when synaptic changes are already established, show a long-lasting but mild pro-inflammatory profile and an intrinsic resistance to phagocytic stimuli when cultured in the absence of neurons. Cortical microglia show a biphasic response, with initial unresponsiveness *in vivo* and *in vitro* to the synaptic alterations presented by neurons from VPA animals and a late microgliosis in juvenile animals. Specifically, in the presence of neurons, cortical microglia display a normal morphological pattern and promote dendritic outgrowth. In line with their adaptive response, microglia show an increase in miRNA processing enzymes that may participate in anti-inflammatory processes. However, *in vivo*, juvenile VPA animals show microgliosis in the PFC. Interestingly, the microgliosis at the juvenile period of VPA animals is concomitant with astrogliosis. Astrocytes isolated from VPA animals show a broader long-lasting pro-inflammatory profile, including an increased expression of pro-inflammatory cytokines and a decrease in miRNA processing enzymes. More importantly, microglia-astroglia crosstalk enables microglia pro-inflammatory profile and exacerbates astrogliosis without engaging glial cells in response to phagocytic stimuli.

Regarding the synaptic changes in the PFC, juvenile VPA animals evidence a greater number of excitatory synapses. This is in accordance with previous reports showing increased

glutamatergic synaptic proteins (Kim et al., 2013) and hyper-connectivity and hyper-plasticity (Rinaldi et al., 2008) in this brain region of juvenile VPA animals. Interestingly, PFC activation impairs social behavior (Benekareddy et al., 2018). Remarkably, this alteration is revealed early during the postnatal period since SYN and vGLUT-1 immunolabeling increase at PND3. Particularly, an increase in vGLUT-1 expression could also suggest a different maturation synaptic stage in this brain region of VPA animals (Minelli et al., 2003; Farhy-Tselnicker and Allen, 2018). Similarly, electrophysiological alterations in the PFC of VPA animals have been reported early in development (Walcott et al., 2011). This synapse pattern seen *in vivo* in the PFC of VPA rats is reproduced *in vitro* by neurons grown in the absence of glia, supporting the idea of neuronal priming (Traetta et al., 2021). Cortical neurons isolated from VPA animals show a greater number of SYN and PSD-95 synaptic clusters, indicating an increase in the number of glutamatergic synapses *in vitro*. In line with this notion, it has been reported that prenatal exposure to VPA enhances the differentiation of glutamatergic synapses during cortical development (Kim et al., 2017). Our results show that prenatal exposure to VPA primes cortical neurons from VPA animals and that these cells have the intrinsic capability to mimic *in vitro* the synaptic changes seen *in vivo* in the PFC of VPA animals. Moreover, neurons from VPA animals develop a more complex dendritic arbor. In accordance with these results, Schafer et al. (2019) have shown that cortical neurons obtained from iPSC from patients with ASD show altered chronology differentiation and greater dendritic complexity.

Recently, impairments in synaptic pruning have been proposed as the main trigger for ASD. Genetic manipulation of microglia during development proved to lead to phenotypes resembling ASD core symptoms (Zhan et al., 2014; Filipello et al., 2018). Particularly, in our study, although isolated microglia from VPA animals exhibit a mild pro-inflammatory profile *in vitro*, at PND3, microglia from VPA animals display a typical morphology of early stages of development (Ueno et al., 2013). However, juvenile VPA rats show a higher proportion of unramified cells in the PFC, suggesting microglial activation. This chronology of microgliosis *in vivo* is in accordance with what was observed in patients with ASD, where microgliosis is not evident at an early age but appears throughout development (Lee et al., 2017). Moreover, the reactive profile of microglia of juvenile VPA animals in cortical areas agrees with that in other reports in VPA animals (Bronzuoli et al., 2018) and in patients with ASD (Morgan et al., 2010; Tetreault et al., 2012; Suzuki et al., 2013).

Our *in vitro* findings imply long-lasting changes in cortical microglia toward a pro-inflammatory profile when grown in the absence of neurons. Cortical microglia isolated from VPA animals when synaptic changes have already occurred (PND3) exhibit a reactive profile in culture conditions, similar to what occurs *in vivo* in juvenile stages. Besides, mild pro-inflammatory microglia from VPA animals still respond to a pro-inflammatory stimulus (LPS) but show resistance to a phagocytic challenge. These alterations could result from epigenetic alterations produced by VPA exposure directly on microglia since microglia colonization begins around E10, and elevated protein synthesis in these cells leads to autism-like behavior (Xu et al., 2020). However, in the hippocampus, where there are no obvious synaptic alterations at an early age, microglia isolated from VPA animals are not affected (Traetta et al., 2021). Indeed, the microglia phenotype could be induced by the abnormal neuronal microenvironment (Marshall et al., 2014; Lenz and Nelson, 2018). In line with this hypothesis, findings in patients suggest that glial alterations are associated with neuronal alterations (Morgan et al., 2012). Likewise, when the microglia from VPA animals are grown *in vitro*, devoid of neuronal factors during its differentiation, they show a reactive morphology, suggesting that the abnormal environment before isolation may have a long-term impact on the *in vitro* culture.

Interestingly, neuron-microglia co-cultures show that cortical microglia isolated from VPA animals are adapted to their neuronal milieu. In the presence of neurons isolated from VPA animals, microglia from VPA animals show a non-reactive morphological profile, similar to that of the neuron-microglia co-cultures obtained from control animals. Besides, microglia isolated from VPA animals mimic the neurite outgrowth effects of control microglia (Zhang and Fedoroff, 1996) regardless of the neuronal substrate. However, microglia isolated from control animals acquire a different morphological profile when exposed to neurons isolated from VPA animals by promoting dendritic shortening and reducing the dendritic tree. These findings suggest that microglia from control animals can differentiate between the VPA and control neuronal substrates, while cortical microglia from VPA animals are insensitive or adapted to their neuronal substrate. These results highlight the incapability of microglia from VPA animals to restore synaptic alterations since they are unable to differentiate neuronal substrates and respond to a phagocytic stimulus (synaptosomes). In fact, microglia are essential for refining circuits (Stevens et al., 2007) and inhibiting excessive cortical transmission (Badimon et al., 2020). This microglial adaptation to the neuronal milieu may contribute to the absence of microgliosis in the PFC of VPA animals at PND3.

An intriguing result is that although microglia isolated from VPA animals seem adapted to neuronal cues, microgliosis has been consistently described in the PFC of juvenile VPA animals along with astrogliosis (Codagnone et al., 2015; Bronzuoli et al., 2018). Interestingly, astrocytes acquire adult morphology during postnatal development (Farhy-Tselnicker and Allen, 2018). Indeed, at the neonatal period, the PFC of both control and VPA animals evidence radial structures and very few astrocytes with mature morphology. However, at the juvenile stage, robust astrogliosis is found in the PFC of VPA animals (Codagnone et al., 2015; Bronzuoli et al., 2018), which is consistent with findings in cortical areas in patients with ASD (Laurence and Fatemi, 2005; Vargas et al., 2005; Fatemi et al., 2008). Our *in vitro* findings disclose that cortical astrocytes isolated from VPA animals display a reactive morphological pattern along with a pro-inflammatory cytokine profile. Moreover, astrocytes from VPA animals show an imbalanced miRNA processing machinery, suggesting an extensive alteration in the regulation of the pro-inflammatory gene expression program. It is worth mentioning

that dysregulation of miRNA expression machinery has been associated with pro-inflammatory profiles in different diseases of the central nervous system (Sun et al., 2019). Consequently, cortical astrocytes from VPA animals evidence long-lasting changes when differentiated *in vitro* in the absence of neuronal signals. Remarkably, astrocyte maturation in the cerebral cortex depends on vGLUT-1-expressing synapses (Morel et al., 2014). As this glutamate transporter is increased in the PFC of VPA rats at PND3, such neuronal change could impact astrocytes during postnatal maturation. In agreement with our findings, Voineagu et al. (2011) have shown that the astrocytic changes observed in patients are not related to genetic alterations associated with ASD, suggesting that they are a consequence of neuronal alterations or environmental events.

In addition, we show that the presence of astrocytes enables microglia from VPA animals to display a pro-inflammatory profile similar to that observed *in vivo* at PND35. In turn, microglia from VPA animals also exacerbate astrocyte reactivity. Furthermore, microglia-astroglia interaction does not allow the engagement of microglia in response to phagocytic stimuli. These results suggest that cortical microglia from VPA animals in the presence of astrocytes are not able to counteract changes in synapse number. It is known that bidirectional communication between microglia and astrocytes plays a key role in neuroinflammation (Zhang et al., 2010; Matta et al., 2019; Matejuk and Ransohoff, 2020). Herein, we provide evidence of a distinctive microglia-astroglia crosstalk in VPA animals responsible for microgliosis and exacerbation of astrogliosis. In fact, active microglia induce reactive astrocytes by secreting diverse cytokines, such as IL1, IL6, and TNFα (Zhang et al., 2010; Liddelow et al., 2017). In turn, reactive astrocytes release gliotransmitters such as ATP to trigger microglia activation (Coco et al., 2003; Bianco et al., 2005; Davalos et al., 2005) and cytokines that may modulate microglia inflammatory profile (Kettenmann et al., 2013). Microglia and astroglia from VPA animals showed a particular cytokine expression profile and a profound alteration of the miRNA processing machinery that may reveal a complex altered microglia-astroglia crosstalk in the PFC of VPA animals. It has been shown that microglia-astrocyte interaction is crucial for the proper synaptic development of the thalamus and spinal cord (Vainchtein et al., 2018). Thus, future studies of this crosstalk may reveal interesting targets that could be modulated.

To sum up, our findings are the first to show *in vitro* long-lasting changes in cortical microglia and astroglia induced by prenatal exposure to VPA. Cortical microglia from VPA animals are insensitive or adapted to the neuronal milieu and incapable of responding to phagocytic stimuli. Microglia-astroglia communication in VPA animals enables a microglial pro-inflammatory program and exacerbates astrogliosis without engaging microglia in response to phagocytic stimuli. Thus, we provide evidence that cortical microglia are not able to counteract synaptic changes and that microglia-astroglia crosstalk is a key player in neuroinflammation observed in experimental models and patients with ASD. Our study highlights cortical microglia-astroglia communication as a new mechanism implicated in neuroinflammation in ASD; consequently, we propose this crosstalk as a potential target for interventions in this disorder.

DATA AVAILABILITY STATEMENT

The original contributions presented in the study are included in the article/**Supplementary Material**; further inquiries can be directed to the corresponding author.

ETHICS STATEMENT

The animal study was reviewed and approved by Ethics Committee for the Care and Use of Laboratory Animals of the School of Pharmacy and Biochemistry at the Universidad de Buenos Aires (Approval No. 180613-1 and 2320).

AUTHOR CONTRIBUTIONS

AR conceived and designed the study. MET contributed to experimental design. MET, NAU, SCZ, DGC and AR performed the experiments. NAU contributed to the design of behavioral tests and performed the transmission electron microscopy study. SCZ contributed to the design and performance of flow cytometry experiments. DGC performed RT-PCR assays. AJR gave advice on glial primary culture experiments and contributed to the design of RT-PCR assays. MET and AR wrote the first draft of the manuscript. MET, SCZ, AJR and AR discussed results. NAU, SCZ and AJR revised the first draft of the manuscript. All authors contributed to the revision of the final version of the manuscript and read and approved the submitted version.

FUNDING

This study was supported by grants to AR (Agencia Nacional de Promoción Científica y Tecnológica (ANPCYT; PICT2014-1769 and 2018–2504), Consejo Nacional de Investigaciones Científicas y Técnicas (CONICET; PIP 11220130100212CO), and Universidad de Buenos Aires (UBA; UBACyT 20020170100478BA)). The funders had no role in study design, data collection and analysis, decision to publish, or preparation of the manuscript.

ACKNOWLEDGMENTS

The authors thank Biot. Andrea Pecile and Marianela Ceol for animal care.

SUPPLEMENTARY MATERIAL

The Supplementary Material for this article can be found online at: https://www.frontiersin.org/articles/10.3389/fphar.2021.707859/full#supplementary-material

REFERENCES

Acaz-Fonseca, E., Ortiz-Rodriguez, A., Azcoitia, I., Garcia-Segura, L. M., and Arevalo, M. A. (2019). Notch Signaling in Astrocytes Mediates Their Morphological Response to an Inflammatory Challenge, [Internet]. *Cell Death Discov.* 5, 85, 2019 . Available from: https://www.ncbi.nlm.nih.gov/pmc/articles/PMC6447583/. doi:10.1038/s41420-019-0166-6

Allen, N. J., and Eroglu, C. (2017). Cell Biology of Astrocyte-Synapse Interactions. *Neuron* 96 (3), 697–708. doi:10.1016/j.neuron.2017.09.056

American Psychiatric Association (2013). *Diagnostic and Statistical Manual of Mental Disorders: DSM-5™*. 5th ed.. Arlington, VA, US: American Psychiatric Publishing, Inc., 947. xliv.

Anney, R., Klei, L., Pinto, D., Regan, R., Conroy, J., Magalhaes, T. R., et al. (2010). A Genome-wide Scan for Common Alleles Affecting Risk for Autism. *Hum. Mol. Genet.* 19 (20), 4072–4082. doi:10.1093/hmg/ddq307

Araque, A., and Navarrete, M. (2010). Glial Cells in Neuronal Network Function. *Philos. Trans. R. Soc. Lond. B Biol. Sci.* 365 (1551), 2375–2381. doi:10.1098/rstb.2009.0313

Auzmendi, J., Moffatt, L., and Ramos, A. J. (2020). Predicting Reactive Astrogliosis Propagation by Bayesian Computational Modeling: the Repeater Stations Model. *Mol. Neurobiol.* 57 (2), 879–895. doi:10.1007/s12035-019-01749-9

Badimon, A., Strasburger, H. J., Ayata, P., Chen, X., Nair, A., Ikegami, A., et al. (2020). Negative Feedback Control of Neuronal Activity by Microglia. *Nature* 586 (7829), 417–423. doi:10.1038/s41586-020-2777-8

Benekareddy, M., Stachniak, T. J., Bruns, A., Knoflach, F., von Kienlin, M., Künnecke, B., et al. (2018). Identification of a Corticohabenular Circuit Regulating Socially Directed Behavior. *Biol. Psychiatry* 83 (7), 607–617. doi:10.1016/j.biopsych.2017.10.032

Betancur, C., Sakurai, T., and Buxbaum, J. D. (2009). The Emerging Role of Synaptic Cell-Adhesion Pathways in the Pathogenesis of Autism Spectrum Disorders. *Trends Neurosci.* 32 (7), 402–412. doi:10.1016/j.tins.2009.04.003

Bianco, F., Pravettoni, E., Colombo, A., Schenk, U., Möller, T., Matteoli, M., et al. (2005). Astrocyte-derived ATP Induces Vesicle Shedding and IL-1 Beta Release from Microglia. *J. Immunol.* 174 (11), 7268–7277. doi:10.4049/jimmunol.174.11.7268

Bohatschek, M., Kloss, C. U., Kalla, R., and Raivich, G. (2001). *In Vitro* model of Microglial Deramification: Ramified Microglia Transform into Amoeboid Phagocytes Following Addition of Brain Cell Membranes to Microglia-Astrocyte Cocultures. *J. Neurosci. Res.* 64 (5), 508–522. doi:10.1002/jnr.1103

Bourgeron, T. (2015). From the Genetic Architecture to Synaptic Plasticity in Autism Spectrum Disorder. *Nat. Rev. Neurosci.* 16 (9), 551–563. doi:10.1038/nrn3992

Bronzuoli, M. R., Facchinetti, R., Ingrassia, D., Sarvadio, M., Schiavi, S., Steardo, L., et al. (2018). Neuroglia in the Autistic Brain: Evidence from a Preclinical Model. *Mol. Autism* 9, 66. doi:10.1186/s13229-018-0254-0

Chini, M., and Hanganu-Opatz, I. L. (2021). Prefrontal Cortex Development in Health and Disease: Lessons from Rodents and Humans. *Trends Neurosci.* 44 (3), 227–240. doi:10.1016/j.tins.2020.10.017

Chung, W. S., Clarke, L. E., Wang, G. X., Stafford, B. K., Sher, A., Chakraborty, C., et al. (2013). Astrocytes Mediate Synapse Elimination through MEGF10 and MERTK Pathways. *Nature* 504 (7480), 394–400. doi:10.1038/nature12776

Coco, S., Calegari, F., Pravettoni, E., Pozzi, D., Taverna, E., Rosa, P., et al. (2003). Storage and Release of ATP from Astrocytes in Culture. *J. Biol. Chem.* 278 (2), 1354–1362. doi:10.1074/jbc.M209454200

Codagnone, M. G., Podestá, M. F., Uccelli, N. A., and Reinés, A. (2015). Differential Local Connectivity and Neuroinflammation Profiles in the Medial Prefrontal Cortex and Hippocampus in the Valproic Acid Rat Model of Autism. *Dev. Neurosci.* 37 (3), 215–231. doi:10.1159/000375489

Davalos, D., Grutzendler, J., Yang, G., Kim, J. V., Zuo, Y., Jung, S., et al. (2005). ATP Mediates Rapid Microglial Response to Local Brain Injury *In Vivo*. *Nat. Neurosci.* 8 (6), 752–758. doi:10.1038/nn1472

De Rubeis, S., He, X., Goldberg, A. P., Poultney, C. S., Samocha, K., Cicek, A. E., et al. (2014). Synaptic, Transcriptional and Chromatin Genes Disrupted in Autism. *Nature* 515 (7526), 209–215. doi:10.1038/nature13772

Dheen, S. T., Kaur, C., and Ling, E. A. (2007). Microglial Activation and its Implications in the Brain Diseases. *Curr. Med. Chem.* 14 (11), 1189–1197. doi:10.2174/092986707780597961

Dixon, M. L., Thiruchselvam, R., Todd, R., and Christoff, K. (2017). Emotion and the Prefrontal Cortex: An Integrative Review. *Psychol. Bull.* 143 (10), 1033–1081. doi:10.1037/bul0000096

Farhy-Tselnicker, I., and Allen, N. J. (2018). Astrocytes, Neurons, Synapses: a Tripartite View on Cortical Circuit Development, [Internet]. *Neural Dev.* 13, 7, 2018 . Available from: https://www.ncbi.nlm.nih.gov/pmc/articles/PMC5928581/. doi:10.1186/s13064-018-0104-y

Fatemi, S. H., Folsom, T. D., Reutiman, T. J., and Lee, S. (2008). Expression of Astrocytic Markers Aquaporin 4 and Connexin 43 Is Altered in Brains of Subjects with Autism. *Synapse* 62 (7), 501–507. doi:10.1002/syn.20519

Fernández-Arjona, M. del. M., Grondona, J. M., Fernández-Llebrez, P., and López-Ávalos, M. D. (2019). Microglial Morphometric Parameters Correlate with the Expression Level of IL-1β, and Allow Identifying Different Activated Morphotypes. *Front. Cel Neurosci.* 13, 472. doi:10.3389/fncel.2019.00472

Filipello, F., Morini, R., Corradini, I., Zerbi, V., Canzi, A., Michalski, B., et al. (2018). The Microglial Innate Immune Receptor TREM2 Is Required for Synapse Elimination and Normal Brain Connectivity. *Immunity* 48 (5), 979–e8. doi:10.1016/j.immuni.2018.04.016

Geschwind, D. H., and Flint, J. (2015). Genetics and Genomics of Psychiatric Disease. *Science* 349 (6255), 1489–1494. doi:10.1126/science.aaa8954

Guang, S., Pang, N., Deng, X., Yang, L., He, F., Wu, L., et al. (2018). Synaptopathology Involved in Autism Spectrum Disorder. *Front. Cel Neurosci.* 12, 470. doi:10.3389/fncel.2018.00470

Hol, E. M., and Pekny, M. (2015). Glial Fibrillary Acidic Protein (GFAP) and the Astrocyte Intermediate Filament System in Diseases of the central Nervous System. *Curr. Opin. Cel Biol* 32, 121–130. doi:10.1016/j.ceb.2015.02.004

Hoogland, I. C., Houbolt, C., van Westerloo, D. J., van Gool, W. A., and van de Beek, D. (2015). Systemic Inflammation and Microglial Activation: Systematic Review of Animal Experiments. *J. Neuroinflammation* 12, 114. doi:10.1186/s12974-015-0332-6

Hu, C., Chen, W., Myers, S. J., Yuan, H., and Traynelis, S. F. (2016). Human GRIN2B Variants in Neurodevelopmental Disorders. *J. Pharmacol. Sci.* 132 (2), 115–121. doi:10.1016/j.jphs.2016.10.002

Hutsler, J. J., and Zhang, H. (2010). Increased Dendritic Spine Densities on Cortical Projection Neurons in Autism Spectrum Disorders. *Brain Res.* 1309, 83–94. doi:10.1016/j.brainres.2009.09.120

Iossifov, I., O'Roak, B. J., Sanders, S. J., Ronemus, M., Krumm, N., Levy, D., et al. (2014). The Contribution of De Novo Coding Mutations to Autism Spectrum Disorder. *Nature* 515 (7526), 216–221. doi:10.1038/nature13908

Kettenmann, H., Kirchhoff, F., and Verkhratsky, A. (2013). Microglia: New Roles for the Synaptic Stripper. *Neuron* 77 (1), 10–18. doi:10.1016/j.neuron.2012.12.023

Kim, K. C., Choi, C. S., Gonzales, E. L. T., Mabunga, D. F. N., Lee, S. H., Jeon, S. J., et al. (2017). Erratum: Valproic Acid Induces Telomerase Reverse Transcriptase Expression during Cortical Development. *Exp. Neurobiol.* 26 (5), 252–265. doi:10.5607/en.2017.26.5.252 Erratum in: (2017). Exp Neurobiol. 26 (6), 399.

Kim, K. C., Kim, P., Go, H. S., Choi, C. S., Park, J. H., Kim, H. J., et al. (2013). Male-specific Alteration in Excitatory post-synaptic Development and Social Interaction in Pre-natal Valproic Acid Exposure Model of Autism Spectrum Disorder. *J. Neurochem.* 124 (6), 832–843. doi:10.1111/jnc.12147

Kirkley, K. S., Popichak, K. A., Afzali, M. F., Legare, M. E., and Tjalkens, R. B. (2017). Microglia Amplify Inflammatory Activation of Astrocytes in Manganese Neurotoxicity. *J. Neuroinflammation* 14 (1), 99. doi:10.1186/s12974-017-0871-0

Kreutzberg, G. W. (1996). Microglia: a Sensor for Pathological Events in the CNS. *Trends Neurosci.* 19 (8), 312–318. doi:10.1016/0166-2236(96)10049-7

Laurence, J. A., and Fatemi, S. H. (2005). Glial Fibrillary Acidic Protein Is Elevated in superior Frontal, Parietal and Cerebellar Cortices of Autistic Subjects. *Cerebellum* 4 (3), 206–210. doi:10.1080/14734220500208846

Leblond, C. S., Nava, C., Polge, A., Gauthier, J., Huguet, G., Lumbroso, S., et al. (2014). Meta-analysis of SHANK Mutations in Autism Spectrum Disorders: a Gradient of Severity in Cognitive Impairments. *Plos Genet.* 10 (9), e1004580. doi:10.1371/journal.pgen.1004580

Lee, A. S., Azmitia, E. C., and Whitaker-Azmitia, P. M. (2017). Developmental Microglial Priming in Postmortem Autism Spectrum Disorder Temporal Cortex. *Brain Behav. Immun.* 62, 193–202. doi:10.1016/j.bbi.2017.01.019

Lenz, K. M., and Nelson, L. H. (2018). Microglia and Beyond: Innate Immune Cells as Regulators of Brain Development and Behavioral Function. *Front. Immunol.* 9, 698. doi:10.3389/fimmu.2018.00698

Liao, X., Liu, Y., Fu, X., and Li, Y. (2020). Postmortem Studies of Neuroinflammation in Autism Spectrum Disorder: a Systematic Review. *Mol. Neurobiol.* 57, 3424. doi:10.1007/s12035-020-01976-5

Liddelow, S. A., Guttenplan, K. A., Clarke, L. E., Bennett, F. C., Bohlen, C. J., Schirmer, L., et al. (2017). Neurotoxic Reactive Astrocytes Are Induced by Activated Microglia. *Nature* 541 (7638), 481–487. doi:10.1038/nature21029

Liddelow, S. A., Marsh, S. E., and Stevens, B. (2020). Microglia and Astrocytes in Disease: Dynamic Duo or Partners in Crime?. *Trends Immunol.* 41 (9), 820–835. doi:10.1016/j.it.2020.07.006

Lin, Y. C., Frei, J. A., Kilander, M. B., Shen, W., and Blatt, G. J. (2016). A Subset of Autism-Associated Genes Regulate the Structural Stability of Neurons. *Front. Cel Neurosci.* 10, 263. doi:10.3389/fncel.2016.00263

Lively, S., and Schlichter, L. C. (2018). Microglia Responses to Pro-inflammatory Stimuli (LPS, IFNγ+TNFα) and Reprogramming by Resolving Cytokines (IL-4, IL-10). *Front. Cel Neurosci*, 12, 215. doi:10.3389/fncel.2018.00215

Marshall, G. P., Deleyrolle, L. P., Reynolds, B. A., Steindler, D. A., and Laywell, E. D. (2014). Microglia from Neurogenic and Non-neurogenic Regions Display Differential Proliferative Potential and Neuroblast Support. *Front. Cel Neurosci* 8, 180. doi:10.3389/fncel.2014.00180

Matejuk, A., and Ransohoff, R. M. (2020). Crosstalk Between Astrocytes and Microglia: An Overview. *Front. Immunol.* 11, 1416. doi:10.3389/fimmu.2020.01416

Matta, S. M., Hill-Yardin, E. L., and Crack, P. J. (2019). The Influence of Neuroinflammation in Autism Spectrum Disorder. *Brain Behav. Immun.* 79, 75–90. doi:10.1016/j.bbi.2019.04.037

McCarthy, K. D., and de Vellis, J. (1980). Preparation of Separate Astroglial and Oligodendroglial Cell Cultures from Rat Cerebral Tissue. *J. Cel Biol.* 85 (3), 890–902. doi:10.1083/jcb.85.3.890

Minelli, A., Edwards, R. H., Manzoni, T., and Conti, F. (2003). Postnatal Development of the Glutamate Vesicular Transporter VGLUT1 in Rat Cerebral Cortex. *Brain Res. Dev. Brain Res.* 140 (2), 309–314. doi:10.1016/s0165-3806(02)00617-x

Miyamoto, A., Wake, H., Ishikawa, A. W., Eto, K., Shibata, K., Murakoshi, H., et al. (2016). Microglia Contact Induces Synapse Formation in Developing Somatosensory Cortex. *Nat. Commun.* 7, 12540. doi:10.1038/ncomms12540

Modabbernia, A., Velthorst, E., and Reichenberg, A. (2017). Environmental Risk Factors for Autism: an Evidence-Based Review of Systematic Reviews and Meta-Analyses. *Mol. Autism* 8, 13. doi:10.1186/s13229-017-0121-4

Morel, L., Higashimori, H., Tolman, M., and Yang, Y. (2014). VGluT1+ Neuronal Glutamatergic Signaling Regulates Postnatal Developmental Maturation of Cortical Protoplasmic Astroglia. *J. Neurosci.* 34 (33), 10950–10962. doi:10.1523/JNEUROSCI.1167-14.2014

Morgan, J. T., Chana, G., Abramson, I., Semendeferi, K., Courchesne, E., and Everall, I. P. (2012). Abnormal Microglial-Neuronal Spatial Organization in the Dorsolateral Prefrontal Cortex in Autism. *Brain Res.* 1456, 72–81. doi:10.1016/j.brainres.2012.03.036

Morgan, J. T., Chana, G., Pardo, C. A., Achim, C., Semendeferi, K., Buckwalter, J., et al. (2010). Microglial Activation and Increased Microglial Density Observed in the Dorsolateral Prefrontal Cortex in Autism. *Biol. Psychiatry* 68 (4), 368–376. doi:10.1016/j.biopsych.2010.05.024

Nicolini, C., and Fahnestock, M. (2018). The Valproic Acid-Induced Rodent Model of Autism. *Exp. Neurol.* 299 (Pt A), 217–227. doi:10.1016/j.expneurol.2017.04.017

Paolicelli, R. C., Bolasco, G., Pagani, F., Maggi, L., Scianni, M., Panzanelli, P., et al. (2011). Synaptic Pruning by Microglia Is Necessary for normal Brain Development. *Science* 333 (6048), 1456–1458. doi:10.1126/science.1202529

Paxinos, G., and Watson, C. (1986). *The Rat Brain in Stereotaxis Coordinates*. 4th ed.. San Diego: Academic Press.

Phillips, G. R., Huang, J. K., Wang, Y., Tanaka, H., Shapiro, L., Zhang, W., et al. (2001). The Presynaptic Particle Web: Ultrastructure, Composition, Dissolution, and Reconstitution. *Neuron* 32 (1), 63–77. doi:10.1016/s0896-6273(01)00450-0

Podestá, M. F., Yam, P., Codagnone, M. G., Uccelli, N. A., Colman, D., and Reinés, A. (2014). Distinctive PSA-NCAM and NCAM Hallmarks in Glutamate-Induced Dendritic Atrophy and Synaptic Disassembly. *PLoS ONE* 9 (10), e108921. doi:10.1371/journal.pone.0108921

Raymond, G. V., Bauman, M. L., and Kemper, T. L. (1996). Hippocampus in Autism: a Golgi Analysis. *Acta Neuropathol.* 91 (1), 117–119. doi:10.1007/s004010050401

Reinés, A., Bernier, L. P., McAdam, R., Belkaid, W., Shan, W., Koch, A. W., et al. (2012). N-cadherin Prodomain Processing Regulates Synaptogenesis. *J. Neurosci.* 32 (18), 6323–6334. doi:10.1523/JNEUROSCI.0916-12.2012

Rinaldi, T., Perrodin, C., and Markram, H. (2008). Hyper-connectivity and Hyper-Plasticity in the Medial Prefrontal Cortex in the Valproic Acid Animal Model of Autism. *Front. Neural Circuits* 2, 4. doi:10.3389/neuro.04.004.2008

Ritzel, R. M., Patel, A. R., Grenier, J. M., Crapser, J., Verma, R., Jellison, E. R., et al. (2015). Functional Differences between Microglia and Monocytes after Ischemic Stroke. *J. Neuroinflammation* 12, 106. doi:10.1186/s12974-015-0329-1

Rollenhagen, A., and Lübke, J. H. R. (2013). "Dendrites: A Key Structural Element of Neurons," in *Neuroscience in the 21st Century*. Editor D. W. Pfaff (New York, NY: Springer), 179–217. doi:10.1007/978-1-4614-1997-6_11

Rosciszewski, G., Cadena, V., Auzmendi, J., Cieri, M. B., Lukin, J., Rossi, A. R., et al. (2019). Detrimental Effects of HMGB-1 Require Microglial-Astroglial Interaction: Implications for the Status Epilepticus -Induced Neuroinflammation. *Front. Cel Neurosci.* 13, 380. doi:10.3389/fncel.2019.00380

Rosciszewski, G., Cadena, V., Murta, V., Lukin, J., Villarreal, A., Roger, T., et al. (2018). Toll-Like Receptor 4 (TLR4) and Triggering Receptor Expressed on Myeloid Cells-2 (TREM-2) Activation Balance Astrocyte Polarization into a Proinflammatory Phenotype. *Mol. Neurobiol.* 55 (5), 3875–3888. doi:10.1007/s12035-017-0618-z

Roullet, F. I., Lai, J. K., and Foster, J. A. (2013). In Utero exposure to Valproic Acid and Autism-Aa Current Review of Clinical and Animal Studies. *Neurotoxicol Teratol.* 36, 47–56. doi:10.1016/j.ntt.2013.01.004

Schafer, D. P., Lehrman, E. K., Kautzman, A. G., Koyama, R., Mardinly, A. R., Yamasaki, R., et al. (2012). Microglia Sculpt Postnatal Neural Circuits in an Activity and Complement-dependent Manner. *Neuron* 74 (4), 691–705. doi:10.1016/j.neuron.2012.03.026

Schafer, S. T., Paquola, A. C. M., Stern, S., Gosselin, D., Ku, M., Pena, M., et al. (2019). Pathological Priming Causes Developmental Gene Network Heterochronicity in Autistic Subject-Derived Neurons. *Nat. Neurosci.* 22 (2), 243–255. doi:10.1038/s41593-018-0295-x

Schneider, T., and Przewłocki, R. (2005). Behavioral Alterations in Rats Prenatally Exposed to Valproic Acid: Animal Model of Autism. *Neuropsychopharmacology* 30 (1), 80–89. doi:10.1038/sj.npp.1300518

Sebat, J., Lakshmi, B., Malhotra, D., Troge, J., Lese-Martin, C., Walsh, T., et al. (2007). Strong Association of De Novo Copy Number Mutations with Autism. *Science* 316 (5823), 445–449. doi:10.1126/science.1138659

Sofroniew, M. V., and Vinters, H. V. (2010). Astrocytes: Biology and Pathology. *Acta Neuropathol.* 119 (1), 7–35. doi:10.1007/s00401-009-0619-8

Stevens, B., Allen, N. J., Vazquez, L. E., Howell, G. R., Christopherson, K. S., Nouri, N., et al. (2007). The Classical Complement cascade Mediates CNS Synapse Elimination. *Cell* 131 (6), 1164–1178. doi:10.1016/j.cell.2007.10.036

Stewart, M. G., Popov, V. I., Kraev, I. V., Medvedev, N., and Davies, H. A. (2014). "Structure and Complexity of the Synapse and Dendritic Spine," in *The Synapse: Structure and Function*. Editors V. Pickel and M. Segal (Kidlington: Academic Press), 1–20. doi:10.1016/b978-0-12-418675-0.00001-8

Sun, C., Zhu, L., Ma, R., Ren, J., Wang, J., Gao, S., et al. (2019). Astrocytic miR-324-5p Is Essential for Synaptic Formation by Suppressing the Secretion of CCL5 from Astrocytes. *Cell Death Dis.* 10 (2), 141. doi:10.1038/s41419-019-1329-3

Suzuki, K., Sugihara, G., Ouchi, Y., Nakamura, K., Futatsubashi, M., Takebayashi, K., et al. (2013). Microglial Activation in Young Adults with Autism Spectrum Disorder. *JAMA Psychiatry* 70 (1), 49–58. doi:10.1001/jamapsychiatry.2013.272

Tamashiro, T. T., Dalgard, C. L., and Byrnes, K. R. (2012). Primary Microglia Isolation from Mixed Glial Cell Cultures of Neonatal Rat Brain Tissue. *J. Vis. Exp.* 15 66, e3814. doi:10.3791/3814

Tetreault, N. A., Hakeem, A. Y., Jiang, S., Williams, B. A., Allman, E., Wold, B. J., et al. (2012). Microglia in the Cerebral Cortex in Autism. *J. Autism Dev. Disord.* 42 (12), 2569–2584. doi:10.1007/s10803-012-1513-0

Traetta, M. E., Codagnone, M. G., Uccelli, N. A., Ramos, A. J., Zárate, S., and Reinés, A. (2021). Hippocampal Neurons Isolated from Rats Subjected to the Valproic Acid Model Mimic *In Vivo* Synaptic Pattern: Evidence of Neuronal Priming during Early Development in Autism Spectrum Disorders. *Mol. Autism* 12 (1), 23. doi:10.1186/s13229-021-00428-8

Ueno, M., Fujita, Y., Tanaka, T., Nakamura, Y., Kikuta, J., Ishii, M., et al. (2013). Layer V Cortical Neurons Require Microglial Support for Survival during Postnatal Development. *Nat. Neurosci.* 16 (5), 543–551. doi:10.1038/nn.3358

Vainchtein, I. D., Chin, G., Cho, F. S., Kelley, K. W., Miller, J. G., Chien, E. C., et al. (2018). Astrocyte-derived Interleukin-33 Promotes Microglial Synapse Engulfment and Neural Circuit Development. *Science* 359 (6381), 1269–1273. doi:10.1126/science.aal3589

Vargas, D. L., Nascimbene, C., Krishnan, C., Zimmerman, A. W., and Pardo, C. A. (2005). Neuroglial Activation and Neuroinflammation in the Brain of Patients with Autism. *Ann. Neurol.* 57 (1), 67–81. doi:10.1002/ana.20315

Varol, D., Mildner, A., Blank, T., Shemer, A., Barashi, N., Yona, S., et al. (2017). Dicer Deficiency Differentially Impacts Microglia of the Developing and Adult Brain. *Immunity* 46 (6), 1030. doi:10.1016/j.immuni.2017.05.003

Villarreal, A., Seoane, R., González Torres, A., Rosciszewski, G., Angelo, M. F., Rossi, A., et al. (2014). S100B Protein Activates a RAGE-dependent Autocrine Loop in Astrocytes: Implications for its Role in the Propagation of Reactive Gliosis. *J. Neurochem.* 131 (2), 190–205. doi:10.1111/jnc.12790

Voineagu, I., Wang, X., Johnston, P., Lowe, J. K., Tian, Y., Horvath, S., et al. (2011). Transcriptomic Analysis of Autistic Brain Reveals Convergent Molecular Pathology. *Nature* 474 (7351), 380–384. doi:10.1038/nature10110

Walcott, E. C., Higgins, E. A., and Desai, N. S. (2011). Synaptic and Intrinsic Balancing during Postnatal Development in Rat Pups Exposed to Valproic Acid In Utero. *J. Neurosci.* 31 (37), 13097–13109. doi:10.1523/JNEUROSCI.1341-11.2011

Walker, F. R., Beynon, S. B., Jones, K. A., Zhao, Z., Kongsui, R., Cairns, M., et al. (2014). Dynamic Structural Remodelling of Microglia in Health and Disease: a Review of the Models, the Signals and the Mechanisms. *Brain Behav. Immun.* 37, 1–14. doi:10.1016/j.bbi.2013.12.010

Xu, Z. X., Kim, G. H., Tan, J. W., Riso, A. E., Sun, Y., Xu, E. Y., et al. (2020). Elevated Protein Synthesis in Microglia Causes Autism-like Synaptic and Behavioral Aberrations. *Nat. Commun.* 11 (1), 1797. doi:10.1038/s41467-020-15530-3

Zárate, S. C., Traetta, M. E., Codagnone, M. G., Seilicovich, A., and Reinés, A. G. (2019). Humanin, a Mitochondrial-Derived Peptide Released by Astrocytes, Prevents Synapse Loss in Hippocampal Neurons. *Front. Aging Neurosci.* 11, 123. doi:10.3389/fnagi.2019.00123

Zhan, Y., Paolicelli, R. C., Sforazzini, F., Weinhard, L., Bolasco, G., Pagani, F., et al. (2014). Deficient Neuron-Microglia Signaling Results in Impaired Functional Brain Connectivity and Social Behavior. *Nat. Neurosci.* 17 (3), 400–406. doi:10.1038/nn.3641

Zhang, D., Hu, X., Qian, L., O'Callaghan, J. P., and Hong, J. S. (2010). Astrogliosis in CNS Pathologies: Is There A Role for Microglia?. *Mol. Neurobiol.* 41 (0), 232–241. doi:10.1007/s12035-010-8098-4

Zhang, S. C., and Fedoroff, S. (1996). Neuron-microglia Interactions *In Vitro*. *Acta Neuropathol.* 91 (4), 385–395. doi:10.1007/s004010050440

Conflict of Interest: The authors declare that the research was conducted in the absence of any commercial or financial relationships that could be construed as a potential conflict of interest.

Publisher's Note: All claims expressed in this article are solely those of the authors and do not necessarily represent those of their affiliated organizations, or those of the publisher, the editors and the reviewers. Any product that may be evaluated in this article, or claim that may be made by its manufacturer, is not guaranteed or endorsed by the publisher.

Copyright © 2021 Traetta, Uccelli, Zárate, Gómez Cuautle, Ramos and Reinés. This is an open-access article distributed under the terms of the Creative Commons Attribution License (CC BY). The use, distribution or reproduction in other forums is permitted, provided the original author(s) and the copyright owner(s) are credited and that the original publication in this journal is cited, in accordance with accepted academic practice. No use, distribution or reproduction is permitted which does not comply with these terms.

frontiers in Pharmacology

ORIGINAL RESEARCH
published: 18 August 2021
doi: 10.3389/fphar.2021.706439

Galectin-3 Deletion Reduces LPS and Acute Colitis-Induced Pro-Inflammatory Microglial Activation in the Ventral Mesencephalon

*Ana M. Espinosa-Oliva[1], Pablo García-Miranda[2], Isabel María Alonso-Bellido[1], Ana E. Carvajal[2], Melania González-Rodríguez[3], Alejandro Carrillo-Jiménez[1], Arturo J. Temblador[4], Manuel Felices-Navarro[1], Irene García-Domínguez[1], María Angustias Roca-Ceballos[1], María D. Vázquez-Carretero[2], Juan García-Revilla[1], Marti Santiago[1], María J. Peral[2], José Luis Venero[1] and Rocío M. de Pablos[1]**

[1]Instituto de Biomedicina de Sevilla (IBiS), Hospital Universitario Virgen Del Rocío/CSIC/Universidad de Sevilla, Departamento de Bioquímica y Biología Molecular, Facultad de Farmacia, Universidad de, Sevilla, Spain, [2]Departamento de Fisiología, Facultad de Farmacia, Universidad de Sevilla, Sevilla, Spain, [3]Neuroplasticity and Neurodegeneration Laboratory, Ciudad Real Medical School, CRIB, Universidad de Castilla-La Mancha, Ciudad Real, Spain, [4]Laboratory of Virology and Chemotherapy, Department of Microbiology, Immunology and Transplantation, Rega Institute for Medical Research, Leuven, Belgium

Parkinson's disease is a highly prevalent neurological disorder for which there is currently no cure. Therefore, the knowledge of risk factors as well as the development of new putative molecular targets is mandatory. In this sense, peripheral inflammation, especially the originated in the colon, is emerging as a predisposing factor for suffering this disease. We have largely studied the pleiotropic roles of galectin-3 in driving microglia-associated immune responses. However, studies aimed at elucidating the role of galectin-3 in peripheral inflammation in terms of microglia polarization are lacking. To achieve this, we have evaluated the effect of galectin-3 deletion in two different models of acute peripheral inflammation: intraperitoneal injection of lipopolysaccharide or gut inflammation induced by oral administration of dextran sodium sulfate. We found that under peripheral inflammation the number of microglial cells and the expression levels of pro-inflammatory mediators take place specifically in the dopaminergic system, thus supporting causative links between Parkinson's disease and peripheral inflammation. Absence of galectin-3 highly reduced neuroinflammation in both models, suggesting an important central regulatory role of galectin-3 in driving microglial activation provoked by the peripheral inflammation. Thus, modulation of galectin-3 function emerges as a promising strategy to minimize undesired microglia polarization states.

Keywords: galectin-3, microglia, Parkinson's disease, peripheral inflammation, neuroinflammation

OPEN ACCESS

Edited by:
Mariela Fernanda Perez, National University of Cordoba, Argentina

Reviewed by:
Pablo Garrido-Gil, University of Santiago de Compostela, Spain
Yijuang Chern, National Research Program for Biopharmaceuticals, Taiwan

****Correspondence:***
Rocío M. de Pablos
depablos@us.es

Specialty section:
This article was submitted to Neuropharmacology, a section of the journal Frontiers in Pharmacology

Received: *07 May 2021*
Accepted: *06 August 2021*
Published: *18 August 2021*

Citation:
Espinosa-Oliva AM, García-Miranda P, Alonso-Bellido IM, Carvajal AE, González-Rodríguez M, Carrillo-Jiménez A, Temblador AJ, Felices-Navarro M, García-Domínguez I, Roca-Ceballos MA, Vázquez-Carretero MD, García-Revilla J, Santiago M, Peral MJ, Venero JL and de Pablos RM (2021) Galectin-3 Deletion Reduces LPS and Acute Colitis-Induced Pro-Inflammatory Microglial Activation in the Ventral Mesencephalon. Front. Pharmacol. 12:706439. doi: 10.3389/fphar.2021.706439

Abbreviations: BrdU, 5-bromo deoxyuridine; DAI, disease Activity Index; DSS, dextran sulphate sodium; Gal 3, galectin-3; Gal3KO, gal3 null mutant mice; GWAS, genome-wide association studies; IBDs, inflammatory bowel diseases; IL, interleukin; i.p., intraperitoneally; LPS, lipopolysaccharide; MUC-2, anti-mucin-2; PBS, phosphate buffer saline; PD, Parkinson's disease; RT, room temperature; RT-qPCR, real-time quantitative reverse transcription PCR; SN, substantia nigra; TBS, tris-buffered saline; TLR4, toll-like receptor; TNF, tumor necrosis factor; TREM2, triggering receptor expressed on myeloid cells 2; UC, ulcerative colitis; WT, wild type.

INTRODUCTION

Parkinson's disease (PD) is the second most prevalent neurodegenerative disorder with 1 million people affected all over the word (de Rijk et al., 1997). This neurological disorder results from the loss of dopaminergic neurons of the substantia nigra pars compacta (SNpc), which leads to the depletion of dopamine levels in striatum (Kordower et al., 2013). Striatal dopamine loss is responsible for the cardinal symptoms of PD, including tremor, bradikinesia, postural instability and rigidity along with a variety of non-motor symptoms (Kumaresan and Khan 2021). In an effort to decipher the underlying causes of this disease, the scientific community has shown that mitochondrial dysfunction, oxidative stress, excitotoxicity and alterations in the ubiquitin-proteasome system that leads to α-synuclein aggregation, cooperate in the dopaminergic neuronal death that takes place in PD (Gundersen 2020). However, to date there is no treatment capable of curing, or at least, slowing down the progress of this disease. For this reason, it is imperative to know the risk factors of PD as well as discover new molecular targets that improve the treatment options.

Reactive microgliosis, a process long considered secondary to neurodegeneration, is a characteristic typically associated with neurodegenerative diseases, including PD (Heneka et al., 2015). However, with the development of genome-wide association studies (GWAS), convincing evidence has been found on the probable direct involvement of microglia in neurodegeneration processes. Thus, different GWAS studies have identified several risk genes associated with PD strongly related to the innate immune system, including the triggering receptor expressed on myeloid cells 2 (TREM2) (Nalls et al., 2014); (Rayaprolu et al., 2013); (Hirsch and Hunot 2009). Moreover, recent massive transcriptomic studies have provided fundamental clues about the molecular profile of microglia, the immune cells of the central nervous system (CNS), under homeostatic conditions (Butovsky et al., 2014), aging (Hickman et al., 2013); (Galatro et al., 2017); (Grabert et al., 2016) and various models of neurodegeneration (Keren-Shaul et al., 2017); (Krasemann et al., 2017); (Mathys et al., 2017). Recently, Friedman and colleagues have compared the genome-wide transcriptional responses of brain myeloid cells obtained from diverse neuropathological models and identified modules of genes that show similar responses in multiple settings. Among these modules authors highlighted the proliferative, interferon-related, core neuro-degeneration-related and LPS-related modules (Friedman et al., 2018). All these transcriptomic studies surprisingly found a very similar transcriptional pattern in neurodegenerative conditions, characterized by the selective induction of multiple genes, including Itgax (Cd11c), Axl, Clec7a, MHC class II and Lgals3 (galectin-3; Gal3). Gal3 is the only known member of the chimera-type family of galectins. It is involved in the inflammatory response, and its expression is increased in microglial cells upon various neuroinflammatory stimuli (Lalancette-Hébert et al., 2012); (Satoh et al., 2011; Wesley et al., 2013).

We have recently demonstrated that Gal3 can bind to and activate different microglial receptors including TREM2 (Boza-Serrano et al., 2019) and Toll-like receptor (TLR)-4 (Burguillos et al., 2015). We have also shown that Gal3 plays a role in α-synuclein-induced microglial activation (Burguillos et al., 2015); (Boza-Serrano et al., 2014) and that Gal3 regulates inflammatory response in Alzheimer's disease (Boza-Serrano et al., 2019). These data point out Gal3 as a candidate of enormous relevance in the process of microglial activation associated with neurodegeneration and, therefore, its possible involvement in the neuroinflammation that takes place in PD deserves special attention.

Regarding the risk factors of PD, it has been proposed that peripheral inflammation could induce an inflammatory environment in the brain that eventually could lead to neurodegeneration (Herrera et al., 2015). Thus, peripheral injections of the inflammogen lipopolysaccharide (LPS) increase pro-inflammatory cytokine production and induce the death of dopaminergic terminals in the striatum (Beier et al., 2017). Moreover, our group and others have pointed out the possibility that different forms of peripheral inflammation, especially that induced by gut inflammation, increase the death of nigral dopaminergic neurons (Hernández-Romero et al., 2012); (Villarán et al., 2010); (Garrido-Gil et al., 2018); (Herrera et al., 2015). Intriguingly, recent cohort studies have shown an association between PD and inflammatory bowel diseases (IBDs), one of whose typical feature is long-lasting systemic inflammation (Villumsen et al., 2019); (Wan, Zhao, and Wu 2020); (Weimers et al., 2019); (Zhu et al., 2019); (Brudek 2019). Actually, the gut-brain axis hypothesis of PD is gaining a lot of attention, as supported by the exponential increase in the number of papers referring to this topic in the last 10 years (for a review, see (Kaushal, Singh, and Singh 2021).

With all these precedents, the aim of this study was to investigate whether two different models of acute peripheral inflammation are able to induce neuroinflammation in the ventral mesencephalon and the ability of Gal3 to regulate brain inflammation in response to both systemic LPS and oral dextran sulphate sodium (DSS) model of ulcerative colitis (UC).

MATERIAL AND METHODS

Animals and Treatments

12–16 week-old wild type (WT) and Gal3 null mutant mice (Gal3KO) on the C57BL/6 background (Colnot et al., 1998) were obtained from Dr. T. Deierborg from Lund University. Both colonies were maintained at the Centre of Production and Animal Experimentation of the University of Seville. Animals were housed at constant room temperature (RT) of 22 ± 1°C and relative humidity (60%), with a 12 h light-dark cycle and *ad libitum* access to food and water. Experiments were carried out in accordance with the Guidelines of the European Union Directive (2010/63/EU) and Spanish regulations (BOE 34/11370–421, 2013) for the use of laboratory animals; the study was approved by the Scientific Committee of the University of Seville.

For the LPS treatment, 40 mice were divided into four groups: 1) WT group, control WT animals injected intraperitoneally (i.p.) with 100 µl 0.9% sterile saline; 2) WTLPS group, WT animals

injected i.p. with 100 µL LPS (Sigma-Aldrich, St. Louis, MO, United States) in 0.9% sterile saline, at a dose of 1 µg/g for four consecutive days; 3) Gal3KO group, Gal3KO animals injected i.p. with 100 µL 0.9% sterile saline; and 4) Gal3KOLPS group, Gal3KO animals injected i.p. with 100 µL LPS in 0.9% sterile saline, at a dose of 1 µg/g for four consecutive days. Animals were sacrificed 5 days after the first LPS injection.

The acute colitis was induced by oral administration of DSS (molecular weight 36,000–50,000 Da; MP Biomedicals, LLC) at a concentration of 4% in tap water. A total of 40 mice organized into four groups were used: 1) WT group, control WT animals drinking tap water; 2) WTDSS group, WT animals drinking DSS for 10 days; 3) Gal3KO group, Gal3KO animals drinking tap water; and 4) Gal3KODSS group, Gal3KO animals drinking DSS for 10 days. Animals were sacrificed 10 days after the beginning of the treatment.

In order to carry out a clinical evaluation of the inflammation generated by the DSS, the animals were monitored, at the beginning and end of the treatment, based on the named Disease Activity Index (DAI). DAI was assessed according to a standard scoring system, and body weight, stool consistency and rectal bleeding were recorded (Cooper et al., 1993). Loss in body weight was scored as: 0, no weight loss; 1, weight loss of 1–5% from baseline; 2, 5–10%; 3, 10–20%; and 4, >20%. For stool consistency, a score of 0 was assigned for normally formed pellets, 1 for soft pellets not adhering to the anus, two for very soft pellets adhering to the anus and three for liquid stools adhering to the anus. For bleeding, a score of 0 was assigned for no blood, 1 for small spots of blood in stool and dry anus, two for large spots of blood in stool and through anal orifice and three for gross bleeding and largely around the anus. These scores are added together and divided by three, resulting in DAIs ranging from 0 (healthy) to 3 (maximal disease activity). Body weight loss was calculated as the percentage of the initial weight (day 0).

The colon inflammation was assessed by colon length shortening, histological score and by the mRNA expression levels of the pro-inflammatory cytokines interleukin (IL)-1β and tumor necrosis factor (TNF)-α, as described (Carvajal, et al., 2017b). Following sacrifice, the colons were removed, washed with ice-cold saline solution, and measured. For histological analysis, the distal colons were fixed by overnight incubation with phosphate buffer saline (PBS) (in mM, 137 NaCl, 2.7 KCl, 10 Na2HPO4 and 1.8 KH2PO4 pH 7.4) containing 4% para-formaldehyde. Tissues were embedded in paraffin and cut into 5 µm-thick sections that were stained with hematoxylin/eosin. The analysis was performed in a blinded fashion by a validated method (Cooper et al., 1993). Colon damage was graded based on destruction of epithelium, dilatation of crypts, loss of goblet cells, inflammatory cell infiltrate, oedema and crypt abscesses. Each of these parameters is scored on a scale of 0 to 3 and added together to obtain a total severity scoring.

Cell Proliferation Rate

Epithelial cell proliferation rate was quantified by measuring the incorporation into DNA of 5-bromo deoxyuridine (BrdU) as previously described (Carvajal, et al., 2017a). Briefly, mice received an i.p. injection of BrdU (120 mg/kg body weight) and were sacrificed 90 min later. BrdU was detected by immunohistochemistry using an anti-BrdU antibody (1:300; Sigma-Aldrich). Antibody binding was visualized with a biotinylated antibody followed by immunoperoxidase staining. Vectastain ABC peroxidase kit (Vector) and 3,3′-diaminobenzidine were used. The slides were rinsed, mounted and photographed with a Zeiss Axioskop 40 microscope equipped with a SPOT Insight V 3.5 digital camera. Acquired images were analyzed by using Spot Advance 3.5.4.1 program (Diagnostic Instrument, Inc.,). The number of labelled cells was determined in at least 15 crypts well oriented longitudinally per mouse. Crypt cell proliferation rate is expressed as the number of BrdU-positive cells per crypt.

Goblet Cells Staining

The identification and quantification of mature goblet cells in the epithelium of the distal colon was performed by immunohistochemical detection using an anti-mucin-2 (MUC-2) antibody (1:25; Santa Cruz Biotechnology), as described above. The number of positive cells was determined in at least 15 crypts longitudinally well oriented per mouse and the results are expressed as the number of MUC-2 positive cells per crypt.

Real-Time Quantitative Reverse Transcription PCR

SN, striatum and distal colon were dissected from each mouse after 4 (for LPS) or 10 (for DSS) days of treatment, snap frozen in liquid nitrogen and stored at −80°C. Total RNA was extracted using RNeasy® kit (Qiagen). cDNA was synthesized from 1 µg of total RNA using QuantiTect® reverse transcription kit (Qiagen) in 20 µL reaction volume as described by the manufacturer. RT-qPCR was performed with iQ™SYBR® Green Supermix (Bio-Rad Laboratories), 0.4 µM primers and 1 µL cDNA. Controls were carried out without cDNA. Amplification was run in a Mastercycler® ep realplex (Eppendorf) thermal cycler at 94°C for 3 min followed by 35 cycles of 94°C for 30 s, 55°C for 45 s, and 72°C for 45 s, followed by a final elongation step at 72°C for 7 min. Following amplification, a melting curve analysis was performed by heating the reactions from 65 to 95°C in 1°C intervals while monitoring fluorescence. Analysis confirmed a single PCR product with the melting temperature. β-actin served as a reference gene and was used for sample normalization. The primer sequences for Gal3, TNF-α, IL-1β, IL-6, CXCL10, NOS2, COX2, IL-10 and β-actin are shown in **Table 1**. The cycle at which each sample crossed a fluorescence threshold, Ct, was determined, and the triplicate values for each cDNA were averaged. Analyses of RT-qPCR were performed using a comparative Ct method integrated in a Bio-Rad System Software.

Immunohistological Evaluation

For Iba-1 and CD68 staining, animals were perfused through the heart under deep anesthesia (isoflurane) with 150–200 ml of 0.9% sterile saline. After perfusion, brains were removed and fixed in 4% para-formaldehyde in phosphate buffer, pH 7.4. Then they were cryoprotected serially in sucrose in PBS, pH 7.4, first in 10% sucrose for 24 h and then in 30% sucrose until sunk

TABLE 1 | Sense and antisense sequences of the primers used for the analysis of mRNA expression by qPCR. Abbreviations: Gal3, galectin-3; TNF-α, tumor necrosis factor α; NOS2, nitric oxide synthase two; IL, interleukin; CXCL10, C-X-C motif chemokine 10; COX2, cyclooxygenase-2.

Gene	Forward (5′- 3′)	Reverse (5′- 3′)
β-actin	5′-CCACACCCGCCACCAGTTCG-3′	5′-CCCATTCCCACCATCACACC-3′
Gal3	5′-GATCACAATCATGGGCACAG-3′	5′-GTGGAAGGCAACATCATTCC-3′
TNF-α	5′-TGCCTATGTCTCAGCCTCTTC-3′	5′-GAGGCCATTTGGGAACTTCT-3′
NOS2	5′-CTTTGCCACGGACGAGAC-3′	5′-TCATTGTACTCTGAGGGCTGAC-3′
IL-6	5′-GACAAAGCCAGAGTCCTTCAGA-3′	5′-AGGAGAGCAATTGGAAATTGGGG-3′
IL-1β	5′-TGTAATGAAAGACGGCACACC-3′	5′-TCTTCTTTGGGTATTGCTTGG-3′
IL 10	5′-CCAAGCCTTATCGGAAATGA-3′	5′-TTTCACAGGGAGAAATCG-3′
CXCL10	5′-AAGCATGTGGAGGTGCGAC-3′	5′-CTAGGGAGGACAAGGAGGGT-3′
COX2	5′-CCAGGCCGACTAAATCAAGC-3′	5′-GGACAATGGGCATAAAGCTATGG-3′

(2–5 days). The brains were then frozen in isopentane at −80°C. Incubations and washes were in Tris-buffered saline (TBS) or PBS, pH 7.4. All work was performed at RT. Coronal sections (20 μm) were cut on a cryostat at −20°C and mounted in gelatin-coated slides. Sections were washed and then treated with 0.3% hydrogen peroxide in methanol for 20 min and washed again. Sections were then incubated in a solution containing TBS and 1% goat serum (Vector) for 60 min in a humid chamber. Slides were then drained and further incubated with rabbit-derived anti-Iba-1(1:500, Wako) and mouse-derived anti-CD68 (1:100, Invitrogen) in TBS containing 1% serum and 0.25% Triton-X-100 for 24 h. The immunostaining continued incubating the sections for 2 h with biotinylated goat anti-rabbit IgG (1:200, Vector), for Iba-1 or with goat anti-mouse IgG (1:200, Vector) for CD68. The secondary antibody was diluted in TBS containing 0.25% Triton-X-100 and its addition was preceded by three 10 min rinses. Sections were then incubated with the VECTASTAIN®-Peroxidase solution (1:100; Vector). The peroxidase was visualized with a standard diaminobenzidine/hydrogen reaction for 5 min.

Immunohistochemistry Data Analysis

For the measurement of Iba-1 and CD68 immunoreactivity, we used the AnalySIS imaging software (Soft Imaging System GmbH) coupled to a Polaroid DMC camera (Polaroid) attached to a light microscope (Leica Mikroskopie). Cells showing Iba-1 or CD68 immunoreactivity were counted by using five sections per animal systematically distributed through the brain anterior–posterior axis. In each section, a systematic sampling of the area occupied by the Iba-1/CD68 positive cells was made from a random starting point with a grid adjusted to count five fields per section. An unbiased counting frame of known area (40 μm × 25 μm = 1,000 μm^2) was superimposed on the tissue section image under a ×40 objective. The different types of Iba-1-positive cells (displaying different shapes depending on their activation state) in the different treatment conditions were counted as a whole. The entire z-dimension of each section (20 μm in all animals) was sampled; no guard zone was used; hence, the section thickness sampling fraction was 1.

Immunofluorescence

Animals were perfused and sections were prepared as described above. Incubations and washes for all the antibodies were in PBS, pH 7.4. All work was done at RT, unless otherwise noted. Sections were blocked with PBS containing 5% BSA and 1% Triton X-100 for 2 h. The slides were then incubated overnight at 4°C with the primary antibody: sheep-derived anti-Tyrosine hydroxylase (anti-TH, 1:1,000, Novus), rabbit-derived anti-caspase 3 (1:250, Cell Signaling; 1:250), rabbit-derived anti-Iba1 (Wako; 1:1,000) and goat-derived anti-galectin-3 (R&D Systems; 1:500). Primary antibodies were diluted in PBS containing 1% BSA and 1% Triton X-100. After three washes in PBS, sections were incubated with the secondary antibodies, Alexa Fluor® 488, Alexa Fluor® 546 and Alexa Fluor® 647 (Invitrogen; 1:500), for 2 h at room temperature in the dark. Fluorescence images were acquired using a confocal laser scanning microscope (Zeiss LSM seven DUO) and processed using the associated software package (ZEN 2010). Iba-1/galectin-3 and TH/Caspase three co-localizing cells were visualized with Image-J software.

Fluoro Jade C

Before use, slides were dried at RT for 10 min, and washed in 80% ethanol for 5 min and then in 70% ethanol for 2 min. Then slides were washed for 2 min in distilled water and incubated in a solution of 0.06% potassium permanganate solution for 10 min, on a shaker table to ensure consistent background suppression between sections. The slides were then washed in distilled water for 2 min. The staining solution was prepared as described by the manufacturer using a 0.0001% solution of Fluoro jade C (Histo-Chem Inc., Jefferson AR). Hoechst was added to the working solution in a concentration of 1:1,000. After 10 min in the staining solution, the slides were rinsed for 1 min in each of three distilled water washes. Excess water was removed by briefly draining the slides vertically on a paper towel. The slides were then placed on a slide warmer at 50°C for 30 min in darkness (until they were fully dry). The dried slides were cleared by immersion in xylene for 1 min before coverslipping with DPX (VWR International Inc., Poole, England), a non-aqueous, non-fluorescent plastic mounting media.

Statistical Analysis

Results are expressed as mean ± SD. Means were compared by one-way ANOVA followed by the Fisher's LSD test for post hoc multiple range comparisons. We also performed a multifactor

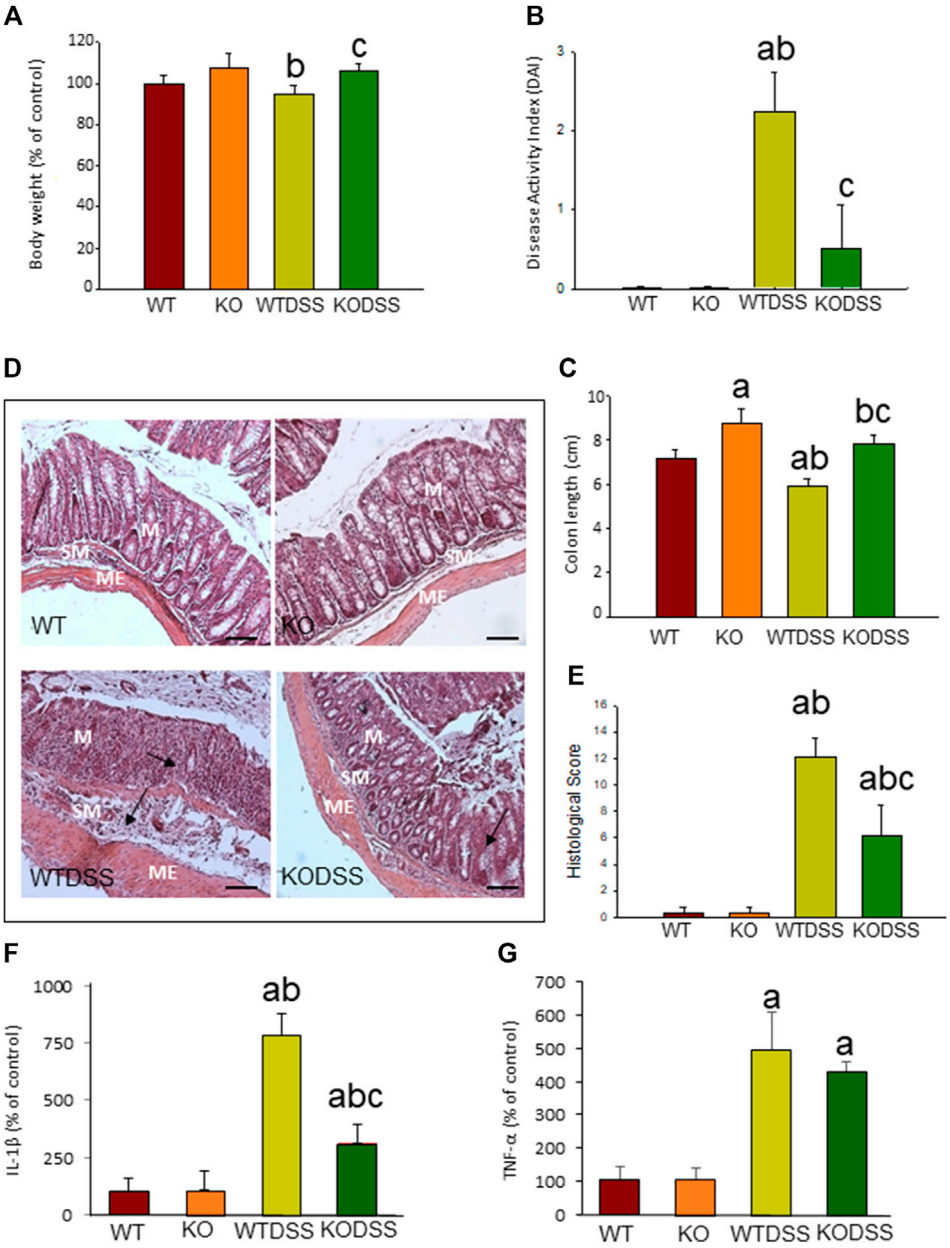

FIGURE 1 | Evaluation of the DSS-induced inflammation in WT and Gal3KO mice. The mice were subjected to 4 % DSS in the drinking water for up to 10 days. Clinical symptoms and indicators of colonic inflammation were assessed at the end of the treatment. Body weight expressed as percentage of control (WT mice) **(A)**; disease activity index (DAI) **(B)**; Length of colon **(C)**; Representative photographs of histological analysis **(D)** performed with hematoxylin/eosin staining in distal colon sections. Scale bar: 200 μm. Alterations such as loss of structure of colonic crypts and infiltration of immune cells are indicated by arrows (M: mucosa; SM: submucosa; ME: muscularis externa); Histological score **(E)**; mRNA relative expression of IL-1β **(F)** and TNF-α **(G)** in distal colon expressed as percentage of control (WT mice). Results are mean ± SD of 10 mice per experimental group. Statistical analysis: One-way ANOVA followed by the Fisher's LSD post hoc test for multiple comparisons was used, with $\alpha = 0.05$: **(a)**, compared with the WT group; **(b)**, compared with the KO group; **(c)**, compared with the WTDSS group; $p < 0.05$ for body weight and mRNA expression, $p < 0.001$ for colon length, DAI and histological score. Abbreviations: WT, wild type mice; WTDSS, wild type mice treated with DSS; KO, Gal3 knockout mice; KODSS, Gal3 knockout mice treated with DSS.

ANOVA to analyze the interactions between the two factors included in the comparisons made in the study: genotype (WT and KO animals) and treatment (control and DSS). These results are summarized in **Supplementary Appendix S1, S2**. An alpha level of 0.05 was used. The Statgraphics Plus 3.0 statistical package was used for the analyses.

RESULTS

Dextran Sulphate Sodium Treatment Induces Acute Colitis

Clinical evaluation of the animals and analysis of the colon damage at the end of the treatment were made, as described in Methods. All DSS-treated mice developed acute colitis with clinical symptoms and colon damage. **Figure 1A** shows that, although the body weight of WTDSS animals did not decrease compared to WT mice, there were differences in the DAI score used for clinical evaluation. DAI score revealed that, while control animals (WT) had 0 points, WTDSS mice were affected, reaching a punctuation of 2.25 ± 0.5 (p <0.001; **Figure 1B**; see **Supplementary Appendix S1** for multifactor ANOVA analysis). We next evaluated the colon length shortening and histological scoring as indicators of colonic inflammation. **Figure 1C** reveals that the colon length significantly decreased in WTDSS mice compared with WT animals (p <0.001; see **Supplementary Appendix S1** for multifactor ANOVA analysis). Histological analysis also showed colon inflammation in WTDSS mice (**Figures 1D,E**). We also carried out RT-qPCR experiments to analyze mRNA expression levels of the pro-inflammatory cytokines IL-1β and TNF-α in the distal colon. **Figures 1F,G** show an increase in both cytokines with the DSS treatment in WT animals (p <0.05, compared to the control WT animals; see **Supplementary Appendix S1** for multifactor ANOVA analysis).

The Absence of *Gal3* Prevents the Development of Severe Dextran Sulphate Sodium -Induced Acute Colitis

To elucidate whether the absence of *Gal3* modifies the disease severity in acute colitis, we compared the response between WT and Gal3KO mice after 10 days of DSS treatment. **Figure 1A** shows that there is a statistical difference (p <0.05) in body weight between WTDSS and Gal3KODSS mice. Hence, animals with complete deletion of *Gal3* showed a 12% increase in body weight (p <0.05, compared with WTDSS mice; see **Supplementary Appendix S1** for multifactor ANOVA analysis). DAI score also revealed that the WTDSS mice were much more affected as compared with Gal3KODSS mice. Results ranged from 2.25 ± 0.5 in WTDSS to 0.5 ± 0.57 in Gal3KODSS (p <0.001; **Figure 1B**; see **Supplementary Appendix S1** for multifactor ANOVA analysis), indicating that the Gal3KODSS mice scarcely had clinical symptoms. Regarding the colon length shortening and histological scoring, **Figure 1C** reveals that the colon length significantly decreased in both WTDSS and Gal3KODSS mice compared with their respective controls without DSS treatment (p <0.001). However, colon shortening was significantly higher in WTDSS mice as compared with Gal3KODSS mice (p <0.001; see **Supplementary Appendix S1** for multifactor ANOVA analysis.). Histological analysis showed colon inflammation in both WTDSS and Gal3KODSS mice, but in WT was much more significant ranging from 12.1 ± 1.4 in WTDSS to 6.2 ± 2.3 in Gal3KODSS (p <0.001; **Figures 1D,E**; see **Supplementary Appendix S1** for multifactor ANOVA analysis). Highlight that in Gal3KODSS mice loss of crypts and infiltration of immune cells was more severe in the colon wall than that seen in WTDSS (**Figure 1D**). RT-qPCR experiments showed an increase in both cytokines with the DSS treatment in both types of mice, but in the Gal3KO, compared to WT, the levels of IL-1β were significantly lower, ranging from 783.9 ± 9.2 in WTDSS to 314.2 ± 82.9 % in Gal3KODSS (p <0.001; **Figures 1F,G**; see **Supplementary Appendix S1** for multifactor ANOVA analysis). According to all these results, Gal3KODSS mice developed a much milder acute colitis compared to WTDSS mice. Thus, *Gal3* deletion might protect against colitis development and associated peripheral inflammation.

Effect of the Absence of *Gal3* on Cell Proliferation and Goblet Cells in the Colon of Dextran Sulphate Sodium -Treated Mice

We then tested whether the decreased susceptibility of the Gal3KODSS mice was associated with processes involved in maintaining the intestinal barrier that prevent the colitis, such as epithelial renewal and mucus production. For that, we evaluated cell proliferation rate and the presence of mature goblet cells in the distal colon epithelium of WT and Gal3KO mice with and without DSS treatment.

BrdU incorporation into DNA was measured to evaluate epithelial cell proliferation rate, as described in Methods. The results showed that BrdU is mainly observed in the nuclei of the cells located in the lower part of the crypts where proliferation occurs (**Figure 2A**). In the **Figure 2B**, the quantification revealed that DSS-induced colitis decreased cell proliferation rate in both, WT and Gal3KO, being this diminution greater in WTDSS mice and therefore indicating that *Gal3* deletion significantly lessened the effect caused by DSS treatment (from 3.85 ± 1.21 in WT to 8.60 ± 0.77 in Gal3KO; p < 0.001; see **Supplementary Appendix S1** for multifactor ANOVA analysis).

We next evaluated mature goblet cells by immunohistochemical detection of MUC-2 as a marker (**Figure 2C**). The quantification of number of MUC-2 positive cells per crypt (**Figure 2D**) revealed that the mature goblet cells and therefore MUC-2 production in the colonic mucosa diminished in the DSS-treated WT and Gal3KO mice (p <0.01), but it decreased significantly more in Gal3KO (from 9.7 ± 0.9 in WT to 8.2 ± 1.2 in Gal3KO; p <0.05; see **Supplementary Appendix S1** for multifactor ANOVA analysis) indicating that *Gal3* deletion, in this case, increased the effect of DSS treatment.

Peripheral Inflammation Induced by Lipopolysaccharide Injection Causes Microglial Activation in the Ventral Mesencephalon

To study the role of peripheral inflammation on the brain, we first took advantage of an established model of peripheral inflammation based on four consecutive daily i.p. doses of LPS

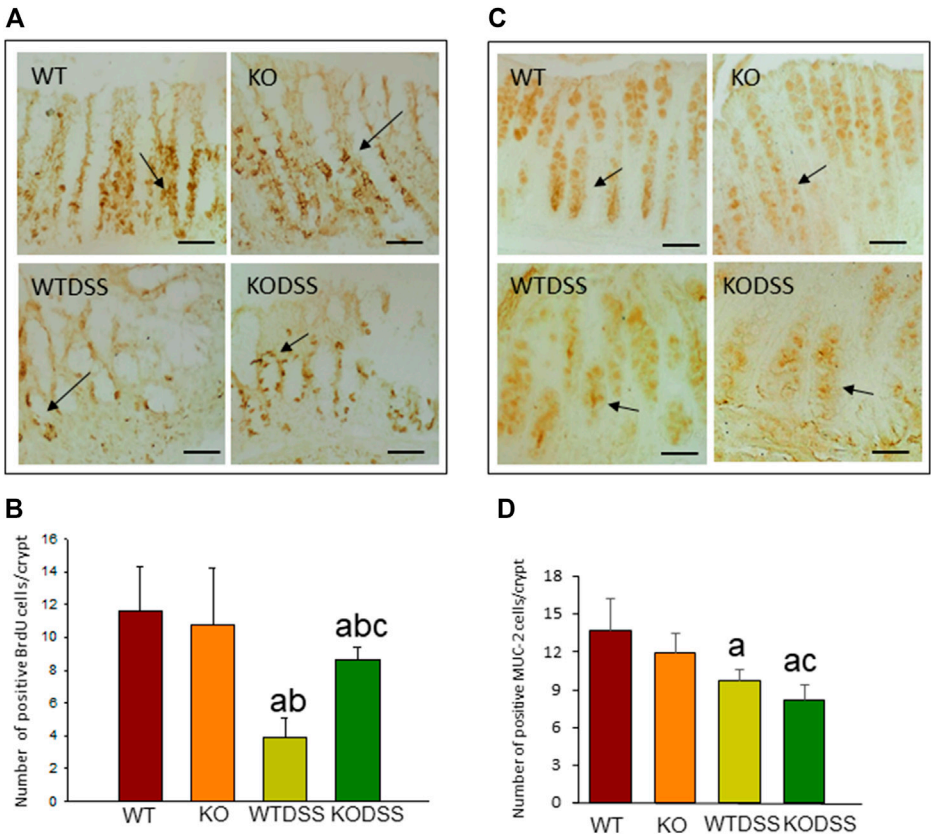

FIGURE 2 | Effect of the DSS treatment on cell proliferation rate and goblet cells in the colon of WT and Gal3KO mice. Representative distal colon sections of cell proliferation rate assessment **(A)**. Examples of BrdU-labelled cells in the crypts are indicated by arrows. Scale bar = 20 μm. Cell proliferation rate expressed as number of BrdU positive cells per colonic crypt **(B)**; Representative distal colon sections of stained goblet cells **(C)**. Arrows indicate MUC-2-labelled goblet cells in the crypts. Quantification is expressed as the number of MUC-2 positive goblet cells per colonic crypt **(D)**. Scale bar: 100 μm. Results are mean ± SD of 10 mice per experimental group. Statistical analysis: One-way ANOVA followed by the Fisher's LSD *post hoc* test for multiple comparisons was used, with $\alpha = 0.05$: **(a)**, compared with the WT group; **(b)**, compared with the KO group; **(c)**, compared with the WTDSS group; $p < 0.001$ for BrdU, $p < 0.05$ for MUC-2. Abbreviations: WT, wild type mice; WTDSS, wild type mice treated with DSS; KO, Gal3 knockout mice; KODSS, Gal3 knockout mice treated with DSS.

and then studied the microglial activation at both cellular and molecular levels. Using immunohistochemistry against Iba-1 (a pan microglia marker) we found that i.p. injection of LPS increased the number of microglial cells 5 days after the beginning of the treatment, in both the striatum (with an increase of 77.8% with respect to the control group, p <0.001; **Figures 3A,C,D**) and SN (with an increase of 118% with respect to the control group, p <0.0001; **Figure 3B**; see **Supplementary Appendix S2** for multifactor ANOVA analysis) from WT animals. Although this increase in microglial cells in response to systemic LPS injection has been previously shown in striatum and cortex (Beier et al., 2017); (García Dominguez et al., 2018), we have extended these results by studying the SN, the most affected structure in PD. The study of microglial activation using immunohistochemistry against CD68 showed that LPS induces an increase of four fold in the number of CD68 positive cells, both in SN (**Figures 4C,D,G**) and striatum (**Figure 4H**). Co-localization of Iba-1 with Gal3 showed that only a few Iba1 positive cells co-localized with Gal3 in response to systemic LPS injections (**Figure 5**).

Microglial activation in the SN and striatum was also studied at the molecular level. Using RT-qPCR, we have evaluated the expression levels of Gal3 and some pro-inflammatory (TNF-α, IL-1β, IL-6, CXCL10, NOS2 and COX2) and anti-inflammatory (IL-10) mediators (**Figures 6(SN),7** (striatum)). Most of these markers were chosen based on single-cell analysis of microglia revealing that upon systemic LPS challenge, microglia acquire a well-defined molecular signature characterized by strong up-regulation of different pro-inflammatory mediators including CXCL10, IL-6, IL-1β, COX2 and TNF (Krasemann et al., 2017). As expected, in SN only WT mice expressed Gal3 (**Figure 6A**). LPS-treatment increased the mRNA levels of Gal3 in the SN for up to three fold (**Figure 6A**; p <0.0001). Moreover, LPS injection produced a strong induction of mRNA expression levels of TNF-α, IL-1β and NOS2, ranging from 233.9 ± 54.8% for NOS2 to 610.9 ± 137.1% for IL-1β in WTLPS mice compared to WT (**Figures 6B,C,F**; p <0.01). In the case of the anti-inflammatory mediator IL-10, the treatment with LPS reduced significantly its expression level in WTLPS mice (p <0.05, compared with the control group; **Figure 6H**; see

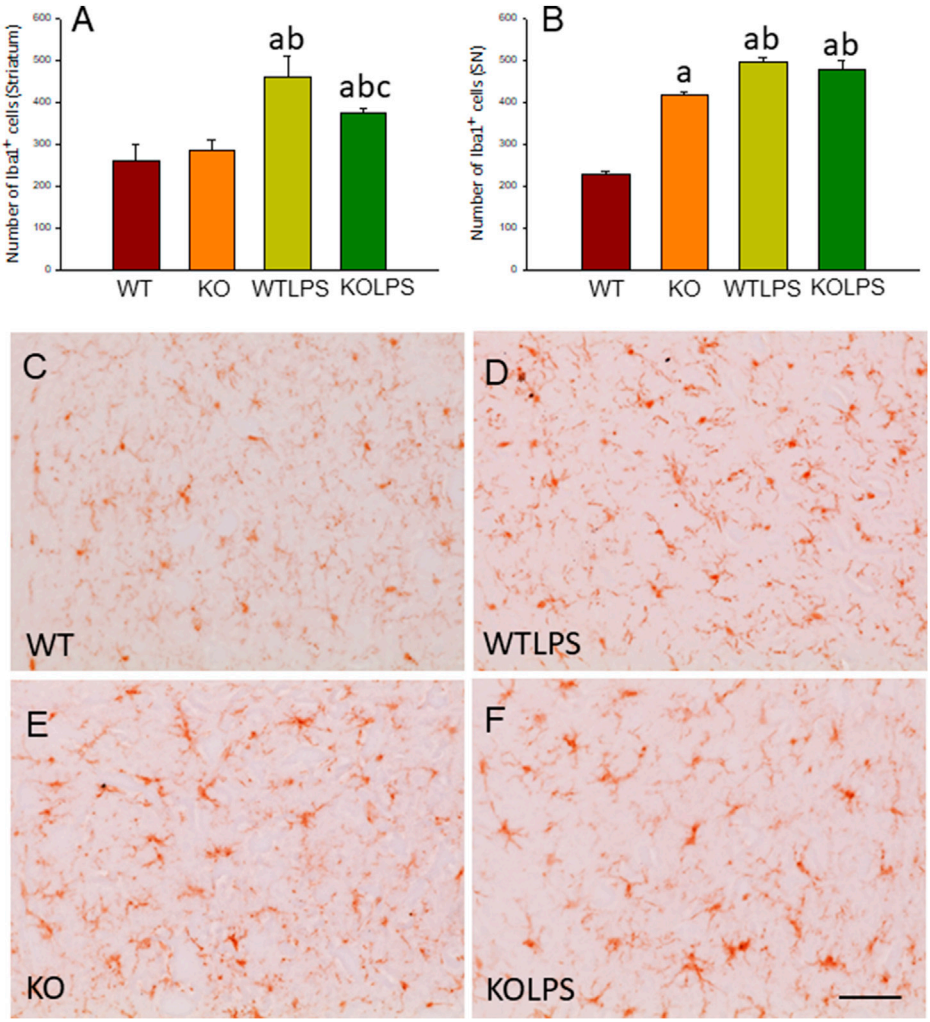

FIGURE 3 | Evaluation of the microglial activation induced by LPS treatment in WT and Gal3KO mice. The effect of LPS was evaluated in striatum **(A)** and SN **(B)** from WT and Gal3KO mice. Results are mean ± SD of at least three mice per experimental group, expressed as the number of Iba1$^+$cells per mm^2. Statistical analysis: One-way ANOVA followed by the Fisher's LSD *post hoc* test for multiple comparisons was used, with $\alpha = 0.05$: **(a)**, compared with WT group; **(b)**, compared with KO group; **(c)**, compared with the WTLPS group; $p < 0.001$ **(C–F)** Representative immunostaining from striatum sections of the different experimental groups. Scale bar: 20 μm. Abbreviations: WT, wild type mice; WTLPS, wild type mice treated with LPS; KO, Gal3 knockout mice; KOLPS, Gal3 knockout mice treated with LPS.

Supplementary Appendix S2 for multifactor ANOVA analysis). In striatum, LPS-treatment increased the mRNA levels of Gal3 (174 ± 36% with respect to the control group; **Figure 7A**; p <0.001). LPS injection also induced an upregulation of TNF-α, IL-1β and NOS2, ranging from 196.96 ± 16.72% for NOS2 to 641.69 ± 114.01% for IL-1β, in WTLPS mice compared to control group (**Figures 7B,C,F**; p <0.001; see **Supplementary Appendix S2** for multifactor ANOVA analysis).

Dextran Sulphate Sodium -Induced Acute Colitis Promotes Microglial Activation in the Ventral Mesencephalon

As stated before, the effect of peripheral injection of LPS in the brain has been already studied (Beier et al., 2017). However, the effect of peripheral inflammation in the brain after DSS treatment has barely been explored. Therefore, we wanted to study neuroinflammation in different structures of CNS with implication in neurodegenerative diseases (cortex, hippocampus, striatum and SN), at both morphological and molecular levels. Using immunohistochemistry against Iba-1 (a pan microglia marker) and CD68 (a marker for microglial activation) we found that the SN was the only structure affected by our UC model (**Figures 8A–D**). Indeed, we failed to detect significant changes in microglia density in the striatum in response to acute DSS, contrary to systemic LPS challenge (**Figure 8C**). We have demonstrated that systemic inflammation induces a fast and transient microglia activation in striatum that may explain the different effects of acute colitis in striatum and SN (García Dominguez et al., 2018). Treatment with DSS induced a significant increase in the number of Iba-1 and CD68 cells in the

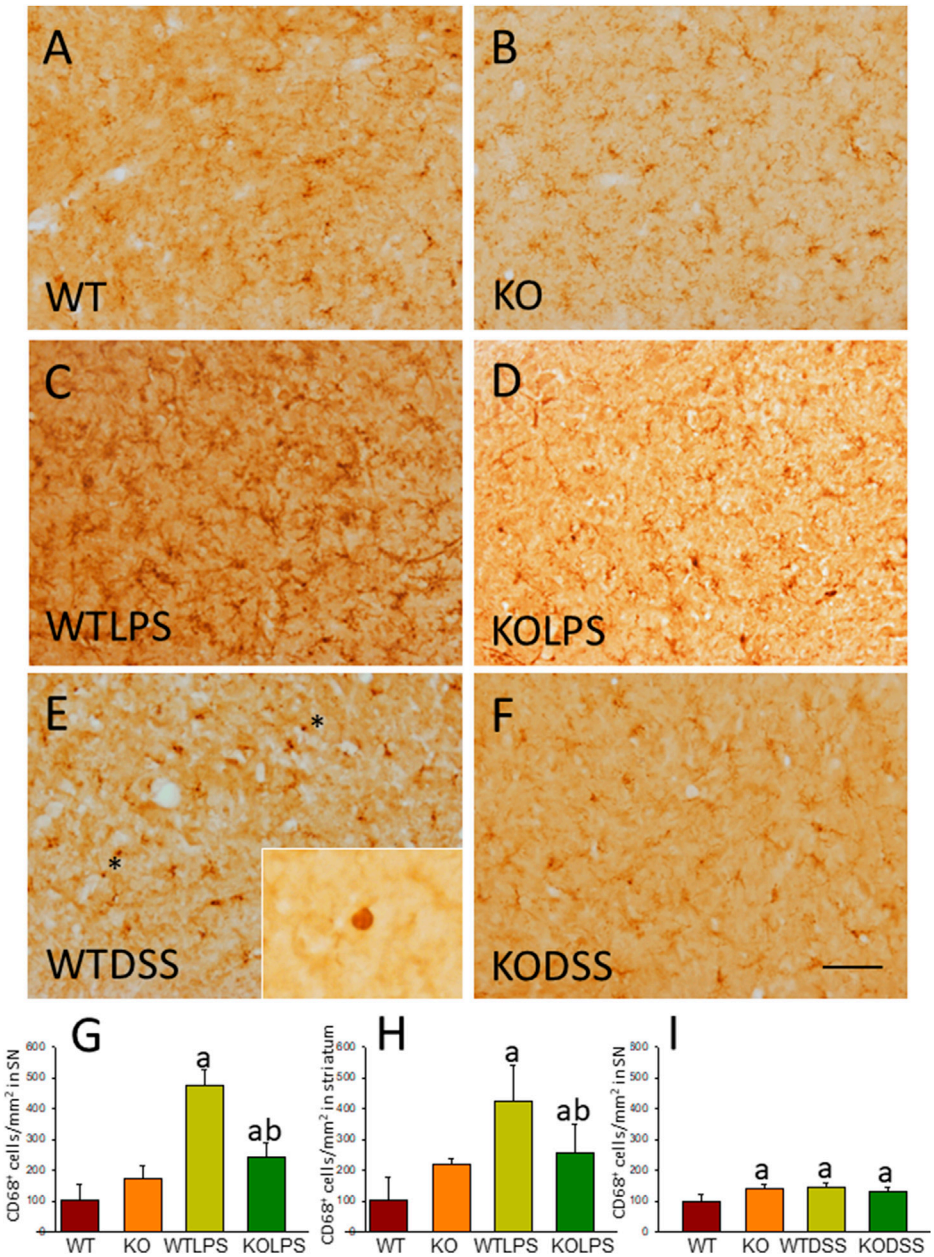

FIGURE 4 | CD68 expression in LPS and DSS treated mice. Representative immunostaining from sections of the different treatments assayed. SN of WT **(A)** animals show a normal pattern of CD68 expression. Gal3KO **(B)** animals show a slight increase in the expression of CD68 in SN. WTLPS animals **(C)** show an increase in the number of CD68 positive cells while the absence of Gal3 in Gal3KOLPS **(D)** animals reduces this induction. Treatment with DSS in WT animals **(E)** also increases the number of CD68 positive cells. Notice the amoeboid morphology typical of highly reactive microglia in WT animals treated with DSS. Absence of Gal3 in DSS treated animals **(F)** do not reduce the number of CD68 positive cells but clearly avoid the presence of highly activated microglia with amoeboid morphology. Scale bar: 125 μm. **(G)** Quantification of the density of CD68 positive cells in SN of LPS treated mice. **(H)** Quantification of the density of CD68 positive cells in the striatum of LPS treated mice. **(I)** Quantification of the density of CD68 positive cells in SN of DSS treated mice. Results are mean ± SD of at least three animals per experimental group, expressed as the number of CD68 positive cells per mm^2. Statistical significance: One-way ANOVA followed by the Fisher's LSD post hoc test for multiple comparisons was used, with $\alpha = 0.05$: **(a)**, compared with the WT group; **(b)**, compared with the WTLPS group; $p < 0.05$. Abbreviations: WT, wild type mice; WTLPS, WT animals treated with LPS; KOLPS, Gal3 knockout mice treated with LPS; WTDSS, wild type mice treated with DSS; KO, Gal3 knockout mice; KODSS, Gal3 knockout mice treated with DSS.

SN of WT animals (203 and 146%, respectively, with respect to the control group; p <0.001; **Figures 4E,I**, **8D,E,G**). When activated, microglial cells change their morphology from resting resident ramified microglia with two or three fine processes to round cells resembling tissue macrophages. After DSS treatment some CD68 positive cells showed a typical round morphology of chronically activated microglia (**Figure 4E**). However, co-localization of Iba-1 with Gal3 showed that only

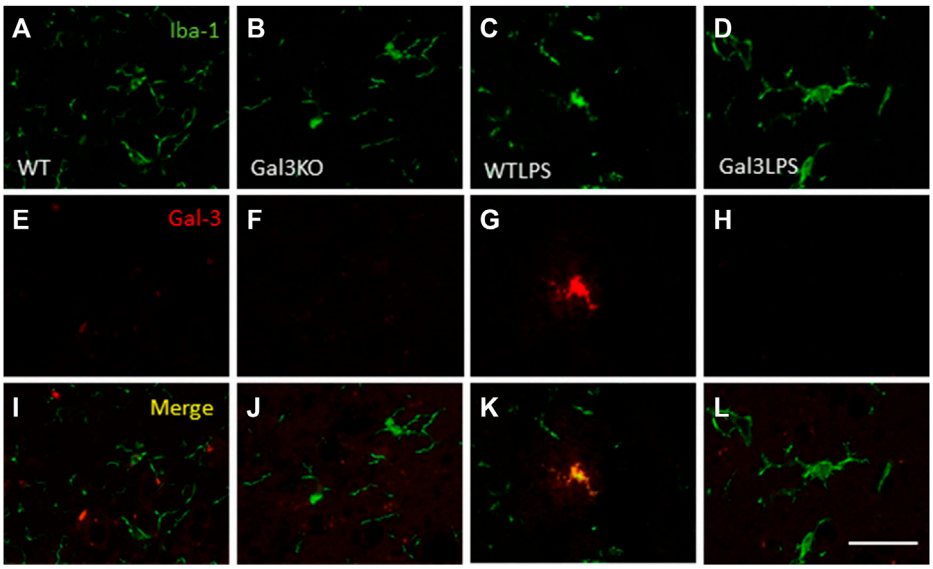

FIGURE 5 | Expression of Gal3 in LPS-activated microglia. Representative images from sections of the different treatments assayed showing immunostaining of Iba1 (green) and Gal3 (red). Only a few Iba1 positive cells co-localized with Gal3 (yellow) in animales WT treated with LPS (K), indicating a not possible DAM phenotype. Scale bar: 75 μm. Abbreviations: WT, wild type mice; WTLPS, wild type mice treated with LPS; Gal3KO, Gal3 knockout mice; Gal3KOLPS, Gal3 knockout mice treated with LPS.

a few Iba1 positive cells co-localized with Gal3 (**Figure 9**). We failed to detect TREM2 expression by microglia after DSS treatment (data not shown). Since expression of TREM2 and Gal3 are features of disease-associated microglia (DAM) (Keren-Shaul et al., 2017); (Krasemann et al., 2017), we may conclude that nigral microglia get activated after acute gut inflammation but they acquire a phenotype different from classical DAM. As previously stated, different microglia modules have been identified under brain disease conditions (Friedman et al., 2018); (Krasemann et al., 2017). Expression of different pro-inflammatory markers potentially neurotoxic have been identified by single-cell analysis after acute systemic inflammation (Krasemann et al., 2017). Consequently, microglial activation in the SN was also studied at the molecular level to analyze if the pro-inflammatory module is induced by mesencephalic microglia under conditions of acute gut inflammation. Hence, using qRT-PCR, we evaluated the expression levels of Gal3 and some pro-inflammatory (TNF-α, IL-1β, IL-6, CXCL10, NOS2 and COX2) and anti-inflammatory (IL-10) mediators (**Figure 10**). As expected, only WT mice expressed Gal3 (**Figure 10A**; p <0.001). Interestingly, DSS-treatment increased the mRNA levels of Gal3 in the SN of WT animals. Moreover, the acute colitis produced a strong induction of mRNA expression levels of TNF-α, IL-1β, IL-6 and CXCL10, ranging from 233.5 ± 24.0% for IL6 to 663.5 ± 195.8% for TNF-α, in WTDSS mice compared to control group (**Figures 10B–E**; p <0.05). In the case of the anti-inflammatory mediator IL-10, the treatment with DSS reduced significantly its expression level in WTDSS mice (p <0.01, compared with the control group; **Figure 10H**). See **Supplementary Appendix S1** for multifactor ANOVA analysis.

Absence of *Gal3* reduces microglial activation in the ventral mesencephalon from LPS or DSS treated mice.

We next studied the effect of deletion of *Gal3* on the neuroinflammation generated by LPS or DSS in each model. Immunohistochemistry against Iba-1 showed that the absence of Gal3 significantly decreased the neuroinflammation caused by LPS only in the striatum (1.2 fold with respect to the WTLPS, p <0.001; **Figures 3A–D**). However, it is interesting to notice that Gal3KO animals have more microglial cells than WT animals in SN. Therefore, if we compare Gal3KO with Gal3KOLPS animals, in SN, no statistical differences were found among these groups. However, multifactor ANOVA analysis showed that there is a positive interaction between genotype and treatment (see **Supplementary Appendix S2**). Consequently, the effect of LPS on the microglial population in the SN depends on the genotype, and the effect of genotype depends on the LPS/saline injection. Besides, the absence of Gal3 significantly decreased the number of microglial cells after DSS treatment in the SN (55.8125 ± 6.7 cells/mm^2 respect to WTDSS; p <0.001; **Figures 8D,G,H**; see **Supplementary Appendix S1** for multifactor ANOVA analysis). When we used CD68 to study microglial activation, we found that the number of cells expressing CD68 decreases around 50% in SN and striatum in Gal3KOLPS animals compared with the WTLPS group (**Figures 4C,D,G,H**). Although we did not find any statistical decrease in the number of CD68 positive cells in Gal3KODSS animals with respect to the WTDSS group (**Figures 8E,F,I**), microglial cells in Gal3KODSS mice did not show the typical round morphology of chronically activated microglia as seen in WTDSS animals (**Figures 8E,F**). Besides, we could not find any statistical differences between Gal3KO and Gal3KODSS animals. In this

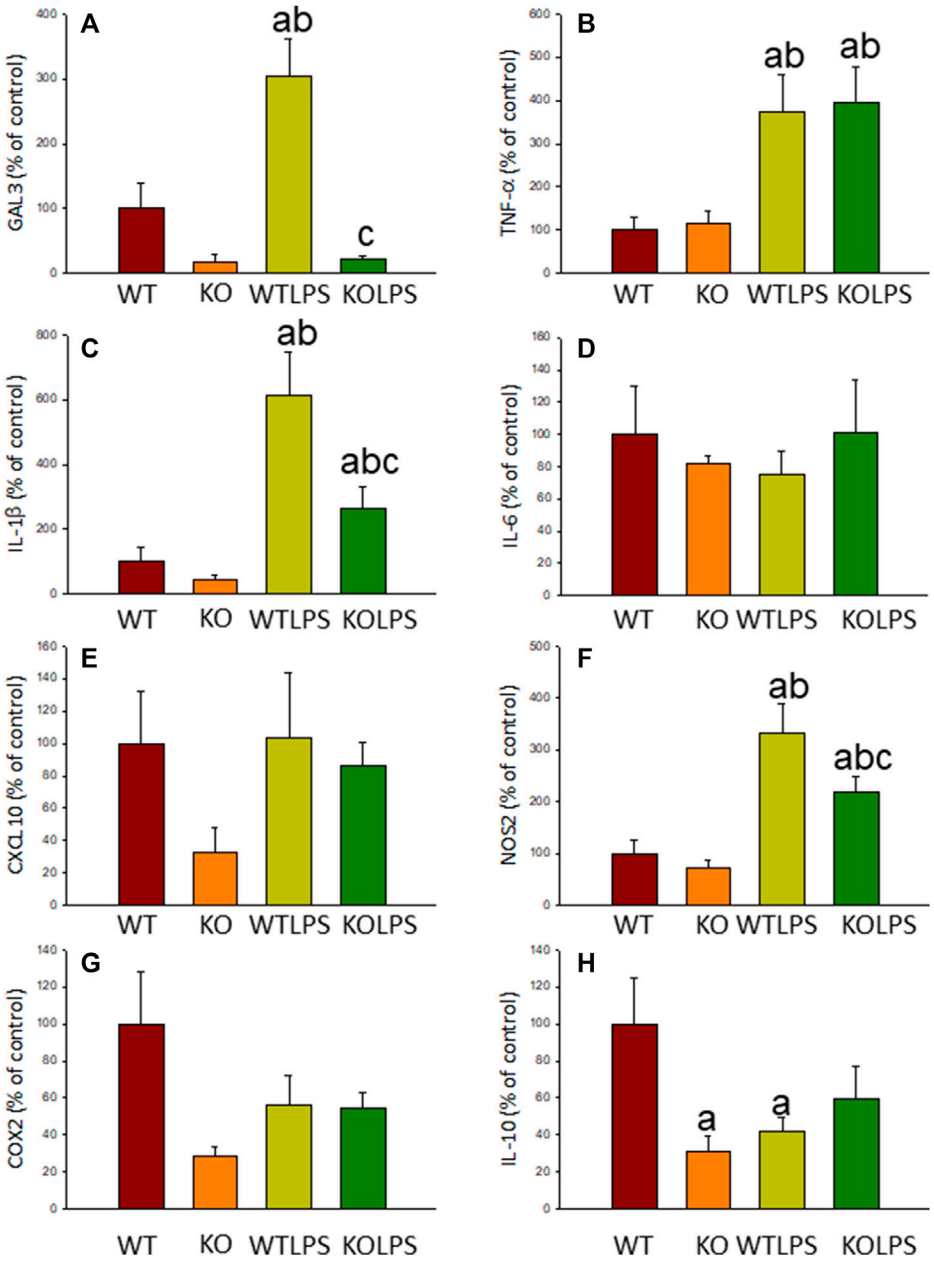

FIGURE 6 | Effect of the LPS treatment on the expression levels of Gal3, TNF-α, IL-1β, IL-6, CXCL10, NOS2, COX2 and IL-10 in SN. Measurement of the effect of the treatment with LPS on the expression levels of mRNA of Gal3 **(A)**, pro-inflammatory mediators such as TNF-α **(B)**, IL-1β **(C)**, IL-6 **(D)**, CXCL10 **(E)**, NOS2 **(F)**, COX2 **(G)** and the anti-inflammatory mediator IL-10 **(H)** in the SN of mice from the different experimental groups by using RT-qPCR. Results are mean ± SD of at least three mice per experimental group, normalized to β-actin and expressed as percentage relative to the WT group. Statistical significance: One-way ANOVA followed by the Fisher's LSD post hoc test for multiple comparisons was used, with $\alpha = 0.05$: **(a)**, compared with the WT group; **(b)**, compared with the KO group; **(c)**, compared with the WTLPS group; $p < 0.05$. Abbreviations: WT, wild type mice; WTLPS, wild type mice treated with LPS; KO, Gal3 knockout mice; KOLPS, Gal3 knockout mice treated with LPS.

case, multifactor ANOVA analysis shows that there is an interaction between the two factors studied (genotype and DSS/water treatment).

Microglial activation in the SN and striatum was also studied at the molecular level, using RT-qPCR (**Figures 5**, **6**, **9**). Interestingly, the LPS and DSS-mediated induction of inflammatory mediators was prevented in GAL3KO animals. Hence, expression levels of IL-1β and NOS2 mRNA were decreased in the SN and striatum of Gal3KOLPS mice compared to WTLPS animals (more than 50% reduction for IL-1β and 25–35% for NOS2; **Figures 5**, **6**). Even though Gal3 deletion failed to alter the number of Iba1 positive microglia in

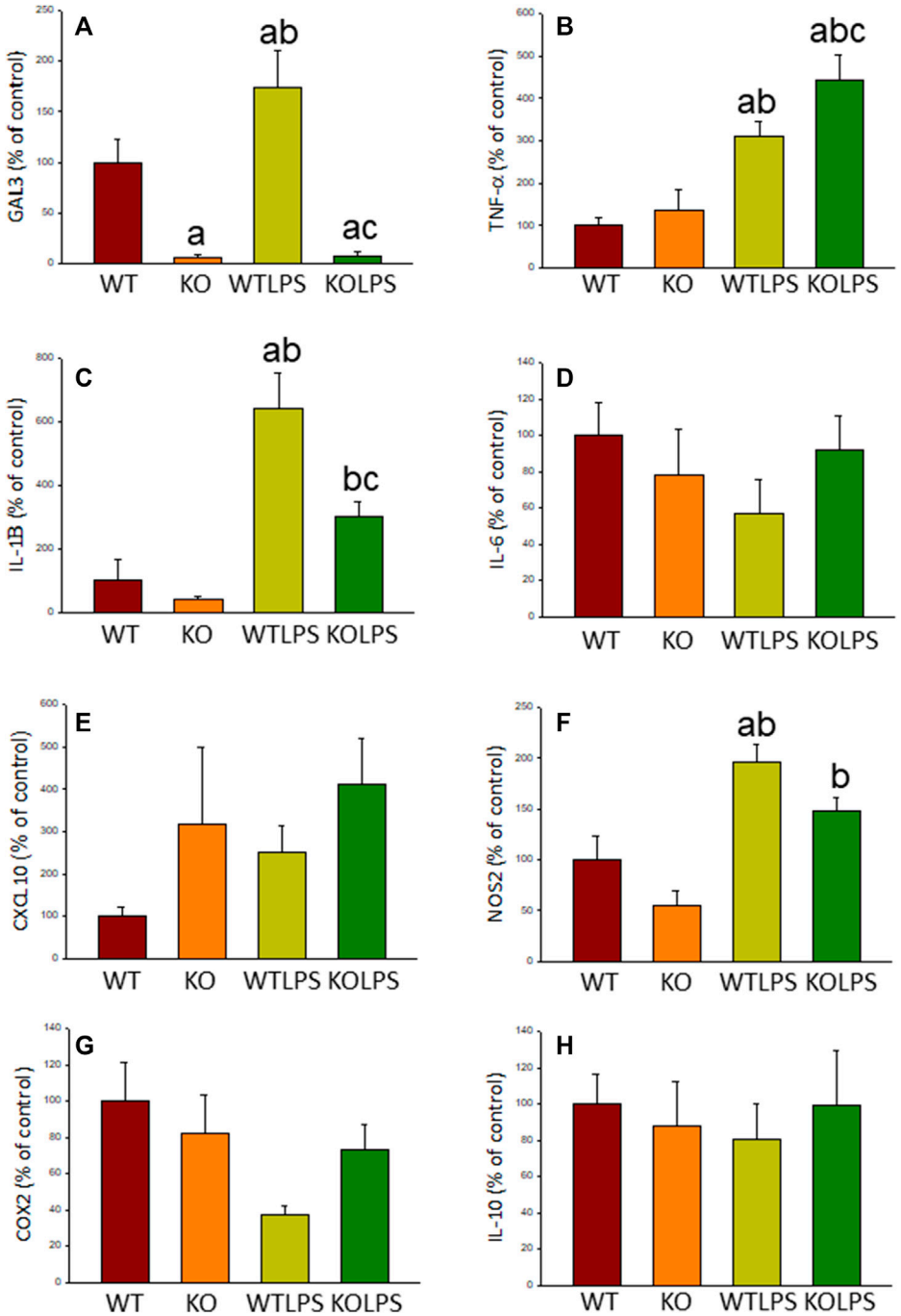

FIGURE 7 | Effect of the LPS treatment on the expression levels of Gal3, TNF-α, IL-1β, IL-6, CXCL10, NOS2, COX2 and IL-10 in striatum. Measurement of the effect of the treatment with LPS on the expression levels of mRNA of Gal3 **(A)**, pro-inflammatory mediators such as TNF-α **(B)**, IL-1β **(C)**, IL-6 **(D)**, CXCL10 **(E)**, NOS2 **(F)**, COX2 **(G)** and the anti-inflammatory mediator IL-10 **(H)** in the striatum of mice from the different experimental groups by using RT-qPCR. Results are mean ± SD of at least three mice per experimental group, normalized to β-actin and expressed as percentage relative to the WT group. Statistical significance: One-way ANOVA followed by the Fisher's LSD *post hoc* test for multiple comparisons was used, with $\alpha = 0.05$: **(a)**, compared with the WT group; **(b)**, compared with the KO group; **(c)**, compared with the WTLPS group; $p < 0.001$. Abbreviations: WT, wild type mice; WTLPS, wild type mice treated with LPS; KO, Gal3 knockout mice; KOLPS, Gal3 knockout mice treated with LPS.

the SN in response to LPS as compared with WPLPS, the molecular analysis support the view that mesencephalic microglia acquire a pro-inflammatory phenotype, which is partially prevented in Gal3KOLPS. It is noteworthy that Gal3 deletion prevented the upregulation of all pro-inflammatory markers analyzed in the SN but not in the gut in response to

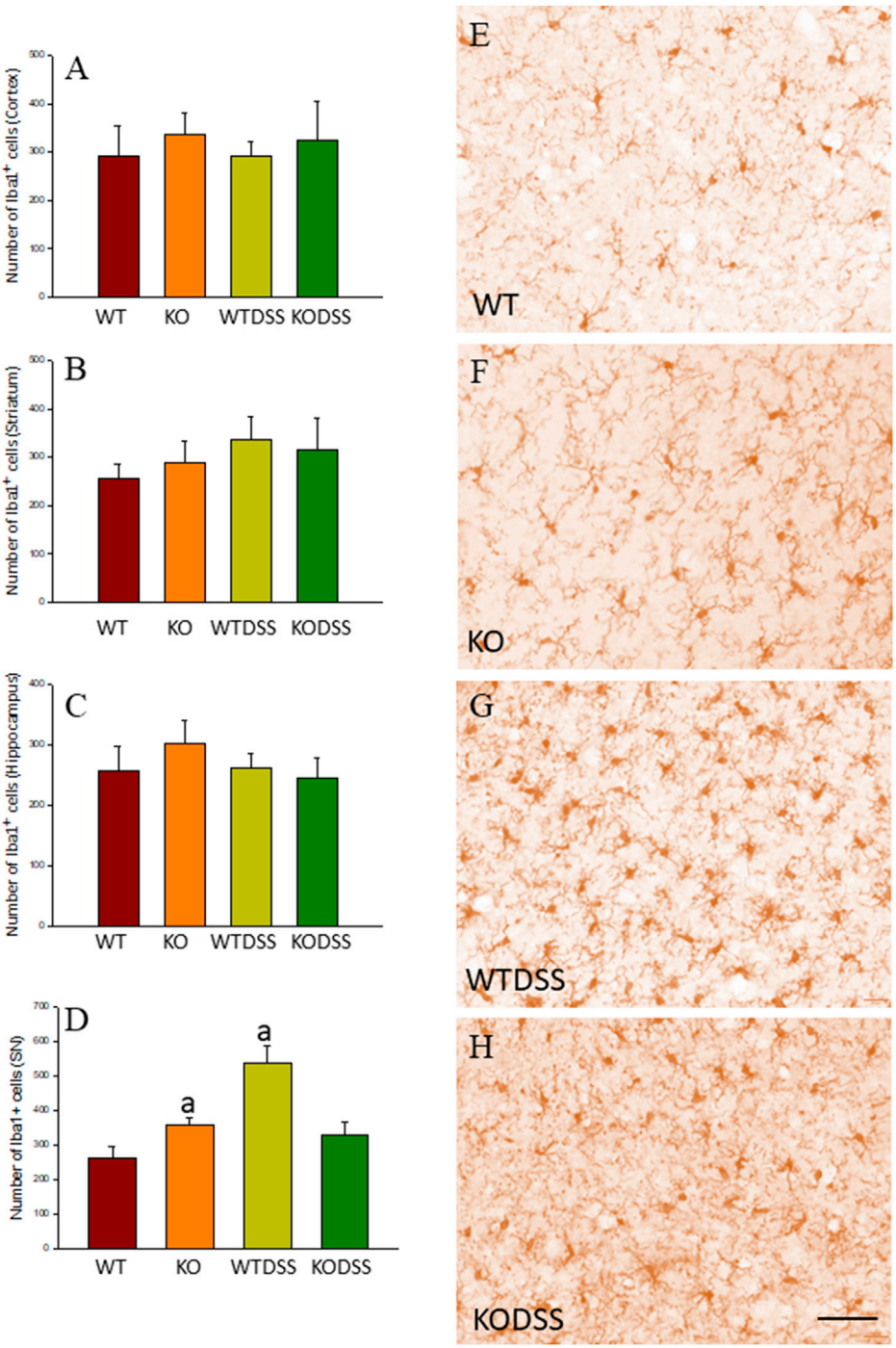

FIGURE 8 | Evaluation of the microglial activation induced by DSS treatment in WT and Gal3KO mice. The effect of peripheral inflammation induced after 10 days of DSS treatment was evaluated in cortex **(A)**, striatum **(B)**, hippocampus **(C)** and SN **(D)** from WT and Gal3KO mice. Results are mean ± SD of at least three mice per experimental group, expressed as the number of Iba1$^+$ cells per mm^2. Statistical significance: One-way ANOVA followed by the Fisher's LSD post hoc test for multiple comparisons was used, with $\alpha = 0.05$: **(a)**, compared with the WT group; $p < 0.001$ **(E–H)** Representative immunostaining from SN sections of the different experimental groups. Scale bar: 20 μm. Abbreviations: WT, wild type mice; WTDSS, wild type mice treated with DSS; KO, Gal3 knockout mice; KODSS, Gal3 knockout mice treated with DSS.

DSS treatment. However, it should be considered the different nature of immune players (microglia vs peripheral immune cells) and focal vs distant areas of inflammation.

Moreover, expression levels of TNF-α, IL-1β, IL-6 and CXCL10 also decreased in the SN of Gal3KODSS mice compared with the WTDSS animals, with reductions ranging

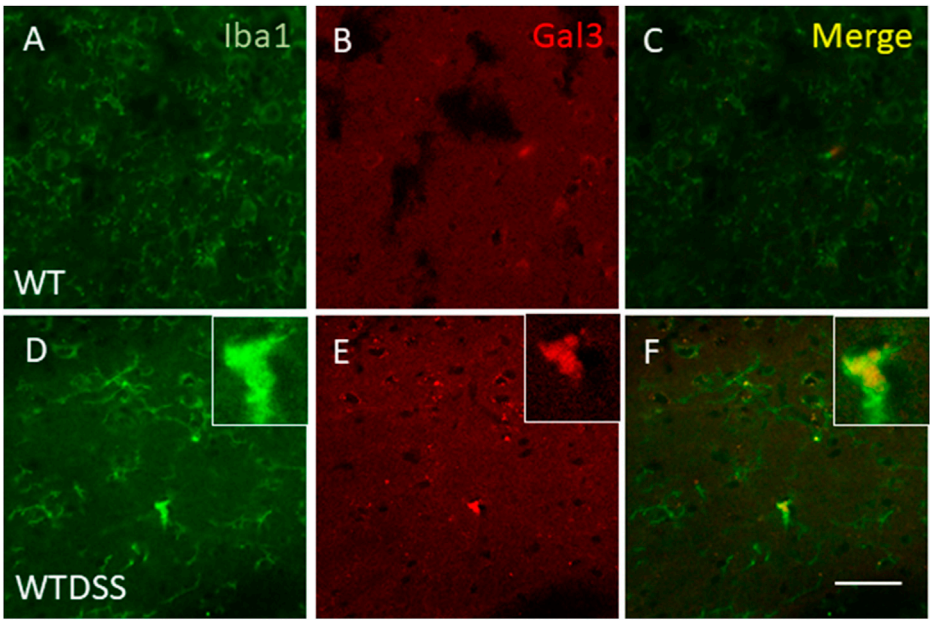

FIGURE 9 | Expression of Gal3 in DSS-activated microglia. Representative images from sections of WT **(A–C)** and WTDSS **(D–F)** animals showing immunostaining of Iba1 (green) and Gal3 (red). As shown, only a few Iba1 positive cells co-localized with Gal3 (yellow) after the treatment with DSS **(F)**. Scale bar: 125 μm. Abbreviations: WT, wild type mice; WTDSS, wild type mice treated with DSS.

from 40% for IL-6–66% for CXCL10 (**Figure 9**). In the case of the anti-inflammatory mediator IL-10, the reduction induced by DSS treatment was also abolished in Gal3KO mice compared with its respective control (**Figure 9H**). See **Supplementary Appendix S1, S2** for multifactor ANOVA analysis.

Peripheral inflammation induced by LPS injection and DSS treatment does not cause dopaminergic neuronal death in the ventral mesencephalon.

We finally wanted to study if the microglial activation induced using the two models of peripheral inflammation was able to produce neuronal death in the SN, the main structure affected in PD. To this end we performed a Fluorojade C staining in order to assess whether LPS injection and/or DSS treatment induce neuronal degeneration. However, we did not find neurodegenerative events following LPS/DSS treatment (**Figures 11E,F,I,J**). We also performed a double immunofluorescence of TH (a dopaminergic neuronal marker) and caspase-3 (an apoptotic marker). Again, we did not find any sign of apoptosis in the TH positive neurons in none of the peripheral inflammation models used (**Figures 11G,H,K,L**).

DISCUSSION

The idea that peripheral inflammation could increase the damage in a previously inflamed brain is not new. We have previously demonstrated that the peripheral inflammation generated by an UC model, as well as a rheumatoid arthritis model, is able to increase the dopaminergic neuronal loss induced by intranigral injection of LPS (Villarán et al., 2010); (Hernández-Romero et al., 2012) or 1-methyl-4-phenyl-1,2,3,6-tetrahydropyridine (García-Domínguez et al., 2018), both models of PD. These studies strongly suggest that peripheral inflammation is a risk factor for the death of nigral dopaminergic neurons in response to different settings.

In the present work, we provide evidence that the inflammatory stimulus caused by either i.p. administration of LPS or by oral administration of DSS was able to produce by itself a similar pattern of neuroinflammation, especially in the SN. This is of special interest, since the SN is the main brain structure affected in PD, suggesting a potential role of peripheral inflammation in the development of this disease. The current results also demonstrate that Gal3 regulates the process involving inflammation either in the periphery or in the SN.

To prove our hypothesis, we first took advantage of an already established model of peripheral inflammation based on the i.p. injection of four consecutive doses of LPS (Beier et al., 2017). It has been previously demonstrated that this paradigm induces microglial activation in the striatum, along with a strong up-regulation of pro-inflammatory mediators in the first 5 days with no apparent neuronal loss, while at 19 days the microglial phenotype changes to an anti-inflammatory state coinciding with the beginning of the death of dopaminergic neurons (Beier et al., 2017). Therefore, we wanted to study the profile of microglial activation in the dopaminergic system, finding that, similarly to previous studies, the number of Iba1 positive cells increased in the striatum 5 days after the first injection of LPS. We completed this study measuring the number of microglial cells in the SN, and found that treatment with LPS increased the number of Iba1 and CD68 positive cells even more than in striatum.

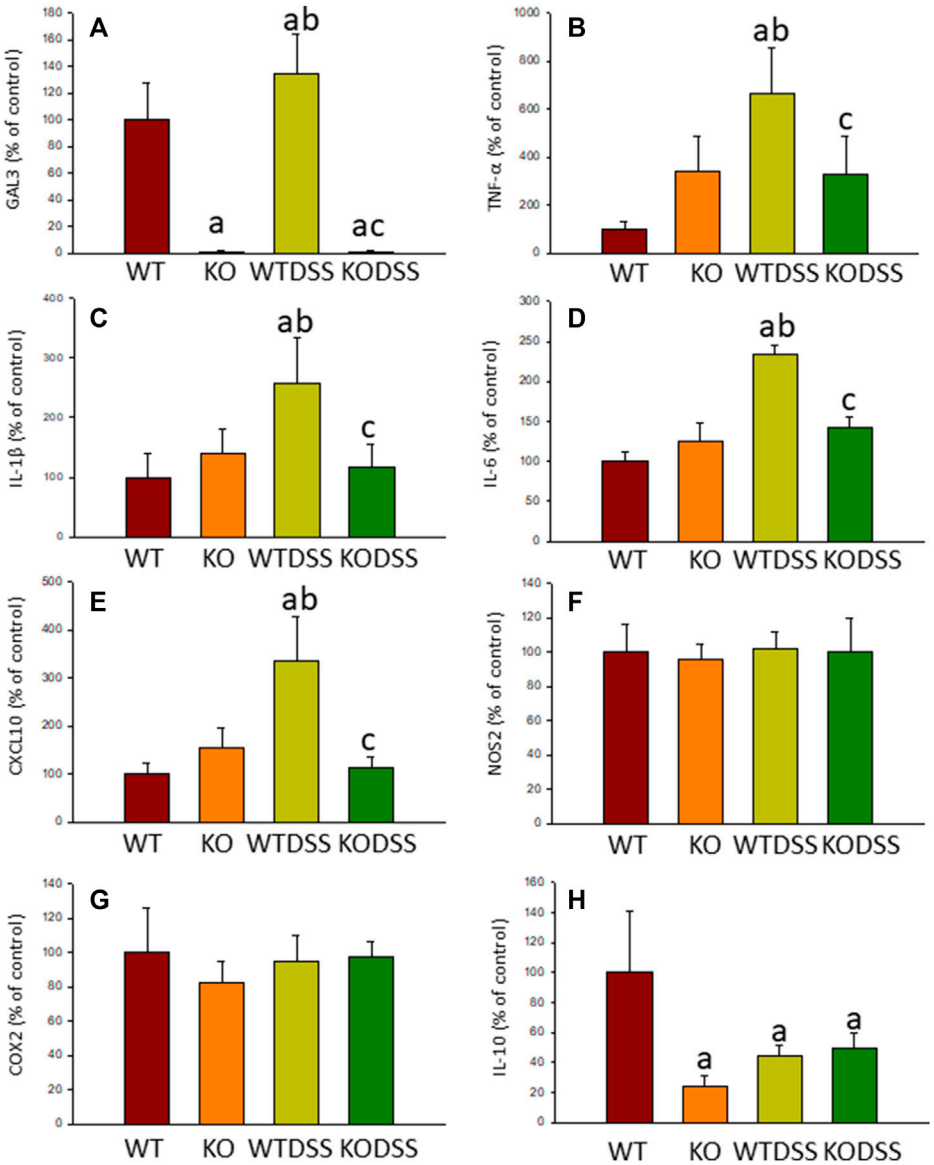

FIGURE 10 | Effect of the DSS treatment on the expression levels of Gal3, TNF-α, IL-1β, IL-6, CXCL10, NOS2, COX2 and IL-10. Measurement of the effect of the treatment with DSS on the expression levels of mRNA of Gal3 **(A)**, pro-inflammatory mediators such as TNF-α **(B)**, IL-1β **(C)**, IL-6 **(D)**, CXCL10 **(E)**, NOS2 **(F)**, COX2 **(G)** and the anti-inflammatory mediator IL-10 **(H)** in the SN of mice from the different experimental groups by using RT-qPCR. Results are mean ± SD of at least three mice per experimental group, normalized to β-actin and expressed as percentage relative to the WT group. Statistical significance: One-way ANOVA followed by the Fisher's LSD *post hoc* test for multiple comparisons was used, with $\alpha = 0.05$: **(a)**, compared with the WT group; **(b)**, compared with the KO group; **(c)**, compared with the WTDSS group; $p < 0.05$. Abbreviations: WT, wild type mice; WTDSS, wild type mice treated with DSS; KO, Gal3 knockout mice; KODSS, Gal3 knockout mice treated with DSS.

We also studied the profile of cytokine expression in the SN 5 days after the first injection of LPS. Using qPCR techniques, we found an overexpression of genes typically related to the pro-inflammatory phenotype of microglia, including TNF-α, IL-1β and NOS2. Several authors have pointed out the key relevance of TNF-α in neurodegenerative conditions (Clark and Vissel 2021). Furthermore, (Qin et al., 2017), have shown that TNF-α levels remain elevated for up to 10 months after a single intraperitoneal dose of 5 mg/kg of LPS (Qin et al., 2007). In addition, various cytokines and immune cells may cause certain damage to dopaminergic neurons (Alrafiah et al., 2019); (Qin et al., 2016). Among them, IL-1 and IL-6 possess a potent pro-inflammatory effect. IL-1β and IL-6 gene polymorphisms play important roles in the occurrence and development of various diseases (Yousefi et al., 2018), including PD (Li et al., 2021).

We also wanted to know whether Gal3 is involved in this process. When we measured the expression of *Gal3* in the SN after the i.p. injections of LPS, we found a strong up-regulation of

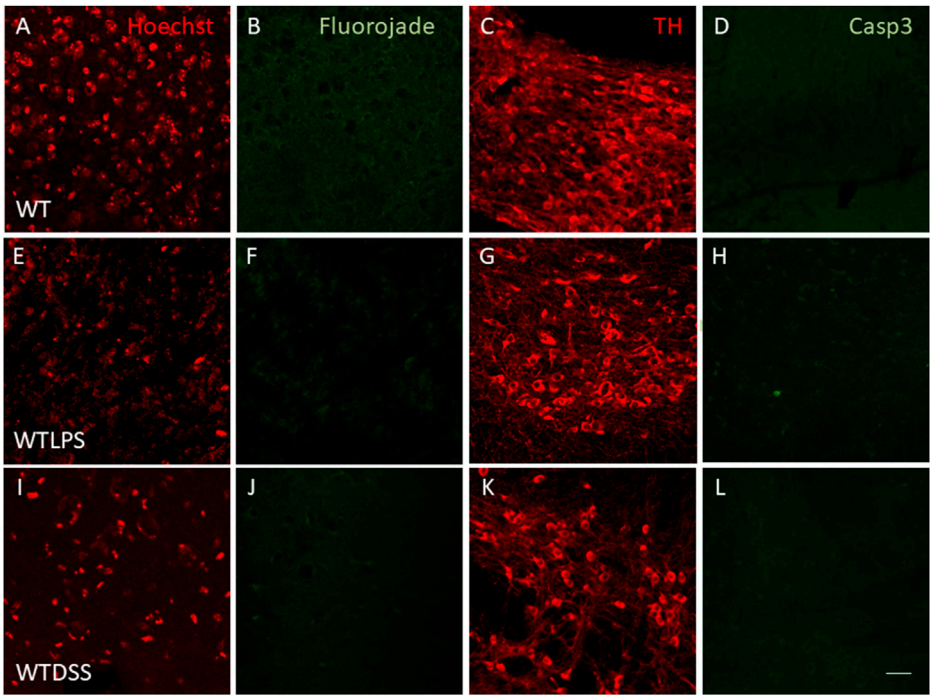

FIGURE 11 | Effect of the treatment with LPS or DSS in the degeneration of dopaminergic neurons. Representative images from sections of WT, WTLPS and WTDSS animals. After 5 days of LPS treatment no signs of neurodegeneration or apoptosis were found **(E–H)** compared to the control group **(A–D)**. After 10 days of treatment with DSS neither neuronal degeneration **(J)** nor signs of apoptosis **(L)** were found compared to the control group **(A–D)**. Scale bar: 150 μm. Abbreviations: WT, wild type mice; WTLPS, WT animals treated with LPS; WTDSS, wild type mice treated with DSS.

this protein, which suggests that Gal3 could be involved in the induction of a specific microglial phenotype after a peripheral inflammatory stimulus. Taking advantage of Gal3KO animals, we also found that absence of *Gal3* decreased the levels of some pro-inflammatory mediators in the SN and striatum, including IL-1β and NOS2, confirming the important role of Gal3 in driving this specific glial response.

To expand these results and go deeper in this issue, we also wondered if this pattern was shared by other pathological conditions that courses with peripheral inflammation. As stated before, the peripheral inflammation that accompanies IBD could be related to the development of PD and may be considered a risk factor for suffering this pathology (Brudek 2019). For this reason, we studied if the inflammatory environment induced by an acute colitis model in mice that resembles an active stage of UC could reach the brain and induce a similar profile of cytokines and if again, Gal3 is involved in this process. For this purpose, we first induced acute colitis through the oral administration of DSS in the drinking water, a model extensively used in the literature (Nascimento et al., 2020).

We first studied the clinical symptoms and colon state of DSS-treated mice and found that the treatment was able to produce an acute inflammatory process. This was supported by multiple markers including a decrease of body weight along with an increase in DAI score, colon shortening, damage in colon and increased mRNA levels of pro-inflammatory cytokines such as IL-1β and TNF-α. Interestingly, it has been previously shown that TNF-α is essential for the transfer of peripheral inflammation to the CNS (Qin et al., 2007).

In our experimental conditions, absence of *Gal3* led to lower inflammatory scores and levels of cytokines, preventing the appearance of symptoms of disease and attenuating the colonic inflammation induced by DSS, revealing an interesting possible role of Gal3 modulating peripheral inflammation. Results regarding Gal3 effects on colonic inflammation are contradictory. For instance, Simovic Markovic et al. (2016) showed an important pro-inflammatory role that Gal3 plays in events that accompany UC, while other authors found that Gal3 reduces the colon inflammation in animal models of experimental colitis (Tsai et al., 2016); (Lippert et al., 2015). More recently, it has been shown that the effects of *Gal3* deletion vary as colon inflammation progresses since Gal3 may direct the polarization of colonic macrophages towards inflammatory or anti-inflammatory phenotype (Volarevic et al., 2019). Moreover, Gal3 seems to be involved in processes that maintain the barrier in the colon. Similar to that reported by other authors (Araki et al., 2010), we observed decreased epithelial cell proliferation in the colon of DSS-treated mice. This alteration causes relevant leaks in the intestinal barrier because it prevents its restoration following injury, promoting colon inflammation and subsequent peripheral inflammation. In this condition, *Gal3* deletion attenuated the inhibition of the proliferation, suggesting that Gal3 could promote the inflammation by reducing epithelial renewal. Gal3 was found to inhibit cell proliferation in

cultured endothelial cells (Zhang et al., 2018) but in other tissues and pathologies Gal3 promoted it (Viguier et al., 2014). On the other hand, according to our results, down-regulation of Gal3 decreases the intestinal epithelial intercellular adhesion (Jiang et al., 2014) which facilitates the proliferation.

Another interesting finding is related to the goblet cells. As expected, DSS treatment decreased the number of goblet cells (MUC-2 positive) in the colon (Kim and Ho 2010). In DSS-treated Gal3KO mice, this decrease was greater, indicating that Gal3 would facilitate MUC-2 production that forms the protective mucus layer contributing to prevent colon inflammation (Kim and Ho 2010). Our finding agrees with the up-regulation of MUC-2 transcription by Gal3 (Song et al., 2005). This effect would be opposite to the observations discussed so far and indicate again that Gal3 might play different roles associated with inflammatory processes as in other tissues and clinical contexts (Sciacchitano et al., 2018). These contradictory effects of Gal3 can be explained by the different subcellular localizations of Gal3 together with its possible post-translational modifications. Actually, Gal3 can be found in the cytoplasm, nucleus, and membranes (Shimura et al., 2004) and can be released into the extracellular space upon certain stimuli such as LPS (Li et al., 2008) and interferon γ (Jeon et al., 2010).

Once we examined the induction of acute colitis in our DSS model and the role that Gal3 plays in this process, we wanted to know whether this peripheral inflammation was able to reach the brain. For this purpose and using immunohistochemistry techniques, we looked for signs of neuroinflammation in several CNS structures typically involved in neurodegenerative diseases, such as cortex, hippocampus, striatum and SN. We found that peripheral inflammation induced a significant increase in the number of microglial cells only in the SN of DSS-treated animals. To shed more light on the nature of the neuroinflammation induced by the gut inflammation, we studied the transcriptional phenotype of microglial cells. Using qPCR, we found that DSS treatment induced the up-regulation of pro-inflammatory mediators in the SN, including again IL-1β and TNF-α. Nevertheless, the pro-inflammatory nature of these markers along with the increased number of $CD68^+$ activated microglial cells supports the view that peripheral inflammation sustains pro-inflammatory microglia.

Once we studied the effect of peripheral inflammation caused by the colitis in the brain, we wanted to decipher the possible role that Gal3 could have in this process. Our results showed that genetic deletion of *Gal3* prevented the increase in microglial cells in the SN as well as the increase in the pro-inflammatory cytokines in response to DSS treatment. This effect could be mediated by the reduction of the gut inflammation, by a reduction of microglial activation, or more likely by the addition of the effects that the deletion of *Gal3* has in both peripheral and central inflammation.

An important question that emerges from our study is how Gal3 regulates brain inflammation associated with systemic inflammation. With the advent of single-cell RNA analysis of microglial cells in disease conditions, a TREM2-dependent microglia phenotype was identified and named either disease-associated phenotype (Keren-Shaul et al., 2017) or microglia neurodegenerative phenotype (Krasemann et al., 2017). A common feature to both phenotypes is upregulation of selective genes including *Trem2*, *Apoe*, *Clec7a*, *Itgax*, *Spp1* and *Lgals3* (Keren-Shaul et al., 2017); (Krasemann et al., 2017); (Mathys et al., 2017). There is controversy whether this microglial phenotype is protective or deleterious (Keren-Shaul et al., 2017); (Krasemann et al., 2017). It has been reasoned that given that loss-of-function mutations of TREM2 confer higher risk of suffering AD and PD, DAM is protective (Keren-Shaul et al., 2017). However, the picture is more complex than thought and, for instance, *Trem2* deletions have been shown to be protective and deleterious depending on the context (García-Revilla et al., 2019). Besides, we have demonstrated that Gal3, which is strongly upregulated in DAM (Krasemann et al., 2017); (Mathys et al., 2017), exerts a noxious role under different brain disease conditions including AD (Boza-Serrano et al., 2019), brain ischaemia (Burguillos et al., 2015) and traumatic brain injury (Yip et al., 2017). Whether the DAM phenotype is neuroprotective or deleterious, it is important to highlight that different microglial modules have been recently identified (Friedman et al., 2018). Among them, those associated with systemic inflammation have been characterized and shown to express high levels of classical pro-inflammatory genes including *Il6*, *Cxcl10*, *Il1b* and *Tnf* (Krasemann et al., 2017). Importantly, both acute models analyzed (LPS and DSS) clearly induced a pro-inflammatory module (Burguillos et al., 2015); (Krasemann et al., 2017). In addition, we failed to detect Gal3 and TREM2 immunoreactivity in activated microglia associated with both peripheral inflammatory conditions. Since DAM or MGnD phenotypes are characterized by strong upregulation of both markers (Keren-Shaul et al., 2017); (Krasemann et al., 2017); (Mathys et al., 2017), our data supports the view that under conditions of peripheral inflammation, Gal3 drives a microglia pro-inflammatory polarization through a peripherally acting mechanisms. Indeed, Gal3 is highly expressed in myeloid cells including monocytes, macrophages, dendritic cells and neutrophils (Díaz-Alvarez and Ortega 2017) and membrane-associated Gal3 plays immune-associated roles under acute and chronic inflammation (Díaz-Alvarez and Ortega 2017).

It is certainly intriguing why gut inflammation induces brain inflammation only in the SN. The maintenance of the gut barrier is synergistically coordinated by the immune system and by the gut microbiota (Donaldson and Mabbott, 2016); (Rooks and Garrett 2016). A breached intestinal barrier may allow gut microbiota–specific immune cells to act as systemic mediators able to penetrate the CNS and hence causing neuroinflammation (Buscarinu et al., 2017); (Pröbstel et al., 2020). Besides, the involvement of the vagus nerve in selectively driving immune response in SN should not be discarded. Indeed, the possibility that PD starts in the ENS and then spreads to the brain via the vagus nerve is consistent with Braak's hypothesis (Braak et al., 2002); (Braak et al., 2003); (Braak et al., 2007).

In conclusion, we provide evidence that peripheral inflammation associated with systemic LPS and gut inflammation polarizes microglia towards a pro-inflammatory phenotype, potentially neurotoxic. Our results support the view that mice lacking Gal3 developed a much milder acute colitis in response to DSS treatment compared to WT mice. Hence, Gal3 deletion might protect from both colitis development and associated peripheral inflammation. Our data does not sustain a classical DAM phenotype under conditions of acute systemic

inflammation (both models) and suggest a prominent role of Gal3 acting peripherally. It is certainly straightforward the selectivity of gut inflammation to solely drive inflammation in the ventral mesencephalon. Given the anatomical gut-brain connection through the vagus nerve, the involvement of this pathway should be considered in spreading inflammation from gut to brain. Indeed, epidemiological studies have demonstrated that IBD patients had an increased risk of suffering subsequent PD (Lin et al., 2016); (Peter et al., 2018); (Villumsen et al., 2019); (Weimers et al., 2019). Finally, we demonstrate that Gal3 is upregulated in the ventral mesencephalon under conditions of acute inflammation. We should consider that elevated serum levels of Gal3 from PD patients have been found (Yazar et al., 2019); (Cengiz et al., 2019) and Gal3 has been identified in the outer layers of Lewy Bodies from PD patients (Flavin et al., 2017), a clear indication that Gal3 may play a yet unidentified role if PD etiology and/or progression. Overall, Gal3 emerges as an important regulator of the immune response, both peripheral and central, and that inhibition of Gal3 may be a potential pharmacological approach to counteract diseases with an inflammatory base, such as PD.

DATA AVAILABILITY STATEMENT

The raw data supporting the conclusions of this article will be made available by the authors, without undue reservation.

ETHICS STATEMENT

The animal study was reviewed and approved by Consejería de Agricultura, Pesca y Desarrollo Rural, Junta de Andalucía.

AUTHOR CONTRIBUTIONS

RP designed the study, wrote the manuscript, analyzed and interpreted the data. JV and MP helped in the design of the study and the writing of the manuscript. AO performed the animal treatments, perfusions and dissection of animal brains. She was also involved in drafting and revising the manuscript. PM and MC performed the colon analysis. IB and AC performed the RP analysis. MG, AJ, AT, MN, ID, MC and JR helped with the performance of the immunohistochemistry and RP analysis. MS were involved in critical revision of the manuscript.

FUNDING

This work was supported by grants from the Spanish Ministerio de Ciencia, Innovación y Universidades (RTI 2018-098830-B-I00), from the Consejería de Economía y Conocimiento of Junta de Andalucía (P18-RT-1372 and US-1264806). MJP, MDVC and PGM were supported by a grant from the Junta de Andalucía (CTS 5884) and AEC by an associated post-doctoral grant.

ACKNOWLEDGMENTS

We thank A.A. Ilundáin for the support provided.

SUPPLEMENTARY MATERIAL

The Supplementary Material for this article can be found online at: https://www.frontiersin.org/articles/10.3389/fphar.2021.706439/full#supplementary-material

REFERENCES

Alrafiah, A., Al-Ofi, E., Obaid, M. T., and Alsomali, N. (2019). Assessment of the Levels of Level of Biomarkers of Bone Matrix Glycoproteins and Inflammatory Cytokines from Saudi Parkinson Patients. *Biomed. Res. Int.* 2019, 2690205. doi:10.1155/2019/2690205

Araki, Y., Mukaisyo, K., Sugihara, H., Fujiyama, Y., and Hattori, T. (2010). Increased Apoptosis and Decreased Proliferation of Colonic Epithelium in Dextran Sulfate Sodium-Induced Colitis in Mice. *Oncol. Rep.* 24, 869–874. doi:10.3892/or.2010.869

Beier, E. E., Neal, M., Alam, G., Edler, M., Wu, L. J., and Richardson, J. R. (2017). Alternative Microglial Activation Is Associated with Cessation of Progressive Dopamine Neuron Loss in Mice Systemically Administered Lipopolysaccharide. *Neurobiol. Dis.* 108, 115–127. doi:10.1016/j.nbd.2017.08.009

Boza-Serrano, A., Reyes, J. F., Rey, N. L., Leffler, H., Bousset, L., Nilsson, U., et al. (2014). The Role of Galectin-3 in α-synuclein-induced Microglial Activation. *Acta Neuropathol. Commun.* 2, 156. doi:10.1186/s40478-014-0156-0

Boza-Serrano, A., Ruiz, R., Sanchez-Varo, R., García-Revilla, J., Yang, Y., Jimenez-Ferrer, I., et al. (2019). Galectin-3, a Novel Endogenous TREM2 Ligand, Detrimentally Regulates Inflammatory Response in Alzheimer's Disease. *Acta Neuropathol.* 138, 251–273. doi:10.1007/s00401-019-02013-z

Braak, H., Del Tredici, K., Bratzke, H., Hamm-Clement, J., Sandmann-Keil, D., and Rüb, U. (2002). Staging of the Intracerebral Inclusion Body Pathology Associated with Idiopathic Parkinson's Disease (Preclinical and Clinical Stages). *J. Neurol.* 249 Suppl 3, III–5. doi:10.1007/s00415-002-1301-4

Braak, H., Del Tredici, K., Rüb, U., de Vos, R. A., Jansen Steur, E. N., and Braak, E. (2003). Staging of Brain Pathology Related to Sporadic Parkinson's Disease. *Neurobiol. Aging* 24, 197–211. doi:10.1016/s0197-4580(02)00065-9

Braak, H., Sastre, M., Bohl, J. R., de Vos, R. A., and Del Tredici, K. (2007). Parkinson's Disease: Lesions in Dorsal Horn Layer I, Involvement of Parasympathetic and Sympathetic Pre- and Postganglionic Neurons. *Acta Neuropathol.* 113, 421–429. doi:10.1007/s00401-007-0193-x

Brudek, T. (2019). Inflammatory Bowel Diseases and Parkinson's Disease. *J. Parkinsons Dis.* 9, S331–S344. doi:10.3233/JPD-191729

Burguillos, M. A., Svensson, M., Schulte, T., Boza-Serrano, A., Garcia-Quintanilla, A., Kavanagh, E., et al. (2015). Microglia-Secreted Galectin-3 Acts as a Toll-like Receptor 4 Ligand and Contributes to Microglial Activation. *Cell Rep* 10, 1626–1638. doi:10.1016/j.celrep.2015.02.012

Buscarinu, M. C., Cerasoli, B., Annibali, V., Policano, C., Lionetto, L., Capi, M., et al. (2017). Altered Intestinal Permeability in Patients with Relapsing-Remitting Multiple Sclerosis: A Pilot Study. *Mult. Scler.* 23, 442–446. doi:10.1177/1352458516652498

Butovsky, O., Jedrychowski, M. P., Moore, C. S., Cialic, R., Lanser, A. J., Gabriely, G., et al. (2014). Identification of a Unique TGF-β-dependent Molecular and Functional Signature in Microglia. *Nat. Neurosci.* 17, 131–143. doi:10.1038/nn.3599

Carvajal, A. E., Serrano-Morales, J. M., Vázquez-Carretero, M. D., García-Miranda, P., Calonge, M. L., Peral, M. J., et al. (2017a). Reelin Protects from colon Pathology by Maintaining the Intestinal Barrier Integrity and Repressing

Tumorigenic Genes. *Biochim. Biophys. Acta Mol. Basis Dis.* 1863, 2126–2134. doi:10.1016/j.bbadis.2017.05.026

Carvajal, A. E., Vázquez-Carretero, M. D., García-Miranda, P., Peral, M. J., Calonge, M. L., and Ilundain, A. A. (2017b). Reelin Expression Is Up-Regulated in Mice colon in Response to Acute Colitis and Provides Resistance against Colitis. *Biochim. Biophys. Acta Mol. Basis Dis.* 1863, 462–473. doi:10.1016/j.bbadis.2016.11.028

Cengiz, T., Türkboyları, S., Gençler, O. S., and Anlar., Ö. (2019). The Roles of Galectin-3 and Galectin-4 in the Idiopatic Parkinson Disease and its Progression. *Clin. Neurol. Neurosurg.* 184, 105373. doi:10.1016/j.clineuro.2019.105373

Clark, I. A., and Vissel, B. (2021). Broader Insights into Understanding Tumor Necrosis Factor and Neurodegenerative Disease Pathogenesis Infer New Therapeutic Approaches. *J. Alzheimers Dis.* 79, 931–948. doi:10.3233/JAD-201186

Colnot, C., Fowlis, D., Ripoche, M. A., Bouchaert, I., and Poirier, F. (1998). Embryonic Implantation in Galectin 1/galectin 3 Double Mutant Mice. *Dev. Dyn.*, 211. 2-L: CO, 306–313. doi:10.1002/(SICI)1097-0177(199804)211:4<306::AID-AJA2>3.0.CO;2-L

Cooper, H. S., Murthy, S. N., Shah, R. S., and Sedergran, D. J. (1993). Clinicopathologic Study of Dextran Sulfate Sodium Experimental Murine Colitis. *Lab. Invest.* 69, 238–249.

de Rijk, M. C., Rocca, W. A., Anderson, D. W., Melcon, M. O., Breteler, M. M., Maraganore, D. M., et al. (1997). A Population Perspective on Diagnostic Criteria for Parkinson's Disease. *Neurology* 48, 1277–1281. doi:10.1212/wnl.48.5.1277

Díaz-Alvarez, L., and Ortega, E. (2017). The Many Roles of Galectin-3, a Multifaceted Molecule, in Innate Immune Responses against Pathogens. *Mediators Inflamm.* 2017, 9247574. doi:10.1155/2017/9247574

Donaldson, D. S., and Mabbott, N. A. (2016). The Influence of the Commensal and Pathogenic Gut Microbiota on Prion Disease Pathogenesis. *J. Gen. Virol.* 97, 1725–1738. doi:10.1099/jgv.0.000507

Flavin, W. P., Bousset, L., Green, Z. C., Chu, Y., Skarpathiotis, S., Chaney, M. J., et al. (2017). Endocytic Vesicle Rupture Is a Conserved Mechanism of Cellular Invasion by Amyloid Proteins. *Acta Neuropathol.* 134, 629–653. doi:10.1007/s00401-017-1722-x

Friedman, B. A., Srinivasan, K., Ayalon, G., Meilandt, W. J., Lin, H., Huntley, M. A., et al. (2018). Diverse Brain Myeloid Expression Profiles Reveal Distinct Microglial Activation States and Aspects of Alzheimer's Disease Not Evident in Mouse Models. *Cel Rep* 22, 832–847. doi:10.1016/j.celrep.2017.12.066

Galatro, T. F., Holtman, I. R., Lerario, A. M., Vainchtein, I. D., Brouwer, N., Sola, P. R., et al. (2017). Transcriptomic Analysis of Purified Human Cortical Microglia Reveals Age-Associated Changes. *Nat. Neurosci.* 20, 1162–1171. doi:10.1038/nn.4597

García-Domínguez, I., Veselá, K., García-Revilla, J., Carrillo-Jiménez, A., Roca-Ceballos, M. A., Santiago, M., et al. (2018). Peripheral Inflammation Enhances Microglia Response and Nigral Dopaminergic Cell Death in an *In Vivo* MPTP Model of Parkinson's Disease. *Front. Cel. Neurosci.* 12, 398. doi:10.3389/fncel.2018.00398

García-Revilla, J., Alonso-Bellido, I. M., Burguillos, M. A., Herrera, A. J., Espinosa-Oliva, A. M., Ruiz, R., et al. (2019). Reformulating Pro-oxidant Microglia in Neurodegeneration. *J. Clin. Med.* 8, 1719. doi:10.3390/jcm8101719

Garrido-Gil, P., Rodriguez-Perez, A. I., Dominguez-Meijide, A., Guerra, M. J., and Labandeira-Garcia, J. L. (2018). Bidirectional Neural Interaction between Central Dopaminergic and Gut Lesions in Parkinson's Disease Models. *Mol. Neurobiol.* 55, 7297–7316. doi:10.1007/s12035-018-0937-8

Grabert, K., Michoel, T., Karavolos, M. H., Clohisey, S., Baillie, J. K., Stevens, M. P., et al. (2016). Microglial Brain Region-dependent Diversity and Selective Regional Sensitivities to Aging. *Nat. Neurosci.* 19, 504–516. doi:10.1038/nn.4222

Gundersen, V. (2020). Parkinson's Disease: Can Targeting Inflammation Be an Effective Neuroprotective Strategy? *Front. Neurosci.* 14, 580311. doi:10.3389/fnins.2020.580311

Heneka, M. T., Carson, M. J., El Khoury, J., Landreth, G. E., Brosseron, F., Feinstein, D. L., et al. (2015). Neuroinflammation in Alzheimer's Disease. *Lancet Neurol.* 14, 388–405. doi:10.1016/S1474-4422(15)70016-5

Hernández-Romero, M. C., Delgado-Cortés, M. J., Sarmiento, M., de Pablos, R. M., Espinosa-Oliva, A. M., Argüelles, S., et al. (2012). Peripheral Inflammation Increases the Deleterious Effect of CNS Inflammation on the Nigrostriatal Dopaminergic System. *Neurotoxicology* 33, 347–360. doi:10.1016/j.neuro.2012.01.018

Herrera, A. J., Espinosa-Oliva, A. M., Oliva-Martin, M. J., Carrillo-Jimenez, A., Venero, J. L., and de Pablos, R. M. (2015). Collateral Damage: Contribution of Peripheral Inflammation to Neurodegenerative Diseases. *Curr. Top. Med. Chem.* 15, 2193–2210. doi:10.2174/1568026615666150610142027

Hickman, S. E., Kingery, N. D., Ohsumi, T. K., Borowsky, M. L., Wang, L. C., Means, T. K., et al. (2013). The Microglial Sensome Revealed by Direct RNA Sequencing. *Nat. Neurosci.* 16, 1896–1905. doi:10.1038/nn.3554

Hirsch, E. C., and Hunot, S. (2009). Neuroinflammation in Parkinson's Disease: a Target for Neuroprotection? *Lancet Neurol.* 8, 382–397. doi:10.1016/S1474-4422(09)70062-6

Jeon, S. B., Yoon, H. J., Chang, C. Y., Koh, H. S., Jeon, S. H., and Park, E. J. (2010). Galectin-3 Exerts Cytokine-like Regulatory Actions through the JAK-STAT Pathway. *J. Immunol.* 185, 7037–7046. doi:10.4049/jimmunol.1000154

Jiang, K., Rankin, C. R., Nava, P., Sumagin, R., Kamekura, R., Stowell, S. R., et al. (2014). Galectin-3 Regulates Desmoglein-2 and Intestinal Epithelial Intercellular Adhesion. *J. Biol. Chem.* 289, 10510–10517. doi:10.1074/jbc.M113.538538

Kaushal, S., Singh, C., and Singh, A. (2021). Involvement of the Gut-Brain axis in Neurological Disorders. *Cnsnddt* 20. doi:10.2174/1871527320666210310141015

Keren-Shaul, H., Spinrad, A., Weiner, A., Matcovitch-Natan, O., Dvir-Szternfeld, R., Ulland, T. K., et al. (2017). A Unique Microglia Type Associated with Restricting Development of Alzheimer's Disease. *Cell* 169, 1276–e17. doi:10.1016/j.cell.2017.05.018

Kim, Y. S., and Ho, S. B. (2010). Intestinal Goblet Cells and Mucins in Health and Disease: Recent Insights and Progress. *Curr. Gastroenterol. Rep.* 12, 319–330. doi:10.1007/s11894-010-0131-2

Kordower, J. H., Olanow, C. W., Dodiya, H. B., Chu, Y., Beach, T. G., Adler, C. H., et al. (2013). Disease Duration and the Integrity of the Nigrostriatal System in Parkinson's Disease. *Brain* 136, 2419–2431. doi:10.1093/brain/awt192

Krasemann, S., Madore, C., Cialic, R., Baufeld, C., Calcagno, N., El Fatimy, R., et al. (2017). The TREM2-APOE Pathway Drives the Transcriptional Phenotype of Dysfunctional Microglia in Neurodegenerative Diseases. *Immunity* 47, 566–e9. doi:10.1016/j.immuni.2017.08.008

Kumaresan, M., and Khan, S. (2021). Spectrum of Non-motor Symptoms in Parkinson's Disease. *Cureus* 13, e13275. doi:10.7759/cureus.13275

Lalancette-Hébert, M., Swarup, V., Beaulieu, J. M., Bohacek, I., Abdelhamid, E., Weng, Y. C., et al. (2012). Galectin-3 Is Required for Resident Microglia Activation and Proliferation in Response to Ischemic Injury. *J. Neurosci.* 32, 10383–10395. doi:10.1523/JNEUROSCI.1498-12.2012

Li, N., Wang, J. X., Huo, T. T., Zhao, J. R., and Wang, T. J. (2021). Associations of IL-1β and IL-6 Gene Polymorphisms with Parkinson's Disease. *Eur. Rev. Med. Pharmacol. Sci.* 25, 890–897. doi:10.26355/eurrev_202101_24657

Li, Y., Komai-Koma, M., Gilchrist, D. S., Hsu, D. K., Liu, F. T., Springall, T., et al. (2008). Galectin-3 Is a Negative Regulator of Lipopolysaccharide-Mediated Inflammation. *J. Immunol.* 181, 2781–2789. doi:10.4049/jimmunol.181.4.2781

Lin, J. C., Lin, C. S., Hsu, C. W., Lin, C. L., and Kao, C. H. (2016). Association between Parkinson's Disease and Inflammatory Bowel Disease: a Nationwide Taiwanese Retrospective Cohort Study. *Inflamm. Bowel Dis.* 22, 1049–1055. doi:10.1097/MIB.0000000000000735

Lippert, E., Stieber-Gunckel, M., Dunger, N., Falk, W., Obermeier, F., and Kunst, C. (2015). Galectin-3 Modulates Experimental Colitis. *Digestion* 92, 45–53. doi:10.1159/000431312

Mathys, H., Adaikkan, C., Gao, F., Young, J. Z., Manet, E., Hemberg, M., et al. (2017). Temporal Tracking of Microglia Activation in Neurodegeneration at Single-Cell Resolution. *Cel Rep* 21, 366–380. doi:10.1016/j.celrep.2017.09.039

Nalls, M. A., Pankratz, N., Pankratz, N., Lill, C. M., Do, C. B., Hernandez, D. G., et al. (2014). International Parkinson's Disease Genomics Consortium (IPDGC), Parkinson's Study Group (PSG) Parkinson's Research: The Organized GENetics Initiative (PROGENI), 23andMe, GenePD, NeuroGenetics Research Consortium (NGRC), Hussman Institute of Human Genomics (HIHG), Ashkenazi Jewish Dataset Investigator, Cohorts for Health and Aging Research in Genetic Epidemiology (CHARGE), North American Brain Expression Consortium (NABEC), United Kingdom Brain Expression Consortium (UKBEC), Greek Parkinson's Disease Consortium, and

Alzheimer Genetic Analysis GroupLarge-Scale Meta-Analysis of Genome-wide Association Data Identifies Six New Risk Loci for Parkinson's Disease. *Nat. Genet.* 46, 989–993. doi:10.1038/ng.3043

Nascimento, R. P. D., Machado, A. P. D. F., Galvez, J., Cazarin, C. B. B., and Maróstica Junior, M. R. (2020). Ulcerative Colitis: Gut Microbiota, Immunopathogenesis and Application of Natural Products in Animal Models. *Life Sci.* 258, 118129. doi:10.1016/j.lfs.2020.118129

Peter, I., Dubinsky, M., Bressman, S., Park, A., Lu, C., Chen, N., et al. (2018). Anti-Tumor Necrosis Factor Therapy and Incidence of Parkinson Disease Among Patients with Inflammatory Bowel Disease. *JAMA Neurol.* 75, 939–946. doi:10.1001/jamaneurol.2018.0605

Pröbstel, A. K., Zhou, X., Baumann, R., Wischnewski, S., Kutza, M., Rojas, O. L., et al. (2020). Gut Microbiota-specific IgA+ B Cells Traffic to the CNS in Active Multiple Sclerosis. *Sci. Immunol.* 5, eabc7191. doi:10.1126/sciimmunol.abc7191

Qin, L., Wu, X., Block, M. L., Liu, Y., Breese, G. R., Hong, J. S., et al. (2007). Systemic LPS Causes Chronic Neuroinflammation and Progressive Neurodegeneration. *Glia* 55, 453–462. doi:10.1002/glia.20467

Qin, X. Y., Zhang, S. P., Cao, C., Loh, Y. P., and Cheng, Y. (2016). Aberrations in Peripheral Inflammatory Cytokine Levels in Parkinson Disease: A Systematic Review and Meta-Analysis. *JAMA Neurol.* 73, 1316–1324. doi:10.1001/jamaneurol.2016.2742

Rayaprolu, S., Mullen, B., Baker, M., Lynch, T., Finger, E., Seeley, W. W., et al. (2013). TREM2 in Neurodegeneration: Evidence for Association of the p.R47H Variant with Frontotemporal Dementia and Parkinson's Disease. *Mol. Neurodegener.* 8, 19. doi:10.1186/1750-1326-8-19

Rooks, M. G., and Garrett, W. S. (2016). Gut Microbiota, Metabolites and Host Immunity. *Nat. Rev. Immunol.* 16, 341–352. doi:10.1038/nri.2016.42

Satoh, K., Niwa, M., Goda, W., Binh, N. H., Nakashima, M., Takamatsu, M., et al. (2011). Galectin-3 Expression in Delayed Neuronal Death of Hippocampal CA1 Following Transient Forebrain Ischemia, and its Inhibition by Hypothermia. *Brain Res.* 1382, 266–274. doi:10.1016/j.brainres.2011.01.049

Sciacchitano, S., Lavra, L., Morgante, A., Ulivieri, A., Magi, F., De Francesco, G. P., et al. (2018). Galectin-3: One Molecule for an Alphabet of Diseases, from A to Z. *Int. J. Mol. Sci.* 19. doi:10.3390/ijms19020379

Shimura, T., Takenaka, Y., Tsutsumi, S., Hogan, V., Kikuchi, A., and Raz, A. (2004). Galectin-3, a Novel Binding Partner of Beta-Catenin. *Cancer Res.* 64, 6363–6367. doi:10.1158/0008-5472.CAN-04-1816

Simovic Markovic, B., Nikolic, A., Gazdic, M., Bojic, S., Vucicevic, L., Kosic, M., et al. (2016). Galectin-3 Plays an Important Pro-inflammatory Role in the Induction Phase of Acute Colitis by Promoting Activation of NLRP3 Inflammasome and Production of IL-1β in Macrophages. *J. Crohns Colitis* 10, 593–606. doi:10.1093/ecco-jcc/jjw013

Song, S., Byrd, J. C., Mazurek, N., Liu, K., Koo, J. S., and Bresalier, R. S. (2005). Galectin-3 Modulates MUC2 Mucin Expression in Human colon Cancer Cells at the Level of Transcription via AP-1 Activation. *Gastroenterology* 129, 1581–1591. doi:10.1053/j.gastro.2005.09.002

Tsai, H. F., Wu, C. S., Chen, Y. L., Liao, H. J., Chyuan, I. T., and Hsu, P. N. (2016). Galectin-3 Suppresses Mucosal Inflammation and Reduces Disease Severity in Experimental Colitis. *J. Mol. Med. (Berl)* 94, 545–556. doi:10.1007/s00109-015-1368-x

Viguier, M., Advedissian, T., Delacour, D., Poirier, F., and Deshayes, F. (2014). Galectins in Epithelial Functions. *Tissue Barriers* 2, e29103. doi:10.4161/tisb.29103

Villarán, R. F., Espinosa-Oliva, A. M., Sarmiento, M., De Pablos, R. M., Argüelles, S., Delgado-Cortés, M. J., et al. (2010). Ulcerative Colitis Exacerbates Lipopolysaccharide-Induced Damage to the Nigral Dopaminergic System: Potential Risk Factor in Parkinson`s Disease. *J. Neurochem.* 114, 1687–1700. doi:10.1111/j.1471-4159.2010.06879.x

Villumsen, M., Aznar, S., Pakkenberg, B., Jess, T., and Brudek, T. (2019). Inflammatory Bowel Disease Increases the Risk of Parkinson's Disease: a Danish Nationwide Cohort Study 1977-2014. *Gut* 68, 18–24. doi:10.1136/gutjnl-2017-315666

Volarevic, V., Zdravkovic, N., Harrell, C. R., Arsenijevic, N., Fellabaum, C., Djonov, V., et al. (2019). Galectin-3 Regulates Indoleamine-2,3-dioxygenase-dependent Cross-Talk between Colon-Infiltrating Dendritic Cells and T Regulatory Cells and May Represent a Valuable Biomarker for Monitoring the Progression of Ulcerative Colitis. *Cells* 8, 709. doi:10.3390/cells8070709

Wan, Q. Y., Zhao, R., and Wu, X. T. (2020). Older Patients with IBD Might Have Higher Risk of Parkinson's Disease. *Gut* 69, 193–194. doi:10.1136/gutjnl-2018-317103

Weimers, P., Halfvarson, J., Sachs, M. C., Saunders-Pullman, R., Ludvigsson, J. F., Peter, I., et al. (2019). Inflammatory Bowel Disease and Parkinson's Disease: A Nationwide Swedish Cohort Study. *Inflamm. Bowel Dis.* 25, 111–123. doi:10.1093/ibd/izy190

Wesley, U. V., Vemuganti, R., Ayvaci, E. R., and Dempsey, R. J. (2013). Galectin-3 Enhances Angiogenic and Migratory Potential of Microglial Cells via Modulation of Integrin Linked Kinase Signaling. *Brain Res.* 1496, 1–9. doi:10.1016/j.brainres.2012.12.008

Yazar, H. O., Yazar, T., and Cihan, M. (2019). A Preliminary Data: Evaluation of Serum Galectin-3 Levels in Patients with Idiopathic Parkinson's Disease. *J. Clin. Neurosci.* 70, 164–168. doi:10.1016/j.jocn.2019.08.032

Yip, P. K., Carrillo-Jimenez, A., King, P., Vilalta, A., Nomura, K., Chau, C. C., et al. (2017). Galectin-3 Released in Response to Traumatic Brain Injury Acts as an Alarmin Orchestrating Brain Immune Response and Promoting Neurodegeneration. *Sci. Rep.* 7, 41689. doi:10.1038/srep41689

Yousefi, A., Najafi, M., Motamed, F., Mahmoudi, E., Bidoki, A. Z., Sadr, M., et al. (2018). Association of Interleukin-6 and Interleukin-1 Family Gene Polymorphisms in Autoimmune Hepatitis. *Ann. Hepatol.* 17, 1021–1025. doi:10.5604/01.3001.0012.7202

Zhang, L., Li, Y. M., Zeng, X. X., Wang, X. Y., Chen, S. K., Gui, L. X., et al. (2018). Galectin-3- Mediated Transdifferentiation of Pulmonary Artery Endothelial Cells Contributes to Hypoxic Pulmonary Vascular Remodeling. *Cell Physiol. Biochem.* 51, 763–777. doi:10.1159/000495331

Zhu, F., Li, C., Gong, J., Zhu, W., Gu, L., and Li, N. (2019). The Risk of Parkinson's Disease in Inflammatory Bowel Disease: A Systematic Review and Meta-Analysis. *Dig. Liver Dis.* 51, 38–42. doi:10.1016/j.dld.2018.09.017

Conflict of Interest: The authors declare that the research was conducted in the absence of any commercial or financial relationships that could be construed as a potential conflict of interest.

Publisher's Note: All claims expressed in this article are solely those of the authors and do not necessarily represent those of their affiliated organizations, or those of the publisher, the editors and the reviewers. Any product that may be evaluated in this article, or claim that may be made by its manufacturer, is not guaranteed or endorsed by the publisher.

Copyright © 2021 Espinosa-Oliva, García-Miranda, Alonso-Bellido, Carvajal, González-Rodríguez, Carrillo-Jiménez, Temblador, Felices-Navarro, García-Domínguez, Roca-Ceballos, Vázquez-Carretero, García-Revilla, Santiago, Peral, Venero and de Pablos. This is an open-access article distributed under the terms of the Creative Commons Attribution License (CC BY). The use, distribution or reproduction in other forums is permitted, provided the original author(s) and the copyright owner(s) are credited and that the original publication in this journal is cited, in accordance with accepted academic practice. No use, distribution or reproduction is permitted which does not comply with these terms.

Advantages of publishing in Frontiers

OPEN ACCESS
Articles are free to read for greatest visibility and readership

FAST PUBLICATION
Around 90 days from submission to decision

HIGH QUALITY PEER-REVIEW
Rigorous, collaborative, and constructive peer-review

TRANSPARENT PEER-REVIEW
Editors and reviewers acknowledged by name on published articles

Frontiers
Avenue du Tribunal-Fédéral 34
1005 Lausanne | Switzerland

Visit us: www.frontiersin.org
Contact us: frontiersin.org/about/contact

REPRODUCIBILITY OF RESEARCH
Support open data and methods to enhance research reproducibility

DIGITAL PUBLISHING
Articles designed for optimal readership across devices

FOLLOW US
@frontiersin

IMPACT METRICS
Advanced article metrics track visibility across digital media

EXTENSIVE PROMOTION
Marketing and promotion of impactful research

LOOP RESEARCH NETWORK
Our network increases your article's readership